1-1-2014

Part I. Synthetic Investigations of Heterocyclic Natural and Unnatural Compounds Part II. New Approach to Latent Fingerprint Detection on Paper

Jisun Lee
University of Pennsylvania, jlsun@sas.upenn.edu

Part I. Synthetic Investigations of Heterocyclic Natural and Unnatural Compounds Part II. New Approach to Latent Fingerprint Detection on Paper

Abstract
Since the discovery and isolation of the didemnin family of marine depsipeptides in 1981, the synthesis and biological activity of its congeners have been of great interest to the scientific community. Of those, didemnin B was the first marine natural product to reach phase II clinical trials, stimulating many analogue syntheses to date. Almost two decades later, tamandarins A and B were reported and found to possess a structure similar to that of the didemnins. Significant efforts have been devoted to the syntheses of tamandarin analogues to find whether they behaved as didemnin mimics or as individual therapeutic agents. The biological and synthetic significance of the didemnins, tamandarins, and related natural products are discussed in Chapter 1.

The improved second-generation synthesis of the tamandarin B macrocycle and its successful application to the syntheses of three novel tamandarin B side chain analogues are presented in Chapter 2. The results of these investigations could help elucidate the structure-activity relationship as well as mode of action of these natural products.

Chapter 3 deals with the generation of structurally intriguing azabicyclic [3.1.0]- and [4.1.0]aminocyclopropanes and their application in an unprecedented ring-opening conditions to afford corresponding 3-piperidinone and 3-azepinone derivatives which are important pharmaceutical motifs.

Chapter 4 introduces a rapidly growing family of natural diketopiperazine alkaloids: epipolythiodiketopiperazine (ETP) alkaloids, and related synthetic efforts in the generation of these alkaloids. Extensive synthetic investigation towards the formal synthesis of (−)-epicoccin G and other related epidithiodiketopiperazine alkaloids have been conducted. A novel methodology to access the 6-5-6-5-6 pentacyclic framework present in many ETP alkaloids is presented. Further application of this methodology in total synthesis could provide ETP alkaloids that have not been synthesized.

Chapter 5 deals with the development and successful application of 1,2-indanedione functionalized gold nanoparticles in a modified multi-metal deposition process for the development of latent fingerprints on paper. Although a wide variety of ninhydrin-like compounds have been developed as chemical agents for this process over the years, considerable portions of latent fingerprints still escape detection. The new approach provides an alternative method of fingerprint detection that could be utilized in challenging situations.

Degree Type
Dissertation

Degree Name
Doctor of Philosophy (PhD)

Graduate Group
Chemistry

PART I. SYNTHETIC INVESTIGATIONS OF HETEROCYCLIC NATURAL AND UNNATURAL COMPOUNDS

PART II. NEW APPROACH TO LATENT FINGERPRINT DETECTION ON PAPER

Jisun Lee

A DISSERTATION

in

Chemistry

Presented to the Faculties of the University of Pennsylvania

in

Partial Fulfillment of the Requirements for the
Degree of Doctor of Philosophy

2014

Supervisor of Dissertation

_____

Madeleine M. Joullié
Class of 1970 Professor of Chemistry

Graduate Group Chairperson

_____

Gary A. Molander
Hirschmann-Makineni Professor of Chemistry

Dissertation Committee:

Amos B. Smith III, Rhodes-Thompson Professor of Chemistry
William P. Dailey, Associate Professor of Chemistry
David M. Chenoweth, Assistant Professor of Chemistry

PART I. SYNTHETIC INVESTIGATIONS OF HETEROCYCLIC NATURAL AND UNNATURAL COMPOUNDS

PART II. NEW APPROACH TO LATENT FINGERPRINT DETECTION ON PAPER

DEDICATION

To Mom and Dad

For their unconditional love and support

ACKNOWLEDGMENT

I would like to first thank my advisor, Professor Madeleine M. Joullié, for accepting me into her research group even when things were uncertain. Although I had a rough start of my graduate career, she always supported me in all my endeavors and gave me creative freedom in all my projects. I deeply respect and appreciate her for all that she has done for her students and me over the years. I would also like to thank my committee members, Professor Smith, Professor Dailey, and Professor Chenoweth for always keeping me on my toes and reminding me to always put in my best effort. Of course, I have to thank my Bryn Mawr crew. Professor Malachowski introduced me to synthetic organic chemistry research. I still remember the day when he showed me how to set up a Birch reduction on large scale—it was the coolest, yet scariest thing ever. Thank you for teaching me the ins and outs of organic chemistry research and how to behave in a research lab in general. I also thank Dr. Nerz-Stormes for her love and support since the beginning of my undergraduate years at Bryn Mawr. I was overwhelmed with joy and sadness after I took her final exam, just because I have enjoyed her course that much. I thank her for always encouraging me and also taking me back this past year to teach along side of her. And of course, Dr. Frank Mallory and Dr. Sally Mallory for their support since Bryn Mawr as well as until today. I would not have come to Penn or survived Penn Chemistry if it wasn't for both Dr. Mallorys! Thank you so much for believing in me and being there for me when things were tough. I would also like to thank my former Joullié group members, especially Dr. Ken Lassen, Dr. Simon Berritt, Dr. Brandon Kelley, and Megan Potteiger, for making my graduate experience enjoyable.

As for chemistry buddies, I thank everyone that I started my graduate career with, especially Dr. Gretchen Stanton, Dr. Kevin Cheng, and Dr. Nga Nguyen for always being there for me in times of sadness and happiness. I would also like to extend my appreciation and special thanks to Dr. Simon Berritt for being there since I first joined the Joullié group, you have been my biggest supporter and I look forward to many more fun and adventurous days with you. Thank you for reminding me not to take myself too seriously and to enjoy chemistry for what it is. I want to thank my parents for all that they've done for me. You have made all of this possible, and every bit of this work is dedicated to you. Thank you for all your prayers and believing in the greater purpose of things. Thank you for reminding me that there is no such thing as coincidence, and that I could not have done any of this on my own. I also have to acknowledge that my mom is the first person who introduced me to the lab setting. It was some crazy times working in her lab alongside her students during my sophomore year. I would consider my life a success if I could become like you one day—you've showed me how to balance work and family life and do both well. And I thank my dad for being the silent but strong supporter in all that I do, and putting up with me changing my mind so many times about med school. Thank you for reminding me that the grass may not always be greener on the other side. Finally, to all the others that I have failed to mention individually, I thank you for helping me arrive at this point in my life and hopefully I could now stop making excuses about being too busy to hang out…

ABSTRACT

PART I. SYNTHETIC INVESTIGATIONS OF HETEROCYCLIC NATURAL AND UNNATURAL COMPOUNDS

PART II. NEW APPROACH TO LATENT FINGERPRINT DETECTION ON PAPER

Jisun Lee

Madeleine M. Joullié

Since the discovery and isolation of the didemnin family of marine depsipeptides in 1981, the synthesis and biological activity of its congeners have been of great interest to the scientific community. Of those, didemnin B was the first marine natural product to reach phase II clinical trials, stimulating many analogue syntheses to date. Almost two decades later, tamandarins A and B were reported and found to possess a structure similar to that of the didemnins. Significant efforts have been devoted to the syntheses of tamandarin analogues to find whether they behaved as didemnin mimics or as individual therapeutic agents. The biological and synthetic significance of the didemnins, tamandarins, and related natural products are discussed in Chapter 1.

The improved second-generation synthesis of the tamandarin B macrocycle and its successful application to the syntheses of three novel tamandarin B side chain analogues are presented in Chapter 2. The results of these investigations could help elucidate the structure-activity relationship as well as mode of action of these natural products.

Chapter 3 deals with the generation of structurally intriguing azabicyclic [3.1.0]- and [4.1.0]aminocyclopropanes and their application in an unprecedented ring-opening

conditions to afford corresponding 3-piperidinone and 3-azepinone derivatives which are important pharmaceutical motifs.

Chapter 4 introduces a rapidly growing family of natural diketopiperazine alkaloids: epipolythiodiketopiperazine (ETP) alkaloids, and related synthetic efforts in the generation of these alkaloids. Extensive synthetic investigation towards the formal synthesis of (−)-epicoccin G and other related epidithiodiketopiperazine alkaloids have been conducted. A novel methodology to access the 6-5-6-5-6 pentacyclic framework present in many ETP alkaloids is presented. Further application of this methodology in total synthesis could provide ETP alkaloids that have not been synthesized.

Chapter 5 deals with the development and successful application of 1,2-indanedione functionalized gold nanoparticles in a modified multi-metal deposition process for the development of latent fingerprints on paper. Although a wide variety of ninhydrin-like compounds have been developed as chemical agents for this process over the years, considerable portions of latent fingerprints still escape detection. The new approach provides an alternative method of fingerprint detection that could be utilized in challenging situations.

TABLE OF CONTENTS

Chapter 1: Didemnins, tamandarins and related natural products

1.1) Discovery and isolation

Marine invertebrates of the class Ascidiacea (phylum Chordata, subphylum Urochordata) have been found to produce nitrogen-containing metabolites that often exhibit potent anticancer properties.[1,2] Of such, ascidians, more commonly known as sea squirts or tunicates, are marine invertebrates that are characterized by a tough outer tunic and their ability to attach themselves to rocks and shells. Ascidians possess a fascinating defense mechanism in which they produce secondary metabolites that significantly reduce predation on both adults and larvae. This chemical defense mechanism is crucial in allowing the release of large larvae during daylight periods when the larvae have the greatest probability to select appropriate settlement sites when exposure to fish predation is the highest.

The colonial ascidian *Trididemnum solidum* (Figure 1.1) is found in a broad range of geographical locations, and forms large mats, actively growing and harming live coral.[3] Larvae of *Trididemnum solidum* have been found to owe their unpalatability to chemical rather than structural defenses. The didemnins (**1**-**5**, Figure 1.2) were isolated from *Trididemnum solidum*, including several from *Trididemnum cyanophorum*, in which the presence of didemnin cyclic peptides in the larvae supports a chemical defense.[4,5,6,7,8,9,10,11,12] Interestingly, there are chemical differences between larvae and adults, where the larvae contain only four of the six didemnins found in the adult colonies.

The larvae either receive a selected transfusion of adult chemistry or synthesize secondary metabolites to better adapt to or enhance their chance of survival.[3] Comparison of the chemistries of the larvae and the colonies that produce them should aid in the identification of factors affecting secondary metabolites at different life stages.[13] Of note, studies by Lindquist, Hays, and Fenical suggest that ascidians may be able to avoid autotoxicity from their chemical defense mechanism by possessing a well-developed circulatory system that allow the encapsulation of bioactive compounds within blood cells.[3,13]

Figure 1.1 Photographs of *Tridemnum solidum* and *Aplidium albicans*: (a) *Tridemnum solidum*, (b) *Tridemnum solidum* overgrowing an Agaricia coral species, and (c) *Aplidium albicans*.
Sources: (a) Photograph courtesy of François Rebufat. Reprinted from http://www.pictolife.net/photos.php?table=ascidies. (b) Photograph courtesy of Miriam C. Goldstein, Scripps Institution of Oceanography. (c) Photograph courtesy of PharmaMar, S.A Sociedad Unipersonal. All rights reserved.

1.2) Structural features

The didemnins (**1**-**5**, Figure 1.2) are a family of cyclic depsipeptides isolated from tunicates of the family *Didemnidae*, while as aplidine or dehydrodidemnin B (**4**, Figure 1.2) was extracted from the ascidian *Aplidium albicans* (Figure 1.1).[14] While these ascidians were found in the Caribbean and Mediterranean coasts, the tamandarins (**6**, **7**, Figure 1.2) were isolated from an unidentified Brazilian marine ascidian also from the family *Didemnidae*.[15,16] Interestingly, although the two species that generated these ascidians were found in remote geographic locations, they were found to use a common method to defend their vulnerable larvae by producing structurally similar, but not

identical depsipeptides (Figure 1.2).[17] More recently, another didemnin congener, *N*,*N*'-methyleno-didemnin A, was isolated from *Tridemnum solidum*.[18]

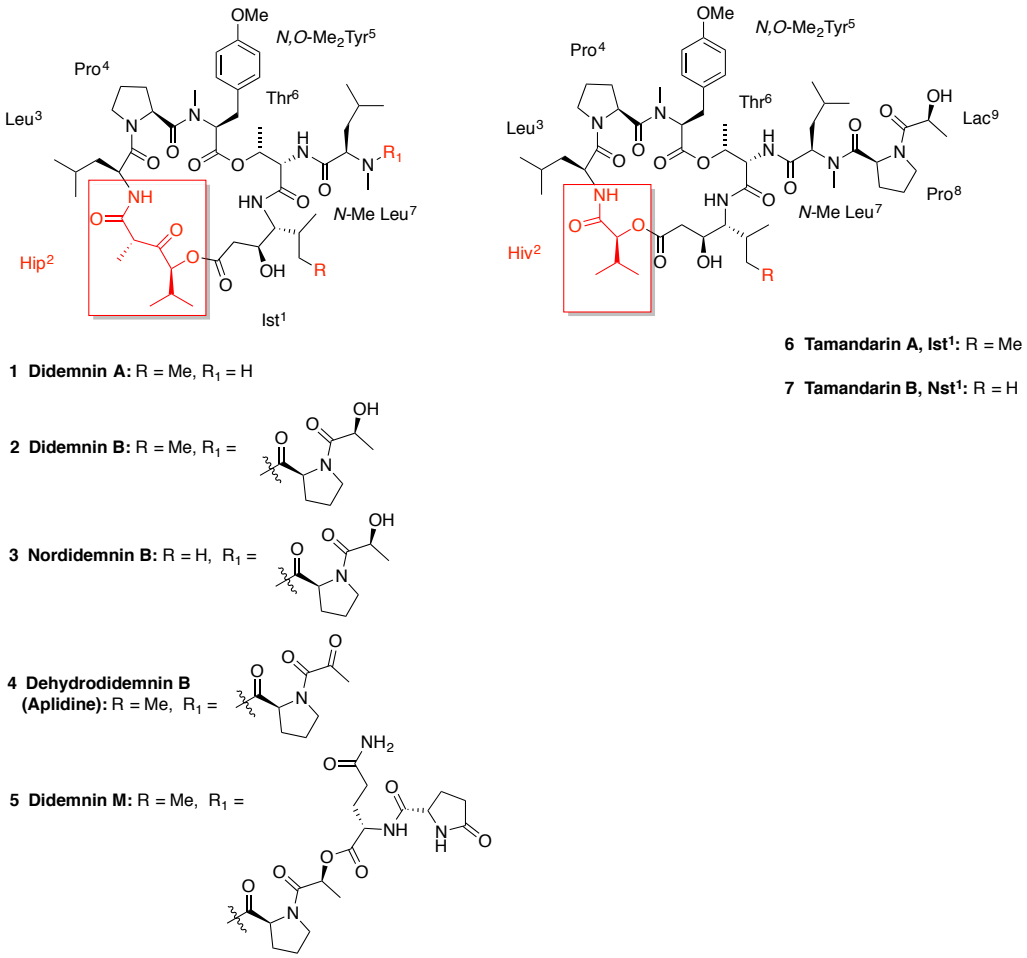

Figure 1.2. Structures of naturally occurring didemnins and tamandarins.

Tamandarins A (**6**) and B (**7**) are closely related to **2** and nordidemnin B (**3**), respectively, varying only by the presence of α-hydroxyisovaleric acid (Hiv^2) instead of the [α-(α-hydroxyisovaleryl)propionic acid] (Hip^2) present in all didemnin congeners (Figure 1.2). Didemnins and tamandarins display similar biological properties, which suggest that the propionic acid unit leads to only a minor conformational modification. Tamandarin A contains an isostatine residue (Ist^1) in the macrocycle, while tamandarin B possess a

norstatine residue (Nst[1]) (Figure 1.2). Extensive conformational studies to assess the ring modifications in **6** showed that tamandarin A is rigid, and that all peptide bonds have *trans* conformations, as in **2**.[15] Furthermore, the keto group, present in the Hip[2] unit but absent in the Hiv[2] unit, does not seem to affect the bioactivity even though it was believed that its position, extending outwards from the macrocycle, allowed it to interact with its associated protein targets.[19] It is of interest to note that removal of the stereogenic methyl group in didemnin B led to complete loss of bioactivity, while its absence in the tamandarins does not affect the bioactivity. This suggests that its absence in the didemnins may produce a change in conformation that could be due to enolization.

1.3) Function as chemical defense agents in nature

Perhaps one of the most important ecological questions is the effect of consuming chemically defended prey on the fitness of marine consumers and consequently the evolution of effective chemical defenses in marine prey.[20] *Tridemnum solidum* larvae are recognized and avoided by marine predators. When ingested at ecologically realistic doses, they can decrease or destroy consumer fitness. The ascidian tunic is the first physical and chemical defense barrier against microbial and fungal organisms, fouling organisms, and predation.[3]

In 2003, Joullié and coworkers synthesized fluorescent analogues of didemnin B (**8**) and tamandarin A (**9**, Figure 1.3) to investigate the potential chemical defense mechanisms of tunicates of the family *Didemnidae*.[17]

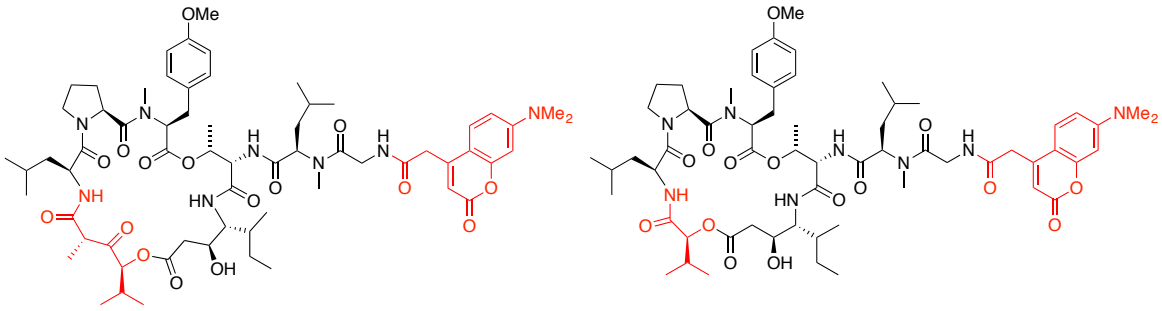

8 Fluorescent didemnin B **9 Fluorescent tamandarin A**

Figure 1.3. Fluorescent probes developed from the didemnin and tamandarin depsipeptides.

When mosquito larvae containing the fluorescent derivatives were fed to six species of fish, a rapid response was observed, where the rate of absorption and physiological processing were the same for both synthetic products. The effect was dependent on the dose, leading to association of the larval species with distaste, and after five daily feedings, 50% of the fish that consumed 50 ± 4 ng of depsipeptide avoided the treated larvae. Predator fitness increased with their ability to recognize the treated larvae, but produced an overall decrease in hunting. Ingestion and absorption of the treated larvae resulted in accumulation of fluorescent material in the joint tissue of the fish. This was the first report that showed that didemnin B and tamandarin A fluorescent probes **8** and **9**, although structurally different, possessed similar activity (Figure 1.3).

1.4) Crystallographic and NMR studies

Only three crystal structures for the cyclic depsipetides have been elucidated to date, which includes didemnin B (**2**),[19] didemnin A (**1**),[21] and the cyclic depsipeptide backbone (Figure 1.4).[22] The features of these structures may be relevant to their biological activity, especially as conformational consistency from crystal to solution structure is well established in a range of solvents.[9,19,23,24,25]

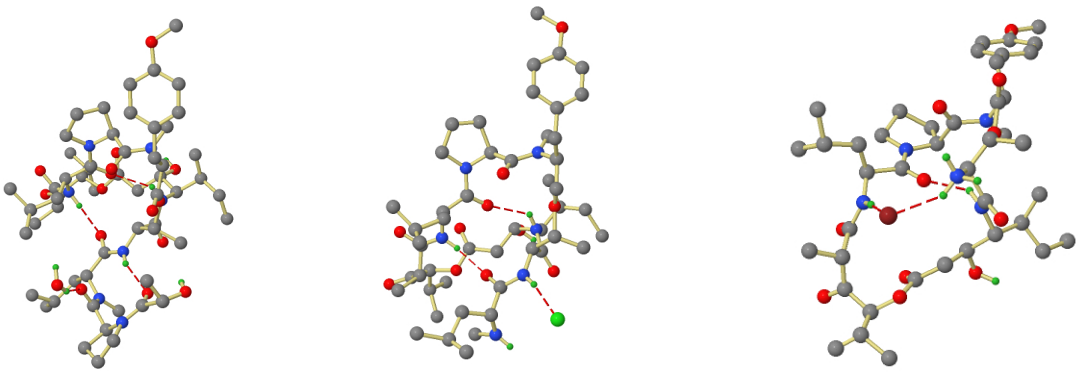

(a) didemnin B (b) didemnin A (c) didemnin B macrocyclic salt

Figure 1.4. Computer-generated representations of (a) didemnin B (**2**); (b) didemnin A (**1**); (c) didemnin B macrocyclic salt. These structures were generated using a Java application called Jmol, an open-source Java viewer for chemical structures in 3D. (http://www.jmol.org/).

Didemnin B (**2**) exhibits an irregular shape, described as a "bent figure eight" (Figure 1.4). There are three hydrogen bonds stabilizing the structure: a) the only hydrogen bond in the macrocycle that stretches from the L-proline carbonyl to the isostatine NH (3.020 Å), b) the hydrogen bond in the linear chain goes from the lactyl proline carbonyl to the NH of *N*-Me-D-leucine (3.087 Å) which is responsible for the β(II)-turn of the side chain, and c) finally the strongest hydrogen bond which links the linear side chain to the backbone (2.90 Å), stretches from the NH of the macrocycle leucine to the *N*-Me-D-leucine carbonyl of the side chain.

All oxygen atoms in the macrocycle point away from the interior of the cavity, which explains why **2** is not an ionophore and does not complex alkali cations. Didemnin B (**2**) also forms three strong hydrogen bonds with a water molecule. Moreover, although Hossain and coworkers originally recognized more than one group on **2** that could bind to receptors, they suggested that the linear peptide chain, particularly the lactylproline moiety, was the most significant structural feature for the biological activity.[19]

The crystal structure and packing of didemnin A (**1**) are different from those of **2**, because the molecules form a dimeric pair, in which each molecule preserves the folded conformation of a "bent figure eight." They are also stabilized by two intramolecular hydrogen bonds similar to hydrogen bonds present in didemnin B (a and c mentioned above), but stronger (2.83 Å *vs.* 3.02 Å and 2.88 Å *vs.* 2.90 Å), suggesting a more rigid macrocycle. An analysis of selected torsional angles also showed some variations.[21]

Finally, the crystal structure for the macrocycle hydrobromide salt, Figure 1.4 (c), displays a more flattened oval shape, due to lack of a side chain. Two separate conformations were identified, where one of them more closely resembled didemnin B. A comparison of the torsional angles also showed good agreement with those of didemnin B for only one of the two conformations. The bromide ion was situated in the center of the molecule, suggesting possible ionophoric properties.[22]

Spectroscopic properties of both didemnins and tamandarins have been well investigated in conjugation with their discovery.[16] However, recent reports in this area are few, since the earlier investigation of **4** revealed the existence of two slowly interconverting conformers that could only be resolved by HPLC.[26] The conformers are due to hydrogen bonding from the NH of Thr^6 and the two carbonyls of the pyruvyl unit, resulting in restricted rotation around the pyruvyl-proline bond of the side chain. The different hydrogen bonds result in *cis* (with keto carbonyl) and *trans* (with amide carbonyl) isomers for aplidine (Figure 1.5) but do not affect the three-dimensional structure of the macrocycle.

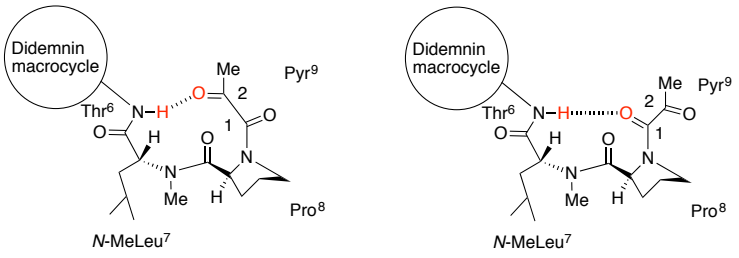

Figure 1.5. Hydrogen bonds between Thr^6-NH and the pyruvyl unit of aplidine (**4**) in the *cis*- and *trans*- conformation.

Didemnin B (**2**), which has a lactyl unit instead of a pyruvyl unit, exists as only one major conformer in solution with either $CDCl_3$ or DMSO-d_6 as the NMR solvent. However, the *cis-/trans*- isomers of aplidine (**4**) exist as a 45:55 mixture in $CDCl_3$. Interestingly, a more recent NMR study of aplidine (**4**) in DMSO-d_6 done by Cárdenas and coworkers shows four interconverting structures in a ratio of 47:33:13:7, and represents the first observation of conformational isomers for the didemnins.[27] The major isomers are the same *cis*- and *trans*- isomers observed in $CDCl_3$, but with a preference for *cis*. The minor isomers arise from similar *cis*/*trans* isomers in structures in which the *N*-Me-D-Leu^7-Pro^8 is the *cis* isomer. It is important to note that all conformational isomers retain the three-dimensional structure of **4**, but a significant difference in the disposition of the side chain is observed between the major and minor pairs of conformations. In the major isomers, the side chains adopt the well-established type II β-turn-like conformation, while as in the minor conformations, due to the presence of the *N*-Me-D-Leu^7-Pro^8 *cis*-amide bond, the side chains adopt an open, extended conformation that cannot form a hydrogen bond to the macrocycle. The authors believe that this finding may suggest that the adoption of a β-turn-type conformation in the didemnin side chain may not be the only prerequisite for biological activity.

1.5) Biological activity and clinical trials

In 1981 Rinehart and coworkers isolated didemnin B (**2**) from extracts of the tunicate *Tridemnum solidum*, and this compound went through preclinical and clinical trials as an anticancer, antiviral, and immunosuppressive drug.[28] Although it was the first compound that was characterized from a marine source to go into clinical trials for human diseases, the NCI trials were terminated in 1990 due to toxicity issues.[3] While some progress was made in understanding its protein biosynthesis and structure/activity relationships (SARs), the complex mechanistic issues of antitumor potency still need to be elucidated.[16]

Didemnin B was found to induce apoptosis in a wide range of transformed cell lines, while resting normal lymphocytes were unaffected by exposure to the drug.[29] In order to investigate whether cell transformation, and/or cell proliferation was necessary for the drug to induce apoptosis, the effect of didemnin B on freshly harvested human lymphocytes before and after stimulation with concanavalin A was examined. Excitingly, didemnin B induced apoptosis in normal lymphocytes only after mitogenic stimulation, warranting further examination for its potential use as a chemotherapeutic agent, especially for the treatment of leukemia.[29]

Aplidine (**4**) is one of the most biologically active metabolites from an ascidian of the genus *Aplidium*.[30] It is widely known as an antitumor agent, which is currently obtained by chemical synthesis. It is also PharmaMar's second most advanced compound, and is currently in phase II clinical trials for solid and hematological malignant neoplasms, T

cell lymphoma, and myelofibrosis, and in phase III clinical trials for multiple myeloma.[3] In 2003, the European Commission granted approval to PharmaMar SA Sociedad Unipersonal, Spain, to use aplidine in the treatment of acute lymphoblastic leukemia.[31] Moreover, the Food and Drug Administration (FDA) has accepted the proposal made by PharmaMar for the production process of the drug Aplidin®. Unlike didemnin B (**2**), which was not successful in clinical trials, aplidine (**4**) showed no cardiotoxicity and exhibited stronger antitumor activity.[32,33,34,35]

1.6) Structural modifications of didemnins

On the basis of spatial relationships, three particular sites of the didemnin macrocycle were considered essential for the biological activity: the tyrosine side chain of the tetrapeptide region, the hydroxyl group of isostatine, and the side chain attached to the amino group of threonine. These three regions were found to be at the periphery of the macrocycle as established by X-ray and solution conformation of **2**.[3] In an effort to better understand the structure-activity relationships of the didemnins, several analogues were prepared with modifications in the side chain, Hip-isostatine region, tetrapeptide region, and macrocycle backbone. These investigations were thoroughly reviewed by Dr. Matthew Vera.[36]

Although several modifications in the Hip-isostatine region were reported, results consistently showed low tolerance for changes in this region, as all analogues exhibited dramatically decreased bioactivity, albeit with small differences between cytotoxicity and immunosuppressive activity.[16] Nordidemnin B (**3**) was the only congener with a structural modification in this portion of the macrolide, in which isostatine was replaced

by norstatine without affecting the bioactivity.[12,37] Another successful modification in this region was displayed in the tamandarins, which contain a drastically modified Hip^2 residue. The tamandarins showed comparable bioactivity with respect to didmenin B.[15]

With regards to the modifications in the macrocyclic backbone, it was originally thought that the ester group in the macrocycle was a source of instability, hence the replacement of this group with an amide was the focus of several investigations.[3] Although replacement of the Thr^6 ester resulted in a significant decrease in cytotoxicity, replacement of both Thr^6 and Hip^2 ester groups or replacement with a short chain, such as diaminopropionic acid, did not alter the cytotoxicity.[38]

The approach of using covalent linkers to replace amino acids that do not participate in receptor activation has led to the syntheses of comparable or more active analogues. Joullié and coworkers synthesized the first reduced ring analogue, where three important moieties were kept in their bioactive conformations.[39] Specifically, the leucine-proline portion of the macrocycle was replaced with a *n*-butyl linker. However, no biological data were given for this compound (**12**, Figure 1.6). Another conformationally constrained analogue (**11**) was synthesized shortly thereafter, in which the isostatine moiety was replaced by a (*S,S,S*)-β-hydroxy-γ-aminocyclohexanecarboxylic acid, to probe the biological conformation of didemnin B.[40] This constrained analogue (**11**) was tested for protein biosynthesis inhibition and showed about 20-fold decrease in activity with respect to didemnin B.[3]

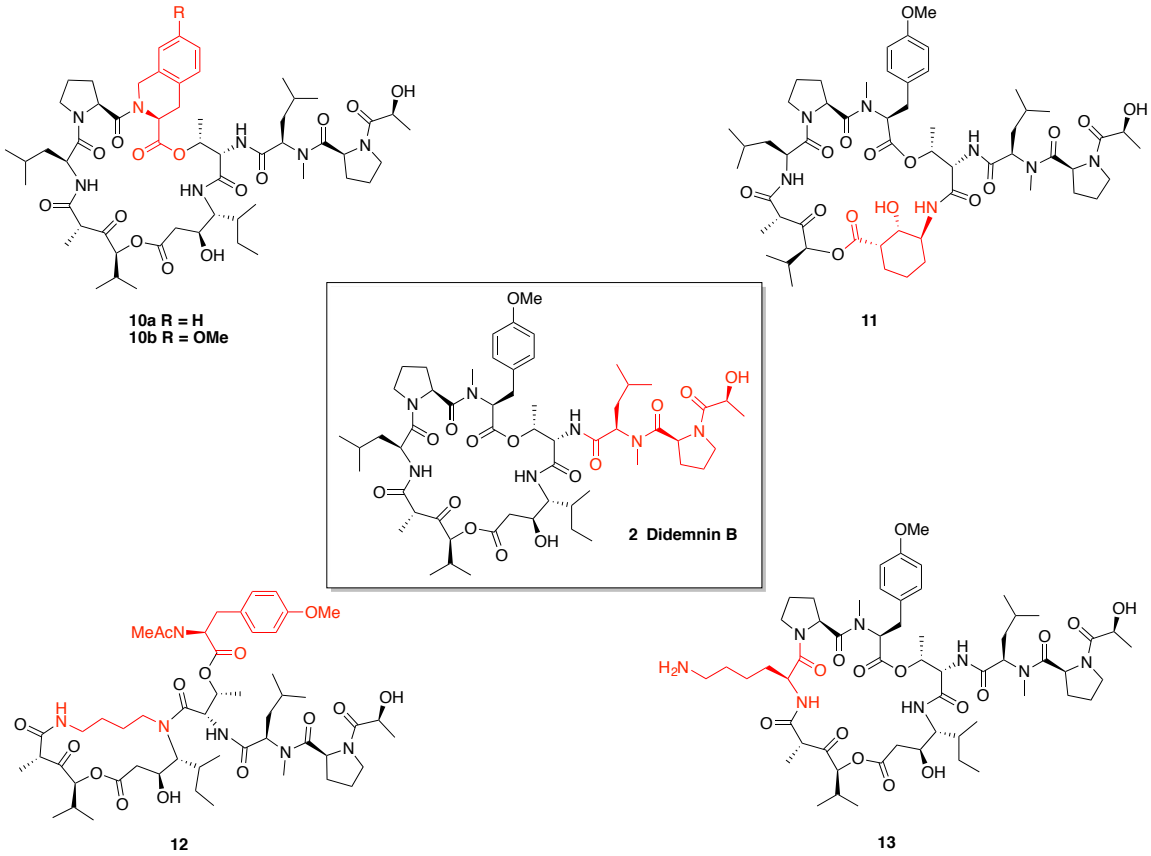

Figure 1.6. Modifications in the macrocyclic backbone of didemnin B.

Based on the X-ray data of didemnin B that was obtained earlier, the tyrosine side chain was thought to be involved in binding to the receptor since it protrudes outward from the molecule (Figure 1.4).[19] Therefore, Joullié and coworkers synthesized a didemnin B analogue (**10a**) containing Tic (L-1,2,3,4-tetrahydroisoquinoline-3-carboxylic acid) as a conformationally restrained replacement for tyrosine, which showed comparable potency as a protein biosynthesis inhibitor.[41] Two other didemnin B analogues were subsequently synthesized, in which the tyrosine moiety was replaced with *N*-Me-leucine and *N*-Me-phenylalanine.[42] These analogues were found to retain both antitumor activity and the ability to inhibit protein synthesis, suggesting that variations in this region are tolerated. With these encouraging results, another constrained analogue (L-1,2,3,4-tetrahydro-7-

methoxyisoquinoline-3-carboxylic acid)didemnin B (**10b**) was synthesized. [43] Interestingly, the results showed that the MeO-Tic was less active but also less toxic than the Tic. Taken together, these results support the hypothesis that this residue exists in a hydrophobic pocket of the target protein that must be filled by the protein-ligand complex to achieve optimal binding.[3]

Schreiber and coworkers were interested in investigating the mechanisms behind the various bioactivity displayed by didemnin B in the mid 1990s. Three particular biological activities of didemnin B was of interest: its ability to inhibit protein synthesis, induce G_1 cell cycle arrest, and suppress a mixed lymphocyte reaction. Interestingly, these activities ranged in effective concentrations over five orders of magnitude, suggesting that they may be mediated by different mechanisms.[44] In order to elucidate these mechanisms, Schreiber and coworkers characterized proteins that bind didemnin B, and found that a major intracellular didemnin-binding protein is the translation elongation factor 1α (EF-1α).[45] They reported that didemnin B binds uniquely to the activated GTP-bound form of EF-1α, albeit with modest affinity.[45] To investigate the mechanisms involved in the cytostatic and immunosuppressive activities displayed by didemnin B observed at low concentrations, Schreiber and coworkers sought out for additional didemnin-binding proteins.[44] They successfully purified and cloned a new didemnin-binding protein with sequence similarity to palmitoyl protein thioesterase (PPT).[44] Both EF-1α and PPT1 are the only didemnin-binding proteins isolated to date, where the study utilized side chain modifications of didemnin A (**1**).[3] As this immobilized didemnin had a substantially modified side chain that lacks the important lactylproline unit, it is possible that

molecular targets mediating other activities did not recognize the immobilized didemnin. Therefore, a didemnin macrocycle that could be attached at a position that would free the side chain was of interest. To address this hypothesis, [Lys^3]didemnin B was synthesized (**13**, Figure 1.6). Although the analogue showed a drop in potency, its residual antiproliferative and cytotoxic activities suggested potential use for the compound.[46]

Compared to analogues generated from modifications of the macrocycle, there have been numerous analogues generated from modifications in the side chains, since they could be more efficiently synthesized (**14**-**23**, Figure 1.7). Modifications in the side chain region were also found to be beneficial in that the corresponding analogues displayed diverse effects on bioactivity.[16] More specifically, the side chain amide bond between *N*-Me-D-leucine^7 and L-proline^8 is known to be an important site, because acylation on the leucine residue was thought to play a role in bioactivity.[3] The use of amide surrogates is one way to modify the bioactivity of peptides, and the ψ[CH_2NH]amide surrogate is generally known as one of the simplest isosteres of the amide bond. Hence, the amide bond between *N*-Me-D-leucine^7 and L-proline^8 was replaced by the ψ[CH_2NH]amide surrogate, with lactyl (**20**) or pyruvyl (**21**) residues at the terminal position (Figure 1.7). The corresponding biological data showed that although **21** was unstable, **20** displayed an increase in growth inhibition and a large increase in cytotoxicity.[47] Since the ψ[CH_2NH]amide surrogate (**20**) exhibited comparable bioactivity to that of didemnin B, this result suggests that the *N*-acylation of *N*-Me-D-leucine^7 is not a strict requirement for intact biological activity and that the presence of a basic nitrogen is tolerated.[3]

In the hopes of evaluating protein biosynthesis inhibition, benzophenone-based didemnin photoaffinity labeling reagents, such as **23**, were synthesized and tested.[46] All the analogues that were generated were shown to retain functional activity, although compounds having longer linkers were less reactive. These compounds were then evaluated in the NCI-60 tumor cell screen, where all the analogues were found to have potency comparable to didemnin B regardless of chain length.[38]

Yet another approach in clarifying the mode of action (MOA) of didemnin B was undertaken. Developing a receptor-binding assay using radiolabeled didemnin ligand was thought to be crucial in establishing the relationship between binding to a given receptor and a given biological effect. Furthermore, a radioactive didemnin analogue could be a useful probe molecule for studying a variety of related phenomena, including drug metabolism, cell-uptake, and interaction with other macromolecules.[16] The placement of tritium on the didemnin B molecule was carefully thought out, since it would be undesirable to alter the stereo-electronic nature of the ligand. Thus, a peptide containing an unsaturated proline residue was synthesized and subsequently subjected to catalytic tritiation, furnishing radioactive didemnin B side chain, which was then coupled to an advanced macrocyclic intermediate to yield [3,4-ditritioPro^{8}]didemnin B analogue (**22**, Figure 1.7).[16] As expected, the tritiated analogue was found to be equipotent with the natural didemnin B as an *in vitro* protein biosynthesis inhibitor.[16] However, one surprising result was the failure to observe direct binding between tritiated didemnin B and purified EF-1α which was comparable to either the IC_{50} value obtained for protein biosynthesis inhibition in cell-free assay or the dissociation constant estimated by

Schreiber and coworkers.[16] Only after extensive experimentation was any binding interaction was verified, indicating that binding affinity was substantially lower than expected. This also suggests that the role of EF-1α in mediating the protein biosynthesis inhibition was more complex than previously expected.[16]

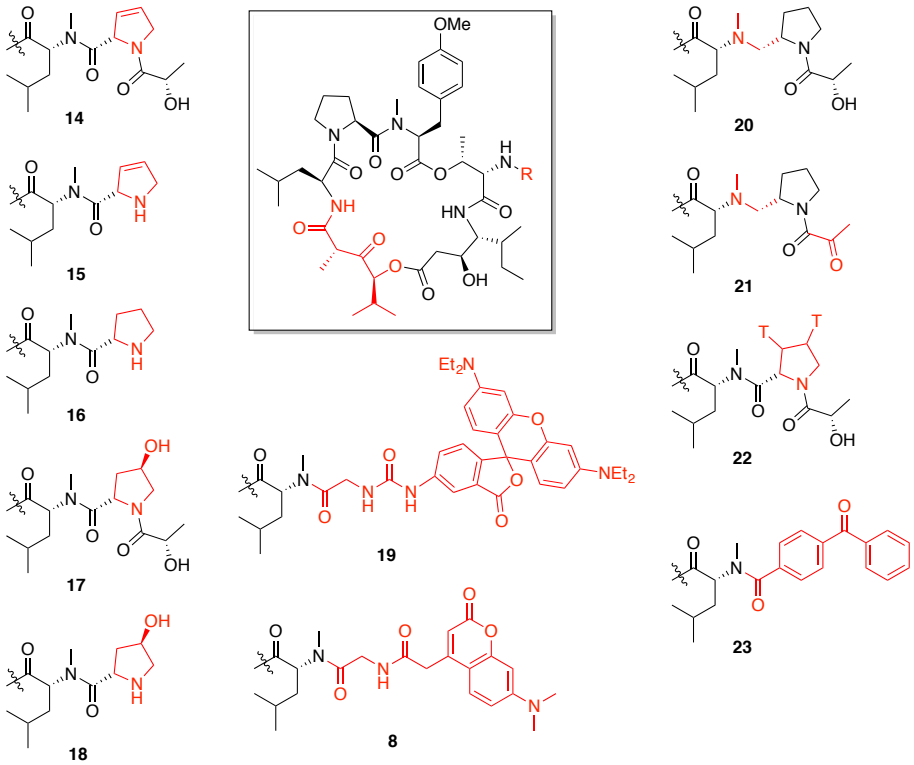

Figure 1.7. Modifications in the side chain of didemnin B (**2**).

1.7) Structural modifications of tamandarins

Upon isolation and characterization of tamandarins, Fenical and coworkers reported that tamandarin A (**6**) retained similar levels of *in vitro* antitumor activity in clonogenic assays and protein inhibition properties.[15] However, no biological data were reported for tamandarin B (**7**) due to the isolation of insufficient material. This problem ignited a synthetic program designed to prepare both natural products, as well as a number of relevant analogues having the same biologically active side chains present in the

didemnins.[3] All equivalent structural modifications resulted in comparable biological properties, although the cytotoxicities of tamandarin A and B being somewhat higher than that of didemnin B.[48] As mentioned above, fluorescence studies revealed similar behavior for both depsipeptide families.[17]

Since modifications in the tetrapeptide region of didemnin B were found to be tolerated, two tamandarin B analogues were prepared by Joullié and coworkers in which the *N,O*-Me_2Tyr^5 residue was replaced with *N*-Me-phenylalanine (*N*-$MePhe^5$) (**24**) and (*S*)-2-methylamino-3-(naphthalen-2-yl)propanoic acid (*N*-$MeNaphth^5$) (**26**) (Figure 1.8). These two analogues were evaluated in a panel of 14 tumor cell lines and compared to the results from tamandarin B.[49] The two analogues were found to perform better than tamandarin B, and showed similar *in vitro* cytotoxicities relative to each other, suggesting that changes to the macrocyclic scaffold at position 5 with more lipophilic aromatic amino acids were well tolerated.[3] Also, although studies have been done in which D-proline was substituted for L-proline, tolerance for other modifications at the Pro^4 and Thr^6 positions had not been investigated.[9] Therefore, the Ala^4-tamandarin B (**25**) and Ser^6-tamandarin B (**27**) were prepared by Joullié and coworkers.[50] It was found that modifications at the *N,O*-Me_2Thr^5 residue and at the Thr^6 position were well tolerated and even displayed enhanced cytotoxic activity against several human tumor cell lines.[3] However, the substitution of Pro^4 by alanine resulted in significantly reduced activity, suggesting that conformational and spatial effects are critical for antitumor activity (Figure 1.8).

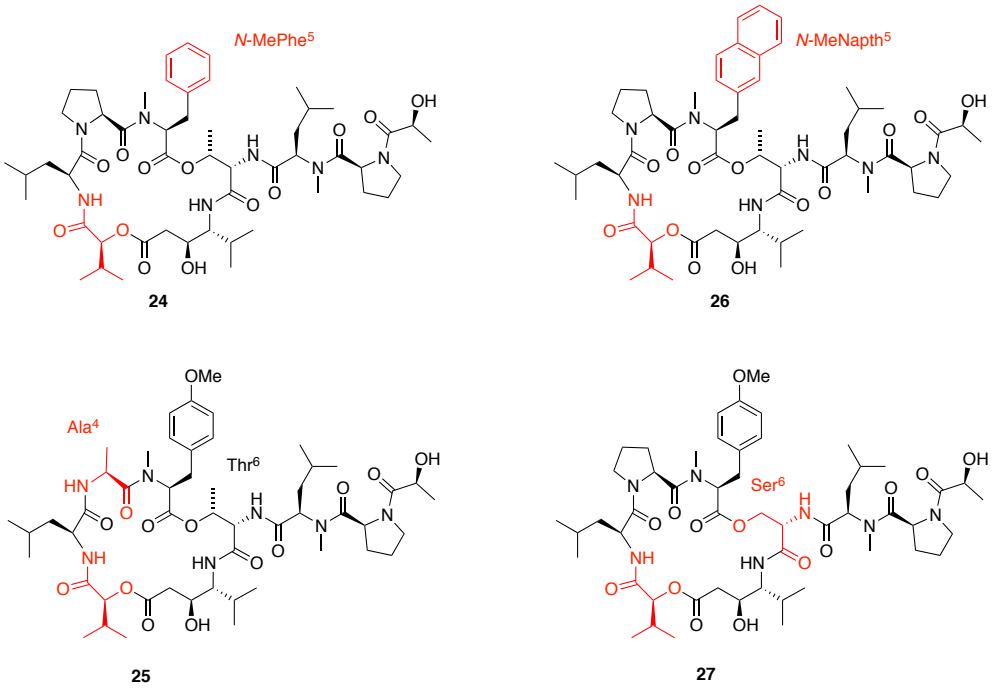

Figure 1.8. Tamandarin modifications.

In 2010, Joullié and coworkers successfully synthesized three novel tamandarin B analogues and tested their corresponding biological activities, which will be discussed in detail in Chapter 2.

1.8) Synthetic studies of didemnins, aplidine, tamandarins and related compounds

1.8.1) Syntheses of didemnin analogues

Since 1987, there have been several total syntheses of the didemnins, where the synthetic strategies differ mainly by the site of the macrocyclic ring closure and the choice of coupling reagent employed (Figure 1.9).

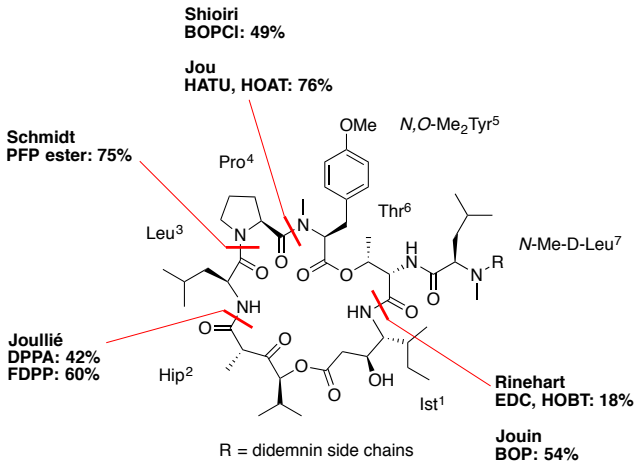

Figure 1.9. Cyclization sites for the didemnins by various groups, their choice of coupling reagent, and yield.

The first total synthesis of the didemnins was achieved by Rinehart in 1987. The site of macrocylization that they chose was at the Ist[1]-Thr[6] junction using EDC as the coupling reagent (Figure 1.9). There were some drawbacks to this synthesis besides the modest yield for the key macrocylization step. The synthesis was not conducted in a stereocontrolled manner, in that the methyl group of the Hip[2] residue was carried through the synthesis as a mixture of epimers, which was only eventually resolved by HPLC at the final steps of the synthesis.[51] Furthermore, the side chain was installed earlier on in the synthesis, rather than after the macrocylization step, which would have made the synthesis more convergent. Although this synthetic route lacked overall efficiency, Rinehart's total synthesis was an important contribution, especially given that clinical trials of didemnin B were already underway with no other synthetic route yet available. Moreover, didemnin B is the less abundant congener of *Tridemnum solidum*, making isolation of the natural product not an effective option at the time.[16]

Schmidt's synthesis of the didemnins afforded one of the highest-yielding macrocyclizations reported in the didemnin field (Figure 1.9).[52,53,54] Another key feature

of this synthesis was that it included a stereocontrolled preparation of the isostatine residue, and a synthetic route to the expensive D-*allo*-isoleucine to allow more synthetic flexibility to generate analogues from a common late-stage intermediate.[16] Interestingly, Schmidt and coworkers also found that epimerization of the undesired (*2R*)-epimer to the desired (*2S*)-epimer of the Hip^2 moiety could be done under either acidic (with TFA) or basic (with DBU) conditions in quantitative yield.[52,53,54]

Shioiri and coworker's synthetic strategy was similar to the Rinehart and Schmidt syntheses, because they also deferred the issue of stereocontrol within the Hip^2 moiety until after cyclization.[16] More specifically, they utilized Schmidt's epimerization conditions to obtain the desired epimer towards the end of their synthesis. However, Shioiri's synthesis is distinguished by a successful use of BOPCl mediated macrocylization protocol employing a secondary amine as their nucleophile (Figure 1.9).[55]

Joullié's synthesis differed conceptually from the previously discussed synthetic efforts in that it incorporated strategic elements of stereocontrol at both the Ist^1 and Hip^2 moieties from the outset.[56] Although this led to additional post-cyclization manipulation of advanced intermediates that lengthened the approach, the synthesis did not rely on the inversion of the methyl group configuration at Hip^2. Like the Schmidt synthesis, Joullié's method did not incorporate the *N*-Me-D-Leu^7 residue of the side chain into the synthesis of the macrolide, which allowed them to synthesize various analogues.[16]

Jouin's synthetic approach to the stereochemical challenges of the Hip[2] and norstatine fragments were generally similar to other efforts within the field.[57] However, their synthesis was somewhat different due to the fact that they synthesized nordidemnin B (**3**) (Figure 1.2). The synthesis of nordidemnin B was particularly important, because it permitted a direct biological comparison with didemnin B. They also utilized a late stage coupling of the side chain, which permitted the synthesis of several analogues for the purpose of defining structure-activity trends.[16] Jouin and coworkers were also able to dramatically increase the yield of macrocyclization by employing a relatively newer coupling reagent (Figure 1.9).

Jou and coworkers accomplished the most recent syntheses of didemnins in 1997.[58] Jou's synthesis of didemnin A (**1**) and dehydrodidemnin B (**4**) successfully employed more modern coupling reagents, which led to high cyclization yields comparable to that of Schmidt's (Figure 1.9). Their use of uronium and phosphonium salt-based coupling reagents ushered the increasing popularity of using HATU, HBTU, and PyBroP in very demanding coupling reactions.[16]

1.8.2) Didemnin M

Didemnin M (**5**) was first reported in 1994 by Banaigs, who originally named it didemnin H (Figure 1.2).[11] It was found to possess potent *in vitro* antitumor and immunosuppressive activities. While no total synthesis of this molecule was reported since isolation, a few semi-synthetic methods have been published.[59,60,61,62] Joullié developed a route to an analogue with a simplified didemnin macrocycle and the

didemnin M side chain,[59] while Crews devised a solution and solid phase semi-synthetic route to didemnin M.[62] Rinehart, however, used a different approach in their semi-synthetic route to didemnin M.[16] They used didemnin B as the natural product starting point, and their synthesis worked inward from the terminal residue instead of working outward (Scheme 1.1).[3]

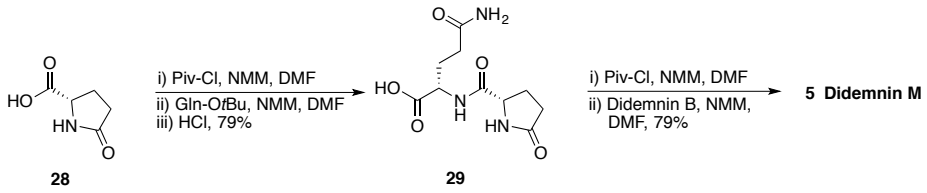

Scheme 1.1. Rinehart's semi-synthetic route to didemnin M.

Rinehart synthesized didemnin M using a three-step, one pot procedure starting from *p*Glu-OH (**28**) and didemnin B (**2**) (Scheme 1.1). Activation of *p*Glu-OH (**28**) as a mixed anhydride, followed by condensation with Gln-O*t*Bu, afforded the desired amide bond. Acidic workup removed the ester group to give the desired acid (**29**). Finally, mixed anhydride formation followed by addition of didemnin B yielded didemnin M (**5**) in 79% yield.[60]

1.8.3) Didemnin B amide bond surrogate (ψ[CH_2NH_2]) analogue

As discussed in previous sections, Joullié and coworkers synthesized several side chain analogues of didemnin B, in which the most biologically active being the amide bond surrogate (ψ[CH_2NH_2]) analogue (**20**, Figure 1.7). The major structural difference is the reduction of the proline carbonyl to a methylene group.[47,63] The synthesis began with *N*-methylation of *N*-Boc-D-Leu-OBn (**30**) followed by Boc removal and subsequent reductive amination with *N*-Boc-prolinal to afford amine **32** in good yield (Scheme 1.2).

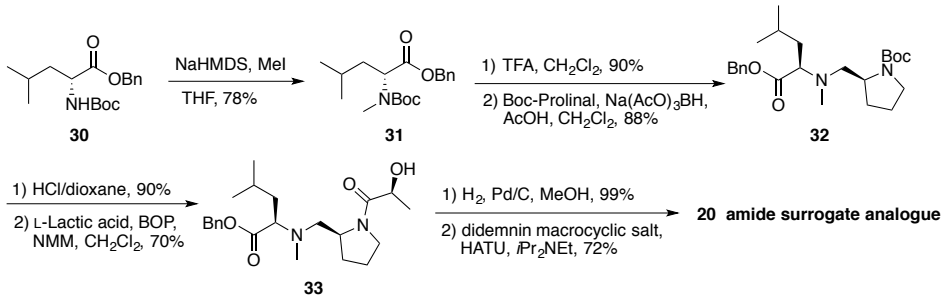

Scheme 1.2. Synthesis of ψ[CH_2NH_2] surrogate analogue of didemnin B.

Removal of the Boc group, followed by coupling to L-lactic acid afforded the fully functionalized side chain (**33**). Finally, hydrogenolysis, followed by coupling to the didemnin marocyclic salt yielded the desired amide surrogate analogue (**20**) (Scheme 1.2).

1.8.4) Synthesis of the tamandarin macrocycle

Both tamandarins A and B were first synthesized by Joullié and coworkers using convergent syntheses that utilized the same cyclization strategy to form the parent macrocycles.[48,64,65] The retrosynthetic analysis divided the parent natural products into the protected macrocycle (**34**) and the side chain acid (**35**) (Scheme 1.3).

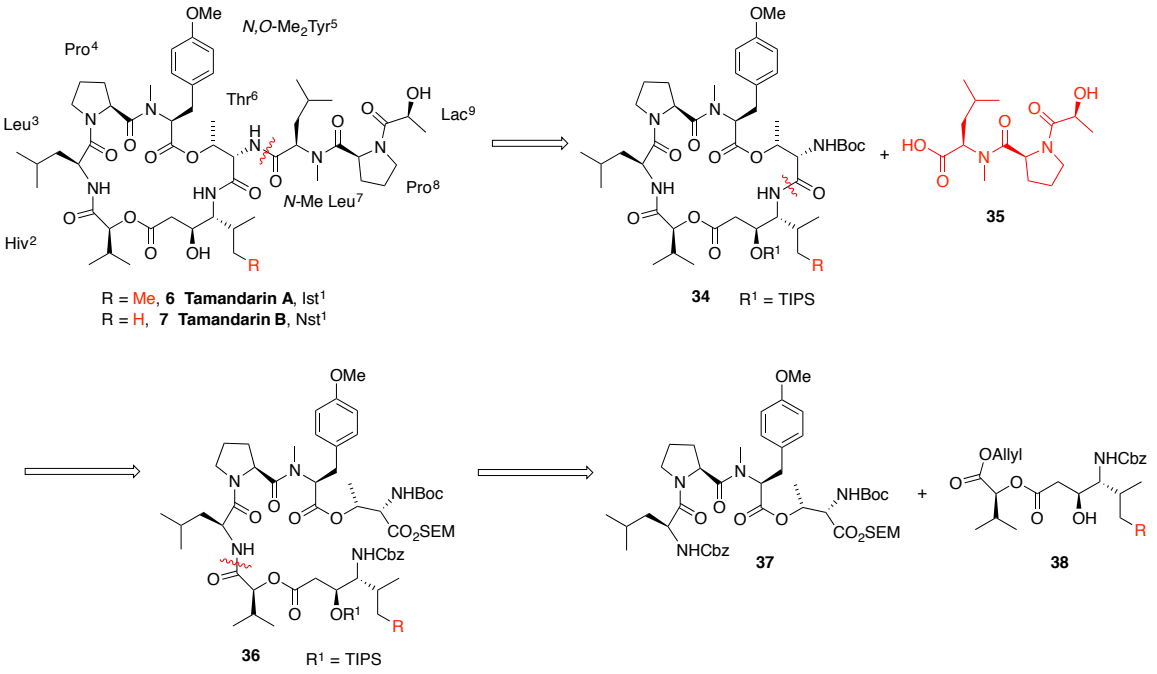

Scheme 1.3. Joullié's retrosynthetic analysis of tamandarins A and B.

Unlike their didemnin synthesis discussed in previous sections (Figure 1.9), the point of macrocyclization for the two tamandarin syntheses was at the Thr[6]-Nst/Ist[1] junction (Scheme 1.3). Cleavage of the linear precursor **36** at the Leu[3]-Hiv[2] junction formed the corresponding tetrapeptide **37** and allyl ester **38**. The greatest challenge in the syntheses of tamandarins A and B was the low yielding macrocyclization (23% yield using HATU as the coupling reagent).[48,64,65] Nonetheless, the syntheses of the two natural products proved to be essential for biological evaluation in relation to various didemnin analogues.

1.8.5) Synthesis and activity of tamandarin A analogues

Two additional analogues using the tamandarin A macrocycle and the side chains of didemnin M and dehydrodidemnin B were synthesized by Joullié using similar synthetic strategies (Figure 1.10).[48]

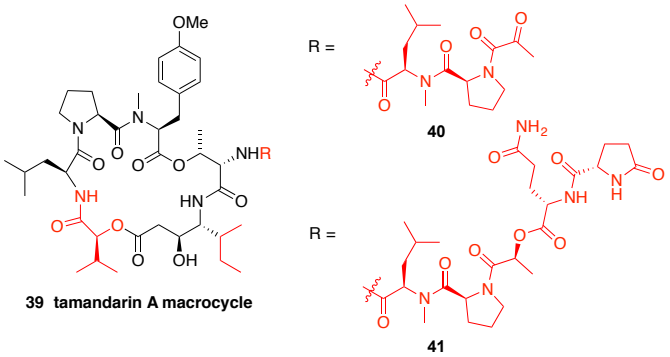

Figure 1.10. Tamandarin A analogues.

Both compounds were submitted to the NCI-60 tumor cell screen for *in vitro* testing. The cytotoxicity data showed that these compounds were more potent than didemnin B, where the tamadarin A/dehydrodidemnin B analogue (**40**) being the most potent, followed by the tamandarin A/didemnin M analogue (**41**), and finally tamandarin B (Table 1.1).[66]

Table 1.1. Biological activity of selected compounds

Compound	GI_{50}	LC_{50}
didemnin B	13 nM	3.8 μM
tamandarin B	2.3 nM	1.4 μM
tamandarin A/dehydrodidemnin B	1 nM	2.7 μM
tamandarin A/didemnin M	4 nM	7.6 μM

GI_{50} = median lethal dose, 50%; growth inhibitory power; **LC_{50}** = lethal concentration, 50%.

1.8.6) Synthesis and activity of tamandarin B macrocyclic analogues

As mentioned in previous sections, Joullié and coworkers synthesized two tamandarin B macrocyclic analogues in 2006, in which the *N,O*-Me_2Thr^5 residue was replaced by a *N*-MePhe residue in one analogue (**24**) and a *N*-MeNapth reside in the other (**26**, Figure 1.8). Interestingly, the site of macrocyclization was different for the syntheses of these analogues (Figure 1.11).[67] The *N*-MePhe^5 analogue was synthesized by using an approach similar to that of tamandarin A and B, in which the macrocyclization took place

at the Nst[1]-Thr[6] junction, albeit in low yield (16%). For the *N*-MeNapth[5] analogue, however, the site of macrocyclization was at the Pro[4]-*N*-MePhe[5] junction, which resulted in significantly higher yield (65%).[3] As discussed above, the two new analogues performed better than tamandarin B when their cytotoxicities were evaluated in a panel of 14 tumor cell lines.

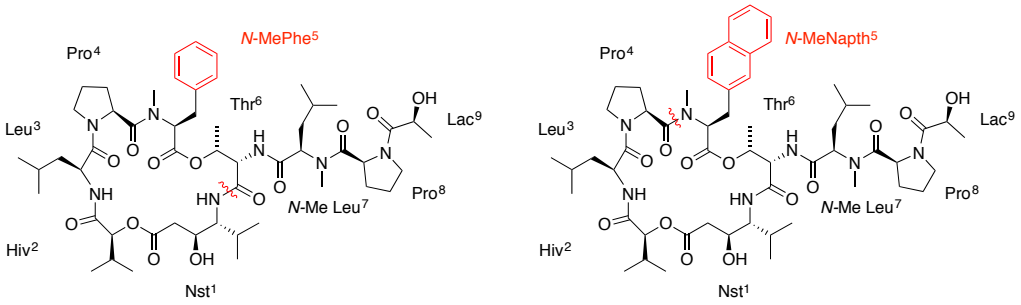

Figure 1.11. Tamandarin B analogues highlighting site of macrocylization.

In another study, Joullié and coworkers synthesized yet another two additional macrocyclic analogues Ala[4] tamandarin B (**25**) and Ser[6] tamandarin B (**27**, Figure 1.8).[50] Based on the success of the macrocyclization of the *N*-MeNapth[5] analogue, they selected the Pro[4]-*N*-MePhe[5] function as the site of macrocyclization for these analogues. These analogues were tested against the same panel of 14 tumor cell lines as briefly mentioned above, and the results suggested that the proline residue is essential for biological activity, whereas modification at Thr[6] could be moderately tolerated.[3]

1.9) Conclusions

Didemnin B (**2**) was the most investigated of all didemnin congeners in order to develop this class of compounds for therapeutic use. Although the development of didemnin B as a therapeutic agent was discontinued during phase II trials due to undesirable neuromuscular effects and cardiotoxicity, it undoubtedly paved the way for scientists to

better understand the mode of action of this family of natural products. Furthermore, significant amount of effort has been devoted to the syntheses of various tamandarin analogues to test whether the tamandarins would act as mere didemnin mimics or as individual therapeutic agents. In order to fully elucidate the structure-activity relationship as well as mode of action of these natural products, synthetically efficient generation of more side chain analogues of tamandarin B could be of great value.

1.10) References

[1] Wang, W., Namikoshi, M. "Bioactive Nitrogenous Metabolites from Ascidians." *Heterocycles* **2007**, *74*, 53-88.

[2] Pawlik, J. R. "Marine Invertebrate Chemical Defenses." *Chem. Rev.* **1993**, *93*, 1911-1922.

[3] Lee, J., Currano, J. N., Carroll, P. J., Joullié, M. M. "Didemnins, tamandarins and related natural products." *Nat. Prod. Rep.* **2012**, *29*, 404-424.

[4] Rinehart, K. L. *US Patent*, 4 493 796-A, **1985**.

[5] Rinehart, K. L. "Antitumor compounds from tunicates." *Med. Res. Rev.* **2000**, *20*, 1-27.

[6] Rinehart, K. L., Jr., Gloer, J. B., Cook, J. C., Jr., Mizsak, S. A. & Scahill, T. A. "Structures of the Didemnins, Antiviral and Cytotoxic Depsipeptides from a Caribbean Tunicate." *J. Am. Chem. Soc.* **1981**, *103*, 1857-1859.

[7] Rinehart, K. L., Jr. *et al.* "Didemnins: Antiviral and Antitumor Depsipeptides from a Caribbean Tunicate." *Science* **1981**, *212*, 933-935.

[8] Rinehart, K. L., Jr., Gloer, J. B., Wilson, G. R., Hughes, G. J., Li, L. H., Renis, H. E., McGovern, J. P. "Antiviral and antitumor compounds from tunicates." *Fed. Proc.* **1983**, *42*, 87-90.

[9] Abou-Mansour, E., Boulanger, A., Badre, A., Bonnard, I., Banaigs, B., Combaut, G., Francisco, C. "[Tyr^5]didemnin B and [D-Pro^4]didemnin B; Two New Natural Didemnins with a Modified Macrocycle." *Tetrahedron* **1995**, *51*, 12591-12600.

[10] Banaigs, B., Abou-Mansour, E., Bonnard, I., Boulanger, A., Francisco, C. "[Hysp^2] and [Hap^2]Didemnin B, two new [Hip^2]-modified didemnin B from the tunicate *Tridemnum cyanophorum*." *Tetrahedron* **1999**, *55*, 9559-9574.

[11] Boulanger, A., Abou-Mansour, A., Badre, B., Banaigs, G., Combaut, G., Francisco, C. "The complete spectra assignment of didemnin H a new constituent of the tunicate *Tridemnum* cyanophorum." Tetrahedron *Lett.* **1994**, *35*, 4345-4348.

[12] Jouin, P., Poncet, J., Dufour, M.-N., Pantaloni, A. & Castro, B. "Synthesis of the Cyclodepsipeptide Nordidemnin B, a Cytotoxic Minor Product Isolated from the Sea Tunicate *Tridemnum cyanophorum*." *J. Org. Chem.* **1989**, *54*, 617-627.

[13] Lindquist, N., Hay, M. E., Fenical, W. "Chemical defense of ascidians and their conspicuous larvae." *Ecol. Monogr.* **1992**, *62*, 547-568.

[14] Rinehart, K. L., Lithgow-Bertelloni, A. M. *PTC Int. Pat*., WO 9104985-A1, **1991**.

[15] Vervoort, H., Fenical, W. & de A. Epifanio, R. "Tamandarins A and B: New Cytotoxic Depsipeptides from a Brazilian Ascidian of the Family *Didemnidae*." *J. Org. Chem.* **2000**, *65*, 782-792.

[16] Vera, M. D. & Joullie, M. M. "Natural Products as Probes of Cell Biology: 20 Years of Didemnin Research." *Med. Res. Rev.* **2002**, *22*, 102-145.

[17] Joullié, M. M.; Leonard, M. S.; Portonovo, P.; Liang, B.; Ding, X.; LaClair, J. J. "Chemical Defense in Ascidians of the Didemnidae Family." Bioconjugate Chem. 2003, 14, 30-37.

[18] Molinski, T. F., Ko, J., Reynolds, K. A., Lievens, S. C., Skarda, K. R. "*N*,*N*'-methyleno-didemnin A from the ascidian Tridemnum solidum. Complete NMR assignments and confirmation of the imidazolidinone ring by strategic analysis of 1J(CH)." *J. Nat. Prod.* **2011**, *74,* 882-887.

[19] Hossain, M. B., van der Helm, D., Antel, J., Sheldrick, G. M., Sanduja, S. K., Weinheimer, A. J. "Crystal and molecular structure of didemnin B, and antiviral and cytotoxic depsipeptide." *Proc. Natl. Acad. Sci. U. S. A.* **1988**, *85*, 4118-4122.

[20] Lindquist, N., Hay, M. E. "Can small rare prey be chemically defended? The case for marine larvae." *Ecology* **1995**, *76*, 1347-1358.

[21] Bilayethossain, M., van der Helm, D., Antel, J., Sheldrick, G. M., Weinheimer, A. J., Sanduja, S. K. "Crystal and molecular structure of didemnin A, an antiviral depsipeptide." *Int. J. Peptide Protein Res.* **1996**, *47*, 20-27.

[22] Mayer, S. C., Carroll, P. J., Joullié, M. M. "The cyclic depsipeptide backbone of the didemnins." *Acta Crystallogr., Sect. C: Cryst. Struct. Commun.* **1995**, *C51*, 1609-1614.

[23] Kessler, H., Mronga, S., Will, M., Schmidt, U. "Solution structure of [Me-L-Leu^7]Didemnin B determined by NMR spectroscopy and refined by MD calculation." *Helv. Chim. Acta* **1990**, *73*, 25-47.

[24] Kessler, H., Will, M., Antel, J., Beck, H., Sheldrick, G. M. "Conformational analysis of didemnins. A multidisciplinary approach by means of X-Ray, NMR, molecular-dynamics, and molecular-mechanics techniques." *Helv. Chim. Acta* **1989**, *72*, 530-555.

[25] Searle, M. S., Hall, J. G., Kyratzis, I., Wakelin, L. P. G. "Didemnin B conformation and dynamics of an antitumour and antiviral depsipeptide studied in solution by ^{1}H and ^{13}C NMR spectroscopy." *Int. J. Pept. Protein Res.* **1989**, *34*, 445-454.

[26] Cárdenas, F., Thormann, M., Feliz, M., Caba, J.-M., Lloyd-Williams, P., Giralt, E. "Analysis of dehydrodidemnin B (Aplidine) by NMR spectroscopy and molecular mechanics/dynamics calculations." *J. Org. Chem.* **2001**, *66*, 4580-4584.

[27] Cárdenas, F., Caba, J. M., Feliz, M., Lloyd-Williams, P., Giralt, E. "Analysis of conformational equilibria in aplidine using selective excitation 2D NMR spectroscopy and molecular mechanics/dynamics calculations." *J. Org. Chem.* **2003**, *68*, 9554-9562.

[28] Nuijen, B., Bouma, M., Manada, C., Jimeno, J. M., Schellens, J. H., Bult, A., Beijnen, J. H. "Pharmaceutical development of anticancer agents derived from marine sources." *Anticancer Drugs* **2000**, *11*, 793-811.

[29] Baker, M. A., Grubb, D. R., Lawen, A. "Didemnin B induces apoptosis in proliferating but not resting peripheral blood mononuclear cells." *Apoptosis* **2002**, *7*, 407-412.

[30] Zubia, E., Ortega, M. J., Salva, J. "Natural products chemistry in marine ascidians of the genus aplidium." *Mini-Rev. Org. Chem.* **2005**, *2*, 389-399.

[31] Annual report of the European Medicines Agency 2005, Management Board Report EMEA/MB/63019/2006, European Medicines Agency, London, 2006.

[32] Gómez-Fabre, P. M., de Pedro, E., Medina, M. A., Núñez de Castro, I., Márquez, J. "Polyamine contents of human breast cancer cells treated with the cytotoxic agents chlorpheniramine and dehydrodidemnin B." *Cancer Lett.* **1997**, *113*, 141-144.

[33] Lobo, C. G., Garcia,-Pozo, S. G., Núñez de Castro, I., Alonso, F. "Effect of dehydrodidemnin B on human colon carcinoma cell lines." *Anticancer Res.* **1997**, *17*, 333-336.

[34] Newman, D. J., Cragg, G. M. "Marine natural products and related compounds in clinical and advanced preclinical trials." *J. Nat. Prod.* **2004**, *67*, 1216-1238.

[35] Urdiales, J. L., Morata, P., Núñez de Castro, I., Sánchez-Jiménez, F. "Antiproliferative effect of dehydrodidemnin B (DDB), a depsipeptide isolated from Mediterranean tunicates." *Cancer Lett.* **1996**, *102*, 31-37.

[36] Vera, M. D. "Synthetic and Medicinal Chemistry of the Didemnins", University of Pennsylvania, Philadelphia, PA, **2000**.

[37] Jouin, P., Poncet, J., Dufour, M. N., Aumelas, A., Pantaloni, A., Cros, S., Francois, G. "Antineoplastic activity of didemnin congeners: nordidemnin and modified chain analogues." *J. Med. Chem.* **1991**, *34*, 486-491.

[38] Marchini, S., Chiorino, G., Faircloth, G. T., D'Incalci, M. "Changes in gene expression profile induced by the anticancer agent Aplidine in Molt-4 leukemic cell lines." *J. Biol. Regul. Homeostatic Agents* **2002**, *16*, 241-248.

[39] Ramanjulu, J. M., Ding, X., Li, W.-R., Joullié, M. M. "Synthesis of a reduced ring analog of didemnin B." *J. Org. Chem.* **1997**, *62*, 4961-4969.

[40] Xiao, D., Vera, M. D., Liang, B., Joullié, M. M. "Total synthesis of a conformationally constrained didemnin B analog." **2001**, *66*, 2734-2742.

[41] Pfizenmayer, A., Ramanjulu, J. M., Vera, M., Ding, X., Xiao, D., Chen, W. C., Joullié, M. M., Tandon, D., Toogood, P. L. "Synthesis and biological activity of [Tic(5)]didemnin B." *Bioorg. Med. Chem. Lett.* **1998**, *8*, 3653-3656.

[42] Pfizenmayer, A., Ramanjulu, J. M., Vera, M. D., Ding, D., Xiao, D., Chen, W.-C., Joullié, M. M. "Synthesis and biological activities of [*N*-MeLeu^5]- and [*N*-MePhe^5]-didemnin B." *Tetrahedron* **1999**, *55*, 313-334.

[43] Tarver, Jr., J. E., Pfizenmayer, A. J., Joullié, M. M. "Total syntheses of conformationally constrained didemnin B analogues. Replacement of *N*,*O*-dimethyltyrosine with L-1,2,3,4-tetrahydroisoquinoline, and L-1,2,3,4-tetrahydro-7-methoxyisoquinoline." *J. Org. Chem.* **2001**, *66*, 7575-7587.

[44] Crews, C. M., Lane, W. S. & Schreiber, S. L. "Didemnin binds to the protein palmitoyl thioesterase responsible for infantile neuronal ceroid lipofuscinosis." *Proc. Natl. Acad. Sci. USA* **1996**, *93*, 4316-4319.

[45] Crews, C. M., Collins, J. L., Lane, W. S., Snapper, M. L. & Schreiber, S. L. "GTP-dependent Binding of the Antiproliferative Agent Didemnin to Elongation Factor 1α." *J. Biol. Chem.* **1994**, *269*, 15411-15414.

[46] Vera, M. D., Pfizenmayer, A. J., Ding, X., Xiao, D. & Joullie, M. M. "[Lys^3]Didemnins as Potential Affinity Ligands." *Bioorg. Med. Chem. Lett.* **2001**, *11*, 13-16.

[47] Ding, X. *et al.* "Structure-Activity Relationships of Side-Chain Modified Didemnins." *Bioorg. Med. Chem. Lett.* **2001**, *11*, 231-234.

[48] Liang, B., Richard, D. J., Portonovo, P. & Joullie, M. M. "Total Syntheses and Biological Investigations of Tamandarins A and B and Tamandarin A Analogs." *J. Am. Chem. Soc.* **2001**, *123*, 4469-4474.

[49] Adrio, J., Cuevas, C., Manzanares, I. & Joullie, M. M. "Synthesis and Biological Evaluation of Tamandarin B Analogues." *Org. Lett.* **2006**, *8*, 511–514.

[50] Adrio, J., Cuevas, C., Manzanares, I. & Joullie, M. M. "Total Synthesis and Biological Evaluation of Tamandarin B analogues." *J. Org. Chem.* **2007**, *72*, 5129–5138.

[51] Rinehart, K. L., Jr. *et al.* "Total Synthesis of Didemnins A, B and C." *J. Am. Chem. Soc.* **1987**, *109*, 6846-6848.

[52] Schmidt, U., Kroner, M. & Griesser, H. "Total Synthesis of the Didemnins - 1. Synthesis of the Peptolide Ring." *Tetrahedron Lett.* **1988**, *29*, 3057-3060 and 4407-4408.

[53] Schmidt, U., Kroner, M. & Griesser, H. "Total Synthesis of The Didemnins -2. Synthesis of Didemnin A, B, C and Prolyldidemnin A." *Tetrahedron Lett.* **1988**, *29*, 4407-4408.

[54] Schmidt, U., Kroner, M. & Griesser, H. "Total Synthesis of the Didemnins; III. Synthesis of Protected (2*R*, 3*S*)-Alloisoleucine and (3*S*, 4*R*, 5*S*)-Isostatine Derivatives-Amino Acids from Hydroxy Acids." *Synthesis* **1989**, 832-835.

[55] Hamada, Y., Kondo, Y., Shibata, M. & Shioiri, T. "Efficient Total Synthesis of Didemnins A and B." *J. Am. Chem. Soc.* **1989**, *111*, 669-673.

[56] Li, W.-R., Ewing, W. R., Harris, B. D. & Joullié, M. M. "Total Synthesis and Structural Investigations of Didemnins A, B, and C." *J. Am. Chem. Soc.* **1990**, *112*, 7659-7672.

[57] Jouin, P., Poncet, J., Dufour, M.-N., Pantaloni, A. & Castro, B. "Synthesis of the Cyclodepsipeptide Nordidemnin B, a Cytotoxic Minor Product Isolated from the Sea Tunicate *Tridemnum cyanophorum*." *J. Org. Chem.* **1989**, *54*, 617-627.

[58] Jou, G., Gonzales, I., Albericio, F., Lloyd-Williams, P. & Giralt, E. "Total Synthesis of Dehydrodidemnin B. Use of Uronium and Phosphonium Salt Coupling Reagents in Peptide Synthesis in Solution." *J. Org. Chem.* **1997**, *62*, 354-366.

[59] Liang, B., Vera, M. D. & Joullié, M. M. "Total Synthesis of [(2*S*)-Hiv^2]Didemnin M." *J. Org. Chem.* **2000**, *65*, 4762-4765.

[60] Rinehart, K. L. & Katauskas, A. J. "Semi-synthetic studies toward didemnin analogues." WO patent 9817275 **1998**.

[61] Rinehart, K. L., Sakai, R., Stroh, J. G. *US Pat*., 4 948 791, **1990**; *Chem. Abstr*. **1991**, 114: p. 214413h.

[62] Wen, J. J. & Crews, C. M. "Towards the semi-synthesis of didemnin M. Solution and solid phase syntheses of the pseudotetrapeptide: pGlu-Gln psi COO Ala-Pro- OH." *Tetrahedron Lett.* **1998**, *39*, 779-782.

[63] Ding, X. "Total Synthesis of Didemnin B Analogs", University of Pennsylvania, Philadelphia, PA, **2000**.

[64] Joullié, M. M., Portonovo, P., Liang, B. & Richard, D. J. "Total Synthesis of Tamandarin B." *Tetrahedron Lett.* **2000**, *41*, 9373-9376.

[65] Liang, B., Portonovo, P., Vera, M. D., Xiao, D. & Joullié, M. M. "The First Total Synthesis of (−)-Tamandarin A." *Org. Lett,* **1999**, *1*, 1319-1322.

[66] K. M. Lassen, "The synthesis and biological evaluation of tamandarin B analogues", University of Pennsylvania, Philadelphia, PA, **2011**.

[67] Adrio, J., Cuevas, C., Manzanares, I. & Joullie, M. M. "Synthesis and Biological Evaluation of Tamandarin B Analogues." *Org. Lett.* **2006**, *8*, 511–514.

Chapter 2: Preparation of Tamandarin B/Didemnin Hybrid Analogues

2.1) Second-generation synthesis of the tamandarin B macrocycle

Developing an improved strategy that could address synthetic challenges that were present in the first synthesis of tamandarin B macrocycle[1] was thought to be crucial, since the structure-activity relationship as well as mode of action of these natural products still remained unclear. An efficient synthesis would allow the generation of various analogues that could be tested in a timely manner. One of the main synthetic challenges was to devise a consistently high yielding macrocyclization methodology. When Joullié and coworkers synthesized two tamandarin B macrocyclic analogues in 2006, two different methods of cyclization were used (Figure 2.1).

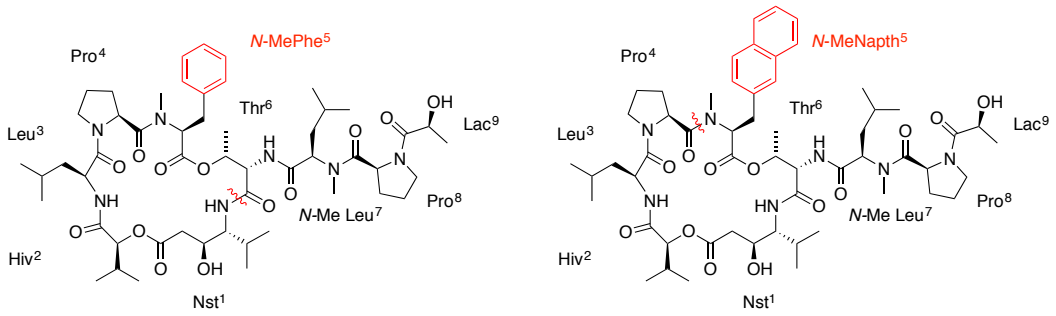

Figure 2.1. Tamandarin B analogues highlighting site of macrocyclization.

Interestingly, the site of macrocyclization utilized for *N*-MePhe[5] analogue was at the Nst[1]-Thr[6] junction, while as in the *N*-MeNapth[5] analogue, the Pro[4]-*N*-MePhe[5] junction was chosen instead.[2,3] The corresponding yields for this step varied drastically, as the former methodology provided 16% yield, while the other afforded 65%.[2,3] Furthermore, previous didemnin syntheses also showed that macrocyclization at the Pro[4]-*N*-MePhe[5] junction generally resulted in higher yields.[4,5]

Another synthetic challenge was to devise a convergent synthesis that would increase the overall efficiency. In the first-generation synthesis, the linear precursor (**1**) was formed by two main fragments (tetrapeptide (**2**) and Nst/Hiv (**3**)) (Scheme 2.1). Dividing the macrocycle into three fragments would make its synthesis more accessible and convergent, as it would shorten the longest linear sequence.

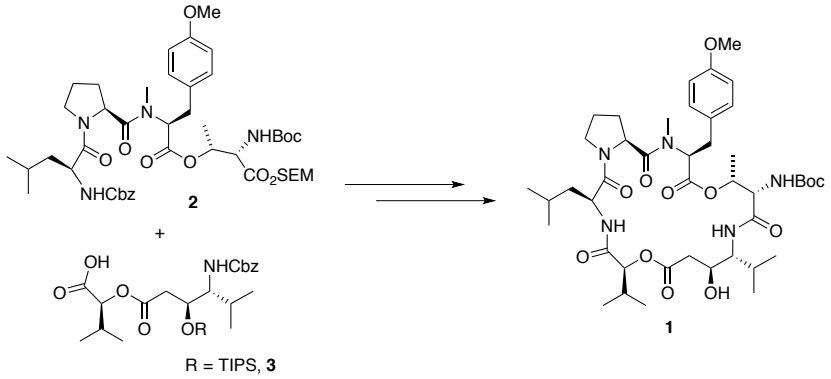

Scheme 2.1. Two-fragment approach to tamandarin B macrocycle.

Finally, the last synthetic challenge was to develop an efficient protecting group strategy. One particular difficulty in the route was the removal of an allyl group to form a carboxylic acid, a step that proved to be low yielding and had to be carried on through another step as an impure mixture.[2,3] The synthetic strategy lacked protecting group orthogonality, as forming the free linear precursor before cyclization took two steps (Scheme 2.2).

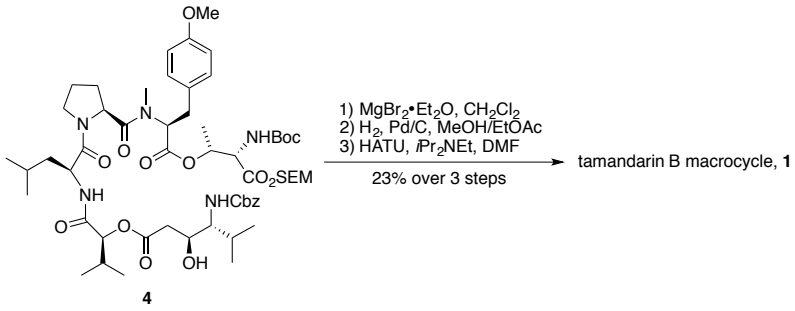

Scheme 2.2. First-generation approach towards tamandarin B macrocycle.

A protecting group strategy that allows for a one step removal of the terminal protecting groups would make the synthesis more efficient. More specifically, a new protecting group strategy that entails quantitative removal of all protecting groups so that the resulting product could be used without further purification would be of great value.

In an effort to improve the previous approaches, a second-generation retrosynthesis was proposed (Scheme 2.3).[6]

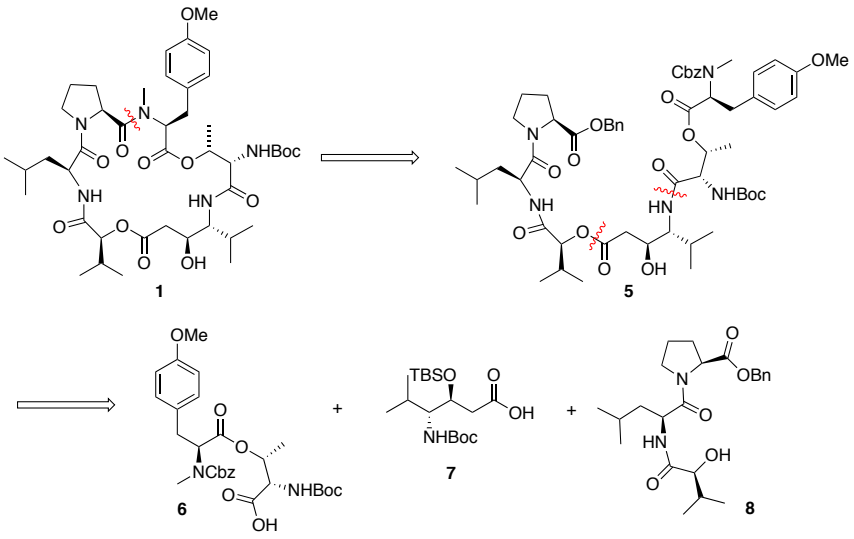

Scheme 2.3. Second-generation retrosynthesis of tamandarin B macrocycle.

The site of macrocyclization at the Pro[4]-Me_2Tyr[5] junction was chosen based on previous studies. The linear precursor (**5**) could be further divided into three fragments: Tyr-Thr acid (**6**), norstatine acid (**7**), and Hiv-Leu-Pro-OBn (**8**). The terminal protecting groups of linear precursor **5** were the benzyl ester and Cbz carbamate, which would allow simultaneous removal of both protecting groups under hydrogenolysis conditions. The Hiv[2] residue was incorporated into **5**, requiring fewer protection/deprotection steps than in the first-generation synthesis. Finally, the TBS and Boc protecting groups on the norstatine fragment (**7**) could be simultaneously removed under acidic conditions, thereby increasing the efficiency of synthesis.[7]

The forward synthesis was commenced with the synthesis of Hiv-Leu-Pro-OBn fragment (**12**) (Scheme 2.4). Pro-OBn•HCl (**12**) was coupled to Boc-Leu using diethylcyanophosphonate (DEPC) as the coupling reagent.[4] DEPC was the particular coupling reagent that was utilized in previous syntheses, and was proven to afford higher yields compared to dicyclohexylcarbodiimide (DCC)[2] or 4-(4,6-dimethoxy[1,3,5]triazi-2-yl)methylmorpholinium chloride (DMTMM)[8]. Removal of the Boc group under acidic conditions afforded the corresponding amine HCl salt, which was directly coupled to 2*S*-hydroxyisovaleric acid (**11**) to afford alcohol **12** in 93% yield.

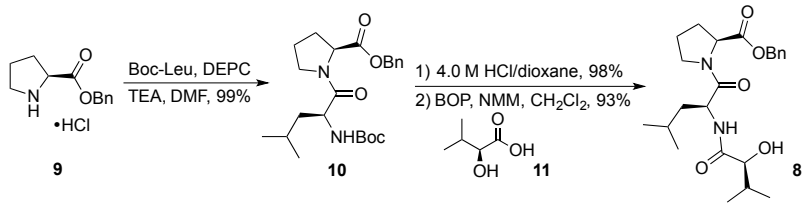

Scheme 2.4. The synthesis of fragment **8**.

The norstatine fragment (**7**) was synthesized next. The carboxylic acid of *N*-Boc-D-valine (**12**) was activated as its pentafluorophenylester (PfP) (**13**) using pentafluorophenyl trifluoroacetate (Scheme 2.5). The lithium enolate of methyl acetate was condensed onto the activated ester to form the β-ketomethyl ester (**14**). The resulting ketone was reduced using KBH_4 to afford the corresponding β-hydroxymethyl ester (**15**) as a mixture of separable diastereomers (major diastereomer shown). The alcohol was then protected as its TBS ether to yield **16**. Finally, lithium hydroxide mediated hydrolysis of the methyl ester resulted in norstatine fragment **7**.

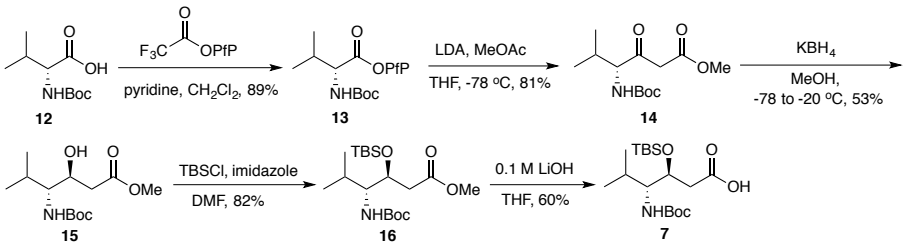

Scheme 2.5. Synthesis of norstatine fragment **7**.

The final fragment to be synthesized was the Tyr-Thr acid (**6**) (Scheme 2.6). Methylation of commercially available *N*-Cbz-L-Tyr (**17**) under basic conditions followed by hydrolysis of the resulting methyl ester afforded acid (**18**). Following Joullié's previous synthesis of didemnin B macrocycle,[9] **18** was esterified with *N*-Boc-L-Thr-OSEM (**19**) using isopropenyl chloroformate to yield **20**. The SEM group was chosen as the ideal protecting group because of its previous success in the synthesis of the didemnins and the first generation synthesis of tamandarins A and B.[1,9] Unfortunately, removal of the SEM group proved to be difficult under standard conditions ($MgBr_2 \bullet Et_2O$)[10], where the only product of this reaction was removal of the Boc group on the adjacent nitrogen. When fluoride based reagents, such as HF•pyridine, TAS-F, and TBAF on silica gel were used, no apparent reaction occurred.

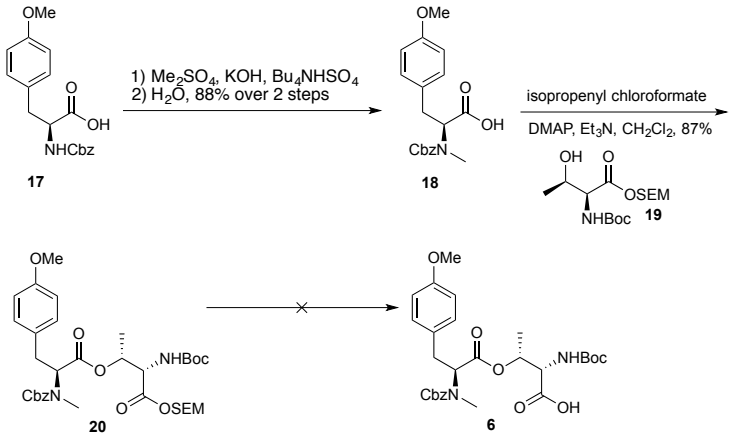

Scheme 2.6. First attempt at the synthesis of fragment **6**.

These unforeseen results led to the reconsideration of protecting group strategy. An allyl group was used as the protecting group for the Tyr-Thr acid fragment instead of the SEM group (Scheme 2.7).

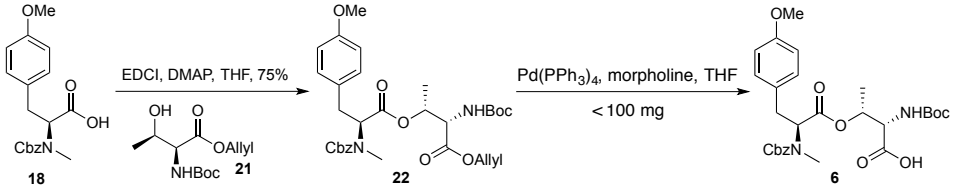

Scheme 2.7. Second attempt at the synthesis of fragment **6**.

Esterification of acid **18** with *N*-Boc-L-Thr-OAllyl (**21**) was accomplished by EDCI rather than isopropenyl chloroformate, since it afforded a higher yield of the desired allyl ester (**22**) (75% *vs*. <40%). However, this new protecting group strategy also presented problems. Removal of the allyl group using catalytic palladium was achievable only at small scales. On scales less than 100 mg, the reaction went to completion in about 6 h, while at larger scales, the rate of the reaction significantly slowed down and never went to completion even after 3 days. Increased catalyst loading or increased addition of morpholine did not improve the transformation.

Yet another revision in the protecting group strategy was made, where the allyl group was changed to a methyl group. Methyl ester is generally not a popular protecting group used in macrocyclic peptide syntheses due to concerns of regioselective removal of the methyl ester under hydrolysis conditions in the presence of other ester fragments in the molecule. For instance, using standard conditions, such as lithium hydroxide, to hydrolyze the methyl ester would likely hydrolyze the Tyr-Thr ester bond in **24** (Scheme 2.8). In 2007, Nicolaou and coworkers reported a mild hydrolysis methodology using

trimethyltin hydroxide to selectively hydrolyze methyl esters in the presence of other esters.[11] The desired substrate (**24**) was synthesized *via* esterification of the acid **18** with *N*-Boc-Thr-OMe (**23**) using EDCI as the coupling reagent (Scheme 2.8). Surprisingly, when Nicolaou's methodology was utilized in the present system, the hydrolysis of the methyl ester (**24**) afforded the desired acid (**6**) in almost quantitative yield in only 3 h.

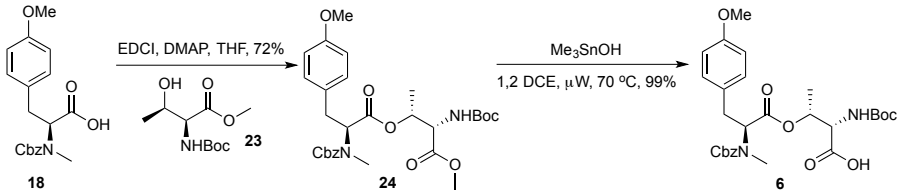

Scheme 2.8. The synthesis of Tyr-Thr fragment (**6**).

Finally, with all three desired fragments made, the next step was to synthesize the linear precursor (**5**). Esterification of acid **7** and alcohol **8** using EDCI and DMAP unfortunately led to poor reaction yields of <20% of the product (**25**) (Scheme 2.9). Using other coupling reagents, such as DCC, isopropenyl chloroformate, or isobutyl chloroformate instead of EDC only led to a similar result.[7]

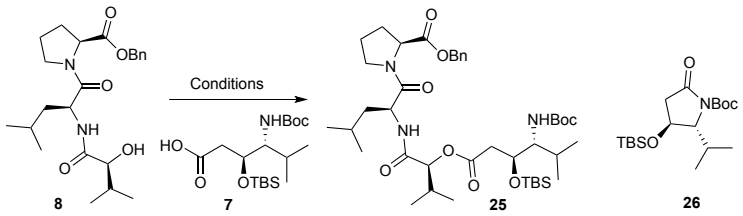

Scheme 2.9. Initial attempts at formation of **25**.

In all cases, undesired side product (**26**) was formed in a higher yield. The side product lactam **26** is the result of intramolecular cyclization of the activated intermediate of acid **7**. This problem was also present in the first generation synthesis of tamandarins A and B[1] on a similar substrate as well as on the analogue synthesis on the exact same reaction[2]. Hence, a modification to the norstatine acid was deemed necessary. The simplest solution to this challenge would be to decrease the nucleophilicity of the Boc protected nitrogen

by the formation of *N*,*O*-isopropylidene acetal with the neighboring alcohol. This portion of the investigation was done by Dr. Kenneth M. Lassen, and it is described in detail in his dissertation.[7] After much optimization to form the desired *N*,*O*-isopropylidene acetal (**27**), the best condition was the use of stoichiometric (±)-10-camphorsulfonic acid in 2,2-dimethoxypropane and acetone at room temperature, which resulted in 56% yield (Scheme 2.10). The methyl ester (**27**) was then hydrolyzed to **28** with lithium hydroxide in quantitative yield.

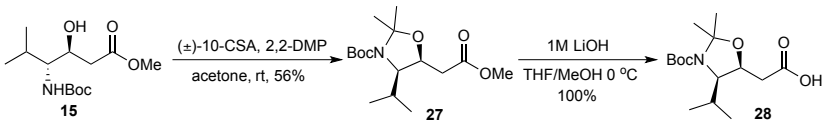

Scheme 2.10. Synthesis of acid **28**.

Satisfyingly, with the acid **28** in hand, esterification with alcohol **8** afforded a 94% yield of **29** using the original conditions of EDCI and DMAP, completely suppressing the formation of the undesired lactam **26** (Scheme 2.11).

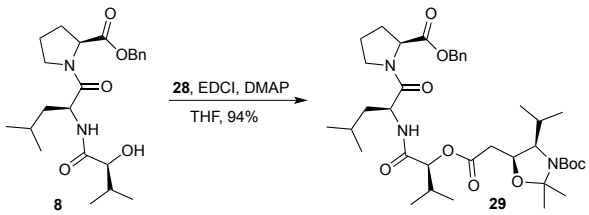

Scheme 2.11. Synthesis of **29**.

The next steps involved removing the Boc group, fragmenting the *N*,*O* acetal, and coupling the resulting amine salt to acid **6** to form the linear precursor (**5**). Under protic acid conditions, both the Boc group and the *N*,*O* acetal were removed in less than 2 h to afford the corresponding amine HCl salt, which was then subsequently coupled to **6** using BOP as the coupling reagent to afford the desired linear precursor (**5**) in 76% yield (Scheme 2.12).

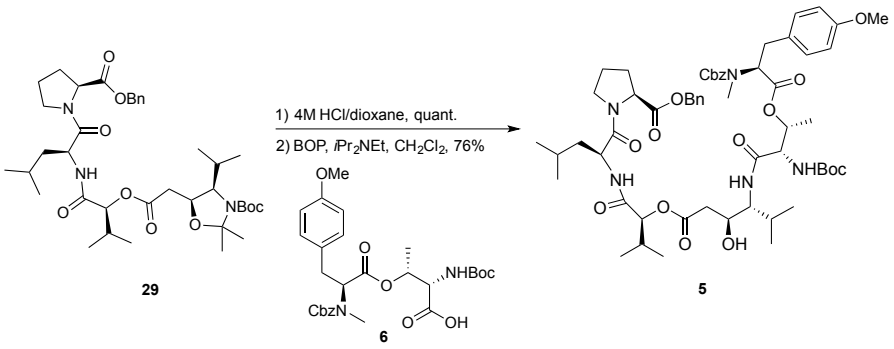

Scheme 2.12. Synthesis of linear precursor **5**.

With the protected linear precursor **5** in hand, the next step was to remove both the Cbz and benzyl protecting groups in one transformation. Initial hydrogenolysis attempts using 10% Pd/C at ambient temperature and 1atm resulted in quantitative yield, although the reaction took 2 days to reach full conversion. When the reaction was conducted at 45 psi using a Parr hydrogenator, the reaction was completed in 4 h, but the yield decreased to 80%. Finally, replacing 10% Pd/C with 10% $Pd(OH)_2/C$ allowed the reaction to go to full conversion in 10 h, under 1 atm (Scheme 2.13). It is important to note that hydrogenolysis labile protecting groups were used purposefully on the linear precursor for synthetic convenience, as most hydrogenolysis often result in very clean reactions, making column chromatography purification unnecessary.

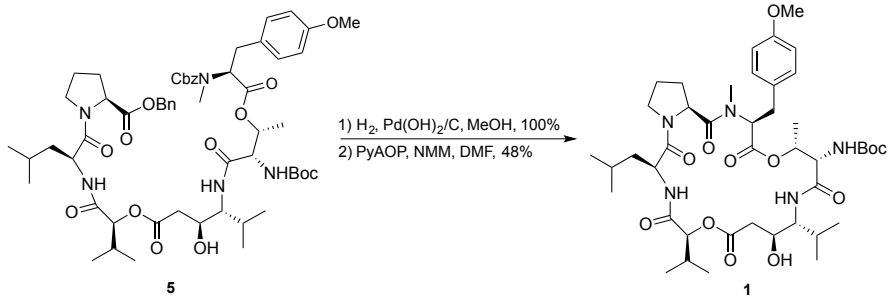

Scheme 2.13. Formation of macrocycle **1**.

Perhaps one of the most important steps of the reaction—the macrocyclizaiton step was next to be investigated. Based on previous knowledge of Shioiri's accomplishment in his

didemnin B synthesis,[4] BOPCl was the first coupling reagent that was utilized in our many attempts at macrocyclization. More specifically, Shioiri's exact reaction conditions were used, where Et_3N was used as the base in CH_2Cl_2 at 1 mM concentration. Unfortunately, unlike Shioiri's successful yield (76%), the present system only resulted in 18% yield. The significant decrease in yield could be attributed to the difference in the linear precursor. First of all, the didemnins possess a 23-membered ring macrocycle, while as tamandarin B has a 21-membered ring. Secondly, the two molecules were functionalized differently, where Shioiri protected the alcohol of the norstatine as its TBS ether, while as in the present system, the secondary alcohol was left unprotected. Furthermore, his synthesis also had the Me-Leu[7] residue of the side chain in place prior to cyclization. Taken together, these seemingly small structural differences may result in vastly different conformations of the molecule in solution that could inhibit the molecule from cyclization. Since such structural behavior is exceedingly difficult to predict, the only viable option was to try a different known macrocyclization method.

The next set of conditions that was tried was the one used by Giralt in his synthesis of dehydrodidemnin B, where he employed HATU, HOAt, and *i*Pr_2NEt in THF.[5] Giralt's conditions gave a slightly improved 23% yield. The only deviation from his step was the ring size and dilution. Interestingly, Giralt's macrocyclization was done at 1.15 M in THF, which seemed too concentrated for an intramolecular reaction. Therefore when his conditions were utilized, they were conducted in a much more dilute 1 mM concentration in the hopes of promoting the desired reaction. However, similar to the present system, Giralt also left the norstatine alcohol unprotected and the Thr[6] protected as a Boc group.

Changing the amine base to NMM and solvent to CH_3CN also did not improve the yield (25%). The next set of conditions that was tried was DMTMM, NMM in acetonitrile, which only resulted in a 20% yield.[12] Yet another condition was tried, where T3P, *i*Pr_2NEt, CH_2Cl_2 was used.[13] Although the resultant yield increased to 30%, one more coupling reagent was investigated. When PyAOP[14,15] and NMM in DMF at 1 mM concentration was used, the yield resulted in a much significant increase (49%), though the reaction took 48 h (Scheme 2.13). However, this set of condition was deemed most optimal, as the reaction proved to be highly scalable.

The second-generation synthesis of the tamandarin B macrocycle was completed in a longest linear sequence of 10 steps and an overall yield of 6.6%.[6] This was a significant improvement in comparison to the first-generation synthesis, which was 12 steps and afforded an overall yield of 3.2%.

2.2) Synthesis of three tamandarin B/didemnin hybrid analogues

As discussed in the previous chapter, the natural product didemnin M, [16] dehydrodidemnin B,[5, 17] and Ψ[CH_2NH] didemnin B [18] are potent molecules with interesting biological activities. When the analogues containing the tamandarin A/didemnin M[19] side chain and tamandarin A/dehydrodidemnin B[1] side chain were made, *in vitro* testing of these molecules showed similar activity to that of the parent natural products. However, the tamandarin B versions of these compounds have never been made. Therefore, with a new and improved second-generation synthesis of the tamandarin B macrocycle in hand, a relatively more efficient generation of these biologically intriguing analogues was available. This study would ultimately help determine the effects of side

chain structure on the biological activity of tamandarin B and may produce compounds with potential therapeutic value. The synthetic strategy to access these analogues was to selectively couple the side chain to the macrocyclic amine salt as the final step of the synthesis (Figure 2.2).

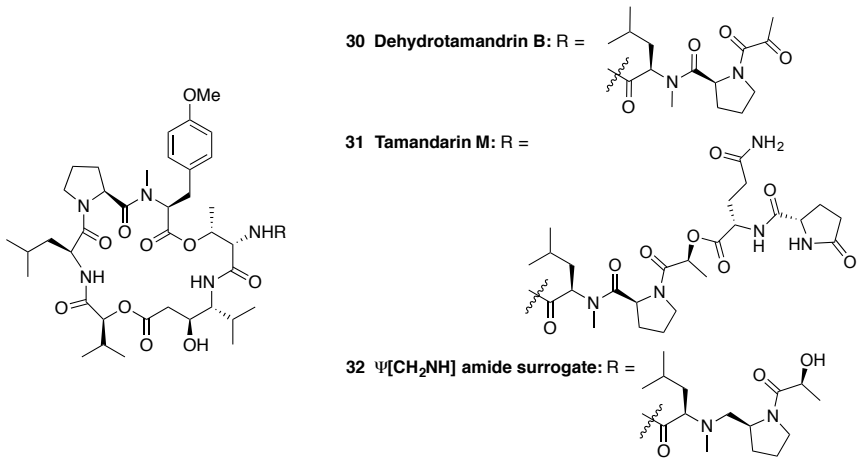

Figure 2.2. Structure of tamandarin B/didemnin hybrid analogues.

These particular side chains have been previously synthesized by Joullié and coworkers[1,18,19] using three different routes each having a distinctive strategy.[7] A more unified approach, which allows the production of these side chains from as many common intermediates as possible, would be highly beneficial.

2.2.1) Synthesis of dehydrotamandarin B

Synthesis of dehydrotamandarin B commenced with the protection of L-leucine (**33**) as its Boc carbamate (Scheme 2.14). Benzyl ester formation followed by *N*-methylation, and subsequent Boc group removal under acidic conditions afforded **34**. BOP-Cl mediated coupling with Boc-proline resulted in good yield. Removal of the Boc group, followed by BOP mediated coupling to lactic acid afforded **36**. Oxidation of the secondary alcohol **36**

using Dess-Martin periodinane and subsequent hydrogenolysis of its benzyl ester yielded the desired free acid side chain **37**.

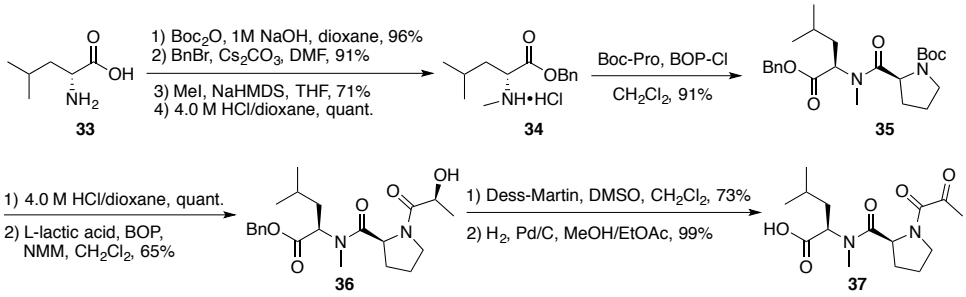

Scheme 2.14. Synthesis of dehydrodidemnin B side chain.

This side chain synthesis was two steps shorter than the previous synthesis and proved to be more synthetically efficient. The free acid side chain (**37**) was then coupled to the tamandarin B macrocyclic HCl salt via BOP mediated coupling, affording **30** in good yield (Scheme 2.15).[20]

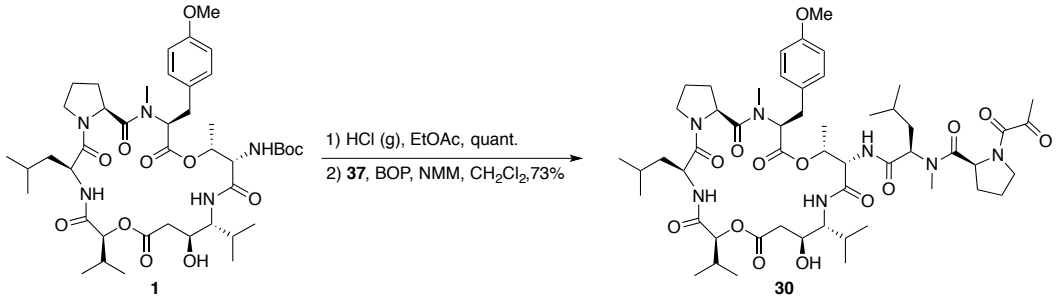

Scheme 2.15. Completion of dehydrotamandarin B analogue synthesis.

2.2.2) Synthesis of tamandarin M

Synthesis of tamandarin M side chain began with a common intermediate (**36**) used in the dehydrodidemnin B side chain synthesis, thereby making this synthesis more convergent (Scheme 2.16). The alcohol **36** was esterified with BocGln(Xan)OH[21] to afford **38**. Removal of the Boc and xanthyl groups under acidic conditions, followed by condensation with *N*-Cbz-*p*-GlnOPfP, yielded the fully functionalized side chain.

Hydrogenolysis conditions removed the Cbz and benzyl groups to afford the desired free side chain **40**.

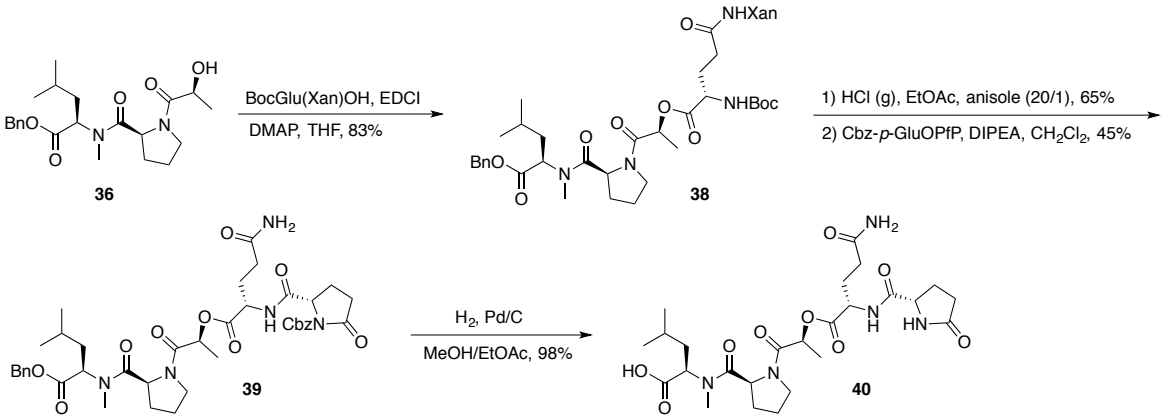

Scheme 2.16. Synthesis of didemnin M side chain.

Synthesis of tamandarin M was completed using the same set of reagents employed in the synthesis of dehydrotamandarin B (Scheme 2.17). Removal of the Boc group of the tamandarin B macrocycle, followed by coupling with the free acid side chain **40** using BOP as the coupling reagent, afforded tamandarin M analogue (**31**) in 81% yield.[20] It is important to note that the final coupling step was a great improvement over the 32% obtained in the corresponding reaction with the tamandarin A macrocyclic salt.[19]

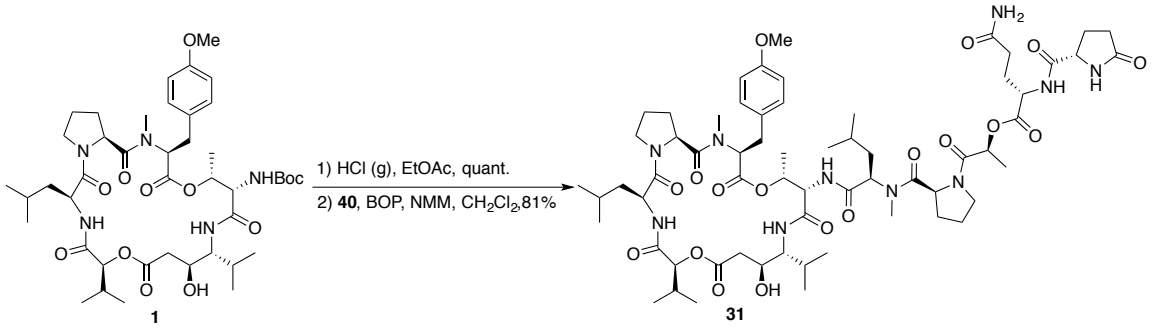

Scheme 2.17. Completion of tamandarin B analogue synthesis.

2.2.3) Synthesis of Ψ[CH_2NH]tamandarin B analogue

The final tamandarin B/didemnin hybrid analogue synthesized was the Ψ[CH_2NH]tamandarin B analogue. Commercially available *N*-Boc-L-proline (**41**) was converted to the corresponding aldehyde (**42**) using a known reduction/oxidation sequence (Scheme 2.18).[7] Reductive amination of **42** with the amine salt **34**, previously utilized in the synthesis of dehydrotamandarin B, led to **43**.[22] Subsequent Boc removal followed by amide bond formation between the corresponding amine salt and L-lactic acid yielded the protected side chain **44**. Finally, benzyl group removal afforded the desired side chain **45**.

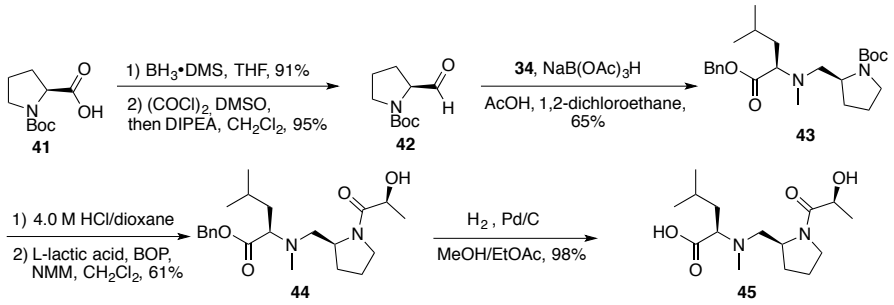

Scheme 2.18. Synthesis of Ψ[CH_2NH]tamandarin B side chain.

Unlike the previous tamandarin B analogue syntheses, the free acid side chain (**45**) was coupled to the tamandarin B macrocyclic salt in good yield using HATU as the coupling reagent based on the premise that HATU afforded higher yield than BOP (Scheme 2.19).[20]

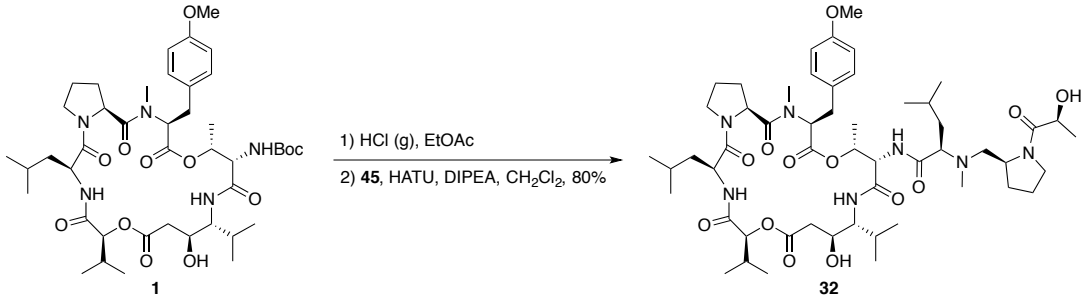

Scheme 2.19. Completion of Ψ[CH_2NH]tamandarin B analogue synthesis.

2.3) Activity of tamandarin B/didemnin hybrid analogues.

All three tamandarin B/didemnin hybrid analogues were tested in the NCI-60 tumor cell screen. Dehydrotamandarin B (**30**) performed well in the cell based assays with GI_{50} values of less than 10 nM in 23 of the 60 cell lines tested, along with LC_{50} values greater than 1 mM in 55 of the 60 lines tested.[7] Ψ[CH_2NH]tamandarin B (**32**) tested comparably, with GI_{50} values less than 10 nM in 28 of the 60 cell lines and LC_{50} values of greater than 1 mM in 48 of the 60 cell lines tested.[7] Interestingly, tamandarin M (**31**) proved to be the most potent analogue in these tests. It displayed GI_{50} values of less than 10 nM in all of the cell lines tested, and LC_{50} values of greater than 1 mM in 45 of the 60 cell lines.[7] With these impressive preliminary results, a collaboration began with the Crews laboratory at Yale University to further study the bioactivity of these analogues. Dehydrotamandarin B (**30**) and tamandarin M (**31**) were tested for activity in HeLa cells and for immunosuppressive reactivity *via* mixed lymphocyte reaction. Dehydrotamandarin B (**30**) displayed an IC_{50} of 0.608 nM in HeLa cells, and gave an IC_{50} of 0.765 nM in the mixed lymphocyte reaction.[7] In accordance with previous biological activity studies, **31** showed extremely potent activity in both assays, where in HeLa cells it displayed an IC_{50} of 0.851 fM and in mixed lymphocyte reaction it displayed an IC_{50} of 1.78 fM.[7] Next, the tamandarin B macrocyclic salt and the M side chain (**40**) were tested separately. Surprisingly, while the tamandarin B macrocyclic salt was inactive (IC_{50} >>10 nM), the free acid M side chain (**40**) showed good activity, with an IC_{50} of 0.385 nM.[7]

2.4) Conclusions

The second-generation synthesis of the tamandarin B macrocycle was successfully accomplished. The number of synthetic steps was reduced, and the overall yield was doubled relative to the first-generation synthesis. These findings will inevitably aid in the generation of more diverse tamandarin B analogues in the future. For example, combinatorial syntheses of side chain analogues using high-throughput experimentation would efficiently provide necessary compounds for further biological testing. Based on our previous knowledge from the didemnins, three particular side chain analogues were synthesized in high yields and showed impressive *in vitro* biological activities. While these results are promising, the source of biological activity is still unclear, and the mechanism of action of this class of natural products still needs to be elucidated. One particularly interesting result was the activity of the free acid M side chain (**40**), while the tamandarin B macrocyclic salt was found to be comparably inactive. Rigorous biological studies on the free acid M side chain should be done in order to assess its potential therapeutic value. Since the generation of the side chain is synthetically simpler in comparison to the macrocycle, further biological testing could be done in more time efficient manner. Taken together, more interesting experiments could be built upon our findings in the hopes of ultimately discovering new therapeutics.

2.5) Experimental results

General Methods. All reactions were performed under an argon atmosphere except where otherwise noted. Tetrahydrofuran was distilled over sodium-benzophenone, dichloromethane was distilled over calcium hydride, DMF in Acroseal bottles were used without further purification prior to use. Flash chromatography was carried out on Merck silica gel 60 (240-400 mesh) using the solvent conditions listed under individual experiments. Analytical thin-layer chromatography was performed on Merck silica gel (60F-254) plates (0.25 mm). Visualization was effected with ultraviolet light, phosphomolybdic acid, ammonium molybdate, or ninhydrin stain. Proton magnetic resonance spectra (^{1}H NMR) and Carbon magnetic resonance spectra (^{13}C NMR) were performed on a Bruker DRX-500 operating at 500 and 125 MHz respectively. Infrared spectra (IR) were obtained on a Perkin-Elmer 281-B spectrometer. High resolution mass spectra (HRMS) were obtained on a Micromass Autospec or a Waters LCTOF-Xe premier. Optical rotations were measured on a Jasco P-1010 polarimeter.

General procedure for removal of benzyl and Cbz groups. The desired substrate was dissolved in a 1:1 mixture of anhydrous MeOH/EtOAc (0.1 M). To this solution was added 10% Pd/C (10% wt). The reaction was monitored by TLC and was filtered through a pad of Celite when complete. Removal of solvent under reduced pressure provided the product, which was used without further purification.

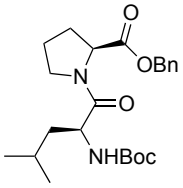

***N*-Boc-Leu-Pro-OBn (10).** Proline benzyl ester hydrochloride (115 mg, 0.48 mmol) and Boc-leucine (100 mg, 0.43 mmol) were dissolved in anhydrous DMF (3 mL) and cooled to 0 °C. To this mixture was added DEPC (72 mL, 0.48 mmol) and triethylamine (120 mL, 0.86 mmol). The resulting reaction was allowed to warm to room temperature and stir overnight. The mixture was diluted with ethyl acetate (15 mL) and washed with 10% citric acid (10 mL), saturated $NaHCO_3$ (10 mL), water (10 mL) and brine (10 mL). The organic layer was dried over Na_2SO_4, filtered, and concentrated. Purification by column chromatography (10% acetone/hexanes) led to the product as a yellow oil (178 mg, 98%). R_f 0.32 (30% acetone/hexanes); ^{1}H NMR (500 MHz, $CDCl_3$) δ 0.82 (d, *J*=6.7 Hz, 3H), 0.88 (d, *J*=6.5 Hz, 3H), 1.34 (s, 9H), 1.66 (septet, *J*=6.7 Hz, 1H), 1.92 (m, 3H), 2.12 (m, 2H), 3.50 (m, 1H), 3.68 (q, *J*=9.2 Hz, 1H), 4.38 (q, *J*=7.6 Hz, 1H), 4.50 (dd, *J*=8.5, 3.9 Hz, 1H), 4.59 (s, 1H), 5.05 (m, 1H), 5.10 (m, 2H), 7.25 (m, 5H); ^{13}C NMR (125 MHz, $CDCl_3$) δ 21.9, 23.6, 24.8, 25.1, 29.2, 42.2, 46.9, 50.5, 65.2, 67.1, 79.7, 127.2, 127.6, 127.6, 128.5, 128.6, 135.8, 141.6, 156.0, 172.1; IR (cm^{-1}) 3311, 2958, 2871, 1745, 1708, 1647, 1499, 1437, 1168; HRMS (ESI) *m/z* calculated for $C_{23}H_{34}N_2O_5Na$ $(M + Na)^+$: 441.2366, found: 441.2355; $[\alpha]_D^{21.6}$ 59.97 (c 0.90, $CHCl_3$).

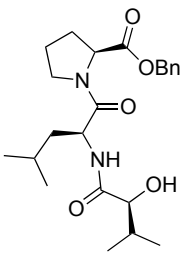

Hiv-Leu-Pro-OBn (8). *N*-Boc-Leu-Pro-OBn (100 mg, 0.24 mmol) was

dissolved in 4.0 M HCl in dioxane (3 mL) and the solution was allowed to stir at room temperature for 3 h at which point the reaction solvent was removed to yield the salt as a white solid, which was used without further purification. The salt (94 mg, 0.24 mmol) was dissolved in anhydrous dichloromethane (1 mL) and cooled to 0 °C. To this was added hydroxyisovaleric acid **11** (33 mg, 0. 28 mmol), NMM (66 mL, 0.59 mmol), and BOP (116 mg, 0.26 mmol). The reaction was then allowed to warm to room temperature and stir overnight. The mixture was diluted with ethyl acetate (20 mL), and washed with 10% HCl (10 mL), saturated $NaHCO_3$ (10 mL), and brine (10 mL). The organic layer was dried over Na_2SO_4, filtered and concentrated to yield the crude product. Purification by column chromatography (20 → 40% acetone/hexanes) yielded the product as a yellow oil (101 mg, quantitative). R_f 0.36 (30% acetone/hexanes); ^{1}H NMR: (500 MHz, $CDCl_3$) δ 0.81 (d, *J*=6.45 Hz, 3H), 0.89 (m, 6H), 0.97 (d, *J*=6.55 Hz, 3H), 1.45 (t, *J*=9.69 Hz, 1H), 1.57 (t, *J*=9.99 Hz, 1H), 1.65 (m, 1H), 1.99 (m, 3H), 2.17 (m, 3H), 3.58 (d, *J*=7.70 Hz, 1H), 3.76-3.79 (m, 1H), 3.93 (s, 1H), 4.50 (s, 1H), 4.76 (m, 1H), 5.03-5.15 (m, 2H), 7.31 (m, 5H); ^{13}C NMR: (125 MHz, $CDCl_3$) δ 15.5, 19.2, 21.6, 23.3, 24.6, 24.8, 28.9, 31.6, 40.8, 46.9, 48.4, 59.0, 66.9, 75.9, 128.1, 128.3, 128.5, 135.5, 171.5, 172.0, 175.9; IR (cm^{-1}): 3382, 2960, 2873, 1745, 1639, 1520, 1454, 1260, 1173, 1261; HRMS (ESI) *m/*z calculated for $C_{23}H_{34}N_2O_5Na$ $(M + Na)^+$: 441.2365, found: 441.2359; $[\alpha]_D^{23.6}$ -91.71 (c 0.60, CH_2Cl_2).

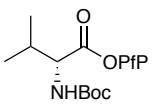

***N*-Boc-D-Val-OPfP (13).** Boc-D-Valine (8.41 g, 38.70 mmol) was dissolved in anhydrous dichloromethane (97 mL) and cooled to 0 °C. To this solution was added

distilled pyridine (3.42 mL, 42.8 mmol) and pentafluorophenyl trifluoroacetate (8.0 mL, 46.4 mmol). The reaction was allowed to warm to room temperature and stir overnight. The reaction was quenched with saturated NH_4Cl and allowed to stir for 15 min. The mixture was diluted with dichloromethane (30 mL) and the layers were separated. The organic layer was washed with 10% $KHSO_4$ (20 mL), saturated $NaHCO_3$ (20 mL), and brine (20 mL). The organic layer was dried over $MgSO_4$, filtered and concentrated to yield the product as an oil that eventually formed a white foam upon standing. The product was used without further purification (13.01 g, 87%).

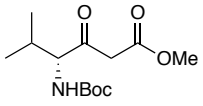

β-Ketoester (14). *n*-Butyllithium (52.0 mL, 130.69 mmol, 2.5 M in hexanes) was added to distilled diisopropylamine (18.0 mL, 130.69 mmol) in anhydrous tetrahydrofuran (70 mL) at 0 °C and allowed to stir for 30 min at which time it was cooled to -78 °C. Methyl acetate (10.4 mL, 130.69 mmol) was added dropwise to this solution to form the lithium enolate. The mixture was stirred for 1 h. In a separate flask, PfP ester **13** (11.65 g, 30.39 mmol) was dissolved in anhydrous tetrahydrofuran (98 mL) and cooled to -78 °C. The PfP ester solution was transferred to the lithium enolate solution via cannula. The reaction was allowed to stir at -78°C for 3 h at which time the cooling bath was removed and the reaction was quenched with saturated NH_4Cl (40 mL). The mixture was allowed to warm to room temperature and is diluted with dichloromethane (100 mL). The organic layer was washed with 10% HCl (40 mL), saturated $NaHCO_3$ (40 mL), and brine (40 mL). The organic layer was dried over Na_2SO_4, filtered, and evaporated to yield the crude product as an orange oil. Purification by

column chromatography (5→10→15% EtOAc/hexanes) yielded the product as a yellow oil (6.86 g, 83%). R_f 0.56 (30% EtOAc/Hexanes); ^{1}H NMR: (500 MHz, $CDCl_3$) δ 0.77-1.03 (m, 6H), 1.43 (s, 9H), 2.22 (m, 1H), 3.56 (s, 2H), 3.73 (s, 3H), 4.30 (s, 1H), 5.02 (d, *J*=7.03 Hz, 1H); ^{13}C NMR: (125 MHz, $CDCl_3$) δ 17.6, 19.7, 28.3, 29.5, 46.9, 52.4, 64.3, 80.0, 158.8, 167.1, 202.0; IR (cm $^{-1}$): 3373, 2933, 2967, 1748, 1715, 1643, 1367, 1170, 1019; HRMS (ESI) *m/z* calculated for $C_{13}H_{23}NO_5Na$ $(M+Na)^+$: 296.1474, found: 296.1486; $[\alpha]_D^{21.1}$ 15.94 (c 2.0, $CHCl_3$).

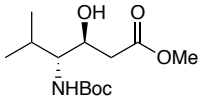

β-Hydroxyester (15). β-Ketoester **14** (6.86 g, 25.10 mmol) was dissolved in anhydrous methanol (251 mL) and cooled to -78 °C. To this solution was added potassium borohydride (4.74 g, 87.84 mmol) and the reaction was stirred at -78 °C for 20 min. The temperature of the reaction was then increased to -20 °C for an additional 1 h. The cooling bath was removed and glacial acetic acid (3 mL) was added and the mixture was allowed to stir until all solids dissolved. The solvent was evaporated and the remaining residue was dissolved in EtOAc/H_2O (1:1, 100 mL). The organic layer was separated and dried over Na_2SO_4, filtered, and concentrated to yield the crude product. Purification by column chromatography (5→40% EtOAc/hexanes) afforded the product as a white solid (3.65 g, 53%). R_f 0.34 (30% EtOAc/hexanes); ^{1}H NMR: (500 MHz, $CDCl_3$) δ 0.85 (d, *J*=6.80 Hz, 3H), 0.91 (d, *J*=6.85 Hz, 3H), 1.41 (s, 9H), 2.08 (m, 1H), 2.45 (dd, *J*=16.3, 9.0 Hz, 1H), 2.45 (dd, *J*=16.3, 2.25 Hz, 1H), 3.25 (d, *J*=4.95 Hz, 1H), 3.49 (m, 1H), 3.68 (s, 3H), 3.89 (s, 1H), 4.41 (d, *J*=9.64 Hz, 1H); ^{13}C NMR: (125 MHz, $CDCl_3$) δ 16.2, 20.1, 27.5, 28.3, 38.2, 51.9, 58.8, 79.5, 156.4, 173.6; IR (cm^{-1}): 3450,

3370, 2964, 1718, 1694, 1524, 1367, 1172; HRMS (ESI) *m/z* calculated for $C_{13}H_{25}NO_5Na$ $(M + Na)^+$: 298.1631, found: 298.1630; $[\alpha]_D^{21.1}$ -4.16 (c 0.75, CH_2Cl_2).

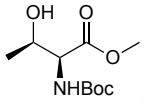

***N*-Boc-Thr-OMe (23).** *N*-Boc-Thr (100 mg, 0.46 mmol) was dissolved in anhydrous DMF (2 mL). To this was added methyl iodide (57 mL, 0.91 mmol) and sodium carbonate (145 mg, 1.37 mmol). The reaction was allowed to stir overnight then was diluted with ethyl acetate (20 mL) and washed with water (2 x 10 mL), 10% HCl (10 mL), and brine. The organic layer was dried over Na_2SO_4, filtered, and concentrated to yield the product, which was used without any further purification (92 mg, 86%). R_f 0.26 (30% EtOAc/hexanes); ^{1}H NMR (500 MHz, $CDCl_3$) δ 1.25 (d, *J*=6.36Hz, 1.46 (s, 9H), 1.93 (s, 9H), 3.78 (s, 3H), 4.28 (m, 2H) 5.27 (bs, 1H); ^{13}C NMR: (125 MHz, $CDCl_3$) δ 14.1, 19.8, 28.2, 52.3, 58.7, 60.3, 80.0, 156.1, 171.9; IR (cm^{-1}): 3436, 2979, 2935, 1744, 1718, 1510, 1368, 1167; HRMS (ESI) *m/z* calculated for $C_{10}H_{19}NO_5Na$ $(M + Na)^+$: 256.1161; found: 256.1162; $[\alpha]_D^{21.4}$ -8.77 (c 0.75, CH_2Cl_2).

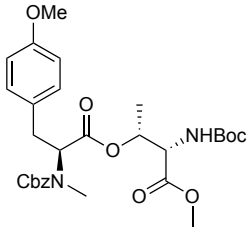

Cbz-*N,O*-Dimethyltyrosine-*O*-Boc-threonine-OMe (24). Cbz-*N,O*-Dimethyltyrosine (176 mg, 0.51 mmol) and *N*-Boc-Thr-OMe (**23**) (92 mg, 0.39 mmol) were dissolved in anhydrous tetrahydrofuran (4.5 mL) and cooled to 0 °C. To this was added EDCI (98 mg, 0.51 mmol) and DMAP (96 mg, 0.79 mmol). The reaction was

allowed to warm to room temperature and stir for 24 h. The reaction was diluted with ethyl acetate (20 mL) and washed with 10% HCl (10 mL), saturated $NaHCO_3$ (10 mL), and brine (10 mL). The organic layer was dried over Na_2SO_4, filtered and concentrated to yield the crude product. Purification by column chromatography (20% ethyl acetate/hexanes) yielded the product as an oil (202 mg, 92%). R_f 0.50 (30% acetone/hexanes); ^{1}H NMR: (500 MHz, $CDCl_3$) δ 1.25 (m, 3H), 1.43 (s, 9H), 2.75 (m, 3H), 2.83-2.97 (m, 1H), 3.17 (m, 1H), 3.67 (m, 3H), 3.75 (s, 3H), 4.42 (s, 1H), 4.75 (d, *J*=6.03 Hz, 1H), 5.03-5.11 (m, 2H), 5.25 (d,*J*=9.05 Hz, 1H), 5.39 (s, 1H), 6.77 (d, *J*=7.80 Hz, 2H), 6.95-7.10 (m, 2H), 7.29 (m, 5H); ^{13}C NMR (125 MHz, $CDCl_3$) δ 16.9, 28.2, 31.9, 34.1, 52.5, 55.1, 56.9, 60.4, 67.3, 71.6, 80.2, 113.9, 127.5, 127.6, 127.8, 127.9, 128.4, 128.8, 129.7, 129.8, 136.6, 155.9, 156.4, 158.3, 169.8, 170.4; IR (cm^{-1}): 3350, 2978, 1746, 1712, 1514, 1248, 1166; HRMS (ESI) *m/z* Calculated for $C_{29}H_{38}N_2O_9Na$ $(M+Na)^+$: 581.2475, found: 581.2475; $[\alpha]_D^{22.0}$ -13.90 (c 0.9, CH_2Cl_2).

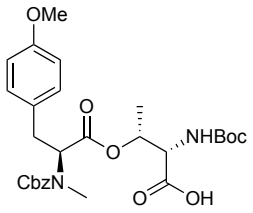

Cbz-*N,O*-Dimethyltyrosine-*O*-Boc-threonine-OH (6). Methyl ester **24** (279 mg, 50 mmol) was dissolved in anhydrous 1,2-dichloroethane (5.6 mL) in a microwave vial. To this was added trimethyltin hydroxide (361 mg, 200 mmol) and the reaction vessel was heated in a microwave reactor (3 h, 70 °C, 100 W). The solvent was evaporated and the remaining residue was dissolved in ethyl acetate (20 mL). This solution was washed with 10% $KHSO_4$ (10 mL) and brine (10 mL). The organic layer

was dried over Na_2SO_4, filtered and concentrated to yield the product as a white solid which was used without further purification (268 mg, 99%).

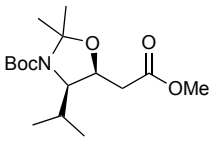

Oxazolidine methyl ester (27). β-Hydroxy ester **15** (2.01g, 7.3 mmol) was dissolved in acetone (18.5 mL) and 2,2-dimethoxypropane (18.5 mL). To this solution was added 10 (±)-camphorsulfonic acid (1.69 g, 7.3 mmol). The reaction was allowed to stir at room temperature for 24 h, at which time it was diluted with ethyl acetate (75 mL) and washed with saturated $NaHCO_3$ (40 mL), and brine (40 mL). The organic layer was dried over Na_2SO_4, filtered and concentrated to yield the crude product. Purification by column chromatography (0→10% EtOAc/hexanes) yielded the product as an oil (1.28g, 56%). R_f 0.65 (20% EtOAc/hexanes); ^{1}H NMR: (500 MHz, $CDCl_3$) δ 0.84 (d, *J*=5.05 Hz, 6H), 1.35 (s, 9H), 1.43 (s, 6H), 1.72 (m, 1H), 2.54 (m, 2H), 3.59 (s, 3H), 3.66-3.80 (m, 1H), 4.36 (d, *J*=6.54 Hz, 1H); ^{13}C NMR: (125 MHz, $CDCl_3$) δ 19.0, 21.5, 23.1, 24.7, 25.9, 26.6, 28.2, 34.2, 51.6, 62.9, 73.0, 79.4, 92.7, 153.1, 170.9; IR (cm^{-1}): 2971, 2930, 1742, 1697, 1375, 1173; HRMS (ESI) *m/z* calculated for $C_{16}H_{29}NO_5Na$ $(M+Na)^+$: 338.1944, found: 338.1953; $[\alpha]_D^{22.5}$ +24.34 (c 0.9 CH_2Cl_2).

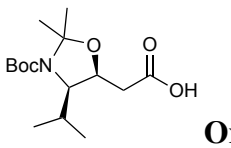

Oxazolidine carboxylic acid (28). Oxazolidine **27** (1.28 g, 4.10 mmol) was dissolved in 1:1 THF/MeOH (20 mL) and cooled to 0 °C. To this was added 0.1M LiOH (8 mL) dropwise. The reaction was allowed to warm to room temperature and stir overnight. The solvent was evaporated and the remaining aqueous solution was acidified

with 10% $KHSO_4$. This solution was then extracted with ethyl acetate (3 x 30 mL) and the combined aqueous extracts were dried over Na_2SO_4, filtered and concentrated to yield the product (1.22 g, quantitative) as an oil which was used without further purification.

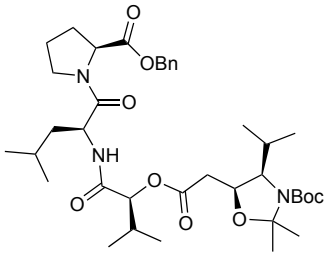

Coupled oxazolidine (29). Hiv-Leu-Pro-OBn (**8**) (50 mg, 0.119 mmol) and carboxylic acid **28** (40 mg, 0.131 mmol) were dissolved in anhydrous tetrahydrofuran (1 mL) and cooled to 0 °C. To this solution was added EDCI (27 mg, 0.143 mmol) and DMAP (1.4 mg, 0.0119 mmol). The reaction was allowed to warm to room temperature and stir overnight. The reaction was diluted with ethyl acetate (50 mL) and washed with 10% HCl (20 mL), saturated $NaHCO_3$ (20 mL), and brine (20 mL). The organic layer was dried over Na_2SO_4, filtered and concentrated to yield the crude product. Purification by column chromatography (20→40% EtOAc/hexanes) yielded the product as a white solid (78 mg, 94%). R_f 0.25 (30% EtOAc/hexanes); ^1H NMR (500 MHz, $CDCl_3$) δ 0.85-0.99 (m, 18H), 1.44 (s, 9H), 1.52 (m, 6H), 1.40 (m, 1H), 1.86 (s, 2H), 1.99 (m, 3H), 2.13-2.31 (m, 2H), 2.76 (d, *J*= 5.85 Hz, 2H), 3.56 (q, *J*= 7.45 Hz, 1H), 3.70 (m, 1H), 3.87 (s, 1H), 4.41 (m, 1H) 4.51 (dd, *J*=8.52, 4.23 Hz, 1H), 4.88 (q, *J*= 8.20 Hz, 1H), 5.00-5.19 (m, 3H), 6.66 (d, *J*= 8.70 Hz, 1H), 7.31 (m, 5H); ^{13}C NMR (125 MHz, $CDCl_3$) δ 17.0, 18.7, 21.7, 23.3, 24.6, 24.8, 28.3, 28.9, 30.6, 34.9, 42.1, 46.8, 48.5, 58.8, 63.2, 66.9, 67.8, 72.8, 78.3 79.8, 92.9, 128.1, 128.4, 128.5, 135.5, 164.9, 168.8, 169.9, 170.6, 171.6; IR (cm^{-1}): 3306, 2966, 2935, 2876, 1745, 1694, 1648, 1451, 1367, 1173; HRMS

(ESI) *m/z* calculated for $C_{38}H_{60}N_3O_9$ $(M + H)^+$: 702.4251, found: 702.4330; $[\alpha]_D^{19.6}$ -42.04 (c 1.00, CH_2Cl_2).

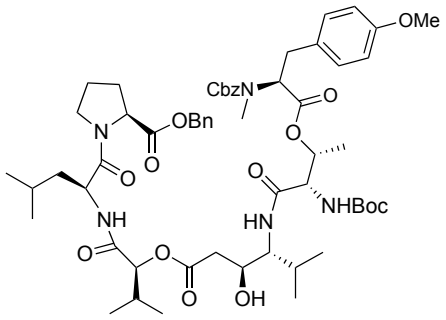

Protected linear precursor (5). Coupled oxazolidine **29** (215 mg, 0.306 mmol) was dissolved in 4.0 M HCl in dioxane (5 mL) and allowed to stir for 3 h. The solvent was evaporated and to the residue was added Et_2O and the solution was subsequently evaporated and kept under reduced pressure overnight to yield the HCl salt as a white solid. The HCl salt (183 mg, 0.306 mmol) was dissolved in anhydrous dichloromethane (3.8 mL) and the solution was cooled to 0 °C. Acid **6** (200 mg, 0.367 mmol), BOP (169 mg, 0.383 mmol), and *i*Pr_2NEt (187 mL, 1.07 mmol) were added successively to the reaction flask. The reaction was allowed to warm to room temperature and stir for 24 h. The mixture was diluted with ethyl acetate (10 mL) and washed with 10% HCl (5 mL), saturated $NaHCO_3$ (5 mL), and brine (5 mL). The organic layer was dried over Na_2SO_4, filtered, and concentrated to yield the crude product. Purification by column chromatography (30→40% EtOAc/hexanes) yielded the product as an amorphous solid (251 mg, 76%). R_f 0.28 (30% acetone/hexanes); ^{1}H NMR (500 MHz, $CDCl_3$) δ 0.74-0.98 (m, 18H), 1.22 (d, *J*=5.34 Hz, 3H), 1.43 (s, 9H), 1.64 (m, 2H), 1.96 (m, 5H), 2.17 (m, 3H), 2.54 (m, 1H), 2.70 (m, 1H), 2.80 (m, 3H), 2.94 (m, 1H), 3.19 (dd, *J*=12.9, 5.2 Hz, 1H), 3.58 (m, 1H), 3.63 (s, 1H), 3.73 (s, 3H), 3.80 (m, 1H), 4.04 (t,

J= 6.70 Hz, 1H), 4.10 (m, 1H), 4.35 (s, 1H), 4.45 (m, 1H), 4.77-4.89 (m, 2H), 4.92 (d, *J*=4.81 Hz, 1H), 5.00 (m, 2H), 5.05-5.14 (m, 1H), 5.19 (m, 1H), 5.26 (m, 1H), 5.50 (d, *J*= 8.44 Hz, 1H), 6.74 (d, *J*= 8.00 Hz, 2H), 7.01 (m, 2H), 7.29 (m, 10H), 7.46 (m, 1H); ^{13}C NMR (125 MHz, $CDCl_3$) δ 13.6, 16.9, 17.7, 18.3, 18.5, 19.1, 20.2, 20.9, 21.1, 23.3, 24.7, 28.1, 28.8, 30.4, 31.9, 34.0, 38.7, 40.1, 46.9, 48.4, 55.1, 58.9, 64.3, 66.9, 67.3, 68.6, 70.2, 78.6, 80.2, 113.9, 127.6, 127.9, 128.1, 128.4, 128.5, 129.7, 129.8, 135.4, 156.1, 156.8, 158.3, 169.9, 170.0, 171.3, 171.6, 171.9; IR (cm^{-1}): 3329, 2961, 2935, 2875, 1744, 1686, 1637, 1514, 1454, 1248, 1173; HRMS (ESI) *m/z* calculated for $C_{58}H_{81}N_5O_{15}Na$ $(M+Na)^+$: 1110.5627, found: 1110.5609; $[\alpha]_D^{20.2}$ -44.34 (c 1.00, CH_2Cl_2).

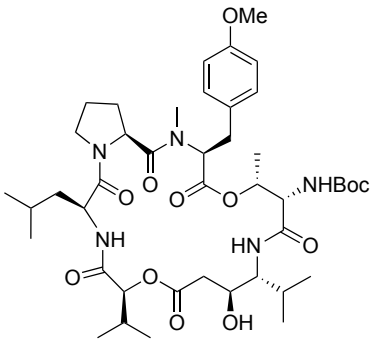

Tamandarin B macrocycle (1). Protected linear precursor **5** (40 mg, 0.037 mmol) was dissolved in anhydrous methanol (4 mL). To this was added 10% $Pd(OH)_2/C$ (4 mg, 10% wt.). The flask was evacuated, purged with hydrogen for three cycles, and allowed to stir overnight. The reaction mixture was diluted with dichloromethane (15 mL) and the solution was filtered through a pad of Celite, and concentrated to yield the product (32 mg, quantitative) as a white solid, which was used without further purification. This deprotected product (32 mg, 0.037 mmol) was dissolved in anhydrous DMF (37 mL) and cooled to 0 °C. To this was added PyAOP (33 mg, 0.063 mmol) and NMM (20 mL, 0.19 mmol). The reaction was allowed to warm to

room temperature and stir overnight. After 24 h additional PyAOP (19 mg, 0.36 mmol) and NMM (4 μL) were added and the reaction was stirred for an additional 24 h. To the reaction mixture was added water (50 mL). This solution was then extracted with EtOAc (4 x 50 mL). The combined organic phases were washed with 10% $KHSO_4$ (30 mL), 5% $NaHCO_3$ (30 mL), and brine (30 mL). The organic layer was dried over Na_2SO_4, filtered and evaporated to yield the crude product. Purification by column chromatography (40% EtOAc/CH_2Cl_2) afforded the product (14 mg, 48%) as a white solid. R_f 0.2 (50% EtOAc/CH_2Cl_2); ^{1}H NMR (500 MHz, $CDCl_3$) δ 0.80- 1.03 (m, 18H), 1.25 (d, *J*= 6.45 Hz, 3H), 1.43 (s, 9H), 1.53-1.71 (m, 4H), 1.73-1.80 (m, 4H), 1.96-2.21 (m, 4H), 2.46 (dd, *J*=16.96, 6.72 Hz), 2.56 (s, 3H), 2.85-2.94 (m, 1H), 3.14 (dd, *J*= 14.44, 10.89 Hz,1H), 3.36 (dd, *J*= 14.22, 4.32 Hz, 1H), 3.55 (dd, *J*= 10.47, 4.47 Hz, 1H), 3.64 (d, *J*= 6.00 Hz, 2H), 3.70 (t, *J*= 9.29 Hz, 1H), 3.77 (s, 3H), 3.98 (t, *J*= 6.16 Hz, 1H), 4.32 (dd, *J*= 10.37, 3.12 Hz, 1H), 4.58 (dd, *J*= 7.85, 4.60 Hz, 1H), 4.88 (t, *J*= 9.92 Hz, 1H), 4.95 (m, 2H), 5.00 (dd, *J*= 6.30, 3.20 Hz, 1H), 6.82 (d, *J*= 8.44 Hz, 2H), 7.06 (d, *J*= 8.44 Hz, 2H), 7.53 (d, *J*= 9.64 Hz, 1H), 7.95 (d, *J*= 8.49 Hz, 1H); ^{13}C NMR (125 MHz, $CDCl_3$) δ 15.1, 18.0, 18.5, 20.2, 20.7, 23.5, 24.9, 27.6, 28.0, 30.4, 34.0, 38.5, 38.9, 46.7, 48.3, 55.2, 55.8, 57.1, 60.3, 65.8, 68.9, 71.4, 79.2, 80.2, 114.1, 129.9, 130.3, 155.8, 158.6, 168.6, 169.7, 170.4, 171.3, 171.6, 172.8; IR (cm^{-1}): 3341, 2961, 2873, 1741, 1669, 1636, 1514, 1166; HRMS (ESI) *m/z* calculated for $C_{43}H_{68}N_5O_{12}$ $(M+H)^+$: 846.4864, found: 846.4869; $[\alpha]_D^{18.7}$ -90.1 (c 0.7, CH_2Cl_2).

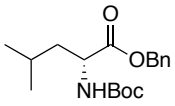

Boc-D-Leucine benzyl ester (46). D-Leucine (5 g, 38.1 mmol) was

suspended in 1 M NaOH (76 mL) and dioxane (23 mL) and cooled to 0 °C. To this was added Boc anhydride (9.15 g, 41.9 mmol) in dioxane (30 mL). The resulting reaction was allowed to warm to room temperature and stir overnight. The reaction mixture was diluted with water (100 mL) and extracted with hexanes (3 x 100 mL). The remaining aqueous layer was acidified with solid citric acid and extracted with ethyl acetate (3 x 100 mL). The organic extracts were washed with water (50 mL), brine (50 mL) and dried over $MgSO_4$. Filtration and concentration under reduced pressure led to the product as clear oil (8.51 g, 97%) that was used directly in the next step. The Boc protected product (8.51 g, 36.8 mmol) was dissolved in anhydrous DMF (75 mL) and cooled to 0 °C. To this solution was added cesium carbonate (12.0 g, 36.8 mmol) and the reaction was allowed to stir for 20 min. Benzyl bromide (4.37 mL, 36.8 mmol) was added to the reaction mixture via syringe. This mixture was allowed to warm to room temperature and stir overnight. Water (300 mL) was added to the reaction and was then extracted with hexanes (3 x 150 mL). The combined organic extracts were washed with water, brine, and dried over $MgSO_4$. Concentration under reduced pressure led to the product as a clear oil (10.76 g, 91%): R_f 0.41 (10% EtOAc/hexanes); ^{1}H NMR (500 MHz, $CDCl_3$) δ 0.92 (d, *J*= 4.10 Hz, 3H), 0.93 (d, *J*= 4.10 Hz), 1.46 (s, 9H), 1.49 (m, 1H), 1.65 (m, 2H), 4.49 (s, 1H), 4.89 (s, 1H), 5.16 (q, *J*= 13.4 Hz, 2H), 7.32 (m, 5H); ^{13}C NMR (125 MHz, $CDCl_3$) δ 21.9, 22.8, 24.8, 28.3, 41.7, 52.1, 66.9, 79.8, 128.1, 128.3, 128.5, 135.7, 155.5, 173.5; IR (neat, cm^{-1}): 3365, 2958, 1718, 1508, 1366, 1251, 1164; HRMS (ESI) *m/z* calculated for $C_{18}H_{27}NO_4Na$ $(M+Na)^+$: 344.1838, found: 344.1850; $[\alpha]_D^{22.8}$ +32.56 (c 1.12, MeOH).

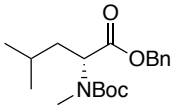

***N*-Me-*N*-Boc-D-Leucine benzyl ester (47).** *N*-Boc-Leucine benzyl ester **46** (3.61 g, 11.2 mmol) was dissolved in anhydrous tetrahydrofuran (56 mL) and cooled to 0 °C. Methyl iodide (3.54 mL, 56.2 mmol) was added to this solution followed by 1M NaHMDS (16.8 mL, 16.8 mmol). The reaction mixture was allowed to warm to room temperature and stir overnight. The reaction was quenched by addition of saturated ammonium chloride (50 mL). The reaction mixture was extracted with diethyl ether (2 x 50 mL). The combined organic phases were washed with 10% HCl (30 mL), saturated $NaHCO_3$ (30 mL), brine (30 mL), and dried over $MgSO_4$. The solvent was evaporated to yield the crude product as a brown oil. Purification by column chromatography (2→4% EtOAc/hexanes) yielded the product as a clear oil (2.76g, 73%): R_f 0.40 (10% EtOAc/hexanes); ^{1}H NMR (500 MHz, $CDCl_3$) δ 0.92 (d, *J*= 6.55 Hz, 3H), 0.94 (d, *J*= 5.83 Hz, 3H), 1.43 (s, 9H), 1.56 (m, 1H), 1.68 (m, 2H), 2.79 (m, 3H), 4.6-4.8 (m, 1H), 5.15 (m, 2H), 7.33 (m, 5H); ^{13}C NMR (125 MHz, $CDCl_3$) δ 21.2, 23.7, 24.6, 28.2, 32.4, 37.4, 56.0, 57.2, 66.5, 80.1, 127.3, 128.2, 128.5, 135.7, 155.4, 156.2, 172.26; IR (neat, cm^{-1}) 2958, 1740, 1702, 1455, 1391, 1367, 1323, 1156, 970; HRMS (ESI) *m/z* calculated for $C_{19}H_{29}NO_4Na$ $(M + Na)^+$: 358.1995, found: 358.1990; $[\alpha]_D^{24.8}$ +23.96 (c 1.0, MeOH).

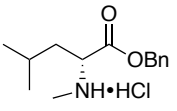

***N*-Me-D-Leucine benzyl ester hydrochloride (34).** *N*-Me-*N*-Boc-D-Leucine benzyl ester (6.47 g, 19.29 mmol) was dissolved in 4.0 M HCl in dioxane (20 mL) at room temperature. The reaction was complete after 2 h. The solvent was evaporated to yield the product (5.24 g, quantitative) as a white solid, which was used

without further purification.

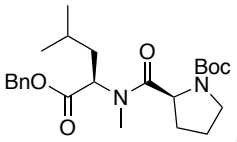

***N*-Boc-Proline-*N*-Me-D-Leucine benzyl ester (35).** Boc-Proline (2.99 g, 13.9 mmol) was dissolved in anhydrous dichloromethane (46 mL) and cooled to -15 °C. To this solution was added BOP-Cl (3.72 g, 14.6 mmol) and NMM (1. 64 mL, 14.8 mmol). This mixture was stirred for 30 minutes, then *N*-methyl-D-leucine-benzyl ester hydrochloride (3.78 g, 13.9 mmol) and NMM (5 mL, 45.9 mmol) were added. The reaction was allowed to warm to room temperature and stir for 24 h. The mixture was diluted with ethyl acetate (100 mL), washed with 10% HCl (30 mL), saturated $NaHCO_3$ (30 mL), brine (30 mL), dried over $MgSO_4$, and filtered. After solvent evaporation the crude product was purified by column chromatography (10→20% acetone/hexanes) to yield the product (4.75 g, 92%) as a white solid: R_f 0.5 (30% acetone/hexanes); ^{1}H NMR (500 MHz, $CDCl_3$) δ 0.91 (m, 6H) 1.40 (m, 9H), 1.63 (s, 1H) 1.70-1.78 (m, 1H), 1.79-2.20 (m, 3H), 3.02 (m, 3H) 3.37- 3.48 (m, 1H), 3.53-3.69 (m, 1H), 4.60 (dd, *J*=8.59, 3.39 Hz), 5.14 (m, 2H), 7.32 (m, 5H); ^{13}C NMR (125MHz, $CDCl_3$) δ 21.2, 23.3, 25.1, 28.2, 30.4, 31.7, 32.6, 37.8, 46.4, 55.2, 57.1, 66.7, 79.5, 128.1, 128.5, 135.6, 153.9, 171.6, 173.3; IR (neat, cm^{-1})**:** 2958, 2931, 2872, 1741, 1699, 1661, 1396, 1169; HRMS (ESI) *m/z* calculated for $C_{24}H_{36}N_2O_5Na$ $(M + Na)^+$: 455.2522, found: 455.2515; $[\alpha]_D^{25.8}$ -1.54 (c 1.0, CH_2Cl_2).

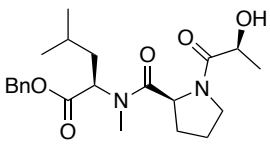

L-Lactyl-L-Prolyl-*N*-methyl-D-Leucine benzyl ester (36). Benzyl

ester **35** (300 mg, 0.69 mmol) was dissolved in 4.0 M HCl in dioxane (3 mL) and allowed to stir at room temperature for 2 h. The solvent was removed and the resulting salt was re-dissolved in anhydrous CH_2Cl_2 (3 mL) and cooled to 0 °C. To this solution was added L-lactic acid (52 μL, 0.69 mmol), BOP (368 mg, 0.83 mmol), and NMM (0.31 mL, 2.78 mmol). The mixture was allowed to warm to room temperature and stir overnight. The reaction was diluted with CH_2Cl_2 (25 mL) and washed with 10% HCl (10 mL), saturated $NaHCO_3$ (10 mL), and brine (10 mL). The organic phase was dried over Na_2SO_4, filtered, and concentrated. The crude product was purified by column chromatography (25% acetone/hexanes) to yield the product (0.172 g, 61%) as a clear oil: R_f 0.48 (50% acetone/hexanes); ^{1}H NMR (500 MHz, $CDCl_3$) δ 0.78-1.01 (m, 6H), 1.33 (m, 6H), 1.43 (m, 2H), 1.74 (m, 2H), 1.91 (m, 2H), 2.09 (m, 2H), 3.01 (s, 3H), 3.52 (t, *J*=6.75 Hz, 2H), 4.29 (q, *J*=5.98 Hz, 1H), 5.15 (m, 3H), 7.31 (m, 5H); ^{13}C NMR (125 MHz, CDCl3) δ 20.4, 21.3, 23.1, 24.8, 28.3, 32.1, 37.4, 46.5, 55.6, 568, 65.5, 66.6, 128.0, 128.4, 128.6, 135.6, 171.1, 172.1, 173.2; IR (neat, cm^{-1}): 3415, 2957, 2873, 1739, 1651, 1456, 1129, 843; HRMS (ESI) *m/z* calculated for $C_{22}H_{32}N_2O_5Na$ $(M + Na)^+$: 427.2209, found: 427.2194; $[\alpha]_D^{25.6}$ -14.07 (c 0.76, $CHCl_3$).

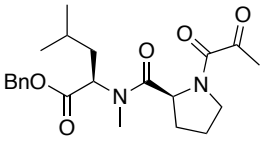

Pyruvyl-Prolyl-*N*-methyl-D-Leucine benzyl ester (48). Lactyl-Prolyl-*N*-methyl-D-Leucine benzyl ester **36** (120 mg, 0.296 mmol) was dissolved in anhydrous dichloromethane (1 mL) and dimethyl sulfoxide (0.30 mL). To this solution was added Dess-Martin periodinane (629 mg, 1.48 mmol). The reaction was allowed to

stir for 24 h at which time it was quenched with 5% $Na_2S_2O_3$ (5 mL) and diluted with Et_2O (25 mL). The organic layer was separated and washed with saturated $NaHCO_3$ (5 mL), water (5 mL), dried over Na_2SO_4, filtered and concentrated. The crude product was purified by column chromatography (20% acetone/hexanes) to yield the product (87 mg, 73%) as a yellow oil: R_f 0.27 (30% acetone/hexanes); ^{1}H NMR ($CDCl_3$, 500 MHz) δ 0.91 (m, 6H), 1.43 (m, 1H), 1.60-1.90 (m, 6H), 2.20-2.45 (m, 3H), 2.81-3.10 (m, 3H), 3.52-3.92 (m, 2H), 4.92 (m, 1H), 5.04-5.22 (m, 3H), 7.36 (m, 3H); ^{13}C NMR ($CDCl_3$, 125 MHz) δ 21.2, 22.3, 23.3, 24.9, 26.1, 31.1, 32.1 37.2, 47.5, 57.8, 58.5, 66.9, 128.1, 128.3, 128.5, 136.5, 163.6, 170.9 172.6, 198.7; IR (neat, cm^{-1}): 3460, 2958, 2873, 1739, 1715, 1652, 1455, 1206; HRMS (ESI) *m/z* calculated for $C_{22}H_{30}N_2O_5Na$ $(M + Na)^+$: 425.2052, found: 425.2040; $[\alpha]_D^{20.5}$ -2.58 (c 0.96, $CHCl_3$).

Procedure for preparation of tamandarin B macrocyclic salt. Macrocycle (14 mg, 0.017 mmol) was dissolved in ethyl acetate (4 mL) and cooled to -30 °C. HCl gas was bubbled over this solution while keeping the temperature at -30 °C for 10 min. The flow of HCl gas was stopped and stirring continued at -30 °C for an additional 30 min. The temperature was raised to 0 °C for 1 h. At this point TLC showed that the starting material had been consumed. The solvent was removed under reduced pressure to yield the macrocyclic salt (13 mg, quantitative) as a yellow solid, which was used without further purification.

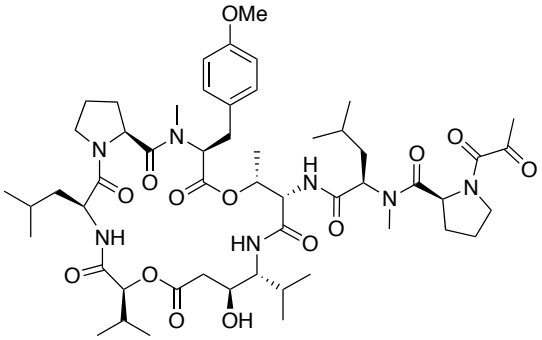

Dehydrotamandarin B (30). The tamandarin B macrocyclic salt (8.0 mg, 0.010 mmol) was dissolved in anhydrous dichloromethane (1 mL) and cooled to 0 °C. To this solution was added side chain (**37**) (5.0 mg, 0.015 mmol), BOP (7.0 mg, 0.15 mmol) and NMM (4.5 mL, 0.041 mmol). The reaction was allowed to warm to room temperature and stir overnight. The reaction was quenched with brine (4 mL) and the mixture was extracted with EtOAc (3 x 10 mL). The organic phase was washed with 10% HCl (5 mL), 5% $NaHCO_3$ aq. (5 mL), brine (5 mL), dried over Na_2SO_4, filtered and concentrated to yield the crude product. The product was purified by reverse phase HPLC (10% MeOH/H_2O→100% MeOH gradient over 40 min) to yield the product (8 mg, 73%) as a white solid. R_f 0.26 (30% acetone/hexanes); ^{1}H NMR (500 MHz, $CDCl_3$) δ 0.78-1.07 (m, 24H), 1.25 (m, 10H) 1.40 (t, *J*= 7.49 Hz, 3H), 1.45 (m, 1H), 1.61 (m, 5H), 1.72-2.28 (m, 10H), 2.43-2.50 (m, 1H), 2.53-2.62 (m, 3H), 3.03-3.12 (m, 3H), 3.13-3.20 (m, 1H), 3.55-3.74 (m, 3H), 3.79 (s, 3H), 3.81-3.89 (m, 1H), 3.91-4.04 (m,1H), 4.28-4.40 (m, 1H), 4.63 (m, 1H), 4.89 (t, *J*= 10.17 Hz, 1H), 5.05 (d, *J*=4.49 Hz, 1H), 5.16-5.27 (m, 1H), 5.28-5.36 (m, 1H), 6.84 (m, 2H), 7.08 (d, *J*= 7.91 Hz, 2H), 7.42-7.56 (m, 1H), 7.72-7.85 (m, 1H); ^{13}C NMR (125 MHz, $CDCl_3$) δ 14.1, 16.6, 17.0, 17.4, 18.9, 20.4, 20.8, 21.4, 22.7, 23.5, 23.8, 24.9, 26.3, 27.1, 28.0, 29.4, 29.7, 30.0, 30.6, 31.2, 34.0, 35.8, 38.7, 39.2, 46.7, 48.7, 48.8, 54.7, 55.2, 56.9, 57.3, 58.3, 58.9, 66.0, 70.9, 78.7,

114.1, 129.8, 130.3, 158.6, 161.3, 168.6, 169.6, 170.4, 170.5, 171.7, 172.2, 172.9, 173.9, 201.11. IR (cm^{-1}) 3340, 2957, 2926, 2871, 1741, 1662, 1636, 1514, 1457, 1170, 1078; HRMS (ESI) *m/z* calcd for $C_{53}H_{81}N_7O_{14}Na$ $(M + Na)^+$: 1062.5739, found: 1062.5760; $[\alpha]_D^{17.0}$ -18.68 (c 0.2, CH_2Cl_2).

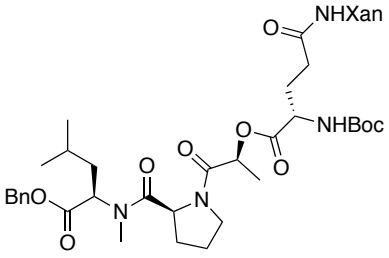

N^2-Boc-N^5-Xanthyl-Glutaminyl-*O*-L-Lactyl-L-Prolyl-*N*-methyl-D-Leucine benzyl ester (38). L-Lactyl-L-Prolyl-*N*-methyl-D-Leucine benzyl ester **36** (2.24 g, 5.5 mmol) was dissolved in anhydrous tetrahydrofuran (30 mL) and cooled to 0 °C. To this solution was added N^2-Boc-N^5-glutamine (3.07 g, 7.2 mmol), followed by EDCI (1.48 g, 7.7 mmol) and DMAP (1.34 g, 11 mmol). The reaction was allowed to warm to room temperature and stir overnight. EtOAc (50 mL) was added and the solution was washed sequentially with 10% HCl (25 mL), saturated $NaHCO_3$ (25 mL), brine (25 mL), dried over $MgSO_4$, filtered, and concentrated. The crude product was purified by column chromatography (15→20% acetone/hexanes) to yield the product (3.70 g, 83%) as a white solid: R_f 0.54 (50% acetone/hexanes); ^1H NMR (500 MHz, $CDCl_3$) δ 0.73 (t, *J*= 6.63 Hz, 2H), 0.80 (d, *J*= 6.50 Hz, 2H), 0.86 (d, *J*= 6.65 Hz, 3H), 0.97 (dd, *J*= 16.2, 6.53 Hz, 1H), 1.35 (d, *J*= 5.85 Hz, 3H), 1.43 (s, 9H), 1.60-1.69 (m, 2H), 1.78-1.88 (m, 2H), 1.88-2.20 (m, 3H), 2.22-2.42 (m, 2H), 2.70 (m, 3H), 2.89-2.98 (m, 1H), 3.43-3.69 (m, 2H), 3.72 (t, *J*= 6.25 Hz, 2H), 4.31-4.64 (m, 1H), 4.91 (m, 2H), 5.11 (m, 2H), 6.50 (m, 1H), 7.00-7.12 (m, 4H), 7.18-7.37 (m, 7H), 7.39- 7.51 (m, 2H); ^{13}C

NMR (125 MHz, $CDCl_3$) δ 11.4, 14.1, 16.0, 21.3, 22.5, 23.1, 24.9, 25.3, 28.3, 29.0, 31.5, 32.0, 34.6, 36.0, 37.3, 43.5, 46.7, 55.8, 56.7, 66.3, 116.2, 121.2, 123.3, 123.5, 127.9, 128.4, 128.8, 129.4, 135.7, 151.1, 168.6, 170.1, 171.9, 172.1; IR (neat, cm^{-1}): 3305, 2959, 1743, 1712, 1652, 1481, 1456, 1258; HRMS (ESI) *m/z* calculated for $C_{45}H_{56}N_4O_{10}Na$ (M + Na^+): 835.3894, found: 835.3992; $[\alpha]_D^{24.0}$ -27.24 (c 0.89, $CHCl_3$).

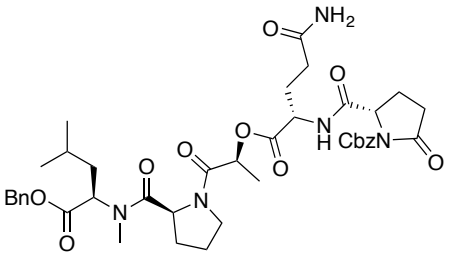

Protected tamandarin M side chain (39). *N*^{2}-Boc-*N*^{5}-Xanthyl-glutaminyl-*O*-L-Lactyl-L-Prolyl-*N*-methyl-D-Leucine benzyl ester (407 mg, 0.50 mmol) was dissolved in ethyl acetate (4.75 mL) and anisole (0.25 mL) and cooled to -20 °C. Gaseous HCl was bubbled in the reaction mixture over a 5 min period, and the reaction changed colors from yellow to red. The resulting mixture was allowed to stir at -20 °C for 1 h and at 0 °C for another 1 h. Argon was then bubbled through the solution as it was allowed to warm to room temperature. The solvent was evaporated and the remaining residue was triturated with diethyl ether (10 mL) to produce a white solid, which was obtained by filtration. The remaining ether solution was evaporated and triturated again to produce a second crop of the hydrochloride salt. The product was isolated as a white solid (0.182 g, 64%) that was used in the next step without further purification. The HCl salt (0.182 g, 32 mmol) was dissolved in anhydrous dichloromethane (1.4 mL) and cooled to 0 °C. To this solution was added *N*-Cbz-pGlu-OPfP (0.140 g, 32 mmol) and *i*Pr_2NEt (225 μL, 1.28 mmol). The mixture was allowed to

warm to room temperature and stir overnight. The reaction was quenched with brine (3 mL) and diluted with CH_2Cl_2 (5 mL). The layers were separated and the aqueous layer was extracted with CH_2Cl_2 (3 x 5 mL). The combined organic extracts were washed with 10 % HCl (5 mL), 5% $NaHCO_3$ aq. (5 mL), and brine (5 mL). The organic layer was dried ($MgSO_4$), filtered and concentrated to yield the crude product which was purified by column chromatography (1→5% MeOH/CH_2Cl_2) to yield the product (77 mg, 31%) as a white solid: R_f 0.41 (10% MeOH/CH_2Cl_2); ^{1}H NMR ($CDCl_3$, 500 MHz) δ 0.86 (d, *J*= 6.52 Hz, 3H), 0.91 (d, *J*= 6.67 Hz, 3H), 1.38 (m, 1H), 1.44-1.57 (m, 3H), 1.69-1.79 (m, 3H), 1.93-2.33 (m, 9H), 2.35-2.47 (m, 2H), 2.68 (t, *J*= 9.87 Hz, 1H), 2.71 (t, *J*= 9.97 Hz, 1H), 2.99 (s, 3H), 3.57 (q, *J*= 7.68 Hz, 1H), 3.70 (q, *J*= 7.75 Hz, 1H), 4.46-4.60 (m, 2H), 4.86 (dd, *J*= 8.40, 4.76 Hz, 1H, 5.05-5.28 (m, 4H), 5.42 (m, 1H), 6.93 (s, 1H), 7.24-7.39 (m, 10H), 7.51 (d, *J*= 6.55 Hz, 1H); ^{13}C NMR ($CDCl_3$, 125 MHz) δ 15.8, 21.1, 22.2, 23.2, 24.9, 25.1, 27.1, 28.3, 31.1, 31.3, 31.6, 37.4, 46.7, 51.9, 55.0, 57.2, 59.5, 66.8, 68.2, 69.2, 127.9, 128.2, 128.5, 128.6, 135.1, 135.5, 151.3, 168.6, 170.7, 171.1, 171.5, 171.9, 173.5, 175.6; IR (neat, cm^{-1}): 3432, 3328, 3214, 2951, 1791, 1742, 1661, 1452, 1304, 1189; HRMS (ESI) *m/z* calculated for $C_{40}H_{51}N_5O_{11}Na$ $(M + Na)^+$: 800.3483, found: 800.3495; $[\alpha]_D^{27.0}$ -57.03 (c 0.77, $CHCl_3$).

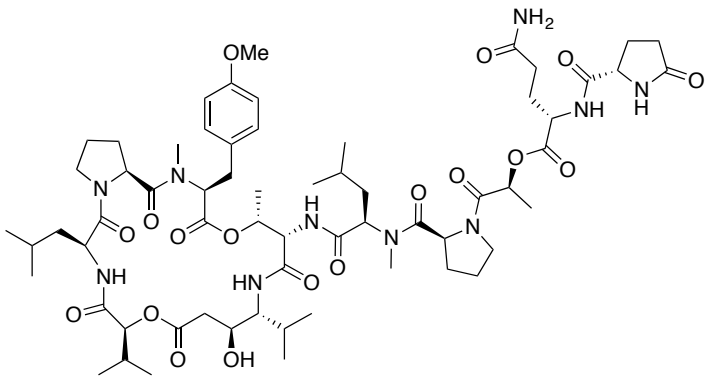

Tamandarin M (31). The tamandarin B macrocyclic salt (10.0 mg, 0.013 mmol) was dissolved in anhydrous dichloromethane (1 mL) and cooled to 0 °C. To this solution was added side chain **40** (11.0 mg, 0.019 mmol), BOP (9.0 mg, 0.019 mmol), and NMM (6.0 μL, 0.051 mmol). The reaction was allowed to warm to room temperature and stir overnight. The reaction was quenched with brine (4 mL) and the resulting mixture was extracted with EtOAc (3 x 10 mL). The organic phase was washed with 10 % HCl (5 mL), 5% $NaHCO_3$ aq. (5 mL), brine (5 mL), dried over Na_2SO_4, filtered, and concentrated to yield the crude product. The product was purified by reverse phase HPLC (10% MeOH/H_2O→100% MeOH gradient over 40 min) to yield the product (13 mg, 81%) as a white solid. R_f 0.21 (50% EtOAc/CH_2Cl_2); ^{1}H NMR (500 MHz, $CDCl_3$) δ 0.76-1.05 (m, 24H), 1.15-1.32 (m, 10H), 1.36-1.42 (m, 5H), 1.46 (d, *J*= 7.07 Hz, 2H), 1.52-1.66 (m, 3H), 1.72 (m, 2H), 1.89 (m, 2H), 1.96-2.31 (m, 9H), 2.34-2.46 (m, 2H), 2.54 (s, 3H), 2.61 (m, 1H), 2.92 (m, 1H), 2.97 (s, 2H), 3.06-3.16 (m, 2H), 3.32 (dd, *J*= 14.16, 3.95 Hz, 1H), 3.53-3.74 (m, 4H), 3.77 (s, 3H), 3.87 (m, 2H), 4.15 (t, *J*= 4.16 Hz, 1H), 4.49 (m, 2H), 4.57 (dd, *J*= 7.73, 4.68 Hz, 1H), 4.74 (t, *J*= 7.05 Hz, 1H), 4.87 (m, 1H), 4.91 (d, *J*= 5.05 Hz, 1H), 5.01 (m, 1H), 5.11 (q, *J*= 6.70 Hz, 1H), 5.25 (dd, *J*= 9.45, 6.00 Hz, 1H), 5.94 (s, 1H), 6.81 (d, *J*= 8.30 Hz, 2H), 7.05 (d, *J*= 8.35 Hz, 2H), 7.75 (d, *J*= 9.40 Hz, 1H), 7.80 (d, *J*= 9.80 Hz, 1H), 8.52 (d,

J= 6.35 Hz, 1H). ^{13}C NMR (125 MHz, $CDCl_3$) δ 14.2, 15.9, 16.1, 16.9, 17.9, 18.8, 20.3, 20.9, 21.4, 22.7, 23.6, 23.7, 24.6, 24.9, 25.7, 27.2, 27.9, 28.8, 29.3, 29.7, 30.2, 31.1, 31.8, 31.9, 34.0, 26.1, 38.6, 39.2, 39.5, 46.8, 47.1, 48.3, 51.8, 53.8, 54.3, 55.3, 56.3, 56.6, 56.8, 57.0, 58.4, 66.1, 68.7, 69.5, 71.2, 79.4, 114.1, 129.8, 130.4,158.6, 168.8, 169.4, 169.5, 170.5, 170.8, 171.1, 171.3, 172.6, 173.3, 173.5, 176.5, 178.8; IR (cm^{-1}) 3337, 2958, 1928, 2873, 1741, 1662, 1636, 1514, 1456, 1248; HRMS (ESI) *m/z* calculated for $C_{63}H_{96}N_{10}O_{18}Na$ $(M + Na)^+$: 1303.6802, found: 1303.6832; $[\alpha]_D^{17.0}$ -35.49 (c 0.65, CH_2Cl_2).

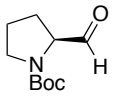

***N*-Boc-Prolinal (42).** This compound was prepared according to a procedure by Reed.[23] The obtained product was in good agreement with the reported spectra and physical characteristics.

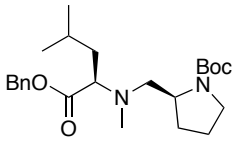

***N*-Boc-Pro Ψ($NHCH_2$) *N*-methyl-D-leucine-benzyl ester (43).** Boc-Prolinal (**42**) (430 mg, 2.15 mmol) and *N*-methyl leucine benzyl ester (**34**) (508 mg, 2.15 mmol) were dissolved in anhydrous 1,2-dichloroethane (5 mL). The reaction was cooled to 0 °C and acetic acid (0.5 mL) was added and the solution and stirred for 20 min. Sodium triacetoxyborohydride (637 mg, 3.01 mmol) was added to the reaction and the mixture was allowed to warm to room temperature and to stir for 3 h. The reaction was quenched with saturated NH_4Cl and diluted with CH_2Cl_2 (15 mL). The organic layer was washed with 10% HCl (10 mL), 5% $NaHCO_3$ aq. (10 mL), brine (10 mL), dried over

Na_2SO_4, filtered, and concentrated to yield the crude product. The crude product was purified by column chromatography (10→20% EtOAc/hexanes) to afford the product (580 mg, 65%) as a yellow oil: R_f 0.68 (30% EtOAc/hexanes); ^{1}H NMR (500 MHz, $CDCl_3$) δ 0.89 (m, 6H), 1.42 (s, 9H), 1.56 (m, 1H), 1.68 (m, 1H), 1.80 (m, 4H), 2.30 (m, 4H), 2.51-2.80 (m, 1H), 3.31 (m, 3H), 3.70-3.95 (m, 1H), 5.13 (m, 2H), 7.35 (m, 5H); ^{13}C NMR (125 MHz, $CDCl_3$) δ 22.4, 22.9, 24.7, 28.5, 36.8, 39.2, 40.3, 46.1, 55.9, 66.1, 79.1, 128.2, 128.3, 128.5, 136.0, 154.4, 172.8; IR (neat, cm^{-1}): 2958, 2873, 1731, 1694, 1456, 1394, 1171; HRMS (ESI) *m/z* Calculated for $C_{24}H_{38}N_2O_4Na$ $(M + Na)^+$: 441.2730, found: 441.2741; $[\alpha]_D^{22.0}$ +10.7 (c 0.8, $CHCl_3$).

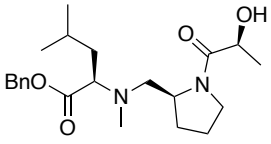

L-Lactyl-Pro Ψ(NHCH$_2$) *N*-methyl-D-leucine benzyl ester (44). *N*-Boc-Pro Y(NHCH$_2$) *N*-methyl-D-leucine-benzyl ester (**43**) (0.128 g, 0.316 mmol) was dissolved in 4.0 M HCl in dioxane (5 mL). The reaction was stirred for 2 h and the solvent was evaporated to yield the hydrochloride salt in quantitative yield. The resulting salt (0.122 g, 0.316 mmol) was dissolved in anhydrous dichloromethane (2 mL) and cooled to 0 °C. To this solution was added L-lactic acid (25 μL, 0.332 mmol), BOP (0.154 g, 0.348 mmol), and NMM (173 μL, 1.58 mmol). The reaction was allowed to warm to room temperature and stir overnight. The reaction was diluted with EtOAc (20 mL) and washed with 10% HCl (10 mL), 5% $NaHCO_3$ aq. (10 mL), and brine (10 mL). The organic layer was dried over Na_2SO_4, filtered, and concentrated to yield the crude product. The crude product was purified by column chromatography (20→50%

EtOAc/hexanes) to yield the product (75 mg, 61%) as a yellow oil: R_f 0.30 (50% EtOAc/hexanes); ^{1}H NMR (500 MHz, $CDCl_3$) δ 0.83-0.92 (m, 6H), 1.29 (d, *J*= 6.55 Hz, 3H), 1.38-1.70 (m, 4H), 1.76-2.01 (m, 4H), 2.28-2.48 (m, 5H), 2.64-2.87 (m, 1H), 3.24-3.50 (m, 3H), 4.06-4.40 (m, 1H), 5.12 (d, *J*= 4.75 Hz, 2H), 7.33 (m, 5H); ^{13}C NMR (125 MHz, $CDCl_3$) δ 20.3, 20.9, 22.3, 22.7, 23.4, 23.9, 24.8, 27.7, 29.6, 37.4, 38.4, 46.0, 56.6, 65.4, 66.0, 128.1, 128.3, 128.4, 135.8, 172.5, 173.6; IR (neat, cm^{-1}): 3426, 2957, 2925, 2863, 1731, 1639, 1452, 1127; HRMS (ESI) *m/z* calculated for $C_{22}H_{35}N_2O_4$ $(M + H)^+$: 391.2597, found: 391.2585; $[\alpha]_D^{19.0}$ -1.55 (c 0.58, $CHCl_3$).

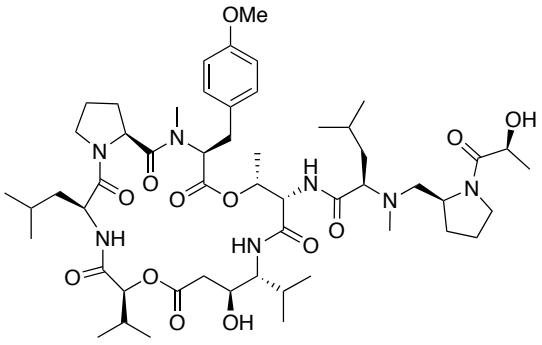

Ψ[CH_2NH] Amide surrogate tamadarin B (32). The tamandarin B macrocyclic salt (15.0 mg, 0.019 mmol) was dissolved in anhydrous dichloromethane (1 mL) and cooled to 0 °C. To this solution was added side chain **45** (12 mg, 0.038 mmol), HATU (12 mg, 0.031 mmol), and *i*Pr_2NEt (14 μL, 0.077 mmol). The reaction was allowed to warm to room temperature and stir overnight. The reaction was diluted with EtOAc (15 mL) and washed with 10% HCl (5 mL), 5% $NaHCO_3$ aq. (5 mL), brine (5 mL), dried over Na_2SO_4, filtered and concentrated to yield the product (15 mg, 83 %) as a white solid. R_f 0.46 (10 % MeOH/CH_2Cl_2); ^{1}H NMR (500 MHz, $CDCl_3$) δ 0.0-1.05 (m, 24H), 1.19 (m, 1H), 1.25 (t, *J*= 7.09 Hz, 3H),1.29-1.39 (m, 5H), 1.40-1.52 (m, 3H), 1.57-1.81 (m, 5H), 1.82-2.05 (m, 3H), 2.07-2.18 (m, 3H), 2.33 (d,

J= 10.00 Hz, 3H), 2.41 (m, 1H), 2.53 (s, 2H), 2.77 (s, 3H), 2.89 (m, 1H), 3.12 (m, 2H), 3.28-3.50 (m, 3H), 3.52-3.71 (m, 3H), 3.76 (s, 3H), 3.94 (m, 1H), 4.26 (m, 2H), 4.56 (m, 2H), 4.84 (d, *J*= 6.05 Hz, 2H), 5.01 (m, 1H), 6.80 (d, *J*= 8.15 Hz, 2H), 7.05 (d, *J*= 7.95 Hz, 2H), 7.62 (d, *J*= 9.15 Hz, 1H) 7.68 (d, *J*= 8.34 Hz, 1H), 7.77 (d, *J*= 8.53 Hz, 1H), 8.00 (t, *J*= 8.90 Hz, 1H); ^{13}C NMR (125 MHz, $CDCl_3$) δ 15.5, 16.5, 18.1,18.5, 20.3, 20.8, 21.1, 22.0, 22.6, 23.0, 23.5, 24.4, 24.9, 25.1 25.6, 27.6, 28.0, 30.3, 34.1, 36.0, 36.7, 38.6, 45.8, 46.4, 46.8, 48.3, 54.5, 56.4, 57.1, 57.2, 58.9, 63.6, 64.6, 65.1, 65.4, 65.8, 68.8, 69.3, 71.3, 79.3, 114.0, 129.8, 130.4, 158.6, 165.8, 168.8, 169.8, 170.3, 171.2, 172.5, 172.9, 173.2; IR (cm^{-1}) 3339, 2956, 2920, 2868, 1742, 1661, 1654, 1633, 1511, 1094; HRMS (ESI) *m/z* calculated for $C_{53}H_{86}N_7O_{13}$ $(M + H)^+$: 1028.6284, found: 1028.6300; $[\alpha]_D^{18.0}$ -65.55 (c 0.34, CH_2Cl_2).

2.6) References

[1] Liang, B., Richard, D. J., Portonovo, P. & Joullie, M. M. "Total Syntheses and Biological Investigations of Tamandarins A and B and Tamandarin A Analogs." *J. Am. Chem. Soc.* **2001**, *123*, 4469-4474.

[2] Adrio, J., Cuevas, C., Manzanares, I. & Joullie, M. M. "Synthesis and Biological Evaluation of Tamandarin B Analogues." *Org. Lett.* **2006**, *8*, 511–514.

[3] Adrio, J., Cuevas, C., Manzanares, I. & Joullie, M. M. "Total Synthesis and Biological Evaluation of Tamandarin B analogues." *J. Org. Chem.* **2007**, *72*, 5129–5138.

[4] Hamada, Y., Kondo, Y., Shibata, M. & Shioiri, T. "Efficient Total Synthesis of Didemnins A and B." *J. Am. Chem. Soc.* **1989**, *111*, 669-673.

[5] Jou, G., Gonzales, I., Albericio, F., Lloyd-Williams, P. & Giralt, E. "Total Synthesis of Dehydrodidemnin B. Use of Uronium and Phosphonium Salt Coupling Reagents in Peptide Synthesis in Solution." *J. Org. Chem.* **1997**, *62*, 354-366.

[6] Lassen, K. M., Lee, J. & Joullie, M. M. "An efficient synthesis of the tamandarin B macrocycle." *Tetrahedron Lett.* **2010**, *51*, 1635-1638.

[7] K. M. Lassen, "The synthesis and biological evaluation of tamandarin B analogues", University of Pennsylvania, Philadelphia, PA, **2011**.

[8] Long, C. M. "Investigations of Novel Ascidian Metabolites" Ph. D. thesis, University of Pennsylvania, Philadelphia, **2006**.

[9] Li, W.-R., Ewing, W. R., Harris, B. D. & Joullié, M. M. "Total Synthesis and Structural Investigations of Didemnins A, B, and C." *J. Am. Chem. Soc.* **1990**, *112*, 7659-7672.

[10] Chen, W.-C., Vera, M. D. & Joullié, M. M. "Mild, selective cleavage of amino acid

and peptide [beta]-(trimethylsilyl)ethoxymethyl (SEM) esters by magnesium bromide." *Tetrahedron Lett.* **1997**, *38*, 4025-4028.

[11] Nicolaou, K. C., Estrada, A. A., Zak, M., Lee, S. H. & Safina, B. S. "A mild and selective method for the hydrolysis of esters with trimethyltin hydroxide." *Angew. Chem., Int. Ed. Engl.* **2005**, *44*, 1378-1382.

[12] Kunishima, M., Kawachi, C., Iwasaki, F., Terao, K. & Tani, S. "Synthesis and characterization of 4-(4,6-dimethoxy-1,3,5-triazin-2-yl)-4-methylmorpholinium chloride." *Tetrahedron Lett.* **1999**, *40*, 5327-5330.

[13] Hiebl, J. *et al.* "Large-scale synthesis of hematoregulatory nonapeptide SK&F 107647 by fragment coupling." *J. Pept. Res.* **1999**, *54*, 54-65.

[14] Carpino, L. A., Elfaham, A., Minor, C. A., Albericio, F. "Advantageous Applications of Azabenzotriazole (Triazolopyridine)-Based Coupling Reagents to Solid-Phase Peptide-Synthesis." *J. Chem. Soc., Chem. Commun.* **1994**, 201-203.

[15] HoegJensen, T., Holm, A. & Sorensen, H. "Peptide thioacylation with high stereochemical preservation." *Synthesis* **1996**, 383-&.

[16] Rinehart, K. L. & Katauskas, A. J. "Semi-synthetic studies toward didemnin analogues." WO patent 9817275 **1998**.

[17] Rinehart, K. L. & Lithgow-Bertelloni, A. M. P. in *GB patent W22026,**1990*** Vol. 115 (ed Appl. WO 91 04 PTC Int, 985) 248086q (GB, 1991).

[18] Ding, X. *et al.* "Structure-Activity Relationships of Side-Chain Modified Didemnins." *Bioorg. Med. Chem. Lett.* **2001**, *11*, 231-234.

[19] Liang, B., Vera, M. D. & Joullié, M. M. "Total Synthesis of [(2*S*)-Hiv^2]Didemnin M."

J. Org. Chem. **2000**, *65*, 4762-4765.

[20] Lassen, K. M., Lee, J. & Joullie, M. M. "Synthetic Studies of Tamandarin B Side Chain Analogues." *J. Org. Chem.* **2010**, *75*, 3027-3036.

[21] Atherton, E. *et al.* "Peptide synthesis. Part 3. Comparative solid-phase syntheses of human [small beta]-endorphin on polyamide supports using t-butoxycarbonyl and fluorenylmethoxycarbonyl protecting groups." *J. Chem. Soc., Perkin Trans. 1* **1983**, 65-73.

[22] Abdel-Magid, A. F., Carson, K. G., Harris, B. D., Maryanoff, C. A. & Shah, R. D. "Reductive Amination of Aldehydes and Ketones with Sodium Triacetoxyborohydride. Studies on Direct and Indirect Reductive Amination Procedures." *J. Org. Chem.* **1996**, *61*, 3849-3862.

[23] Reed, P. E. & Katzenellenbogen, J. A. "Synthesis of proline-valine pseudodipeptide enol lactones, serine protease inhibitors." *J. Org. Chem.* **1991**, *56*, 2624-2634.

2.7) Appendix A. Nuclear Magnetic Resonance and Infrared Spectra Relevant to Chapter 2

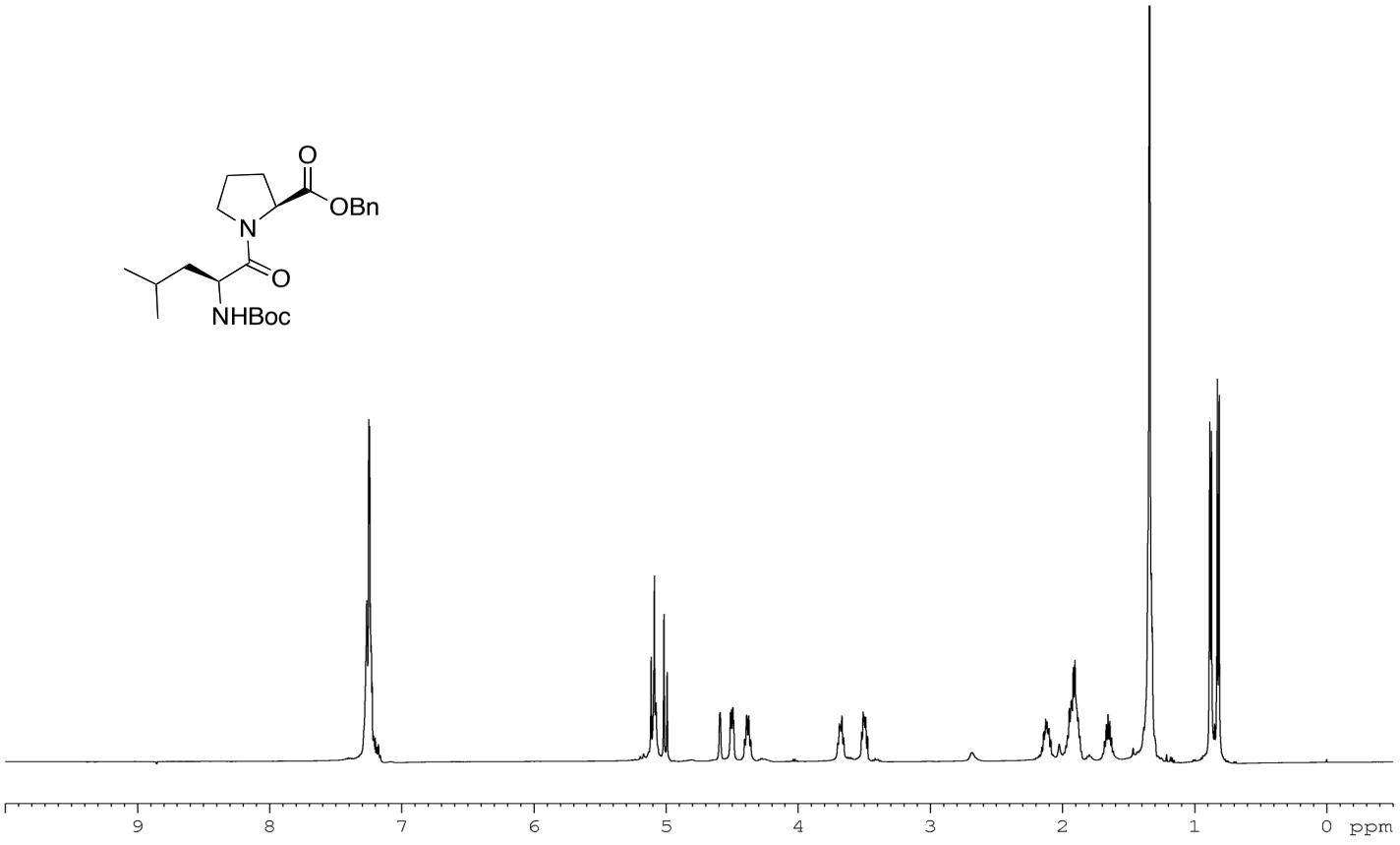

Figure 1: ^{1}H NMR ($CDCl_3$, 500 MHz) of **10**

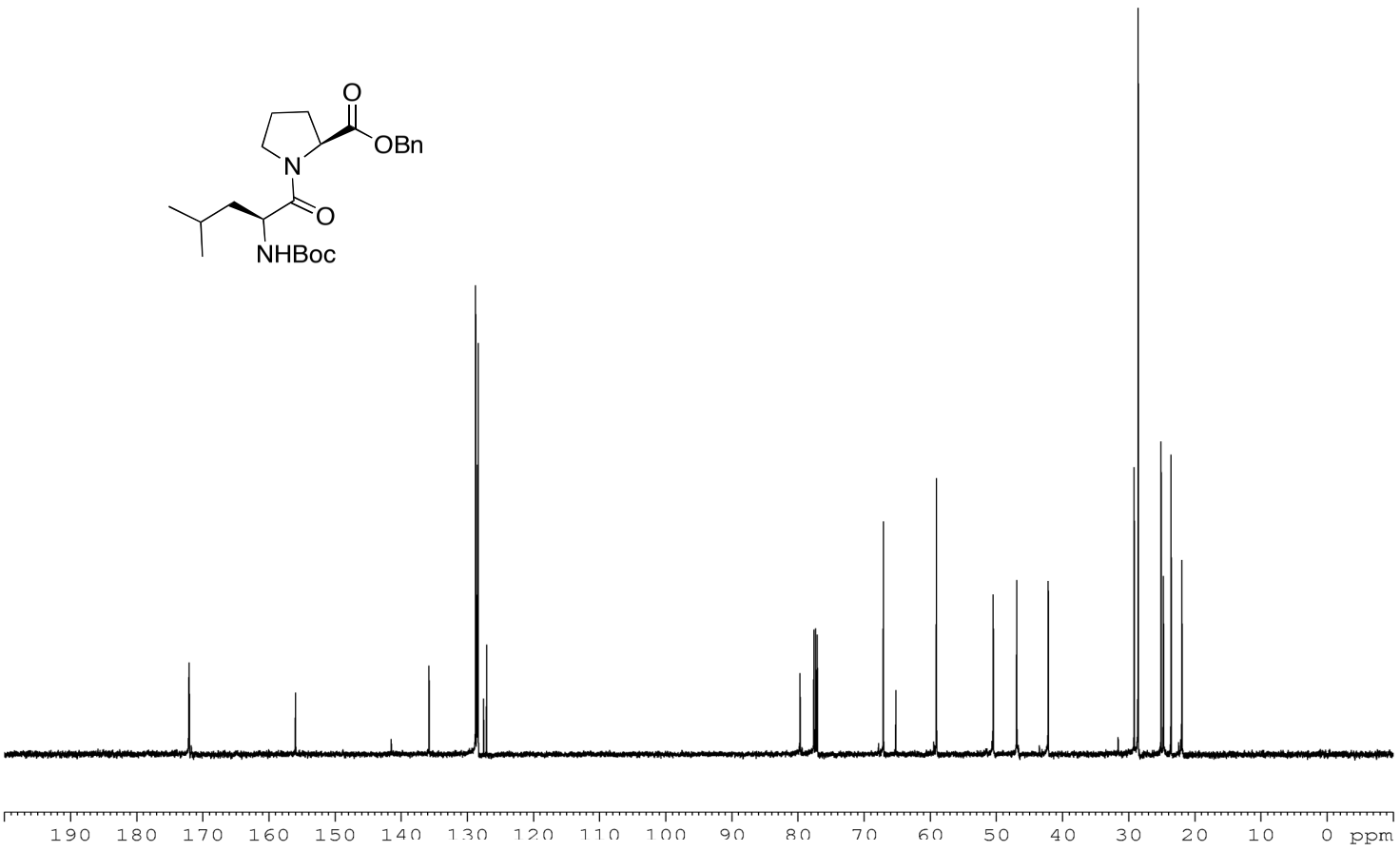

Figure 2: ^{13}C NMR ($CDCl_3$, 125 MHz) of **10**

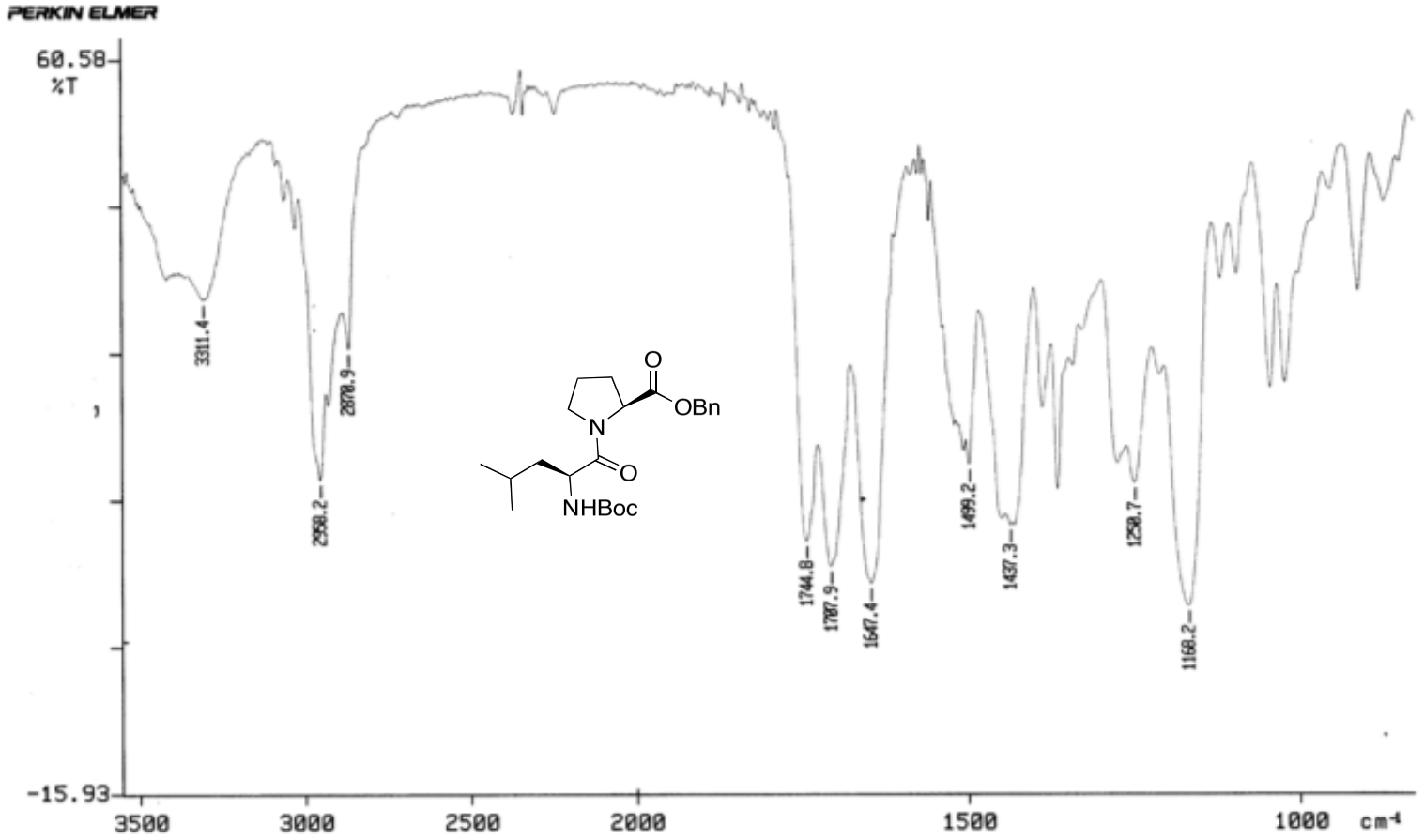

Figure 3: Infrared spectra (neat) of **10**

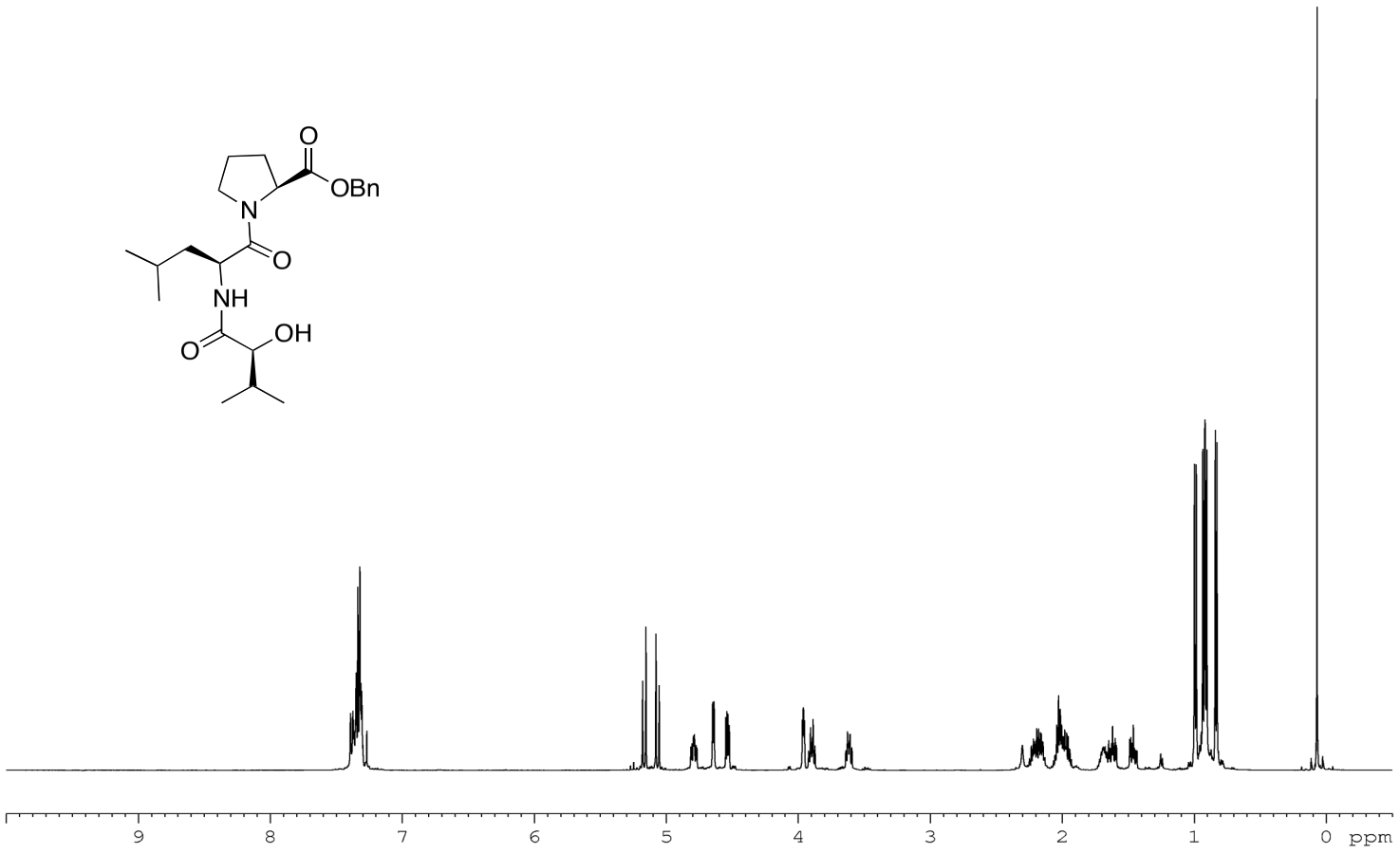

Figure 4: ^{1}H NMR ($CDCl_3$, 500 MHz) of **8**

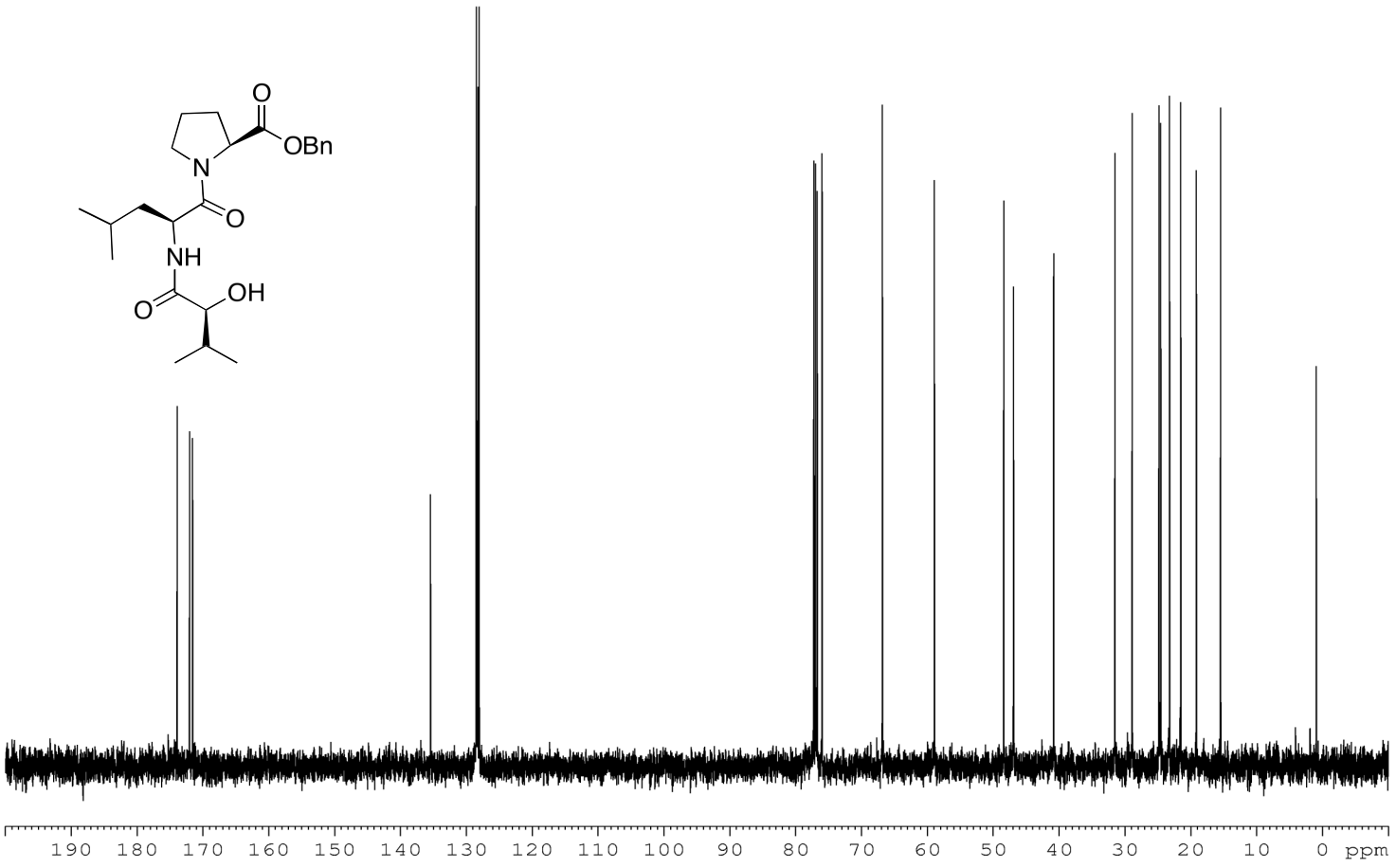

Figure 5: ^{13}C NMR ($CDCl_3$, 125 MHz) of **8**

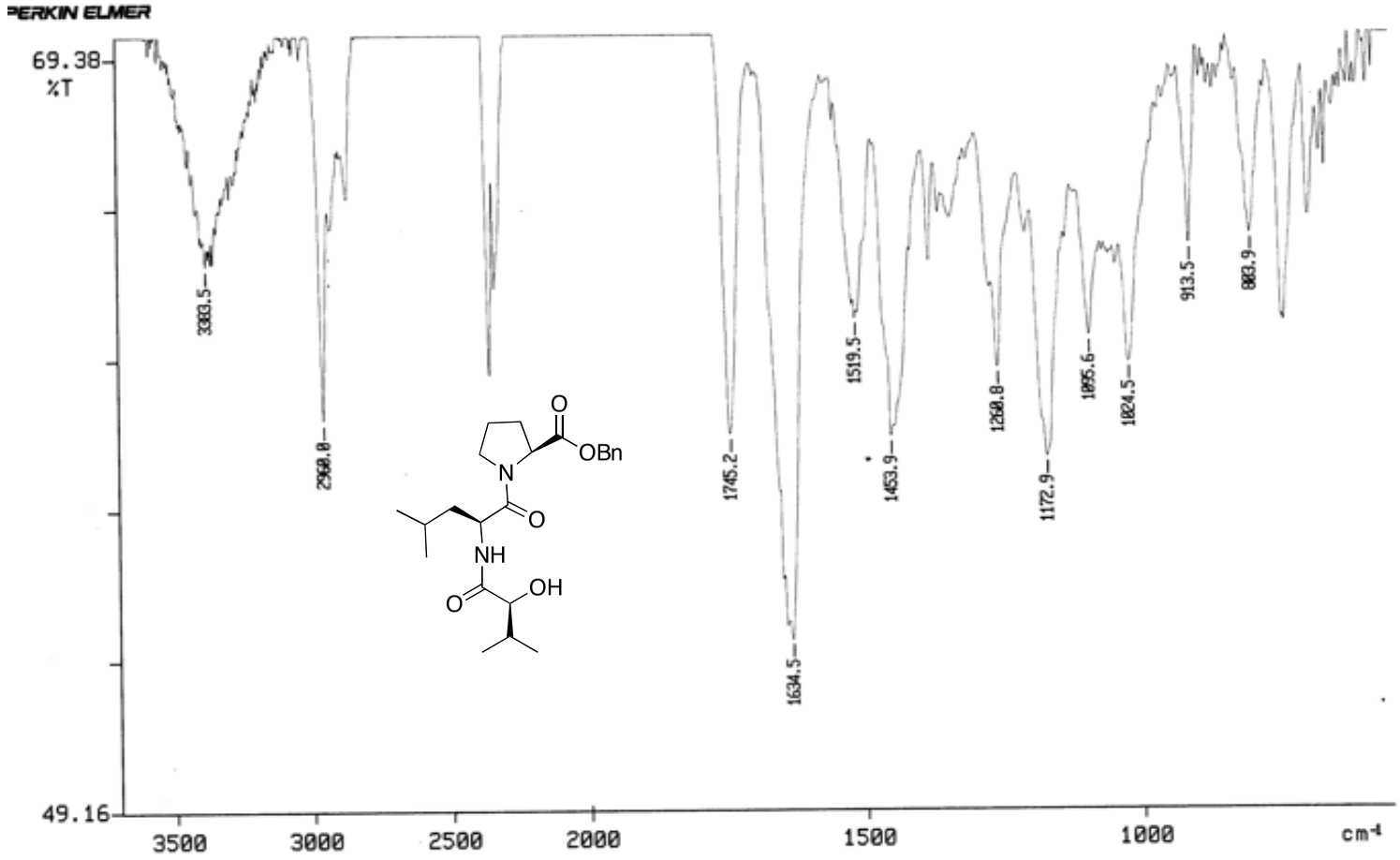

Figure 6: Infrared spectra (neat) of **8**

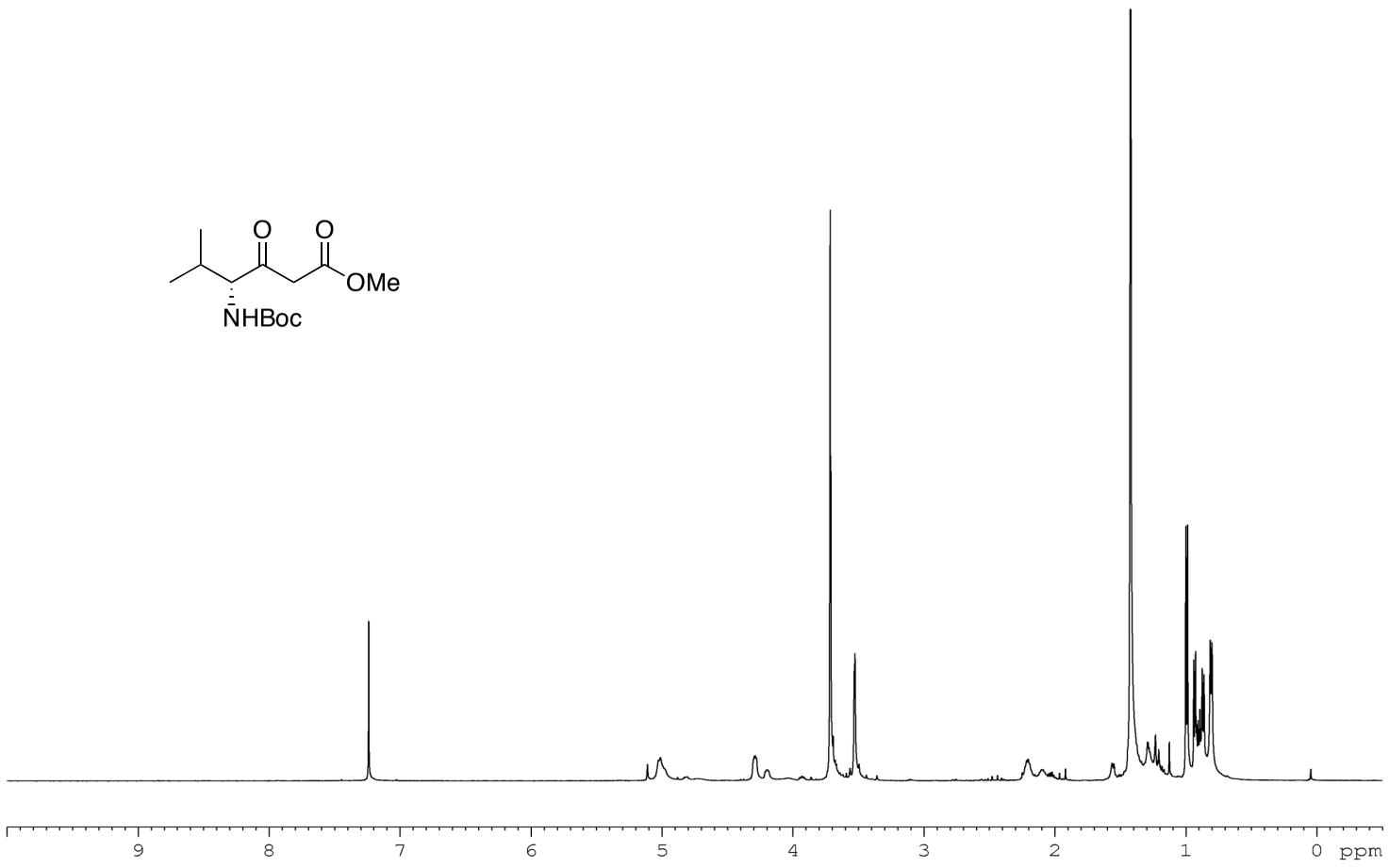

Figure 7: ^{1}H NMR ($CDCl_3$, 500 MHz) of **14**

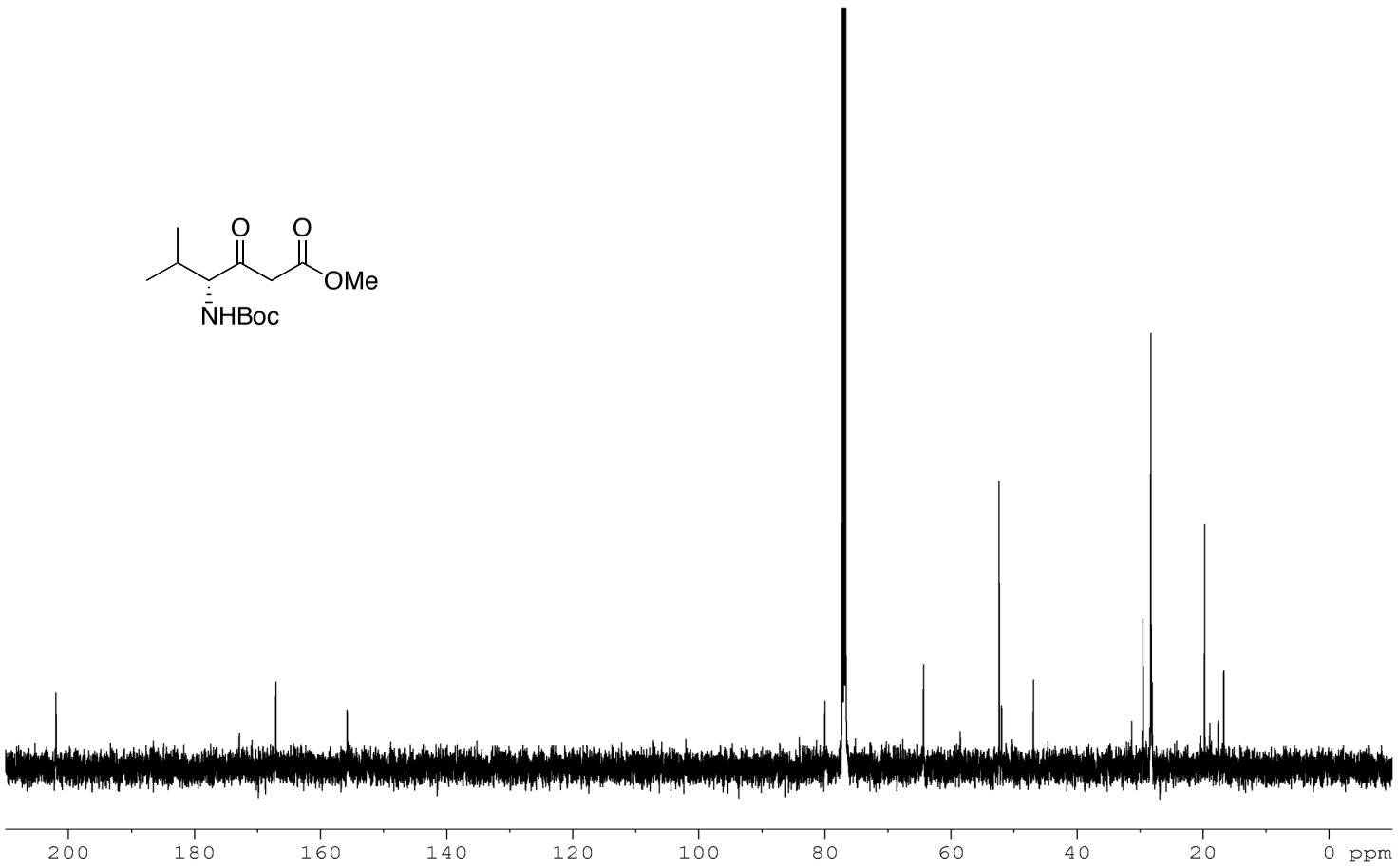

Figure 8: ^{13}C NMR ($CDCl_3$, 125 MHz) of **14**

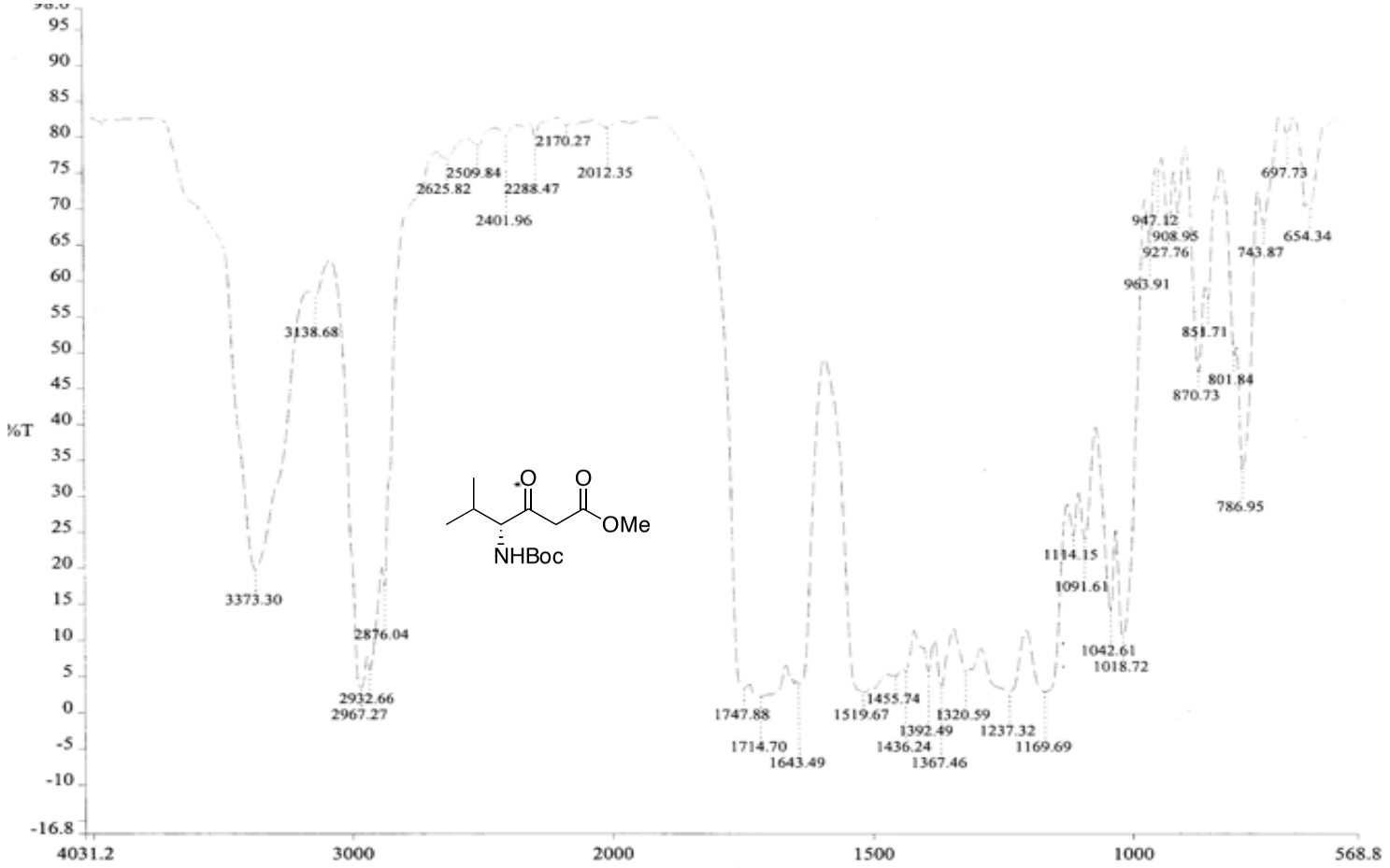

Figure 9: Infrared spectra (neat) of **14**

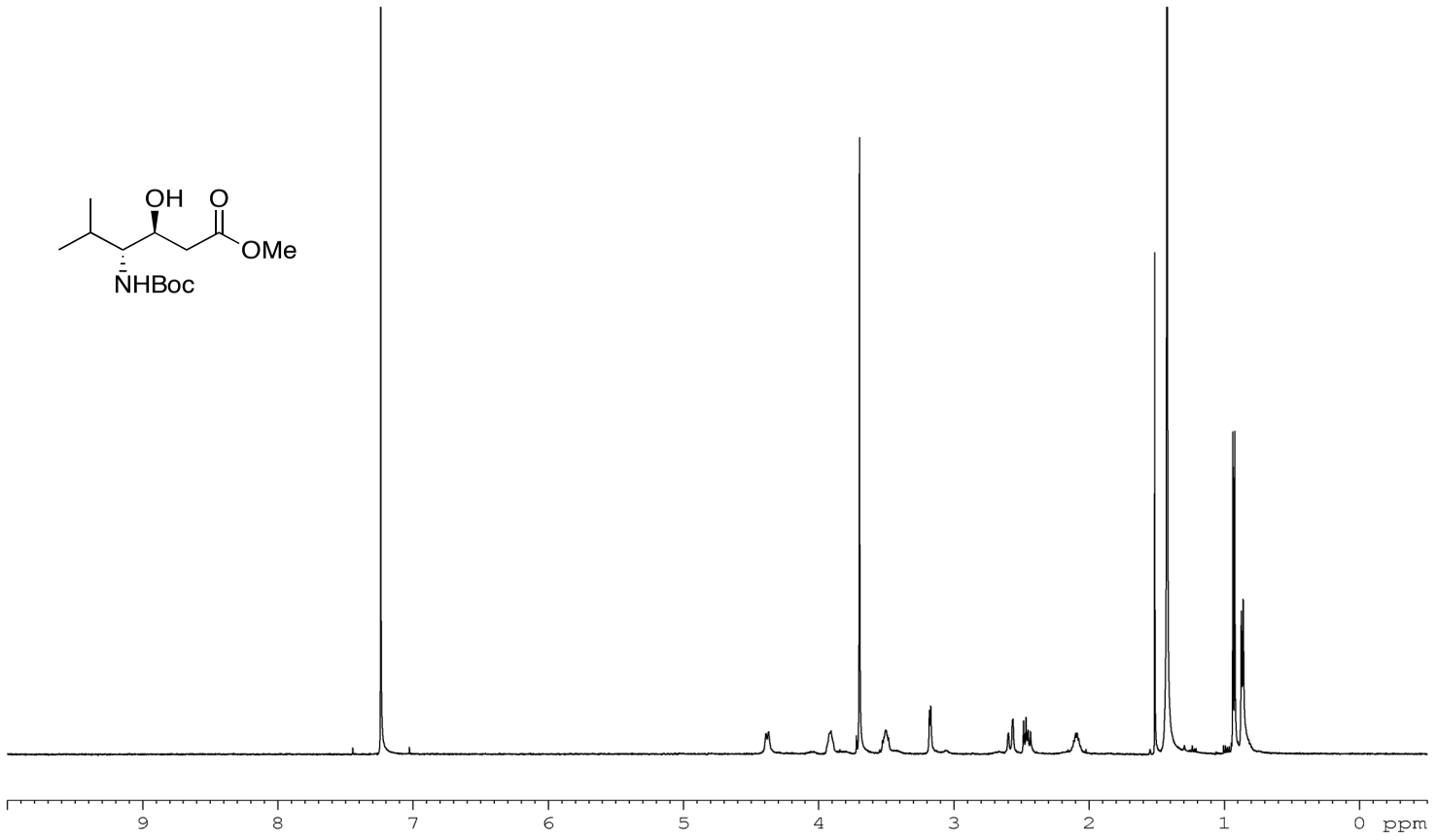

Figure 10: ^{1}H NMR ($CDCl_3$, 500 MHz) of **15**

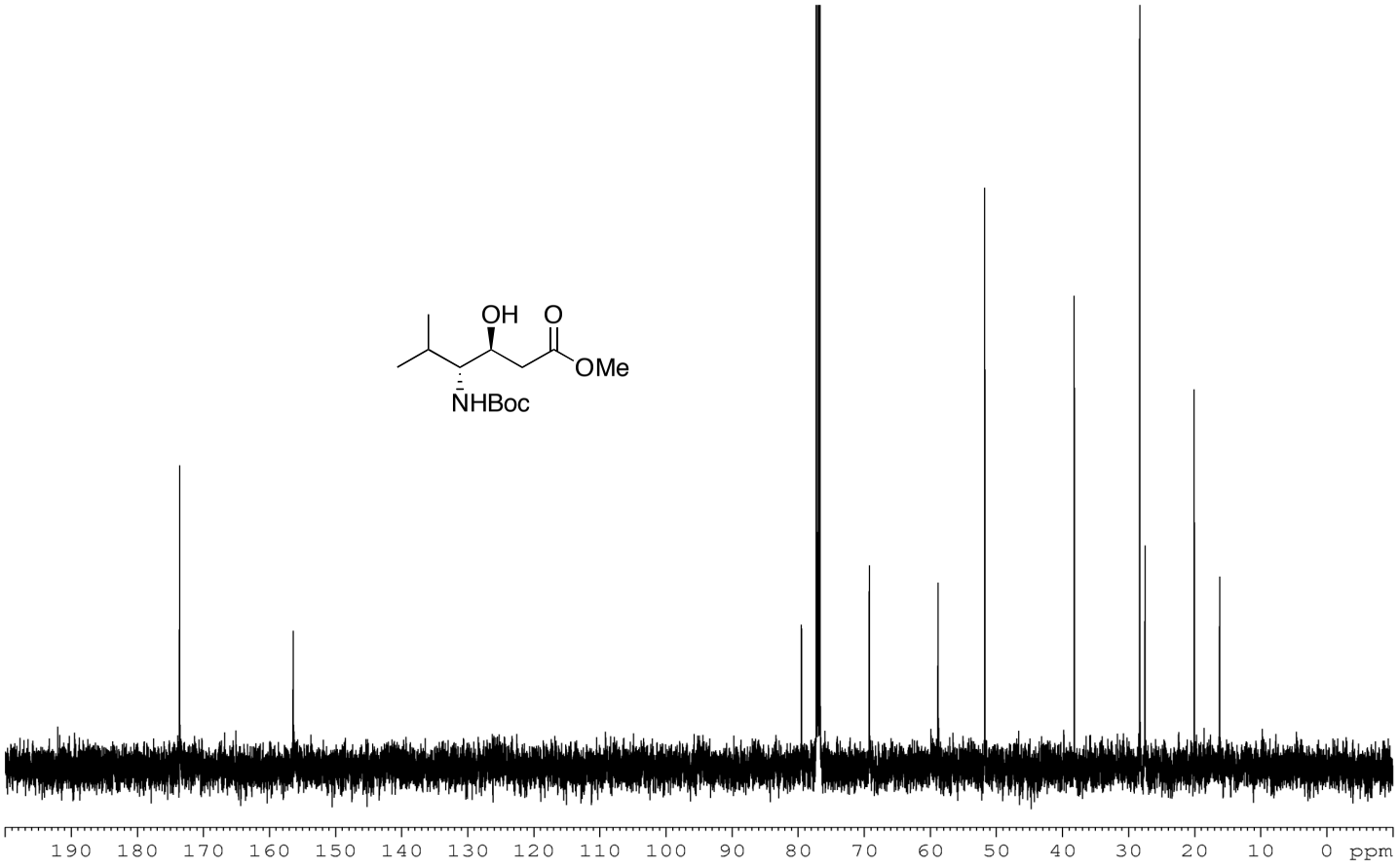

Figure 11: ^{13}C NMR ($CDCl_3$, 125 MHz) of **15**

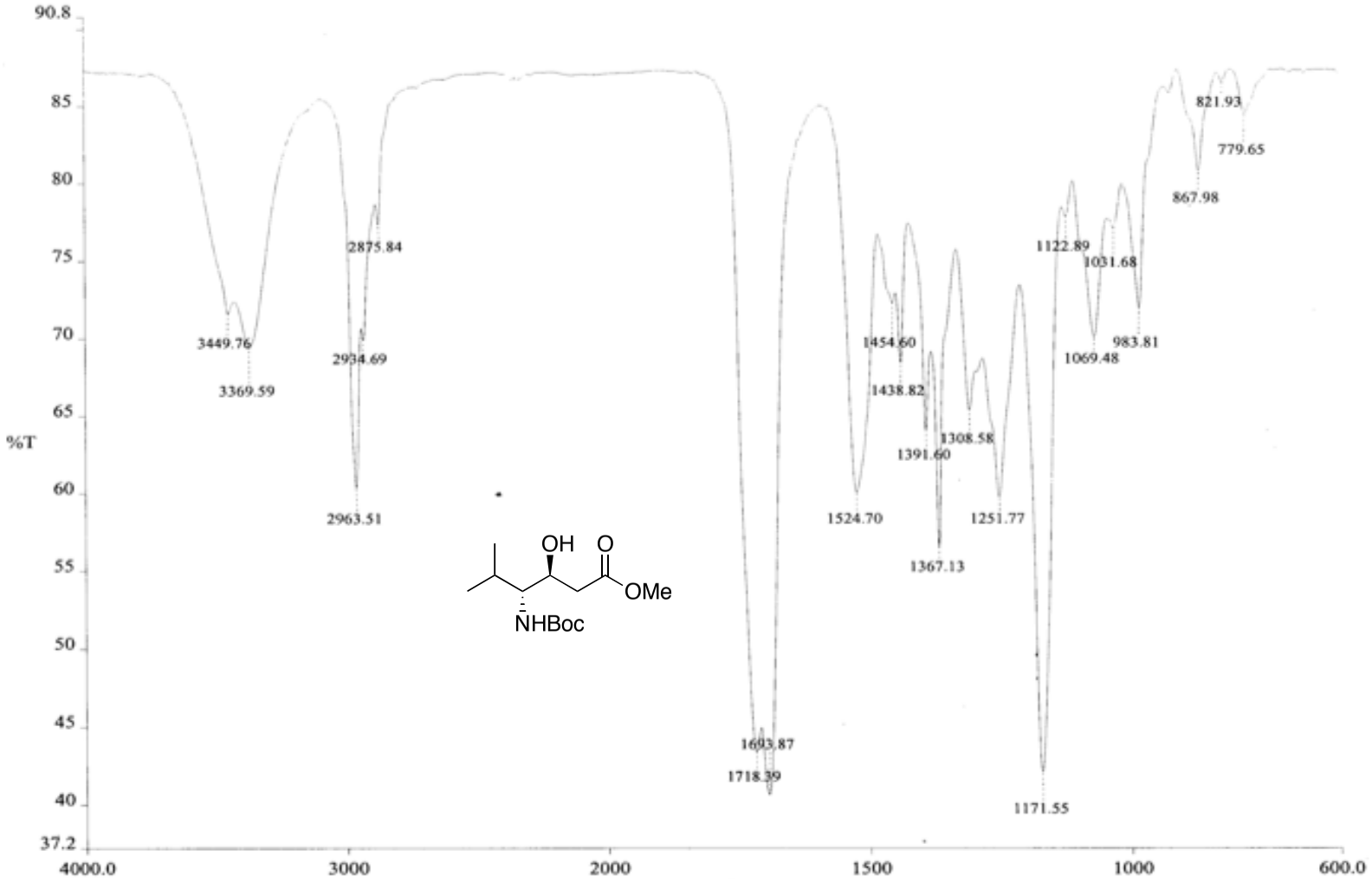

Figure 12: Infrared spectra (neat) of **15**

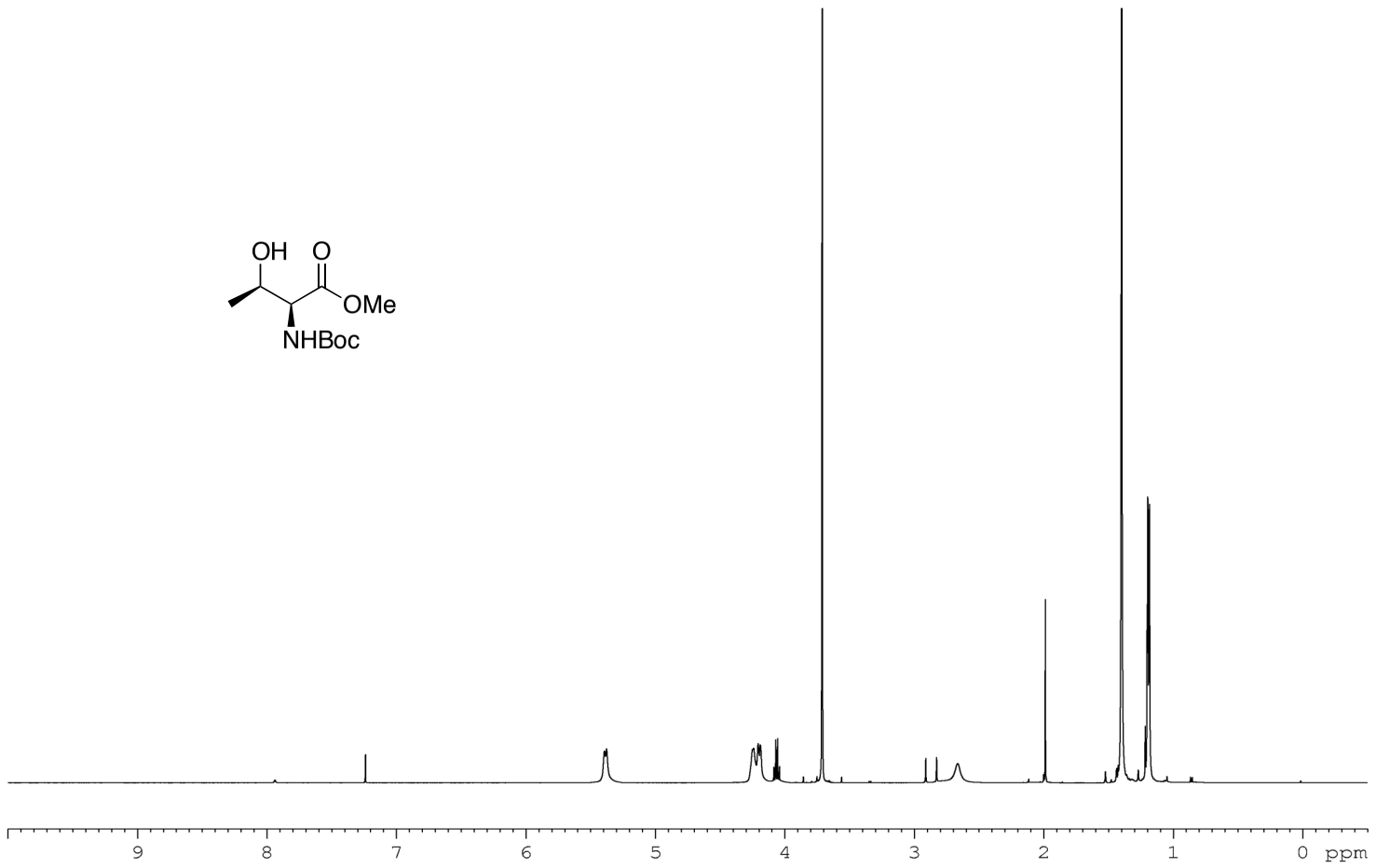

Figure 13: ^{1}H NMR ($CDCl_3$, 500 MHz) of **23**

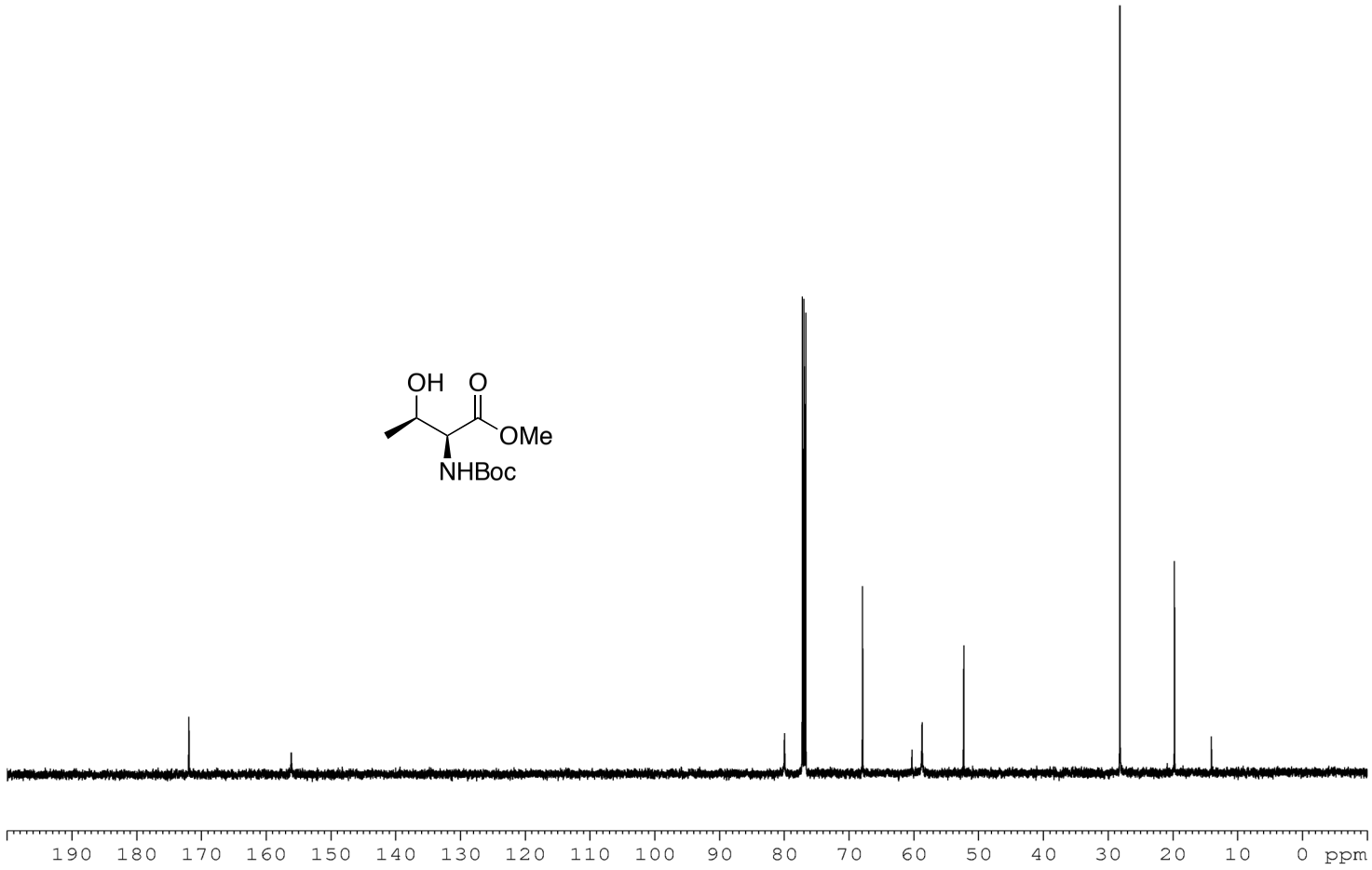

Figure 14: ^{13}C NMR ($CDCl_3$, 125 MHz) of **23**

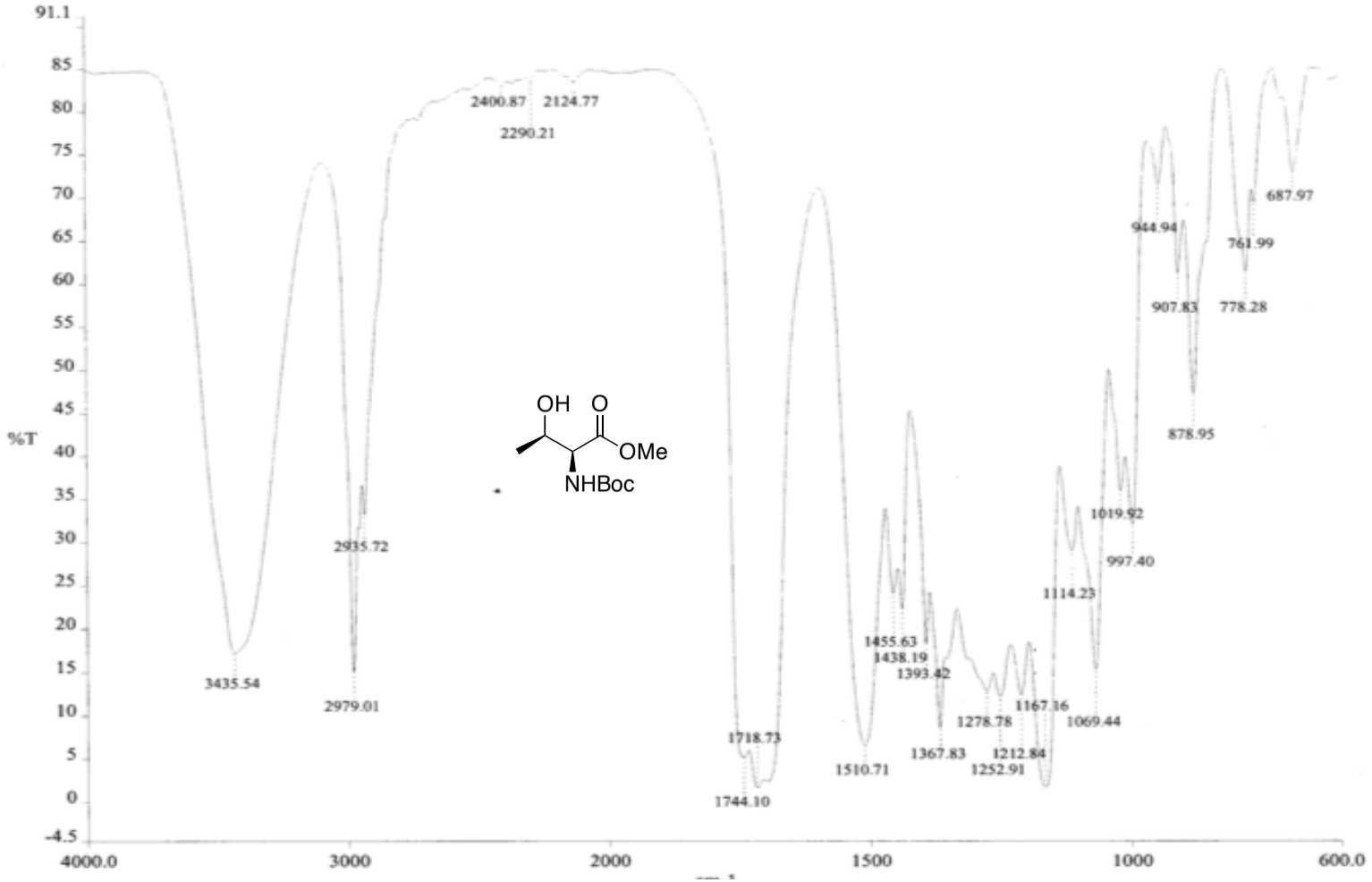

Figure 15: Infrared spectra (neat) of **23**

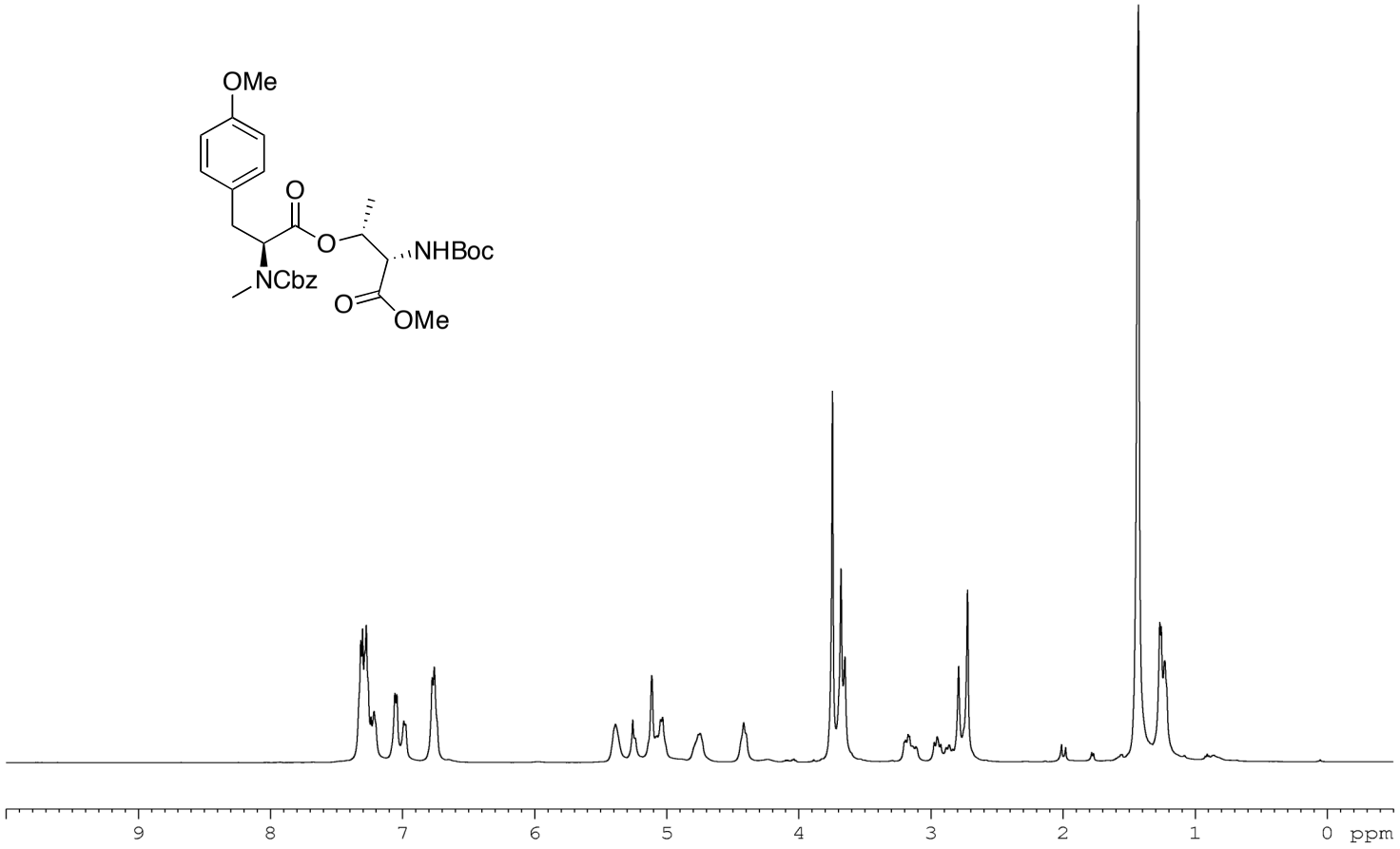

Figure 16: ^{1}H NMR ($CDCl_3$, 500 MHz) of **24**

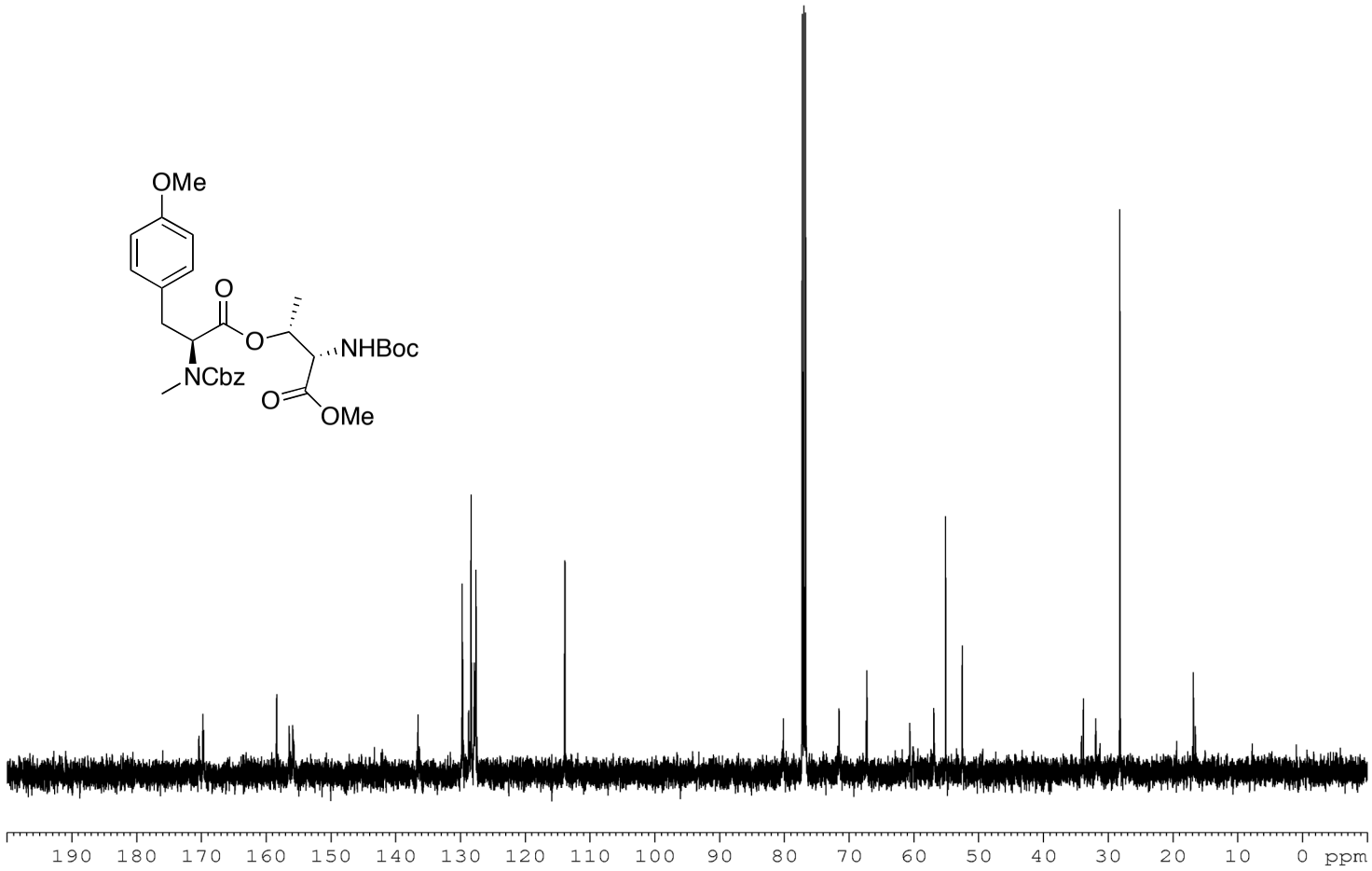

Figure 17: ^{13}C NMR ($CDCl_3$, 125 MHz) of **24**

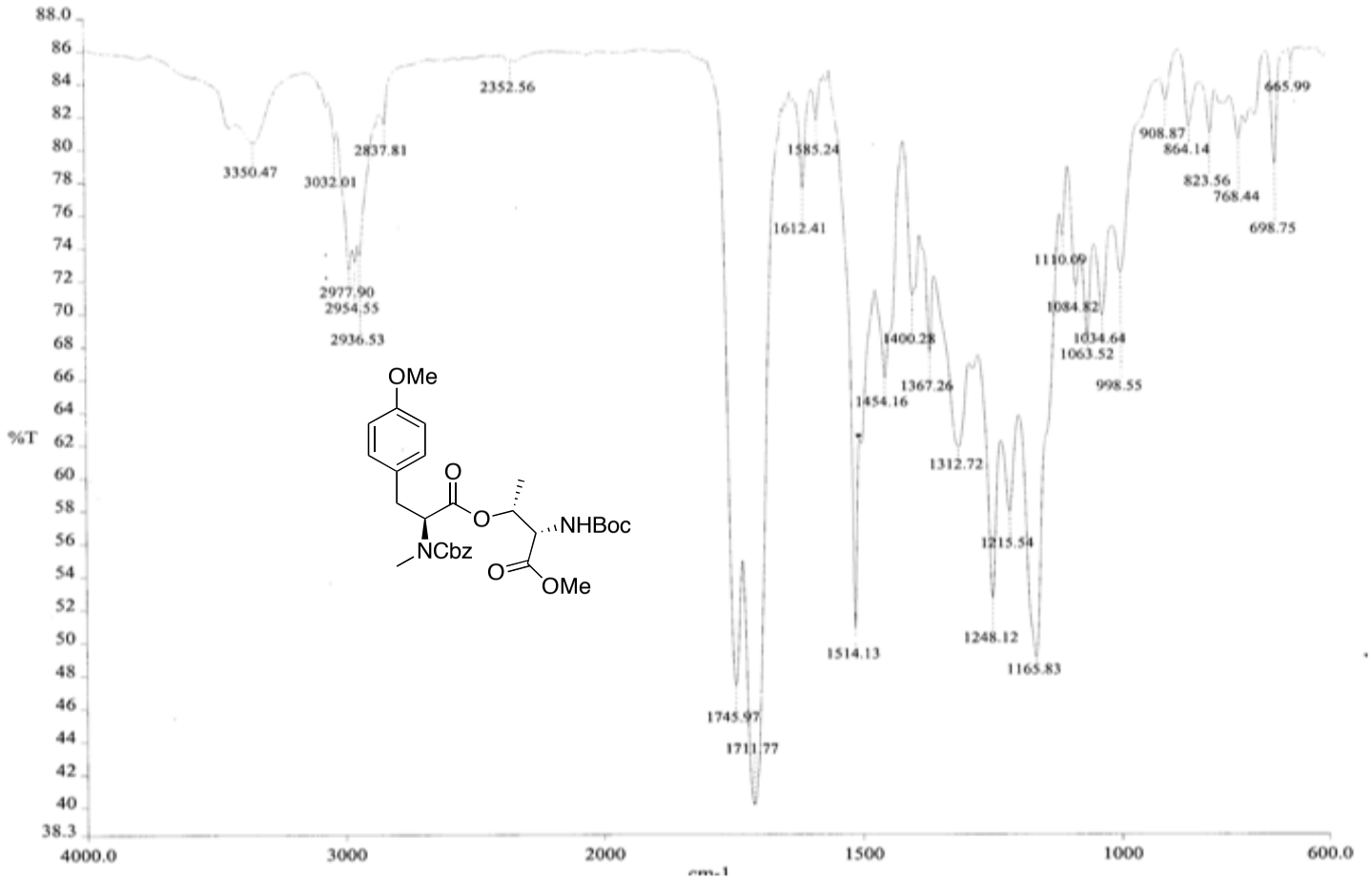

Figure 18: Infrared spectra (neat) of **24**

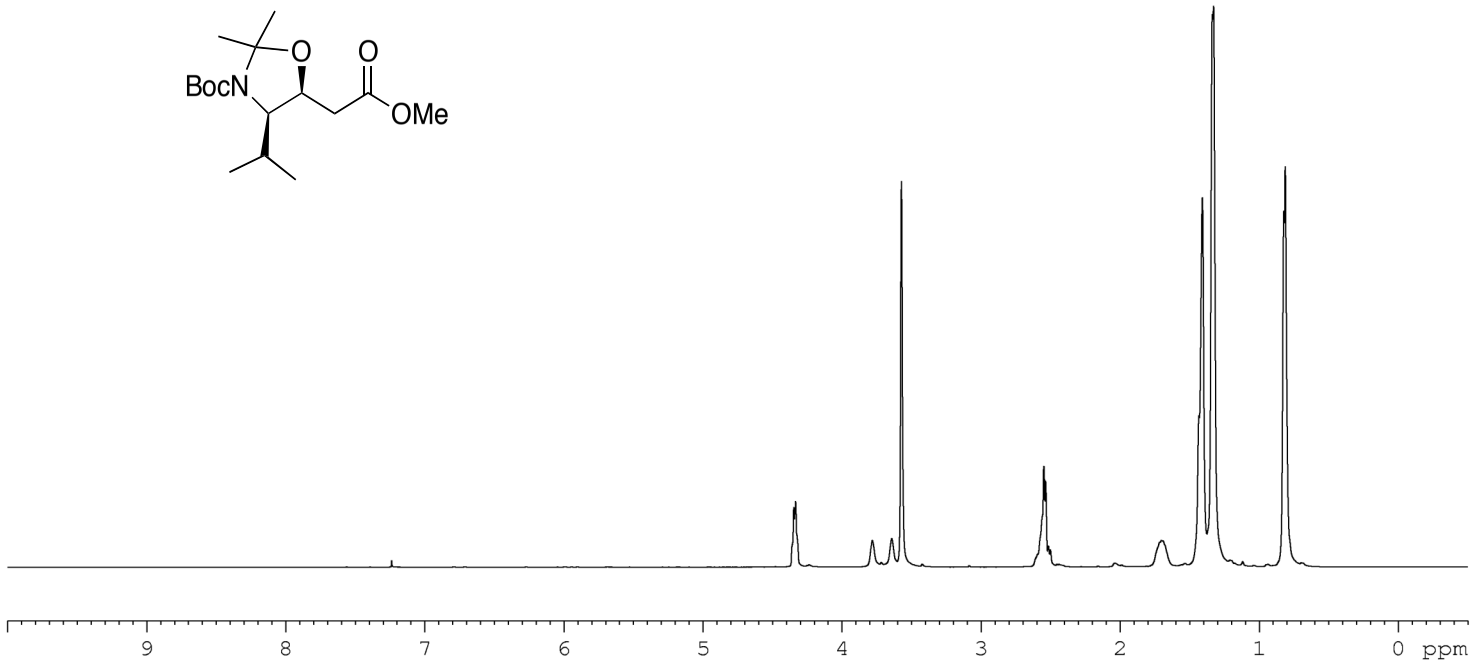

Figure 19: ^{1}H NMR ($CDCl_3$, 500 MHz) of **27**

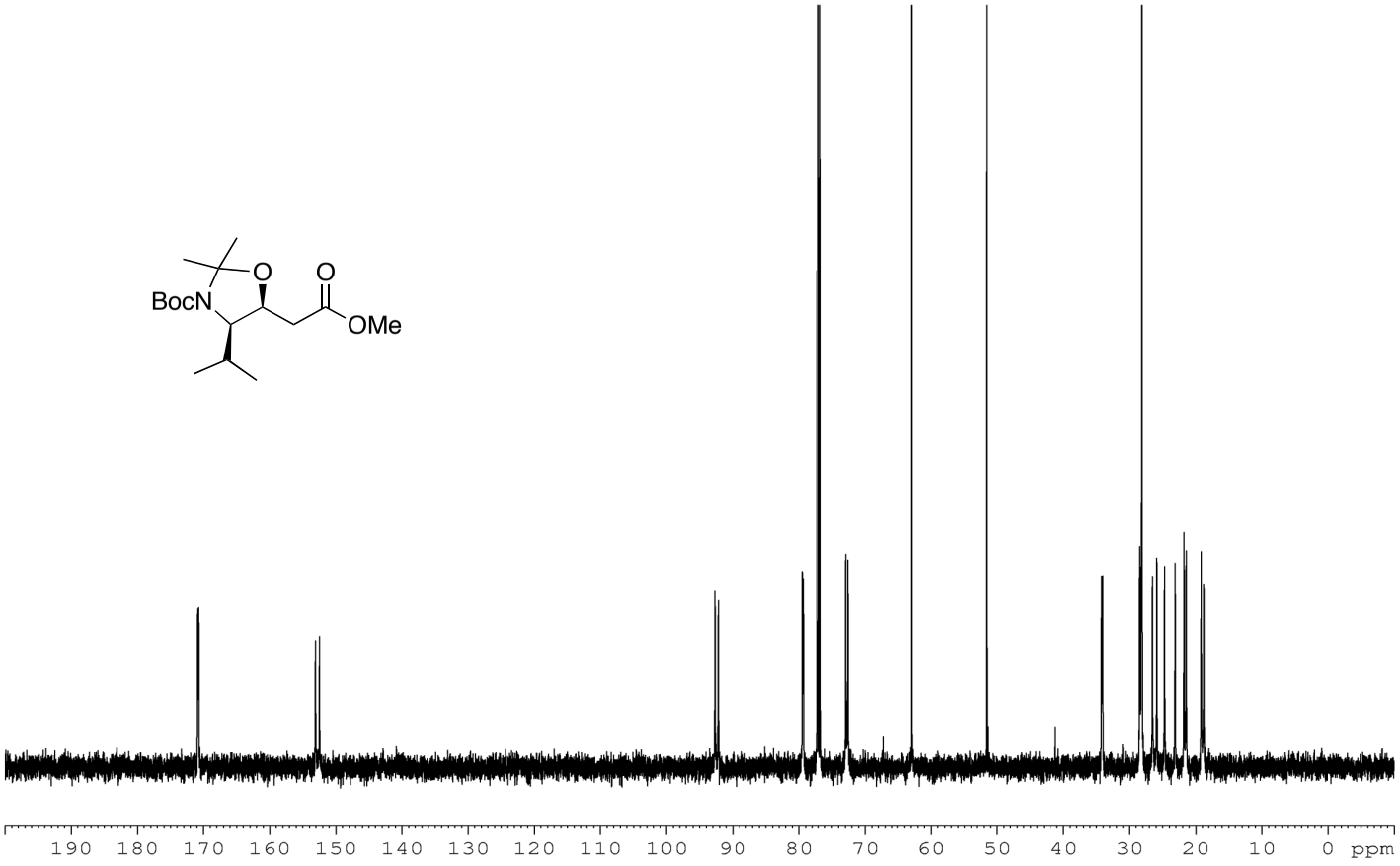

Figure 20: ^{13}C NMR ($CDCl_3$, 125 MHz) of **27**

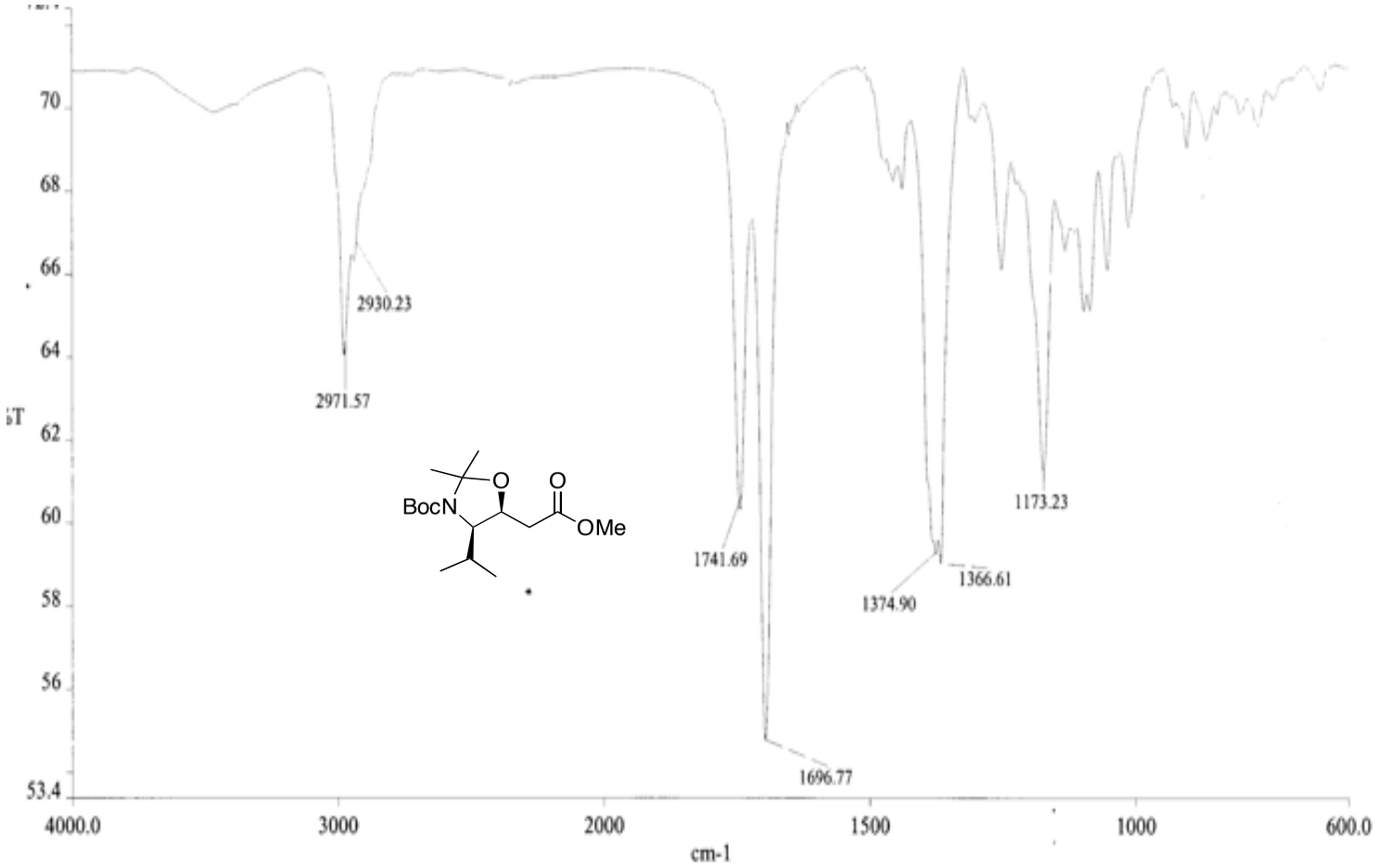

Figure 21: Infrared spectra (neat) of **27**

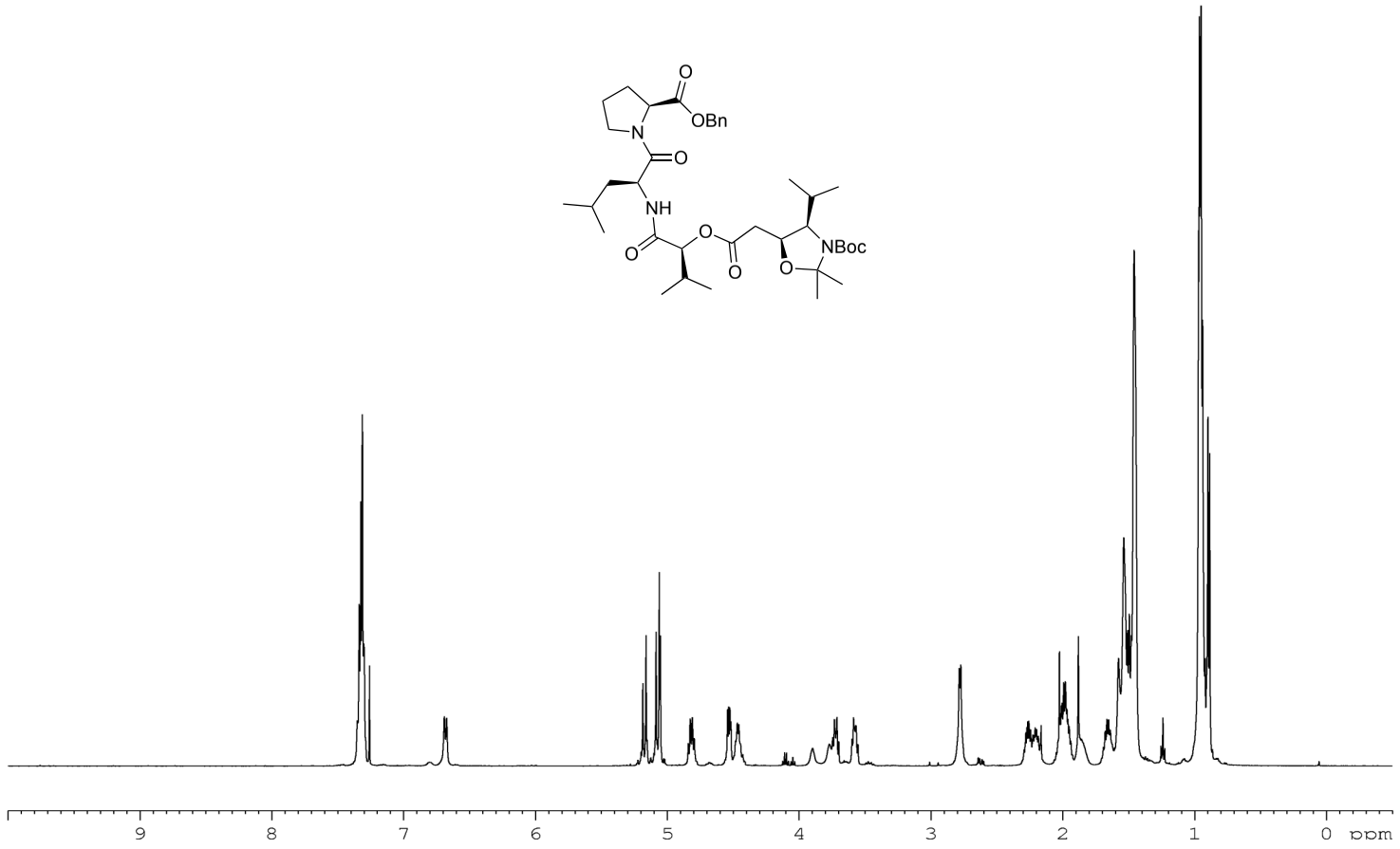

Figure 22: ^{1}H NMR ($CDCl_3$, 500 MHz) of **29**

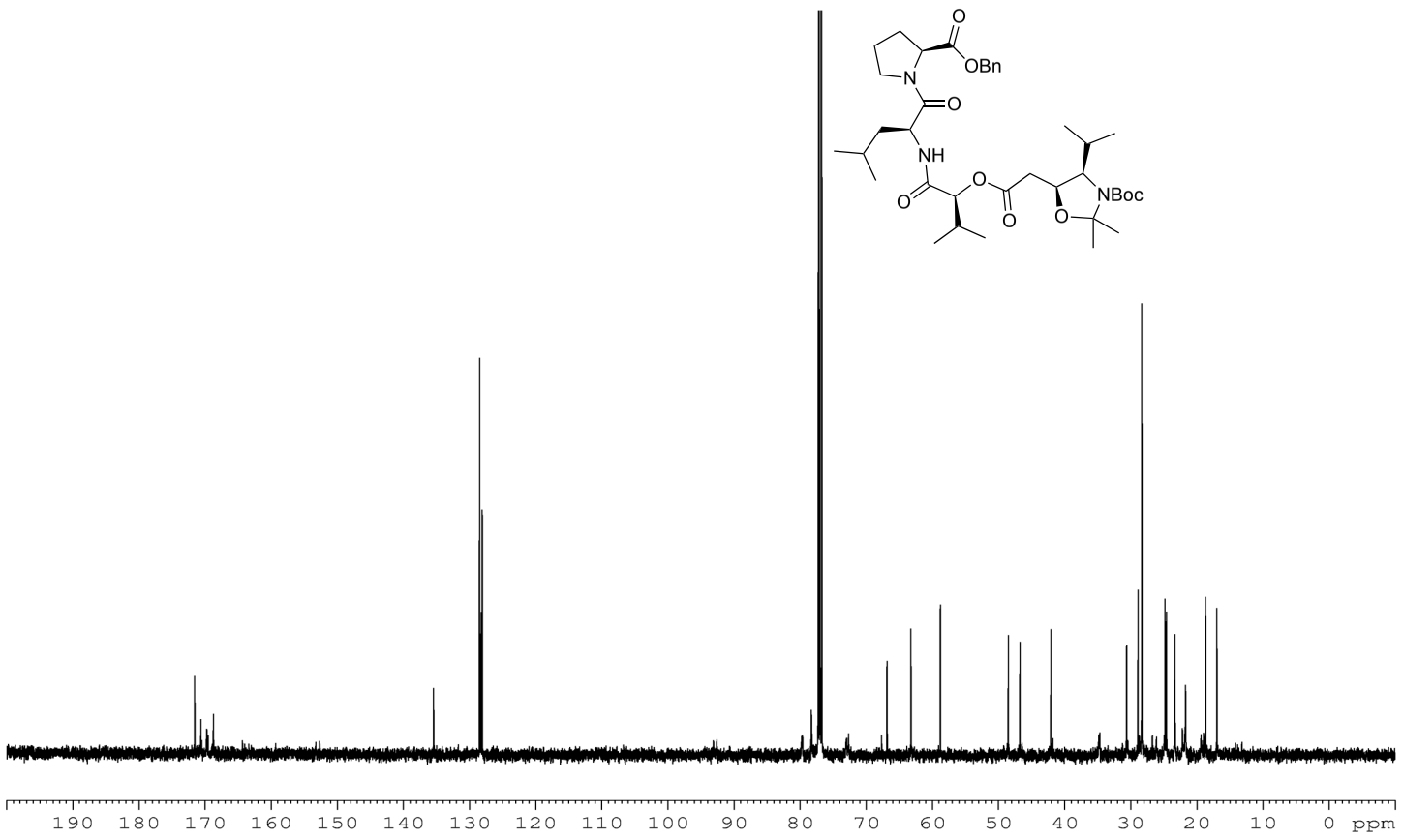

Figure 23: ^{13}C NMR ($CDCl_3$, 125 MHz) of **29**

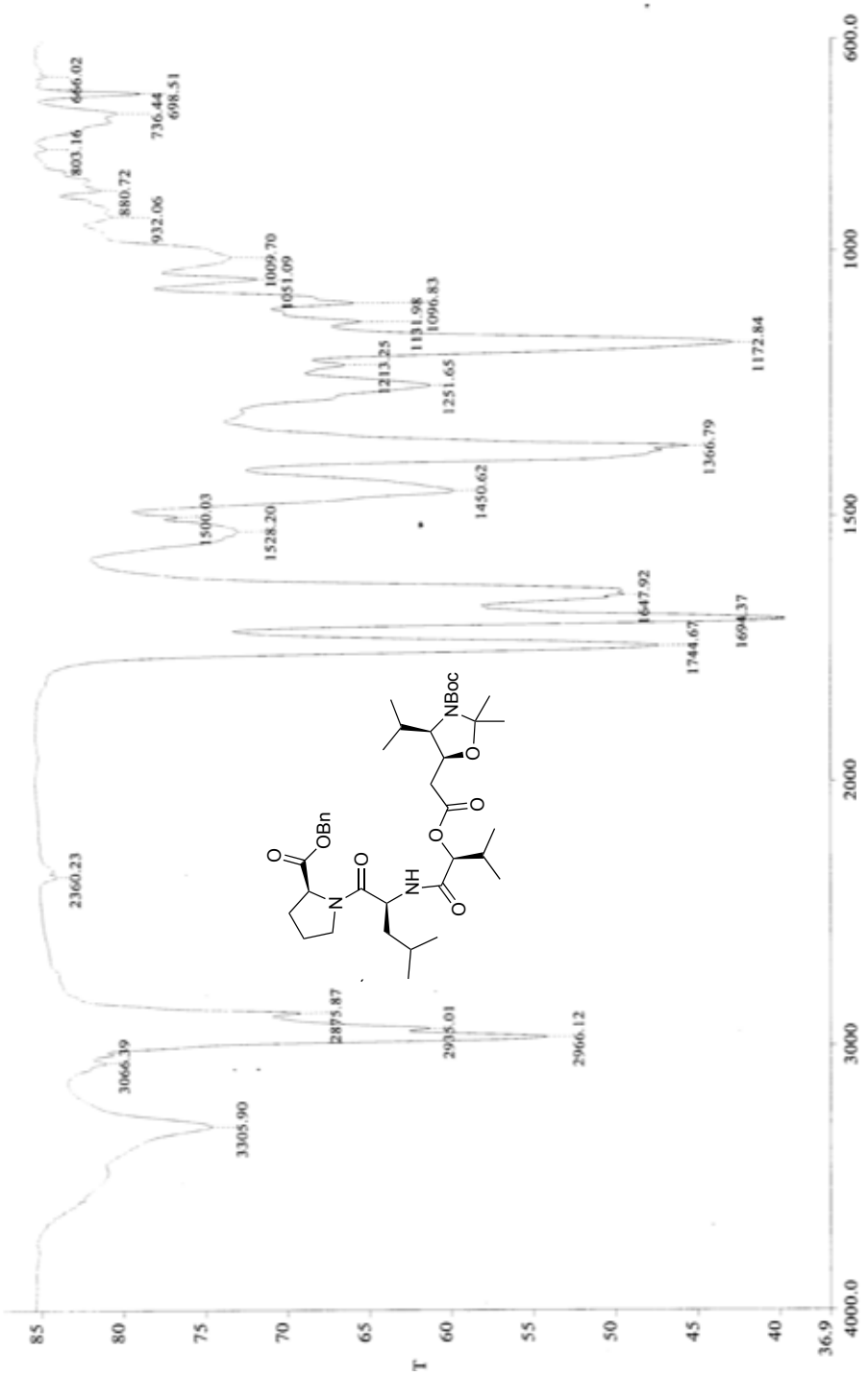

Figure 24: Infrared spectra (neat) of **29**

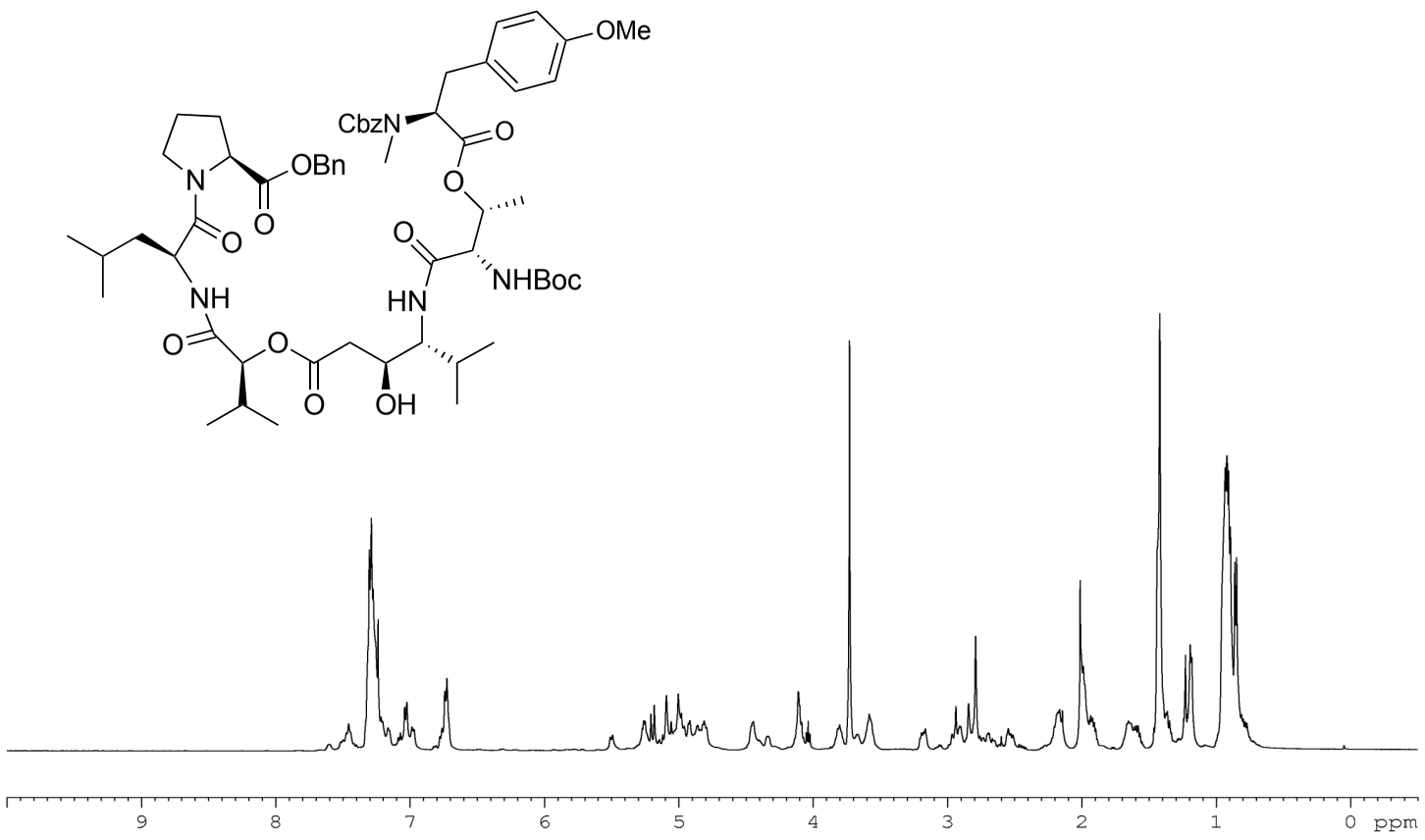

Figure 25: ^{1}H NMR ($CDCl_3$, 500 MHz) of **5**

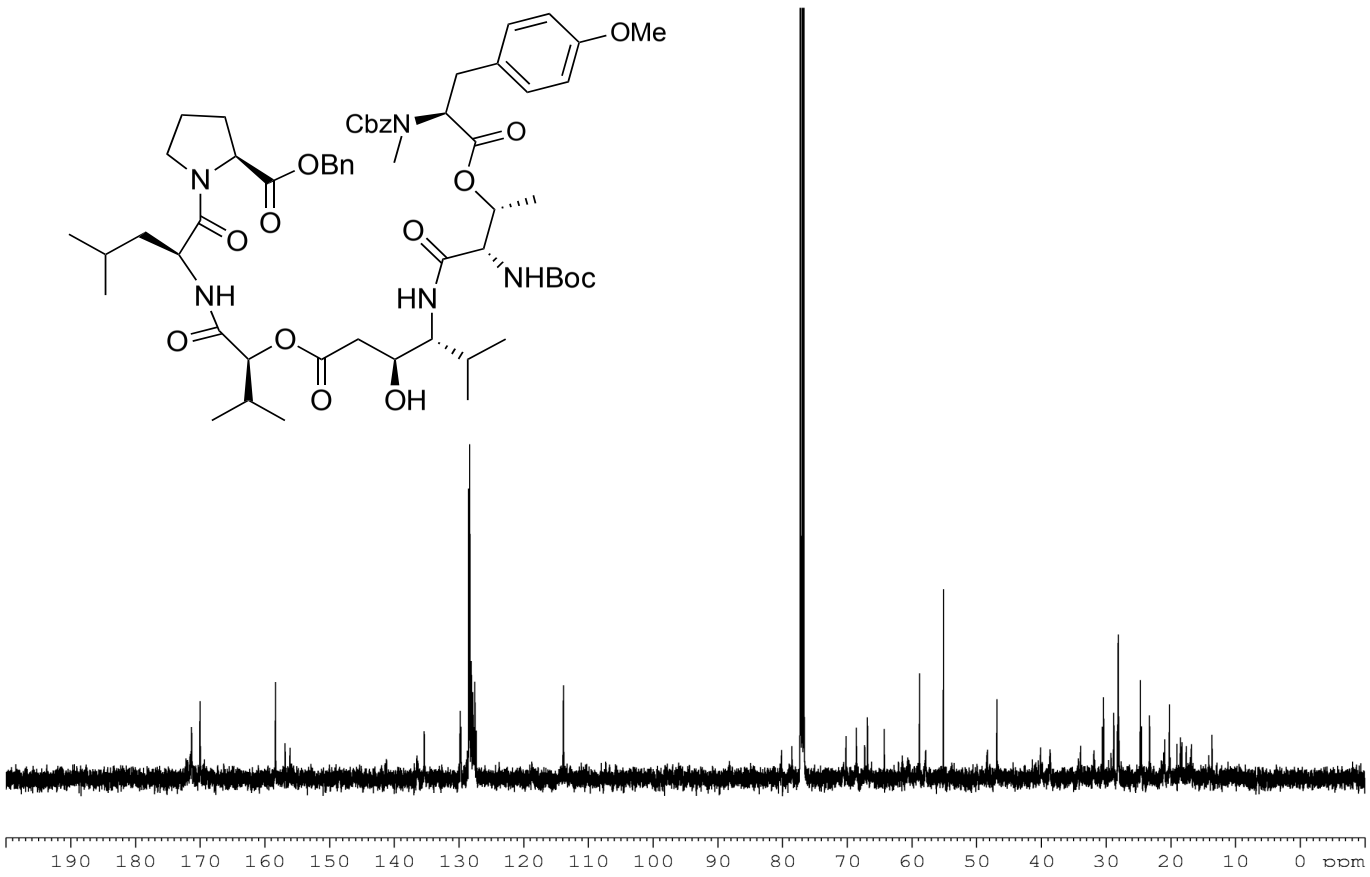

Figure 26: ^{13}C NMR ($CDCl_3$, 125 MHz) of **5**

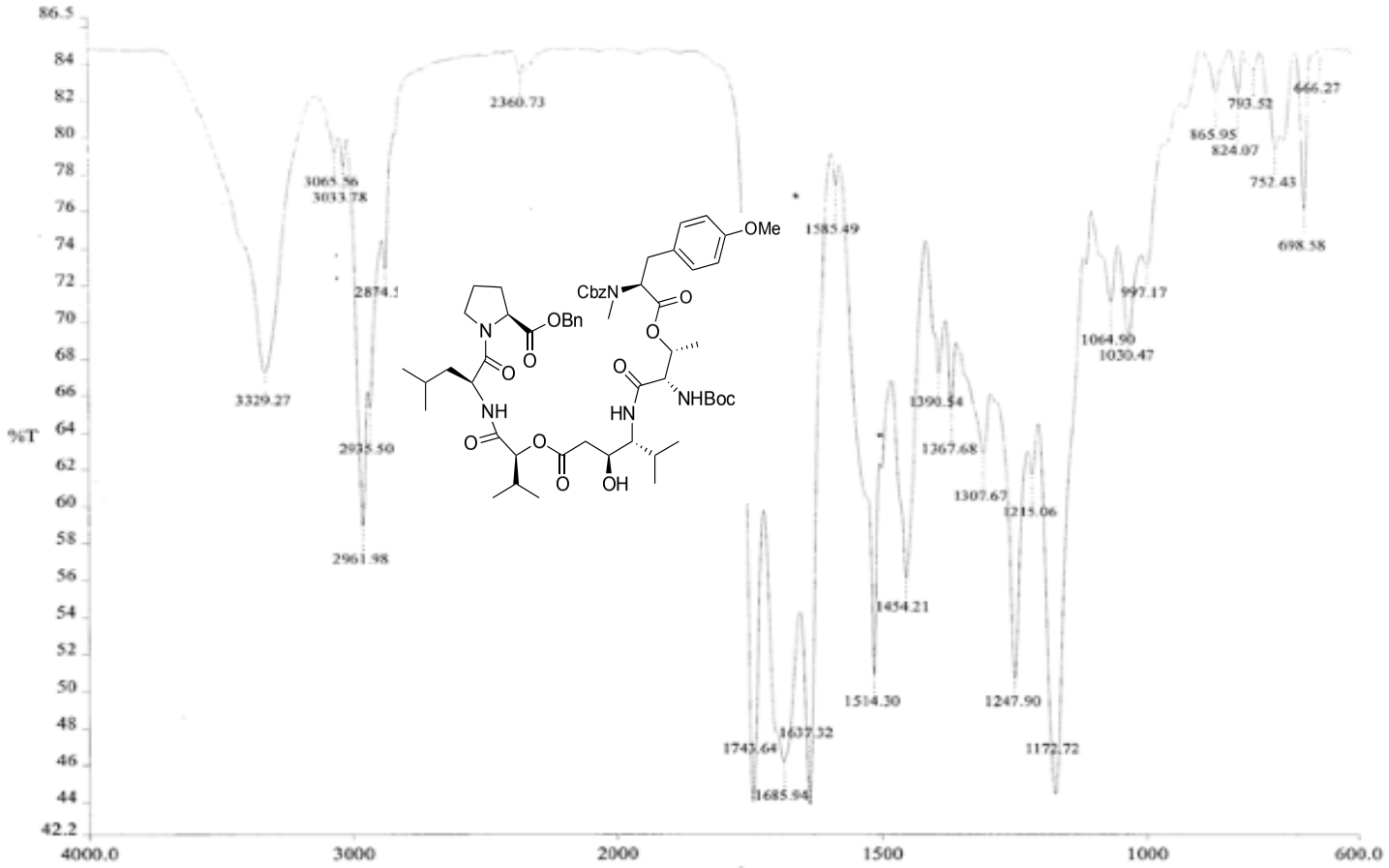

Figure 27: Infrared spectra (neat) of **5**

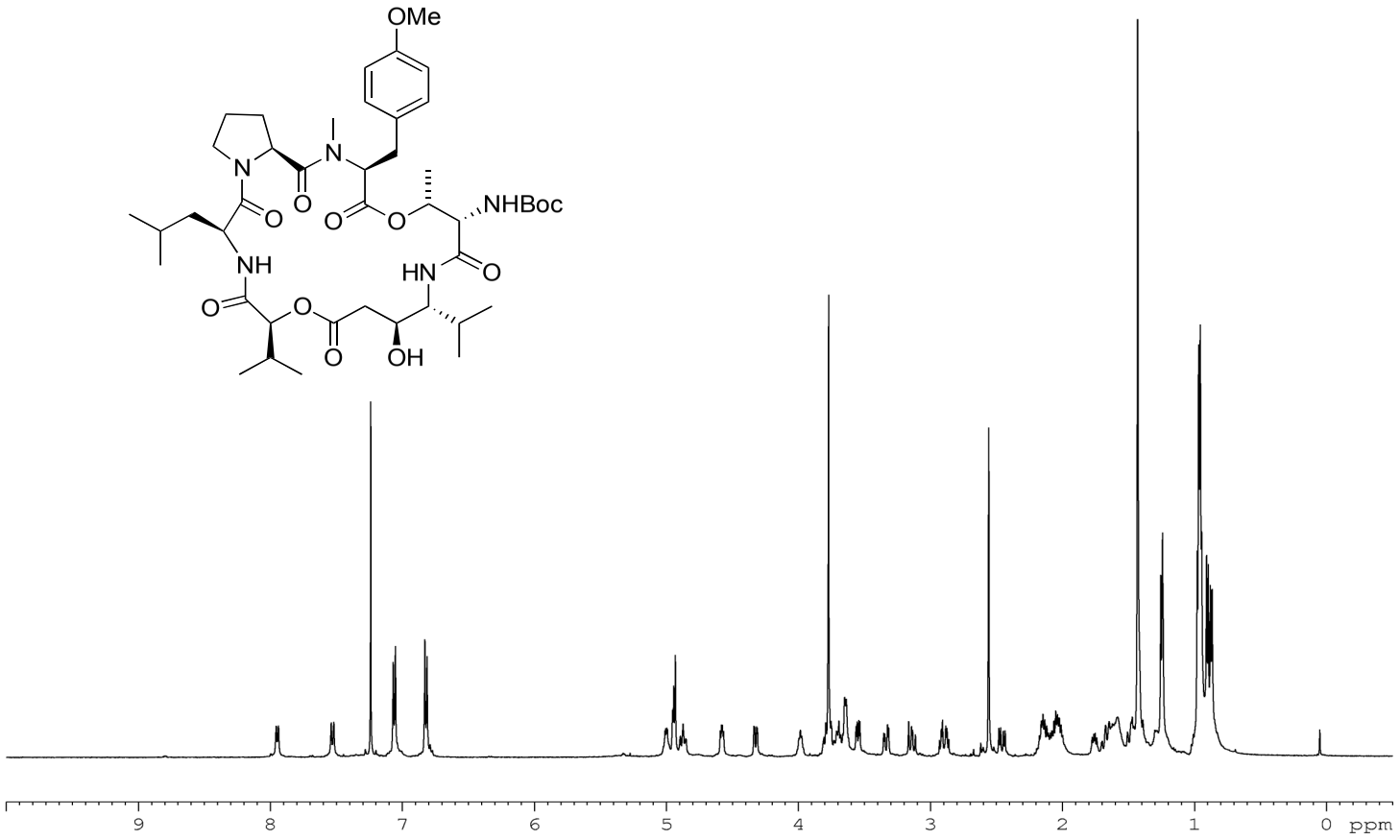

Figure 28: ^{1}H NMR ($CDCl_3$, 500 MHz) of **1**

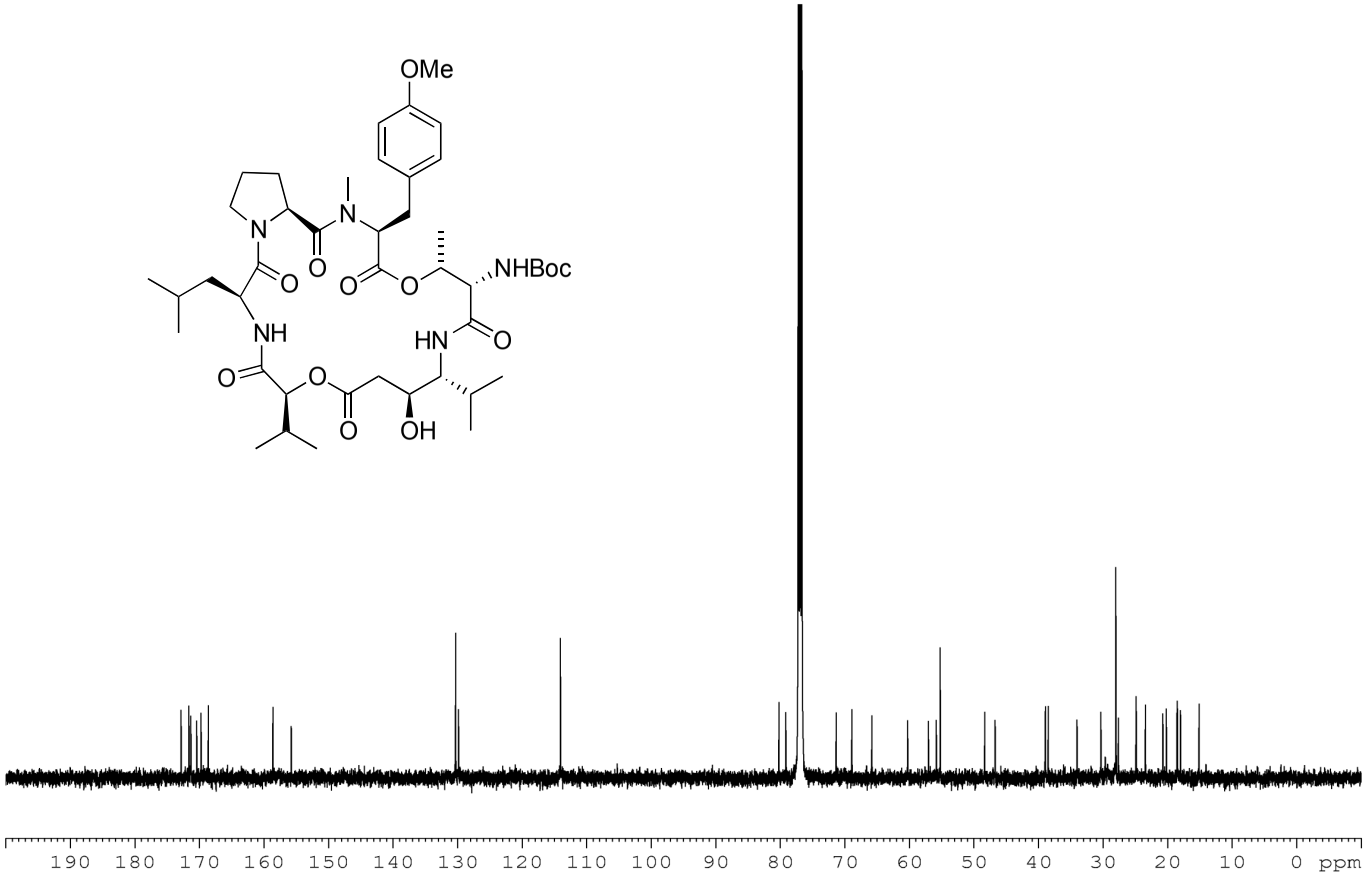

Figure 29: ^{13}C NMR ($CDCl_3$, 125 MHz) of **1**

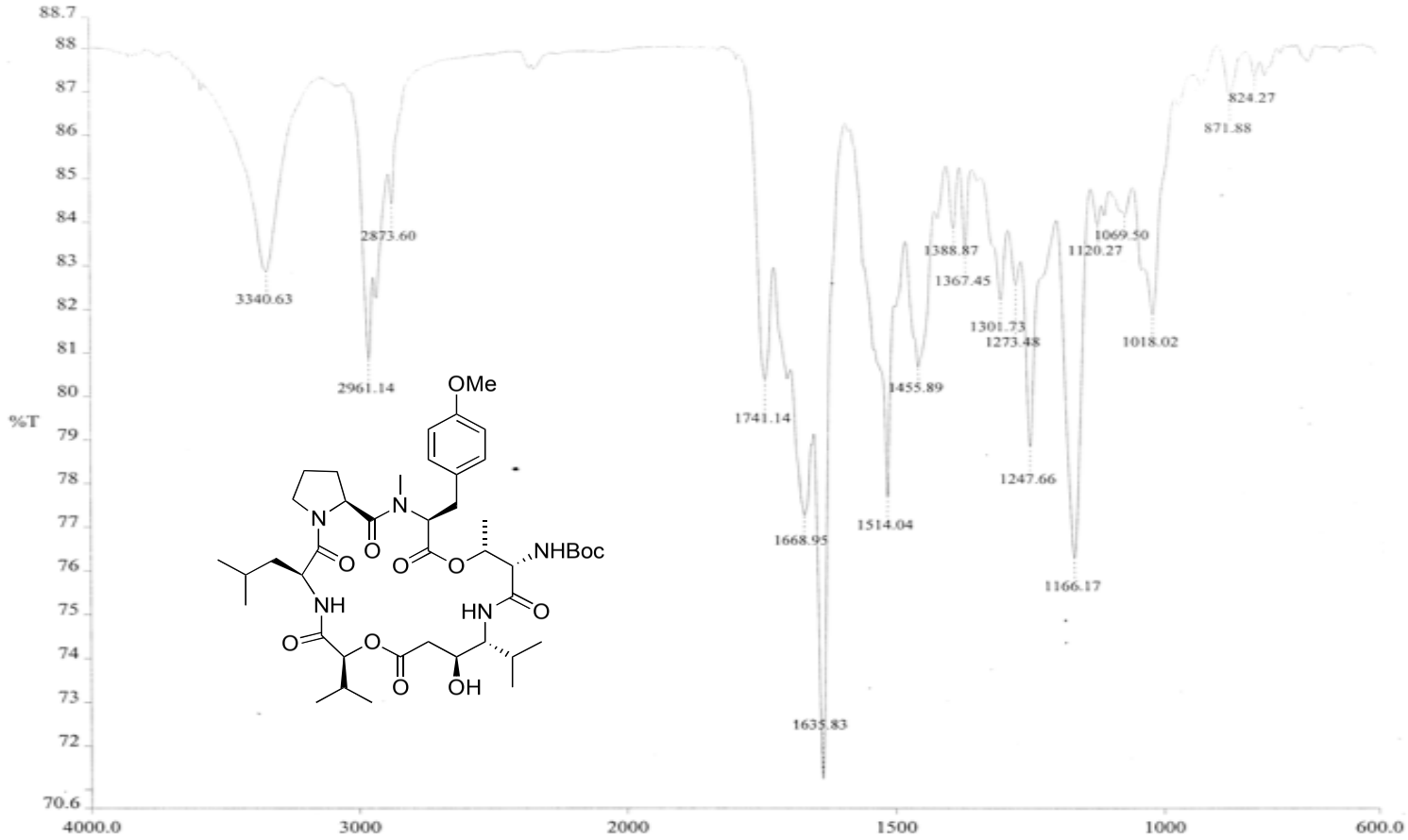

Figure 30: Infrared spectra (neat) of **1**

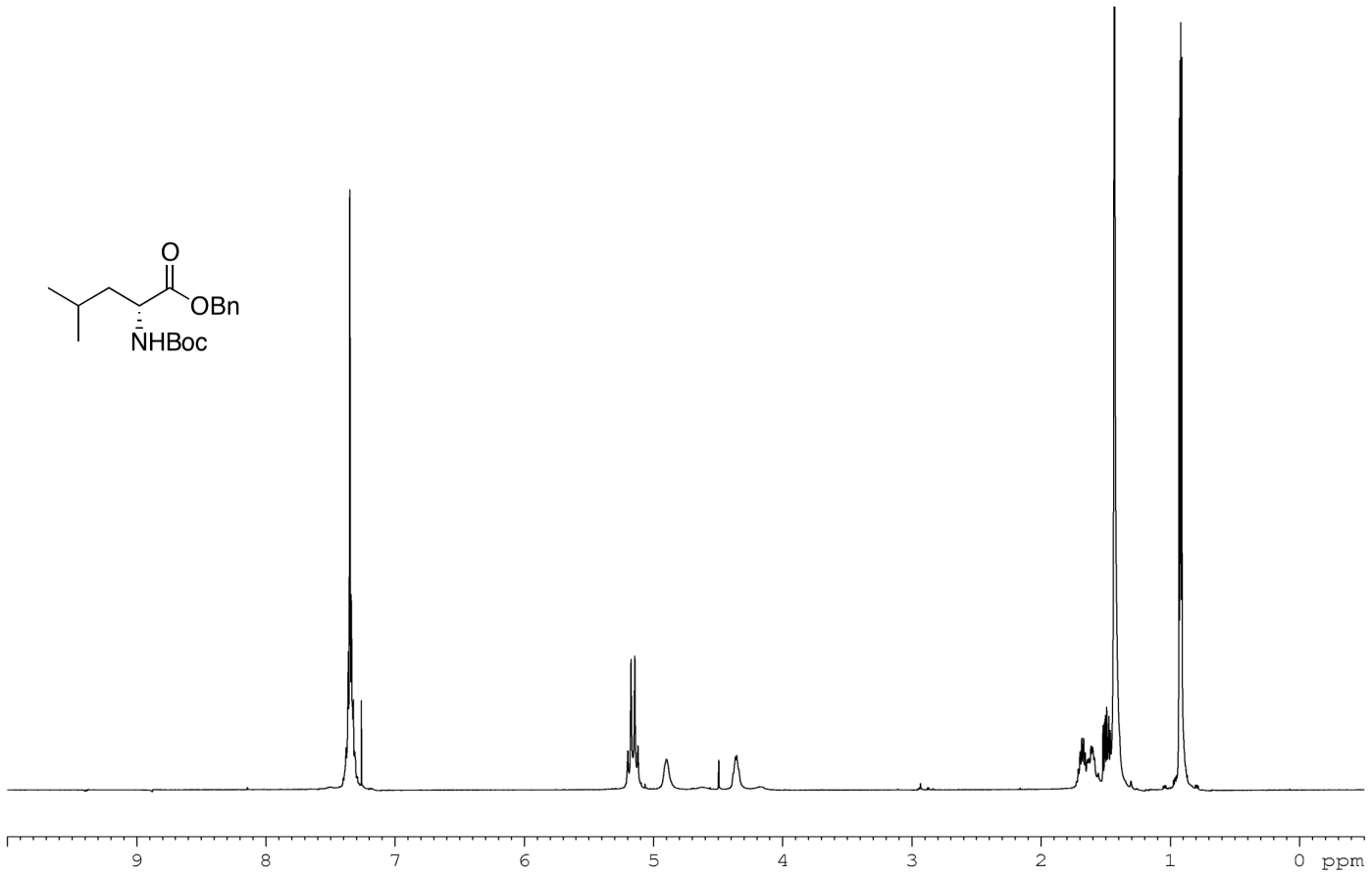

Figure 31: ^{1}H NMR ($CDCl_3$, 500 MHz) of **46**

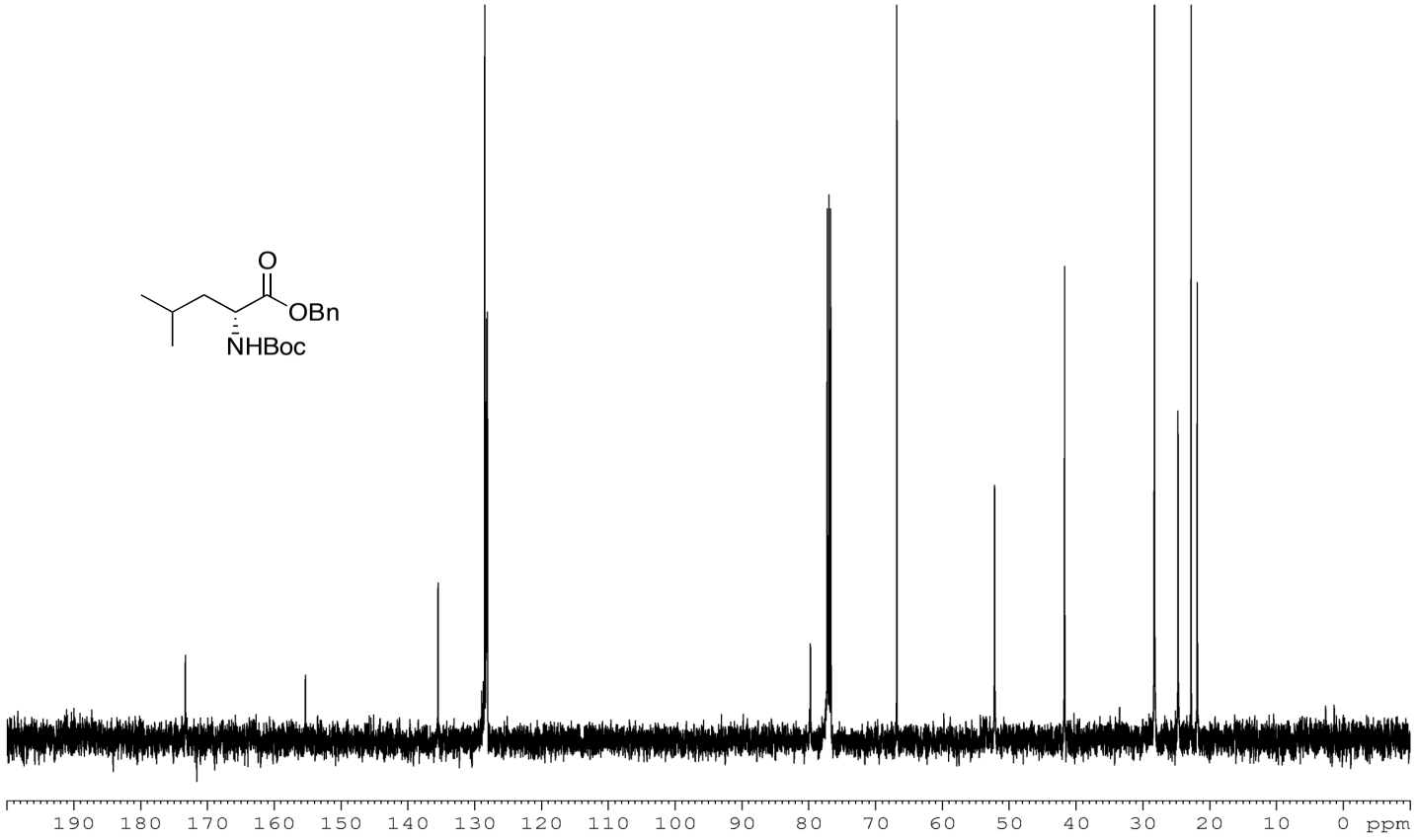

Figure 32: ^{13}C NMR ($CDCl_3$, 125 MHz) of **46**

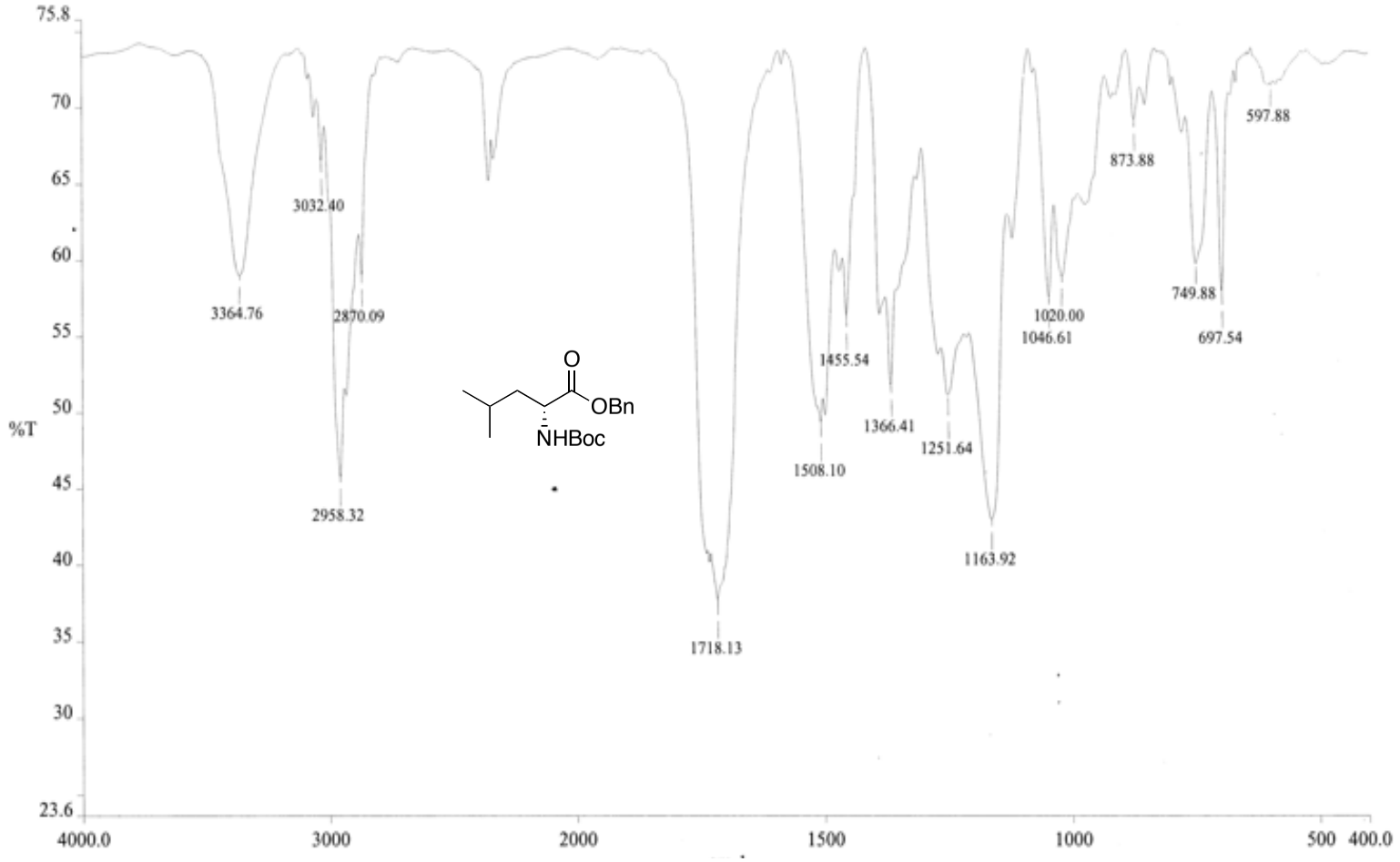

Figure 33: Infrared spectra (neat) of **46**

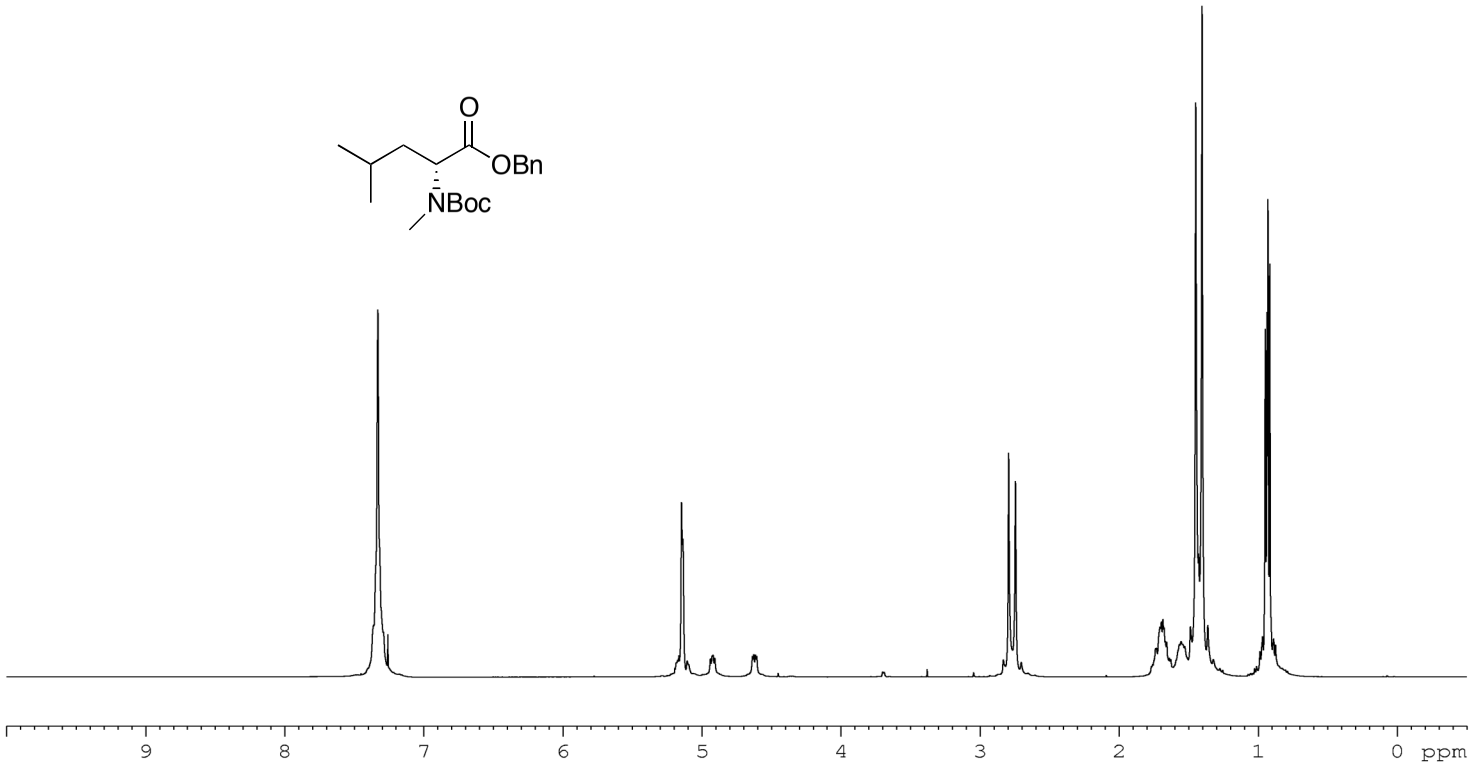

Figure 34: ^{1}H NMR ($CDCl_3$, 500 MHz) of **47**

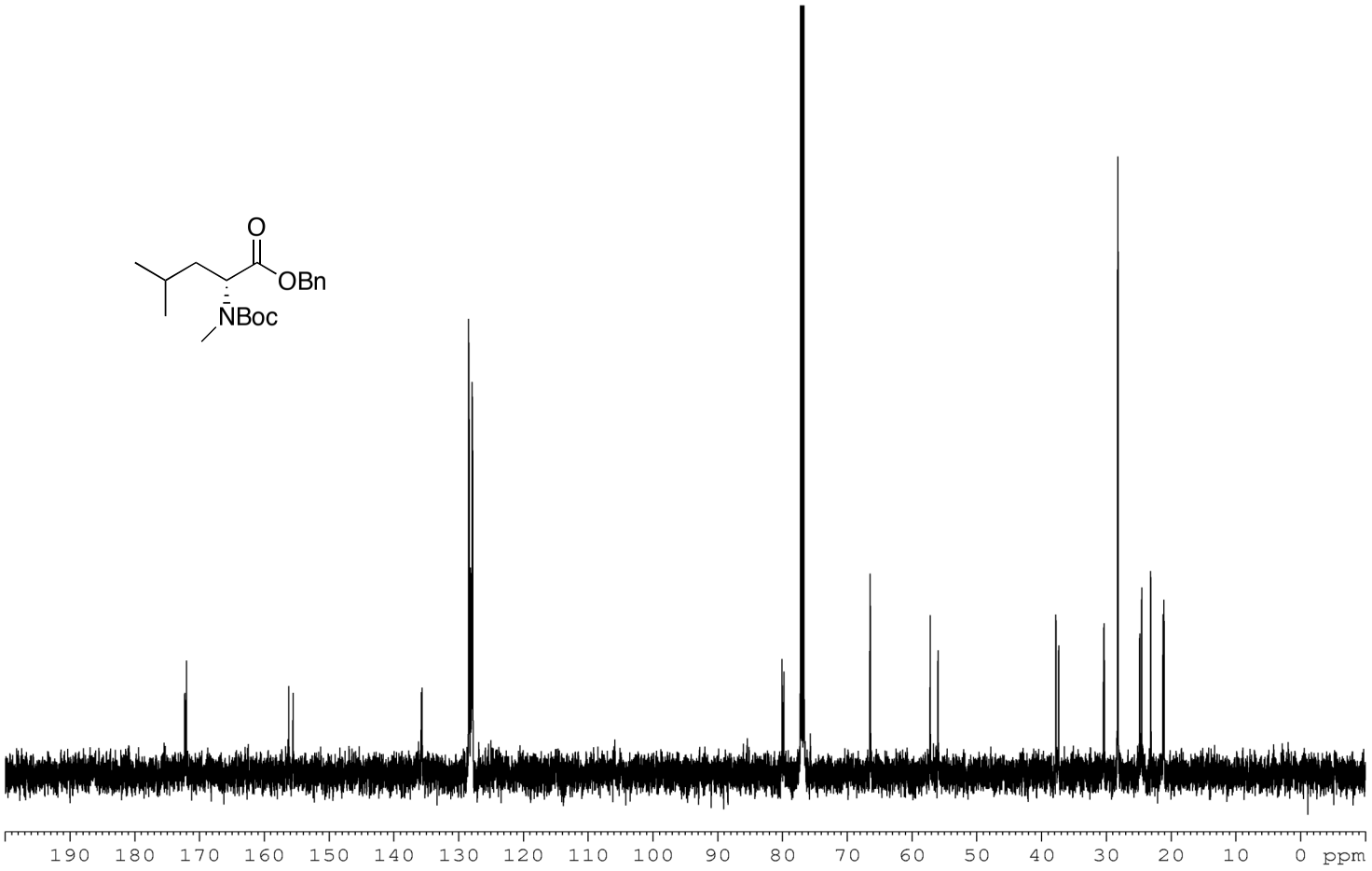

Figure 35: ^{13}C NMR ($CDCl_3$, 125 MHz) of **47**

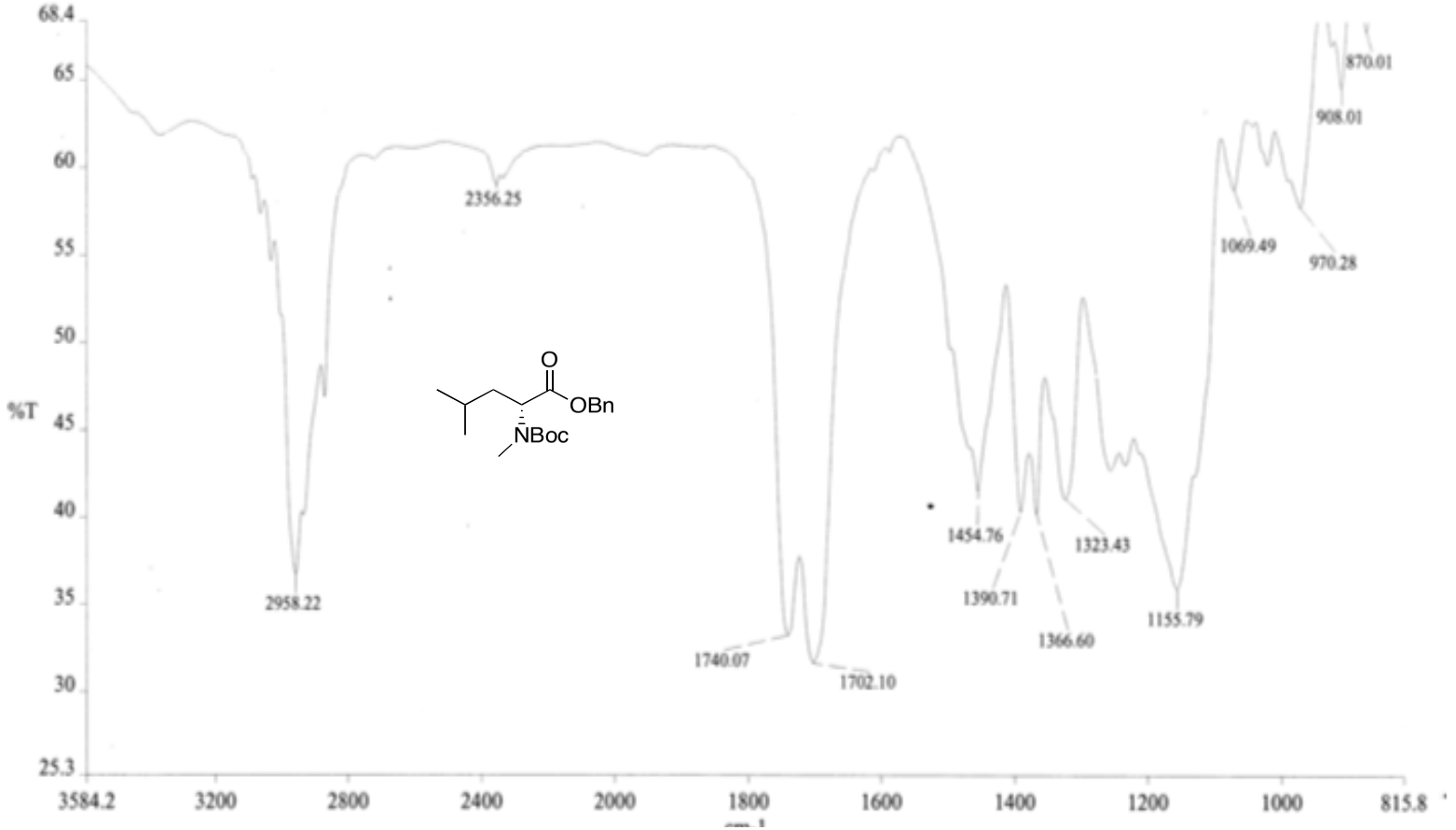

Figure 36: Infrared spectra (neat) of **47**

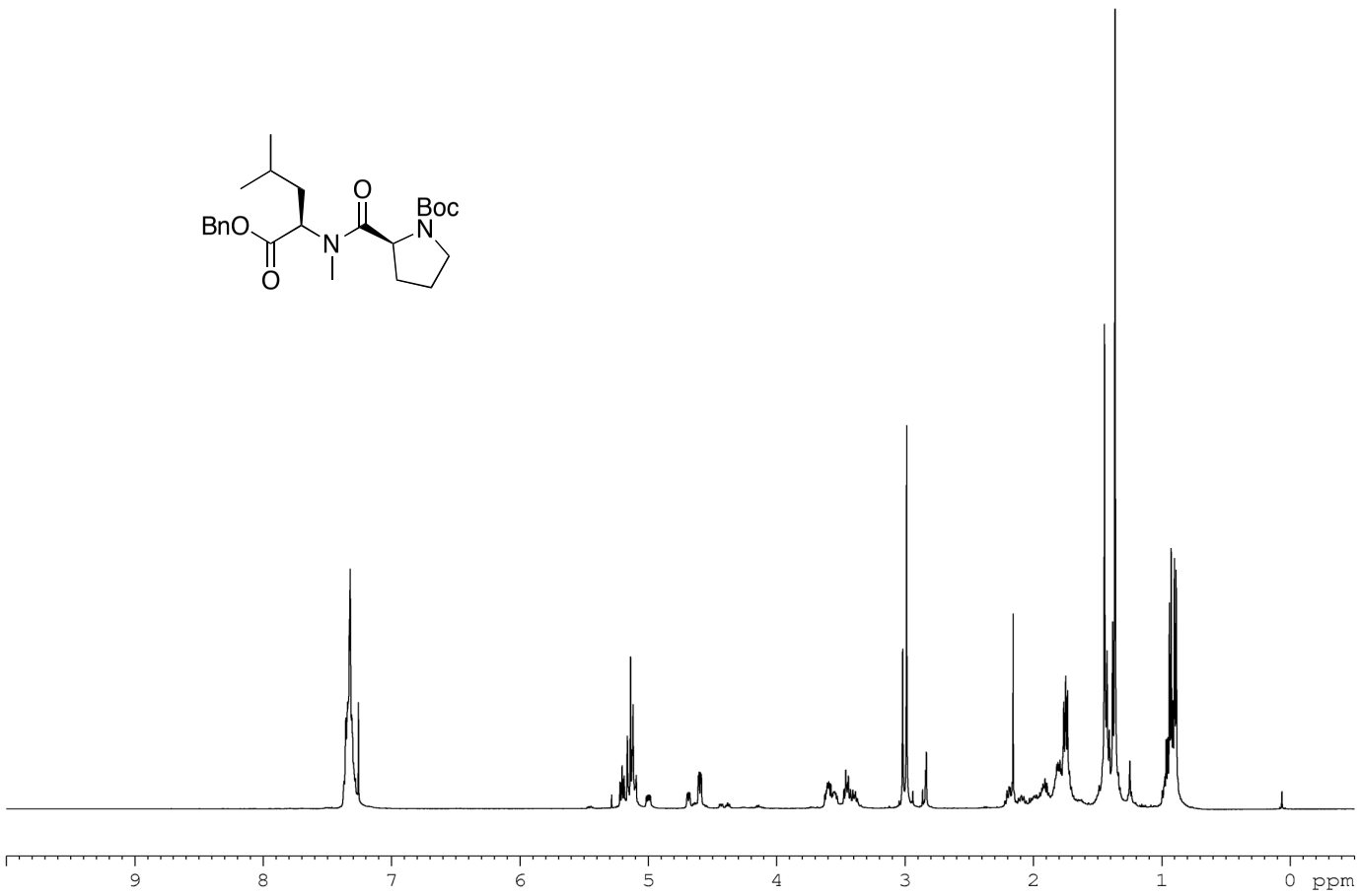

Figure 37: ^{1}H NMR ($CDCl_3$, 500 MHz) of **35**

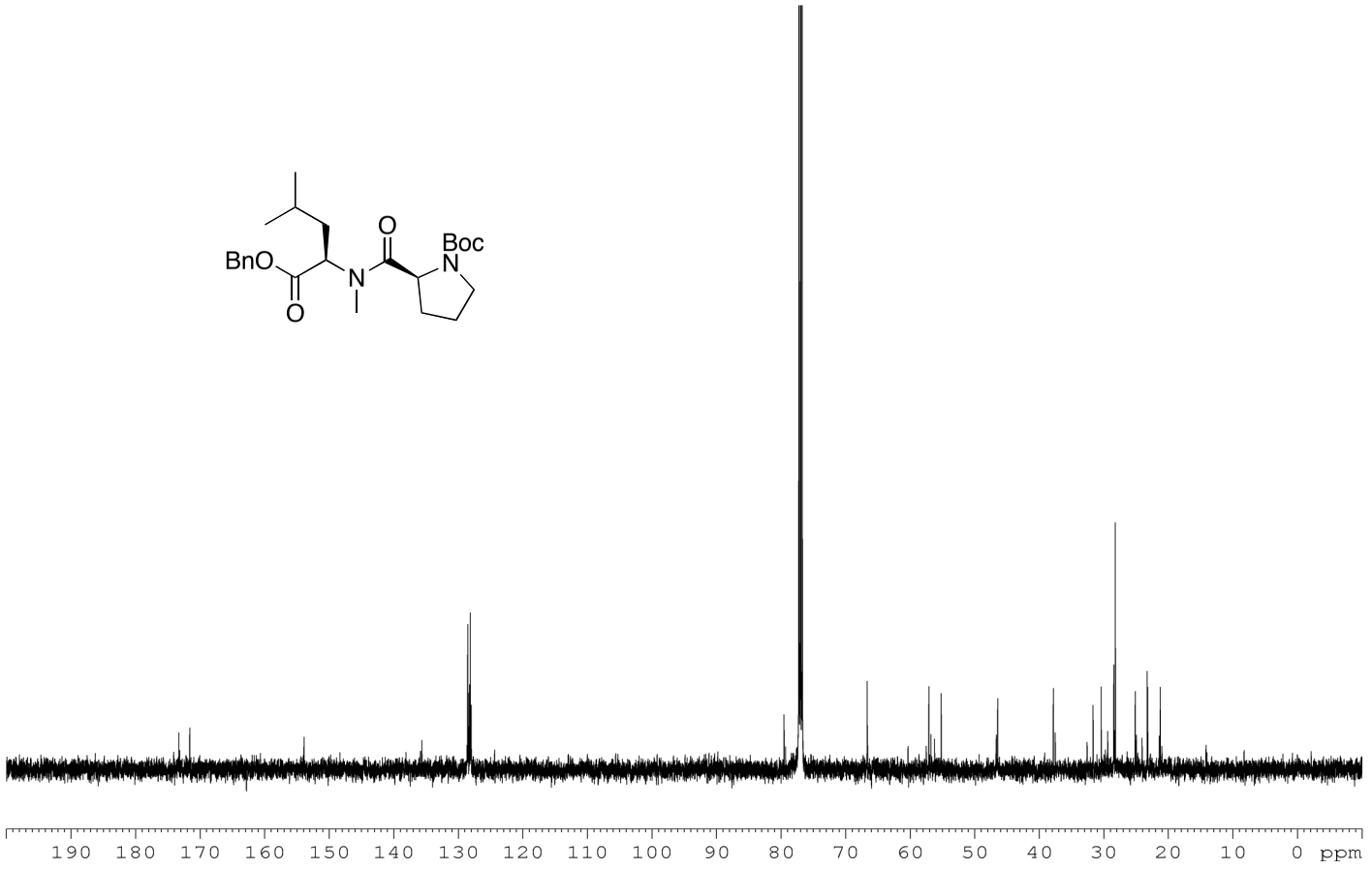

Figure 38: ^{13}C NMR ($CDCl_3$, 125 MHz) of **35**

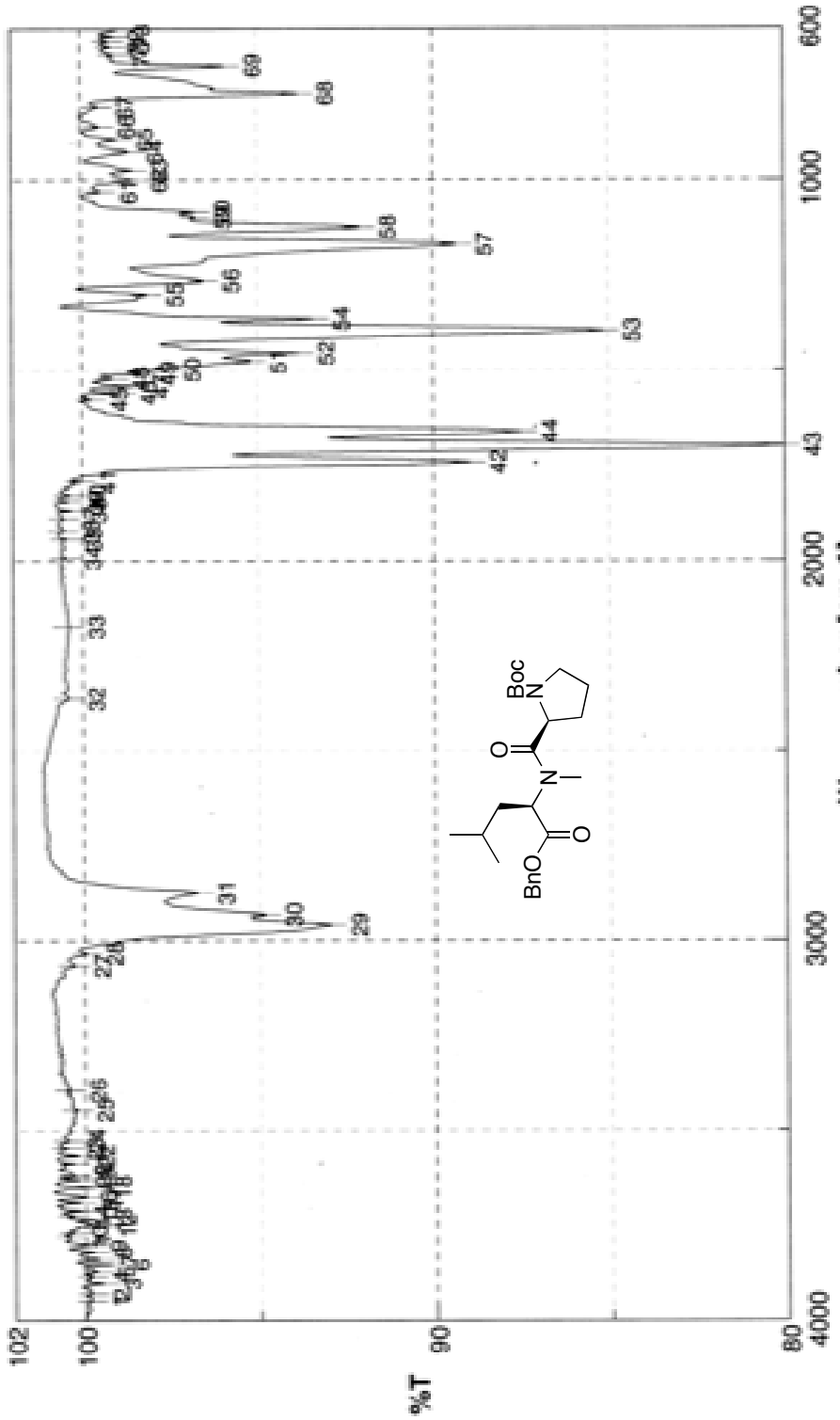

Figure 39: Infrared spectra (neat) of **35**

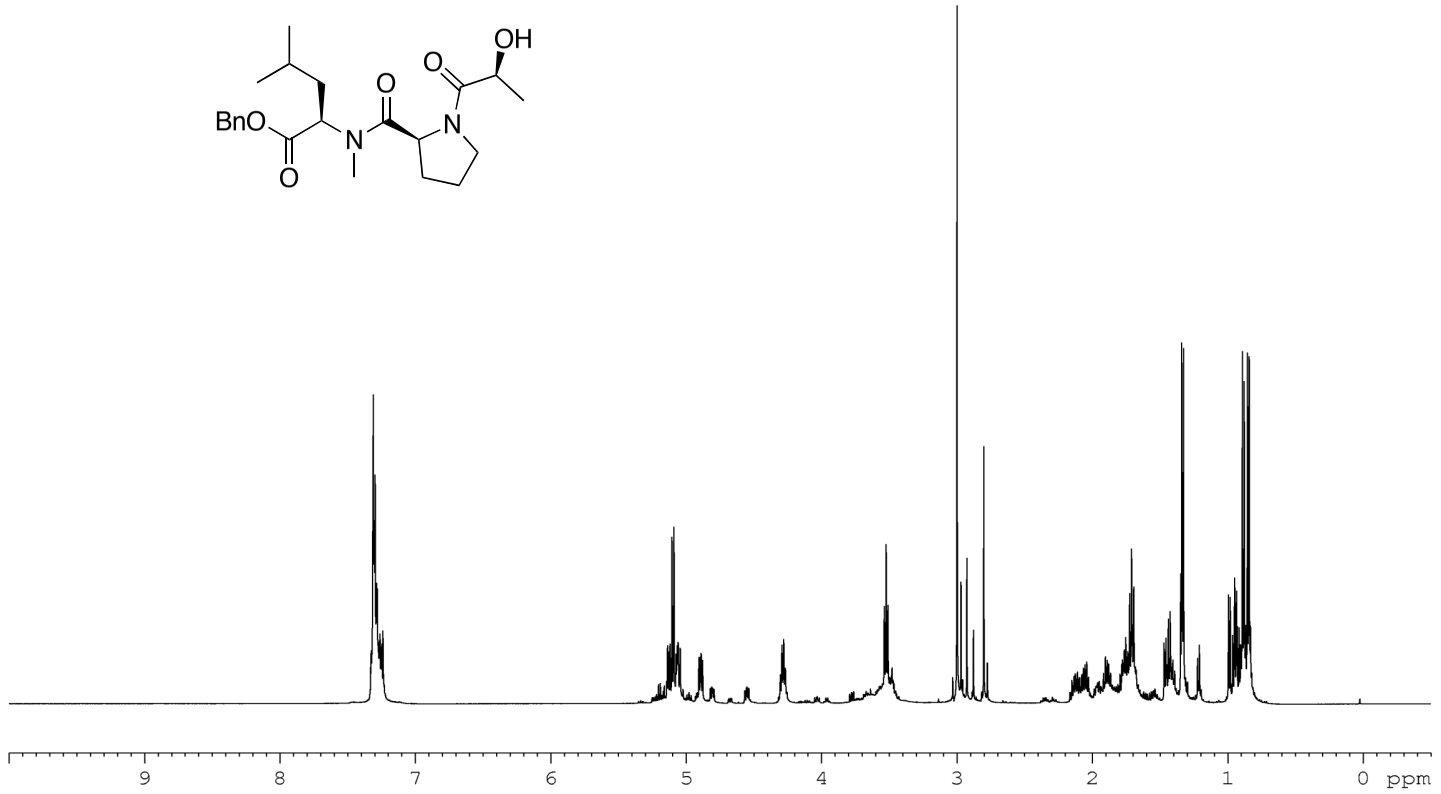

Figure 40: ^{1}H NMR ($CDCl_3$, 500 MHz) of **36**

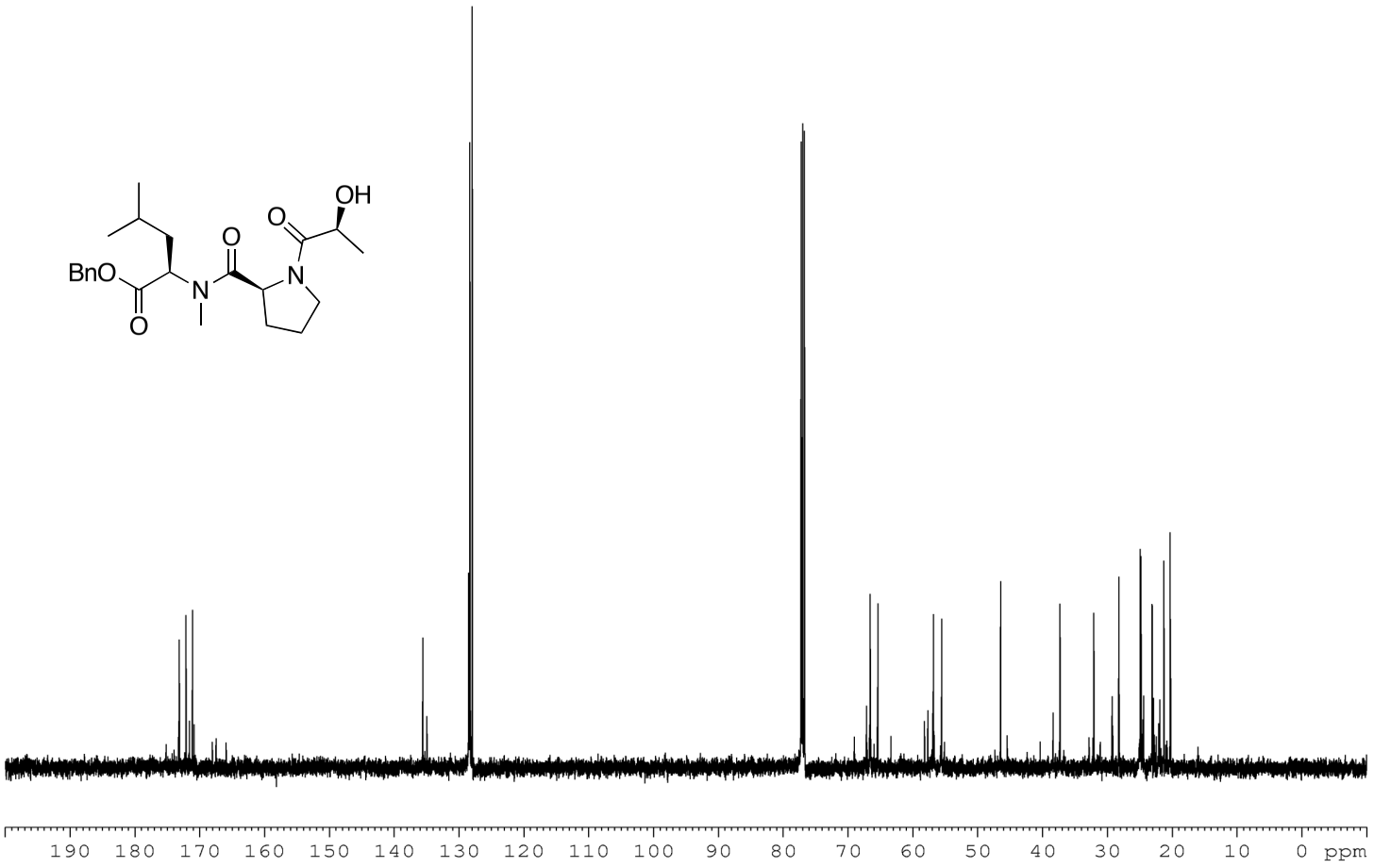

Figure 41: ^{13}C NMR ($CDCl_3$, 125 MHz) of **36**

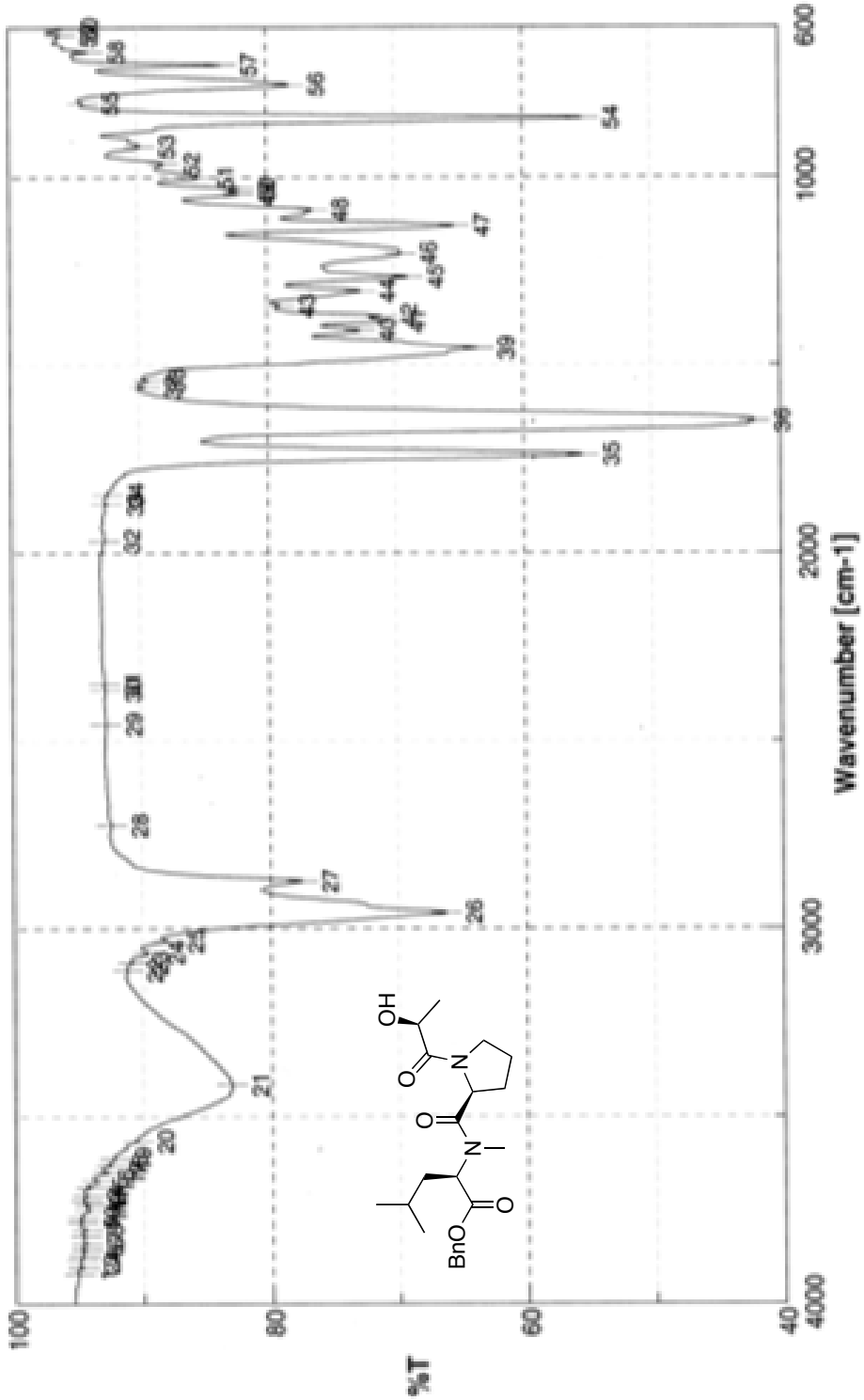

Figure 42: Infrared spectra (neat) of **36**

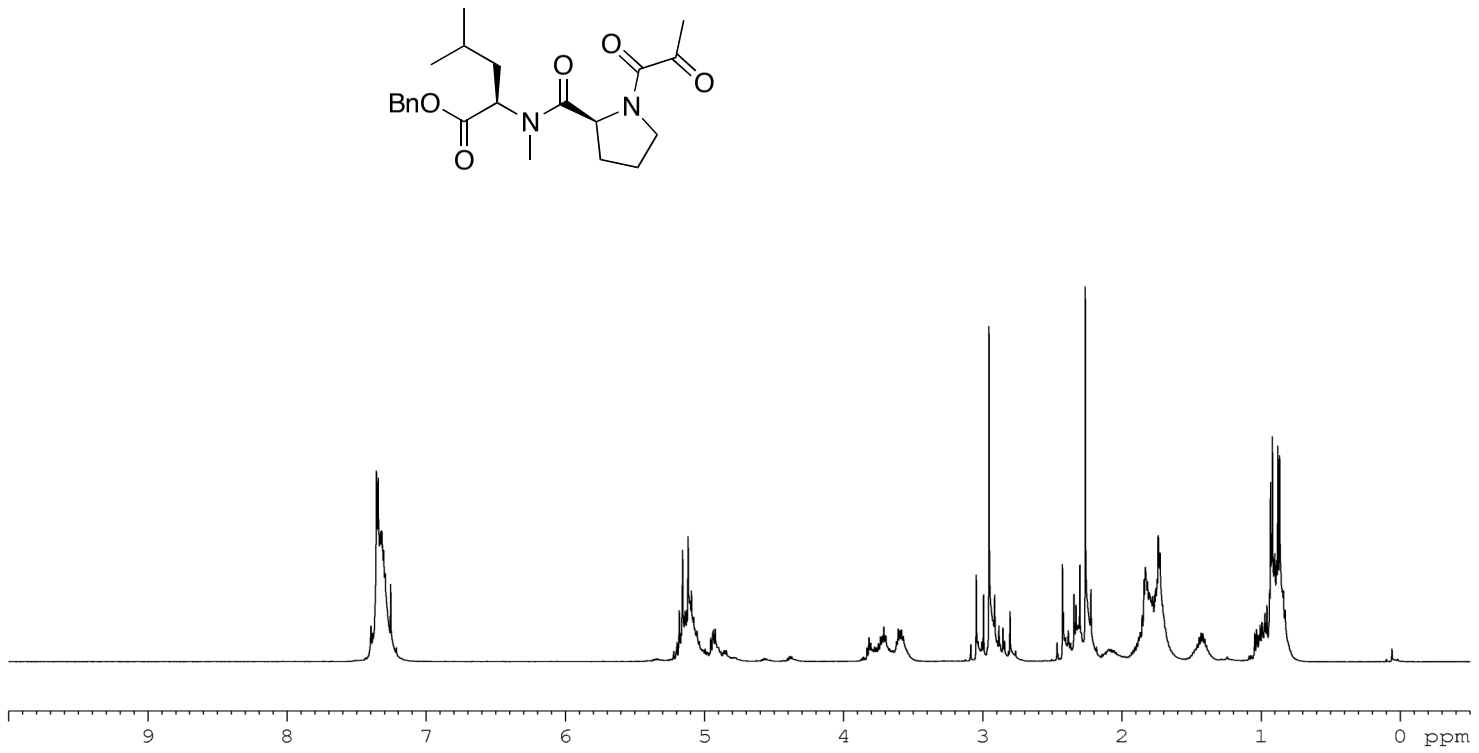

Figure 43: ^{1}H NMR ($CDCl_3$, 500 MHz) of **48**

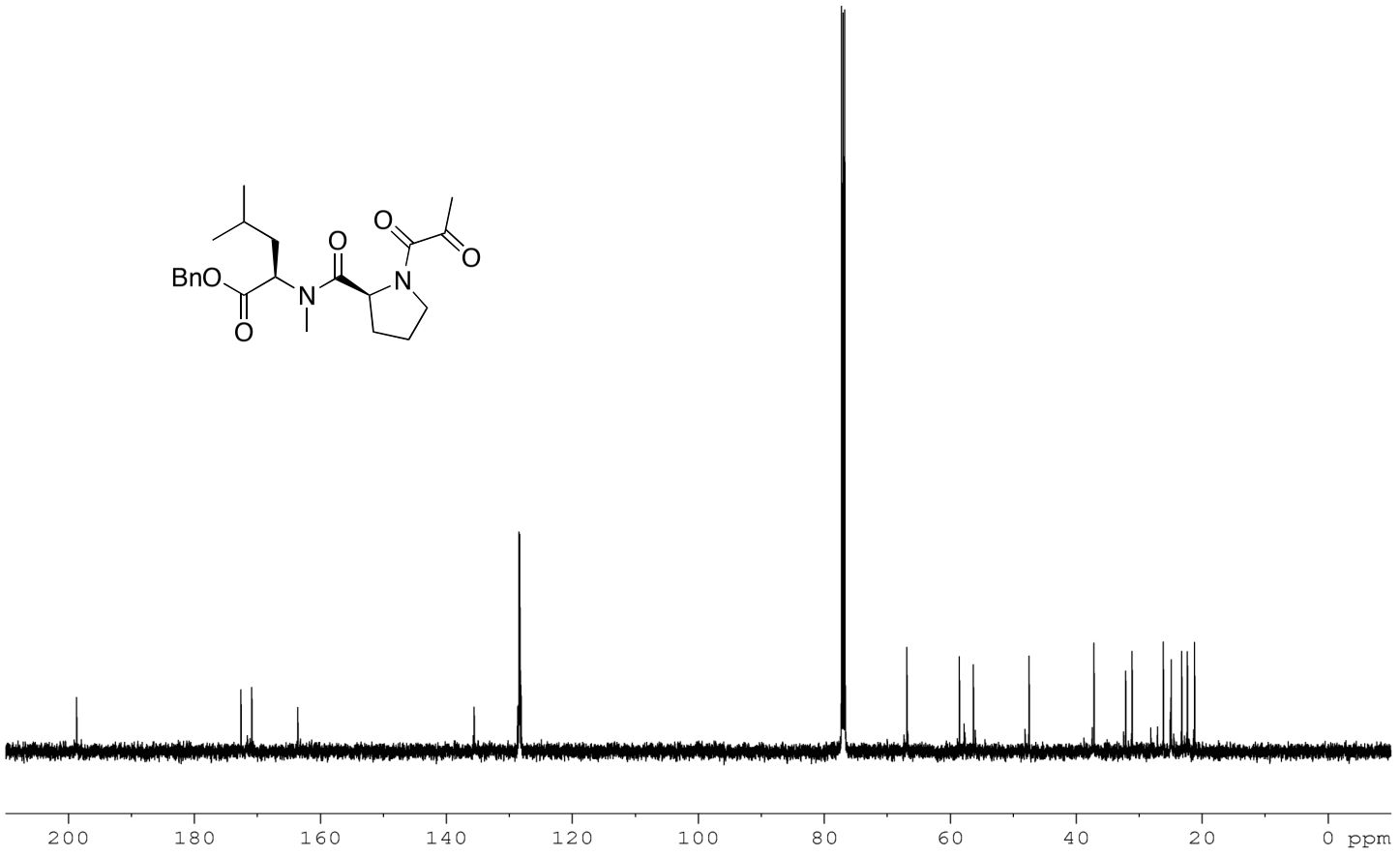

Figure 44: ^{13}C NMR ($CDCl_3$, 125 MHz) of **48**

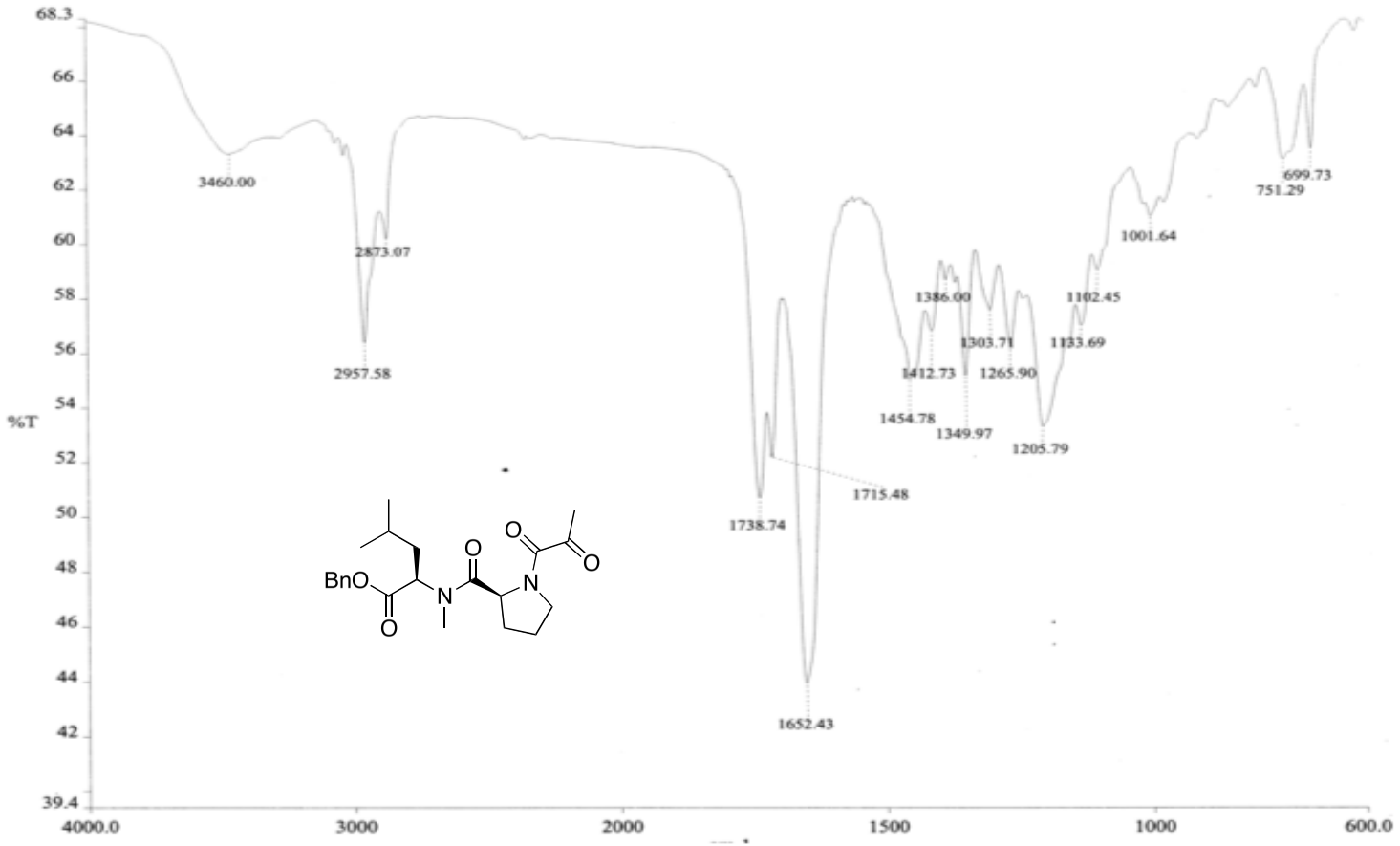

Figure 45: Infrared spectra (neat) of **48**

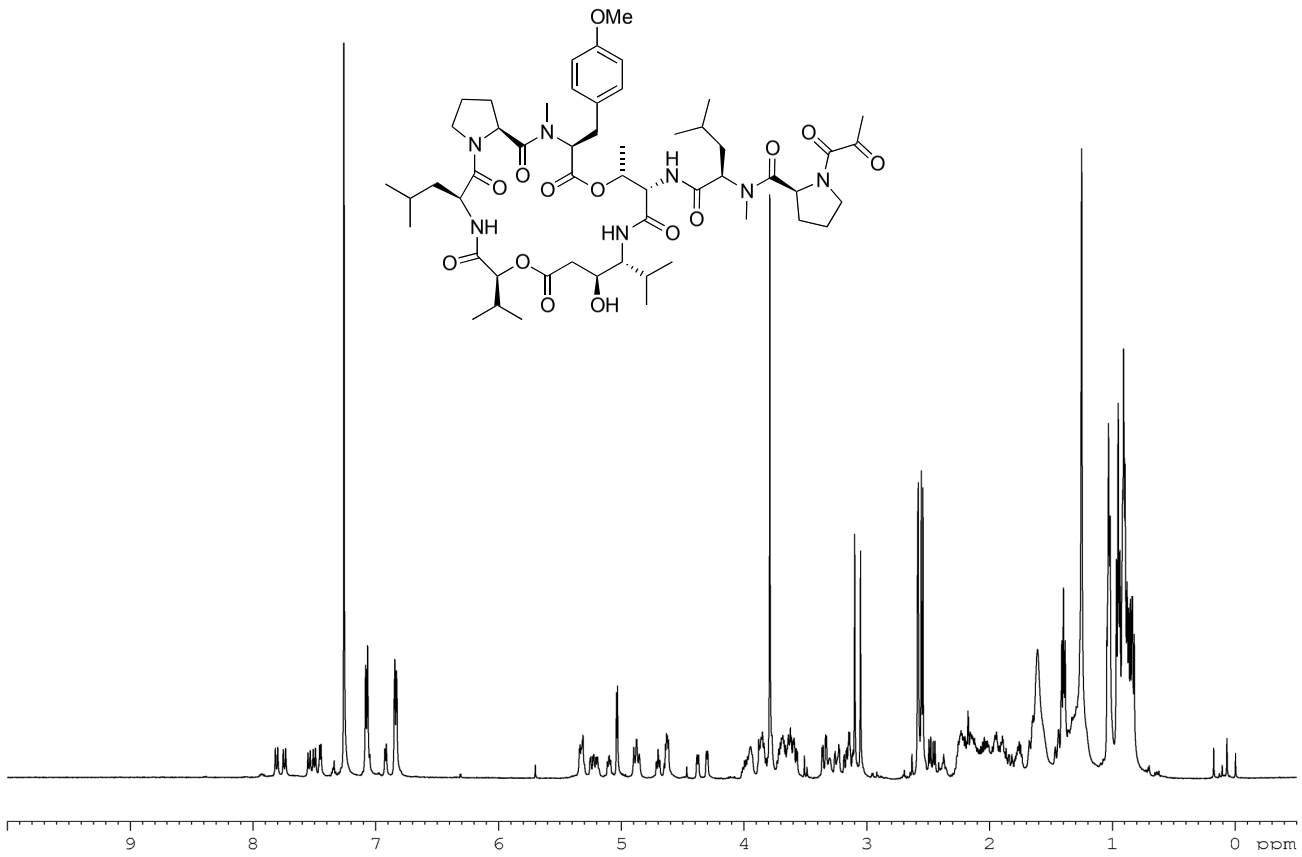

Figure 46: ^{1}H NMR ($CDCl_3$, 500 MHz) of **30**

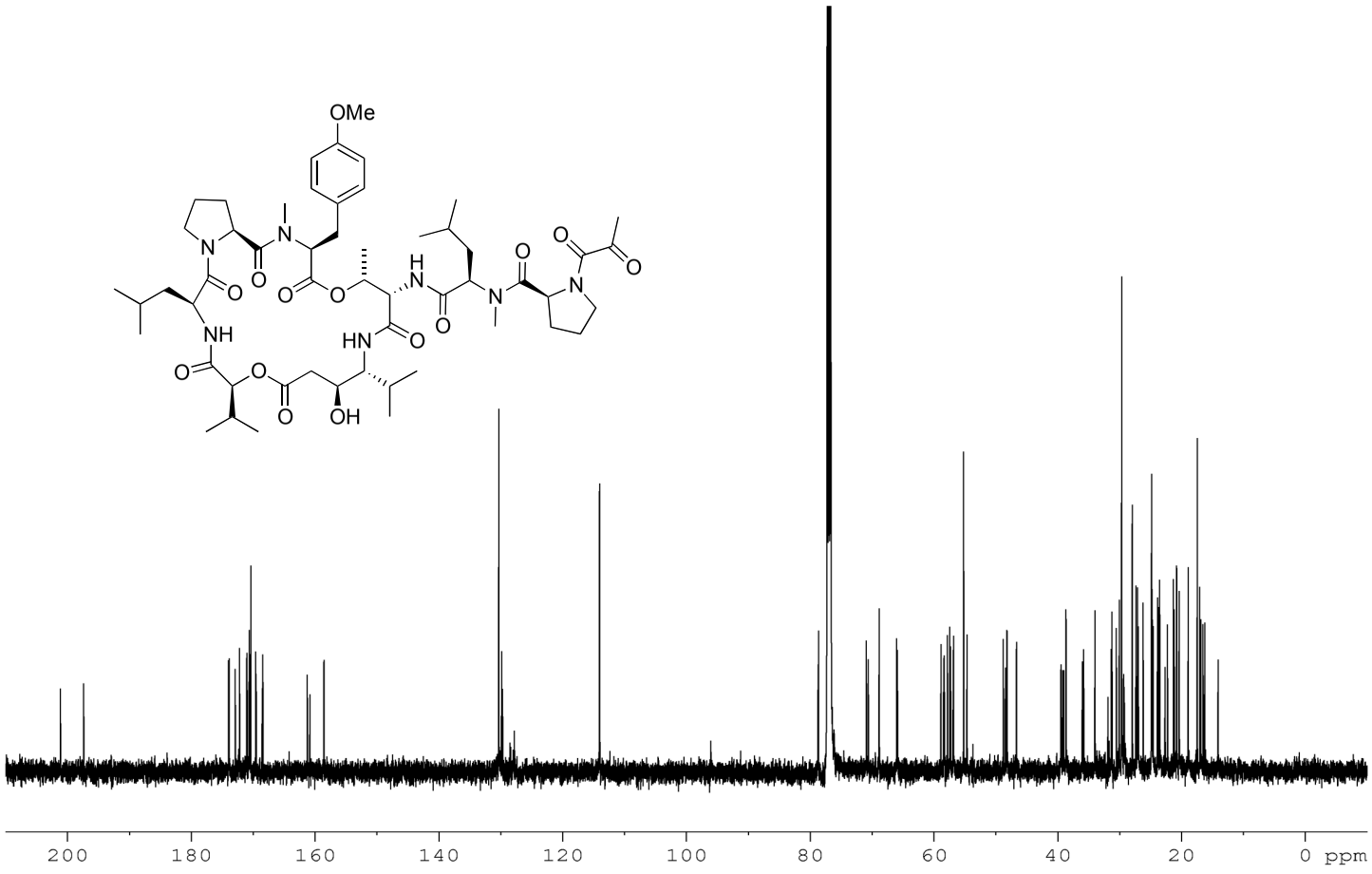

Figure 47: ^{13}C NMR ($CDCl_3$, 125 MHz) of **30**

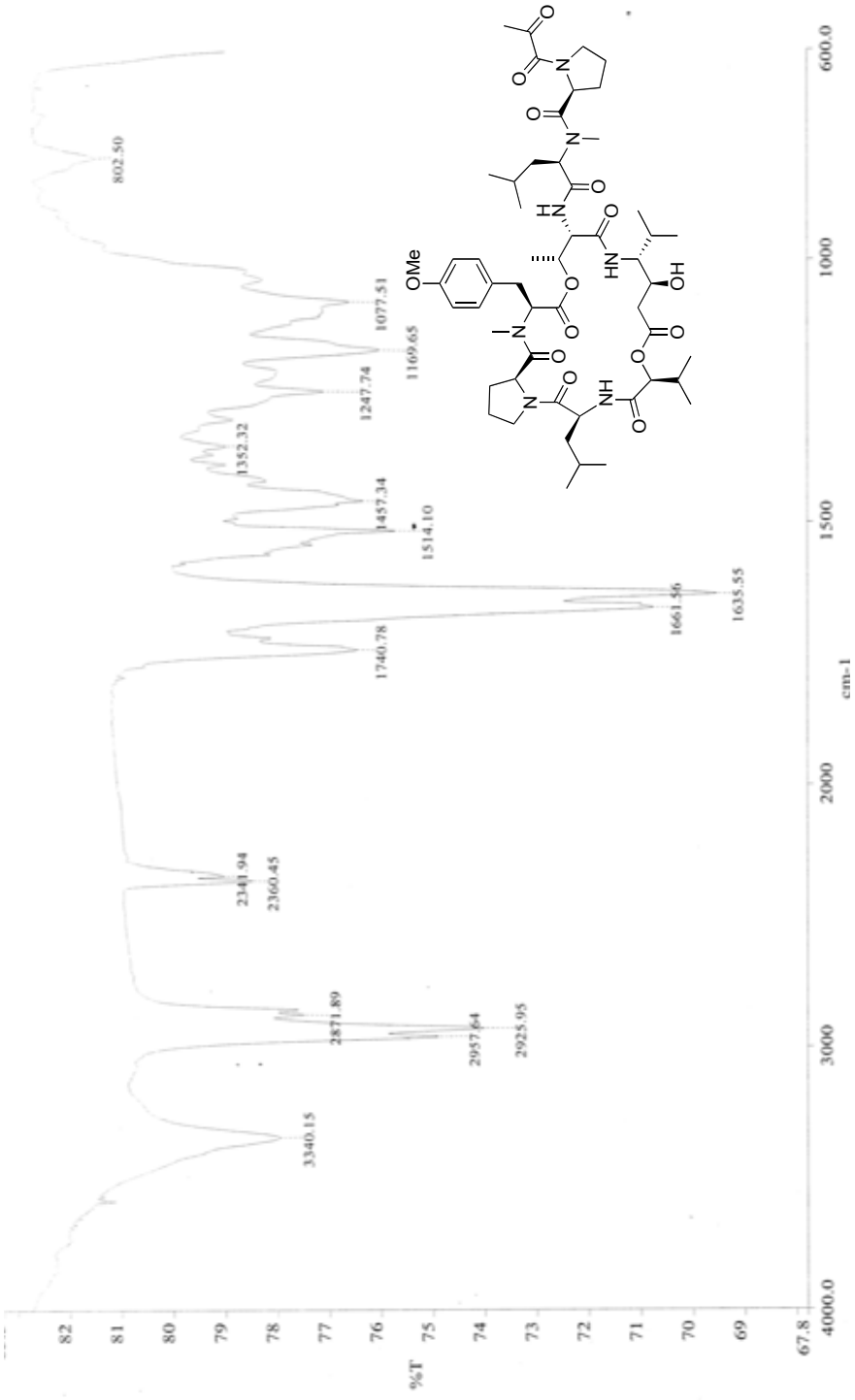

Figure 48: Infrared spectra (neat) of **30**

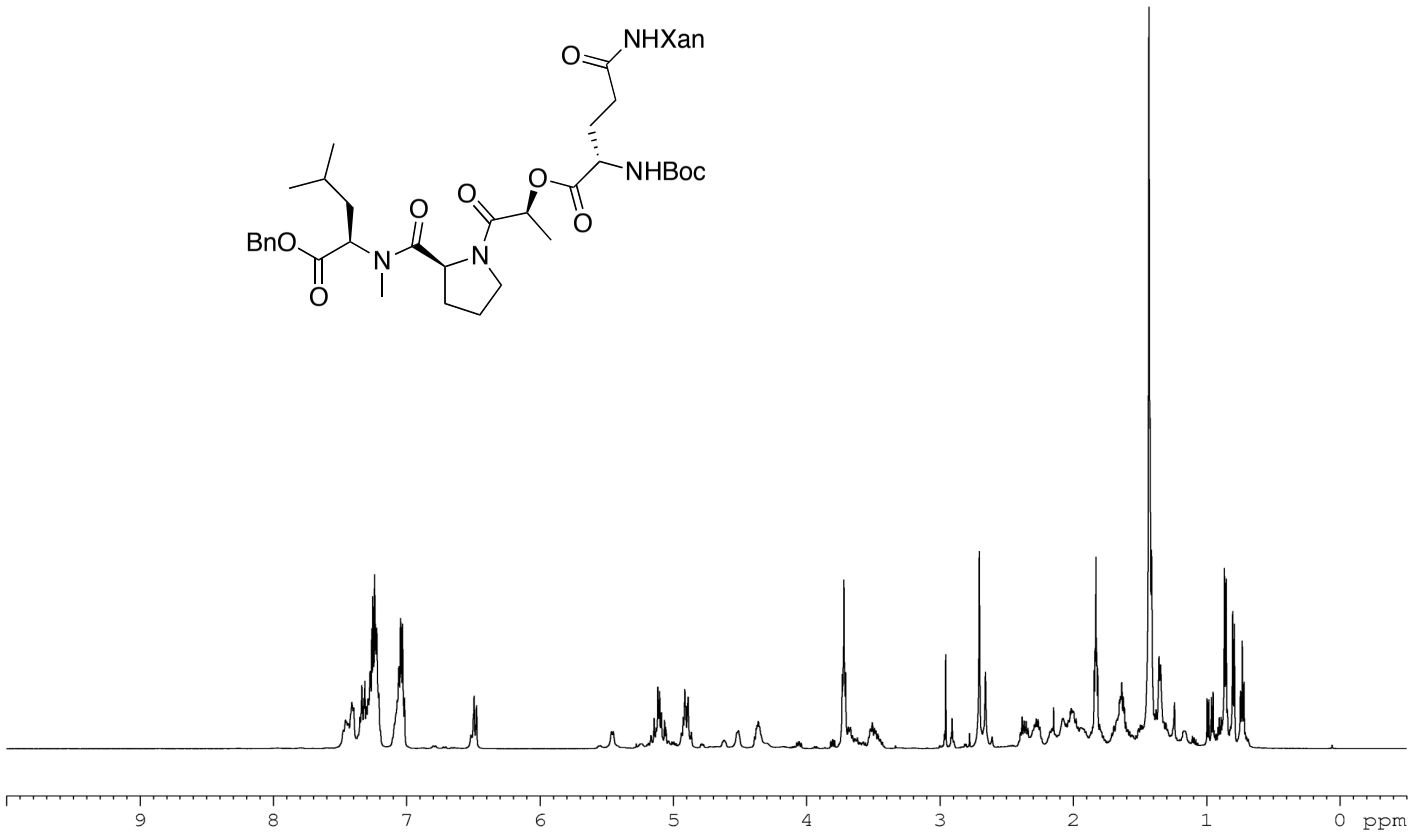

Figure 49: ^{1}H NMR ($CDCl_3$, 500 MHz) of **38**

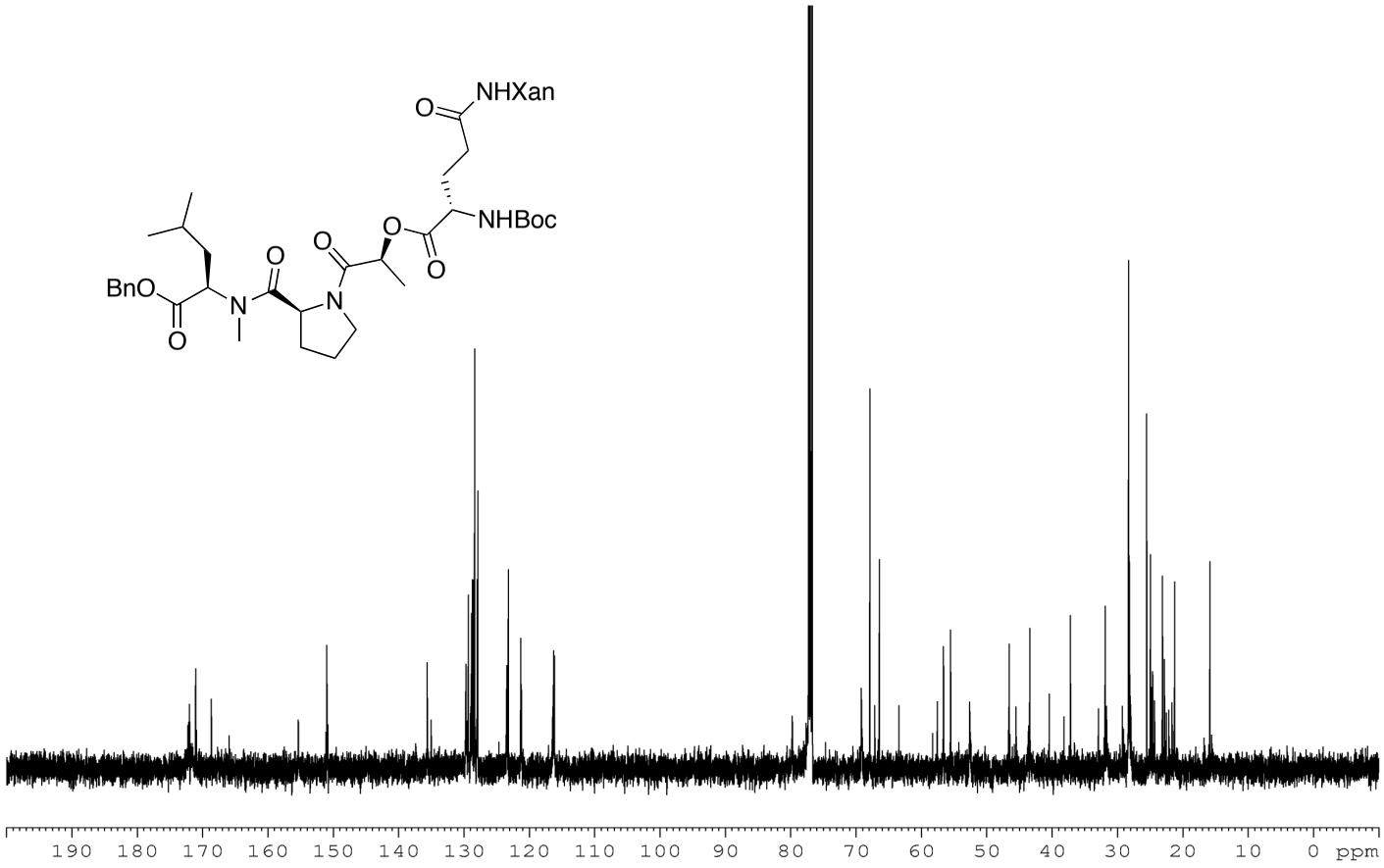

Figure 50: ^{13}C NMR ($CDCl_3$, 125 MHz) of **38**

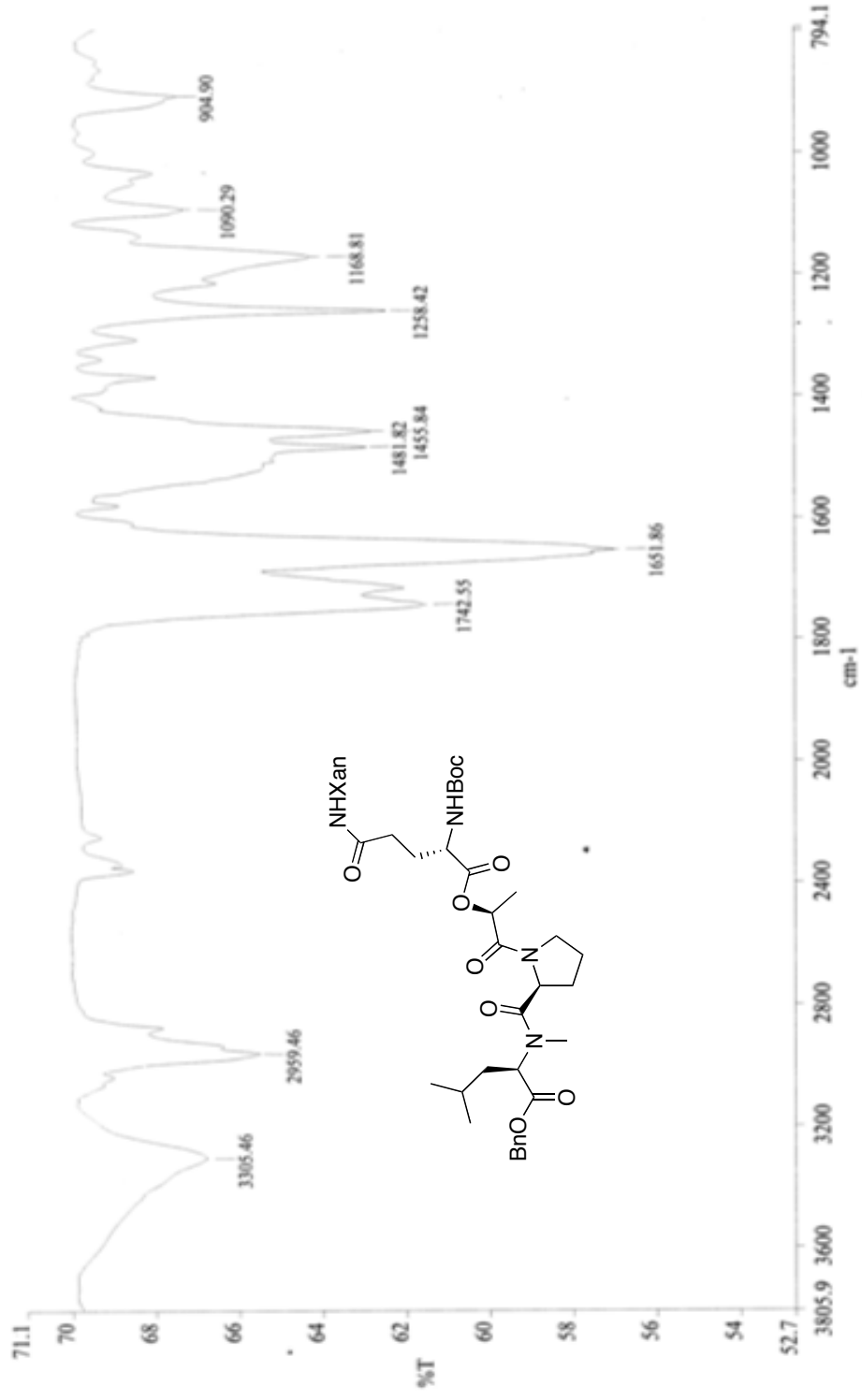

Figure 51: Infrared spectra (neat) of **38**

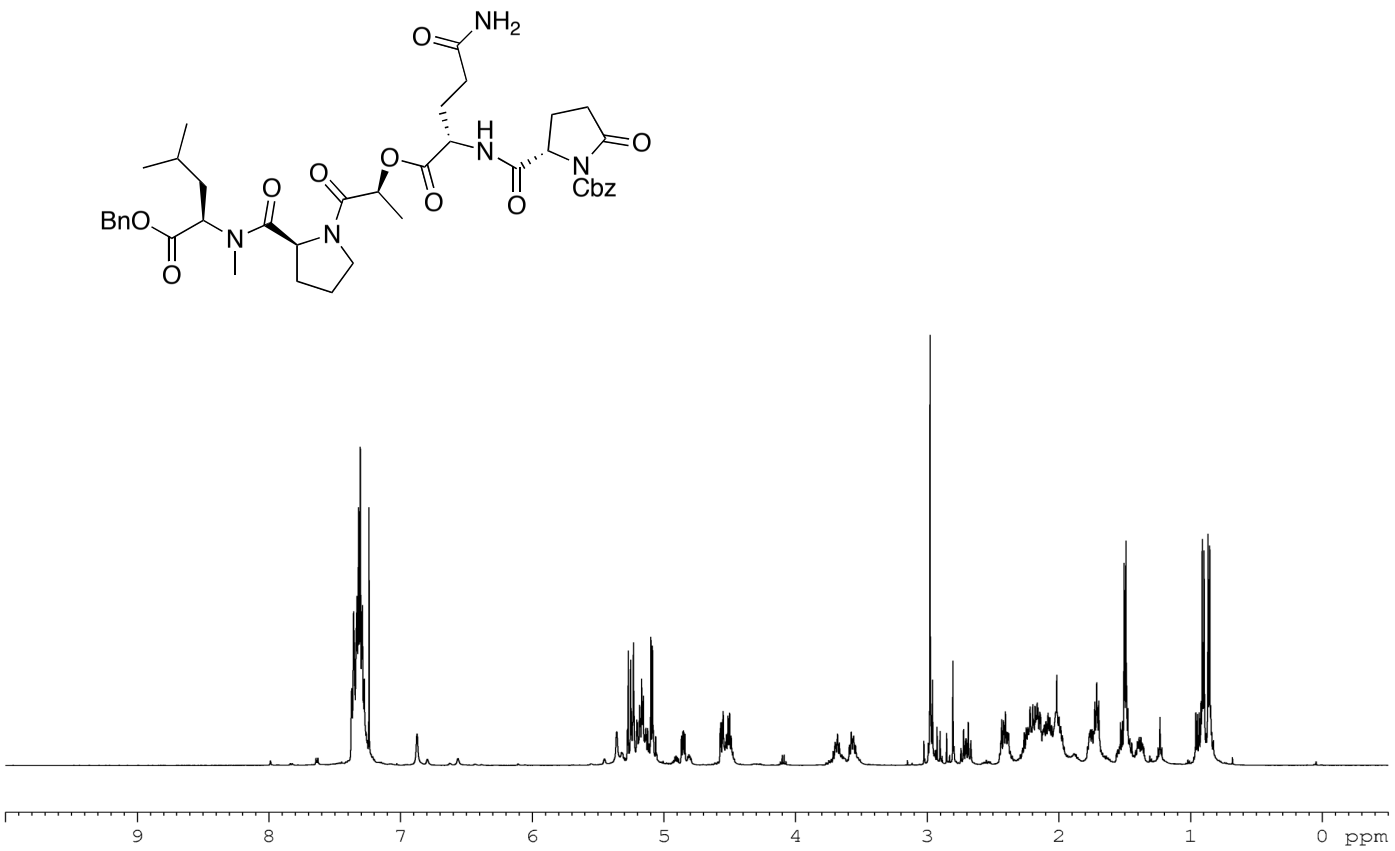

Figure 52: ^{1}H NMR ($CDCl_3$, 500 MHz) of **39**

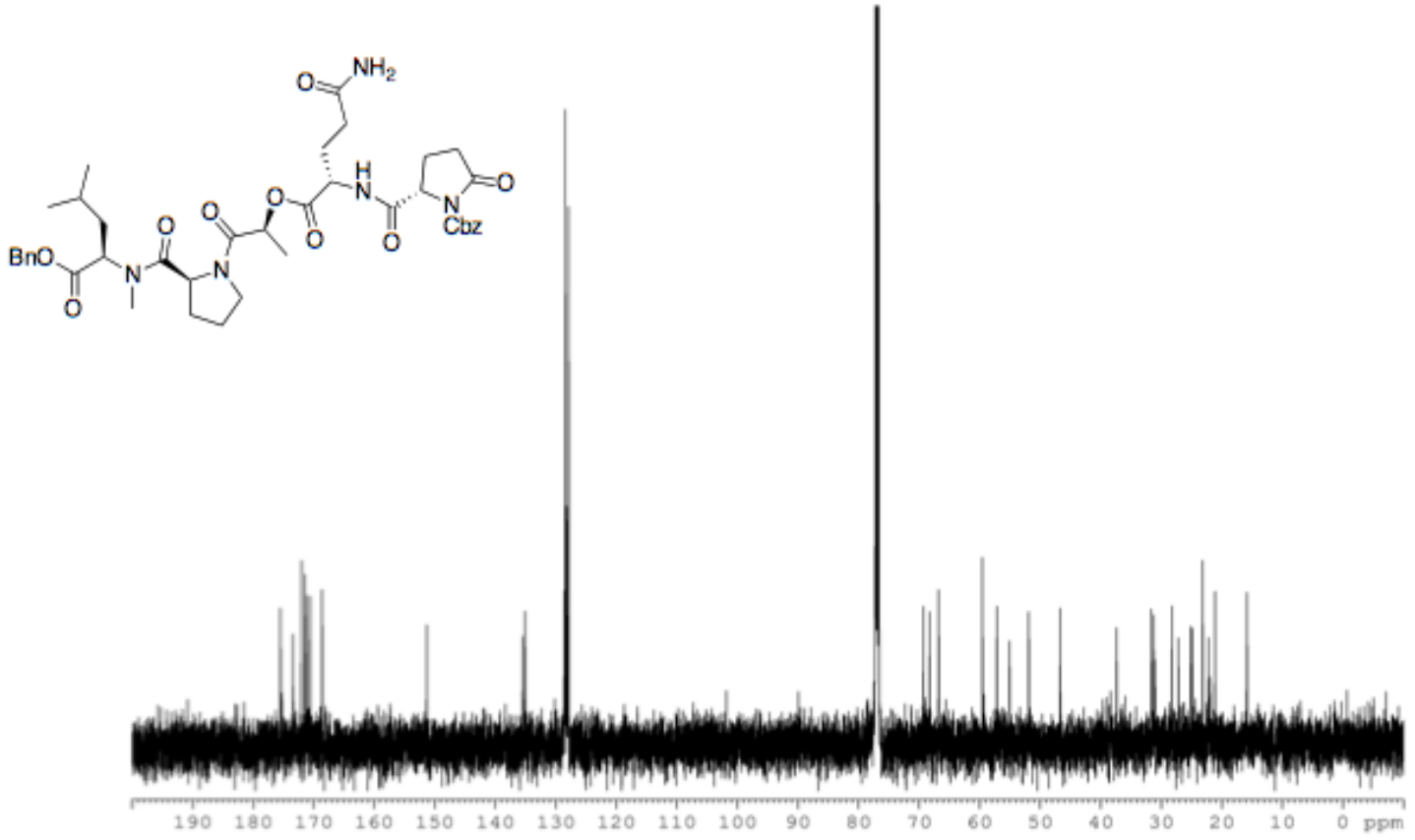

Figure 53: ^{13}C NMR ($CDCl_3$, 125 MHz) of **39**

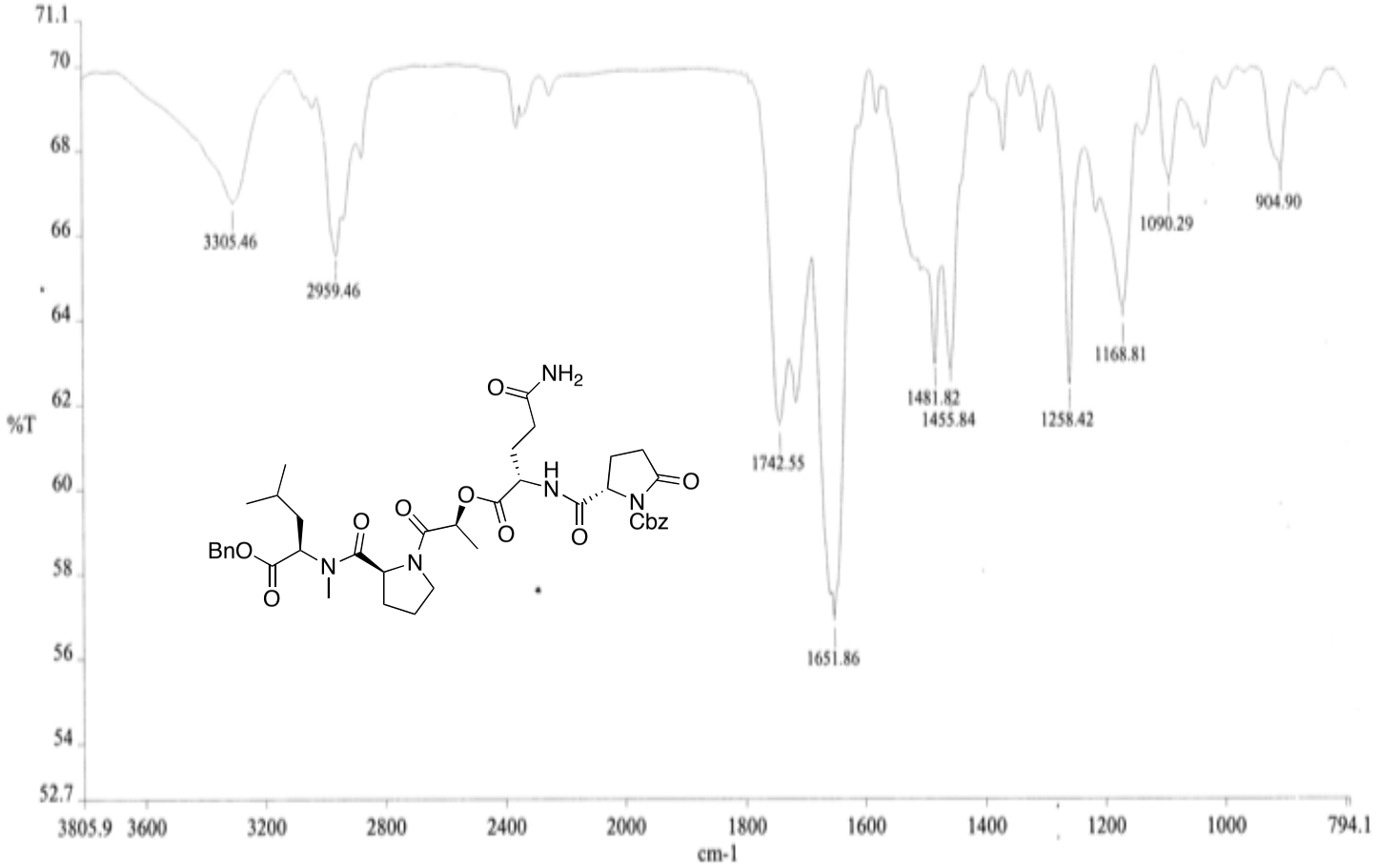

Figure 54: Infrared spectra (neat) of **39**

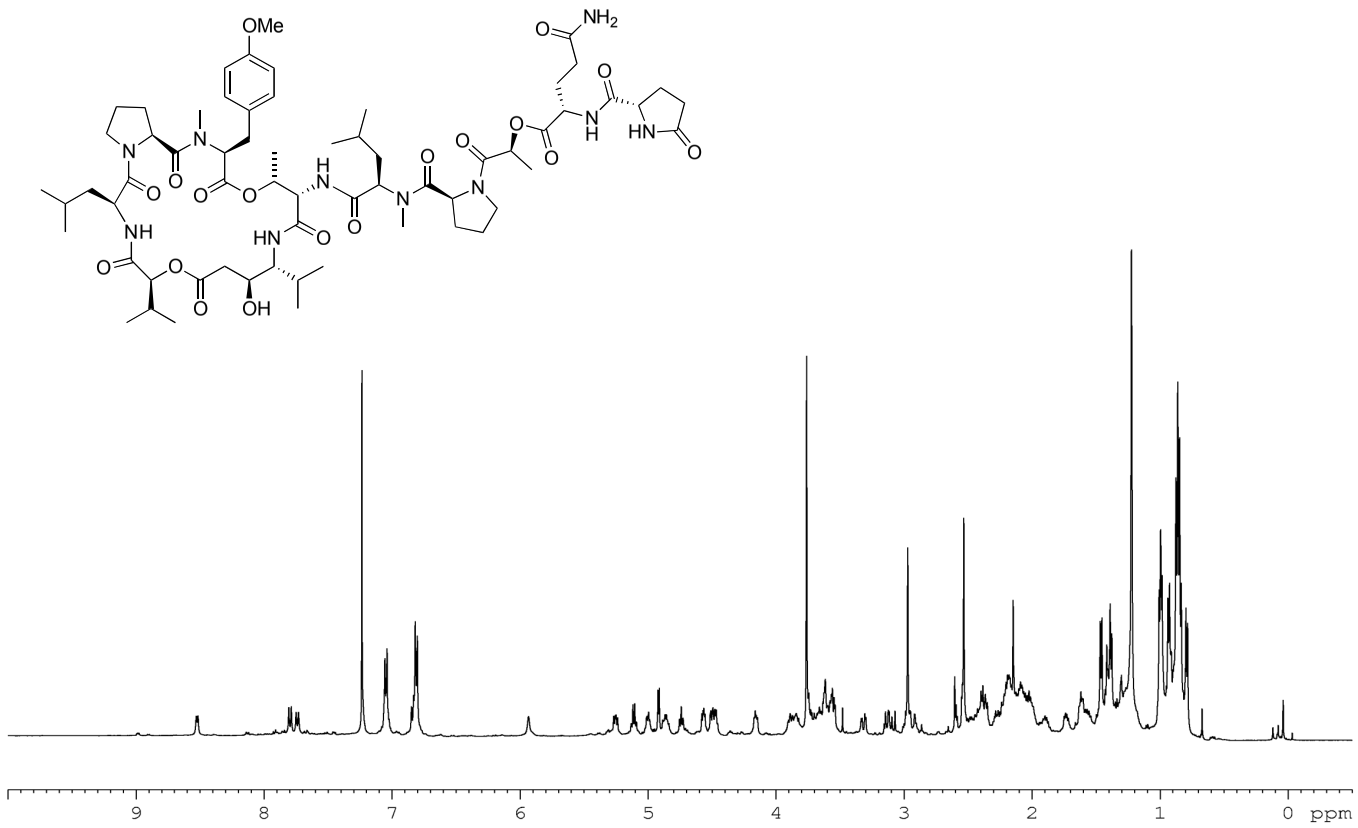

Figure 55: ^{1}H NMR ($CDCl_3$, 500 MHz) of **31**

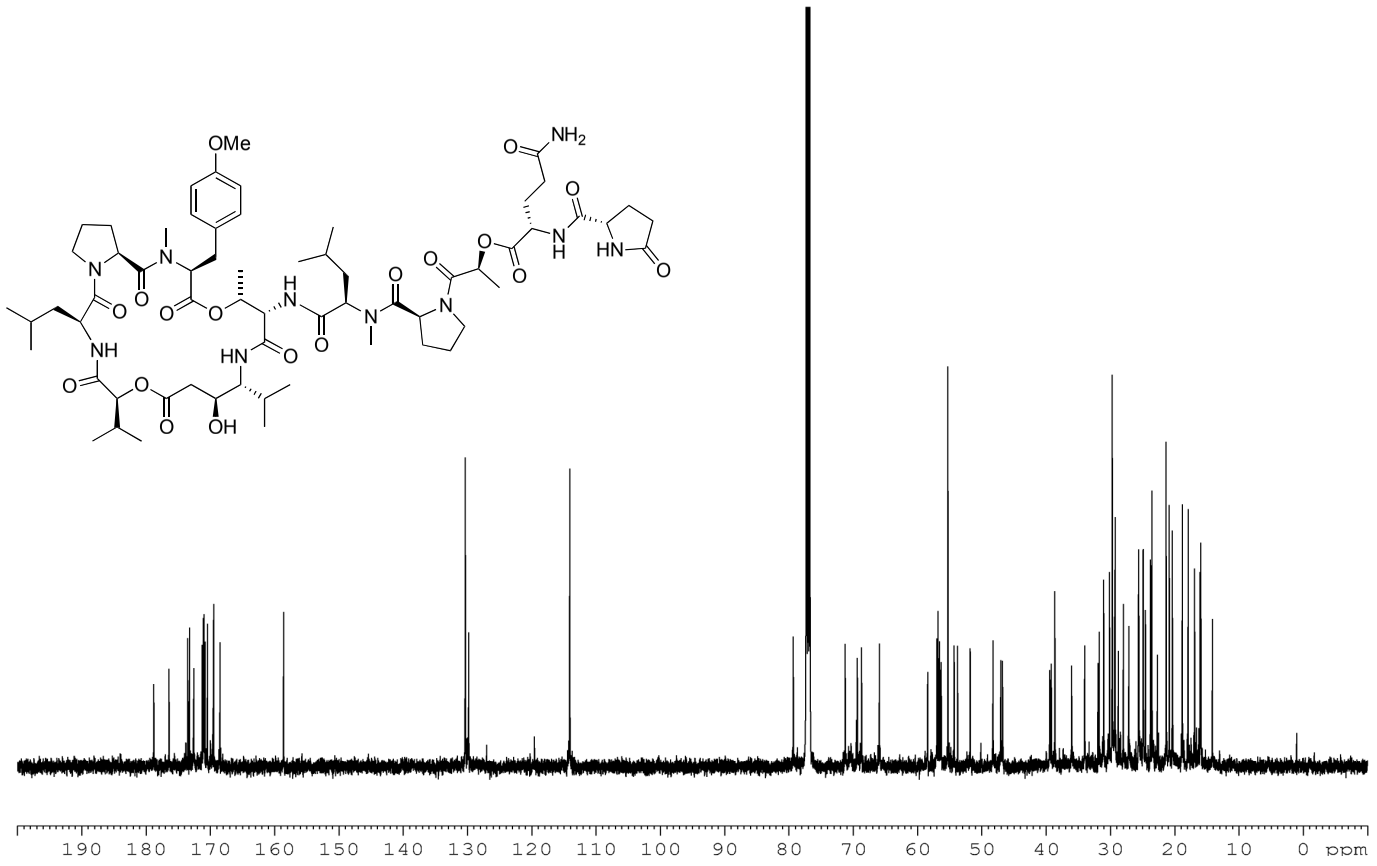

Figure 56: ^{13}C NMR ($CDCl_3$, 125 MHz) of **31**

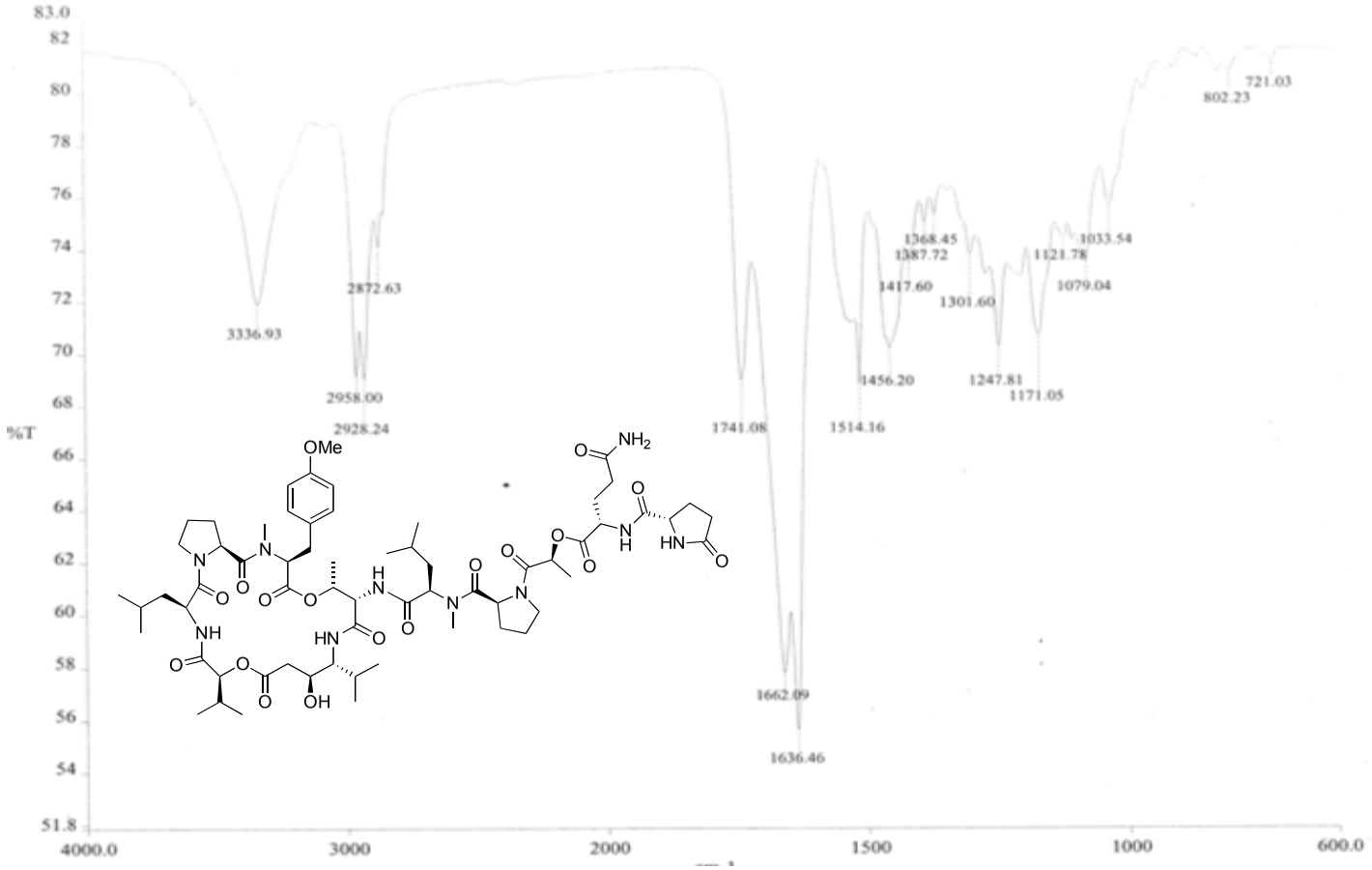

Figure 57: Infrared spectra (neat) of **31**

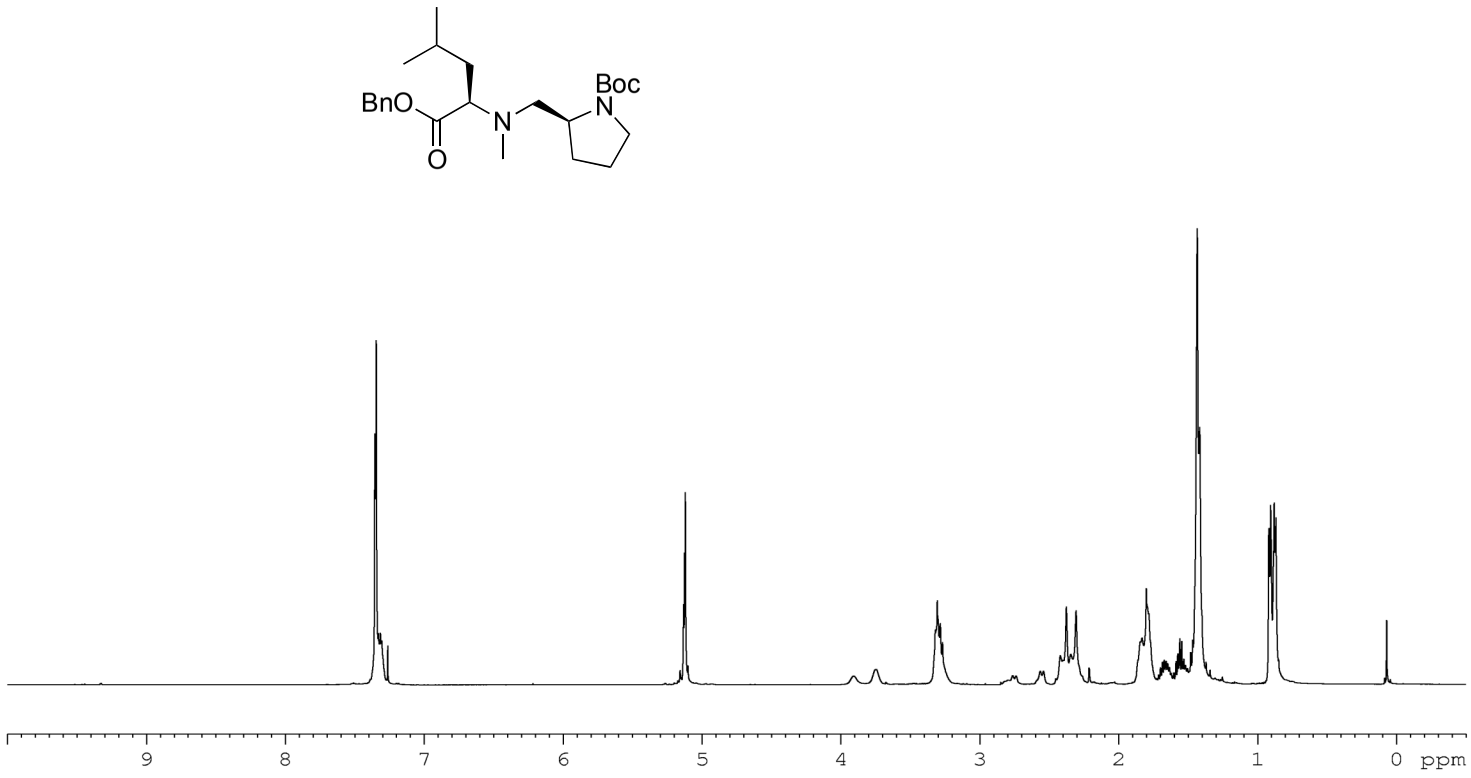

Figure 58: ^{1}H NMR ($CDCl_3$, 500 MHz) of **42**

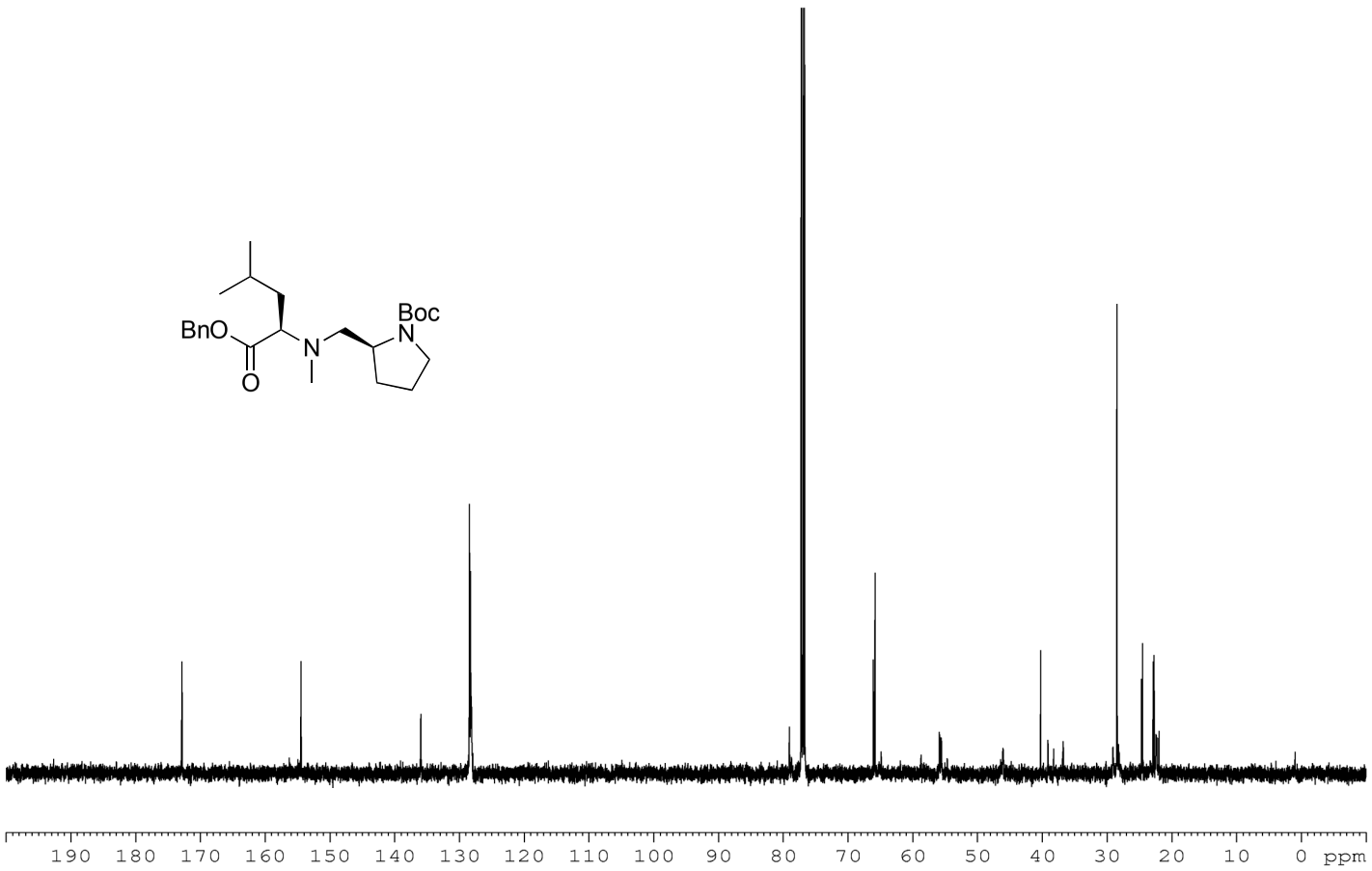

Figure 59: ^{13}C NMR ($CDCl_3$, 125 MHz) of **42**

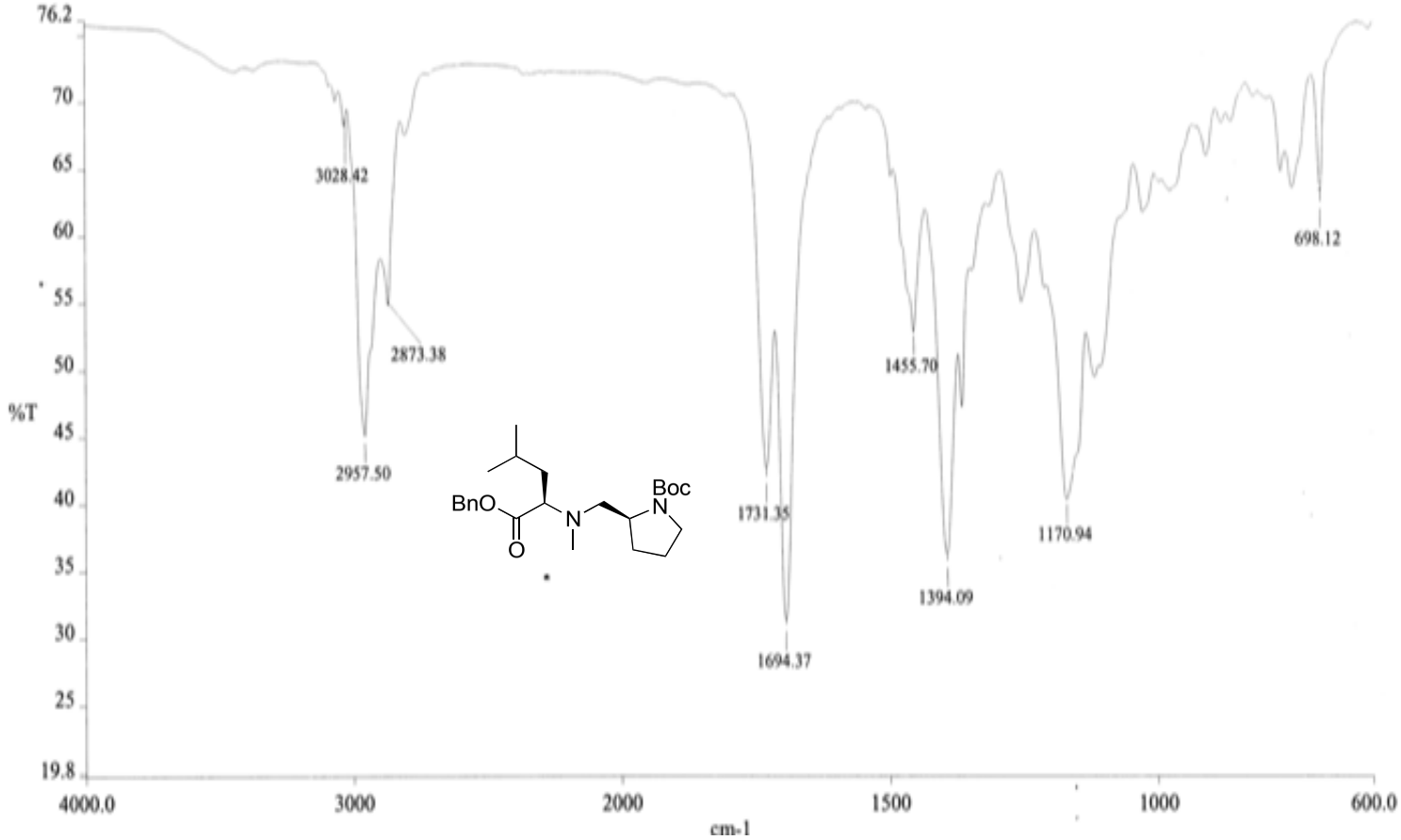

Figure 60: Infrared spectra (neat) of **42**

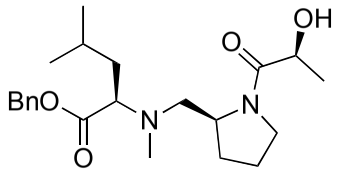

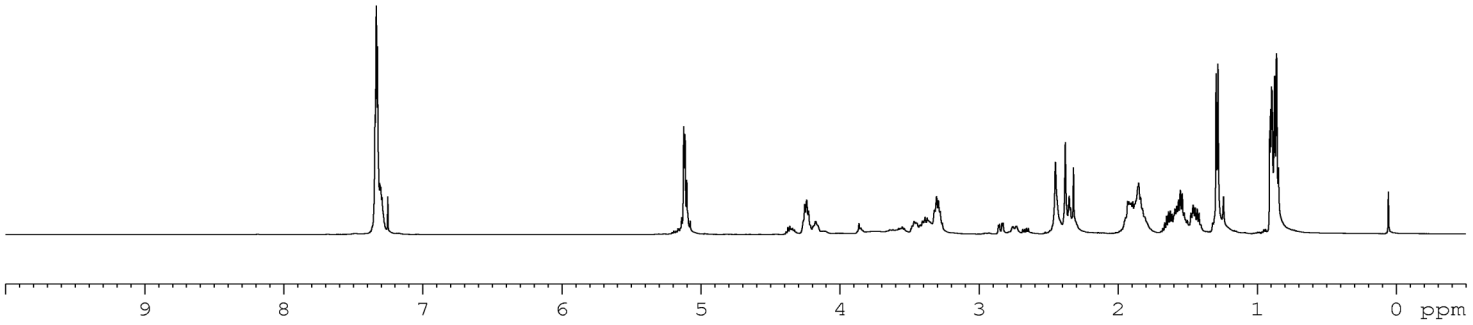

Figure 61: ^{1}H NMR ($CDCl_3$, 500 MHz) of **44**

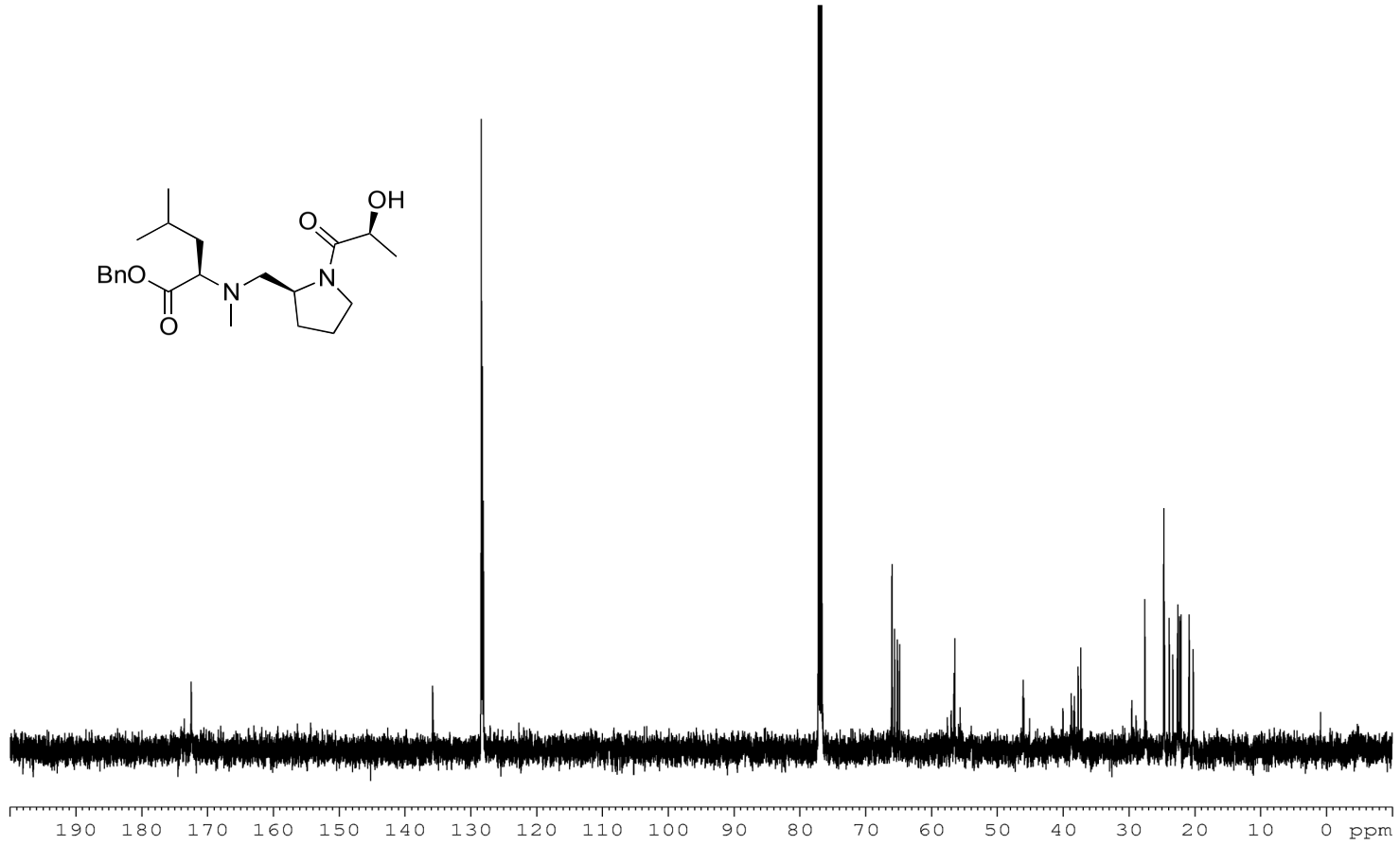

Figure 62: ^{13}C NMR ($CDCl_3$, 125 MHz) of **44**

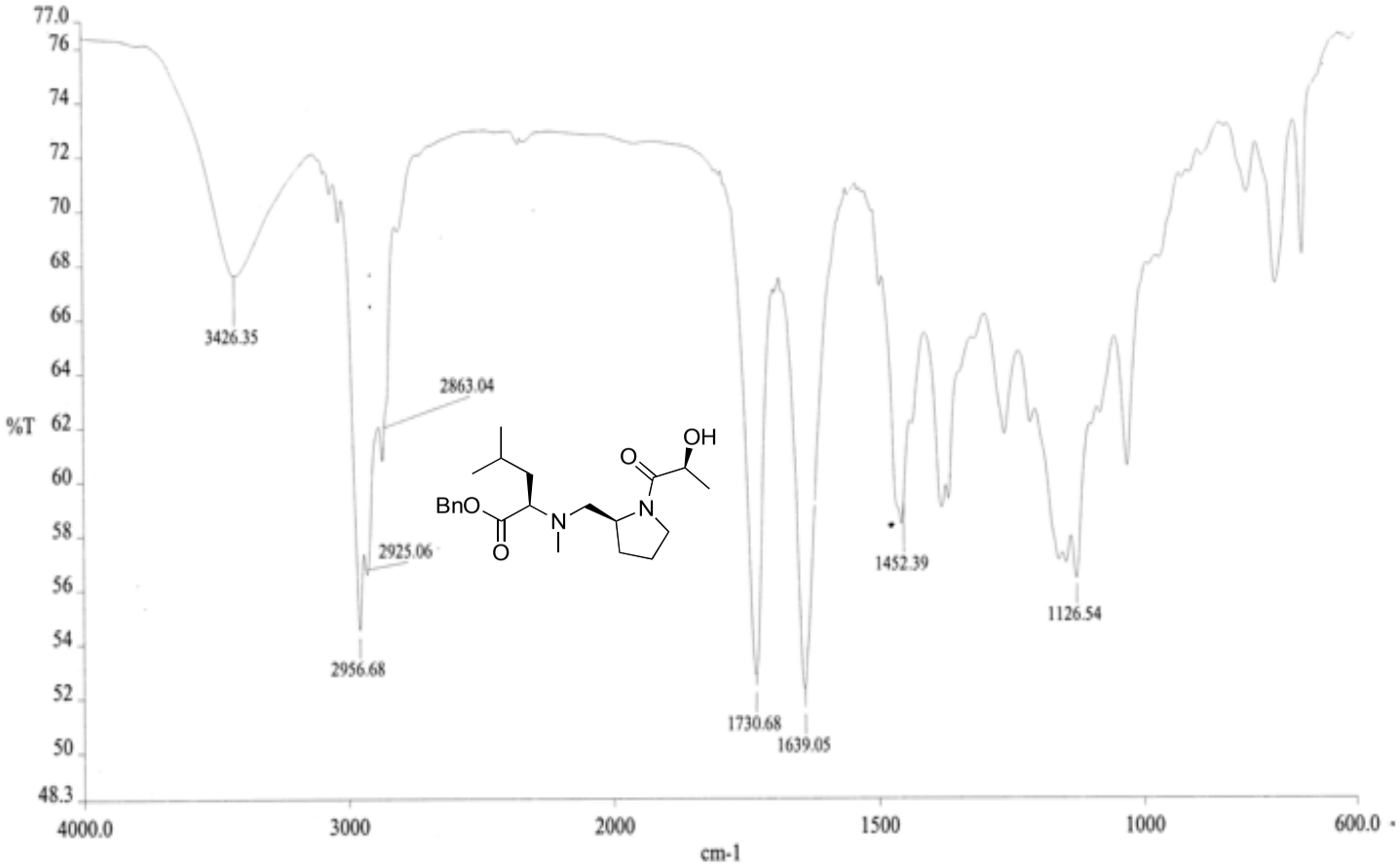

Figure 63: Infrared spectra (neat) of **44**

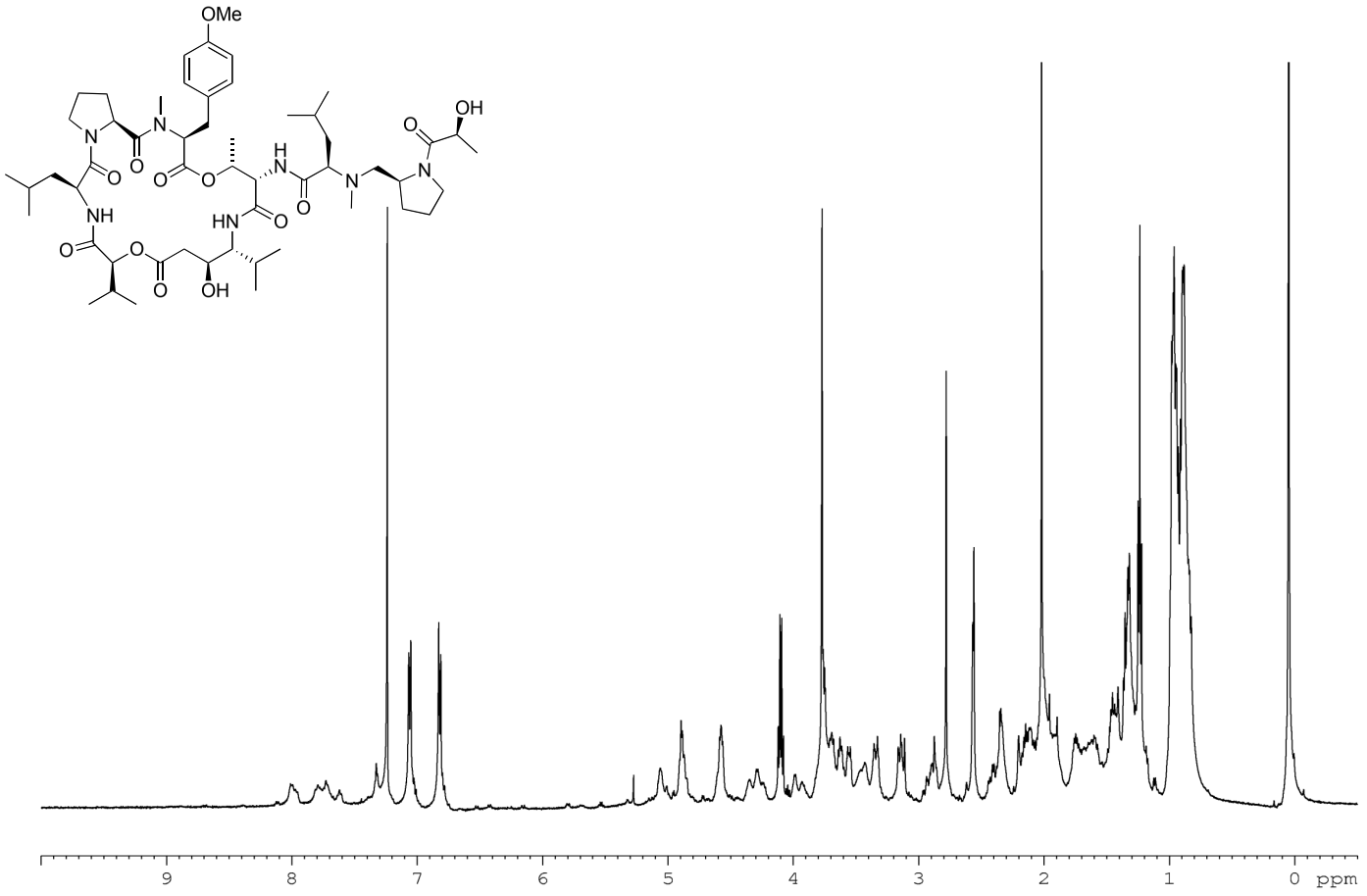

Figure 64: ^{1}H NMR ($CDCl_3$, 500 MHz) of **32**

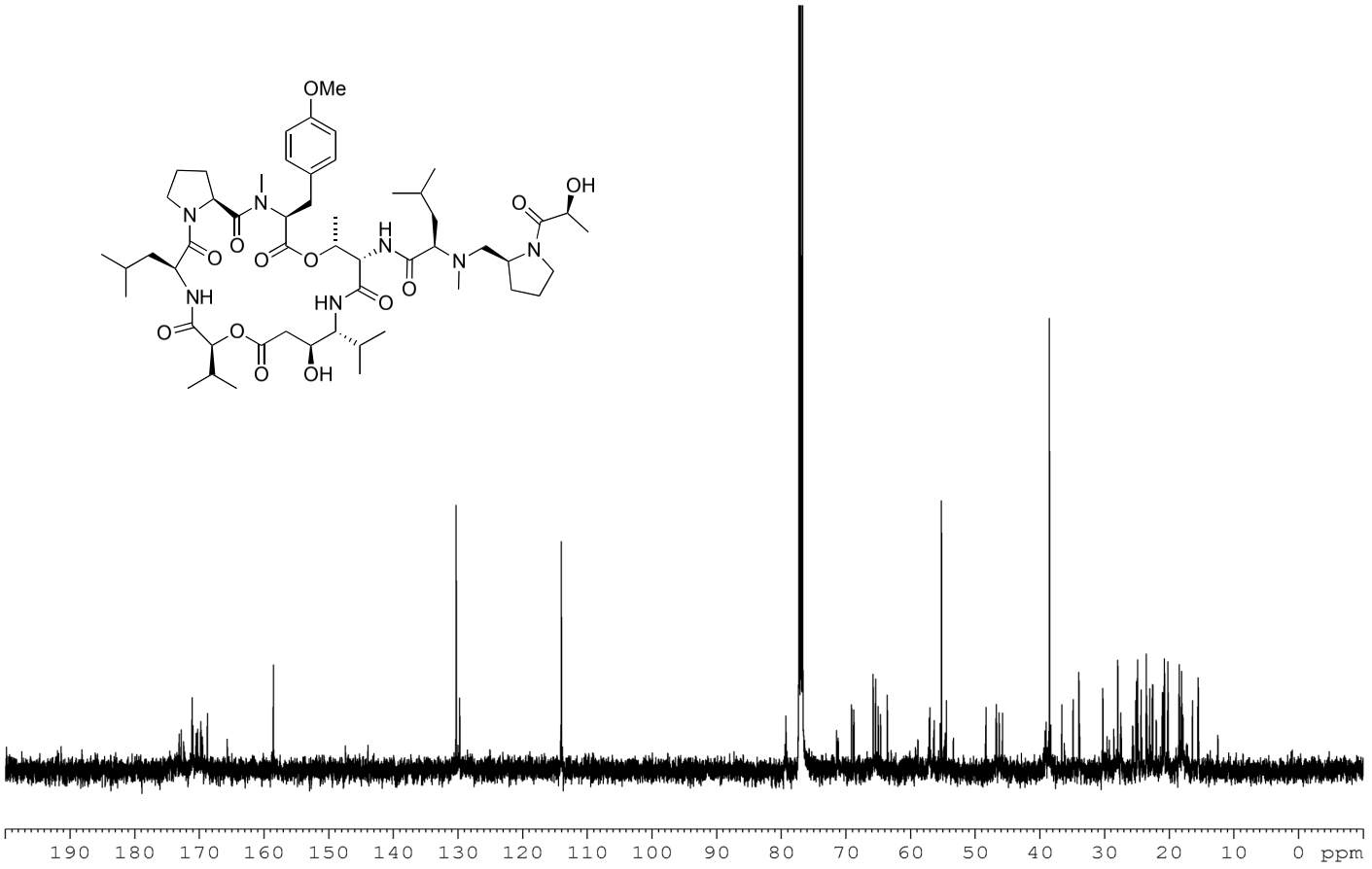

Figure 65: ^{13}C NMR ($CDCl_3$, 125 MHz) of **32**

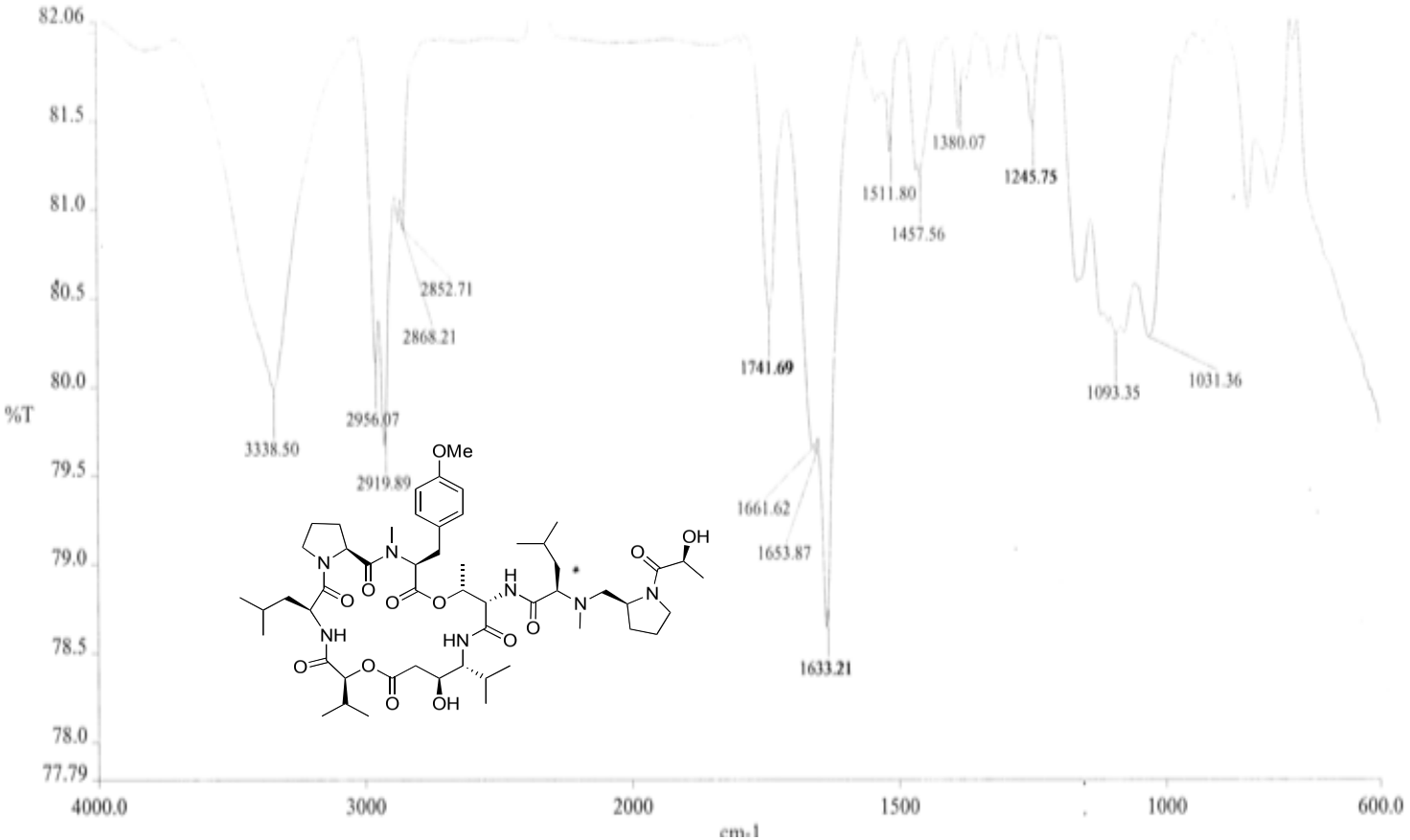

Figure 66: Infrared spectra (neat) of **32**

Chapter 3: Synthesis of 3-piperidinone and 3-azepinone derivatives *via* ring-opening of azabicyclic [3.1.0]-and [4.1.0]aminocyclopropanes

3.1) Synthesis of [3.1.0]-and [4.1.0]azabicycles via intramolecular Kulinkovich cyclopropanation of amino acid derivatives

Since its discovery, the Kulinkovich reaction[1] has been generally utilized to access a number of biologically and structurally interesting cyclopropanols and aminocyclopropanes from simple starting materials. The original Kulinkovich protocol[1] provided means to obtain hydroxycyclopropanes. This protocol was further expanded by de Meijere and coworkers to provide *N,N*-dialkylcyclopropylamines from *N,N*-dialkylamides.[2] Subsequent discovery of the ligand exchange for the generation of various substituted titanacyclopropane intermediates[3] further improved the methodology and expanded the scope of the reaction.[4] Reports of intramolecular cyclopropanations were then reported by Sato and Cha.[5] More specifically, Cha and coworkers investigated intramolecular cyclopropanation of ω-vinyl esters as well as ω-vinyl amides.[5d] Accordingly, Joullié[6] and de Meijere[7] also utilized intramolecular Kulinkovich reaction to access various bicyclic aminocyclopropanes.

In their synthesis of bicyclic *N,N*-dimethylcyclopropylamines, Joullié and coworkers utilized intermediates that were made from proteinogenic amino acids, such as phenylalanine, tyrosine, and tryptophan.[6a] The proposed mechanism is as follows.[6a] Reaction of $ClTi(O\textit{i}Pr)_3$ with 2 equivalents of cyclopentylmagnesium chloride affords titanacyclopropane intermediate **4** (Scheme 3.1). Subsequent olefin exchange with allyl compound **1** leads to titanacyclopropane intermediate **5** and **7**. The following step, **5** to **6**

and **7** to **8** involves position-selective expansion of the titanacyclopropane ring by insertion of the amide carbonyl moiety between Ti and the more substituted carbon. The most favorable conformation (**5**) has the α-substituent of the amide group in a β-position and *anti* to the hydrogen of the most substituted carbon of the titanacyclopropane. This carbon retains its stereochemical integrity in the corresponding bicyclic intermediate (**6**). Conversion of **6** to major product **2** occurs with retention of configuration of the carbon carrying the dimethylamino group. The final conversion to the desired aminocyclopropane rather than the cyclopropanol could be explained by the oxophilicity of titanium and the poor leaving group properties of the amine.

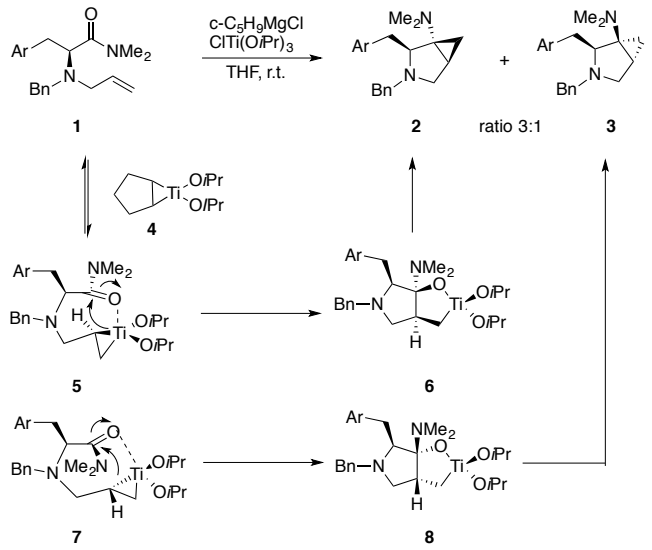

Scheme 3.1. Proposed mechanism and diastereoselectivity of products.

Starting materials for the intramolecular Kulinkovich reaction were generated by amino acids (Scheme 3.2).[6a] An aromatic amino acid (**9**) was converted to the corresponding methyl ester, which then underwent reductive amination with benzaldehyde and sodium borohydride triacetate to afford the secondary amine **10**. Subsequent allylation followed by aminolysis of the methyl ester furnished the amide **1**, which was then treated under intramolecular aminocyclopropanation reaction to afford two diastereomeric bicyclic

compounds, **2** and **3** in isolated yields ranging from 78-83%. The diastereomeric ratio obtained was approximately 3:1 for all amino acid variants.

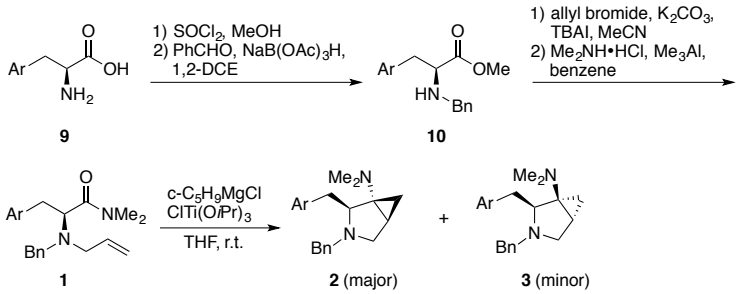

Scheme 3.2. General synthetic scheme to generate azabicyclic [3.1.0]aminocyclopropanes.

The absolute configuration of one of the major bicyclic compounds was determined by X-Ray analysis.[6a] Using a similar synthetic approach, [4.1.0] bicyclic systems were also made from phenylalanine and protected serine (Scheme 3.3).[6b] Homoallylation of **11** using Grieco's procedure [8] followed by aminolysis of the methyl ester afforded corresponding *N*-homoallylated products (**12**). Intramolecular aminocyclopropanation reaction of **12** furnished the desired [4.1.0] adducts **13** and **14** in greater diastereoselectivity (9:1) compared to [3.1.0] systems. The corresponding yields for this step were also acceptable (61-74%).

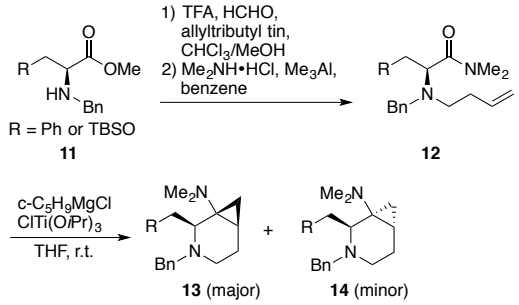

Scheme 3.3. General synthetic scheme to generate azabicyclic [4.1.0]aminocyclopropanes.

3.2) Ring-opening of bicyclic [3.1.0]-and [4.1.0]aminocyclopropanes

Generally, ring-opening of cyclopropanols is a relatively facile process compared to ring-opening of tertiary aminocyclopropanes, [9] which requires high temperatures, [10]

photooxidative, or aerobic oxidative conditions.[11] In 1973, in their pursuit of exploring aminocyclopropanes as synthetic homologues of enamines, Kuehne observed that unlike alkoxycyclopropanes, aminocyclopropanes are resistant to ring-opening under strongly acidic and basic conditions.[10] However, heating the bicyclic [3.1.0]- or [4.1.0]aminocyclopropanes at high temperatures in aqueous methanol in a sealed tube afforded the desired ring-opened ketones (Scheme 3.4).

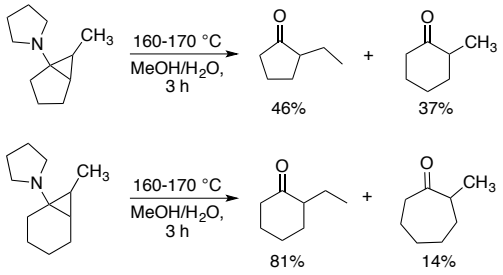

Scheme 3.4. Kuehne's thermolysis/hydrolysis ring-opening conditions.

The direction of cyclopropane ring-opening was found to favor protonation at the least substituted carbon, resulting predominantly in methylation rather than ring-expanded product (Scheme 3.4).[10] The relative increase in the ring-expanded product for bicyclic [3.1.0]aminocyclopropane relative to [4.1.0]-system could be attributed to more thermodynamically favorable release of ring strain. Efforts toward lowering the activation temperature for this reaction was also investigated by using 10% Pd/C as the adsorbing surface agent under refluxing aqueous methanol conditions. Interestingly, although the reaction time increased (1-2 days), Kuehne observed increased formation of ring-opened products, while almost completely suppressing the formation of ring-expanded products. For bicyclic [3.1.0]aminocyclopropane system, no ring-expanded product was observed, while as for [4.1.0]-system, only 3% of the ring-expanded product was formed.[10]

In 1997, photosensitized oxidative ring-opening of tertiary aminocyclopropanes were reported by Cha and coworkers.[11a] They envisioned applying the well-known, rapid rearrangement of cyclopropylcarbinyl radical to homoallyl radical on tertiary cyclopropylamines to obtain the corresponding cyclopropylamine cation radical. This process is known in the literature for cyclopropanol and cyclopropylthiols. Furthermore, analogous ring opening of cyclopropylamine radical cation has been implicated in the inactivation of cytochrome P-450 and monoamine oxidase by enzymatic oxidation of cyclopropylamines, establishing the potential of using aminium radicals for the ring-opening process.[11a] Tertiary amines have been widely utilized as efficient electron donors in electron transfer processes with excited states of various organic substrates due to their low ionization and oxidation potentials. Therefore, the photoinduced one-electron oxidation allows a convenient method for generating an amine radical cation. Cha and coworkers observed 1,4-dicyanobenzene (DCB) photosensitized oxidation of cyclopropylamine in degassed solution of 10:1 MeCN/MeOH containing K_2CO_3 by irradiation (254 or 300 nm) to give the corresponding ketone in good yield (Scheme 3.5).[11a]

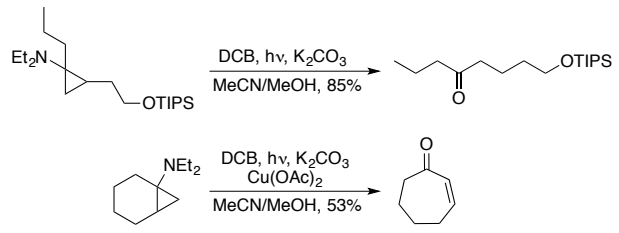

Scheme 3.5. Ring-opening under photosensitized oxidative conditions.

Although this methodology worked well for various monocyclic tertiary amines, application to bicyclic [4.1.0]aminocyclopropanes was unsuccessful. Addition of $Cu(OAc)_2$ provided the desired ring-opened product, albeit in low starting material

conversion.[11a] The proposed mechanism of this reaction is shown in Scheme 3.6. Initial formation of the tertiary aminium radical occurs by photoinduced electron transfer from the tertiary amine to DCB. The amine radical cation then undergoes either decay by back electron transfer or ring-opening to generate the β-iminium carbon radical. Subsequent hydrogen atom abstraction followed by aqueous workup affords the observed ring-opened ketone.[11a] The source of the H-atom for the abstraction process was proven by deuterium studies.

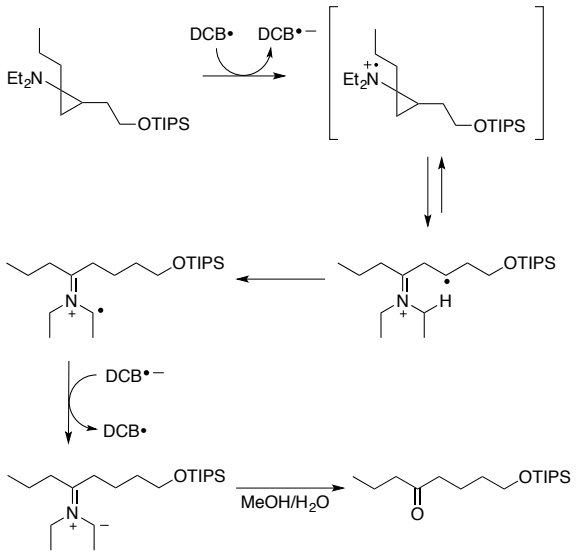

Scheme 3.6. Proposed mechanism for photosensitized oxidative ring-opening.

Cha and coworkers then developed a stereocontrolled synthesis of bicyclo[5.3.0]decan-3-ones, employing intramolecular Kulinkovich cyclopropanation of olefin-tethered amides followed by a tandem ring-expansion-cyclization sequence of the resulting bicyclic aminocyclopropanes by aerobic oxidation.[11b] As an extension to their previous study, they utilized *p*-anisidine as one of the substituents on the amine of the bicyclic [4.1.0]aminocyclopropane system in the hopes of lowering the amine oxidation potential. The lower potential was confirmed *via* cyclic voltammetry (CV). Their rationale was that

by lowering the oxidative potential, the formation of the tertiary aminium radical would be more facile. Surprisingly, they observed their intramolecular Kulinkovich adduct (**15**) to undergo oxidative ring-opening during silica gel column chromatography (Scheme 3.7). Since molecular oxygen was the only oxidant present, they examined the use of silica gel and fluorocarbon solvents which are known to possess high solubility of oxygen.[11b] Silica gel was indeed found to be an important component, as the cyclization took 3 days in the absence of silica gel in acetonitrile as opposed to 1 day. As expected, use of fluorinated solvent accelerated the reaction in the presence of silica gel to 1 h.

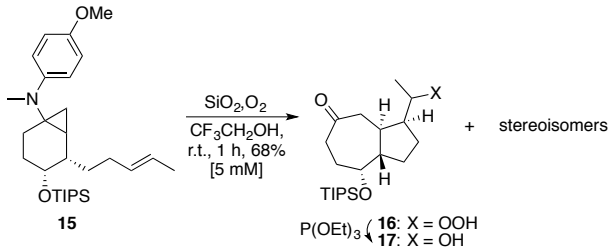

Scheme 3.7. Synthesis of bicyclo[5.3.0]decan-3-one by aerobic oxidation of cyclopropylamines.

Particularly noteworthy is the good diastereoselectivity (17:1) for **17** (as 1:1 epimers at the hydroxyl stereocenter following reduction with triethyl phosphite).[11b] Also, when *N*-phenyl derivative instead of *N*-*p*-anisidine derivative (**15**) was used under identical reaction conditions, it was found to be completely unreactive. Therefore, the presence of *N*-*p*-anisidine moiety is crucial to this methodology. The proposed mechanism is as follows (Scheme 3.8). Initial formation of the tertiary aminium radical **A** and superoxide occurs via one-electron oxidation with molecular oxygen. Subsequent ring cleavage generates the ring-expanded β-immonium carbon radical **B**, which then undergoes 5-hexenyl cyclization to afford **C**. The observed stereochemistry involving the *trans*-fused ring junction and the *cis*-side chain is believed to arise from the chair-like conformation having the alkenyl side chain equatorial.[11b] Finally, trapping of the resultant radical by

oxygen affords the peroxy radical **D** as a 1:1 epimeric mixture. Although the precise mechanistic pathway for the last step is unknown, an electron transfer between the peroxy radical **D** and tertiary amine **15** could be involved as the chain propagation step. Alternatively, the hydroperoxide could be formed by an electron transfer with superoxide.[11b] Aqueous workup furnishes the desired ketone **16** (Scheme 3.8).[11b]

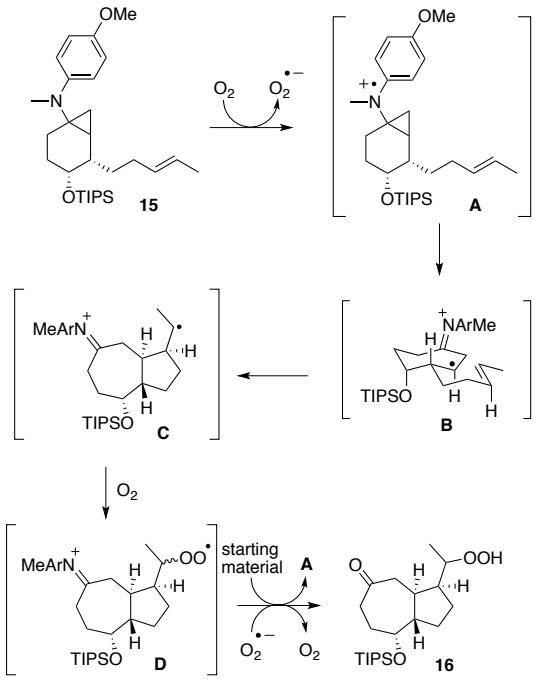

Scheme 3.8. Proposed mechanism for the synthesis of bicyclo[5.3.0]decan-3-one by aerobic oxidation of cyclopropylamines.

3.3) Ring-opening of azabicyclic [3.1.0]-and [4.1.0]aminocyclopropanes

Ring-opening of azabicyclic [3.1.0]-and [4.1.0]aminocyclopropanes affords 3-piperidinone and 3-azepinone derivatives respectively (Figure 3.1). Both piperidinones and azepinones are well-known in the literature for being biologically important motifs. More specifically, piperidinones are often used as intermediates in organic synthesis,[12] and azepinone moieties are found in pharmaceutically and biologically important

compounds.[13] Furthermore, azepinones are often synthetically challenging compounds due to their nitrogen-containing seven-membered ring.[14]

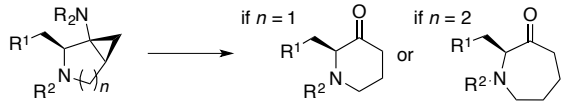

Figure 3.1. Ring-opening of azabicyclic [3.1.0]-and [4.1.0]aminocyclopropanes.

Based on known literature precedence,[10,11] we began our studies by testing traditional (i.e., SiO_2 and $FeCl_3$, pyridine, DMF) oxidative ring-opening of the strained aminocyclopropanes, which only resulted in decomposition of starting material.[15] Furthermore, following Cha's work,[11b] *N*-*p*-anisidine derivative was synthesized and employed under oxidative conditions, but these conditions also resulted in decomposition (Figure 3.2).[15]

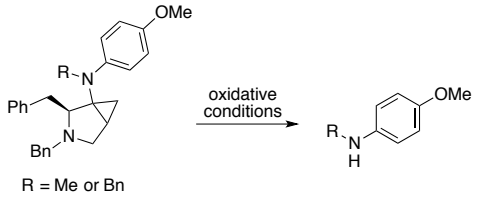

Figure 3.2. Failed ring-opening attempt under oxidative conditions.

Hence, a different approach was considered based on the work of Schulte-Wülwer and coworkers.[16] We envisioned that formation of the highly reactive *N*-chloroaminocyclopropane derivative followed by reaction with CuCl could induce a nitrogen radical formation/cleavage event (Scheme 3.9).[17]

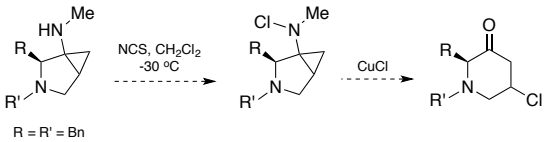

Scheme 3.9. CuCl approach to radical-induced cleavage of cyclopropylamines.

When previously synthesized phenylalanine aminocyclopropane[6] was employed in the proposed methodology, the desired selective monodeprotection of the *N*-

methylbenzylamine and subsequent chlorination were unsuccessful. More specifically, traditionally palladium-catalyzed hydrogenolysis displayed poor selectivity over the two secondary amines, and the subsequent chlorination product was highly unstable upon isolation. Therefore, in order to establish orthogonality within the route, the cyclic amine was protected as its benzenesulfonamide (Scheme 3.10).[17]

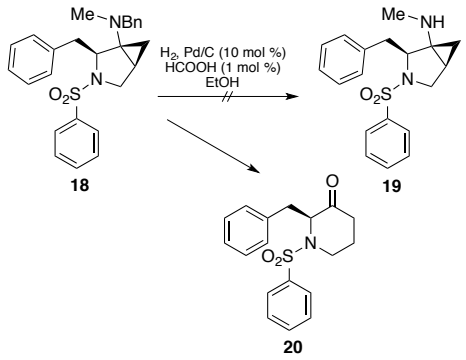

Scheme 3.10. Pd/C catalyzed hydrogenolysis/fragmentation.

Synthesis of azabicyclic [3.1.0]aminocyclopropane sulfonamide (**18**) was accomplished using previously reported methods[6] with minor changes in amine protecting group. We then turned our attention to hydrogenolysis of the benzylamine in order to proceed with *N*-chlorination. Although palladium-on-carbon catalyzed hydrogenolysis of benzylamines is generally known to be slow compared to hydrogenolysis of benzyl ethers, this process could be expedited in the presence of a protic acid.[17] Therefore, **18** was treated with 10% Pd/C in the presence of formic acid under an atmosphere of hydrogen. Surprisingly, instead of affording the debenzylated product (**19**), the ring-opened product (**20**) was obtained in synthetically useful yield (Scheme 3.10). The ring-opening presumably occurs *via* debenzylation followed by protonation of the cyclopropane ring followed by hydrolysis of the intermediate imine to the ketone.[17]

Next, we synthesized a variety of azabicyclic [3.1.0]- and [4.1.0]aminocyclopropanes using a modified procedure to test the scope of the reaction (Scheme 3.11).

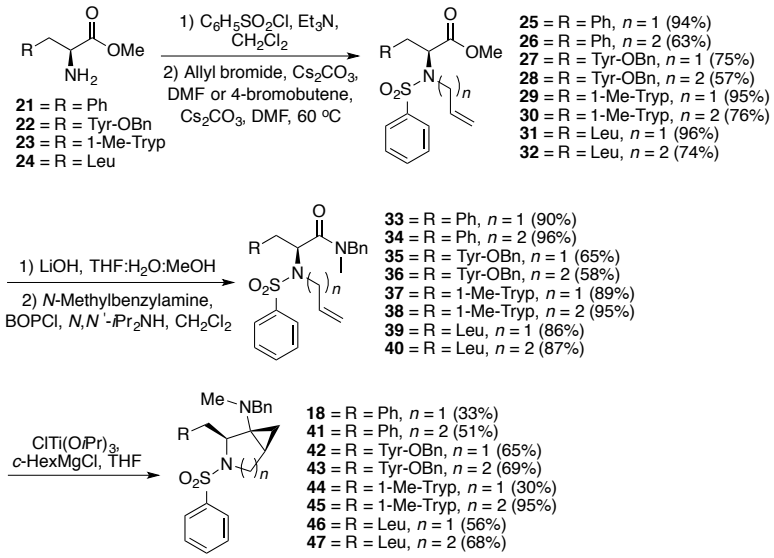

Scheme 3.11. Synthesis of azabicyclic [3.1.0]- and [4.1.0]aminocyclopropane derivatives.

The syntheses of allylsulfonamides (n = 1) **25**, **27**, **29**, and **31** proceeded in good yields, where as the corresponding homoallylsulfonamides (n = 2) were found to be less reactive under the same reaction conditions due to the reduced nucleophilicity of the sulfonamide nitrogen and resulted in lower yields.[17] Other homoallylation conditions were explored with various bases such as *n*-BuLi, LiHMDS, and NaH, but they resulted solely in the recovery of starting material. Reductive alkylation with allyltributylstannane[6b] also only afforded starting material, even after prolonged reaction times. Saponification of the methyl ester followed by BOPCl mediated coupling of the acid and *N*-methylbenzylamine afforded **33**-**40** in good yields considering this difficult coupling. Finally, exposure of the allylsulfonamide or homoallylsulfonamide under previously established[6] intramolecular Kulinkovich conditions furnished the corresponding aminocyclopropanes in moderate to good yields. It is important to note that for certain

homoallylsulfonamide substrates, it was necessary to replace $ClTi(O\textit{i}Pr)_3$ with $MeTi(O\textit{i}Pr)_3$ to obtain the desired product, since the former resulted in no reaction.[7c] The general decrease in yield observed for the synthesis of azabicyclic [3.1.0] ring system compared to that of [4.1.0] system could be attributed to increase in ring strain of five-membered compared to six-membered ring formations.[17]

With the various Kulinkovich adducts in hand, the scope of the ring-opening reaction was investigated. Exposure of the aminocyclopropanes to 10% Pd/C and catalytic amount of formic acid (88% solution) afforded the corresponding 3-piperidinone and 3-azepinone derivatives in satisfactory yields (Table 3.1).[17]

Table 3.1. Scope of ring-opening reactions of azabicyclic [3.1.0]- and [4.1.0]aminocyclopropanes.

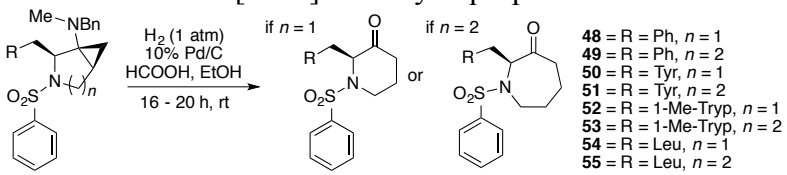

48 = R = Ph, n = 1
49 = R = Ph, n = 2
50 = R = Tyr, n = 1
51 = R = Tyr, n = 2
52 = R = 1-Me-Tryp, n = 1
53 = R = 1-Me-Tryp, n = 2
54 = R = Leu, n = 1
55 = R = Leu, n = 2

entry	R	n	10% Pd/C	HCOOH (equiv.)	yield (%)[a]
1		1	0.1	0.01	65
2		2	0.2	0.01	62
3[b]	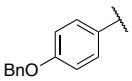	1	0.1	0.01	75
4[b]	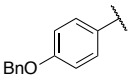	2	0.1	0.01	76
5	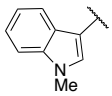	1	0.1	0.01	69
6	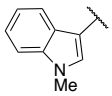	2	0.2	0.01	27
7		1	0.1	0.01	64
8		2	0.5	0.01	42
9		1	0.5	0	no product formation[c]
10		1	0	neat	no reaction[d]
11		1	0.1	neat	no reaction[d]

[a] Silica gel chromatography yields
[b] Benzyl ether moiety of tyrosine transformed to afford the corresponding alcohol under the reaction conditions
[c] Reaction time was prolonged to 48h
[d] Recovery of starting material

The presence of catalytic amounts of both palladium and formic acid proved to be essential for the reaction (Table 3.1). For instance, subjecting the cyclopropylamine to a solution of formic acid resulted in recovery of starting material, proving the need for palladium (entry 10, Table 3.1). Alternatively, when the cyclopropylamine was subjected

under a hydrogen atmosphere with catalytic amount of palladium in the absence of formic acid, only insignificant amount of debenzylated amine was obtained over prolonged reaction time (entry 9, Table 3.1). Moreover, the importance of catalytic addition of formic acid was evident when the cyclopropylamine was exposed under a hydrogen atmosphere with catalytic amount of palladium in neat formic acid (entry 11, Table 3.1). Overall, the ring-opening methodology on various azabicyclic [3.1.0] and [4.1.0] substrates proved to be generally acceptable, whereas in some cases the formation of 3-piperidinone is more favorable than 3-azepinone (Table 3.1). This observation could be attributed to the well-accepted fact that six-membered ring formations are more favorable than seven-membered ring formations.[17] More specifically, 3-azepinone formations of structurally more complex tryptophan and leucine derivatives (entries 6 and 8, Table 3.1) resulted in lower yields in comparison to the respective formations of 3-piperidinone (entries 5 and 7, Table 3.1).

3.4) Conclusions

Though there have been reports[18,19] of ring-opening of monocyclic aminocyclopropanes under catalytic hydrogenolysis conditions in the literature, ring-opening of corresponding azabicylic aminocyclopropanes under the same conditions was known to be synthetically challenging. To the best of our knowledge, no ring-opening reactions of azabicylic aminocyclopropanes have been reported under the conditions presented, thus establishing novelty in our methodology.[17] The optimized reaction condition is rather mild in that it does not require heating or the use of harsh oxidants. Furthermore, the use of a sulfonamide as a protecting group may also provide interesting antimicrobial activities

when coupled with the conformationally constrained Kulinkovich products. These interesting substrates could be tested for biological activity in due course.

3.5) Experimental results

General Methods. All reactions were performed under an argon atmosphere except where otherwise noted. Tetrahydrofuran was distilled over sodium-benzophenone, dichloromethane was distilled over calcium hydride, DMF in Acroseal bottles were used without further purification prior to use. Flash chromatography was carried out on Merck silica gel 60 (240-400 mesh) using the solvent conditions listed under individual experiments. Analytical thin-layer chromatography was performed on Merck silica gel (60F-254) plates (0.25 mm). Visualization was effected with ultraviolet light or phosphomolybdic acid (PMA) stain. Proton magnetic resonance spectra (^{1}H NMR) and Carbon magnetic resonance spectra (^{13}C NMR) were performed on a Bruker DRX-500 operating at 500 and 125 MHz respectively. Infrared spectra (IR) were obtained on a Perkin-Elmer 281-B spectrometer. High resolution mass spectra (HRMS) were obtained on a Micromass Autospec or a Waters LCTOF-Xe premier. Optical rotations were measured on a Jasco P-1010 polarimeter.

General methodology of *N*-allylsulfonamide formation:

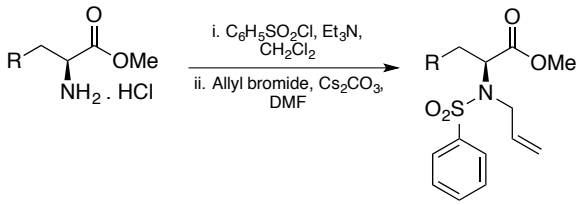

To a solution of (L)-amino acid methyl ester hydrochloride salt (14 mmol) in dichloromethane (0.2 M) was added triethylamine (28 mmol) and benzenesulfonyl

chloride (15.4 mmol). The solution was stirred until TLC analysis showed the reaction to be complete. The reaction was quenched with H_2O (10 mL) and the organics washed sequentially with 10% HCl (10 mL), $NaHCO_3$ (20 mL), and brine (20 mL). The organic layer was dried over $MgSO_4$ and reduced *in vacuo*. The crude material was subjected to silica gel flash chromatography to afford the corresponding sulfonamide.

To a solution of sulfonamide (2.3 mmol) in DMF (0.15 M) was added Cs_2CO_3 (3.5 mmol), and the resultant mixture stirred for 30 mins. Allyl bromide (4.7 mmol) was added in one portion *via* syringe, and the mixture stirred until TLC analysis indicated reaction completion. The solvent was removed *in vacuo* and the residue was dissolved in EtOAc, washed with H_2O (2 x 10 mL) and the organics dried over Na_2SO_4 and reduced *in vacuo*. The crude material was subjected to silica gel flash chromatography to yield the corresponding allylsulfonamide.

General methodology of *N*-homoallylsulfonamide formation:

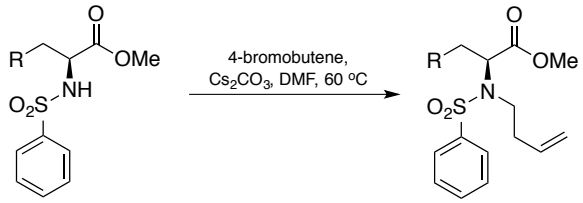

To a solution of sulfonamide (1.7 mmol) in DMF (0.02 M) was added Cs_2CO_3 (1.7 mmol), and the resultant mixture stirred at 60 ºC for 30 mins. To this mixture was added 4-bromobutene (3.5 mmol) dropwise *via* syringe, and the mixture stirred for a further 6 hrs. After this time the solvent was removed *in vacuo* and the residue was dissolved in EtOAc, washed with H_2O (2 x 10 mL) and the organics dried over Na_2SO_4 and reduced *in vacuo*. The crude material was subjected to silica gel flash chromatography to yield the corresponding homoallylsulfonamide.

General methodology of (*S*)-2-(*N*-allylphenylsulfonamido)-*N*-benzyl-*N*-methyl amide formation:

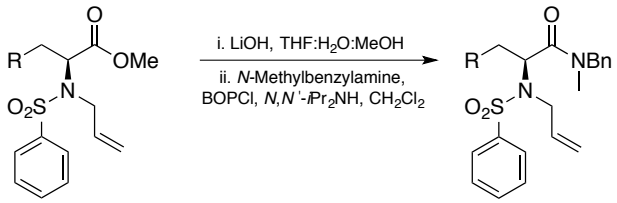

The *N*-allylsulfonamide (1.8 mmol) was dissolved in an equal mixture of THF, MeOH, and H_2O (0.1 M) and cooled to 0 ºC. To this was added $LiOH \cdot H_2O$ (5.4 mmol) and the stirred reaction mixture was warmed to room temperature over 3 hrs. After this time the volatiles were reduced *in vacuo* and the aqueous layer washed with Et_2O (10 mL). The aqueous portion was acidified to pH 3 with 10% HCl solution and extracted with EtOAc (3 x 30 mL). The organics were dried over Na_2SO_4 and reduced *in vacuo* to provide the crude acid, which was carried on without further purification.

The crude acid (1.4 mmol) was dissolved in CH_2Cl_2 (0.2 M) and cooled to 0 ºC under an argon atmosphere. To this solution was added *N*-methylbenzylamine (1.5 mmol), BOPCl (1.6 mmol), and Et_3N (1.7 mmol). The resultant solution was stirred for 12 hrs and after this time diluted with EtOAc (10 mL) and washed with 10% HCl (5 mL), sat. $NaHCO_3$ (10 mL), and brine (10 mL). The organics were dried over Na_2SO_4 and reduced *in vacuo* and the crude material was subjected to silica gel flash chromatography to afford the corresponding *N*-methylamide.

General methodology of (*S*)-*N*-benzyl-2-(*N*-(but-3-en-1-yl)phenylsulfonamido)-*N*-methyl amide formation:

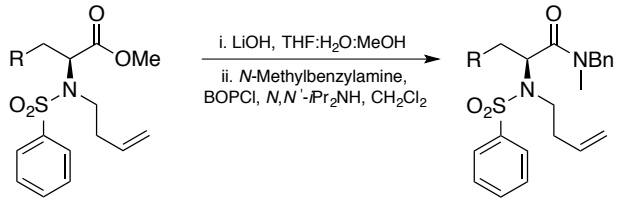

The sulfonamide (0.4 mmol) was dissolved in an equal mixture of THF, MeOH, and H_2O (0.1 M) and cooled to 0 ºC. To this was added $LiOH{\cdot}H_2O$ (1.1 mmol) and the stirred reaction mixture was warmed to rt over 3 hrs. After this time the volatiles were reduced *in vacuo* and the aqueous layer washed with Et_2O (10 mL). The aqueous portion was acidified to pH 3 with 10% HCl solution and extracted with EtOAc (3 x 20 mL). The organics were dried over Na_2SO_4 and reduced *in vacuo* to provide the crude acid, which was carried on without further purification.

The crude acid (0.2 mmol) was dissolved in CH_2Cl_2 (0.2 M) and cooled to 0 ºC under an argon atmosphere. To this solution was added *N*-methylbenzylamine (0.25 mmol), BOPCl (0.25 mmol), and Et_3N (0.26 mmol). The resultant solution was stirred for 12 hrs and after this time diluted with EtOAc (10 mL) and washed with 10% HCl (5 mL), sat. $NaHCO_3$ (10 mL), and brine (10 mL). The organics were dried over Na_2SO_4 and reduced *in vacuo* and the crude material was subjected to silica gel flash chromatography to afford the corresponding *N*-methylamide.

General methodology of azabicyclic [3.1.0] aminocyclopropane formation:

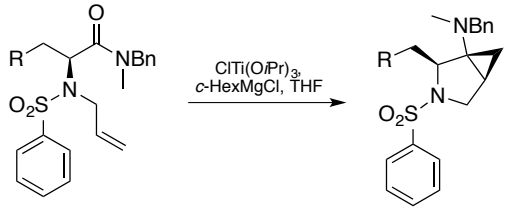

To a solution of the *N*-methylamide (1.1 mmol) in THF (0.1M) under an argon atmosphere was added $ClTi(OiPr)_3$ (1.1 mL, 1M) dropwise *via* syringe. To this solution was added cyclohexylMgCl or cyclohexylMgBr (2.5 mL, 2M) dropwise *via* syringe pump addition over 1 hr. The solution gradually changed color from colorless to dark yellow and finally black over the course of 3 hrs. TLC analysis showed reaction completion, and the reaction mixture was poured onto ice water (20 mL) and stirred for 15 mins. The crude mixture was filtered thorough celite to remove titanium residues, and the two layers separated. The aqueous layer was extracted once with EtOAc (20 mL) and the combined organics washed with brine (20 mL) and dried over Na_2SO_4. The crude mixture was subjected to silica gel flash chromatography to isolate the corresponding major diastereomer aminocyclopropane.

General methodology of azabicyclic [4.1.0] aminocyclopropane formation:

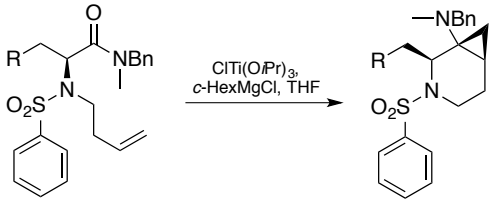

To a solution of the *N*-methylamide (0.3 mmol) in THF (0.05M) under an argon atmosphere was added $ClTi(OiPr)_3$ or $MeTi(OiPr)_3$ (1.3 mL, 0.3M) dropwise *via* syringe. To this solution was added cyclohexylMgCl or cyclohexyl MgBr (0.8 mL, 2M) dropwise *via* syringe pump addition over 1 hr. The solution gradually changed color from colorless to dark yellow and finally black over the course of 4 hrs. TLC analysis showed reaction completion, and the reaction mixture was poured onto ice water (20 mL) and stirred for 15 mins. The crude mixture was filtered thorough celite to remove titanium residues, and the two layers separated. The aqueous layer was extracted once with

EtOAc (20 mL) and the combined organics washed with brine (20 mL) and dried over Na_2SO_4. The crude mixture was subjected to silica gel flash chromatography to isolate the corresponding major diastereomer aminocyclopropane.

General methodology of 3-piperidinone formation:

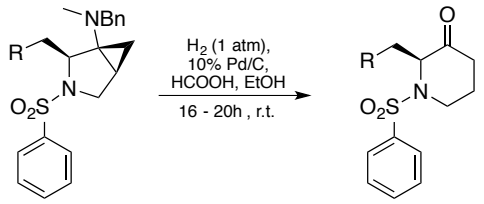

A solution of aminocyclopropane (21 mg, 38 μmol) in EtOH (0.4 mL, 0.1M) was charged with 10% Pd/C (4 mg, 3.8 μmol) and 88% formic acid (14.6 μL, 0.3 μmol) and the system purged with H_2 three times. The mixture was stirred for 16-20 hrs at room temperature under an atmosphere of H_2, after which time the inorganic material was removed *via* filtration and the solvent reduced *in vacuo*. The crude material was subjected to silica gel flash chromatography to give the corresponding piperidinone.

General methodology of 3-azepinone formation:

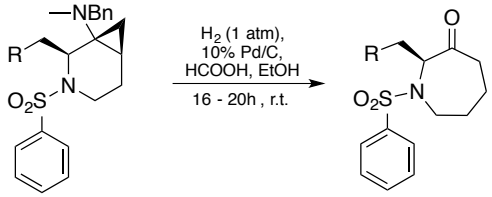

A solution of aminocyclopropane (21 mg, 38 μmol) in EtOH (0.4 mL, 0.1M) was charged with 10% Pd/C (4 mg, 3.8 μmol) and 88% formic acid (14.6 μL, 0.3 μmol) and the system purged with H_2 three times. The mixture was stirred for 16-20 hrs at room temperature under an atmosphere of H_2, after which time the inorganic material was removed *via* filtration and the solvent reduced *in vacuo*. The crude material was subjected to silica gel flash chromatography to give the corresponding 3-azepinone.

Specific experimental procedures & characterizations

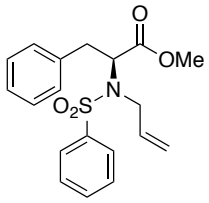

(*S*)-methyl 2-(*N*-allylphenylsulfonamido)-3-phenylpropanoate (25).

Following general procedure for *N*-allylsulfonamide formation, in a solution of the known sulfonamide[i] (0.50 g, 1.56 mmol) in DMF (10.4 mL) was added Cs_2CO_3 (0.76 g, 2.35 mmol) at room temperature. After 30 min, allylbromide (0.27 mL, 3.13 mmol) was added, and the resulting mixture was left to stir at room temperature for 6 h to afford the crude *N*-allylphenylsulfonamide upon work-up. Purification by silica gel chromatography (20% ethyl acetate in hexanes) gave the title compound as light orange oil (0.56 g, quant.). R_f = 0.4 (20% ethyl acetate in hexanes). $[\alpha]_D^{29.4} = -37.6$ (*c* = 0.5 CH_2Cl_2). FTIR (thin film) cm^{-1}: 3065, 3029, 2952, 1743, 1641, 1604, 1585, 1497, 1479, 1447, 1420, 1346, 1288, 1224, 1162, 1128, 1091, 1072, 1057, 1031, 999, 928, 875, 836, 743, 700, 690, 613, 596, 573, 510. HRMS (ESI) m/z calcd. $C_{19}H_{21}NO_4NaS$ $[M+Na]^+$ 382.1089, found 382.1081. ^{1}H-NMR (500 MHz; $CDCl_3$): δ 7.69 (dd, *J* = 8.4, 1.3 Hz, 2H), 7.53 (dd, *J* = 7.7, 1.4 Hz, 1H), 7.44-7.41 (m, 2H), 7.30-7.19 (m, 5H), 5.73 (ddt, *J* = 17.0, 10.3, 6.5 Hz, 1H), 5.20 (dd, *J* = 17.2, 1.4 Hz, 1H), 5.11 (dd, *J* = 10.2, 1.3 Hz, 1H), 4.84 (t, *J* = 7.6 Hz, 1H), 3.98-3.86 (m, 2H), 3.47-3.46 (m, 3H), 3.32 (dd, *J* = 14.0, 7.7 Hz, 1H), 2.98 (dd, *J* = 14.1, 7.6 Hz, 1H). ^{13}C-NMR ($CDCl_3$, 125 MHz): 170.9, 140.1, 136.8, 134.6, 132.6, 129.3, 128.9, 128.7, 127.6, 127.0, 118.2, 61.0, 52.1, 48.5, 36.7.

[i] Ruano, J. L. G.; Parra, A.; Yuste, F.; Mastranzo, V. M. *Synthesis* **2008**, *2*, 311.

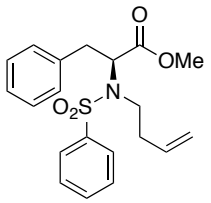

(*S*)-methyl 2-(*N*-(but-3-en-1-yl)phenylsulfonamido)-3-phenylpropanoate (26). Following the general procedure for *N*-homoallylsulfonamide formation, in a solution of the known sulfonamide[i] (0.54 g, 1.70 mmol) in DMF (85 mL) was added Cs_2CO_3 (0.55 g, 1.70 mmol), and the resultant mixture stirred at 60 ºC for 30 mins. To this mixture was added 4-bromobutene (0.35 mL, 3.50 mmol) dropwise *via* syringe, and the mixture stirred for a further 6 hrs. Upon work-up, the crude product was obtained as an oil. Purification by silica gel chromatography (15% ethyl acetate in hexanes) afforded the title compound as an oil (0.33 g, 53%). R_f = 0.3 (15% ethyl acetate in hexanes). $[\alpha]_D^{28.5}$ = –36.8 (*c* = 0.4 $CHCl_3$). FTIR (thin film) cm^{-1}: 3065, 3029, 3003, 2978, 2951, 1742, 1641, 1604, 1585, 1496, 1479, 1446, 1345, 1289, 1222, 1163, 1130, 1090, 1072, 1000, 920, 839, 740, 699, 691, 598, 574, 556, 511. HRMS (ESI) m/z calcd. $C_{20}H_{23}NO_4NaS$ $[M+Na]^+$ 396.1245, found 396.1254. ^{1}H-NMR (500 MHz; $CDCl_3$): δ 7.73 (d, *J* = 7.2 Hz, 2H), 7.54 (tt, *J* = 7.4, 1.5 Hz, 1H), 7.44 (t, *J* = 7.9 Hz, 2H), 7.29-7.18 (m, 6H), 5.70 (ddt, *J* = 17.1, 10.3, 6.8 Hz, 1H), 5.08-5.02 (m, 2H), 4.79 (dd, *J* = 8.2, 7.1 Hz, 1H), 3.46-3.42 (m, 3H), 3.37 (ddd, *J* = 15.3, 10.3, 5.3 Hz, 1H), 3.31-3.25 (m, 2H), 2.94 (dd, *J* = 13.9, 7.0 Hz, 1H), 2.43-2.27 (m, 2H). ^{13}C-NMR ($CDCl_3$, 125 MHz): 170.9, 140.0, 136.6, 134.8, 132.7, 129.2, 128.9, 128.7, 127.5, 127.1, 117.2, 61.2, 52.1, 45.5, 37.0, 35.0.

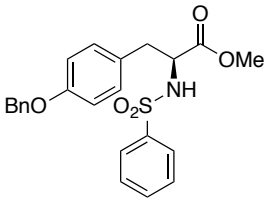

(*S*)-methyl 3-(4-(benzyloxy)phenyl)-2-(phenylsulfonamido)propanoate (22). Following general procedure of *N*-sulfonamide formation, to a solution of *O*Bn-tyrosine methyl ester hydrochloride salt (4.5 g, 14 mmol) in CH_2Cl_2 (28 mL) was added triethylamine (4 mL, 28 mmol) and benzenesulfonyl chloride (2 mL, 15.4 mmol). The solution was stirred for 30 min, whereupon TLC analysis showed the reaction to be complete. The reaction was quenched with H_2O (10 mL) and the organics washed sequentially with 10% HCl (10 mL), $NaHCO_3$ (20 mL), and brine (20 mL). The organic layer was dried over $MgSO_4$, filtered, and reduced *in vacuo* to afford a white solid that was recrystallized from Et_2O to give the title compound (5.1 g, 86%) as a white crystalline solid. Rf = 0.45 (30% ethyl acetate in hexanes). $[\alpha]_D^{18.6}$ = +2.46 (*c* = 1.09 $CHCl_3$). FTIR (thin film) cm^{-1}: 3290, 1740, 1613, 1586, 1513, 1448, 1350, 1329, 1249, 1164, 1155. HRMS (ESI) m/z calcd. $C_{23}H_{23}NNaO_5S$ $[M+Na]^+$ 444.1195, found 448.1182. ^{1}H-NMR (500 MHz; $CDCl_3$): δ 7.76-7.74 (m, 2H), 7.52 (tt, *J* = 7.4, 1.6 Hz, 1H), 7.45-7.36 (m, 7H), 7.32 (ddt, *J* = 7.6, 2.5, 2.1 Hz, 1H), 6.98-6.95 (m, 2H), 6.85-6.82 (m, 2H), 5.01 (d, *J* = 6.8 Hz, 3H), 4.18 (dt, *J* = 9.2, 5.9 Hz, 1H), 3.47 (s, 3H), 2.97 (dd, *J* = 5.9, 1.6 Hz, 2H). ^{13}C-NMR ($CDCl_3$, 125 MHz): 171.1, 158.0, 139.6, 136.9, 132.6, 130.4, 128.9, 128.5, 127.9, 127.4, 127.1, 127.0, 114.9, 69.9, 56.7, 52.3, 38.5.

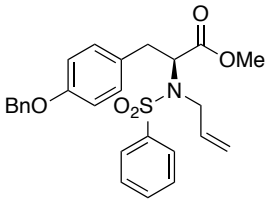

(*S*)-methyl 2-(*N*-allylphenylsulfonamido)-3-(4-(benzyloxy)phenyl)propanoate (27). Following the general procedure of *N*-allylsulfonamide formation, to a solution of sulfonamide **22** (1 g, 2.3 mmol) in DMF (16 mL, 0.15 M) was added Cs_2CO_3 (1.1g, 3.5 mmol), and the resultant mixture stirred at RT for 30 mins, whereupon a color change of white to straw yellow was observed. Allylbromide (0.4 mL, 4.7 mmol) was added and the mixture stirred for a further 1 hr. TLC analysis indicated reaction completion. The solvent was removed *in vacuo* and the residue was dissolved in EtOAc, washed with H_2O (2 x 10 mL) and the organics dried over Na_2SO_4 and reduced *in vacuo*. The crude material was subjected to silica gel chromatography (20% ethyl acetate in hexanes) to yield the allylsulfonamide **10** (0.8 g, 75%) as a clear oil. R_f = 0.3 (20% ethyl acetate in hexanes). $[\alpha]_D^{20.2} = -26.55$ (*c* = 1.0 $CHCl_3$). FTIR (thin film) cm^{-1}: 3007, 3064, 3022, 2950, 1741, 1640, 1611, 1584, 1512, 1447, 1345, 1243, 1160, 1091, 1024. HRMS (ESI) m/z calcd. $C_{26}H_{28}NNaO_5S$ $[M+Na]^+$ 466.1688, found 466.1686. ^{1}H-NMR (500 MHz; $CDCl_3$): δ 7.72-7.70 (m, 2H), 7.52 (t, *J* = 7.4 Hz, 1H), 7.46-7.38 (m, 6H), 7.32 (t, *J* = 7.23 Hz, 1H), 7.10 (d, *J* = 8.57 Hz, 2H), 6.88 (d, *J* = 8.59 2H), 5.74 (ddt, *J* = 17.0, 10.4, 6.4 Hz, 1H), 5.19 (dd, *J* = 17.2, 1.2 Hz, 1H), 5.12-5.10 (m, 1H), 5.03 (s, 2H), 4.77 (t, *J* = 7.6 Hz, 1H), 3.93 (qd, *J* = 17.3, 6.3 Hz, 2H), 3.48 (s, 3H), 3.25 (dd, *J* = 14.1, 7.8 Hz, 1H), 2.92 (dd, *J* = 14.1, 7.5 Hz, 1H). ^{13}C-NMR ($CDCl_3$, 125 MHz): 170.8, 157.7, 140.1, 137.0, 134.5, 132.4, 130.2, 128.9, 128.6, 128.5, 127.8, 127.43, 127.41, 127.0, 117.9, 114.9, 69.9, 61.0, 53.3, 51.8, 48.3, 35.8

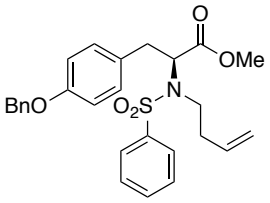

(*S*)-methyl 3-(4-(benzyloxy)phenyl)-2-(*N*-(but-3-en-1-yl)phenylsulfonamido)propanoate (28). Following the general procedure for *N*-homoallylsulfonamide formation, to a solution of sulfonamide **22** (0.7 g, 1.7 mmol) in DMF (70 mL) was added Cs_2CO_3 (0.5 g, 1.7 mmol), and the resultant mixture stirred at 60 ºC for 30 mins. To this mixture was added 4-bromobutene (0.3 mL, 3.5 mmol) dropwise *via* syringe, and the mixture stirred for a further 6 hrs. Aqueous work-up afforded the crude material which was subjected to silica gel chromatography (5% ethyl acetate in hexanes) to afford the title compound as a clear oil (0.4 g, 57%). R_f = 0.3 (20% ethyl acetate in hexanes). $[\alpha]_D^{20.2} = -26.55$ (c = 1.0 $CHCl_3$). FTIR (thin film) cm^{-1}: 3007, 3064, 3022, 2950, 1741, 1640, 1611, 1584, 1512, 1447, 1345, 1243, 1160, 1091, 1024. HRMS (ESI) m/z calcd. $C_{26}H_{28}NNaO_5S$ $[M+Na]^+$ 466.1688, found 466.1686. ^{1}H-NMR (500 MHz; $CDCl_3$): δ 7.76-7.72 (m, 2H), 7.53 (t, J = 7.4 Hz, 1H), 7.45-7.36 (m, 7H), 7.34 (dt, J = 11.6, 5.6 Hz, 1H), 7.11 (d, J = 8.6 Hz, 2H), 6.89 (d, J = 8.6 Hz, 2H), 5.72 (ddt, J = 17.1, 10.3, 6.8 Hz, 1H), 5.09-5.01 (m, 4H), 4.75 (t, J = 8.0 Hz, 1H), 3.47-3.42 (m, 3H), 3.41-3.27 (m, 2H), 3.25 (dt, J = 14.2, 7.2 Hz, 1H), 2.90 (dd, J = 14.0, 6.9 Hz, 1H), 2.46-2.28 (m, 2H). ^{13}C-NMR ($CDCl_3$, 125 MHz): 170.8, 157.7, 140.1, 137.0, 134.5, 132.4, 130.2, 128.9, 128.6, 128.5, 127.8, 127.43, 127.41, 127.0, 117.9, 114.9, 69.9, 61.0, 53.3, 51.8, 48.3, 35.8.

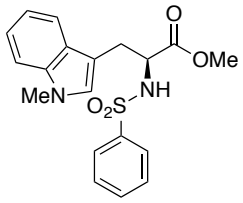

(*S*)-methyl 3-(1-methyl-1H-indol-3-yl)-2-(phenylsulfonamido)propanoate (23). Following the general procedure for *N*-allylphenylsulfonamide formation, the sulfonamide was synthesized by treating (2*S*)-2-Amino-3-(1-methyl-1*H*-indol-3-yl)propionic acid methyl ester hydrochloride (1.06 g, 4.56 mmol) in CH_2Cl_2 (23 mL) with triethylamine (0.73 mL, 11.4 mmol), and benzenesulfonyl chloride (0.58 mL, 4.56 mmol) at room temperature for 6 h to afford the crude sulfonamide product. Purification by silica gel column (35% ethyl acetate in hexanes) afforded the sulfonamide as a tan solid (1.51 g, 89%). R_f = 0.2 (30% ethyl acetate in hexanes). $[\alpha]_D^{27.3} = +7.2$ (*c* = 1.1 CH_2Cl_2). FTIR (thin film) cm^{-1}: 3283, 3057, 2952, 1744, 1615, 1585, 1550, 1475, 1447, 1331, 1277, 1253, 1204, 1164, 1129, 1092, 1012, 944, 916, 848, 822, 743, 721, 688, 591, 564, 522. HRMS (ESI) m/z calcd. $C_{19}H_{20}N_2O_4NaS$ $[M+Na]^+$ 395.1041, found 395.1048. ^{1}H-NMR (500 MHz; $CDCl_3$): δ 7.73 (d, *J* = 7.9 Hz, 2H), 7.52-7.49 (m, 1H), 7.41 (dd, *J* = 6.8, 5.7 Hz, 3H), 7.26-7.18 (m, 2H), 7.06 (dd, *J* = 7.9, 7.0 Hz, 1H), 6.88-6.86 (m, 1H), 5.14 (t, *J* = 0.3 Hz, 1H), 4.29-4.26 (m, 1H), 3.71 (s, 3H), 3.42 (s, 3H), 3.24 (d, *J* = 5.4 Hz, 2H). ^{13}C- NMR ($CDCl_3$, 125 MHz): 171.6, 139.9, 137.0, 132.7, 129.0, 128.1, 127.9, 127.2, 121.9, 119.4, 118.7, 109.4, 107.4, 56.3, 52.5, 32.9, 29.4.

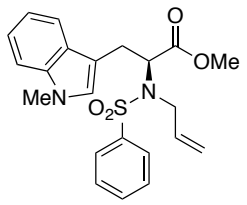

(*S*)-methyl 2-(*N*-allylphenylsulfonamido)-3-(1-methyl-1*H*-indol-3-yl)propanoate (29). Following general procedure for *N*-allylsulfonamide formation, sulfonamide **23** (0.5 g, 1.34 mmol) in DMF (9 mL) was added Cs_2CO_3 (0.66 g, 2.01 mmol) at room temperature. After 30 min, allylbromide (0.23 mL, 2.68 mmol) was added, and the resulting mixture was left to stir at room temperature for 6 h to afford the crude *N*-allylphenylsulfonamide. Purification by silica gel chromatography (20% ethyl acetate in hexanes) afforded the title compound as yellow oil (0.55 g, quant.). Rf = 0.4 (30% ethyl acetate in hexanes). $[\alpha]_D^{30.1} = -2.9$ (*c* = 0.8 CH_2Cl_2). FTIR (thin film) cm^{-1}: 3057, 3026, 2950, 1741, 1640, 1616, 1585, 1554, 1475, 1446, 1375, 1331, 1287, 1254, 1222, 1204, 1162, 1131, 1091, 1072, 1013, 999, 927, 879, 832, 742, 714, 690, 669, 585. HRMS (ESI) m/z calcd. $C_{22}H_{24}N_2O_4NaS$ $[M+Na]^+$ 435.1354, found 435.1363. ^{1}H-NMR (500 MHz; $CDCl_3$): δ 7.68 (d, *J* = 8.0 Hz, 2H), 7.58-7.47 (m, 2H), 7.38-7.36 (m, 2H), 7.27-7.20 (m, 3H), 7.13-7.10 (m, 1H), 6.93-6.79 (m, 1H), 5.77 (ddt, *J* = 16.9, 10.4, 6.4 Hz, 1H), 5.18 (d, *J* = 17.2 Hz, 1H), 5.07 (d, *J* = 10.2 Hz, 1H), 4.87 (t, *J* = 7.5 Hz, 1H), 4.03-3.90 (m, 2H), 3.67 (s, 3H), 3.46 (s, 4H), 3.12 (dd, *J* = 14.8, 7.3 Hz, 1H). ^{13}C-NMR ($CDCl_3$, 125 MHz): 171.3, 140.4, 137.0, 134.9, 132.5, 128.8, 128.0, 127.7, 127.5, 121.8, 119.2, 118.8, 118.0, 109.4, 109.2, 60.0, 52.1, 48.4, 32.8, 26.7.

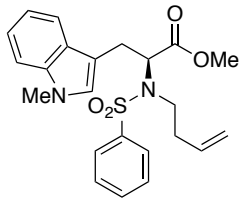

(*S*)-methyl 2-(*N*-(but-3-en-1-yl)phenylsulfonamido)-3-(1-methyl-1*H*-indol-3-yl)propanoate (30). Following the general procedure for *N*-homoallylsulfonamide formation, in a solution of sulfonamide **23** (0.50 g, 1.34 mmol) in DMF (67 mL) was added Cs_2CO_3 (0.44 g, 1.34 mmol), and the resultant mixture stirred at 60 ºC for 30 mins. To this mixture was added 4-bromobutene (0.28 mL, 2.77 mmol) dropwise *via* syringe, and the mixture stirred for a further 6 hrs. Upon work-up, the crude product was obtained as an oil. Purification by silica gel chromatography (20% ethyl acetate in hexanes) afforded the title compound as an oil (0.36 g, 63%). R_f = 0.3 (20% ethyl acetate in hexanes). $[\alpha]_D^{26.2} = +4.1$ (*c* = 0.5 $CHCl_3$). FTIR (thin film) cm^{-1}: 3059, 2950, 1741, 1640, 1615, 1553, 1475, 1446, 1375, 1342, 1254, 1222, 1203, 1162, 1132, 1090, 1073, 1012, 922, 838, 811, 741, 690, 666, 583, 550. HRMS (ESI) m/z calcd. $C_{23}H_{26}N_2O_4NaS$ $[M+Na]^+$ 449.1511, found 449.1528. ^{1}H-NMR (500 MHz; $CDCl_3$): δ 7.72 (d, *J* = 8.5 Hz, 2H), 7.57-7.49 (m, 2H), 7.39 (t, *J* = 7.1 Hz, 2H), 7.27-7.22 (m, 3H), 7.11 (t, *J* = 7.4 Hz, 1H), 6.88 (s, 1H), 5.74-5.65 (m, 1H), 5.04-4.99 (m, 2H), 4.84 (t, *J* = 7.5 Hz, 1H), 3.68 (s, 3H), 3.41 (s, 5H), 3.32 (dd, *J* = 10.2, 5.0 Hz, 1H), 3.10 (dd, *J* = 14.8, 7.2 Hz, 1H), 2.46-2.28 (m, 2H). ^{13}C-NMR ($CDCl_3$, 125 MHz): 171.3, 140.1, 137.0, 134.9, 132.5, 128.8, 127.8, 127.7, 127.5, 121.9, 119.3, 118.7, 117.1, 109.4, 109.1, 60.1, 52.0, 45.4, 35.3, 32.8, 26.9.

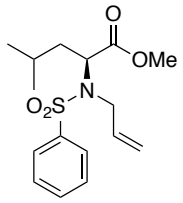

(*S*)-methyl 2-(*N*-allylphenylsulfonamido)-4-methylpentanoate (31). Following general procedure for *N*-allylsulfonamide formation, in a solution of the known sulfonamide[ii] (1.94 g, 7.01 mmol) in DMF (45 mL) was added Cs_2CO_3 (3.32 g, 10.5 mmol) at room temperature. After 30 min, allylbromide (1.15 mL, 14.0 mmol) was added, and the resulting mixture was left to stir at room temperature for 6 h to afford the crude *N*-allylphenylsulfonamide. Purification by silica gel chromatography (20% ethyl acetate in hexanes) gave the title compound as clear oil (2.11 g, 93%). R_f = 0.6 (30% ethyl acetate in hexanes). $[\alpha]_D^{27.2} = -64.1$ (*c* = 4.7 CH_2Cl_2). FTIR (thin film) cm^{-1}: 3069, 2956, 2868, 1742, 1447, 1345, 1165, 1090, 1048, 926, 869, 746, 690. HRMS (ESI) m/z calcd. $C_{16}H_{24}NO_4S$ $[M+H]^+$ 326.1426, found 326.1420. ^{1}H-NMR (500 MHz; $CDCl_3$): δ 7.83 (d, *J* = 7.9 Hz, 2H), 7.56 (t, *J* = 7.4 Hz, 1H), 7.50-7.47 (m, 2H), 5.88 (dddd, *J* = 17.2, 10.1, 7.2, 5.5 Hz, 1H), 5.17 (d, *J* = 17.2 Hz, 1H), 5.10 (d, *J* = 10.2 Hz, 1H), 4.61 (dd, *J* = 9.4, 5.6 Hz, 1H), 3.99 (dd, *J* = 16.6, 5.5 Hz, 1H), 3.82 (dd, *J* = 16.7, 7.2 Hz, 1H), 3.46 (s, 3H), 1.73-1.57 (m, 3H), 0.95 (d, *J* = 6.4 Hz, 3H), 0.89 (d, *J* = 6.6 Hz, 3H). ^{13}C-NMR ($CDCl_3$, 125 MHz): 172.0, 140.0, 135.8, 132.7, 128.9, 127.6, 117.4, 58.1, 52.0, 48.3, 39.2, 24.3, 22.7, 21.4.

[ii] Karrer, P.; Kehl, W. *Helv. Chim. Acta.* **1930**, *13*, 50.

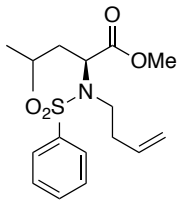

(*S*)-methyl 2-(*N*-(but-3-en-1-yl)phenylsulfonamido)-4-methylpentanoate (32). Following the general procedure for *N*-homoallylsulfonamide formation, in a solution of the known sulfonamide[ii] (0.50 g, 1.75 mmol) in DMF (88 mL) was added Cs_2CO_3 (0.57 g, 1.75 mmol), and the resultant mixture stirred at 60 ºC for 30 mins. To this mixture was added 4-bromobutene (0.37 mL, 3.61 mmol) dropwise *via* syringe, and the mixture stirred for a further 6 hrs. Upon work-up, the crude product was obtained as an oil. Purification by silica gel chromatography (10% ethyl acetate in hexanes) afforded the title compound as an oil (0.29 g, 49%). R_f = 0.2 (5% ethyl acetate in hexanes). $[\alpha]_D^{24.5}$ = –64.5 (*c* = 1.5 CH_2Cl_2). FTIR (thin film) cm^{-1}: 3065, 2955, 2868, 1742, 1635, 1447, 1344, 1269, 1248, 1165, 1152, 1090, 922, 740, 690. HRMS (ESI) m/z calcd. $C_{17}H_{26}NO_4S$ $[M+H]^+$ 340.1583, found 340.1597. ^{1}H-NMR (500 MHz; $CDCl_3$): δ 7.83 (d, *J* = 7.2 Hz, 3H), 7.58-7.55 (m, 1H), 7.51-7.47 (m, 3H), 5.77-5.69 (m, 1H), 5.09-5.02 (m, 2H), 4.57 (dd, *J* = 9.4, 5.5 Hz, 1H), 3.44-3.40 (m, 3H), 3.34 (ddd, *J* = 15.5, 10.7, 4.9 Hz, 1H), 3.18 (ddd, *J* = 15.6, 10.7, 5.2 Hz, 1H), 2.58-2.51 (m, 1H), 2.33-2.24 (m, 1H), 1.74-1.56 (m, 4H), 0.96 (dd, *J* = 9.6, 6.5 Hz, 7H). ^{13}C-NMR ($CDCl_3$, 125 MHz): 171.9, 139.8, 135.0, 132.7, 128.9, 127.6, 117.1, 58.2, 52.0, 45.5, 39.6, 35.8, 24.6, 23.0, 21.7.

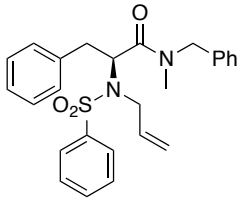

(*S*)-2-(*N*-allylphenylsulfonamido)-*N*-benzyl-*N*-methyl-3-phenylpropanamide (33). Following the general procedure for the amide formation, The

N-allylsulfonamide **25** (0.54 g, 1.57 mmol) was dissolved in an equal mixture of THF, MeOH, and H_2O (0.1 M) and cooled to 0 ºC. To this was added $LiOH{\cdot}H_2O$ (0.19 g, 4.55 mmol) and the stirred reaction mixture was warmed to room temperature over 3 hrs. After this time the volatiles were reduced *in vacuo* and the aqueous layer washed with Et_2O. The aqueous portion was acidified to pH 3 with 10% HCl solution and extracted with EtOAc. The organics were dried over Na_2SO_4 and reduced *in vacuo* to provide the crude acid, which was carried on without further purification. The crude acid (0.54 g, 1.57 mmol) was dissolved in CH_2Cl_2 (8 mL) and cooled to 0 ºC under an argon atmosphere. To this solution was added *N*-methylbenzylamine (0.22 mL, 1.73 mmol), BOPCl (0.48 g, 1.89 mmol), and Et_3N (0.26 mL, 1.89 mmol). The resultant solution was stirred for 12 hrs. Aqueous work-up afforded the crude material which was purified by silica gel chromatography (20% ethyl acetate in hexanes) to afford the title compound as a white solid (0.56 g, 80%). R_f = 0.3 (20% ethyl acetate in hexanes). $[\alpha]_D^{24.1} = -35.1$ (*c* = 0.7 CH_2Cl_2). FTIR (thin film) cm^{-1}: 3063, 3028, 2931, 1649, 1494, 1446, 1342, 1162, 1090, 1020, 928, 846, 799, 772, 730, 698, 596, 568. HRMS (ESI) m/z calcd. $C_{26}H_{28}N_2O_3NaS$ $[M+Na]^+$ 471.1718, found 471.1720. ^{1}H-NMR (500 MHz; $CDCl_3$): δ 7.86-7.84 (m, 2H), 7.60-7.49 (m, 3H), 7.26-7.12 (m, 8H), 7.04-7.03 (m, 1H), 6.92-6.90 (m, 1H), 6.64 (d, *J* = 7.7 Hz, 1H), 5.85 (dtt, *J* = 16.6, 11.0, 5.6 Hz, 1H), 5.17-5.08 (m, 2H), 4.14-4.02 (m, 3H), 3.36-3.28 (m, 1H), 2.73 (rotameric d, 3H). ^{13}C-NMR ($CDCl_3$, 125 MHz): 169.2, 140.4, 136.6, 136.5, 135.7, 133.0, 129.8, 129.6, 129.3, 128.8, 128.7, 128.6, 128.1, 127.5, 127.0, 126.5, 117.3, 57.4, 56.7, 52.8, 51.4, 47.5, 47.2, 36.8, 35.5, 34.8, 34.4.

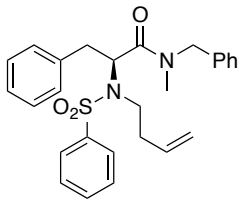

(*S*)-*N*-benzyl-2-(*N*-(but-3-en-1-yl)phenylsulfonamido)-*N*-methyl-3-phenylpropanamide (34). Following the general procedure for the amide formation, the sulfonamide **26** (0.33 g, 0.88 mmol) was dissolved in an equal mixture of THF, MeOH, and H_2O (0.1 M) and cooled to 0 ºC. To this was added $LiOH{\cdot}H_2O$ (0.10, 2.42 mmol) and the stirred reaction mixture was warmed to rt over 3 hrs. After this time the volatiles were reduced *in vacuo* and the aqueous layer washed with Et_2O. The aqueous portion was acidified to pH 3 with 10% HCl solution and extracted with EtOAc. The organics were dried over Na_2SO_4 and reduced *in vacuo* to provide the crude acid, which was carried on without further purification. The crude acid (0.30 g, 0.84 mmol) was dissolved in CH_2Cl_2 (4.2 mL) and cooled to 0 ºC under an argon atmosphere. To this solution was added *N*-methylbenzylamine (0.12 mL, 0.93 mmol), BOPCl (0.26 g, 1.01 mmol), and Et_3N (0.14 mL, 1.01 mmol). The resultant solution was stirred for 12 hrs and after this time diluted with EtOAc and washed with 10% HCl, sat. $NaHCO_3$, and brine. The organics were dried over Na_2SO_4 and reduced *in vacuo* and the crude material was subjected to silica gel flash chromatography (15% ethyl acetate in hexanes) to afford the corresponding *N*-methylamide as an opaque oil (0.36 g, 93%). R_f = 0.32 (15% ethyl acetate in hexanes). $[\alpha]_D^{26.7} = -33.3$ (c = 0.8 $CHCl_3$). FTIR (thin film) cm^{-1}: 3064, 3029, 3003, 2933, 1739, 1650, 1584, 1495, 1480, 1447, 1415, 1344, 1243, 1224, 1162, 1128, 1090, 1051, 1028, 999, 923, 863, 802, 751, 727, 697, 635, 609, 571. HRMS (ESI) m/z calcd. $C_{27}H_{30}N_2O_3NaS$ $[M+Na]^+$ 485.1875, found 485.1884. ^{1}H-NMR (rotamers present)

(500 MHz; $CDCl_3$): δ 7.88 (t, *J* = 8.3 Hz, 2H), 7.61-7.58 (m, 1H), 7.54 (dd, *J* = 9.6, 5.7 Hz, 2H), 7.25-7.11 (m, 8H), 6.92-6.90 (m, 1H), 6.61 (d, *J* = 7.4 Hz, 1H), 5.75 (d, *J* = 6.9 Hz, 1H), 5.11-5.02 (m, 3H), 4.09-4.06 (m, 1H), 3.57 (d, *J* = 0.2 Hz, 1H), 3.46 (dt, *J* = 11.8, 6.1 Hz, 1H), 3.30 (q, *J* = 11.8 Hz, 2H), 2.79 (s, *J* = 19.0 Hz, 3H), 2.47-2.38 (m, 3H). ^{13}C-NMR (rotamers present) ($CDCl_3$, 125 MHz): 168.8, 140.1, 136.2, 134.9, 132.9, 129.6, 129.4, 129.3, 129.2, 129.0, 128.9, 128.6, 128.6, 128.5, 128.5, 127.9, 127.3, 127.3, 127.2, 126.8, 126.2, 116.8, 56.7, 51.4, 35.7, 35.5, 34.7.

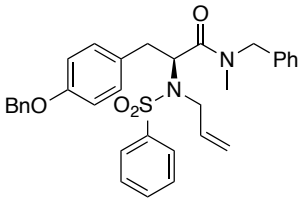

(*S*)-2-(*N*-allylphenylsulfonamido)-*N*-benzyl-3-(4-(benzyloxy)phenyl)-*N*-methylpropanamide (35). Following the general procedure for the amide formation, the *N*-allylsulfonamide **27** (0.8 g, 1.8 mmol) was dissolved in an equal mixture of THF, MeOH, and H_2O (0.1 M) and cooled to 0 ^oC. To this was added $LiOH{\cdot}H_2O$ (0.2 g, 5.4 mmol) and the stirred reaction mixture was warmed to room temperature over 3 hrs. The volatiles were reduced *in vacuo* and the aqueous layer was washed with Et_2O. The aqueous portion was acidified to pH 3 with 10% HCl solution and extracted with EtOAc. The organics were dried over Na_2SO_4 and reduced *in vacuo* to provide the crude acid, which was carried on without further purification. The crude acid (0.6 g, 1.4 mmol) was dissolved in CH_2Cl_2 (7 mL, 0.2 M) and cooled to 0 ºC under an argon atmosphere. To this solution was added *N*-methylbenzylamine (0.2 mL, 1.5 mmol), BOPCl (0.4 g, 1.6 mmol), and Et_3N (0.2 mL, 1.7 mmol). The resultant solution was stirred for 12 hrs and after this time diluted with EtOAc (10 mL) and washed with 10% HCl (5 mL), sat. $NaHCO_3$ (10 mL), and brine (10 mL). The organics were dried over

Na_2SO_4 and reduced *in vacuo* and the crude material was subjected to flash chromatography (20% ethyl acetate in hexanes) to afford the *N*-methylamide **18**, as a white foam (0.3 g, 43%). R_f = 0.3 (20% ethyl acetate in hexanes). $[\alpha]_D^{20.0}$ = –60.17 (*c* = 0.61 $CHCl_3$). FTIR (thin film) cm^{-1}: 3063, 3030, 2979, 1650, 1609, 1583, 1510, 1446, 1340, 1241, 1160, 1108, 1090, 1020, 924. HRMS (ESI) m/z calcd. $C_{33}H_{34}N_2NaO_4S$ $[M+Na]^+$ 577.2137, found 577.2154. ^{1}H-NMR (500 MHz; $CDCl_3$): (Rotamers present) δ 7.85-7.81 (m, 2H), 7.60-7.54 (m, 1H), 7.54-7.48 (m, 2H), 7.48-7.44 (m, 1H), 7.43-7.36 (m, 3H), 7.36-7.31 (m, 1H), 7.25-7.19 (m, 2H), 7.12-7.09 (m, 1H), 7.06-7.02 (m, 1H), 6.97-6.91 (m, 2H), 6.84-6.79 (m, 2H), 6.66-6.64 (m, 1H), 5.90-5.80 (m, 1H), 5.27-5.22 (m, 1H), 5.12-5.04 (m, 2H), 5.04-5.00 (m, 1H), 4.64 (d, *J* = 14.6 Hz, 1H), 4.34-4.29 (m, 1H), 4.16-4.01 (m, 2H), 3.29-3.21 (m, 1H), 2.77-2.68 (m, 3H), 2.58-2.55 (m, 1H). ^{13}C-NMR ($CDCl_3$, 125 MHz): 169.1,168.3, 157.6, 140.4, 140.3, 136.9, 135.5, 134.9, 132.7, 132.6, 130.5, 130.4, 129.1, 129.0, 128.9, 128.6, 128.54, 128.51, 128, 36, 127.96, 127.9, 127.27, 127.22, 127.16, 126.2, 117.0, 114.8, 69.9, 57.2, 56.4, 52.5, 51.1, 47.2, 35.8, 34.5, 34.4, 34.1.

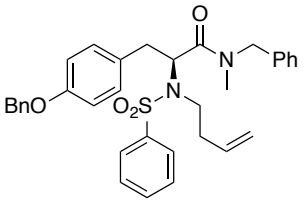

(*S*)-*N*-benzyl-3-(4-(benzyloxy)phenyl)-2-(*N*-(but-3-en-1-yl)phenylsulfonamido)-*N*-methylpropanamide (36). Following the general procedure for the amide formation, the sulfonamide **28** (0.2 g, 0.4 mmol) was dissolved in an equal mixture of THF, MeOH, and H_2O (0.1 M) and cooled to 0 ^oC. To this was added $LiOH{\cdot}H_2O$ (0.05 g, 1.1 mmol) and the mixture was warmed to room temperature over 3

hrs. The volatiles were removed *in vacuo* and the aqueous layer was washed with Et_2O. The aqueous portion was acidified to pH 3 with 10% HCl solution and extracted with EtOAc. The organics were dried over Na_2SO_4 and reduced *in vacuo* to provide the crude acid, which was carried on without further purification. The crude acid (0.1 g, 0.2 mmol) was dissolved in CH_2Cl_2 (1 mL, 0.2 M) and cooled to 0 ºC under an argon atmosphere. To this solution was added *N*-methylbenzylamine (30 µL, 0.25 mmol), BOPCl (60 mg, 0.25 mmol), and Et_3N (30 µL, 0.26 mmol). The resultant solution was stirred for 12 hrs and after this time diluted with EtOAc and washed with 10% HCl, sat. $NaHCO_3$, and brine. The organics were dried over Na_2SO_4 and reduced *in vacuo* and the crude material was subjected to flash chromatography (10% ethyl acetate in hexanes) to afford the *N*-methylamide **19** as a clear oil (77 mg, 74%). R_f = 0.25 (10% ethyl acetate in hexanes). $[\alpha]_D^{20.0}$ = –38.72 (*c* = 1.2 $CHCl_3$). FTIR (thin film) cm^{-1}: 3065, 3032, 2999, 2997, 2950, 2870, 1741, 1641, 1611, 1584, 1512, 1446, 1345, 1242, 1129, 1090. HRMS (ESI) m/z calcd. $C_{34}H_{36}N_2NaO_4S$ $[M+Na]^+$ 591.2293, found 591.2293. ^{1}H-NMR (500 MHz; $CDCl_3$): δ 7.80-7.74 (m, 2H), 7.51-7.46 (m, 1H), 7.44-7.39 (m, 2H), 7.39-7.21 (m, 5H), 7.14-7.09 (m, 2H), 7.02-7.00 (m, 1H), 6.96-6.94 (m, 1H), 6.86-6.81 (m, 2H), 6.75-6.70 (m, 2H), 6.56 (d, *J* = 7.3 Hz, 1H), 5.71-5.62 (m, 1H), 5.05-5.00 (m, 1H), 5.00-4.90 (m, 4H), 4.78 (dd, *J* = 11.1, 3.2 Hz,), 4.64-4.61 (m, 1H), 4.01-3.97 (m, 1H), 3.52-3.46 (m, 1H), 3.41-3.33 (m, 1H), 3.19-3.11 (m, 1H), 2.71-2.64 (m, 3H), 2.42-2.25 (m, 3H). ^{13}C-NMR ($CDCl_3$, 125 MHz): 168.5, 140.1, 136.9, 136.3, 134.9, 134.8, 132.8, 130.6, 130.4, 130.1, 129.2, 129.17, 129.13, 128.6, 128.57, 128.55, 128.4, 127.97, 127.95, 127.6, 127.39, 127.38, 127.28, 127.25, 126.9, 126.2, 116.7, 114.8, 69.9, 56.6, 51.3, 44.4, 34.7, 34.4.

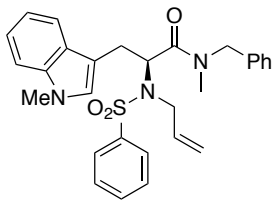

(*S*)-2-(*N*-allylphenylsulfonamido)-*N*-benzyl-*N*-methyl-3-(1-methyl-1*H*-indol-3-yl)propanamide (37). Following the general procedure for the amide formation, The *N*-allylsulfonamide **29** (0.56 g, 1.36 mmol) was dissolved in an equal mixture of THF, MeOH, and H_2O (0.1 M) and cooled to 0 ºC. To this was added $LiOH{\cdot}H_2O$ (0.17 g, 4.09 mmol) and the stirred reaction mixture was warmed to room temperature over 3 hrs. After this time the volatiles were reduced *in vacuo* and the aqueous layer washed with Et_2O. The aqueous portion was acidified to pH 3 with 10% HCl solution and extracted with EtOAc. The organics were dried over Na_2SO_4 and reduced *in vacuo* to provide the crude acid, which was carried on without further purification. The crude acid (0.56 g, 1.40 mmol) was dissolved in CH_2Cl_2 (7 mL) and cooled to 0 ºC under an argon atmosphere. To this solution was added *N*-methylbenzylamine (0.2 mL, 1.53 mmol), BOPCl (0.43 g, 1.67 mmol), and Et_3N (0.23 mL, 1.67 mmol). The resultant solution was stirred for 12 hrs. Aqueous work-up afforded the crude material which was purified by silica gel chromatography (25% ethyl acetate in hexanes) to afford the title compound as a solid (0.55 g, 79%). R_f = 0.25 (25% ethyl acetate in hexanes). $[\alpha]_D^{27.4} = -7.4$ (*c* = 0.8 CH_2Cl_2). FTIR (thin film) cm^{-1}: 3059, 2931, 1736, 1648, 1551, 1475, 1446, 1375, 1330, 1252, 1204, 1161, 1090, 1012, 927, 839, 775, 740, 691, 614, 581. HRMS (ESI) m/z calcd. $C_{29}H_{31}N_3O_3NaS$ $[M+Na]^+$ 524.1984, found 524.1962. ^{1}H-NMR (500 MHz; $CDCl_3$): δ 7.86 (dd, *J* = 20.7, 8.1 Hz, 2H), 7.57-7.46 (m, 4H), 7.27-7.16 (m, 5H), 7.10 (dd, *J* = 7.8, 7.0 Hz, 1H), 6.93 (s, 1H), 6.86 (d, *J* = 6.8 Hz,

1H), 6.76 (s, 1H), 6.56 (d, *J* = 7.6 Hz, 1H), 5.92-5.85 (m, 1H), 5.28-5.24 (m, 2H), 5.10-5.08 (m, 1H), 4.69 (d, *J* = 14.6 Hz, 1H), 4.38-4.33 (m, 1H), 4.19 (d, *J* = 0.6 Hz, 1H), 3.93 (d, *J* = 14.6 Hz, 1H), 3.63 (d, *J* = 9.5 Hz, 3H), 3.46-3.43 (m, 1H), 2.84 (dd, *J* = 13.5, 4.0 Hz, 1H), 2.71 (s, 1H), 2.59 (s, 2H). ^{13}C-NMR ($CDCl_3$, 125 MHz): 169.9, 140.7, 140.7, 136.9, 135.9, 132.9, 129.2, 129.2, 128.5, 128.5, 128.4, 127.6, 126.6, 121.8, 121.7, 119.3, 117.2, 109.4, 55.9, 55.3, 52.8, 51.3, 47.3, 47.1, 34.9, 34.3, 32.7, 26.7, 25.7.

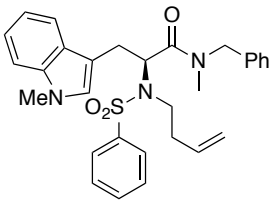

(*S*)-*N*-benzyl-2-(*N*-(but-3-en-1-yl)phenylsulfonamido)-*N*-methyl-3-(1-methyl-1*H*-indol-3-yl)propanamide (38). Following the general procedure for the amide formation, the sulfonamide **30** (0.36 g, 0.84 mmol) was dissolved in an equal mixture of THF, MeOH, and H_2O (0.1 M) and cooled to 0 ºC. To this was added $LiOH{\cdot}H_2O$ (0.1, 2.3 mmol) and the stirred reaction mixture was warmed to rt over 3 hrs. After this time the volatiles were reduced *in vacuo* and the aqueous layer washed with Et_2O. The aqueous portion was acidified to pH 3 with 10% HCl solution and extracted with EtOAc. The organics were dried over Na_2SO_4 and reduced *in vacuo* to provide the crude acid, which was carried on without further purification. The crude acid (0.31 g, 0.75 mmol) was dissolved in CH_2Cl_2 (3.8 mL) and cooled to 0 ºC under an argon atmosphere. To this solution was added *N*-methylbenzylamine (0.11 mL, 0.82 mmol), BOPCl (0.23 g, 0.9 mmol), and Et_3N (0.12 mL, 0.9 mmol). The resultant solution was stirred for 12 hrs and after this time diluted with EtOAc and washed with 10% HCl, sat. $NaHCO_3$, and brine. The organics were dried over Na_2SO_4 and reduced *in vacuo* and the crude material was subjected to silica gel flash chromatography (25% ethyl acetate in

hexanes) to afford the corresponding *N*-methylamide as yellow oil (0.35 g, 90%). R_f = 0.27 (25% ethyl acetate in hexanes). $[\alpha]_D^{27.8} = -13.6$ (*c* = 0.6 $CHCl_3$). FTIR (thin film) cm^{-1}: 3061, 3028, 2930, 1648, 1585, 1551, 1475, 1446, 1375, 1330, 1252, 1204, 1160, 1131, 1089, 1071, 1012, 999, 924, 855, 811, 740, 692, 665, 630, 613, 581, 547, 507. HRMS (ESI) m/z calcd. $C_{30}H_{33}N_3O_3NaS$ $[M+Na]^+$ 538.2140, found 538.2133. ^{1}H-NMR (500 MHz; $CDCl_3$): δ 7.58-7.47 (m, 4H), 7.37-7.10 (m, 6H), 6.94-6.86 (m, 2H), 6.77 (s, 1H), 6.56 (d, *J* = 7.6 Hz, 1H), 5.79-5.72 (m, 1H), 5.21 (dd, *J* = 11.0, 3.9 Hz, 1H), 5.14-5.01 (m, 3H), 4.74 (d, *J* = 14.6 Hz, 1H), 4.00 (t, *J* = 15.3 Hz, 1H), 3.59-3.41 (m, 6H), 2.75-2.67 (m, 4H), 2.54-2.39 (m, 2H). ^{13}C-NMR ($CDCl_3$, 125 MHz): 169.7, 140.5, 136.9, 136.7, 135.2, 132.9, 129.3, 128.5, 128.5, 128.4, 128.0, 127.5, 127.4, 126.6, 121.8, 119.3, 118.7, 116.9, 109.4, 108.8, 56.1, 55.4, 52.8, 51.5, 44.5, 35.7, 35.0, 34.5, 32.7, 26.1.

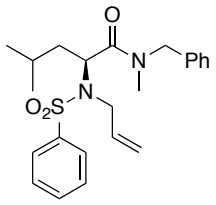

(*S*)-2-(*N*-allylphenylsulfonamido)-*N*-benzyl-*N*,4-dimethylpentanamide (39). Following the general procedure for the amide formation, The *N*-allylsulfonamide **31** (2.0 g, 6.16 mmol) was dissolved in an equal mixture of THF, MeOH, and H_2O (0.1 M) and cooled to 0 ºC. To this was added $LiOH{\cdot}H_2O$ (0.77 g, 18.4 mmol) and the stirred reaction mixture was warmed to room temperature over 3 hrs. After this time the volatiles were reduced *in vacuo* and the aqueous layer washed with Et_2O. The aqueous portion was acidified to pH 3 with 10% HCl solution and extracted with EtOAc. The organics were dried over Na_2SO_4 and reduced *in vacuo* to provide the crude acid, which was carried on without further purification. The crude acid (1.90 g,

6.10 mmol) was dissolved in CH_2Cl_2 (30 mL) and cooled to 0 ºC under an argon atmosphere. To this solution was added *N*-methylbenzylamine (0.86 mL, 6.71 mmol), BOPCl (1.77 g, 6.95 mmol), and Et_3N (1.0 mL, 7.32 mmol). The resultant solution was stirred for 12 hrs. Aqueous work-up afforded the crude material which was purified by silica gel chromatography (20% ethyl acetate in hexanes) to afford the title compound as a clear oil (1.80 g, 71%). R_f = 0.36 (20% ethyl acetate in hexanes). $[\alpha]_D^{23.8} = -10.4$ (*c* = 1.7 CH_2Cl_2). FTIR (thin film) cm^{-1}: 3064, 3028, 2957, 2868, 1653, 1447, 1339, 1163, 1089, 1015, 920, 742, 691. HRMS (ESI) m/z calcd. $C_{23}H_{31}N_2O_3S$ $[M+H]^+$ 415.2055, found 415.2051. ^{1}H-NMR (500 MHz; $CDCl_3$): δ 7.80-7.75 (m, 2H), 7.58-7.45 (m, 3H), 7.39-7.27 (m, 4H), 7.23-7.16 (m, 2H), 5.91-5.85 (m, 1H), 5.23-5.16 (m, 1H), 5.09-5.04 (m, 1H), 4.95 (dd, *J* = 3.8, 2.8 Hz, 1H), 4.58-4.55 (m, 1H), 4.36-4.20 (m, 2H), 4.14-3.99 (m, 1H), 3.09-2.90 (m, 3H), 1.67-1.57 (m, 2H), 1.38-1.26 (m, 1H), 0.94-0.86 (m, 4H), 0.69 (d, *J* = 6.5 Hz, 1H), 0.60 (d, *J* = 6.6 Hz, 1H). ^{13}C-NMR ($CDCl_3$, 125 MHz): 170.5, 140.2, 136.9, 136.1, 132.8, 129.1, 128.8, 128.3, 127.6, 127.6, 127.5, 126.7, 116.9, 100.1, 54.2, 52.9, 51.4, 47.6, 38.5, 34.8, 24.8, 22.4, 22.2.

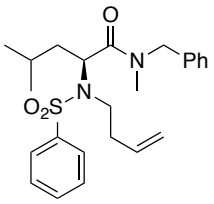

(*S*)-*N*-benzyl-2-(*N*-(but-3-en-1-yl)phenylsulfonamido)-*N*,4-dimethylpentanamide (40). Following the general procedure for the amide formation, the sulfonamide **32** (0.58 g, 1.71 mmol) was dissolved in an equal mixture of THF, MeOH, and H_2O (0.1 M) and cooled to 0 ºC. To this was added $LiOH{\cdot}H_2O$ (0.2, 4.7 mmol) and the stirred reaction mixture was warmed to room temperature over 3 hrs.

After this time the volatiles were reduced *in vacuo* and the aqueous layer washed with Et_2O. The aqueous portion was acidified to pH 3 with 10% HCl solution and extracted with EtOAc. The organics were dried over Na_2SO_4 and reduced *in vacuo* to provide the crude acid, which was carried on without further purification. The crude acid (0.54 g, 1.66 mmol) was dissolved in CH_2Cl_2 (8.3 mL) and cooled to 0 ºC under an argon atmosphere. To this solution was added *N*-methylbenzylamine (0.23 mL, 1.82 mmol), BOPCl (0.51 g, 1.99 mmol), and Et_3N (0.3 mL, 1.99 mmol). The resultant solution was stirred for 12 hrs and after this time diluted with EtOAc and washed with 10% HCl, sat. $NaHCO_3$, and brine. The organics were dried over Na_2SO_4 and reduced *in vacuo* and the crude material was subjected to silica gel flash chromatography (15% ethyl acetate in hexanes) to afford the corresponding *N*-methylamide as an oil (0.55 g, 77%). R_f = 0.3 (15% ethyl acetate in hexanes). $[\alpha]_D^{25.8} = -6.0$ (*c* = 1.3 CH_2Cl_2). FTIR (thin film) cm^{-1}: 3065, 2956, 2869, 1653, 1447, 1342, 1164, 1090, 1048, 996, 923, 811, 740, 693, 587, 550. HRMS (ESI) m/z calcd. $C_{24}H_{33}N_2O_3S$ $[M+H]^+$ 429.2212, found 429.2194. ^{1}H-NMR (500 MHz; $CDCl_3$): δ 7.81 (d, *J* = 8.4 Hz, 1H), 7.77 (d, *J* = 7.2 Hz, 1H), 7.58-7.55 (m, 1H), 7.50-7.47 (m, 2H), 7.37 (t, *J* = 7.5 Hz, 1H), 7.32-7.19 (m, 6H), 5.74-5.66 (m, 1H), 5.11-4.99 (m, 2H), 4.87-4.84 (m, 1H), 4.62 (d, *J* = 14.6 Hz, 1H), 4.33 (d, *J* = 15.0 Hz, 1H), 3.51-3.44 (m, 1H), 3.33-3.23 (m, 1H), 3.05 (s, 3H), 2.37-2.32 (m, 2H), 1.84-1.75 (m, 1H), 1.04 (t, *J* = 6.7 Hz, 1H), 0.86 (dd, *J* = 8.6, 6.8 Hz, 4H), 0.68 (d, *J* = 6.6 Hz, 1H), 0.55 (d, *J* = 6.7 Hz, 1H). ^{13}C-NMR ($CDCl_3$, 125 MHz): 170.0, 140.1, 136.9, 135.2, 132.9, 129.2, 129.0, 128.8, 128.4, 128.4, 127.7, 127.6, 127.5, 126.7, 119.6, 116.8, 54.3, 51.7, 44.6, 35.6, 35.0, 25.2, 22.7, 22.5.

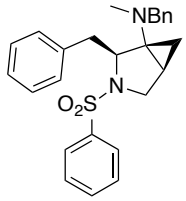

(1*R*,2*S*,5*S*)-*N*,2-dibenzyl-*N*-methyl-3-(phenylsulfonyl)-3-azabicyclo[3.1.0]hexan-1-amine (18). Following the general procedure for azabicyclic [3.1.0] formation, to a solution of the *N*-methylamide **33** (0.25 g, 0.56 mmol) in THF (5.6 mL) under an argon atmosphere was added $ClTi(OiPr)_3$ (0.56 mL, 1M) dropwise *via* syringe. To this solution was added cyclohexylMgCl (1.25 mL, 2M) dropwise *via* syringe pump addition over 1 hr. After 12 hrs, the reaction mixture was poured onto ice water and stirred for 15 mins. The crude mixture was filtered thorough celite, and the two layers separated. The aqueous layer was extracted once with EtOAc and the combined organics washed with brine and dried over Na_2SO_4. The crude mixture was subjected to silica gel flash chromatography (15% ethyl acetate in hexanes) to isolate the corresponding major diastereomer aminocyclopropane (0.08 g, 33%). $R_f = 0.5$ (20% ethyl acetate in hexanes). $[\alpha]_D^{25.9} = +49.87$ (*c* = 0.4 $CHCl_3$). FTIR (thin film) cm^{-1}: 3062, 3027, 2931, 2879, 2791, 1758, 1718, 1603, 1585, 1495, 1474, 1446, 1342, 1166, 1123, 1095, 1030, 999, 750, 719, 699, 613, 603, 582, 571. HRMS (ESI) m/z calcd. $C_{26}H_{29}N_2O_2S$ $[M+H]^+$ 433.1950, found 433.1936. ^{1}H-NMR (500 MHz; $CDCl_3$): δ 7.87 (d, *J* = 8.1 Hz, 2H), 7.58 (dq, *J* = 16.4, 7.8 Hz, 4H), 7.39 (d, *J* = 7.7 Hz, 2H), 7.33 (t, *J* = 7.2 Hz, 2H), 7.27-7.22 (m, 6H), 7.13 (s, 3H), 6.82 (d, *J* = 7.5 Hz, 2H), 4.00 (dd, *J* = 8.4, 3.1 Hz, 1H), 3.56 (dd, *J* = 14.4, 2.8 Hz, 1H), 3.39 (s, 2H), 3.21 (d, *J* = 13.8 Hz, 1H), 3.06 (dd, *J* = 14.2, 8.51 Hz, 1H), 2.76-2.73 (m, 1H), 1.70 (d, *J* = 4.3 Hz, 3H), 1.36 (dt, *J* = 8.6, 4.3 Hz, 1H), 0.98-0.96 (m, 1H), 0.85-0.83 (m, 1H). ^{13}C-NMR ($CDCl_3$, 125 MHz):139.3, 138.6, 136.4,

132.8, 129.9, 129.2, 129.0, 128.6, 128.3, 127.9, 127.6, 127.7, 127.0, 126.6, 126.3, 60.7, 58.7, 58.3, 51.6, 39.4, 37.9, 23.3, 18.2.

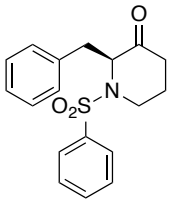

(*S*)-2-benzyl-1-(phenylsulfonyl)piperidin-3-one (48). Following the general procedure for 3-piperidinone formation, a solution of aminocyclopropane **18** (74 mg, 0.17 mmol) in EtOH (2 mL) was charged with 10% Pd/C (18 mg, 0.02 mmol) and 88% formic acid (79 μL, 1.7 μmol) and the system purged with H_2 three times. The mixture was stirred for 20 hrs at room temperature under an atmosphere of H_2, after which time the inorganic material was removed *via* filtration and the solvent reduced *in vacuo*. The crude material was subjected to silica gel flash chromatography (15% ethyl acetate in hexanes) to give the corresponding piperidinone as light yellow solid (29 mg, 52%). R_f = 0.17 (25% ethyl acetate in hexanes). $[\alpha]_D^{20.2}$ = +18.69 (*c* = 1.16, $CHCl_3$). FTIR (thin film) cm^{-1}: 2951, 2930, 1720, 1447, 1346, 1314, 1157, 1095, 954, 748, 690. HRMS (ESI) m/z calcd. $C_{18}H_{19}NNaO_3S$ $[M+Na]^+$ 352.0984, found 352.0990. ^{1}H-NMR (500 MHz; $CDCl_3$): δ 7.58 (d, *J* = 8.1 Hz, 2H), 7.50 (t, *J* = 6.9 Hz, 1H), 7.40-7.37 (m, 2H), 7.23 (dd, *J* = 5.7, 4.1 Hz, 3H), 7.09-7.08 (m, 2H), 4.58 (t, *J* = 6.7 Hz, 1H), 3.76-3.71 (m, 1H), 3.22-3.21 (m, 1H), 3.07-3.05 (m, 2H), 2.37-2.21 (m, 2H), 1.81-1.63 (m, 2H). ^{13}C-NMR ($CDCl_3$, 125 MHz): 206.5, 140.0, 136.1, 132.8, 129.6, 129.3, 128.8, 127.2, 127.2, 65.7, 40.6, 37.9, 36.9, 23.1.

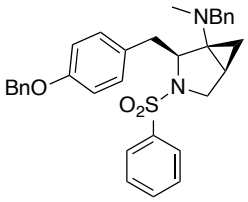

(1*R*,2*S*,5*S*)-*N*-benzyl-2-(4-(benzyloxy)benzyl)-*N*-methyl-3-(phenylsulfonyl)-3-azabicyclo[3.1.0]hexan-1-amine (42). Following the general procedure for azabicyclic [3.1.0] formation, to a solution of the *N*-methylamide **35** (0.5 g, 1.1 mmol) in THF (11 mL, 0.1M) under an argon atmosphere was added $ClTi(OiPr)_3$ (1.1 mL, 1M) dropwise *via* syringe. To this solution was added cyclohexylMgBr (2.5 mL, 2M) dropwise *via* syringe pump addition over 1 hr. The solution gradually changed color from colorless to dark yellow and finally black over the course of 3 hrs. TLC analysis showed reaction completion, and the reaction mixture was poured onto ice water and stirred for 15 mins. The crude mixture was filtered thorough celite, and the two layers were separated. The aqueous layer was extracted once with EtOAc and the combined organics washed with brine and dried over Na_2SO_4. The crude mixture was subjected to flash chromatography (20% ethyl acetate in hexanes) to afford two diastereomers as a 1.3:1 ratio (0.3g, 62%) as a golden oil. R_f = 0.25 (20% ethyl acetate in hexanes). $[\alpha]_D^{19.4}$ = +51.06 (*c* = 0.67 $CHCl_3$). FTIR (thin film) cm^{-1}: 3368, 3029, 2929, 1609, 1583, 1510, 1446, 1380, 1341, 1239, 1165, 1094, 1026, 806. HRMS (ESI) m/z calcd. $C_{33}H_{35}N_2NaO_3S$ $[M+Na]^+$ 539.2368, found 539.2363. ^{1}H-NMR (500 MHz; $CDCl_3$): δ 7.89 (t, *J* = 7.8 Hz, 2H), 7.59 (dq, *J* = 16.1, 7.8 Hz, 3H), 7.48 (t, *J* = 8.5 Hz, 2H), 7.46-7.33 (m, 7H), 7.23-7.14 (m, 3H), 6.99 (d, *J* = 8.4 Hz, 2H), 6.89 (d, *J* = 6.1 Hz, 2H), 5.12-5.07 (m, 2H), 3.98 (dd, *J* = 7.8, 2.6 Hz, 1H), 3.51 (dd, *J* = 14.3, 2.8 Hz, 1H), 3.44-3.39 (m, 2H), 3.28 (d, *J* = 13.7 Hz, 1H), 3.10 (dd, *J* = 14.3, 8.0 Hz, 1H), 2.88 (d, *J* = 13.7 Hz,

1H), 1.77 (s, 3H), 1.37 (t, *J* = 4.3 Hz, 1H), 1.00-0.95 (m, 1H), 0.85 (q, *J* = 4.9 Hz, 1H). ^{13}C-NMR ($CDCl_3$, 125 MHz): 157.3, 139.2, 137.0, 136.3, 132.7, 130.89, 130.87, 128.93, 128.44, 127.9, 127.7, 127.6, 127.4, 127.3, 126.6, 114.6, 69.9, 60.6, 58.5, 58.3, 51.6, 38.4, 38.01, 23.1, 18.1.

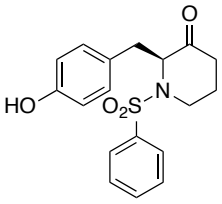

(*S*)-2-(4-hydroxybenzyl)-1-(phenylsulfonyl)piperidin-3-one (50). A solution of aminocyclopropane **42** (21 mg, 38 μmol) in EtOH (0.4 mL, 0.1M) was charged with 10% Pd/C (4 mg, 3.8 μmol) and 88% formic acid (14.6 μL, 0.3 μmol) and the system purged with H_2 three times. The mixture was stirred for 20 hrs at room temperature under an atmosphere of H_2, after which time the inorganic material was removed *via* filtration and the solvent reduced *in vacuo*. The crude material was subjected to flash chromatography (30% ethyl acetate in hexanes) to give the title compound (10.1 mg, 55%). R_f = 0.3 (30% ethyl acetate in hexanes). $[\alpha]_D^{17.1} = +3.95$ (*c* = 0.19, $CHCl_3$). FTIR (thin film) cm^{-1}: 3401, 2924, 1715, 1614, 1516, 1447, 1313, 1264, 1155, 1091, 931. HRMS (ESI) m/z calcd. $C_{24}H_{21}NNaO_4S$ $[M+Na]^+$ 382.1079, found 382.1074. ^{1}H-NMR (500 MHz; $CDCl_3$): δ 7.64 (d, *J* = 7.7 Hz, 2H), 7.53 (t, *J* = 7.3 Hz, 1H), 7.43 (t, *J* = 7.7 Hz, 2H), 6.97 (d, *J* = 8.2 Hz, 2H), 6.70 (d, *J* = 8.2 Hz, 2H), 4.98 (s(*b*), 1H), 4.54 (t, *J* = 6.8 Hz, 1H), 3.76 (dt, *J* = 14.0, 4.8 Hz, 1H), 3.24 (ddd, *J* = 14.2, 9.8, 4.4 Hz, 1H), 3.02 (d, *J* = 6.9 Hz, 2H), 2.35-2.23 (m, 2H), 1.77-1.66 (m, 2H), 1.26 (d, *J* = 8.7 Hz, 2H). ^{13}C-NMR ($CDCl_3$, 125 MHz): 207.3, 154.7, 140.2, 132.6, 130.4, 129.1, 127.8, 127.0, 115.5, 65.7, 40.8, 36.6, 33.1, 30.9, 14.1, 14.0.

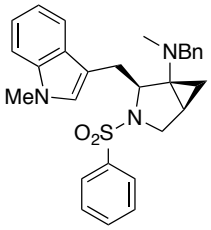

(1*R*,2*S*,5*S*)-*N*-benzyl-*N*-methyl-2-((1-methyl-1*H*-indol-3-yl)methyl)-3-(phenylsulfonyl)-3-azabicyclo[3.1.0]hexan-1-amine (44). Following the general procedure for azabicyclic [3.1.0] formation, to a solution of the *N*-methylamide **37** (0.25 g, 0.49 mmol) in THF (5 mL) under an argon atmosphere was added $ClTi(O\textit{i}Pr)_3$ (0.5 mL, 1M) dropwise *via* syringe. To this solution was added cyclohexylMgCl (1.12 mL, 2M) dropwise *via* syringe pump addition over 1 hr. After 12 hrs, the reaction mixture was poured onto ice water and stirred for 15 mins. The crude mixture was filtered thorough celite, and the two layers separated. The aqueous layer was extracted once with EtOAc and the combined organics washed with brine and dried over Na_2SO_4. The crude mixture was subjected to silica gel flash chromatography (20% ethyl acetate in hexanes) to isolate the corresponding major diastereomer aminocyclopropane as an orange oil (0.07 g, 30%). R_f = 0.32 (20% ethyl acetate in hexanes). $[\alpha]_D^{25.5}$ = +56.26 (*c* = 0.4, $CHCl_3$). FTIR (thin film) cm^{-1}: 3058, 3027, 2930, 2883, 2795, 1615, 1473, 1446, 1377, 1342, 1251, 1217, 1165, 1128, 1095, 1073, 1031, 829, 742, 719, 694, 666, 613, 590, 570. HRMS (ESI) m/z calcd. $C_{29}H_{32}N_3O_2S$ $[M+H]^+$ 486.2215, found 486.2211. ^{1}H-NMR (500 MHz; $CDCl_3$): δ 7.91 (d, *J* = 6.9 Hz, 2H), 7.77 (d, *J* = 7.9 Hz, 1H), 7.58-7.50 (m, 3H), 7.29 (d, *J* = 8.2 Hz, 1H), 7.21 (dd, *J* = 8.1, 1.1 Hz, 1H), 7.13 (ddd, *J* = 7.9, 7.0, 0.9 Hz, 1H), 7.08-7.07 (m, 3H), 7.02 (s, 1H), 6.71-6.69 (m, 2H), 4.15 (dd, *J* = 8.4, 3.0 Hz, 1H), 3.74-3.68 (m, 3H), 3.64-3.60 (m, 1H), 3.46 (dd, *J* = 10.1, 5.8 Hz, 1H), 3.39-3.37 (m, 1H), 3.15-3.11 (m, 2H), 2.66 (d, *J* = 13.7 Hz, 1H), 1. 58 (s, 3H), 1.34 (q, *J* = 6.8 Hz, 1H), 1.26-1.20 (m, 1H). ^{13}C-

NMR ($CDCl_3$, 125 MHz): 139.4, 137.1, 136.9, 132.7, 129.0, 128.6, 128.0, 127.9, 127.72, 127.71, 126.5, 121.4 119.3, 118.8, 110.9, 109.1, 60.0, 59.1, 58.2, 51.7, 37.7, 32.6, 29.1, 23.4, 18.4.

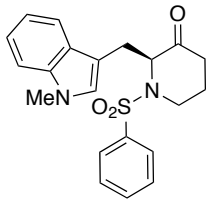

(*S*)-2-((1-methyl-1*H*-indol-3-yl)methyl)-1-(phenylsulfonyl)piperidin-3-one (52). Following the general procedure for 3-piperidinone formation, a solution of aminocyclopropane **44** (55 mg, 0.11 mmol) in EtOH (1.1 mL) was charged with 10% Pd/C (12 mg, 0.01 mmol) and 88% formic acid (52 μL, 1.1 μmol) and the system purged with H_2 three times. The mixture was stirred for 20 hrs at room temperature under an atmosphere of H_2, after which time the inorganic material was removed *via* filtration and the solvent reduced *in vacuo*. The crude material was subjected to silica gel flash chromatography (20% ethyl acetate in hexanes) to give the corresponding piperidinone (28 mg, 65%). R_f = 0.3 (20% ethyl acetate in hexanes). $[\alpha]_D^{25.6}$ = +32.6 (*c* = 1.34, $CHCl_3$). FTIR (thin film) cm^{-1}: 3057, 3026, 2928, 1720, 1615, 1552, 1474, 1447, 1425, 1376, 1348, 1319, 1248, 1160, 1131, 1093, 1012, 956, 925, 881, 858, 745, 719, 690, 667, 650, 587, 568. HRMS (ESI) m/z calcd. $C_{21}H_{23}N_2O_3S$ $[M+H]^+$ 383.1429, found 383.1447. ^{1}H-NMR (500 MHz; $CDCl_3$): δ 7.61 (dd, *J* = 8.4, 1.2 Hz, 2H), 7.48 (dt, *J* = 17.4, 8.0 Hz, 2H), 7.33 (t, *J* = 7.8 Hz, 2H), 7.22-7.17 (m, 2H), 7.07 (ddd, *J* = 7.9, 6.8, 1.1 Hz, 1H), 6.76 (s, 1H), 4.62 (t, *J* = 6.6 Hz, 1H), 3.78 (dt, *J* = 14.4, 4.8 Hz, 1H), 3.68-3.63 (m, 3H), 3.28-3.22 (m, 3H), 2.26 (td, *J* = 9.8, 6.3 Hz, 2H), 1.75-1.65 (m, 2H). ^{13}C-NMR ($CDCl_3$, 125

MHz): 206.9, 140.1, 136.8, 132.5, 129.0, 127.8, 127.7, 126.9, 126.8, 121.7, 119.3, 118.8, 109.2, 108.5, 64.9, 40.7, 36.8, 32.7, 28.0, 23.1.

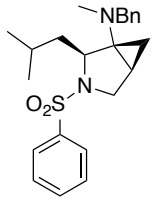

(1*R*,2*S*,5*S*)-*N*-benzyl-2-isobutyl-*N*-methyl-3-(phenylsulfonyl)-3-azabicyclo[3.1.0]hexan-1-amine (46). Following the general procedure for azabicyclic [3.1.0] formation, to a solution of the *N*-methylamide **39** (0.5 g, 1.21 mmol) in THF (12 mL) under an argon atmosphere was added $ClTi(OiPr)_3$ (1.21 mL, 1M) dropwise *via* syringe. To this solution was added cyclohexylMgCl (2.71 mL, 2M) dropwise *via* syringe pump addition over 1 hr. After 12 hrs, the reaction mixture was poured onto ice water and stirred for 15 mins. The crude mixture was filtered thorough celite, and the two layers separated. The aqueous layer was extracted once with EtOAc and the combined organics washed with brine and dried over Na_2SO_4. The crude mixture was subjected to silica gel flash chromatography (15% ethyl acetate in hexanes) to isolate the corresponding major diastereomer aminocyclopropane as a dark orange oil (0.27 g, 56%). R_f = 0.6 (30% ethyl acetate in hexanes). $[\alpha]_D^{25.9} = +80.2$ (*c* = 0.6, CH_2Cl_2). FTIR (thin film) cm^{-1}: 3063, 3029, 2954, 2867, 2794, 1494, 1468, 1446, 1342, 1166, 1123, 1094, 1071, 1028, 750, 717, 693, 615, 595, 570. HRMS (ESI) m/z calcd. $C_{23}H_{31}N_2O_2S$ $[M+H]^+$ 399.2106, found 399.2106. ^{1}H-NMR (500 MHz; $CDCl_3$): δ 7.85 (d, *J* = 6.8 Hz, 2H), 7.60-7.52 (m, 3H), 7.24-7.18 (m, 3H), 7.07 (d, *J* = 6.7 Hz, 2H), 3.72 (dd, *J* = 6.8, 4.8 Hz, 1H), 3.43 (s,), 3.40 (d, *J* = 3.6 Hz, 2H), 3.34 (s, 1H), 2.12-2.08 (m, 1H), 2.00-1.94 (m, 4H), 1.62 (dt, *J* = 13.8, 6.8 Hz, 1H), 1.45 (dt, *J* = 7.5, 3.9 Hz, 1H), 1.04 (dd, *J* = 8.3, 6.6

Hz, 8H), 0.94 (t, J = 5.1 Hz, 2H). ^{13}C-NMR ($CDCl_3$, 125 MHz): 139.3, 137.2, 132.8, 129.1, 128.3, 128.3, 128.0, 127.1, 60.1, 58.9, 58.6, 52.4, 43.2, 38.6, 25.4, 25.2, 23.9, 23.0, 22.3, 17.5.

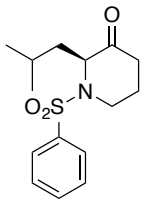

(*S*)-2-isobutyl-1-(phenylsulfonyl)piperidin-3-one (54). Following the general procedure for 3-piperidinone formation, a solution of aminocyclopropane **46** (0.22 g, 0.56 mmol) in EtOH (5.6 mL) was charged with 10% Pd/C (0.06 g, 0.06 mmol) and 88% formic acid (0.26 mL, 5.6 μmol) and the system purged with H_2 three times. The mixture was stirred for 20 hrs at room temperature under an atmosphere of H_2, after which time the inorganic material was removed *via* filtration and the solvent reduced *in vacuo*. The crude material was subjected to silica gel flash chromatography (20% ethyl acetate in hexanes) to give the corresponding piperidinone (0.11 g, 64%). R_f = 0.5 (30% ethyl acetate in hexanes). $[\alpha]_D^{26.4}$ = +38.9 (c = 0.6, CH_2Cl_2). FTIR (thin film) cm^{-1}: 3066, 2958, 2871, 1719, 1585, 1468, 1447, 1422, 1388, 1349, 1317, 1289, 1249, 1164, 1128, 1091, 1072, 999, 939, 880, 849, 755, 733, 716, 691, 655, 591, 572, 508. HRMS (ESI) m/z calcd. $C_{15}H_{22}NO_3S$ $[M+H]^+$ 296.1320, found 296.1320. ^{1}H-NMR (500 MHz; $CDCl_3$): δ 7.82-7.80 (m, 2H), 7.59-7.56 (m, 1H), 7.53-7.49 (m, 2H), 4.40-4.37 (m, 1H), 3.91-3.86 (m, 1H), 3.39 (ddd, J = 14.8, 11.0, 3.9 Hz, 1H), 2.38 (ddd, J = 16.0, 11.2, 6.3 Hz, 1H), 2.12-2.07 (m, 1H), 1.82-1.78 (m, 1H), 1.71-1.57 (m, 3H), 1.44 (ddd, J = 13.6, 7.7, 6.1 Hz, 1H), 0.94 (dd, J = 19.1, 6.5 Hz, 7H). ^{13}C-NMR ($CDCl_3$, 125 MHz): 207.2, 140.7, 133.0, 129.5, 127.2, 63.1, 39.6, 39.5, 36.1, 24.5, 23.6, 22.9, 21.9

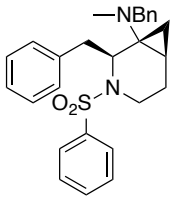

(1*R*,2*S*,6*R*)-*N*,2-dibenzyl-*N*-methyl-3-(phenylsulfonyl)-3-azabicyclo[4.1.0]heptan-1-amine (41). Following the general procedure for azabicyclic [4.1.0] aminocyclopropane formation, to a solution of the *N*-methylamide **34** (0.36 g, 0.78 mmol) in THF (15.7 mL) under an argon atmosphere was added $ClTi(O\textit{i}Pr)_3$ (0.78 mL, 1M) dropwise *via* syringe. To this solution was added cyclohexylMgCl (1.76 mL, 2M) dropwise *via* syringe pump addition over 1 hr. After 12 hrs, the reaction mixture was poured onto ice water and stirred for 15 mins. The crude mixture was filtered thorough celite, and the two layers were separated. The aqueous layer was extracted once with EtOAc and the combined organics washed with brine and dried over Na_2SO_4. The crude mixture was subjected to silica gel flash chromatography (15% ethyl acetate in hexanes) to isolate the corresponding major diastereomer aminocyclopropane as a light yellow solid (0.18 g, 51%). R_f = 0.4 (20% ethyl acetate in hexanes). $[\alpha]_D^{25.8}$ = +14.8 (*c* = 0.4, $CHCl_3$). FTIR (thin film) cm^{-1}: 3063, 3027, 2926, 2857, 2788, 1651, 1603, 1495, 1447, 1319, 1273, 1219, 1155, 1114, 1089, 1074, 1028, 979, 938, 908, 859, 786, 747, 720, 694, 630, 591, 570, 519. HRMS (ESI) m/z calcd. $C_{27}H_{31}N_2O_2S$ $[M+H]^+$ 447.2106, found 447.2107. ^{1}H-NMR (500 MHz; $CDCl_3$): δ 7.40-7.37 (m, 1H), 7.33-7.30 (m, 2H), 7.28-7.22 (m, 8H), 7.21-7.18 (m, 4H), 5.05-5.02 (m, 1H), 3.70-3.67 (m, 1H), 3.33 (dd, *J* = 14.8, 5.9 Hz, 1H), 2.84 (dd, *J* = 14.0, 4.9 Hz, 1H), 2.69 (dd, *J* = 14.1, 9.9 Hz, 1H), 2.59 (ddd, *J* = 14.8, 12.8, 3.5 Hz, 1H), 2.22-2.13 (m, 4H), 1.61-1.57 (m, 1H), 1.27 (dt, *J* = 10.4, 5.4 Hz, 2H), 0.86-0.83 (m, 1H), 0.72 (t, *J* = 5.8 Hz, 1H). ^{13}C-NMR ($CDCl_3$, 125 MHz):

140.7, 139.7, 138.5, 132.1, 129.9, 128.8, 128.6, 128.5, 128.3, 127.4, 126.9, 126.7, 58.8, 58.8, 52.0, 48.6, 40.1, 37.6, 35.8, 22.4, 21.3, 15.8.

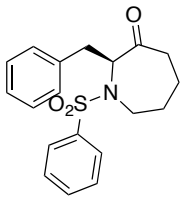

(*S*)-2-benzyl-1-(phenylsulfonyl)azepan-3-one (49). Following the general procedure for 3-azepinone formation, a solution of aminocyclopropane **41** (49 mg, 0.11 mmol) in EtOH (1.1 mL) was charged with 10% Pd/C (60 mg, 0.06 mmol) and 88% formic acid (52 μL, 1.1 μmol) and the system purged with H_2 three times. The mixture was stirred for 20 hrs at room temperature under an atmosphere of H_2, after which time the inorganic material was removed *via* filtration and the solvent reduced *in vacuo*. The crude material was subjected to silica gel flash chromatography (25% ethyl acetate in hexanes) to give the corresponding 3-azepinone as a light yellow solid (18 mg, 49%). R_f = 0.37 (20% ethyl acetate in hexanes). $[\alpha]_D^{26.1} = +19.5$ (*c* = 0.75 $CHCl_3$). FTIR (thin film) cm^{-1}: 3063, 3029, 2931, 2875, 1723, 1651, 1603, 1585, 1496, 1447, 1333, 1291, 1260, 1213, 1163, 1097, 1073, 1031, 999, 982, 950, 929, 906, 849, 784, 752, 721, 691, 651, 591, 555. HRMS (ESI) m/z calcd. $C_{19}H_{22}NO_3S$ $[M+H]^+$ 344.1320, found 344.1314. ^{1}H-NMR (500 MHz; $CDCl_3$): δ 7.54-7.48 (m, 3H), 7.37 (t, *J* = 7.8 Hz, 2H), 7.22-7.18 (m, 3H), 7.07-7.06 (m, 2H), 4.69 (t, *J* = 6.2 Hz, 1H), 3.60-3.54 (m, 1H), 3.19-3.10 (m, 2H), 3.02 (dd, *J* = 13.9, 7.4 Hz, 1H), 2.29-2.21 (m, 1H), 2.03-1.97 (m, 1H), 1.10-1.04 (m, 1H), 0.94 (d, *J* = 6.6 Hz, 3H). ^{13}C-NMR ($CDCl_3$, 125 MHz): 210.2, 139.4, 137.0, 132.6, 132.5, 129.7, 129.1, 129.0, 128.5, 127.0, 126.9, 65.5, 40.3, 39.8, 38.0, 27.7, 13.7.

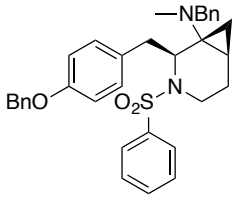

(1*R*,2*S*,6*R*)-*N*-benzyl-2-(4-(benzyloxy)benzyl)-*N*-methyl-3-azabicyclo[4.1.0]heptan-1-amine (43). To a solution of the *N*-methylamide **36** (0.2 g, 0.3 mmol) in THF (7.5 mL, 0.05M) under an argon atmosphere was added $ClTi(OiPr)_3$ (1.3 mL, 0.3M) dropwise *via* syringe. To this solution was added cyclohexylMgBr (0.8 mL, 2M) dropwise *via* syringe pump addition over 1 hr. After 4 hrs, the reaction mixture was poured onto ice water and stirred for 15 mins. The crude mixture was filtered thorough celite, and the two layers were separated. The aqueous layer was extracted once with EtOAc and the combined organics washed with brine and dried over Na_2SO_4. The crude mixture was subjected to flash chromatography (10% ethyl acetate in hexanes) to afford the cyclopropane **13** (0.1g, 48%) as a golden oil. R_f = 0.26 (10% ethyl acetate in hexanes). $[\alpha]_D^{19.5} = -1.45$ (*c* = 0.33 $CHCl_3$). FTIR (thin film) cm^{-1}: 3294, 3005, 3063, 3030, 2927, 2855, 1742, 1648, 1610, 1584, 1511, 1453, 1375, 1320, 1242, 1155, 1089, 1026. HRMS (ESI) m/z calcd. $C_{34}H_{37}N_2NaO_3S$ $[M+Na]^+$ 553.2525, found 553.2521. ^{1}H-NMR (500 MHz; $CDCl_3$): δ 7.51-7.22 (m, 15H), 7.10 (t, *J* = 13.8 Hz, 2H), 6.88 (q, *J* = 10.3 Hz, 2H), 5.07-5.03 (m, 2H), 5.01 (dd, *J* = 9.6, 4.8 Hz, 1H), 3.39 (dd, *J* = 14.6, 5.7 Hz, 1H), 2.80 (dt, *J* = 13.4, 6.3 Hz, 1H), 2.72-2.58 (m, 2H), 2.26-2.18 (m, 3H), 1.64-1.57 (m, 1H), 1.32-1.22 (m, 2H), 0.87 (dd, *J* = 9.8, 5.2 Hz, 1H), 0.74 (t, *J* = 5.8 Hz, 1H). ^{13}C-NMR ($CDCl_3$, 125 MHz): 157.5, 140.7, 139.5, 137.0, 131.8, 130.6, 130.5, 129.0, 128.5, 128.4, 128.3, 128.0, 127.9, 127.4, 127.3, 127.1, 126.9, 126.6, 114.7, 70.2, 69.9, 58.6, 51.9, 48.3, 39.0, 37.4, 35.6, 35.4, 25.3, 24.0, 22.4, 21.0, 15.5.

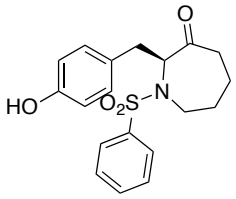

(*S*)-2-(4-hydroxybenzyl)-1-(phenylsulfonyl)azepan-3-one (51). A solution of aminocyclopropane **43** (21 mg, 38 μmol) in EtOH (0.4 mL) was charged with 10% Pd/C (4 mg, 3.8 μmol) and 88% formic acid (14.6 μL, 0.3 μmol) and the system purged with H_2 three times. The mixture was stirred for 20 hrs at room temperature under an atmosphere of H_2, after which time the inorganic material was removed *via* filtration and the solvent reduced *in vacuo*. The crude material was subjected to flash chromatography (30% ethyl acetate in hexanes) to give azepan-3-one **35** (10.1 mg, 55%). R_f = 0.3 (30% ethyl acetate in hexanes). $[\alpha]_D^{17.1} = +3.95$ (*c* = 0.19, $CHCl_3$). FTIR (thin film) cm^{-1}: 3401, 2924, 1715, 1614, 1516, 1447, 1313, 1264, 1155, 1091, 931. HRMS (ESI) m/z calcd. $C_{24}H_{21}NNaO_4S$ $[M+Na]^+$ 382.1079, found 382.1074. ^{1}H-NMR (500 MHz; $CDCl_3$): δ 7.60 (t, *J* = 14.6 Hz, 2H), 7.51 (q, *J* = 7.7 Hz, 1H), 7.44-7.39 (m, 2H), 6.95 (d, *J* = 8.3 Hz, 2H), 6.69 (d, *J* = 8.4 Hz, 2H), 4.52 (t, *J* = 7.4 Hz, 1H), 3.85 (d, *J* = 14.7 Hz, 1H), 3.43-3.37 (m, 1H), 2.98 (qd, *J* = 14.6, 7.4 Hz, 2H), 2.45 (dquintet, *J* = 12.6, 6.3 Hz, 1H), 2.07-1.95 (m, 2H), 1.83 (ddd, *J* = 10.8, 5.7, 2.8 Hz, 1H). ^{13}C-NMR ($CDCl_3$, 125 MHz): 207.3, 154.7, 140.2, 132.6, 130.4, 129.1, 127.8, 127.0, 115.5, 65.7, 40.8, 36.6, 33.1, 30.9, 14.1, 14.0.

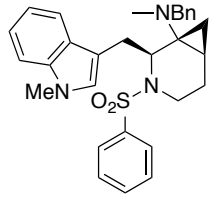

(1*R*,2*S*,6*R*)-*N*-benzyl-*N*-methyl-2-((1-methyl-1*H*-indol-3-yl)methyl)-3-(phenylsulfonyl)-3-azabicyclo[4.1.0]heptan-1-amine (45). Following the general

procedure for azabicyclic [4.1.0] aminocyclopropane formation, to a solution of the *N*-methylamide **38** (0.34 g, 0.66 mmol) in THF (13.3 mL) under an argon atmosphere was added $ClTi(OiPr)_3$ (0.66 mL, 1M) dropwise *via* syringe. To this solution was added cyclohexylMgCl (1.50 mL, 2M) dropwise *via* syringe pump addition over 1 hr. After 12 hrs, the reaction mixture was poured onto ice water and stirred for 15 mins. The crude mixture was filtered thorough celite, and the two layers were separated. The aqueous layer was extracted once with EtOAc and the combined organics washed with brine and dried over Na_2SO_4. The crude mixture was subjected to silica gel flash chromatography (20% ethyl acetate in hexanes) to isolate the corresponding major diastereomer aminocyclopropane as a light yellow solid (0.23 g, 69%). R_f = 0.3 (20% ethyl acetate in hexanes). $[\alpha]_D^{28.2} = +14.2$ (*c* = 0.5, $CHCl_3$). FTIR (thin film) cm^{-1}: 3059, 3026, 2930, 2855, 2789, 1615, 1585, 1555, 1493, 1473, 1446, 1424, 1376, 1343, 1323, 1271, 1252, 1217, 1154, 1126, 1089, 1063, 1027, 1012, 981, 935, 861, 794, 738, 695, 665, 632, 614, 585, 562, 525. HRMS (ESI) m/z calcd. $C_{30}H_{34}N_3O_2S$ $[M+H]^+$ 500.2372, found 500.2371. ^{1}H-NMR (500 MHz; $CDCl_3$): δ 7.62 (d, *J* = 7.9 Hz, 1H), 7.30-7.06 (m, 13H), 6.75 (s, 1H), 5.01 (t, *J* = 7.0 Hz, 1H), 3.66-3.59 (m, 5H), 3.50 (dt, *J* = 14.0, 6.3 Hz, 1H), 2.90 (t, *J* = 6.9 Hz, 2H), 2.73-2.67 (m, 1H), 2.22-2.16 (m, 4H), 1.90-1.86 (m, 1H), 1.75-1.70 (m, 1H), 1.65 (d, *J* = 13.7 Hz, 1H), 1.55-1.52 (m, 1H), 1.31-1.23 (m, 4H), 0.85 (dd, *J* = 9.6, 5.1 Hz, 1H), 0.79 (t, *J* = 5.8 Hz, 1H). ^{13}C-NMR ($CDCl_3$, 125 MHz): 141.0, 139.9, 136.9, 131.6, 128.4, 128.2, 128.2, 127.7, 126.8, 126.8, 121.6, 119.1, 119.0, 110.9, 109.3, 77.4, 70.4, 58.6, 51.1, 48.5, 37.6, 36.1, 35.7, 32.7, 29.5, 25.6, 24.3, 23.2, 21.3.

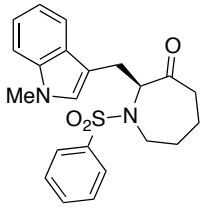

(*S*)-2-((1-methyl-1*H*-indol-3-yl)methyl)-1-(phenylsulfonyl)azepan-3-one (53). Following the general procedure for 3-azepinone formation, a solution of aminocyclopropane **45** (70 mg, 0.14 mmol) in EtOH (1.4 mL) was charged with 10% Pd/C (30 mg, 0.03 mmol) and 88% formic acid (65 μL, 1.4 μmol) and the system purged with H_2 three times. The mixture was stirred for 20 hrs at room temperature under an atmosphere of H_2, after which time the inorganic material was removed *via* filtration and the solvent reduced *in vacuo*. The crude material was subjected to silica gel flash chromatography (25% ethyl acetate in hexanes) to give the corresponding 3-azepinone as a yellow solid (15 mg, 27%). R_f = 0.3 (30% ethyl acetate in hexanes). $[\alpha]_D^{24.8}$ = +14.7(*c* = 0.3, $CHCl_3$). FTIR (thin film) cm^{-1}: 3058, 2924, 2852, 1722, 1646, 1615, 1585, 1551, 1470, 1446, 1377, 1328, 1290, 1260, 1217, 1159, 1094, 1073, 1036, 954, 925, 898, 849, 802, 742, 722, 690, 667, 647, 627, 583, 567. HRMS (ESI) m/z calcd. $C_{22}H_{25}N_2O_3S$ $[M+H]^+$ 397.1586, found 397.1588. ^{1}H-NMR (500 MHz; $CDCl_3$): δ 7.56-7.55 (m, 2H), 7.48 (dt, *J* = 7.8, 0.4 Hz, 2H), 7.35-7.32 (m, 2H), 7.24-7.19 (m, 3H), 7.09-7.06 (m, 1H), 6.69 (s, 1H), 4.71-4.69 (m, 1H), 3.65 (d, *J* = 7.3 Hz, 3H), 3.64-3.60 (m, 1H), 3.31-3.28 (m, 2H), 3.18-3.15 (m, 1H), 2.23-2.19 (m, 1H), 1.94-1.90 (m, 1H), 1.05-1.00 (m, 1H), 0.93-0.90 (m, 2H). ^{13}C-NMR ($CDCl_3$, 125 MHz): 210.9, 139.9, 136.9, 132.5, 129.0, 128.3, 127.9, 126.9, 121.8, 119.4, 119.3, 109.6, 109.2, 65.2, 40.8, 40.1, 32.8, 29.9, 28.3, 27.9, 14.0.

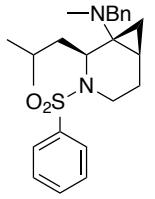

(1*R*,2*S*,6*R*)-*N*-benzyl-2-isobutyl-*N*-methyl-3-(phenylsulfonyl)-3-azabicyclo[4.1.0]heptan-1-amine (47). Following the general procedure for azabicyclic [4.1.0] aminocyclopropane formation, to a solution of the *N*-methylamide **40** (0.27 g, 0.62 mmol) in THF (12.5 mL) under an argon atmosphere was added $ClTi(OiPr)_3$ (0.62 mL, 1M) dropwise *via* syringe. To this solution was added cyclohexylMgCl (1.40 mL, 2M) dropwise *via* syringe pump addition over 1 hr. After 12 hrs, the reaction mixture was poured onto ice water and stirred for 15 mins. The crude mixture was filtered thorough celite, and the two layers were separated. The aqueous layer was extracted once with EtOAc and the combined organics washed with brine and dried over Na_2SO_4. The crude mixture was subjected to silica gel flash chromatography (15% ethyl acetate in hexanes) to isolate the corresponding major diastereomer aminocyclopropane (0.18 g, 68%). R_f = 0.7 (30% ethyl acetate in hexanes). $[\alpha]_D^{28.6} = +65.2$ (*c* = 0.6, CH_2Cl_2). FTIR (thin film) cm^{-1}: 3064, 3027, 3005, 2954, 2867, 2837, 2787, 2704, 2333, 1961, 1896, 1813, 1651, 1602, 1586, 1494, 1467, 1447, 1416, 1366, 1331, 1291, 1272, 1244, 1224, 1162, 1129, 1089, 1072, 1063, 1028, 1004, 983, 951, 927, 854, 825, 789, 736, 696, 669, 630, 612, 584, 568, 551, 515, 466. HRMS (ESI) m/z calcd. $C_{24}H_{33}N_2O_2S$ $[M+H]^+$ 413.2263, found 413.2260. ^{1}H-NMR (500 MHz; $CDCl_3$): δ 7.89 (d, *J* = 7.4 Hz, 2H), 7.53-7.43 (m, 4H), 7.28-7.19 (m, 8H), 4.68 (d, *J* = 10.4 Hz, 1H), 3.69 (d, *J* = 12.8 Hz, 1H), 3.54 (d, *J* = 12.8 Hz, 1H), 3.45 (dd, *J* = 15.0, 5.6 Hz, 1H), 2.57 (ddd, *J* = 15.0, 13.1, 3.3 Hz, 1H), 2.13 (s, 4H), 1.83 (tt, *J* = 12.8, 6.2 Hz, 1H), 1.68 (ddtd, *J* = 13.2, 9.9, 6.6, 3.3

Hz, 1H), 1.51 (ddd, J = 18.0, 14.9, 11.7 Hz, 3H), 1.14-1.09 (m, 2H), 1.06 (d, J = 6.4 Hz, 3H), 0.88 (d, J = 6.7 Hz, 3H), 0.69 (dd, J = 9.7, 5.1 Hz, 1H), 0.56 (t, J = 5.7 Hz, 1H). ^{13}C-NMR ($CDCl_3$, 125 MHz): 141.3, 139.4, 132.3, 128.8, 128.7, 128.3, 128.1, 128.1, 127.3, 127.0, 126.7, 58.8, 48.5, 48.1, 43.4, 37.4, 35.5, 24.6, 24.1, 21.9, 21.7, 21.0, 14.9.

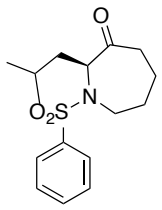

(*S*)-2-isobutyl-1-(phenylsulfonyl)azepan-3-one (55). Following the general procedure for 3-azepinone formation, a solution of aminocyclopropane **47** (47 mg, 0.11 mmol) in EtOH (1.2 mL) was charged with 10% Pd/C (62 mg, 0.06 mmol) and 88% formic acid (54 μL, 1.2 μmol) and the system purged with H_2 three times. The mixture was stirred for 20 hrs at room temperature under an atmosphere of H_2, after which time the inorganic material was removed *via* filtration and the solvent reduced *in vacuo*. The crude material was subjected to silica gel flash chromatography (15% ethyl acetate in hexanes) to give the corresponding 3-azepinone (15 mg, 42%). R_f = 0.3 (20% ethyl acetate in hexanes). $[\alpha]_D^{28.4}$ = +20.9 (c = 1.5, $CHCl_3$). FTIR (thin film) cm^{-1}: 3299, 3066, 2958, 2931, 2871, 1717, 1651, 1585, 1447, 1341, 1318, 1290, 1267, 1233, 1166, 1091, 1072, 1032, 999, 981, 931, 884, 838, 748, 730, 691, 633, 585, 571. HRMS (ESI) m/z calcd. $C_{16}H_{23}NO_3NaS$ $[M+Na]^+$ 332.1287, found 332.1287.^{1}H-NMR (500 MHz; $CDCl_3$): δ 7.77 (d, J = 7.9 Hz, 2H), 7.48-7.47 (m, 3H), 4.40-4.37 (m, 1H), 3.90-3.86 (m, 1H), 3.47-3.41 (m, 1H), 2.51-2.48 (m, 1H), 1.78-1.74 (m, 1H), 1.70-1.62 (m, 2H), 1.49-1.47 (m, 1H), 1.44-1.39 (m, 1H), 1.24-1.22 (m, 1H), 1.08-1.04 (m, 1H), 0.94-0.79 (m, 10H).

^{13}C-NMR ($CDCl_3$, 125 MHz): 208.2, 140.7, 132.8, 129.3, 129.2, 127.1, 63.2, 40.2, 39.5, 39.1, 33.2, 24.4, 22.7, 21.9, 14.0.

3.6) References

[1] (a) Kulinkovich, O. G., Sviridov, S. V., Vasilevskii, D. A., Prityтskaya, T. S., "Reaction of ethylmagnesium bromide with carboxylic acid esters in the presence of tetraisopropoxytitanium." *Zh. Org. Khim.* **1989**, *25*, 2244-2245. (b) Kulinkovich, O. G., Sviridov, S. V., Vasilevskii, D. A., "Titanium(IV) isopropoxide-catalyzed formation of 1-substituted cyclopropanols in the reaction of ethylmagnesium bromide with methyl alkanecarboxylates." *Synthesis* **1991**, *3*, 234.

[2] Chaplinski, V., deMeijere, A. "A versatile new preparation of cyclopropylamines from acid dialkylamides." *Angew. Chem. Int. Ed. Engl.* **1996**, *35*, 413-414.

[3] (a) Kulinkovich, O. G., Savchenko, A. I., Sviridov, S. V., Vasilevski, D. A. "Titanium(IV) isopropoxide-catalyzed reaction of ethylmagnesium bromide with ethyl acetate in the presence of styrene." *Mendeleev Commun.* **1993**, *6*, 230-231. (b) Epstein, O. L., Savchenko, A. I., Kulinkovich, O. G. "Titanium(IV) isopropoxide-catalyzed reaction of alkylmagnesium halides with ethyl acetate in the presence of styrene. Non-hydride mechanism of ligand exchange in the titanacyclopropanes." *Tetrahedron Lett.* **1999**, *40*, 5935-5938.

[4] (a) Chaplinski, V., Winsel, H., Kordes, M., de Meijere, A. "A new versatile reagent for the synthesis of cyclopropylamines including 4-azaspiro[2.n]alkanes and bicyclo[n.1.0]alkylamines." *Synlett* **1997**, 111-114. (b) Williams, C. M., Chaplinski, V., Schreiner, P. R., de Meijere, A. "Unexpected titanium shifts during cyclopropanation of

N,N-dibenzylformamide with ligand-exchanged titanium-alkadiene complexes." *Tetrahedron Lett.* **1998**, *39*, 7695-7698.

[5] (a) Okamoto, S., Iwakubo, M., Kobayashi, K., Sato, F. "Efficient and practical method for synthesizing *N*-heterocyclic compounds using intramolecular nucleophilic acyl substitution reactions mediated by Ti(O-*i*-Pr)$_4$/2*i*-PrMgX reagent. Synthesis of quinolones, pyrroles, indoles, and optically active *N*-heterocycles including allopumiliotoxin alkaloid 267A." *J. Am. Chem. Soc.* **1997**, *119*, 6984-6990. (b) Kasatkin, A., Kobayashi, K., Okamoto, S., Sato, F. "Synthesis of 1-hydroxybicyclo[n.1.0]alkanes (n = 3 and 4) and their silyl ethers from olefinic esters via tandem intramolecular nucleophilic acyl substitution and intramolecular carbonyl addition reactions mediated by Ti(OPr-i)$_4$2PrMgCl reagent." *Tetrahedron Lett.* **1996**, *37*, 1849-1852. (c) Kasatkin, A., Sato, F. "Diastereoselective synthesis of *trans*-1,2-disubstituted cyclopropanols from homoallyl or bis-homoallyl esters via tandem intramolecular nucleophilic acyl substitution and intramolecular carbonyl addition reactions mediated by Ti(OPr-*i*)$_4$/2 *i*-PrMgBr reagent." *Tetrahedron Lett.* **1995**, *36*, 6079-6082. (d) Jong, S. U., Lee, J., Cha, J. K. "A new route to seven-and eight-membered carbocycles." *Tetrahedron Lett.* **1997**, *38*, 5233-5236.

[6] (a) Cao, B., Xiao, D., Joullié, M. M. "Synthesis of bicyclic cyclopropylamines by intramolecular cyclopropanation of *N*-allylamino acid dimethylamides." *Org. Lett.* **1999**, *1*, 1799-1801. (b) Faler, C. A., Cao, B., Joullié, M. M. "Synthesis of bicyclic cyclopropylamines from amino acid derivatives." *Heterocycles* **2006**, *67*, 519-522.

[7] (a) Tebben, G.-D., Rauch, K., Stratmann, C., Williams, C. M., de Meijere, A. "Intramolecular titanium-mediated aminocyclopropanation of terminal alkenes: Easy access to various substituted azabicyclo[n.1.0]alkanes." *Org. Lett.* **2003**, *5*, 483-485. (b) Gensini, M., de Meijere, A. "Cyclopropane-annelated azaoligoheterocycles by Ti-mediated intramolecular reductive cyclopropanation of cyclic amino acid amides." *Chem.—Eur. J.* **2004**, *10*, 785-790. (c) Gensini, M., Kozhushkov, S. I., Yufit, D. S., Howard, J. A. K., Es-Sayed, M., de Meijere, A. "3-Azabicyclo[3.1.0]hex-1-ylamines by Ti-mediated intramolecular reductive cyclopropanation of *alpha*-(*N*-allylamino)-substituted *N,N*-dialkylcarboxamides and carbonitriles." *Eur. J. Org. Chem.* **2002**, 2499-2507.

[8] Grieco, P. A., Bahsas, A. "Reactions of allylstannanes with in situ generated immonium salts in protic solvent: A facile aminomethano destannylation process." *J. Org. Chem.* **1987**, *52*, 1378-1380.

[9] Most recent review on Kulinkovich reaction and its applications: Wolan, A., Six, Y. "Synthetic transformation mediated by the combination of titanium(IV) alkoxides and grignard reagents: selectivity issues and recent applications. Part 1: reactions of carbonyl derivatives and nitriles." *Tetrahedron* **2010**, *66,* 15-61.

[10] Kuehne, M. E., King, J. C. "Cyclopropylamines as intermediates in a new method for alkylation of aldehydes and ketones." *J. Org. Chem.* **1973**, *38*, 304-311.

[11] (a) Lee, J., Sun U, J., Blackstock, S. C., Cha, J. K. "Facile ring opening of tertiary aminocyclopropanes by photooxidation." *J. Am. Chem. Soc.* **1997**, *119*, 10241-10242. (b) Lee, H. B., Sung, M. J., Blackstock, S. C., Cha, J. K. "Radical cation-mediated

annulation. Stereoselective construction of bicyclo[5.3.0]decan-3-ones by aerobic oxidation of cyclopropylamines." *J. Am. Chem. Soc.* **2001**, *123*, 11322-11324.

[12] Weintraub, P. M., Sabol, J. S., Kane, J. M., borcherding, D. R. "Recent advances in the synthesis of piperidones and piperidines." *Tetrahedron* **2003**, *59*, 2953-2989.

[13] Wang, H., Matsuhashi, H., Doan, B. D., Goodman, S. N., Ouyang, X., Clarck, W. M., Jr. "Large-scale synthesis of SB-462795, a cathepsin K inhibitor: the RCM-based approaches." *Tetrahedron* **2009**, *65*, 6291-6303.

[14] Dubinina, G. G., Yoshida, W. Y., Chain, W. J. "On the preparation of azepinones." *Tetrahedron Lett.* **2010**, *51*, 5325-5327.

[15] C. A. Faler, "Synthesis and applications of cyclopropylamines and cyclopropanols from Ti-mediated cyclopropanation", University of Pennsylvania, Philadelphia, PA, 2007.

[16] Schulte-Wülwer, I. A., Helaja, J., Göttlich, R. "Copper(I)-catalyzed intramolecular addition of *N*-chloroamides to double bonds; an efficient synthesis of lactams from unsaturated amides." *Synthesis* **2003**, 1886-1890.

[17] Lee, J., Berritt, S., Prier, C. K., Joullié, M. M. "Facile ring-opening of azabicyclic[3.1.0]-and [4.1.0]aminocyclopropanes to afford 3-piperidinone and 3-azepinone." *Org. Lett.* **2011**, *13*, 1083-1085.

[18] Ishikawa, S., Sheppard, T. D., D'Oyley, J. M., Kamimura, A., Motherwell, W. B. "A rapid route to aminocyclopropanes via carbamatoorganozinc carbenoids." *Angew. Chem. Int. Ed.* **2013**, *52*, 10060-10063.

[19] de Meijere, A., Williams, C. M., Kourdioukov, A., Sviridov, S. V., Chaplinski, V., Kordes, M., Savchenko, A. I., Stratmann, C., Noltemeyer, M. "Mono- and disubstituted

N,N-dialkylcyclopropylamines from dialkylformamides via ligand-exchanged titanium-alkene complexes." *Chem.—Eur. J.* **2002**, *8*, 3789-3810.

3.7) Appendix B. Nuclear Magnetic Resonance and Infrared Spectra Relevant to Chapter 3

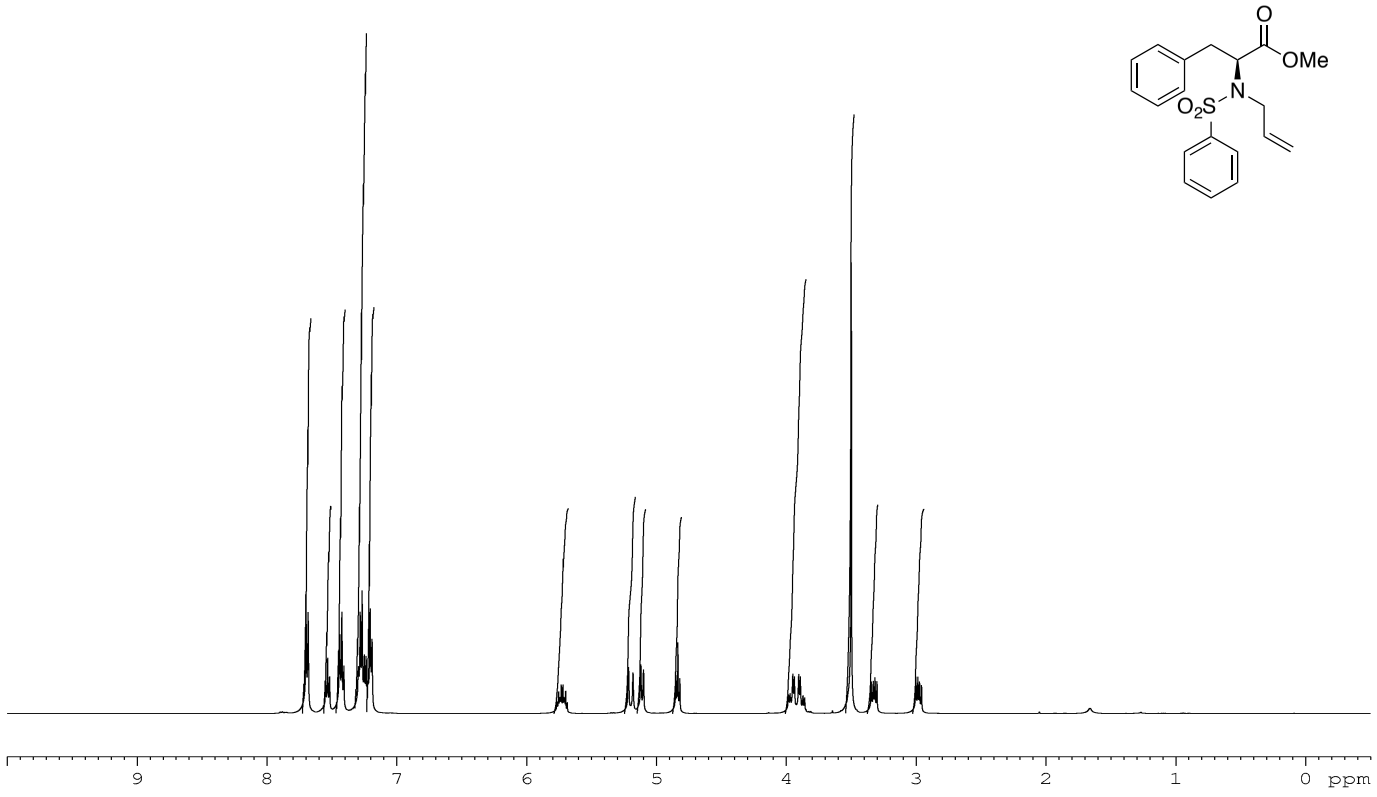

Figure 1: ^{1}H NMR ($CDCl_3$, 500 MHz) of **25**

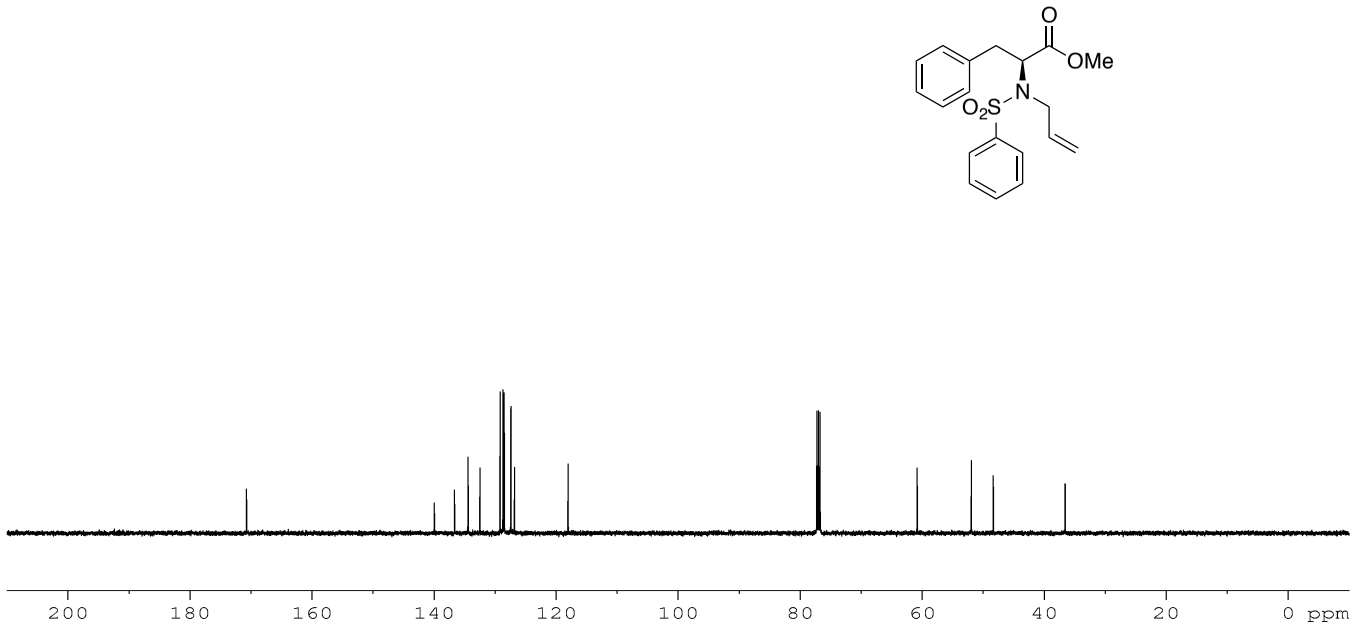

Figure 2: ^{13}C NMR ($CDCl_3$, 125 MHz) of **25**

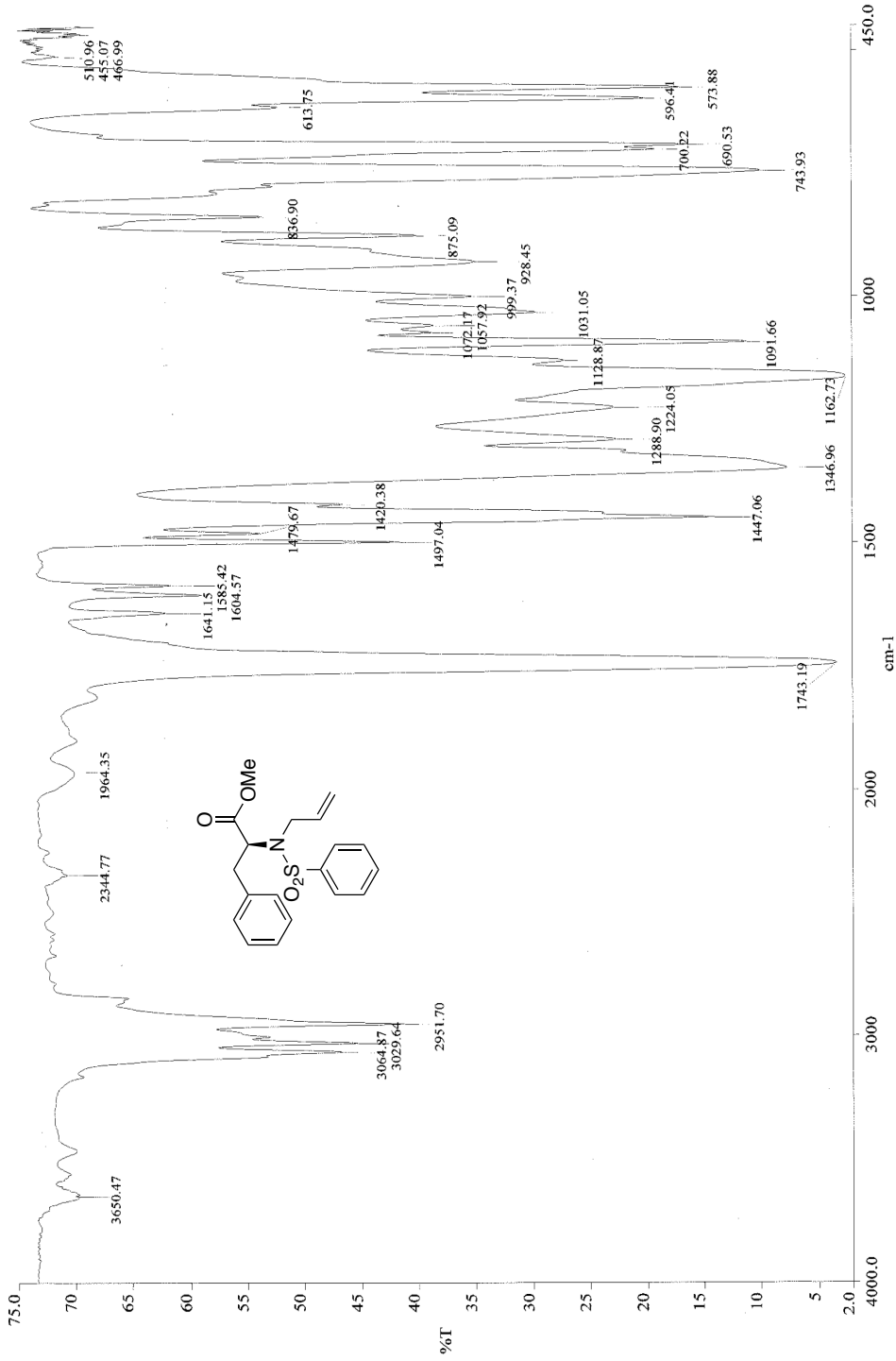

Figure 3: Infrared spectra (neat) of **25**

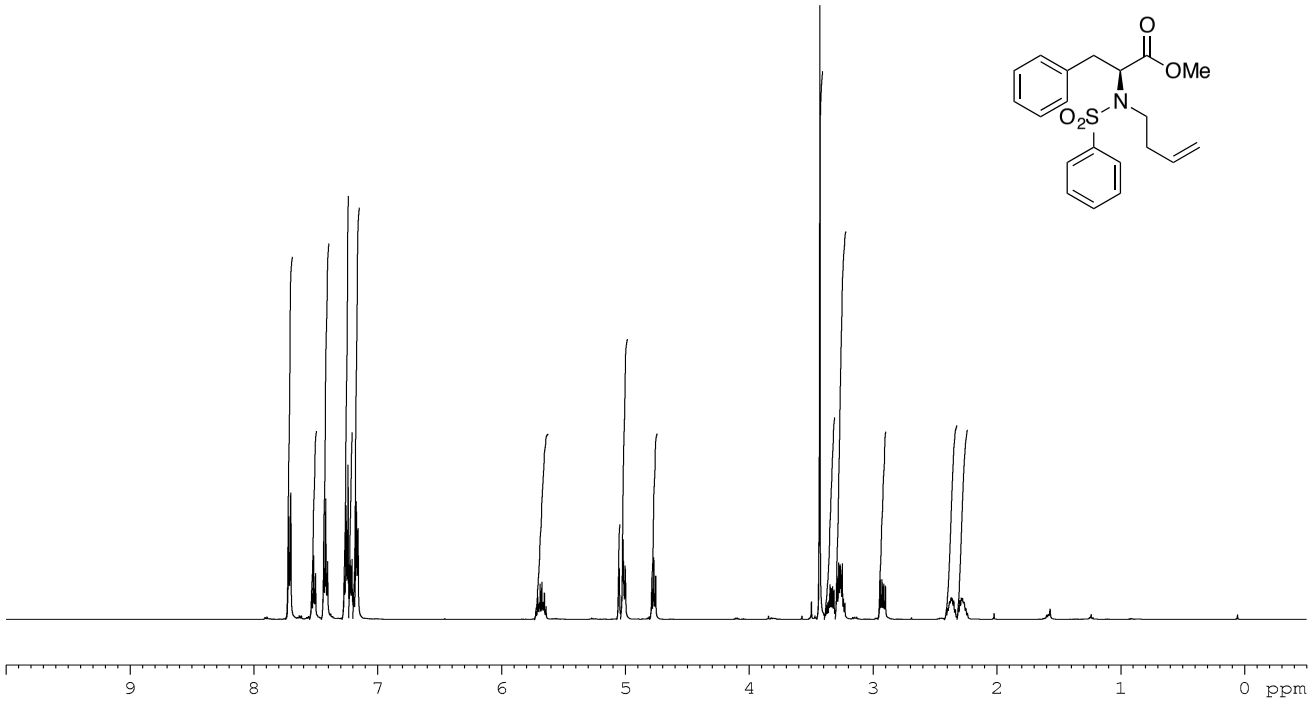

Figure 4: ^{1}H NMR ($CDCl_3$, 500 MHz) of **26**

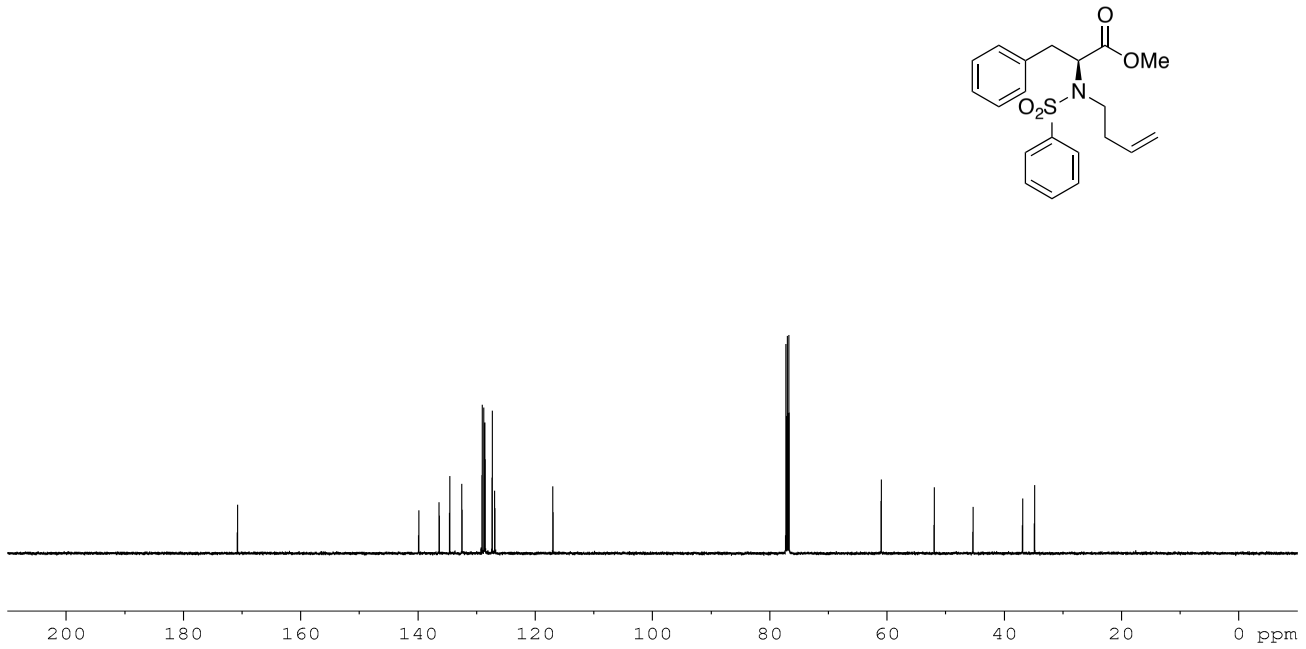

Figure 5: ^{13}C NMR ($CDCl_3$, 125 MHz) of **26**

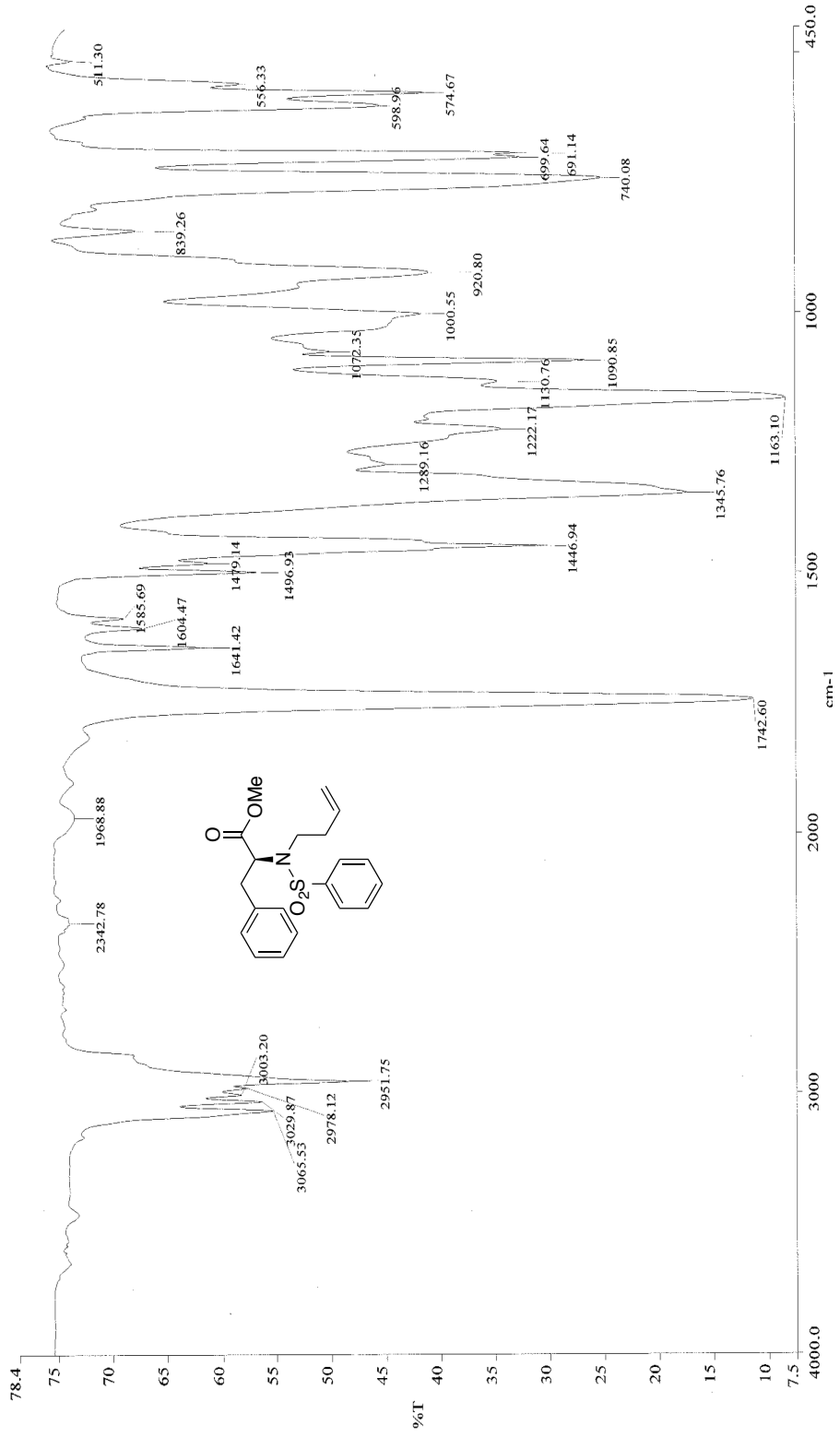

Figure 6: Infrared spectra (neat) of **26**

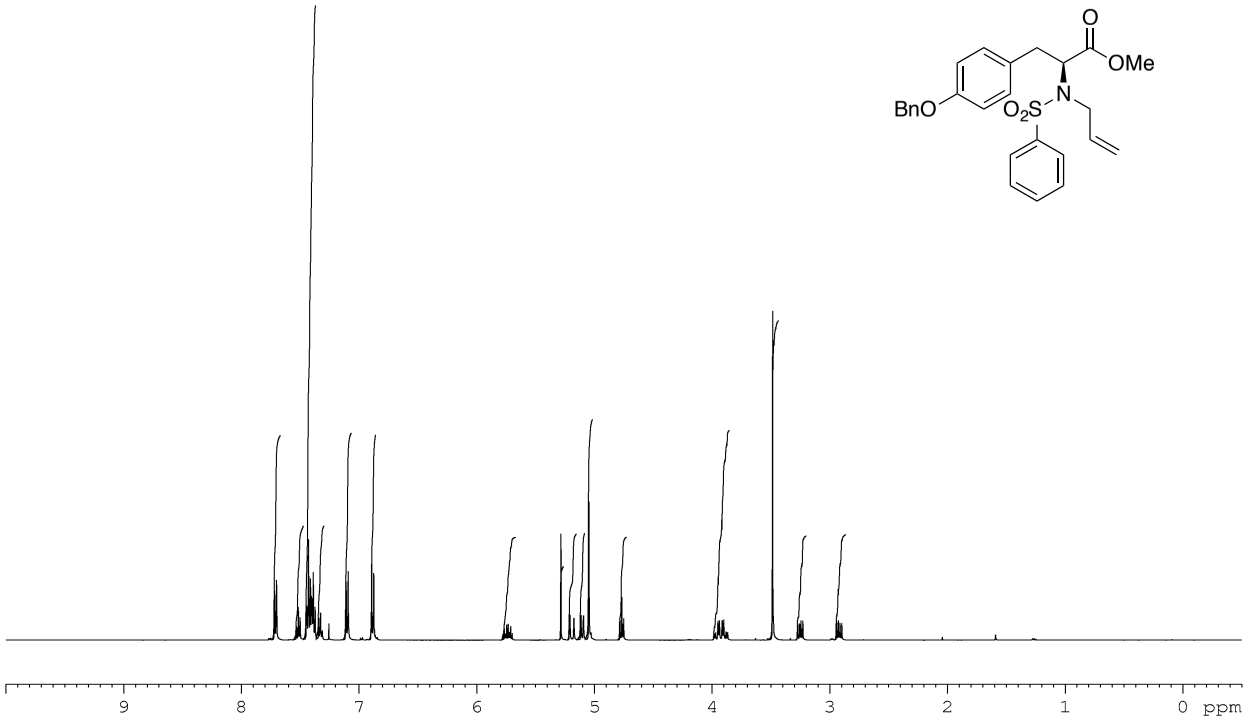

Figure 7: ^{1}H NMR ($CDCl_3$, 500 MHz) of **27**

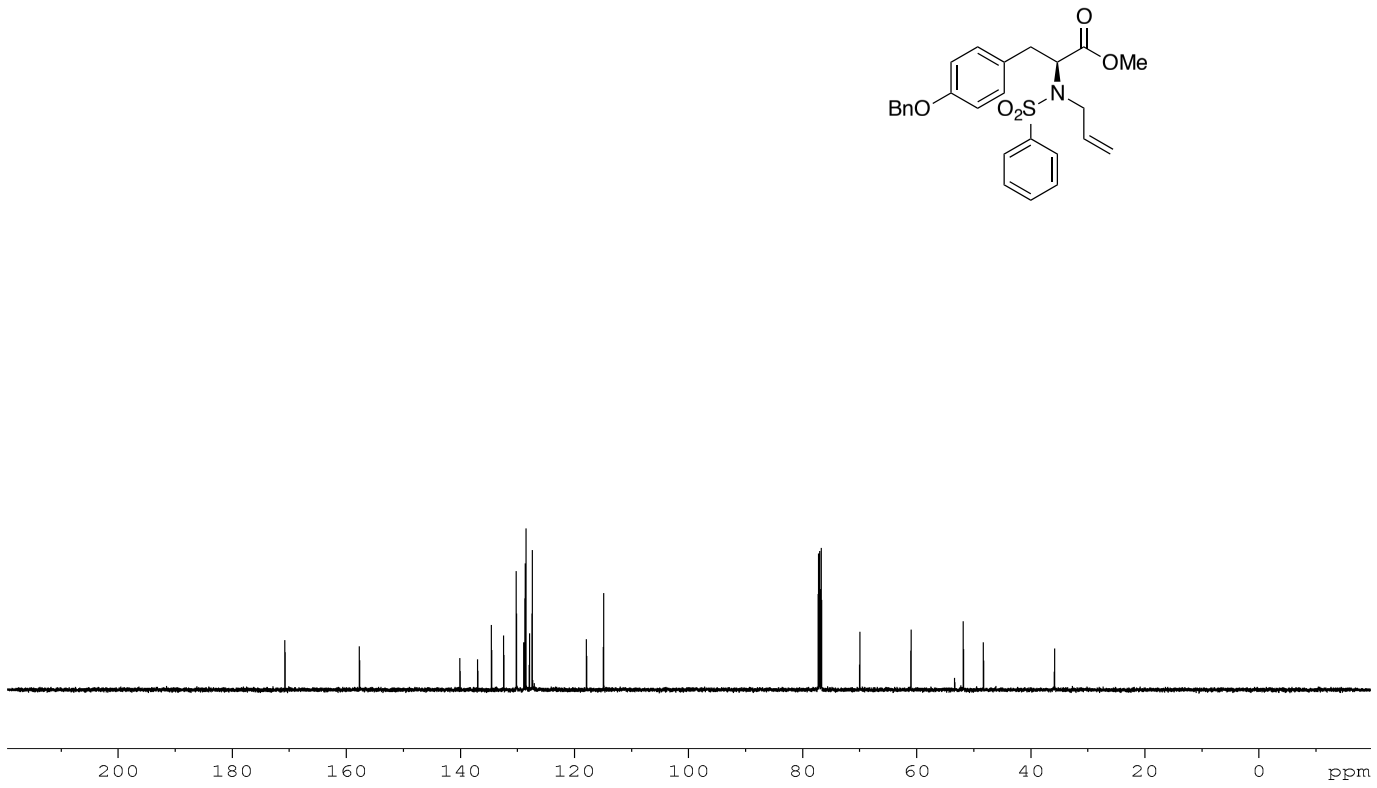

Figure 8: ^{13}C NMR ($CDCl_3$, 125 MHz) of **27**

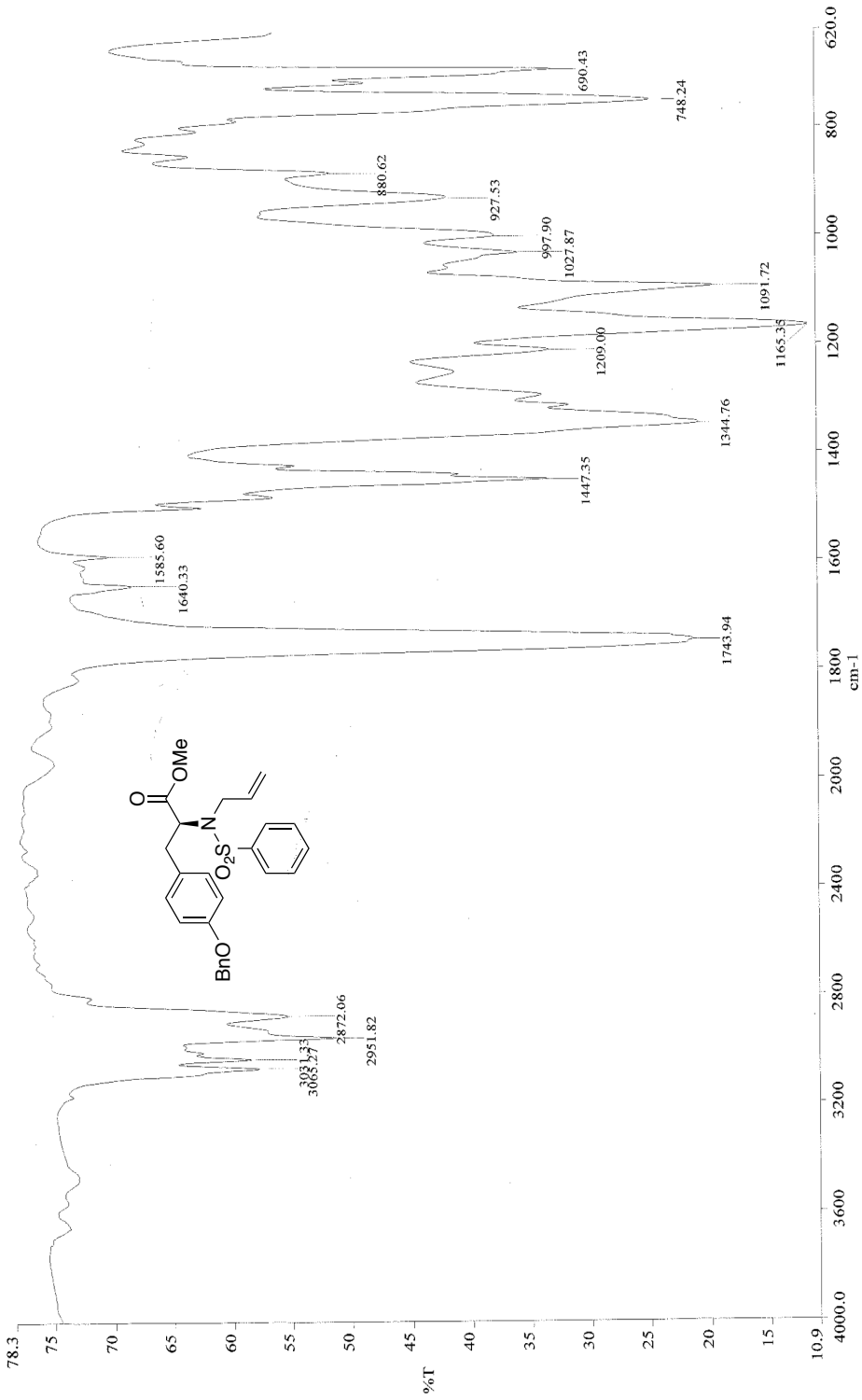

Figure 9: Infrared spectra (neat) of **27**

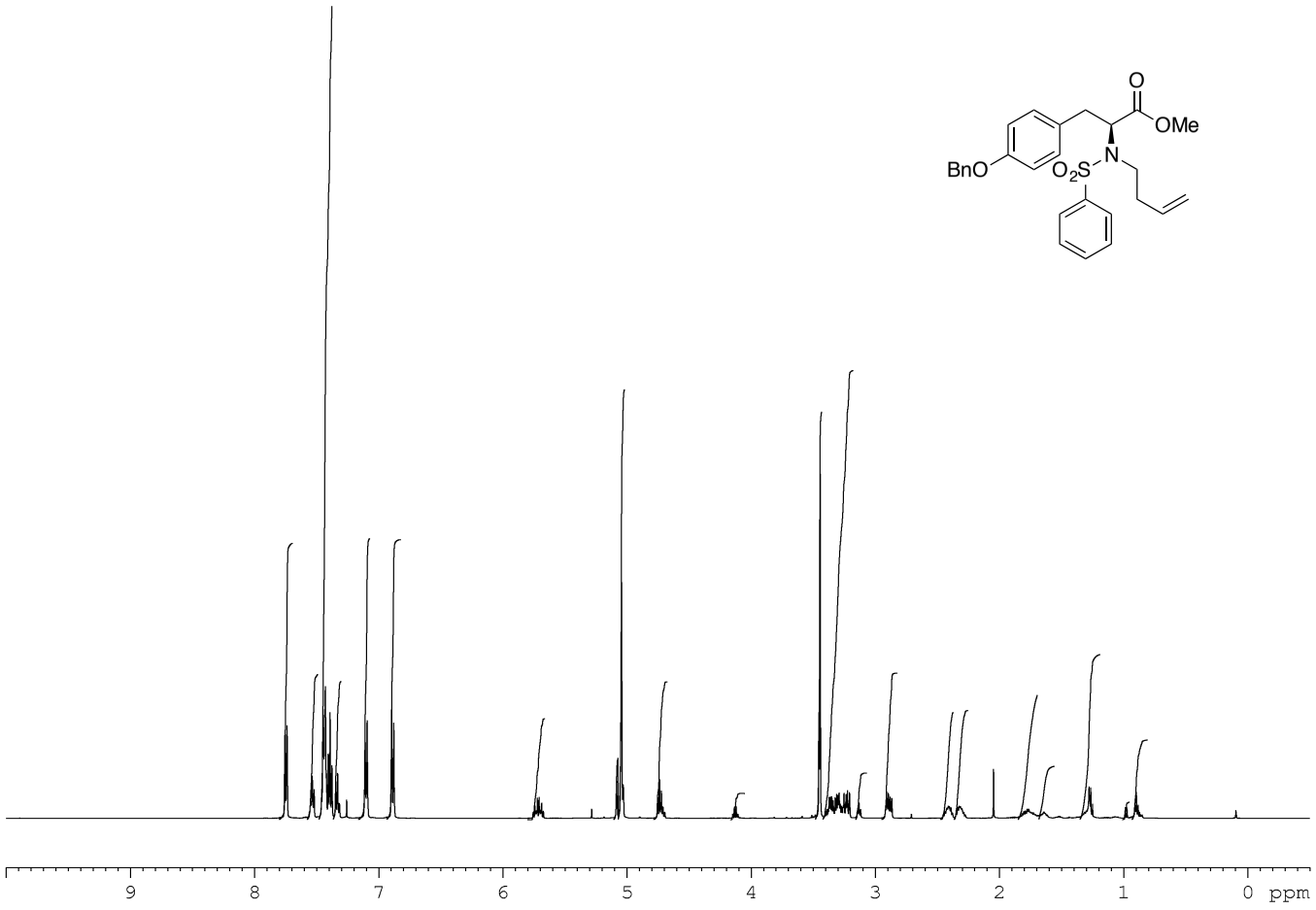

Figure 10: ^{1}H NMR ($CDCl_3$, 500 MHz) of **28**

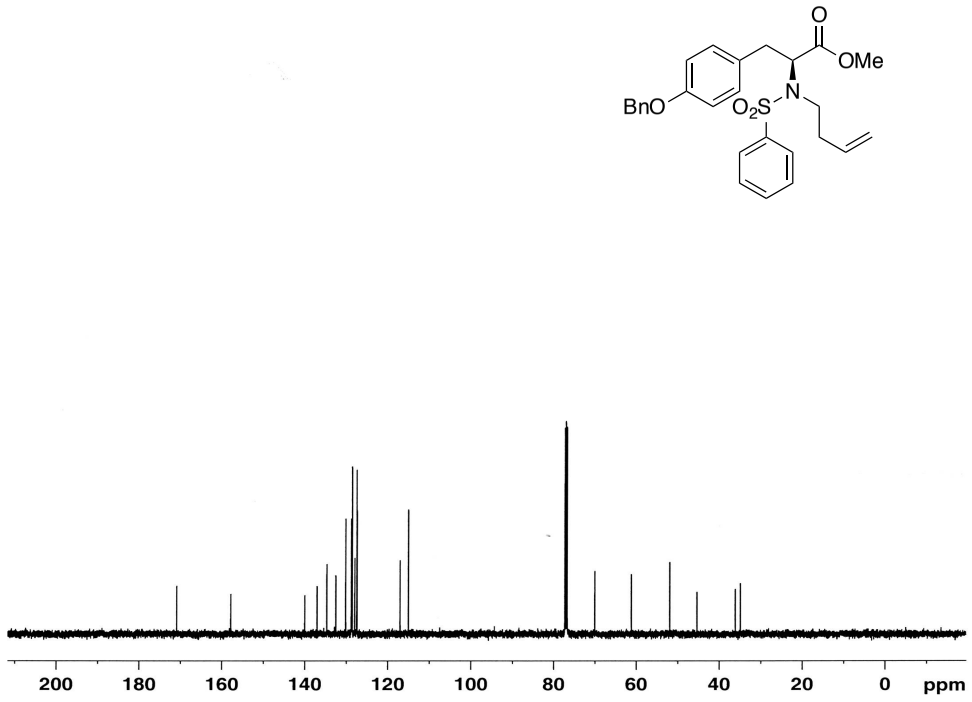

Figure 11: ^{13}C NMR ($CDCl_3$, 125 MHz) of **28**

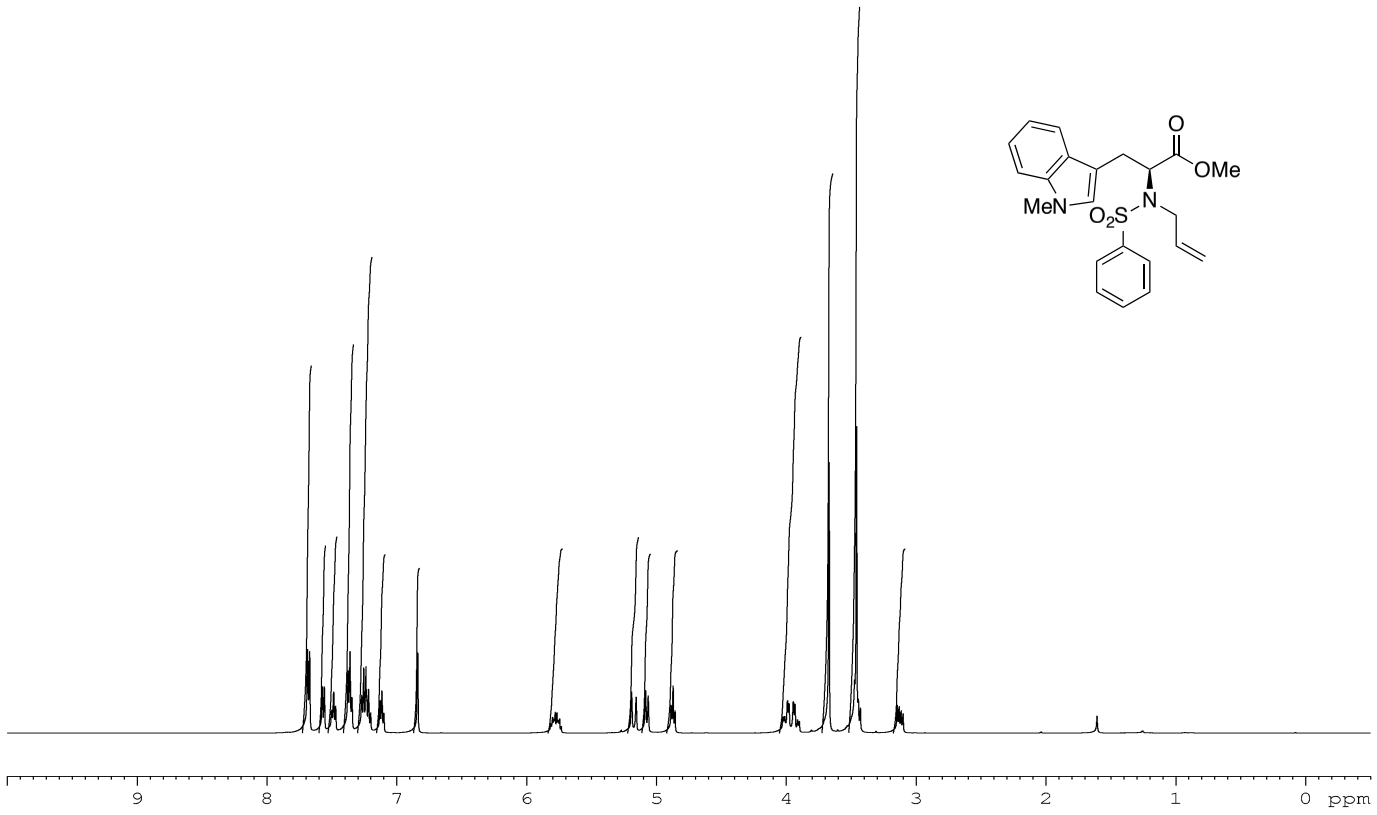

Figure 12: ^{1}H NMR ($CDCl_3$, 500 MHz) of **29**

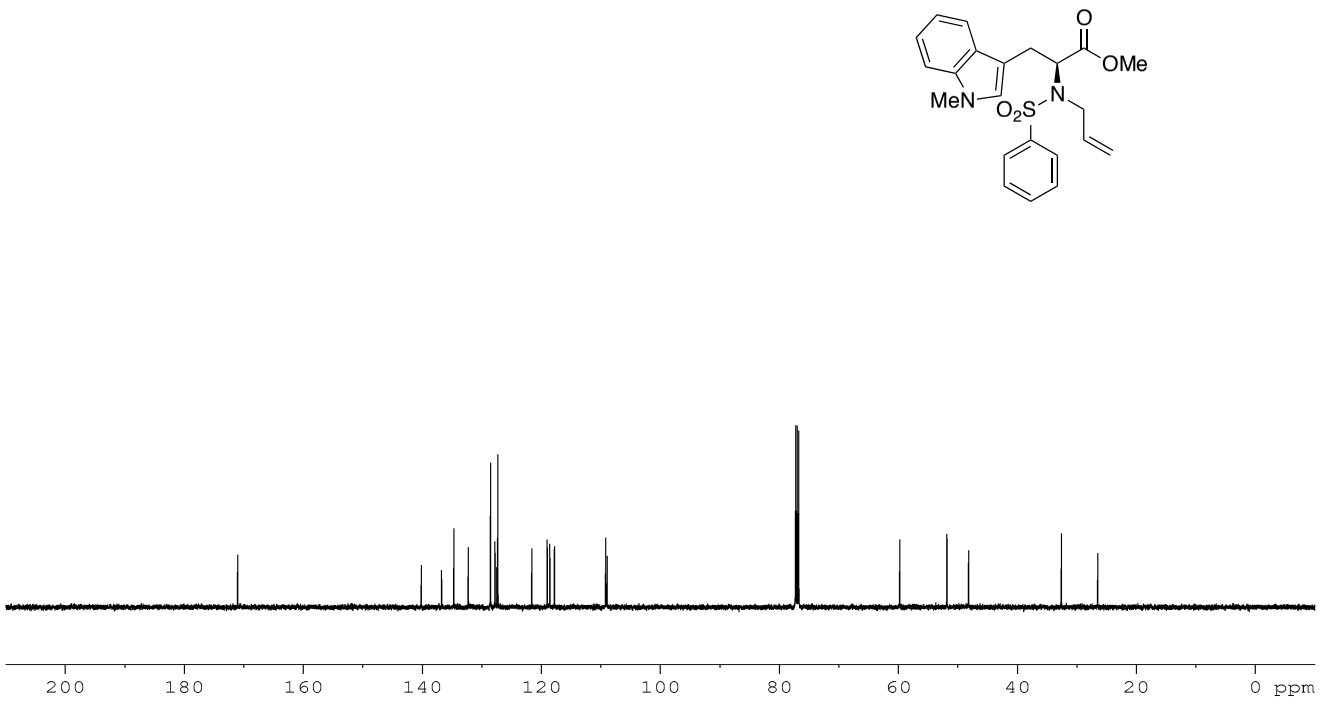

Figure 13: ^{13}C NMR ($CDCl_3$, 125 MHz) of **29**

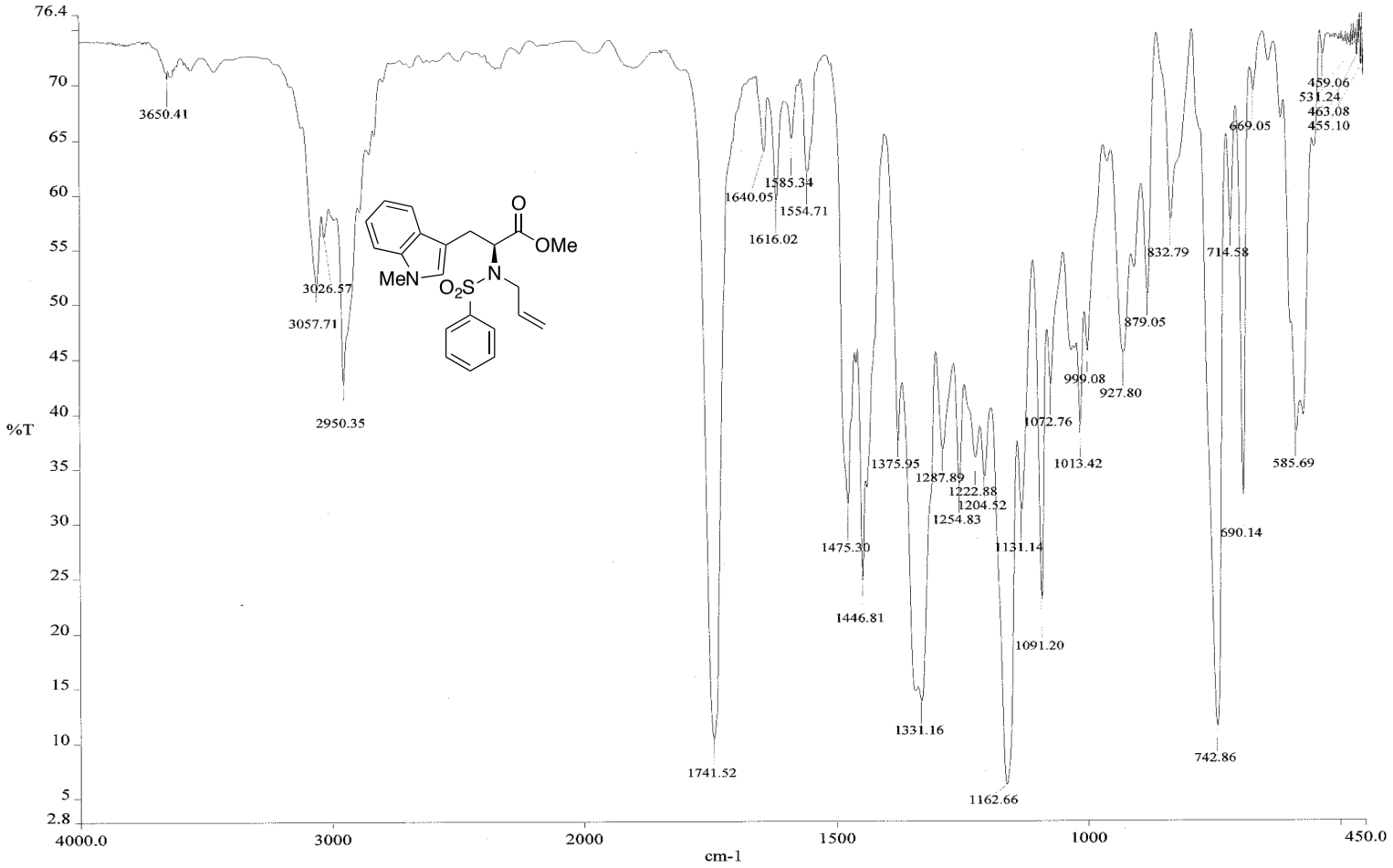

Figure 14: Infrared spectra (neat) of **29**

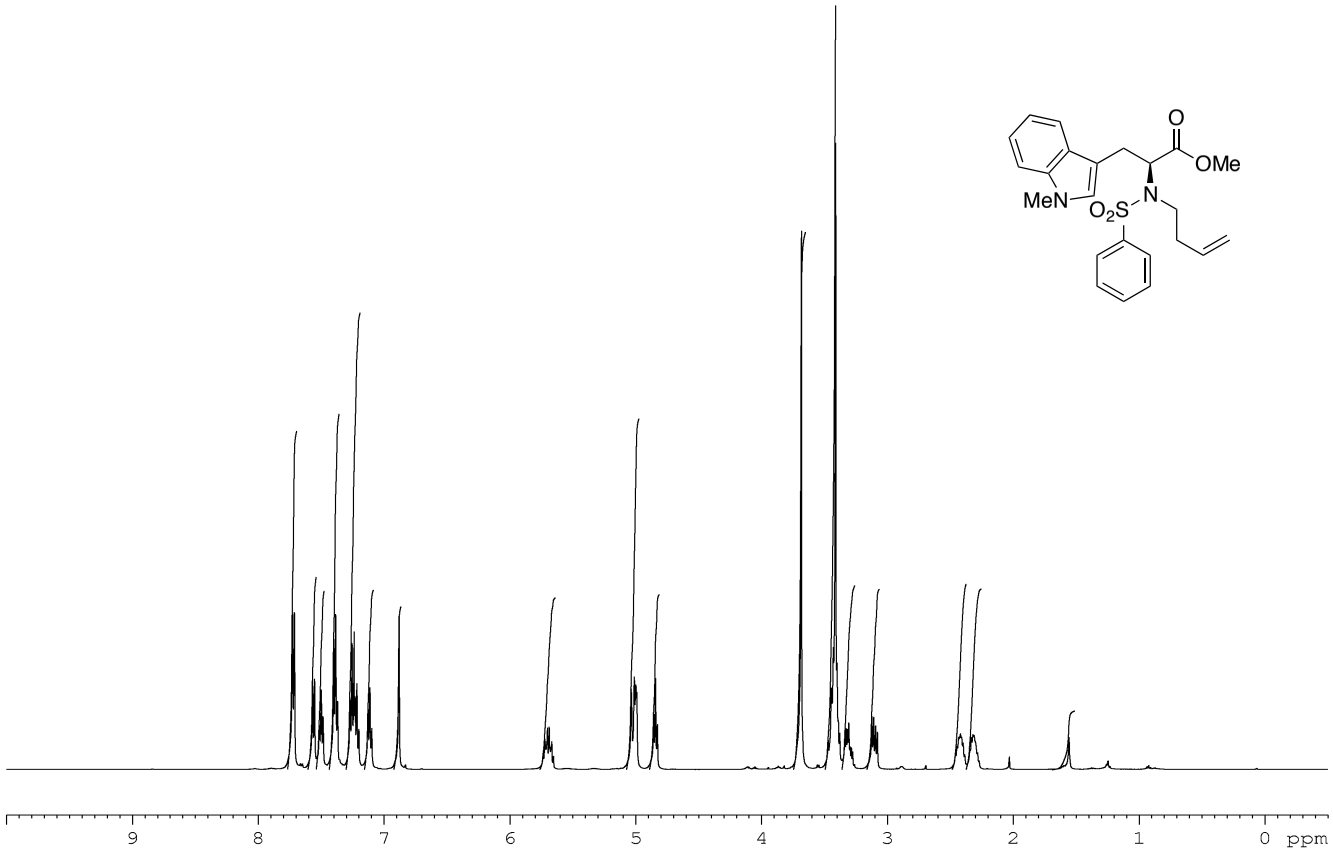

Figure 15: ^{1}H NMR ($CDCl_3$, 500 MHz) of **30**

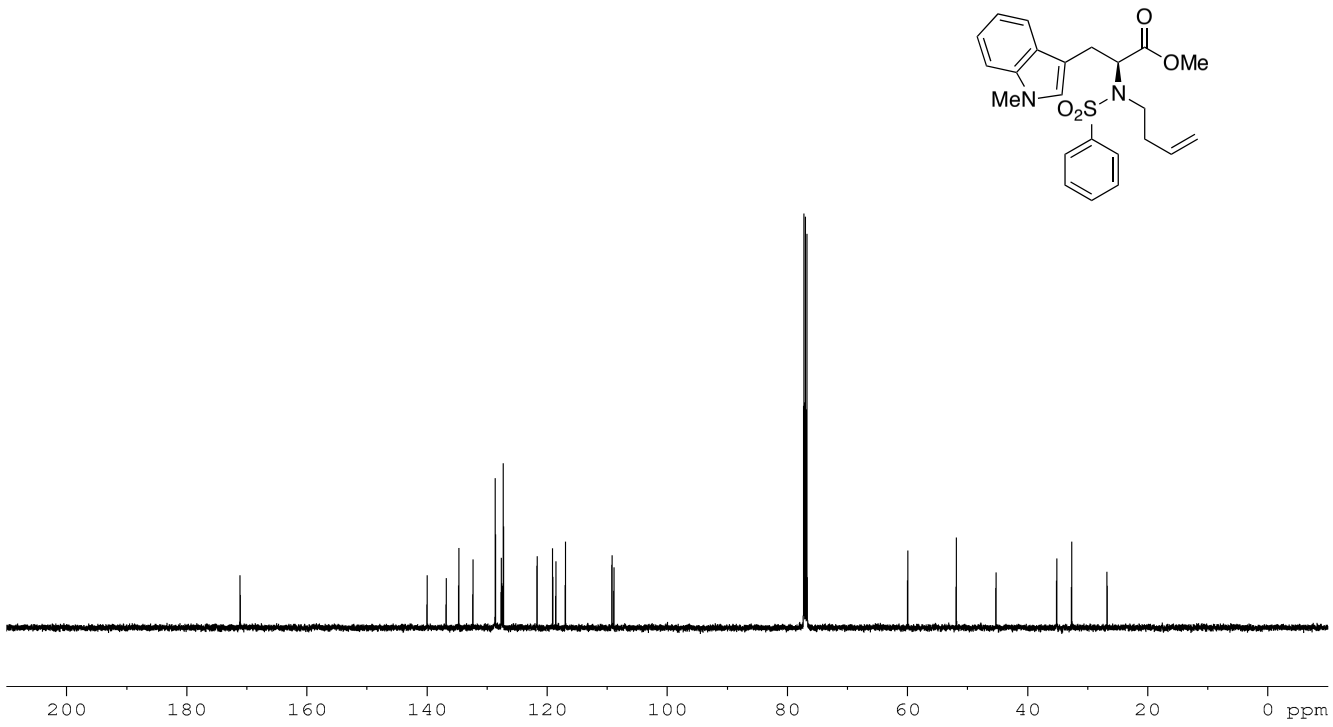

Figure 16: ^{13}C NMR ($CDCl_3$, 125 MHz) of **30**

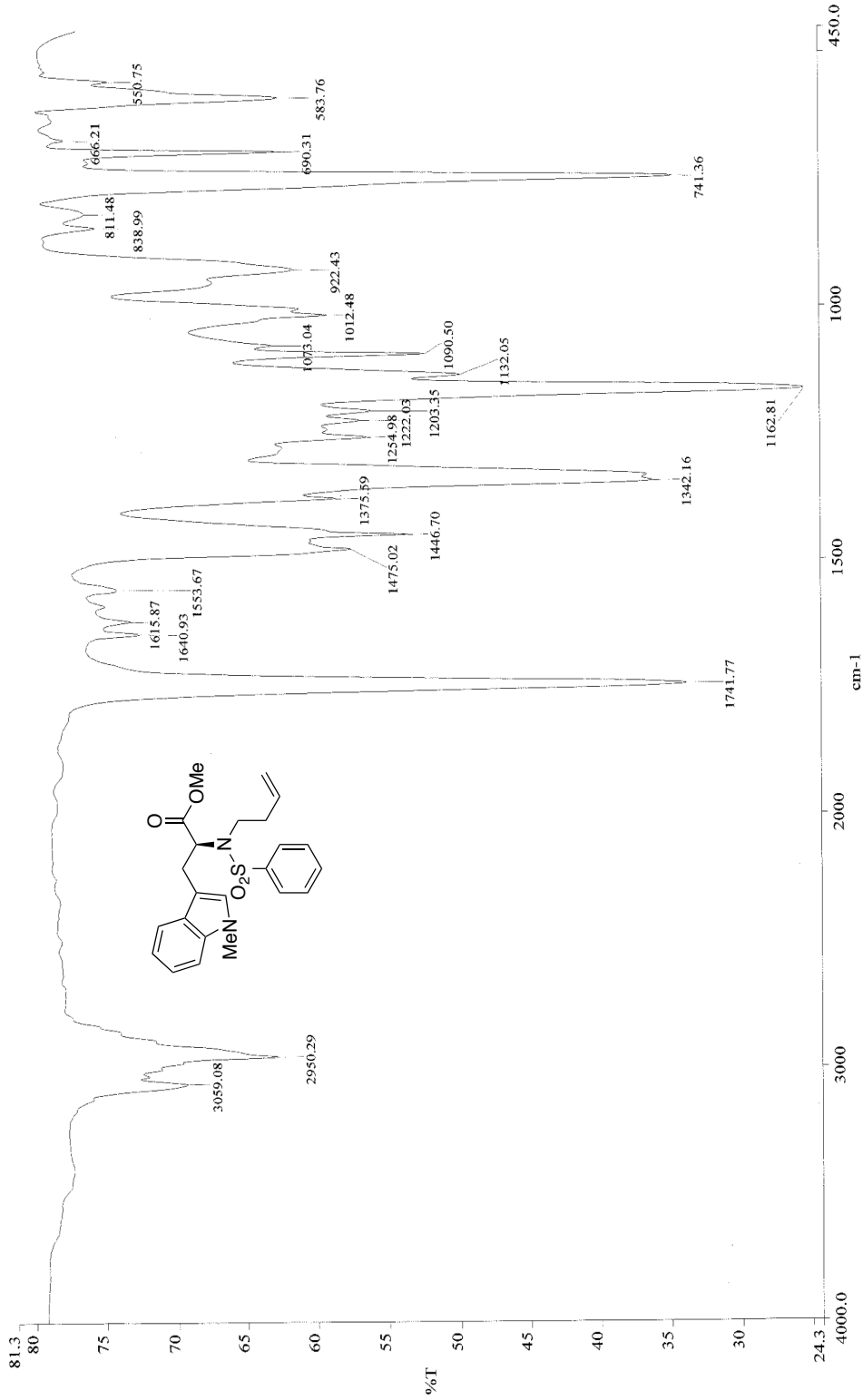

Figure 17: Infrared spectra (neat) of **30**

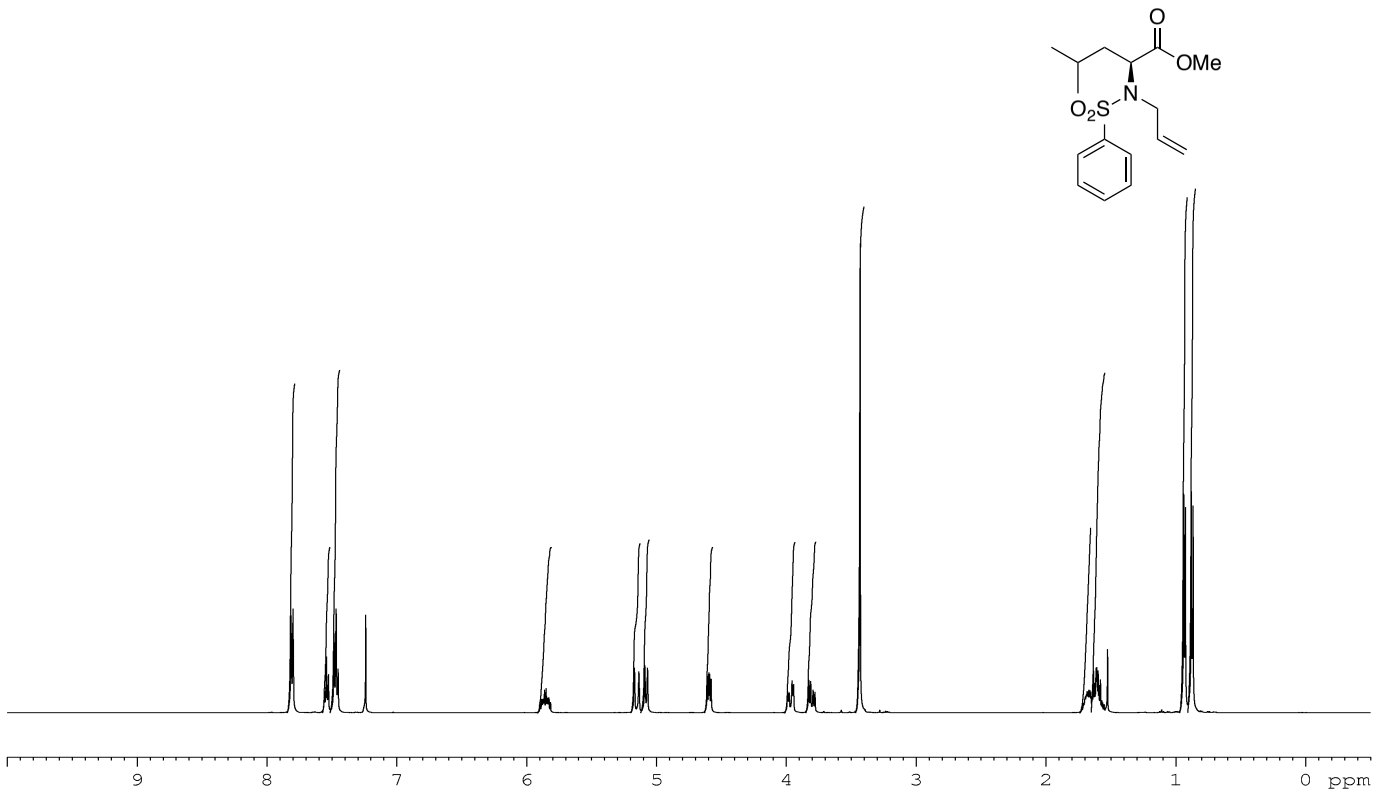

Figure 18: ^{1}H NMR ($CDCl_3$, 500 MHz) of **31**

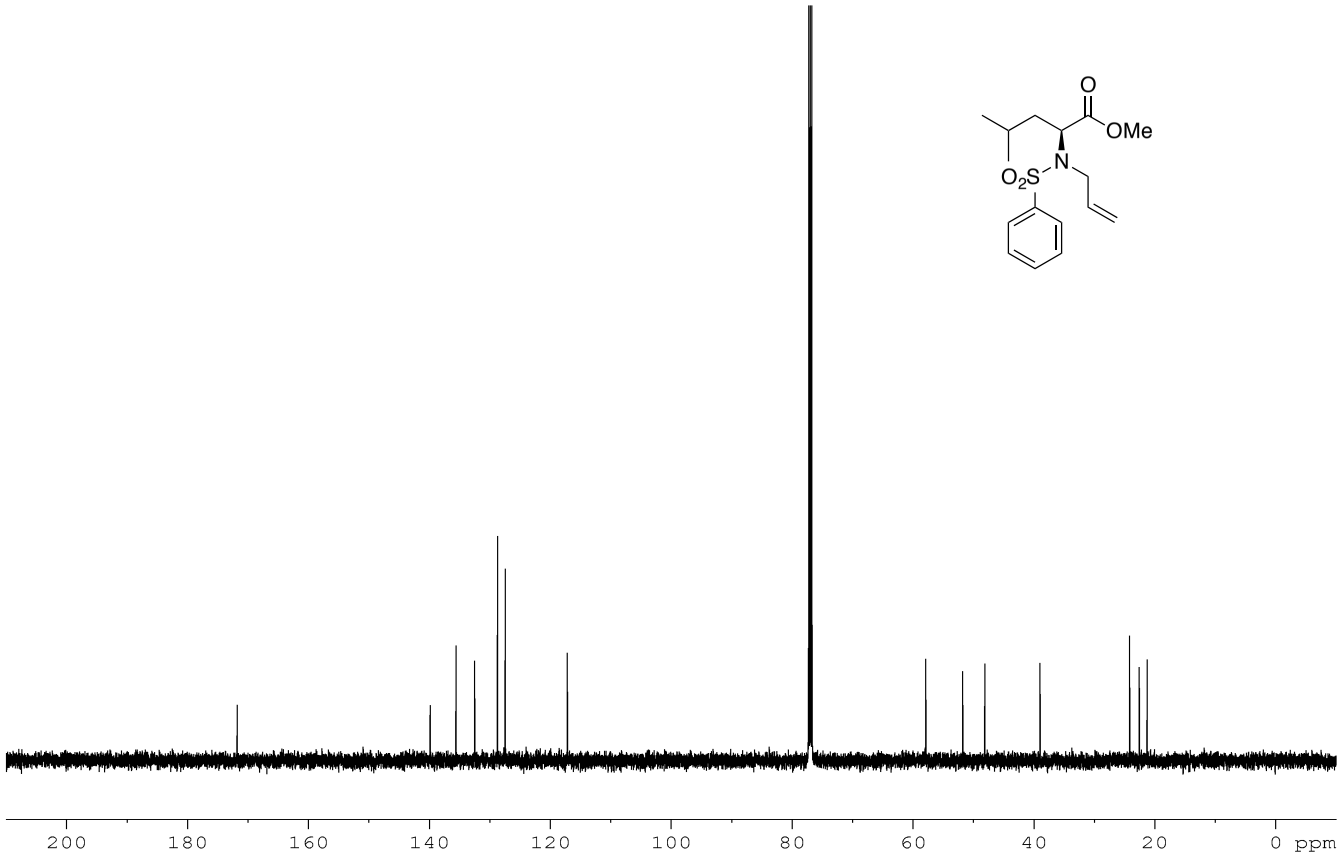

Figure 19: ^{13}C NMR ($CDCl_3$, 125 MHz) of **31**

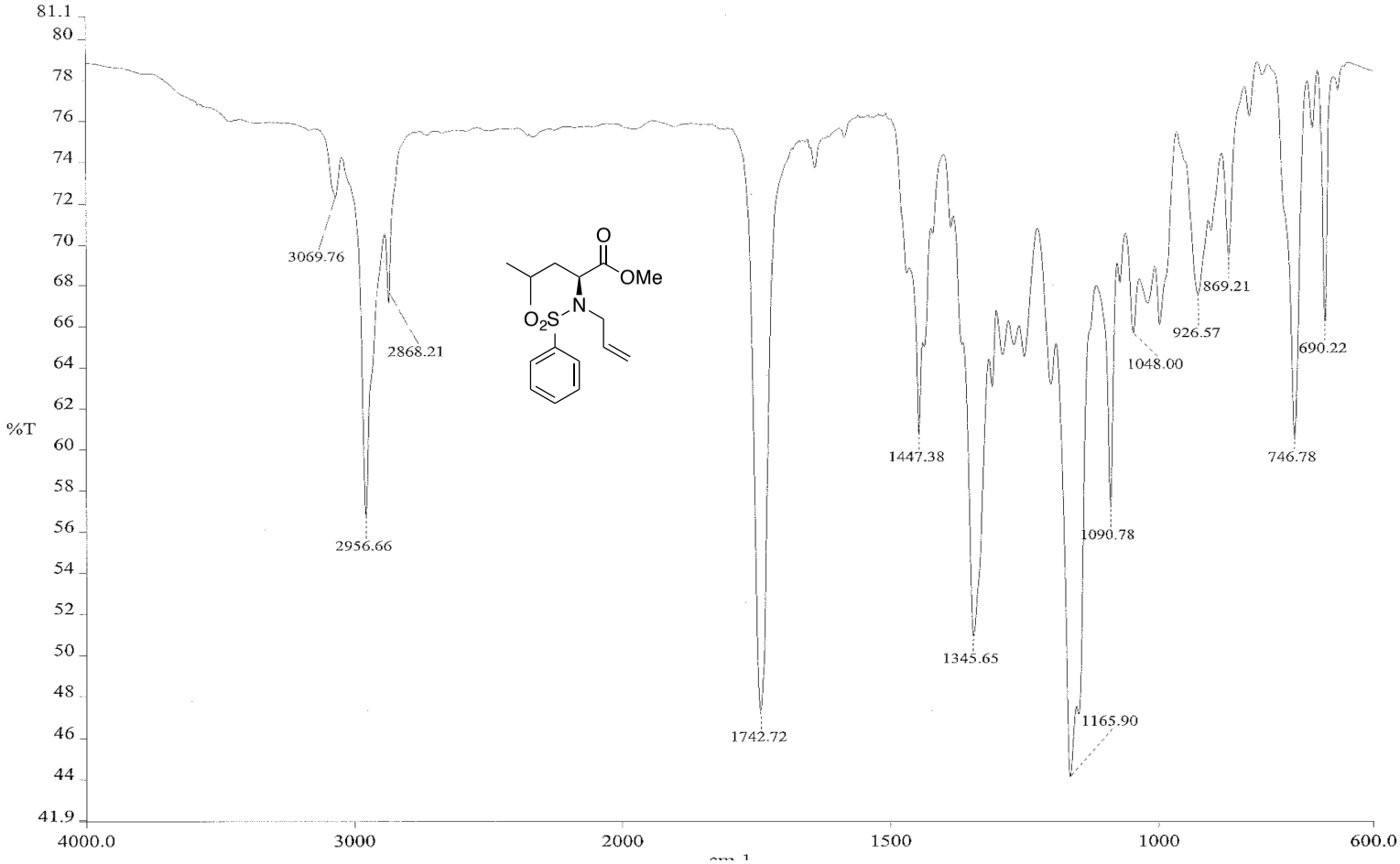

Figure 20: Infrared spectra (neat) of **31**

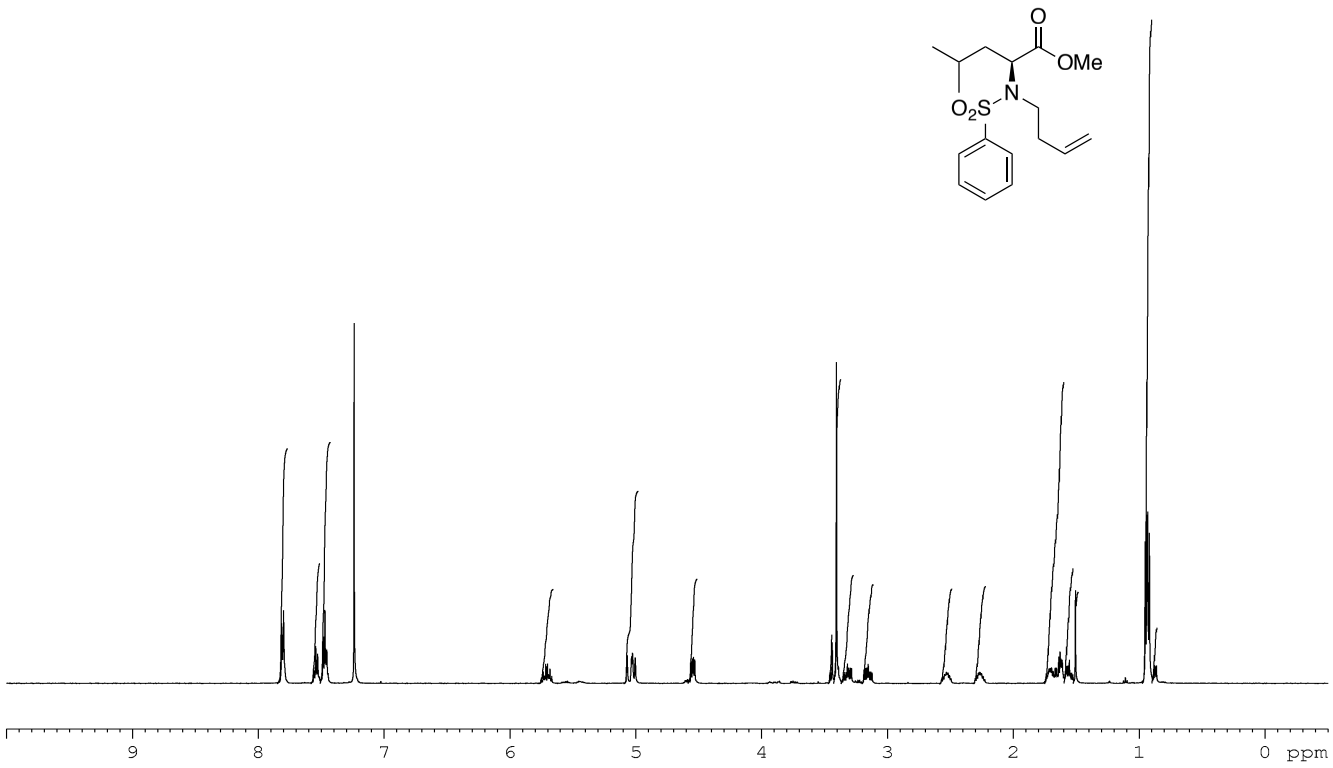

Figure 21: ^{1}H NMR ($CDCl_3$, 500 MHz) of **32**

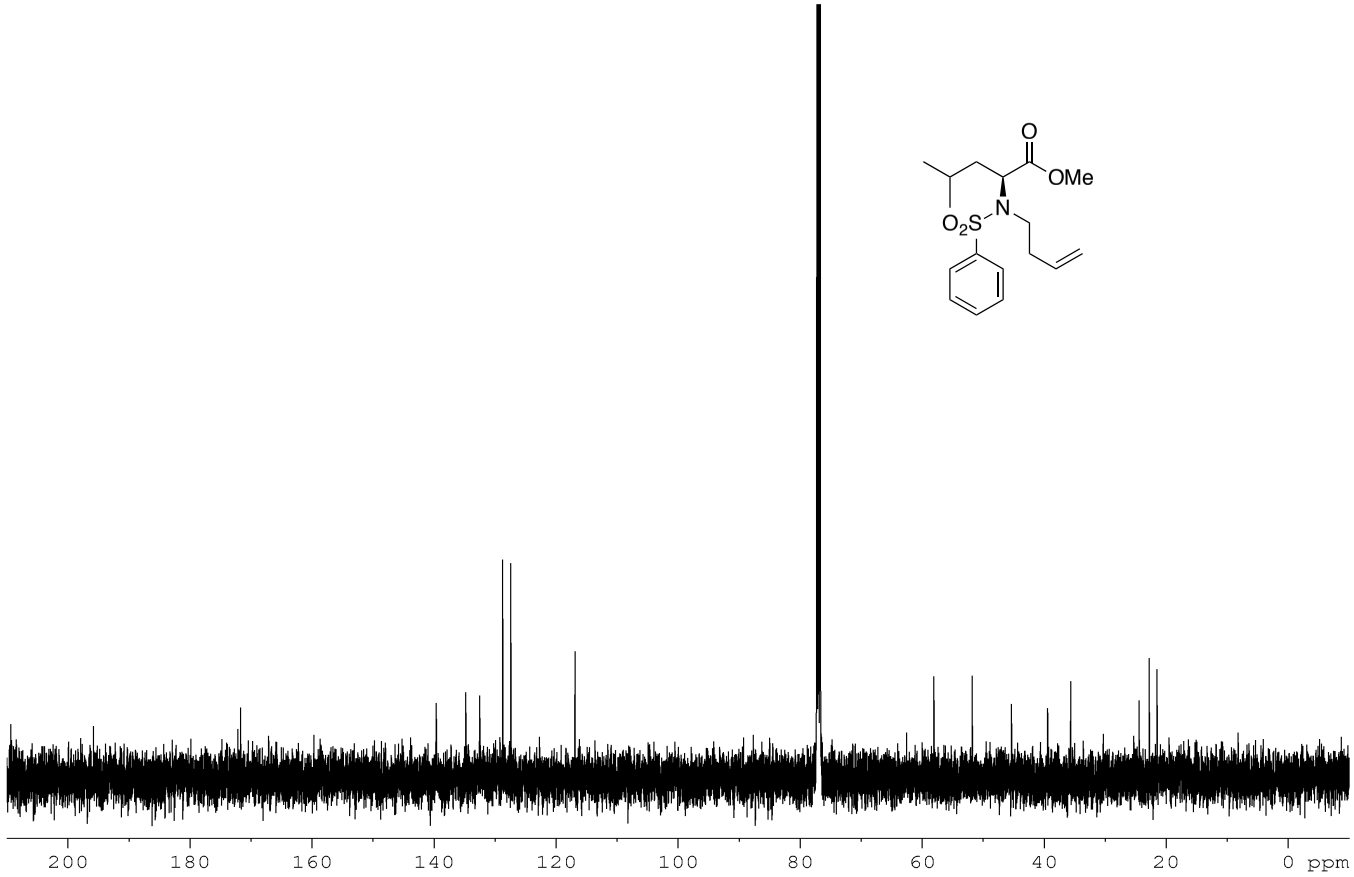

Figure 22: ^{13}C NMR ($CDCl_3$, 125 MHz) of **32**

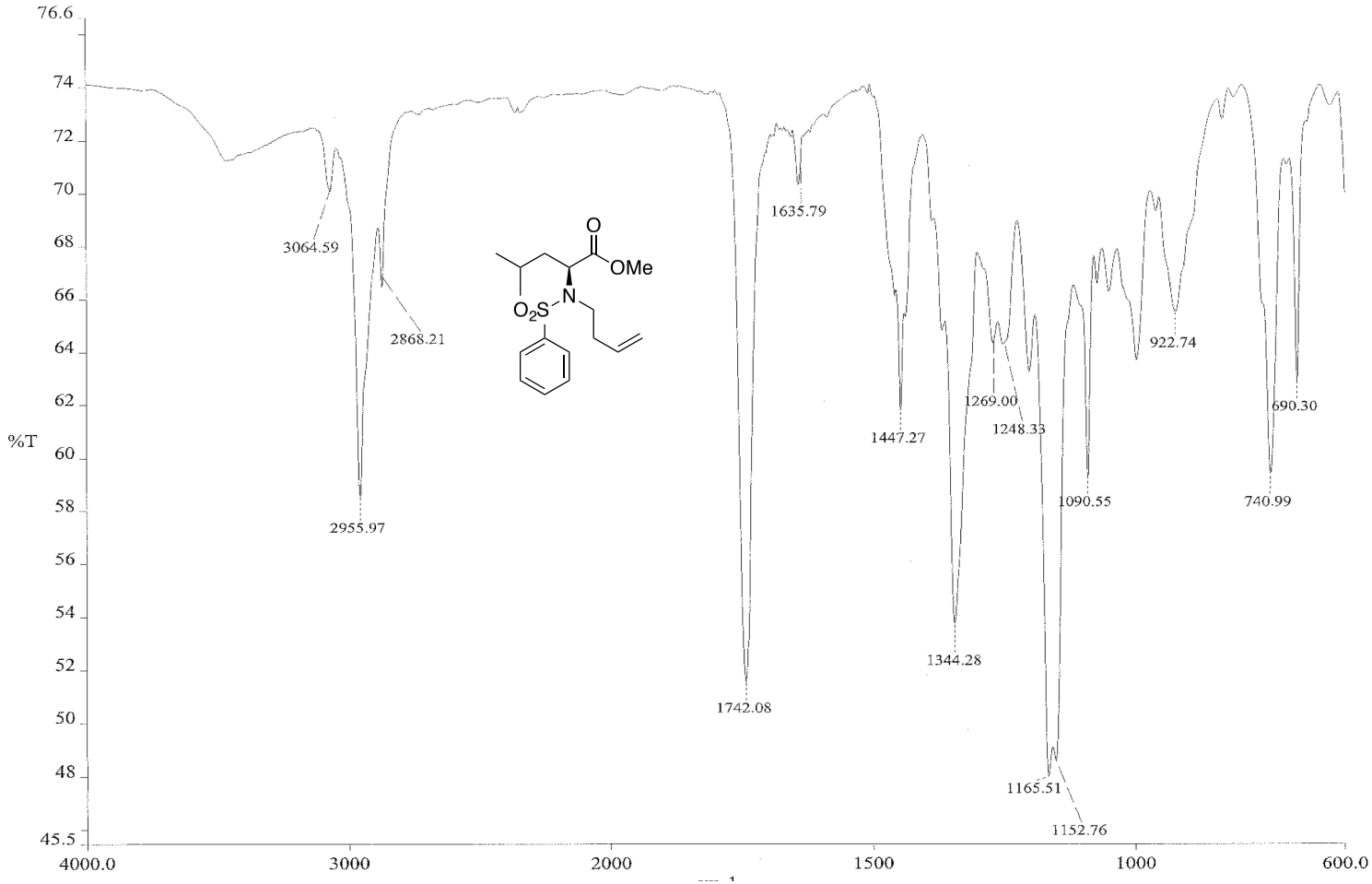

Figure 23: Infrared spectra (neat) of **32**

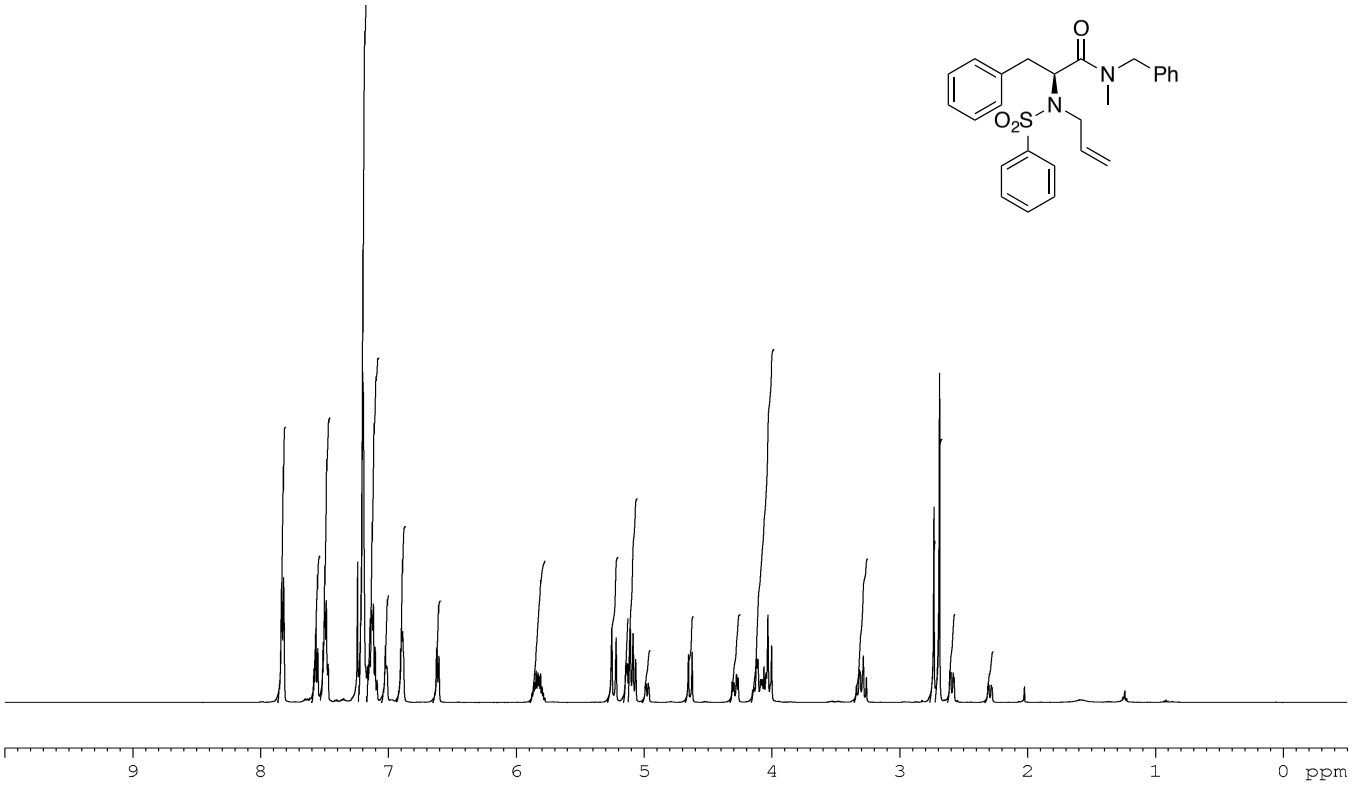

Figure 24: ^{1}H NMR ($CDCl_3$, 500 MHz) of **33**

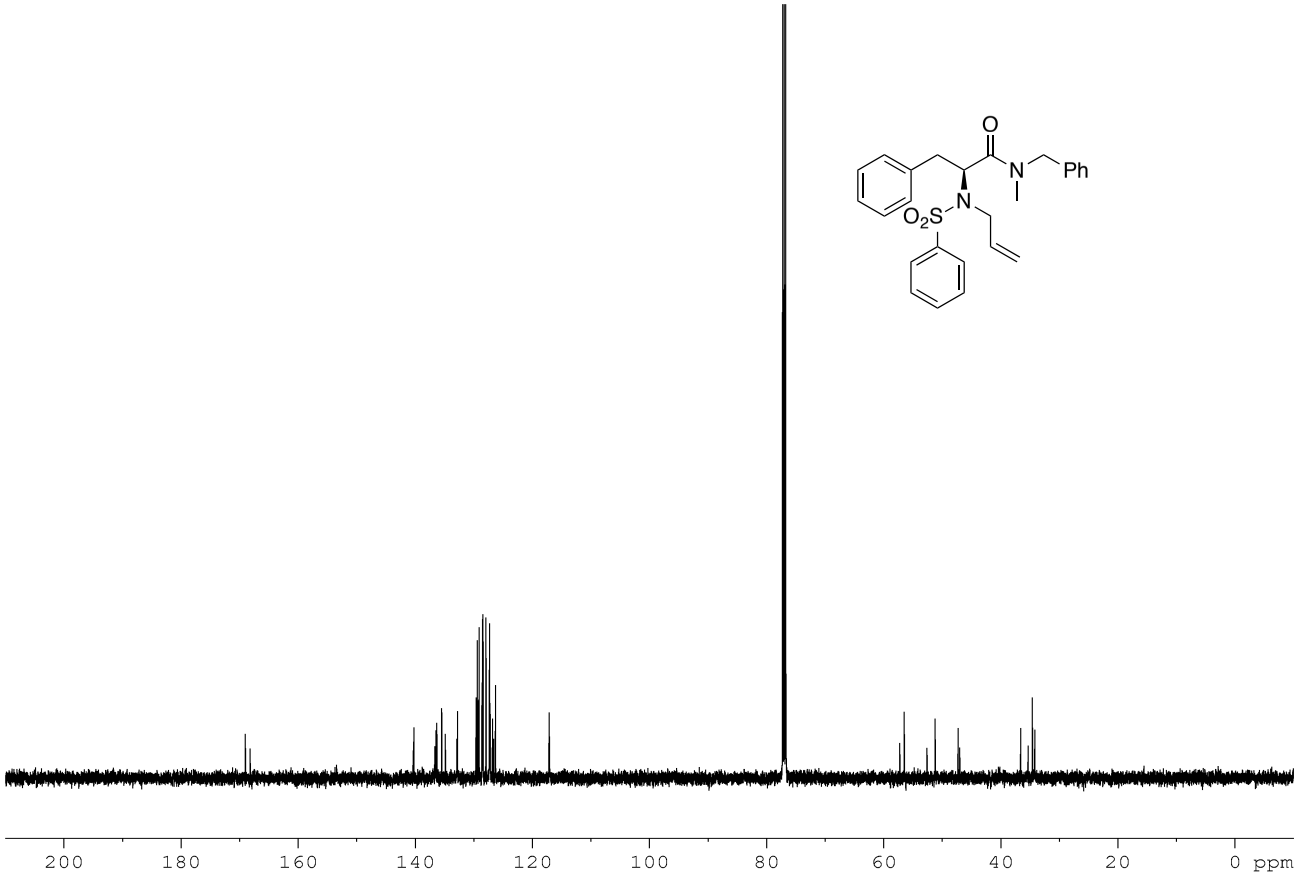

Figure 25: ^{13}C NMR ($CDCl_3$, 125 MHz) of **33**

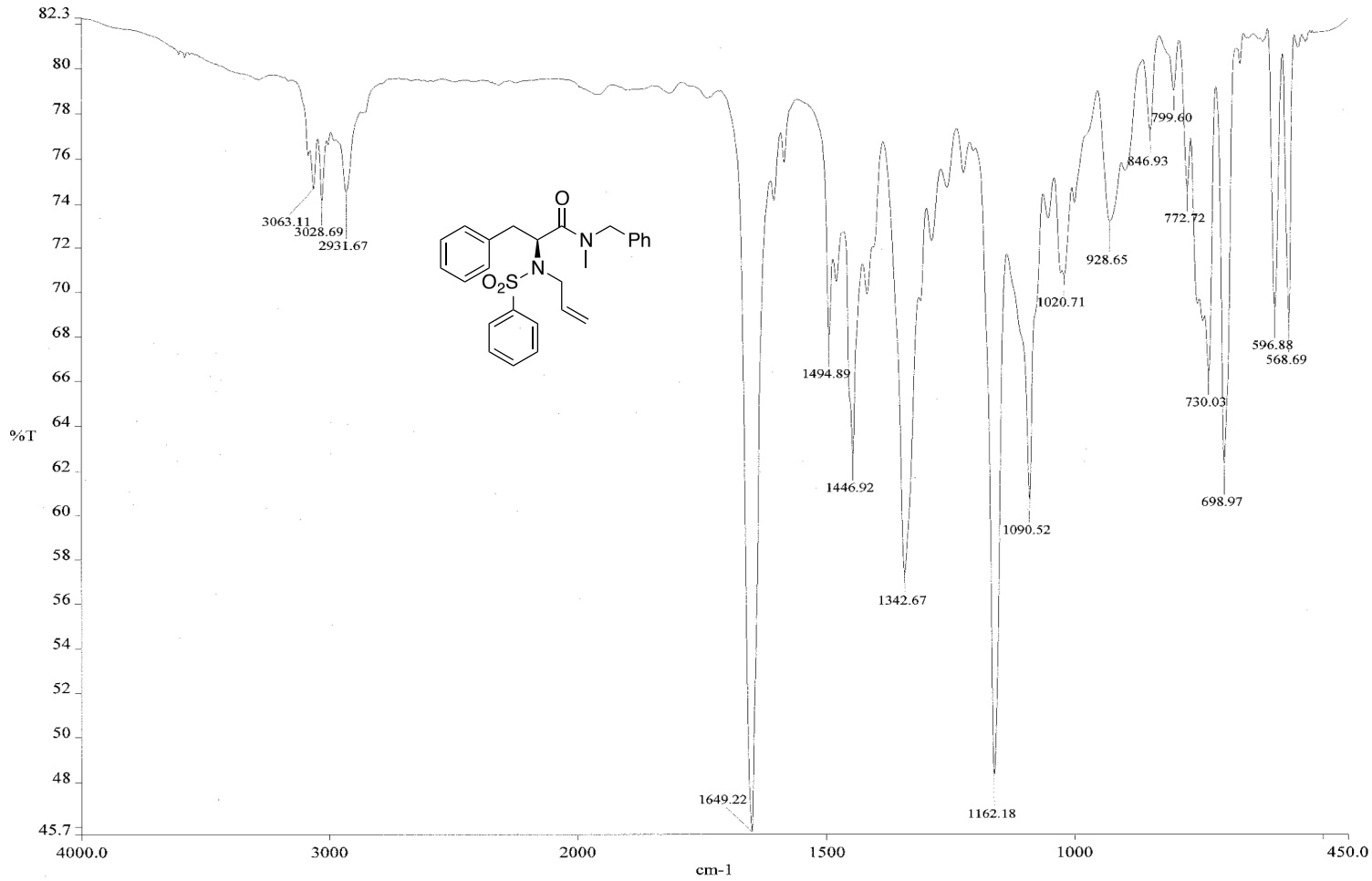

Figure 26: Infrared spectra (neat) of **33**

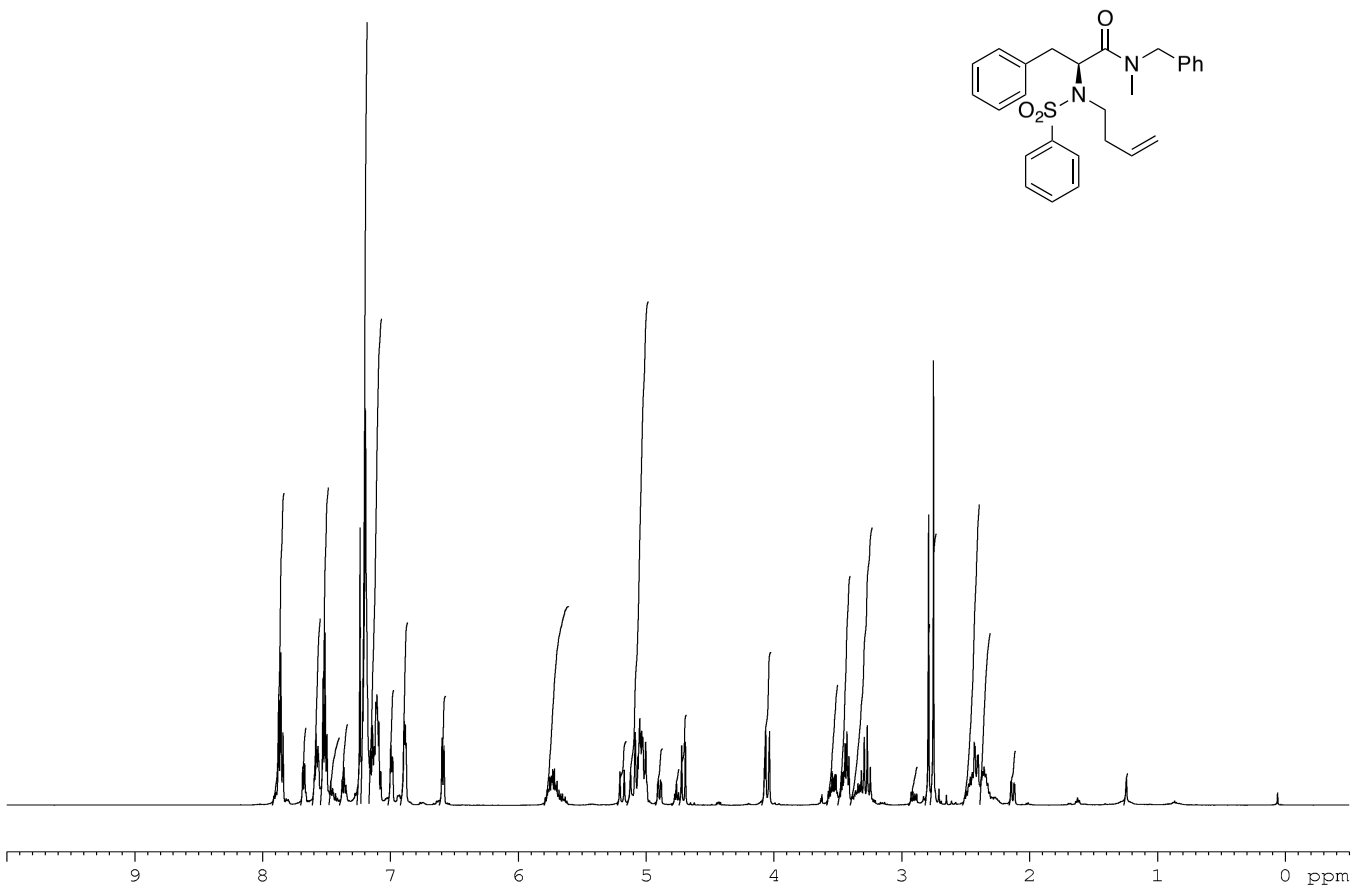

Figure 27: ^{1}H NMR ($CDCl_3$, 500 MHz) of **34**

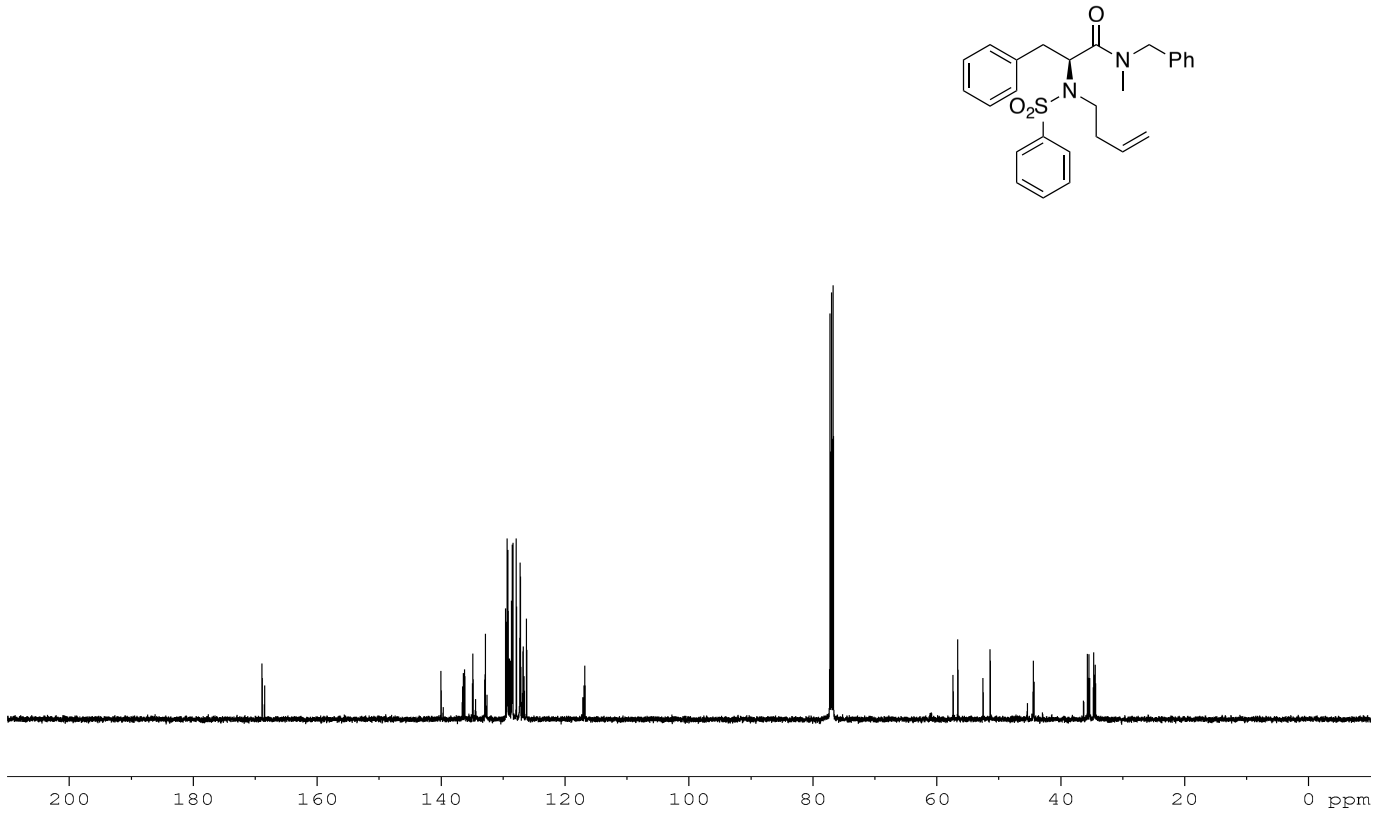

Figure 28: ^{13}C NMR ($CDCl_3$, 125 MHz) of **34**

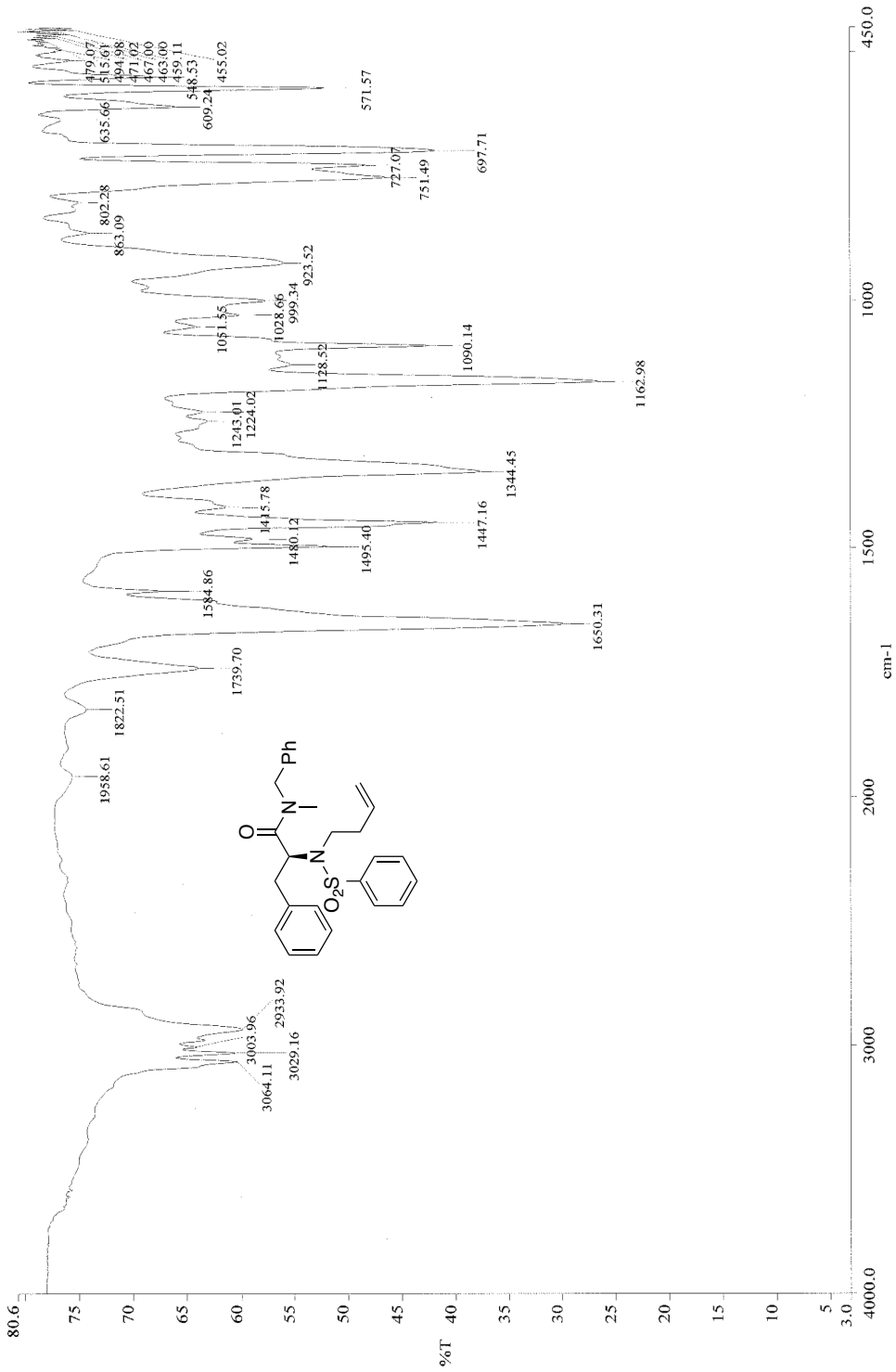

Figure 29: Infrared spectra (neat) of **34**

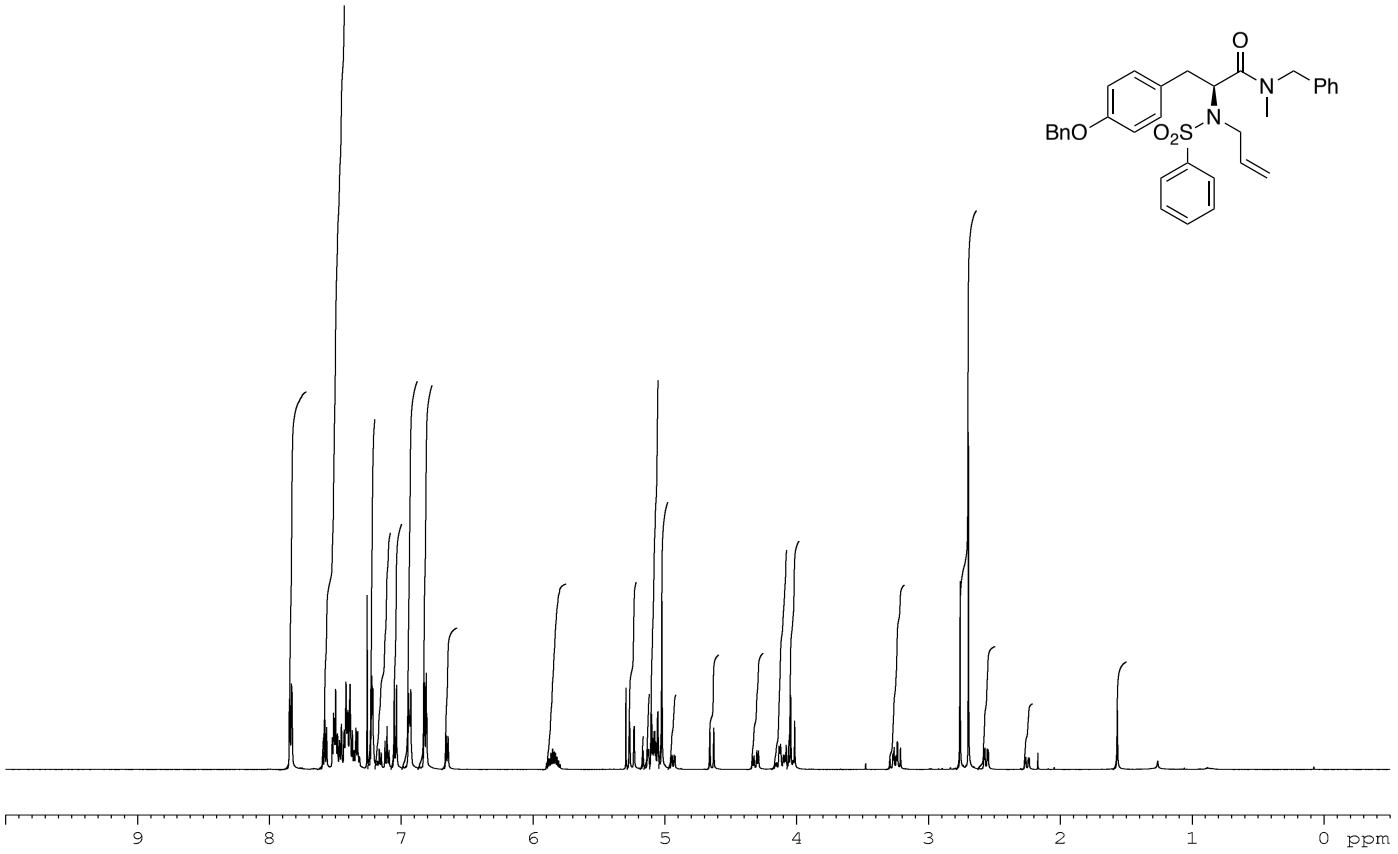

Figure 30: ^{1}H NMR ($CDCl_3$, 500 MHz) of **35**

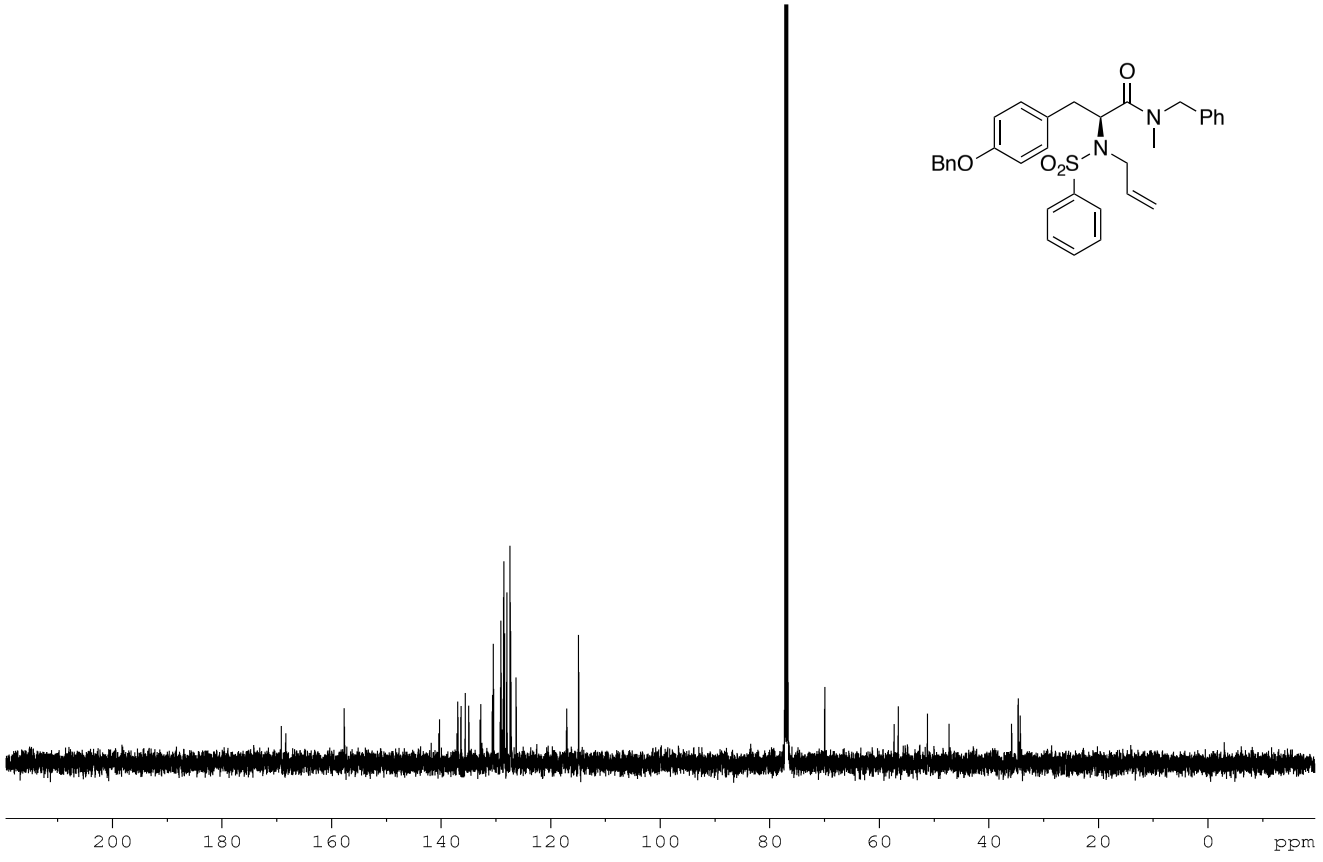

Figure 31: ^{13}C NMR ($CDCl_3$, 125 MHz) of **35**

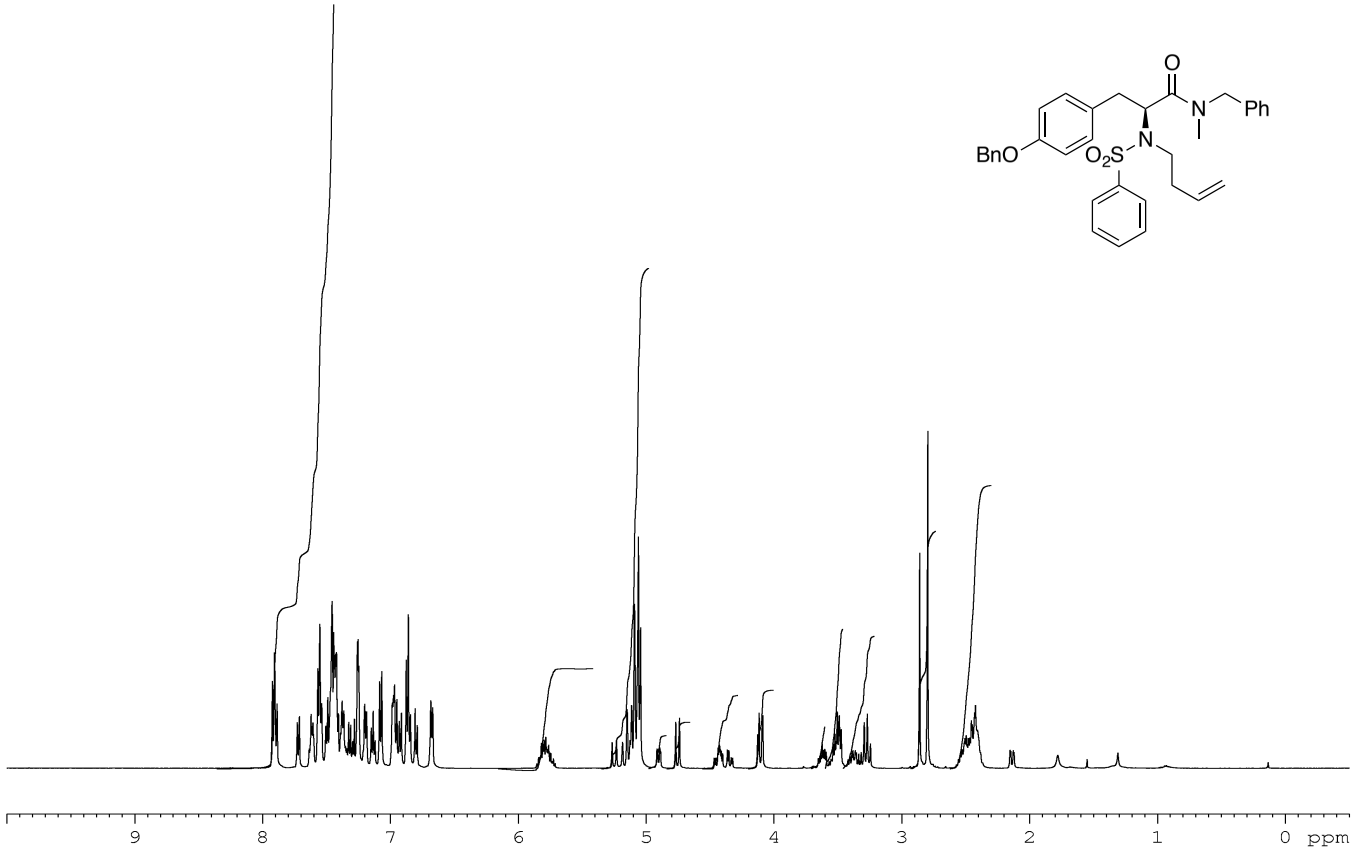

Figure 32: ^{1}H NMR ($CDCl_3$, 500 MHz) of **36**

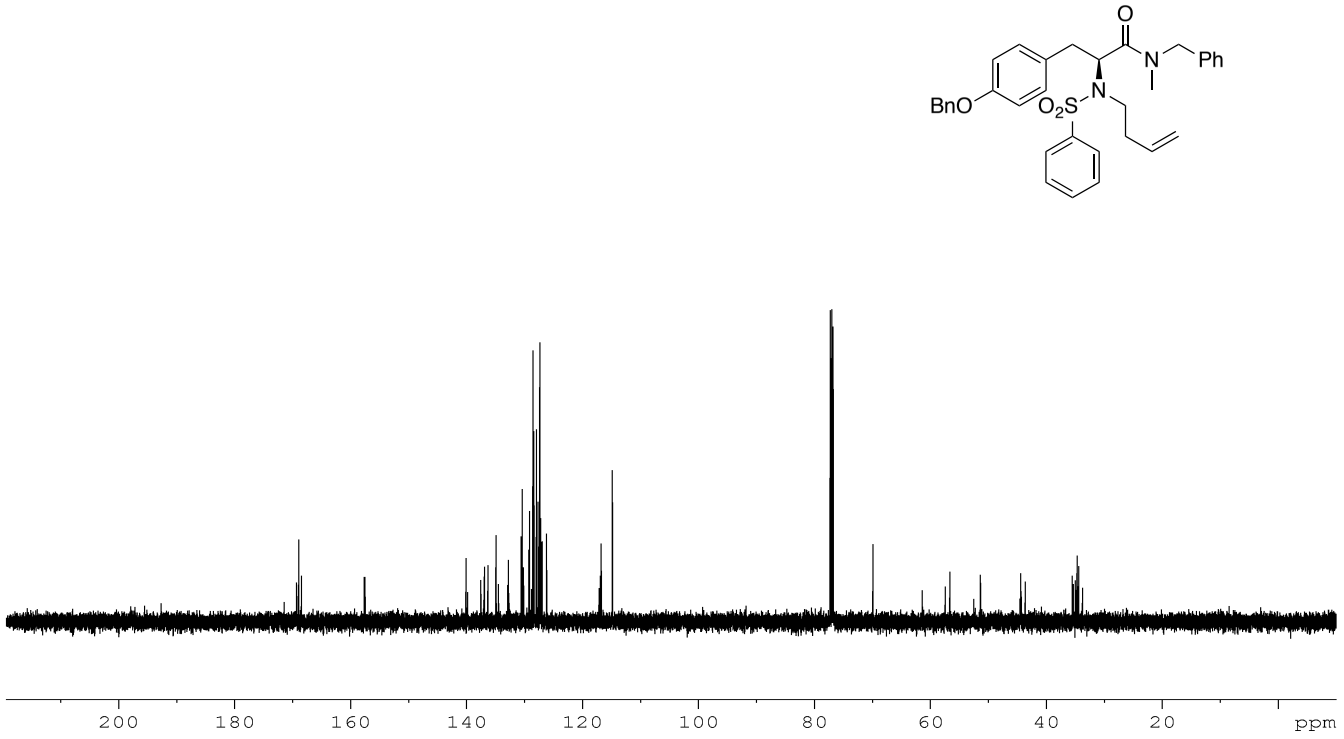

Figure 33: ^{13}C NMR ($CDCl_3$, 125 MHz) of **36**

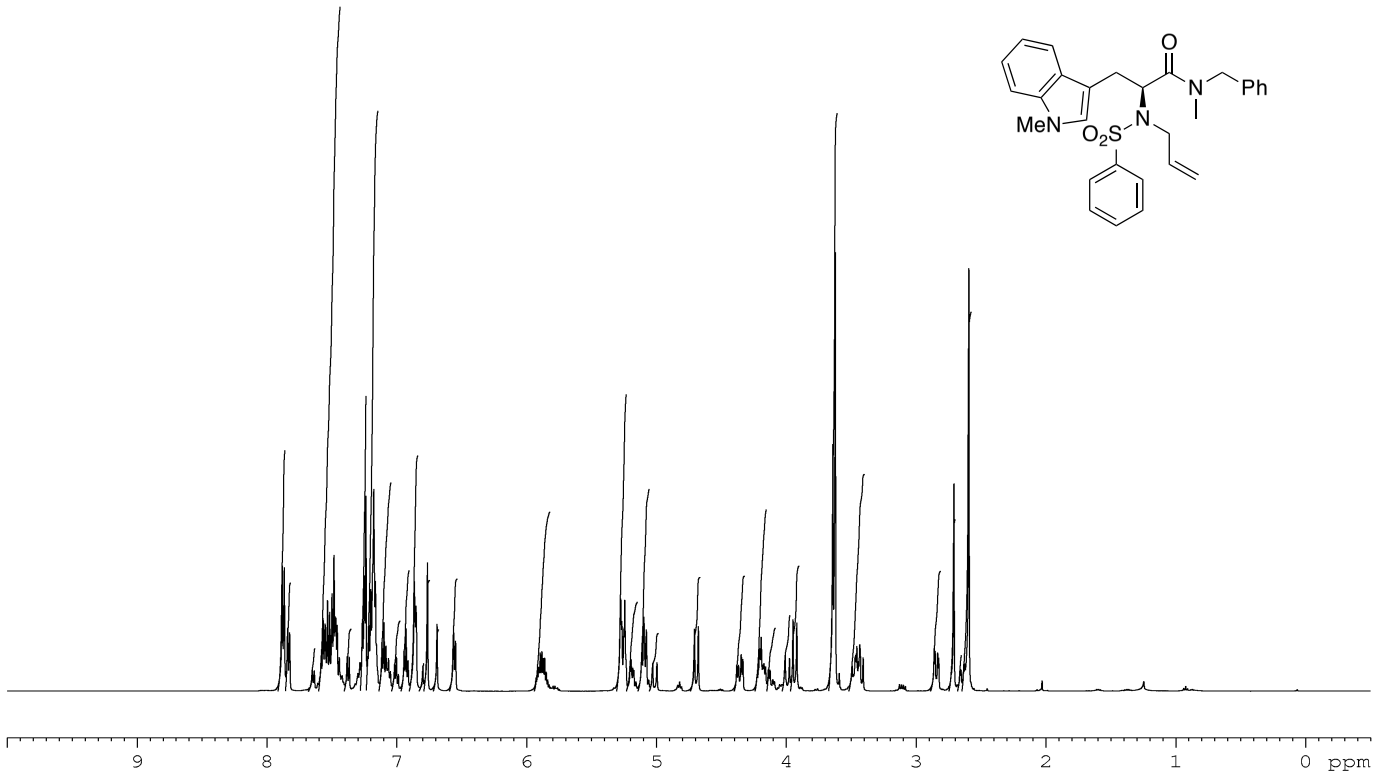

Figure 34: ^{1}H NMR ($CDCl_3$, 500 MHz) of **37**

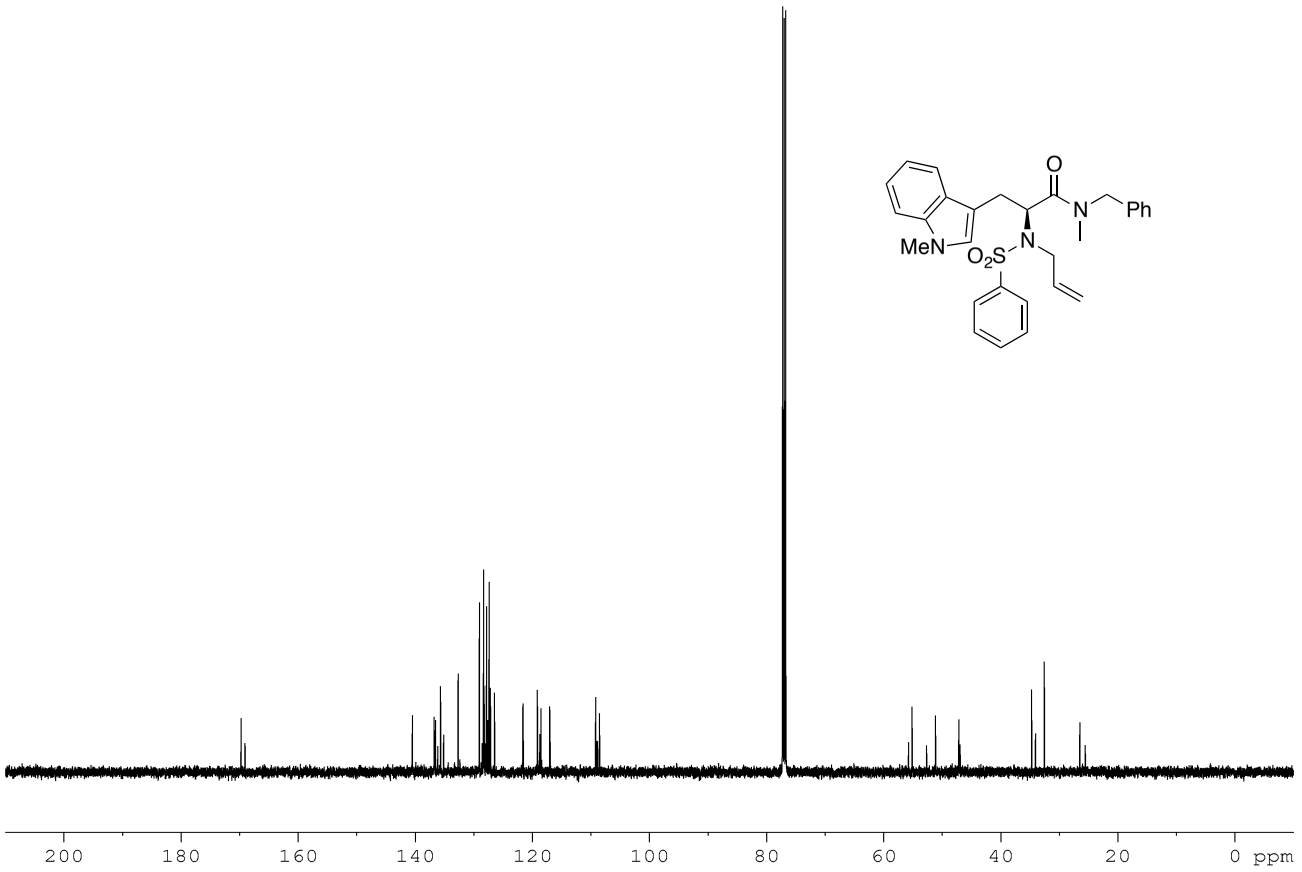

Figure 35: ^{13}C NMR ($CDCl_3$, 125 MHz) of **37**

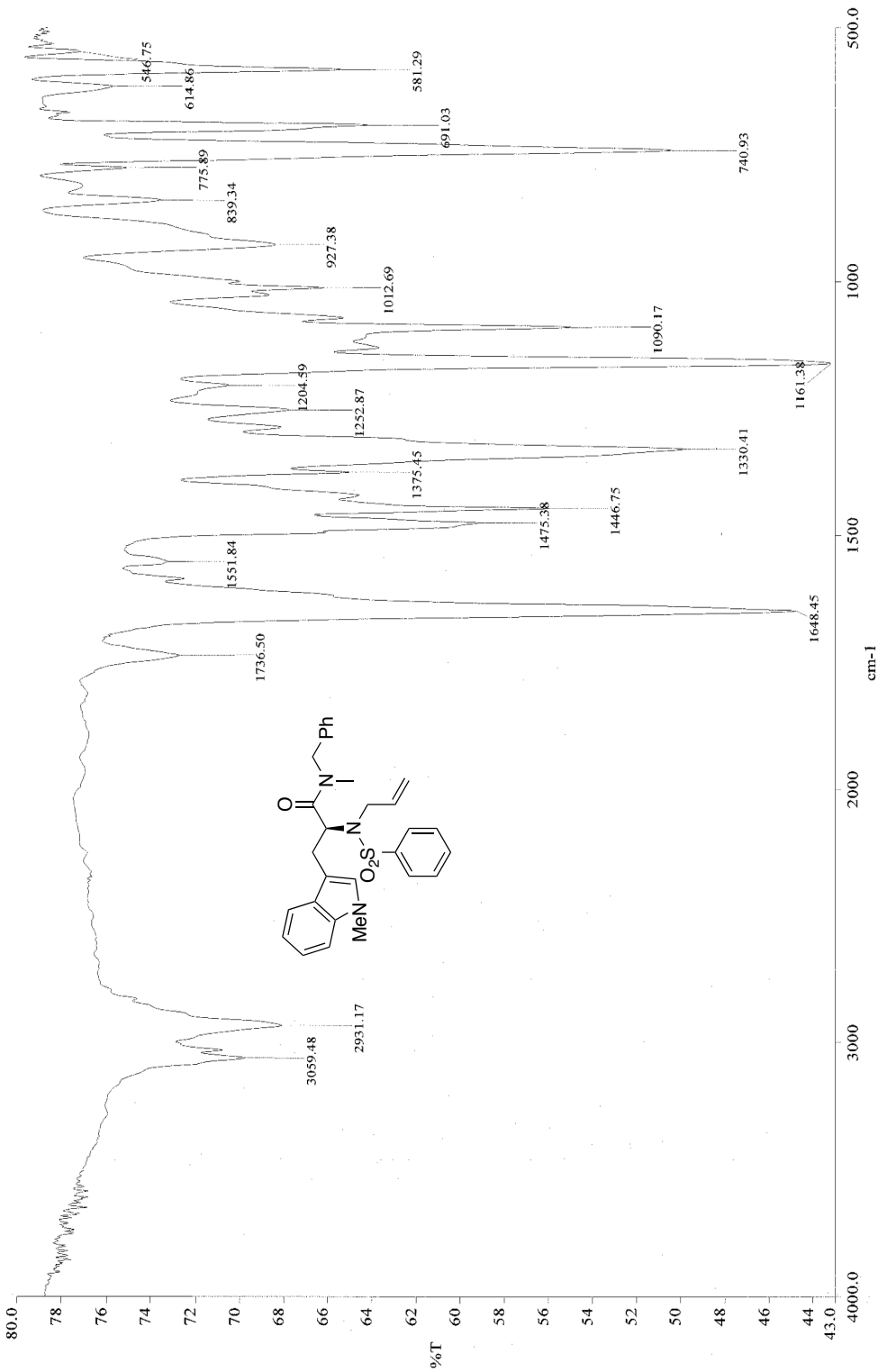

Figure 36: Infrared spectra (neat) of **37**

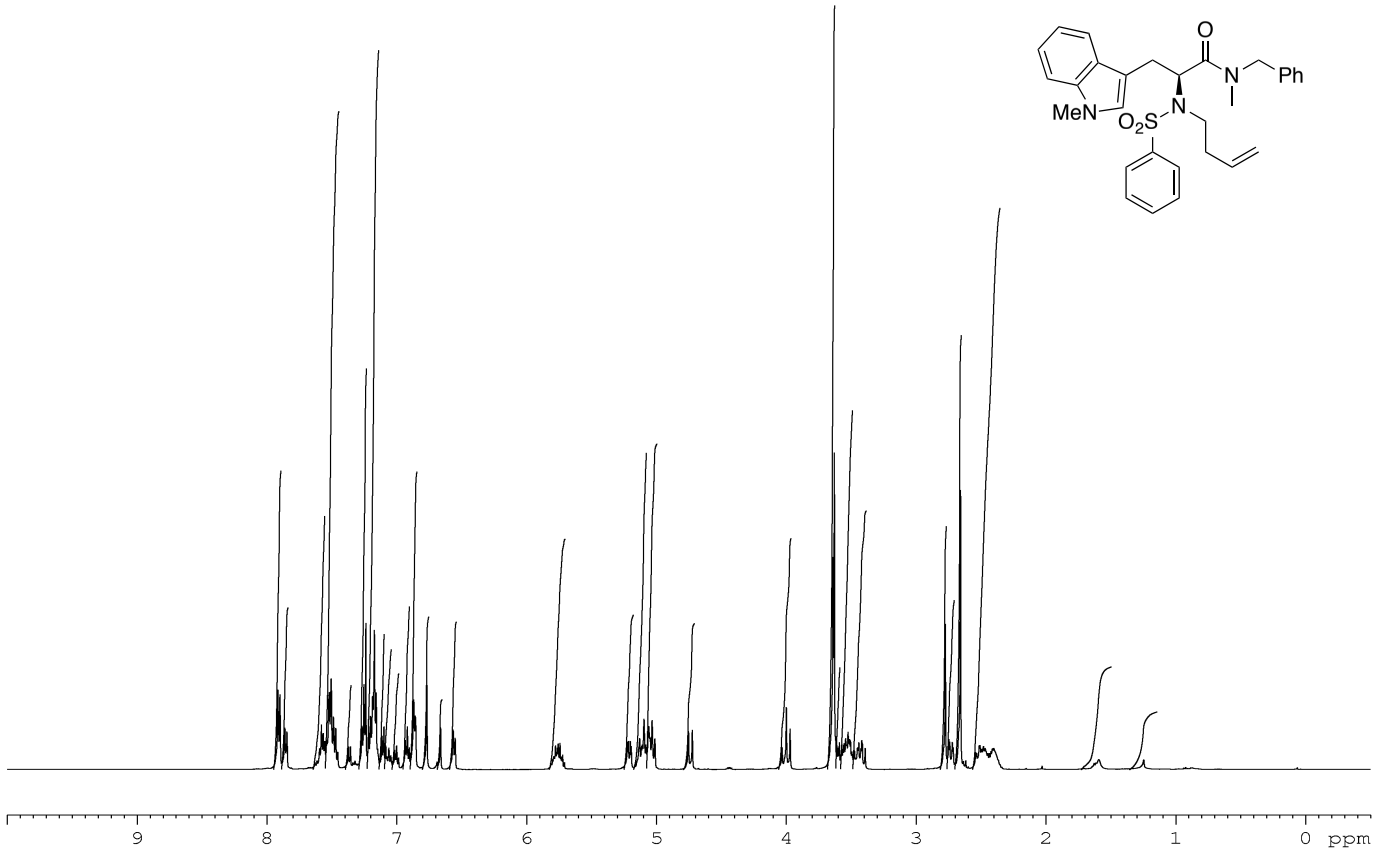

Figure 37: ^{1}H NMR ($CDCl_3$, 500 MHz) of **38**

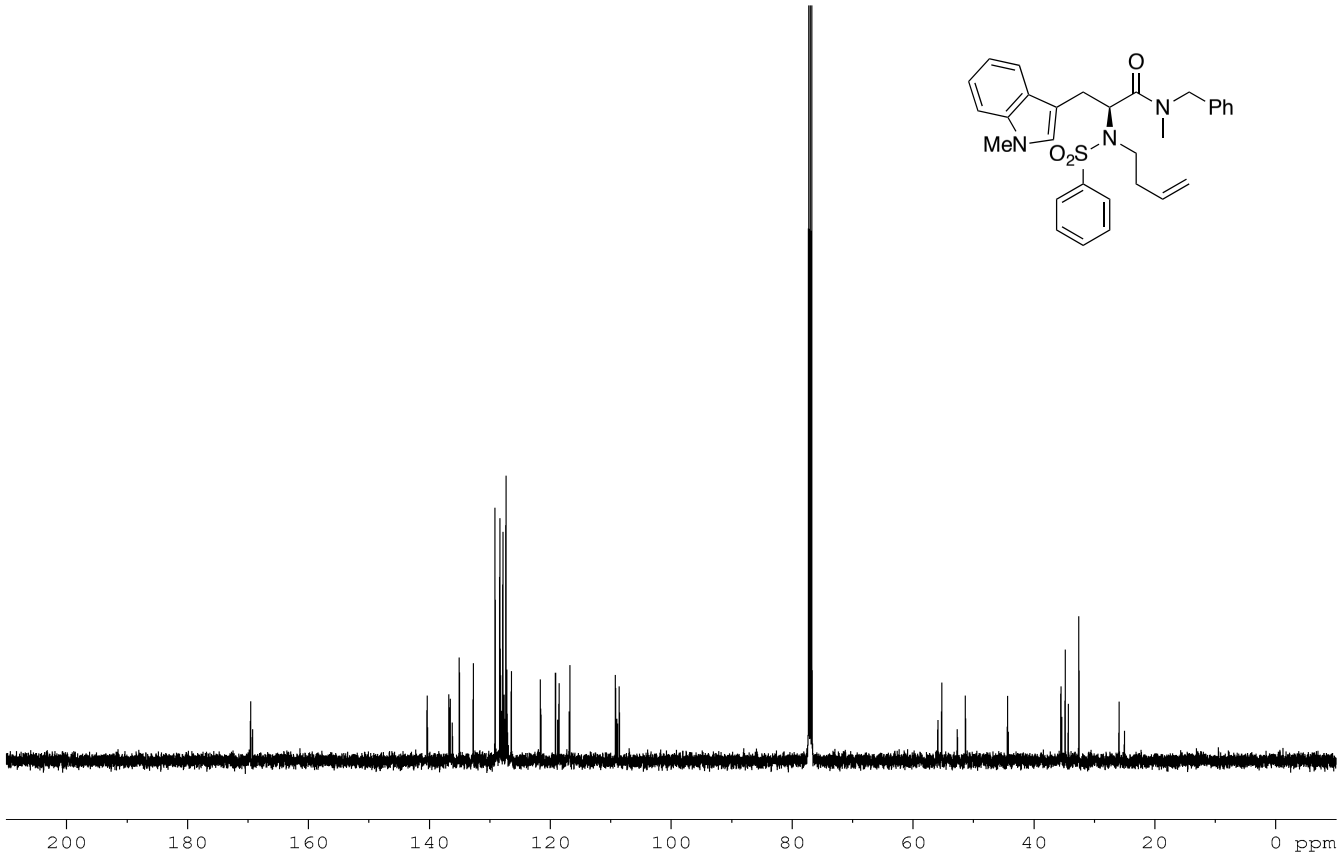

Figure 38: ^{13}C NMR ($CDCl_3$, 125 MHz) of **38**

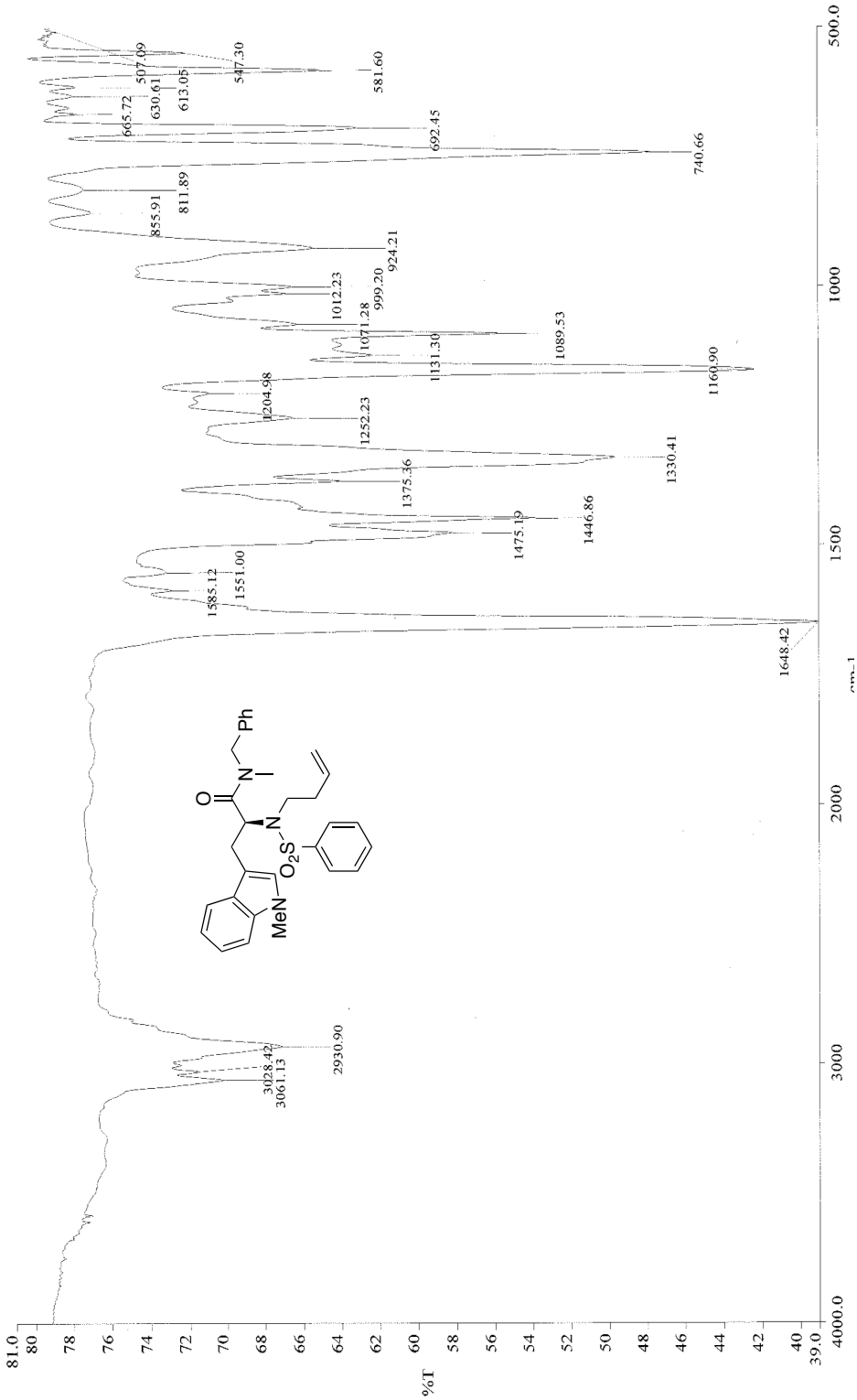

Figure 39: Infrared spectra (neat) of **38**

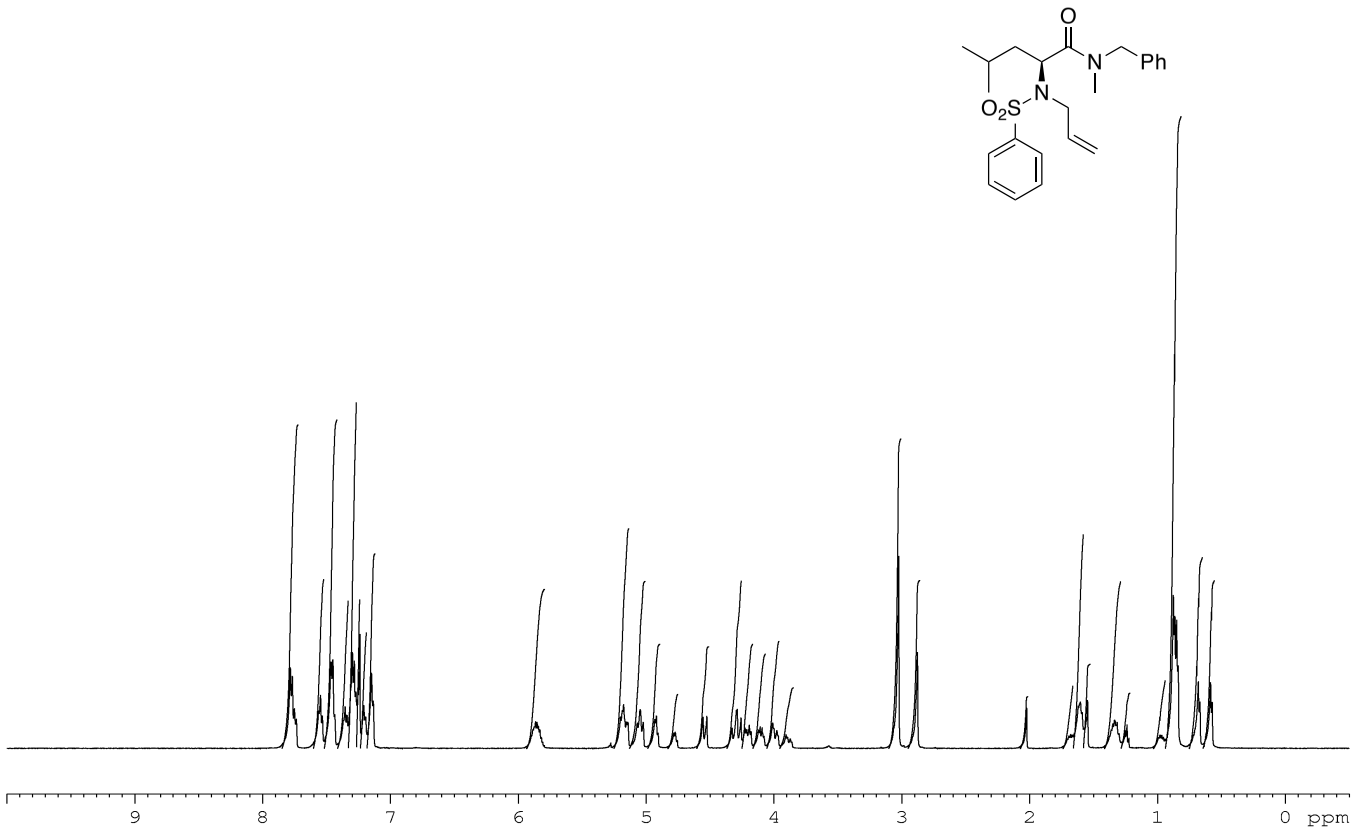

Figure 40: ^{1}H NMR ($CDCl_3$, 500 MHz) of **39**

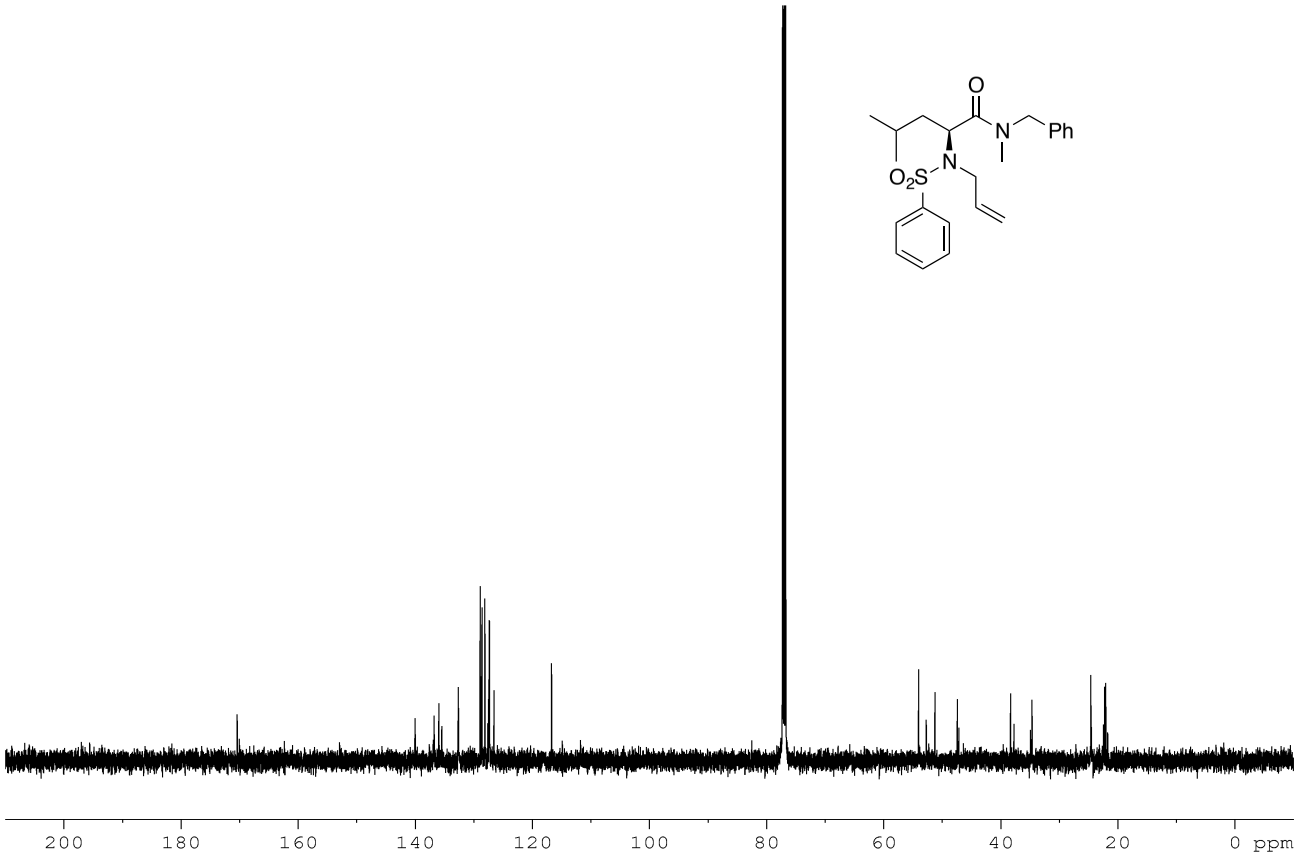

Figure 41: ^{13}C NMR ($CDCl_3$, 125 MHz) of **39**

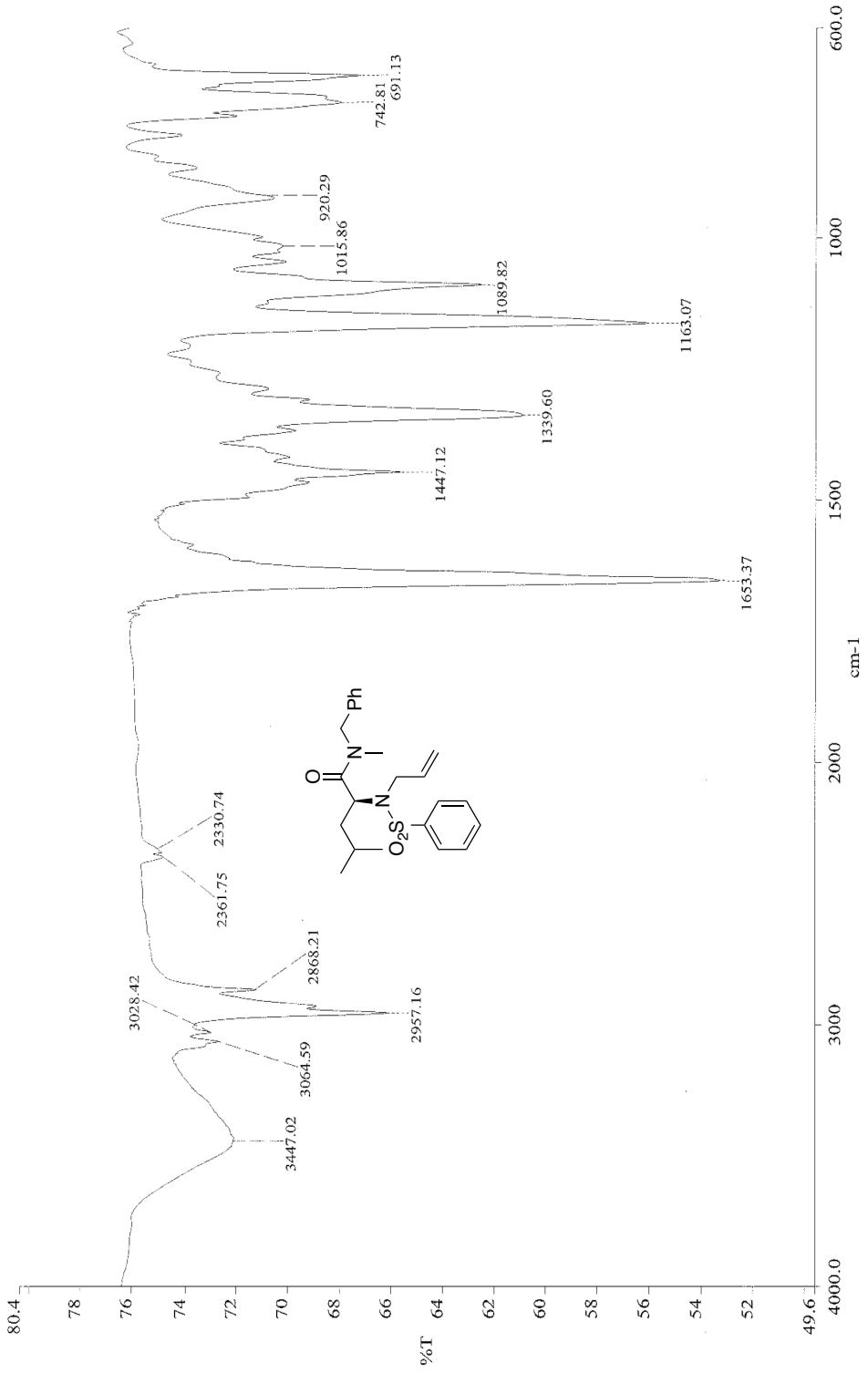

Figure 42: Infrared spectra (neat) of **39**

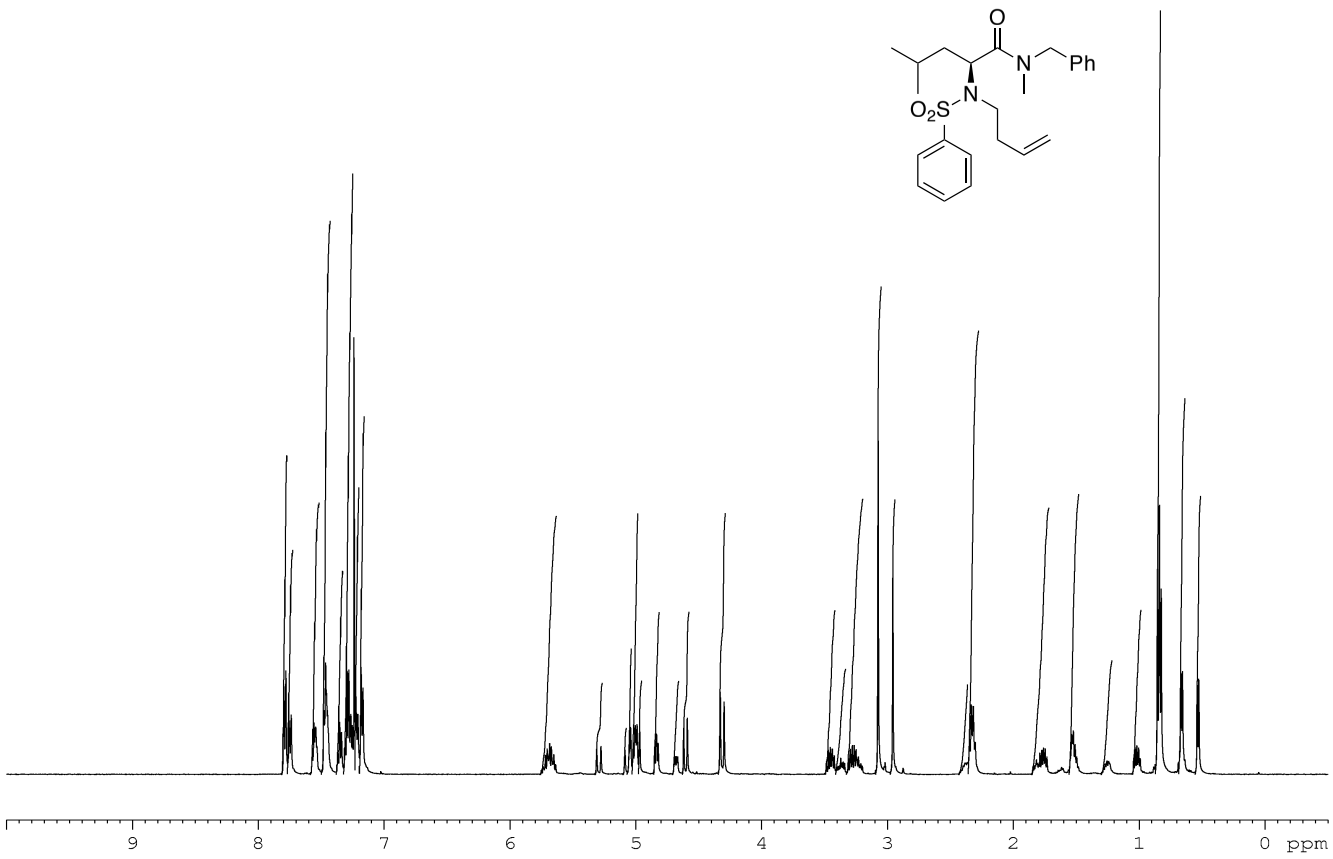

Figure 43: ^{1}H NMR ($CDCl_3$, 500 MHz) of **40**

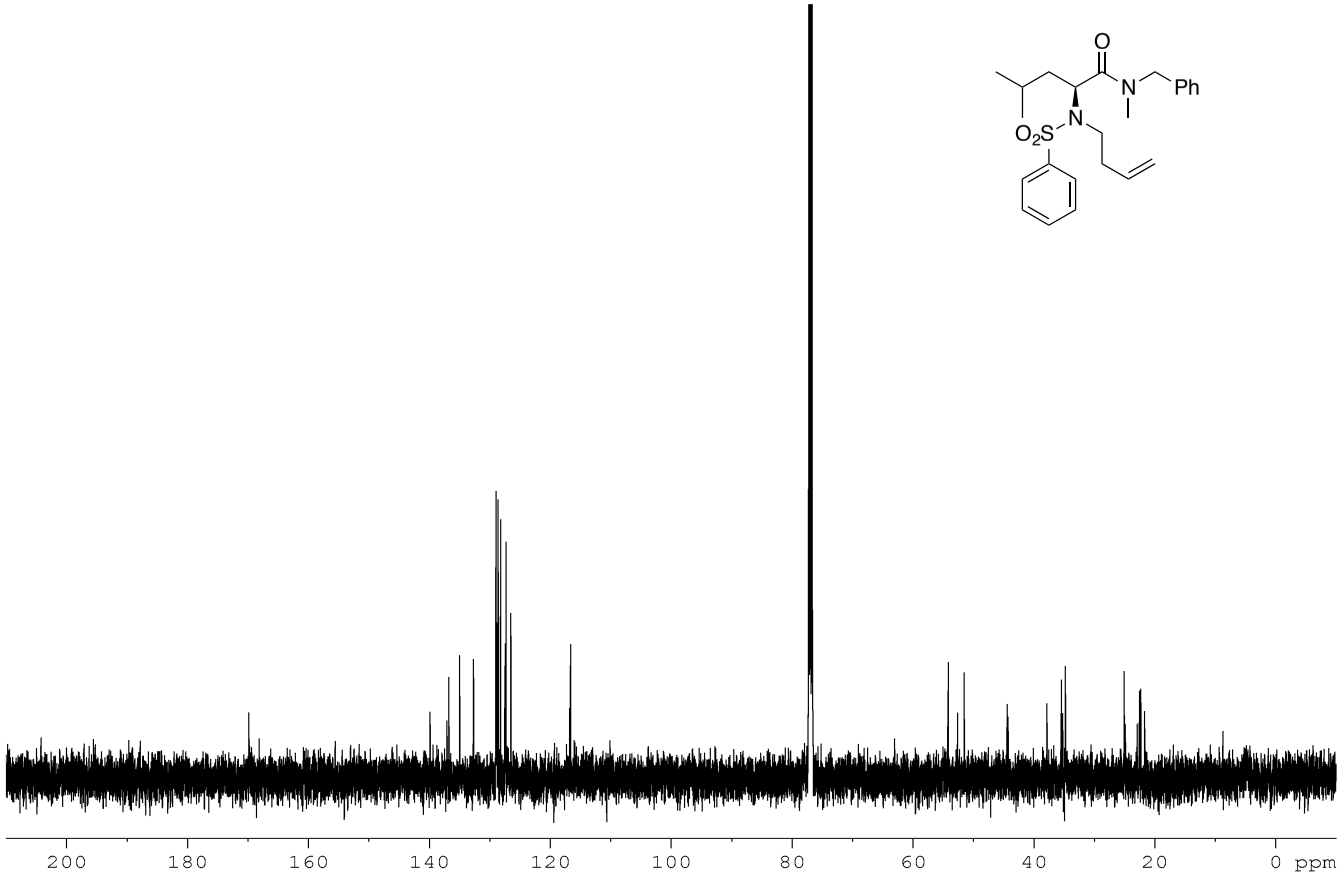

Figure 44: ^{13}C NMR ($CDCl_3$, 125 MHz) of **40**

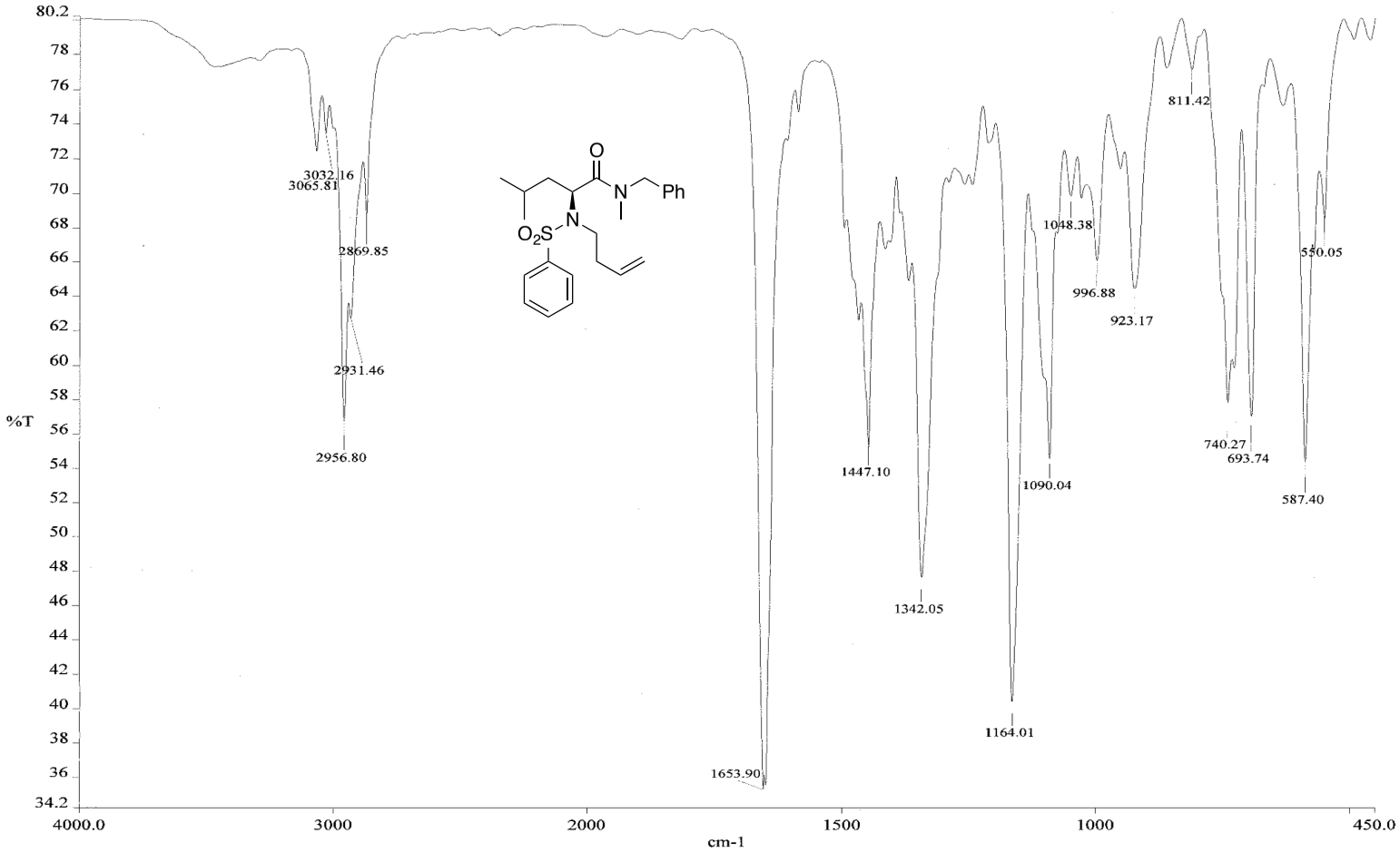

Figure 45: Infrared spectra (neat) of **40**

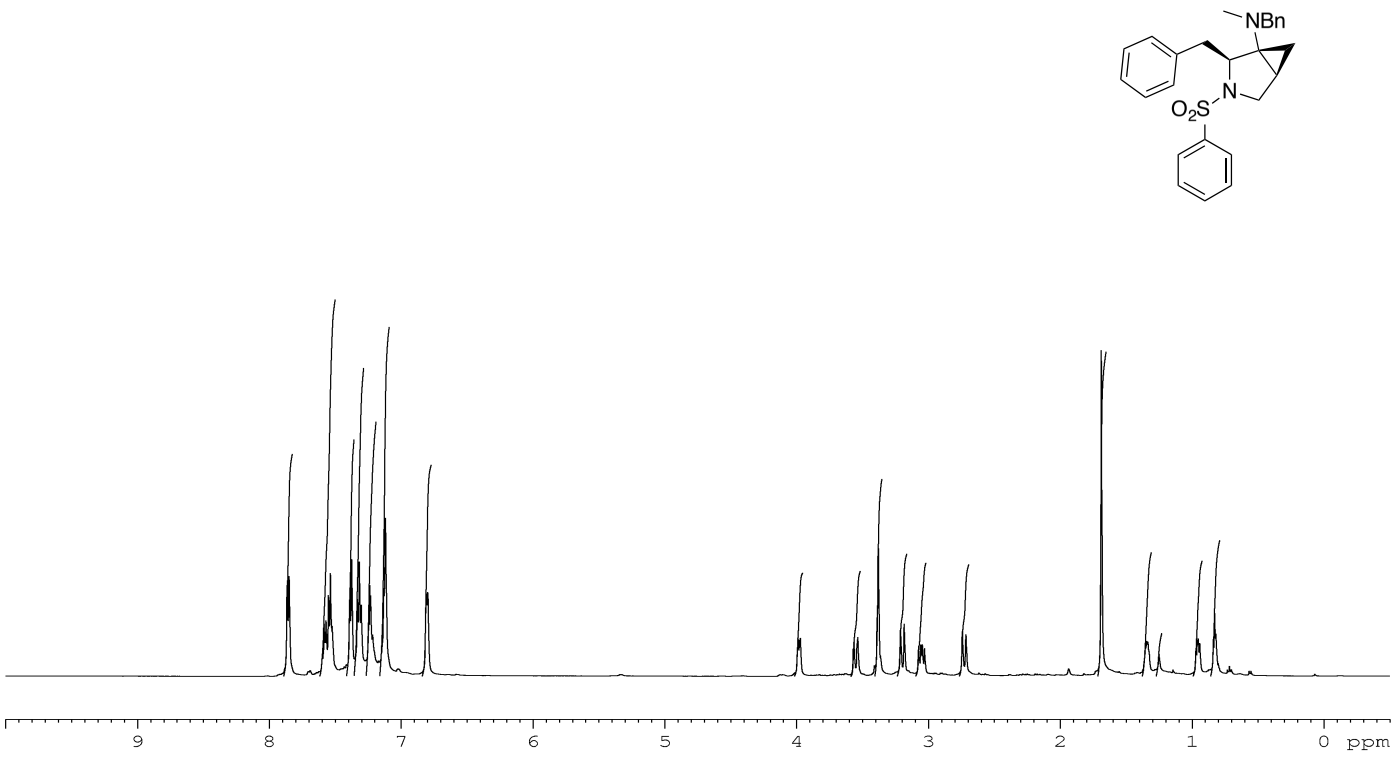

Figure 46: ^{1}H NMR ($CDCl_3$, 500 MHz) of **18**

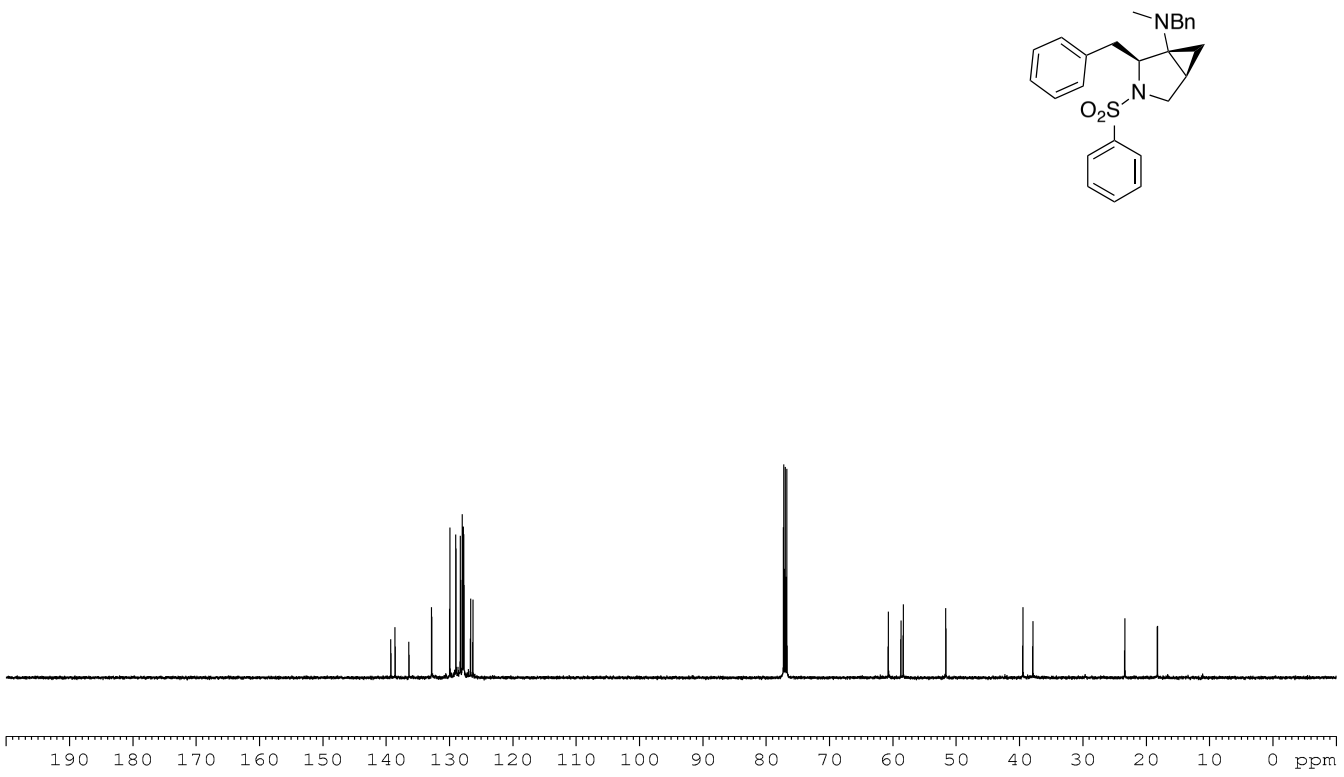

Figure 47: ^{13}C NMR ($CDCl_3$, 125 MHz) of **18**

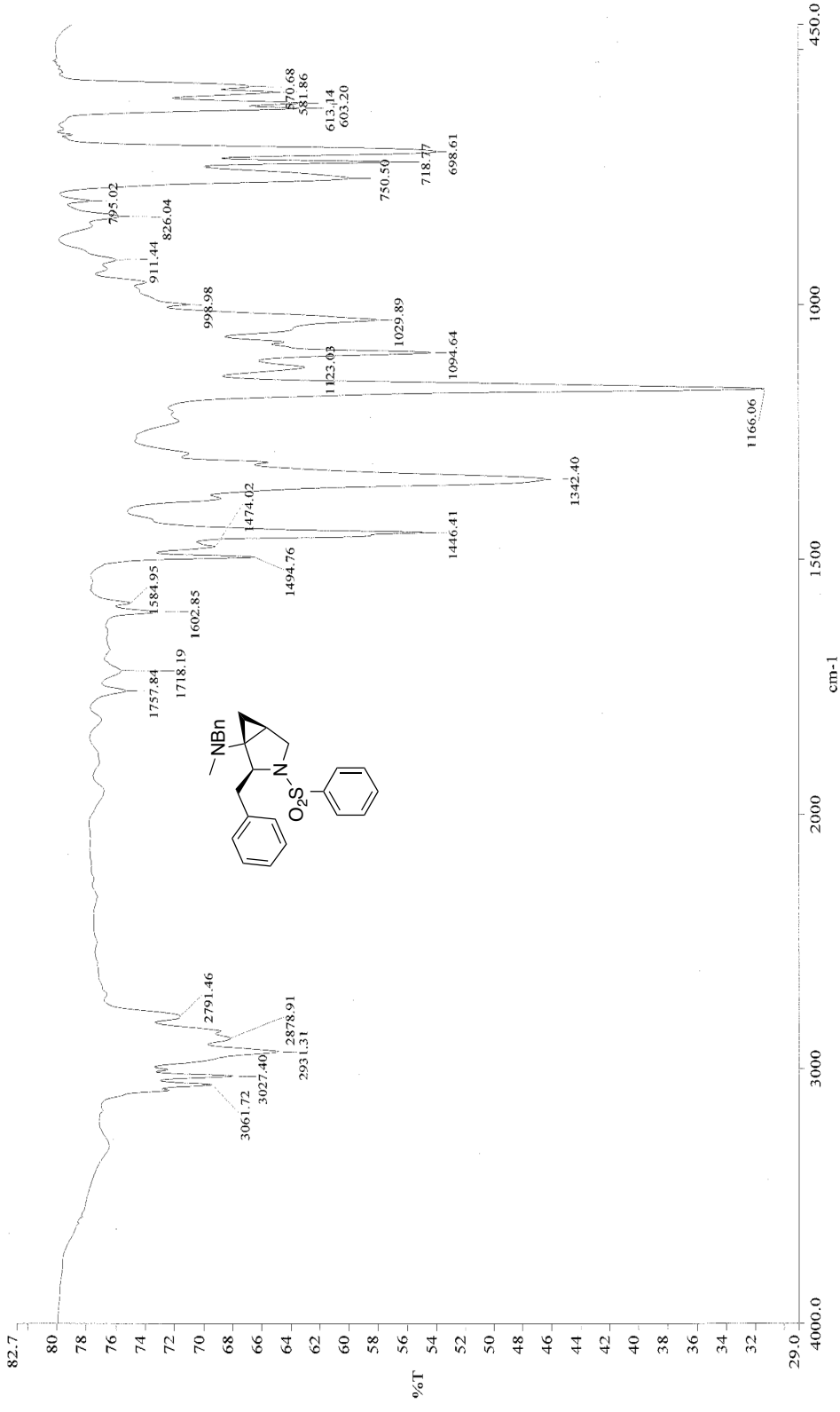

Figure 48: Infrared spectra (neat) of **18**

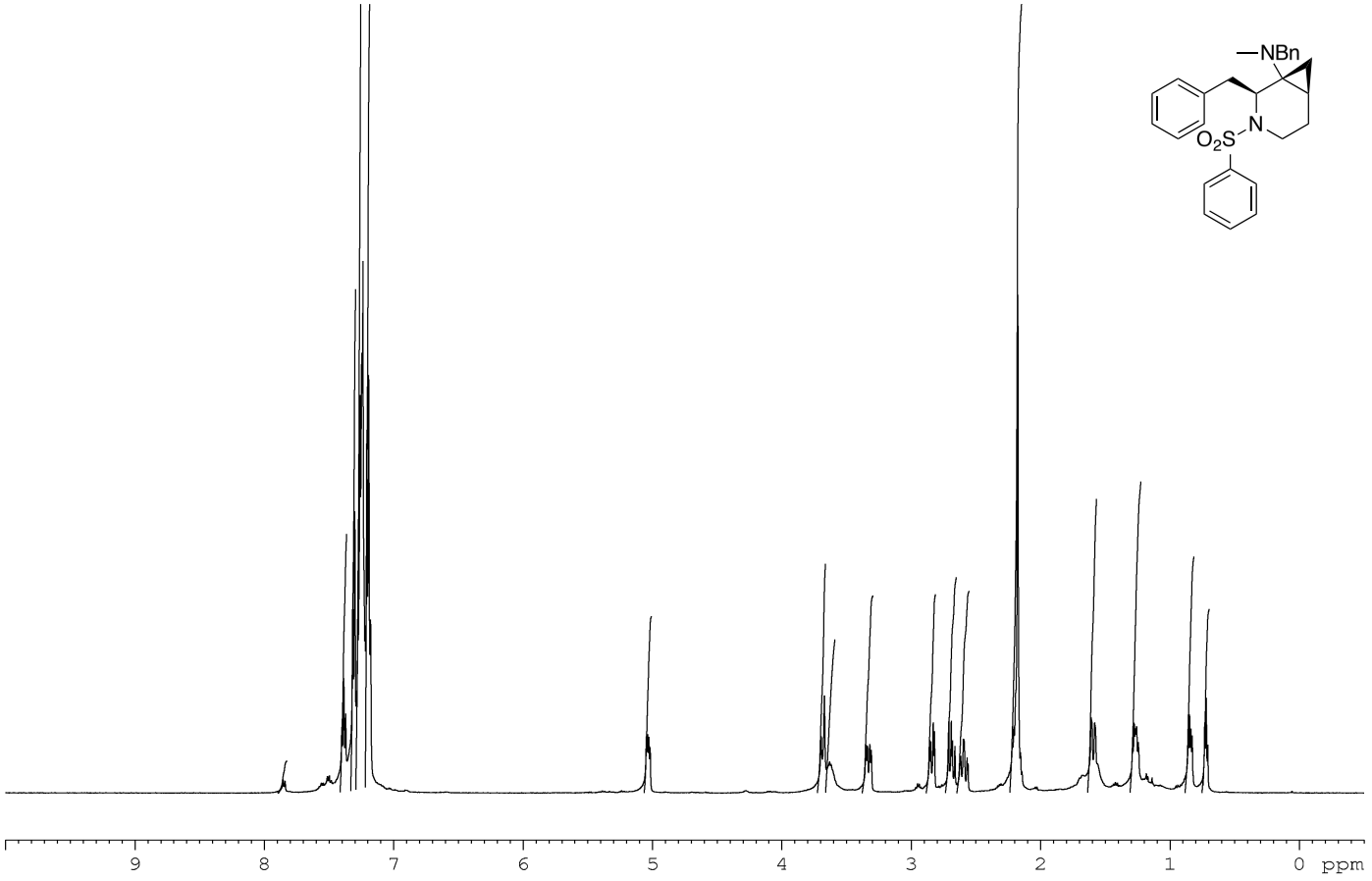

Figure 49: ^{1}H NMR ($CDCl_3$, 500 MHz) of **41**

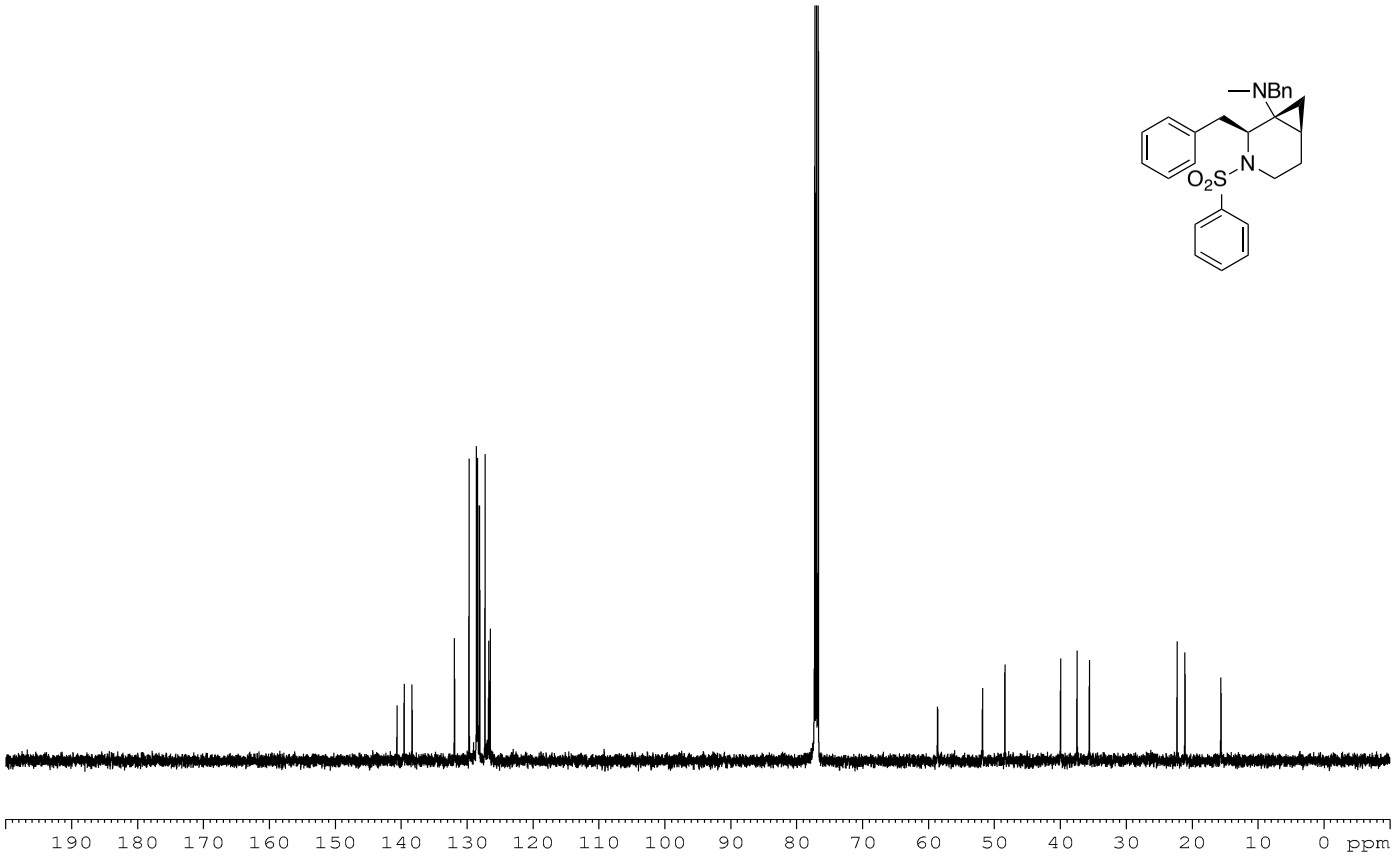

Figure 50: ^{13}C NMR ($CDCl_3$, 125 MHz) of **41**

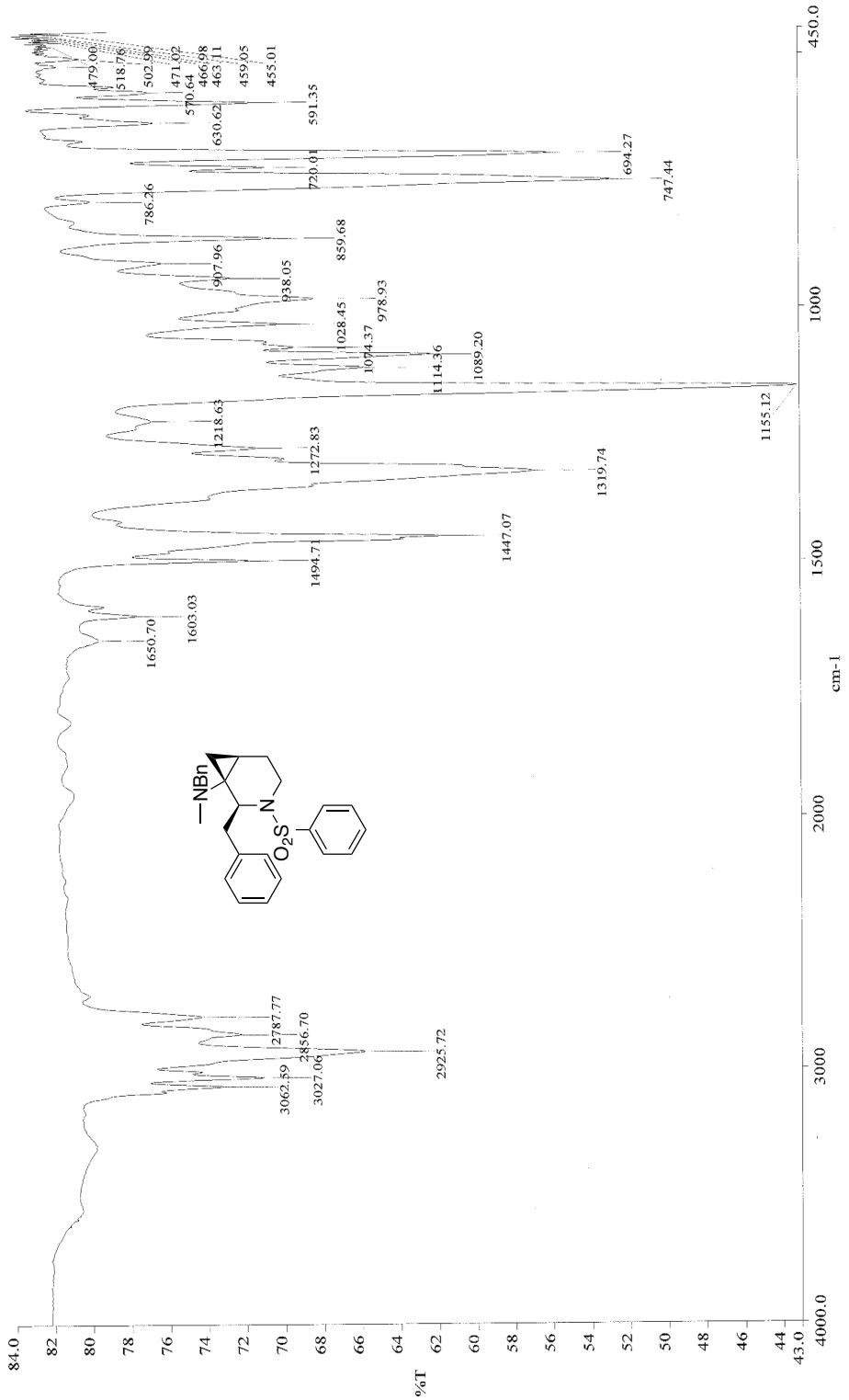

Figure 51: Infrared spectra (neat) of **41**

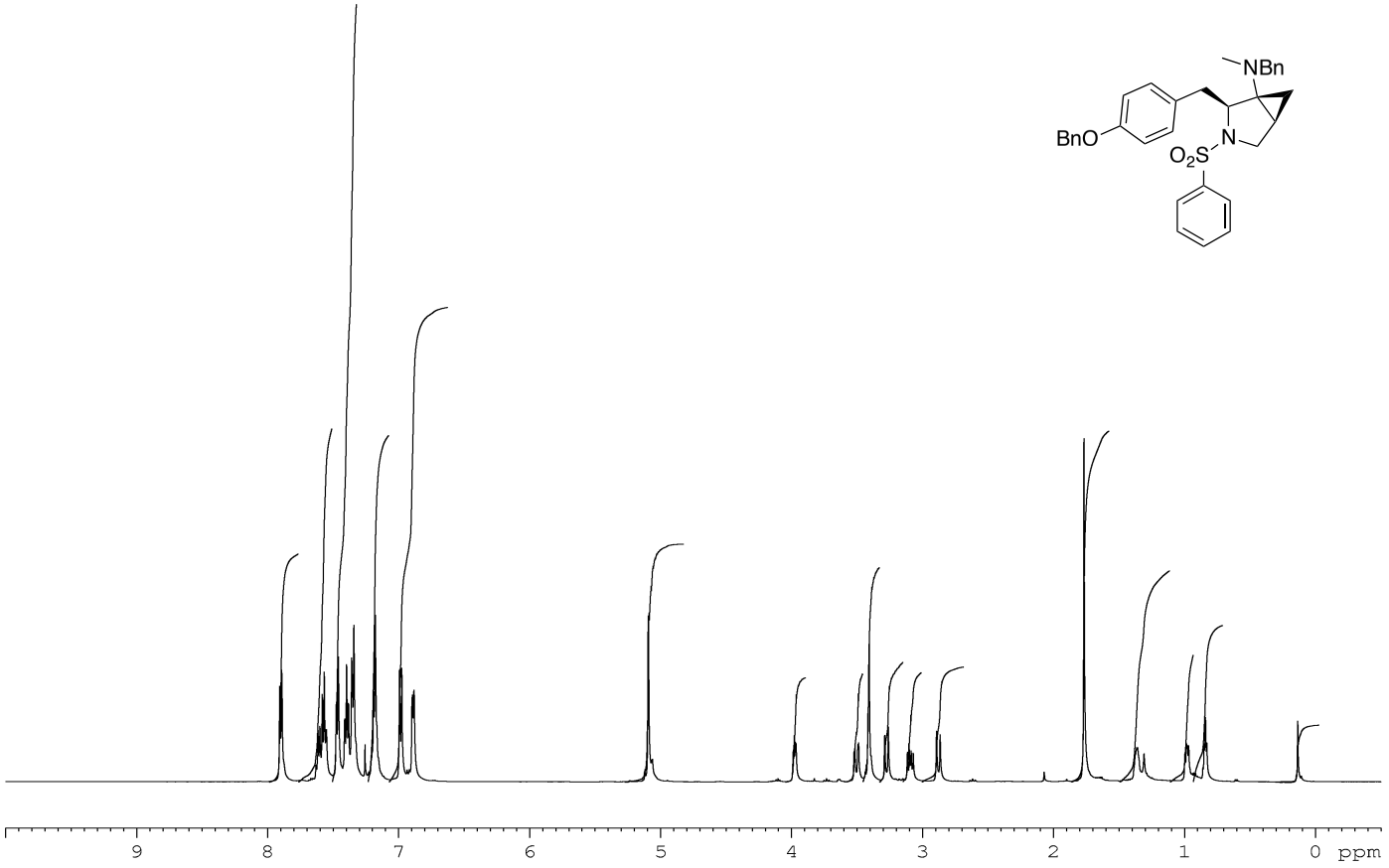

Figure 52: ^{1}H NMR ($CDCl_3$, 500 MHz) of **42**

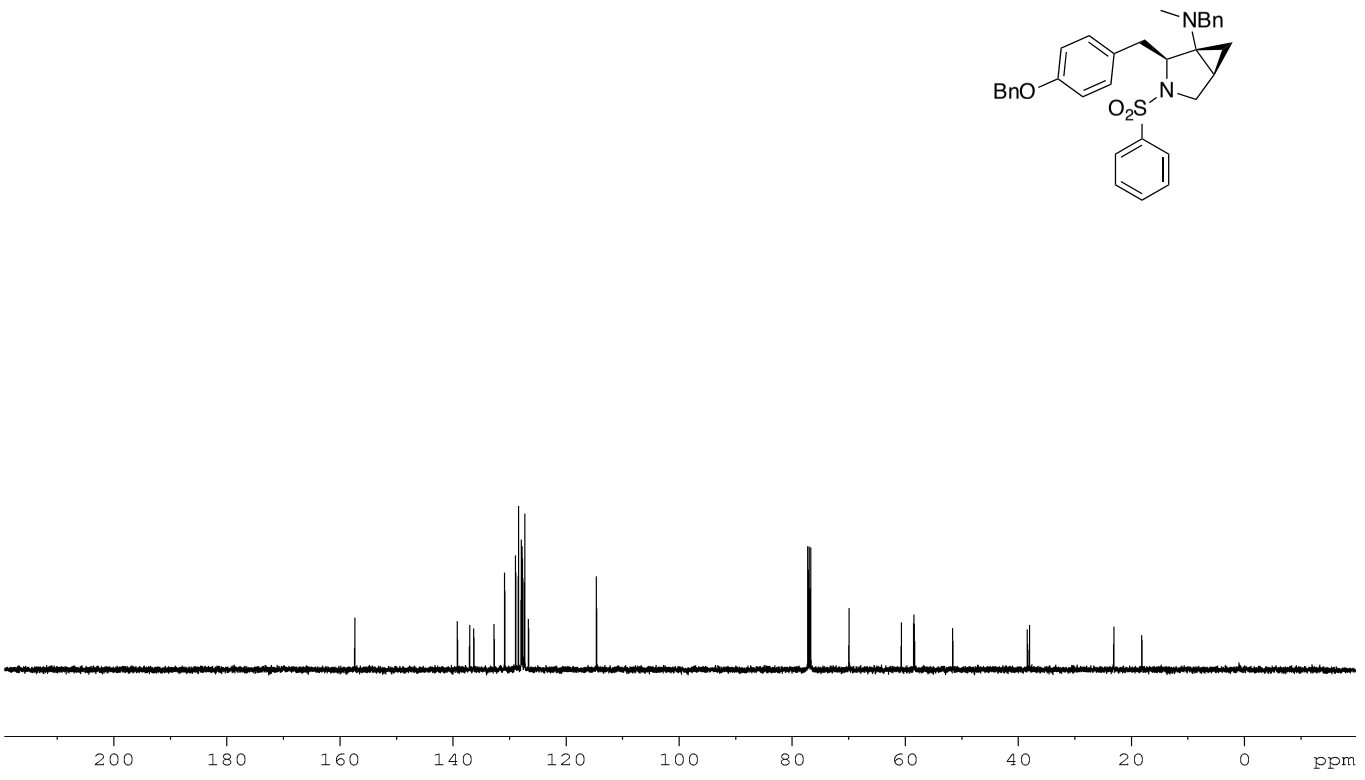

Figure 53: ^{13}C NMR ($CDCl_3$, 125 MHz) of **42**

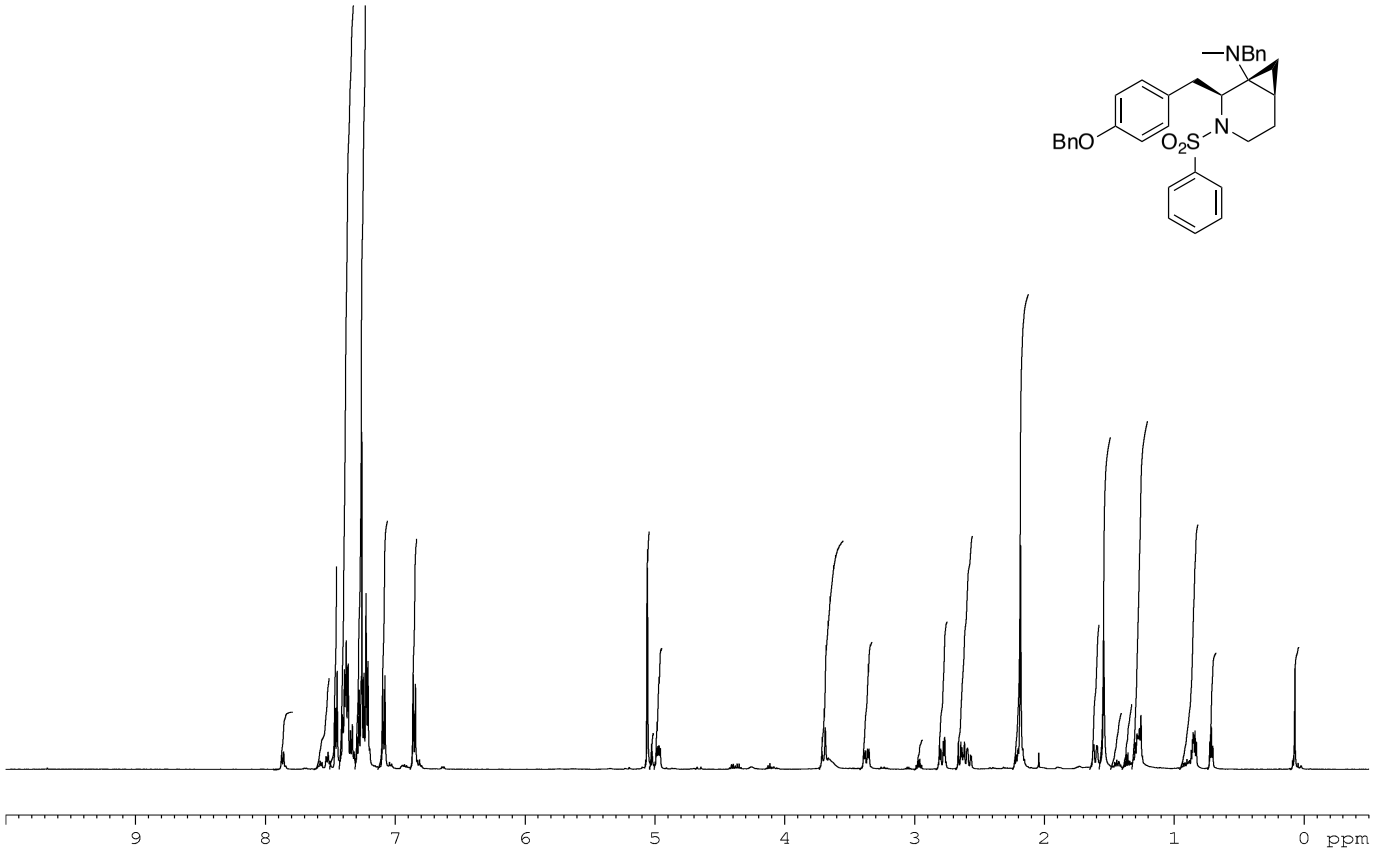

Figure 54: ^{1}H NMR ($CDCl_3$, 500 MHz) of **43**

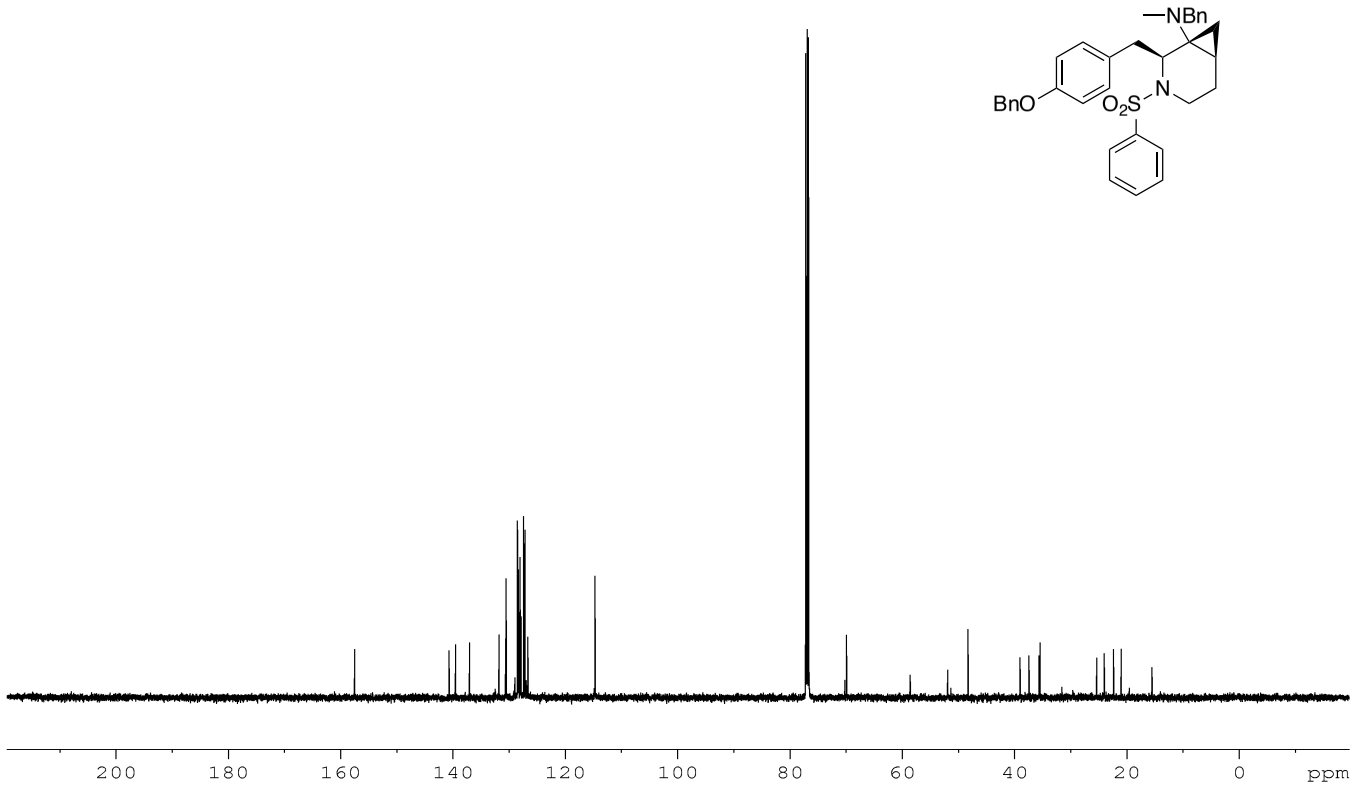

Figure 55: ^{13}C NMR ($CDCl_3$, 125 MHz) of **43**

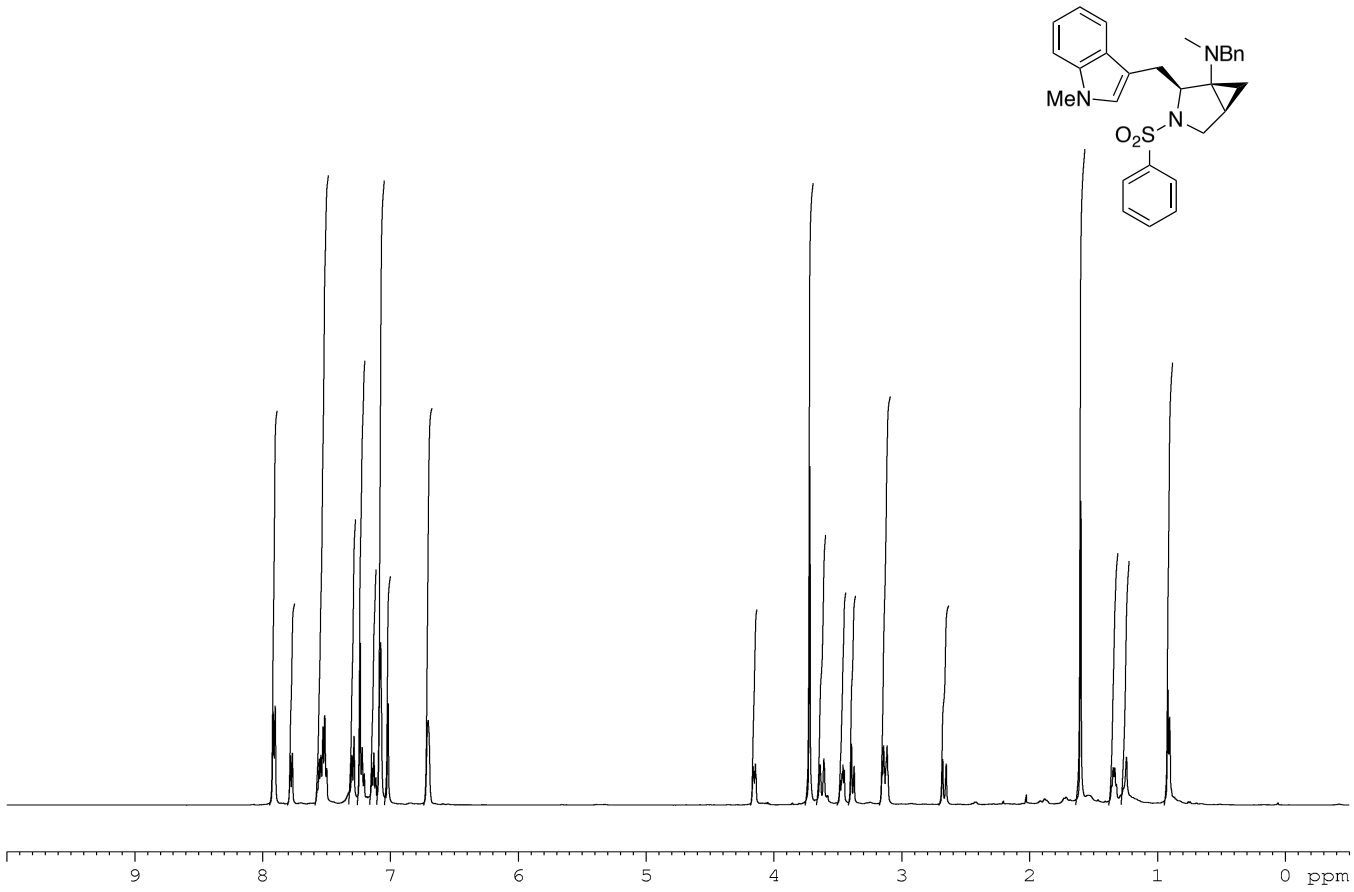

Figure 56: ^{1}H NMR ($CDCl_3$, 500 MHz) of **44**

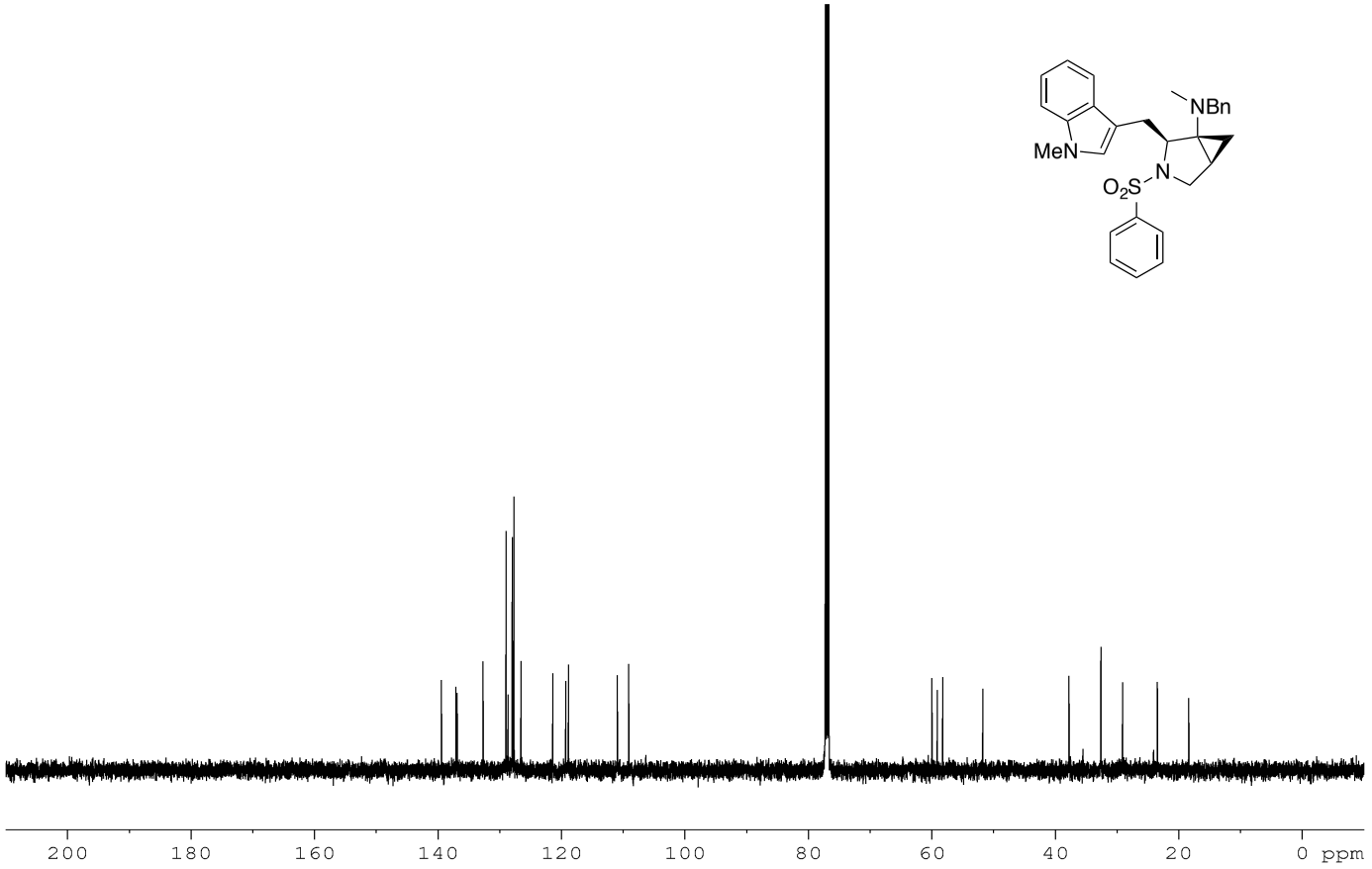

Figure 57: ^{13}C NMR ($CDCl_3$, 125 MHz) of **44**

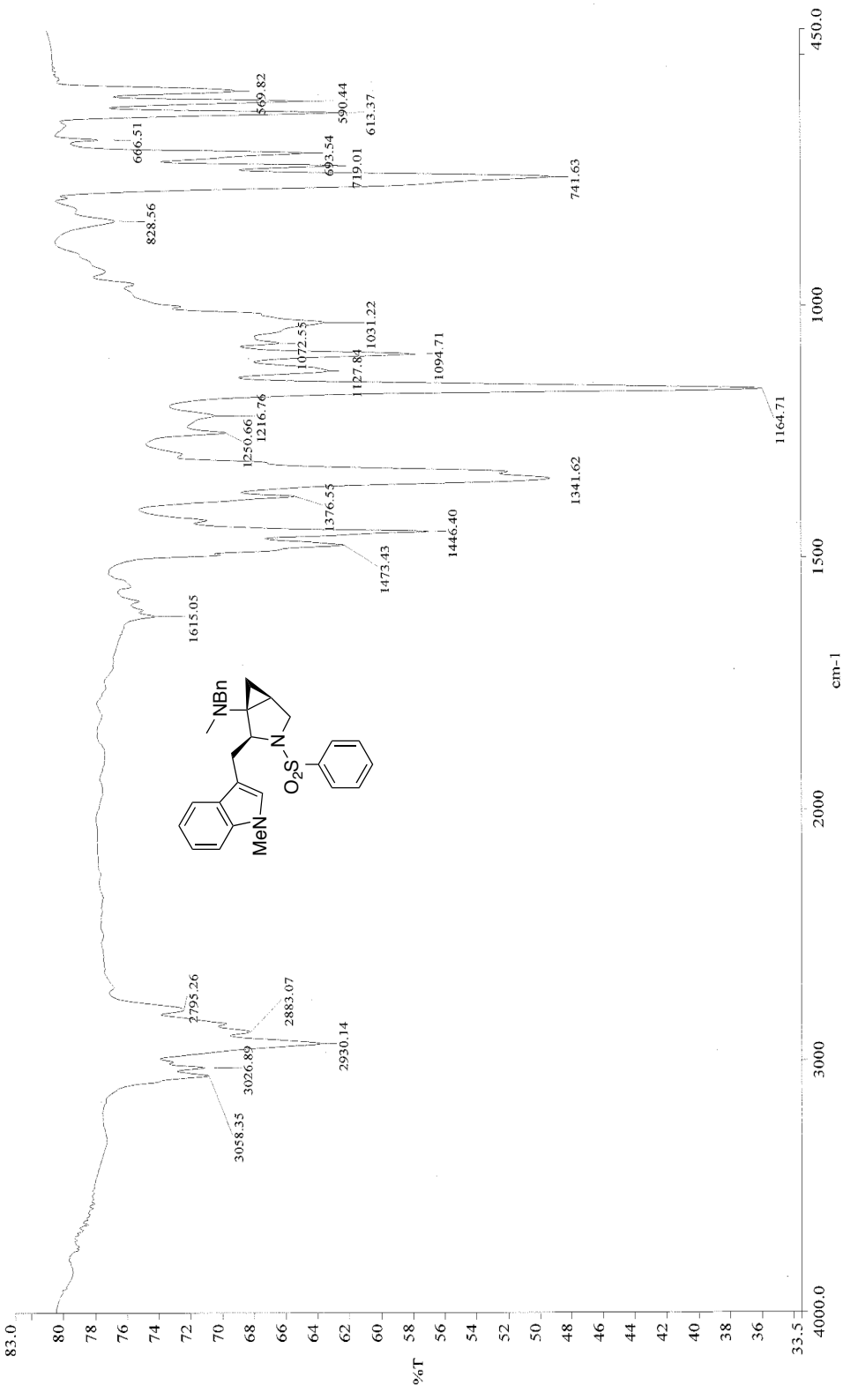

Figure 58: Infrared spectra (neat) of **44**

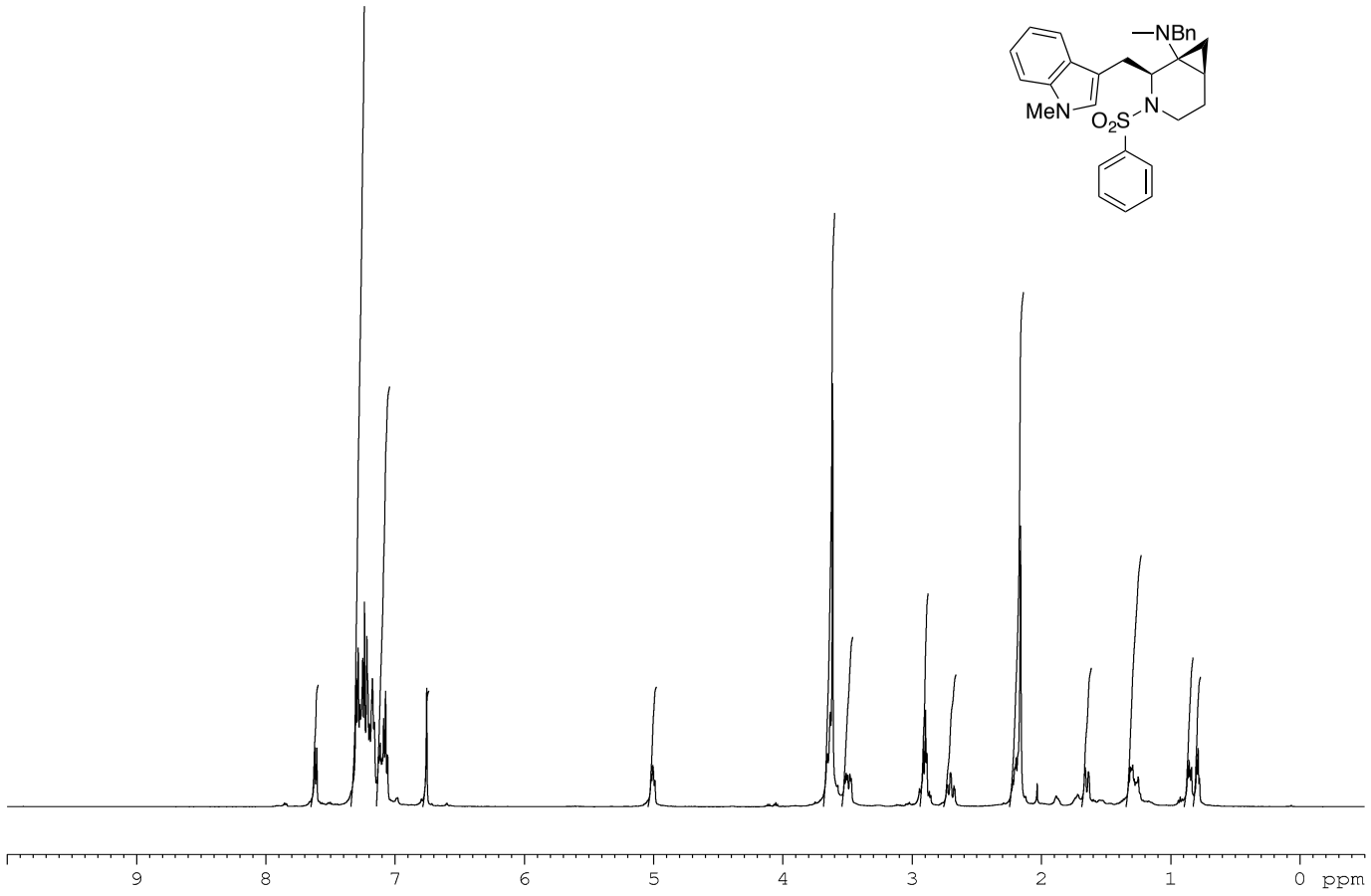

Figure 59: ^{1}H NMR ($CDCl_3$, 500 MHz) of **45**

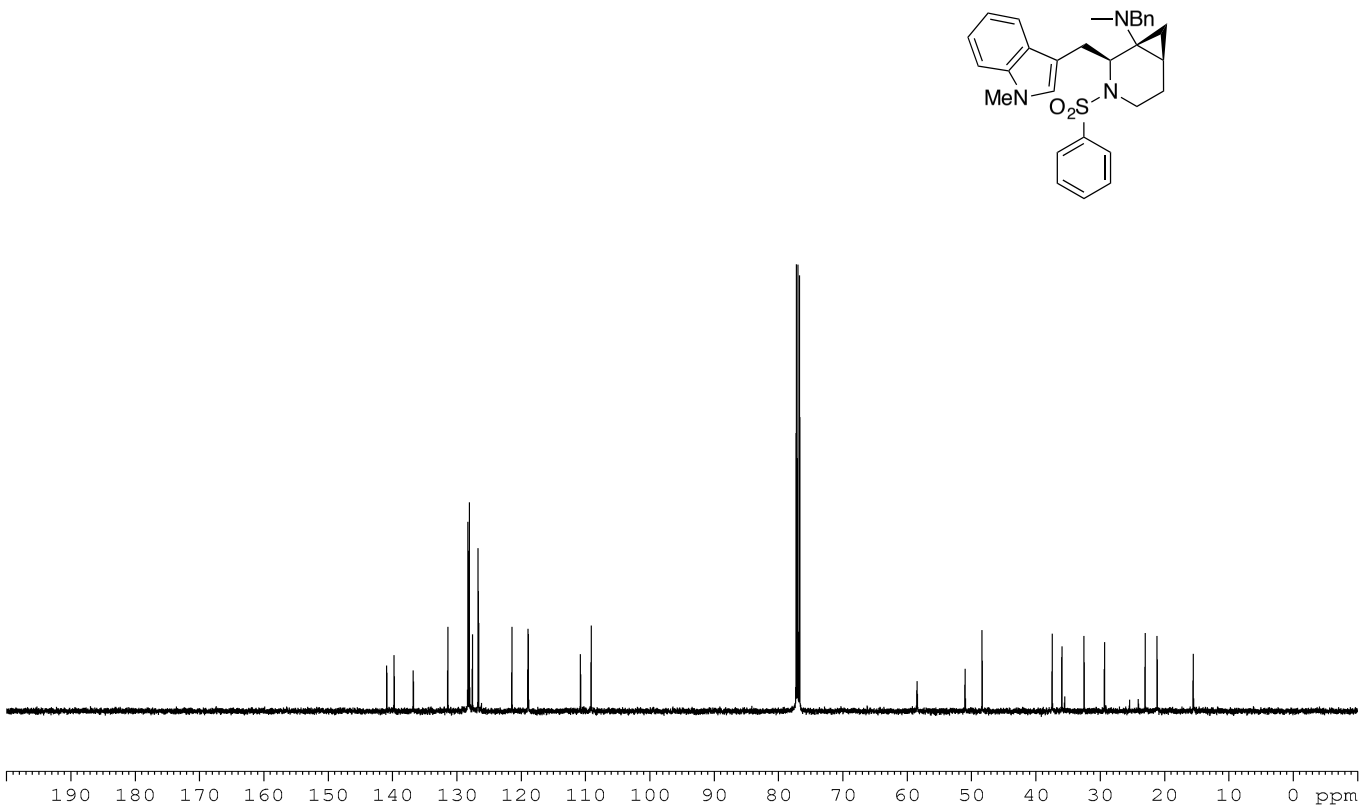

Figure 60: ^{13}C NMR ($CDCl_3$, 125 MHz) of **45**

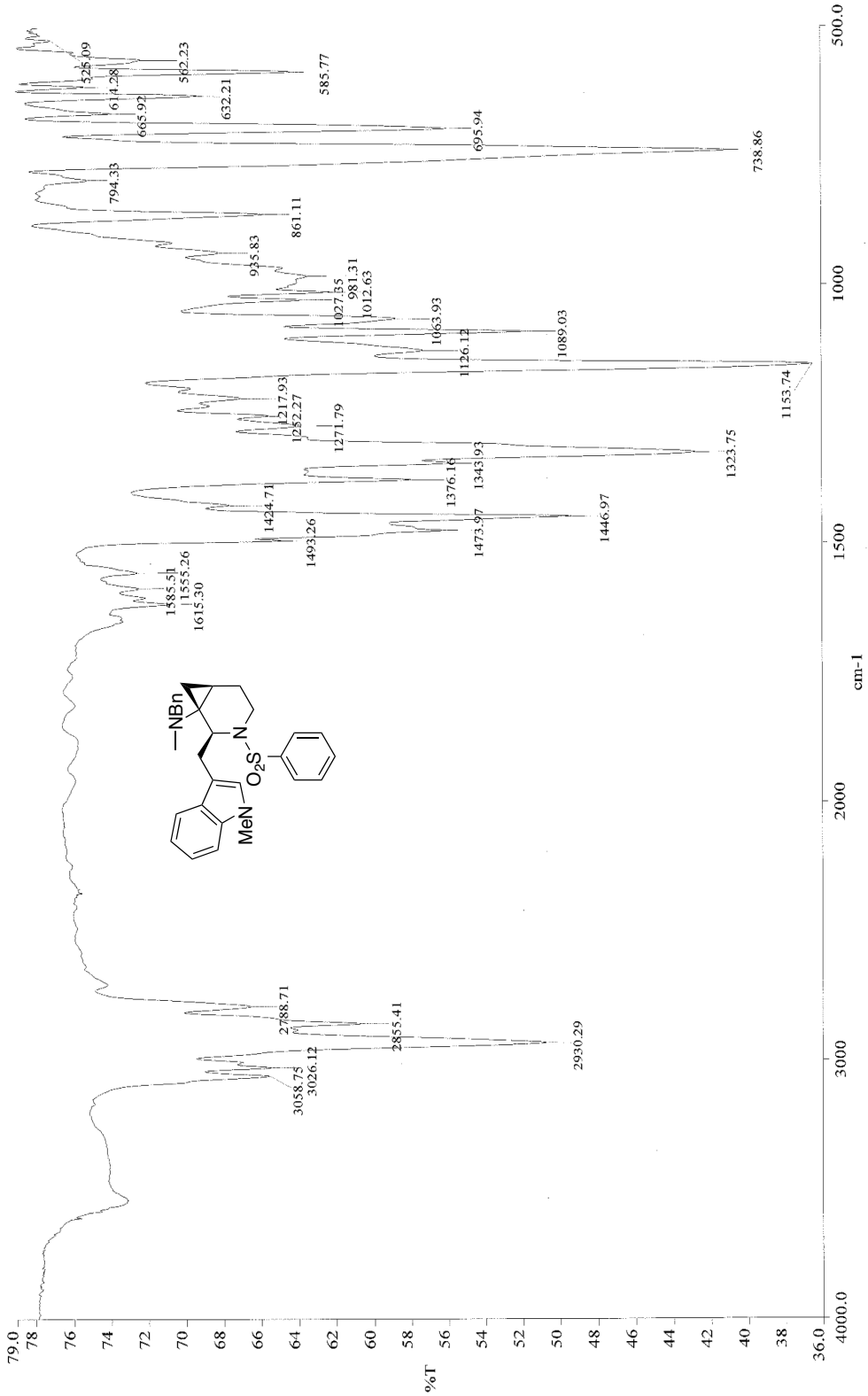

Figure 61: Infrared spectra (neat) of **45**

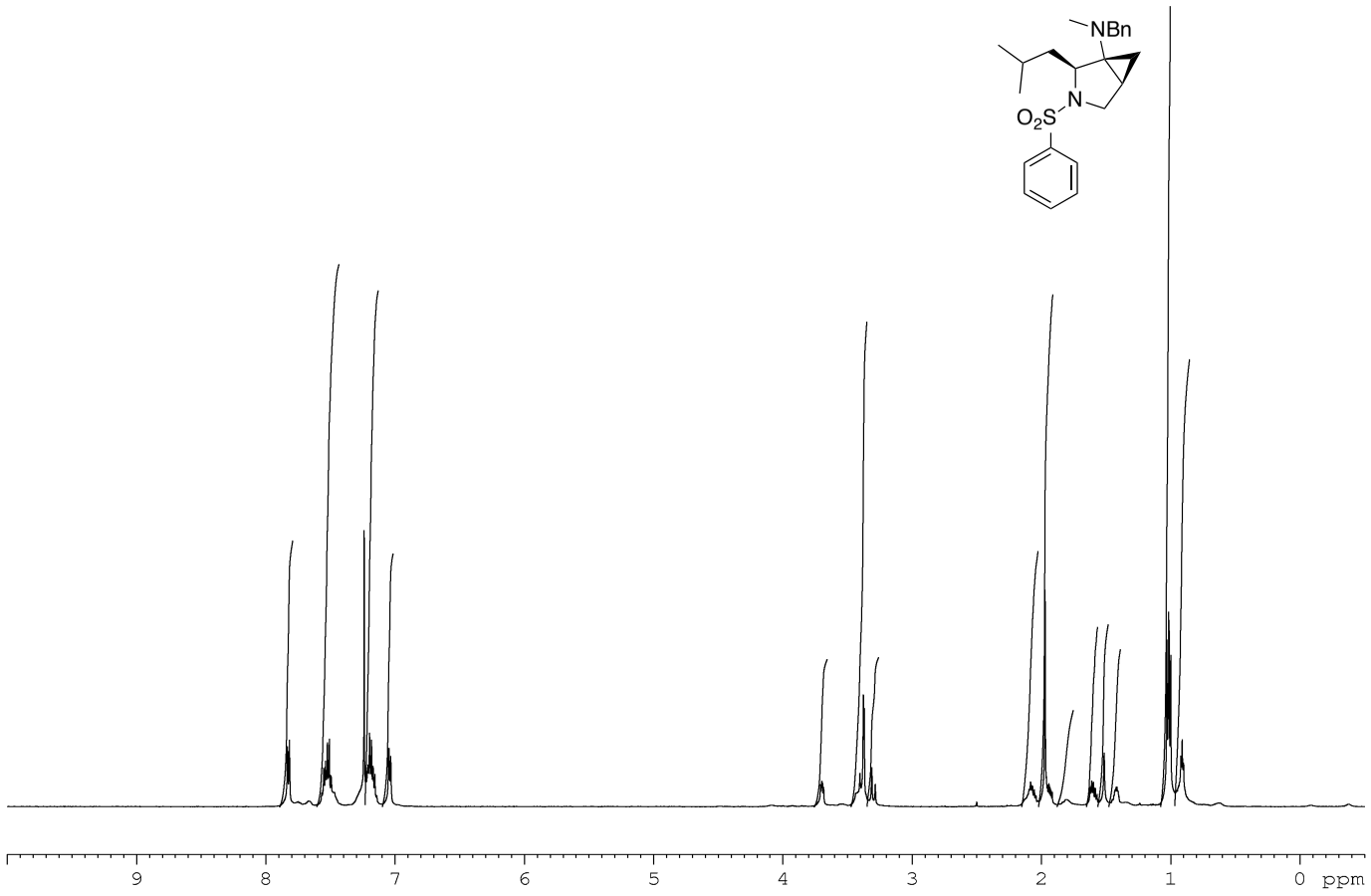

Figure 62: ^{1}H NMR ($CDCl_3$, 500 MHz) of **46**

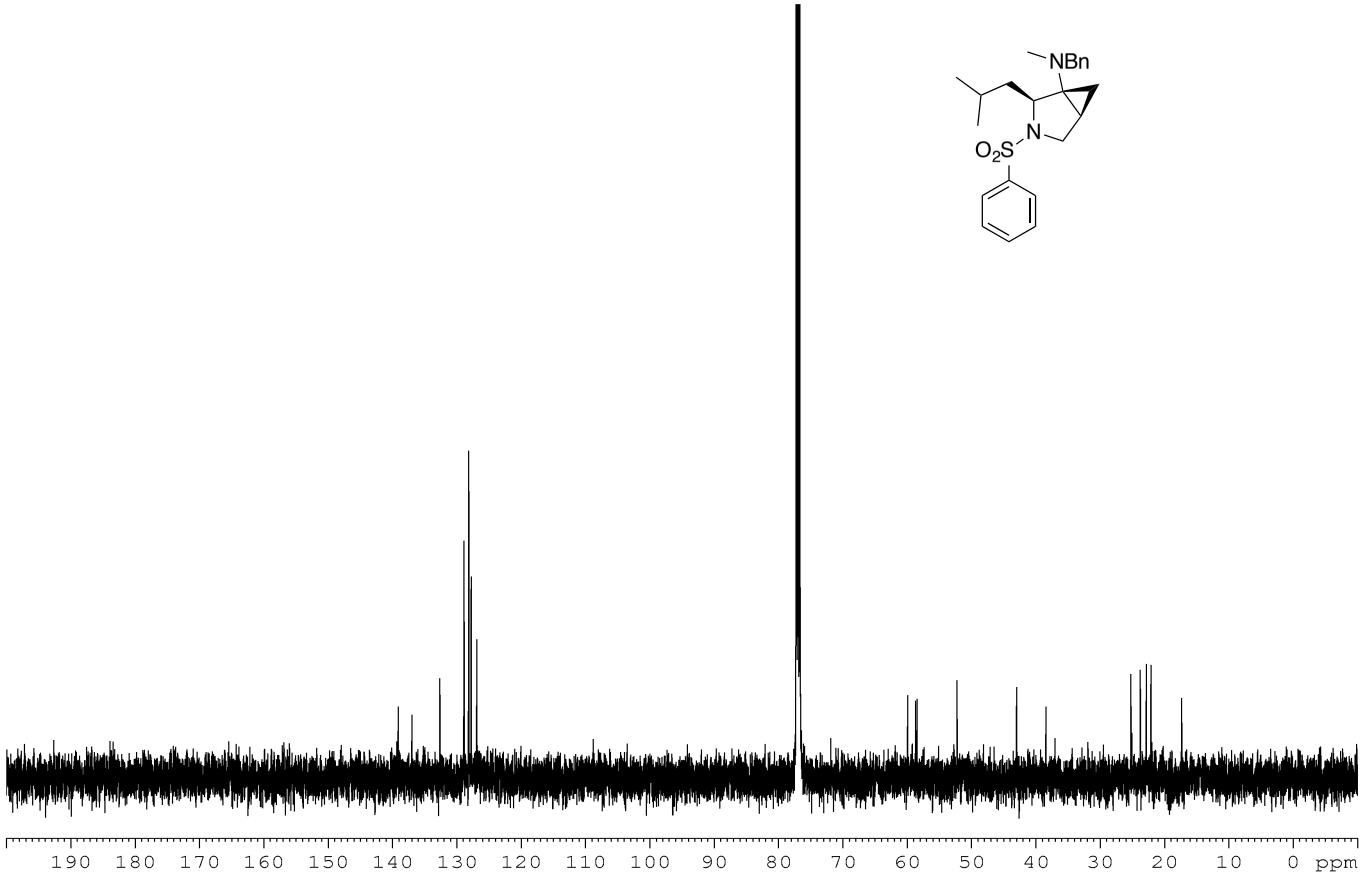

Figure 63: ^{13}C NMR ($CDCl_3$, 125 MHz) of **46**

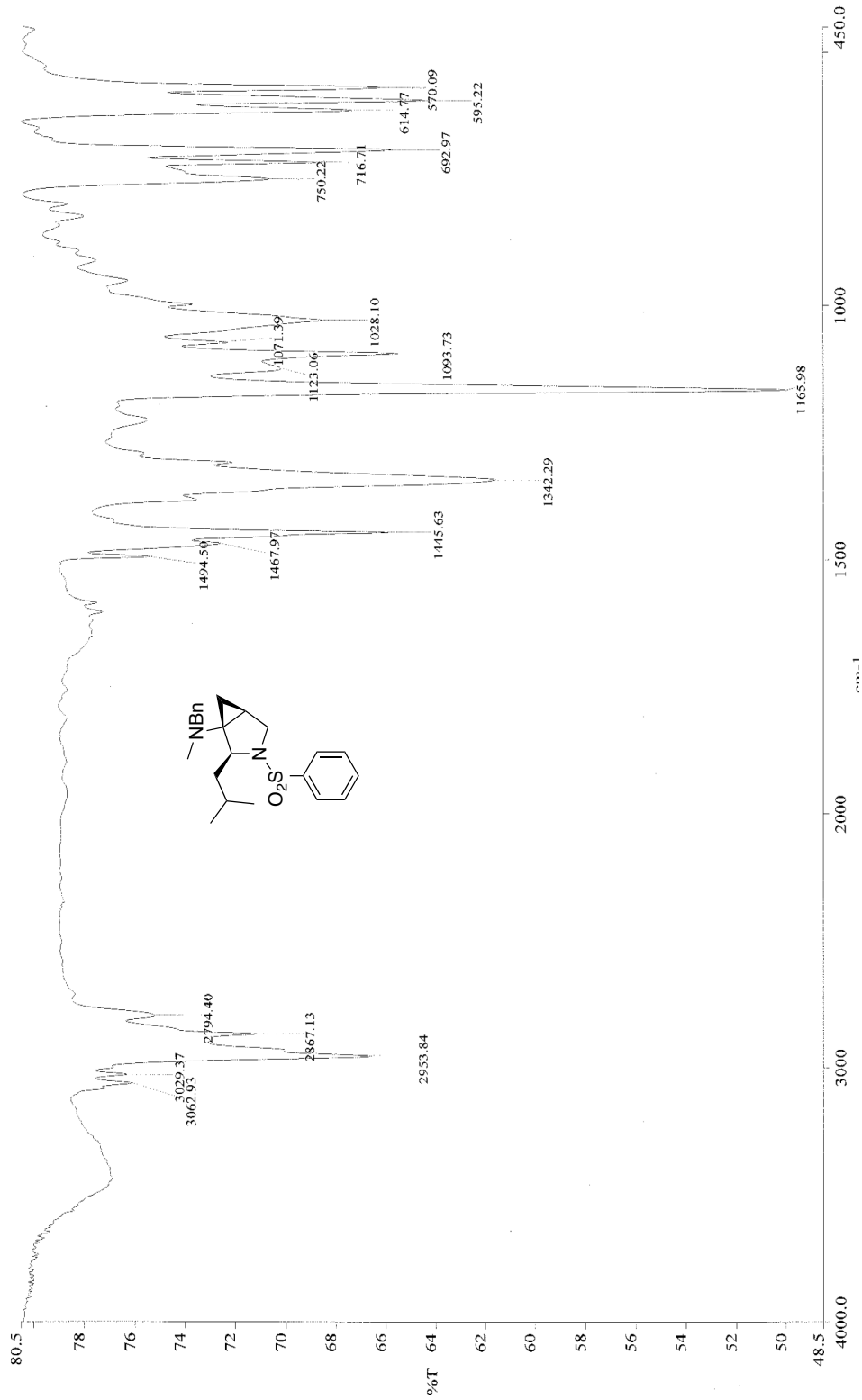

Figure 64: Infrared spectra (neat) of **46**

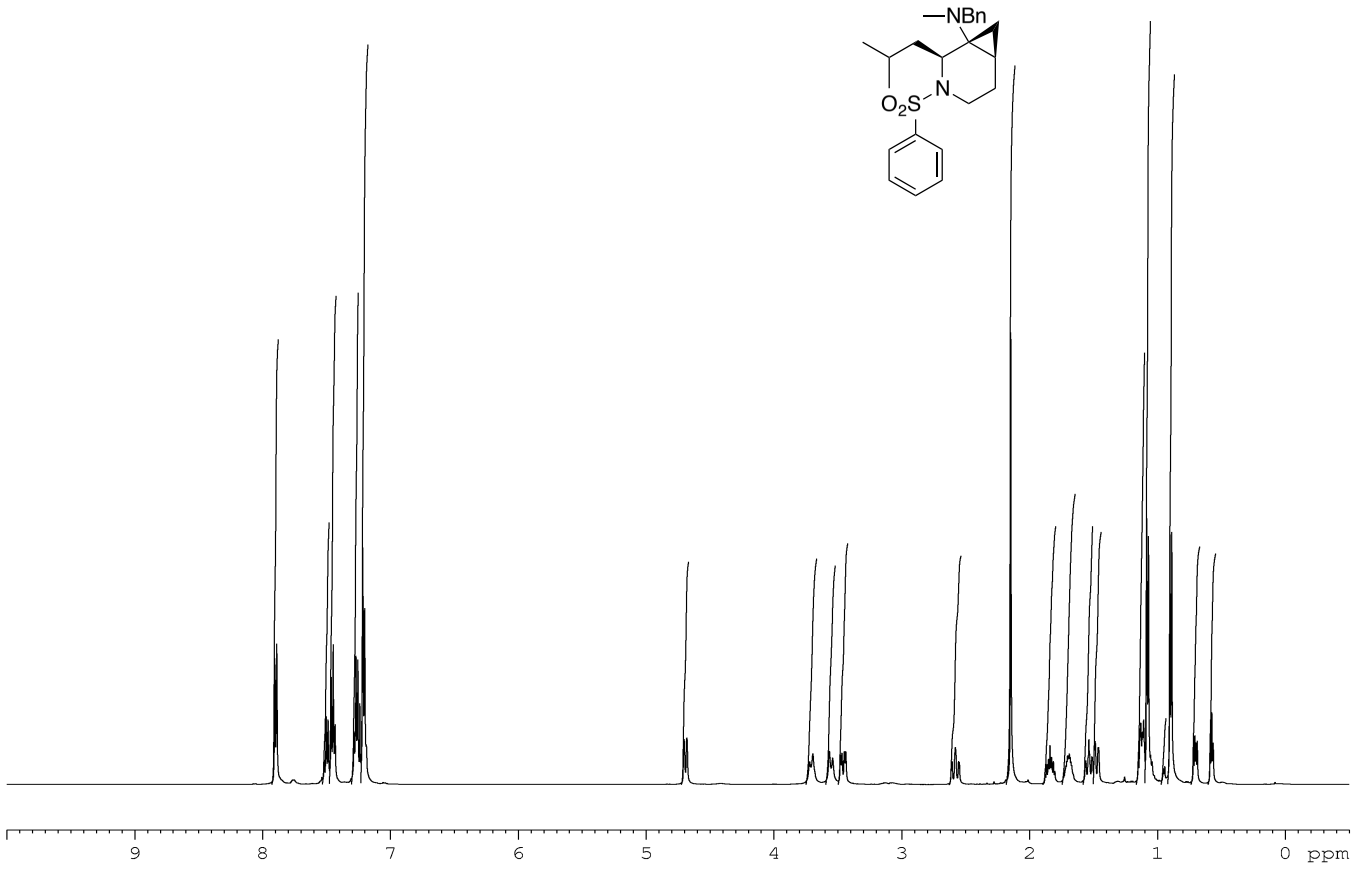

Figure 65: ^{1}H NMR ($CDCl_3$, 500 MHz) of **47**

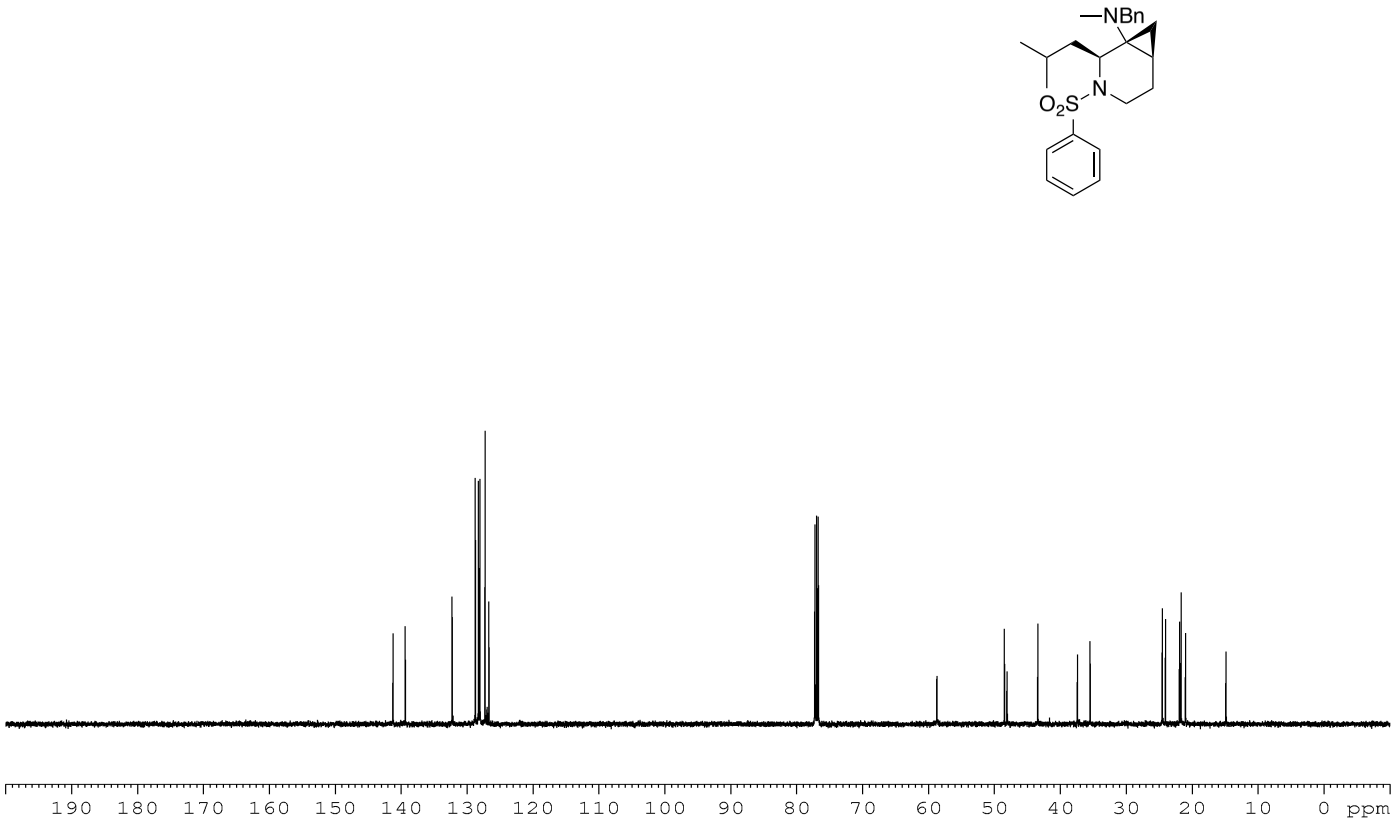

Figure 66: ^{13}C NMR ($CDCl_3$, 125 MHz) of **47**

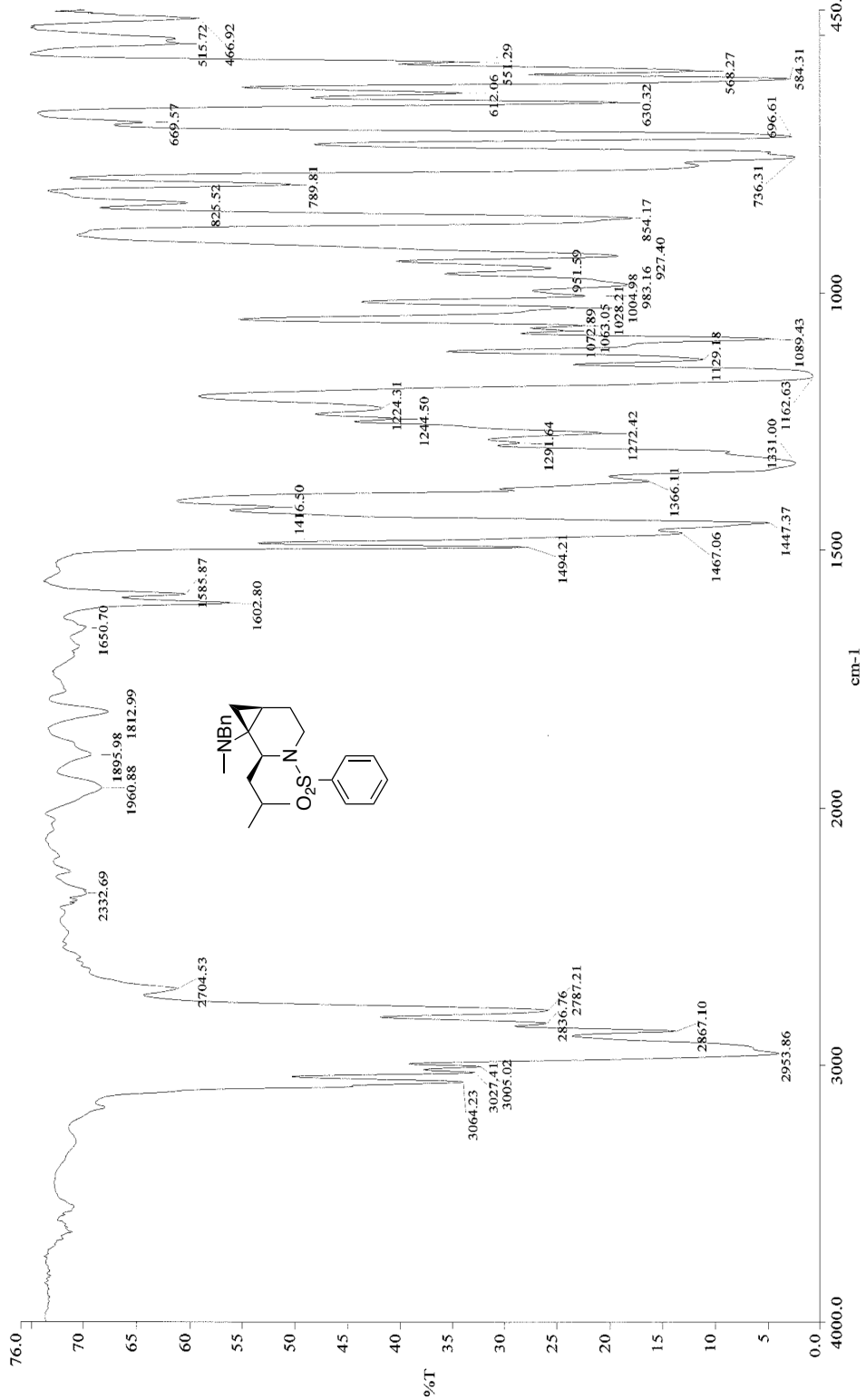

Figure 67: Infrared spectra (neat) of **47**

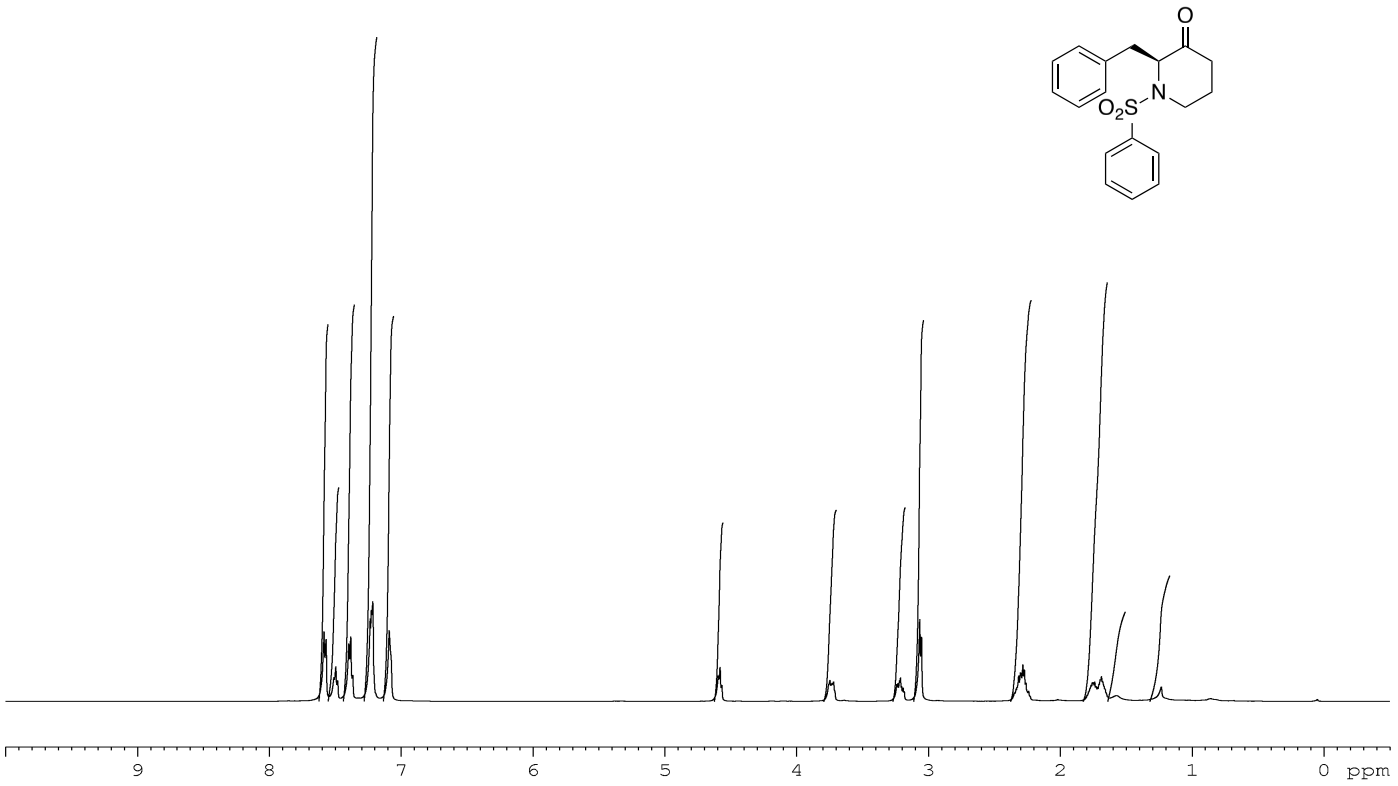

Figure 68: ^{1}H NMR ($CDCl_3$, 500 MHz) of **48**

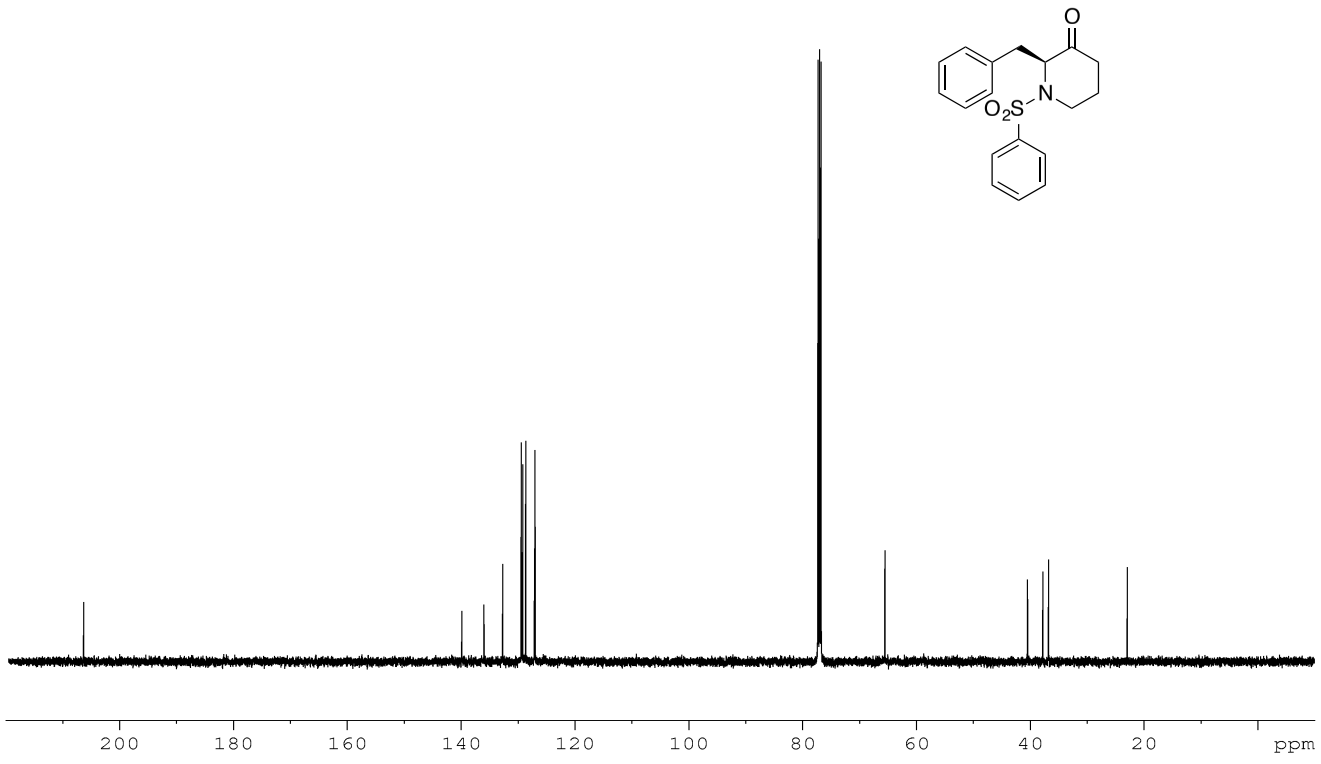

Figure 69: ^{13}C NMR ($CDCl_3$, 125 MHz) of **48**

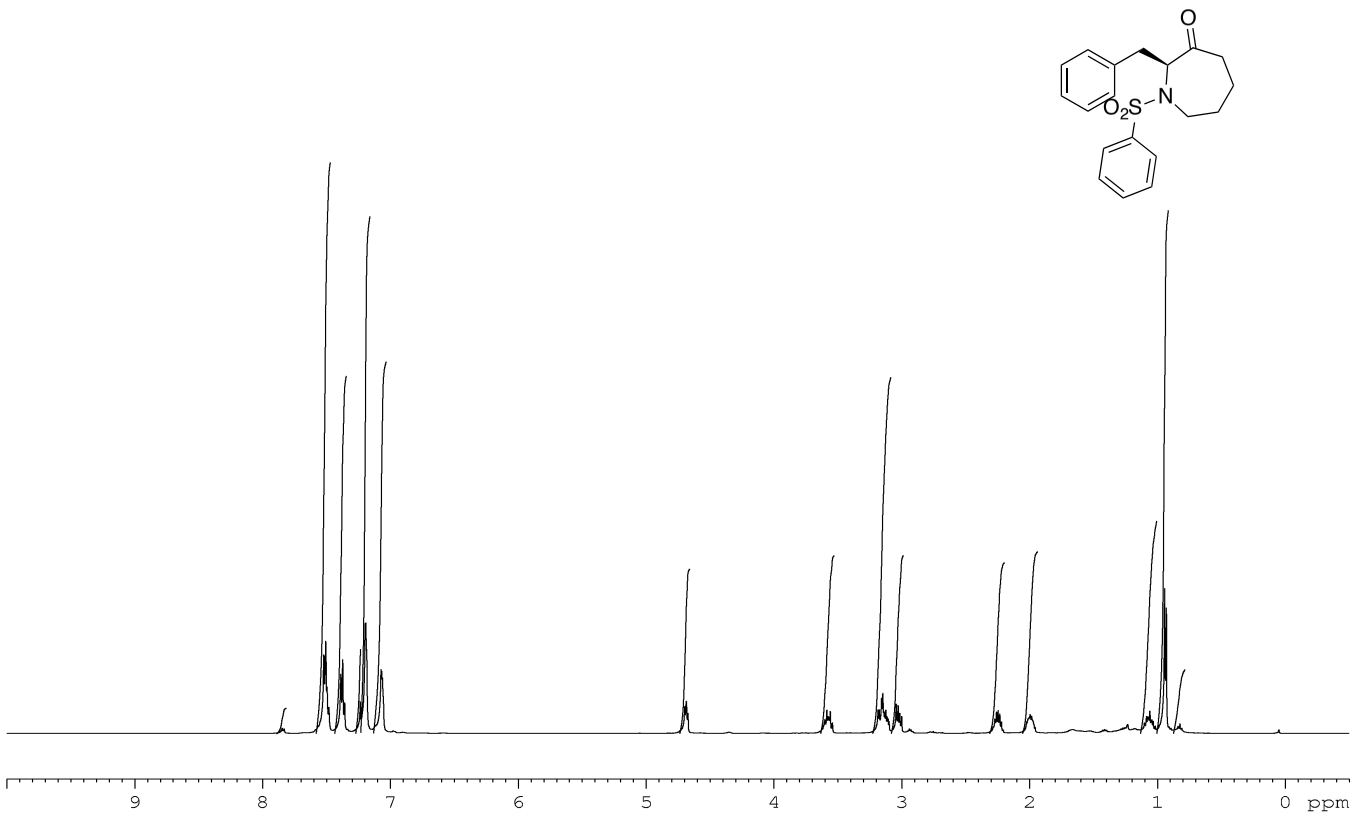

Figure 70: ^{1}H NMR ($CDCl_3$, 500 MHz) of **49**

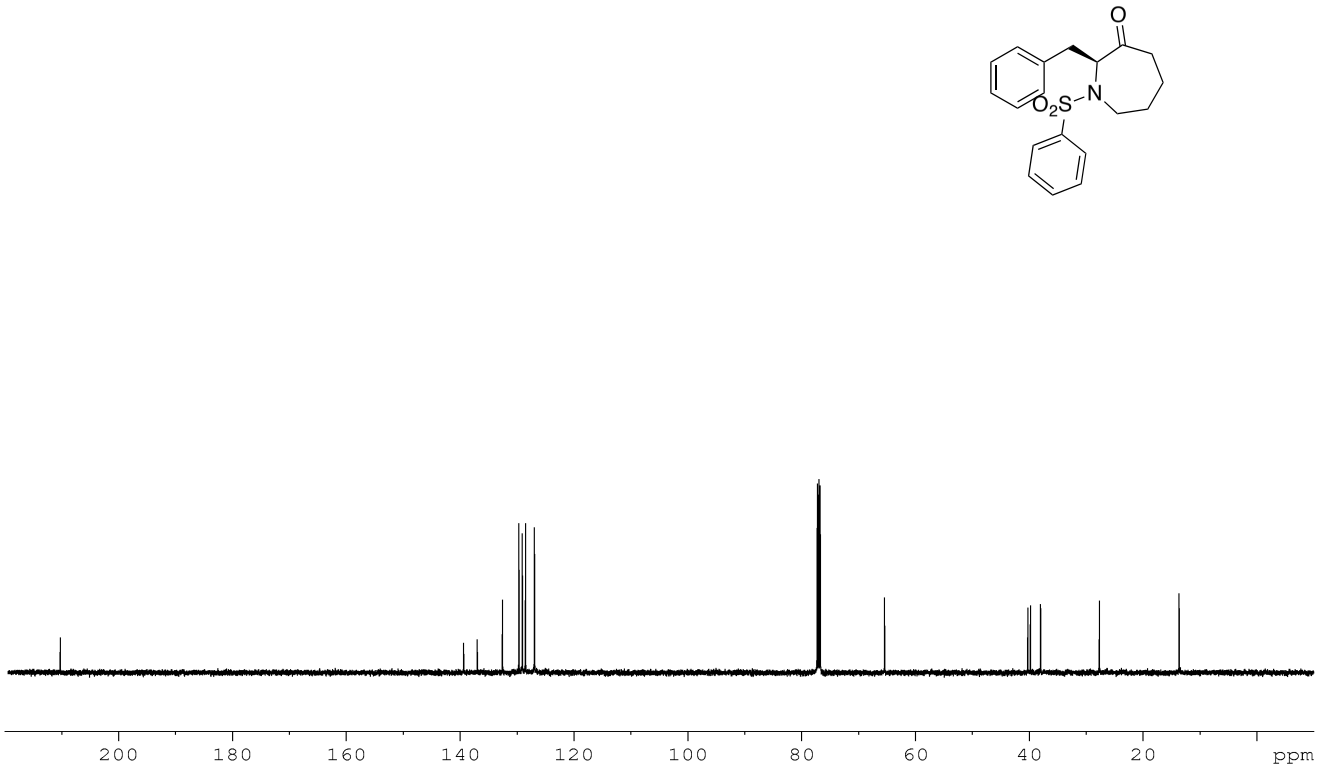

Figure 71: ^{13}C NMR ($CDCl_3$, 125 MHz) of **49**

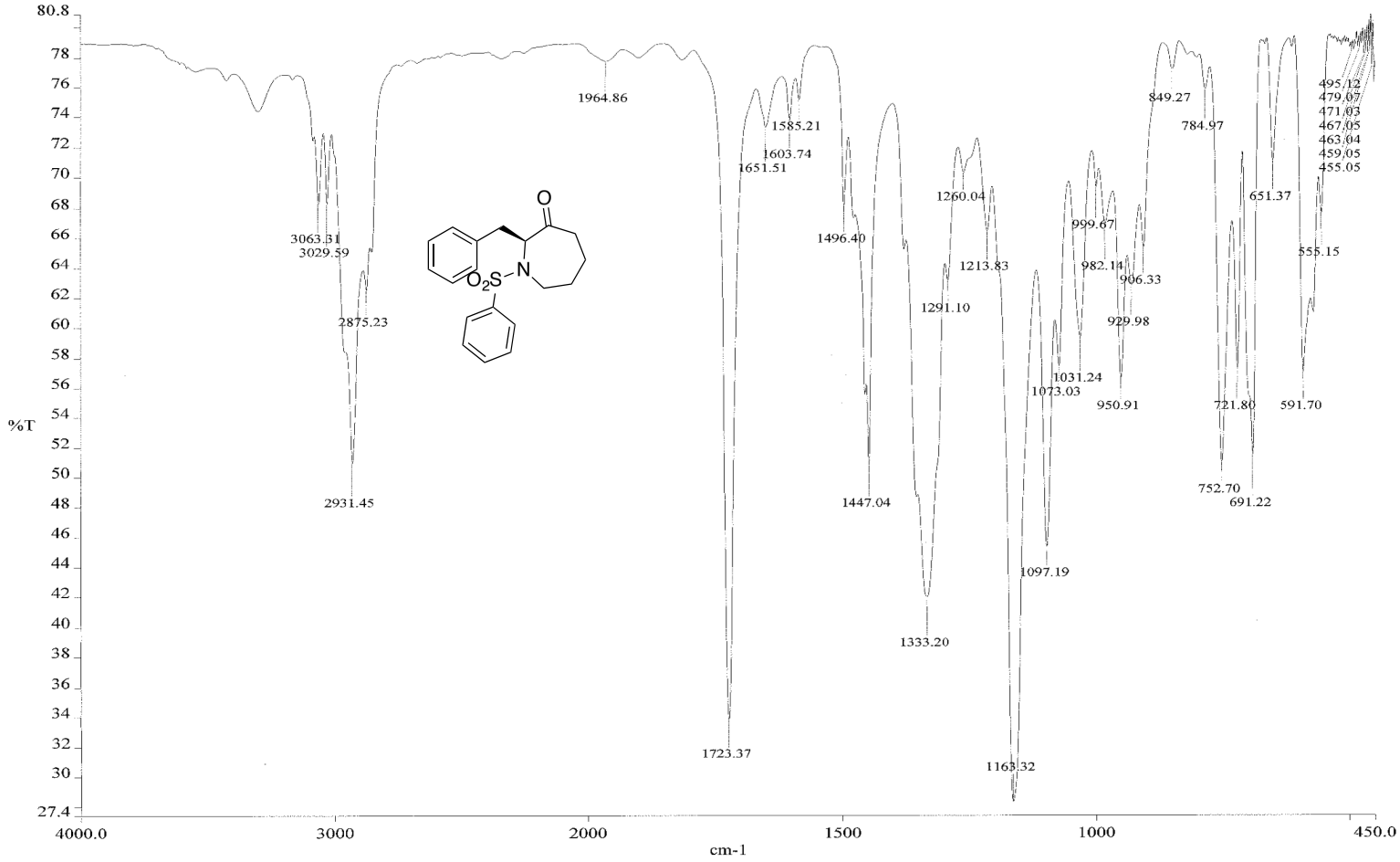

Figure 72: Infrared spectra (neat) of **49**

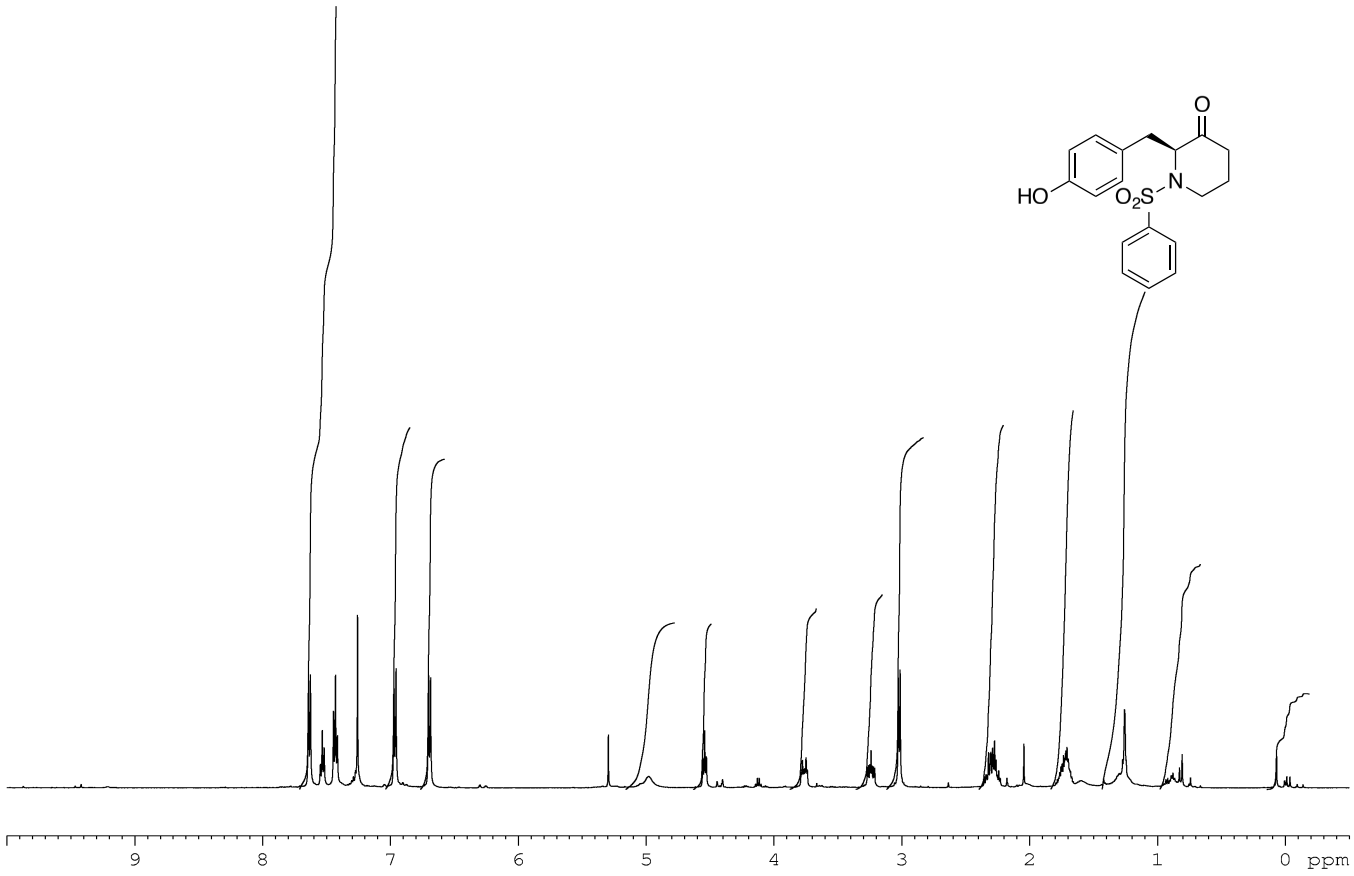

Figure 73: ^{1}H NMR ($CDCl_3$, 500 MHz) of **50**

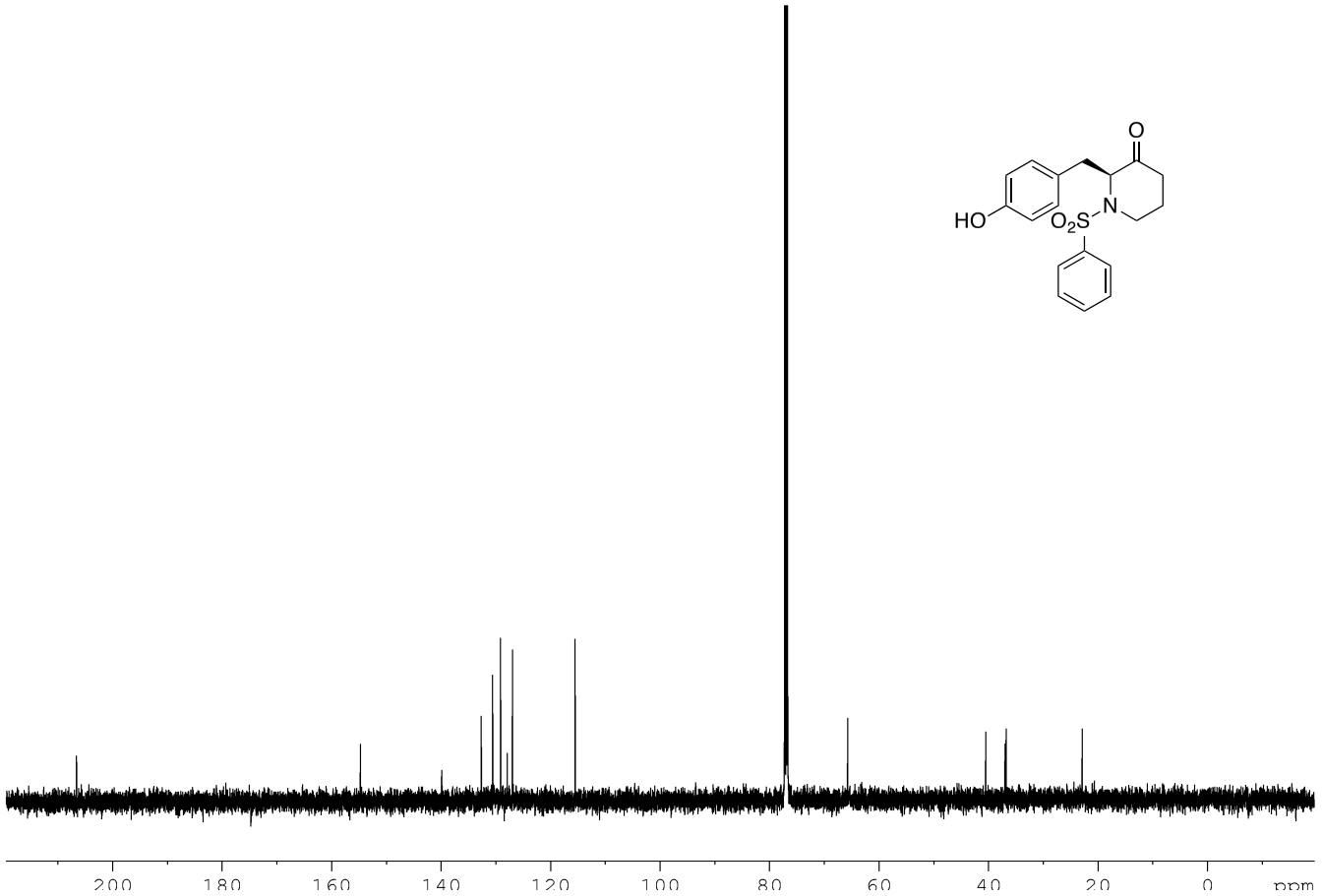

Figure 74: ^{13}C NMR ($CDCl_3$, 125 MHz) of **50**

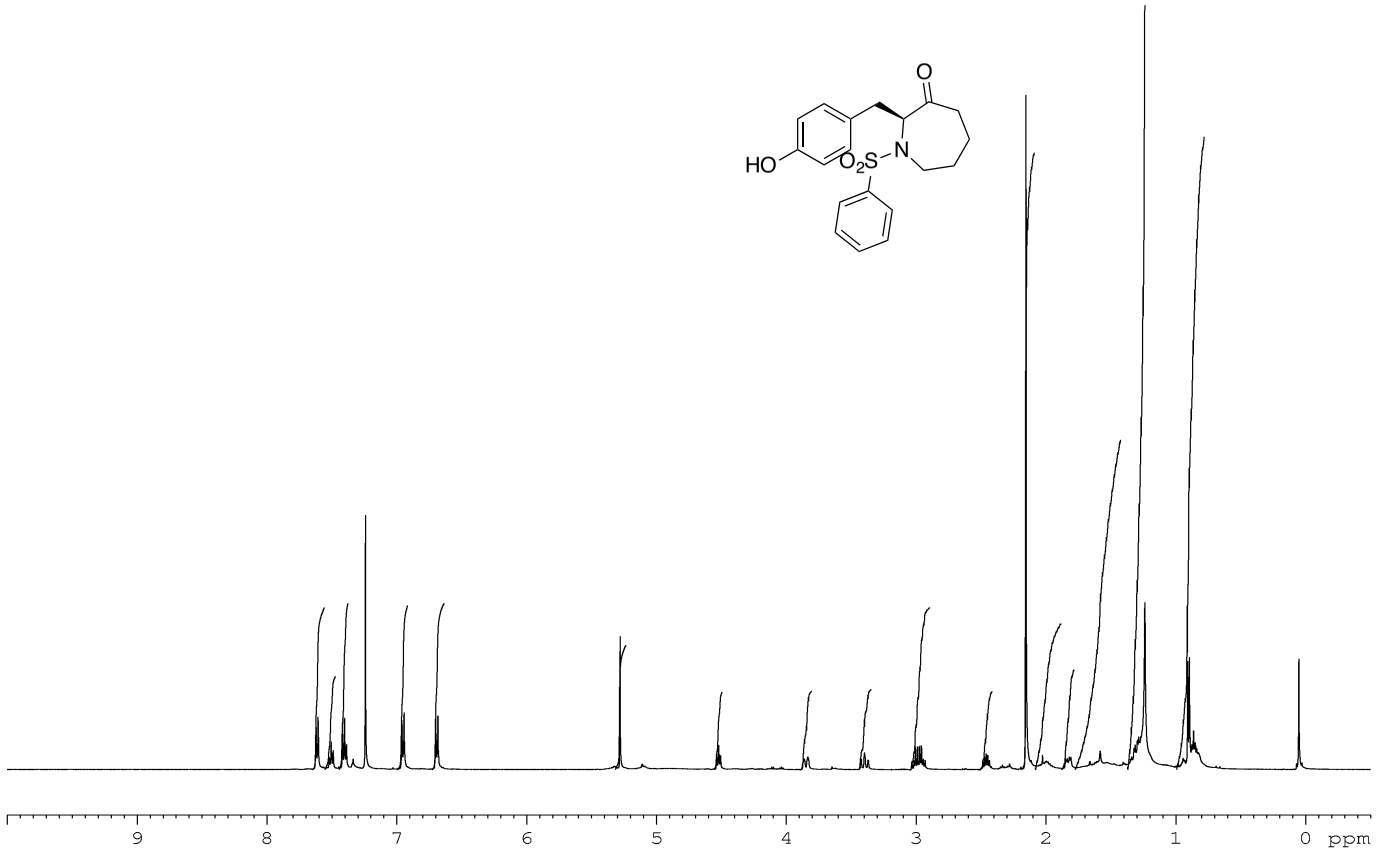

Figure 75: ^{1}H NMR ($CDCl_3$, 500 MHz) of **51**

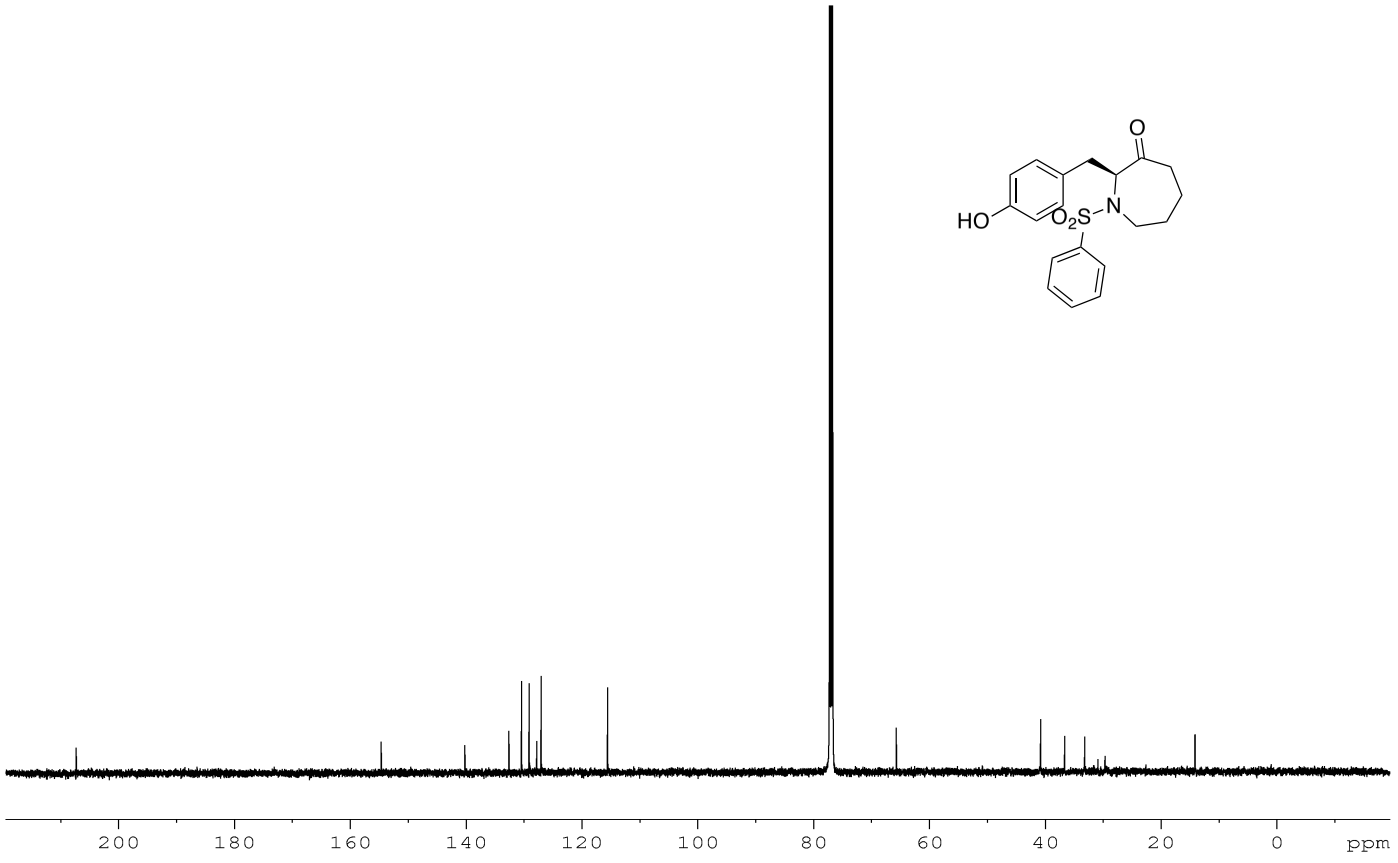

Figure 76: ^{13}C NMR ($CDCl_3$, 125 MHz) of **51**

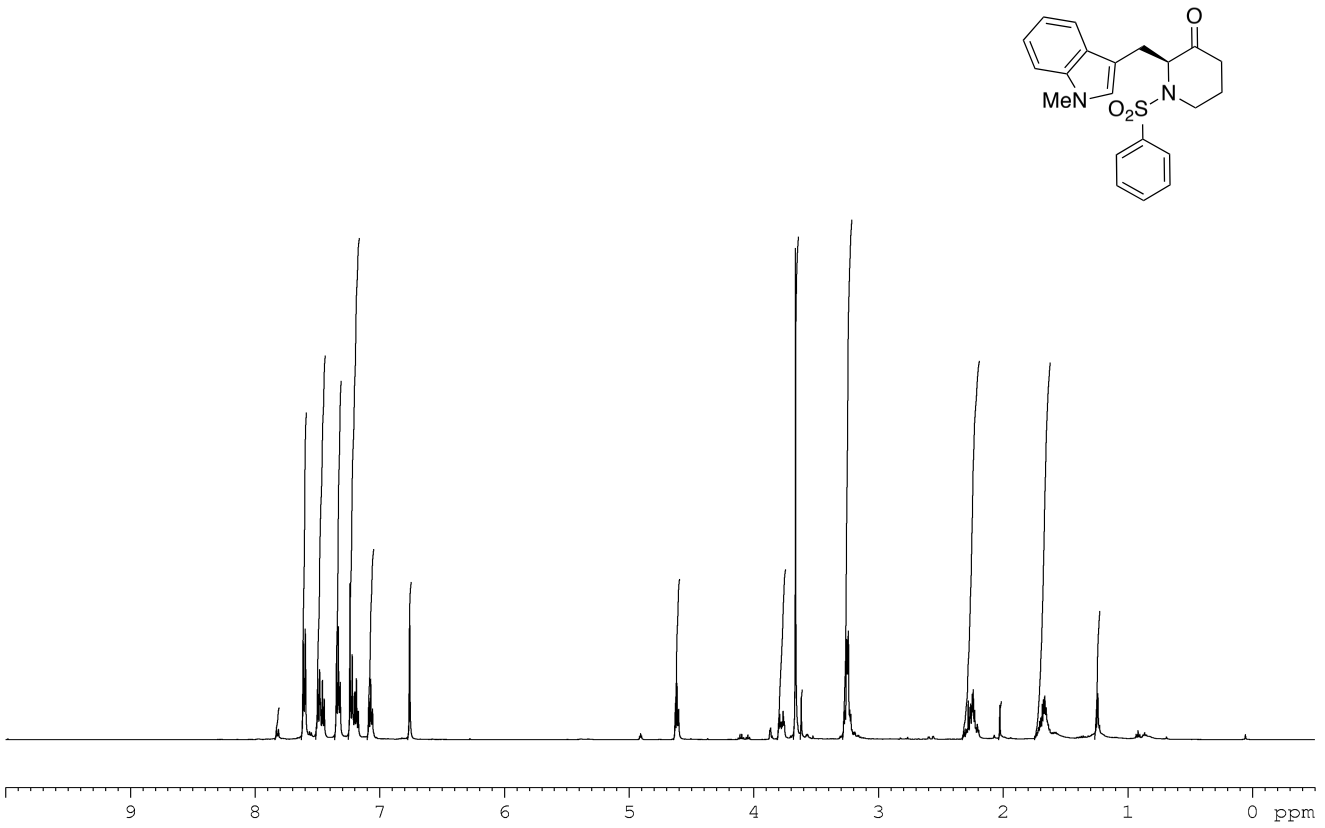

Figure 77: ^{1}H NMR ($CDCl_3$, 500 MHz) of **52**

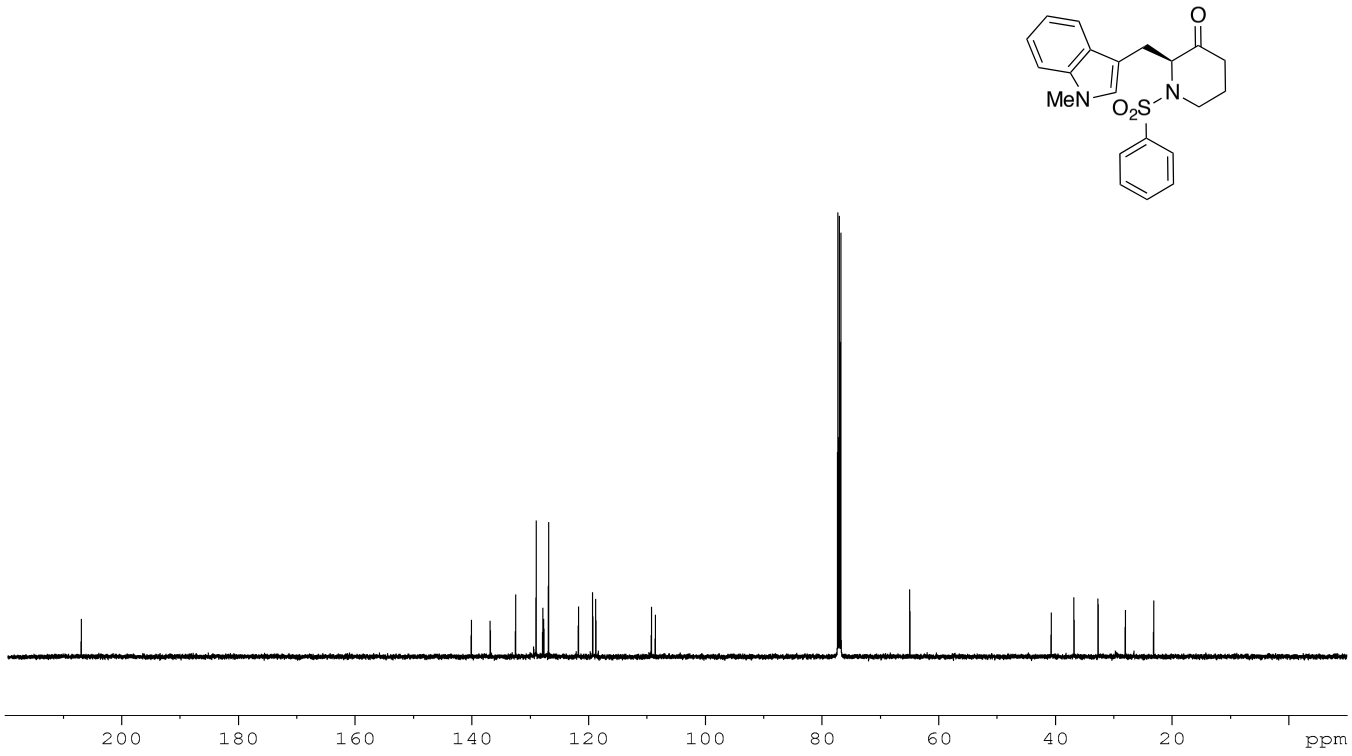

Figure 78: ^{13}C NMR ($CDCl_3$, 125 MHz) of **52**

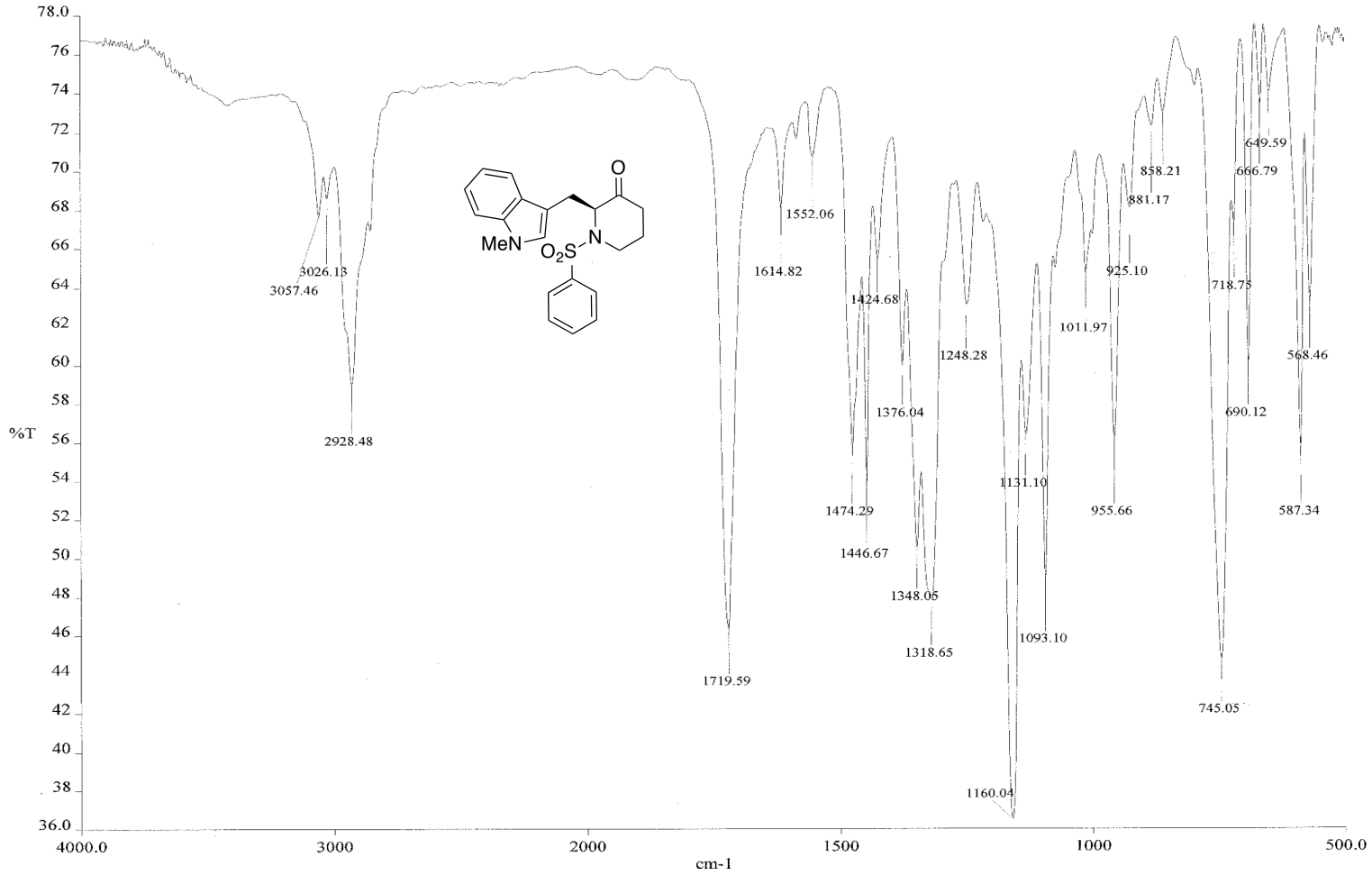

Figure 79: Infrared spectra (neat) of **52**

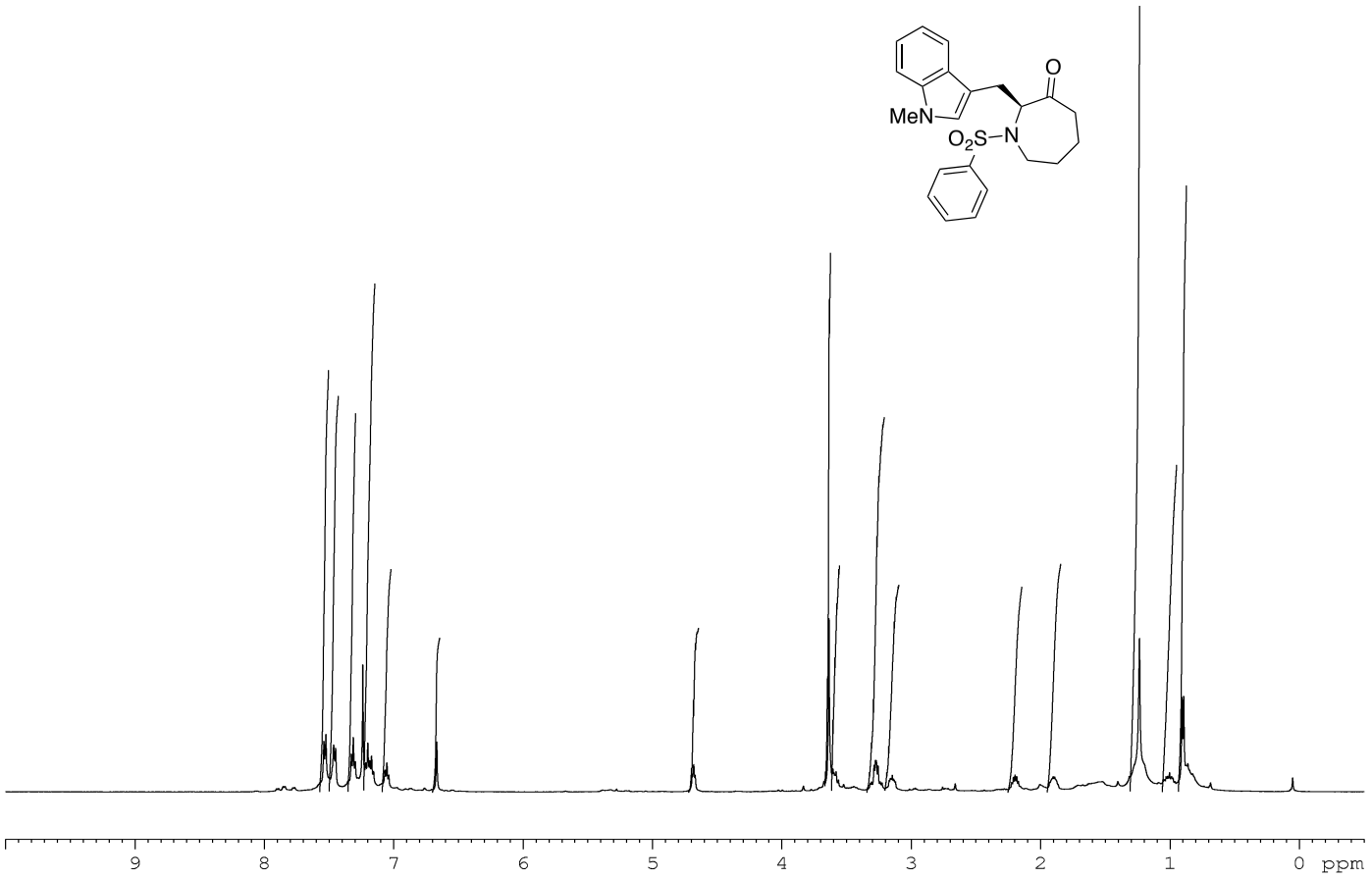

Figure 80: ^{1}H NMR ($CDCl_3$, 500 MHz) of **53**

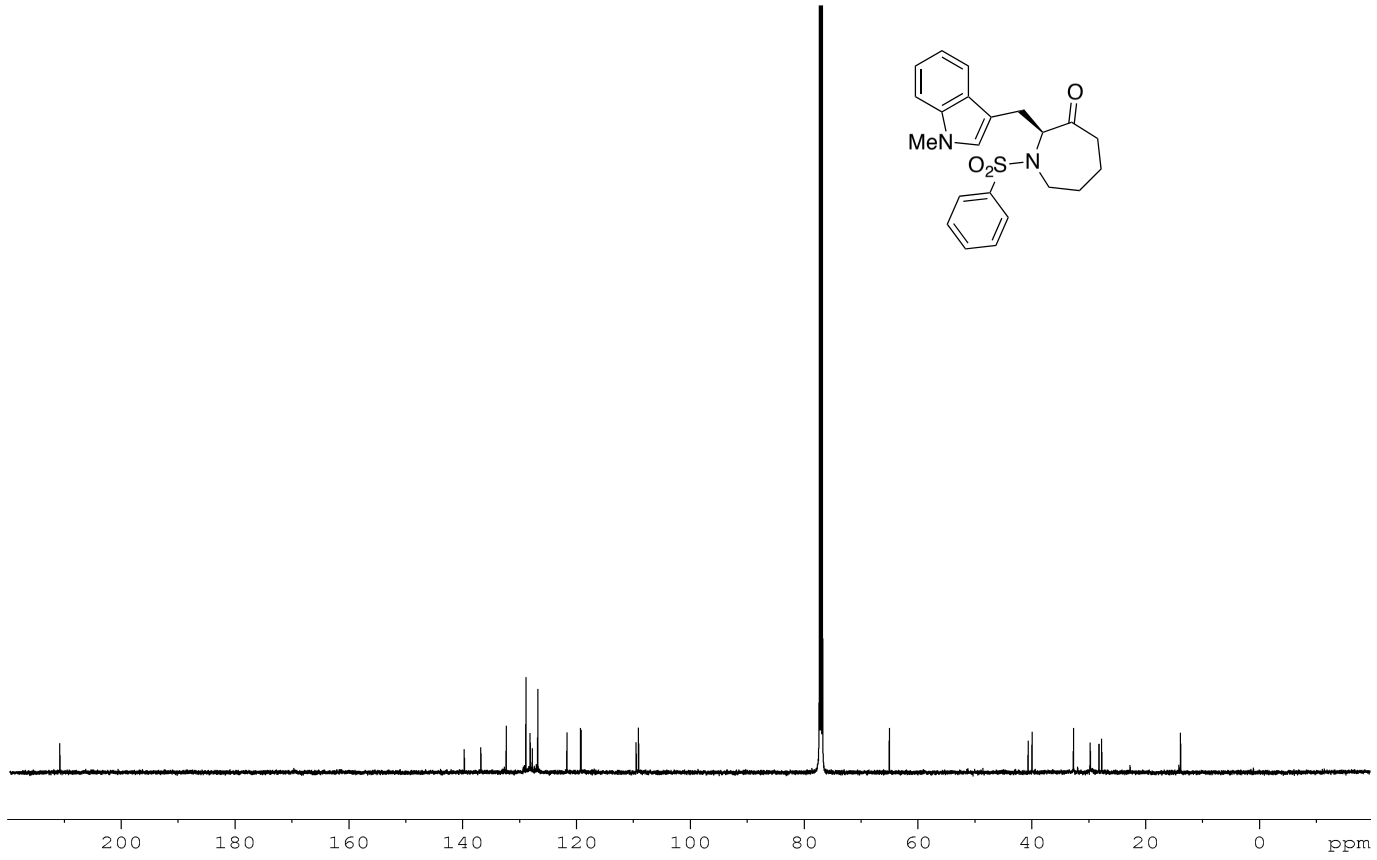

Figure 81: ^{13}C NMR ($CDCl_3$, 125 MHz) of **53**

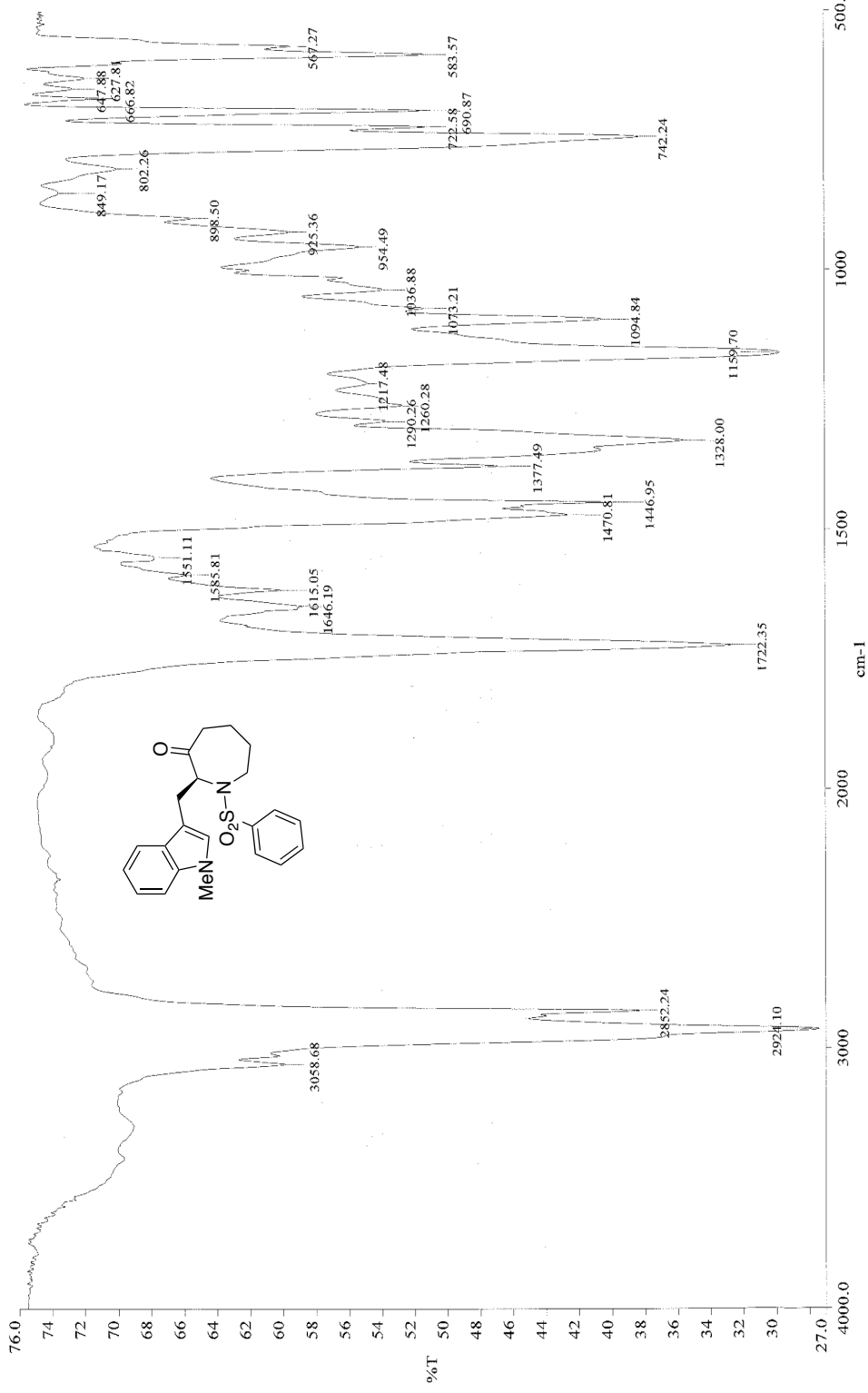

Figure 82: Infrared spectra (neat) of **53**

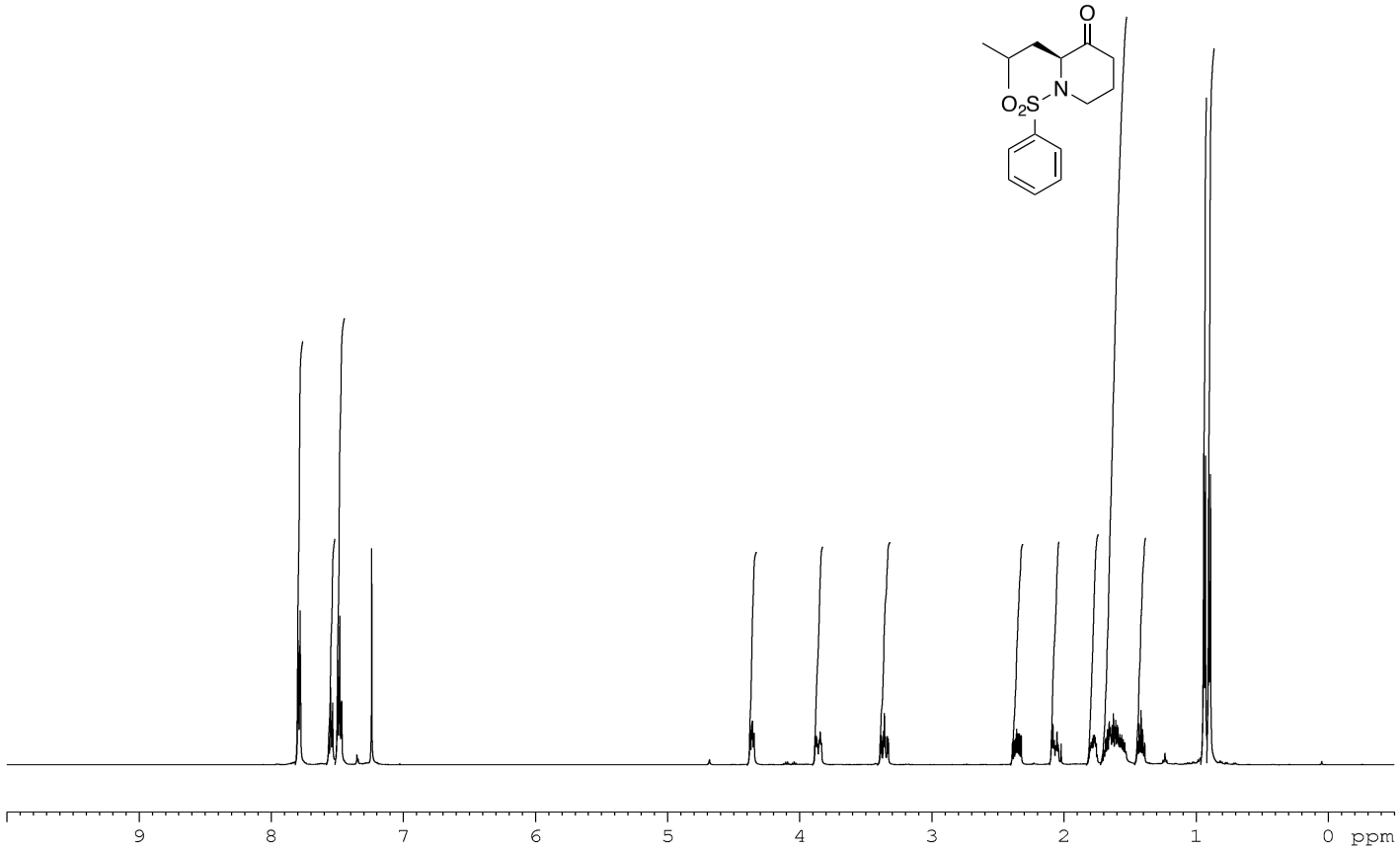

Figure 83: ^{1}H NMR ($CDCl_3$, 500 MHz) of **54**

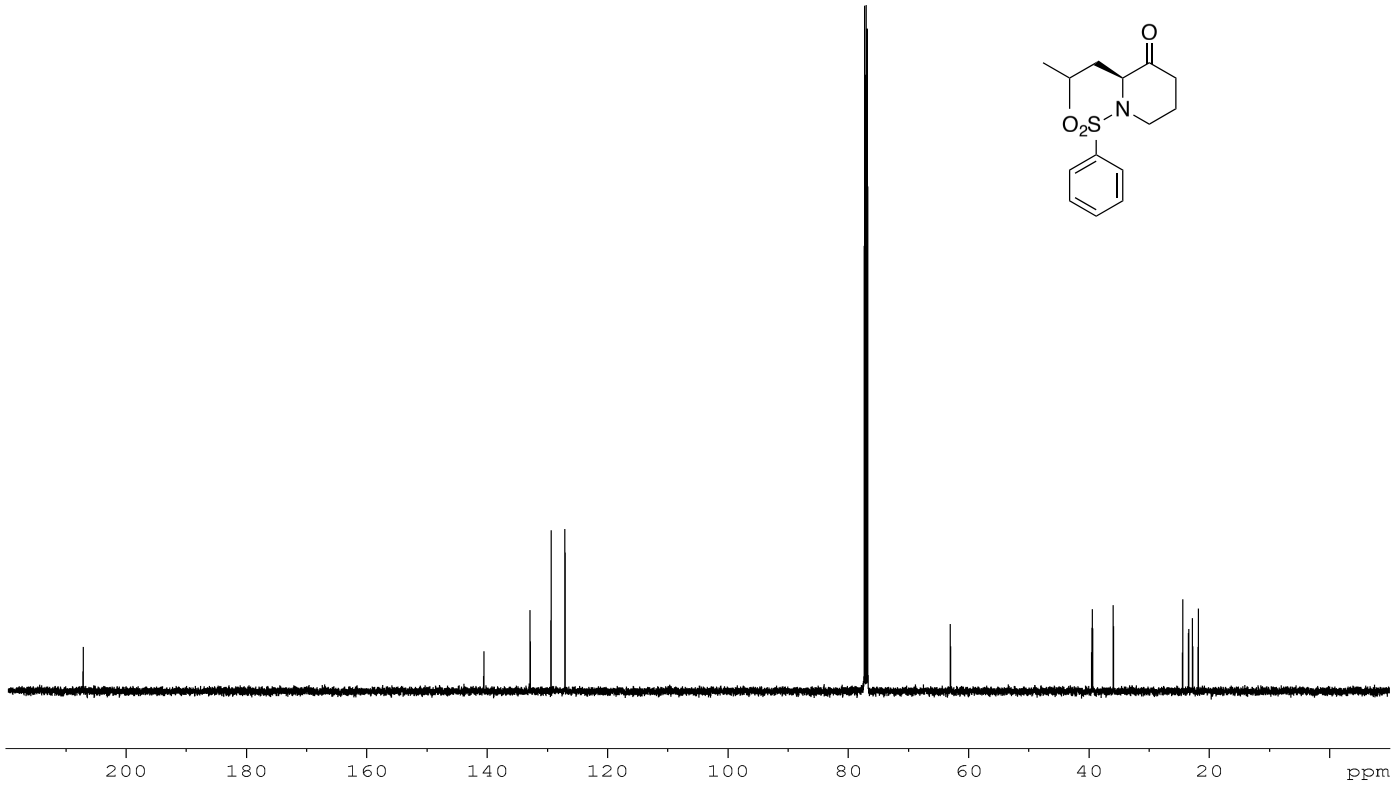

Figure 84: ^{13}C NMR ($CDCl_3$, 125 MHz) of **54**

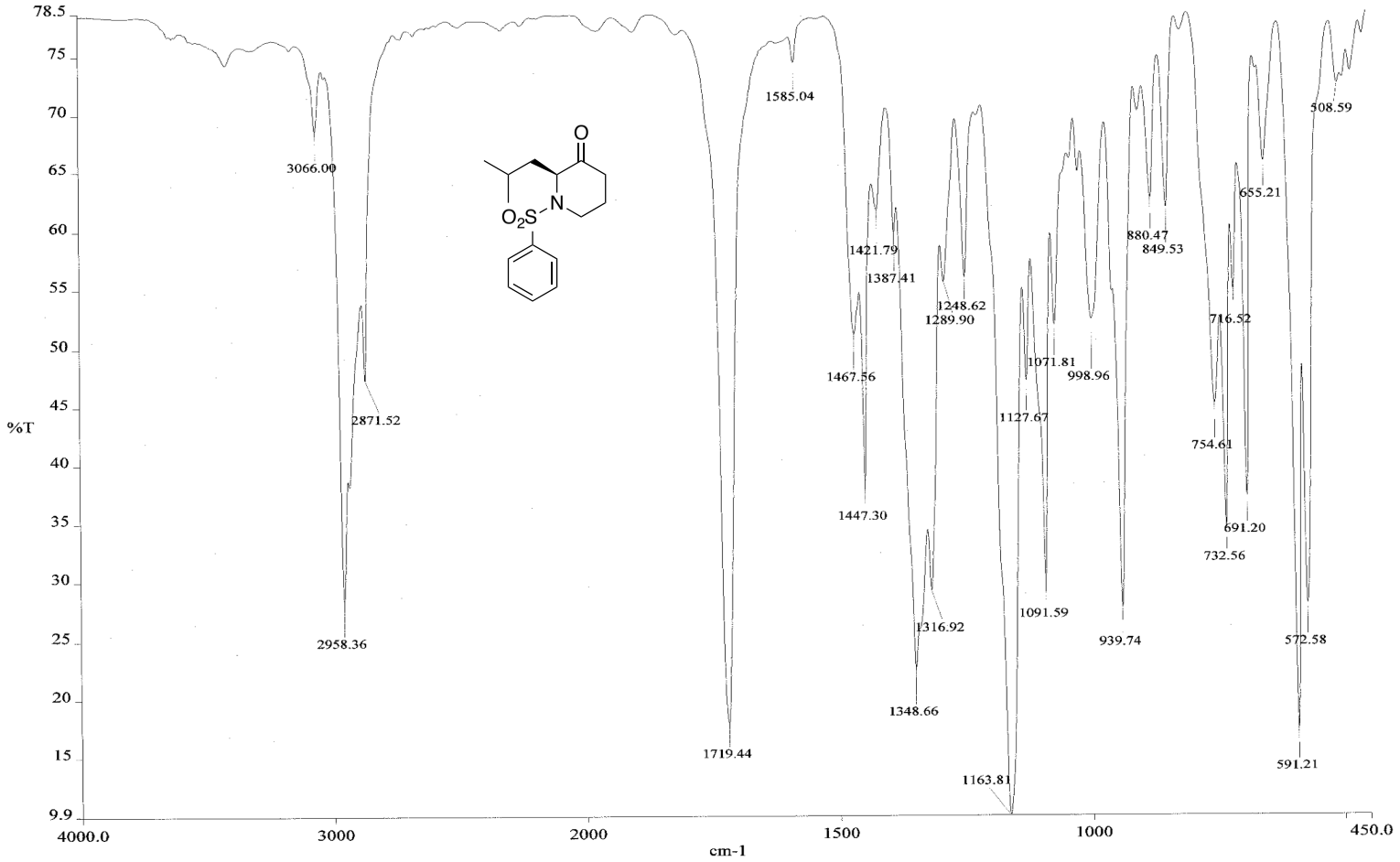

Figure 85: Infrared spectra (neat) of **54**

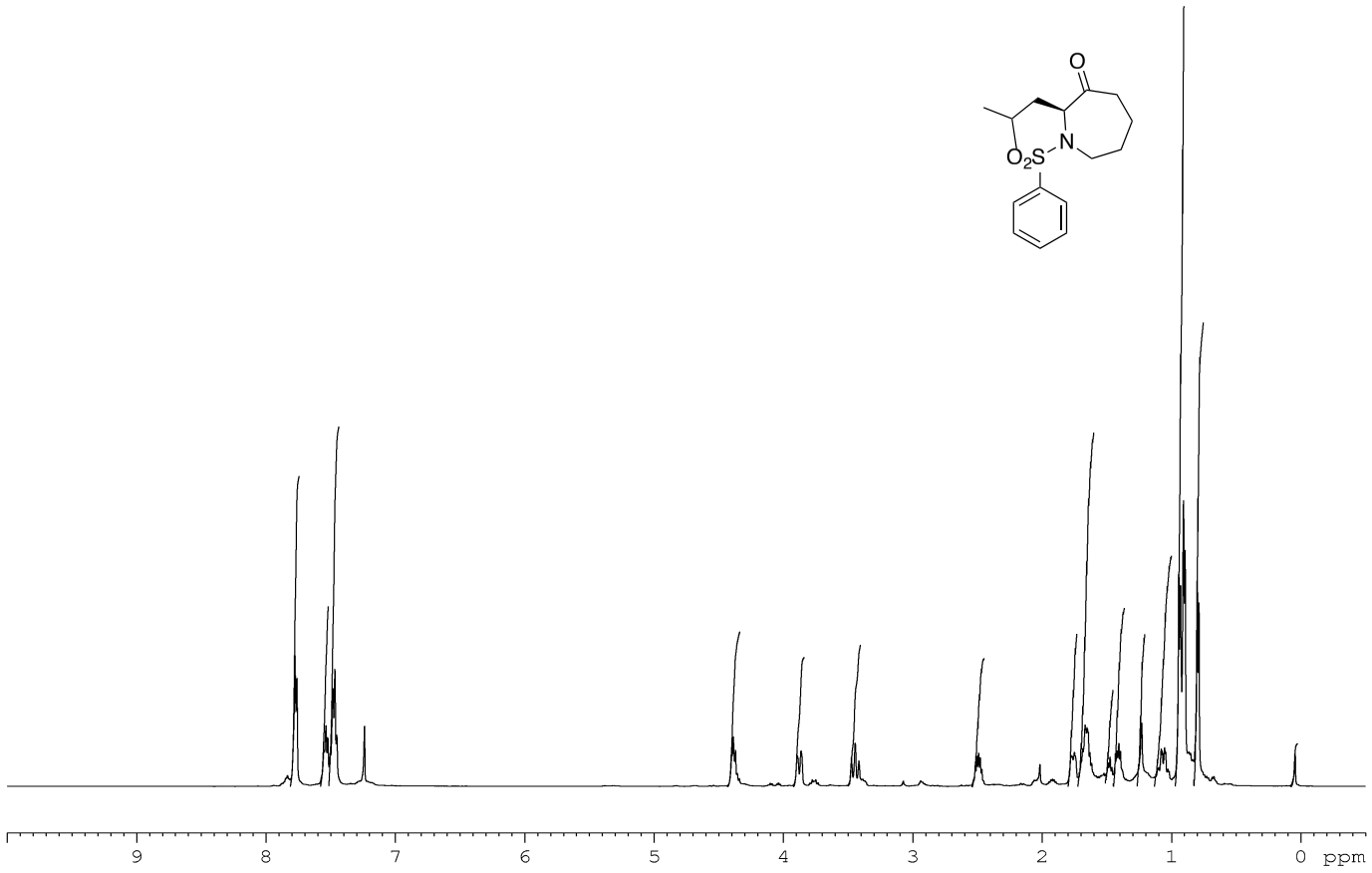

Figure 86: ^{1}H NMR ($CDCl_3$, 500 MHz) of **55**

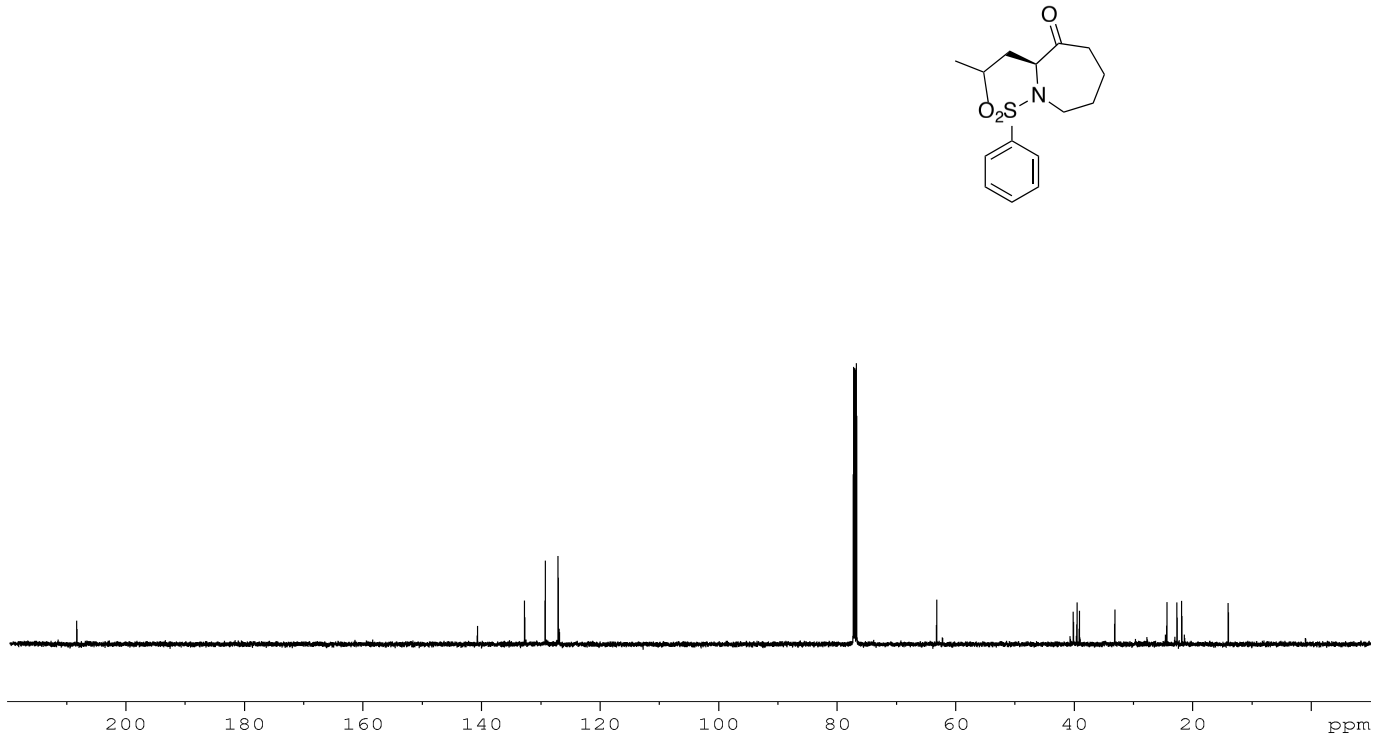

Figure 87: ^{13}C NMR ($CDCl_3$, 125 MHz) of **55**

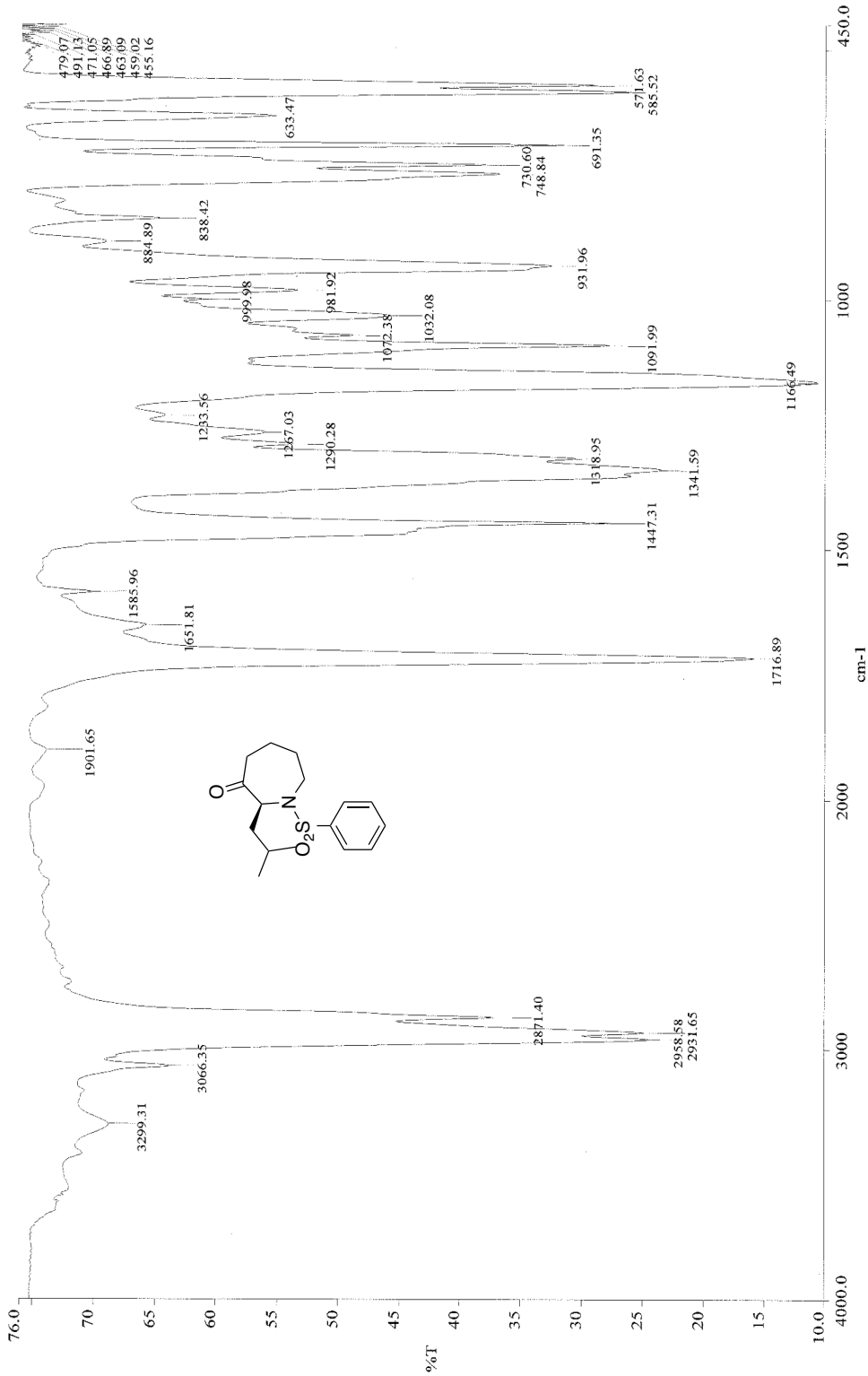

Figure 88: Infrared spectra (neat) of **55**

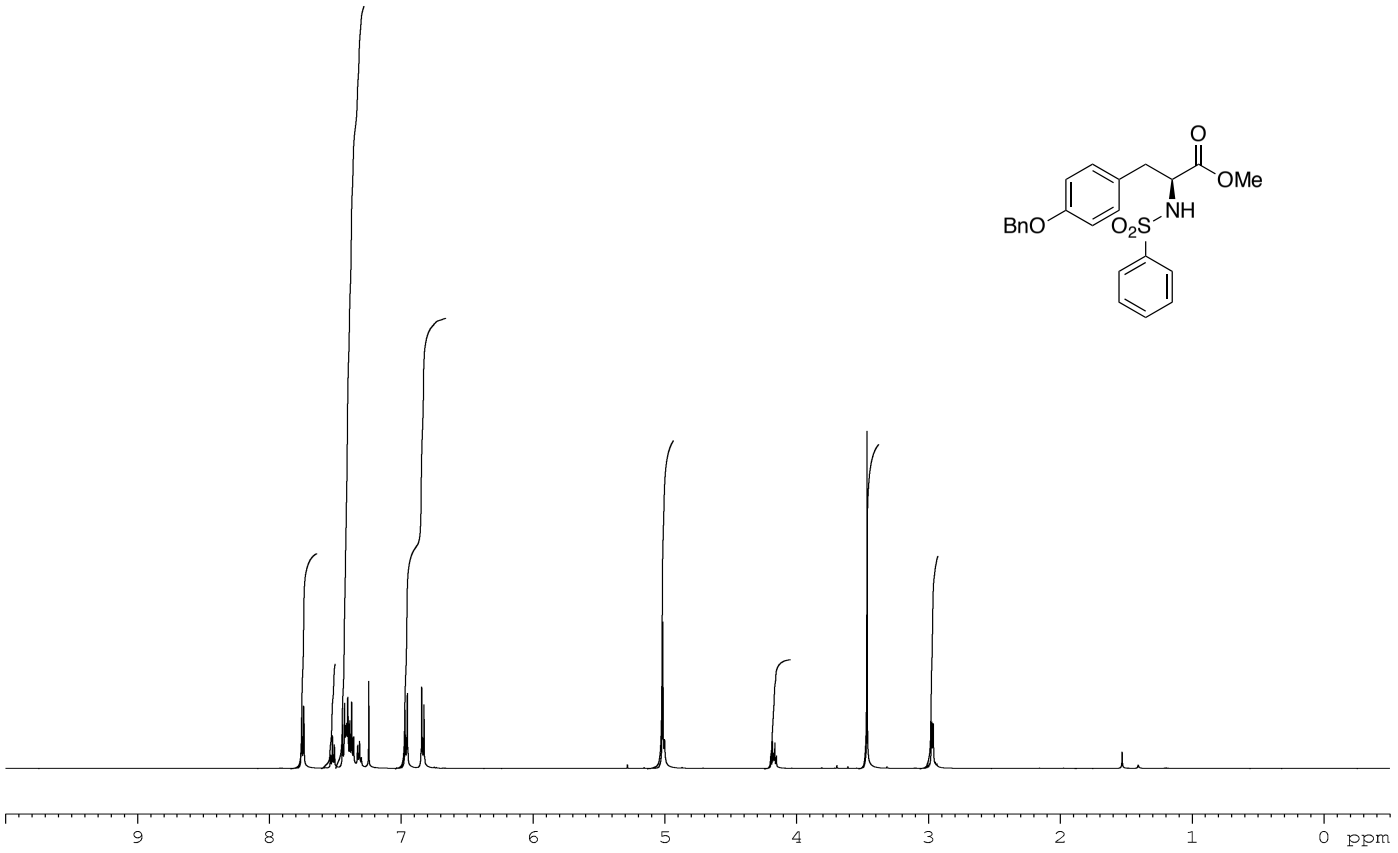

Figure 89: ^{1}H NMR ($CDCl_3$, 500 MHz) of **22**

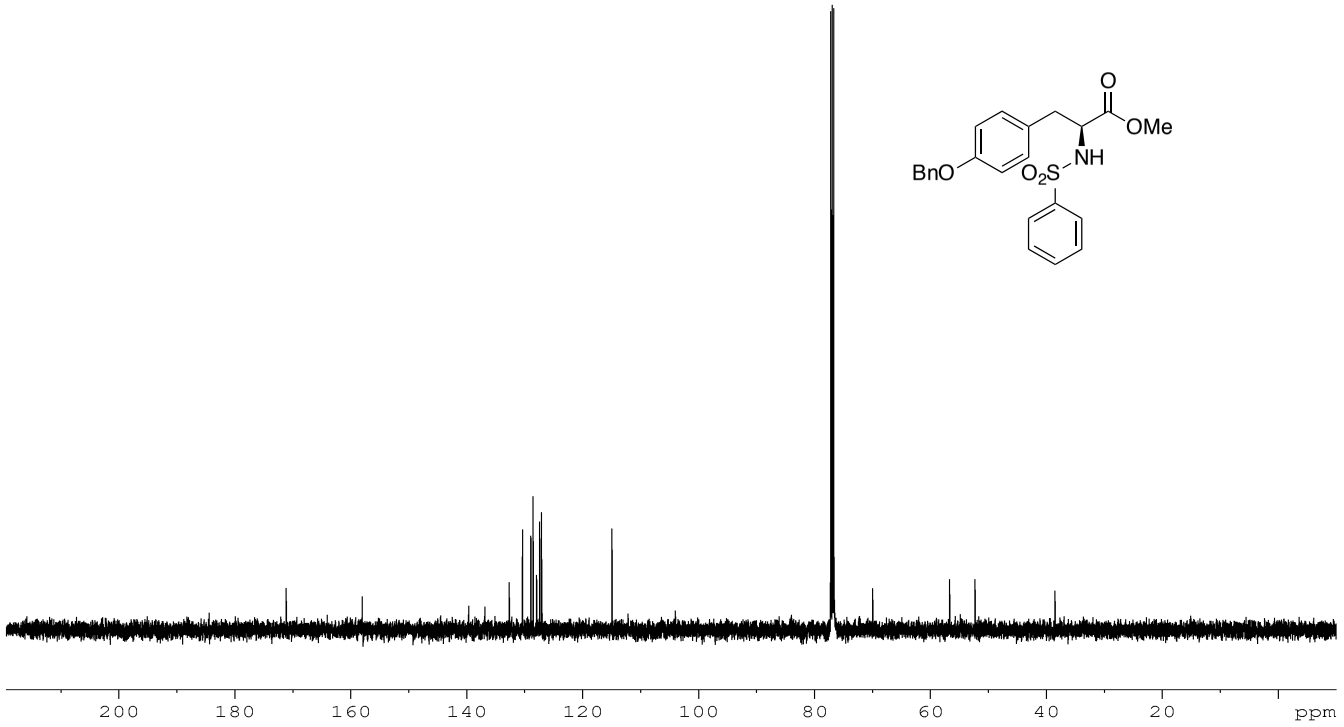

Figure 90: ^{13}C NMR ($CDCl_3$, 125 MHz) of **22**

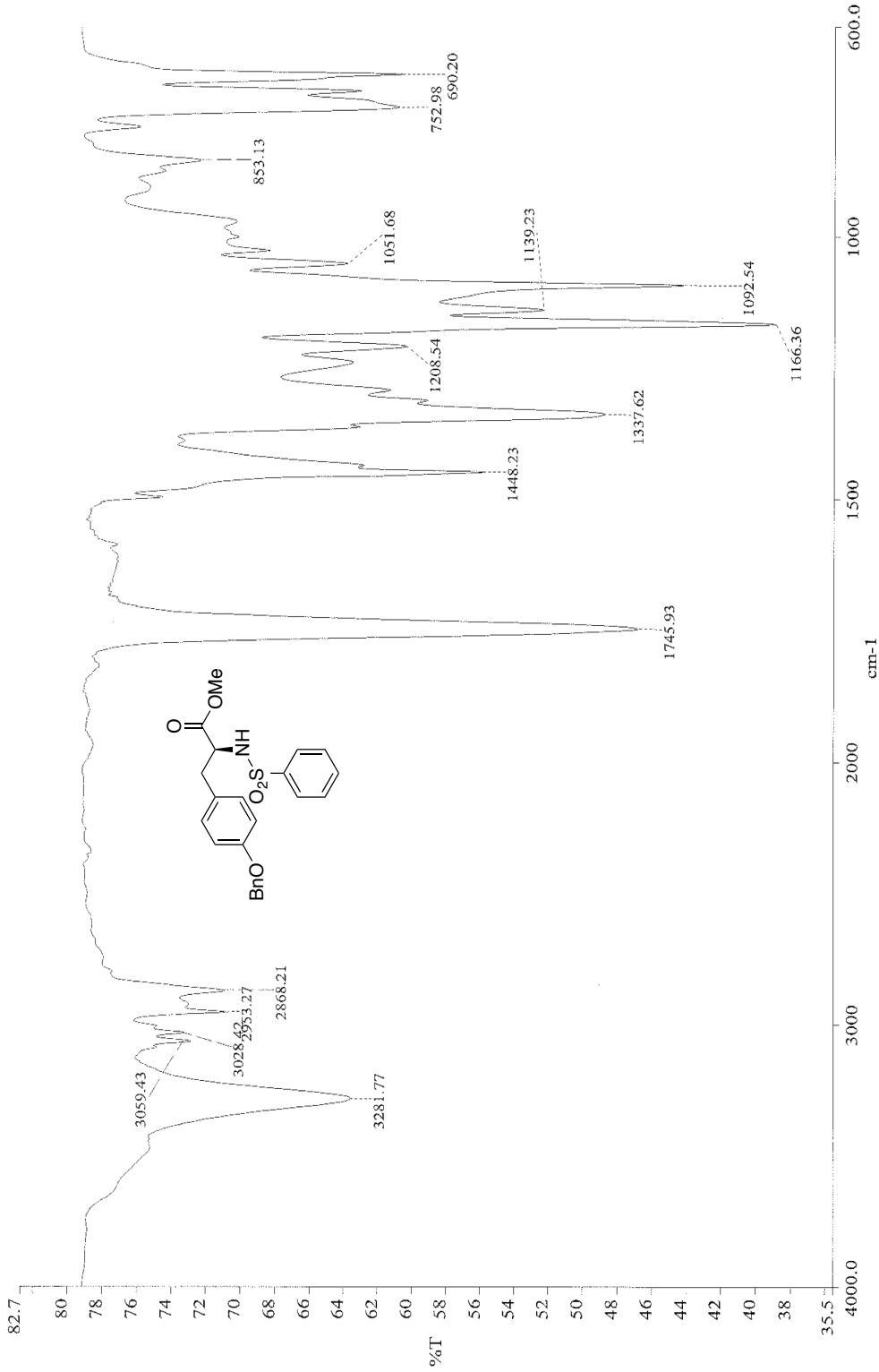

Figure 91: Infrared spectra (neat) of **22**

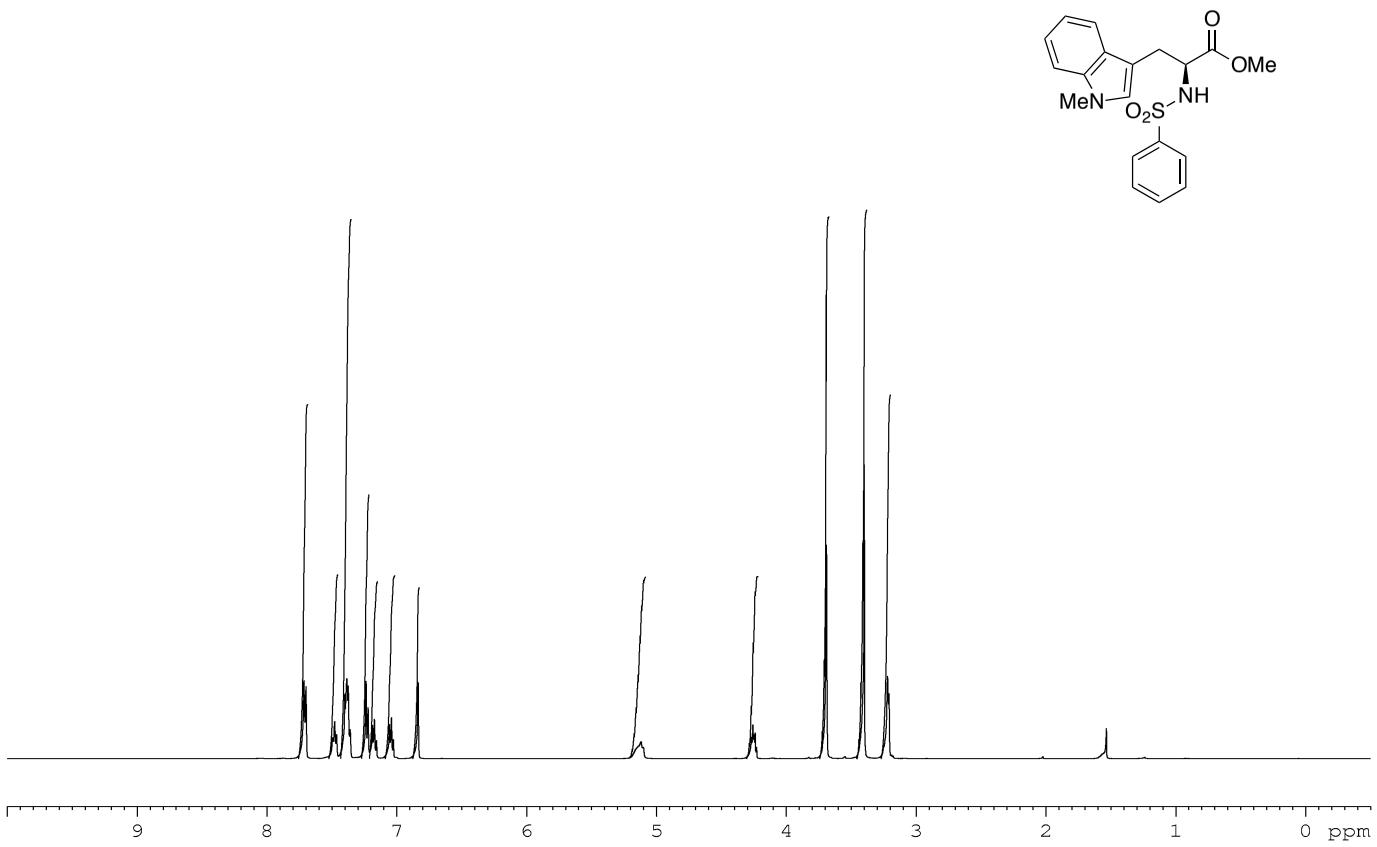

Figure 92: ^{1}H NMR ($CDCl_3$, 500 MHz) of **23**

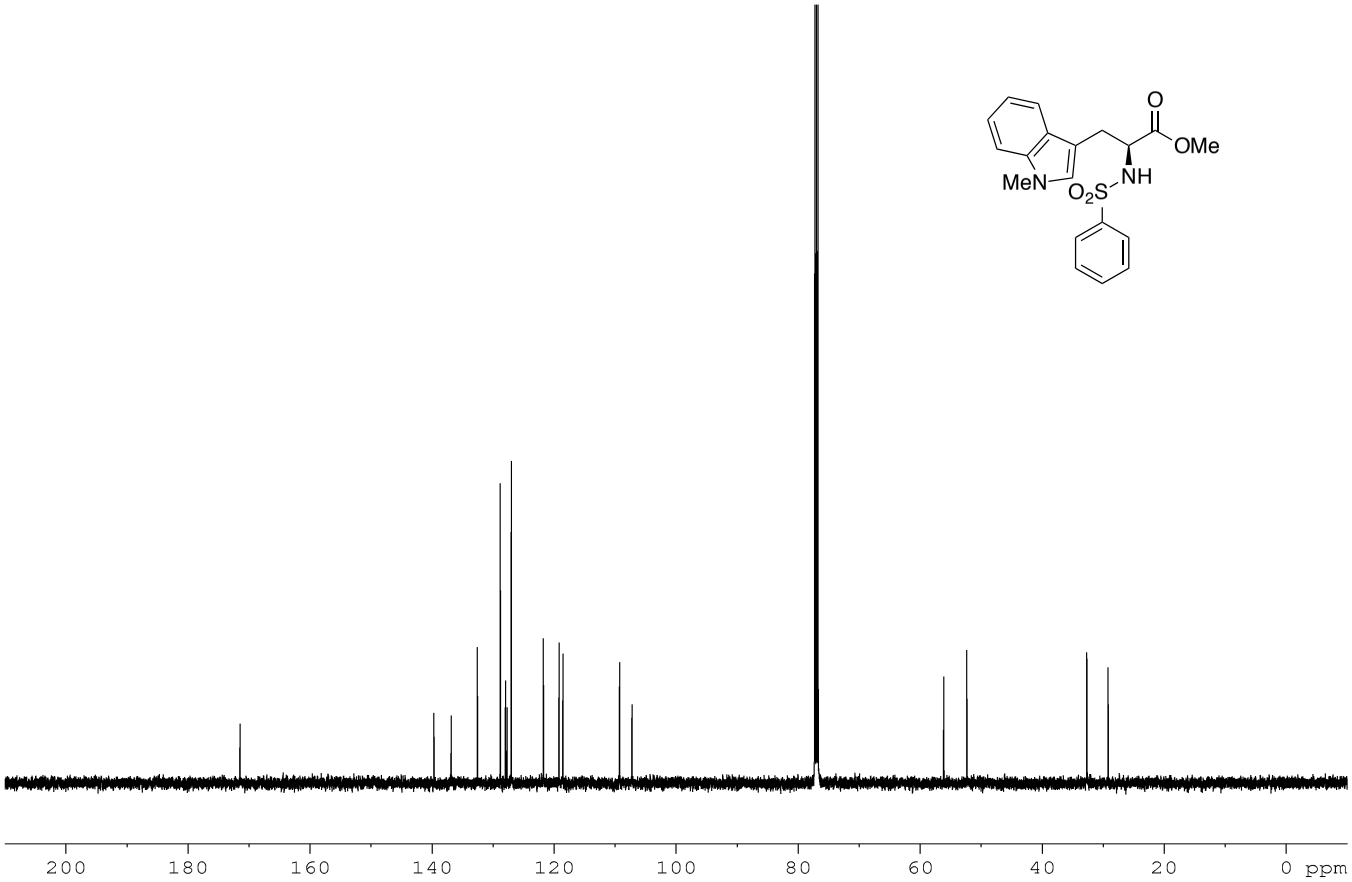

Figure 93: ^{13}C NMR ($CDCl_3$, 125 MHz) of **23**

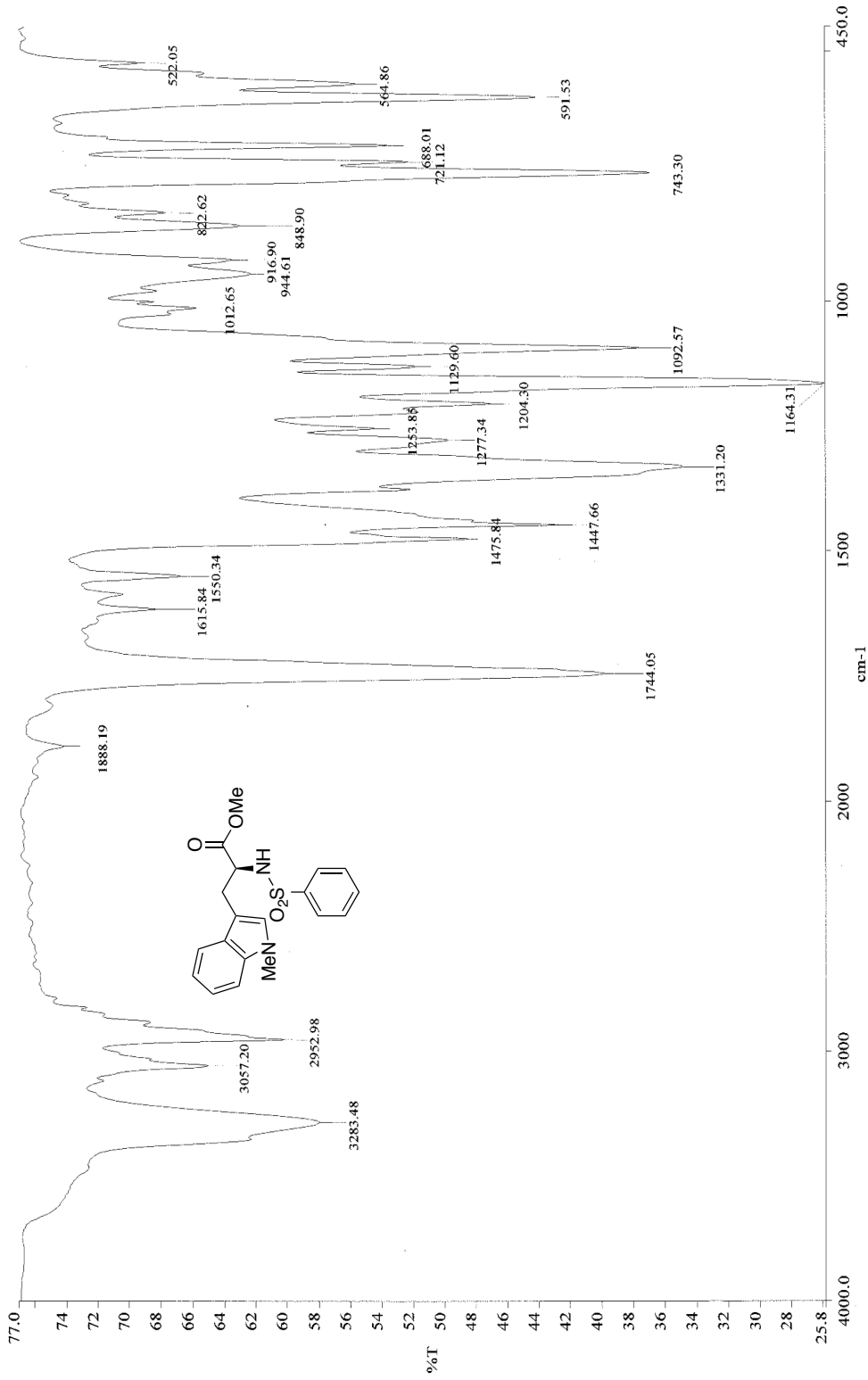

Figure 94: Infrared spectra (neat) of **23**

Chapter 4: Synthetic investigations toward the formal synthesis of (−)-epicoccin G and related epidithiodiketopiperazine alkaloids

4.1) Biological significance of epidithiodiketopiperazine alkaloids

Epipolythiodiketopiperazine (ETP) alkaloids constitute a rapidly growing family of natural diketopiperazine alkaloids, most of which are classified as fungal secondary metabolites (Figure 4.1).[1,2,3] Diketopiperazines (DKPs) are the central precursors to ETPs, and are believed to be biosynthesized from amino acids either by nonribosomal peptide synthases (NRPS) or by tRNA-dependent enzymes called cyclodipeptide synthases (CDPS).[3] ETPs are formed by oxidative modifications of corresponding DKPs. In addition to their unique structural features, ETP alkaloids possess a wide range of biological activities, including cytotoxic, antibacterial, antimicrobial, antitumor, apoptotic, antivirus, antiallergic, and antimalarial activities.[1] However, the underlying molecular mechanisms of these biological activities have yet to be fully elucidated.

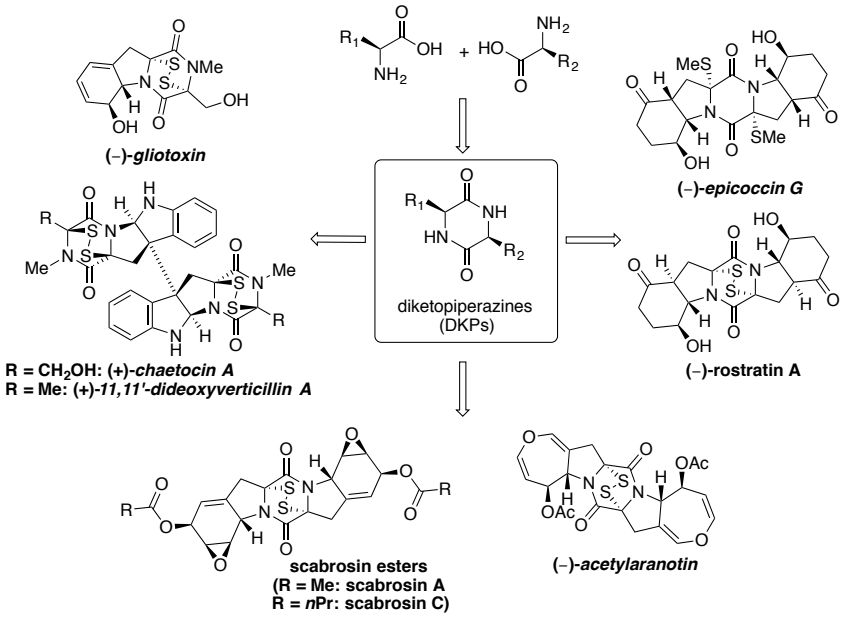

Figure 4.1. Diversity of bridged diketopiperazine alkaloids.

The oldest and perhaps most well-known ETP alkaloid is gliotoxin, which was isolated in 1943 (Figure 4.1).[4] The chemical structure of gliotoxin was incorrectly assigned until 1958, when Woodward and coworkers were able to establish the correct structure that included the unprecedented disulfide bridge in the DKP core *via* degradation studies.[5] The total synthesis of (±)-gliotoxin was subsequently accomplished by Fukuyama and Kishi in 1976[6] and the synthesis of the optically active form of gliotoxin immediately followed in 1981.[7] The variety of biological properties, such as antiviral, antibacterial, and immunosuppressive activities, displayed by gliotoxin are thought to be a direct consequence of the reactivity of the disulfide bridge, which is capable of generating reactive oxygen species as well as engaging in protein conjugation (Figure 4.2).[3,8]

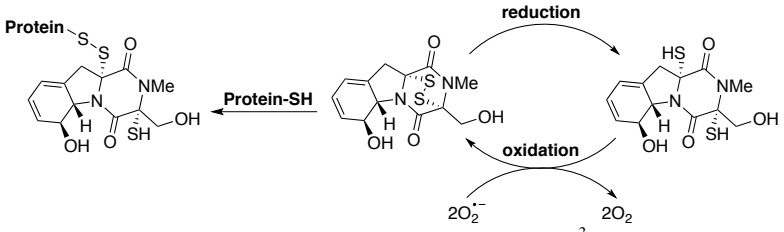

Figure 4.2. Bioactivity of gliotoxin.[3]

The most intriguing questions in the biosynthesis of gliotoxin were the mode of incorporation of the sulfur atoms and the way the disulfide bridge is formed. These two questions remained unanswered for over half a century due to limitations in existing methodologies.[3] For instance, the ease of disulfide bridge formation by air oxidation of DKP-derived *cis*-dithiols as shown by many synthetic studies, poses an important question of whether it is formed by spontaneous or an enzyme-catalyzed transformation. Molecular genetics approach became a popular method used to elucidate the biosynthesis of natural products in the last two decades.[3] This approach connects the secondary metabolites to their encoding genes. Rather than synthesizing isotopically labeled

precursors and intermediates, the genes and enzymes encoded by them are the main targets, which provides deeper insight into nature's chemical craftsmanship.[3] In 2005, the full genome sequencing of *Aspergillus fumigatus* was accomplished, enabling the identification of the 12 gene cluster that is responsible for the biosynthesis of gliotoxin.[9] The largest of these genes, *gliP*, was subsequently shown to code for a multimodular NRPS, which is responsible for the formation of the DKP that consists of L-phenylalanine and L-serine.[10] Following this discovery, in a series of seminal publications from 2010-2013, Hertweck and coworkers achieved the landmark elucidation of all the remaining key steps in the biosynthesis of gliotoxin, from the introduction of the sulfur atoms into the DKP to the formation of the disulfide bridge.[11] Most notably, in 2010, Hertweck[11a] and Doyle[12] groups independently showed that the formation of the disulfide bridge in gliotoxin is catalyzed by an FAD-dependent homodimeric enzyme GliT, which uses molecular oxygen as the stoichiometric oxidant to oxidize the dithiol to the disulfide (Figure 4.2). The X-ray structures of GliT as well as two related thiol oxidases were solved by Huber and Groll in collaboration with Hertweck recently, further proving the unequivocal mechanism behind the formation of the disulfide bridge.[13] Taken together, these findings provide crucial foundations to further understand the biosynthesis of not only gliotoxin, but other related natural ETP alkaloids as well. Furthermore, by understanding the biosynthesis of these interesting natural products, implications in development of future therapeutics could be made.

4.2) Previous syntheses of epidithiodiketopiperazine alkaloids

During the 1970s, Kishi published a series of landmark total syntheses of ETP alkaloids, which includes (±)-dehydrogliotoxin,[14] (±)-sporidesmin A,[15] (±)-gliotoxin,[6] and (±)-hyalodendrin.[7] The main synthetic strategy featured an inside-out approach, in which the ETP core was formed in the early stage of the synthesis followed by its elaboration to the corresponding target compounds. This strategy was carefully designed, since the methodologies that existed at the time to incorporate sulfur atoms in the DKP involved the use of harsh reaction conditions,[16] which may be detrimental if employed at later stages of the synthesis. Therefore, Kishi reasoned that sulfur should be incorporated earlier on, protected, and then revealed in the final stages of the synthesis.[7] Similar to his synthetic approach undertaken for the syntheses of (±)-dehydrogliotoxin[14] and (±)-sporidesmin A[15], Trown's methodology[16a] was utilized to obtain dithiol **2** from DKP **1** *en route* to the synthesis of (±)-gliotoxin. (Scheme 4.1).[6] More specifically, MOM protection of the DKP nitrogen followed by radical bromination using NBS and benzoyl peroxide (BPO), and subsequent elimination, and nucleophilic displacement with potassium thioacetate afforded a mixture of *cis* and *trans* isomers of dithioacetate. Hydrolysis of the thioesters afforded the dithiol **2**. Reaction with *p*-anisaldehyde in the presence of boron trifluoride etherate gave a 1:1 diastereomeric mixture of thioacetal **(±)-3**. *N*-alkylation with Michael acceptor **4** furnished the intermediate **(±)-5** as a mixture of diastereomers. After functional group manipulations to generate benzylic chloride **(±)-6**, lithiation followed by intramolecular alkylation provided intermediate **(±)-7**, completing the formation of carbon skeleton. Finally, benzyl ether deprotection and subsequent oxidation unraveled the disulfide bridge, completing the synthesis of (±)-gliotoxin.[6]

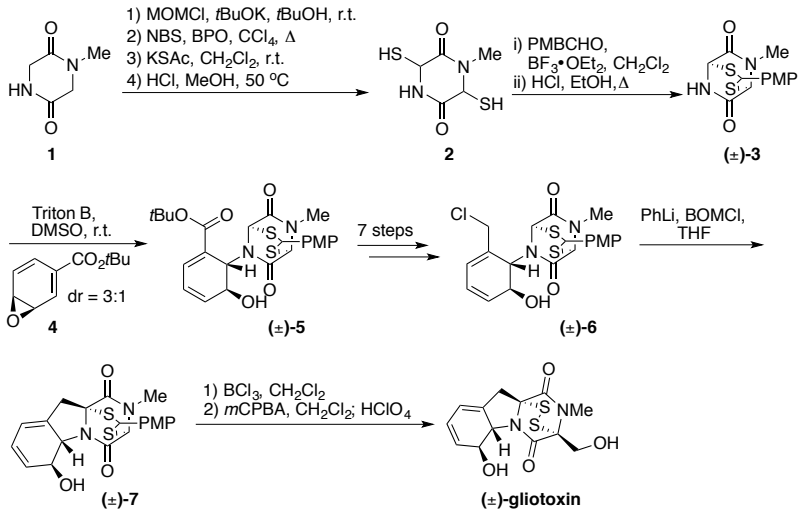

Scheme 4.1. Kishi's synthesis of (±)-gliotoxin.[6]

Another pivotal synthesis of ETP alkaloid was reported in 2009 by the Movassaghi group in their total synthesis of (+)-11,11'-dideoxyverticillin A (Figure 4.1).[17] Although the dimeric subset of ETP alkaloids in which their compound belongs to has been known for nearly 4 decades since the isolation of (+)-chaetocin A[18] and (+)-verticillin A[19], there was no known synthesis of such compounds, marking their accomplishment as the first example of chemical synthesis of a dimeric ETP alkaloid (Figure 4.1). (+)-11,11'-dideoxyverticillin A was first isolated in 1999 from a marine-derived fungus of the genus *Penicillum*.[17] In addition to its cytotoxicity, the alkaloid possess relatively potent tyrosine kinase-inhibitory activity of the epidermal growth factor receptor (IC_{50} = 0.14 nM).[17] Movassaghi's elegant synthesis was biosynthetically inspired, in that it was based on Kirby's findings of radio-labeled amino acid feeding experiments and his hypothesis for gliotoxin biosynthesis.[17] As mentioned above, elucidating biosynthesis of gliotoxin was a rapidly growing research area at the time, and feeding experiments were especially popular approach taken by researchers before molecular genetics approach was introduced. Therefore, unlike Kishi's strategy[6], Movassaghi planned his synthesis to

employ thiolation and subsequent disulfide bridge formation to be carried out after the complete assembly of the carbon framework (Scheme 4.2).

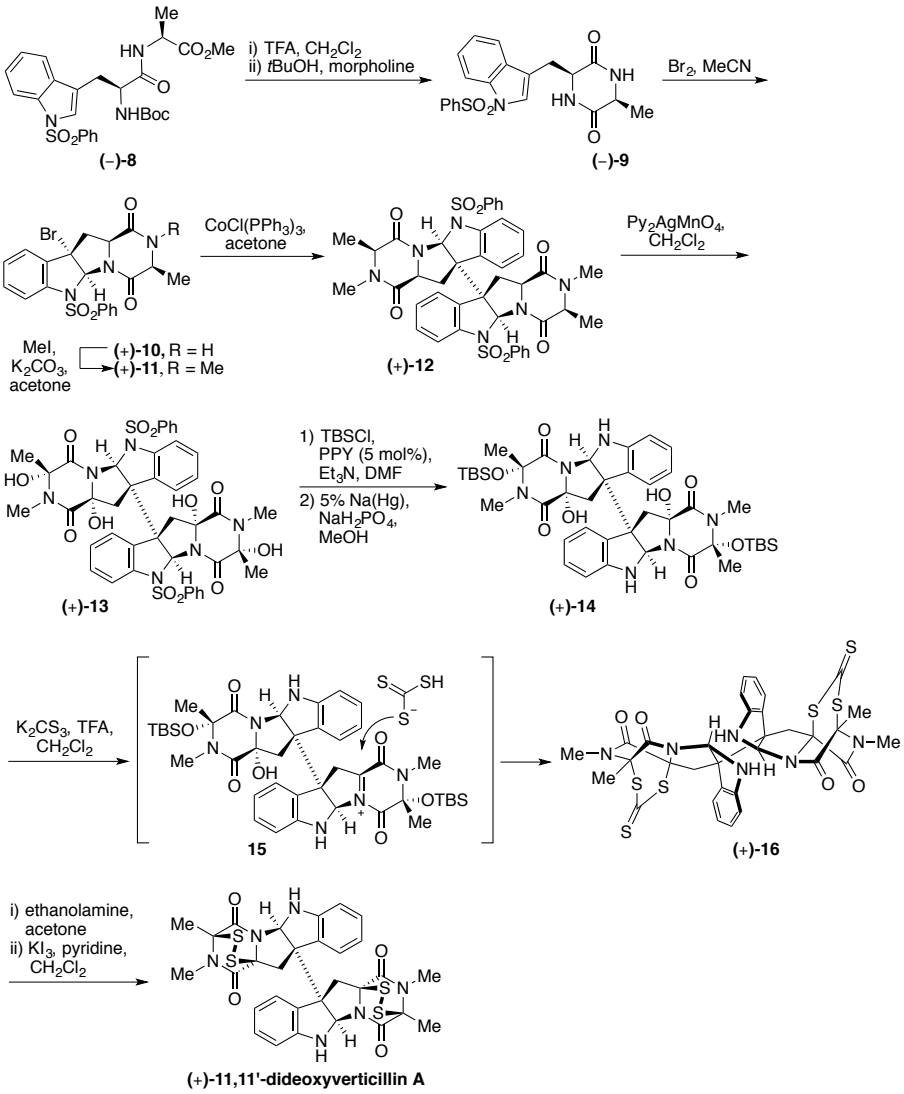

Scheme 4.2. Movassaghi's total synthesis of (+)-11,11'-dideoxyverticillin A.

The dimeric DKP **(+)-12** was synthesized in six steps from commercially available amino acid derivatives (Scheme 4.2).[17] Sequential treatment of the dipeptide **(−)-8** under acidic conditions followed by cyclization afforded the desired *cis*-DKP **(−)-9**. Subsequent exposure to molecular bromine furnished the monomeric tetracyclic bromide **(+)-10**. Treatment of tetracyclic bromide **(+)-10** under methylation conditions gave the base-

sensitive dimerization precursor **(+)-11**. Reductive dimerization of the tertiary benzylic bromide **(+)-11** using previously established methodology[20] afforded the key dimeric octacyclic intermediate **(+)-12**. Based on their biosynthetic hypothesis, the tetrahydroxylation step was a critical part of their synthesis in order to incorporate sulfur atoms in their DKP. After much screening, they found bis(pyridine)-silver(I) permanganate (Py_2AgMnO_4) to be the optimal reagent to obtain the desired oxidized dimeric octacycle **(+)-13** as a single diastereomer.[17] Not surprisingly, the tetraol intermediate **(+)-13** was highly sensitive to acidic and basic conditions. Therefore, careful control of reaction conditions was vital in order to keep the integrity of the oxidized dimeric octacyclic system. Silyl protection of the tetraol **(+)-13** was realized as the best option. Using Fu's (*R*)-(+)-4-pyrrolidinopyridinyl (pentamethylcyclopentadienyl)iron (PPY) catalyst[21], the selective silyl protection was achieved. At this juncture, Schmidt's protocol[16d] of installing the disulfide bridge was attempted and accomplished in low yield. Most of the intermediates that were involved in the last few steps were not only highly labile and prone to decomposition, but also the use of pressurized toxic hydrogen sulfide led them to seek an alternative strategy. Interestingly, the Movassaghi group opted to use potassium trithiocarbonate as the reagent to deliver a sulfurated product poised for mild unveiling of the desired tetrathiol at an advanced stage.[17] The desired dimeric bisdithiepanethione **(+)-16** was obtained, likely *via* kinetic trapping of iminium ion **15** followed by intramolecular dithiepanethione formation. Addition of ethanolamine rapidly afforded the corresponding diaminotetrathiol, which was then treated with aqueous hydrochloric acid in dichloromethane followed by immediate addition of potassium triiodide to furnish the final compound (+)-11,11'-dideoxyverticillin A (Scheme 4.2). X-

ray analysis confirmed the stereochemistry of their title compound.[17] Since this landmark paper, the Movassaghi group reported more syntheses of structurally similar ETP alkaloids and has obtained interesting biological information of such compounds.[22] More specifically, they found that chemical ablation of the sulfur bridge in naturally occurring alkaloids or the synthesis of such analogues without the sulfur atoms at the α-α'-positions of the DKP result in biologically inactive compounds, further augmenting previous biological studies that suggested the importance of sulfur moiety in ETP alkaloids.[22b]

In 2011, Nicolaou and coworkers reported the total synthesis of (−)-epicoccin G (Figure 4.1).[23] (−)-Epicoccin G was isolated from the endophytic fungus *Epicoccum nigrum* in 2009, and it was shown to exhibit anti-HIV activity in C8166 cells (IC_{50} = 13.5 mM).[23] This ETP alkaloid possesses an interesting 6-5-6-5-6 diketopiperazine framework, which is also found in other similar natural products, such as rostratin B and exserohilone. Unlike the aforementioned ETP alkaloids, (−)-epicoccin G exhibits C_2 symmetry, allowing for a general two-directional synthetic strategy. Interestingly, the incorporation of sulfur atoms was done in the intermediate stages of their synthesis, rather than in the beginning[6] or the end[17] of the synthesis as discussed in previous syntheses. The timing of the introduction of sulfur moieties in the molecule was deemed crucial, since early introduction of sulfur may not allow functional group tolerance for subsequent steps, while late installation should be avoided due to higher reactivity of the ketone groups (relative to the DKP moiety) under basic conditions needed for the sulfenylation step.[23] The synthesis of key intermediate **26** began with a known enone **18** through a two-step

procedure from *N*-Boc-L-tyrosine **17** (Scheme 4.3.[24,23] Deoxygenation of the enone **18** was accomplished through a three-step sequence involving acetylation, zinc reduction, and base-induced isomerization of the resulting β,γ-unsaturated ketone to afford the desired bicyclic enone **19**. Subsequent Luche reduction of this enone gave the hydroxyl *N*-Boc methyl ester **20**, which was treated under either acidic or basic conditions to afford the corresponding hydroxy amine **21** and hydroxy acid **22**, respectively. Dimerization *via* BOPCl-mediated coupling of **21** and **22** resulted in the *N*-Boc methyl ester amide **23**. Deprotection of the amine followed by Et_3N-induced intramolecular ring closure gave the corresponding DKP **24**. Conversion of the bisallylic alcohol **24** to the bistrifluoroacetate **25** followed by Pd(0) mediated allylic elimination furnished the desired key intermediate **26**.[23]

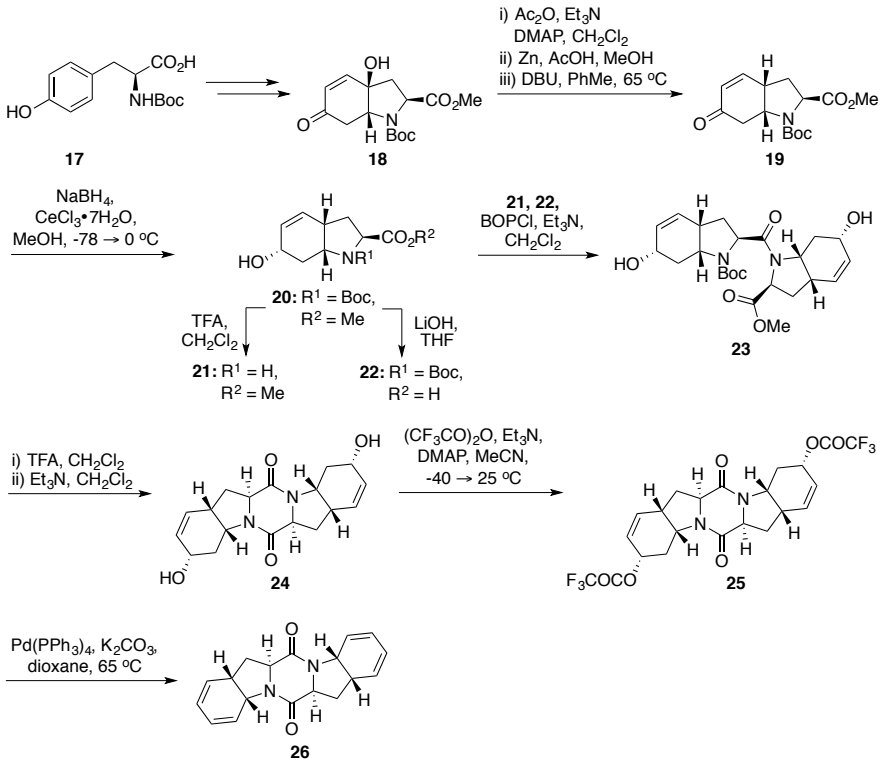

Scheme 4.3. Nicolaou's synthesis of bisdiene key intermediate.

With the bisdiene key intermediate **26** in hand, various known sulfenylation protocols were screened. However, classical sulfenylation methods[16] failed to provide the desired sulfenylated product. Instead they developed and successfully utilized a modified version of Schmidt's sulfenylation method.[16c] The modified protocol entailed pretreatment of S_8 with 3 equiv. of NaHMDS at ambient temperature followed by sequential addition of **26** and an additional 2 equiv. of NaHMDS to obtain a mixture of oligosulfenylated compounds **27**, which was then subjected to reduction with $NaBH_4$ followed by quenching of the resulting dianion with MeI to obtain the desired bismethylthio derivative **28** (Scheme 4.4). The stereochemical configuration of **28** was confirmed by NOESY correlations.[23] Subsequent reaction of **28** with singlet oxygen (generated from triplet oxygen and light in the presence of *meso*-tetraphenylporphyrin (TPP) as a sensitizer) afforded bisendoperoxide **29**, which underwent regioselective Kornblum—DeLaMare rearrangement upon in situ treatment with DBU to furnish bishydroxy enone **30**. Finally, catalytic hydrogenation of **30** furnished (−)-epicoccin G.

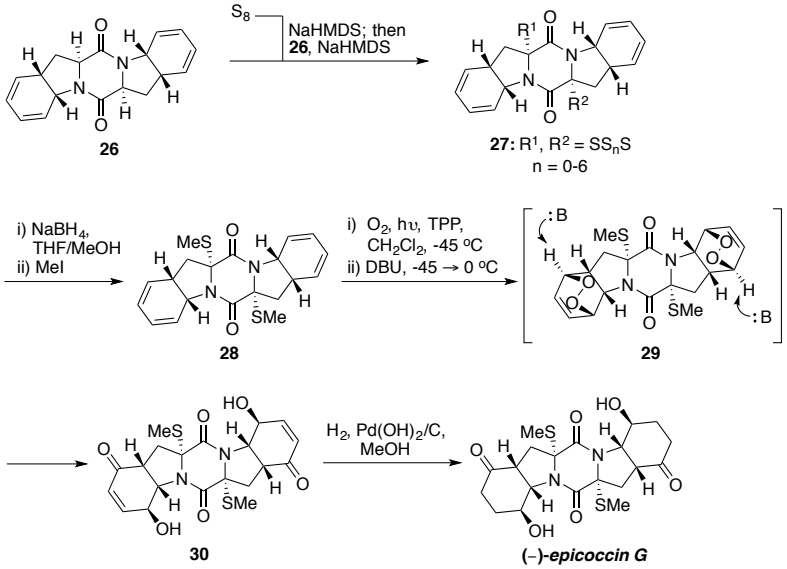

Scheme 4.4. Completion of the total synthesis of (−)-epicoccin G.

In the same report, they also synthesized 8,8'-*epi*-*ent*-rostratin B from the common bisdiene intermediate **26** using slight variation of the synthetic protocol.[23] Following this seminal report, further publications ensued, further demonstrating the effectiveness of their modified Schmidt sulfenylation protocol in synthesizing structurally similar ETP alkaloids.[25]

Although syntheses of ETP alkaloids were known since the 1970s[6], their popularity have been exponentially growing since Movassaghi's landmark paper in 2009.[17] For example, Overman reported the syntheses of various indole based ETP alkaloids similar in structure to that of Movassaghi's dideoxyverticillin A in 2011 and in 2013, where he employed functionalized trioxopiperazine as the key intermediate.[26] Another example to note is, (−)-acetylaranotin, a C_2 symmetric ETP alkaloid (Figure 4.1), which was synthesized by Reisman followed shortly thereafter by Tokuyama in 2012.[27] Both groups utilized approaches similar to Nicolaou's,[23] where they synthesized functionalized bicyclic monomer followed by dimerization to the corresponding DKP using amide coupling methods.[27] On other hand, they also used approaches similar to Movassaghi's[17,22] in that they left the sulfenylation to the end of their syntheses, where they used yet another variation of Nicolaou's version of the Schmidt protocol.[27]

4.3) Various synthetic approaches to dethiolated ETP alkaloid framework

Many efforts have been made by various groups to provide alternative ways to easily access symmetric and unsymmetric ETP alkaloids. Although their focus was not necessarily to provide novel sulfenylation methods, they have nonetheless afforded synthetic variety towards this class of compounds.

Bräse made a significant contribution towards the synthesis of C_2 symmetric as well as unsymmetric ETP alkaloids since 2007.[28] Of note, he has generated a unique methodology to synthesize symmetric and unsymmetric DKPs *via* phosphite-promoted dimerization of corresponding unprotected amino acids.[28a] In 2008, he reported the preparation of functionalized hexahydroindoles *via* intramolecular Diels-Alder reaction,[28b] which he made further improvements in 2011.[28e] As displayed elegantly in previous syntheses of ETP alkaloids,[23,27] development of new methodologies to functionalized hexahydroindoles are important, since they could serve as building blocks for 6-5-6-5-6 framework present in C_2 symmetric ETP alkaloids. In 2010, Bräse reported a unified strategy targeting various ETP alkaloids, such as exserohilone, gliotoxin, the epicoccins, the epicorazines, rostratin A, and aranotin, by the use of one common precursor **31** that was generated from L-pyroglutamic acid in five steps (Scheme 4.5).[28d] Briefly, isomerization of the terminal alkene of **31** followed by a 1,2-addition of vinyl Grignard afforded the corresponding lactol, which was treated under ring closing metathesis (RCM) conditions to provide the *cis*-annelated cyclohexenone which is the monomer of epicorazin B. Protection of the alcohol in the epicorazin B monomer followed by diastereoselective reduction of the ketone moiety, and further protecting group manipulation gave epicoccin F monomer, which ultimately underwent Pd^0-catalyzed Tsuji-Trost elimination conditions to furnish the gliotoxin and apoaranotin monomer. Alternatively, hydrogenolysis of epicorazin B monomer afforded epicoccin A-D, and G monomer. The aranotin monomer was constructed by enol ether-olefin RCM of an intermediate derived from the ring opened of the lactol **32**, while as the exserohilone

and epicorazin A monomer was obtained from epimerization at C4 and C5 of the proline derivative derived from the same intermediate **32**, followed by RCM. Finally, the exserohilone and epicorazin A monomer was converted to rostratin A monomer *via* series of protecting group manipulations, diastereoselective reduction of the ketone moiety, and hydrogenolysis.

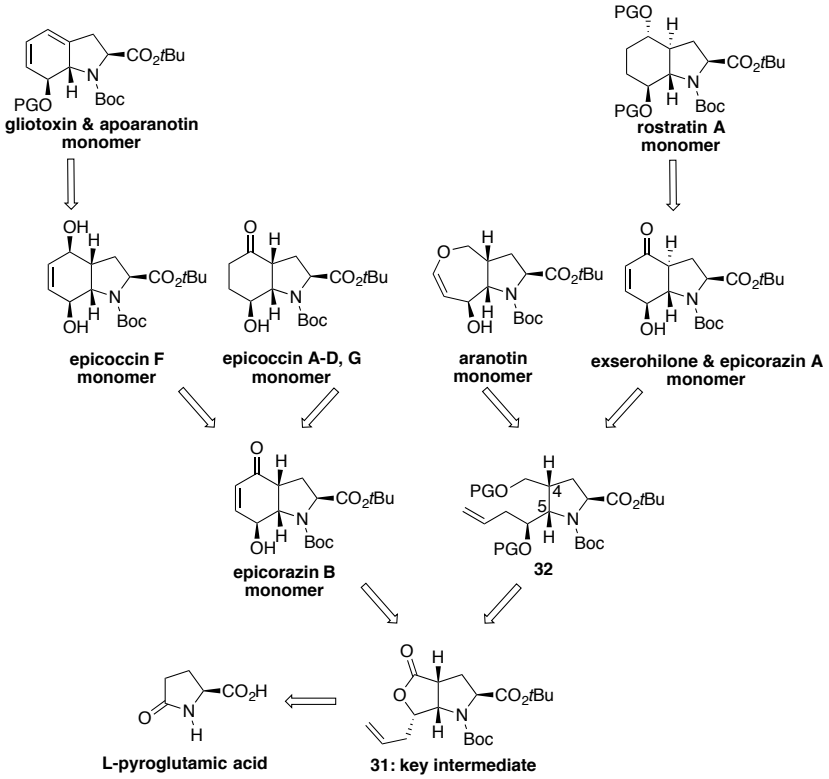

Scheme 4.5. Bräse's retrosynthetic analysis of various ETP alkaloids from one key intermediate. PG = protecting group.

As a proof of principle, using their previous dimerization methodology,[28a] they synthesized the dethio analogue of the epicoccins A, C, and D **33** (Scheme 4.6).

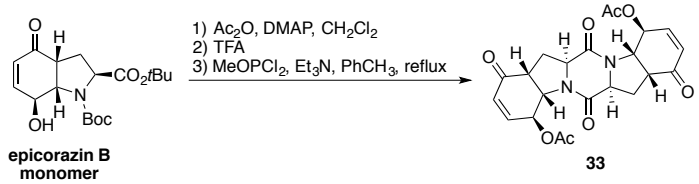

Scheme 4.6. Assembly of the core **33** found in epicoccins A, C, and D.

Diver's group were also interested in employing their previous methodology towards the synthesis of the scabrosins (Figure 4.1), which is another class of ETP alkaloid that possess a potential as anticancer agents.[29] Cyclohexadiene **34** was synthesized using their previously developed tandem enyne metathesis (Scheme 4.7).[29] Subsequent Pd(II)-promoted chloroacetoxylation using Bäckvall's conditions[30] followed by base-catalyzed cyclization afforded functionalized indoline **36**. Using similar set of reactions as discussed in previous total syntheses of ETP alkaloids, they successfully synthesized the pentacyclic core (**37**) displayed in the scabrosins. The stereochemistry of the pentacycle **37** was confirmed by X-ray analysis.[29]

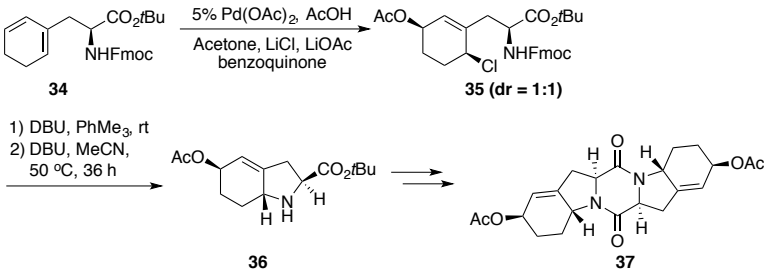

Scheme 4.7. Diver's efforts toward the synthesis of the scabrosins.

Recently, Carreira reported a novel strategy to access the core structure of 6-5-6-5-6 framework present in various ETP alkaloids using his previously developed methodology as the key step of the synthesis.[31] Alcohol **38** was synthesized in four steps from bromoacrolein using Corey and Loh's enantioselective Diels-Alder protocol (Scheme 4.8).[32] Swern oxidation afforded the corresponding unstable aldehyde *in situ*, which was trapped under low temperatures *via* direct double condensation with *N,N'*-diacetylDKP **39** to give olefin **40**. This double condensation could also be done step-wise. Using a slightly modified version of their previously reported conditions, the double intramolecular opening of the oxabicyclio[2.2.1]heptenes proceeded smoothly to furnish

pentacycle **41**, which was directly deprotected under basic conditions to give **42**.[31] X-ray analysis of **42** established the correct assignment of the structure. Since many ETP alkaloids contain pyrrolidines, protecting group exchanged version of **42** was subjected under hydrogenation conditions to afford **43** as a single diastereomer.[31]

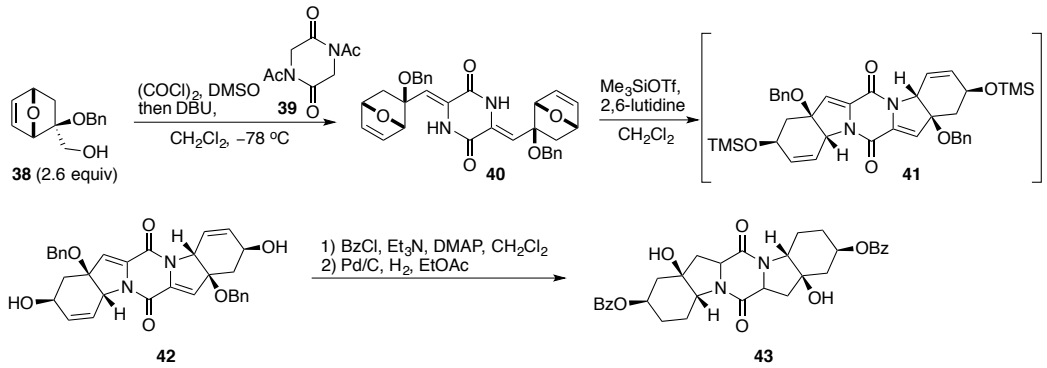

Scheme 4.8. Carreira's synthesis of pentacyclic framework.

4.4) Retrosynthetic analysis

As discussed in previous sections, the most commonly used synthetic strategy to access C_2 symmetric ETP alkaloids is *via* late-stage dimerization of functionalized bicyclic monomer (A,B rings) with the requisite stereochemistry already built into the system followed by installation of the disulfide bridge as one of the last remaining steps (Figure 4.3). Although quite a number of C_2 symmetric ETP alkaloids have been reported in the literature,[33] only few[23,25] have been synthesized in recent years (Figure 4.3).

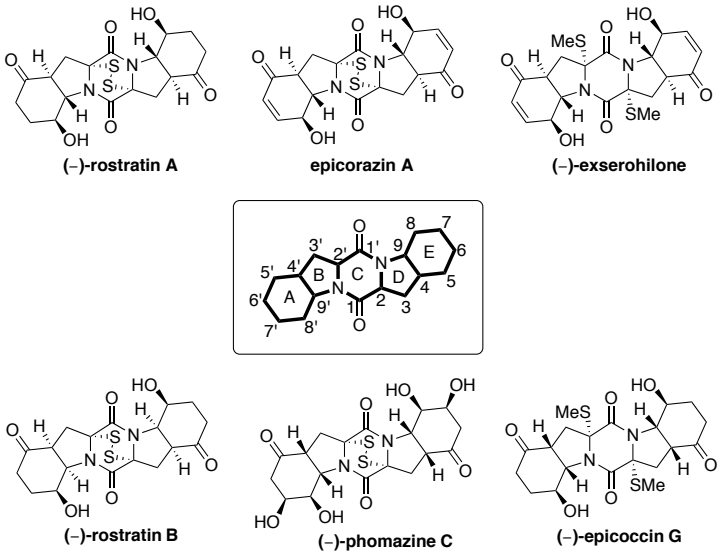

Figure 4.3. Structurally similar C_2 symmetric ETP alkaloids.[33]

We were initially interested in developing a novel strategy that could lead to the total synthesis of rostratins A and B.[33a] We envisaged a drastically different approach to access C_2 symmetric pentacyclic framework from a single synthetic transformation of a common key intermediate utilizing a diastereoselective double intramolecular Diels-Alder (IMDA) reaction (Figure 4.4). Depending on the chiral catalyst employed in the reaction, one could obtain either the *cis* (*exo* adduct) or *trans* (*endo* adduct) fused ring system, where the *cis* A,B ring system leads to rostratin B and the *trans* A,B ring system leads to rostratin A.

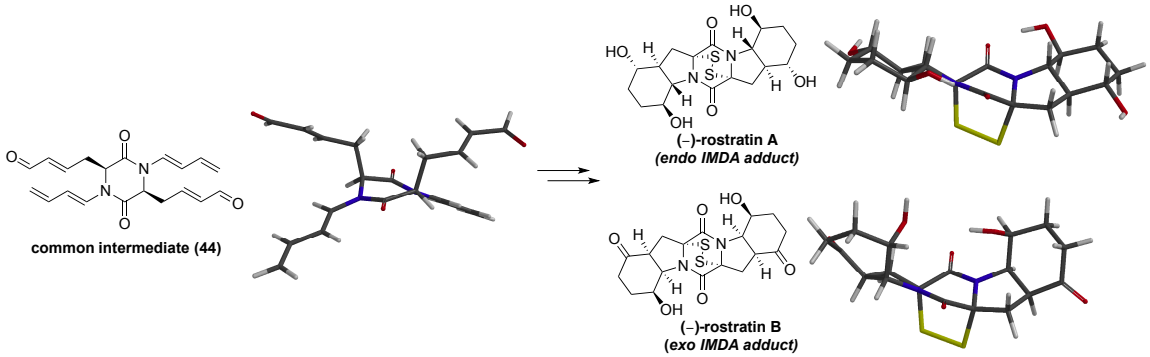

Figure 4.4. Novel approach to C_2 symmetric pentacyclic system in rostratins A & B. (Optimized at HF/AM1 level of theory using Spartan 04)

The common intermediate IMDA precursor (**44**) could be derived from transition metal mediated C-N coupling of **45** and **46** (Scheme 4.9). DKP **46** could be obtained from intramolecular dimerization of modified L-aspartic acid derivative. Diastereoselective IMDA of **44** could either afford the *endo* adduct **47** or the *exo* adduct **48**. Secondary alcohol in 8,8'-positions of rostratins A and B could be derived from corresponding epoxides **49** and **50**. Secondary alcohol or ketone functionalities present in 5,5'-positions of rostratins A and B respectively could arise from a decarbonylation-oxygenation sequence from the aldehyde in **47** and **48**. Finally, disulfide bridge formation would be achieved last, as early incorporation would not display functional group tolerance.

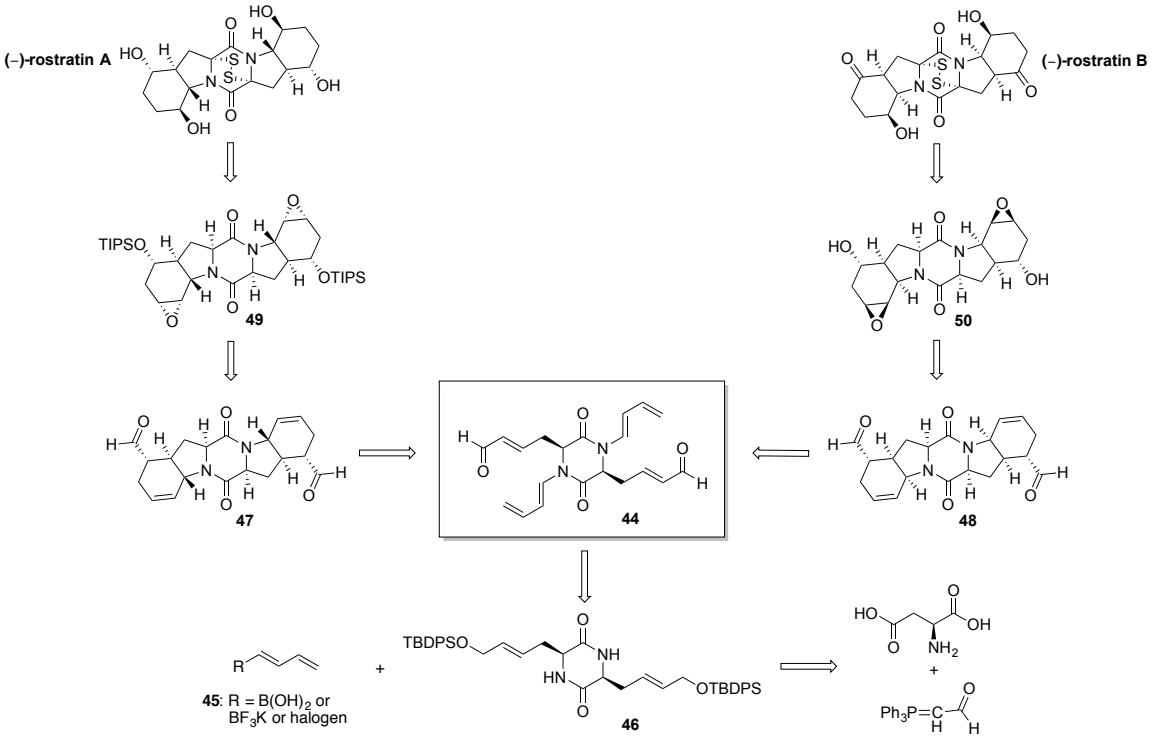

Scheme 4.9. Retrosynthetic analysis of rostratins A and B.

4.5) Synthesis of IMDA precursor

Sutherland's method[34] was utilized to obtain allylic alcohol **(+)-54** starting from L-aspartic acid (Scheme 4.10). One-pot esterification followed by mono-Boc protection of commercially available L-aspartic acid led to the corresponding protected amino acid in good yield. Further treatment with di-*tert*-butyl dicarbonate in the presence of catalytic amounts of DMAP afforded *N,N*-di*tert*-butoxycarbonyl L-aspartic acid dimethyl ester **(−)-51**. As noted by Sutherland,[34a] the di-Boc protection of the amine allows excellent regioselective manipulation of the ester functional groups, which is also a well-known method. Regioselective reduction of the β-methyl ester **(−)-51** afforded the L-aspartic acid aldehyde **(−)-52** in good yield. Selective removal of one of the Boc-protecting groups is required for the Wittig reaction to obtain the *E*-α,β-unsaturated aldehyde **(+)-53** for steric reasons. Hence, **(+)-53** was obtained *via* mono-Boc deprotection using lithium bromide followed by two-carbon homologation using a Wittig reaction with the stabilized ylide. Subsequent reduction of the terminal aldehyde led to the desired allylic alcohol **(+)-54** in good yield.

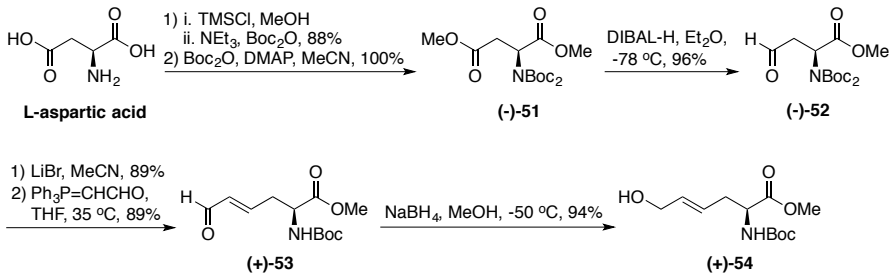

Scheme 4.10. Synthesis of allylic alcohol **(+)-54**.

Initially, we sought out to employ a combination of Bräse's dimerization protocol[28a] and method to install 1,3-butadiene moiety[28b] (Scheme 4.11). Protection of the allylic alcohol **(+)-54** followed by Boc removal and subsequent condensation of the resulting amine with

crotonaldehyde would afford the corresponding imine. The conjugated imine could then isomerize to the desired enamine **56** upon treatment with base. Saponification of the methyl ester (**56**) followed by Bräse's dimerization protocol[28a] should afford the corresponding DKP **58**. Unfortunately, although protection of allylic alcohol **(+)-54** was successful, subsequent Boc removal proved to be problematic. Treatment of **(+)-54** with zinc bromide led to removal of both Boc and SEM protecting groups due to prolonged reaction time. Other methods (SiO_2, μW irradiation) to mildly and selectively remove the Boc group were attempted without much success.

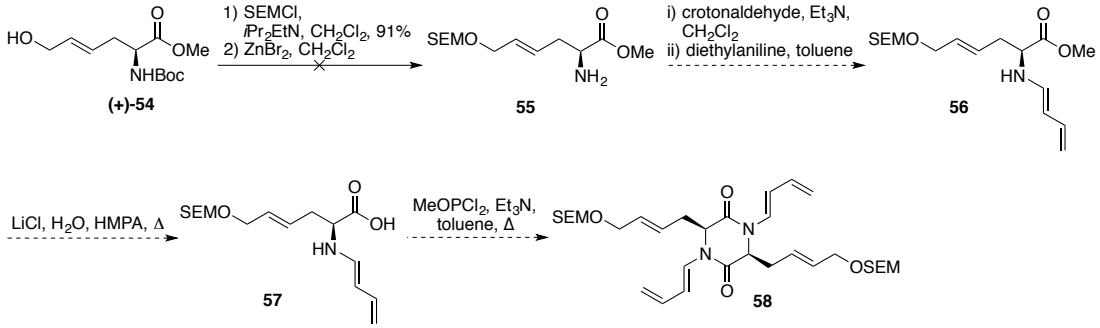

Scheme 4.11. First attempt to utilize Bräse's methodology.

Therefore, a change in protecting group was deemed necessary. The more robust and less acid and base sensitive TBDPS ether intermediate **(+)-59** was synthesized (Scheme 4.12). Although the desired Boc removal proceeded in good yield, subsequent one-pot enamine (**60**) formation resulted in complete decomposition of material, which could be attributed to the instability of enamine.

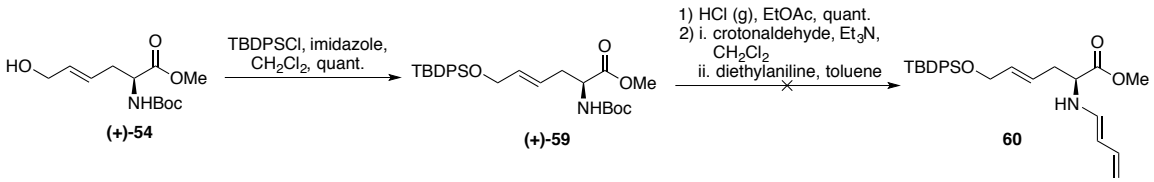

Scheme 4.12. Second attempt to utilize Bräse's methodology.

A more traditional route to form the desired DKP was envisioned instead, in which the silyl ether **(+)-59** could either be treated under acidic conditions to afford the Boc removed amine salt, or under saponification conditions to afford the corresponding acid, which could then undergo amide bond formation reaction to afford the dipeptide **(+)-63** (Scheme 4.13). The Boc group on the dipeptide would be removed, followed by intramolecular cyclization to form the desired DKP.

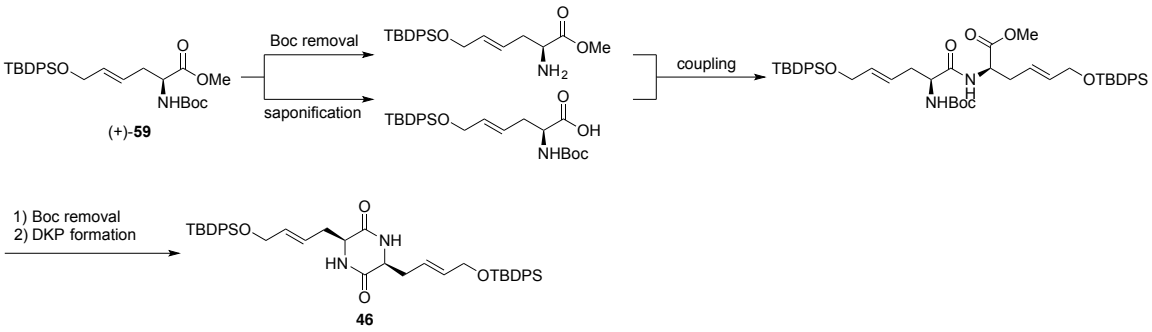

Scheme 4.13. Proposed synthesis of DKP intermediate.

Initially, few acidic conditions (HCl (g), HCl in dioxane, TFA), were attempted to remove the Boc group of **(+)-59**, and proceeded equally well. However, based on previous experience in forming amine salts, TFA amine salts tend to be more operationally convenient, as they tend to be less hygroscopic. Therefore, TFA amine salt was utilized. For the saponification step, other conditions such as LiOH, 1M NaOH, and Me_3SnOH were tried, but the use of $KOSiMe_3$ proved to be most efficient, as the reaction time was drastically shortened (4 h-overnight to 2 h). Although Me_3SnOH was relatively efficient reagent (4 h μW irradiation), it is not as cost effective in comparison to $KOSiMe_3$, and the use of μW irradiation makes the reaction not as scalable. For the coupling step, other conditions were screened in the beginning using the HCl amine salt and acid derived from various saponification reactions (Table 4.1).

Table 4.1. Coupling reaction conditions.[a]

Coupling reagent	Base	Solvent	Yield (%)[d]
BOP	NMM	CH_2Cl_2	20
EDC, HOBt	NMM	DMF	39
EDC, HOBt	Et_3N	CH_2Cl_2	22
EDC, HOBt[b]	$NaHCO_3$[c]	DMF	20
EDC, HOBt	DMAP (cat.)	DMF	25
Ipcf[d]	DMAP, Et_3N	CH_2Cl_2	17
DEPC	Et_3N	DMF	35
DEPBT	Et_3N	CH_2Cl_2	30
HATU	iPr$_2$EtN	DMF	17

[a] General procedure: amine HCl salt (1 equiv.), acid (1.1 equiv.), coupling reagent (1.1 – 1.2 equiv.), base (2 – 2.5 equiv.), at 0.1 M concentration, rt, overnight.
[b] Activated the acid as the pentafluorophenyl ester.
[c] $NaHCO_3$ was used in 5 equivalents.
[d] Isolated yield.
[d] Isopropyl chloroformate

The surprisingly low yielding coupling step led to a thorough investigation of reaction parameters. The major side product of the reaction was the mono TBDPS cleaved dipeptide. The precise timing of when TBDPS group removal was occurring was examined. The use of non-nucleophilic base ($NaHCO_3$, Et_3N, iPr$_2$EtN) did not improve the overall yield of the reaction, suggesting TBDPS removal was occurring prior to the coupling step (Table 4.1). In order to minimize the likelihood of TBDPS removal, the Boc deprotection step was conducted at lower temperatures using anhydrous conditions. As for the saponification step, use of milder, non-nucleophilic base, $KOSiMe_3$, significantly minimized the undesired side reaction, thereby improving the overall yield. Interestingly, the rate of the saponification was increased with $KOSiMe_3$ in comparison to more traditional hydroxide based reagents. When all these precautions were taken, the subsequent coupling step proceeded in much improved yield to afford the desired dipeptide **(+)-63** (Scheme 4.14). Since the initial screening of coupling step resulted in very similar yields, it could be assumed that the use of other coupling reagents beside BOP would result in comparable yields.

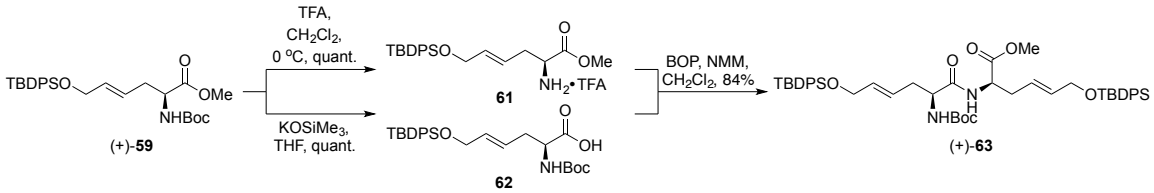

Scheme 4.14. Optimized synthesis of dipeptide **(+)-63**.

With the desired dipeptide **(+)-63** in hand, DKP formation was investigated next. Acidic conditions similar to Boc removal of **(+)-59** worked well on **(+)-63**, and provided the corresponding TFA amine salt. However, the subsequent intramolecular cyclization to form the DKP was not a trivial transformation. Since DKPs are well-known in the literature,[35] there are numerous ways to synthetically access them. However, success in finding the optimum set of conditions depends on the substituents that make up the DKP ring, which may not necessarily be obvious. There were few concerns with the present system. First of all, due to decrease in reactivity of primary amines as nucleophiles in comparison to secondary or tertiary amines, the overall progress of the desired cyclization could be more difficult. Secondly, certain DKPs could isomerize[36] more readily than others to yield a mixture of diastereomers. Eguchi and Kakuta determined thermodynamic constants in the equilibrium of the isomerization of various DKPs and found that DKPs that contain acyclic substituents (such as *cyclo*(Ala-Ala), *cyclo*(Leu-Leu), etc.) exist in almost 1:1 ratio of *cis* and *trans* isomers, since they tend to be very flexible and could adopt various boat and planar conformations that are not discrete and easily interconvertible.[36] On the other hand, DKPs that have cyclic substituents (such as *cyclo*(Pro-Pro)), predominantly exist as *cis* isomers, due to the added steric constraints.[36] Unfortunately, since the present system contains acyclic substituents, it was expected that the diastereoselectivity would not be as favorable. Finally, the concentration of the

intramolecular reaction was surprisingly not consistent in the literature.[35] Although intramolecular cyclization reactions are generally performed at dilute concentrations, documented DKP forming methods displayed various concentrations. Therefore, much attention was given towards optimization of this step. Movassaghi's conditions[17] were investigated first using excess morpholine in a non-nucleophilic solvent, *t*-butanol (entry 1, Table 4.2). At high dilution, the reaction was sluggish, although it did provide modest yield of the desired *cis* DKP (entries 1-5, Table 4.2). Slight increase in temperature, prolonged reaction time, and portion-wise addition of morpholine did not affect the yield significantly (entries 2-3, Table 4.2). A solvent effect was suggested when the reaction was performed in CH_2Cl_2 instead of *t*-butanol (entries 5-6, Table 4.2). Increasing the overall concentration also did not affect the yield (entry 7, Table 4.2). Potential use of alternative amines and inorganic bases were screened using high-throughput experimentation (96-well plate: 8 solvents, 12 bases), which suggested the use of NMM, TBD, and 2,6-lutidine in MeCN as a possible substitute. Alternative ways of activating the carbonyl moiety of the methyl ester electrophile was investigated by saponification of **(+)-63**, followed by pentafluorophenyl (pfp) ester formation using standard conditions. The product was then Boc deprotected and utilized in the reaction with various bases (entries 10-13, Table 4.2). Unfortunately, amine bases (NMM, TBD, 2,6-lutidine) and inorganic bases ($NaHCO_3$, K_2CO_3) produced a decrease in yield, recovery of starting material, or decomposition (major side products being TBDPS removed products) (entries 8-15, Table 4.2). Interestingly, using standard amide bond formation methods (entry 16, Table 4.2) resulted in no reaction, which may be due in part to increased sterics of the substrate. Lewis acid activation of the carbonyl moiety was explored *via* high-

throughput screening using eight different Lewis acids ($AlCl_3$, $BiOTf_3$, $CoCl_2$, $FeCl_3$, $Sc(OTf)_3$, $SnCl_2$, $Yb(OTf)_3$, $ZnBr_2$) in three different solvents (*t*-BuOH, *i*-PrOH, 1,2-DCE), which generally led to decomposition of material or no reaction. The most promising condition from the screen was scaled-up and tested (entry 21, Table 4.2), which resulted in significant formation of TBDPS removed side products.

Table 4.2. Screening of DKP formation methodology.

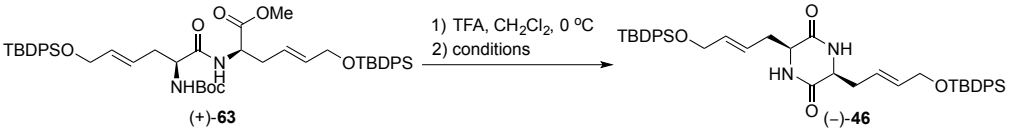

(+)-**63** (–)-**46**

Entry	Reagent (equiv.)	Solvent [M]	Temp (°C)	Time	Yield (%)[a]
1	Morpholine (50)	*t*-butanol [0.02]	rt	5 d	55
2	Morpholine (50)	*t*-butanol [0.02]	30	7 d	43
3[b]	Morpholine (50)	*t*-butanol [0.01]	30	13 d	46
5	Morpholine (14)	*t*-butanol [0.05]	rt	18 h	32
6	Morpholine (14)	CH_2Cl_2 [0.05]	rt	3.5 d	20
7	Morpholine (14)	*t*-butanol [0.19]	rt	5 d	39
8	NMM (3)	*t*-butanol [0.01]	reflux	18 h	32
9	NMM (3)	*t*-butanol [0.06]	122	1 h	Decomposition
10[c]	TBD (1)	MeCN [0.01]	0 → rt	5 h	25
11[d]	TBD (2.2)	MeCN [0.05]	0	2 d	7
12[d]	2,6-lutidine (0.5)	MeCN [0.05]	rt	18 h	Decomposition
13[e]	5% $NaHCO_3$ (1)	CH_2Cl_2 [0.01]	0 → rt	5 h	36
14	(sat.) $NaHCO_3$	EtOAc [0.1]	rt	18 h	No reaction
15	K_2CO_3 (4)	EtOH [0.1]	reflux	20 h	Decomposition
16[e]	BOP (1.2), NMM (2)	CH_2Cl_2 [0.01]	rt	20 h	No reaction
17	2M NH_3 in MeOH (5)	MeOH [0.1]	rt	3 d	36
18	--	2M NH_3 in MeOH [0.01]	reflux	6 h	29
19	DMAP (0.2), NH_4OH (15% of MeOH)	MeOH [0.06]	rt	6 d	33
20	DMAP (0.2), NH_4OH (10% of MeOH)	MeOH [0.1]	rt	18 h	53
21[f]	$Sc(OTf)_3$ (1.5)	1,2-DCE [0.05]	30	2 d	Decomposition

[a] Isolated yield of *cis* diastereomer. Reaction monitored by ^1H NMR and TLC analysis.
[b] Portion-wise addition (10 equiv.) of morpholine over time.
[c] Methyl ester hydrolyzed to acid then activated as pentafluorophenyl (pfp) ester before use, 1 h at 0 °C, then 4 h at rt.
[d] Methyl ester hydrolyzed to acid then activated as pfp ester before use.
[e] Methyl ester hydrolyzed to acid before use.
[f] TFA amine salt substrate was free-based prior to use.

Following a method used by Danishefsky,[37] NH_3 in MeOH was used at varying concentration and temperature, which only led to a decrease in yield (entries 17-18, Table 4.2). Surprisingly, use of NH_4OH in MeOH, a method utilized in our group in the past[38]

with catalytic DMAP at increased concentration not only significantly reduced the reaction time, but it also resulted in a highest yield that was comparable to that of the initial conditions (entry 20, Table 4.2).

With this promising result, the diastereoselectivity of the reaction was investigated (Table 4.3). Although use of lower amounts of morpholine at higher concentrations generally led to an increase in overall yield, the diastereoselectivity decreased (entries 1-3, Table 4.3). Interestingly, shorter reaction times resulted in higher diastereoselectivity (entry 2, Table 4.3), suggesting the possible epimerization of *cis* to *trans* diastereomer with time. This possibility was tested in previous experiments, where the reaction was held at lower temperatures (entries 10 & 13, Table 4.2). However, in those cases, the reaction rate tended to be sluggish. To further probe this result, the reaction was initiated at −78 ^{o}C and held at 0 ^{o}C for 1 d (entry 4, Table 4.3), which did not seem to drastically affect the diastereoselective outcome. From the NH_4OH series, the best result was obtained when 5% NH_4OH was used in MeOH (entry 7, Table 4.3). Of note, there seemed to be some beneficial effect in free-basing the TFA amine salt prior to use.

Table 4.3. DKP formation optimization.

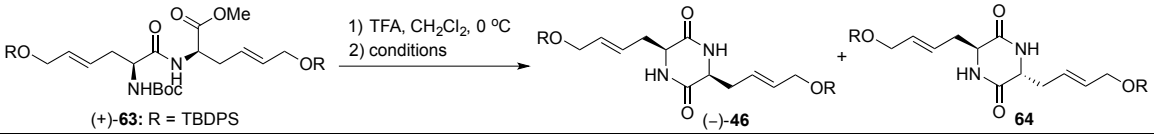

(+)-**63**: R = TBDPS (−)-**46** **64**

Entry	Reagent (equiv.)	Solvent [M]	Temp (^{o}C)	Time	Yield (%)[a]	*dr* = *cis*:*trans*
1	Morpholine (35)	*t*-butanol [0.06]	rt	4 d	48	1.3:1
2	Morpholine (14)	*t*-butanol [0.19]	rt	20 h	65	1.66:1
3	Morpholine (14)	*t*-butanol [0.19]	rt	2 d	86	1.09:1
4	2M NH_3 in MeOH (50)	MeOH [0.1]	−78→0	1 d	61	1.31:1
5	DMAP (0.2), NH_4OH (10% of MeOH)	MeOH [0.06]	rt	2 d	52	1.51:1
6	NH_4OH (3.5% of MeOH)	MeOH [0.06]	rt	3 d	74	1.68:1
7[b]	NH_4OH (5% of MeOH)	MeOH [0.11]	rt	3 d	82	2.3:1

[a] Isolated total yields of both diastereomers.
[b] TFA amine salt substrate was free-based prior to use.

Finally, with optimized conditions for DKP formation in hand, various enamide forming methods were explored in order to install the requisite diene moiety on the DKP for IMDA. Using crotonaldehyde as the 1,3-butadiene precursor was revisited, as the stability of enamide was expected to be higher than that of the corresponding enamine (Scheme 4.12). Furthermore, synthesizing *N*-dienyl lactams and using them in intermolecular Diels-Alder reactions with electron deficient alkenes have been reported in the literature.[39] Hoping that DKPs would react in similar manner as lactams, the method was probed using *cyclo*(Gly/Gly) and crotonaldehyde (Scheme 4.15). Unfortunately, the desired reaction did not proceed and resulted in decomposition and recovery of unreacted crotonaldehyde. Model DKP **(+)-65** was synthesized and tested using same reaction conditions, but it also led to decomposition of starting material. (Synthesis of **(+)-65** will be discussed later.) Specifically, the TBDPS group was removed during the course of the reaction, and the crude reaction mixture did not contain any 1,3-butadiene moieties. These results may be due to the fact that the nitrogen of the amide moiety in DKPs is less nucleophilic than that of lactams. To further support the hypothesis, 2-pyrrolidone was reacted under the same conditions, and as expected, resulted in higher yield (56%) (Scheme 4.15).

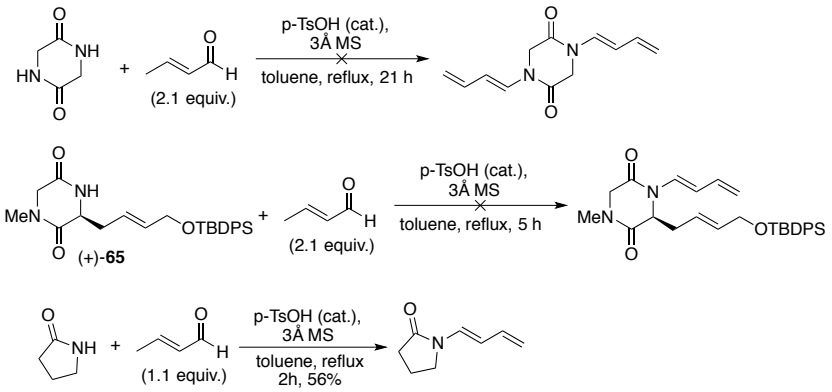

Scheme 4.15. Attempted synthesis of doubly *N*-dienylated DKP.

Undeterred, the use of transition metal catalysis was investigated next. Gooβen's hydroamidation protocol[40] was recently reported at that time. The general procedure does not require a glove box, especially when tri-*n*-butylphosphine is substituted with its HBF_4 adduct, making it more air-stable and easy to handle. The active catalyst is generated *in situ* from ruthenium(III) chloride hydrate, tri-*n*-butylphosphine, DMAP, and K_2CO_3. The catalyst was shown to effectively promote the addition of secondary amides to terminal alkynes under formation of (*E*)-*anti*-Markovnikov enamides in good yield. When *cyclo*(Gly/Gly) was reacted under Gooβen's optimized conditions using two different terminal alkynes, the corresponding products were formed in low yields (Scheme 4.16). Unfortunately, when **64** was reacted under the same conditions for prolonged period of time, only starting material DKP was recovered along with an unknown minor side product (Scheme 4.16). Although Gooβen reported the reaction of *cyclo*(Gly/Gly) with 1-hexyne to undergo at much higher yield (71%)[40], this result was not obtained even after several trials.

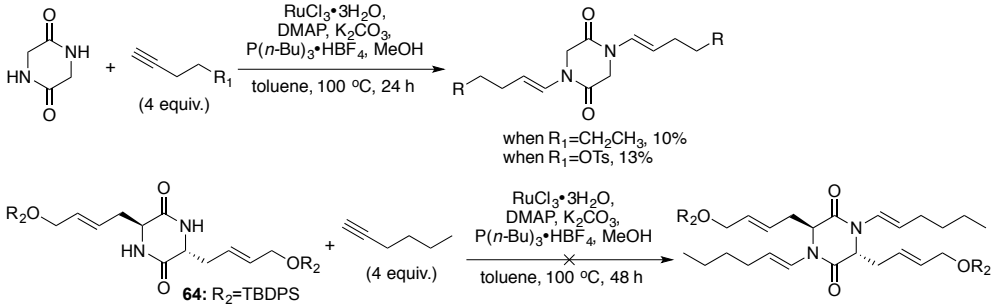

Scheme 4.16. Attempted use of Gooβen's hydroamidation protocol.

During the same year, Batey published a method[41] utilizing copper oxidative conditions to form enamides in good yields. More specifically, in their methodology, potassium alkenyltrifluoroborate salts undergo cross-coupling with amides to afford enamides using

catalytic amount of copper(II) acetate under mild oxidative conditions. The reaction could be set up on the bench top as all reagents are air stable. To probe the reactivity of DKPs under the reported conditions, *cyclo*(Gly/Gly) was tested with various alkenyl trifluoroborate salts (Scheme 4.17). Application of Batey's methodology successfully provided the desired doubly coupled DKP product in high yields when known alkenyl trifluoroborate salts were used. With this promising lead, the actual 1,3-butadiene substrate, **66**, was synthesized and employed, which resulted in a synthetically useful yield of the desired product (Scheme 4.17). According to Batey's report[41], if the amide substrate has a low pK_a (pK_a =13-17 in DMSO), it is possible that *N*-methylimidazole serves as a base, leading to deprotonation of the amide proton and subsequent coordination of the deprotonated species to copper. While as with higher pK_a (pK_a =20-24 in DMSO) amide substrates, *N*-methylimidazole may not serve this role, and instead its direct coordination to copper may result in inhibition of the desired coupling reaction. For the present system, addition of a catalytic amount of *N*-methylimidazole (20 mol%) did not improve the yield, and actually shut down the desired reaction. This observation suggests that the amide proton of the DKP may not possess a relatively low pK_a value.

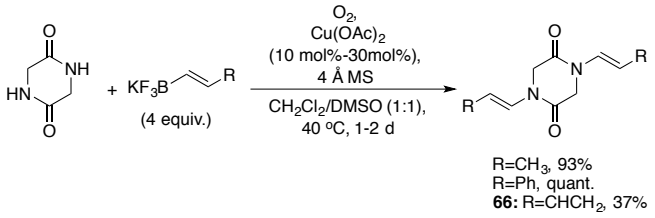

Scheme 4.17. Application of Batey's protocol to test system.

The 1,3-butadiene trifluoroborate salt **66** can be easily accessed in four steps starting from 3-butyn-1-ol in good yields (Scheme 4.18). Mesylation of the alcohol followed by hydroboration[42] installs the corresponding pinacol boronate ester, which is then

immediately eliminated to afford the unstable 1,3-butadiene pinacol boronate ester **68**.[43] Rapid conversion of the pinacol boronate ester **68** to the trifluoroborate[44] affords **66** in good yield. Although much more stable than the pinacol boronate ester **68**, once synthesized, **66**'s lifetime is limited, and should be kept at cold temperatures up to few weeks to prevent undesired polymerization or Diels-Alder reaction with itself,[45] which could be detected by ^{1}H NMR and physical color change over time.

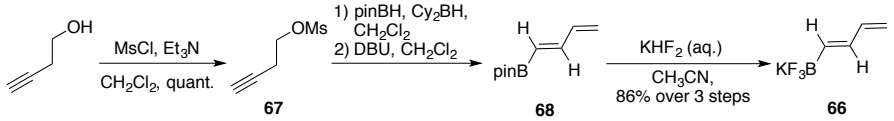

Scheme 4.18. Synthesis of 1,3-butadiene trifluoroborate salt **67**.

Due to the success of application of Batey's protocol[41] to simple DKPs, the actual substrate DKP **(−)-64** and coupling partner trifluoroborate **66** was employed (Scheme 4.19). The copper loading was increased (10 mol% to 30 mol%), as previous experiments with *cyclo*(Gly/Gly) showed slight increase in yield with higher copper loading. The desired reaction occurred at a synthetically useful yield.

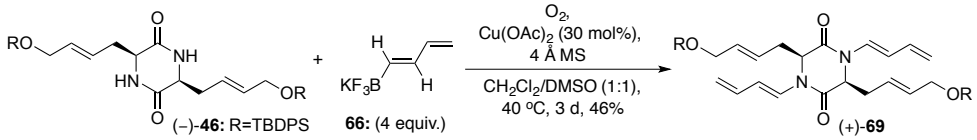

Scheme 4.19. Application of Batey's protocol.

For further optimization, various reaction parameters were varied throughout an extensive time period to achieve consistent results (Table 4.4). Generally, the amount of **66** added to the reaction seemed to affect the overall yield (Entry 1, Table 4.4). Concentration of the reaction also affected the yield and efficiency of the reaction (Entries 1, 13, 20, Table 4.4). Since the reaction is a bimolecular cross-coupling reaction, it could be assumed that higher concentration would result in better yield. However,

substrate solubility appeared to be one of the greatest concerns of the reaction. When the solvent was varied, it led to dramatic decrease in yield (Entries 9-12, 15, 25, Table 4.4), which strongly implies the importance of solubility of the substrates. This finding is in accordance with Batey's report,[41] as he also found the importance of solubilizing both the copper salt, trifluoroborate salt, as well as the amide substrate. As implied from the test reaction with *cyclo*(Gly/Gly), amine base additives did not improve the yield (Entries 2 & 19, Table 4.4). The role of 4 Å molecular sieves (MS) was studied next. Batey had speculated that they may serve as a catalyst for hydrogen peroxide decomposition, or aid in the re-oxidation of copper by oxygen, or may facilitate ligand exchange on boron during transmetallation.[41] When other zeolites were used[46] in the reaction (Entries 5-8, Table 4.4), only starting material was recovered from the reaction even after prolonged period of time. When no 4 Å MS were used (Entry 4, Table 4.4), only trace amount of mono-coupled product was observed, further supporting the importance of having 4 Å MS in the reaction. Interestingly, when the 4 Å MS were thoroughly dried and activated (flame dried under vacuum), and the reaction was set up in the glove box scrupulously excluding the presence of moisture or water (Entry 21, Table 4.4), only starting material was recovered. This led to an investigation of water or moisture effect on the reaction conditions. When water was purposefully added to the reaction (Entry 3, Table 4.4), the yield dramatically decreased. However, when 4 Å MS were used directly from the bottle without further drying or activation, the yield was maintained or increased (Entry 13, Table 4.4) from the initial reaction condition (Scheme 4.19). These results support Batey's hypothesis[41] on the role of 4 Å MS, in that they may have roles other than to serve as simple dessicants. Moreover, since at least one of fluoride ions from the

trifluoroborate should be replaced by hydroxide for the transmetalation to occur, a source of water should be present in the reaction.[41,47] Perhaps using "wet" 4 Å MS provide just enough water for successful transmetalation. However, during the course of the investigation, the partially optimized reaction suddenly failed to provide consistent results (Entry 13, Table 4.4). This disappointing result led to a set of thorough experimentation where each component of the reaction was examined. From previous results, although more equivalents of **66** seemed to result in higher yields, there seemed to be not much effect from 4-5 equivalents (Entries 13,14, Table 4.4). The reason for excess **66** may be due to the instability of **66**, since the limited shelf-life of **66** was already noticed during its synthesis. Perhaps some of **66** undergo the desired cross-coupling reaction, but some other portions of it could slowly oxidize, dimerize, or polymerize, which is reasonable considering the prolonged reaction times. Since the rate of the reaction seemed to be rather sluggish (up to 14 d), a portion-wise addition of **66** was thought to be advantageous (Entry 14, Table 4.4). In terms of copper loading, 0.3 equivalent appeared to be the most optimal loading, as decreasing (Entries 18, 21-23, Table 4.4) or increasing (Entry 24, Table 4.4) amount of copper resulted in dramatically lower yields. In Batey's report,[41] he specifically noted the use of $Cu(OAc)_2$ that is of 97% purity as opposed to 99.9% purity, since extensive studies showed that catalytic presence of Cr(II) in $Cu(OAc)_2$ of 97% purity facilitates the reaction. This was proven to be the case in the present system as well (Entry 21, Table 4.4). Oxygen supply was tested next. According to Batey, higher yields were obtained when the reaction was conducted under a slightly positive oxygen pressure using a gas manifold equipped with an oil bubbler, with the oxygen gas supplied from a cylinder passed through drierite, as opposed to using

oxygen balloon or air.[41] However, there seemed to be not much difference between using oxygen balloon or direct oxygen supply in terms of yield, although the rate in some cases was accelerated. Use of air, however, did decrease the rate and the yield of the reaction. To test the importance of solubilizing oxygen in the reaction mixture, 2,2,2-trifluoroethanol was used in conjugation with DMSO, since fluorinated solvents are generally known to dissolve and contain oxygen better (Entry 16, Table 4.4). Unfortunately, this solvent change actually decreased the yield. Substituting 1,2-dichloroethane for dichloromethane was tolerated, as long as some amount of DMSO was used in conjugation. The use of DMSO is likely due to its ability to solvate the trifluoroborate salt. However, if the amount of DMSO is increased, the reaction is known to be inhibited, as DMSO could also act as a ligand to copper.[41] Use of 1,2-dichloroethane was found to be more beneficial than dichloromethane, since less evaporation occurred over time at 40 ^{o}C.

Table 4.4. Copper-oxidative coupling reaction optimization.

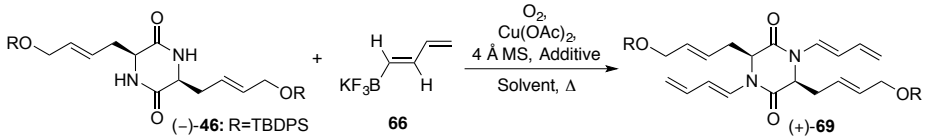

Entry	66 (equiv.)	$Cu(OAc)_2$ (equiv.)	Solvent [M]	Additive	Temp (^{o}C)	Time	Yield[a] (%)
1	3.3	0.3	DMSO:DCM [0.1]	None	40	21 h	0[b]
2	4	0.3	DMSO:DCM [0.25]	Et_3N (2 equiv.)	40	3 d	20
3	4	0.3	DMSO:DCM [0.25]	H_2O (2% v/v)	40	2 d	18
4	4	0.3	DMSO:DCM [0.25]	No sieves	40	3 d	0[c]
5	4	0.3	DMSO:DCM [0.25]	3Å MS[d]	40	3 d	0
6	4	0.3	DMSO:DCM [0.25]	Neutral Alumina[d]	40	3 d	0
7	4	0.3	DMSO:DCM [0.25]	SiO_2[d]	40	3 d	0
8	4	0.3	DMSO:DCM [0.25]	Celite[d]	40	3 d	0
9	4	0.3	DCE [0.25]	None	50	38 h	0[c]
10	4	0.3	DCE [0.12]	None	40	2 d	0[e]
11	4	0.3	DCE [0.25]	MeOH (10 equiv.)	50	38 h	0[c]
12	4	0.3	MeOH [0.25]	None	50	38 h	0[c]
13	4	0.3	DMSO:DCM [0.25]	None	40	1-13d	2-75[g]
14	5 then 2[f]	0.3	DMSO:DCM [0.25]	None	40	14 d	0-98[g]
15	5	0.3	DCM [0.25]	None	40	1 d	0
16	5	0.3	DMSO:TFE [0.25]	None	40	4 d	9

17	5	0.3	DMSO:DCE [0.25]	None	40	10 d	86
18	3	0.2	25%DMSO:DCE [0.25]	None	50	8 d	30[h]
19	3	0.2	25%DMSO:DCE [0.25]	NMI (0.4 equiv.)	50	8 d	0[c]
20	3	0.2	25%DMSO:DCE [0.75]	None	40	42 h	33
21	4	0.1	DMSO:DCM [0.25]	None	40	1 d	0[i]
22	5	0.1	DMSO:DCM [0.25]	None	40	30 h	41
23	5	0.1	DMSO:DCM [0.25]	None	40	1.5 d	0
24	5	1	DMSO:DCM [0.25]	None	40	2.5 d	9
25	4	4	DCE:H_2O 10:1 [0.07]	None	40	2 h	0[j]

[a] Isolated yields. Otherwise specified, 4Å MS used in twice the amount relative to **66**.
[b] 21% of mono-coupled product was isolated.
[c] Trace amount of mono-coupled product was detected.
[d] Effect of different types of zeolites were investigated, used in the place of 4Å MS.
[e] Reaction vessel sonicated for 5-10 min to facilitate solubility.
[f] Added 5 equiv. first, then additional 2 equiv. after 2-5 days.
[g] Effect of O_2 supply tested. Used balloons or connected directly to O_2 cylinder passed through drierite.
[h] Obtained ~30% of mono-coupled product as well.
[i] Used $Cu(OAc)_2$ (99.9% purity), reaction set up in the glovebox, 4Å MS thoroughly dried and activated.
[j] Reaction vessel charged with headspace of air, μW irradiation, 200 Watts, 300 psi.

In line with the importance of solvation of all substrates, 1,2-dichloroethane was used with water, and subjected under microwave irradiation for more effective heating (Entry 25, Table 4.4), which only led to recovery of starting material DKP, and protodeboronated and polymerized **66**. Finally, rigorous stirring and large surface area with 5 equivalents of **66**, 0.3 equivalent of $Cu(OAc)_2$, in 1:1 ratio of DMSO and 1,2-dichloroethane gave the more consistent result (Entry 17, Table 4.4), albeit in 10 days. Effective stirring is generally accepted as a crucial component in copper oxidative couplings (Chan-Lam type), since it facilitates oxygen solvation in the reaction mixture. Interestingly, in some cases, when dichloromethane was used instead of 1,2-dichloroethane, slight oxidation of the product DKP **(+)-69** was observed by ^{1}H NMR. This may be due to the fact that over prolonged reaction time, dichloromethane may be more efficient in solubilizing oxygen, thereby facilitating oxidation of the 1,3-butadiene moiety. There may be a so-called "Goldilocks" modulation at play in terms of solubility, since too much solubility of oxygen (use of TFE or DCM instead of DCE) leads to oxidized side products, while as too little (MeOH, or use of air) impedes the reaction. A

multivariate high-throughput experimentation was done to scope out the chemical space of this transformation. The screens tested the possibility of using alternative copper sources ($Cu(OTf)_2$, $Cu(NO_3)_2$), amine base/ligand additives (NMI, 1,10-phenanthroline, pyridine, Et_3N), and solvents (dioxane, MeOH, chlorobenzene). The results from the screens suggested that $Cu(OAc)_2$ is the optimal copper source, no addition of base/ligand was necessary, and mixture of DMSO and DCE (25% DMSO in DCE or 1:1 mixture) was tolerated.

Although the specific copper oxidation states, spatial orientation of the complexes, and the sequence of events in the catalytic cycle remains to be clarified, Batey proposed a generic mechanism[41] for the reaction based on supporters[48] of the involvement of Cu(III) intermediate in the catalytic cycle (Figure 4.5). As mentioned, replacement of at least one of the fluoride ions from **B** must occur to afford the boron intermediate **C**, which then forms a bridging M-O-B species[47b] that is required for the transmetalation step. Based on Stahl's work[48b] oxidation by molecular oxygen of Cu(I) species **D** to Cu(III) is believed to occur in a stepwise fashion *via* Cu(II). Transmetalation of **C** and coordination of amide substrate **A** may occur either at the Cu(II) or Cu(III) oxidation states, which leads to **E**. Finally, rapid reductive elimination of **E** furnishes the product enamide **F** and regenerates Cu(I) species **A**. As discussed earlier, the role of 4 Å MS could be to aid in the decomposition of hydrogen peroxide, re-oxidation of copper by oxygen, or facilitate ligand exchange on boron.[41]

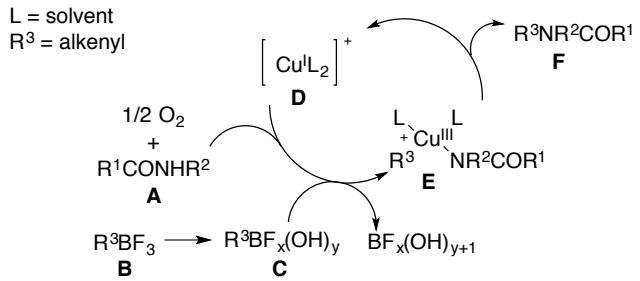

Figure 4.5. Generic mechanism proposed by Batey.[41]

To further prove the importance of this reaction over other well-known copper oxidative cross-coupling reactions, a Chan-Lam type reaction was conducted (Scheme 4.20). The desired product was not obtained under standard conditions even after 5 days.

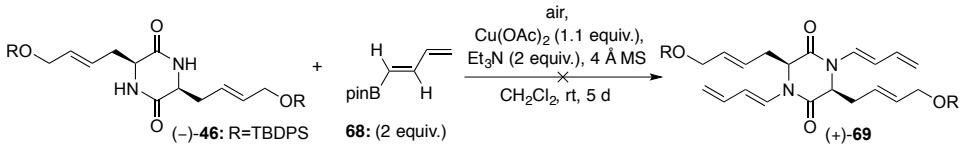

Scheme 4.20. Attempt to use Chan-Lam type cross-coupling.

A model system was developed to test the feasibility of key steps in the synthesis. The model system **(+)-65** contains half of the actual system, where the other half is left unsubstituted (Scheme 4.21). BOPCl-mediated amide formation with common intermediate acid **62** and sarcosine ethyl ester hydrochloride salt **70** affords the dipeptide **(+)-71**. Subsequent Boc removal followed by intramolecular cyclization furnishes the model system DKP **(+)-65** in excellent yield. Interestingly, the DKP formation did not experience the diastereoselectivity problems seen in the actual system. The presence of two TBDPS groups on the actual system may have some influence on the diastereoselectivity of the reaction. Furthermore, the copper-oxidative coupling step was not problematic, as it consistently resulted in good yields. This may be reasonable, since coupling of one 1,3-butadiene moiety may be thermodynamically much easier than *bis* coupling.

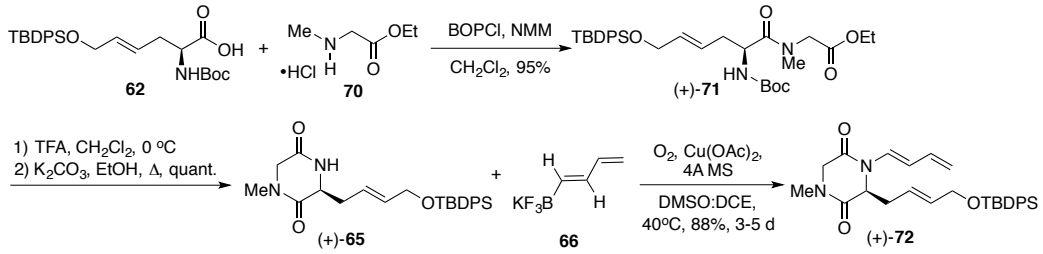

Scheme 4.21. Synthesis of model system coupled DKP **(+)-72**.

Subsequent removal of TBDPS occurred in excellent yield to afford the allylic alcohol **(+)-73** (Scheme 4.22). Optimal condition for the oxidation step was obtained with Dess-Martin periodinane (DMP) to obtain the unstable IMDA precursor **74**. Other oxidants such as MnO_2 and $BaMnO_4$ were sluggish in comparison to DMP, where the starting material was completely consumed only after 4 d along with decomposed or polymerized material. Due to instability of **74**, it was crucial to develop an efficient oxidative condition that would rapidly furnish the desired product in good yield. DMP was the reagent of choice, since the transformation occurred in about 20-30 min. A short plug silica gel column was required promptly after the reaction in order to minimize iodinane contamination.

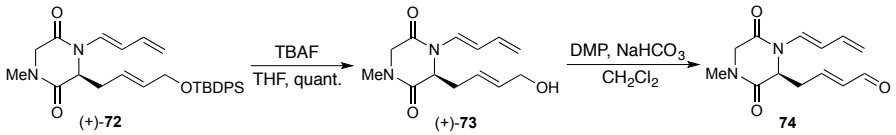

Scheme 4.22. Synthesis of model IMDA precursor **74**.

Optimized conditions obtained from model system DKP **74** translated well to the actual system (Scheme 4.23) to afford the desired IMDA precursor **44**. Similar to experimental results obtained using the model system, use of other oxidation reagents, such as $BaMnO_4$, MnO_2, and Ley oxidation reagents (TPAP, NMO, 4Å MS), resulted in decomposition or polymerization due to sluggish conversion of the starting material to

the highly unstable product **44**. Interestingly, Parikh—Doering oxidation (SO_3•pyr, DMSO, Et_3N) gave comparable results to that of DMP oxidation. While as, IBX was not as reactive as DMP, and resulted in lower yield. IMDA precursor **44** had to be used immediately after a prompt, short silica gel plug column to prevent decomposition/polymerization which occurred rapidly at room temperature.

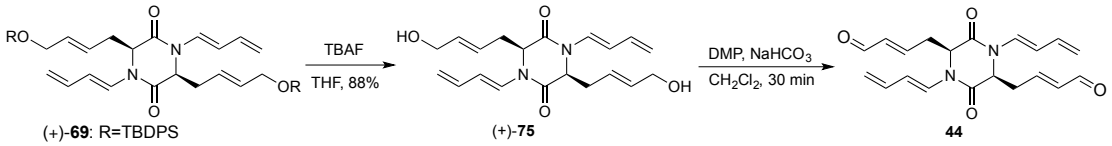

Scheme 4.23. Synthesis of IMDA precursor **44**.

4.6) Investigation of IMDA reaction

IMDA reactions are one of the most popular reactions utilized in many total syntheses to date.[49] There are two types of IMDA based on the point of connection between the diene and the dienophile (Figure **4.6**). The system under investigation is in the category of Type I IMDA, since the dienophile is tethered from the terminus of the diene. The less prevalent Type II IMDA have the dienophile tethered from an internal position on the diene (Figure **4.6**), which results in the formation of bridged bicycles that contain highly strained bridgehead double bonds (*anti*-Bredt alkene). Unlike Type I IMDAs, predicting the diastereoselectivity of type II IMDAs is simpler, since substrates with bridging chains of three or four atoms cyclize exclusively to give *syn* products, due to lower energy of the transition state in comparison to that of the *anti* diastereomer.[50]

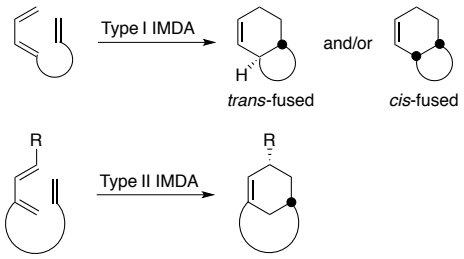

Figure 4.6. Type I vs. Type II IMDA.

For Type I IMDAs, the nature of the diene, dienophile, and tether could dictate the stereo- and regioselective outcome of these reactions (Figure 4.7). In other words, depending on the orientation of the diene and the dienophile on the ends of the tether could lead to the formation of the *endo* or *exo* IMDA adduct. Therefore, we envisioned the utilization of a common IMDA precursor **44** that could lead to the formation of either *endo* or *exo* IMDA adduct depending on the type of organocatalyst employed. Due to the abundance of *endo* selective organocatalysts, investigation of synthetic route towards (−)-rostratin A was conducted first.

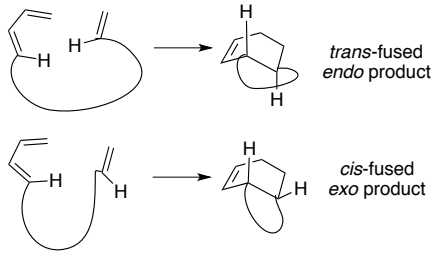

Figure 4.7. Formation of *trans*-fused *vs*. *cis*-fused products in Type I IMDA.

Inspired by MacMillan's successful application of his second-generation imidazolidinone catalyst[51a] in the key IMDA step in the synthesis of marine metabolite solanapyrone D (Scheme 4.24),[51b] use of his organocatalyst was envisioned for the present system hoping to achieve high diastereoselectivity. In particular, the synthetic utility of MacMillan's protocol was demonstrated by the preparation of various [4.3.0]- and [4.4.0]cycloadducts in good yield, enantio-and diastereoselectivity.[51b]

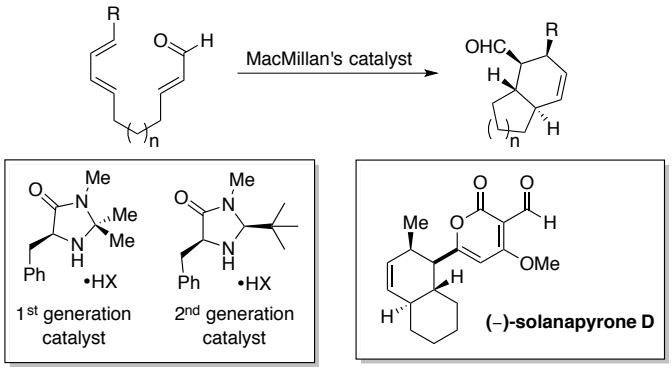

Scheme 4.24. Application of MacMillan's catalyst in his synthesis of (−)-solanapyrone D.[51b]

MacMillan's catalysts function as the LUMO-lowering activator of α,β-unsaturated carbonyl of aldehydes *via* the reversible formation of iminium ion. In terms of selectivity, MacMillan utilized a MM3 force field simulation to show that his first-generation catalyst and the aldehyde selectively form an *E*-iminium ion, where the hydrogen atom in the α-position is able to avoid unfavorable interactions with the geminal methyl groups of the catalyst.[52] The unfavorable interaction would be more pronounced by a *t*-butyl group present in his second-generation catalyst (Figure **4.8**). Consequently, the diene approaches the iminium ion preferably from the *si* face.

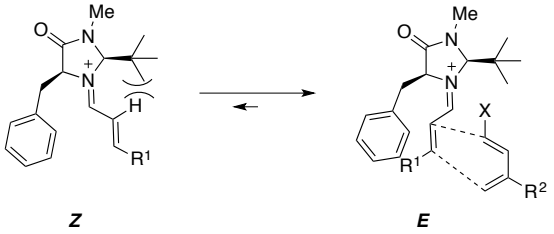

Figure 4.8. Selectivity explanation displayed using MacMillan's catalyst.

Taken together, when applied to the present system, the MacMillan's second-generation catalyst should give predominantly *endo* adduct, where the diene would approach the dienophile in the *si* face (Scheme **4.25**).

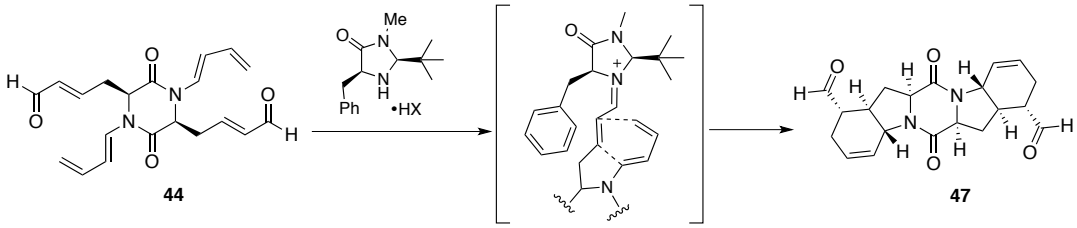

Scheme 4.25. Proposed utilization of MacMillan's catalyst.

Although MacMillan's IMDA protocol has been widely used since his first report,[51b] the reaction lacks generality, in that each IMDA substrate has to be individually studied and optimized for maximal yield and selectivity. Yields are usually reported as percentage conversion as opposed to isolation, due to the propensity of undesired side reaction that could occur during the reaction.[53] There are four main side reactions[53] that should be considered. First, starting materials, such as trienals and tetraenals often polymerize under the reaction conditions. Since the present system contains a trienal moiety, polymerization was a big threat. Furthermore, unsbustituted 1,3-butadienes are notorious for their instability, which could further add to the likelihood of polymerization. Second, since protic acid co-catalysts are used together with the imidazolidinone catalyst, acid catalyzed racemic background reactions could occur. Since the diene and the dienophile are tethered together, dilution effect is not a viable solution in minimizing the racemic background reaction. Since these background reactions go through an achiral transition state, the outcome of the reaction is a racemic mixture of products, decreasing the optical purity (*ee*). Third, the IMDA adducts are prone to epimerization at the aldehyde stereocenter, which could result in an epimer of a diastereomer of the reaction. Since the α-proton of the aldehyde is relatively acidic, it is possible for the basic amine catalyst and/or the conjugate base of the protic acid co-catalyst to readily epimerize the center with time (Scheme 4.26).

Scheme 4.26. Possible epimerization side reaction.[53]

Initial reports from the MacMillan group showed that a considerable amount of aromatic side product was being formed, presumably through dimerization (Scheme 4.27).[53] Following the formation of iminium ion (which is the activated form of the dienophile), the triene could be γ-deprotonated with the conjugate base of the protic acid co-catalyst to form the corresponding dienamine. The dienamine could be sufficiently electron rich to act as a diene and undergo dimerization *via* intermolecular DA. Hydrolysis of the iminium and subsequent elimination and oxidation would afford the aromatized side product. Though this particular side reaction seemed to be a big concern for flexible trienal systems, the system under consideration is not as flexible, so the undesired dimerization may be less likely to occur.

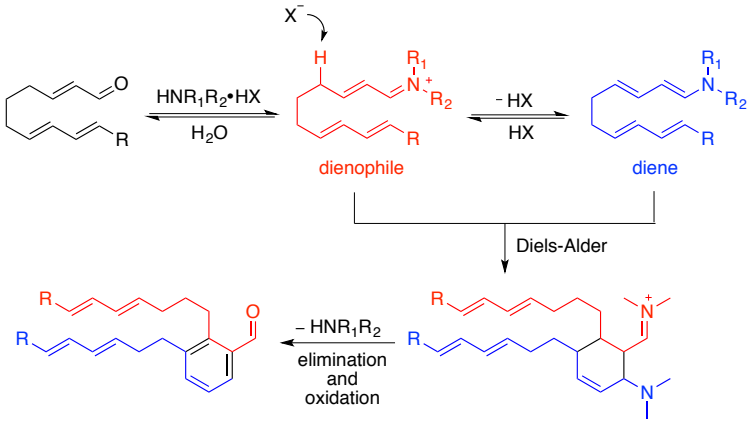

Scheme 4.27. MacMillan's proposed mechanism for the formation of dimerized side products.[53]

The extent of these undesirable side reactions depends on the inherent activity of the IMDA substrate. Fortunately, the side reaction could be somewhat controlled by choice of catalyst, co-catalyst, temperature, and solvent. In terms of the catalyst, MacMillan's second-generation imidazolidinone catalyst was selected based on his results of IMDA

reactions.[51b] In terms of the co-catalyst, more acidic protic acids ($HClO_4$, TfOH) tend to decrease product epimerization and starting material dimerization, due to decreased basicity of the corresponding conjugate base.[53] On the other hand, less acidic co-catalysts (TFA, TCA) tend to minimize acid promoted racemic background reaction and starting material polymerization.[53] Therefore, less acidic co-catalysts are often used for more reactive substrates, while more acidic co-catalysts are used to help activate less reactive substrates. In terms of temperature, less racemic background, epimerization, and dimerization occurs at lower reaction temperatures, which tend to improve product diastereo- and eantioselectivities.[53] However, higher temperatures tend to result in increased yields due to less starting material polymerization. Since starting materials polymerize when the rate of the desired reaction is slow, increasing temperature helps speed up the rate at the cost of obtaining mixtures of diastereomers and enantiomers. Hence, less reactive substrates are run at high temperatures. Finally, extensive studies done by the MacMillan group[53] suggested the importance of water in the reaction. Since water is both a product of iminium formation as well as an agent for iminium hydrolysis, various rate studies were required to find the precise amount of water that would positively affect the reaction outcome. Kinetic studies done in the MacMillan group suggested the optimal solvent to water ratio to be about 98:2 to maximize the rate of catalyst turnover.[53,54] They also found that solvents such as acetonitrile and chloroform effectively reduced the rate of polymerization and increased substrate and catalyst solubility, while butanol and isopropanol effectively minimized the epimerization side reaction.[53]

With these considerations in mind, IMDA using MacMillan's second-generation catalyst was investigated (Table 4.5). Minimizing starting material polymerization and/or decomposition was a challenging task due to highly unstable nature of the IMDA precursor. Polymerization/decomposition was evident at times even prior to setting up the reaction. Therefore, it was crucial for the rate of the IMDA reaction to be much faster than the rate of polymerization/decomposition of the starting material. Although at least three different diastereomers (*endo*, epimer of *endo,* and *exo*) were expected if the cyclization occurred successfully, the initial goal of the optimization was to increase the overall yield. Since it is known[53,54] that optimal solvent mixture is about 95:5 acetonitrile:water or 98:2 acetonitrile:water to maximize the rate of catalyst turnover, such solvent mixtures were used. Generally, use of MacMillan's second-generation catalyst resulted in faster reaction rates in comparison to first-generation catalysts (entries 7-8 & 18, Table 4.5), which resulted in higher yields due to less polymerization and/or decomposition of starting material. Temperature appeared to have an effect on the yield. Yield of the reaction suffered at higher temperatures (entry 3, Table 4.5), which could be attributed to decomposition of material. However, yields decreased at lower temperatures (entries 13 & 16, Table 4.5), which is probably due to decreased rate of the reaction, promoting starting material polymerization. Room temperature seemed to afford the best overall yield, which is likely due to increased rate of the reaction, consequently decreasing the rate of starting material polymerization. This increase in yield may happen at the cost of obtaining poor diastereo- and enantioselectivity. Less acidic co-catalysts (TFA, DCA) led to increased reaction time and decreased yield (entries 7-8 & 18, Table 4.5). Although less acidic co-catalysts were expected to decrease substrate

polymerization, resulting decrease in rate of the desired reaction could have a bigger impact on the overall yield. Kinetic studies done by the MacMillan group strongly implied that the rate of the reaction is directly proportional to acidity of the co-catalyst, since the rate of iminium ion formation is increased with increased acidity of the co-catalyst.[54] Therefore, more acidic co-catalysts (HBF_4, $HClO_4$) afforded comparably better results (entries 6 & 17, Table 4.5). Reaction time was important, as prolonged reaction time led to increased decomposition (entry 12 vs. 11, Table 4.5). Finally, concentration had an unexpected effect on the reaction rate. Since the diene and the dienophile are tethered together, overall concentration was expected to have less of an impact on rate. However, at drastically high concentration (entry 19, Table 4.5), the reaction was fully completed in 2 hours, albeit at the cost of decreased yield, which is probably due to increased decomposition.

Table 4.5. IMDA optimization using MacMillan's catalyst.

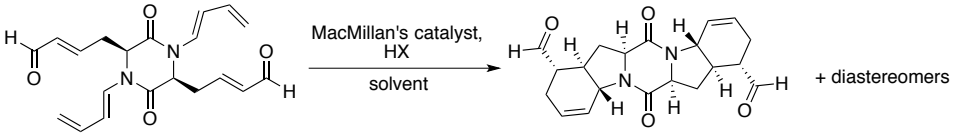

44 47

Entry	Catalyst (mol%)	HX (mol%)	Solvent [M]	Temp (^{o}C)	Time (h)[a]	Yield (%)[b]
1	2nd gen. (50)	$HClO_4$ (50)	MeCN:H_2O 95:5 [0.02]	rt	24	22
2	2nd gen. (20)	$HClO_4$ (20)	MeCN:H_2O 95:5 [0.05]	rt	24	42
3	2nd gen. (40)	$HClO_4$ (40)	MeCN:H_2O 95:5 [0.05]	40	22	<5[c]
4	2nd gen. (40)	$HClO_4$ (40)	MeCN:H_2O 95:5 [0.05]	rt	19	20
5	2nd gen. (40)	HCl (40)	MeCN:H_2O 95:5 [0.05]	rt	19	15
6	2nd gen. (20)	$HClO_4$ (20)	MeCN:H_2O 95:5 [0.1]	rt	21	62
7	1st gen. (40)	DCA (40)	MeCN:H_2O 95:5 [0.1]	rt	120	<30[d]
8	1st gen. (40)	TFA (40)	MeCN:H_2O 98:2 [0.3]	−20→30[e]	72	0[c]
9	2nd gen. (40)	$HClO_4$ (40)	MeCN:H_2O 98:2 [0.35]	4	4.5	36[c]
10	2nd gen. (40)	HCl (40)	MeCN:H_2O 98:2 [0.35]	rt	192	0[c]
11	2nd gen. (40)	HBF_4 (40)	MeCN:H_2O 98:2 [0.35]	rt	4	56[c]
12	2nd gen. (40)	HBF_4 (40)	MeCN:H_2O 98:2 [0.35]	rt	23	36
13	2nd gen. (40)	HBF_4 (40)	MeCN:H_2O 98:2 [0.35]	0→4	6	14[c]
14	2nd gen. (20)	$HClO_4$ (20)	MeCN:H_2O 98:2 [0.4]	rt	6	62
15	2nd gen. (40)	$HClO_4$ (40)	MeCN:H_2O 98:2 [0.4]	rt	18	20[c]
16	2nd gen. (40)	$HClO_4$ (40)	MeCN:H_2O 98:2 [0.4]	−20	24	17[c]
17	2nd gen. (40)	HBF_4 (40)	MeCN:H_2O 98:2 [0.4]	rt	2.5	68
18	1st gen. (40)	TFA (40)	MeCN:H_2O 98:2 [0.5]	rt	48	0[c]
19	2nd gen. (20)	$HClO_4$ (20)	MeCN:H_2O 98:2 [0.6]	rt	2	33[c]

[a] Reaction followed by TLC.
[b] Overall yield (including all diastereomers) over two steps (oxidation and IMDA).
[c] Decomposition/polymerization.
[d] Additional catalyst and HX (20 mol%, total 40 mol%) used after 48 h.
[e] Reaction held at −20 ^{o}C o/n, then 0 ^{o}C o/n, then 5 ^{o}C→rt with addition of more catalyst and HX (20 mol%, total 40 mol%), then 30 ^{o}C o/n

Taken together, the data obtained suggest the use of the second-generation imidazolidinone catalyst, more acidic co-catalysts ($HClO_4$, HBF_4), and a concentrated solvent mixtures (0.35 – 0.4 M) to achieve high overall yield at a faster rate (entries 14 & 17, Table 4.5). The robustness of the optimized conditions was confirmed when applied to the model system (Scheme 4.28).

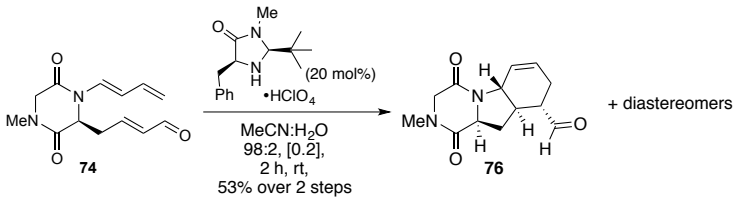

74 76

Scheme 4.28. Application of optimized conditions to the model system.

Derivatives of MacMillan's imidazolidinone catalysts[55] were synthesized and tested, but did not provide comparable results (3 d of reaction time, decomposition). Furthermore, other organocatalysts, such as Corey's oxazaborolidine catalyst,[56] *exo*-selective diarylprolinol silyl ether catalysts,[57] L-proline, and Kündig's chiral ruthenium catalyst[58] all displayed issues in activation of the starting material, which resulted in decomposition due to prolonged reaction time regardless of changes in catalyst loading and solvent concentration. Lewis acids, such as $ZnCl_2$ and Et_2AlCl afforded similar results, where the overall yield of the reaction suffered from either slow reaction rate or decomposition respectively.

Although superior in comparison to other organocatalytic IMDAs, optimized conditions using MacMillan's imidazolidinone catalyst posed difficulties, as the diastereoselectivity of the reaction remains to be elucidated. The reaction afforded a mixture of diastereomeric products that displayed almost identical physical properties, which made determination of diastereomeric ratio by ^{1}H NMR analysis impossible. Furthermore, ^{13}C NMR showed multiple aldehyde carbons, further suggesting the presence of various diastereomers. Attempted separation of individual diastereomers proved to be difficult by both manual and automated (HPLC) column chromatography methods.

In a different approach, the mixture of IMDA cycloadducts was carried on for derivatization with 2,4-dinitrophenylhydrazine (2,4-DNPH), since the resultant hydrazone products would possess visible chromophores (for UV detection) that could aid in the separation process. Furthermore, derivatization could impart relative and absolute stereochemical information as well as enantioselectivity of the IMDA reaction (Scheme 4.29). Gratifyingly, the major hydrazone derivative was isolated (detected by

HRMS and ^{1}H NMR) albeit in small quantities upon HPLC purification. X-ray analysis of the derivative should elucidate the desired absolute stereochemical information.

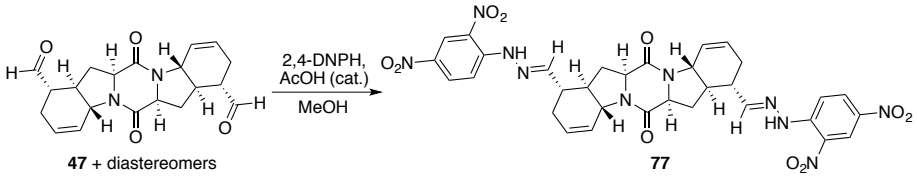

Scheme 4.29. Synthesis of hydrazone derivative.

Alternatively, IMDA by more traditional thermal methods afforded the desired cycloadduct in modest yields (Scheme 4.30). As expected, formation of insoluble decomposed materials was evident as the reaction progressed. To avoid potential polymerization *via* radical mechanism, catalytic amount of 2,6-di-*tert*-butyl-4-methylphenol (BHT) was added as a radical scavenger. The reaction was conducted in a sealed tube, using degassed solvent, and heating in a sand bath. There was an apparent activation barrier, as the cyclization did not occur at lower temperatures (60-80 ^{o}C) even after prolonged reaction time (2 days).

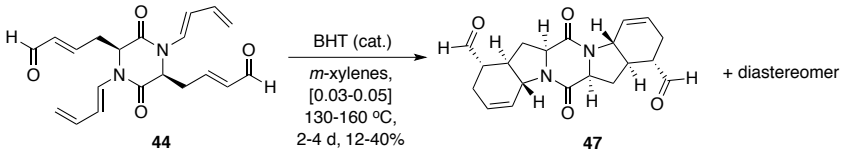

Scheme 4.30. Thermal IMDA reaction.

Since insoluble polymer-like materials were recovered after the reaction even with the addition of BHT, the polymerization might occur by ionic means. A similar conclusion was suggested by Molinski, in his investigation of IMDA in the synthesis of Muironolide A.[59] He proposed that the polymerization could be attributed to the tendency of terminally unsubstituted 1,3-butadiene moiety in tethered systems to polymerize.[59] When terminally substituted 1,3-butadiene IMDA substrates were used, Molinski observed a dramatic increase in yield. However, the use of terminally unsubstituted 1,3-butadienes in

IMDAs are not entirely unprecedented, as Oppolzer illustrated[60] the use of terminally unsubstituted dieneamides in IMDAs as early as 1975, albeit in modest yields.

Although further improvement could be made to obtain better results in terms of diastereoselectivity, taming the highly unstable IMDA precursor towards IMDA cycloaddition was nevertheless an accomplishment on its own.

4.7) Alternative approaches

Due to the apparent instability of the IMDA precursor **44**, in which the rate of substrate polymerization outcompeted the desired cycloaddition reaction, alternative routes to arrive at the 6-5-6-5-6 core of the rostratins were investigated. The observed reactivity of **44** towards polymerization and/or decomposition could arise from highly reactive nature of either the unsubstituted 1,3-butadiene or the α,β-unsaturated aldehyde moieties. Therefore, altering the diene or the dienophile with functional groups that may induce chemical stability towards undesired side reactions that ultimately result in decomposition was explored. Another potential approach would be to switch the position of the diene and dienophile on the DKP, which would afford information on the reactivity of dienamides in comparison to alkyldienes. Moreover, a double *inter*molecular DA on functionalized DKP could be another option. Finally, alternative methods of cycloadditions could be considered, such as cationic radical cyclization and transition metal mediated cyclization.

4.7.1) Alteration of electron-poor dienophile

To assess the reactivity of the α,β-unsaturated aldehyde as the dienophile, alternative electron-poor dienophiles, such as phenyl sulfone, methyl ester, and methyl ketone could be employed in the IMDA reaction (Scheme 4.31).

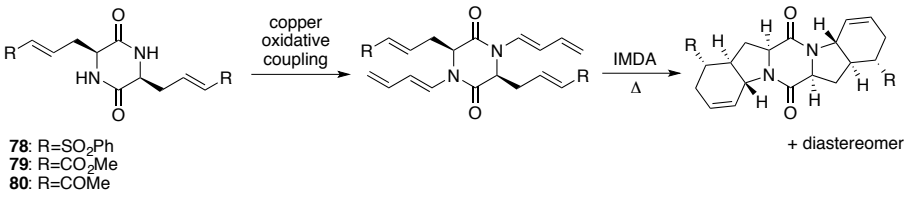

78: R=SO_2Ph
79: R=CO_2Me
80: R=COMe

Scheme 4.31. Use of alternative electron-poor dienophiles for IMDA.

However, use of such dienophiles would limit the scope of IMDA reaction, since organocatalysts that activate *via* iminium ion formation (prolinols, imidazolidinones) cannot be utilized, since esters and ketones are not as reactive as aldehydes. Furthermore, use of phenyl sulfone as the dienophile would be even more limited to thermal IMDA reactions. Nonetheless, these electron-poor alternative dienophiles could be comparably activated towards IMDA.

The synthesis of methyl ketone DKP derivative **80** could not be achieved using previously discussed routes due to the highly reactive nature of methyl ketones towards acidic and basic conditions. Efforts to mask the carbonyl by utilizing reduced forms of the moiety were not productive due to protecting group orthogonality issues (Scheme 4.32). Leaving the secondary alcohol unprotected led to decomposition under *N*-Boc removal conditions.

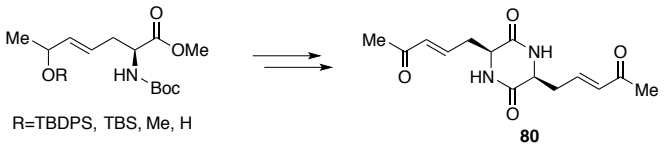

R=TBDPS, TBS, Me, H

80

Scheme 4.32. Proposed synthesis of **80**.

Attention was then given to synthesis of phenyl sulfone and methyl ester derivatives **78** and **79**. The initially proposed synthesis of **78** and **79** was to use cross-metathesis (CM) of known common intermediate **(−)-81**[61] and requisite olefins (Scheme 4.33).

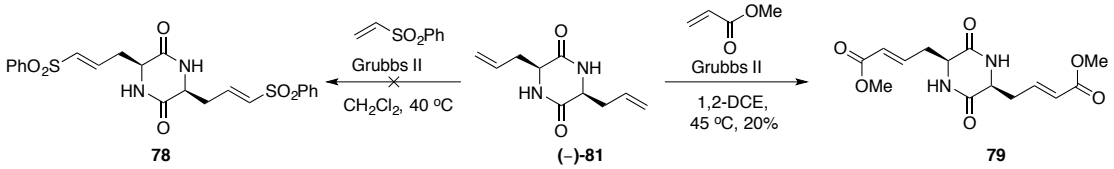

78 **(−)-81** **79**

Scheme 4.33. Attempted synthesis of **78** and **79** using cross-metathesis.

However, due to insurmountable solubility issues of **(−)-81** in solvents that are commonly used in CM (hexanes, toluene, CH_2Cl_2, 1,2-DCE, EtOAc) and other activation issues, the corresponding products could not be obtained in synthetically useful yields (Scheme 4.33). A diverse array of solvents (CH_2Cl_2, 1,2-DCE, EtOAc, DMC, MeOH, acetone, dioxane, and PhMe) and catalysts (Grubbs I & II, Hoveyda-Grubbs I & II, Zhan) were examined at various temperatures (refluxing conditions or in microwave reactor) with a large excess of the coupling partner olefin (>20 equiv. of methyl acrylate or phenyl vinyl sulfone), but none resulted in sufficient quantities of the desired products. Interestingly, when the amide nitrogens of **(−)-81** was protected with benzyl groups, it was readily soluble in standard CM solvents (i.e. CH_2Cl_2), and the reaction could be run at high concentration (0.25 M), which resulted in nearly quantitative yields (Scheme 4.44). However, installation of benzyl moieties on the amide nitrogens of **(−)-81** or DKPs with acyclic substitutions in general, is a well-known unproductive process due to the high propensity of the α-proton epimerization to the more thermodynamic stable *trans* DKP under basic conditions. Furthermore, removal of the benzyl groups may become difficult at later stages of the synthesis, since it often requires harsh reaction conditions.

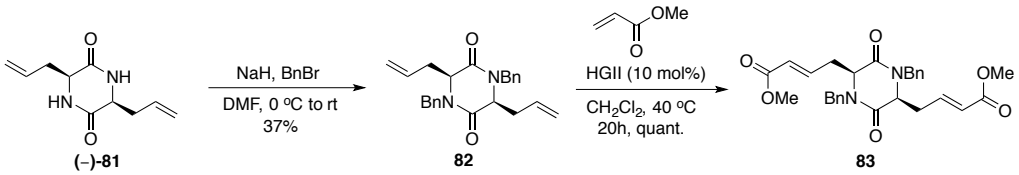

Scheme 4.44. Synthesis of di-benzyl protected **83**.

Fortunately, the phenyl sulfone DKP **(−)-78** was accessed using a similar synthetic route to **(−)-46** starting from a common intermediate **84** (Scheme 4.10) in good yields (Scheme 4.45). Hydrolysis of the methyl ester **(+)-85** to the corresponding acid **87** could be achieved only *via* the use of trimethyltin hydroxide (Me_3SnOH), due to tendency of phenyl sulfone elimination under basic conditions (LiOH, $SiMe_3OH$, $Ba(OH)_2•8H_2O$). Formation of *trans* DKP of **(−)-78** was not observed under the reaction conditions.

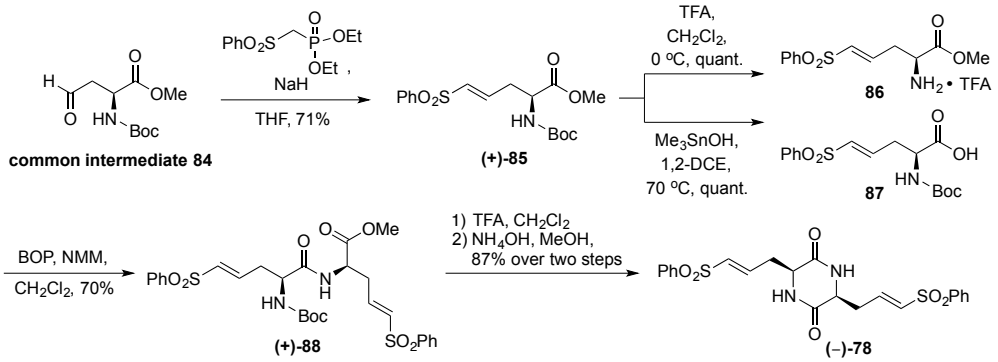

Scheme 4.45. Synthesis of phenyl sulfone DKP **(−)-78**.

Disappointingly, methyl ester DKP **83** could not be obtained using similar routes due to lack of orthogonality in the synthesis. Further synthetic investigation could be done in the future to access **83**.

Nevertheless, with phenyl sulfone DKP **(−)-78** in hand, copper-oxdative coupling with **66** and subsequent thermal IMDA were explored. For the coupling step, previously optimized conditions (Table 4.4) were tested first. Unfortunately, unlike the TBDPS DKP **(−)-46**, activation issues were encountered with **(−)-78**. For instance, complete conversion of starting material was not observed even after 28 days (not shown, reaction

monitored by LRMS). However, prolonged reaction time (>5 days) tend to give rise to oxidized side products that were detected by ^{1}H NMR when aliquots of the reaction were taken at various time points. The nature of oxidized side products could be from both **66** and **(+)-89**, as dienes are notorious for being oxidized upon standing over extended periods of time. Interestingly, slight increase in the O_2 pressure by conducting the reaction under an O_2 manifold increased the formation of oxidized side products (Entry 12, Table 4.6). A Possible reason for using excess **66** in copper-oxidative couplings in both TBDPS DKP **(−)-46** and sulfone DKP **(−)-78** cases could be attributed to oxidation of **66** with time. However, since the oxidation of the product DKP of **(−)-46** was not observed even when the reaction was conducted under slight positive pressure of O_2 over prolonged period of time, suggests the more reactive nature of **(+)-89** under oxidative conditions. Increasing copper catalyst loading (1 equiv.), changing copper catalyst ($Cu(OTf)_2$), increasing amount of **66** (portion-wise addition, 10 equiv.), addition of additives (NMI), and changing solvent mixture (TFE:1,2-DCE) did not result in either increase in conversion or yield (Table 4.6). Difference in electronics of the DKP was considered, since phenyl sulfones are more electron-withdrawing than allyl TBDPS ethers, which would be supported by the relative decrease in pKa value of the amide proton of **(−)-78** in comparison to **(−)-46**. If the pKa was indeed lower, addition of catalytic amounts of amine additives could improve the yield.[41b] However, since this was not the case (Entry 6, Table 4.6), the pKa difference may not be as pronounced as expected. It is possible that the catalytic amount of NMI aided in decomposition of material, since phenyl sulfone moieties are prone to elimination under basic conditions. Nonetheless, the best yield of **(+)-89** was obtained a with slight variation of the

previously optimized protocol (6 equiv. of **66**) in 3 days (Entry 7, Table 4.6). Due to the limited solubility of **(−)-78** in organic solvents, which is a testament of increased polarity of the DKP, dissolution of **(−)-78** had to be ensured prior to addition of other reagents.

Table 4.6. Copper-oxidative coupling optimization for phenyl sulfone derivative.

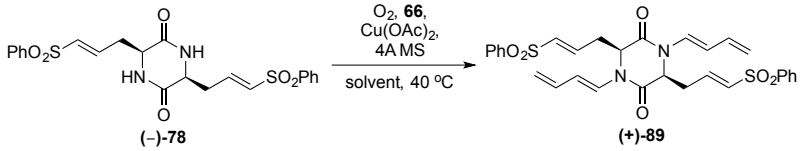

(−)-78 (+)-89

Entry	66 (equiv.)	$Cu(OAc)_2$ (equiv.)	Solvent [M]	Additive	Time (d)	Yield[a] (%)
1	5	30	DMSO:DCM [0.25]	None	1.7	25[b]
2	5	30	DMSO:DCE [0.25]	None	4	42
3	5	30	DMSO:DCE [0.25]	None	5	35
4	5	30	25% DMSO:DCM [0.25]	None	2.8	0
5	5	30	DMSO:TFE [0.25]	None	4	0
6	5	20	DMSO:DCM [0.25]	NMI (40 mol%)	7	0
7	6	30	DMSO:DCM [0.25]	None	3	48
8	5 then 1[c]	30	DMSO:DCM [0.25]	None	5	44
9	5 then 1[d]	30	DMSO:DCM [0.25]	None	16	5
10	5 then 2[e]	30	DMSO:DCM [0.25]	None	15	38
11	5 then 2[e]	20 then 80[f]	DMSO:DCM [0.25]	None	19	<5
12	4 then 2[g]	30	DMSO:DCM [0.25]	None	13	22
13	10	1	DMSO:DCM [0.25]	None	11	0[h]

[a] Isolated yield. O_2 balloon was used in all cases unless specified.
[b] Mono-coupled product was also isolated in 40%.
[c] Additional equivalent of **66** added on day 2.
[d] Additional equivalent of **66** added on day 6.
[e] Additional equivalent of **66** added on day 5 then day 9.
[f] $Cu(OTf)_2$ was used instead. Additional catalyst added on day 3.
[g] Additional equivalent of **66** added on day 4 and 7. Switched to O_2 manifold on day 7.
[h] Reaction done in sealed tube with a headspace of O_2.

With requisite IMDA precursor **(+)-89** in hand, thermal IMDA conditions were investigated. Various solvents (*m*-xylenes, chlorobenzene, 1,2-dichlorobenzene, NMP) were screened at high temperatures (160-190 ^oC). The reactions were generally done in dilute conditions (0.05 M) in a sealed tube. The reaction was heated using either microwave irradiation or sand bath. Microwave irradiation did not necessarily speed up the rate of the reaction, as the presence of starting material (along with decomposed material) was noted even after seven 1 hour cycles at 160 ^oC. Therefore, heating in sand bath was operationally easier as the rate of conversion of the starting material seemed to

be sluggish at high temperatures. Similar to aldehyde IMDA precursor **44**, **(+)-89** also was prone to rapid polymerization/decomposition upon standing. Addition of a catalytic amount of BHT as radical inhibitor seemed to minimize extent of polymerization. The desired cycloadduct was obtained as a mixture of diastereomers in synthetically meaningful yield when NMP was used as solvent, and resulted in less decomposed material (Scheme 4.46).

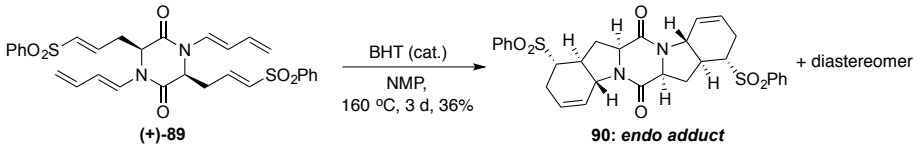

Scheme 4.46. IMDA of sulfone derivative **(+)-89**.

With the exciting result, a potential formal synthesis to Nicolaou's key intermediate[23] was envisioned (Scheme 4.47). Presumably, if the IMDA afforded more of the *endo* adduct, the 4,4'-epimer of Nicolaou's key intermediate could be obtained *via* 1,2-elimination of the phenyl sulfone moiety. Alternatively, if any appreciable amount of *exo* adduct could be obtained and isolated, it would afford the exact stereochemistry observed in his key intermediate. This reaction has synthetic potential, since facile elimination of phenyl sulfone moiety was observed during the synthesis of phenyl sulfone DKP **(−)-78**.

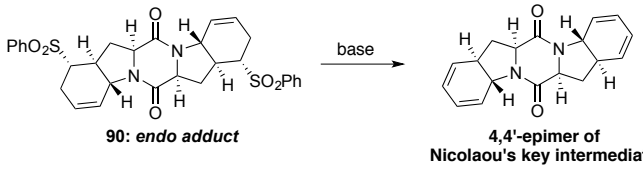

Scheme 4.47**.** Possible formal synthesis of 4,4'-*epi*-epicoccin G.

4.7.2) Alteration of diene

Since lack of terminal substitution, or substitution in general, of the 1,3-butadiene moiety on the tether seemed to impart instability on the IMDA precursors (whether on the aldehyde system **44** or the sulfone system **(+)-89**), synthesizing substituted versions of

1,3-butadiene trifluoroborate **66** may be useful. One of the ways to install substituents is early on the synthesis (Scheme 4.48). The common intermediate alkyne **67** was subjected to known one-pot haloboration conditions[62] to afford the corresponding pinacol boronate **91**. Subsequent elimination of the mesylate followed by conversion to potassium trifluoroborate salt afforded **92** in good yield (Scheme 4.48).

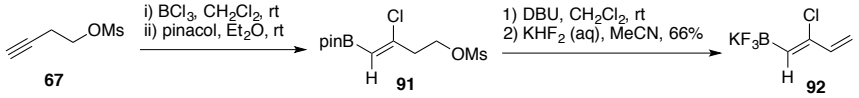

Scheme 4.48. Synthesis of **92**.

However, when the chlorosubstituted diene substrate **92** was used in the copper-oxidative coupling step with TBDPS DKP **(+)-69**, no product was formed using the previously optimized conditions (Scheme 4.49). In fact, only polymerized protodeboronated diene was recovered after 6 days along with unreacted starting material DKP **(+)-69**. Increasing the amount of **92** (10 equiv.) did not afford the coupled product or even the mono-coupled product. A possible explanation may be that the presence of bulky chloride atom on the 2-position of the diene increases sterics of the potassium trifluoroborate salt **92**, thus preventing the desired reaction to occur. Furthermore, Batey's original protocol[41] did not contain any substrates that had electron-withdrawing groups in the potassium alkenyltrifluoroborate moiety, possibly because they are less likely to couple under the given conditions.

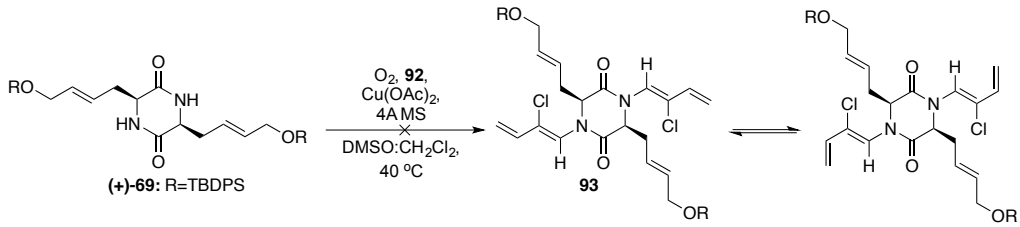

Scheme 4.49. Attempted synthesis of **93**.

Alternative methods of C-N coupling reactions could be attempted in the future to afford the desired product **93**. Furthermore, **92** (Scheme 4.48) is an interesting substrate that could be of use in other syntheses.

A terminal substitution on the diene moiety was envisioned next. Particularly, cross-metathesis (CM) conditions were of interest, since **66** could be utilized as the starting material. Although many different types[63] of reactions with potassium trifluoroborates as the starting materials are known in the literature, they have not been used for CM processes to the best of our knowledge. Initial screening of conditions suggested the use of excess amount of phenyl vinyl sulfone, and more active Hoveyda-Grubbs II catalyst. Since mixtures of potassium trifluoroborates cannot be separated, it was important that the transformation would result in 100% conversion of starting material. ^{1}H NMR detected no starting material **66**, but the presence of the desired product **94** after 6 days (Scheme 4.50).

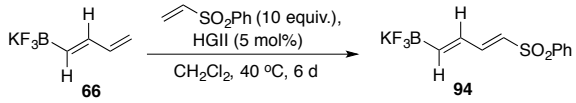

Scheme 4.50. Synthesis of **94**.

However, the reaction has problems. For instance, due to small molecular mass of **66**, and the relatively large molecular mass of the catalyst, 5 mol% catalyst loading is actually a large amount of expensive catalyst (at 1 g of **66**, 196 mg of HGII). Furthermore, since at least 5-fold excess of the potassium trifluoroborate salt is used in the copper-oxidative coupling step, this reaction is not economically viable. Although the sole presence of **94** was detected, the overall yield was not calculated, so it is possible that some of **66** underwent decomposition (*via* protodeboronation) during the course of the reaction,

which would not be entirely unreasonable, since some amount of protodeboronated **66** dimers are present after copper-oxidative coupling conditions at 40 ^{o}C over few days.

Nonetheless, potassium trifluoroborate derivative **94** was synthesized in hopes of utilization in a different cycloadditioin reaction (Scheme 4.51). If the copper-oxidative coupling of **94** with **(−)-81** occurred successfully, the diene moiety would then be electron-poor, while the dienophile moiety would be relatively less electron-poor. Therefore, based on electronic differences, the desired [4+2] cycloaddition could occur under thermal conditions. A mixture of diastereomeric products would be obtained, which could then be utilized towards the synthesis of Nicolaou's key intermediate[23] under elimination conditions as discussed in previous section.

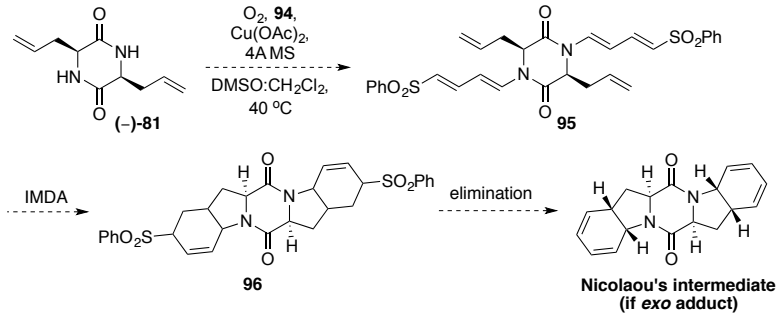

Scheme 4.51. Alternative [4+2] approach.

Although the proposed synthesis was not completed, much synthetic information was gained about the reactivity of alkenyl trifluoroborates under CM conditions.

4.7.3) Intermolecular DA considerations

Alternative approaches in utilizing electron-poor DKPs as dienophiles in intermolecular DA cycloadditions with known dienes were considered, in the intent of using the resulting cycloadducts for allylic C-H amination[64] to furnish the desired 6-5-6-5-6 system (Scheme 4.52).

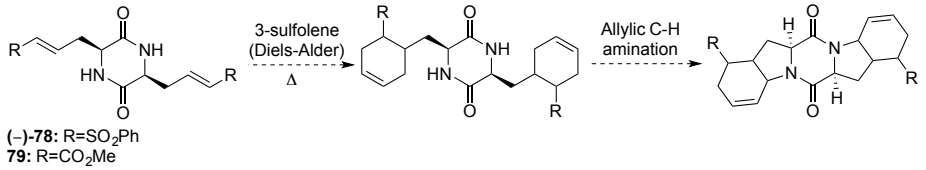

Scheme 4.52. Proposed intermolecular DA.

Unfortunately, the desired DA cycloaddition with 3-sulfolene and either the phenyl sulfone DKP **(−)-78** or methyl ester DKP **79** resulted in either complete recovery of the starting material DKP or decomposition. Various solvents (DMF, NMP, DMSO, chlorobenzene) were tested at high temperatures (reflux, 200 ^{o}C μW irradiation), but none led to detectable amount of the desired cycloadduct. Other dienes (Danishefsky's diene, furan) were reacted without much success. This approach does have some potential problems, such as controlling the diastereoselectivity of both the DA and the allylic C-H amination. It is highly likely to obtain mixture of diastereomers, which may be difficult to separate. However, more extensive investigation could be done for this approach.

4.7.4) Alternative [4+2] cycloadditions

So-called unactivated [4+2] cycloadditions could occur in the presence of heat, high pressure, transition metals, light, or radical cations just to name a few. In particular, transition metal-mediated[65] and radical cationic[66] cycloadditions were of interest for the present study.

Since the reaction of **66** with varying DKP derivatives (TBDPS DKP **(−)-46** and phenyl sulfone DKP **(−)-78**) under copper-oxidative coupling methodology seemed to work reasonably well, coupling of **66** with the alkene DKP **(−)-81** was investigated using previously optimized conditions in hopes of employing the coupled product for transition

metal mediated [4+2] reactions. Not surprisingly, similar issues with activation of starting material DKP and undesired side reactions were encountered. The best yield was obtained using 5 equivalents of **66** (addition of 4 equiv. in the beginning, and additional 1 equiv. after few days), 30 mol% of $Cu(OAc)_2$, in a mixture of DMSO and CH_2Cl_2 at 0.24 M (Scheme 4.53). However, the reaction took 20 days to reach completion at the cost of obtaining oxidized side products and a minor amount of mono-coupled product (26%). Although subsequent [4+2] cycloaddition of **(+)-97** has not been conducted as of yet, it has some promise, since such cycloadditions, especially via transition metal-mediation are known in the literature.[65]

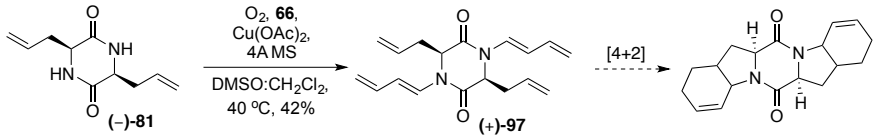

Scheme 4.53. Synthesis of alkene DKP **(−)-81** for [4+2] cycloaddition.

With promising results, alkynyl DKP **(−)-98** was synthesized from L-propargyl glycine derivatives using same synthetic sequence employed in the synthesis of alkene DKP **(−)-81** (Scheme 4.54).

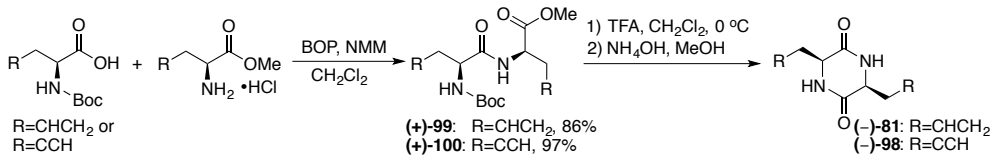

Scheme 4.54. Synthesis of **(−)-81** and **(−)-98**.

However, the alkynyl DKP **(−)-98** did not successfully couple with **66** under various copper-oxidative conditions (Scheme 4.55).

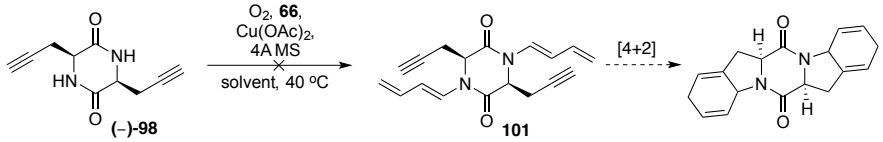

Scheme 4.55. Attempted synthesis of **101** for [4+2] cycloaddition.

A possible explanation for this failed attempt could be that the terminal alkyne of the DKP is coordinating to the copper as a ligand, consequently inhibiting the desired reaction. This hypothesis could be verified by synthesis of terminally substituted alkynyl DKPs in the future. Furthermore, solubility issues of **(−)-98** were apparent especially in comparison to other polar DKPs (**(−)-78** and **(−)-81**). Even with 1:1 ratio of DMSO and CH_2Cl_2, heating of the DKP was needed to achieve dissolution. As discussed earlier, the amount of DMSO cannot be increased for the reaction to occur, since over excess of DMSO could act as a ligand on copper, thereby shutting down the reaction. Nonetheless, if these problems could be resolved, and the subsequent cycloaddition executed, the resulting cycloadduct could be used for the synthesis of scabrosins, since it contains the unsaturation at 4,4'-positions of the 6-5-6-5-6 framework (Scheme 4.7).

Activation of **(+)-69** towards unactivated DA was considered next. Initial data obtained by thermal study[67] of **(+)-69** under common cycloaddition conditions only resulted in apparent removal of TBDPS groups and decomposition of material (Scheme 4.56). Full recovery of starting material was obtained when the reaction was heated at significantly lower temperatures (60 ^oC) for extended periods of time (2 weeks), suggesting the presence of a significant activation barrier to achieve cyclization. Lewis acid ($Cu(OTf)_2$) mediated cycloaddition[65b] at 80 ^oC for 7 days did not afford the desired cycloadduct, but resulted in removal of the TBDPS groups and decomposition.

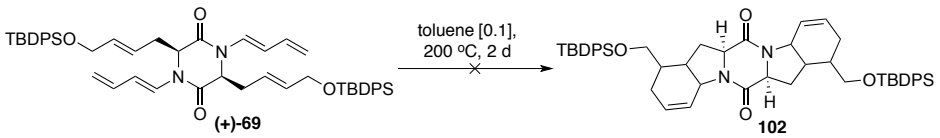

Scheme 4.56. Attempted unactivated DA under thermolysis.

Next, cationic radical cyclization was investigated. Acidic oxidizers, such as tris(*p*-bromophenyl)aminium hexachloroantimonate, generates cationic radicals by abstraction of one electron from the system.[66a] Consequently, the reaction undergoes an electron transfer catalysis (ETC), that could result in cycloadducts that could be obtained by traditional DA reactions. ETC cycloadditions are believed to have activation barriers of 1-5 kcal/mol, often 10-60 kcal/mol lower than the corresponding thermal cycloadditions.[68a] Furthermore, ETCs are good for sterically encumbered substrates especially when such systems fail under thermal conditions.[68b] Generally, substrates that possess lower redox potentials (electron-rich) are more easily oxidized to a cation radical. In terms of mechanism, ETC could be [3+2] or [4+1] (numbers denoting number of electrons in the system, Scheme 4.57).

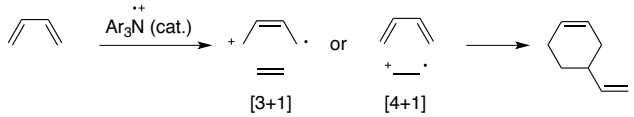

Scheme 4.57. Simplified example of ETC under [3+1] or [4+1].

[3+2] Cycloadditions are symmetry forbidden, step-wise process, and the radical cation is formed from the diene. The diene would be relatively more electron rich in comparison to the dienophile for a [3+2] cycloaddition. On the other hand, [4+1] cycloadditions are symmetry allowed, concerted process, and radical cations are formed from dienophiles. [4+1] Cycloadditions could also occur on systems where the diene and dienophile are identical. In addition, vinylcyclobutane could be obtained and subsequent rearrangement could lead to the same cycloadduct.[68c] Dienes that are in the *s*-cis conformation tend not to react *via* vinylcyclobutane mechanism.[68c]

TBDPS DKP **(+)-69** was tested under ETC conditions using tris(*p*-bromophenyl)aminium hexachloroantimonate as catalyst under standard conditions (Scheme 4.58).[66] The relative redox potential of the diene moiety in comparison to the dienophile on **(+)-69** was speculated, but not measured, as such process would be difficult on a tethered system (using cyclic voltammetry). One possible way to predict the relative redox potential of the diene and the dienophile would be *via* theoretical means (obtaining the relative electron density information by calculation). Furthermore, in order for the reaction to take place, the redox potential of the substrate has to be lower than that of the catalyst for the formation of radical cation. Hence, without such information, the only way to determine if the desired reaction would take place was to conduct the actual experiment. In comparison to thermolysis, ETCs are known to occur rapidly using small amount of catalyst (< 20 mol%) if the redox potential of the substrates are favorable (within minutes). However, this was not observed for the present case. Conversion of the starting material proceeded only after additional amount of catalyst was added (up to 50 mol%) (Scheme 4.58). Even upon stirring overnight with addition of more catalyst (1 equiv. total), the reaction failed to reach completion.

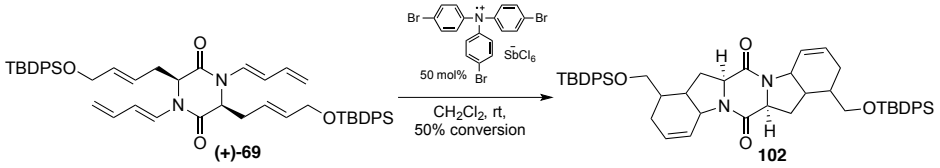

Scheme 4.58. Attempted application of ETC.

Although isolation of unreacted starting material was possible by silica gel chromatography, further purification of the reaction mixture by HPLC did not provide clean isolable material. However, ^{1}H NMR analysis of the minor fraction displayed disappearance of the proton peaks corresponding to the diene moiety, and formation of

methylene protons. The reaction was repeated several times (with addition of catalytic amount of 2,6-lutidine as acid scavenger to determine if the reaction is taking place *via* acidic mechanism or ETC[68d]), but in all cases, there seemed to be an activation issue, as increased catalyst loading and reaction time were required. These results suggest that the current system may not have the favorable redox potential match with the catalyst and/or the diene and dienophile. However, since small amount of what could potentially be the cycloadduct was detected, there may be potential for utilizing ETC using other catalysts (iron-based catalysts) or methods (photoredox).

4.8) Future work

Although the desired double IMDA was accomplished for both aldehyde DKP **44** (using MacMillan's imidazolidinone catalyst and thermolysis) and phenyl sulfone DKP **(+)-89** (using thermolysis) systems, determination of relative and absolute stereochemistry of the adducts is needed. Further efforts toward optimization of IMDA conditions using MacMillan's catalyst could be done to obtain high diastereo- and enantioselectivities.

Furthermore, considerations toward either a formal synthesis (obtaining Nicolaou's key intermediate[23]) or total synthesis of rostratin A could be made using either the aldehyde system or the phenyl sulfone system. Although the yield for the IMDA step (as well as the prior copper-oxidative coupling step) using the phenyl sulfone system is not as comparable, the route to Nicolaou's key intermediate is relatively more obviated than the aldehyde system (Scheme 4.47). For the aldehyde derivative, assuming the major cycloadduct is the *endo* diastereomer **47**, Pinnick oxidation[69] followed by a variation of Barton's decarboxylation-oxygenation protocol[70] of the resulting carboxylic acid, could

furnish alcohol **103** as a mixture of diastereomers (Scheme 4.59). Subsequent oxidation would afford the ketone **104** which could be utilized towards the synthesis of (−)-rostratin B or 9,9'-epimer of (−)-rostratin B. Alternatively, alcohol moiety of **103** could be eliminated, in which case the 4,4'-epimer of Nicolaou's intermediate could be obtained.

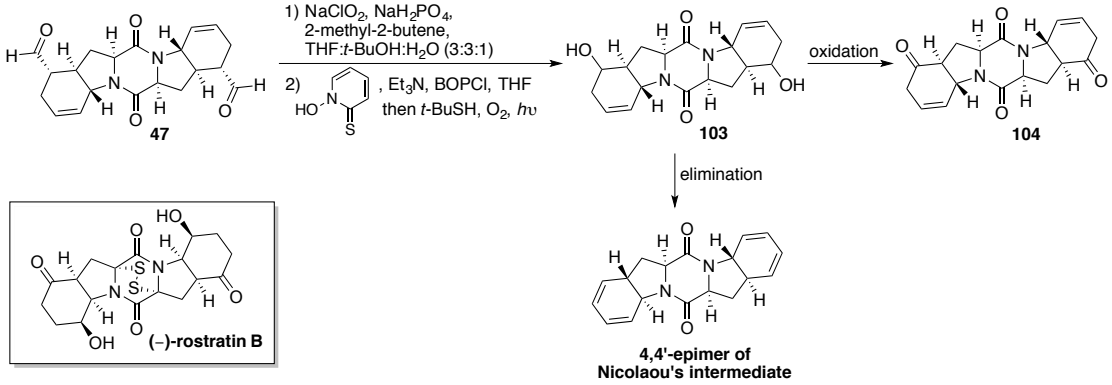

Scheme 4.47. Proposed remaining steps.

Another possible approach would be to use photoredox chemistry in place of Barton's decarboxylation-oxygenation protocol. Recently, a visible-light induced photocatalytic reaction for oxidative C—C bond cleavage of aldehydes to generate corresponding ketones has been reported.[71] This procedure was of interest, since the desired decarbonylation-oxygenation transformation of **47** to **104** could occur in single transformation. The mechanism presumably goes through the reductive quenching cycle (Scheme 4.48). Enamine **A** could be generated *in situ* from the aldehyde and secondary amine, which would then be oxidized to cation radical **B** through the reductive quenching process. Ru(I) could then be oxidized by oxygen in air to regenerate Ru(II) and superoxide species $[O_2]^{\cdot-}$ which would subsequently react with **B** to yield the final product ketone.

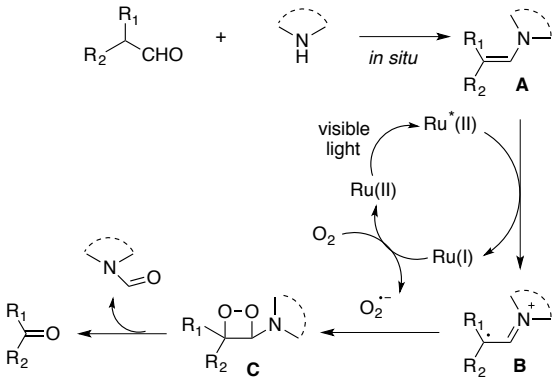

Scheme 4.48. Proposed mechanism of phodoredox reaction.[71]

However, the precise mechanism of the reaction is debatable, since oxygen is a known quencher of the excited state of $Ru(bpy)_3Cl_2$ (*via* energy transfer), which results in singlet oxygen formation. This process would also afford the same C—C cleavage event, suggesting mechanism against the involvement of **B** in the catalytic cycle. Such process was proposed by a different group in the same year,[72] albeit on α-alkoxy aldehydes. Substrates that did not contain the α-alkoxy substituent either afforded poor yields or did not work at all.

A test reaction using one of the substrates reported (Scheme 4.49) in the communication[71] was conducted on an identical scale. Although the reaction presumably reaches near completion in 24 h (by GC), this result was not observed even after 48 h. GCMS and ^1H NMR analysis showed predominant presence of left over starting material and relatively minor formation of the product. Similar results were obtained when the reaction was conducted under slightly positive pressure of oxygen.

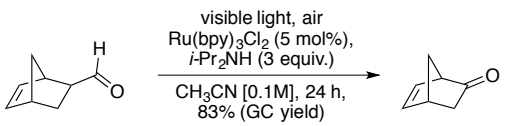

Scheme 4.49. Reported photoredox reaction.

Interestingly, the developed methodology in the report[71] was based only on the use of $Ru(bpy)_3Cl_2$ as photocatalyst, and did not mention the use of any other catalysts. Therefore, alternative photocatalysts ($[Ir(dtbbpy)(ppy)_2][PF_6]$ and Fukuzumi's acridinium-based organic salt[73]) that possess different redox potential were tested and resulted in no improvement in terms of conversion. As the protocol used excess of amine base, prolonged exposure of cycloadduct **47** to such conditions could be detrimental. This was the case when the reaction was applied to the actual system (Scheme 4.50).

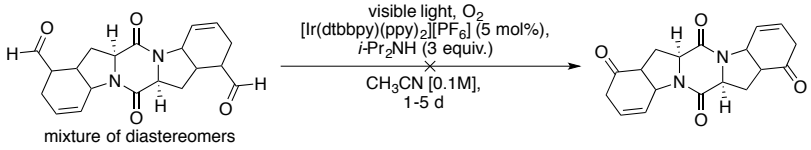

Scheme 4.50. Attempted application of photoredox reaction.

The reaction was conducted using slightly increased wattage (20 W) of compact fluorescent light bulb (CFL) and iridium-based photocatalyst. Iridium-based catalysts are generally known to perform better in terms of oxidation of the enamine to **B** as well as in generating the superoxide species (Scheme 4.48).[74] The progress of the reaction was monitored *via* GCMS over 5 days. Although the reaction did eventually reach full conversion of starting material over 5 days, no product was observed in the final reaction mixture (Scheme 4.50). Instead, ^1H NMR and TLC of the reaction mixture suggested decomposition of material. These results were expected, since the compound would likely decompose under these conditions over prolonged period of time. However, presence of the desired ketone product was detected by GCMS during the course of the reaction, which suggested that the reaction was taking place, but the slow conversion rate decomposed the product. Therefore, further investigation could be done to increase the rate of the desired transformation by screening various photocatalysts with different

redox potential, method of oxygen delivery, alternative light sources, solvents, and amine bases. Extensive screening could also provide information on the possible mechanism of the reaction.

4.9) Conclusions

Various efforts toward the synthesis of ETP alkaloids that contain C_2 symmetric 6-5-6-5-6 framework (rostratins, in particular) have been made. Invaluable information on the reactivity of DKPs was obtained through the process. In particular, optimization of diastereoselective synthesis of acyclic DKPs has been made, which could be a valuable addition to the synthesis of DKP in general. Unprecedented application of Batey's copper-oxdative coupling methodology[41] in total synthesis was successfully demonstrated using newly developed potassium trifluoroborate 1,3-butadiene reagent **66**. This C—N bond forming protocol is superior in comparison to the alternative well-known method of using vinyl iodides and amides under copper catalysis[75] for a few reasons. Firstly, vinyl iodides (or vinyl halogens) are generally not as stable as potassium alkenyltrifluoroborate salts. This difference in stability is even more pronounced for unsubstituted 1,3-butadienes. For instance, when **66** was reacted under known halodeboronation protocols[76] to convert the vinyl trifluoroborate to corresponding vinyl halogens, the reaction only provided decomposed material. Secondly, C—N bond forming methods using vinyl iodides are operationally not as simple as the present protocol, since reactions have to be set up in the absence of moisture and oxygen (in the glovebox, using Schlenk flasks). Finally, copper catalysis using vinyl iodides and amides generally requires heating at high temperatures (90-110 ^{o}C) in the presence of excess base.[75] Such conditions were

reported to result in racemization of chiral DKPs (*via* epimerization of *cis* to *trans*) during the synthesis of tadalafil analogues.[77] Although racemization was minimized when the reaction was conducted at low temperatures (14 ^{o}C) using reduced amount of base and super stoichiometric amount of copper (2 equiv. of CuI) over 15 days, consistently satisfactory yields were not obtained.[77]

Investigation of the key step—double IMDA cycloaddition also provided important information for the potential application of this protocol in the synthesis of other structurally similar ETPs. Although the diastereo- and enantioselectivity of the reactions remain to be determined, promising yields were obtained using MacMillan's imidazolidinone catalyst at relatively short reaction times (2-6 h). The double IMDA reaction is in essence a powerful tool that allows the formation of six new stereocenters in one transformation. Moreover, such multiple asymmetric reactions are known to generally impart increased enantiomeric excess to the final product in comparison with the analogous single transformation.[78] Further investigation of alternative types of cycloaddition reactions could be of value as well, not only in terms of providing alternative methodology, but also for the completion of first total synthesis of rostratins A and B.

4.10) Experimental results

General Methods. All reactions were performed under an argon atmosphere except where otherwise noted. Tetrahydrofuran was distilled over sodium-benzophenone, dichloromethane was distilled over calcium hydride, DMF in Acroseal bottles were used without further purification prior to use. Flash chromatography was carried out on Merck

silica gel 60 (240-400 mesh) using the solvent conditions listed under individual experiments. Analytical thin-layer chromatography was performed on Merck silica gel (60F-254) plates (0.25 mm). Visualization was effected with ultraviolet light or phosphomolybdic acid (PMA) stain. Proton magnetic resonance spectra (^{1}H NMR), Carbon magnetic resonance spectra (^{13}C NMR), Fluorine magnetic resonance spectra (^{19}F NMR), and Boron magnetic spectra (^{11}B NMR) were performed on a Bruker NMR operating at 500, 125, 470, and 128 MHz respectively. All ^{11}B chemical shifts were referenced to external $BF_3.OEt_2$ (0.0 ppm) with a negative sign indicating an upfield shift. Infrared spectra (IR) were obtained on a Perkin-Elmer 281-B spectrometer. High resolution mass spectra (HRMS) were obtained on a Micromass Autospec or a Waters LCTOF-Xe premier. Optical rotations were measured on a Jasco P-1010 polarimeter.

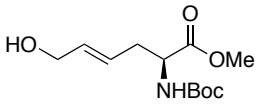

Allylic alcohol (+)-57. To a stirred solution of the known α,β-unsaturated aldehyde **(+)-5**[34] (5.10 g, 19.823 mmol) in anhydrous MeOH (198 mL) at −50 °C was added sodium borohydride (825 mg, 21.805 mmol) in one portion. The resulting mixture was left to stir at −50 °C for 30 min. Upon complete conversion of **(+)-53** (monitored by TLC), the reaction was quenched with aqueous sat. NH_4Cl (75 mL). The resulting layers were separated, and the aqueous layer was extracted with ethyl acetate (120 mL, twice). The organic layers were combined, dried over Na_2SO_4, filtered, and concentrated. Purification by silica gel chromatography (35% EtOAc/Hex) afforded the product as an oil (4.83 g, 94%). R_f = 0.3 (50% EtOAc/Hex). $[\alpha]_D^{19.9} = +23.46$ (*c* = 1.1 CH_2Cl_2). FTIR (thin film) cm^{-1}: 3369, 2978, 2954, 2933, 2870, 1742, 1712, 1518, 1438,

1392, 1367, 1278, 1250, 1216, 1168, 1100, 1052, 1021, 973, 855, 781. HRMS (ESI) m/z calcd. $C_{12}H_{21}NO_5$ $[M+Na]^+$ 282.1317, found 282.1317. ^{1}H-NMR (500 MHz; $CDCl_3$): δ 5.80-5.74 (m, 1H), 5.65-5.59 (m, 1H), 5.08-5.04 (m, 1H), 4.43-4.37 (m, 1H), 4.13 (t, *J* = 5.7 Hz, 2H), 3.77 (s, 3H), 2.62-2.56 (m, 1H), 2.51-2.45 (m, 1H), 1.47 (s, 9H). ^{13}C-NMR ($CDCl_3$, 125 MHz): 172.5, 155.2, 133.6, 125.8, 80.0, 63.1, 53.0, 52.3, 35.3, 28.3.

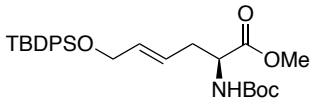

TBDPS ether (+)-59. To a stirred solution of **(+)-57** (2.09 g, 8.060 mmol) in anhydrous CH_2Cl_2 (81 mL) was added TBDPSCl (2.52 mL, 9.672 mmol) followed by imidazole (658 mg, 9.672 mmol). The resulting mixture was left to stir at room temperature overnight. Upon completion, the reaction was diluted with CH_2Cl_2 (100 mL), washed with aqueous 10% HCl (50 mL), aqueous sat. $NaHCO_3$ (50 mL), and brine (50 mL). The organic layer was dried over $MgSO_4$, filtered, and concentrated. Purification by silica gel chromatography (5% → 10% → 15% EtOAc/Hex) afforded the product as an oil (4.0 g, quant.). R_f = 0.55 (20% EtOAc/Hex). $[\alpha]_D^{17.9} = +13.33$ (*c* = 1.0 CH_2Cl_2). FTIR (thin film) cm^{-1}: 3437, 3071, 3049, 2956, 2931, 2894, 2857, 1746, 1718, 1499, 1473, 1461, 1428, 1391, 1365, 1249, 1211, 1168, 1112, 1055, 1027, 972, 823, 740, 702, 613. HRMS (ESI) m/z calcd. $C_{28}H_{39}NO_5Si$ $[M+Cl]^-$ 532.2286, found 532.2278. ^{1}H-NMR (500 MHz; $CDCl_3$): δ 7.75-7.68 (m, 4H), 7.45-7.39 (m, 6H), 5.71-5.56 (m, 2H), 5.03-4.98 (m, 1H), 4.41-4.36 (m, 1H), 4.18-4.17 (m, 2H), 3.74 (s, 3H), 2.56-2.47 (m, 2H), 1.46 (s, 9H), 1.08 (s, 9H). ^{13}C-NMR ($CDCl_3$, 125 MHz): 172.5, 155.1, 135.5, 135.4, 133.6, 133.5, 129.6, 127.6, 123.9, 79.8, 63.9, 53.0, 52.2, 35.1, 28.3, 26.8, 19.2.

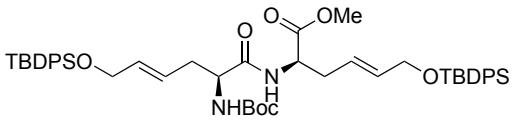

***N*-Boc TBDPS ether dipeptide (+)-63**. To a stirred solution of **(+)-59** (2.67 g, 5.365 mmol) in anhydrous THF (90 mL) was added potassium trimethylsilanolate (2.06 g, 16.094 mmol) in one portion. The resulting mixture was left to stir at room temperature for 2.5 h. Upon full conversion of **(+)-59** (monitored by TLC), aqueous 10% citric acid (30 mL) was added to the reaction and left to stir for additional 10 min. The resulting layers were separated, and the aqueous layer was extracted with ethyl acetate (50 mL, three times). The organic layers were combined, washed with brine (50 mL), dried over Na_2SO_4, filtered, and concentrated. Purification by short plug of silica gel (30% EtOAc/Hex) afforded the corresponding acid **62** as an oil (2.59 g, quant.). In a separate reaction vessel, **(+)-59** (2.82 g, 5.666 mmol) was dissolved in anhydrous CH_2Cl_2 at room temperature with stirring. The solution was then cooled down to 0 ^oC, and TFA (21 mL, 283.3 mmol) was slowly added to the reaction. The resulting mixture was left to stir at 0 ^oC for 45 min. Upon completion, the solvent was evaporated to afford the corresponding amine salt **61** which was used without further purification. In a 100 mL round bottom flask charged with a stir bar, **62** (2.59 g, 5.355 mmol) was dissolved in anhydrous CH_2Cl_2 (21 mL). The reaction flask was foiled, and brought to 0 ^oC. To this was added a portion of NMM (0.59 mL) followed by BOP (2.84 g, 6.426 mmol). In a separate round bottom flask, **61** was dissolved in anhydrous CH_2Cl_2 (33 mL). To this was added rest of NMM (1.18 mL, total NMM used: 1.77 mL, 16.065 mmol) and left to stir at room temperature for 5 min. The *in situ* free-based amine of **61** was then added to the reaction flask containing **62** via cannula addition. The resulting mixture was left to slowly warm to room temperature overnight. The reaction mixture

was diluted with ethyl acetate (100 mL), washed with aqueous 10% $KHSO_4$ (30 mL), aqueous sat. $NaHCO_3$ (30 mL), and brine (30 mL). The organic layer was dried over Na_2SO_4, filtered, and concentrated. Purification by column chromatography (20% EtOAc/Hex) afforded the dipeptide as a colorless oil (3.88 g, 84%). R_f = 0.66 (30% EtOAc/Hex). $[\alpha]_D^{20.9} = +8.83$ (c = 0.45 CH_2Cl_2). FTIR (thin film) cm^{-1}: 3318, 3071, 3049, 2999, 2957, 2931, 2893, 2857, 1746, 1714, 1681, 1514, 1473, 1462, 1428, 1390, 1366, 1249, 1210, 1171, 1112, 1051, 971, 823, 740, 702, 613. HRMS (ESI) m/z calcd. $C_{50}H_{66}N_2O_7Si_2$ $[M+Na]^+$ 885.4306, found 885.4311. ^{1}H-NMR (500 MHz; $CDCl_3$): δ 7.67 (dd, J = 7.8, 1.3 Hz, 8H), 7.44-7.39 (m, 12H), 6.63-6.59 (m, 1H), 5.70-5.56 (m, 4H), 4.95-4.90 (m, 1H), 4.67-4.63 (m, 1H), 4.15-4.14 (m, 4H), 3.71 (s, 3H), 2.57-2.52 (m, 3H), 2.45-2.38 (m, 1H), 1.44 (s, 9H), 1.06 (d, J = 1.0 Hz, 18H).^{13}C-NMR ($CDCl_3$, 125 MHz): 171.7, 170.9, 155.3, 135.4, 135.2, 134.7, 133.6, 133.5, 133.4, 129.62, 129.61, 127.64, 127.62, 127.3, 124.7, 123.5, 80.1, 64.0, 63.8, 54.0, 52.2, 51.9, 35.0, 28.2, 26.8, 26.7, 19.17, 19.15.

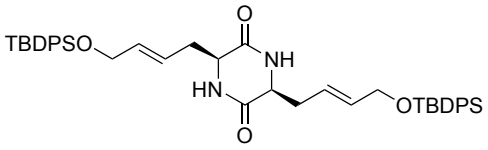

TBDPS ether *cis* DKP (−)-46. To a stirred solution of **(+)-63** (9.8 g, 11.352 mmol) in anhydrous CH_2Cl_2 (45 mL) at −10 °C was added TFA (44 mL, 592.3 mmol). The resulting mixture was left to stir at −10 °C for 1 h. Upon completion (monitored by TLC), the reaction was diluted with ethyl acetate (125 mL), quenched with portion-wise addition of aqueous sat. $NaHCO_3$ (200 mL). The reaction was warmed to room temperature, and the resulting layers were separated. The aqueous layer was extracted with ethyl acetate (150 mL, twice). The organic layers were

then combined, washed with brine (150 mL), dried over Na_2SO_4, filtered, and concentrated. The resulting free-based amine was dissolved in MeOH (103 mL) and to this was added aqueous NH_4OH (5.2 mL). The reaction mixture was left to stir at room temperature for 3 d, or until full conversion of the starting material was evident by ^1H NMR. The reaction was concentrated and directly loaded onto silica gel column for purification (5% → 10% Acetone/CH_2Cl_2) to afford the desired *cis* product as an amorphous solid (3.56 g, 43%). R_f = 0.32 (30% Acetone/Hex). $[\alpha]_D^{19.5} = -78.2$ (*c* = 1.5 CH_2Cl_2). FTIR (thin film) cm^{-1}: 3197, 3070, 3050, 2958, 2930, 2892, 2857, 1665, 1471, 1460, 1427, 1379, 1361, 1331, 1112, 1053, 971, 823, 739, 701, 613. HRMS (ESI) m/z calcd. $C_{44}H_{54}N_2O_4Si_2$ $[M+Na]^+$ 753.3520, found 753.3518. ^1H-NMR (500 MHz; $CDCl_3$): δ 7.69-7.66 (m, 4H), 7.46-7.39 (m, 6H), 5.78-5.63 (m, 3H), 4.21-4.20 (m, 2H), 3.98-3.95 (m, 1H), 2.90-2.84 (m, 1H), 2.40-2.33 (m, 1H), 1.08 (s, 9H).^{13}C-NMR ($CDCl_3$, 125 MHz): 167.2, 135.4, 134.9, 133.46, 133.40, 129.7, 127.7, 123.3, 63.6, 54.0, 36.4, 26.8, 19.1.

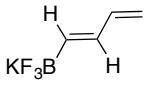

Potassium 1,3-butadiene-1-trifluoroborate salt (66). To a stirred solution of 3-butyn-1-ol (2 mL, 26.423 mmol) in anhydrous CH_2Cl_2 (300 mL) at 0 ^oC was added triethylamine (11 mL, 79.270 mmol) followed by methanesulfonyl chloride (2.66 mL, 34.350 mmol). The resulting solution was left to stir and warm to room temperature over 6 h. Upon completion, the reaction mixture was washed with aqueous 1N HCl (100 mL), brine (100 mL), dried over $MgSO_4$, filtered, and concentrated to afford the corresponding mesylate **67**, which was used in the next step without further purification. To a reaction

vessel charged with a stir bar was added dicyclohexyl borane (538 mg, 3.023 mmol) in a glovebox. The vessel was then removed and put under an argon atmosphere. In a separate round bottom flask, **67** was dissolved in anhydrous CH_2Cl_2 (35 mL), and the resulting solution was added to the reaction vessel containing dicyclohexyl borane[42] via cannula addition. The resulting mixture was brought to 0 ^oC, and to it was added pinacolborane (4.61 mL, 31.745 mmol). The reaction was left to stir and warm to room temperature overnight. The solvent was concentrated under vacuum, and was re-dissolved in anhydrous CH_2Cl_2 (120 mL). To this was added DBU (11.3 mL, 75.590 mmol), and left to stir at room temperature overnight. Upon completion, the solvent was removed, and the crude product was directly loaded onto a plug of silica gel column (10% EtOAc/Hex) to afford **68**[43] as a colorless oil. The pinacolboronate ester **68** was immediately dissolved in acetonitrile (30 mL), and to it was added aqueous 4.5 M KHF_2 (24 mL). The resulting mixture was left to stir at room temperature for 30 min. The solvent was evaporated and the crude product was suspended in hot acetonitrile (50 mL). Hot gravity filtration followed by evaporation of acetonitrile afforded the crude product as a white solid. The solid was further purified by trituration with cold diethyl ether (20 mL). Subsequent vacuum filtration afforded the desired product as a white solid (3.33 g, 90% over three steps). FTIR (neat) cm^{-1}: 3085, 3018, 2987, 2965, 1593, 1260, 1151, 1100, 1013, 973, 920, 745, 637. ^{1}H-NMR (500 MHz; $CDCl_3$): δ 6.35-6.23 (m, 1H), 5.68 (ddt, J = 15.9, 7.4, 3.7 Hz,), 4.96-4.93 (m, 1H), 4.80-4.78 (m, 1H).^{13}C-NMR (acetone-d_6, 125 MHz): 142.7, 136.7, 136.6, 112.6; ^{11}B NMR (128.4 MHz, acetone-d_6) δ 3.3 (q); ^{19}F NMR (470.8 MHz, acetone-d_6) δ −142.0 (q).

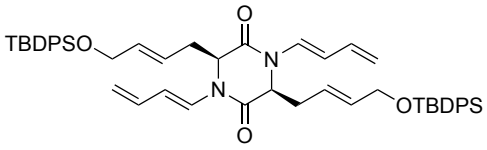

1,3-Butadiene coupled TBDPS DKP (+)-69. A biotage microwave tube was charged with a stir bar, **(−)-46** (320 mg, 0.438 mmol), and freshly prepared **66** (350 mg, 2.185 mmol), $Cu(OAc)_2$ (24 mg, 0.131 mmol), and 4 Å MS (700 mg) on the bench-top. To this was added a 1:1 mixture of 1,2-DCE and DMSO (1.8 mL). The tube was sealed, and the resulting heterogeneous mixture was left to stir at 40 ^oC under O_2 atmosphere until full conversion of **(−)-46** was evident by TLC analysis. The reaction mixture was filtered through a pad of Celite, and was rinsed with portions of ethyl acetate (50 mL). The filtrate was concentrated, and directly loaded onto a silica gel column for purification (10% EtOAc/Hex) to afford the title compound as a white foam (315 mg, 86%). R_f = 0.32 (10% EtOAc/Hex). $[\alpha]_D^{24.3} = +67.0$ (*c* = 0.8 CH_2Cl_2). FTIR (thin film) cm^{-1}: 3069, 2950, 2925, 2856, 1676, 1640, 1427, 1405, 1237, 1112, 1057, 997, 822, 742, 701. HRMS (ESI) m/z calcd. $C_{52}H_{62}N_2O_4Si_2$ $[M+Na]^+$ 857.4146, found 857.4125. ^{1}H-NMR (500 MHz; $CDCl_3$): δ 7.70 (dq, *J* = 6.4, 1.6 Hz, 4H), 7.46-7.39 (m, 6H), 7.36 (s, 1H), 6.39 (dt, *J* = 16.8, 10.3 Hz, 1H), 5.90-5.80 (m, 2H), 5.69 (dt, *J* = 15.3, 4.5 Hz, 1H), 5.22 (d, *J* = 16.9 Hz, 1H), 5.12 (d, *J* = 10.4 Hz, 1H), 4.47 (dd, *J* = 7.2, 4.9 Hz, 1H), 4.21 (d, *J* = 3.4 Hz, 2H), 2.75-2.70 (m, 2H), 1.10 (s, 9H).^{13}C-NMR ($CDCl_3$, 125 MHz): 163.2, 135.5, 135.49, 135.40, 134.7, 134.3, 133.6, 133.5, 133.4, 129.64, 129.63, 127.8, 127.6, 125.9, 124.0, 116.7, 115.4, 63.7, 57.9, 36.1, 26.8,19.1.

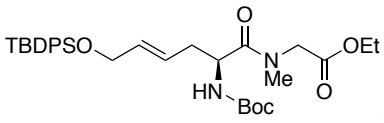

***N*-Boc TBDPS sarcosine dipeptide (+)-71**. To a stirred solution of **62** (1.85 g, 3.824 mmol) in anhydrous CH_2Cl_2 (15 mL) at 0 ^oC was added BOPCl (1.17 g, 4.589 mmol), NMM (1.26 mL, 11.474 mmol), followed by sarcosine ethyl ester hydrochloride salt **70** (646 mg, 4.207 mmol). The resulting mixture was left to stir and warm to room temperature overnight. Upon completion, the reaction was diluted with ethyl acetate (50 mL), washed with aqueous 10% $KHSO_4$ (10 mL), aqueous sat. $NaHCO_3$ (10 mL), brine (10 mL), dried over Na_2SO_4, filtered, and concentrated. Purification by silica gel chromatography (30% EtOAc/Hex) afforded the product as an oil (2.0 g, 93%). R_f = 0.34 (30% EtOAc/Hex). $[\alpha]_D^{21.0} = +6.06$ (*c* = 1.3, CH_2Cl_2). FTIR (thin film) cm^{-1}: 3425, 3314, 3071, 3049, 2961, 2931, 2857, 1748, 1712, 1652, 1487, 1428, 1406, 1391, 1366, 1250, 1171, 1112, 1051, 972, 823, 741, 704, 690, 614, 505, 491. HRMS (ESI) m/z calcd. $C_{32}H_{46}N_2O_6Si$ $[M+H]^+$ 583.3203, found 583.3210. ^{1}H-NMR (500 MHz; $CDCl_3$): δ 7.70-7.68 (m, 4H), 7.45-7.38 (m, 6H), 5.73-5.69 (m, 2H), 5.35 (d, *J* = 8.5 Hz, 1H), 4.73 (q, *J* = 7.2 Hz, 1H), 4.32 (d, *J* = 17.1 Hz, 1H), 4.27-4.16 (m, 4H), 3.90 (d, *J* = 17.3 Hz, 1H), 3.14 (s, 3H), 2.56-2.46 (m, 1H), 2.46-2.35 (m, 1H), 1.44 (s, 9H), 1.27 (t, *J* = 7.1 Hz, 3H), 1.07 (s, 9H).^{13}C-NMR ($CDCl_3$, 125 MHz): 172.4, 168.8, 155.3, 135.5, 133.72, 133.70, 133.1, 129.6, 127.64, 127.61, 124.5, 79.5, 64.2, 61.2, 50.0, 49.7, 36.5, 35.8, 28.4, 26.9, 19.2, 14.2.

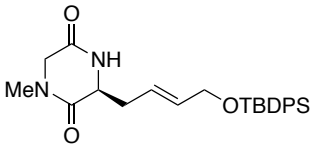

***N*-Methyl mono TBDPS DKP (+)-65**. To a stirred solution of **(+)-71** (2.0 g, 3.51 mmol) in anhydrous CH_2Cl_2 (14 mL) at 0 ^oC was added TFA (14 mL). The resulting mixture was left to stir and warm to room temperature over 1 h. Upon completion, the reaction was concentrated to afford the corresponding amine salt, which was immediately dissolved in EtOH (35 mL). To this was added K_2CO_3 (1.95 g, 14.07 mmol), and the resulting mixture was brought to reflux with stirring overnight. The reaction mixture was filtered through a pad of Celite, rinsed with EtOH (30 mL), and evaporated. Purification by column chromatography (40% Acetone/CH_2Cl_2) afforded the desired product as an amorphous solid (1.5 g, 98%). R_f = 0.4 (40% Acetone/CH_2Cl_2). $\left[\alpha\right]_D^{22.6} = +1.38$ (*c* = 0.9, $CHCl_3$). FTIR (thin film) cm^{-1}: 3070, 2929, 2856, 1687, 1472, 1427, 1330, 1259, 1191, 1112, 976, 822, 741, 703, 614, 504. HRMS (ESI) m/z calcd. $C_{25}H_{32}N_2O_3Si$ $[M+Na]^+$ 459.2080, found 459.2063. ^{1}H-NMR (500 MHz; $CDCl_3$): δ 7.75-7.63 (m, 4H), 7.51-7.39 (m, 6H), 6.67 (s, 1H), 5.76-5.68 (m, 2H), 4.20 (s, 2H), 4.02-4.01 (m, 1H), 3.93 (q, *J* = 23.3 Hz, 2H), 2.96 (s, 3H), 2.70-2.66 (m, 1H), 2.59-2.51 (m, 1H), 1.20-0.95 (m, 9H). ^{13}C-NMR ($CDCl_3$, 125 MHz): 165.5, 165.3, 135.4, 134.9, 133.4, 133.3, 129.7, 127.6, 122.8, 63.6, 54.7, 51.5, 37.3, 33.7, 26.7, 19.1.

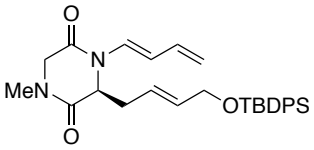

1,3-Butadiene coupled *N*-Methyl mono TBDPS DKP (+)-72. The title compound was synthesized following the procedure used for the synthesis of **(+)-69**. A biotage microwave tube was charged with a stir bar, **(+)-65** (350 mg, 0.802

mmol), and freshly prepared **66** (256 mg, 1.603 mmol), $Cu(OAc)_2$ (44 mg, 0.240 mmol), and 4 Å MS (500 mg) on the bench-top. To this was added a 1:1 mixture of 1,2-DCE and DMSO (3.2 mL). The tube was sealed, and the resulting heterogeneous mixture was left to stir at 40 ^{o}C under O_2 atmosphere until full conversion of **(+)-65** was evident by TLC analysis. The reaction mixture was filtered through a pad of Celite, and was rinsed with portions of ethyl acetate (50 mL). The filtrate was concentrated, and directly loaded onto a silica gel column for purification (40% EtOAc/Hex) to afford the title compound as a yellow oil (344 mg, 88%). R_f = 0.22 (40% EtOAc/Hex). $[\alpha]_D^{21.5} = +2.57$ (c = 0.3 $CHCl_3$). FTIR (thin film) cm^{-1}: 3070, 2957, 2929, 2856, 1676, 1643, 1429, 1406, 1332, 1276, 1237, 1112, 1053, 998, 822, 741, 703, 504. HRMS (ESI) m/z calcd. $C_{29}H_{36}N_2O_3Si$ $[M+Na]^+$ 511.2393, found 511.2395. ^{1}H-NMR (500 MHz; $CDCl_3$): δ 7.66-7.64 (m, 4H), 7.46-7.39 (m, 6H), 7.35 (d, J = 14.7 Hz, 1H), 6.42-6.34 (m, 1H), 5.83 (dd, J = 14.7, 10.4 Hz, 1H), 5.76-5.65 (m, 2H), 5.23 (d, J = 16.9 Hz, 1H), 5.11 (d, J = 9.9 Hz, 1H), 4.54-4.53 (m, 1H), 4.22 (d, J = 17.8 Hz, 1H), 4.15 (s, 2H), 3.85-3.81 (m, 1H), 2.96 (s, 3H), 2.82-2.73 (m, 2H), 1.07 (s, 9H). ^{13}C-NMR ($CDCl_3$, 125 MHz): 165.4, 162.3, 138.0, 135.4, 134.4, 133.2, 133.1, 129.7, 127.8, 127.7, 125.8, 121.3, 116.4, 114.6, 63.4, 57.8, 51.9, 34.0, 33.2, 26.8, 19.2.

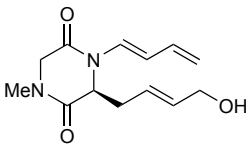

1,3-Butadiene coupled *N*-Methyl mono allyl alcohol DKP (+)-73. To a stirred solution of **(+)-72** (400 mg, 0.818 mmol) in anhydrous THF (8.2 mL) at 0 ^{o}C was added TBAF (1M in THF, 0.9 mL, 0.900 mmol). The resulting mixture was allowed to warm to room temperature over 2.5 h. The solvent was evaporated and directly loaded

onto a silica gel column for purification (50% Acetone/CH_2Cl_2) to afford the title compound as a yellow oil (200 mg, 98%). R_f = 0.4 (50% Acetone/CH_2Cl_2). $[\alpha]_D^{22.1} = +4.30$ (*c* = 0.5 CH_2Cl_2). FTIR (thin film) cm^{-1}: 3411, 3083, 3036, 3000, 2924, 2853, 1669, 1643, 1513, 1435, 1408, 1337, 1278, 1238, 1100, 1085, 1002, 977, 941. HRMS (ESI) m/z calcd. $C_{13}H_{18}N_2O_3$ $[M+Na]^+$ 273.1215, found 273.1219. ^{1}H-NMR (500 MHz; $CDCl_3$): δ 7.32 (d, *J* = 14.7 Hz, 1H), 6.37 (dt, *J* = 16.9, 10.2 Hz, 1H), 5.82 (dd, *J* = 14.7, 10.3 Hz, 1H), 5.75 (dt, *J* = 15.4, 4.9 Hz, 1H), 5.65-5.59 (m, 1H), 5.23 (d, *J* = 16.9 Hz, 1H), 5.11 (d, *J* = 10.2 Hz, 1H), 4.50 (dd, *J* = 4.7, 4.6 Hz, 1H), 4.21 (d, *J* = 18.0 Hz, 1H), 4.09 (d, *J* = 4.7 Hz, 2H), 3.89 (d, *J* = 18.0 Hz, 1H), 3.00 (s, 3H), 2.78-2.68 (m, 2H). ^{13}C-NMR ($CDCl_3$, 125 MHz): 165.2, 162.5, 135.5, 134.3, 125.7, 123.2, 116.7, 114.8, 62.5, 57.7, 51.8, 34.1, 33.3.

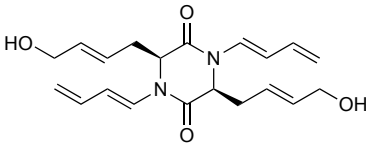

1,3-Butadiene coupled allyl alcohol DKP (+)-75. To a stirred solution of **(+)-69** (1.37 g, 1.640 mmol) in anhydrous THF (33 mL) at 0 °C was added TBAF (1M in THF, 3.44 mL, 3.444 mmol). The resulting mixture was left to stir at 0 °C for 2 h, then warmed to room temperature over additional 1 h. Upon completion, the reaction was quenched with water (0.5 mL) and concentrated. Purification by silica gel column chromatography (20% Acetone/CH_2Cl_2) afforded the title compound as an oil (518 mg, 88%). R_f = 0.3 (20% Acetone/CH_2Cl_2). $[\alpha]_D^{25.9} = +7.36$ (*c* = 0.8 $CHCl_3$). FTIR (thin film) cm^{-1}: 3417, 3084, 3035, 3003, 2972, 2924, 2860, 1672, 1640, 1432, 1406, 1341, 1316, 1286, 1237, 1099, 1000, 974, 939, 898, 756, 665. HRMS (ESI) m/z calcd.

$C_{20}H_{26}N_2O_4$ $[M-H]^-$ 357.1814, found 357.1819. ^{1}H-NMR (500 MHz; $CDCl_3$): δ 7.31 (d, *J* = 14.7 Hz, 1H), 6.41-6.33 (m, 1H), 5.82 (t, *J* = 7.4 Hz, 1H), 5.79 (d, *J* = 4.3 Hz, 2H), 5.28-5.23 (m, 1H), 5.14 (t, *J* = 8.7 Hz, 1H), 4.47 (dd, *J* = 8.7, 4.3 Hz, 1H), 4.15 (d, *J* = 1.4 Hz, 2H), 2.80-2.76 (m, 1H), 2.73-2.65 (m, 1H). ^{13}C-NMR ($CDCl_3$, 125 MHz): 163.8, 134.1, 133.9, 125.8, 125.1, 117.0, 115.5, 62.8, 57.8, 35.8.

General procedure for IMDA using MacMillan's catalyst

To a stirred solution of **(+)-75** (0.405 mmol) in anhydrous CH_2Cl_2 (27 mL) was added $NaHCO_3$ (28.32 mmol) followed by Dess-Martin periodinane (2.427 mmol). The reaction vessel was kept away from light (foiled), and left to stir vigorously at room temperature for 30-40 min. The reaction was quenched with 1:1:1 aqueous sat. $NaHCO_3$/brine/Na_2SO_3 (27 mL) and left to stir until separation of layers was apparent. The resulting layers were separated, and the aqueous layer was extracted with CH_2Cl_2 (20 mL, three times). The organic layers were combined, dried over $MgSO_4$, filtered, and concentrated. The unstable crude bis-aldehyde **44** was immediately loaded onto a short silica gel plug (5% Acetone/CH_2Cl_2) and rapidly separated from excess iodinane. **44** was immediately taken onto the next step without further purification. In a separate flask, the MacMillan catalyst (0.1618 mmol) and protic acid additive (0.1618 mmol) was dissolved in a solution of 98:2 MeCN/H_2O (1.2 mL). The resulting solution was quickly added to the reaction flask containing **44** and a stir bar. The resulting mixture was left to stir at room temperature until full conversion of **44** was apparent by TLC analysis. Upon completion, the reaction mixture was directly loaded onto a silica gel column (90% EtOAc/Hex → 100% EtOAc then 5% MeOH/EtOAc) for isolation of the cycloadduct.

General procedure for thermal IMDA

To a biotage microwave tube equipped with a stir bar under argon was added **(+)-75** (0.245 mmol) in a solution of anhydrous m-xylene (4.9 mL) and BHT (0.012 mmol). The resulting mixture was immediately placed into a pre-heated sand bath at 130-160 ^{o}C, and left to stir for 2 d, or until complete consumption of **(+)-75** was evident by TLC analysis. The reaction mixture was concentrated, and loaded onto a silica gel column (100% EtOAc → 5% MeOH/EtOAc) to isolate the cycloadduct.

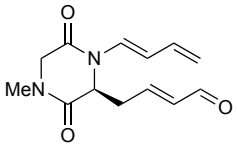

***N*-Methyl mono-aldehyde IMDA precursor (74)**. R_f = 0.22 (10% Acetone/CH_2Cl_2). ^{1}H-NMR (500 MHz; $CDCl_3$): δ 9.53 (dd, *J* = 7.6, 0.6 Hz, 1H), 7.31 (d, *J* = 14.7 Hz, 1H), 6.80-6.73 (m, 1H), 6.40-6.32 (m, 1H), 6.20 (ddd, *J* = 15.6, 7.5, 0.9 Hz, 1H), 5.81 (dd, *J* = 14.6, 10.3 Hz, 1H), 5.24 (d, *J* = 16.9 Hz, 1H), 5.14 (d, *J* = 10.1 Hz, 1H), 4.60 (dd, *J* = 7.2, 4.3 Hz, 1H), 4.15 (d, *J* = 18.2 Hz, 1H), 3.99-3.95 (m, 1H), 3.02 (s, 3H), 2.97 (t, *J* = 5.9 Hz, 1H), 2.95-2.88 (m, 1H). ^{13}C-NMR ($CDCl_3$, 125 MHz): 192.7, 164.2, 161.6, 148.6, 136.3, 133.9, 125.5, 117.4, 115.1, 56.8, 51.6, 34.6, 33.6.

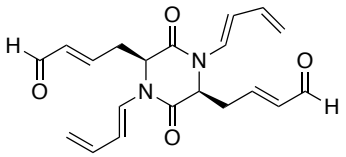

***bis*-Aldehyde IMDA precursor (44)**. R_f = 0.6 (5% Acetone/CH_2Cl_2). ^{1}H-NMR (500 MHz; $CDCl_3$): δ 9.62 (dd, *J* = 7.5, 0.4 Hz, 1H), 7.32 (d, *J* = 14.8 Hz, 1H), 6.93 (dt, *J* = 15.4, 7.6 Hz, 1H), 6.41-6.34 (m, 1H), 6.26-6.21 (m, 1H), 5.80 (dd, *J* = 14.8, 10.2 Hz, 1H), 5.24 (dd, *J* = 44.9, 13.5 Hz, 2H), 4.64 (dd, *J* = 9.8, 4.1

Hz, 1H), 3.11-3.05 (m, 1H), 2.85-2.78 (m, 1H). ^{13}C-NMR ($CDCl_3$, 125 MHz): 192.7, 162.0, 148.9, 135.5, 133.6, 125.1, 118.2, 116.0, 56.7, 36.2.

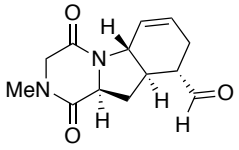

Mono-IMDA cycloadduct (76).[i] R_f = 0.26 (5% MeOH/EtOAc). HRMS (ESI) m/z calcd. $C_{13}H_{16}N_2O_3$ $[M+H]^+$ 249.1239, found 249.1230. ^{1}H-NMR (500 MHz; $CDCl_3$): δ 9.82 (s, 1H), 5.81 (d, *J* = 4.7 Hz, 1H), 5.70-5.62 (m, 1H), 4.40-4.35 (m, 1H), 4.19-3.91 (m, 3H), 3.00 (s, 3H), 2.71-2.65 (m, 1H), 2.51-2.46 (m, 1H), 2.38-2.32 (m, 2H), 2.12-2.08 (m, 2H). ^{13}C-NMR ($CDCl_3$, 125 MHz): 201.3, 165.8, 163.6, 136.7, 118.0, 60.4, 51.4, 49.0, 47.5, 45.9, 33.4, 31.1, 28.9.

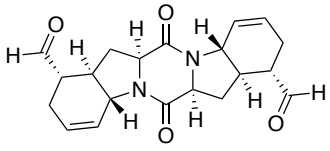

Double IMDA *bis*-aldehyde cycloadduct (47).[ii] R_f = 0.3 (5% MeOH/EtOAc). HRMS (ESI) m/z calcd. $C_{20}H_{22}N_2O_4$ $[M+H]^+$ 355.1658, found 355.1674. ^{1}H-NMR (500 MHz; $CDCl_3$): δ 9.82 (s, 1H), 5.82-5.81 (m, 1H), 5.69-5.61 (m, 1H), 4.39-4.35 (m, 1H), 4.10-4.01 (m, 1H), 3.05-2.99 (m, 1H), 2.79-2.73 (m, 1H), 2.51-2.47 (m, 1H), 2.41-2.34 (m, 1H), 2.05-1.98 (m, 2H). ^{13}C-NMR ($CDCl_3$, 125 MHz): 201.2, 166.7, 136.7, 118.4, 49.1, 46.9, 45.8, 32.2, 29.7, 29.4.

[i] Reported values for ^{1}H and ^{13}C NMR based on major diastereomer.
[ii] Reported values for ^{1}H and ^{13}C NMR based on major diastereomer. ^{13}C NMR spectra shows up to 5 different aldehyde peaks of varying intensity, suggesting presence of diastereomers.

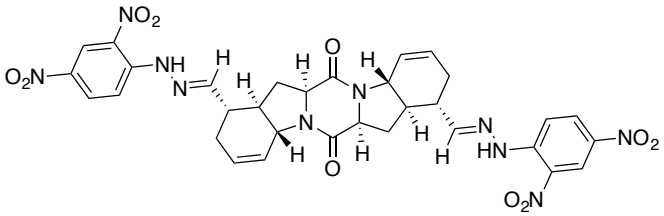

***bis*-Hydrazone derivatized double IMDA cycloadduct (77)**. To a stirred solution of 47 (31 mg, 0.087 mmol) in anhydrous MeOH (0.87 mL) was added 2,4-DNPH (35 mg, 0.175 mmol) followed by AcOH (2 drops). The resulting mixture was left to stir at room temperature for 4 h. Upon completion of the reaction, the solvent was evacuated Purification by HPLC afforded the title compound. R_f = 0.57 (100% EtOAc). HRMS (ESI) m/z calcd. $C_{32}H_{30}N_{10}O_{10}$ $[M+H]^+$ 715.2225, found 715.2219. ^{1}H-NMR (500 MHz; $CDCl_3$): δ 11.09 (s, 1H), 9.13 (d, *J* = 2.6 Hz, 1H), 8.34-8.30 (m, 1H), 7.94 (dd, *J* = 9.6, 2.4 Hz, 1H), 7.61-7.58 (m, 1H), 5.95-5.88 (m, 1H), 5.78-5.66 (m, 1H), 5.26-5.23 (m, 1H), 4.52-4.42 (m, 1H), 2.97-2.87 (m, 1H), 2.85-2.76 (m, 1H), 2.64-2.60 (m, 1H), 2.29-2.22 (m, 2H), 2.09-2.01 (m, 1H).

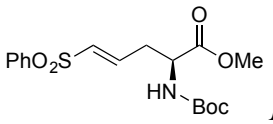

***N*-Boc phenyl sulfone methyl ester (+)-85**. To a suspension of NaH (60% in mineral oil, 543 mg, 16.151 mmol) in anhydrous THF (130 mL) at −10 °C was added drop-wise a solution of diethyl (phenylsulfonyl)methylphosphonate[iii] (4.72 g, 16.151 mmol) in anhydrous THF (30 mL). The resulting mixture was stirred for 30 min at −10 °C. To this was added a solution of the aldehyde **84** (2.87 g, 12.424 mmol) in anhydrous THF (23 mL) drop-wise. The resulting mixture was allowed slowly warm to room temperature and left to stir for 4-5 h. Upon completion, cold aqueous 5% $NaHSO_4$

[iii] Yang, P.-Y., Wang, M., He, C. Y., Yao, S. Q. "Proteomic profiling and potential cellular target identification of K11777, a clinical cysteine protease inhibitor, in *Trypanosoma brucei*." *Chem. Commun.* **2012**, *48*, 835-837.

was added until the pH of the solution reached about 6-7. The resulting biphasic solution was concentrated under vacuum and diluted with water (100 mL). The aqueous layer was extracted with EtOAc (100 mL, three times), washed with aqueous $NaHCO_3$ (120 mL), brine (120 mL), dried over Na_2SO_4, filtered, and concentrated. Purification by silica gel column chromatography (30% → 40% EtOAc/Hex) afforded the title compound as a yellow oil (3.24 g, 71%). R_f = 0.41 (40% EtOAc/Hex). $[\alpha]_D^{21.9} = +44.3$ (*c* = 0.75 $CHCl_3$). FTIR (thin film) cm^{-1}: 3367, 3050, 2978, 2933, 1712, 1632, 1517, 1447, 1392, 1367, 1319, 1250, 1218, 1148, 1086, 1054, 1023, 999, 977, 916, 753, 688, 595, 549. HRMS (ESI) m/z calcd. $C_{17}H_{23}NO_6S$ $[M+Na]^+$ 392.1144, found 392.1147. ^{1}H-NMR (500 MHz; $CDCl_3$): δ 7.87 (d, *J* = 7.6 Hz, 2H), 7.63 (dd, *J* = 13.3, 5.7 Hz, 1H), 7.58-7.53 (m, 2H), 6.92-6.86 (m, 1H), 6.42 (d, *J* = 15.1 Hz, 1H), 5.24-5.23 (m, 1H), 4.49-4.44 (m, 1H), 3.68 (s, 3H), 2.82-2.77 (m, 1H), 2.68-2.62 (m, 1H), 1.42 (s, 9H). ^{13}C-NMR ($CDCl_3$, 125 MHz): 171.4, 155.0, 140.7, 140.1, 133.62, 133.47, 129.3, 127.7, 80.4, 52.7, 52.2, 34.5, 28.2.

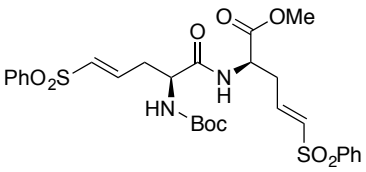

***N*-Boc phenyl sulfone dipeptide (+)-88**. To a stirred solution of **(+)-85** (314 mg, 0.850 mmol) in anhydrous CH_2Cl_2 (3.4 mL) was added TFA (3.4 mL) at room temperature. The resulting mixture was allowed to stir at room temperature for 1 h. The solution was concentrated to afford the TFA amine salt **86**, which was used in the next step without further purification. In a separate reaction vessel, **(+)-85** (282 mg, 0.763 mmol) was dissolved in anhydrous 1,2-DCE (7.6 mL) at room

temperature. To this was added Me_3SnOH (414 mg, 2.290 mmol), and the resulting mixture was brought to 70 ^oC and left to stir for 7 h. The solvent was evaporated under vacuum, and re-dissolved in ethyl acetate (20 mL). The organic layer was washed with aqueous 10% $KHSO_4$ (5 mL), brine (5 mL), dried over Na_2SO_4, filtered, and concentrated to afford the acid **87** as an oil, which was carried onto the next step without further purification. To a foiled round bottom flask containing **87** dissolved in anhydrous CH_2Cl_2 (3 mL) at 0 ^oC was added BOP (424 mg, 0.959 mmol) followed by a portion of NMM (87 mL). In a separate round bottom flask containing **86** dissolved in anhydrous CH_2Cl_2 (5 mL) was added the remainder of NMM (0.17 mL). The *in situ* free-based form of **86** was then added to the flask containing **87** by cannula addition. The resulting mixture was allowed to warm to room temperature and stir overnight. The reaction mixture was diluted with ethyl acetate (20 mL), washed with aqueous 10% $KHSO_4$ (5 mL), aqueous sat. $NaHCO_3$ (5 mL), and brine (5 mL). The organic layer was dried over Na_2SO_4, filtered, and concentrated. Purification by column chromatography (55% EtOAc/Hex) afforded the title compound as an oil (340 mg, 70%). %). R_f = 0.47 (70% EtOAc/Hex). $[\alpha]_D^{22.4} = +33.1$ (*c* = 0.5 CH_2Cl_2). FTIR (thin film) cm^{-1}: 3352, 3059, 2979, 1743, 1710, 1681, 1519, 1447, 1368, 1306, 1290, 1249, 1146, 1085, 1029, 1024, 844, 752, 688, 594, 548. HRMS (ESI) m/z calcd. $C_{28}H_{34}N_2O_9S_2$ $[M+Na]^+$ 629.1603, found 629.1604. ^{1}H-NMR (500 MHz; $CDCl_3$): δ 7.89-7.87 (m, 5H), 7.64-7.61 (m, 2H), 7.54 (t, *J* = 7.7 Hz, 3H), 7.06-7.04 (m, 1H), 6.91 (dt, *J* = 14.9, 7.4 Hz, 1H), 6.84 (dt, *J* = 14.9, 7.5 Hz, 1H), 6.43 (dd, *J* = 14.8, 13.7 Hz, 2H), 5.25-5.17 (m, 1H), 4.67 (td, *J* = 8.0, 4.8 Hz, 1H), 4.31-4.27 (m, 1H), 3.68 (s, 3H), 2.84-2.73 (m, 2H), 2.67-2.52 (m, 2H), 1.44 (s, 9H). ^{13}C-NMR

($CDCl_3$, 125 MHz): 170.6, 170.4, 155.5, 141.2, 140.19, 140.13, 139.9, 133.8, 133.57, 133.51, 133.46, 129.34, 129.31, 127.82, 127.71, 80.90, 52.9, 50.9, 34.2, 33.8, 29.7, 28.2.

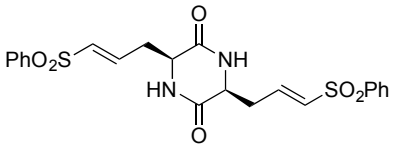

Phenyl sulfone DKP (−)-78. To a stirred solution of **(+)-88** (2.0 g, 3.346 mmol) in anhydrous CH_2Cl_2 (14 mL) at 0 ^oC was added TFA (6.2 mL, 83.648 mmol). The resulting mixture was left to stir at 0 ^oC for 30 min and at room temperature for additional 30 min. Upon completion (monitored by TLC), the reaction mixture was concentrated, and the resulting TFA amine salt was used in the subsequent step without further purification. To a stirred solution of the TFA amine salt in MeOH (51 mL) at 0 ^oC was added aqueous NH_4OH (1.77 mL). The resulting mixture was allowed to warm to room temperature and left to stir until complete consumption of starting material was apparent (monitored by ^1H NMR and TLC). The reaction solution was concentrated and diluted with a 2:1 mixture of EtOAc and acetone (150 mL), which was washed with brine (20 mL). The organic layer was separated, dried over Na_2SO_4, filtered, and concentrated to afford the title compound (1.2 g, 87% over two steps). R_f = 0.66 (100% Acetone). $[\alpha]_D^{22.8} = -21.0$ (c = 0.25 Acetone). FTIR (neat) cm^{-1}: 2360, 2328, 1680, 1667, 1461, 1446, 1342, 1305, 1145, 1085, 822, 758, 715, 688, 670, 613. HRMS (ESI) m/z calcd. $C_{22}H_{22}N_2O_6S_2$ $[M+H]^+$ 475.0998, found 475.0982. ^1H-NMR (500 MHz; DMSO-d_6): δ 8.37 (t, J = 0.3 Hz, 1H), 7.85 (dd, J = 6.9, 1.2 Hz, 2H), 7.76-7.61 (m, 3H), 6.90-6.81 (m, 2H), 4.15-4.12 (m, 1H), 2.66-2.63 (m, 2H). ^{13}C-NMR (DMSO-d_6, 125 MHz): 167.8, 142.7, 140.8, 134.0, 133.1, 130.0, 127.6, 53.2, 34.2.

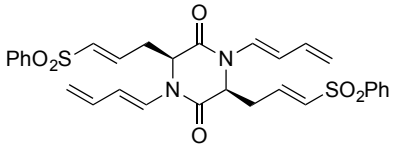

Phenyl sulfone IMDA precursor (+)-89. A biotage microwave tube was charged with a stir bar, **(−)-78** (250 mg, 0.527 mmol), and 1:1 mixture of 1,2-DCE and DMSO (2.1 mL). To this was added freshly prepared **66** (421 mg, 2.634 mmol), $Cu(OAc)_2$ (28 mg, 0.158 mmol), and 4 Å MS (840 mg) on the bench-top. The tube was sealed, and the resulting heterogeneous mixture was left to stir at 40 ^oC under O_2 atmosphere until full conversion of **(−)-78** was evident by TLC analysis. The reaction mixture was filtered through a pad of Celite, and was rinsed with portions of ethyl acetate (80 mL). The filtrate was concentrated, and directly loaded onto a silica gel column for purification (40% EtOAc/Hex) to afford the title compound as a yellow oil (155 mg, 51%). R_f = 0.3 (40% EtOAc/Hex). $[\alpha]_D^{21.9} = +154.7$ (c = 0.7 CH_2Cl_2). FTIR (film) cm^{-1}: 3057, 2923, 2852, 1673, 1642, 1446, 1433, 1407, 1307, 1238, 1146, 1085, 1000, 941, 907, 821, 751, 721, 687, 593, 548. HRMS (ESI) m/z calcd. $C_{30}H_{30}N_2O_6S_2$ $[M+Na]^+$ 601.1443, found 601.1459.^{1}H-NMR (500 MHz; $CDCl_3$): δ 7.90 (dd, J = 8.0, 0.7 Hz, 2H), 7.66-7.63 (m, 1H), 7.58-7.54 (m, 2H), 7.27-7.23 (m, 1H), 7.03-6.95 (m, 1H), 6.56 (d, J = 14.9 Hz, 1H), 6.39-6.30 (m, 1H), 5.81-5.74 (m, 1H), 5.27-5.17 (m, 2H), 4.64-4.62 (m, 1H), 2.98-2.92 (m, 1H), 2.90-2.82 (m, 1H). 13C-NMR (CDCl3, 125 MHz): 161.7, 139.8, 139.2, 134.3, 133.68, 133.63, 129.4, 127.8, 125.2, 118.1, 116.3, 56.4, 34.4.

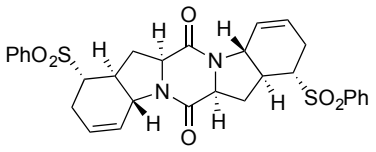

Double IMDA *bis*-phenyl sulfone cycloadduct (90).[iv] The general procedure for thermal IMDA was utilized to obtain the title compound. ^{1}H-NMR (500 MHz; $CDCl_3$): δ 7.98-7.90 (m, 2H), 7.73-7.69 (m, 1H), 7.67-7.59 (m, 2H), 5.89-5.72 (m, 1H), 5.65-5.56 (m, 1H), 4.87-4.73 (m, 1H), 4.34-4.17 (m, 1H), 3.39-3.30 (m, 1H), 2.89-2.75 (m, 1H), 2.70-2.51 (m, 2H), 2.44-2.33 (m, 2H). 13C-NMR (CDCl3, 125 MHz): 165.9, 137.3, 134.2, 129.5, 128.8, 124.8, 124.6, 59.5, 54.2, 32.9, 29.2, 27.9, 20.8.

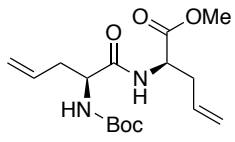

***N*-Boc alkene dipeptide (+)-99**. The general procedure for peptide coupling used in the synthesis of **(+)-63** and **(+)-88** was followed. R_f = 0.61 (40% EtOAc/Hex) $[\alpha]_D^{20.5} = +0.40$ (c = 0.7 $CHCl_3$). FTIR (film) cm^{-1}: 3315, 3079, 3005, 2980, 2954, 2933, 1747, 1661, 1525, 1438, 1391, 1367, 1274, 1250, 1223, 1203, 1168, 1047, 1022, 993, 919, 860. HRMS (ESI) m/z calcd. $C_{16}H_{26}N_2O_5$ $[M+Na]^+$ 349.1739, found 349.1724.^{1}H-NMR (500 MHz; $CDCl_3$): δ 6.89-6.88 (m, 1H), 5.70 (ddt, J = 16.9, 9.8, 6.9 Hz, 1H), 5.62 (dddd, J = 16.8, 6.2, 5.9, 4.3 Hz, 1H), 5.22 (d, J = 7.8 Hz, 1H), 5.11-5.03 (m, 4H), 4.59 (q, J = 6.4 Hz, 1H), 4.18 (dtd, J = 2.0, 1.0, 0.5 Hz, 1H), 3.68 (s, 3H), 2.56-2.38 (m, 4H), 1.38 (s, 9H). ^{13}C-NMR ($CDCl_3$, 125 MHz): 171.8, 171.3, 155.5, 133.0, 132.1, 119.1, 118.8, 79.9, 53.6, 52.3, 51.7, 36.6, 36.3, 28.2.

[iv] Reported values for ^{1}H and ^{13}C NMR based on major diastereomer. ^{13}C NMR spectra shows up to 4 different DKP carbonyl peaks of varying intensity, suggesting presence of diastereomers.

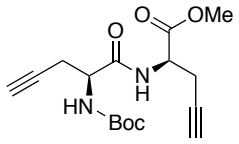

***N*-Boc alkyne dipeptide (+)-100**. The general procedure for peptide coupling used in the synthesis of **(+)-63** and **(+)-88** was followed. R_f = 0.48 (40% EtOAc/Hex). $[\alpha]_D^{20.8} = +47.9$ (*c* = 0.5 CH_2Cl_2). FTIR (film) cm^{-1}: 3295, 2978, 2957, 2932, 1744, 1679, 1515, 1439, 1392, 1368, 1251, 1222, 1167, 1056, 1023, 852, 648. HRMS (ESI) m/z calcd. $C_{16}H_{22}N_2O_5$ $[M+H]^+$ 323.1607, found 323.1607.^{1}H-NMR (500 MHz; $CDCl_3$): δ 7.15-7.14 (m, 1H), 5.35-5.34 (m, 1H), 4.73 (dt, *J* = 7.8, 4.6 Hz, 1H), 4.36-4.35 (m, 1H), 3.79 (s, 3H), 2.83-2.78 (m, 3H), 2.65-2.60 (m, 1H), 2.11 (t, *J* = 2.5 Hz, 1H), 2.03 (dd, *J* = 4.7, 2.1 Hz, 1H), 1.47 (s, 9H). ^{13}C-NMR ($CDCl_3$, 125 MHz): 170.3, 170.0, 155.2, 80.6, 79.10, 79.08, 71.9, 71.6, 60.3, 53.4, 52.8, 50.9, 28.2, 22.3.

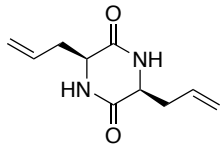

***bis*-Alkene DKP (−)-81**.[61] General procedure for DKP synthesis used in phenyl sulfone DKP **(−)-78** was employed. R_f = 0.45 (10% MeOH/EtOAc). $[\alpha]_D^{21.2} = -82.19$ (*c* = 0.45 MeOH). FTIR (neat) cm^{-1}: 1667, 1457, 1342, 1206, 1138, 922, 844, 802, 725. HRMS (ESI) m/z calcd. $C_{10}H_{14}N_2O_2$ $[M+Na]^+$ 217.0953, found 217.0952.^{1}H-NMR (500 MHz; $CDCl_3$): δ 6.56 (dt, *J* = 0.6, 0.3 Hz, 1H), 5.88-5.73 (m, 1H), 5.47-5.19 (m, 2H), 4.22-4.01 (m, 1H), 2.87-2.77 (m, 1H), 2.53-2.45 (m, 1H). ^{13}C-NMR ($CDCl_3$, 125 MHz): 167.4, 132.1, 120.7, 53.9, 37.9.

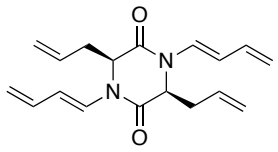

Alkene IMDA precursor (+)-97. A biotage microwave tube was charged with a stir bar, **(−)-81** (50 mg, 0.257 mmol), and 1:1 mixture of CH_2Cl_2 and DMSO (1 mL). To this was added freshly prepared **66** (205 mg, 1.281 mmol), $Cu(OAc)_2$ (14 mg, 0.077 mmol), and 4 Å MS (400 mg) on the bench-top. The tube was sealed, and the resulting heterogeneous mixture was left to stir at 40 ^oC under O_2 atmosphere until full conversion of **(−)-81** was evident by TLC analysis. The reaction mixture was filtered through a pad of Celite, and was rinsed with portions of ethyl acetate (50 mL). The filtrate was concentrated, and directly loaded onto a silica gel column for purification (10% EtOAc/Hex) to afford the title compound as a yellow oil (32 mg, 42%). R_f = 0.29 (10% EtOAc/Hex). $[\alpha]_D^{20.9} = +60.9$ (*c* = 0.45 CH_2Cl_2). FTIR (film) cm^{-1}: 3081, 2922, 2851, 1676, 1641, 1430, 1404, 1314, 1238, 1096, 998, 936, 895, 845. HRMS (ESI) m/z calcd. $C_{18}H_{22}N_2O_2$ $[M+H]^+$ 299.1760, found 299.1758.^{1}H-NMR (500 MHz; $CDCl_3$): δ 7.34 (d, *J* = 14.7 Hz, 1H), 6.44-6.34 (m, 1H), 6.00-5.88 (m, 1H), 5.87-5.79 (m, 1H), 5.30-5.12 (m, 4H), 4.51-4.47 (m, 1H), 2.80-2.66 (m, 2H). ^{13}C-NMR ($CDCl_3$, 125 MHz): 163.1, 134.3, 132.4, 125.9, 119.3, 116.9, 115.5, 57.8, 37.7.

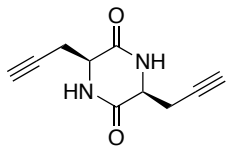

***bis*-Alkyne DKP (−)-98**. General procedure for DKP synthesis used in phenyl sulfone DKP **(−)-78 and** *bis*-alkene DKP **(−)-81** was employed. R_f = 0.7 (100% Acetone). $[\alpha]_D^{21.4} = -41.8$ (*c* = 0.25 DMSO). FTIR (neat) cm^{-1}: 3275, 3210, 3094, 2924, 2853, 1682, 1672, 1440, 1421, 1332, 1223, 1105, 816, 779, 753, 695, 688, 649. ^{1}H-NMR

(500 MHz; DMSO-d_6): δ 8.22 (s, 1H), 4.04 (t, J = 4.4 Hz, 1H), 2.85 (d, J = 1.8 Hz, 1H), 2.71-2.67 (m, 1H), 2.57 (dt, J = 16.9, 3.4 Hz, 1H). ^{13}C-NMR (DMSO-d_6, 125 MHz): 166.3, 80.5, 74.3, 53.4, 23.9.

4.11) References

[1] Iwasa, E., Hamashima, Y., Sodeoka, M. "Epipolythiodiketopiperazine alkaloids: total syntheses and biological activities." *Isr. J. Chem.* **2011**, *51*, 420-433.

[2] Huang, R., Zhou, X., Xu, T., Yang, X., Liu, Y. "Diketopiperazines from marine organisms." *Chem. Biodiversity* **2010**, *7*, 2809-2829.

[3] Amatov, T., Jahn, U. "Gliotoxin: Nature's way of making the epidithio bridge." *Angew. Chem. Int. Ed.* **2014**, *53*, 3312-3314.

[4] Johnson, J. R., Bruce, W. F., Dutcher, J. D. "Gliotoxin, the antibiotic principle of gliocladium fimbriatum. I. Production, physical and biological properties." *J. Am. Chem. Soc.* **1943**, *65*, 2005-2009.

[5] Bell, M. R., Johnson, J. R., Wildi, B. S., Woodward, R. B. "The structure of gliotoxin." *J. Am. Chem. Soc.* **1958**, *80*, 1001-1001.

[6] Fukuyama, T., Kishi, Y. "A total synthesis of gliotoxin." *J. Am. Chem. Soc.* **1976**, *98*, 6723-6724.

[7] Fukuyama, T., Nakatsuka, S.I., Kishi, Y. "Total synthesis of gliotoxin, dehydrogliotoxin, and hyalodendrin." *Tetrahedron* **1981**, *37*, 2045-2078.

[8] Waring, P., Sjaarda, A., Lin, Q. H. "Gliotoxin inactivates alcohol dehydrogenase by either covalent modification or free radical damage mediated by redox cycling." *Biochem. Pharmacol.* **1995**, *49*, 1195-1201.

[9] Nierman, W. C. *et al.* "Genomic sequence of the pathogenic and allergenic filamentous fungus *Aspergillus fumigatus*." *Nature* **2005**, *438*, 1151-1156.

[10] Balibar, C. J., Walsh, C. T. "GliP, a multimodular nonribosomal peptide synthetase in *Aspergillus fumigatus*, makes the diketopiperazine scaffold of gliotoxin." *Biochemistry* **2006**, *45*, 15029-15038.

[11] a) Scharf, D. H., Remme, N., Helnekamp, T., Hortschansky, P., Brakhage, A. A., Hertweck, C. "Transannular disulfide formation in gliotoxin biosynthesis and its role in self-resistance of the human pathogen *Aspergillus fumigatus*." *J. Am. Chem. Soc.* **2010**, *132*, 10136-10141. b) Scharf, D. H., Remme, N., Habel, A., Chankhamjon, P., Scherlach, K., Heinekamp, T., Hortschansky, P., Brakhage, A. A., Hertweck, C. "A dedicated glutathione *S*-transferase mediates carbon-sulfur bond formation in gliotoxin biosynthesis." *J. Am. Chem. Soc.* **2011**, *133*, 12322-12325. c) Scharf, D. H., Chankhamjon, P., Scherlach, K., Heinekamp, T., Roth, M., Brakhage, A. A., Hertweck, C. "Epidithiol formation by an unprecedented twin carbon-sulfur lyase in the gliotoxin pathway." *Angew. Chem. Int Ed.* **2012**, *51*, 10064-10068. d) Scharf, D. H., Chankhamjon, P., Scherlach, K., Heinekamp, T., Willing, K., Brakhage, A. A., Hertweck, C. "Epidithiodiketopiperazine biosynthesis: a four-enzyme cascade converts glutathione conjugates into transannular disulfide bridges." *Angew. Chem. Int. Ed.* **2013**, *52*, 11092-11095.

[12] Schretti, M., Carberry, S., Kavanagh, K., Haas, H., Jones, G. W., O'Brien, J., Nolan, A., Stephens, J., Fenelon, O., Doyle, S. "Self-protection against gliotoxin—a component of the gliotoxin biosynthetic cluster, GliT, completely protects *Aspergillus fumigatus* against exogenous gliotoxin." *PLoS Pathog.* **2010**, *6*, e1000952.

[13] Scharf, D. H., Groll, M., Habel, A., Heinekamp, T., Hertweck, C., Brakhage, A. A., Huber, E. M. "Flavoenzyme-catalyzed formation of disulfide bonds in natural products." *Angew. Chem. Int. Ed.* **2014**, *53*, 2221-2224.

[14] Kishi, Y., Fukuyama, T., Nakatsuka, S. "Total synthesis of dehydrogliotoxin." *J. Am. Chem. Soc.* **1973**, *95*, 6492-6493.

[15] Kishi, Y., Nakatsuka, S., Fukuyama, T., Havel, M. "Total synthesis of sporidesmin A." *J. Am. Chem. Soc.* **1973**, *95*, 6493-6495.

[16] Selected approaches to ETP: (a) Trown, P. W. "Antiviral activity of N,N'-dimethyl-epidithiapiperazinedione, a synthetic compound related to the gliotoxins, LL-S88a and b, chetomin and the sporidesmins." *Biochem. Biophys. Res. Commun.* **1968**, *33*, 402-407. (b) Hino, T., Sato, T. "Synthesis of 3,6-diethoxycarbonyl-3,6-epipolythia-2,5-piperazinedione derivatives." *Tetrahedron Lett.* **1971**, *12*, 3127-3129. (c) Öhler, E., Poisel, H., Tataruch, F., Schmidt, U. "Synthese des epidithio-L-prolyl-L-prolinanhydrids." *Chem. Ber.* **1972**, *105*, 635-641. (d) Öhler, E., Tataruch, F., Schmidt, U. "Über die Einführung von Sauerstoffunktionen in prolyl-prolinanhydrid mit bleitetraacetat: ein neuer weg zum epidisulfid des prolyl-prolinanhydrids." *Chem. Ber.* **1973**, *106*, 396-398.

[17] Kim, J., Ashenhurst, J. A., Movassaghi, M. "Total synthesis of (+)-11,11'-dideoxyverticillin A." *Science* **2009**, *324*, 238-241.

[18] Hauser, D., Weber, H. P., Sigg, H. P. "Isolierung und strukturaufklärung von chaetocin." *Helv. Chim. Acta* **1970**, *53*, 1061-1073.

[19] Katagiri, K., Sato, K., Hayakawa, S., Matsushima, T., Minato H. "Verticillin A, a new anti-biotic from *Verticillium* SF." *J. Antibiot.* **1970**, 23, 420-422.

[20] (a) Movassaghi, M., Schmidt, M. A. "Concise total synthesis of (−)-calycanthine, (+)-chimonanthine, and (+)-follicanthine." *Angew. Chem. Int. Ed.* **2007**, *46*, 3725-3728. (b) Movassaghi, M., Schmidt, M. A., Ashenhurst, J. A. "Concise total synthesis of (+)-win 64821 and (−)-ditryptophenaline." *Angew. Chem. Int. Ed.* **2008**, *47*, 1485-1487.

[21] Ruble, J. C., Fu, G. C. "Enantioselective construction of quaternary stereocenters: rearrangements of *O*-acylated azalactones catalyzed by a planar-chiral derivative of 4-(pyrrolidino)pyridine." *J. Am. Chem. Soc.* **1998**, *120*, 11532-11533.

[22] Selected publications: (a) Kim, J., Movassaghi, M. "General approach to epipolythiodiketopiperazine alkaloids: total synthesis of (+)-chaetocins A and C and (+)-12,12'-dideoxychetracin A." *J. Am. Chem. Soc.* **2010**, *132*, 14376-14378. (b) Boyer, N., Morrison, K. C., Kim, J., Hergenrother, P. J., Movassaghi, M. "Synthesis and anticancer activity of epipolythiodiketopiperazine alkaloids." *Chem. Sci.* **2013**, *4*, 1646-1657. (c) Coste, A., Kim, J., Adams, T. C., Movassaghi, M. "Concise total synthesis of (+)-bionectins A and C." *Chem. Sci.* **2013**, *4*, 3191-3197.

[23] Nicolaou, K. C., Totokotsopoulos, S., Giguère, D., Sun, Y. P., Sarlah, D. "Total synthesis of epicoccin G." *J. Am. Chem. Soc.* **2011**, *133*, 8150-8153.

[24] Wipf, P., Kim, Y. "Studies on the synthesis of *Stemona* alkaloids; stereoselective preparation of the hydroindole ring system by oxidative cyclization of tyrosine." *Tetrahedron Lett.* **1992**, *33*, 5477-5480.

[25] (a) Nicolaou, K. C., Lu, M., Totokotsopoulos, S., Heretsch, P., Giguère, D., Sun, Y. P., Sarlah, D., Nguyen, T. H., Wolf, I. C., Smee, D. F., Day, C. W., Bopp, S., Winzeler, E. A. "Synthesis and biological evaluation of epidithio-, epitetrathio-, and bis-

(methylthio)diketopiperazines: synthetic methodology, enantioselective total synthesis of epicoccin G, 8,8'-*epi*-*ent*-rostratin B, gliotoxin, gliotoxin G, emethallicin e, and haematocin and discovery of new antiviral and antimalarial agents." *J. Am. Chem. Soc.* **2012**, *134*, 17320-17332. (b) Nicolaou, K. C., Giguère, D., Totokotsopoulos, S., Sun, Y.P. "A practical sulfenylation of 2,5-diketopiperazines." *Angew. Chem. Int. Ed.* **2012**, *51*, 728.

[26] (a) DeLorbe, J. E., Jabri, S. Y., Mennen, S. M., Overman, L E., Zhang, F. L. "Enantioselective total synthesis of (+)-gliocladine C: Convergent construction of cyclotryptamine-fused polyoxopiperazines and a general approach for preparing epidithiodioxopiperazines from tiooxopiperazine precursors." *J. Am. Chem. Soc.* **2011**, *133*, 6549-6552. (b) DeLorbe, J. E., Horne, D., Jove, R., Mennen, S. M., Nam, S., Zhang, F. L., Overman, L. E. "General approach for preparing epidithiodioxopiperazines from trioxopiperazine precursors: Enantioselective total syntheses of (+)- and (−)-gliocladine C, (+)-leptosin D, (+)-T988C, (+)-bionectin A, and (+)-gliocladin A." *J. Am. Chem. Soc.* **2013**, *135*, 4117-4128.

[27] (a) Codelli, J. A., Puchlopek, A. L. A., Reisman, S. E. "Enantioselective total synthesis of (−)-acetylaranotin, a dihydrooxepine epidithiodiketopiperazine." *J. Am. Chem. Soc.* **2012**, *134*, 1930-1933. (b) Fujiwara, H., Kurogi, T., Okaya, S., Okano, K., Tokuyama, H. "Total synthesis of (−)-acetylaranotin." *Angew. Chem. Int. Ed.* **2012**, *51*, 13062-13065.

[28] (a) Friedrich, A., Jainta, M., Nieger, M., Bräse, S. "One-pot synthesis of symmetrical and unsymmetrical diketopiperazines from unprotected amino acids." *Synlett*, **2007**, *13*, 2127-2129. (b) Friedrich, A., Jainta, M., Nising, C. F., Bräse, S. "Synthesis of

hexahydroindole carboxylic acids by intramolecular diels-alder reaction." *Synlett*, **2008**, *4*, 589-591. (c) Jainta, M., Nieger, M., Bräse, S. "Facile synthesis and spectroscopic elucidation of 4,11-bis(dehydroxy)-bipolaroamide." *J. Mol. Struct.* **2009**, *921*, 85-88. (d) Gross, U., Nieger, M., Bräse, S. "A unified strategy targeting the thiodiketopiperazine mycotoxins exserohilone, gliotoxin, the epicoccins, the epicorazines, rostratin A and aranotin." *Chem. Eur. J.* **2010**, *16*, 11624-11631. (e) Ruff, B. M., Zhong, S., Nieger, M., Sickert, M., Schneider, C., Bräse, S. "A combined vinylogous mannich/diels-alder approach for the stereoselective synthesis of highly functionalized hexahydroindoles." *Eur. J. Org. Chem.* **2011**, 6558-6566.

[29] Middleton, M. D., Peppers, B. P., Diver, S. T. "Studies directed toward the synthesis of the scabrosins: validation of a tandem enyne metathesis approach." *Tetrahedron* **2006**, *62*, 10528-10540.

[30] Bäckvall, J. E., Nyström, J. E., Nordberg, R. E. "Stereo- and regioselective palladium-catalyzed, 1,4-acetoxychlorination of 1,3-dienes. 1-Acetoxy-4-chloro-2-alkenes as versatile synthons in organic transformations." *J. Am. Chem. Soc.* **1985**, *107*, 3676-3686.

[31] Carreira, E. M., Zipfel, H. F. "An efficient synthesis strategy to the core structure of 6-5-6-5-6-membered epipolythiodiketopiperazines." *Org. Lett.* **2014**, *16*, 2854-2857.

[32] Corey, E. J., Loh, T. P. "Catalytic enantioselective diels-alder addition to furan provides a direct synthetic route to many chiral natural products." *Tetrahedron Lett.* **1993**, *34*, 3979-3982.

[33] (a) Tan, R. X., Jensen, P. R., Williams, P. G., Fenical, W. "Isolation and structure assignments of rostratins A-D, cytotoxic disulfides produced by the marine-derived

fungus *Exserohilum rostratum*." *J. Nat. Prod.* **2004**, *67*, 1374-1382. (b) Baute, M.-A., Deffieux, G., Baute, R., Neveu, A. "New antibiotics from the fungus *Epicoccum nigrum*." *J. Antibiot.* **1978**, *31*, 1099-1101. (c) Sugawara, K., Sugawara, F., Strobel, G. A., Fu, Y., Cun-Heng, H., Clardy, J. "Exserohilone: A novel phytotoxin produced by *Exserohilum holmii*." *J. Org. Chem.* **1985**, *50*, 5631-5633. (d) Zhang, Y., Liu, S., Che, Y., Liu, X. "Epicoccins A-D, epipolythiodioxopiperazines from a *Cordyceps*-colonizing isolate of *Epicoccum nigrum*." *J. Nat. Prod.* **2007**, *70*, 1522-1525. (e) Guo, H., Sun, B., Gao, H., Chen, X., Liu, S., Yao, X., Liu, X., Che, Y. "Diketopiperazines from the *Cordyceps*-colonizing fungus *Epicoccum nigrum*." *J. Nat. Prod.* **2009**, *72*, 2115-2119. (f) Kong, F., Wang, Y., Liu, P., Dong, T., Zhu, W. "Thiodiketopiperazines from the marine-derived fungus *Phoma* sp. OUCMDZ-1847." *J. Nat. Prod.* **2014**, *77*, 132-137.

[34] (a) Fanning, K. N., Sutherland, A. "A facile synthesis of (*S*)-gizzerosine, a potent agonist of the histamine H_2-receptor." *Tetrahedron Lett.* **2007**, *48*, 8479-8481. (b) Padrón, J. M., Kokotos, G., Martín, T., Markidis, T., Gibbons, W. A., Martín, V. S. "Enantiospecific synthesis of a-amino acid semialdehydes: a key step for the synthesis of unnatural unsaturated and saturated a-amino acids." *Tetrahedron: Asymmetry* **1998**, *9*, 3381-3394.

[35] Selected reviews: (a) Dinsmore, C. J., Beshore, D. C. "Recent advances in the synthesis of diketopiperazines." *Tetrahedron* **2002**, *58*, 3297-3312. (b) Borthwick, A. D. "2,5-diketopiperazines: Synthesis, reactions, medicinal chemistry, and bioactive natural products." *Chem. Rev.* **2012**, *112*, 3641-3716.

[36] Eguchi, C., Kakuta, A. "Studies on cyclic dipeptides. I. Thermodynamics of the cis-trans isomerization of the side chains in cyclic dipeptides." *J. Am. Chem. Soc.* **1974**, *96*, 3985-3989.

[37] (a) Schkeryantz, J. M., Woo, J. C. G., Siliphaivanh, P., Depew, K. M., Danishefsky, S. J. "Total synthesis of gypsetin, deoxybrevianamide E, brevianamide E, and tryprostatin B: Novel constructions of 2,3-disubstituted indoles." *J. Am. Chem. Soc.* **1999**, *112*, 11964-11975. (b) Marsden, S. P., Depew, K. M., Danishefsky, S. J. "Stereoselective total syntheses of amauromine and 5-*N*-acetylardeemin. A concise route to the family of "reverse-prenylated" hexahydropyrroloindole alkaloids." *J. Am. Chem. Soc.* **1994**, *116*, 11143-11144.

[38] Shangguan, N., Hehre, W. J., Ohlinger, W. S., Beavers, M. P., Joullié, M. M. "The total synthesis of roquefortine C and a rationale for the thermodynamic stability of isoroquefortine C over roquefortine C." *J. Am. Chem. Soc.* **2008**, *130*, 6281-6287.

[39] (a) Zezza, C., Smith, M. B. "*N*-Dienyl lactams: Preparation and selectivity in the Diels-Alder reaction." *J. Org. Chem.* **1988**, *53*, 1161-1167. (b) Behr, J.-B., Defoin, A., Mahmood, N., Streith, J. "(±)-4-Amino-4,5-dideoxyribose, (±)-4-amino-4-deoxyerythrose, and (±)-dihydroxyproline derivatives from *N*-dienyl-g-lactams." *Helv. Chim. Acta.* **1995**, *78*, 1166-1177."

[40] Gooβen, L. J., Arndt, M., Blanchot, M., Rudolphi, F., Menges, F., Niedner-Schatteburg, G. "A practical and effective ruthenium trichloride-based protocol for the regio- and stereoselective catalytic hydroamidation of terminal alkynes." *Adv. Synth. Catal.* **2008**, *350*, 2701-2707.

[41] (a) Batey, R. A., Bolshan, Y. "Enamide synthesis by copper-catalyzed cross-coupling of amides and potassium alkenyltrifluoroborate salts." *Angew. Chem. Int. Ed.* **2008**, *47,* 2109-2112. (b) Batey, R. A., Bolshan, Y. "Copper-catalyzed cross-coupling of amides and potassium alkenyltrifluoroborate salts: a general approach to the synthesis of enamids." *Tetrahedron* **2010**, *66*, 5283-5294.

[42] Shirakawa, K., Arase, A., Hoshi, M. "Preparation of (*E*)-1-alkenylboronic acid pinacol esters via transfer of alkenyl group from boron to boron." *Synthesis* **2004**, 1814-1820.

[43] Guennouni, N., Rasset-Deloge, C., Carboni, B., Vaultier, M. "Halosulphonylation of unsaturated boronic esters: Access to new electron-deficient alkenes and dienes." *Synlett* **1992**, 581-584.

[44] Molander, G. A., Felix, L. A. "Stereoselective Suzuki-Miyaura cross-coupling reactions of potassium alkenyltrifluoroborates with alkenyl bromides." *J. Org. Chem.* **2005**, *70*, 3950-3956.

[45] De, S., Welker, M. E. "Preparation of 2-BF_3-substituted 1,3-dienes and their Diels-Alder/cross-coupling reactions." *Org. Lett.* **2005**, *7*, 2481-2484.

[46] Importance of type of zeolite in copper-catalyzed reaction is known: Kim, H. Y., Kim, S., Oh, K. "Orthogonal enantioselectivity approaches using homogeneous and heterogeneous catalyst systems: Friedel—Crafts alkylation of indole." *Angew, Chem. Int. Ed.* **2010**, *49*, 4476-4478.

[47] (a) Lennox, A. J. J., Lloyd-Jones, G. C. "Organotrifluoroborate hydrolysis: Boronic acid release mechanism and an acid—base paradox in cross-coupling." *J. Am. Chem. Soc.* **2012**, *134*, 7431-7441. (b) Matos, K., Soderquist, J. A. "Alkylboranes in the Suzuki—

Miyaura coupling: Stereochemical and mechanistic studies." *J. Org. Chem.* **1998**, *63*, 461-470.

[48] (a) Evans, D. A., Katz, J. L., West, T. R. "Synthesis of diaryl ethers through the copper-promoted arylation of phenols with arylboronic acids. An expedient synthesis of thyroxine." *Tetrahedron Lett.* **1998**, *39*, 2937-2940. (b) King, A. E., Brunold, T. C., Stahl, S. S. "Mechanistic study of copper-catalyzed aerobic oxidative coupling of arylboronic esters and methanol: Insights into an organometallic oxidase reaction." *J. Am. Chem. Soc.* **2009**, *131*, 5044-5045.

[49] Selected reviews: (a) Juhl, M., Tanner, D. "Recent application of intramolecular Diels—Alder reactions to natural product synthesis." *Chem. Soc. Rev.* **2009**, *38*, 2983-2992. (b) Merino, P., Marqués-López, E., Tejero, T., Herrera, R. P. "Enantioselective organocatalytic Diels—Alder reactions." *Synthesis* **2010**, 1-26. (c) Moyano, A., Rios, R. "Asymmetric organocatalytic cyclization and cyloaddition reactions." *Chem. Rev.* **2011**, *111*, 4703-4832.

[50] Bear, B. R., Sparks, S. M., Shea, K. J. "The type 2 intramolecular Diels—Alder reaction: Synthesis and chemistry of bridgehead alkenes." *Angew. Chem. Int. Ed.* **2001**, *40*, 820-849.

[51] (a) Graham, T. H., Horning, B. D., MacMillan, D. W. C. "The preparation of (2*R*, 5*S*)-2-*t*-butyl-3,5-dimethylimidazolidin-4-one." *Org. Synth.* **2011**, *88*, 42-54. (b) Wilson, R. M., Jen, W. S., MacMillan, D. W. C. "Enantioselective organocatalytic intramolecular Diels—Alder reactions. The asymmetric synthesis of solanapyrone D." *J. Am. Chem. Soc.* **2005**, *127*, 11616-11617.

[52] Ahrendt, K. A., Borths, C. J., MacMillan, D. W. C. "New strategies for organic catalysts: The first highly enantioselective organocatalytic Diels—Alder reaction." *J. Am. Chem. Soc.* **2000**, *122*, 4243-4244.

[53] W. S. Jen. "Development of new asymmetric organocatalytic methods and progress towards the total synthesis of guanacastepene A." California Institute of Technology, Pasadena, California, 2004.

[54] C. H-M. Larsen. "Investigating imidazolidinone catalysts: Enantioselective organocatalytic Diels—Alder reactions, conjugate additions to access non-natural a-amino acids, and bimodal catalyst activation for the development of organo-cascade reactions." California Institute of Technology, Pasadena, California, 2005.

[55] Kristensen, T. E., Vestli, K., Jakobsen, M. G., Hansen, F. K., Hansen, T. "A general approach for preparation of polymer-supported chiral organocatalysts via acrylic copolymerization." *J. Org. Chem.* **2010**, *75*, 1620-1629.

[56] Zhou, G., Hu, Q.-Y., Corey, E. J. "Useful enantioselective bicyclization reactions using an N-protonated chiral oxazaborolidine as catalyst." *Org. Lett.* **2003**, *5*, 3979-3982.

[57] Hayashi, Y., Samanta, S., Gotoh, H., Ishikawa, H. "Asymmetric Diels—Alder reactions of a,b-unsaturated aldehydes catalyzed by a diarylprolinol silyl ether salt in the presence of water." *Angew. Chem. Int. Ed.* **2008**, *47*, 6634-6637.

[58] Thamapipol, S., Bernardinelli, G., Besnard, C., Kündig, E. P. "Chiral ruthenium lewis acid catalyzed intramolecular Diels—Alder reactions." *Org. Lett.* **2010**, *12,* 5604-5607.

[59] Flores, B., Molinski, T. F. "Assembly of the isoindolinone core of muironolide A by asymmetric intramolecular Diels—Alder cycloaddition." *Org. Lett.* **2011**, *13*, 3932-3935.

[60] Oppolzer, W., Fröstl, W. "A stereoselective approach to *cis*- and *trans*-1,2,3,4,4a,5,6,8a-octahydroquinolines by intramolecular Diels—Alder reactions." *Helv. Chim. Acta.* **1975**, *58*, 590-593.

[61] Porzi, G., Sandri, S. "Synthesis of (3*R*,6*R*)- and (3*S*,6*S*)-3,6-dialkylpiperazin-2,5-dione derivatives as useful intermediates to both (*R*) and (*S*) a-aminoacids." *Tetrahedron: Asymmetry* **1994**, *5*, 453-464.

[62] Guinchard, X., Bugaut, X., Cook, C., Roulland, E. "Palladium(0)-catalyzed cross-coupling of potassium (*Z*)-2-chloroalk-1-enyl trifluoroborates: A chemo- and stereoselective access to (*Z*)-chloroolefins and trisubstituted alkenes." *Chem. Eur. J.* **2009**, *15*, 5793-5798.

[63] Selected publications: (a) Cho, Y. A., Kim, D.-S., Ahn, H. R., Canturk, B., Molander, G. A., Ham, J. "Preparation of potassium azidoaryltrifluoroborates and their cross-coupling with aryl halides." *Org. Lett.* **2009**, *11,* 4330-4333. (b) Molander, G. A., Ham, J., Canturk, B. "Preparation and wittig reactions of organotrifluoroborato phosphonium ylides." *Org. Lett.* **2007**, *9*, 821-824. (c) Kim, D.-S., Bolla, K., Lee, S., Ham, J. "One-pot preparation of hydroxylated potassium organotrifluoroborates and subsequent Jones oxidation to potassium organocarbonyltrifluoroborates." *Tetrahedron* **2011**, *67*, 1062-1070.

[64] Fraunhoffer, K. J., White, M. C. "*syn*-1,2-amino alcohols via diastereoselective allylic C—H amination."*J. Am. Chem. Soc.* **2007**, *129*, 7274-7276.

[65] Selected reviews: (a) Lautens, M., Klute W., Tam, W. "Transition metal-mediated cycloaddition reactions." *Chem. Rev.* **1996**, *96*, 49-92. (b) Reymond, S., Cossy, J. "Copper-catalyzed Diels—Alder reactions." *Chem. Rev.* **2008**, *108*, 5359-5406.

[66] Selected papers: (a) Bellville, D. J., Wirth, D. D., Bauld, N. L. "The cation-radical catalyzed Diels—Alder reaction." *J. Am. Chem. Soc.* **1981**, *103*, 718-720. (b) Rusterholz, D. B., Gorman, D. B., Gassman, P. G. "The intramolecular radical cation induced Diels-Alder reaction in the diene-diene format." *Molecules* **1997**, *2*, 80-86.

[67] Stork, G., West, F., Lee, H. Y., Isaacs, R. C. A., Manabe, S. "The total synthesis of a natural cardenolide: (+)-digitoxigenin." *J. Am. Chem. Soc.* **1996**, *118*, 10660-10661.

[68] (a) Bauld, N. L., Bellville, D. J., Pabon, R., Chelsky, R., Green, G. "Theory of cation-radical pericyclic reactions." *J. Am. Chem. Soc.* **1983**, *105*, 2378-2382. (b) Bellville, D. J., Wirth, D. W., Bauld, N. L. "Cation-radical catalyzed Diels-Alder reaction." *J. Am. Chem. Soc.* **1981**, *103*, 718-720. (c) Pabon, R. A., Bellville, D. J., Bauld, N. L. "Selective cyclobutane adduct formation in competition with Diels-Alder addition in cation radical cycloadditions." *J. Am. Chem. Soc.* **1984**, *106*, 2730-2731. (d) Reynolds, D. W., Lorenz, K. T., Chiou, H. S., Bellville, D. J., Pabon, R. A., Bauld, N. L. "Mechanistic diagnosis of aminium salt initiated Diels-Alder cycloadditions in the diene/diene format." *J. Am. Chem. Soc.* **1987**, *109*, 4960-4968.

[69] Smith, A. B., III., Basu, K., Bosanac, T. "Total synthesis of (−)-okilactomycin." *J. Am. Chem. Soc.* **2007**, *129*, 14872-14874.

[70] Ishihara, J., Nonaka, R., Terasawa, Y., Shiraki, R., Yabu, K., Kataoka, H., Ochiai, Y., Tadano, K. "Total synthesis of (−)-verrucarol." *J. Org. Chem.* **1998**, *63*, 2679-2688.

[71] Sun, H., Yang, C., Gao, F., Li, Z., Xia, W. "Oxidative C—C bond cleavage of aldehydes via visible-light photoredox catalysis." *Org. Lett.* **2013**, *15*, 624-627.

[72] Hu, B., Li, Y., Li, Z., Meng, X. "Aniline mediated oxidative C—C bond cleavage of a-alkoxy aldehydes in air and a model reaction for the synthesis of a-(D)-amino acid derivatives." *Org. Biomol. Chem.* **2013**, *11*, 4138-4141.

[73] Fukuzumi, S., Kotani, H., Ohkubo, K. "Electron-transfer state of 9-mesityl-10-methylacridinium ion with a much longer lifetime and higher energy than that of the natural photosynthetic reaction center." *J. Am. Chem. Soc.* **2004**, *126*, 1600-1601.

[74] Prier, C. K., Rankic, D. A, MacMillan, D. W. C. "Visible light photoredox catalysis with transition metal complexes: Applications in organic synthesis." *Chem. Rev.* **2013**, *113*, 5322-5363.

[75] Selected references: (a) Shen, R., Porco, J. A., Jr., "Synthesis of enamides related to the salicylate antitumor macrolides using copper-mediated vinylic substitution." *Org. Lett.* **2000**, *2*, 1333-1336. (b) Jiang, L., Job, G. E., Klapars, A., Buchwald, S. L. "Copper-catalyzed coupling of amides and carbamates with vinyl halides." *Org. Lett.* **2003**, *5*, 3667-3669.

[76] (a) Molander, G. A., Cavalcanti, L. N. "Metal-free chlorodeboronation of organotrifluoroborates" *J. Org. Chem.* **2011**, *76*, 7195-7203. (b) Yao, M.-L., Kabalka, G. W., Blevins, D. W., Reddy, M. S., Yong, L. "Halodeboronation of organotrifluoroborates using tetrabutylammonium tribromide or cesium triiodide." *Tetrahedron* **2012**, *68*, 3738-3743.

[77] Beghyn, T., Hounsou, C., Deprez, B. P. "PDE5 inhibitors: An original access to novel potent arylated analogues of tadalafil." *Bioorg. Med. Chem. Lett.* **2007**, *17*, 780-792.

[78] Enquist, J. A., Jr., Stoltz, B. M. "The total synthesis of (−)-cyanthiwigin F by means of double catalytic enantioselective alkylation."*Nature* **2008**, *453*, 1228-1231.

4.12) Appendix C. Nuclear Magnetic Resonance and Infrared Spectra Relevant to Chapter 4

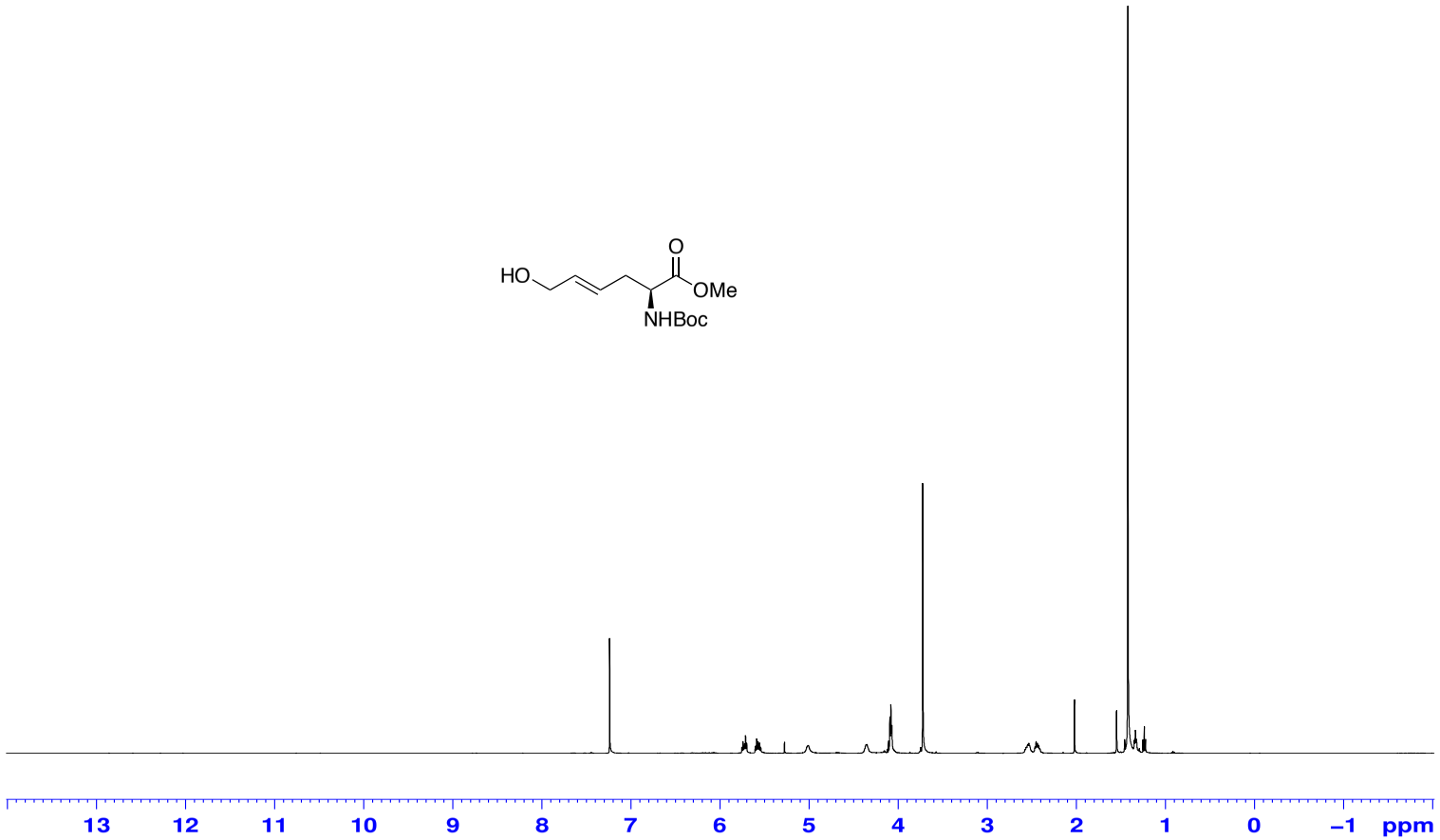

Figure 1: ^{1}H NMR ($CDCl_3$, 500 MHz) of **(+)-57**

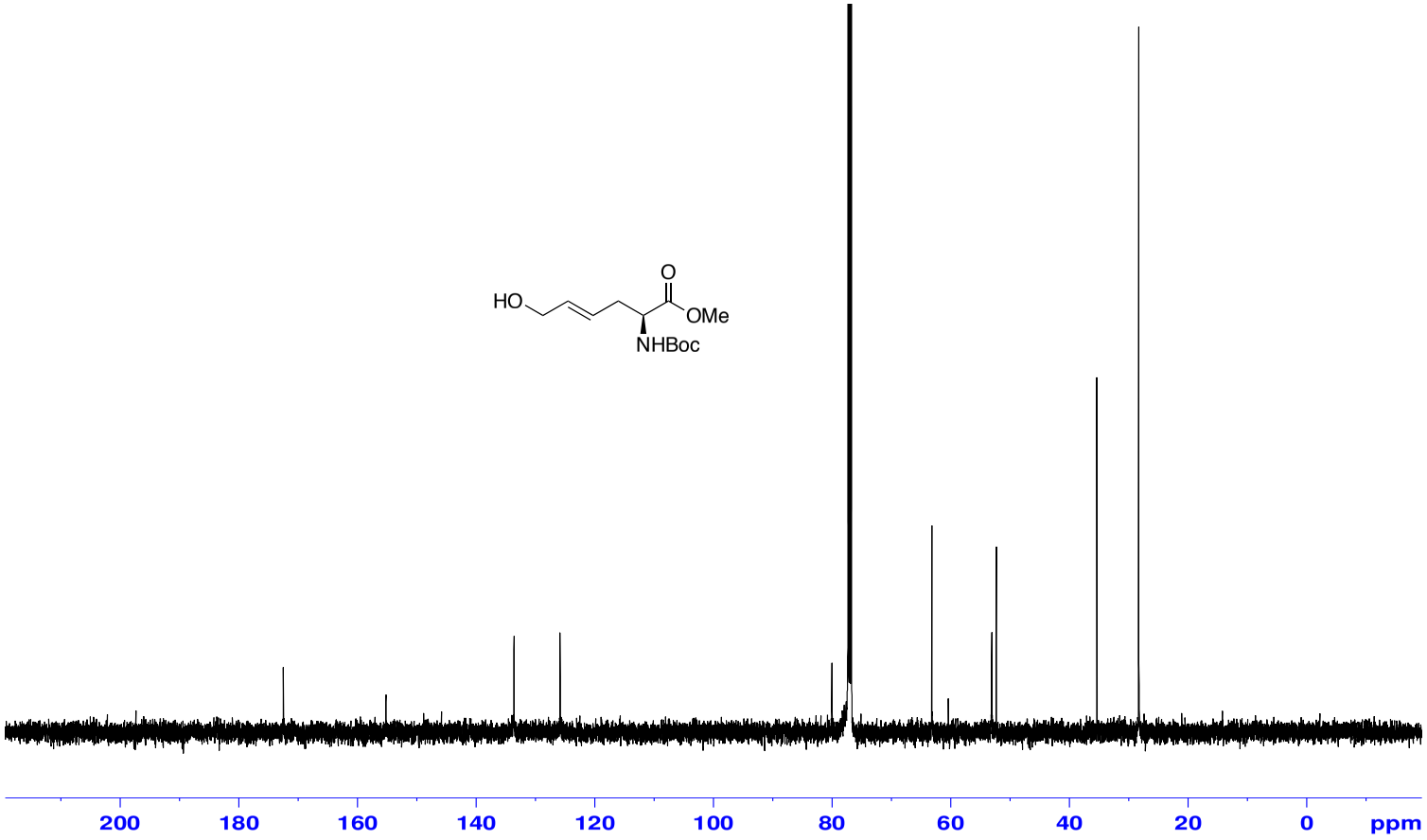

Figure 2: ^{13}C NMR ($CDCl_3$, 125 MHz) of **(+)-57**

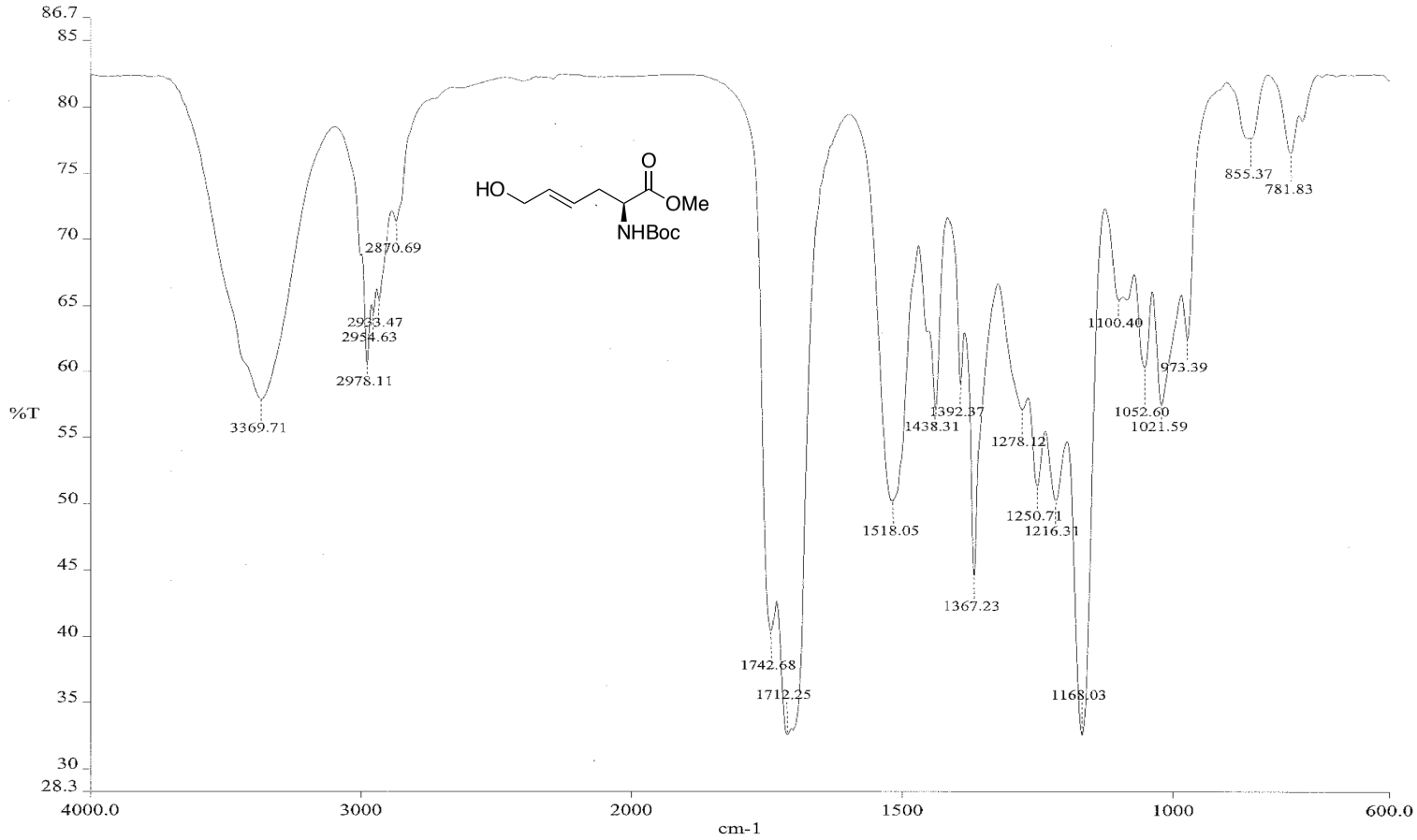

Figure 3: Infrared spectra (neat) of **(+)-57**

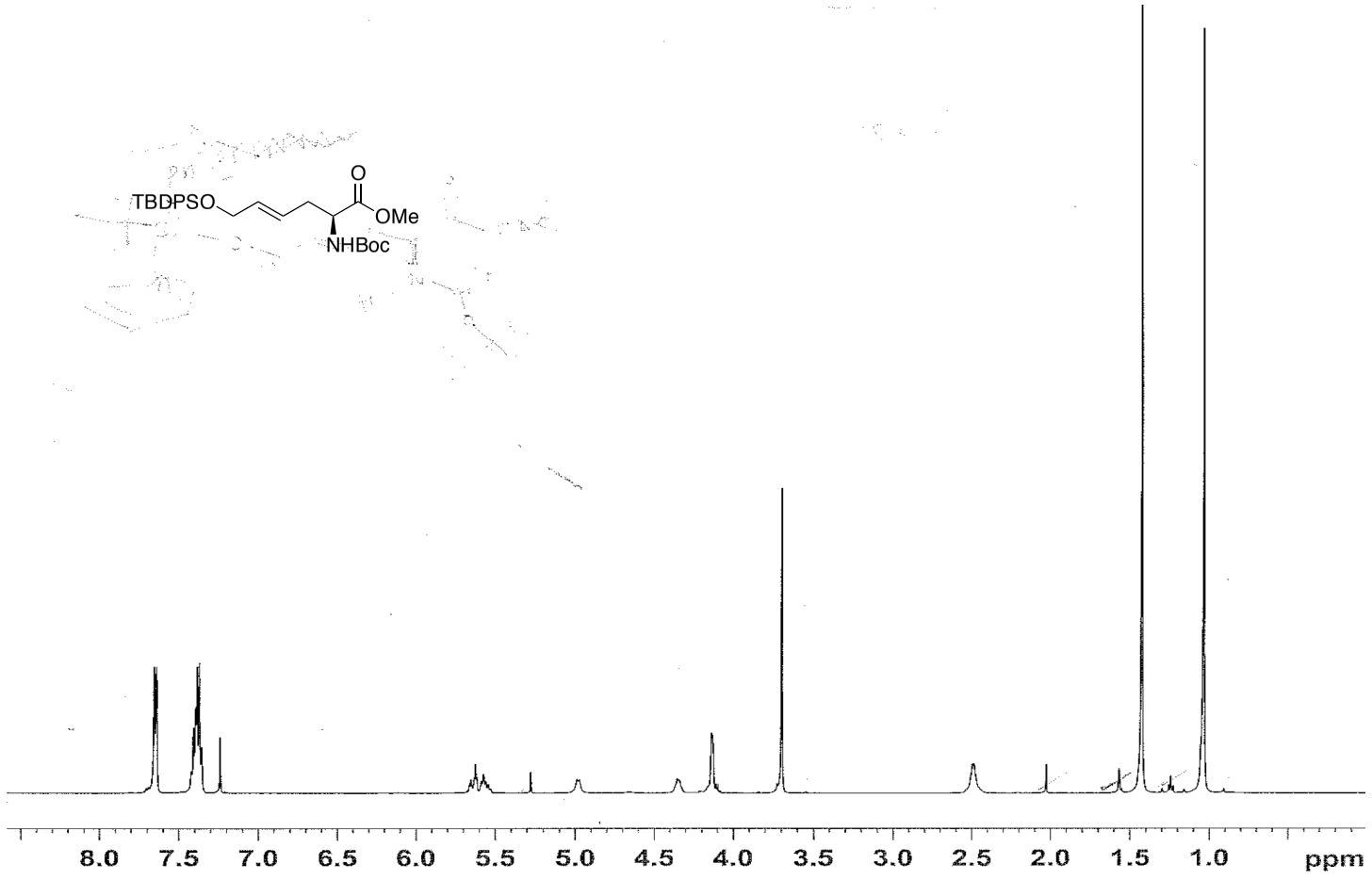

Figure 4: ^{1}H NMR ($CDCl_3$, 500 MHz) of **(+)-59**

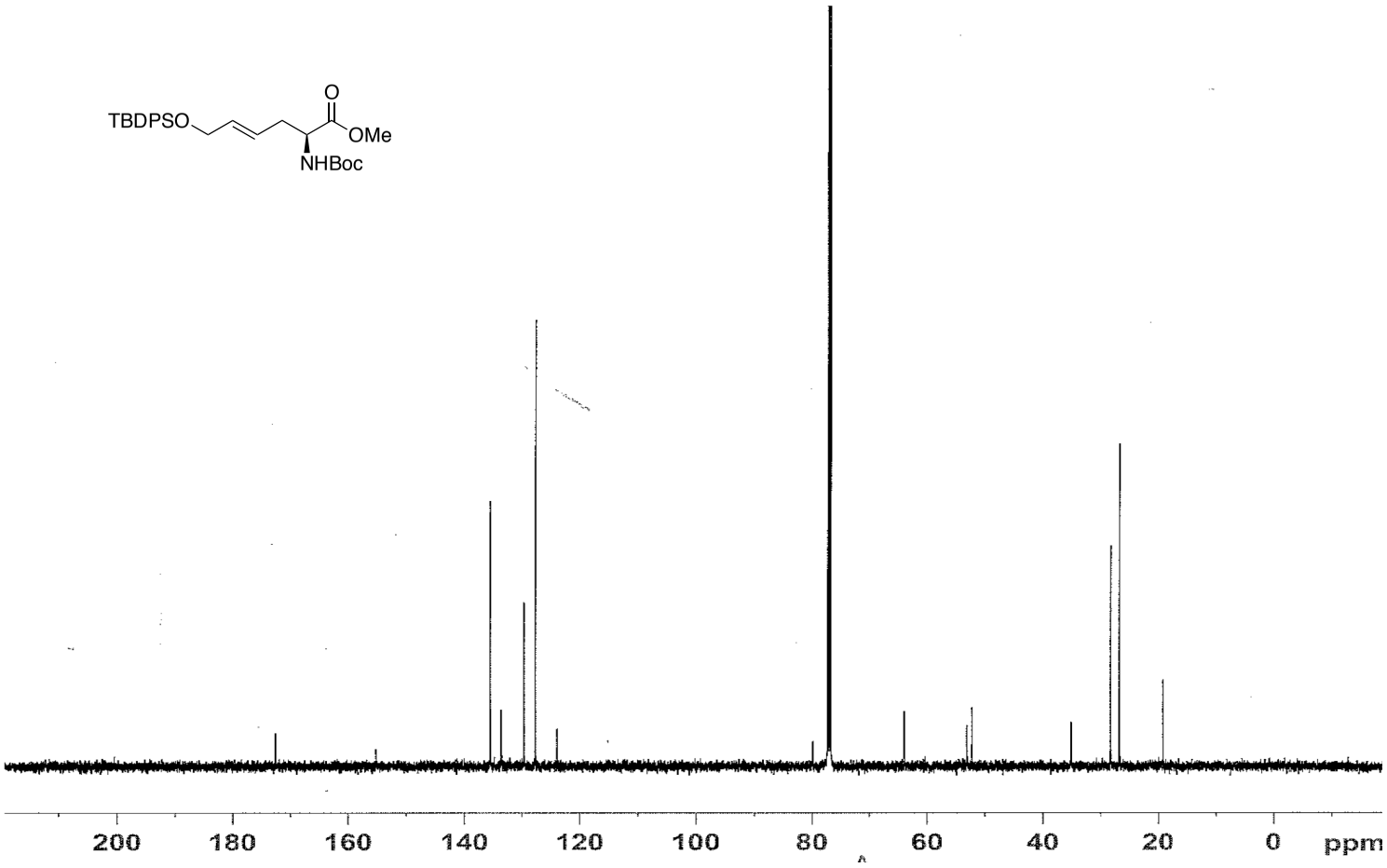

Figure 5: ^{13}C NMR ($CDCl_3$, 125 MHz) of **(+)-59**

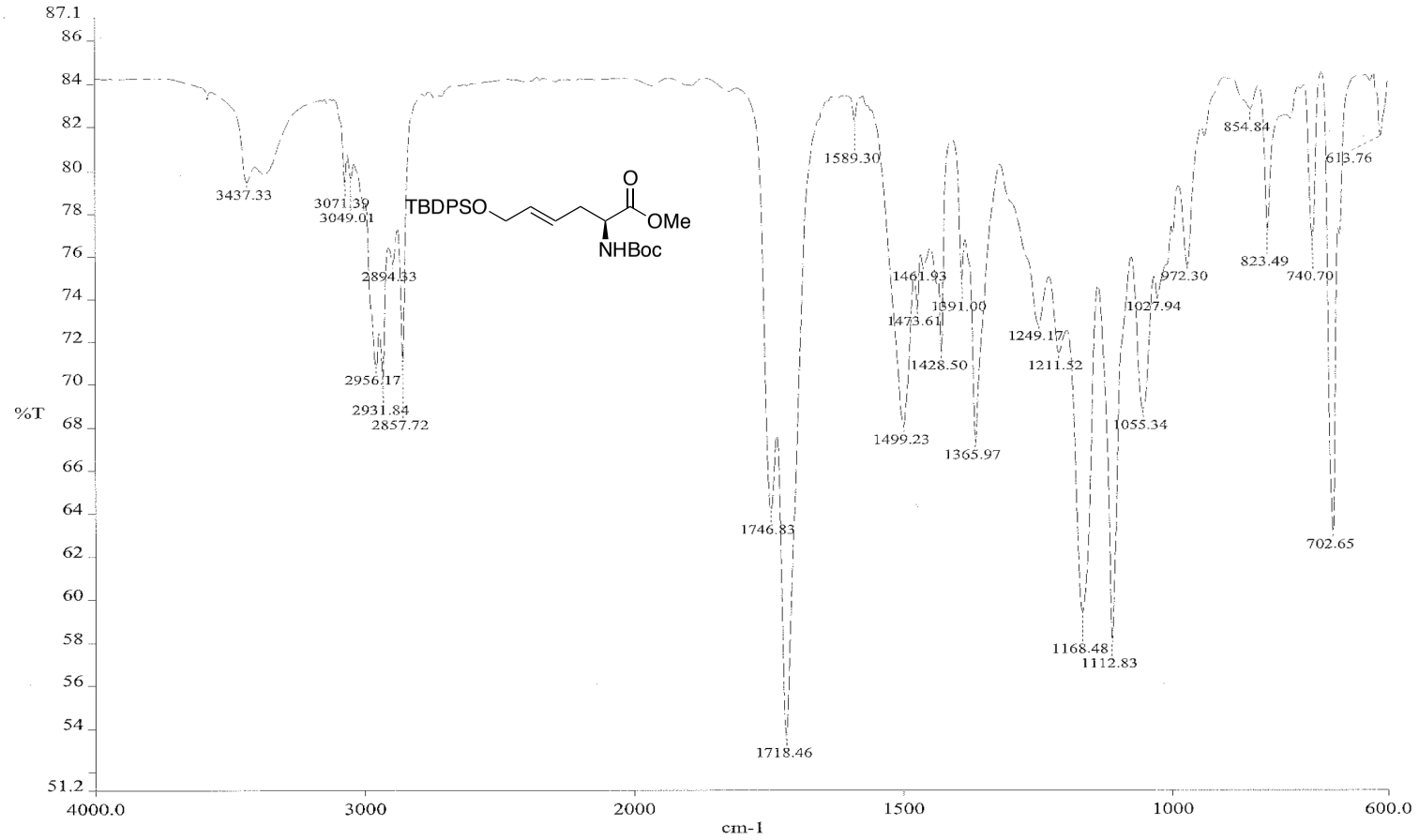

Figure 6: Infrared spectra (neat) of **(+)-59**

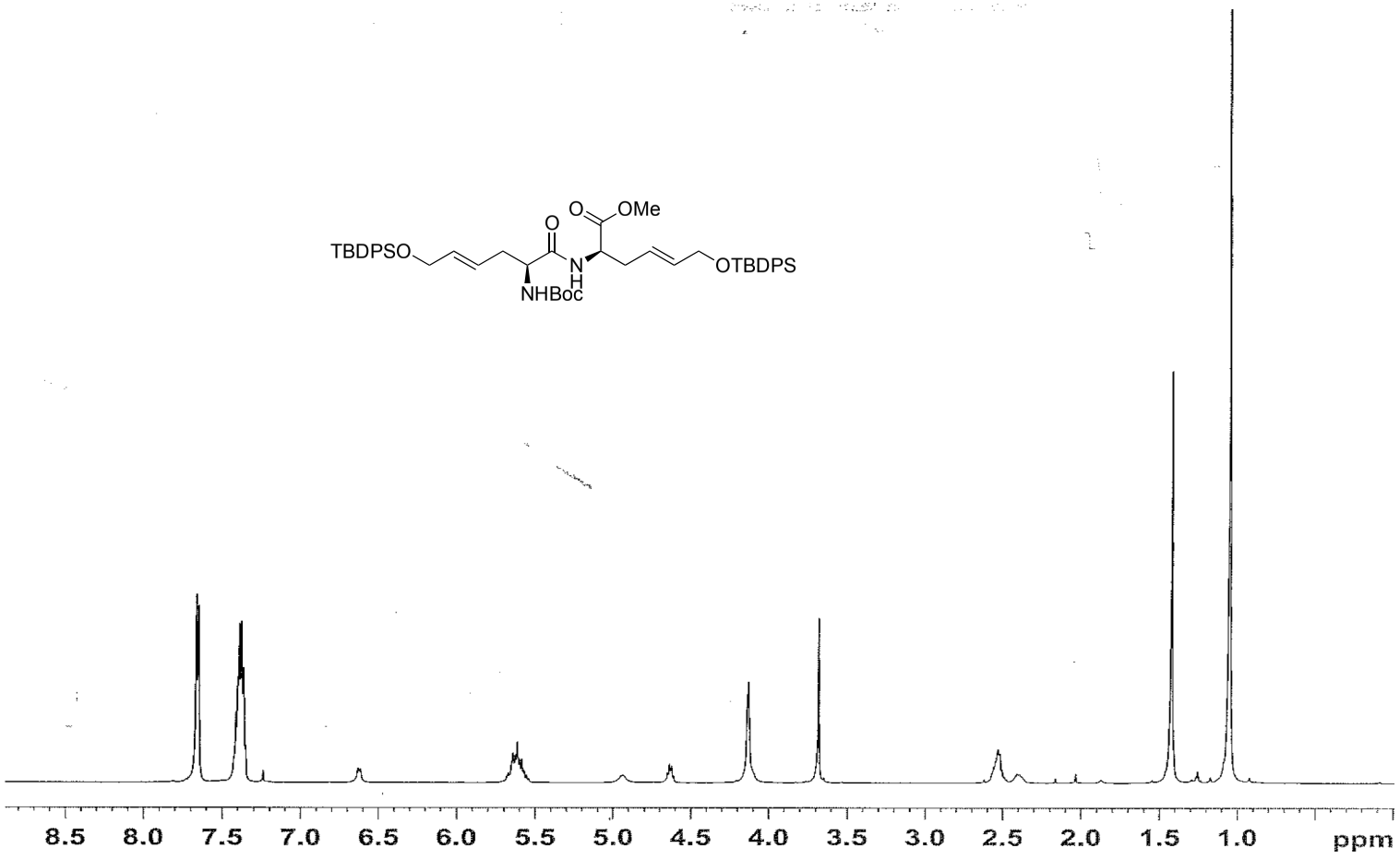

Figure 7: ^{1}H NMR ($CDCl_3$, 500 MHz) of **(+)-63**

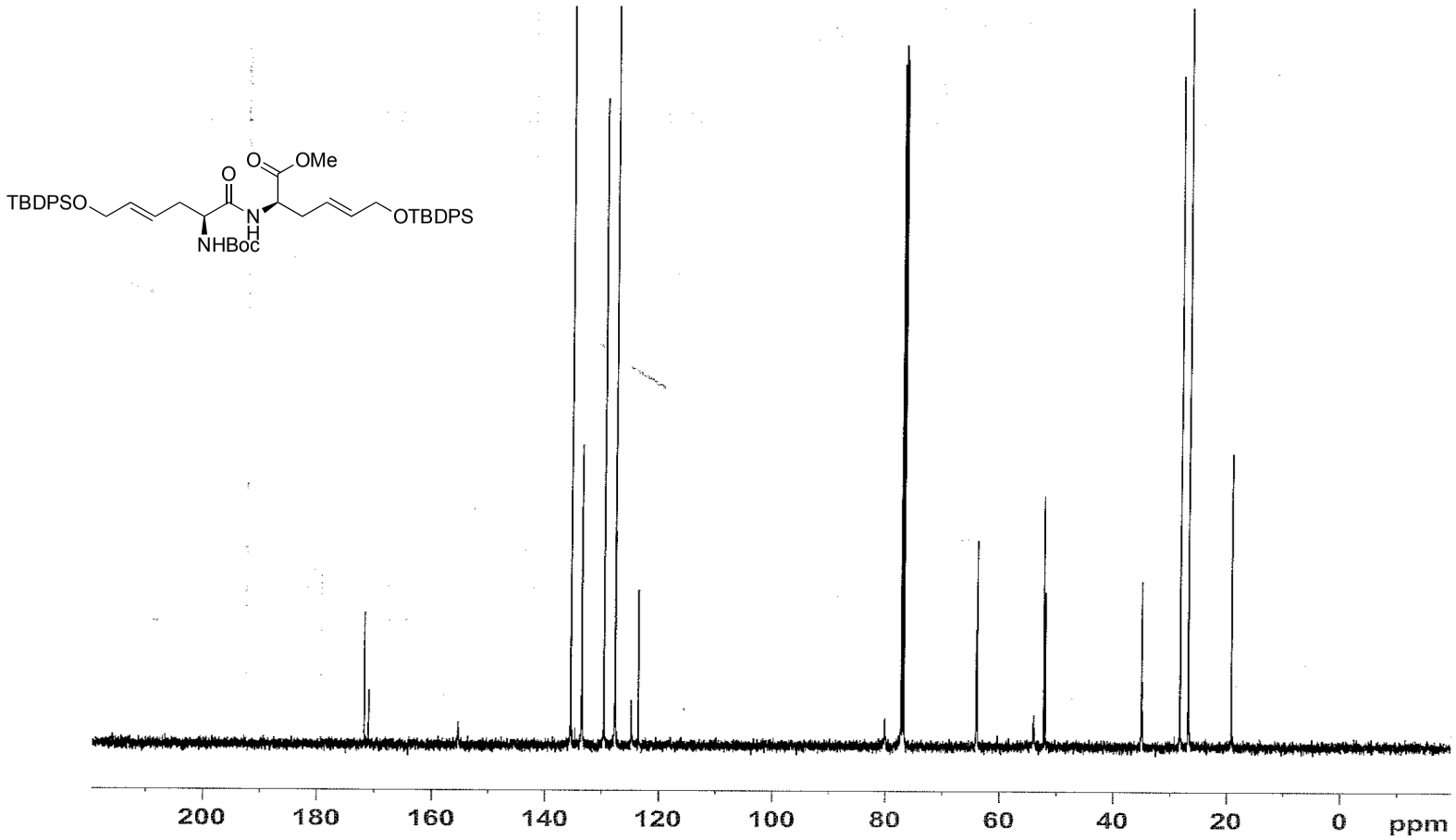

Figure 8: ^{13}C NMR ($CDCl_3$, 125 MHz) of **(+)-63**

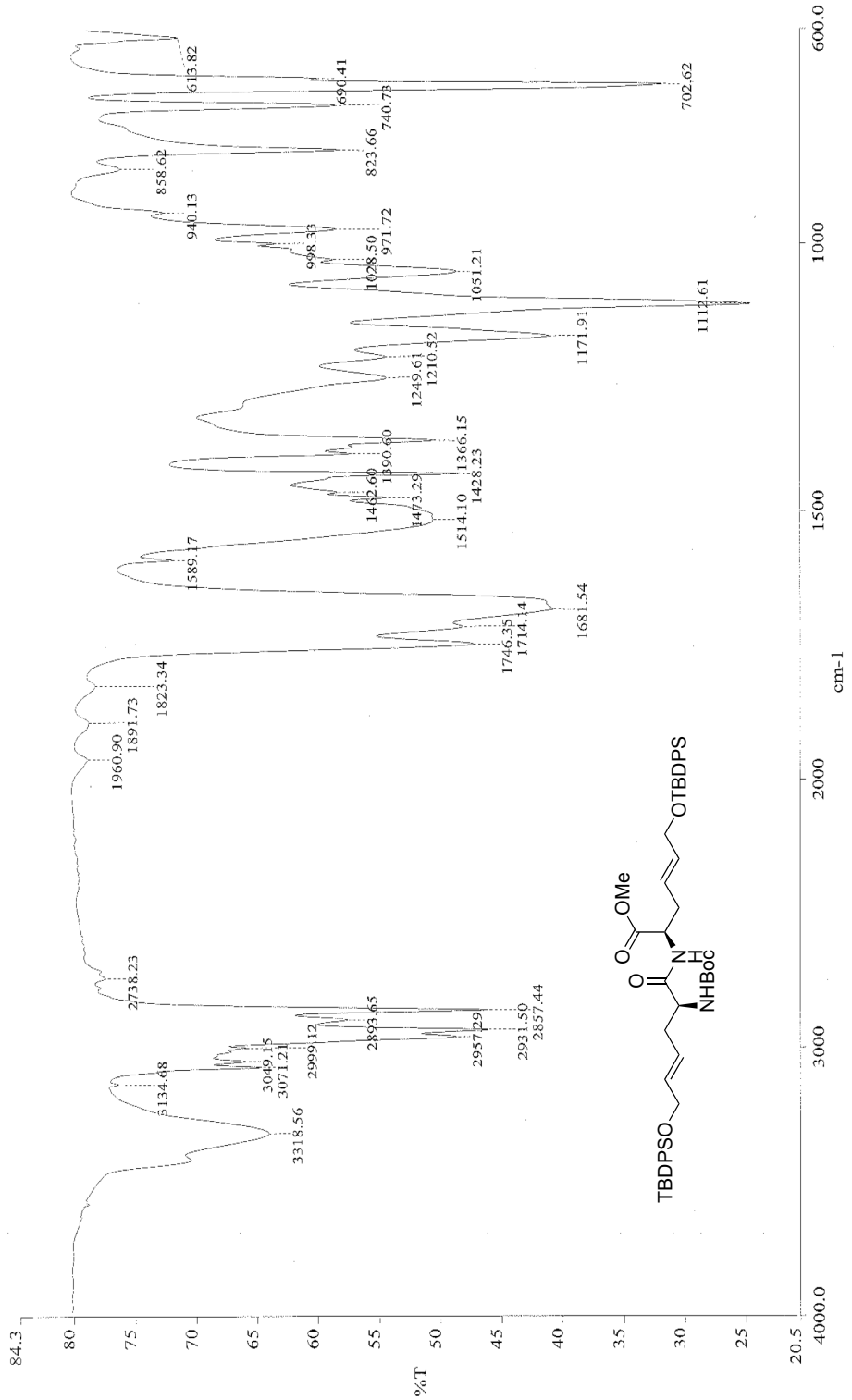

Figure 9: Infrared spectra (neat) of (+)-**63**

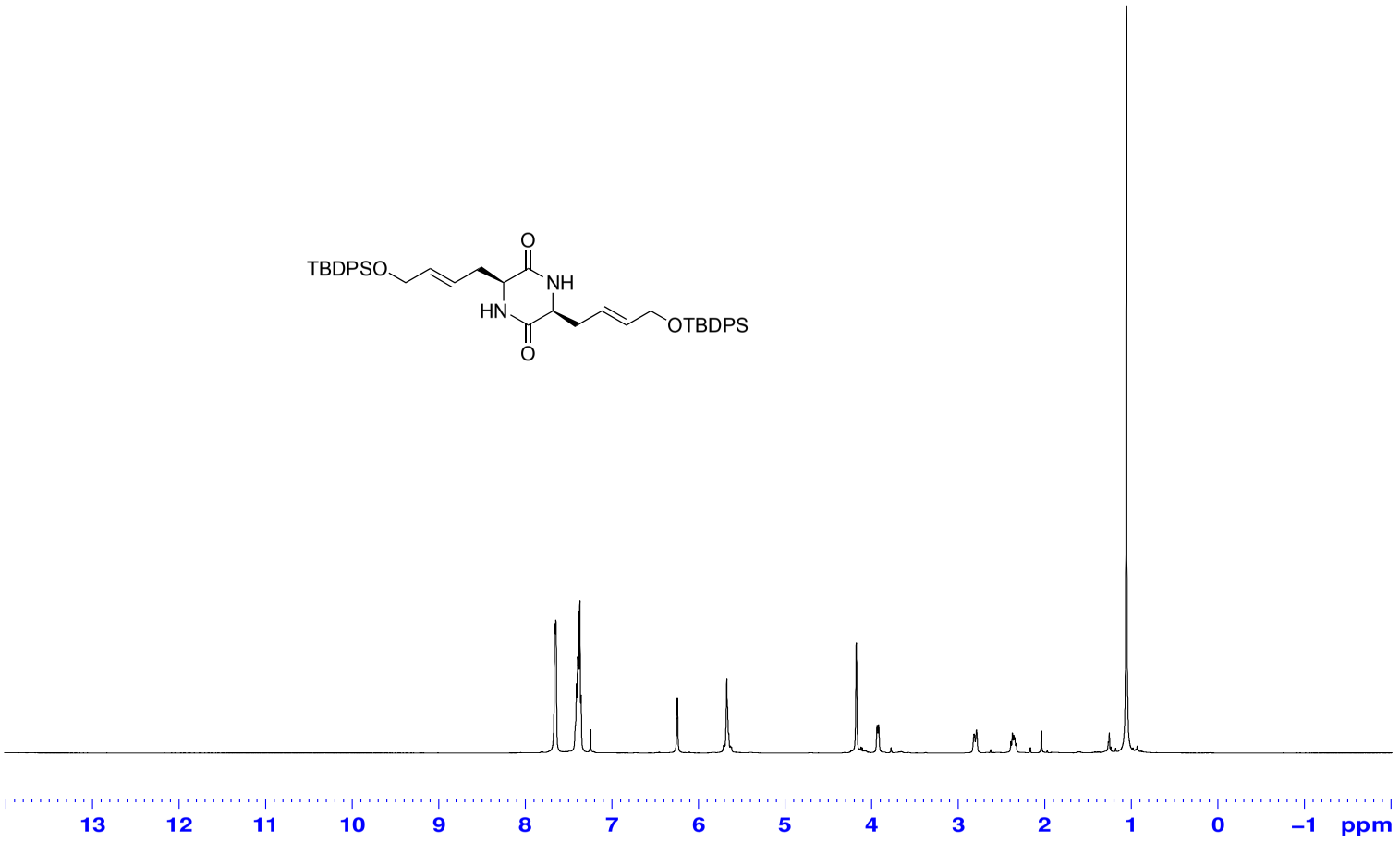

Figure 10: ^{1}H NMR ($CDCl_3$, 500 MHz) of **(−)-46**

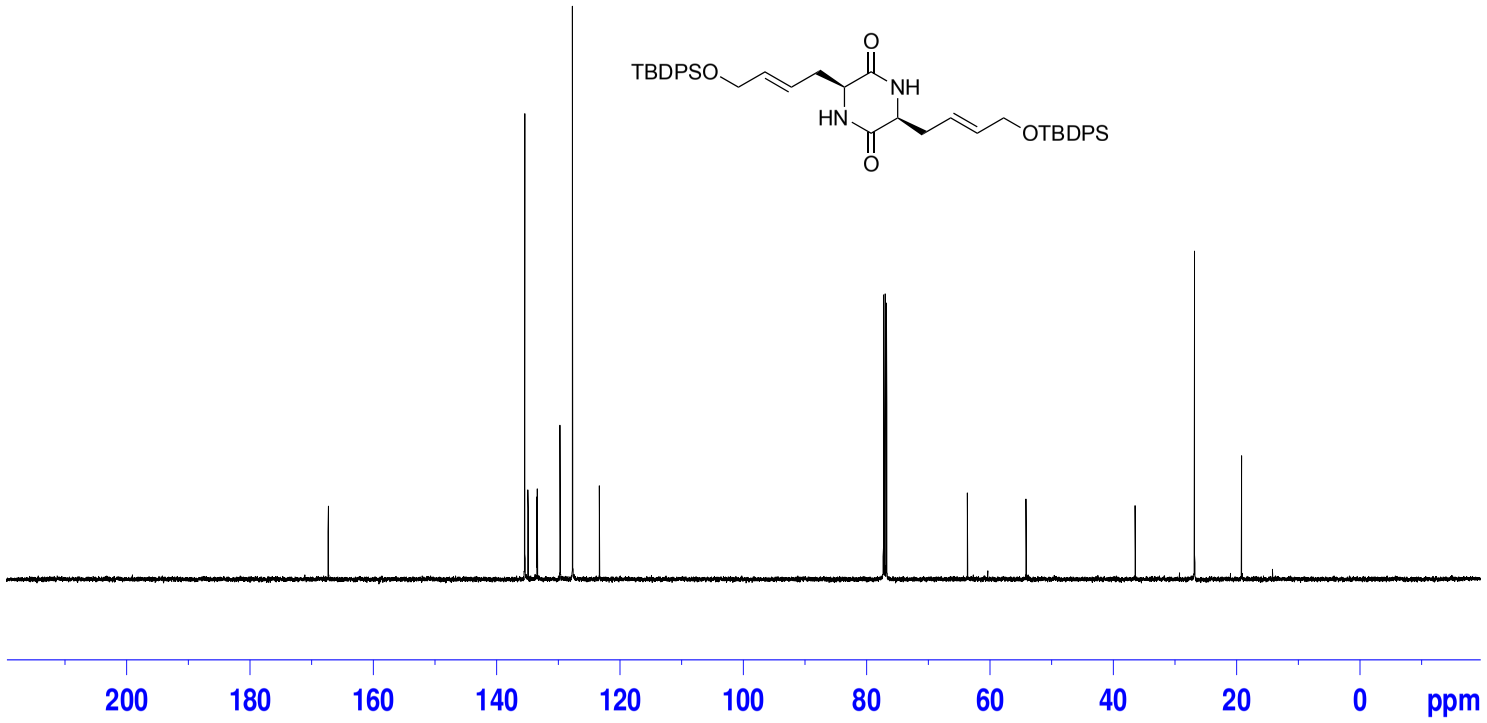

Figure 11: ^{13}C NMR ($CDCl_3$, 125 MHz) of **(−)-46**

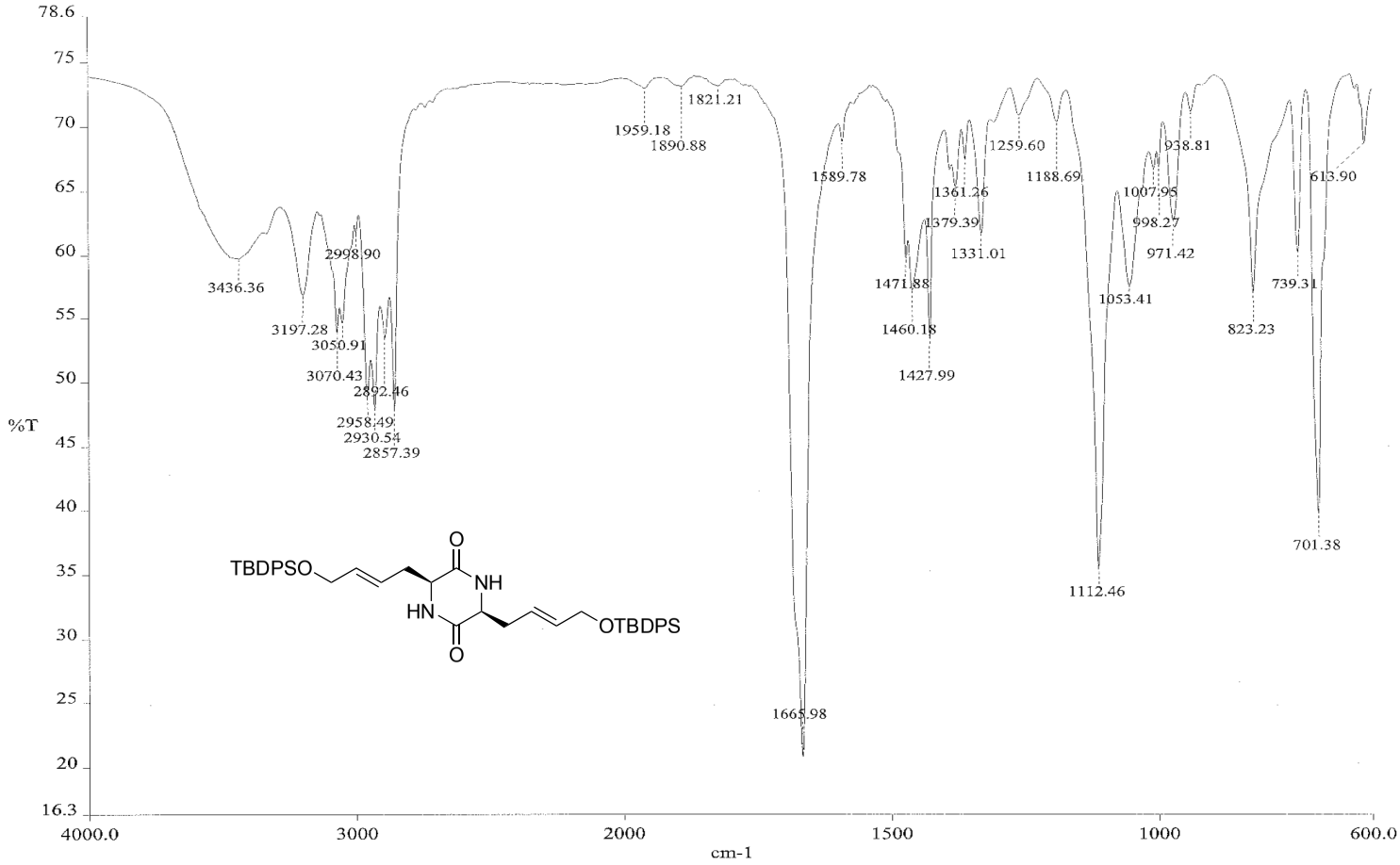

Figure 12: Infrared spectra (neat) of **(−)-46**

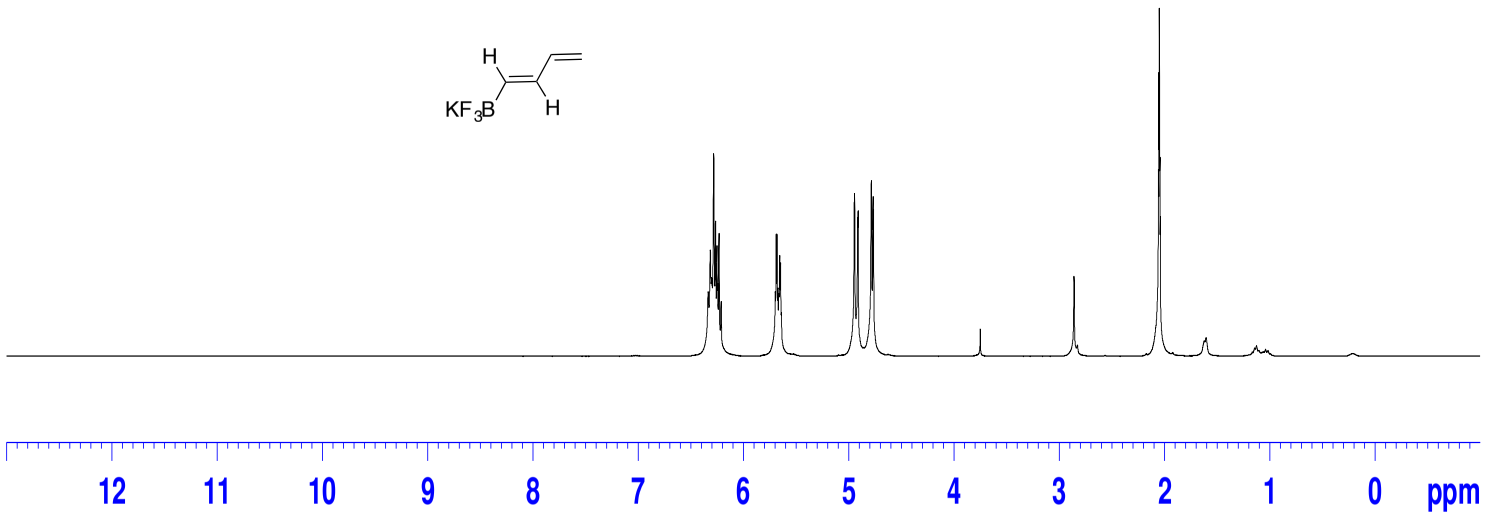

Figure 13: ^{1}H NMR (Acetone-d_6, 500 MHz) of **66**

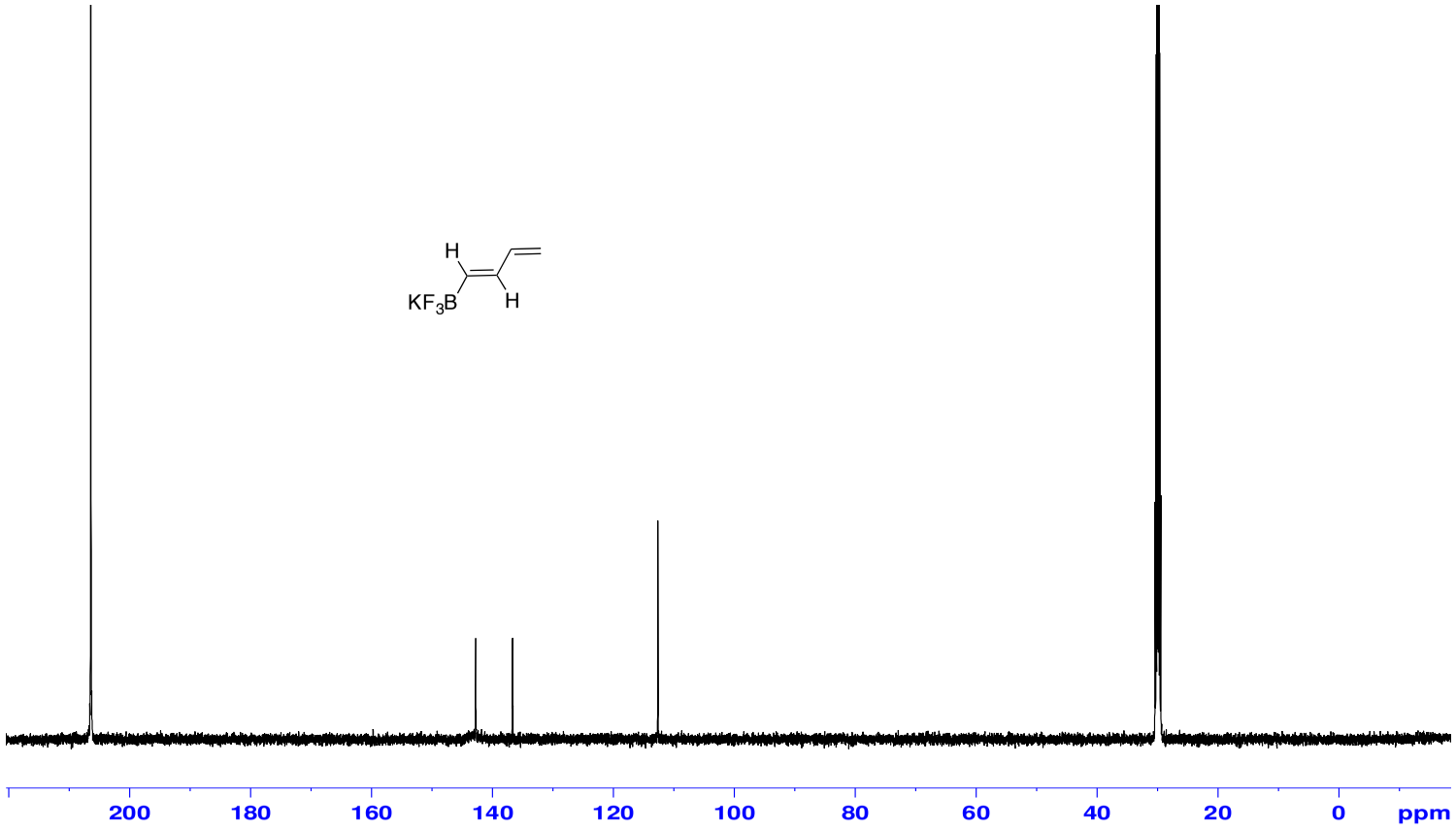

Figure 14: ^{13}C NMR (Acetone-d_6, 125 MHz) of **66**

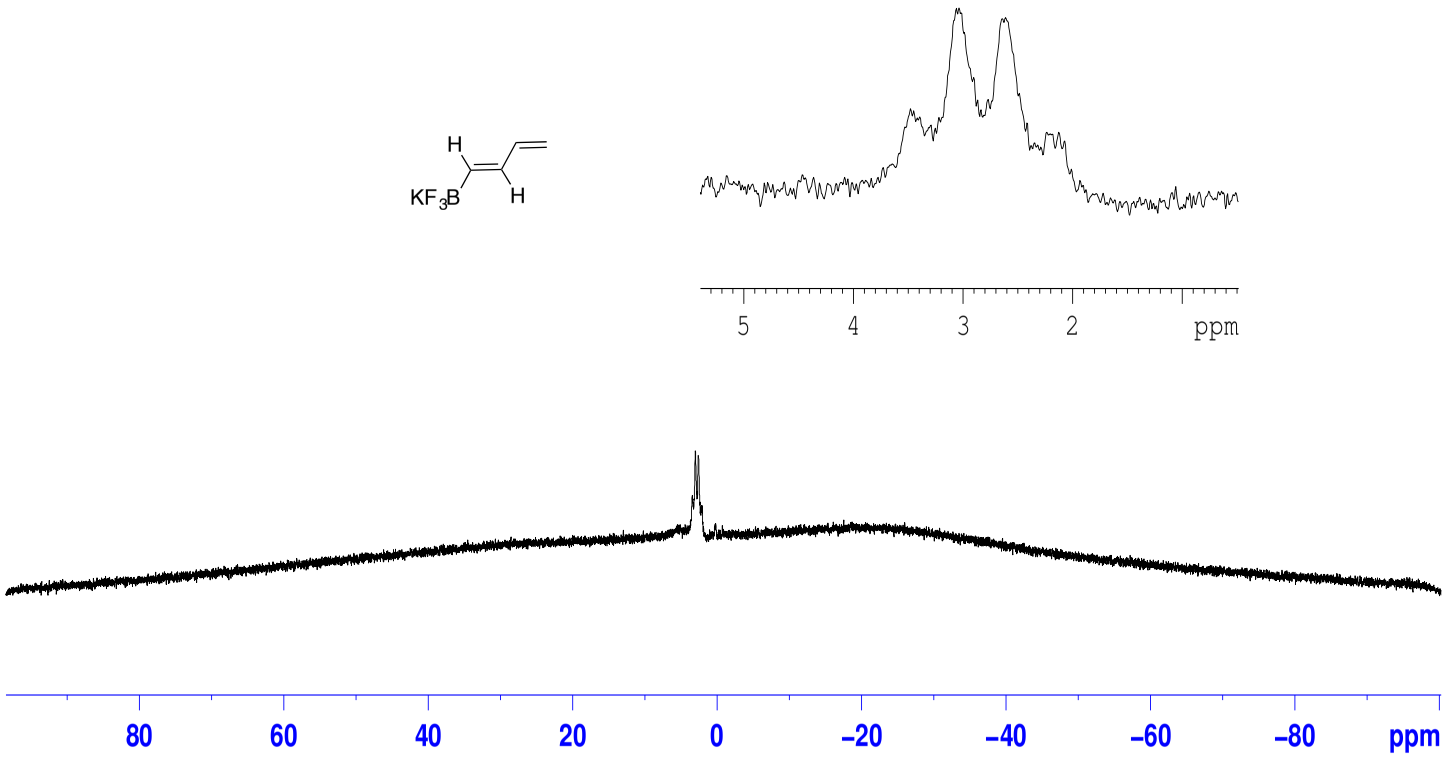

Figure 15: ^{11}B NMR (Acetone-d_6, 128.4 MHz) of **66**

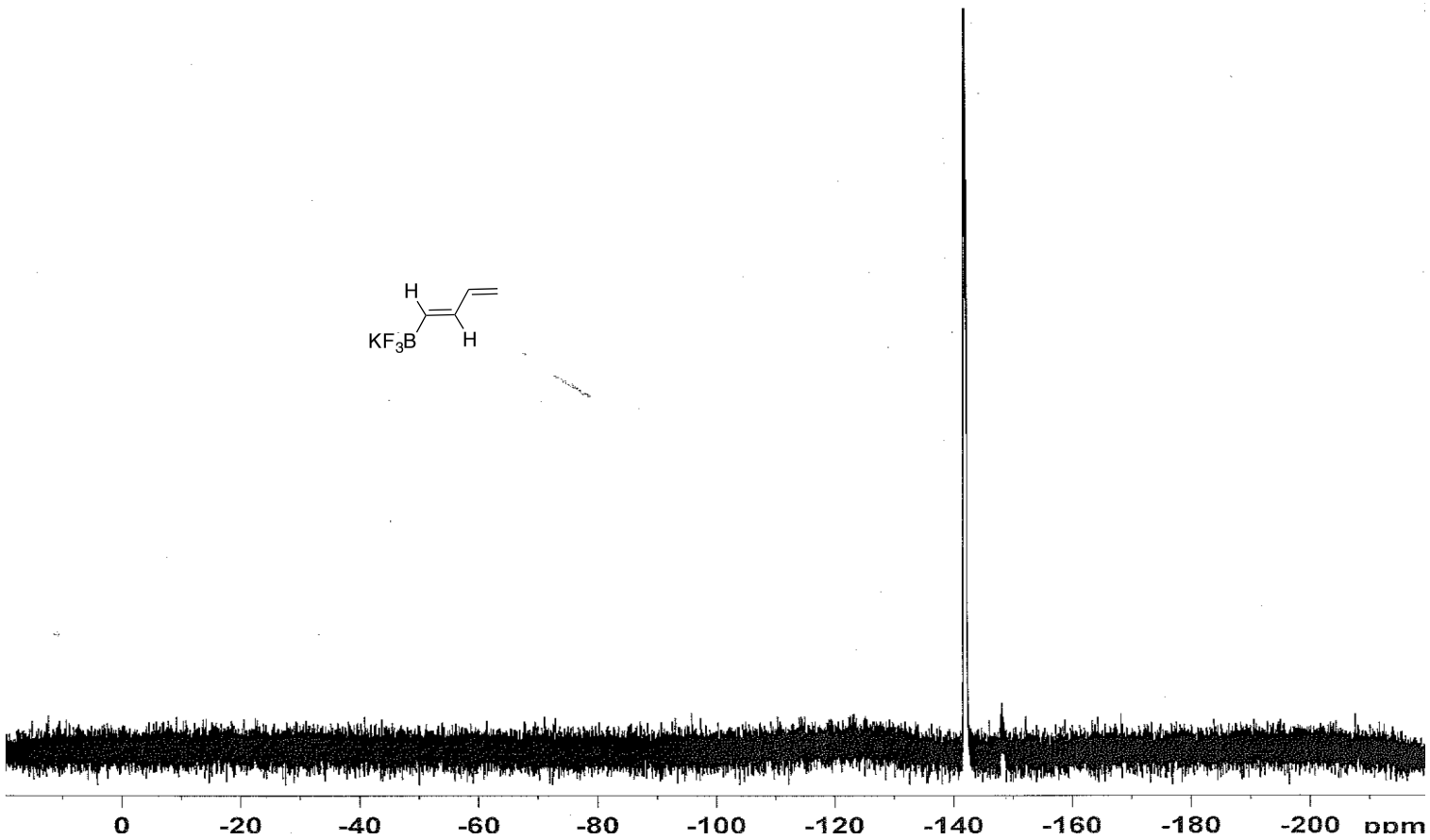

Figure 16: ^{19}F NMR (Acetone-d_6, 470.8 MHz) of **66**

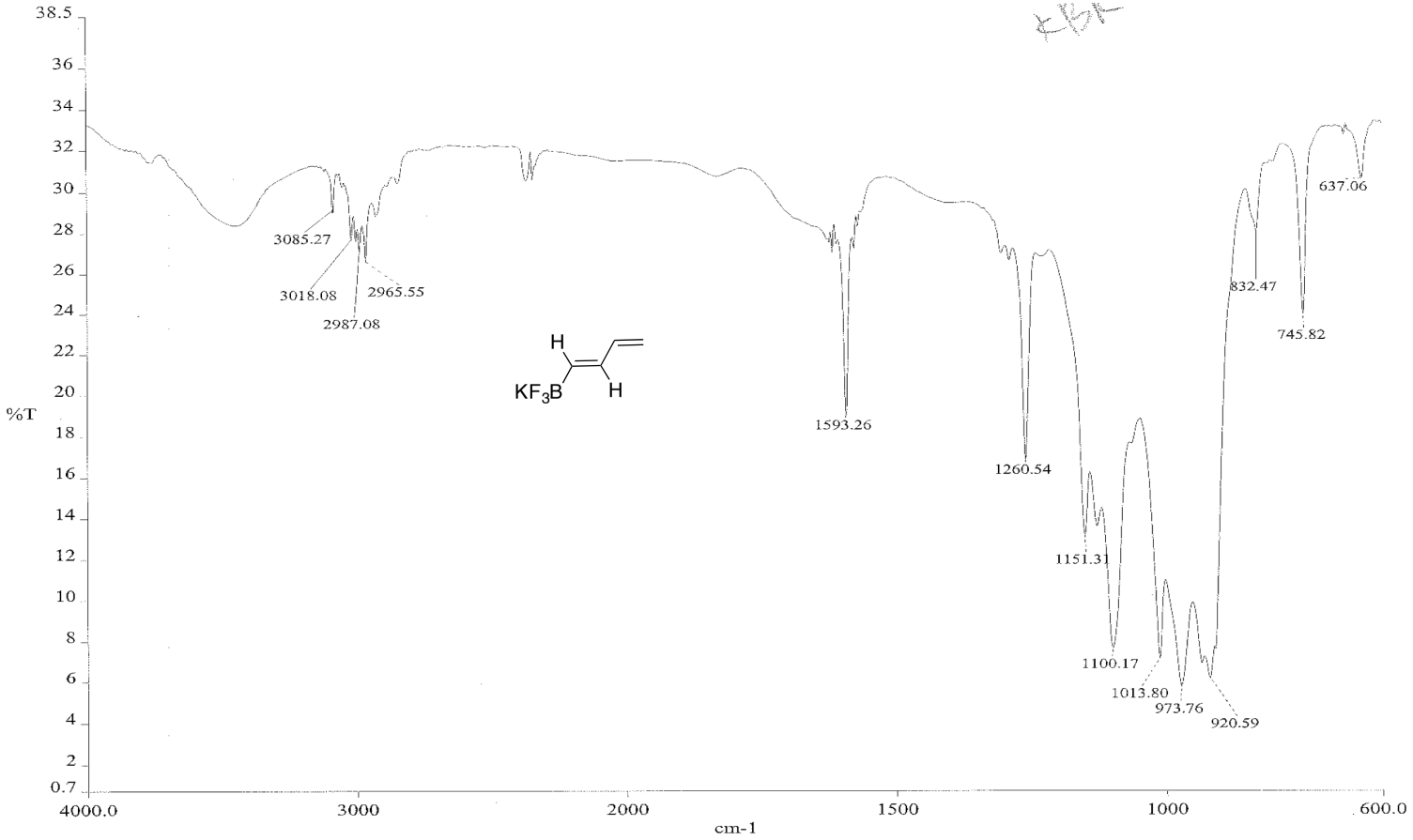

Figure 17: Infrared spectra (KBr) of **66**

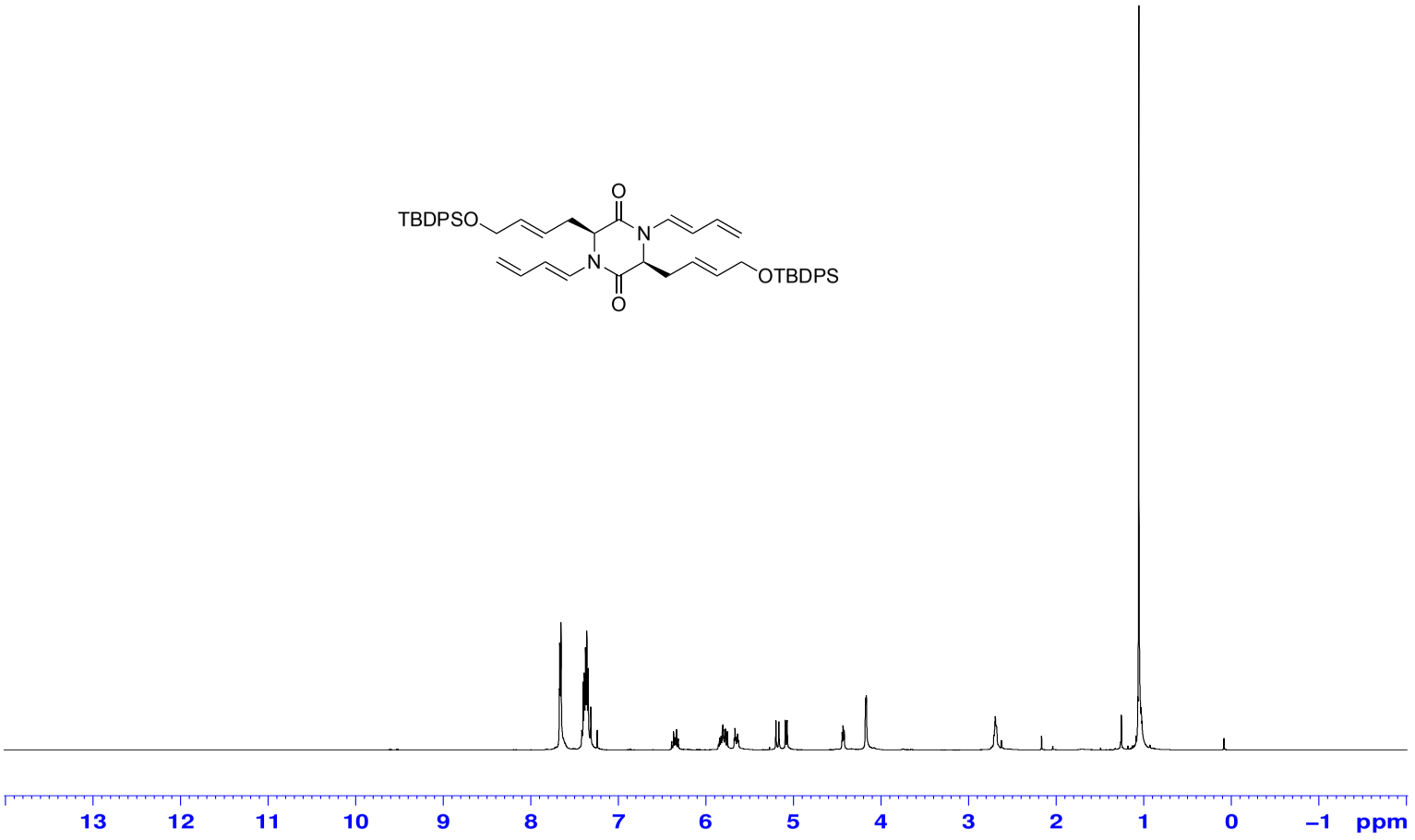

Figure 18: ^{1}H NMR ($CDCl_3$, 500 MHz) of **(+)-69**

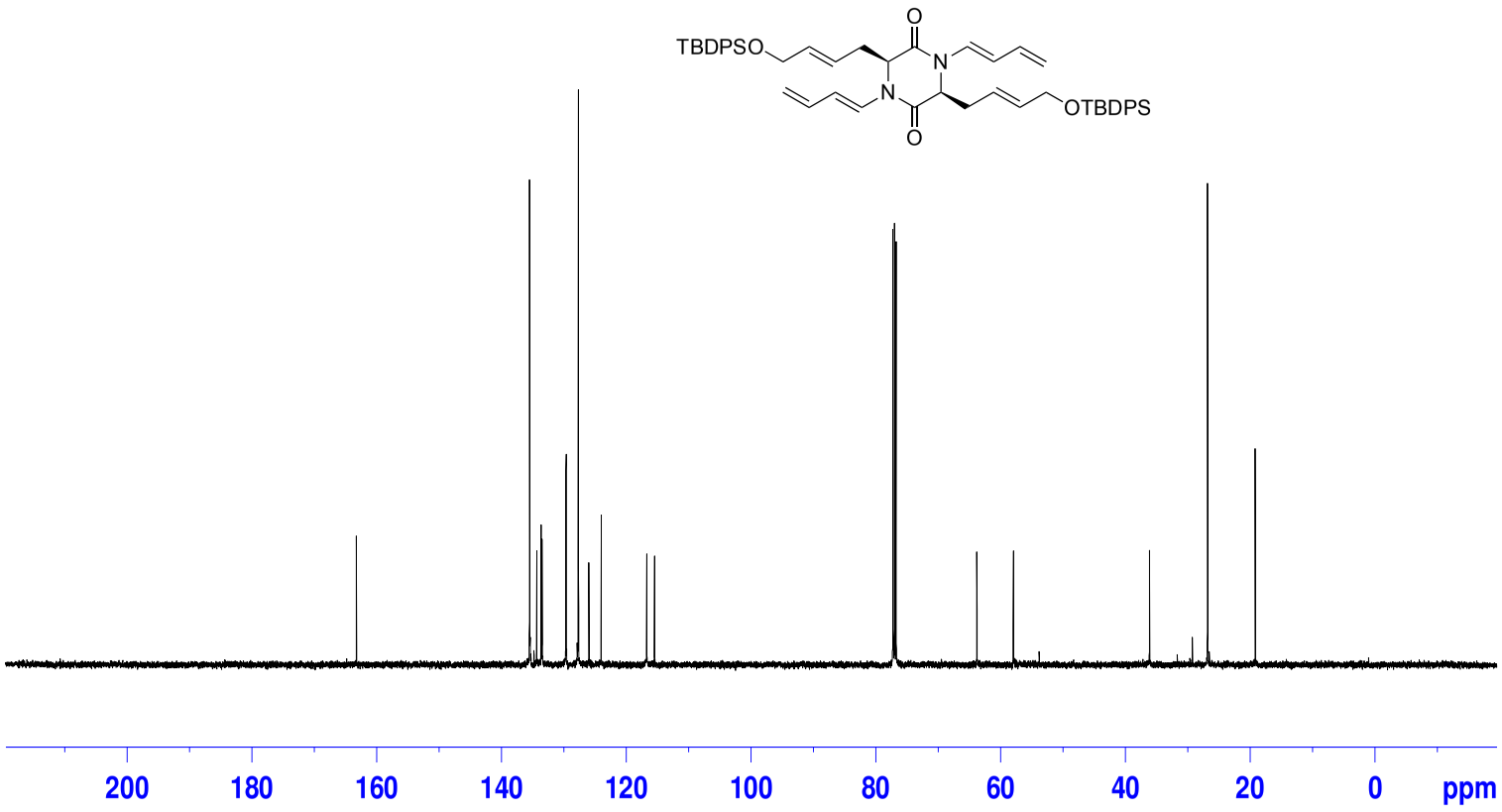

Figure 19: ^{13}C NMR ($CDCl_3$, 125 MHz) of **(+)-69**

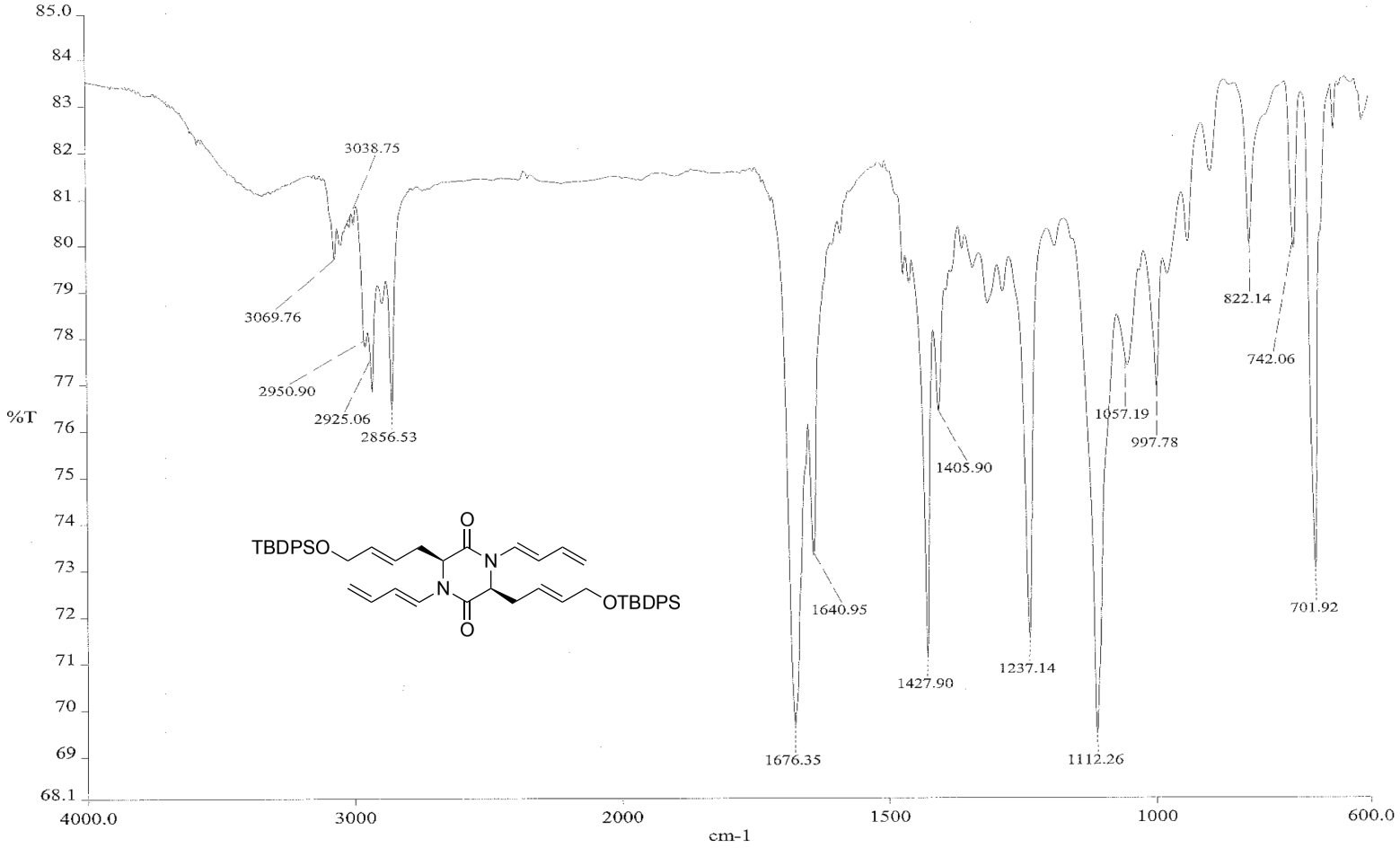

Figure 20: Infrared spectra (neat) of **(+)-69**

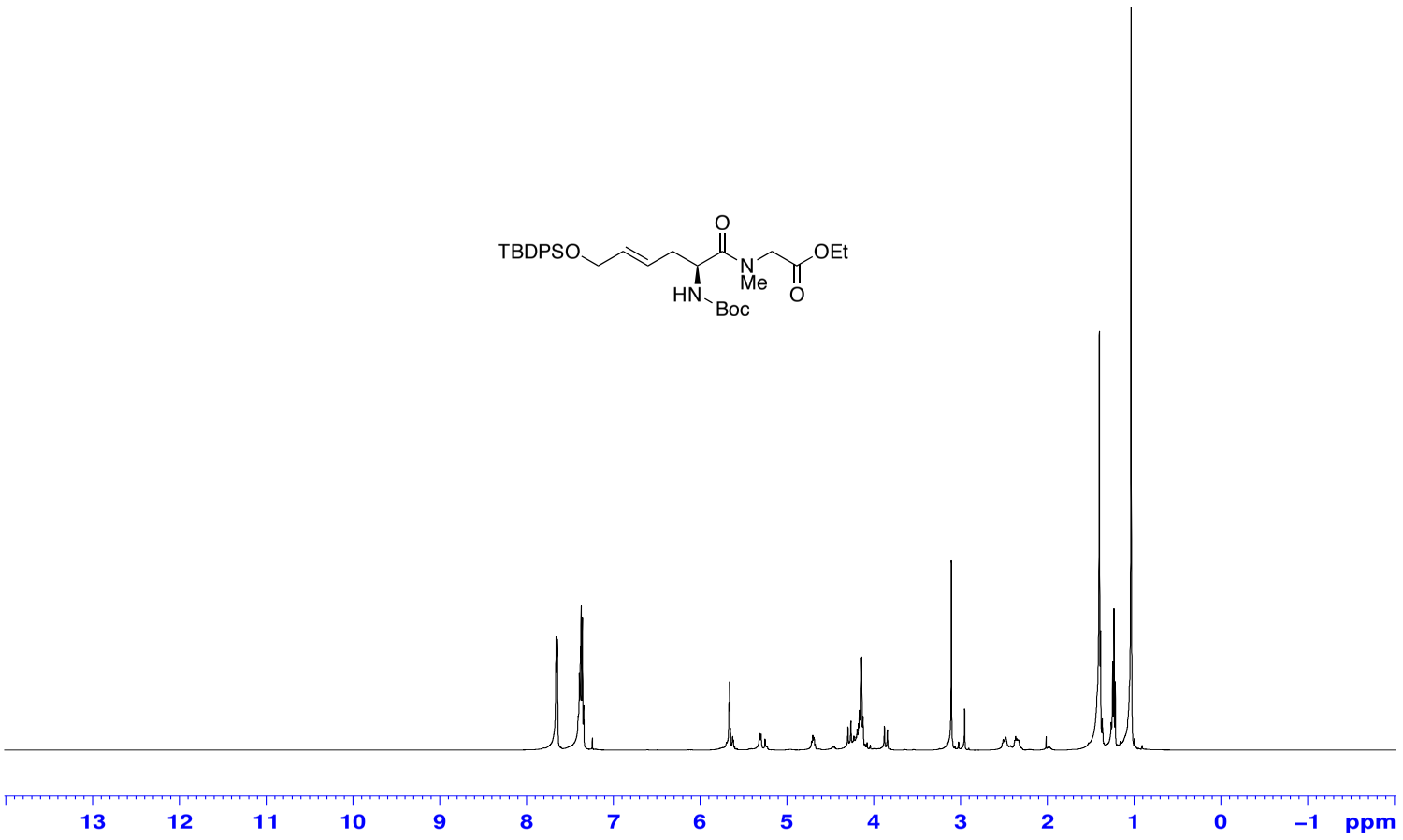

Figure 21: ^{1}H NMR ($CDCl_3$, 500 MHz) of **(+)-71**

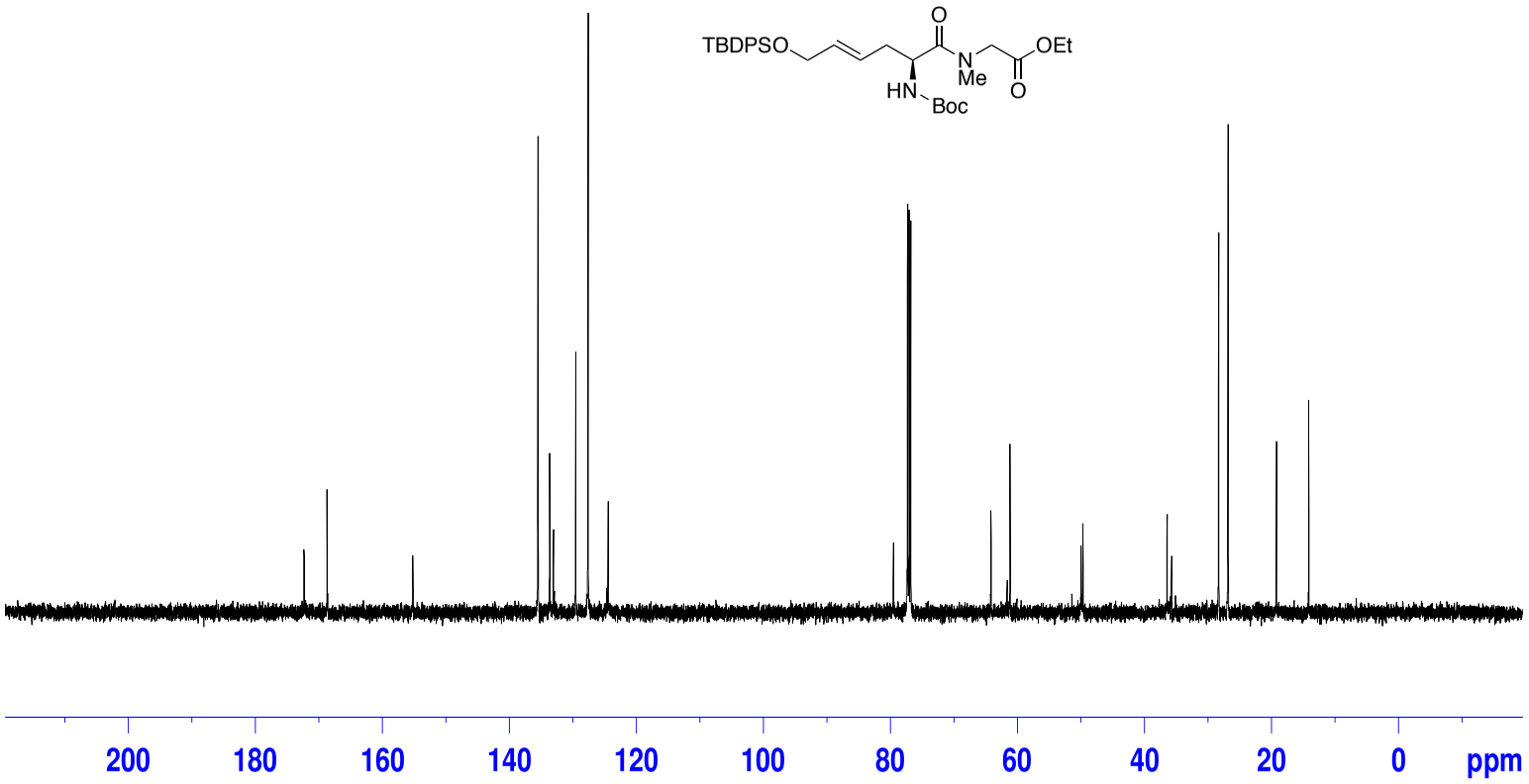

Figure 22: ^{13}C NMR ($CDCl_3$, 125 MHz) of **(+)-71**

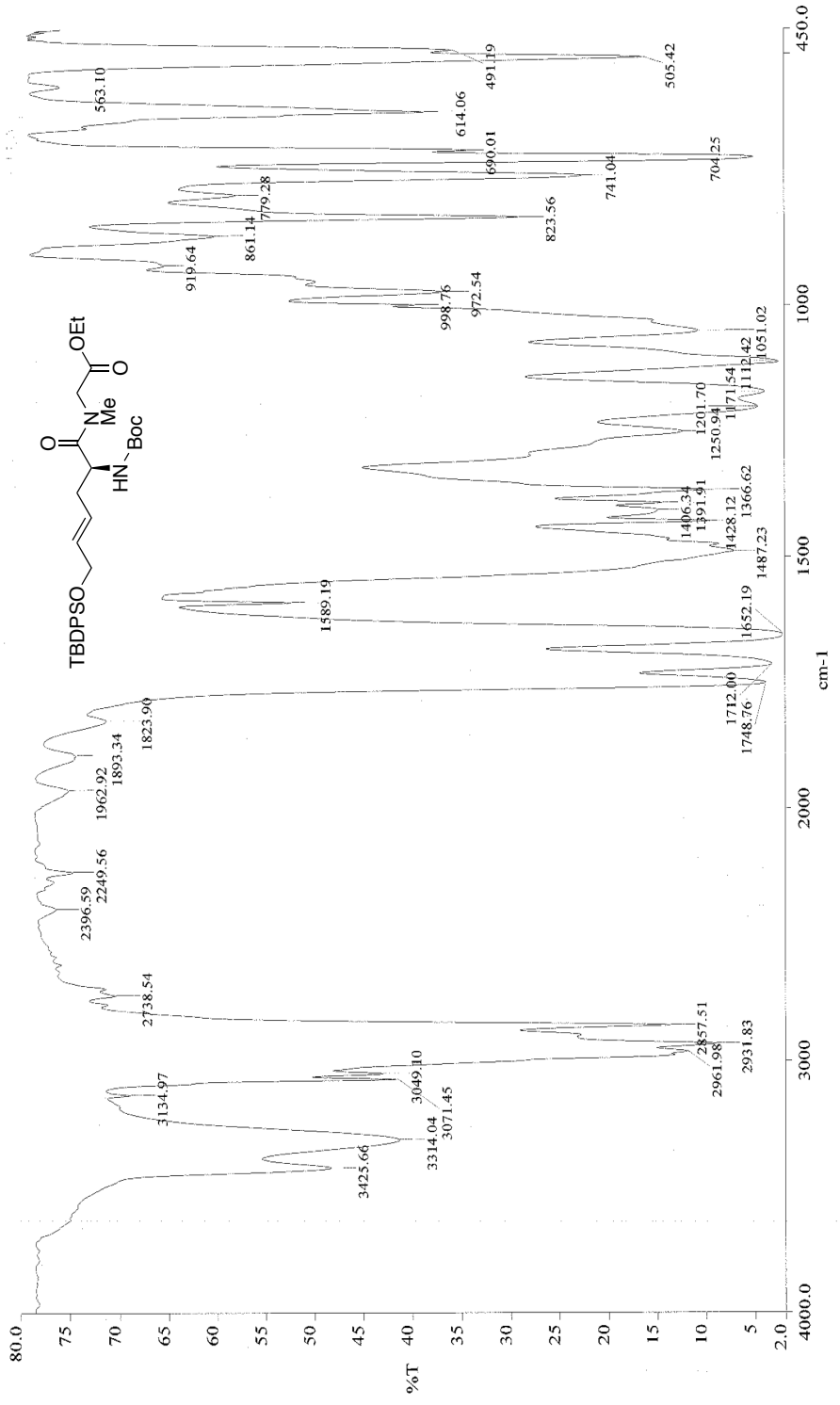

Figure 23: Infrared spectra (neat) of **(+)-71**

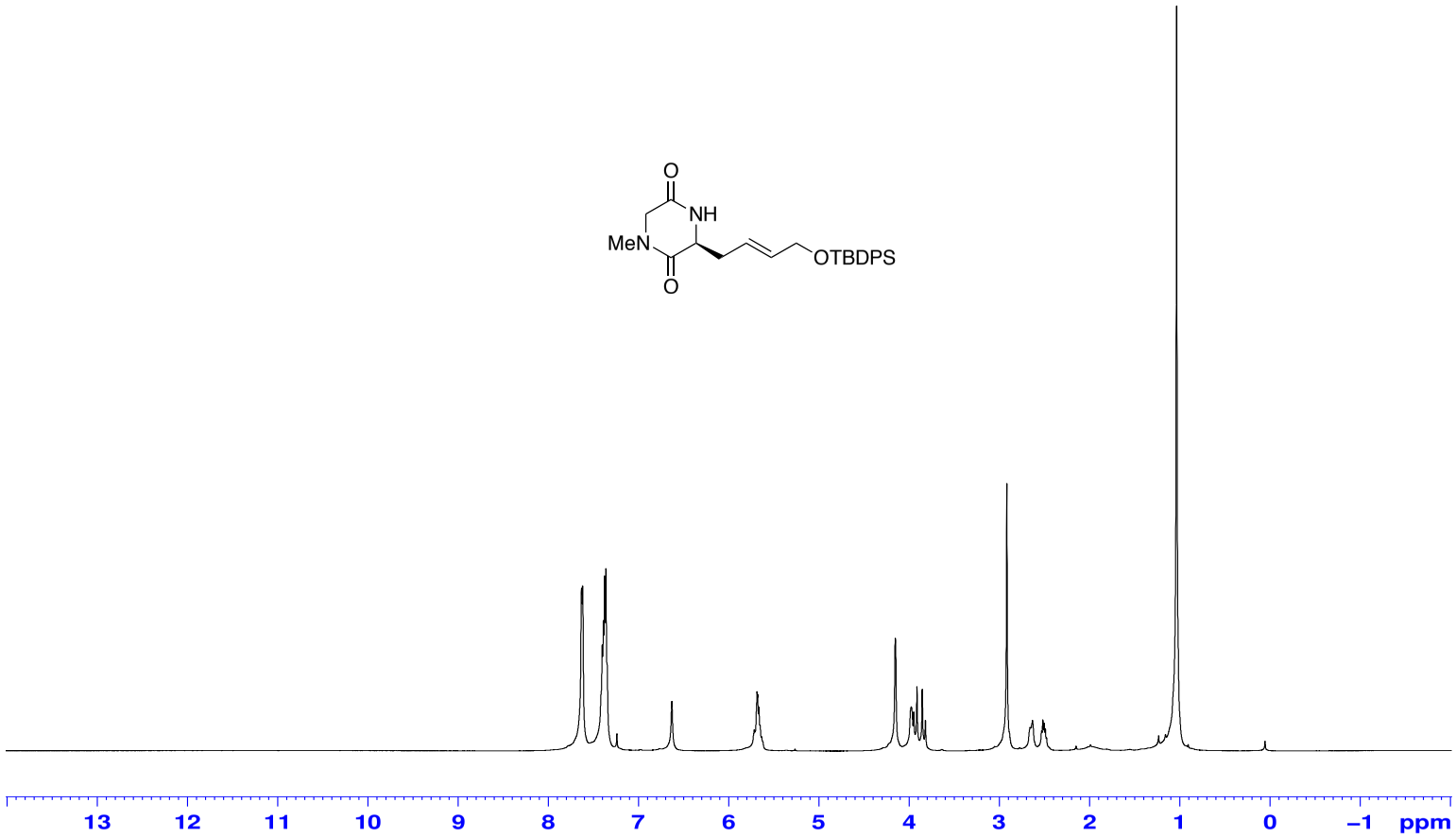

Figure 24: ^{1}H NMR ($CDCl_3$, 500 MHz) of **(+)-65**

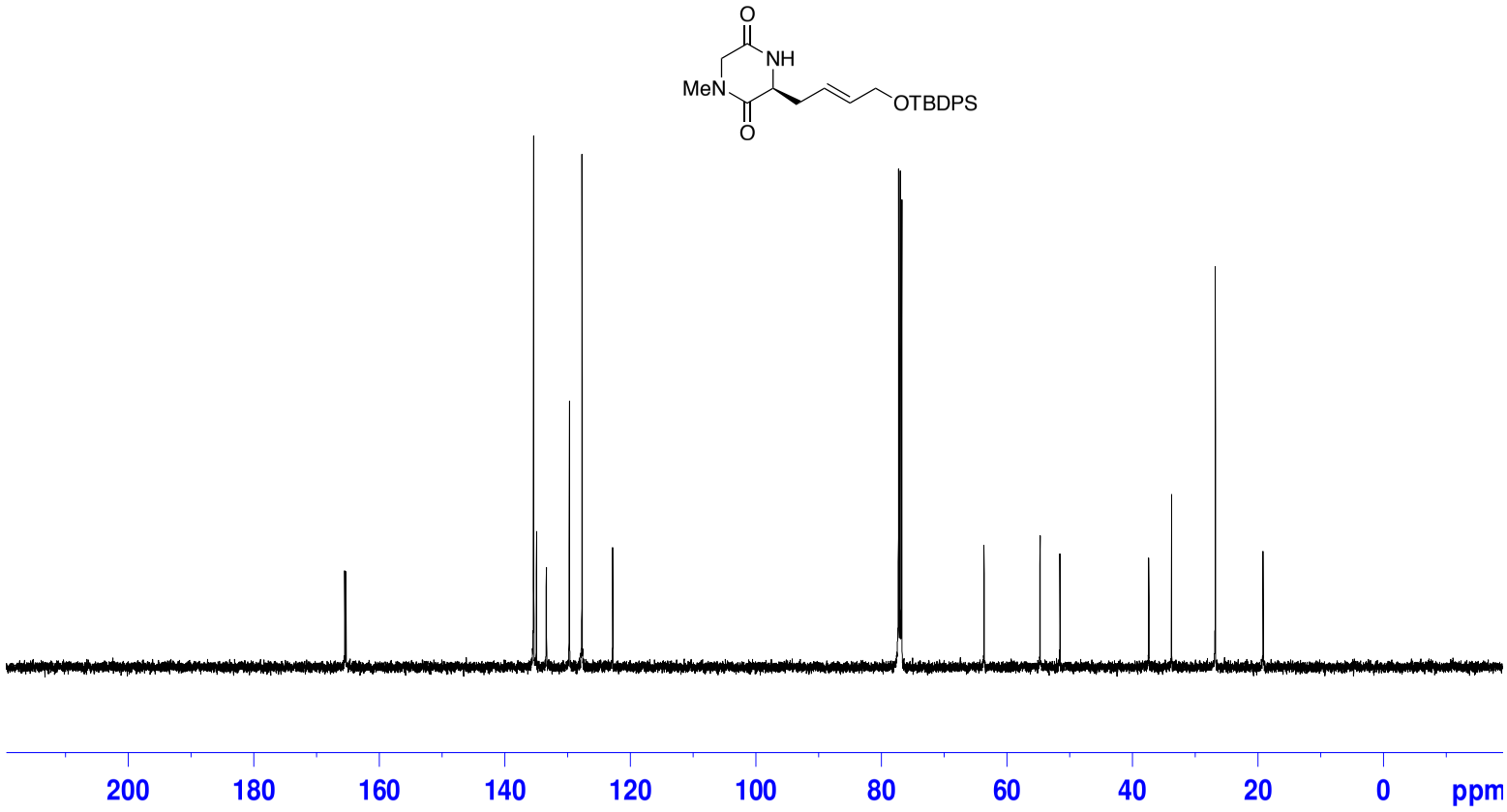

Figure 25: ^{13}C NMR ($CDCl_3$, 125 MHz) of **(+)-65**

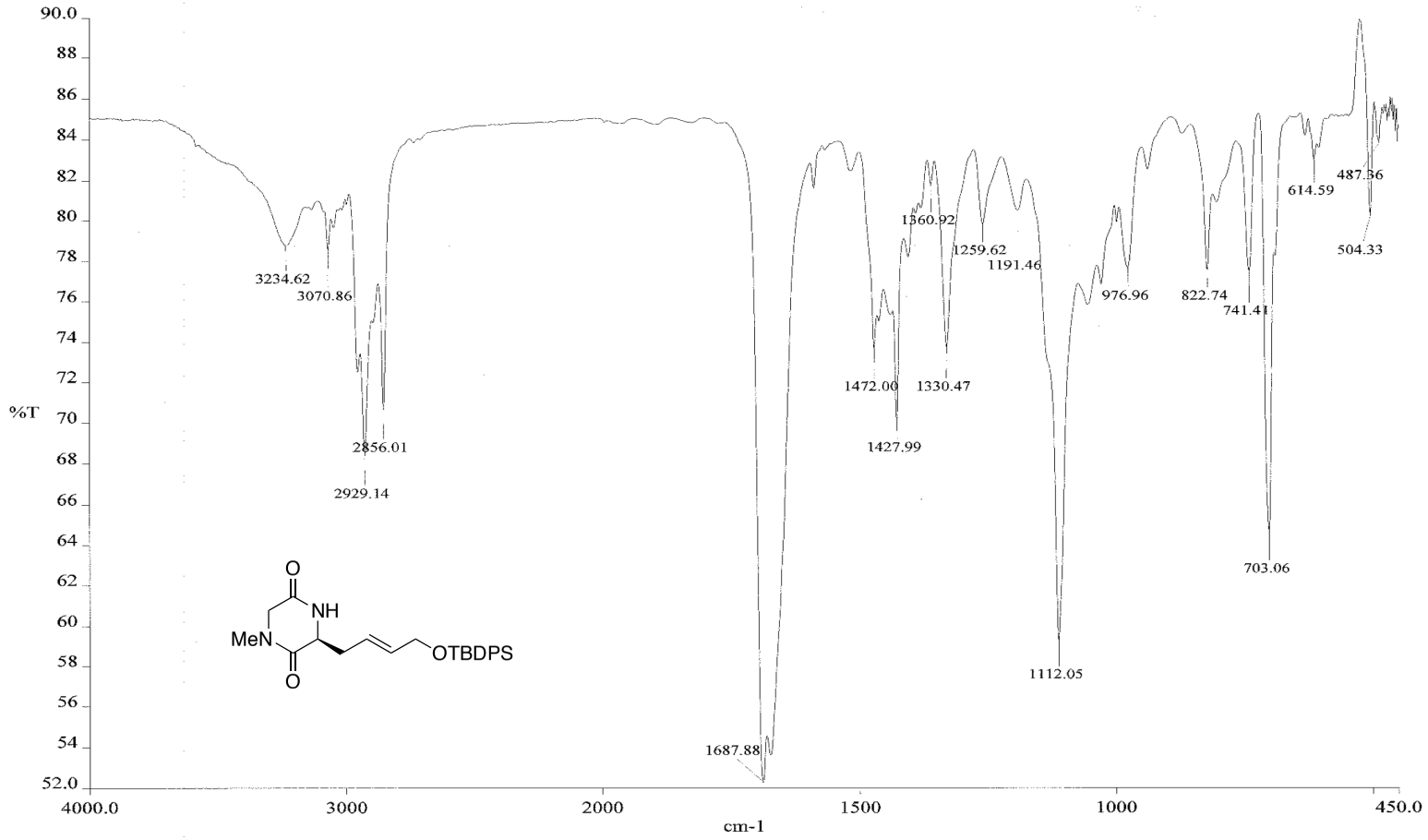

Figure 26: Infrared spectra (neat) of **(+)-65**

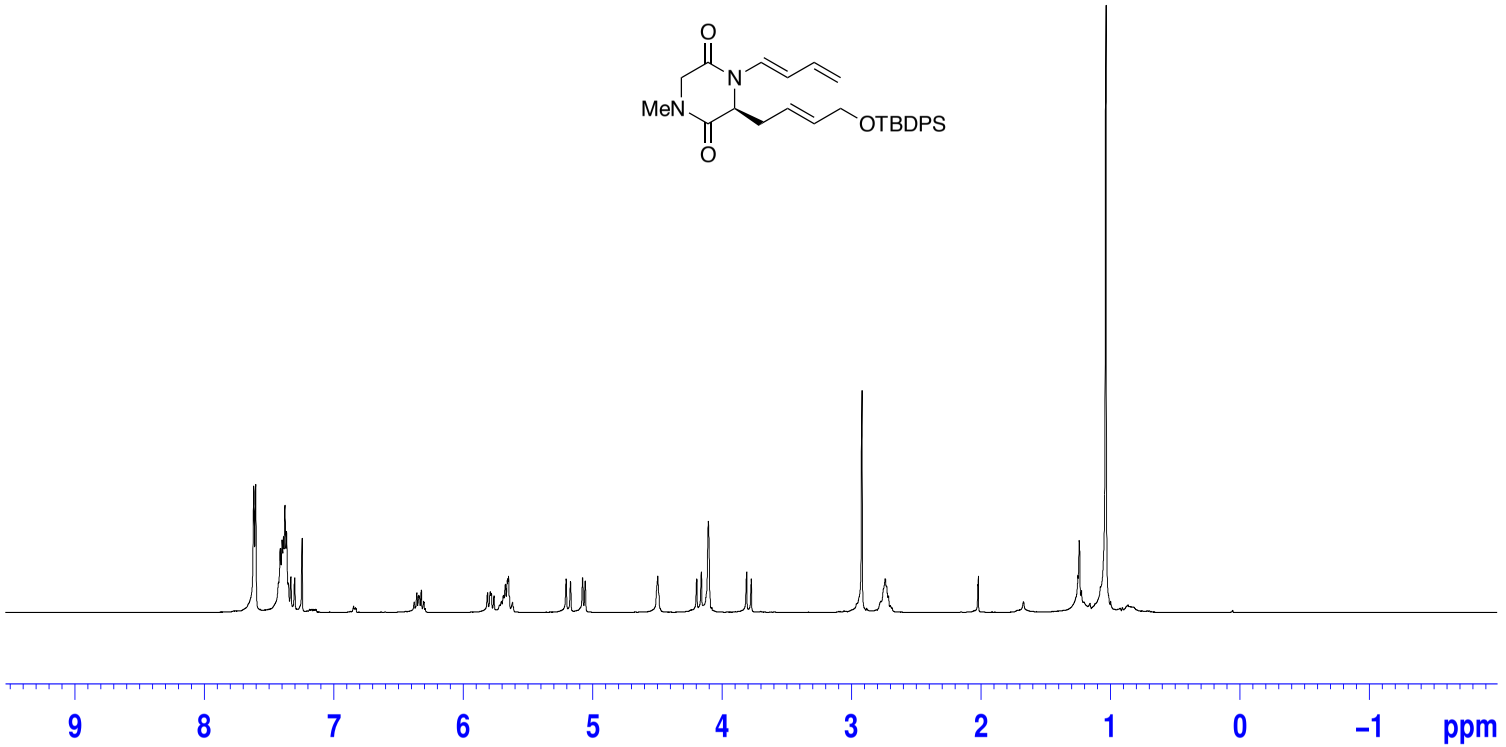

Figure 27: ^{1}H NMR ($CDCl_3$, 500 MHz) of **(+)-72**

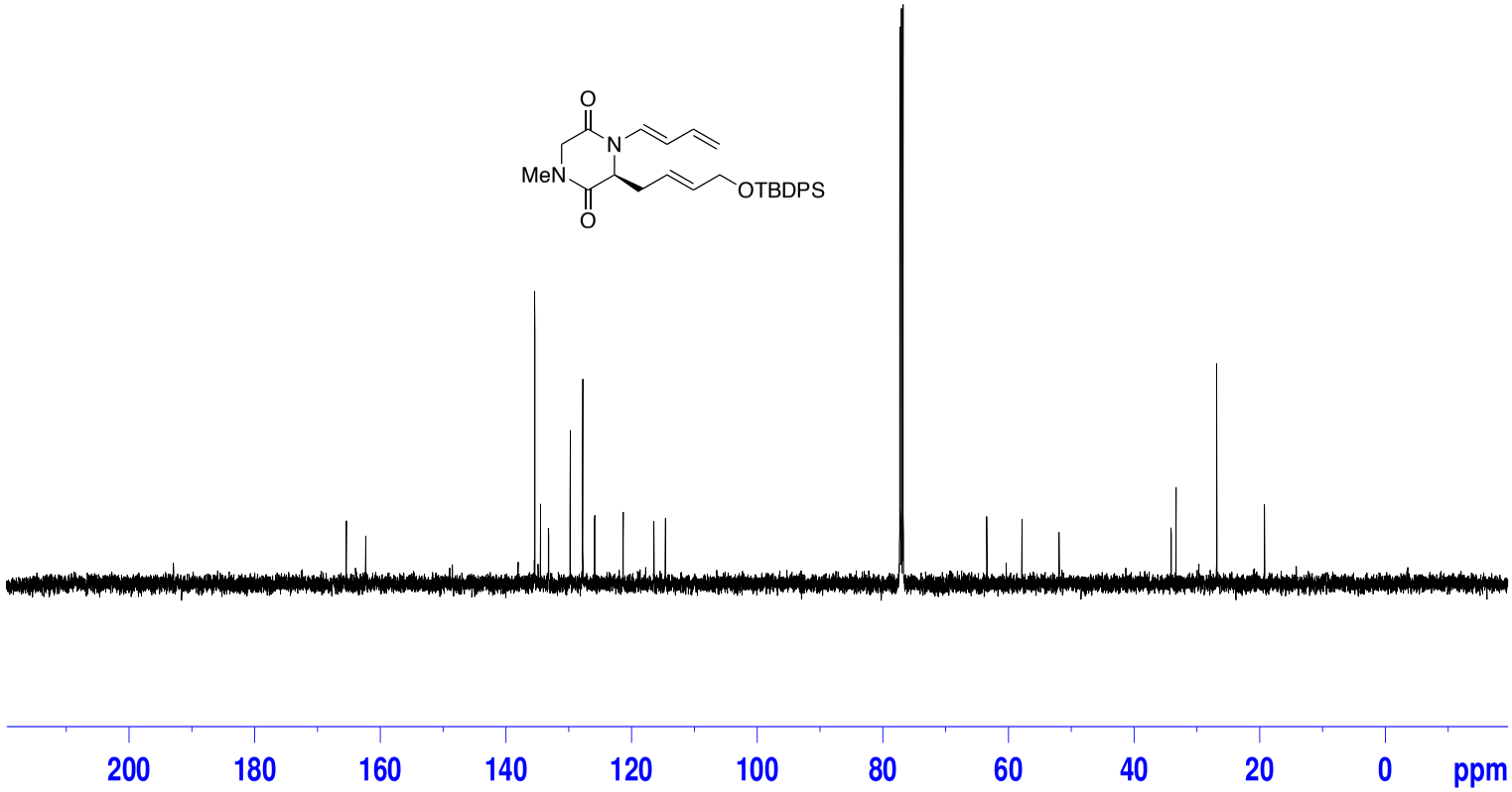

Figure 28: ^{13}C NMR ($CDCl_3$, 125 MHz) of **(+)-72**

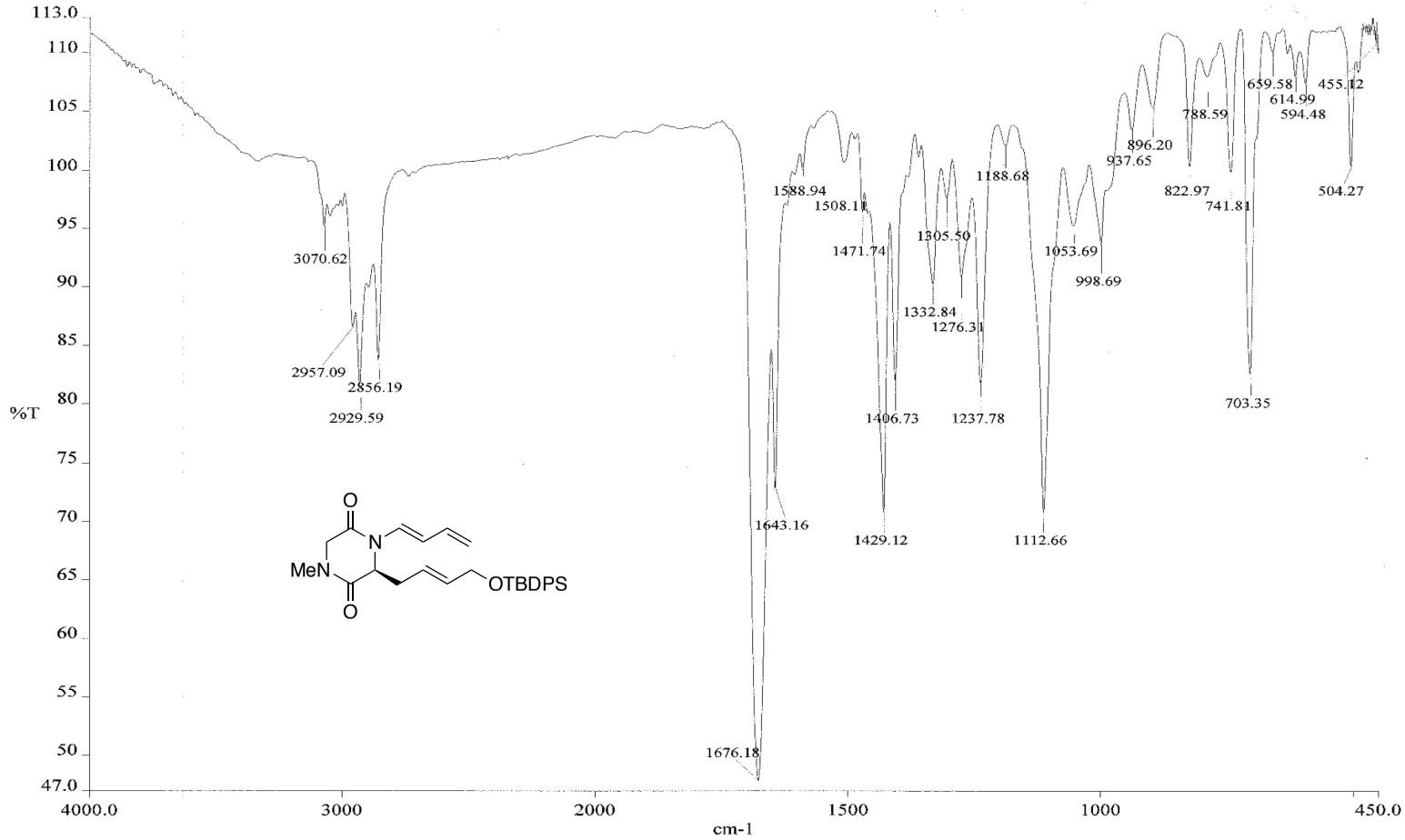

Figure 29: Infrared spectra (neat) of **(+)-72**

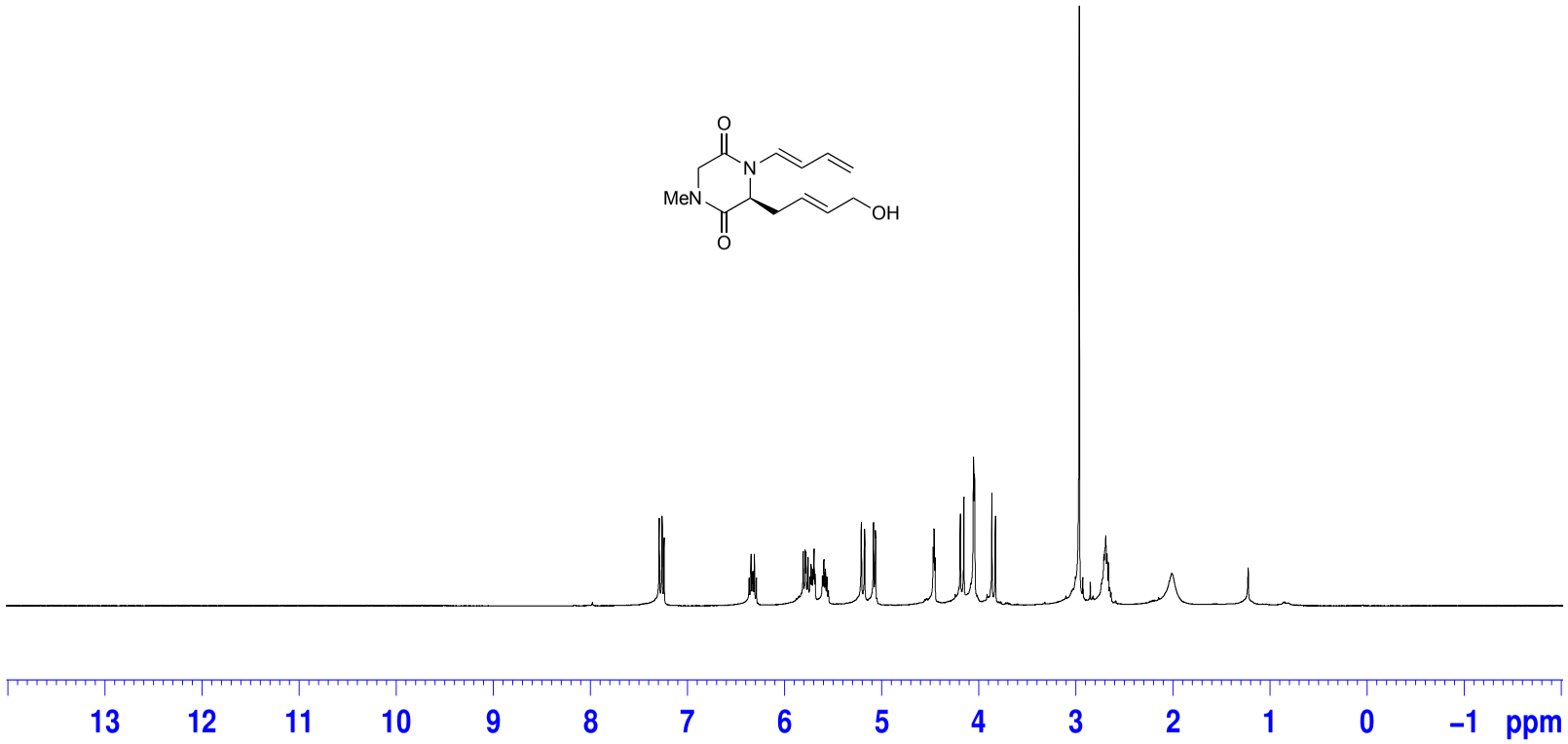

Figure 30: ^{1}H NMR ($CDCl_3$, 500 MHz) of **(+)-73**

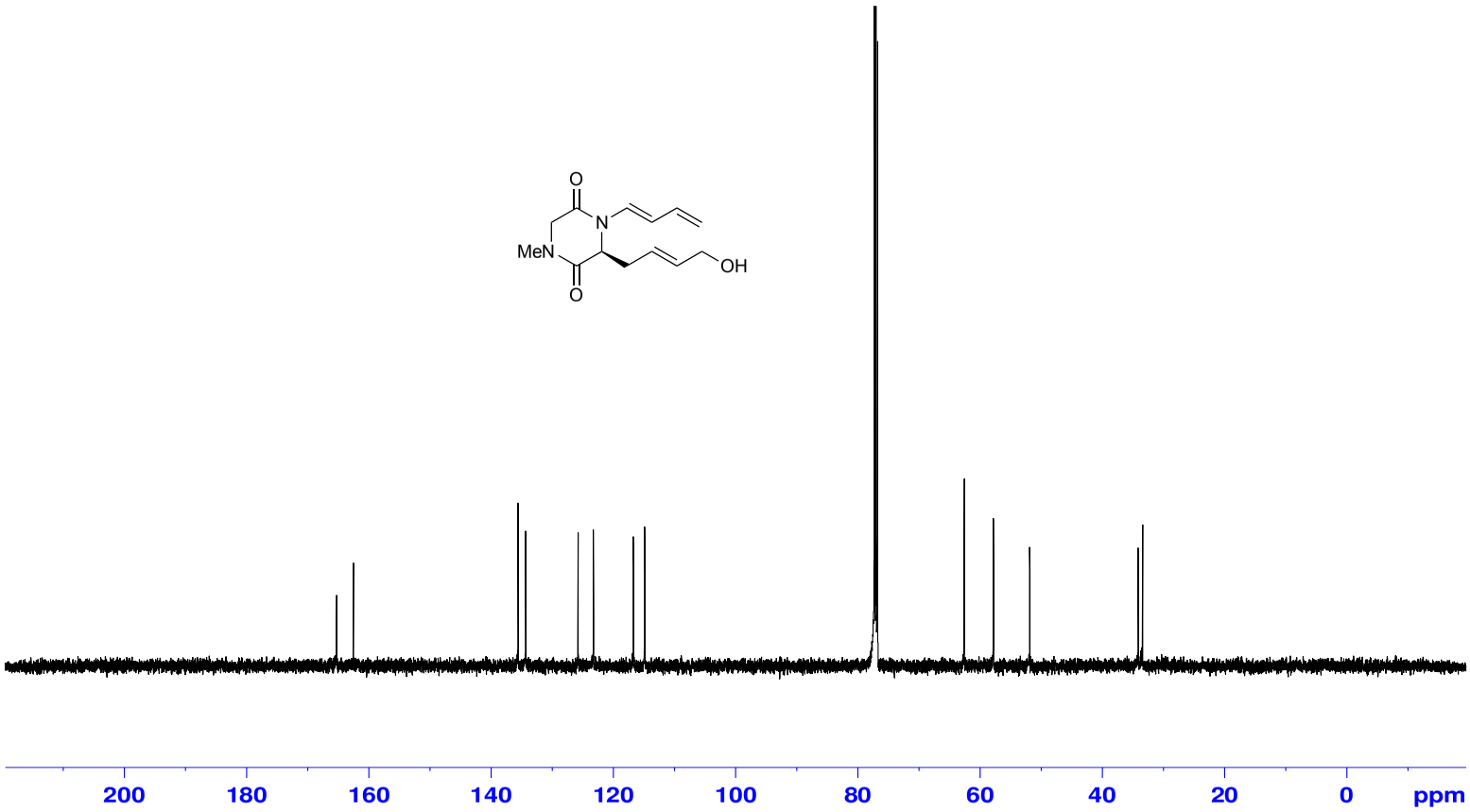

Figure 31: ^{13}C NMR ($CDCl_3$, 125 MHz) of **(+)-73**

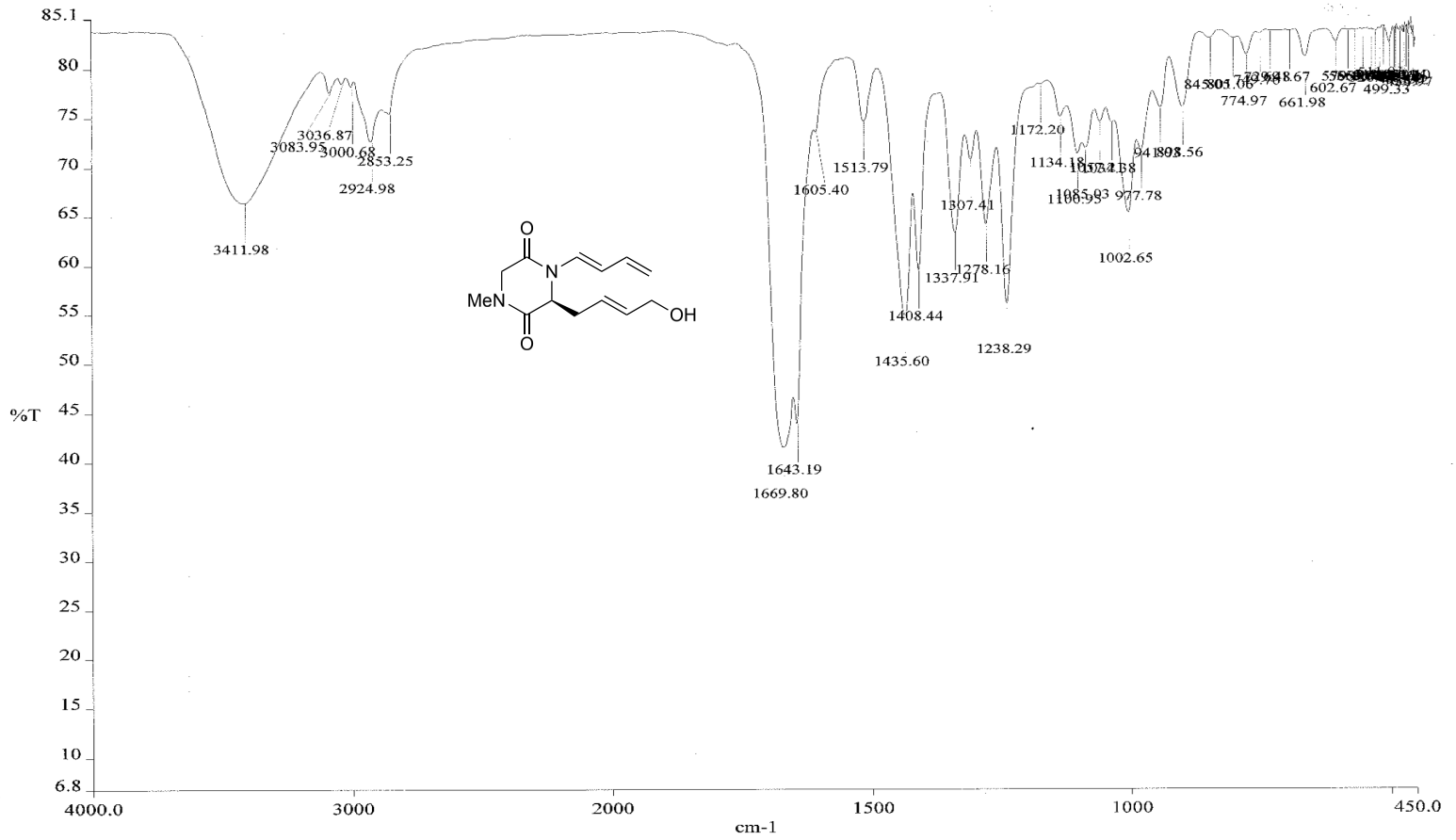

Figure 32: Infrared spectra (neat) of **(+)-73**

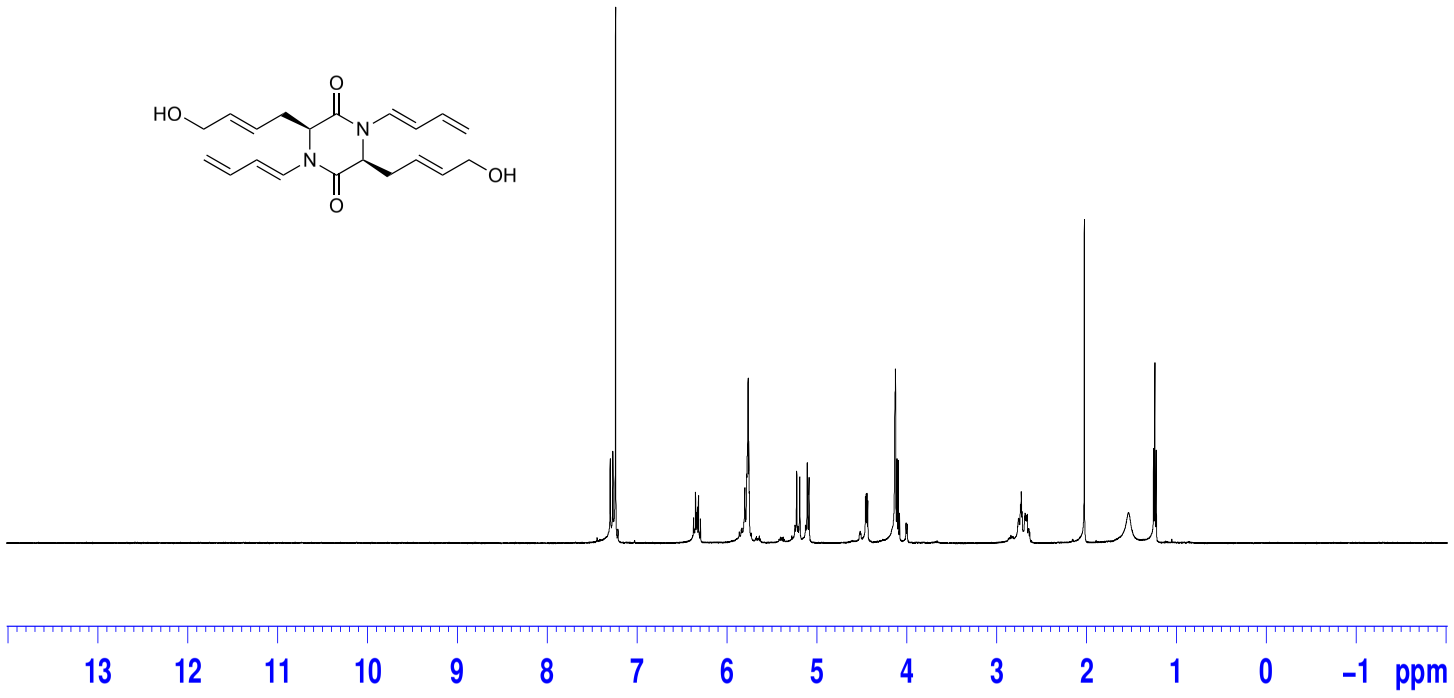

Figure 33: ^{1}H NMR ($CDCl_3$, 500 MHz) of **(+)-75**

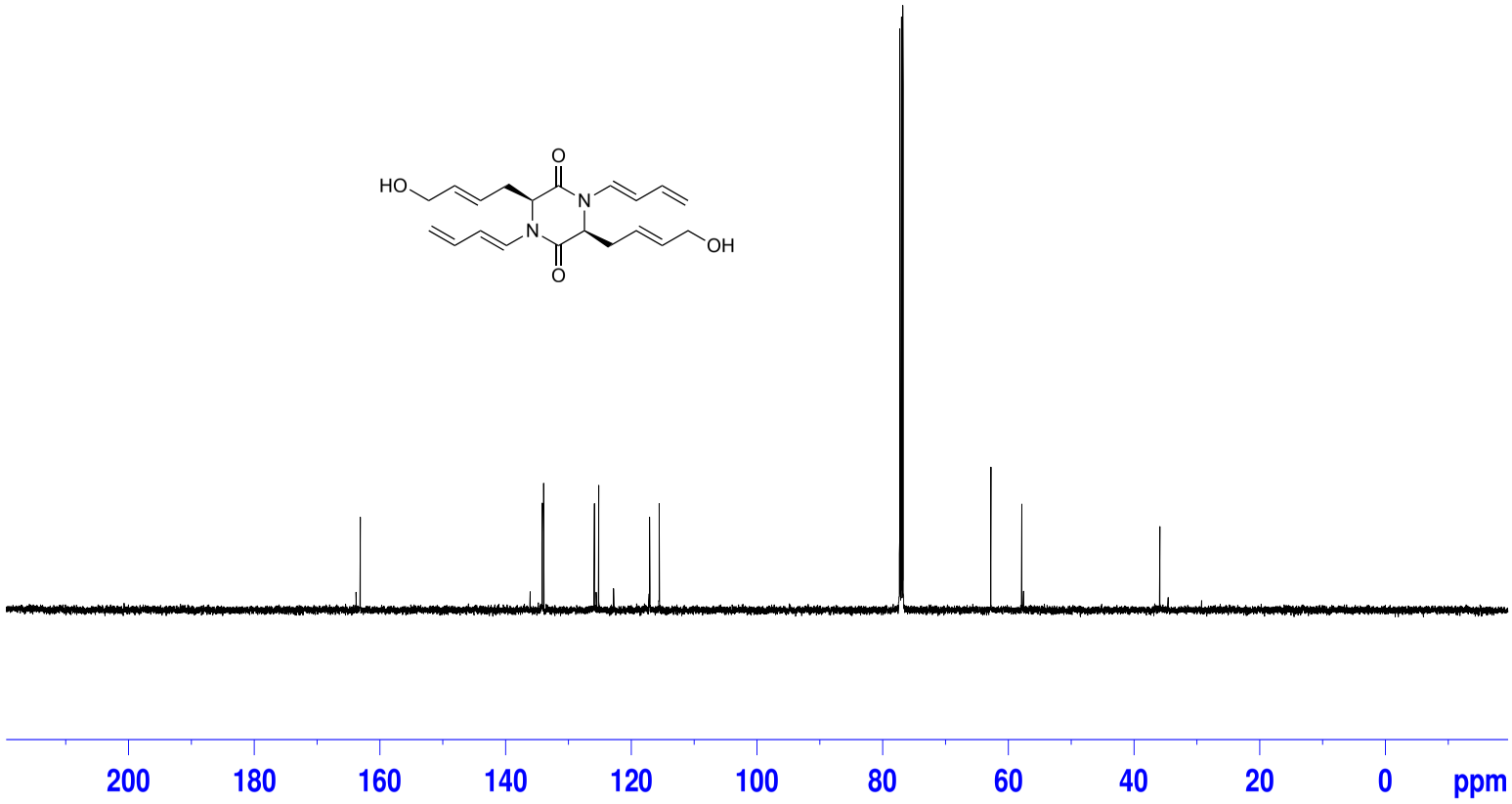

Figure 34: ^{13}C NMR ($CDCl_3$, 125 MHz) of **(+)-75**

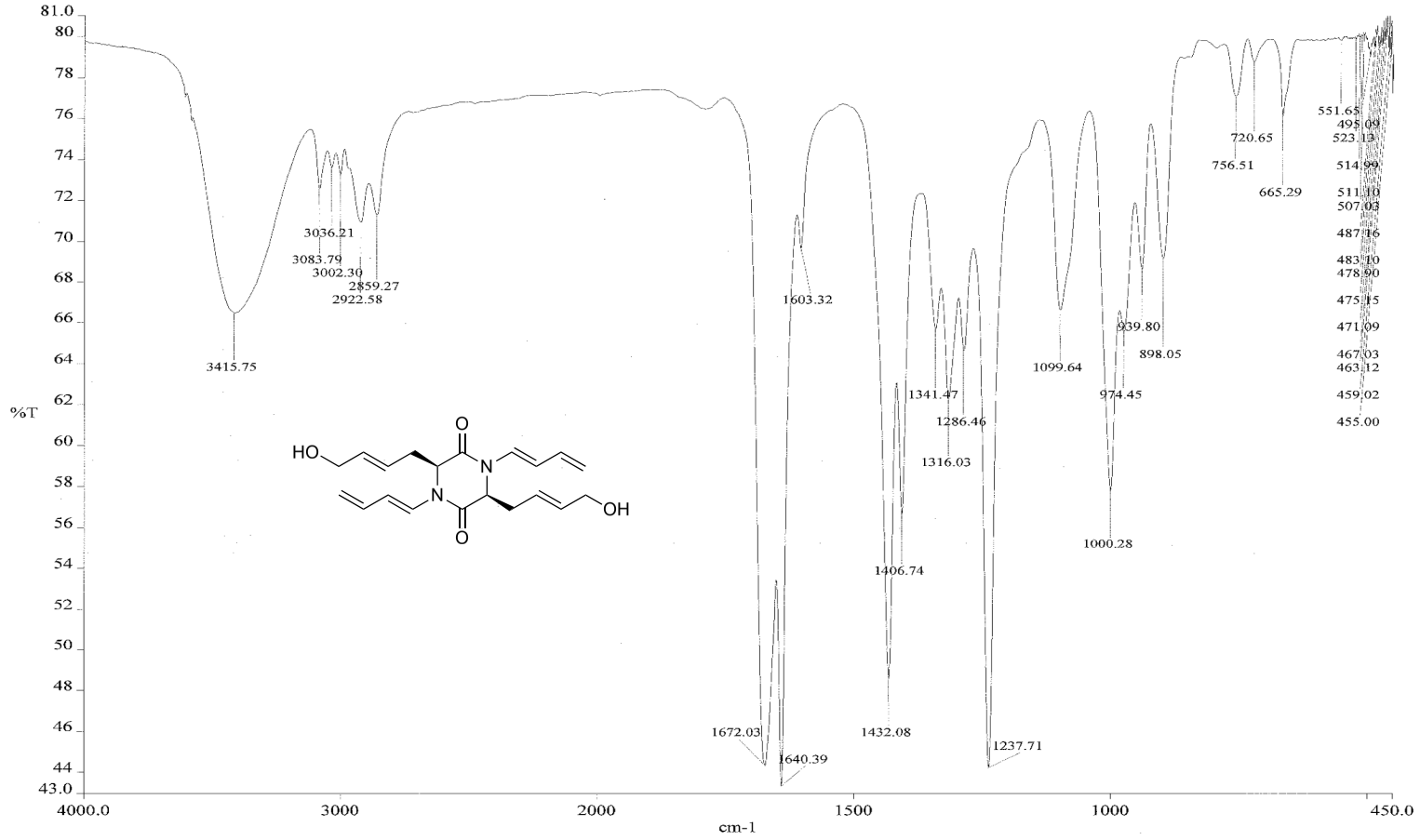

Figure 35: Infrared spectra (neat) of **(+)-75**

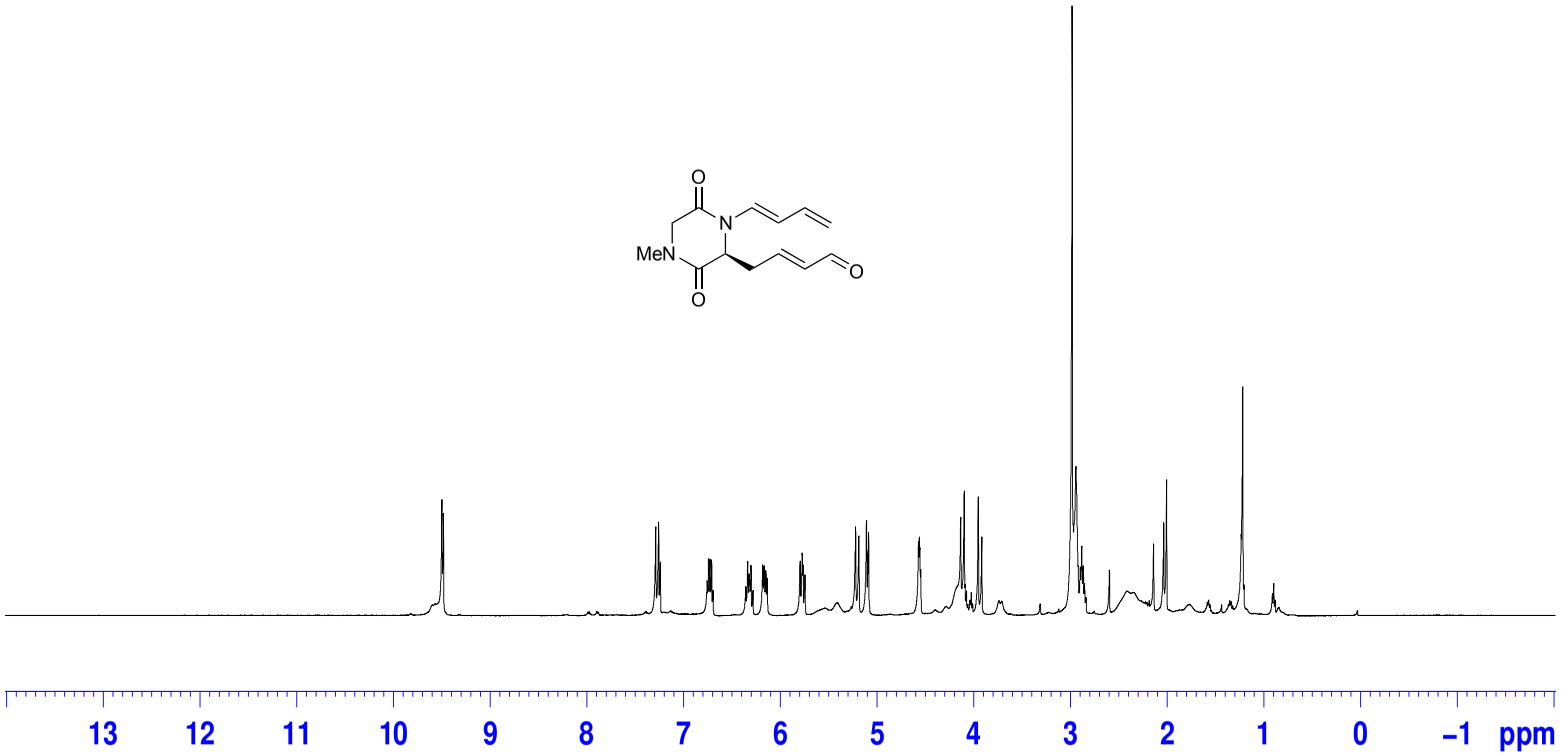

Figure 36: ^{1}H NMR ($CDCl_3$, 500 MHz) of **74**

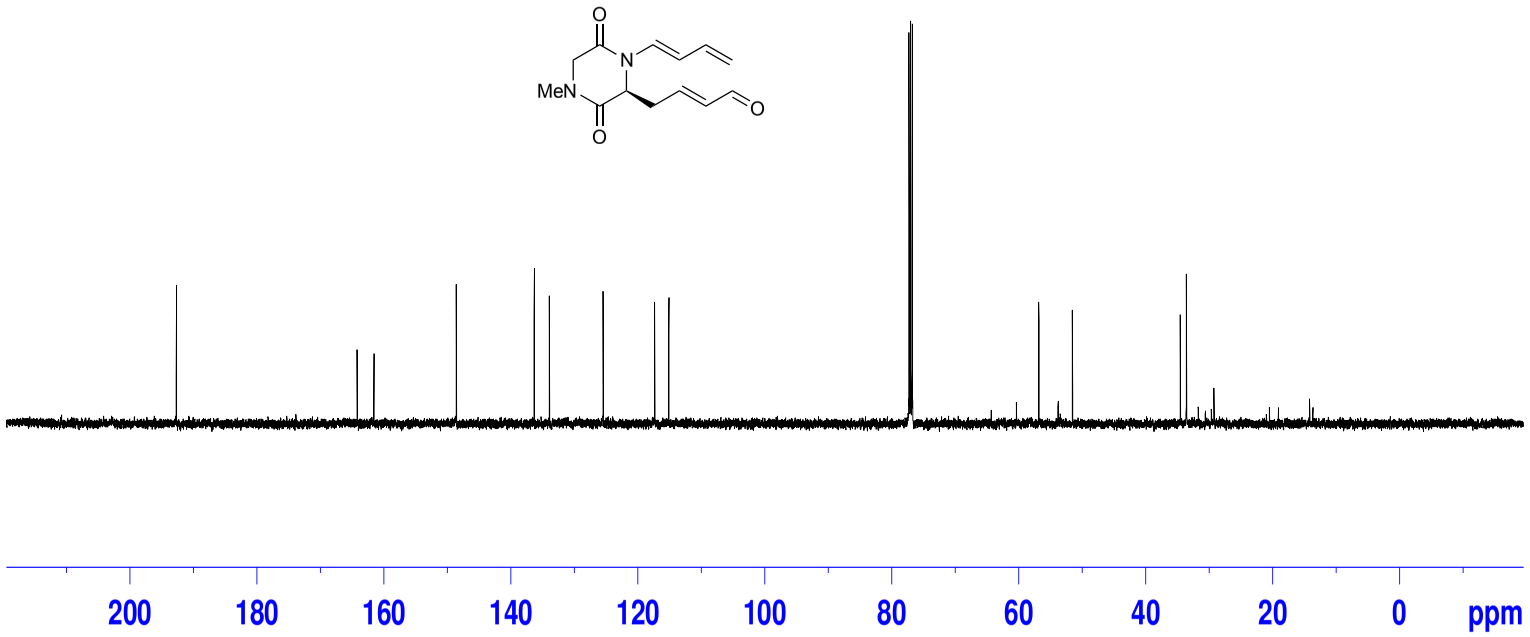

Figure 37: ^{13}C NMR ($CDCl_3$, 125 MHz) of **74**

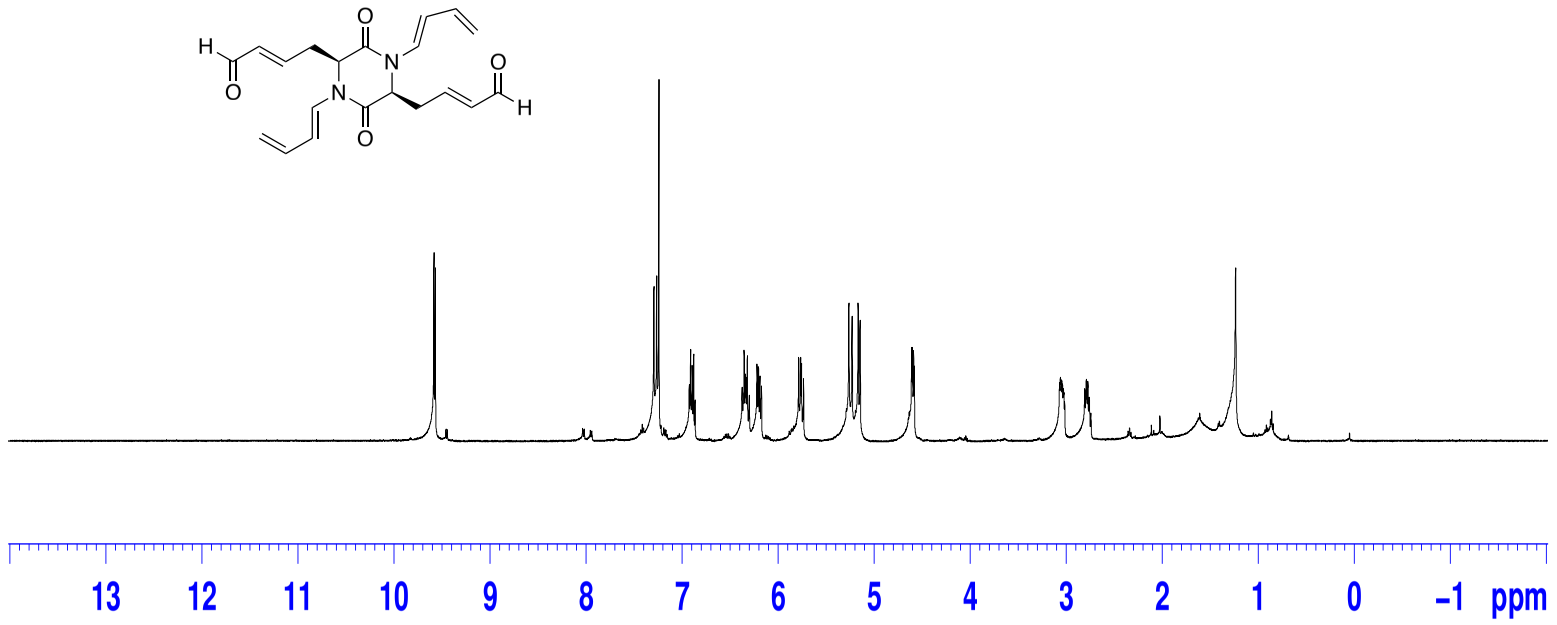

Figure 38: ^{1}H NMR ($CDCl_3$, 500 MHz) of **44**

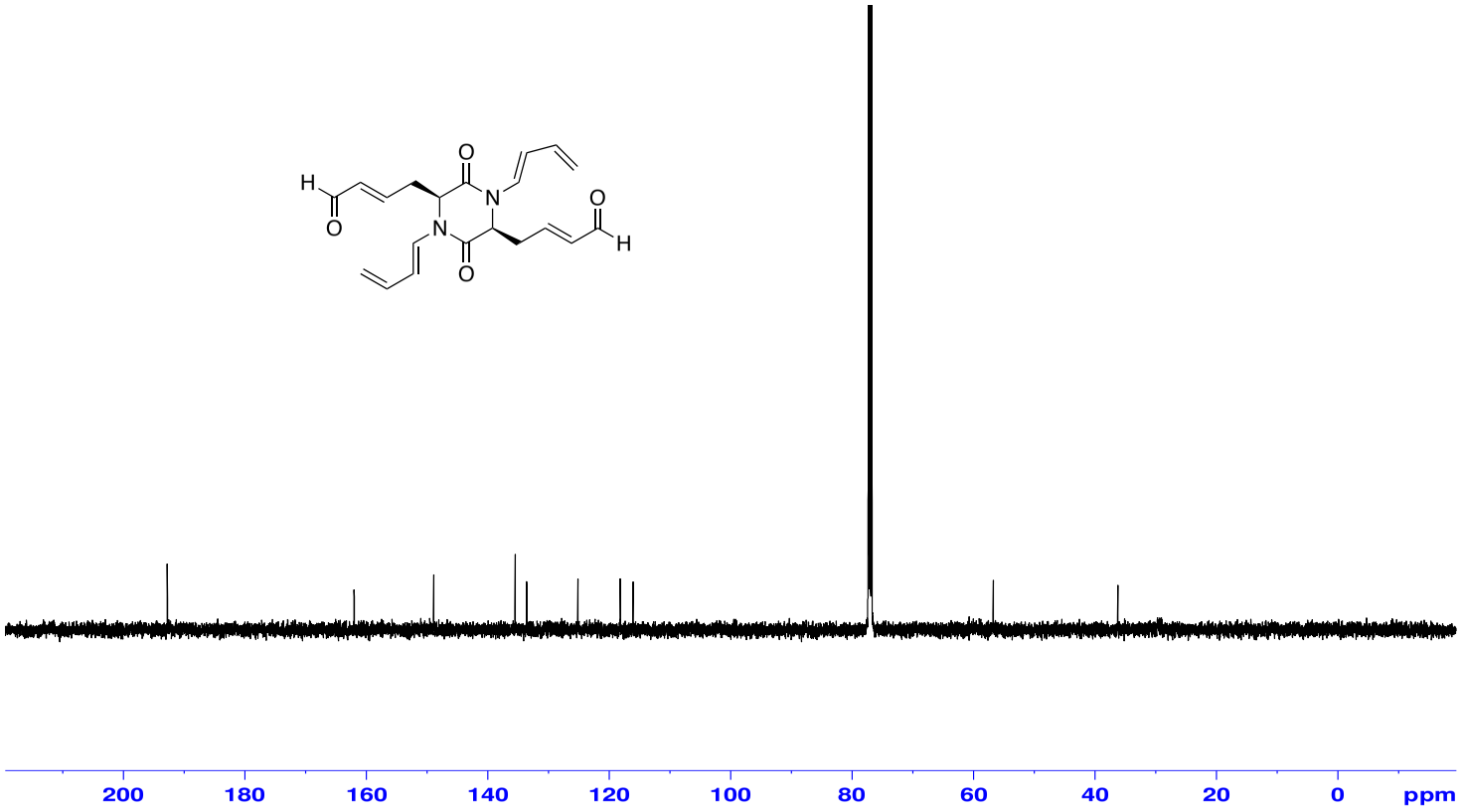

Figure 39: ^{13}C NMR ($CDCl_3$, 125 MHz) of **44**

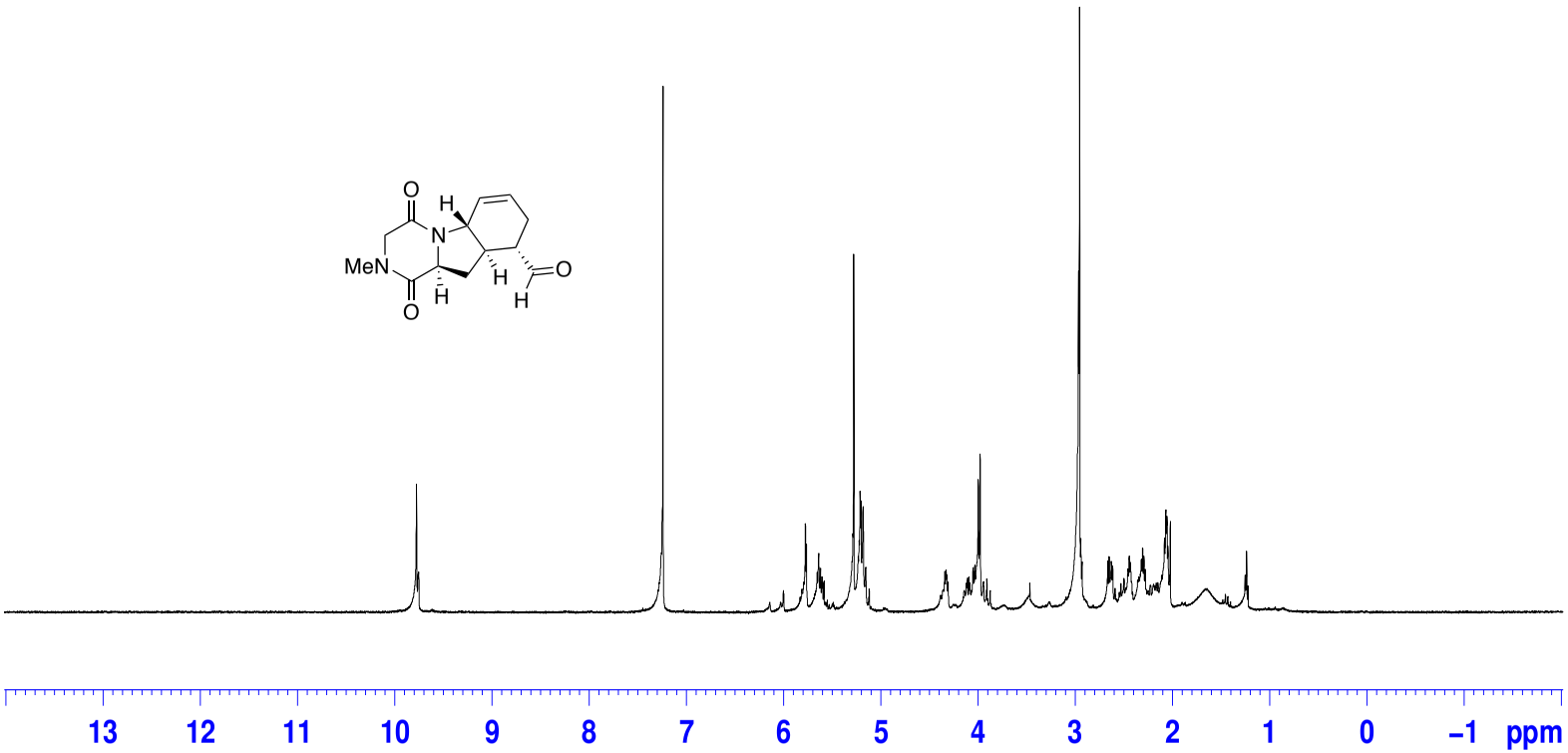

Figure 40: ^{1}H NMR ($CDCl_3$, 500 MHz) of **76**

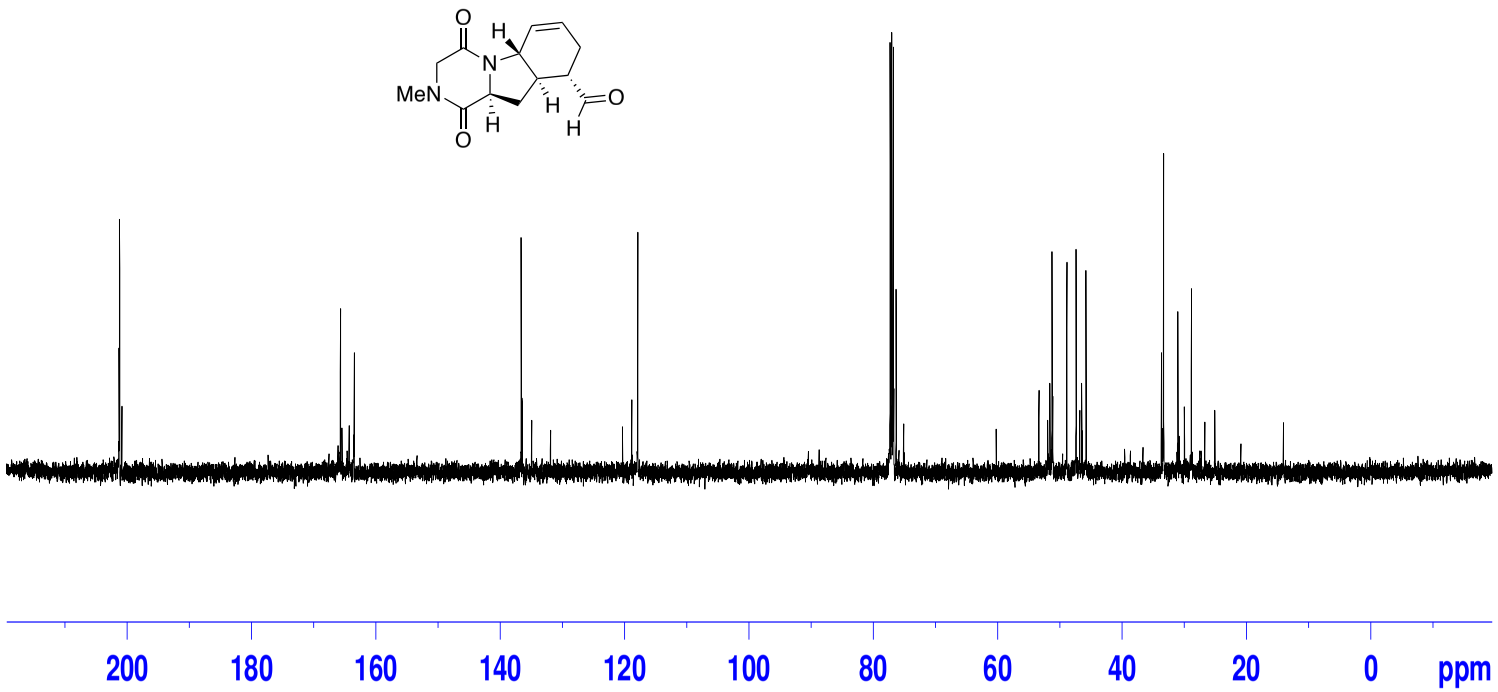

Figure 41: ^{13}C NMR ($CDCl_3$, 125 MHz) of **76**

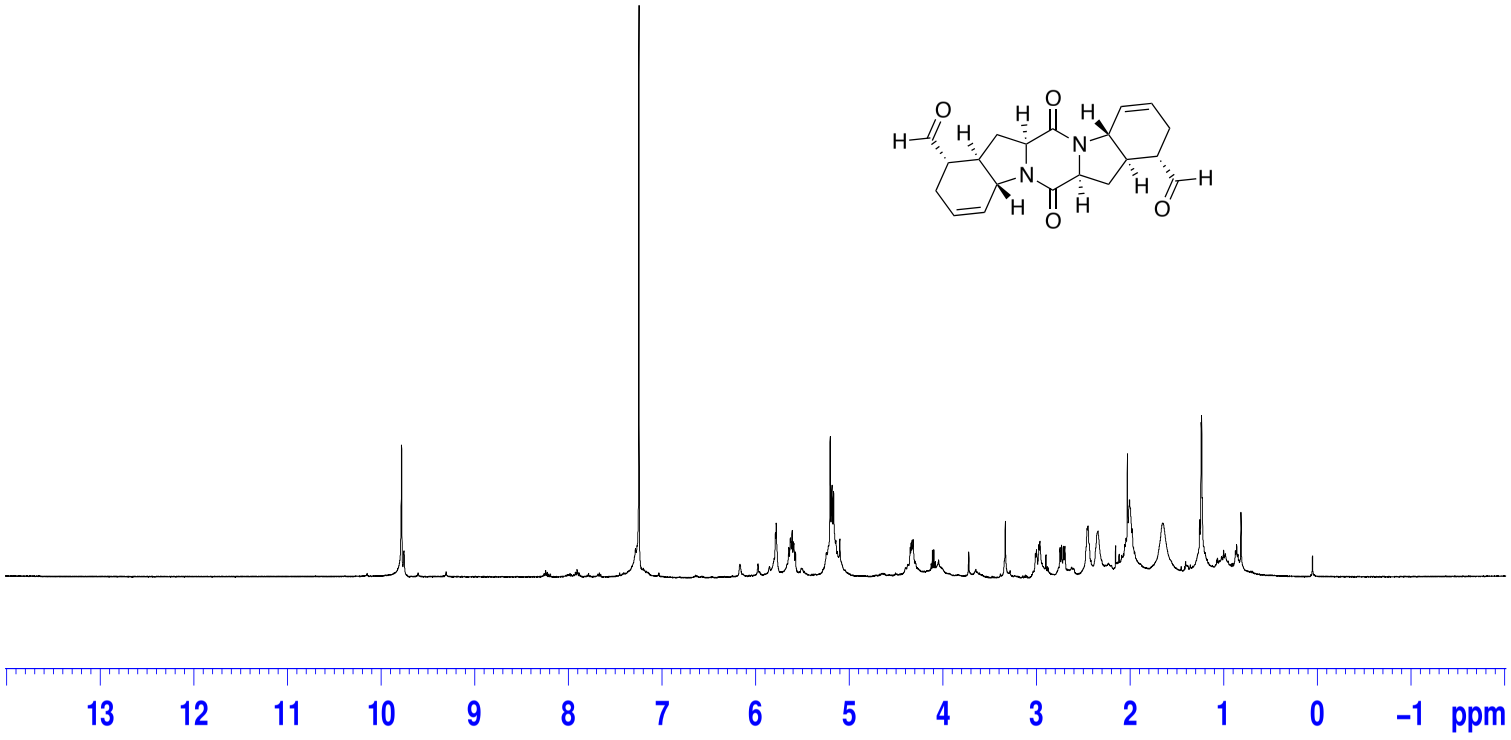

Figure 42: ^{1}H NMR ($CDCl_3$, 500 MHz) of **47**

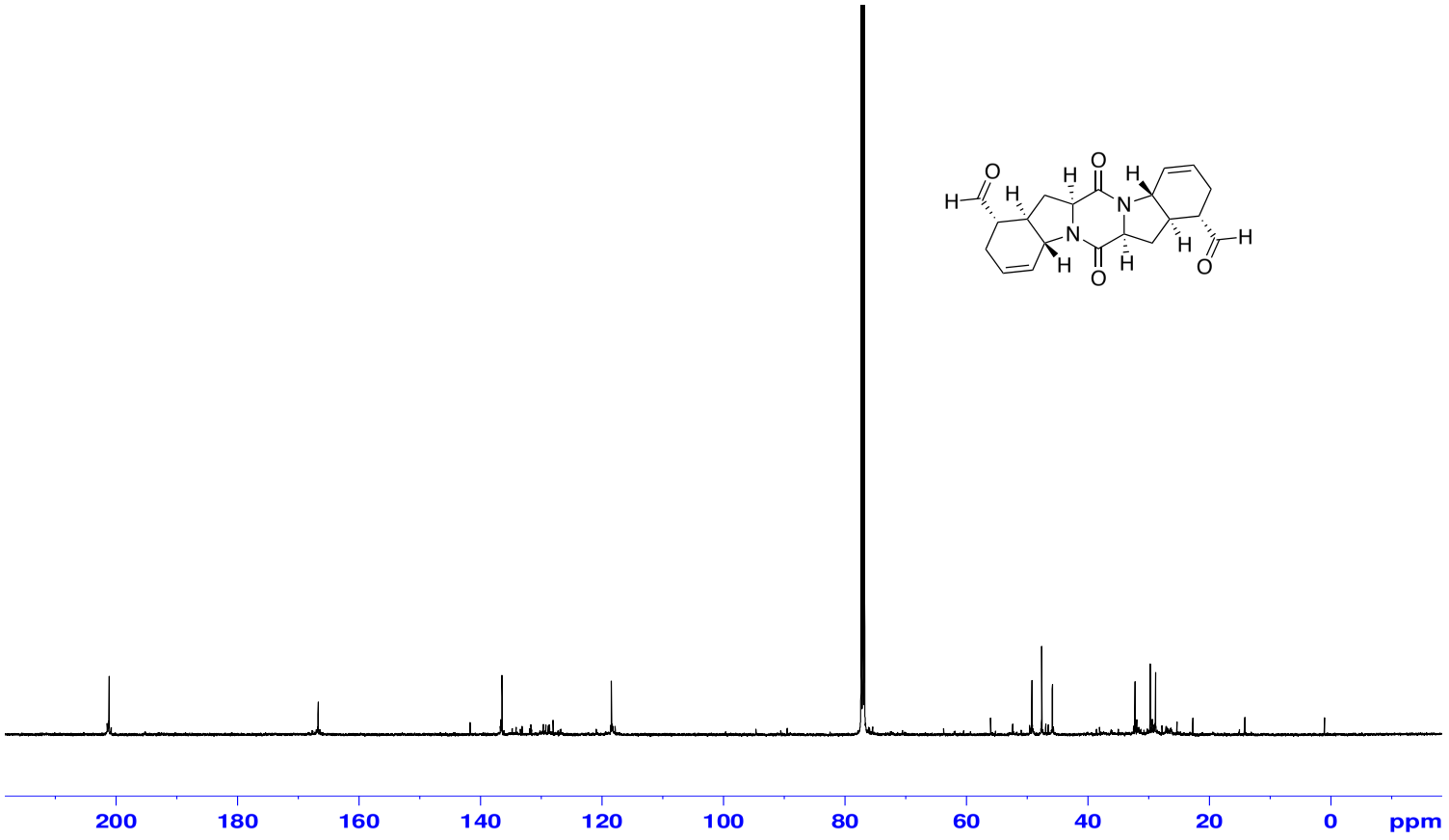

Figure 43: ^{13}C NMR ($CDCl_3$, 125 MHz) of **47**

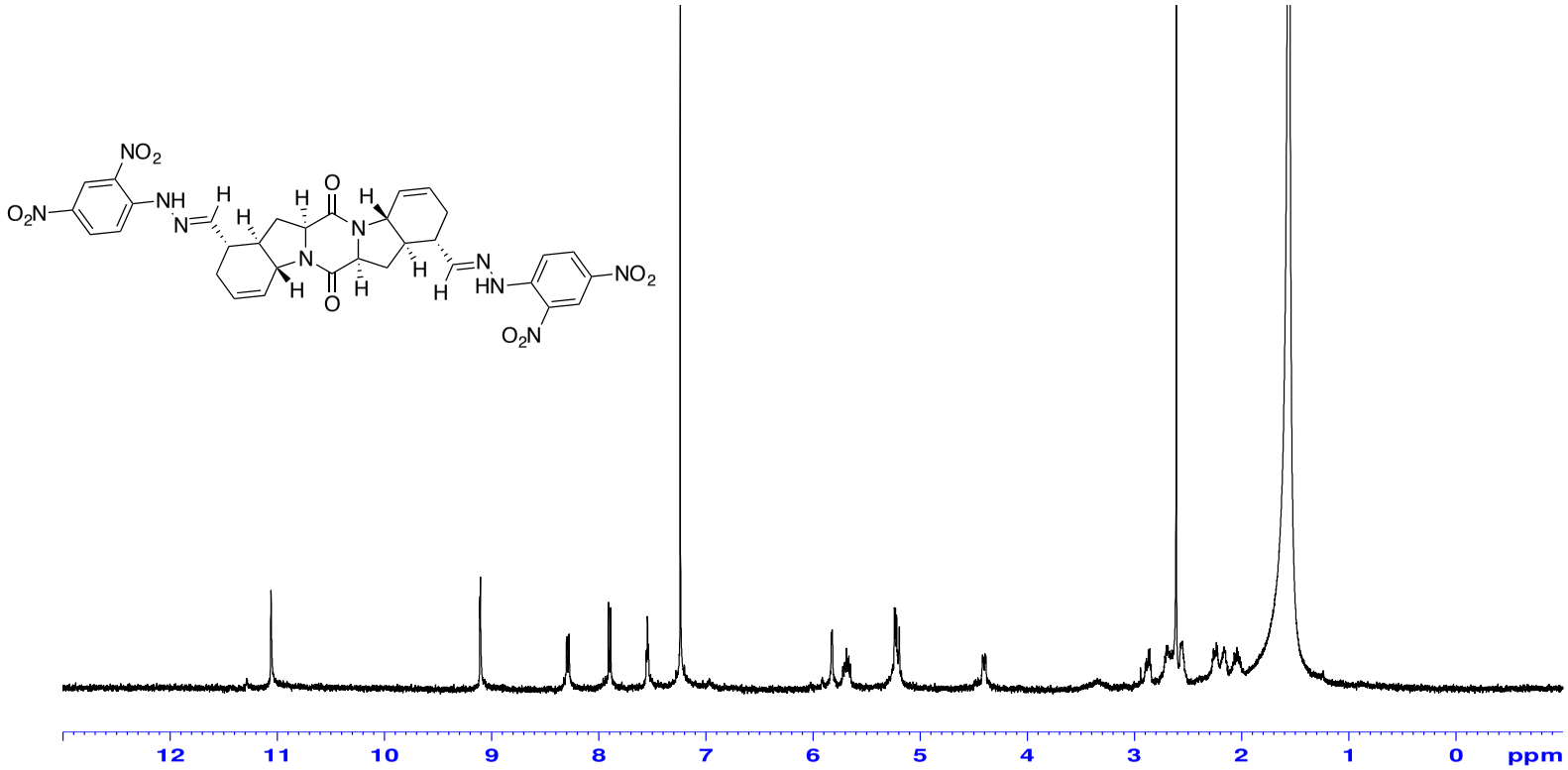

Figure 44: ^{1}H NMR ($CDCl_3$, 500 MHz) of **77**

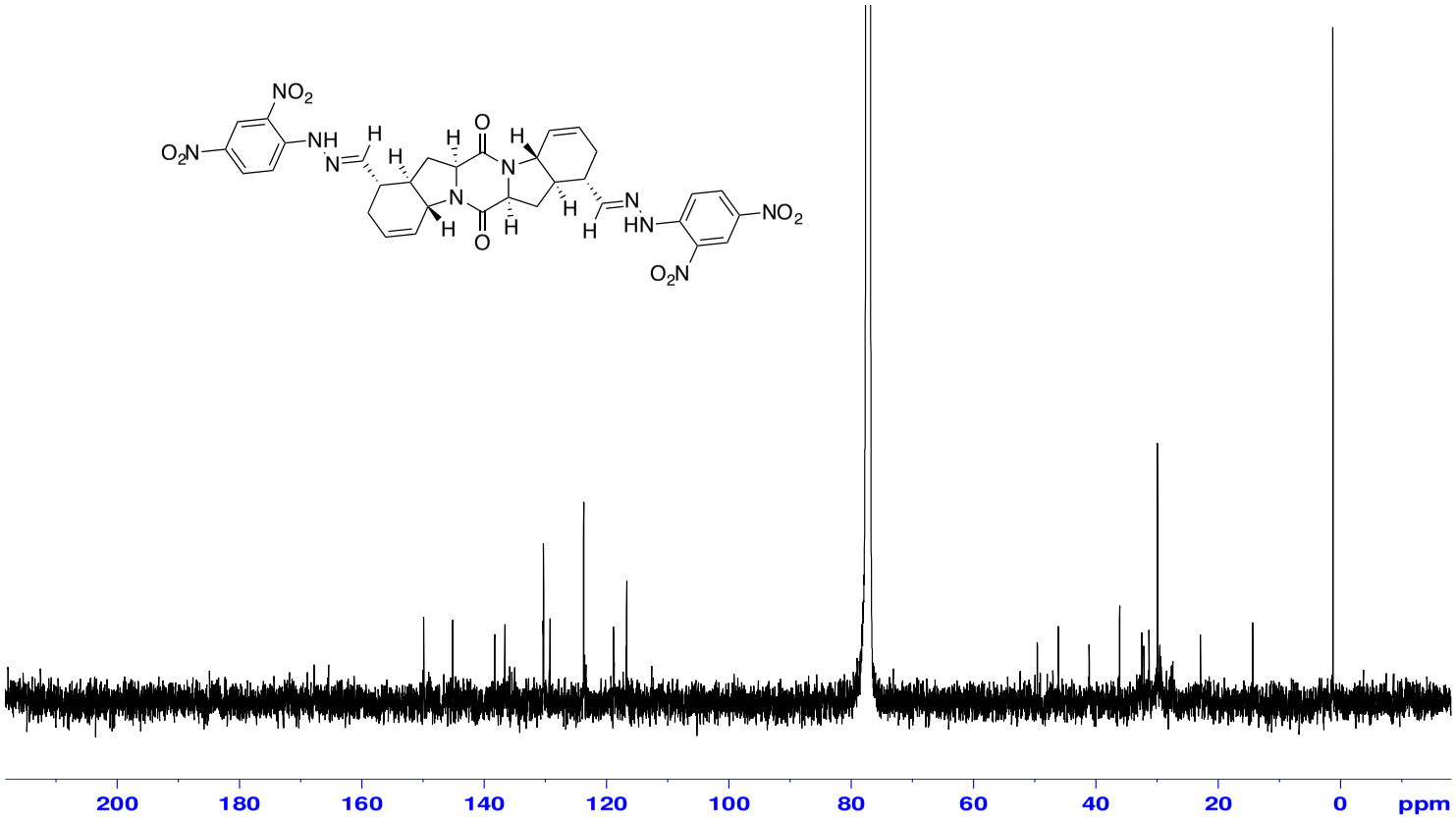

Figure 45: ^{13}C NMR ($CDCl_3$, 125 MHz) of **77**

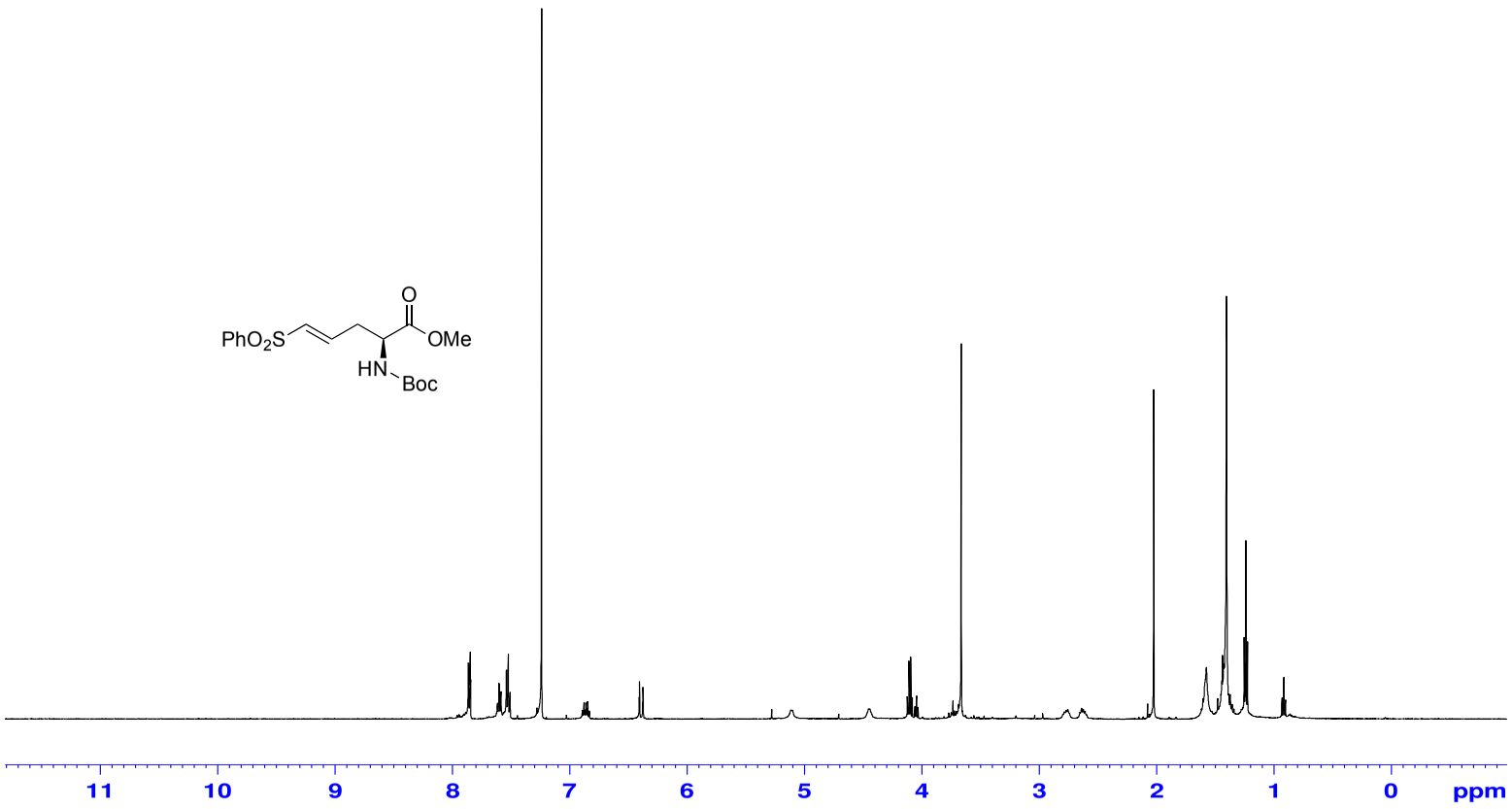

Figure 46: ^{1}H NMR ($CDCl_3$, 500 MHz) of **(+)-85**

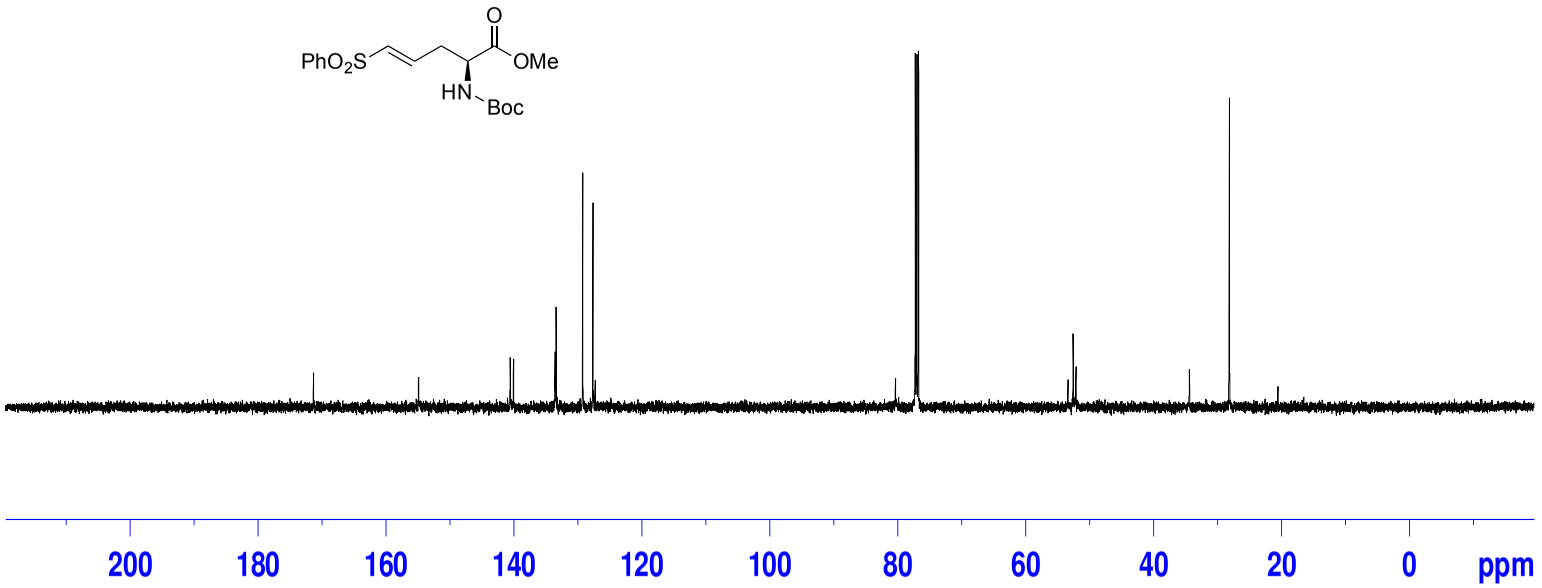

Figure 47: ^{13}C NMR ($CDCl_3$, 125 MHz) of **(+)-85**

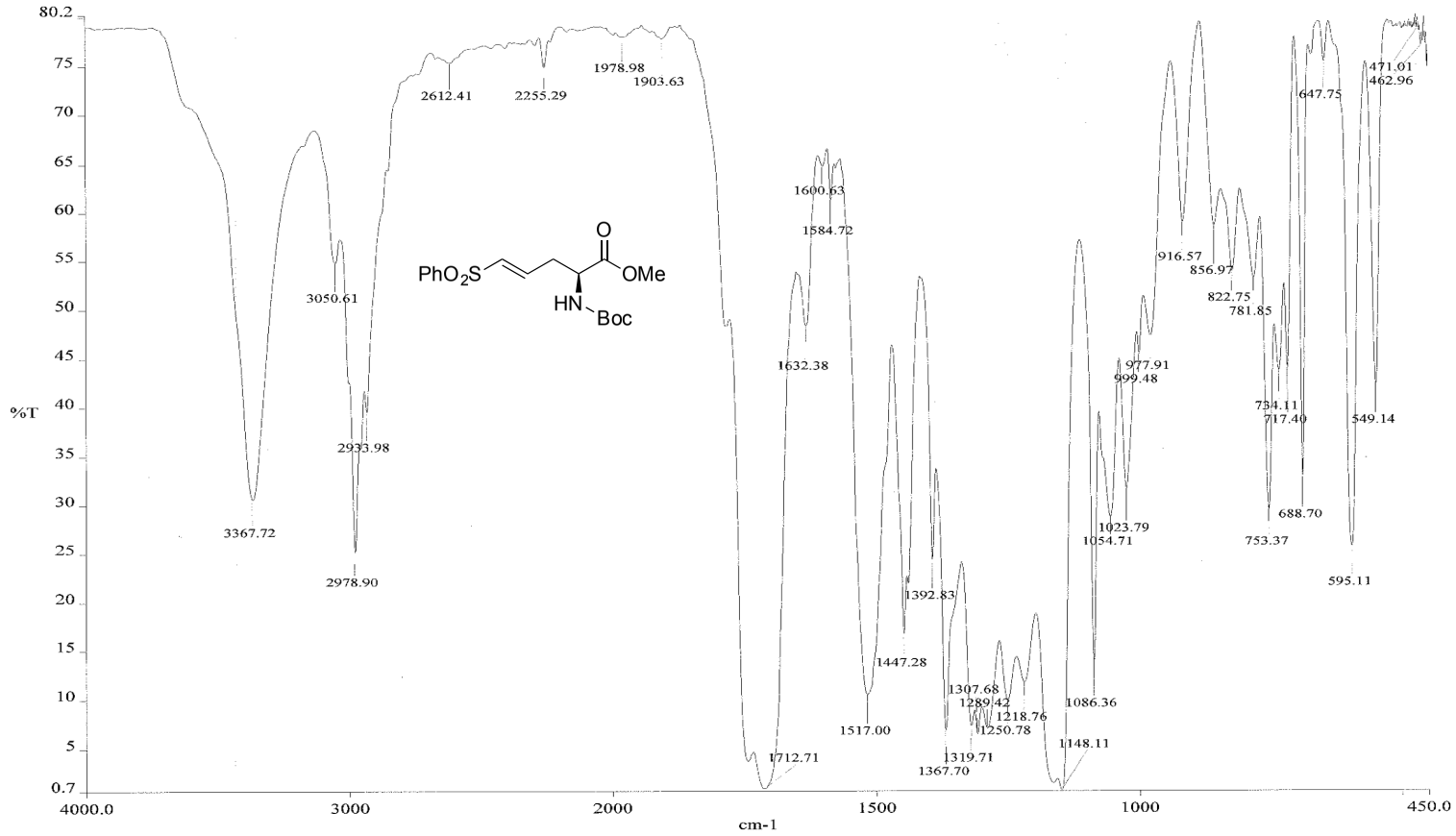

Figure 48: Infrared spectra (neat) of **(+)-85**

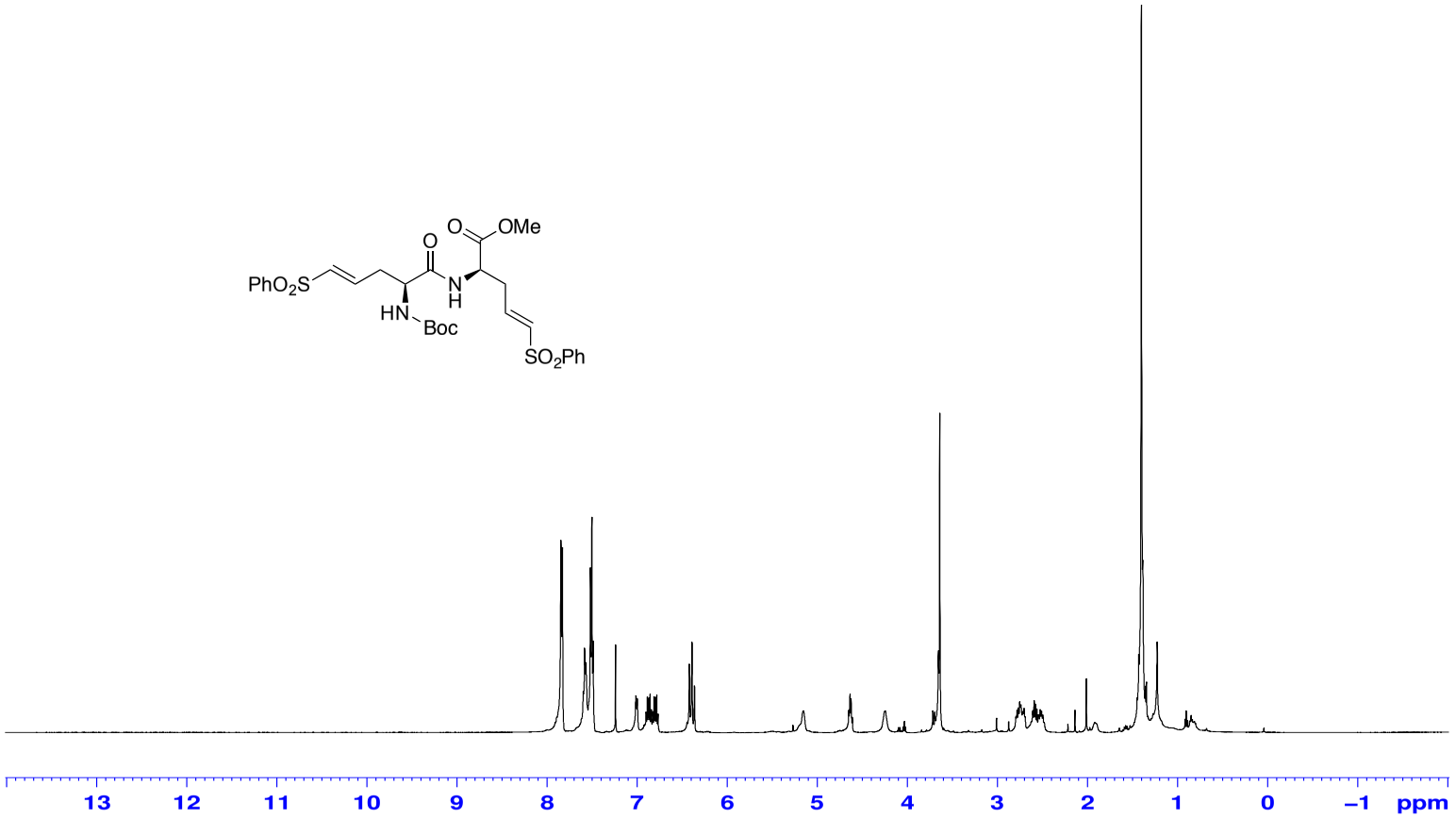

Figure 49: ^{1}H NMR ($CDCl_3$, 500 MHz) of **(+)-88**

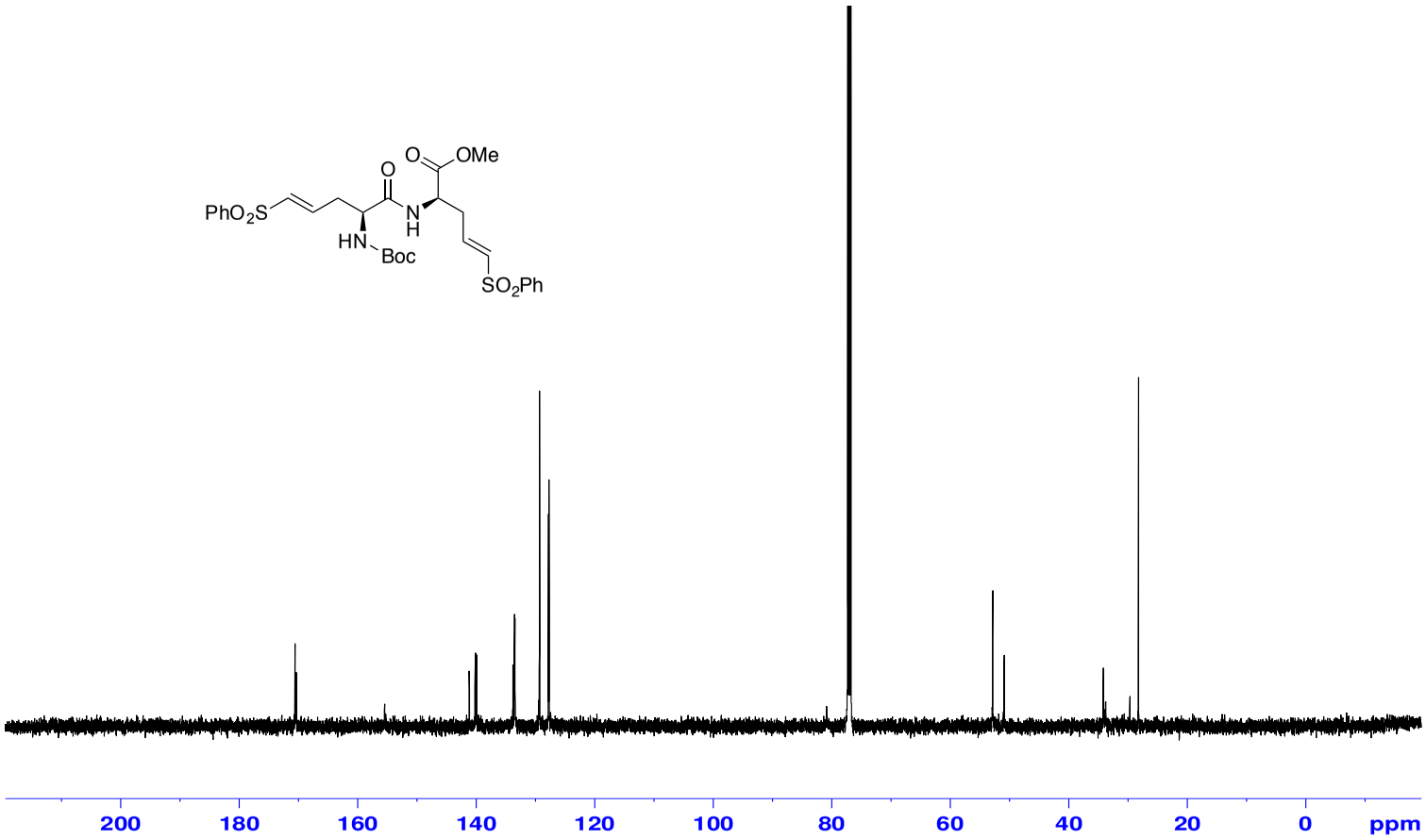

Figure 50: ^{13}C NMR ($CDCl_3$, 125 MHz) of **(+)-88**

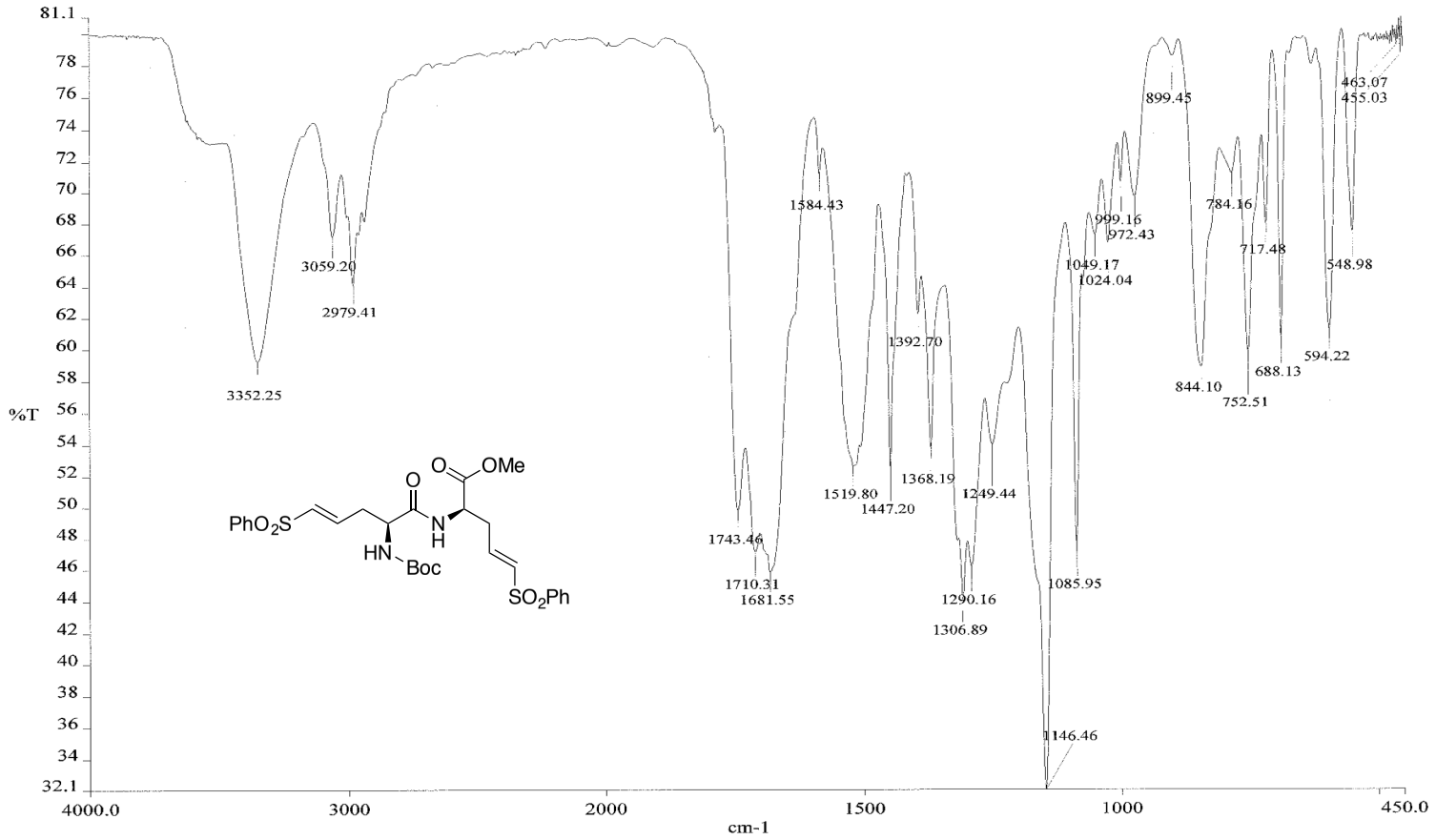

Figure 51: Infrared spectra (neat) of **(+)-88**

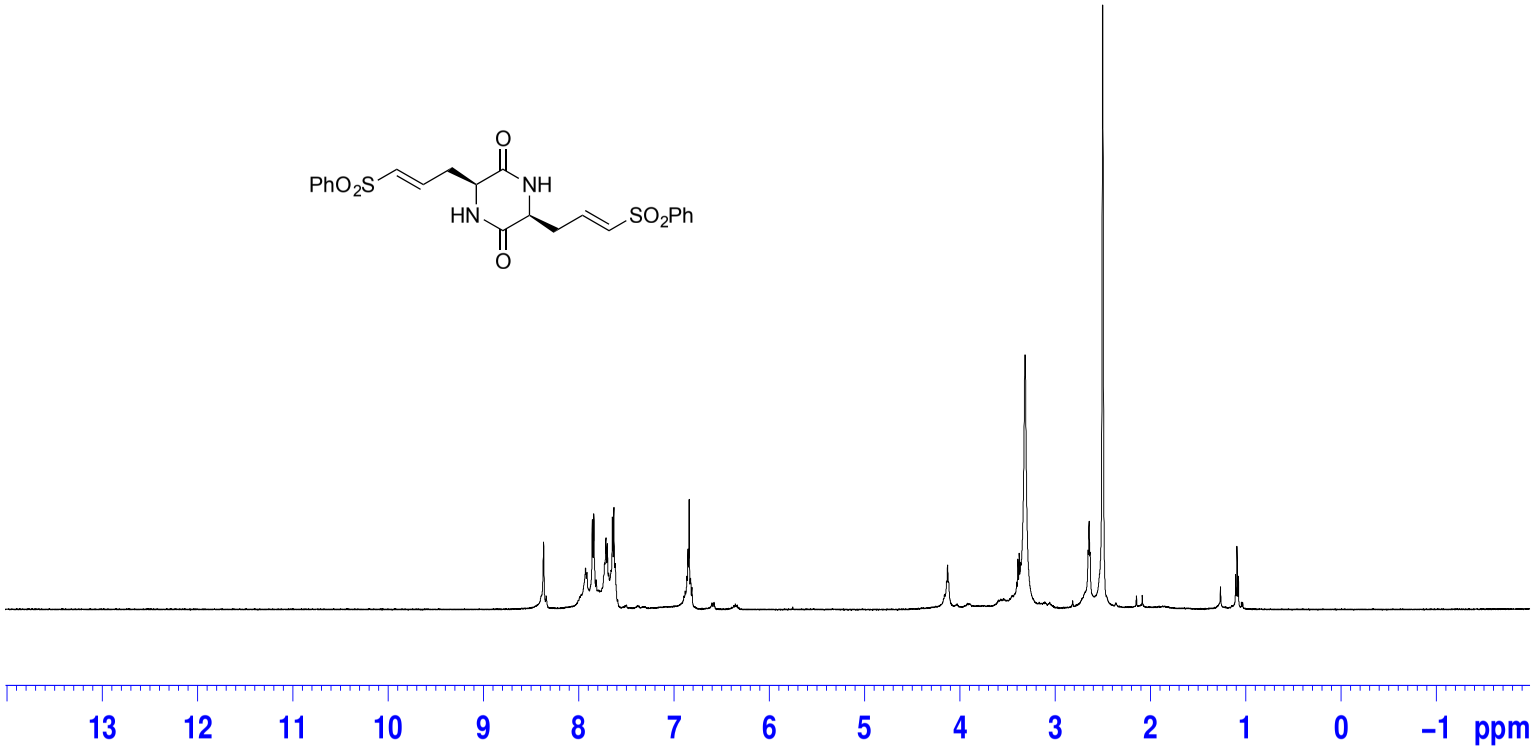

Figure 52: ^{1}H NMR (DMSO-d_6, 500 MHz) of **(−)-78**

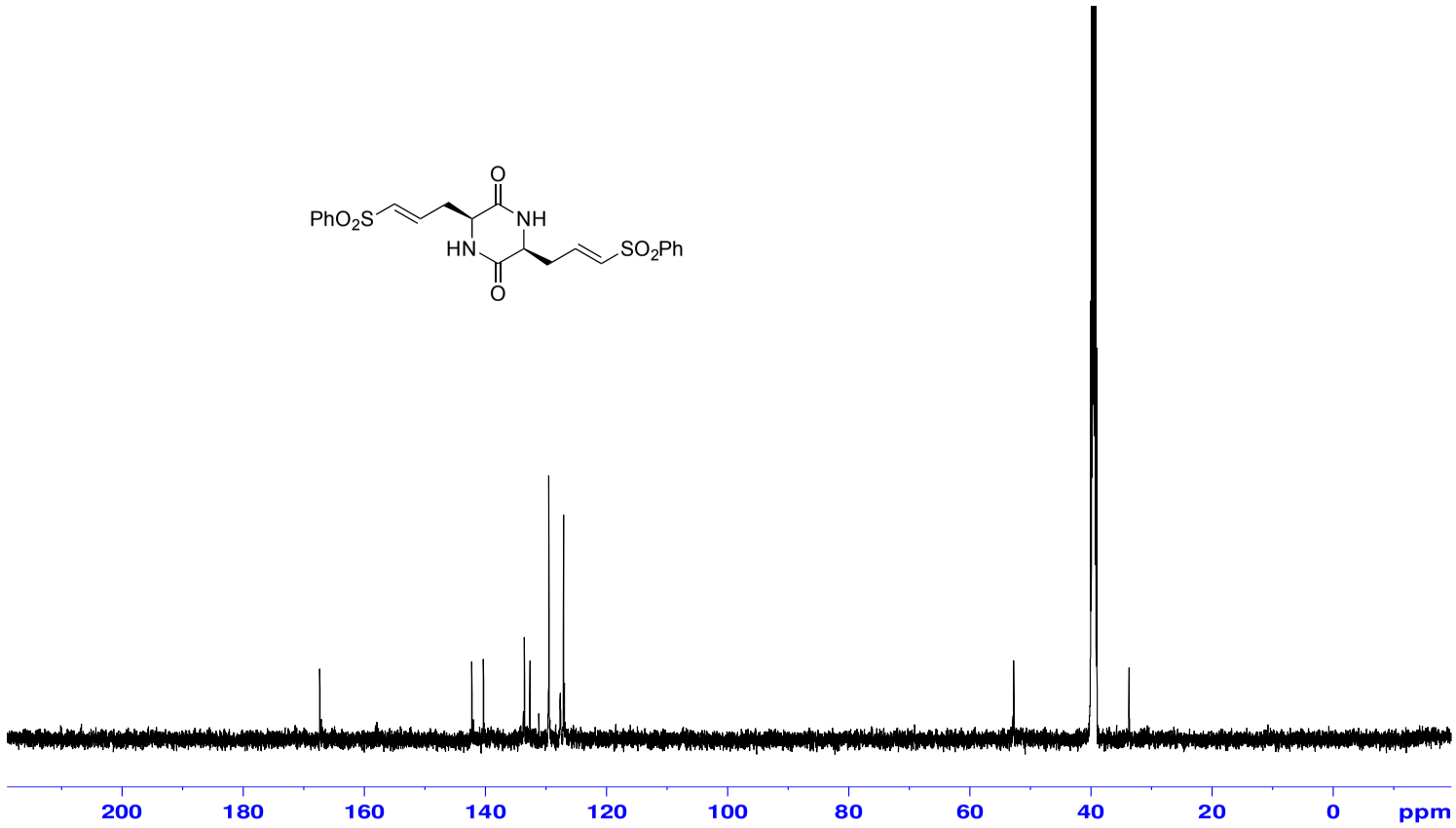

Figure 53: ^{13}C NMR (DMSO-d_6, 125 MHz) of **(−)-78**

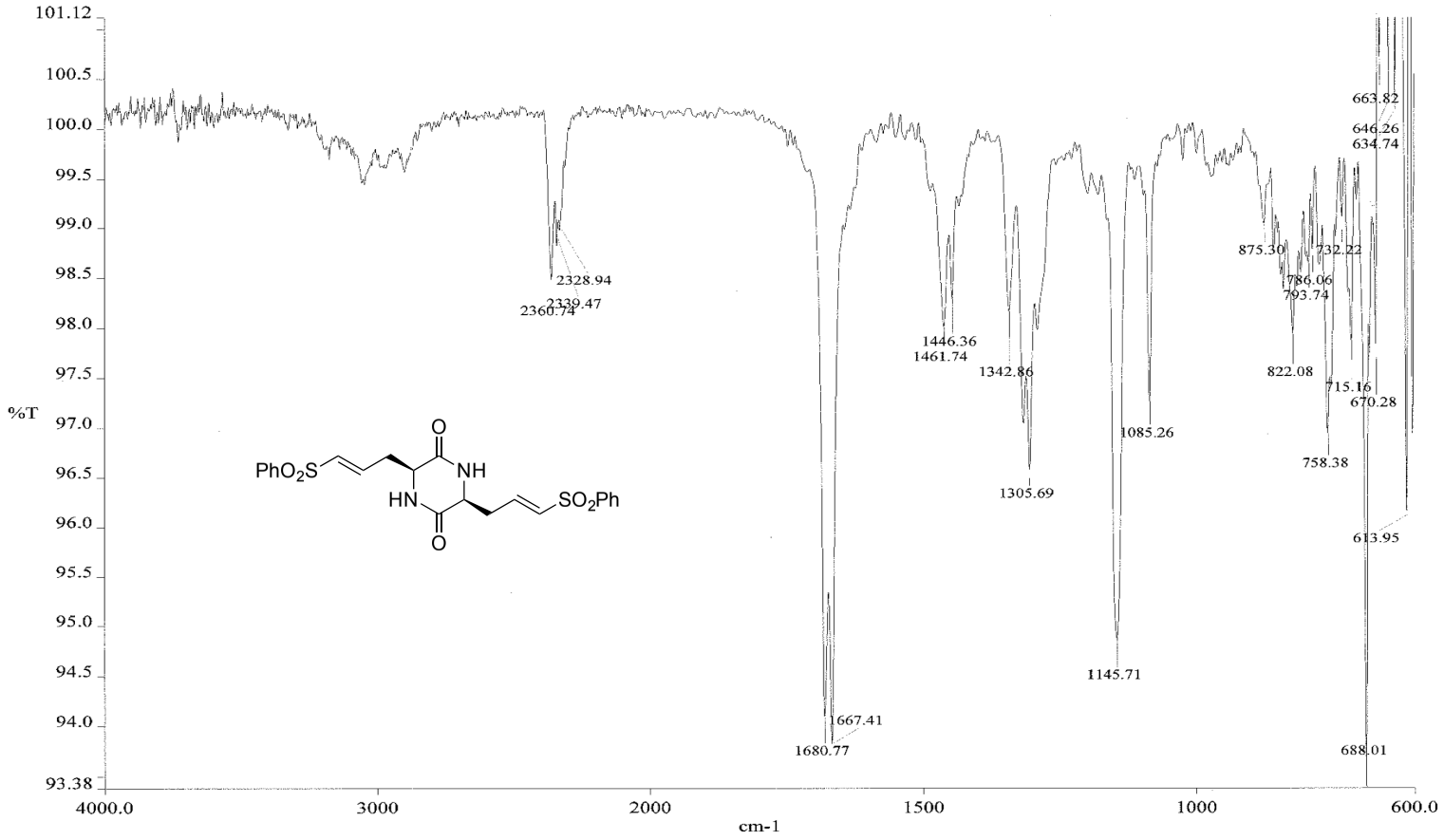

Figure 54: Infrared spectra (neat) of **(−)-78**

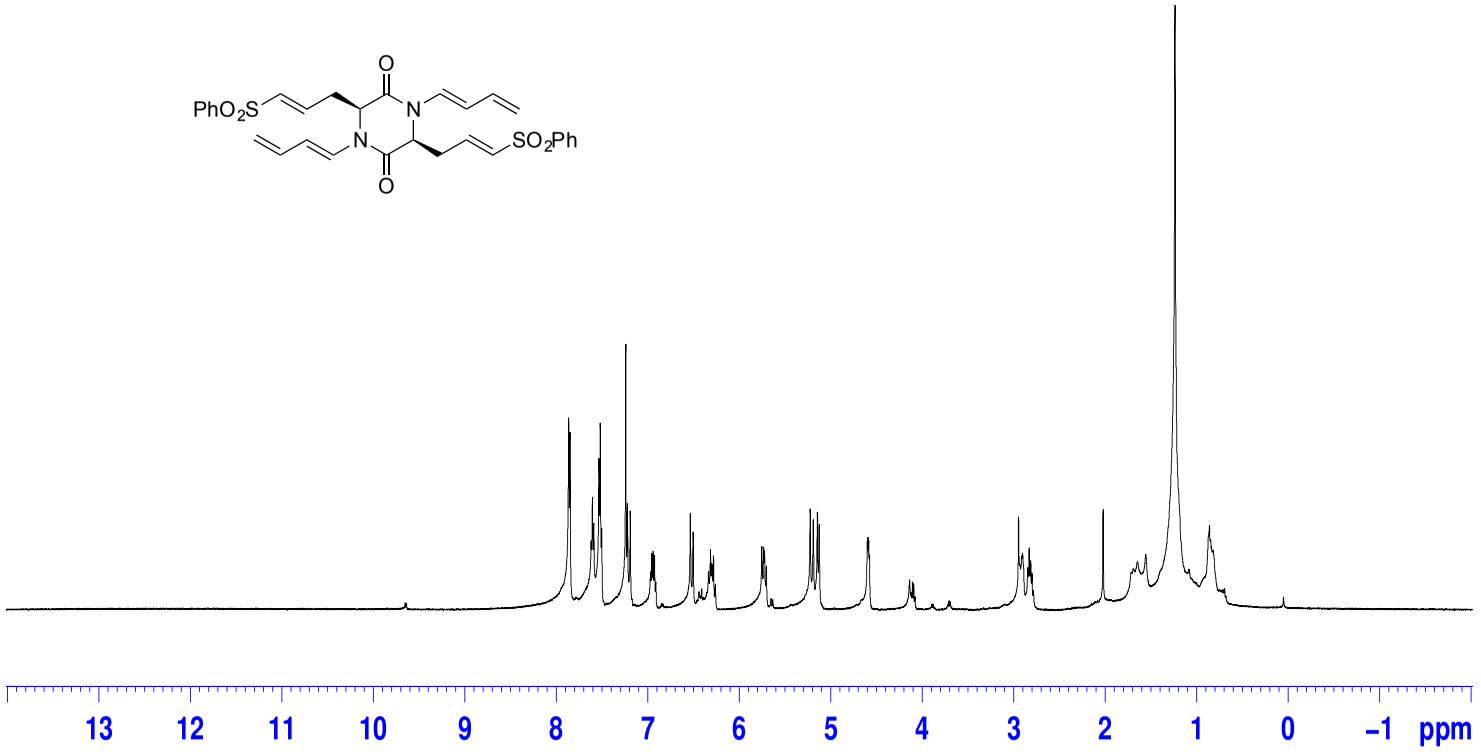

Figure 55: ^{1}H NMR ($CDCl_3$, 500 MHz) of **(+)-89**

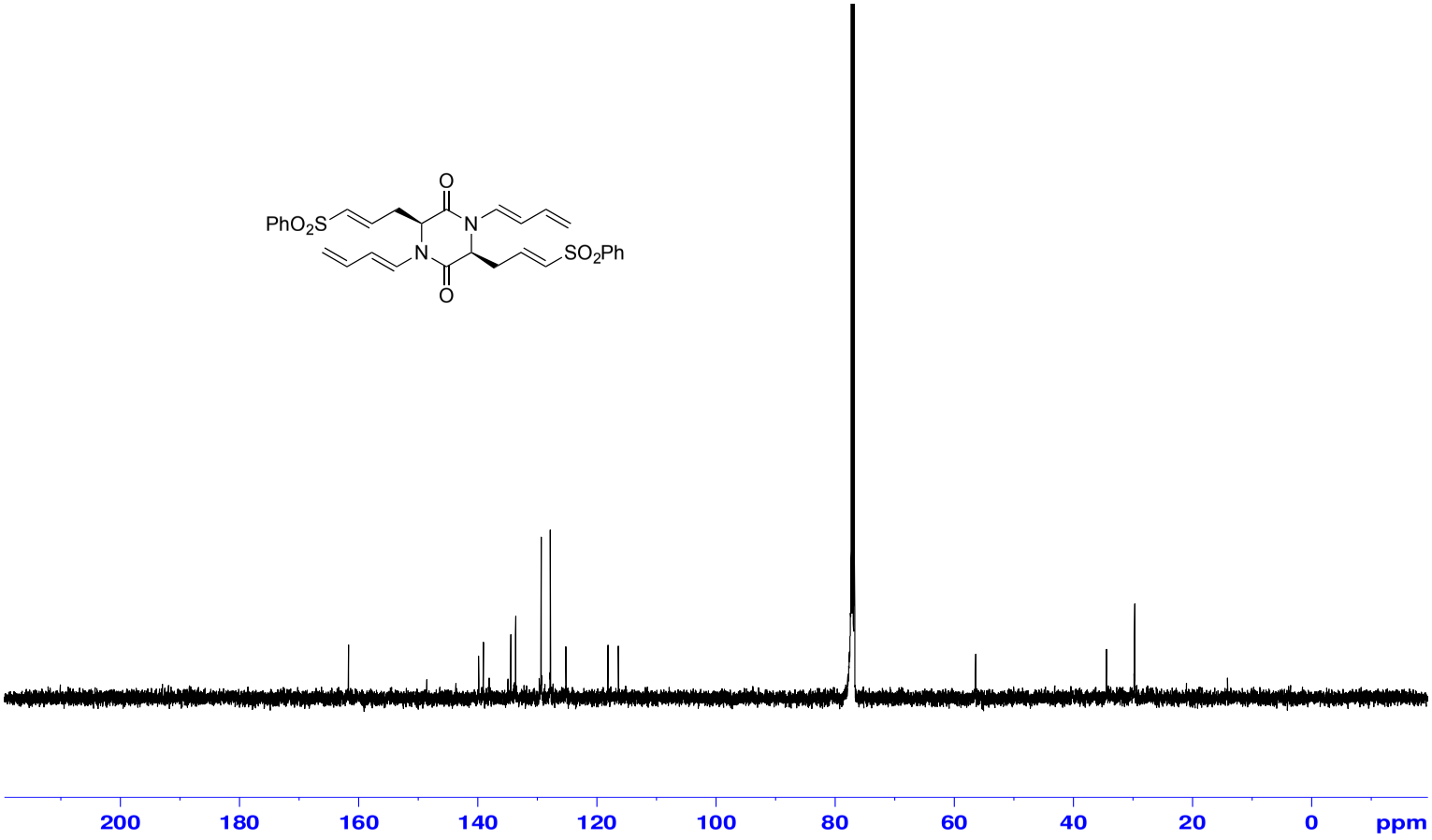

Figure 56: ^{13}C NMR ($CDCl_3$, 125 MHz) of **(+)-89**

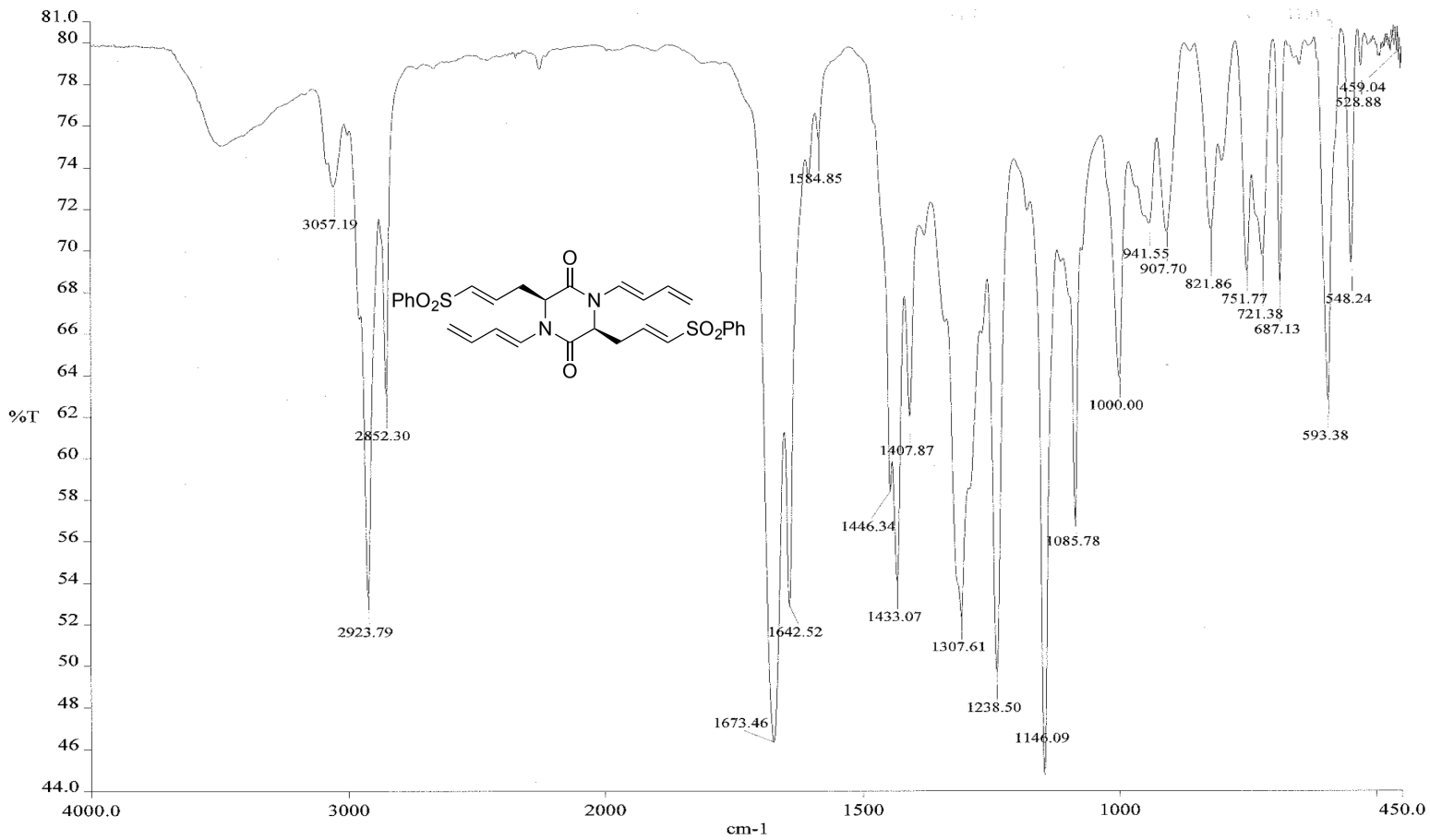

Figure 57: Infrared spectra (neat) of **(+)-89**

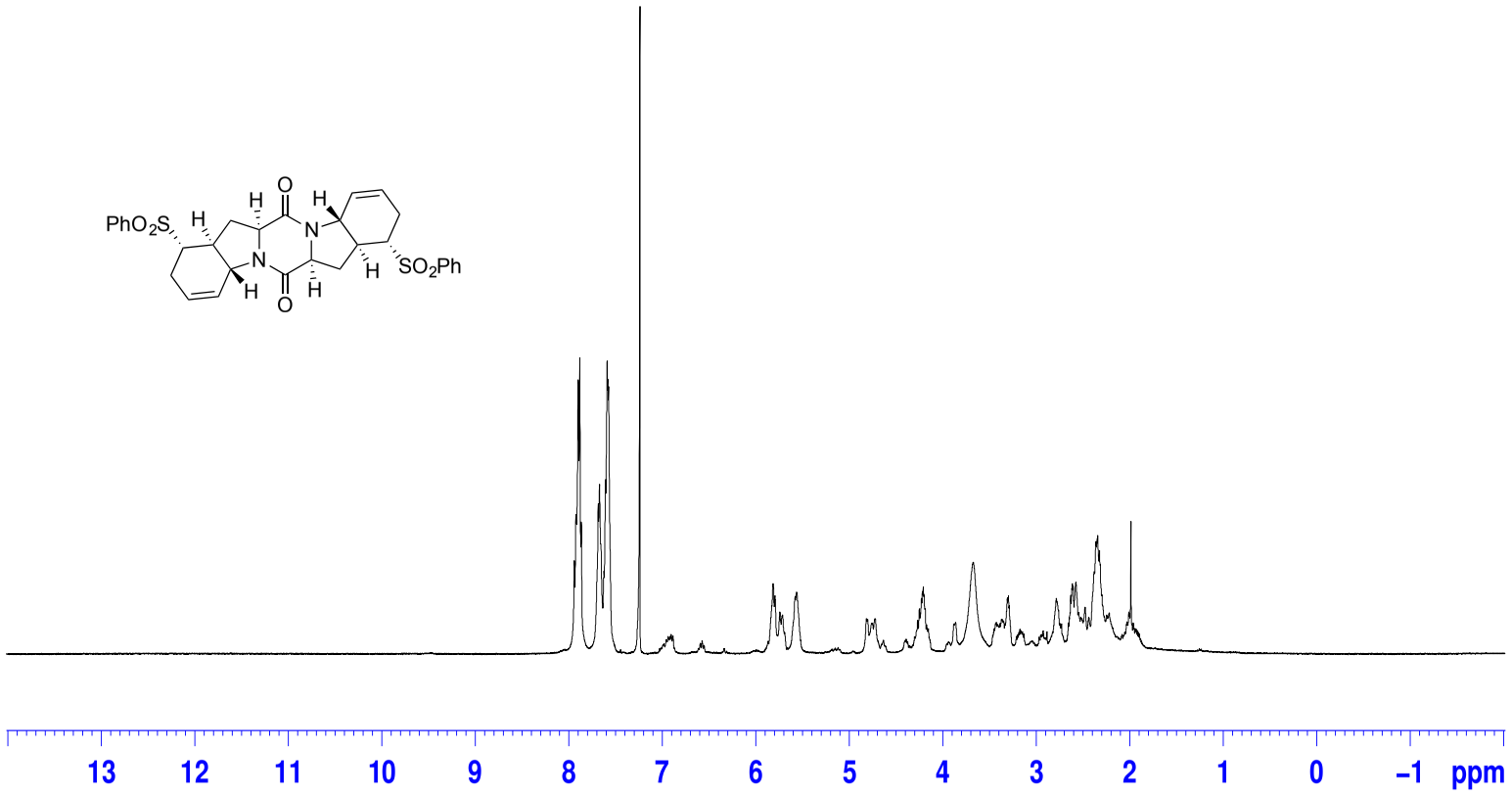

Figure 58: ^{1}H NMR ($CDCl_3$, 500 MHz) of **90**

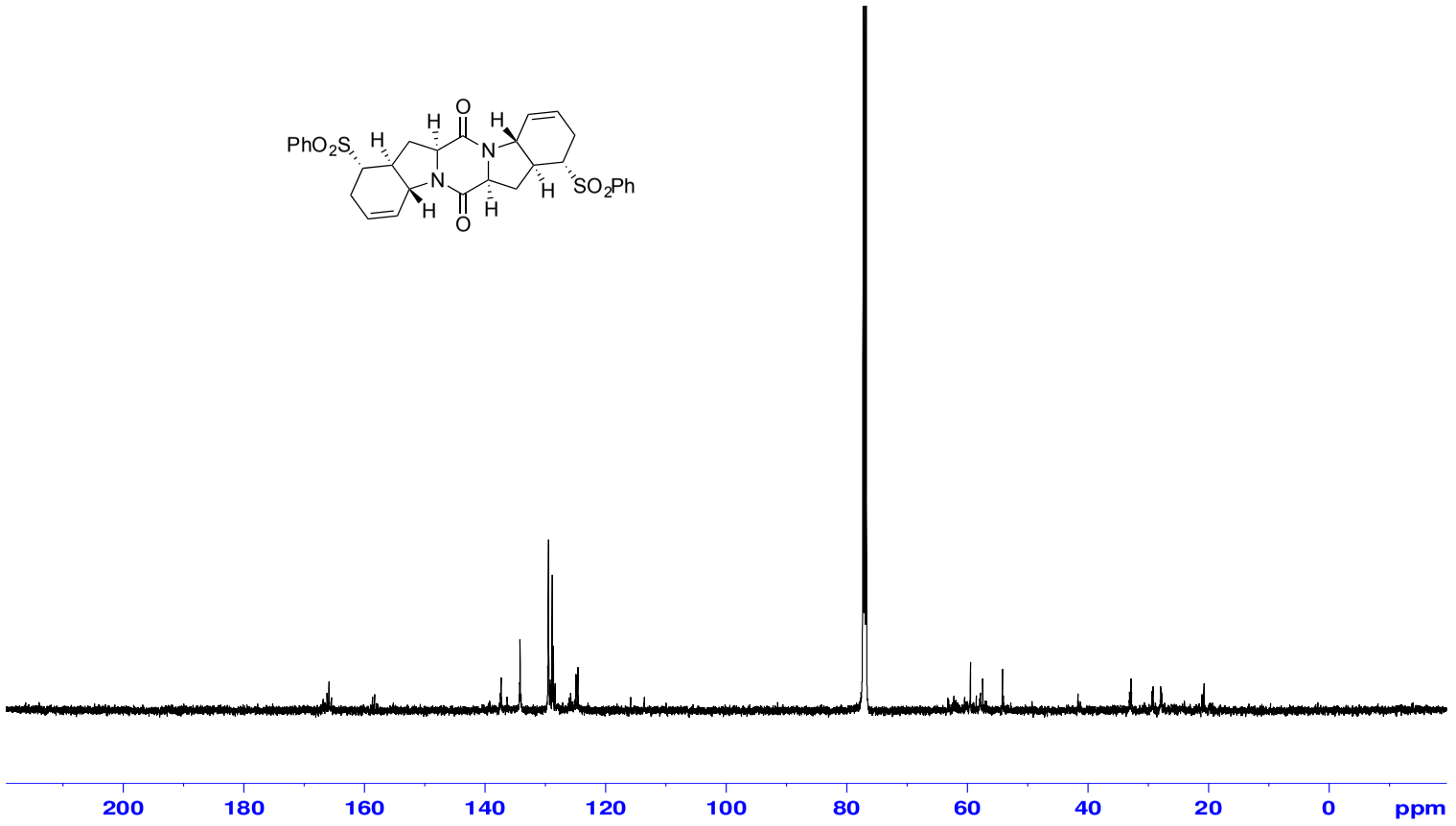

Figure 59: ^{13}C NMR ($CDCl_3$, 125 MHz) of **90**

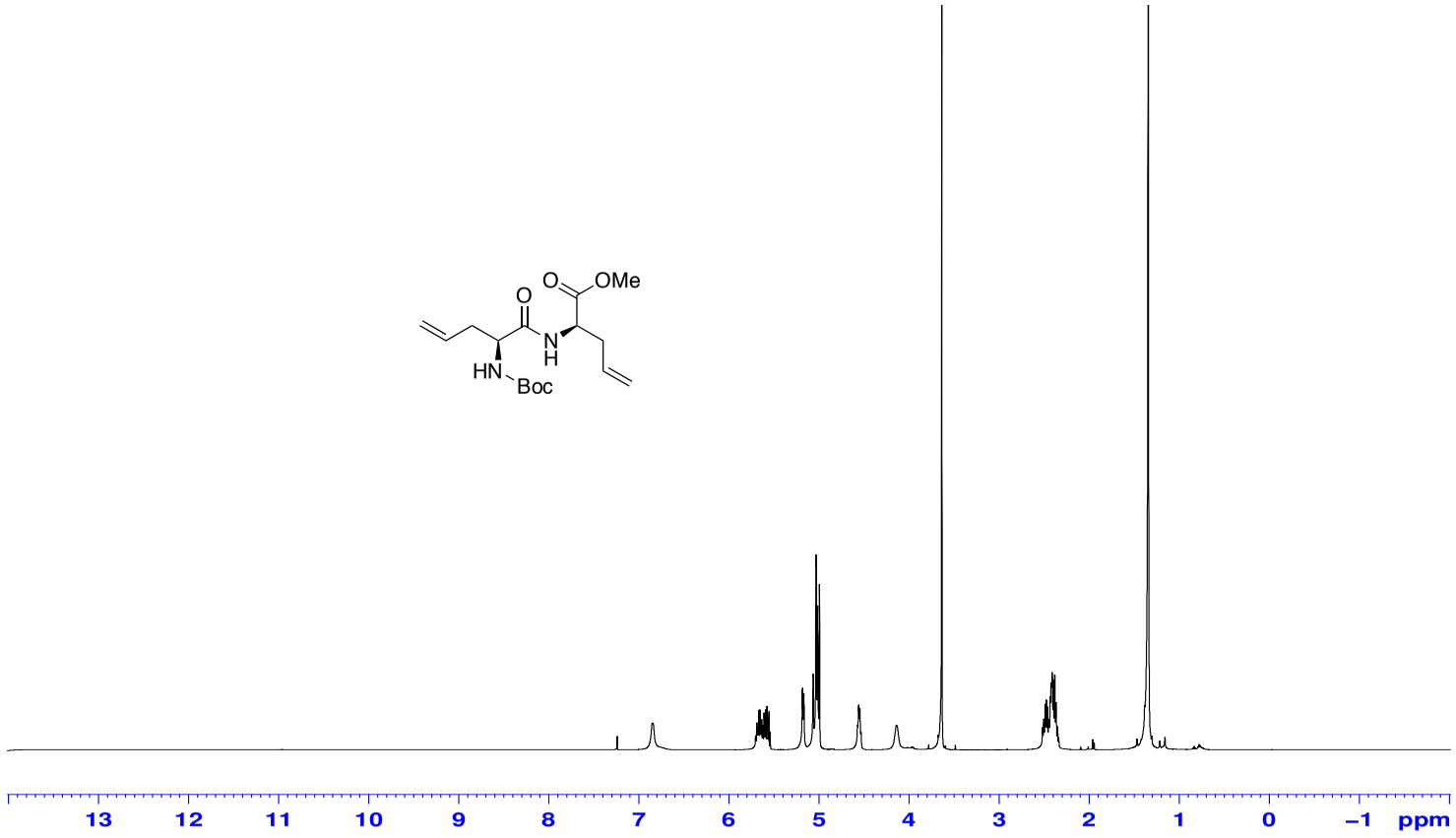

Figure 60: ^{1}H NMR ($CDCl_3$, 500 MHz) of **(+)-99**

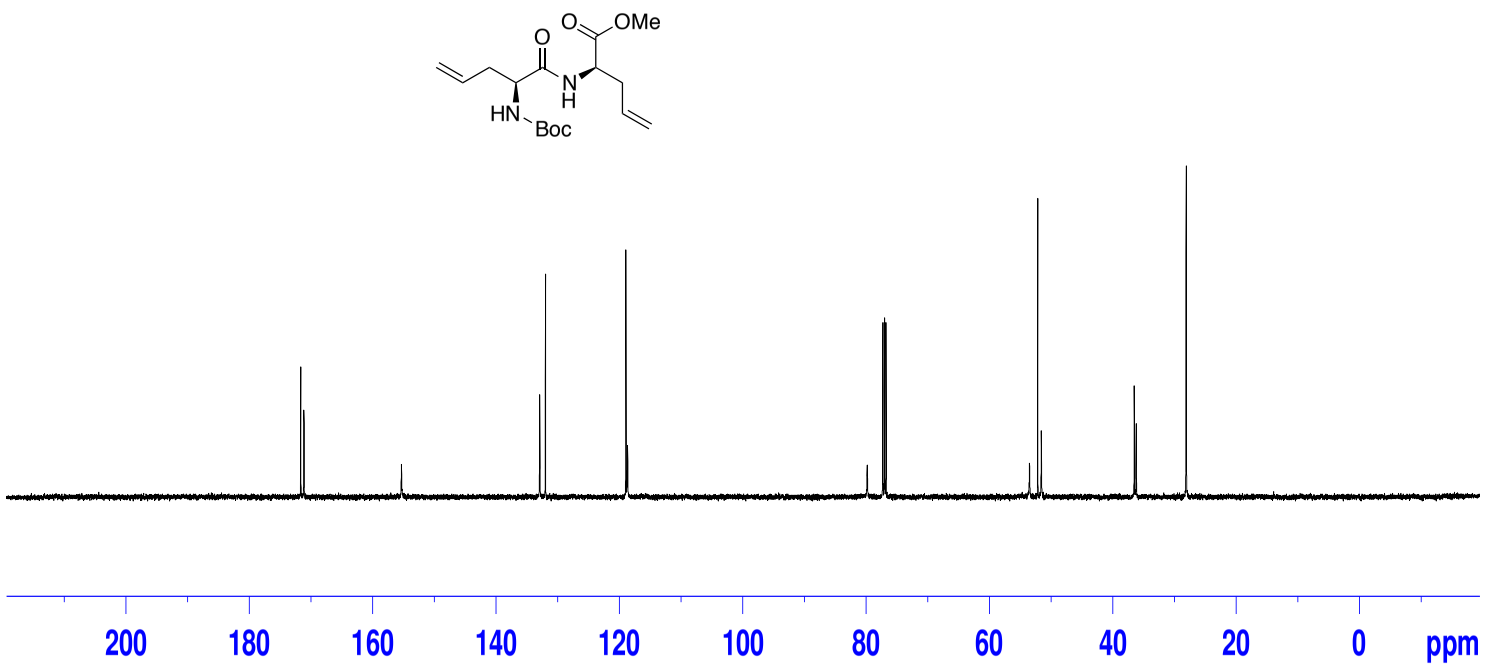

Figure 61: ^{13}C NMR ($CDCl_3$, 125 MHz) of **(+)-99**

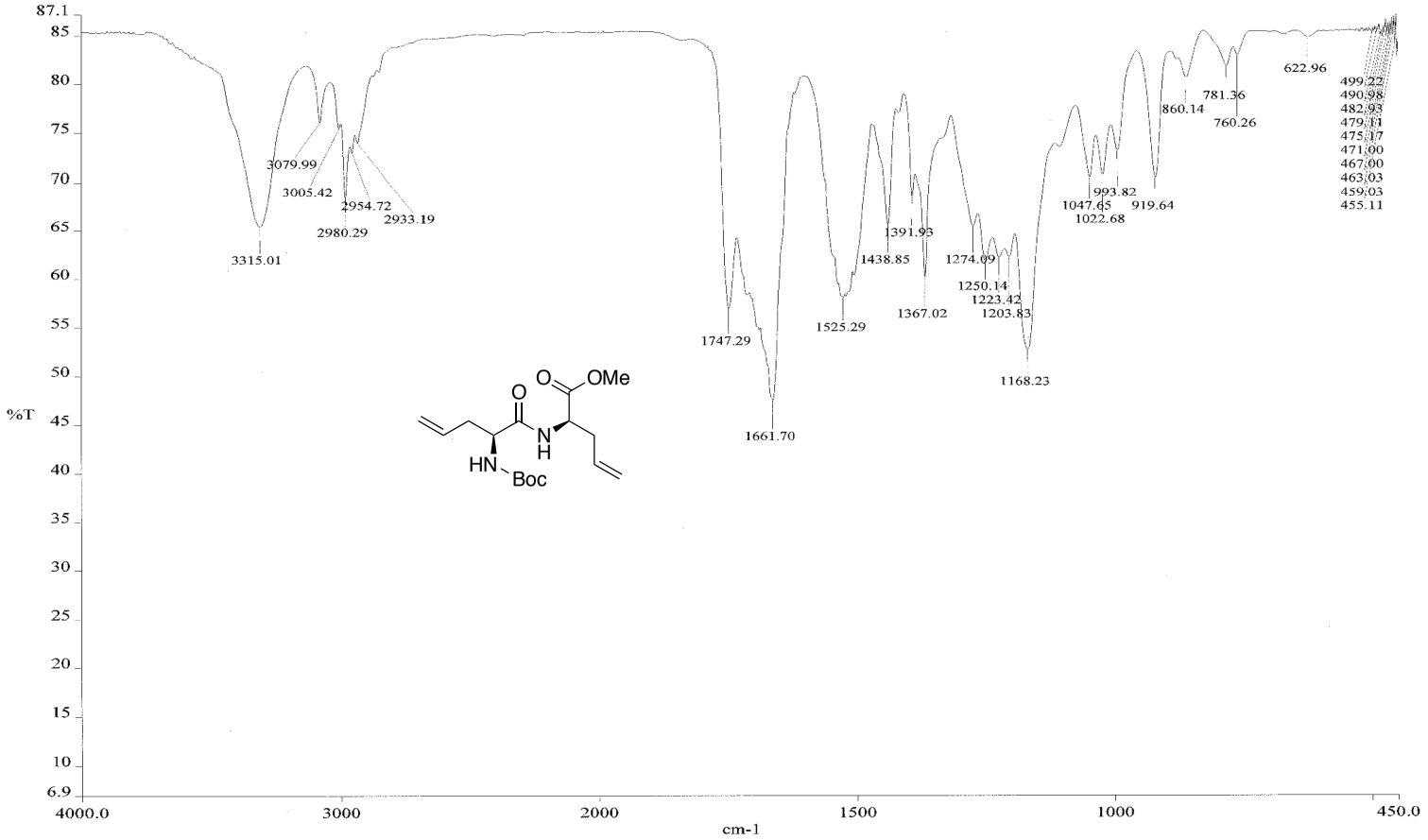

Figure 62: Infrared spectra (neat) of **(+)-99**

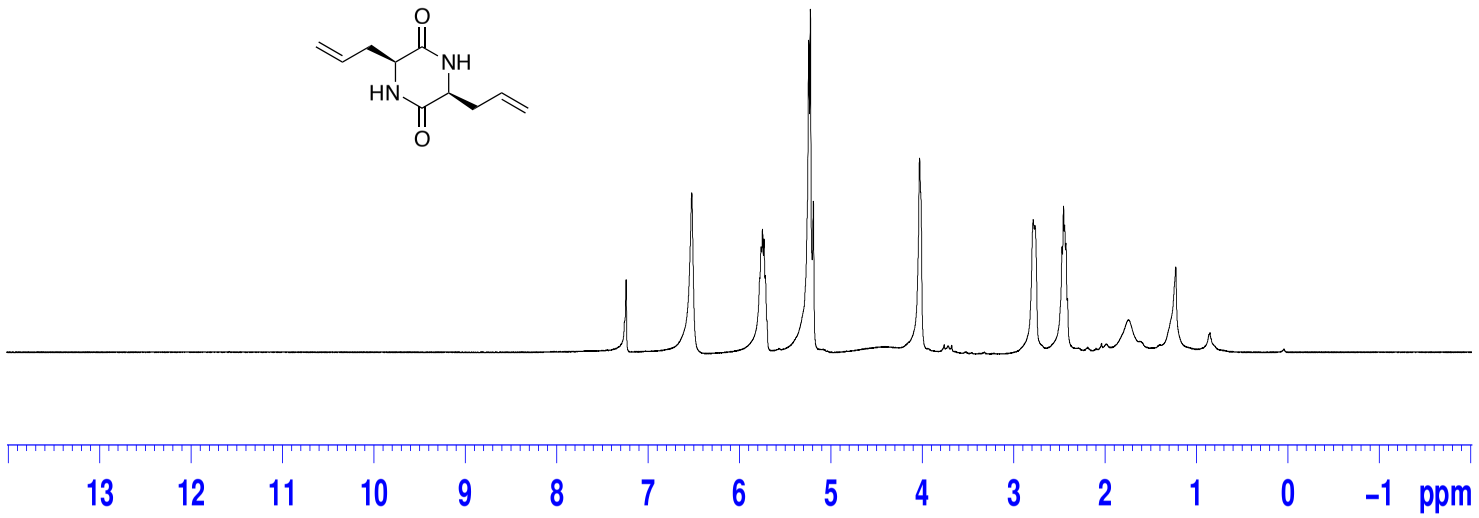

Figure 63: ^{1}H NMR ($CDCl_3$, 500 MHz) of **(−)-81**

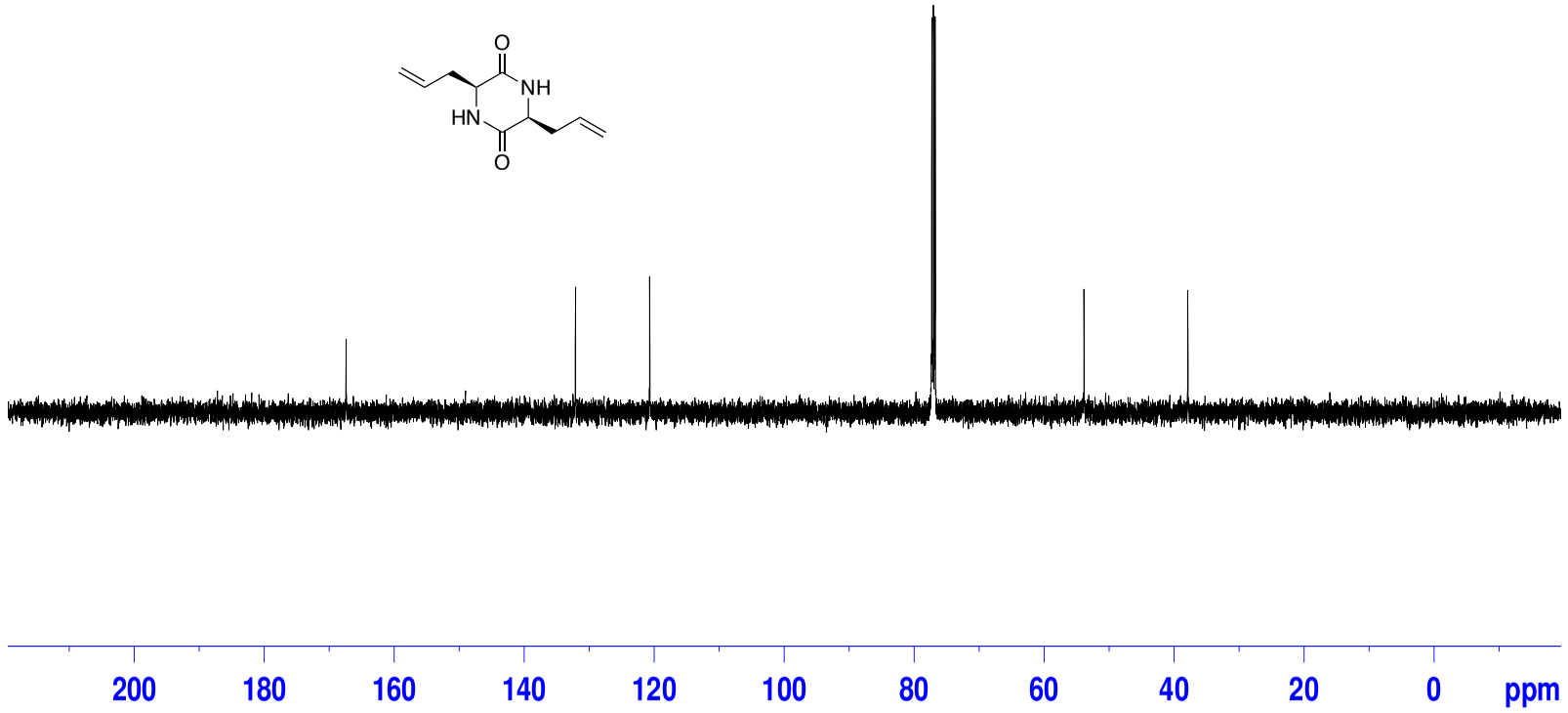

Figure 64: ^{13}C NMR ($CDCl_3$, 125 MHz) of **(−)-81**

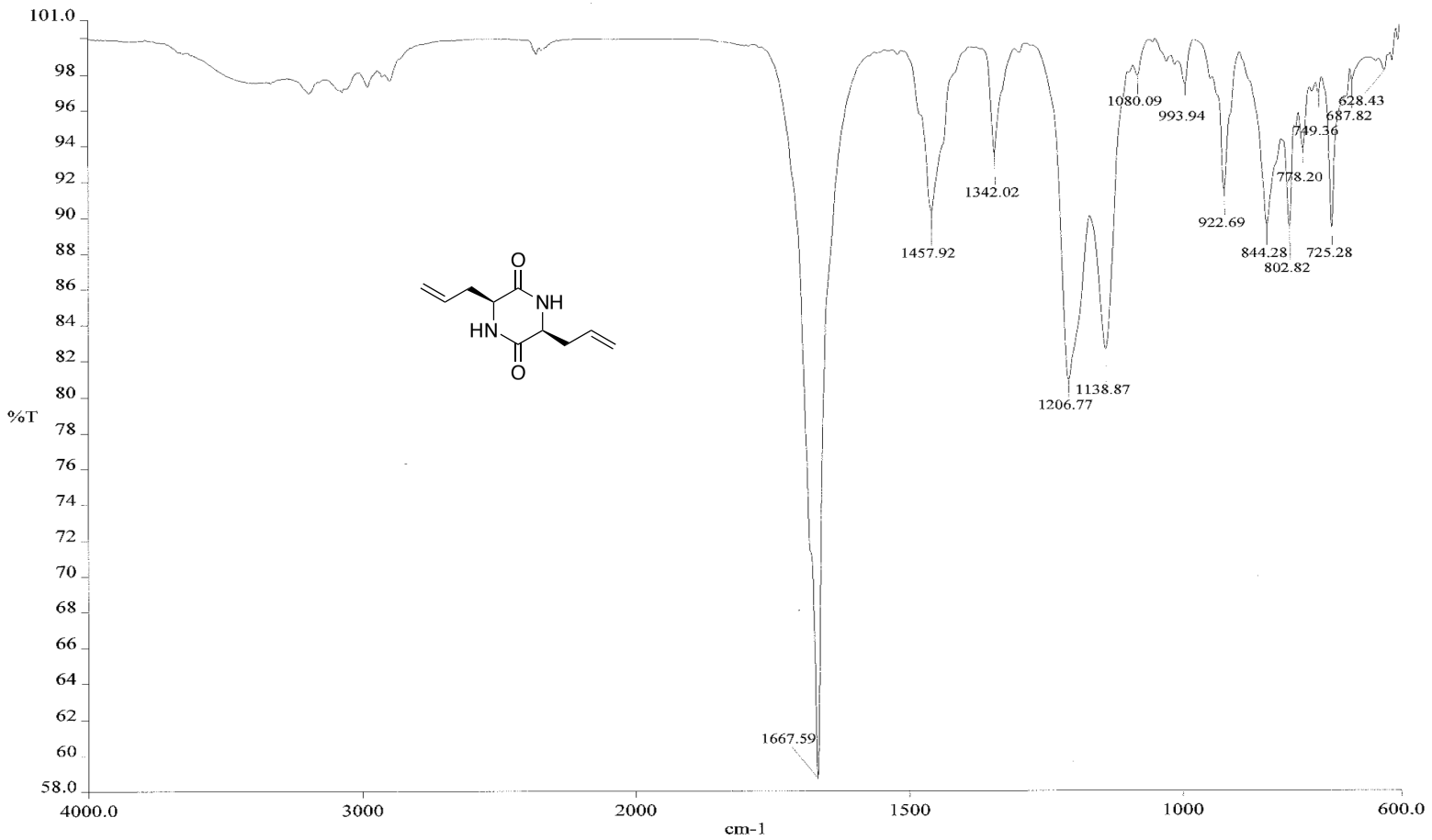

Figure 65: Infrared spectra (neat) of **(−)-81**

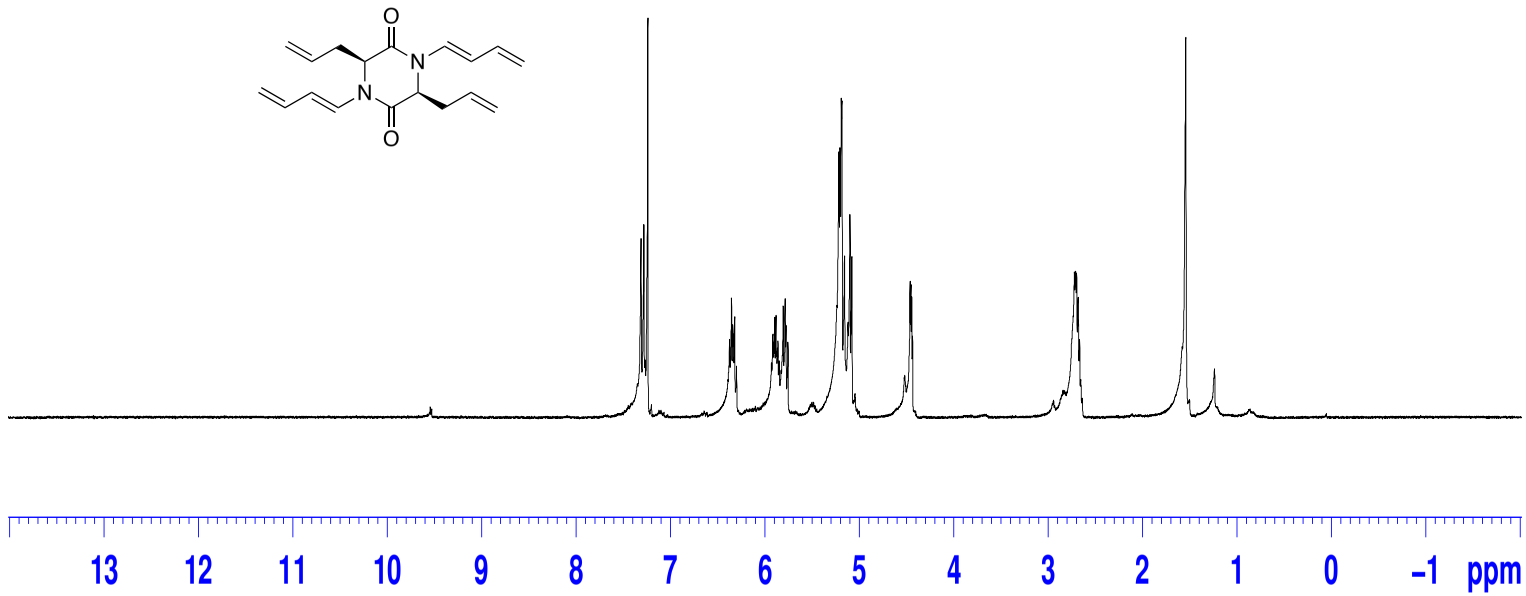

Figure 66: ^{1}H NMR ($CDCl_3$, 500 MHz) of **(+)-97**

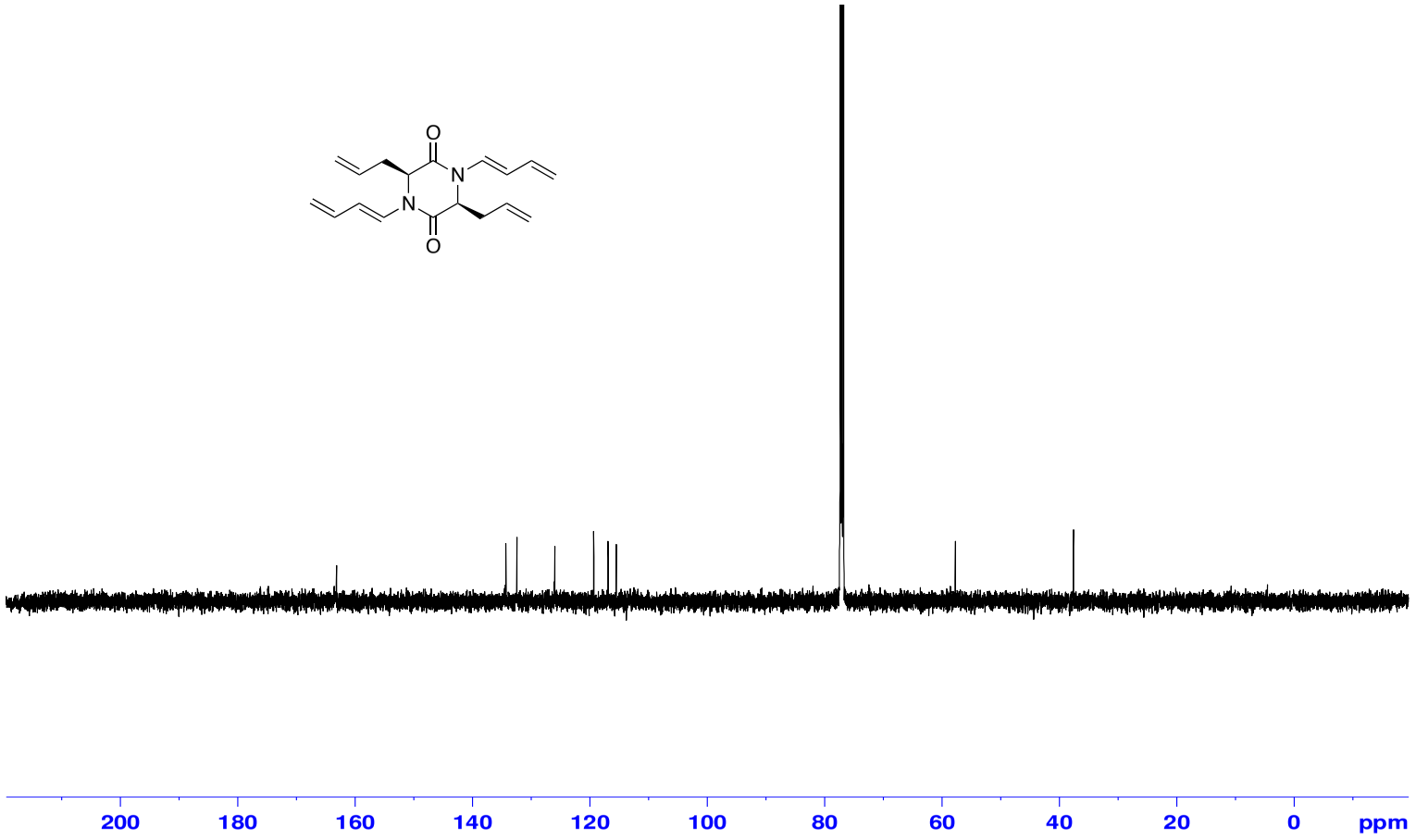

Figure 67: ^{13}C NMR ($CDCl_3$, 125 MHz) of **(+)-97**

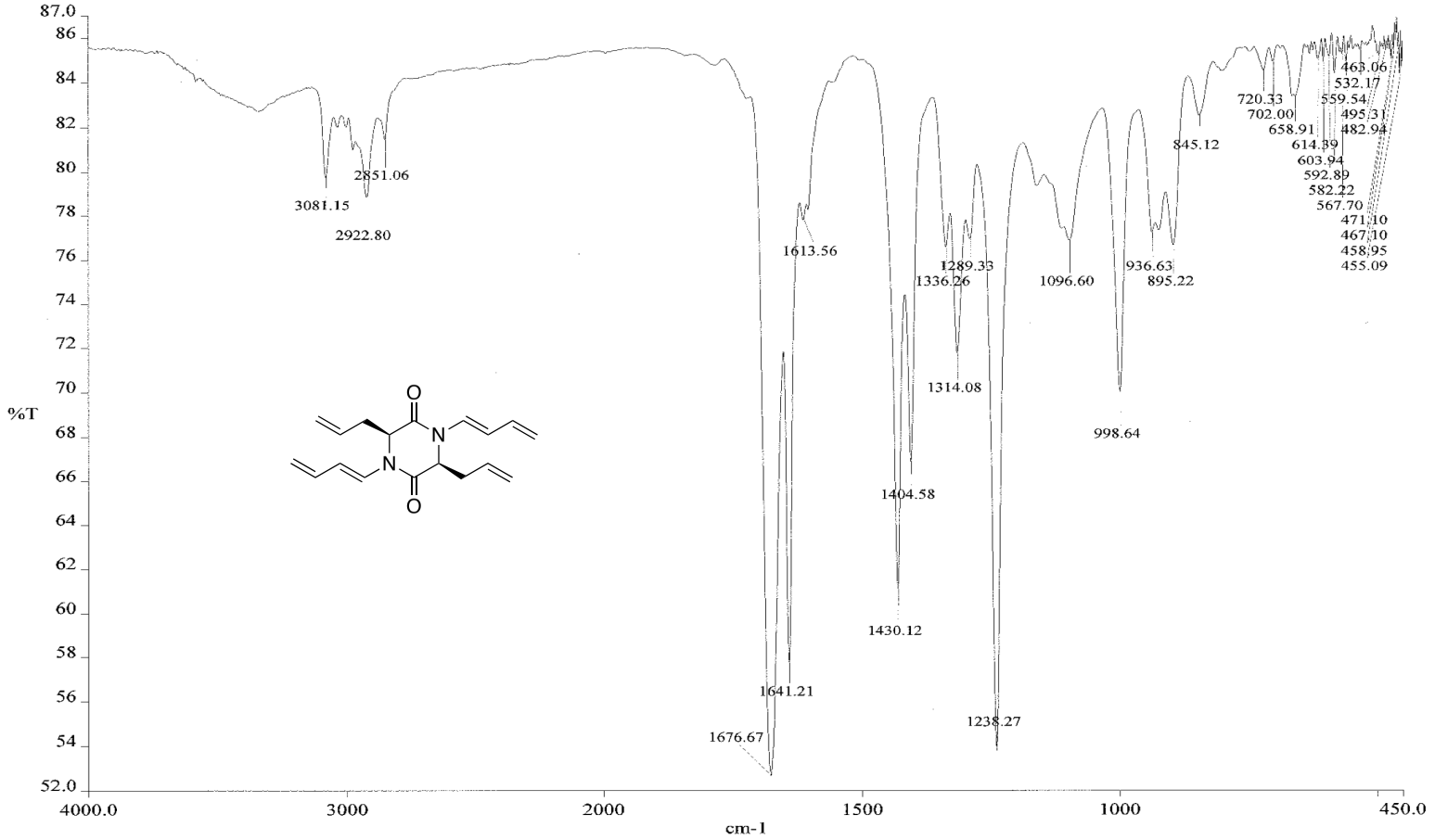

Figure 68: Infrared spectra (neat) of **(+)-97**

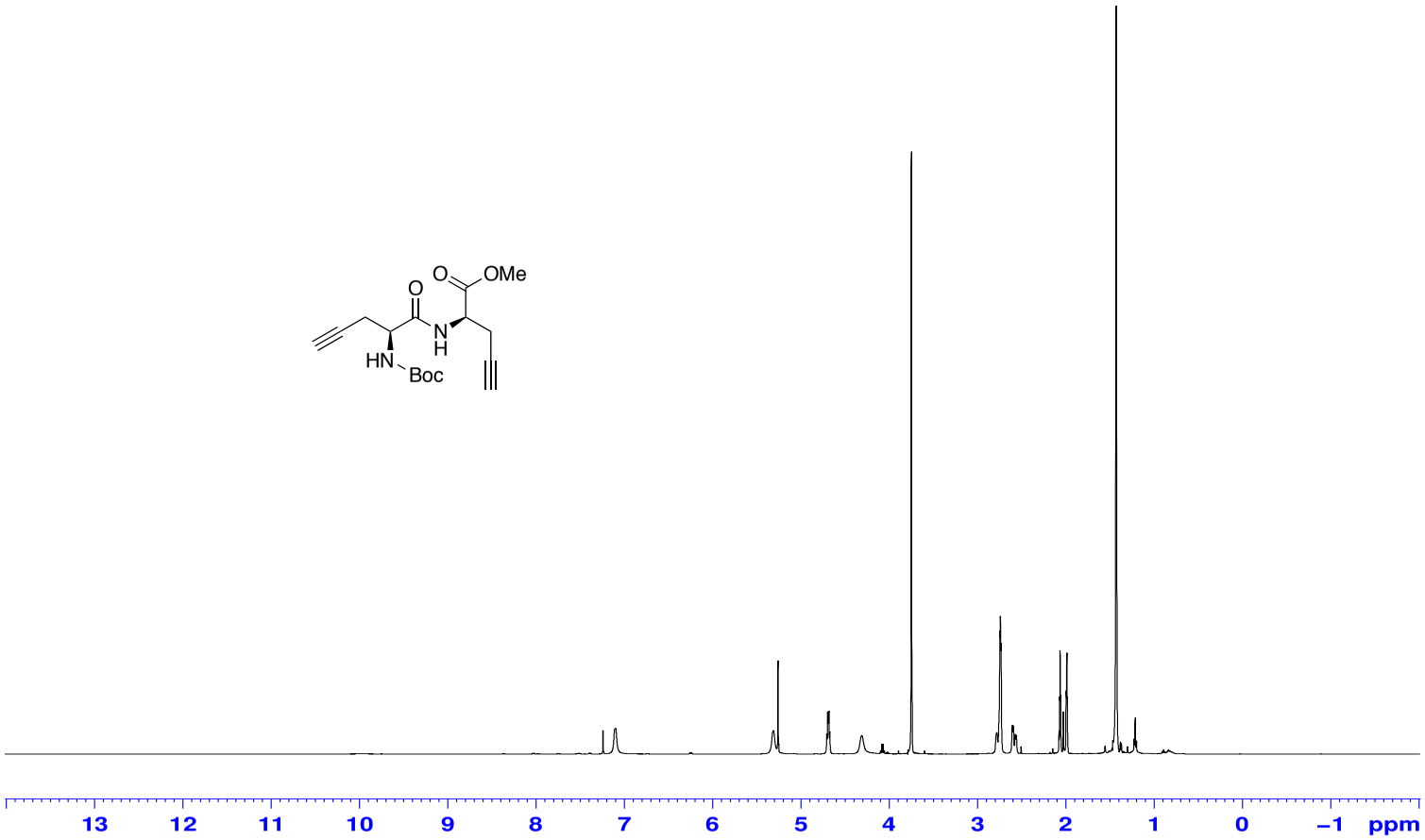

Figure 69: ^{1}H NMR ($CDCl_3$, 500 MHz) of **(+)-100**

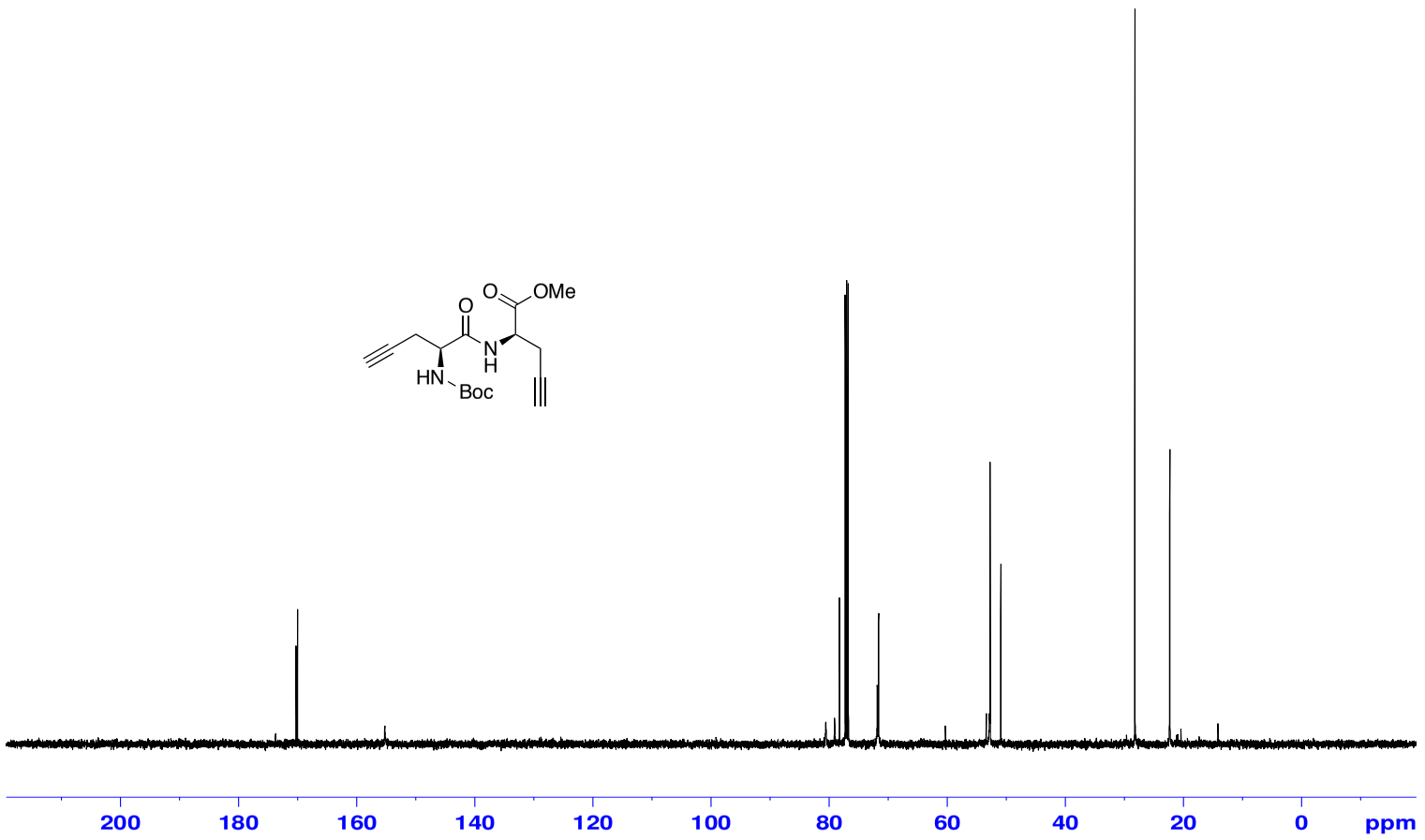

Figure 70: ^{13}C NMR ($CDCl_3$, 125 MHz) of **(+)-100**

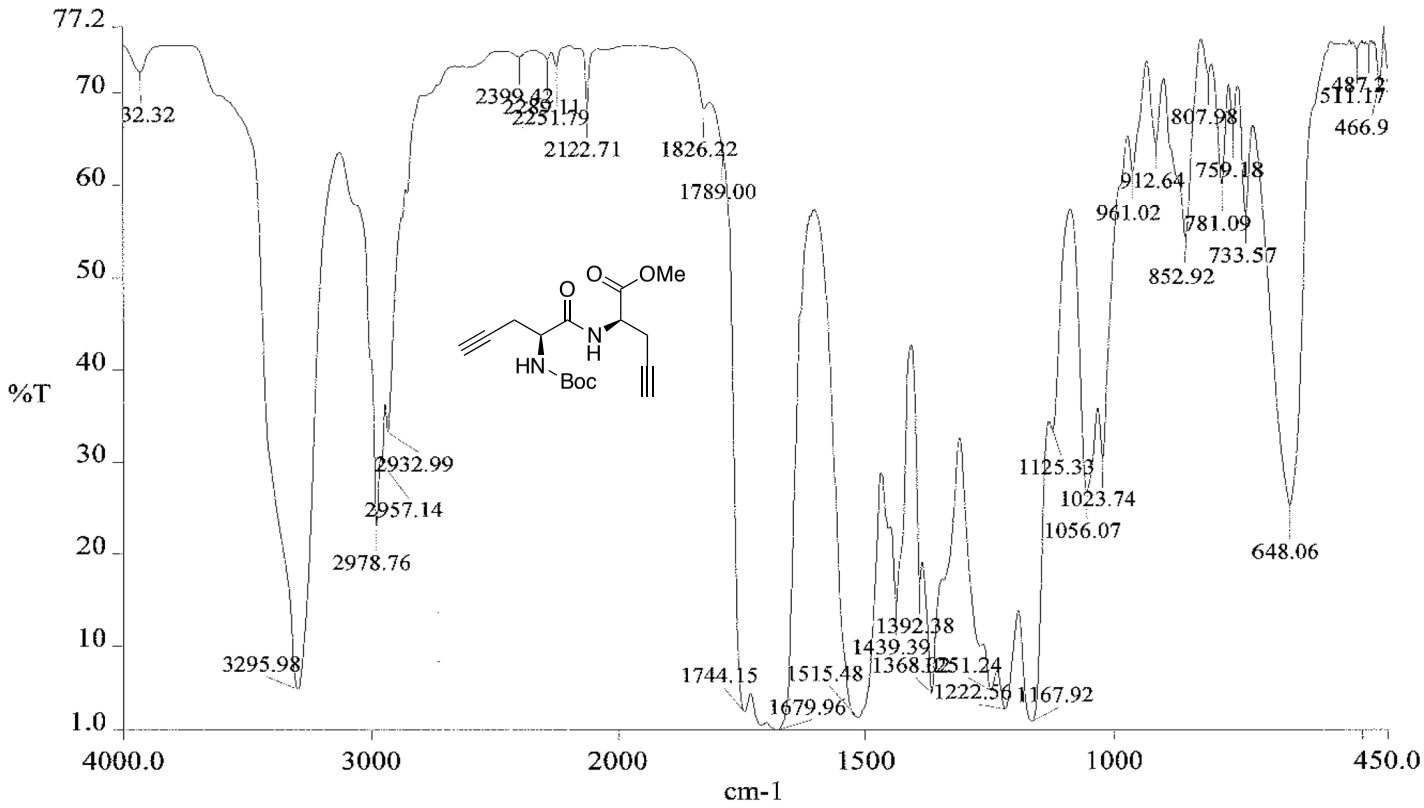

Figure 71: Infrared spectra (neat) of **(+)-100**

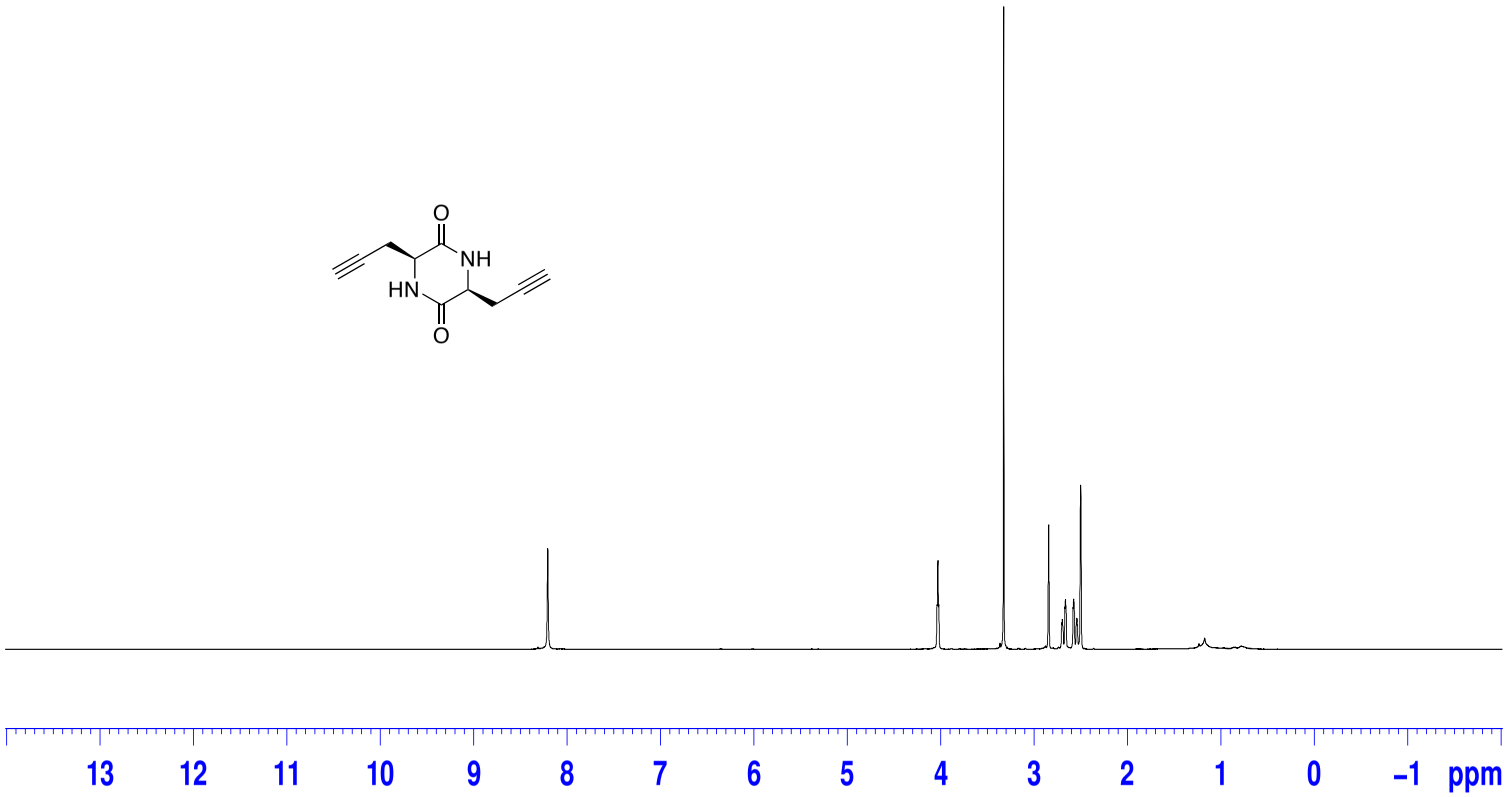

Figure 72: ^{1}H NMR (DMSO-d_6, 500 MHz) of **(−)-98**

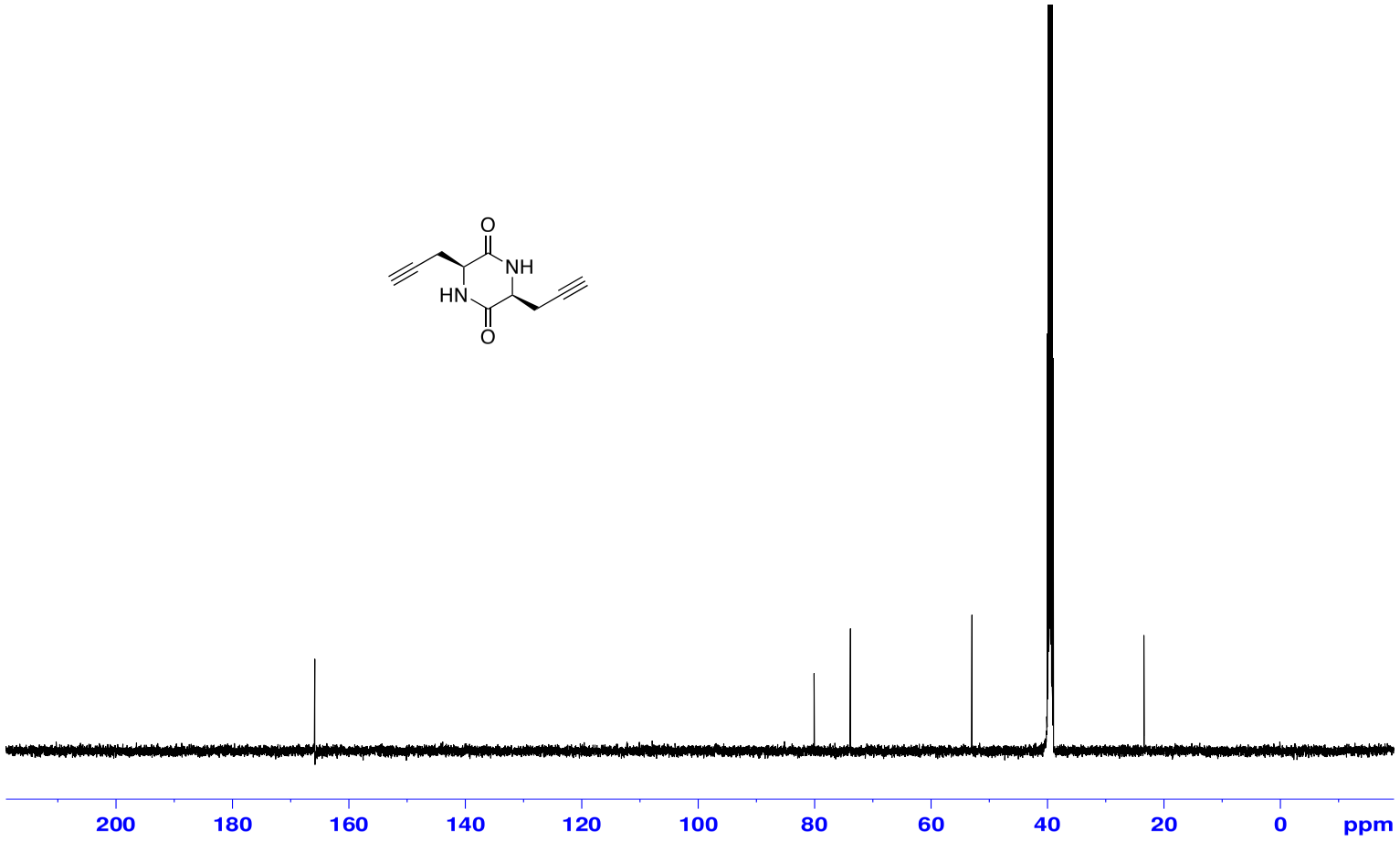

Figure 73: ^{13}C NMR (DMSO-d_6, 125 MHz) of **(−)-98**

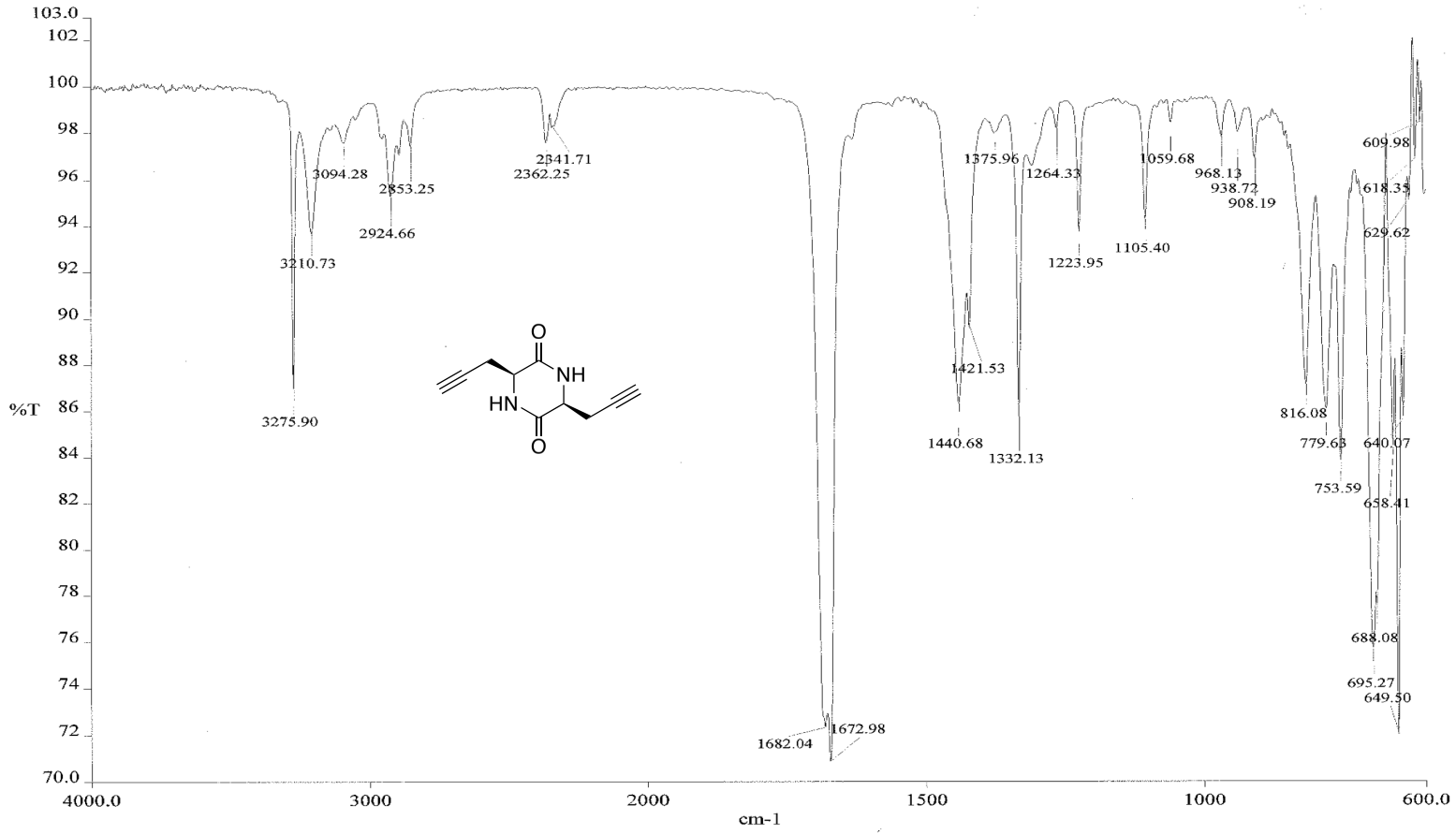

Figure 74: Infrared spectra (neat) of **(−)-98**

Chapter 5: Development of novel 1,2-indanedione fingerprint reagents

5.1) Significance and background of latent fingerprint detection

The central dogma of forensic science: "Every contact leaves a trace" was first introduced by Edmond Locard, a pioneer of forensic science (also regarded as the Sherlock Holmes of France), in what is known as the Locard's exchange principle.[1] Needless to say, fingerprint detection is a crucial area in forensic science. A variety of physical and chemical methods have been developed over the years for the visualization of latent (hidden) fingerprints.[2] Chemical techniques are amongst the most sensitive techniques available today, and can be applied on many surfaces, porous or non-porous and on a large variety of materials (paper, plastic, wood, etc.). Of considerable importance are chemical techniques applied for paper and related cellulosic materials, since our society relies heavily on such materials for official documents, currency printing, wrapping, packaging, etc. More specifically, these methods rely upon the detection of the amino acids present in natural skin secretions. When a fingerprint is deposited on paper substrates, the amino acids are believed to bind to the cellulose of the paper, which preserves an impression of the friction ridge patterns.[2] These impressions are classified into two main groups—visible and latent. Visible marks are remnants of colored contaminant on the skin (blood, oil, ink), which leaves a positive visible impression. Latent marks, on the other hand, are invisible friction ridge impressions that are the result of transfer of skin secretions and non-visible surface contaminants on the porous substrates. Of the two, latent fingerprints are the most common type of evidence

found at crime scenes, and the most problematic, because they require methods to develop fingerprints that can be visualized and recorded.

For the purpose of latent fingerprint detection, eccrine and sebaceous glands are the most important glands that are responsible for skin secretions within the dermis.[2] Eccrine (sweat) glands are found on the palms of the hands, consequently contributing as the major aqueous component of a latent fingerprint. The palms also contain sebaceous secretions as a contaminant due to interactions with the face and hair. Varying degrees of combination of eccrine and sebaceous glands are present in latent deposits depending on the individual (Table 5.1). Human sweat contains a wide range of amino acids, where the exact composition depends upon the individual and a variety of other factors including general health, diet, gender and age.[3] When transferred to the surface of a paper substrate, amino acids have a great affinity for cellulose and tend to be stable over a prolonged period of time (>20 years).[2]

Table 5.1. Summarized constituents of eccrine and sebaceous skin secretions.[2,3]

Secretion	**Constituents**	
	Organic	**Inorganic**
Eccrine	Amino acids	Water (>98%)
	Proteins	Chloride
	Urea	Metal ions (Na^+, K^+, Ca^{2+})
	Uric acid	Sulfate
	Lactic acid	Phosphate
	Sugars	Hydrogen carbonate
	Creatinine	Ammonia
	Choline	
Sebaceous	Glycerides	
	Fatty acids	
	Wax esters	
	Squalene	
	Sterol esters	
	Sterols	

Since the amino acid composition of a fingerprint could vary depending on the individual, non-specific amino acid sensitive reagents are often considered for fingerprint detection.

According to Bramble and Brennan, there are three key requirements that any successful fingerprint detection reagent should have: (1) a suitable medium for the reagent (2) a method of transport for the reagent onto the item of interest (spraying, dipping) (3) using suitable reaction conditions (without destroying the evidence).[4] Generally, amino acid sensitive reagents are dissolved in a carrier solvent with or without additives (acetic acid, metal salts). An ideal solvent is volatile (to readily dry the substrate), non-toxic, non-flammable, and non-polar in order to avoid dissolving inks on treated documents.[2] For these reasons, 1-methoxynonafluorobutane (HFE 7100) is usually the carrier solvent of choice, although depending on the reagent, combination of formulations could be used to allow dissolution of the reagent. Most known reagents often require heat to develop latent fingerprints. Depending on the reagent, the method of heating could be varied, such as using an oven, domestic iron, or laundry press.[2] Furthermore, in certain cases, humidity was found to improve the development of fingerprints.[2] Finally, the developed latent fingerprint is then examined and recorded for identification. The method of examining and recording the developed prints could vary depending on the characteristics of the reagent employed. For instance, photoluminescence could be measured by illuminating the developed fingerprint with a filtered light source (or laser) and visualizing through appropriate filters.[2] Although such visualization methods may allow detection of even weak prints, it is not favorable, due to utilization of highly specialized and expensive instrumentation that are not readily accessible.

5.2) Common amino acid sensitive reagents

5.2.1) Ninhydrin

Although ninhydrin was synthesized and discovered by Ruhemann in 1910,[5] it was not until the mid 1950s when it was applied as the first amino acid sensitive reagent for the detection of latent fingerprints.[6] Ruhemann observed a color change after ninhydrin came in contact with his skin, leaving a purple mark.[5] This purple compound was subsequently known as "Ruhemann's purple."[2] The accepted general mechanism for the reaction of ninhydrin and an amino acid was proposed by Friedman and Williams,[7] and was later confirmed by Grigg[8] using X-ray studies (Scheme 5.1). Condensation of the amine portion of the amino acid on the central carbonyl of ninhydrin affords Schiff's base **1**, which then undergoes decarboxylation (Strecker degradation) to yield resonance-stabilized 1,3-dipolar species **2** and **3**. Subsequent proton transfer followed by hydrolysis affords 2-amino intermediate **5**. Condensation with another molecule of ninhydrin then furnishes Ruhemann's purple.

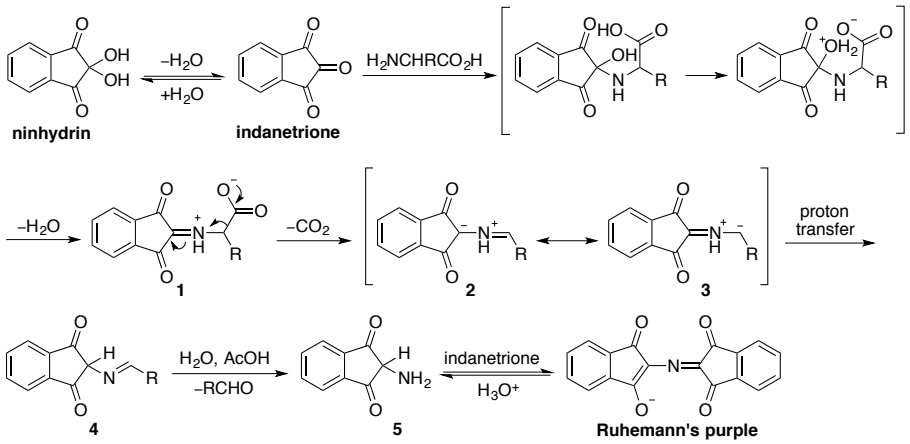

Scheme 5.1. Mechanism of Ruhemann's purple synthesis.

Ninhydrin can be applied to paper substrates by several different ways, but the most popular method is dipping the paper into a solution of ninhydrin. Upon exposure to

ninhydrin, heat and humidity are applied to accelerate the development process. Since prolonged exposure to light could fade ninhydrin developed prints, samples are usually allowed to develop in the dark at room temperature in order to obtain maximum sensitivity and minimal background staining.[9] The main limitation to this procedure is that full development of prints could often take weeks. In order to address this issue, initial efforts were made to alter the formulation of carrier solvent used to dissolve ninhydrin. However, unsatisfactory improvements were made by simple change of formulation methods, which ultimately ushered a wide variety of synthetic efforts towards generation of ninhydrin analogues.[9] Introduction of various substituents and extension of the conjugated system in such analogues showed for the first time that these modifications could produce an increase in molar extinction coefficients, resulting in more sensitive reagents and inducing shifts in the absorption maxima which resulted in change in the color of the Ruhemann's purple complex.[9,10] Alternatively, Ruhemann's purple prints could be complexed with various metal salts which could alter the color of the print. In 1982, Herod and Menzel observed that ninhydrin developed fingerprints changed color as well as became highly fluorescent (observed under an argon laser) when treated with zinc chloride solutions.[11] This was a pivotal discovery in the realm of fingerprint detection. Converting nonfluorescent ninhydrin developed prints into highly fluorescent prints allowed for improvement in contrast on a variety of backgrounds as well as heightened sensitivity (photoluminescence). Such post-treatment of Ruhemann's purple prints with metals has been widely used since then, especially in the detection of weak ninhydrin prints. It has been shown that zinc(II) and cadmium (II) salts complex with Ruhemann's purple to give luminescent products with slightly different properties

(Scheme 5.2). Soon thereafter, it was discovered that the intensity of the luminescence could be further improved if the prints are cooled in liquid nitrogen prior to observation.[12]

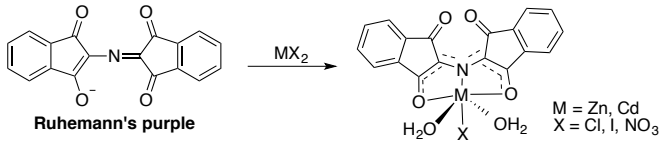

Scheme 5.2**.** Complexation of Ruhemann's purple with metals.

Although the use of fluorescence-based detection methods on ninhydrin/metal treated prints have been popular since its discovery, much attention was given to the synthesis of novel ninhydrin analogues, with the intention of obtaining highly colored Ruhemann's purple species that also exhibit fluorescence without secondary metal treatment, in order to simplify the visualization process. Of the various ninhydrin analogues that were synthesized, the most prominent analogues were 1,8-diazafluorene-9-one (DFO) and 1,2-indanedione, since they produced both color and intense luminescence upon reaction with amino acids in fingerprints without requiring further treatment.[2]

5.2.2) 1,8-Diazafluoren-9-one (DFO)

Although DFO was known since 1950,[13a] it was not until 1990[14] when Grigg and Pounds introduced DFO as an alternative amino acid detecting reagent. Although DFO is not a direct analogue of ninhydrin, it behaves similarly when reacting with amino acids (Scheme 5.3). DFO has only one central carbonyl moiety that is adjacent to two fused pyridine rings on each side that act similarly as neighboring dipoles of the 1,3-diketones in ninhydrin. Upon reaction with amino acids, it produces a red product, which is analogous to Ruhemann's purple.[9,14]

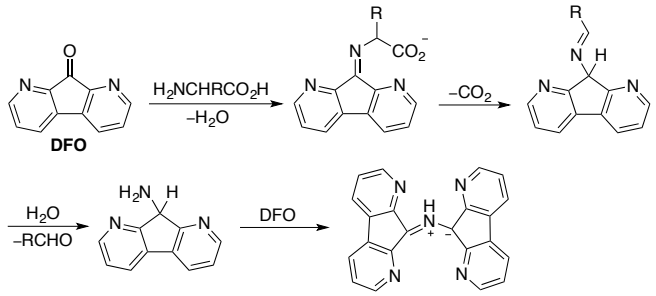

Scheme 5.3. Proposed reaction mechanism of DFO with an amino acid.

Unlike ninhydrin, DFO developed fingerprints were found to be highly fluorescent without secondary post-treatment with metal salts. Although the sensitivity was increased, there were practicality issues related with using DFO as a reagent. For instance, although commercially available, DFO is significantly more expensive than ninhydrin and requires the use of specialized light sources (prints viewed and photographed with a 520 nm (green) excitation filter and 590 nm (red) observation filter) for observation of fingerprints.[9] Furthermore, the development of DFO treated fingerprints requires carefully timed application of relatively high temperature (100-180 ^{o}C) and dry heat in order to avoid thermal decomposition.[2,9] In certain cases, DFO failed to develop all the prints and hence necessitated a secondary treatment with ninhydrin in order to maximize the number and quality of fingerprints. These shortcomings are believed to be the result of a slower reaction with amino acids when compared to ninhydrin. Moreover, efforts toward developing DFO analogues have not resulted in significant improvements.[9,14]

5.2.3) 1,2-Indanedione

In 1997, Joullié reported the ability of 1,2-indanedione to react with amino acids present in latent fingerprints.[15] The reaction results in a pale pink color with intense room-temperature luminescence comparable to that of DFO.[2,15] Extensive mechanistic studies were conducted[16,17] in order to elucidate the reaction pathway. In particular, the

involvement of 1,3-dipolar species of various geometries has been unequivocally confirmed through subsequent cycloaddition studies with *N*-methylmaleimide.[17] The proposed mechanism involves similar reaction pathway to that of DFO and ninhydrin that involves formation of imine intermediate followed by Strecker degradation to obtain 2-amino-1-indanone, which could then react further with another equivalent of 1,2-indanedione to produce a pink Ruhemann's purple analogue referred to as Joullié's pink (Scheme 5.4).[2,18]

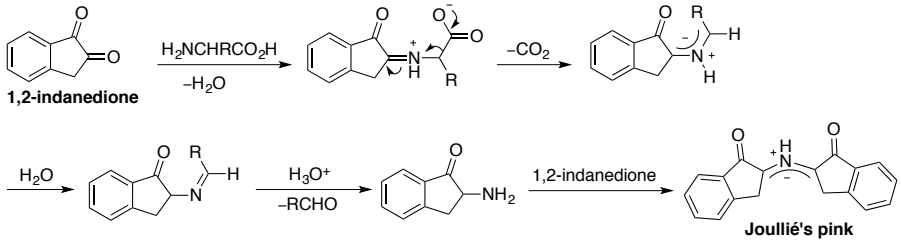

Scheme 5.4. Proposed reaction mechanism of 1,2-indanedione and an amino acid.

As was the case for ninhydrin, when 1,2-indanedione developed fingerprints were treated with zinc or cadmium chloride, the luminescence intensity of the corresponding product was increased, and the color of the product became a darker pink color, improving contrast.[15] Alternatively, zinc chloride could be added in the solution of 1,2-indanedione to provide similar results.[15a] However, inconsistencies in the formulation of 1,2-indanedione solutions across research labs in the world necessitated an optimized protocol that would be universally accepted.[2] It was found that depending on the formulation, varying results were obtained, suggesting usefulness or lack there of, of using 1,2-indanedione as an alternative to ninhydrin or DFO. Moreover, the observed discrepancy was suggested to be the result of differing climate of the research labs (it was believed that humidity plays a big role on development of fingerprints) and/or varying constituents of paper.[19] Formulations from early investigations used methanolic

solutions,[15] although later research recommended limiting the amount of methanol or other alcohols in 1,2-indanedione solutions due to resultant hemiketal formation that could interfere in the desired reaction with amino acids.[2,17,20] Furthermore, fingerprints developed using methanolic solutions often resulted in smudging of the image, thereby reducing the detail of the ridges.[21] Investigations on the effect of different carrier solvents (methanol, petroleum ether, HFE 7100, etc.) on the development of latent fingerprints strongly suggested the use of HFE 7100 over other solvents due to increased luminescence and lower health and safety risks.[2,19,20] In contrast, in some studies, petroleum ether based formulation was found to develop fingerprints that were darker in color and stronger in luminescence in comparison to HFE 7100 based formulation.[22] However, as suggested from the proposed mechanism of action (Scheme 5.4) use of acetic acid as an acidic additive to the formulation is less debated, and is rather well accepted to date to produce better results.[2] Furthermore, studies suggested the importance of relative humidity and moisture content of the paper substrate on the development of latent fingerprints, which may explain the observed results obtained from various countries with differing climatic conditions.[2,19] Although heating of 1,2-indanedione treated fingerprints is not necessary (24-48 h at room temperature for development), the reaction could be accelerated by heating with either an oven or dry heat/laundry press.[2,21] The most accepted conditions to obtain optimum development is to treat 1,2-indanedione developed fingerprints with laundry press at 160-165 ^{o}C for 10 seconds.[2]

In 2011, a study was conducted to elucidate the role of zinc(II) ions and cellulose substrates in the reaction of 1,2-indanedione and amino acids.[23] As was the case for

Ruhemann's purple, zinc(II) ions were initially thought to form a complex with Joullié's pink upon post treatment.[15] However, concentration studies of zinc chloride and its effect on development of fingerprints suggested that the primary role of zinc(II) ions in the 1,2-indanedione-amino acid reaction is that of a Lewis acid catalyst.[24] More specifically, a minor red shift in the absorption spectrum as well as decrease in luminescence and color intensity was observed at high concentrations of zinc chloride, which suggests the catalytic role of zinc chloride.[24] This hypothesis was formulated primarily through anecdotal observations of fingerprints developed using 1,2-indanedione-zinc chloride in various forensic laboratories and have not been confirmed in the literature.[23] Therefore, a careful investigation was conducted[23] in order to determine if the reaction of 1,2-indanedione with amino acids on cellulose proceeds *via* the same mechanism proposed earlier[17] which was done in solution. Three amino acids (L-alanine, L-phenylalanine, and L-leucine) were chosen for the study and were mixed with cellulose to produce amino acid-impregnated cellulose that would mimic the conditions observed on paper substrates.[23] A solution of 1,2-indanedione with or without catalytic amount of zinc chloride (1:2:0 or 10:10:1, or 10:20:1 molar ratios of amino acid-1,2-indanedione-zinc chloride was used) was added to the amino acid-impregnated cellulose and was mixed at room temperature in the dark for 1 h. The resulting reaction products were extracted and analyzed by mass spectrometry (ESI-MS), ^{13}C-MAS-NMR, and UV-Vis.[23] Of the three amino acids studied, the reaction between L-leucine and 1,2-indanedione/zinc(II) (10:10:1 ratio) resulted in the greatest reaction rate, which was implied from the low relative abundance of ions attributable to 1,2-indanedione and early stage reaction intermediates (the ESI-MS results were obtained *via* direct injection immediately

following extraction of reaction mixture from cellulose).[23] Furthermore, an increase in the relative abundance of the Joullié's pink ion was observed with the addition of zinc chloride dramatically improving the reaction rate.[23] The involvement of a new intermediate was subsequently proposed (Scheme 5.5).[23] Since the presence of the proposed intermediate was never detected in any of the reaction conditions that had zinc chloride as an additive, it was suggested that the addition of zinc(II) ions leads to the rapid conversion of the proposed intermediate to 2-amino-1-indanone.[23] From their results, they claimed that zinc chloride acts as a Lewis acid catalyst that stabilizes the 1,3-dipole intermediate during the hydrolytic conversion to 2-amino-1-indanone in low humidity environments.[23] Addition of stoichiometric amount of zinc chloride did not result in improved luminescence through complex formation, but decreased the rate of the reaction and overall yield of Joullié's pink instead.

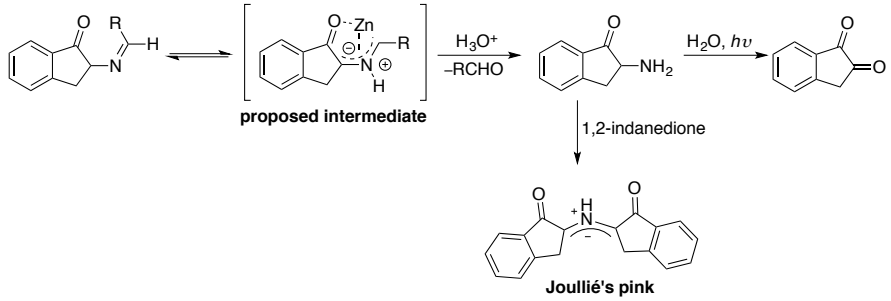

Scheme 5.5. Proposed reaction pathway to Joullié's pink from the imine intermediate.[23]

In order to further support the involvement of 2-amino-1-indanone moiety in the reaction pathway, 2-amino-1-indanone was synthesized using known methods and reacted with 1,2-indanedione in solution on cellulose at room temperature in a 160 ^{o}C oven. UV-Vis spectroscopy, fluorescence spectroscopy, and NMR spectroscopy (HSQC) confirmed the formation of Joullié's pink.[23] When 2-amino-1-indanone was added to cellulose and heated under the same conditions, an unexpected formation of Joullié's pink was

observed, indicating a possible secondary reaction pathway that occurs by slow deamination of 2-amino-1-indanone to form 1,2-indanedione under warm humid conditions (Scheme 5.5).[23] Taken together, these results support the generally accepted reaction mechanistic pathway of 1,2-indanedione and amino acids, and suggest a specific role of zinc chloride as a Lewis acid catalyst. Furthermore, the success of the 1,2-indanedione reaction is dependent upon the relative humidity of the laboratory environment, since decomposition of Joullié's pink was observed under excessive humidity (nearing saturation of the paper substrate). Prolonged heating at relatively high temperatures (70-100 ^{o}C) in low humidity conditions was also found to be detrimental in the development of fingerprints, as the only products that were formed were non-fluorescence oligomeric byproducts.[23] Finally, the role of cellulose was found to be similar to that of a surface catalyst, since it is believed to orient the intermediates in the optimum reaction geometry (through hydrogen bonding), and retain water molecules close to the reaction site to improve the reaction rate.[23] Trace metals present in the commercial paper stocks may also act as a Lewis acid catalyst in the same manner as zinc(II) ions. Although the presence of Joullié's pink was identified by mass, UV, and fluorescence,[23] full characterization still needs to be accomplished in order to validate various hypotheses that were proposed to date. For instance, the initial hypothesis of complexation of zinc with Joullié's pink[15] cannot be completely disregarded.

In terms of determining the overall performance of 1,2-indanedione as a fingerprint detection reagent in comparison to ninhydrin and DFO, there seems to be no clear answer. Using a sequence of combination of reagents has been popularized as well, and in certain

cases, performed better than using a single reagent.[2] A recent study conducted in Australia[25] evaluated two particular fingerprint detection sequences on porous surfaces: 1) 1,2-indanedione—$ZnCl_2$ followed by ninhydrin, physical developer (PD) and the lipid stain Nile red; and 2) DFO followed by ninhydrin, PD and Nile red. The obtained results indicated negligible difference in the performance between the two sequences across all paper types and all time periods evaluated. However, when considering individual reagents, 1,2-indanedione—$ZnCl_2$ developed better quality fingerprints than DFO.[25] In terms of enhancement, ninhydrin had a greater enhancement effect on DFO developed prints rather than 1,2-indanedione—$ZnCl_2$. Although the use of Nile red was proposed in the beginning of the trials, since Nile red did not develop any additional fingerprints at the end of each sequence, it was excluded in the sequences.[25] The optimum sequence that was suggested was the use of 1,2-indanedione—$ZnCl_2$ followed by ninhydrin and PD for development of fingerprints on Australian paperstock.[25]

5.3) Development of alternative fingerprint detecting methods

Although a wide variety of ninhydrin-like compounds have been developed since its discovery, considerable portions of latent fingerprints still escape detection. The main limitation of the existing methods is their stoichiometric nature: as long as the reaction assumes a stoichiometric pathway, there is an upper limit to the sensitivity. Furthermore, latent fingerprints often do not contain enough amino acids (or other relevant components such as lipids), so even the most sensitive reagents fail to produce a sufficiently meaningful mark through a direct chemical reaction with fingerprint components. Although much attention has been given to developing optimal formulation conditions,

success of developing latent fingerprints seems to depend heavily on environmental factors (relative humidity of the laboratory, paper stock of the country, sweat content of individual's fingerprint, etc.) that are difficult to control. Moreover, apart from ninhydrin, amino acid sensitive reagents that have been identified thus far[26] rely on luminescence in order to view latent fingerprints, significantly limiting general accessibility (Table 5.2).

Table 5.2. Conditions for observing photoluminescence of latent fingerprints using common amino acid sensitive reagents.[2]

Reagent	Excitation band	Viewing conditions
Ninhydrin—$ZnCl_2$	490 nm	Orange goggles
DFO	505 nm	Orange goggles
	530 nm	Red goggles
	555 nm	Red goggles
1,2-Indanedione—$ZnCl_2$	505 nm	Orange goggles

There are methods other than using amino acid sensitive chemical reagents in developing latent fingerprints. One notable method is the use of silver physical developer (Ag-PD), which is a process that utilizes metastable silver colloid that develops latent prints on wet, porous surfaces such as paper and cardboard.[27] The developer deposits a black silver precipitate along the fingerprint ridges by associating or reacting with the lipid material present in the fingerprint residue. In a typical formulation, a solution of ferrous and ferric ions, also containing citric acid and a detergent, is mixed with a solution of silver nitrate to generate a citrate-stabilized silver colloid through an electroless reaction in which the Fe^{2+} ions reduce the Ag^{+} ions *in situ*.[27] As already mentioned, Ag-PD could be used after ninhydrin or other amino acid sensitive reagent processing in order to amplify the obtained image or obtain more prints. Prints developed using Ag-PD appear as dark ridges on lighter/white background, creating enough contrast that allows visualization under visible light. Although the process negates the use of expensive, specialized light sources for visualization, it suffers from instability of the developing solution (shelf-life

of Ag-PD solution is limited and should be freshly prepared for best results) and poor reproducibility.

Multimetal deposition (MMD)[28] is a variation of the process, in which a latent fingerprint is enhanced by gold nanoparticles stabilized by citrate ions in aqueous medium, and then treated with Ag-PD. The gold nanoparticles adhere to the fingerprint residue and are believed to catalyze the precipitation of metallic silver from the Ag-PD solution.[28] The affinity of gold nanoparticles to the fingerprint residue is thought to be the result of an ionic interaction between the negatively charged gold colloids and the positively charged components of the fingerprint residue at low pH.[28] Advantages of using MMD is based on its sensitivity, specifically with aged fingerprints, and in the fact that it works on porous as well as non-porous surfaces. However, the main drawback of the process is that it is considered to be labor-intensive (involving several steps to obtain working solution, exposure of prints to six different solutions) and it only produces dark grey to black fingerprints, which could be problematic when dealing with dark and/or patterned surfaces. Therefore, a modification of the process known as single-metal deposition (SMD) was developed, where the enhancement of gold colloids by precipitation of silver was replaced by gold-based growth of the nanoparticles.[29] Efforts towards discovering improved fingerprint development techniques that are based on nanochemical processes are ongoing, and they all suggest the involvement of adherence of nanoparticles to fingerprint residues.[30]

Based on earlier reports by Vijayamohanan,[31] in which dodecanethiol stabilized gold nanoparticles were found to be adsorbed onto activated hydrophobic surfaces *via* hydrophobic interactions, Almog reported[32] that sebum-rich fingerprint deposits could serve as hydrophobic surface for such interactions with various alkanethiol stabilized gold nanoparticles. Ag-PD was used as a post-treatment process, in which the gold nanoparticles that have been adsorbed onto the fingerprint ridges catalyzes silver reduction from the Ag-PD solution, allowing the precipitation of Ag^0 on the ridges, significantly enhancing the developed fingerprints as a result.[32] Although the two step development process is similar to MMD, since the nanoparticles adsorb onto the fingerprint ridges *via* hydrophobic interactions rather than ionic interactions, the underlying mechanism is considered to be different. Moreover, the average size of the gold nanoparticles that were synthesized were of 2-3 nm, which is smaller than the gold nanoparticles often used in MMD process (~14 nm).[32] Best results were obtained using a 0.04% (w/v) solution of the alkanethiol stabilized gold nanoparticle solutions in petroleum ether. Of the three different lengths of the alkanethiol chain tested (10-, 14-, and 18-carbon chains), the longest chain, octadecanethiol, provided the best result, where the aggregation of gold nanoparticles occurred fastest and in greatest amount as observed by scanning electron microscopy (SEM).[32] However, all three chains resulted in positive latent fingerprint detection after post treatment with Ag-PD. The obtained results using paper substrates translated well onto non-porous surfaces (silicon wafers). To test the generality of using metallic nanoparticles, petroleum ether solution of CdSe/ZnS nanoparticles (~3 nm size) stabilized by octadecaneamine were synthesized.[32] Although successful development of fingerprints were obtained for non-porous, silicon wafer

substrates, the process did not work for paper substrates. Interestingly, post treatment with Ag-PD was unnecessary as the CdSe/ZnS treated fingerprints were fluorescent, and consequently visible under UV illumination using optical microscopy.[32]

In 2010, with the intension of extending his previous findings, Almog reported the synthesis of various thiohemiketals of ninhydrin and 1,2-indanedione as potential fingerprint developing reagents.[18] The premise of the study was to use the known reaction of ninhydrin and 1,2-indanedione with amino acids that would furnish the corresponding colored Ruhemann's purple or Joullié's pink, and by having thioether linkages on the compounds, the overall reaction would expel the corresponding thiol alkyl chain that would then presumably stay on the fingerprint ridges and react with gold nanoparticles, further enhancing the contrast.[18] With regards to the synthesis of thiohemiketals, formation of thioketals were not observed in the case of ninhydrin even in the presence of excess thiol. However, in the case of 1,2-indanedione, formation of only thioketals was observed under the same conditions. Several thiohemiketal analogues of ninhydrin were synthesized and reported, however, none of the presumably synthesized thioketal of 1,2-indanedione was reported or characterized.[18] A possible reason for this discrepancy may be due to the fact that the thioketal version of 1,2-indanedione presumably did not react with amino acids or latent fingerprints on paper.[18] Nonetheless, the thiohemiketal analogues of ninhydrin did react with alanine (stereochemistry not specified) to produce Ruhemann's purple (noticed visually), and the presence of thiols in the reaction mixture was detected by GCMS (Scheme 5.6).

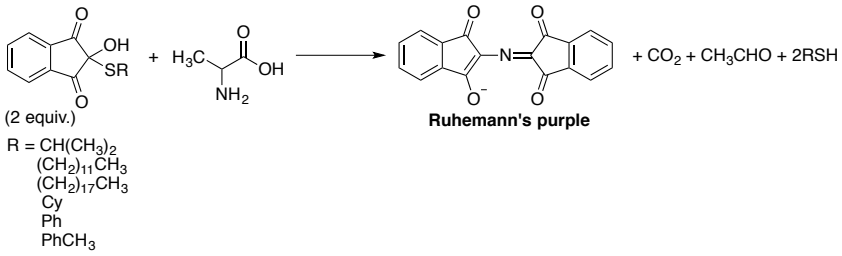

Scheme 5.6. Reaction of thiohemiketals of ninhydrin and alanine.

Amongst the analogues, there was an apparent difference in the rate of the reaction (monitored visibly). For instance, analogues containing longer alkyl chains reacted slowly in comparison to shorter chains. Furthermore, the thiohemiketal analogues of ninhydrin developed latent fingerprints on paper that was comparable to that of ninhydrin.[18] The use of ketals of ninhydrin in the reaction with amino acids is not entirely unprecedented, since another group reported the reaction of hemiketals of ninhydrin with amino acids to form Ruhemann's purple and two equivalents of alcohol per amino acid as early as 1991.[33] Nonetheless, since the proposed hypothesis of using the thiohemiketal analogues of ninhydrin in conjugation with gold nanoparticles was not tested, the viability of this approach remains uncertain.

Shortly thereafter, Almog reported yet another approach[34] to develop latent fingerprints on paper using a similar protocol, but with a different reagent. A bifunctional reagent was devised, in which it is composed of an active polar head (acyl pyridazine) that has high affinity to cellulose (main ingredient of paper), and a long alkyl chain tail containing a sulfur group at the terminal end that could stabilize gold nanoparticles (Scheme 5.7).

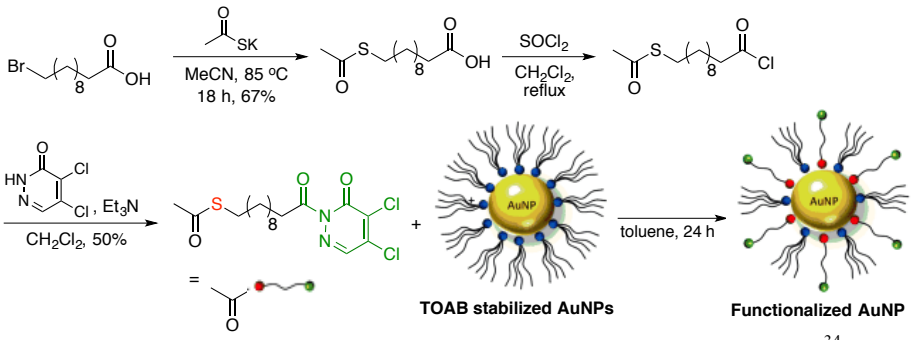

Scheme 5.7. Almog's synthesis of functionalized gold nanoparticles.[34]

Since the head portion of the molecule that has a long alkylthiol chain adheres preferentially to the paper rather than to the sebaceous fingerprint material, further treatment with Ag-PD would darken the paper, leaving the fingerprint ridges uncolored, resulting in a white on black fingerprint image. This so-called "negative image" was hypothesized to be superior in comparison to conventional methods, since the current approach is based on interactions with cellulose rather than the sebaceous fingerprint, which could be varied depending on the sweat content of the individual (Figure 5.1). Although their previous work with octadecanethiol stabilized gold nanoparticles[32] produced good quality fingerprints using conventional methods (gold nanoparticle exposure followed by Ag-PD, targeting sebaceous fingerprints, thereby producing black on white image), they claim that their process lacked consistency due to variability in fingerprint residue composition.[34] The desired fingerprint image was obtained rather quickly using the new process, where the image was obtained after 5 min of treatment with the gold nanoparticles followed by 40-60 s with Ag-PD. Prolonged exposure to Ag-PD solution resulted in darkening of the entire paper, where the silver eventually precipitated on the fingerprint ridges as well. Since the method is based on sebaceous fingerprints (lipid containing hydrophobic prints), eccrine fingerprints (amino acid containing prints) did not work under the same reaction conditions.

Figure 5.1. Comparison between conventional fingerprint image (left) and "negative" image (right) obtained by Almog *et al*.[34]

In an attempt to provide an explanation of the particular interaction that could be occurring with acyl pyridazine moiety of the reagent and cellulose of the paper, two particular classes of gold nanoparticle ligands were synthesized. The first class had functional end groups that are known to form hydrogen bonds (glucose, acetylthioalkoxy benzaldehydes, etc.), while the second class had polar end groups that cannot hydrogen bond (tetrachlorobenzene). Each compound was functionalized with gold nanoparticles and was tested for visualization of sebaceous fingerprints on paper using the same methodology. The authors found that negative fingerprint images were obtained by the first class (ligands with hydrogen bonding motifs), while conventional, positive fingerprint images were obtained by the second class (non-hydrogen bonding motifs). None of the aforementioned obtained images or any of the gold nanoparticle derivatives (other than their main acyl pyridazine reagent) were characterized or referenced in the article.[34] Nonetheless, the fingerprint image that was obtained using their bifunctional ligand containing an acyl pyridazine moiety suggested successful application of this protocol.

More recently, Almog reported another example of negative development of latent fingerprints using a slightly different set of reagents.[35] The method utilized commercially available mercaptocarboxylic acids as ligands to gold nanoparticles rather than the

previously mentioned acyl pyridazine containing ligand. There are apparent advantages in using commercially available mercaptocarboxylic acids—namely the fact that they are commercially available, thus not requiring synthesis and purification to obtain the ligand. Furthermore, the solvent mixture (CH_3CN/DMSO) utilized for the formulation of their previous ligand[34] was an undesirable system for document examinations, since it dissolved ink.[35] Since most mercaptocarboxylic acids that were examined are soluble in water, such problem was not encountered (Figure 5.2). Mercaptocarboxylic acids retain the desired bifunctional behavior of the ligand, since the carboxylic acid serves as the active head that hydrogen bonds to cellulose, and the thiol serves as the active tail that binds to gold nanoparticles, resulting in negative fingerprint images. Although seemingly unconventional, there is precedent[36] in using a variety of mercatocarboxylic acids as ligands to gold nanoparticles.

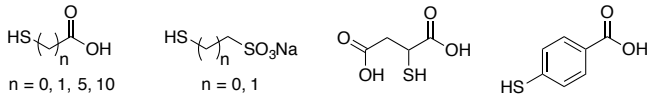

Figure 5.2. Mercaptocarboxylic acids and salts examined by Almog.[35]

All the gold nanoparticle functionalized mercaptocarboxylic ligands were dissolved in water (in the case of 10-carbon chain mercaptocarboxylic ligand, minimal amount of THF was used for dissolution and was further diluted with water to obtain 5% v/v THF in water) for the formulation. Apart from functionalized gold nanoparticles of 5-carbon and 10-carbon chain mercaptocarboxylic ligands, the desired negative fingerprint image was obtained after post treatment with Ag-PD. Best results were obtained using 3-mercaptopropionic acid as the ligand, since fresh and 14 month old latent sebaceous fingerprints were developed with good contrast and resolution. However, gold nanoparticles capped with 6-mercaptohexanoic acid (5-carbon chain ligand) failed to

develop fingerprints, as the entire paper was stained without any distinction. Interestingly, gold nanoparticles capped with 11-mercaptoundecanoic acid produced a positive fingerprint image, in which the gold nanoparticles was preferentially bound to the sebaceous ridges of the fingerprint rather than to the cellulose, which was in line with their previous studies.[32] Although there was no explanation provided for the failure of 6-mercaptohexanoic acid as a ligand for fingerprint development, the obtained results suggested that the appearance of the fingerprint as positive or negative could be tuned *via* the length of ligand on gold nanoparticles.[35]

5.4) Design and synthesis of novel 1,2-indanedione reagents

5.4.1) Proposed methodology and design of novel bifunctional reagent

As discussed in previous sections, the use of amino acid detecting reagents alone for the development of latent fingerprints on paper is not advantageous due to their stoichiometric nature. Since amino acids and the sweat content on a given fingerprint varies drastically depending on the individual and the climate, this prevents even the most sensitive reagents from producing sufficiently meaningful mark through direct chemical reaction. As long as the reaction assumes a stoichiometric pathway, where an equivalent of the reagent (i.e. ninhydrin) reacts with an equivalent of the substrate (amino acid), there is an upper limit to the sensitivity. Furthermore, other factors such as relative humidity of the laboratory in which the development is conducted, formulation conditions, accessibility to specialized equipment (light sources such as lasers) could

affect the outcome. Therefore, utilization of nanotechnology, such as the MMD process, for the development of latent fingerprints could be a promising alternative.

In this context, development of a new highly sensitive, non-stoichiometric gold nanoparticle-based technology following the basic principle of MMD was envisioned. In particular, employing bifunctional reagents similar to that of Almog's[34,35] where one end of the reagent would react with the fingerprint ridges, while the other end would react with gold nanoparticles were envisaged. Since these novel reagents would act as ligands on the gold nanoparticles, in theory, each gold nanoparticle could have many of these ligands appended on them, where the opposite end would seek out amino acids of the fingerprint, thereby increasing the sensitivity *via* catalytic amplification. The resulting ternary complex could then catalyze silver deposition from the Ag-PD, generating a high-contrast fingermark that could be visualized without the use of specialized light source.

In terms of the bifunctional reagent design, based on the well-known use of 1,2-indanedione and our particular familiarity of the reagent, 1,2-indanedione was selected as the "head" portion of the bifunctional reagent. The "tail" portion would be a long alkylthiol chain that is connected to the aromatic ring of 1,2-indanedione. Taken together, the 1,2-indanedione portion would react with amino acids of the fingerprint, and long alkylthiol chain would act as stabilizing ligands on gold nanoparticles (Figure 5.3). Unlike previously mentioned bifunctional reagents that could only target either amino acids or hydrophobic lipids, this reagent could in theory react with both amino acids

(eccrine) as well as lipids (sebaceous) of the fingerprint, increasing the likelihood of latent fingerprint detection on paper substrates.

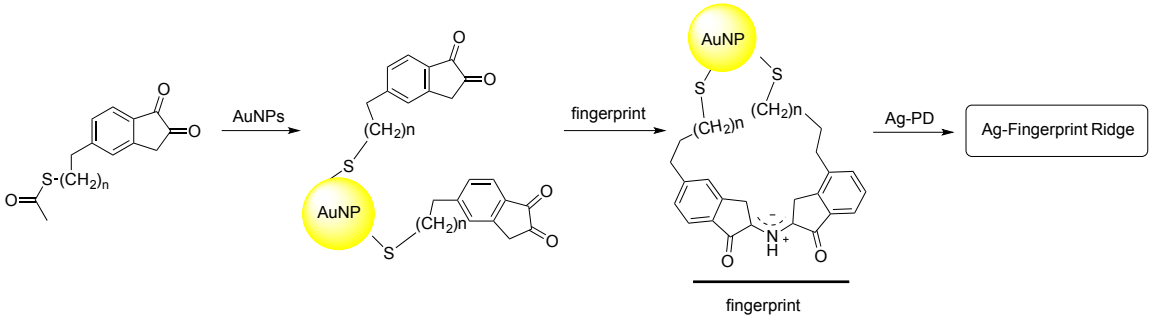

Figure 5.3. General schematic for proposed development of latent fingerprints.

5.4.2) First-generation synthesis

A general route for synthesizing 1,2-indanedione derivatives was developed using commercially available 5-hydroxyindanone as the starting material (Scheme 5.8). Side chain attachment followed by removal of TBS group afforded the corresponding alchols **6** and **7**, which was subsequently transformed into the thioester **8** and **9** by Mitsunobu reaction. Oxime formation using previously developed methods[15,17] followed by conversion to the corresponding ketone[15,17] furnished the functionalized 1,2-indanedione derivative **14**. Although generation of three particular derivatives with varying side chain lengths (n = 10, 12, 14) was envisioned using this methodology, unexpected problems were encountered during the last two steps of the synthesis, thereby limiting the overall efficiency of the synthetic sequence.

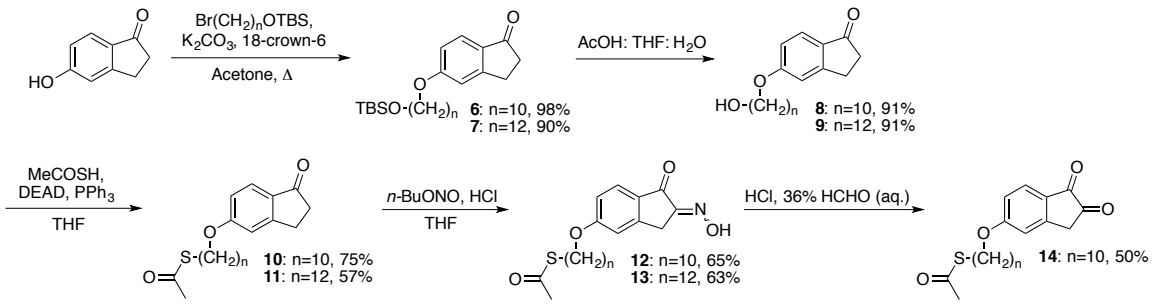

Scheme 5.8. First generation synthesis of 1,2-indanedione analogues.

In particular, for the oxime formation step, various solvents were screened (CH_2Cl_2, THF, EtOH, EtOH:CH_2Cl_2), and the best result was obtained using THF. In terms of the reagent, comparable results were obtained using isopentyl nitrite instead of *n*-butyl nitrite. The main side reactions that were in competition with the desired transformation were the cleavage of the C-O bond in the molecule and removal of the thioacetate group. These unfavorable processes could be attributed to the presence of protic acid (HCl) in the reaction. Similar problems were encountered in the final step of the synthetic sequence, since HCl in aqueous conditions was used. Furthermore, the final product was found to be unstable on silica gel during the duration of the column chromatography, which did not allow effective separation of the desired product from the side products. Other reactions using different set of reagents were explored in hopes of avoiding the use of protic acids. In particular, oxidative deoximating reactions[37] were investigated using Dess-Martin periodinane (DMP), MnO_2, and dichloramine-T.[38] Oxidation by MnO_2 proved to be sluggish and did not result in full conversion of the starting material. As for DMP and dichloramine-T, although the desired product was detected in the reaction mixture (verified by ^{1}H NMR, ^{13}C NMR, and LRMS), the pure product was unable to be isolated *via* silica gel chromatography (due to instability) from the side products of the oxidation. As an alternative, resin bound pyridinium dichromate [poly(vinylpyridinium dichromate)] was synthesized[39] and tested, but the reaction failed to reach full conversion even after prolonged period of time (1 week). Other deoximation methods, such as deoximation by hydrolysis with copper chloride[40] only resulted in side chain cleaved material.

Interestingly, when the present protocol was applied to a derivative bearing a polyethylene glycol (PEG) side chain (Scheme 5.9), side chain cleavage was not observed for the last two steps of the synthesis. This could be attributed to hydrogen bonding interactions in solution that may orient the PEG chain in a manner to protect the C-O bond linkage. Based on previous synthesis, minor changes were made in the synthetic sequence to ensure good yields. For instance, the Mitsunobu step was not utilized due to inconsistency in yield amongst the analogues (Scheme 5.8). Instead, alcohol **16** was converted to the tosylate, which was then substituted by thioacetate to afford **17** (Scheme 5.9). Use of TMSCl in place of HCl for the oxime formation step furnished the desired oxime **18** in excellent yield. Subsequent deoximation under the same conditions used in prior synthesis afforded the desired 1,2-indanedione analogue **19** in good yield. Silica gel column chromatography was not required for the last two steps, since a simple aqueous work-up allowed the isolation of pure material. Although side chain cleaved side product was not observed, minor presence of acetate removed thiol 1,2-indanedione product was observed by NMR and LCMS. However, removal of the acetate group was not a major concern, since such process takes place in the following step (functionalizing gold nanoparticles with 1,2-indanedione analogue as ligand) *in situ*.

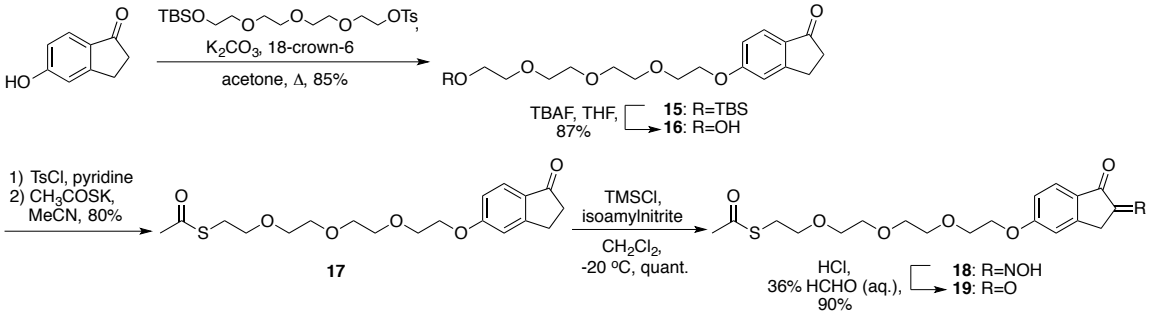

Scheme 5.9. Synthesis of 1,2-indanedione PEG analogue.

Although the 1,2-indanedione PEG side chain analogue afforded synthetically good results, an improved protocol for attaching alkyl side chains was desired. The PEG side chain could display enhanced solubility in water or other polar solvents, while as long alkyl side chains could display the opposite solubility, which would ultimately allow the investigation of various formulations for development of latent fingerprints.

5.4.3) Second-generation synthesis

Variation in the bond linkage between the phenyl ring of 1,2-indanedione and the side chain was deemed necessary, in order to circumvent the undesirable side reactions that were occurring under aqueous protic acid conditions in the last step of the synthesis. An alternative solution to the problem was devised, in which a C-C bond linkage was substituted for the problematic C-O bond. The well-known Suzuki-Miyaura reaction was employed to form the desired C-C bond between the sp^2 carbon of the aromatic ring and the sp^3 carbon of the alkyl chain using a known protocol.[41] In particular, commercially available 5-bromo-1-indanone was coupled with a 10-carbon chain potassium alkyltrifluoroborate using slightly modified version of the palladium catalyst (Scheme 5.10). The requisite side chain was synthesized following the synthetic sequence used by Dreher and Molander.[41] The use of Buchwald's 1st generation preformed palladium catalyst (RuPhosPd(II)phenethylamine)[42] was of particular interest due to ease of operation. Aryl bromide was used instead of aryl chloride, since aryl bromides are generally considered to be more reactive as an electrophile in comparison to aryl chlorides. The desired coupled product **20** was obtained in comparable yields using the modified version of the protocol.[41]

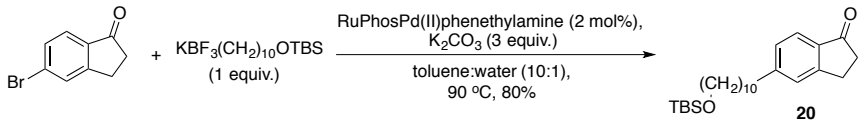

Scheme 5.10. Suzuki-Miyaura coupling of 5-bromo-1-indanone and alkyltrifluoroborate.

Since 5-bromo-1-indanone was more expensive than the chloro- derivative at the time, quick optimization of the reaction was conducted (Table 5.3). Although the original protocol was proved to be general[41] in terms of the nature of the electrophile (Br, Cl, I, OTf), a clear difference between the aryl bromide and the chloride was observed in the present case, especially when the 1st generation RuPhos precatalyst was used (Entries 1 & 2, Table 5.3). The aryl chloride was unable to react even under higher preformed catalyst loadings (Entry 3, Table 5.3). Interestingly, when palladium acetate was used instead, the reaction was able to proceed with the aryl chloride as the substrate. Minor differences were observed amongst the different types of phosphine catalyst, although SPhos gave the best yield (Entries 4,6,7, Table 5.3). Increasing the amount of palladium acetate did not improve the yield (Entry 5, Table 5.3). The 2nd generation SPhos precatalyst[43] afforded comparable results, suggesting the improved reactivity in comparison to the 1st generation preformed catalyst (Entry 8, Table 5.3).

Table 5.3. Optimization of cross-coupling reaction.

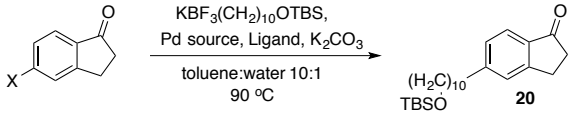

Entry	X	Pd source	Ligand (mol%)	Yield[b]
1	Br	1st generation RuPhos precatalyst (2 mol%)	-	80%
2	Cl	1st generation RuPhos precatalyst (2 mol%)	-	No reaction
3	Cl	1st generation RuPhos precatalyst (10 mol%)	-	No reaction
4	Cl	$Pd(OAc)_2$ (2 mol%)	RuPhos (4 mol%)	62%
5	Cl	$Pd(OAc)_2$ (4 mol%)	RuPhos (8 mol%)	49%
6	Cl	$Pd(OAc)_2$ (2 mol%)	SPhos (4 mol%)	70%
7	Cl	$Pd(OAc)_2$ (2 mol%)	XPhos (4 mol%)	49%
8	Cl	2nd generation SPhos precatalyst[c] (2 mol%)	-	57%

[a] Reaction conditions: 1 equiv. electrophile, 1 equiv. trifluoroborate, 3 equiv. K_2CO_3, at 0.25 M concentration.
[b] Isolated yield.
[c] Chloro(2-dicyclohexylphosphino-2′,6′-dimethoxy-1,1′-biphenyl)[2-(2′-amino-1,1′-biphenyl)]palladium(II).

With the optimized condition in hand, synthesis of potassium alkyltrifluoroborate side chains of varying lengths was commenced. Based on the PEG side chain analogue synthesis (Scheme 5.9), appending a tosylate moiety at the opposite end of the alkyl trifluoroborate chain was desired in order to achieve synthetic efficiency. Accordingly, following the general procedure,[41] various alkyl side chains were synthesized in good yields (Scheme 5.11). Apart from 12- and 14-carbon chain starting materials, commercially available alcohols were used as starting materials. Tosylation of the alcohol followed by iridium-mediated borylation afforded the corresponding pinacol boronate esters in good yields. Conversion of the boronate esters to the corresponding potassium trifluoroborates resulted in acceptable yields of the final side chain products.

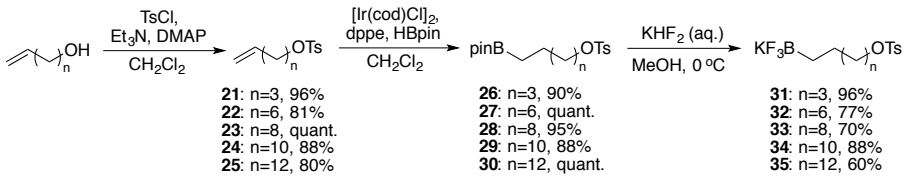

Scheme 5.11. Synthesis of potassium trifluoroborate alkyl side chains.

With the requisite alkyl side chains, the synthesis of 1,2-indanedione analogues was conducted following the general synthetic sequence (Scheme 5.12). Slight variability in terms of yield was observed for the cross-coupling reaction, which may be attributed to the various side chain lengths. In general, longer side chains afforded modest yields in comparison to shorter ones. Subsequent displacement of the tosylate with potassium thioacetate generated analogues **41**-**45** in good yields. Formation of the oxime followed by conversion to the desired 1,2-indanedione occurred in near quantitative yields without the need of performing silica gel column chromatography purifications. Similar to

previous syntheses (Scheme 5.9), removal of thioacetate group was observed as a minor side product in the last step.

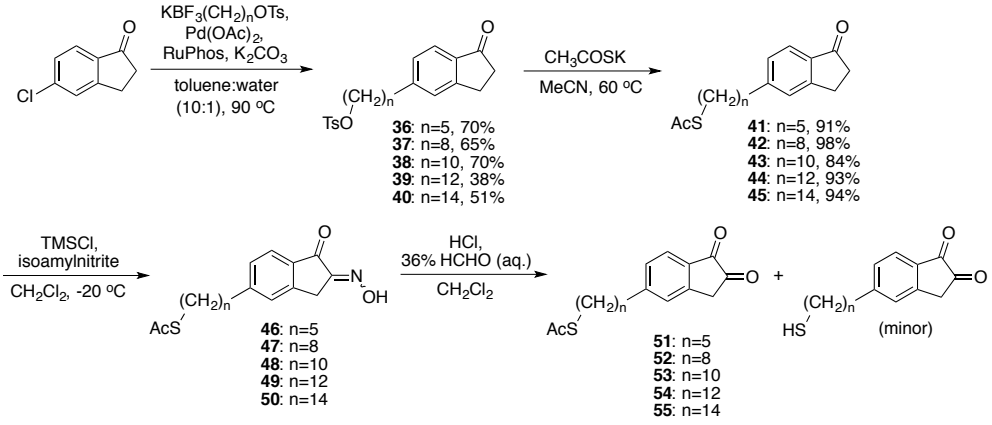

Scheme 5.12. Second generation synthesis of 1,2-indanedione analogues.

The second-generation synthesis was proved to be more synthetically efficient in comparison to the first-generation synthesis not only in terms of number of steps (5 steps *vs.* 4 steps), but also in terms of overall yield. Furthermore, by changing the linkage between the aromatic ring of the 1,2-indanedione and the side chain, the undesired side reactions were not observed, allowing ease of isolation of the desired material by simple aqueous work-up conditions rather than column chromatography purification.

5.5) Progress towards developing latent fingerprints using 1,2-indanedione analogues

In order to assess the ability of the newly generated 1,2-indanedione analogues to detect amino acids, a spot test was performed. The spot test consisted of using a strip of Whatman filter paper that has been impregnated with drops of a weak solution of L-leucine (0.2% w/v in a mixture of 3:7 dioxane/water), which was air-dried. The paper substrate was then dipped into solutions containing either ninhydrin (0.05% w/v solution of ninhydrin in petroleum ether with a drop of AcOH), 1,2-indanedione (0.05% w/v

solution of 1,2-indandione in petroleum ether with a drop of AcOH and catalytic amount of $ZnCl_2$), or the 10-carbon chain analogue **53** (0.05% w/v solution of **53** in petroleum ether with a drop of AcOH and catalytic amount of $ZnCl_2$). The treated paper strip was then air-dried and heated using a steam iron until the spots were visible (1 min). As expected, the ninhydrin treated substrates displayed the characteristic purple colored spots where L-leucine was present (Figure 5.4b). 1,2-Indanedione treated substrates displayed light orange to pink colored spots in comparison. However, paper substrates treated with **53** initially showed almost no visible color development (Figure 5.4a). The spots were made visible only after subsequent post treatment with ninhydrin (Figure 5.4b). Such practices are well-documented in the literature,[2] where weakly developed fingerprints are augmented by post treatment with ninhydrin. Likewise, when 1,2-indanedione treated substrate was post treated with ninhydrin, the color of the spots changed to a darker hue (Figure 5.4b). In all cases, the observed contrast for the developed spots increased over time when the samples were place in an environment away from light (Figure 5.4c).

Figure 5.4. Spot test results; **a)** Initial treatment with **53** (left), post treatment with ninhydrin (right) **b)** Ninhydrin (left), 1,2-indanedione with ninhydrin post treatment (middle), **53** with ninhydrin post treatment (right) **c)** After 24 h.

The results obtained from the spot test with L-leucine suggest that the activity of 1,2-indanedione portion of **53** with amino acids is retained in the presence of a long alkyl side

chain. With this promising result in hand, **53** was chosen as the representative ligand to be functionalized onto gold nanoparticles. Functionalization of gold nanoparticles with **53** was first attempted following a modified Brust protocol[44] used by Almog.[34] Although the synthesis of gold nanoparticles stabilized by tetraoctylammonium bromide was evident (observation of characteristic deep red color upon reduction with $NaBH_4$), subsequent ligand exchange with **53** was unsuccessful. An alternative protocol[45] to synthesize gold colloids stabilized by dodecyldimethylammonium bromide (DDAB) followed by ligand exchange was tested. The protocol was part of a study that was conducted to test the efficacy of digestive ripening with various alkanethiols. Since digestive ripening is a method used to transform highly polydispersed gold nanoparticles to monodispersed gold nanoparticles of decreased average particle size, relatively lower concentration of the surfactant (DDAB) was purposefully used for the study. The authors reasoned that by using a low concentration of DDAB, the removal of DDAB would be easier before the digestive ripening step, and it would also lead to highly polydispersed gold nanoparticles that could be used to observe the decrease in polydispersity after disgestive ripening. Likewise, for the present system, the use of lower concentration of DDAB could allow the subsequent ligand exchange with **53** to occur more easily. However, the digestive ripening step was not followed, since the effect of polydispersity of gold nanoparticles on the development on latent fingerprints on paper has not been determined. Nonetheless, when the protocol was applied in the current system using **53**, the desired functionalized gold nanoparticles were successfully obtained, albeit with prolonged reaction time for ligand exchange. Longer reaction time was expected, since majority of **53** still contained the thioacetate moiety as opposed to the thiol group, which

readily forms strong bonds with gold nanoparticles.[46] Various attempts were made for the removal of the acetate group with no success. Conditions used to convert thioesters to thiols require the use of aqueous media in protic acid or nucleophilic conditions, which only led to the formation of undesired corresponding acetals or decomposition of the material. The precise size of the acquired gold nanoparticles was not determined, since it was assumed that highly polydispersed gold colloids would be obtained. UV-Vis data (λ_{max} = ~530 nm) supported the presence of gold nanoparticles, since the observed λ_{max} was in the region that is characteristic of gold nanoparticles.

With the promising result in hand, detection of latent fingerprint on paper was attempted, following Almog's general procedure.[34] Fingerprints were deposited on a paper substrate (fingerprints that are not "charged" with oily residue (sebaceous) and the paper was subsequently soaked in an aqueous solution of maleic acid for about 5 min to eliminate calcium carbonate on paper. If the calcium carbonate is not removed, the entire paper turns black upon treatment with Ag-PD (i.e. spontaneous silver deposition). The treated paper substrate was air-dried, and dipped into a solution of the functionalized gold nanoparticles in acetonitrile for about 10 min. Subsequent post treatment with Ag-PD solution for 1-2 min gave rise to visible fingerprint ridges (Figure 5.5).

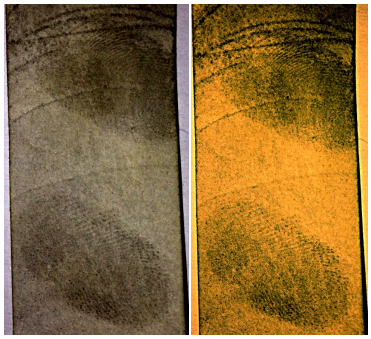

Figure 5.5. Latent fingerprints developed on paper substrate (original image-left, photo enhanced contrast image-right).

Since a "positive" fingerprint image was obtained, in which the silver deposition was more apparent on the ridges of the fingerprint in comparison to the background, the desired reaction of the 1,2-indanedione portion of **53** with the amino acid residue of the fingerprint may be taking precedence over the reaction of 1,2-indanedione with cellulose. Furthermore, although fingerprints that were not "charged" (eccrine fingerprints) were deposited, due to the presence of along alkyl chain on **53**, the observed image could be further amplified by hydrophobic interactions as well.[34,35]

5.6) Conclusions

Novel 1,2-indanedione analogues were successfully synthesized using a concise, four-step protocol. The 10-carbon chain 1,2-indanedione analogue **53** was functionalized onto gold nanoparticles and used to develop latent fingerprints on paper substrates. With the promising preliminary results at hand, further efforts toward optimization of the development protocol will be made. For instance, the effect of gold nanoparticle dispersity on fingerprint development could be studied using the 1,2-indanedione analogues of varying chain lengths. Formulation of the functionalized gold nanoparticle could be optimized as well in order to use solvents that will produce acceptable images without dissolving ink. Use of other sulfur containing compounds as ligands to gold

nanoparticles could be investigated, since the use of thioacetates resulted in prolonged reaction times. Moreover, much work remains to be done in order to fully elucidate the mechanism in which the newly developed reagents are undergoing with residues of latent fingerprints.

Development of latent fingerprints on paper is still an ongoing research area, since there is no universal reagent that detects fingerprints. The outcome of the developed fingerprint could vary on many external factors that are difficult to control. For instance, a recent study using 1,2-indanedione with $ZnCl_2$ suggested that there is a correlation between the grade and the age of the developed print, age of the donor, and the washing of hands.[47] In order to address such issues, existing fingerprint developing processes, such as Ag-PD,[48] are still evolving to achieve optimal formulation conditions. With the rapid advances in nanotechnology, there is a high demand for developing methods using modified MMD processes. Therefore, the proposed current approach in using functionalized 1,2-indanedione analogues as tunable ligands on gold nanoparticles followed by Ag-PD processing could be an important contribution to the area of latent fingerprint detection on paper.

5.7) Experimental results

General Methods. All reactions were performed under an argon atmosphere except where otherwise noted. Tetrahydrofuran was distilled over sodium-benzophenone, dichloromethane was distilled over calcium hydride, DMF in Acroseal bottles were used without further purification prior to use. Flash chromatography was carried out on Merck silica gel 60 (240-400 mesh) using the solvent conditions listed under individual

experiments. Analytical thin-layer chromatography was performed on Merck silica gel (60F-254) plates (0.25 mm). Visualization was effected with ultraviolet light or phosphomolybdic acid (PMA) stain. Proton magnetic resonance spectra (^{1}H NMR), Carbon magnetic resonance spectra (^{13}C NMR), Fluorine magnetic resonance spectra (^{19}F NMR), and Boron magnetic spectra (^{11}B NMR) were performed on a Bruker NMR operating at 500, 125, 470, and 128 MHz respectively. All ^{11}B chemical shifts were referenced to external BF_3•OEt_2 (0.0 ppm) with a negative sign indicating an upfield shift. Infrared spectra (IR) were obtained on a Perkin-Elmer 281-B spectrometer. High resolution mass spectra (HRMS) were obtained on a Micromass Autospec or a Waters LCTOF-Xe premier. Optical rotations were measured on a Jasco P-1010 polarimeter. 5-hydroxy-1,2-indanedione was prepared following the procedure by Petrovskaia.[i] All other starting materials and reagents were purchased from Sigma-Aldrich, TCI, Acros, or Strem unless specified.

General procedure for alkyl side chain synthesis for first generation synthesis

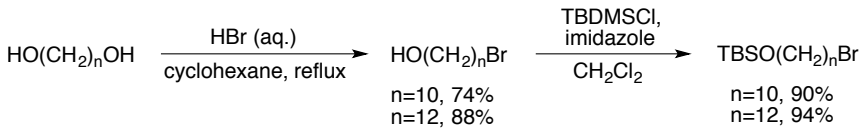

Following the protocol reported by Suzuki *et al*,[ii] to a solution of the diol (5.74 mmol) dissolved in cyclohexane (25 mL) at room temperature was added aqueous HBr (141.4 mmol). The resulting mixture was brought to reflux with stirring for 6 h or until

[i] O. G. Petrovskaia, "Design and synthesis of chromogenic and fluorogenic reagents for amino acid detection." University of Pennsylvania, Philadelphia, PA, 1999.
[ii] Luu, B., Bagnard, D., Hanibali, M., Yamada, M., Suzuki, H. Hydroquinone long-chain derivative and/or phenoxy long-chain derivative and pharmaceutical preparation comprising the same. EP1854777 (A1), November 14, 2007.

completion (monitored by TLC). The reaction mixture was cooled to room temperature and extracted with diethyl ether. The organic layers were combined and washed with aqueous sat. $NaHCO_3$, brine, and dried over $MgSO_4$. Filtration followed by concentration under vacuum afforded a clear oil. Further purification by silica gel chromatography afforded the desired product. ^{1}H NMR spectra of the 10- and 12-carbon derivative were in good accordance with the reported data.[1]

To a solution of the bromoalcohol (4.216 mmol) in anhydrous CH_2Cl_2 (10 mL) was added TBDMSCl (6.324 mmol) followed by imidazole (6.324 mmol) at room temperature. The resulting solution was left to stir for 48 h at room temperature. After removal of the solvent, the residue was dissolved in ethyl acetate and washed with aqueous 10% $KHSO_4$ and dried over Na_2SO_4, filtered, and concentrated. Silica gel chromatography purification afforded the desired product as a clear, colorless oil. ^{1}H NMR spectra of 10- and 12-carbon derivative were in good accordance with the reported data.[iii,iv]

General procedure for chain attachment for first generation synthesis

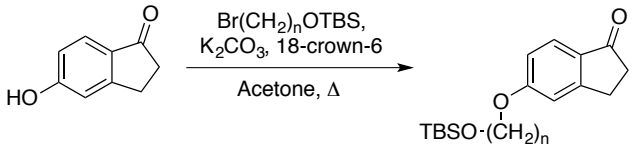

To a stirred solution of 5-hydroxy-1-indanone (100 mg, 0.675 mmol) in anhydrous

[iii] Goulaouic-Dubois, C., Guggisberg, A., Hesse, M. "Samarium diiodide induced ring enlargement of azidocyclododecanones to various marocyclic lactams." *Tetrahedron* **1995**, *51*, 12035-12046.

[iv] Maharvi, G. M., Edwards, A. O., Fauq, A. H. "Chemical synthesis of deuterium-labeled and unlabeled very long chain polyunsaturated fatty acids." *Tetrahedron Lett.* **2010**, *51*, 6426-6428.

acetone (20 mL) was added the 10-carbon chain (261 mg, 0.742 mmol), K_2CO_3 (233 mg, 1.687 mmol), and 18-crown-6 (1.3 mg, 0.005 mmol). The resulting mixture was brought to reflux and left to stir for 24 h. The solvent was evaporated, dissolved in CH_2Cl_2 (30 mL), washed with H_2O (10 mL), back-extracted the aqueous layer with CH_2Cl_2 (10 mL, 3 times). The organic layers were combined and dried over $MgSO_4$, filtered, and concentrated. Silica gel chromatography purification (10% Ethyl acetate/Hexanes) afforded the chain attached indanone **6**.

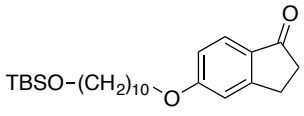

10-Carbon chain TBS ether (6). R_f 0.28 (10% EtOAc/Hex); ^{1}H NMR: (500 MHz, $CDCl_3$) δ 7.70 (d, *J* = 9.13 Hz, 1H), 6.91 (dd, *J* = 6.1, 2.1 Hz, 2H), 4.05 (t, *J* = 6.5 Hz, 2H), 3.64 (t, *J* = 6.5 Hz, 2H), 3.09 (dd, *J* = 7.46, 4.21 Hz, 2H), 2.70-2.67 (m, 2H), 1.86-1.81 (m, 2H), 1.61-1.44 (m, 6H), 1.44-1.28 (m, 8H), 1.04 (s, 9H), 0.13 (s, 6H); ^{13}C NMR: (125 MHz, $CDCl_3$) δ 205.2, 164.9, 158.1, 130.2, 125.3, 115.6, 110.3, 68.4, 63.3, 63.0, 36.4, 32.84, 32.79, 29.5, 29.45, 29.38, 29.3, 29.0, 25.9, 25.8, 25.76, 25.71, 18.35; IR (cm^{-1}): 2929, 2856, 1709, 1601, 1489, 1471, 1443, 1406, 1388, 1360, 1332, 1303, 1257, 1143, 1100, 1006, 836, 812, 775; HRMS (ESI) *m/*z calculated for $C_{25}H_{42}O_3Si$ $(M + Na)^+$: 441.2801, found: 441.2808.

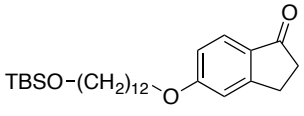

12-Carbon chain TBS ether (7). R_f 0.57 (20% EtOAc/Hex); ^{1}H NMR: (500 MHz, $CDCl_3$) δ 7.71-7.69 (m, 1H), 6.92-6.90 (m, 2H), 4.04 (t, *J* = 6.51 Hz, 2H), 3.61 (td, *J* = 6.63, 0.98 Hz, 2H), 3.11-3.09 (m, 2H), 2.70-2.67 (m, 2H), 1.84-1.81 (m, 2H), 1.54-1.47 (m, 4H), 1.39-1.27 (m, 14H), 0.91 (s, 9H), 0.06 (s, 6H); ^{13}C NMR: (125

MHz, $CDCl_3$) δ 205.2, 164.9, 158.1, 130.2, 125.3, 115.6, 110.3, 68.5, 63.3, 36.4, 32.9, 29.6, 29.5, 29.4, 29.3, 29.1, 26.0, 25.9, 25.86, 25.81, 18.4; IR (cm^{-1}): 2924, 2853, 1701, 1608, 1583, 1475, 1438, 1388, 1329, 1259, 1244, 1146, 1101, 1019, 875, 835, 773; HRMS (ESI) *m/z* calculated for $C_{27}H_{46}O_3Si$ $(M + Na)^+$: 469.3114, found: 469.3120.

General procedure for TBS removal for first generation synthesis

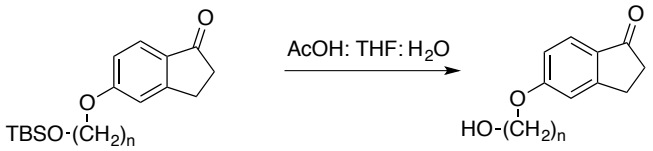

A solution of 10-carbon chain TBS ether **6** (2.7 g, 6.544 mmol) in 3:3:1 mixture of acetic acid:THF:H_2O (170 mL) was stirred at room temperature overnight. Ethyl acetate (200 mL) was added to the reaction mixture. The organic layer was carefully washed with 5% aq. $NaHCO_3$ (100 mL) to neturalize the solution (checked by pH). The organic layer was then washed with 1M HCl (100 mL), brine, dried over $MgSO_4$, filtered and concentrated. Silica gel chromatography purification (30% → 50% EtOAc/Hexanes) afforded the desired alcohol **8**.

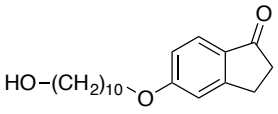

10-Carbon chain alcohol (8). R_f 0.72 (30% Acetone/Hex); ^1H NMR: (500 MHz, $CDCl_3$) δ 7.70 (d, *J* = 9.14 Hz, 1H), 6.92-6.90 (m, 2H), 4.05 (t, *J* = 6.54 Hz, 2H), 3.66 (td, *J* = 6.63, 0.93 Hz, 2H), 3.11-3.09 (m, 2H), 2.70-2.68 (m, 2H), 1.85-1.80 (m, 2H), 1.61-1.56 (m, 2H), 1.50-1.44 (m, 4H), 1.41-1.32 (m, 10H); ^{13}C NMR: (125 MHz, $CDCl_3$) δ 205.2, 164.9, 158.1, 130.3, 125.3, 115.6, 110.3, 68.4, 63.0, 36.4, 32.8, 29.51, 29.46, 29.4, 29.3, 29.0, 25.9, 25.8, 25.7; IR (cm^{-1}): 3411, 2916, 2851, 1686,

1672, 1607, 1595, 1469, 1439, 1401, 1339, 1305, 1259, 1106, 1092, 1049, 1019, 859, 836, 811, 716; HRMS (ESI) *m/*z calculated for $C_{19}H_{28}O_3$ $(M + H)^+$: 305.2117, found: 305.2129.

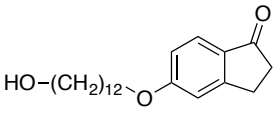

12-Carbon chain alcohol (9). R_f 0.21 (2% EtOAc/CH_2Cl_2); ^1H NMR: (500 MHz, $CDCl_3$) δ 7.69 (d, *J* = 9.33 Hz, 1H), 6.92-6.90 (m, 2H), 4.04 (t, *J* = 6.54 Hz, 2H), 3.69-3.65 (m, 2H), 3.11-3.09 (m, 2H), 2.72-2.67 (m, 2H), 1.87-1.80 (m, 2H), 1.62-1.56 (m, 4H), 1.52-1.45 (m, 2H), 1.42-1.28 (m, 14H), 1.26-1.21 (m, 1H); ^{13}C NMR: (125 MHz, $CDCl_3$) δ 205.3, 164.8, 158.1, 130.1, 125.3, 115.6, 110.2, 68.4, 63.0, 36.4, 32.7, 29.6, 29.5, 29.4, 29.3, 29.0, 25.9, 25.8, 25.7; IR (cm^{-1}): 3420, 2915, 2851, 1686, 1672, 1605, 1583, 1473, 1439, 1401, 1336, 1305, 1258, 1147, 1107, 1094, 1055, 1039, 1023, 1000, 860, 834, 810, 715, 651, 568; HRMS (ESI) *m/*z calculated for $C_{21}H_{32}O_3$ $(M + Na)^+$: 355.2249, found: 355.2255.

General procedure for Mitsunobu reaction for first generation synthesis

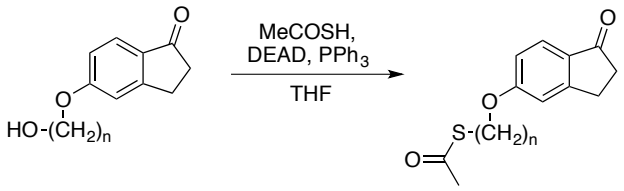

To a mixture of the 10-carbon chain alcohol **8** (90 mg, 0.2956 mmol) and PPh_3 (116 mg, 0.4435 mmol) in anhydrous THF was added drop-wise DEAD (70 mL, 0.4435 mmol). After 5 min, thioacetic acid (42 mL, 0.5913 mmol) was added, and the resulting mixture was stirred at room temperature for 20 h. The solvent was concentrated. Silica gel column chromatography purification (30% EtOAc/Hexanes) afforded the desired product **10**.

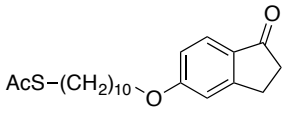

10-Carbon chain thioacetate (10). R_f 0.62 (30% Acetone/Hex); ^{1}H NMR: (500 MHz, $CDCl_3$) δ 7.67 (d, *J* = 9.06 Hz, 1H), 6.89 (t, *J* = 2.23 Hz, 2H), 4.03 (t, *J* = 6.52 Hz, 2H), 3.08 (t, *J* = 5.82 Hz, 2H), 2.86 (t, *J* = 7.36 Hz, 2H), 2.68-2.65 (m, 2H), 2.23, (s, 3H), 1.84-1.76 (m, 2H), 1.57 (dt, *J* = 14.59, 7.30 Hz, 2H), 1.49-1.42 (m, 2H), 1.36-1.24 (m, 12H); ^{13}C NMR: (125 MHz, $CDCl_3$) δ 205.1, 195.9, 164.8, 158.0, 130.1, 125.2, 115.5, 110.2, 68.4, 36.3, 30.5, 29.4, 29.37, 39.30, 29.2, 29.1, 29.0, 28.7, 28.3, 25.9, 25.8, 24.9, 14.0; IR (cm^{-1}): 2918, 2851, 1755, 1698, 1607, 1594, 1470, 1433, 1414, 1305, 1254, 1141, 1119, 1089, 1043, 1014, 968, 855, 830, 807, 717, 636; HRMS (ESI) *m/z* calculated for $C_{21}H_{30}O_3S$ $(M + H)^+$: 363.1994, found: 363.1984.

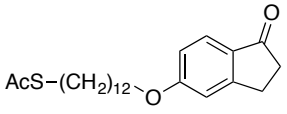

12-Carbon chain thioacetate (11). R_f 0.65 (2% EtOAc/CH_2Cl_2); ^{1}H NMR: (500 MHz, $CDCl_3$) δ 7.69 (d, *J* = 8.99 Hz, 1H), 6.92-6.90 (m, 2H), 4.04 (t, *J* = 6.55, 2H), 3.11-3.09 (m, 2H), 2.88 (t, *J* = 7.35, 2H), 2.68 (ddd, *J* = 5.96, 4.08, 1.83 Hz, 2H), 2.33 (s, 3H), 1.86-1.80 (m, 2H), 1.61-1.55 (m, 2H), 1.51-1.45 (m, 2H), 1.43-1.25 (m, 14H); ^{13}C NMR: (125 MHz, $CDCl_3$) δ 205.2, 195.9, 164.8, 158.0, 130.1, 125.2, 115.5, 110.2, 68.4, 63.9, 38.9, 36.3, 30.5, 29.47, 29.40, 29.2, 29.1, 29.05, 29.03, 28.9, 28.8, 28.7, 28.3, 25.9, 25.8, 24.9, 14.0; IR (cm^{-1}): 2915, 2850, 1755, 1698, 1606, 1487, 1470, 1433, 1414, 1354, 1329, 1305, 1254, 1141, 1089, 1038, 1021, 987, 951, 853, 830, 807, 716, 634, 595; HRMS (ESI) *m/z* calculated for $C_{23}H_{34}O_3S$ $(M + Na)^+$: 413.2126, found: 413.2140.

General procedure for oxime formation for first generation synthesis

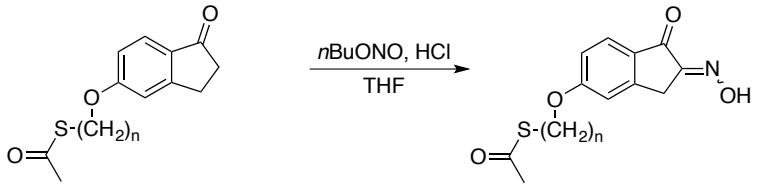

To a solution of 10-carbon thioacetate **10** (86 mg, 0.2372 mmol) in THF (0.5 mL) was added conc. HCl (0.13 mL, 4.278 mmol) followed by *n*Butyl nitrite (77 mL, 0.658 mmol). The resulting mixture was left to stir at room temperature for 2 h (or until completion monitored by TLC). Ethyl acetate (5 mL) was added to the reaction mixture, and the organic layer was washed with H_2O (1 mL), washed with brine (1 mL), dried over $MgSO_4$, filtered, and concentrated. Silica gel chromatography purification (30% EtOAc/Hexanes → 40% → 50%) afforded the desired product **12**.

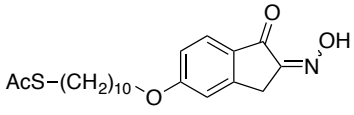

10-Carbon chain oxime (12). R_f 0.28 (40% EtOAc/Hex); ^1H NMR: (500 MHz, $CDCl_3$) δ7.85 (d, *J* = 8.5 Hz, 1H), 6.97-6.94 (m, 2H), 4.08 (t, *J* = 6.5 Hz, 2H), 3.82 (s, 2H), 2.88 (t, *J* = 7.4 Hz, 2H), 2.34 (s, 3H), 1.87-1.81 (m, 2H), 1.61-1.46 (m, 14H), 1.41-1.29 (m, 19H); ^{13}C NMR: (125 MHz, $CDCl_3$) δ 196.2, 187.7, 165.8, 155.2, 149.9, 131.0, 136.6, 116.1, 110.5, 68.6, 30.5, 29.4, 29.3, 29.2, 29.1, 29.0, 28.9, 28.7, 28.4, 25.8; IR (cm^{-1}): 3232, 2925, 2853, 1692, 1601, 1578, 1468, 1344, 1278, 1248, 1108, 1037, 905, 770, 686, 628; HRMS (ESI) *m/*z calculated for $C_{21}H_{29}NO_4S$ $(M + H)^+$: 392.1896, found: 392.1882.

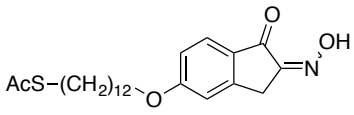

12-Carbon chain oxime (13). R_f 0.36 (40% EtOAc/Hex); ^1H

NMR: (500 MHz, $CDCl_3$) δ 7.84 (d, *J* = 8.4 Hz, 1H), 6.96 (s, 1H), 6.94 (s, 1H), 4.08 (t, *J* = 6.5 Hz, 2H), 3.82 (s, 2H), 2.88 (t, *J* = 7.4 Hz, 2H), 2.34 (s, 3H), 1.87-1.81 (m, 2H), 1.57 (sextet, *J* = 6.4 Hz, 2H), 1.51-1.45 (m, 2H), 1.38-1.29 (m, 15H).; ^{13}C NMR: (125 MHz, $CDCl_3$) δ 196.2, 187.7, 166.0, 155.5, 149.9, 131.1, 126.7, 116.2, 110.6, 68.7, 30.6, 29.49, 29.43, 29.29, 29.15, 29.13, 29.08, 28.99, 28.81, 28.4, 25.92, 25.90; IR (cm^{-1}): 2923, 2852, 1692, 1645, 1601, 1579, 1489, 1471, 1343, 1297, 1248, 1109, 1095, 1037, 771, 684, 628; HRMS (ESI) *m/z* calculated for $C_{23}H_{33}NO_4S$ $(M + Na)^+$: 442.2028, found: 442.2038.

General procedure for synthesis of 1,2-indanedione derivative for first generation synthesis

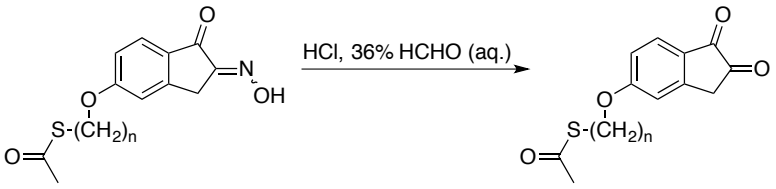

To a suspension of the 10-carbon chain oxime **12** (893 mg, 2.281 mmol) in aqueous formaldehyde (37% in water) (8.6 mL, 116.3 mmol), was added conc. HCl (17 mL, 559.5 mmol). The resulting suspension was vigorously stirred at room temperature overnight. The reaction mixture was diluted with CH_2Cl_2 (20 mL), basified until pH ~5 using aqueous $NaHCO_3$. The aqueous layer was separated and extracted with CH_2Cl_2 (10 mL, 3 times). The organic layers were combined and washed with brine (10 mL), dried over $MgSO_4$, filtered, and concentrated.

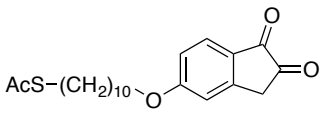

10-Carbon chain 1,2-indanedione analogue (14). R_f 0.6 (40% EtOAc/Hex); ^1H NMR: (500 MHz, $CDCl_3$) δ 7.89 (d, *J* = 8.6 Hz, 1H), 7.00-6.95 (m, 2H),

4.11 (t, J = 6.5 Hz, 2H), 3.57 (s, 2H), 2.87 (t, J = 7.4 Hz, 2H), 2.33 (s, 3H), 1.88-1.82 (m, 2H), 1.57 (dt, J = 14.6, 7.3 Hz, 2H), 1.49-1.45 (m, 2H), 1.37-1.31 (m, 10H); ^{13}C NMR: (125 MHz, $CDCl_3$) δ 200.4, 196.0, 184.6, 166.7, 149.7, 131.3, 128.2, 116.9, 110.7, 69.9, 36.7, 30.6, 29.6, 29.4, 29.38, 29.32, 29.1, 29.09, 29.03, 28.8, 28.7, 25.8; IR (cm^{-1}): 3413, 2826, 2853, 1710, 1691, 1599, 1261, 1105.

Synthesis of functionalized PEG chain

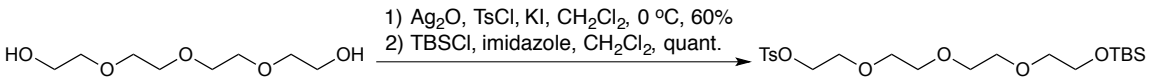

To a stirred solution of tetraethyleneglycol (1 mL, 5.766 mmol) in anhydrous CH_2Cl_2 (58 mL) at 0 ^{o}C was added Ag_2O (2 g, 8.649 mmol) and KI (0.19 mg, 1.154 mmol) followed by portion-wise addition of TsCl (1.2 g, 6.343 mmol). The resulting mixture was kept at 0 ^{o}C for 10 min. The reaction mixture was then filtered through a pad of silica gel and evaporated. Silica gel chromatography purification (30% Acetone/CH_2Cl_2) afforded the tosylated PEG chain as a colorless oil (1.21 g, 60%). ^{1}H NMR spectra obtained was in good accordance with the reported data.[v]

To a stirred solution of tosylated PEG chain (1.11 g, 3.186 mmol) in anhydrous CH_2Cl_2 (16 mL) was added TBSCl (0.72 g, 4.779 mmol) followed by imidazole (0.33 g, 4.779 mmol). The resulting mixture was left to stir at room temperature overnight. The reaction was diluted with ethyl acetate (40 mL), washed with aqueous 10% $KHSO_4$ (15 mL). The organic layer was separated, and dried over Na_2SO_4, filtered, and concentrated. Silica gel

[v] Rubinshtein, M., James, C. R., Young, J. L., Ma, Y. J., Kobayashi, Y., Gianneschi, N. C., Yang, J. "Facile procedure for generating side chain functionalized poly(α-hydroxy acid) copolymers from aldehydes via a versatile passerini-type condensation." *Org. Lett.* **2010**, *12*, 3560-3563.

chromatography purification (40% EtOAc/Hexanes) afforded the desired functionalized PEG chain as a colorless oil (1.47 g, quant.). ^{1}H NMR spectra obtained was in good accordance with the reported data.[vi]

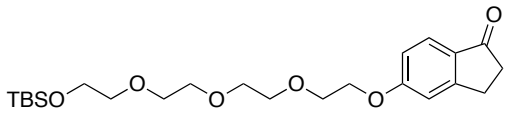

TBS ether PEG chain indanone (15). To a stirred solution of 5-hydroxy-1-indanone (300 mg, 2.025 mmol) in anhydrous acetone (61 mL) was added the functionalized PEG chain (1.0 g, 2.227 mmol), K_2CO_3 (0.7 g, 5.06 mmol), and 18-crown-6 (4 mg, 0.014 mmol). The resulting mixture was brought to reflux and left to stir overnight. The solvent was evaporated, dissolved in CH_2Cl_2 (30 mL), washed with H_2O (10 mL), back-extracted the aqueous layer with CH_2Cl_2 (10 mL, 3 times). The organic layers were combined and dried over $MgSO_4$, filtered, and concentrated. Silica gel chromatography purification (40% EtOAc/Hexanes) afforded the desired product as a yellow oil (759 mg, 85%). R_f 0.23 (40% EtOAc/Hex); ^{1}H NMR: (500 MHz, $CDCl_3$) δ 7.69 (dd, *J* = 9.19, 1.88 Hz, 1H), 6.93 (dd, *J* = 7.20, 1.87 Hz, 2H), 4.23-4.21 (m, 2H), 3.90 (td, *J* = 4.80, 1.45 Hz, 2H), 3.79-3.74 (m, 4H), 3.71 (dd, *J* = 2.85, 1.64 Hz, 2H), 3.67 (d, J = 1.82 Hz, 4H), 3.57 (td, J = 5.43, 1.88 Hz, 2H), 3.09 (t, *J* = 5.39 Hz, 2H), 2.68 (ddt, *J* = 5.75, 3.95, 1.96 Hz, 2H), 0.90 (d, *J* = 1.96 Hz, 9H), 0.07 (d, *J* = 1.95 Hz, 6H); ^{13}C NMR: (125 MHz, $CDCl_3$) δ 205.2, 164.4, 158.0, 130.5, 125.2, 115.6, 110.4, 72.6, 70.8, 70.7, 70.68, 70.63, 69.4, 67.7, 62.6, 36.3, 25.9, 25.8, 25.6, 18.3, -5.2; IR (cm^{-1}): 2928, 1705, 1601, 1488, 1471, 1462, 1443, 1407, 1388, 1360, 1350, 1332,

[vi] Gutiérrez-Nava, M., Masson, P., Nierengarten, J.-F. "Synthesis of copolymers alternating oligophenylenevinylene subunits and fullerene moieties." *Tetrahedron Lett.* **2003**, *44*, 4487-4490.

1304, 1258, 1103, 1030, 1006, 953, 835, 811, 778, 710, 660, 592; HRMS (ESI) *m/*z calculated for $C_{23}H_{38}O_6Si$ $(M + H)^+$: 439.2516, found 439.2523.

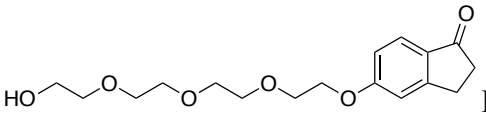

PEG chain indanone (16). To a stirred solution of the TBS ether **15** (659 mg, 1.502 mmol) in anhydrous THF (8 mL) at 0 °C was added TBAF (1M in THF, 3.76 mL, 3.756 mmol). The resulting mixture was kept at 0 °C for 2 h then slowly warmed to room temperature for additional 2 h. The reaction mixture was diluted with ethyl acetate (20 mL), washed with H_2O (10 mL) and brine (10 mL). The organic layer was separated and dried over Na_2SO_4, filtered, and concentrated. Silica gel chromatography purification afforded the alcohol (425 mg, 87%). R_f 0.23 (40% EtOAc/Hex); ^{1}H NMR: (500 MHz, $CDCl_3$) δ 7.70 (d, *J* = 9.24 Hz, 1H), 6.95-6.93 (m, 2H), 4.23 (t, *J* = 4.82 Hz, 2H), 3.90 (t, *J* = 4.81 Hz, 2H), 3.77-3.67 (m, 11H), 3.63 (dd, *J* = 5.12, 3.96 Hz, 2H), 3.10 (t, *J* = 5.91 Hz, 2H), 2.70-2.68 (m, 2H); ^{13}C NMR: (125 MHz, $CDCl_3$) δ; 205.2, 164.4, 158.0, 130.5, 125.3, 115.7, 110.4, 72.4, 70.8, 70.7, 70.6, 70.3, 69.5, 67.7, 61.7, 36.4, 25.8; IR (cm^{-1}): 3449, 3062, 3023, 2919, 2872, 1701, 1599, 1488, 1442, 1406, 1348, 1334, 1305, 1259, 1198, 1127, 1104, 1090, 1032, 953, 885, 837, 809, 710, 650, 592; HRMS (ESI) *m/*z calculated for $C_{17}H_{24}O_6$ $(M + Na)^+$: 347.1471, found: 347.1464.

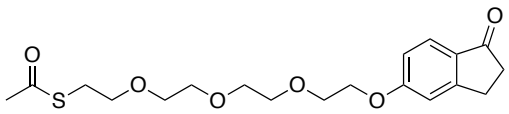

Thioacetate PEG chain indanone (17). To a stirred mixture of the alcohol **16** (420 mg, 1.294 mmol) in pyridine (13 mL) at −5 °C was added TsCl (617 mg, 3.237 mmol). The resulting mixture was kept at −5 °C for 1 h, then

warmed to room temperature over 4 h. The reaction was quenched with 1N HCl (10 mL), and extracted with ethyl acetate (30 mL). The organic layer was washed with 1N HCl (10 mL, three times), aqueous $NaHCO_3$ (10 mL), and brine (10 mL). The organic layer was dried over Na_2SO_4, filtered, and concentrated to afford the crude tosylated product, which was carried on to the next step without further purification. To a stirred solution of the tosylate in anhydrous acetonitrile (78 mL) was added potassium thioacetate (286 mg, 2.504 mmol) in one portion. The resulting mixture was brought to 60 ^oC and left to stir overnight. The reaction was quenched with H_2O (160 mL), and the aqueous layer was extracted with CH_2Cl_2 (200 mL, two times). The combined organic layers were washed with brine (100 mL) and dried over Na_2SO_4, filtered, and concentrated. Silica gel chromatography purification (70% EtOAc/Hexanes) afforded the product as a yellow oil (370 mg, 77%). R_f 0.6 (80% EtOAc/Hex); ^1H NMR: (500 MHz, $CDCl_3$) δ 7.66 (d, J = 9.13 Hz, 1H), 6.91 (t, J = 2.97 Hz, 2H), 4.20 (t, J = 4.79 Hz, 2H), 3.88 (dd, J = 5.17, 4.39 Hz, 2H), 3.74-3.57 (m, 10H), 3.09-3.06 (m, 4H), 2.67-2.64 (m, 2H) 2.31 (s, 3H); ^{13}C NMR: (125 MHz, $CDCl_3$) δ 205.1, 195.3, 164.3, 157.9, 130.4, 125.2, 115.6, 110.3, 70.8, 70.6, 70.4, 70.2, 69.6, 69.4, 67.7, 36.3, 30.4, 28.7, 25.7; IR (cm^{-1}): 2920, 2869, 1701, 1691, 1599, 1487, 1441, 1353, 1332, 1303, 1257, 1196, 1102, 1088, 1055, 1030, 953, 868, 836, 808, 709, 626, 592; HRMS (ESI) *m/z* calculated for $C_{19}H_{26}O_6S$ $(M + Na)^+$: 405.1348, found: 405.1332.

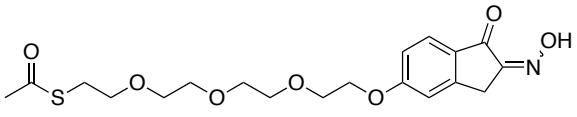

Thioacetate PEG chain oxime (18). To a flask charged with **17** (100 mg, 0.261 mmol) and a stir bar at −20 ^oC was added TMSCl

(33 mL, 0.261 mmol) followed by drop-wise addition of isoamyl nitrite (35 mL, 0.261 mmol). The resulting mixture was left to stir at −20 °C for 30 min. The reaction was quenched with H_2O (1 mL), extracted with ethyl acetate (3 mL), dried over Na_2SO_4, filtered, and concentrated to afford the desired product. R_f 0.2 (80% EtOAc/Hex); ^{1}H NMR: (500 MHz, $CDCl_3$) δ 7.78 (d, *J* = 10 Hz, 1H), 6.94 (d, *J* = 10 Hz, 1H), 6.88 (s, 1H), 4.26 (t, *J* = 5 Hz, 2H), 3.89 (t, *J* = 5 Hz, 2H), 3.74-3.53 (m, 13H), 3.06 (t, *J* = 5 Hz, 2H), 2.33 (s, 3H); ^{13}C NMR: (125 MHz, $CDCl_3$) δ 195.5, 187.7, 165.4, 155.2, 149.7, 131.3, 136.5, 116.2, 110.7, 70.8, 70.7, 70.5, 70.2, 69.7, 69.4, 67.9, 41.6, 30.5, 28.7, 28.3, 22.5; HRMS (ESI) *m/z* calculated for $C_{19}H_{25}NO_7S$ $(M + Na)^+$: 434.1249, found: 434.1261.

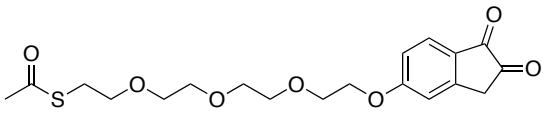

Thioacetate PEG chain 1,2-indanedione (19). To a flask charged with **18** (25 mg, 0.061 mmol) and a stir bar was added formaldehyde (37% in water) (500 mL) and conc. HCl (0.1 mL). The resulting suspension was vigorously stirred overnight. The reaction mixture was diluted with CH_2Cl_2 (2 mL), basified until pH ~5 using aqueous $NaHCO_3$. The aqueous layer was separated and extracted with CH_2Cl_2 (1 mL, 3 times). The organic layers were combined and washed with brine (1 mL), dried over $MgSO_4$, filtered, and concentrated. R_f 0.4 (80% EtOAc/Hex); ^{1}H NMR: (500 MHz, $CDCl_3$) δ 7.89 (d, *J* = 8.58 Hz, 1H), 7.04-7.00 (m, 2H), 4.29 (t, *J* = 4.44 Hz, 2H), 3.93 (t, *J* = 4.28 Hz, 2H), 3.76-3.58 (m, 12H), 3.08 (t, *J* = 6.49 Hz, 2H), 2.33 (s, 3H); ^{13}C NMR: (125 MHz, $CDCl_3$) δ 200.3, 195.4, 184.7, 166.3, 149.7, 131.3, 128.1, 116.9, 111.0, 70.9, 70.6, 70.5, 70.2, 70.0, 69.7, 69.2, 68.2, 36.7, 30.5, 29.6, 28.7; IR (cm^{-1}): 2871, 1761, 1713, 1600, 1489, 1452, 1350, 1257, 1104, 1052, 954,

841; HRMS (ESI) *m/z* calculated for $C_{19}H_{24}O_7S$ $(M + H)^+$: 397.1321, found: 397.1318.

General procedure for synthesis of potassium alkyltrifluoroborate side chains

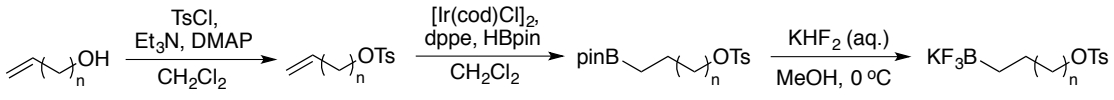

21: n=3, 96%
22: n=6, 81%
23: n=8, quant.
24: n=10, 88%
25: n=12, 80%

26: n=3, 90%
27: n=6, quant.
28: n=8, 95%
29: n=10, 88%
30: n=12, quant.

31: n=3, 96%
32: n=6, 77%
33: n=8, 70%
34: n=10, 88%
35: n=12, 60%

To a stirred solution of 9-decen-1-ol (3 mL, 16.702 mmol) in anhydrous CH_2Cl_2 (30 mL) was added triethylamine (3.5 mL, 25.053 mmol) followed by DMAP (82 mg, 0.668 mmol) and TsCl (3.18 g, 16.702 mmol). The resulting mixture was left to stir at room temperature overnight. The reaction was diluted with water (10 mL) and extracted with chloroform (10 mL, three times). The combined organic layers were washed with aqueous sat. NH_4Cl (10 mL), separated, dried over $MgSO_4$, filtered, and concentrated. Silica gel column chromatography purification (30% EtOAc/Hexanes) afforded **23** as an oil (4.73, 91%).

A 100 mL round bottom flask was charged with $[Ir(cod)Cl]_2$ (146 mg, 0.217 mmol), dppe (173 mg, 0.434 mmol), and a stir bar in a glovebox. The flask was then removed and to it was added a solution of the tosylate **23** (4.5 g, 14.495 mmol) in anhydrous CH_2Cl_2 (48 mL) via cannula addition. The resulting mixture was brought to 0 ^oC, followed by drop-wise addition of pinacolborane (3.15 mL, 21.742 mmol). The reaction mixture was left to stir and allowed to warm to room temperature overnight. The reaction was quenched by water (15 mL), left to stir for 5 min, and the resulting mixture was separated. The aqueous layer was extracted with diethyl ether (15 mL, three times). The combined organic layers were dried over $MgSO_4$, filtered, and concentrated. Purification by silica

gel chromatography (15% EtOAc/Hexanes) afforded the product **28** as an oil (6.12 g, 97%).

To a stirred solution of **28** (4.5 g, 10.357 mmol) in acetonitrile (14 mL) was added aqueous 4.5 M KHF_2 (14 mL). The resulting mixture was left to stir at room temperature for 1 h. The solution was concentrated, and put under vacuum overnight. Hot acetonitrile (100 mL) was added to the solid and filtered by hot gravity filtration (or alternatively, soxhlet extraction). The filtrate was evaporated, re-dissolved in small amount of cold diethyl ether (20 mL) and filtered to afford the desired potassium alkyltrifluoroborate salt **33**.

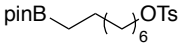

8-Carbon chain pinacolboronate ester (27). R_f 0.65 (20% EtOAc/Hex); ^{1}H NMR: (500 MHz, $CDCl_3$) δ 7.79 (d, *J* = 8.31 Hz, 2H), 7.35 (d, *J* = 8.51 Hz, 2H), 4.04-4.00 (m, 2H), 2.45 (s, 3H), 1.69-1.59 (m, 4H), 1.39-1.22 (m, 20H), 0.75 (t, *J* = 7.82 Hz, 2H); ^{13}C NMR: (125 MHz, $CDCl_3$) δ 144.5, 133.1, 129.7, 127.8, 82.8, 70.6, 32.1, 31.6, 29.0, 28.9, 28.8, 28.7, 25.2, 24.7, 23.8, 22.5, 21.5, 14.0; ^{11}B NMR (128.4 MHz, $CDCl_3$) δ 33.68; IR (cm^{-1}): 2977, 2928, 2857, 1598, 1495, 1466, 1363, 1320, 1272, 1213, 1188, 1177, 1145, 1098, 1019, 966, 936, 845, 815, 664, 577, 555; HRMS (ESI) *m/*z calculated for $C_{21}H_{35}BO_5S$ $(M + H)^+$: 411.2377, found: 411.2372.

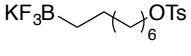

8-Carbon chain potassium trifluoroborate salt (32). ^{1}H NMR: (500 MHz, acetone-d_6) δ 7.81 (d, *J* = 8.18 Hz, 2H), 7.50 (d, *J* = 8.29 Hz, 2H), 4.05 (t, *J* = 6.41 Hz, 2H), 2.47 (s, 3H), 1.63 (dt, *J* = 14.26, 6.90 Hz, 2H), 1.38-1.15 (m, 10H), 0.88 (t, *J* = 7.05 Hz, 2H); ^{13}C NMR: (125 MHz, acetone-d_6) δ 145.7, 134.6, 130.9, 128.7, 83.5, 71.6,

32.9, 32.5, 26.1, 25.3, 25.29, 25.25, 24.8, 23.3, 21.5, 14.4; ^{11}B NMR (128.4 MHz, acetone-d_6) δ 6.03; IR (cm^{-1}): 2916, 2850, 1362, 1175, 1095, 964, 944, 835, 810, 720, 669, 650; HRMS (ESI) *m/*z calculated for $C_{15}H_{23}BF_3O_3S$ $(M - K^+)^+$: 351.1413, found: 351.1406.

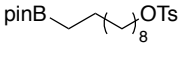

10-Carbon chain pinacolboronate ester (28). R_f 0.43 (10% EtOAc/Hex); ^{1}H NMR: (500 MHz, $CDCl_3$) δ 7.76 (d, *J* = 8.36 Hz, 2H), 7.34-7.32 (m, 2H), 3.99 (t, *J* = 6.52 Hz, 2H), 2.42 (s, 3H), 1.60 (dt, *J* = 14.42, 6.99 Hz, 2H), 1.40-1.34 (m, 2H), 1.26-1.18 (m, 24H), 0.73 (t, *J* = 7.79 Hz, 2H); ^{13}C NMR: (125 MHz, $CDCl_3$) δ 114.5, 133.0, 129.6, 127.7, 82.7, 70.5, 32.2, 31.7, 29.25, 29.23, 29.1, 28.7, 28.6, 25.1, 24.6, 23.8, 22.5, 21.5; ^{11}B NMR (128.4 MHz, $CDCl_3$) δ 33.87; IR (cm^{-1}): 2977, 2855, 1598, 1495, 1466, 1371, 1320, 1271, 1212, 1188, 1177, 1145, 1098, 1019, 1004, 966, 920, 882, 832, 815, 790, 776, 723, 688, 664, 577, 555; HRMS (ESI) *m/*z calculated for $C_{23}H_{39}BO_5S$ $(M + H)^+$: 439.2690, found: 439.2685.

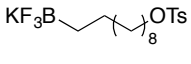

10-Carbon chain potassium trifluoroborate salt (33). ^{1}H NMR: (500 MHz, acetone-d_6) δ 7.84-7.81 (m, 2H), 7.52-7.49 (m, 2H), 4.06 (dt, J = 10.63, 5.0 Hz, 2H), 2.47 (s, 3H), 1.66-1.60 (m, 2H), 1.29-1.18 (m, 14H), 0.15-0.12 (m, 2H); ^{13}C NMR: (125 MHz, acetone-d_6) δ 145.8, 134.5, 130.9, 128.7, 74.8, 71.6, 34.6, 30.8, 30.5, 26.6, 26.1, 25.3, 25.2, 21.6; ^{11}B NMR (128.4 MHz, acetone-d_6) δ 6.06; ^{19}F NMR (470.8 MHz, acetone-d_6) δ −140.95; IR (cm^{-1}): 2918, 2852, 1358, 1188, 1175, 1094, 965, 904, 836, 809, 784, 627.

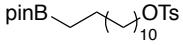

12-Carbon chain pinacolboronate ester (29). R_f 0.34 (10% EtOAc/Hex); ^{1}H NMR: (500 MHz, $CDCl_3$) δ 7.72 (d, *J* = 8.32 Hz, 2H), 7.32 (d, *J* = 8.51 Hz, 2H), 4.00 (t, *J* = 6.54 Hz, 2H), 2.43 (s, 3H), 1.61 (dt, *J* = 14.43, 7.00 Hz, 2H), 1.40-1.17 (m, 30H), 0.74 (t, *J* = 7.77, 2H); ^{13}C NMR: (125 MHz, $CDCl_3$) δ 144.4, 133.2, 129.6, 127.7, 82.7, 70.5, 32.2, 29.5. 29.4, 29.3, 29.2, 28.8, 28.7, 25.2, 24.7, 23.8, 21.4; ^{11}B NMR (128.4 MHz, $CDCl_3$) δ 33.68; IR (cm^{-1}): 2977, 2925, 2853, 1598, 1466, 1364, 1319, 1212, 1188, 1176, 1145, 1098, 1019, 966, 912, 846, 814, 790, 763, 732, 688, 665, 651, 641, 625; HRMS (ESI) *m/*z calculated for $C_{25}H_{43}BO_5S$ $(M + Na)^+$: 489.2822, found: 489.2825.

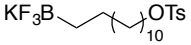

12-Carbon chain potassium trifluoroborate salt (34). ^{1}H NMR: (500 MHz, DMSO-*d*$_6$) δ 7.78 (d, *J* = 8.1 Hz, 2H), 7.49 (d, *J* = 7.9 Hz, 2H), 4.00 (t, *J* = 6.2 Hz, 2H), 2.43 (s, 3H), 1.53 (t, *J* = 6.7 Hz, 2H), 1.19 (s, 18H), -0.04--0.10 (m, 2H); ^{13}C NMR: (125 MHz, DMSO-*d*$_6$) δ 144.8, 132.5, 130.1, 127.5, 70.8, 33.1, 29.4, 29.2, 29.1, 28.9, 28.8, 28.1, 28.0, 25.6, 24.6, 21.0; ^{11}B NMR (128.4 MHz, DMSO-*d*$_6$) δ 6.42; IR (cm^{-1}): 2917, 2850, 1598, 1468, 1363, 1298, 1248, 1188, 1175, 1096, 1021, 965, 946, 918, 836, 809, 793, 720, 669, 642, 626.

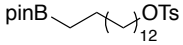

14-Carbon chain pinacolboronate ester (30). R_f 0.67 (20% EtOAc/Hex); ^{1}H NMR: (500 MHz, $CDCl_3$) δ 7.80 (d, *J* = 7.80 Hz, 2H), 7.35 (d, *J* = 7.98 Hz, 2H), 4.05-4.02 (m, 2H), 2.46 (s, 3H), 1.67-1.61 (m, 2H), 1.41 (ddd, *J* = 12.36, 6.78, 6.30 Hz, 2H), 1.30-1.22 (m, 32H), 0.77 (t, *J* = 7.75 Hz, 2H); ^{13}C NMR: (125 MHz, $CDCl_3$) δ 144.5, 133.3, 129.7, 129.5, 127.8, 127.0, 82.8, 70.6, 41.9, 32.4, 29.6, 29.58, 29.55, 29.4, 29.38, 29.36, 28.9, 28.7, 25.3, 24.7, 23.9, 21.5, 14.1; IR (cm^{-1}): 2977, 2925, 2854, 1598, 1466,

1367, 1321, 1188, 1177, 1145, 1097, 1020, 966, 814, 714, 663, 577, 554; HRMS (ESI) *m/z* calculated for $C_{27}H_{47}BO_5S$ $(M + H)^+$: 494.3316, found: 495.3318.

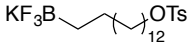

14-Carbon chain potassium trifluoroborate salt (35). ^{1}H NMR: (500 MHz, DMSO-d_6) δ 7.78 (d, *J* = 8.2 Hz, 2H), 7.48 (d, *J* = 7.8 Hz, 2H), 4.00 (t, *J* = 6.3 Hz, 2H), 2.42 (s, 3H), 1.57-1.52 (m, 2H), 1.21-1.16 (m, 22H), -0.06--0.12 (m, 2H); ^{13}C NMR: (125 MHz, DMSO-d_6) δ 144.7, 132.5, 130.1, 127.5, 89.7, 84.5, 70.8, 33.1, 29.4, 29.2, 29.1, 29.0, 28.9, 28.8, 28.7, 28.1, 28.0, 25.6, 24.9, 24.6, 21.0; ; ^{11}B NMR (128.4 MHz, acetone) δ 4.63; IR (cm^{-1}): 2916, 2850, 1364, 1176, 1095, 965, 923, 835, 809, 793, 719, 670.

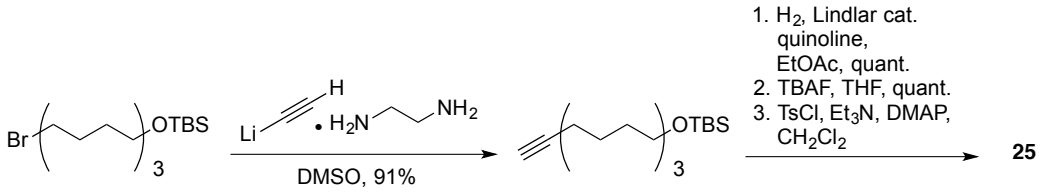

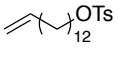

14-Carbon alkene tosylate (25). To a stirred solution of 12-carbon chain bromoalkane (3.57 g, 9.407 mmol) in anhydrous DMSO (21 mL) was added lithium acetylide ethylenediamine complex (1.12 g, 12.229 mmol). The resulting mixture was left to stir at room temperature for 6 h. The reaction was quenched with aqueous sat. NH_4Cl (10 mL). The aqueous layer was extracted with diethyl ether (20 mL, three times). The combined organic layers were washed with water (10 mL), brine (10 mL), and dried over $MgSO_4$, filtered, and concentrated. Purification by silica gel chromatography (100% Hexanes → 5% EtOAc/Hexanes) afforded the known alkyne (2.79 g, 91%). To a solution of the alkyne (2.79 g, 8.595 mmol) in ethyl acetate (43 mL) was added Lindlar's catalyst

(249 mg, 1.203 mmol) followed by quinoline (1 mL, 8.595 mmol). The resulting mixture was stirred under H_2 at room temperature overnight. The reaction mixture was filtered through a bed of Celite and washed with ethyl acetate (10 mL, three times). The filtrate was concentrated. Purification by silica gel chromatography (100% Hexanes → 5% EtOAc/Hexanes) afforded the known alkene as a yellow oil (2.8 g, quant.). To a stirred solution of the TBS ether alkene (2.13 g, 6.521 mmol) in anhydrous THF (44 mL) was added TBAF (1M in THF, 13 mL, 13.042 mmol). The resulting solution was stirred at room temperature for 3 h. The solvent was concentrated and directly loaded onto a silica gel column (20% EtOAc/Hexanes) and afforded the corresponding alcohol (1.38 g, quant.). The desired tosylate **25** was synthesized using the first step of the general procedure to synthesize potassium alkyltrifluoroborate side chains. R_f 0.53 (10% EtOAc/Hex); ^{1}H NMR: (500 MHz, $CDCl_3$) δ 7.80 (d, J = 7.92 Hz, 2H), 7.36 (d, J = 8.24 Hz, 2H), 5.87-5.79 (m, 1H), 5.03-4.93 (m, 2H), 4.03 (td, J = 6.53, 0.72 Hz, 2H), 2.46 (s, 3H), 2.08-2.03 (m, 2H), 1.68-1.62 (m, 2H), 1.41-1.23 (m, 18H); ^{13}C NMR: (125 MHz, $CDCl_3$) δ 144.5, 139.2, 133.3, 129.7, 127.8, 114.0, 70.6, 33.7, 29.5, 29.4, 29.3, 29.1, 28.9, 28.8, 25.6, 25.3, 21.6; IR (cm^{-1}): 2977, 2918, 2850, 1641, 1597, 1495, 1474, 1397, 1357, 1309, 1294, 1190, 1174, 1097, 1042, 1019, 984, 956, 930, 917, 840, 816, 794, 718, 707, 668, 578, 555, 531, 503; HRMS (ESI) *m/*z calculated for $C_{21}H_{34}O_3S$ $(M + H)^+$: 367.2307, found: 367.2306.

General procedure for side chain coupling for second generation synthesis

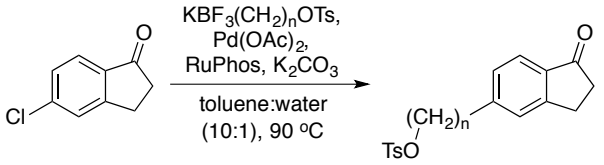

A microwave tube was charged with 5-chloro-1-indanone (100 mg, 0.600 mmol), 10-carbon-potassium alkyltrifluoroborate chain **33** (240 mg, 0.600 mmol), $Pd(OAc)_2$ (3 mg, 0.012 mmol), RuPhos (12 mg, 0.025 mmol), K_2CO_3 (249 mg, 1.801 mmol), and a stir bar. The cap was sealed, and evacuated and purged with Ar (3 cycles). Degassed toluene:H_2O mixture (3 mL) was then added to the microwave tube via syringe and the resulting reaction mixture was heated to 90 ^oC for 36 h. (For larger scale operation, the reaction was set up in a glovebox.) H_2O (1 mL) was added to the reaction, stirred for 5 min, and the resulting layers were separated. The aqueous layer was extracted with ethyl acetate (2 mL, three times). The organic layers were combined, dried over Na_2SO_4, filtered, and concentrated. Purification by silica gel chromatography (20% EtOAc/Hexanes) afforded the coupled product **38** as an amorphous solid (178 mg, 67%).

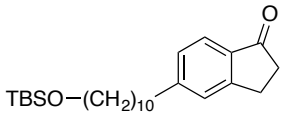

10-Carbon chain TBS ether indanone (20). R_f 0.37 (40% EtOAc/Hex); 1H NMR: (500 MHz, $CDCl_3$) δ 7.68 (d, *J* = 7.84 Hz, 1H), 7.28 (s, 1H), 7.20 (d, *J* = 7.76 Hz, 1H), 3.61 (t, *J* = 6.31 Hz, 2H), 3.12 (t, *J* = 5.77 Hz, 2H), 2.69 (dd, *J* = 10.17, 4.62, 4H), 1.64 (q, *J* = 7.08, 2H), 1.51 (q, *J* = 6.55 Hz, 2H), 1.33-1.29 (m, 12H), 0.90 (s, 9H), 0.05 (s, 6H); ^{13}C NMR: (125 MHz, $CDCl_3$) δ 206.5, 155.6, 150.7, 135.0, 127.9, 126.3, 123.5, 63.2, 36.4, 32.8, 31.2, 29.5, 29.45, 29.42, 29.3, 29.2, 25.9, 25.7, 25.6, 18.3, -5.0; IR (cm^{-1}): 2928, 2855, 1714, 1609, 1470, 1463, 1442, 1406, 1387, 1329, 1280,

1254, 1230, 1098, 1029, 1006, 835, 813, 775, 711; HRMS (ESI) *m/*z calculated for $C_{25}H_{42}O_2Si$ $(M + Na)^+$: 425.2852, found: 425.2849.

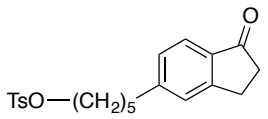

5-Carbon chain tosylate indanone (36). R_f 0.23 (20% EtOAc/Hex); ^{1}H NMR: (500 MHz, $CDCl_3$) δ 7.78 (d, *J* = 8.30 Hz, 2H), 7.67 (d, *J* = 7.85 Hz, 1H), 7.36-7.34 (m, 2H), 7.25 (s, 1H), 7.15 (d, *J* = 7.86 Hz, 1H), 4.03 (t, *J* = 6.41 Hz, 2H), 3.11 (t, *J* = 5.86 Hz, 2H), 2.70-2.65 (m, 4H), 2.45 (s, 3H), 1.76-1.59 (m, 4H), 1.45-1.36 (m. 2H); ^{13}C NMR: (125 MHz, $CDCl_3$) 206.5, 155.7, 149.8, 144.6, 135.1, 133.1, 129.7, 127.9, 127.8, 126.8, 123.6, 70.2, 36.8, 36.0, 30.4, 28.6, 25.6, 24.9, 21.6; IR (cm^{-1}): 2932, 2860, 1708, 1608, 1494, 1440, 1403, 1357, 1281, 1188, 1176, 1097, 1030, 948, 903, 815, 663, 576, 554; HRMS (ESI) *m/*z calculated for $C_{21}H_{24}O_4S$ $(M + H)^+$: 373.1474, found: 373.1473.

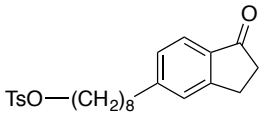

8-Carbon chain tosylate indanone (37). Rf 0.24 (20% EtOAc/Hex); ^{1}H NMR: (500 MHz, $CDCl_3$) δ 7.80 (d, *J* = 8.2 Hz, 2H), 7.68 (d, *J* = 7.8 Hz, 1H), 7.35 (d, *J* = 8.2 Hz, 2H), 7.19 (d, *J* = 7.9 Hz, 1H), 4.03 (t, *J* = 6.5 Hz, 2H), 3.12 (t, *J* = 5.9 Hz, 2H), 2.68 (dd, *J* = 10.3, 4.8 Hz, 4H), 2.46 (s, 3H), 1.64 (dq, *J* = 14.4, 7.2 Hz, 4H), 1.35-1.25 (m, 9H).; ^{13}C NMR: (125 MHz, $CDCl_3$) 206.5, 155.6, 150.5, 144.5, 135.0, 133.2, 129.7, 127.9, 127.8, 126.3, 123.5, 70.5, 36.3, 36.2, 31.1, 29.1, 29.0, 28.8, 28.7, 25;6, 25.2, 21.5; IR (cm^{-1}): 2928, 2856, 1709, 1608, 1495, 1441, 1403, 1359, 1289, 1229, 1188, 1176, 1097, 1030, 941, 815, 664, 577, 555; HRMS (ESI) *m/*z calculated for

$C_{24}H_{30}O_4S$ $(M + H)^+$: 414.1943, found: 414.1943.

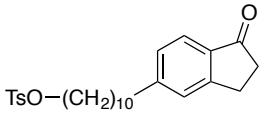

10-Carbon chain tosylate indanone (38). R_f 0.26 (20% EtOAc/Hex); ^1H NMR: (500 MHz, $CDCl_3$) δ 7.70, (d, *J* = 8.27 Hz, 2H), 7.64 (d, *J* = 7.85 Hz, 1H), 7.32 (d, *J* = 8.29 Hz, 2H), 7.26 (s, 1H), 7.17 (d, *J* = 7.85 Hz, 1H), 4.00 (t, *J* = 6.50 Hz, 2H), 3.08 (t, *J* = 5.82 Hz, 2H), 2.68-2.64 (m, 4H), 2.42 (s, 3H), 1.65 (dt, *J* = 14.25, 6.95 Hz, 4H), 1.29-1.21 (m, 12H); ^{13}C NMR: (125 MHz, $CDCl_3$) 206.5, 155.6, 150.6, 144.5, 134.8, 133.0, 129.6, 127.8, 127.6, 126.2, 123.3, 70.5, 36.3, 36.2, 31.1, 29.2, 29.1, 29.0, 28.7, 28.6, 25.5, 25.1, 21.4; IR (cm^{-1}): 2927, 2854, 1709, 1609, 1495, 1465, 1441, 1404, 1359, 1282, 1188, 1176, 1097, 1030, 1020, 957, 927, 814, 664, 576, 555; HRMS (ESI) *m/*z calculated for $C_{26}H_{34}O_4S$ $(M + Na)^+$: 465.2076, found: 465.2079.

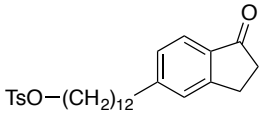

12-Carbon chain tosylate indanone (39). R_f 0.39 (20% EtOAc/Hex); ^1H NMR: (500 MHz, $CDCl_3$) δ 7.80 (d, *J* = 8.0 Hz, 2H), 7.68 (d, *J* = 7.9 Hz, 1H), 7.35 (d, *J* = 8.2 Hz, 2H), 7.20 (d, *J* = 7.8 Hz, 1H), 4.04-4.02 (m, 2H), 3.12 (t, *J* = 5.8 Hz, 2H), 2.71-2.68 (m, 4H), 2.46 (s, 3H), 1.69-1.62 (m, 4H), 1.32-1.23 (m, 17H); ^{13}C NMR: (125 MHz, $CDCl_3$) 206.6, 155.6, 150.7, 144.5, 135.0, 133.2, 129.7, 127.9, 127.8, 126.3, 123.5, 70.6, 36.3, 31.2, 29.5, 29.45, 29.4, 29.3, 29.2, 28.8, 28.7, 25.6, 25.2, 21.5; IR (cm^{-1}): 2977, 2922, 2849, 1704, 1607, 1470, 1434, 1393, 1356, 1323, 1296, 1281, 1246, 1186, 1173, 1097, 1030, 949, 837, 815, 670, 576, 556, 532; HRMS (ESI) *m/*z calculated for $C_{28}H_{38}O_4S$ $(M + H)^+$: 471.2569, found: 471.2550.

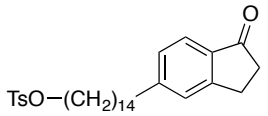

14-Carbon chain tosylate indanone (40). R_f 0.45 (20% EtOAc/Hex); ^{1}H NMR: (500 MHz, $CDCl_3$) δ 7.79 (d, *J* = 8.3 Hz, 2H), 7.67 (d, *J* = 7.8 Hz, 1H), 7.36-7.34 (m, 2H), 7.28 (d, *J* = 0.8 Hz, 1H), 7.19 (d, *J* = 7.9 Hz, 1H), 4.02 (t, *J* = 6.5 Hz, 2H), 3.11 (t, *J* = 5.9 Hz, 2H), 2.71-2.67 (m, 4H), 2.45 (s, 3H), 1.69-1.59 (m, 6H), 1.36-1.18 (m, 18H).; ^{13}C NMR: (125 MHz, $CDCl_3$) 206.6, 155.6, 150.7, 144.5, 134.9, 133.1, 129.7, 127.9, 126.3, 123.4, 70.6, 36.3, 31.2, 29.6, 29.5, 29.47, 29.41, 29.39, 29.3, 29.2, 28.8, 28.7, 25.6, 25.2, 21.5; IR (cm^{-1}): 2917, 2851, 1712, 1607, 1472, 1433, 1360, 1228, 1186, 1171, 1095, 1030, 977, 955, 832, 807, 794, 719, 689, 668, 644; HRMS (ESI) *m/*z calculated for $C_{30}H_{42}O_4S$ $(M + Na)^+$: 521.2702, found: 521.2698.

General procedure for thioacetate synthesis

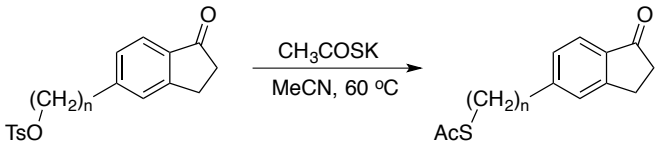

To a stirred solution of tosylate **38** (173 mg, 0.391 mmol) in anhydrous acetonitrile (25 mL) was added potassium thioacetate (89 mg, 0.782 mmol) in one portion. The resulting mixture was then brought to 60 ^{o}C and left to stir overnight. The reaction was quenched by addition of H_2O (40 mL), and extracted with CH_2Cl_2 (50 mL, three times). Organic layers were then combined, washed with brine (50 mL), dried over Na_2SO_4, filtered, and concentrated. Purification by silica gel chromatography (15% EtOAc/Hexanes) afforded **43** as an amorphous solid (114 mg, 84%).

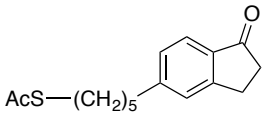

5-Carbon chain thioacetate indanone (41). R_f 0.39 (20% EtOAc/Hex); ^{1}H NMR: (500 MHz, $CDCl_3$) δ 7.65 (d, *J* = 7.8 Hz, 1H), 7.26 (s, 1H), 7.16 (dd, *J* = 7.8, 0.6 Hz, 1H), 3.09 (t, *J* = 5.9 Hz, 2H), 2.84 (t, *J* = 7.3 Hz, 2H), 2.69-2.64 (m, 4H), 2.30 (s, 3H), 1.68-1.56 (m, 4H), 1.43-1.37 (m, 2H).; ^{13}C NMR: (125 MHz, $CDCl_3$) 206.6, 195.9, 155.7, 150.2, 135.1, 127.9, 126.4, 123.6, 36.4, 36.1, 30.68, 30.63, 29.3, 28.9, 28.3, 25.7; IR (cm^{-1}): 2930, 2857, 1710, 1608, 1435, 1353, 1330, 1284, 1230, 1134, 1104, 1030, 956, 813, 627, 586; HRMS (ESI) *m/*z calculated for $C_{16}H_{20}O_2S$ $(M + H)^+$: 277.1262, found: 277.1264.

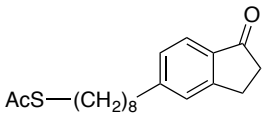

8-Carbon chain thioacetate indanone (42). R_f 0.65 (30% EtOAc/Hex); ^{1}H NMR: (500 MHz, $CDCl_3$) δ 7.65 (d, *J* = 7.8 Hz, 1H), 7.26 (s, 1H), 7.17 (d, *J* = 7.8 Hz, 1H), 3.09 (t, *J* = 5.7 Hz, 2H), 2.84 (t, *J* = 7.3 Hz, 2H), 2.66 (q, *J* = 6.7 Hz, 4H), 2.30 (s, 3H), 1.62 (q, *J* = 7.1 Hz, 2H), 1.55 (quintet, *J* = 7.2 Hz, 2H), 1.31-1.23 (m, 8H); ^{13}C NMR: (125 MHz, $CDCl_3$) 206.3, 195.7, 155.5, 150.4, 134.9, 127.8, 126.2, 123.4, 36.3, 36.2, 31.0, 30.4, 30.0, 29.3, 29.1, 29.0, 28.9, 28.8, 28.5, 25.5; IR (cm^{-1}): 3009, 2926, 2854, 1694, 1608, 1439, 1353, 1330, 1282, 1245, 1230, 1192, 1133, 1105, 1030, 954, 886, 835, 814, 763, 724, 673, 627, 586; HRMS (ESI) *m/*z calculated for $C_{19}H_{26}O_2S$ $(M + H)^+$: 319.1732, found: 319.1729.

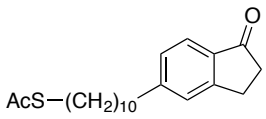

10-Carbon chain thioacetate indanone (43). R_f 0.57 (20%

EtOAc/Hex); ^{1}H NMR: (500 MHz, $CDCl_3$) δ 7.67 (d, *J* = 7.9 Hz, 1H), 7.28 (s, 1H), 7.19 (d, *J* = 7.9 Hz, 1H), 3.11 (t, *J* = 5.8 Hz, 2H), 2.86 (t, *J* = 7.4 Hz, 2H), 2.69-2.66 (m, 4H), 2.32 (s, 3H), 1.63 (dt, *J* = 14.7, 7.4 Hz, 2H), 1.56 (dq, *J* = 14.3, 7.0 Hz, 2H), 1.31 (dd, *J* = 21.5, 15.0 Hz, 10H); ^{13}C NMR: (125 MHz, $CDCl_3$) 206.5, 195.9, 155.6, 150.6, 134.9, 127.9, 126.2, 123.4, 36.3, 31.2, 30.5, 29.4, 29.3, 29.1, 29.0, 28.9, 28.7, 25.6; IR (cm^{-1}): 2921, 2851, 1697, 1686, 1608, 1469, 1444, 1352, 1334, 1294, 1234, 1132, 1106, 1031, 958, 818, 766, 721, 638; HRMS (ESI) *m/*z calculated for $C_{21}H_{30}O_2S$ $(M + Na)^+$: 369.1864, found: 369.1865.

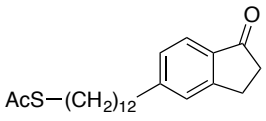

12-Carbon chain thioacetate indanone (44). R_f 0.63 (20% EtOAc/Hex); ^{1}H NMR: (500 MHz, $CDCl_3$) δ 7.69 (d, *J* = 7.8 Hz, 1H), 7.29 (s, 1H), 7.21 (d, *J* = 7.8 Hz, 1H), 3.13 (dd, *J* = 7.6, 4.1 Hz, 2H), 2.88 (t, *J* = 7.4 Hz, 2H), 2.72-2.69 (m, 4H), 2.34 (s, 3H), 1.72-1.62 (m, 2H), 1.61-1.54 (m, 2H), 1.37-1.28 (m, 16H); ^{13}C NMR: (125 MHz, $CDCl_3$) 206.6, 196.0, 155.6, 150.7, 135.0, 128.0, 126.3, 123.5, 36.4, 31.2, 30.6, 29.6, 29.5, 29.49, 29.43, 29.2, 29.1, 29.0, 28.8, 25.7; IR (cm^{-1}): 2917, 2851, 1701, 1686, 1607, 1470, 1443, 1352, 1334, 1295, 1273, 1231, 1193, 1135, 1106, 1031, 959, 903, 818, 766, 719, 639; HRMS (ESI) *m/*z calculated for $C_{23}H_{34}O_2S$ $(M + Na)^+$: 397.2177, found: 397.2177.

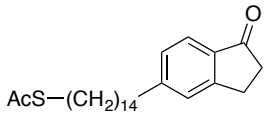

14-Carbon chain thioacetate indanone (45). R_f 0.5 (20% EtOAc/Hex); ^{1}H NMR: (500 MHz, $CDCl_3$) δ 7.69 (d, *J* = 7.8 Hz, 1H), 7.29 (s, 1H), 7.21

(d, J = 7.8 Hz, 1H), 3.12 (dd, J = 5.9, 5.7 Hz, 2H), 2.88 (t, J = 7.4 Hz, 2H), 2.71-2.69 (m, 4H), 2.34 (s, 3H), 1.71-1.62 (m, 2H), 1.61-1.55 (m, 4H), 1.38-1.27 (m, 18H); ^{13}C NMR: (125 MHz, $CDCl_3$) 206.6, 196.0, 155.6, 150.8, 135.0, 128.0, 126.3, 123.5, 36.4, 31.3, 30.6, 29.6, 29.56, 29.53, 29.49, 29.46, 29.2, 29.15, 29.11, 28.8, 25.7; IR (cm^{-1}): 2916, 2849, 1701, 1686, 1607, 1469, 1442, 1428, 1234, 1120, 1030, 958, 818, 654; HRMS (ESI) m/z calculated for $C_{25}H_{38}O_2S$ $(M + Na)^+$: 425.2490, found: 425.2498.

General procedure for oxime synthesis

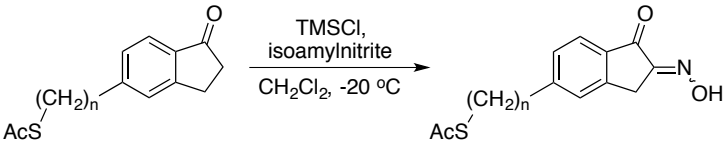

To a stirred solution of indanone **43** (398 mg, 1.148 mmol) in anhydrous CH_2Cl_2 (5 mL) at −20 °C was added TMSCl (0.15 mL, 1.148 mmol) followed by drop-wise addition of isoamy nitrite (0.15 mL, 1.148 mmol). The resulting mixture was left to stir at −20 °C for 1 h. The reaction was quenched by addition of H_2O (1 mL), and the layers were separated. The aqueous layer was extracted with CH_2Cl_2 (3 mL, three times), and the organic layers were combined. The organic layer was washed with brine (2 mL), dried over $MgSO_4$, filtered, and concentrated to afford the oxime **48** (420 mg, quant.).

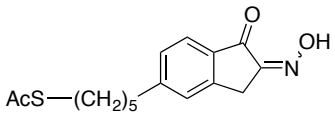

5-Carbon chain thioacetate oxime (46). R_f 0.3 (40% EtOAc/Hex); ^{1}H NMR: (500 MHz, $CDCl_3$) δ 7.82 (d, J = 7.9 Hz, 1H), 7.34 (s, 1H), 7.27 (d, J = 8.0 Hz, 1H), 3.85 (s, 2H), 2.88 (t, J = 7.3 Hz, 2H), 2.73 (t, J = 7.7 Hz, 2H), 2.34 (s, 3H), 1.73-1.60 (m, 5H), 1.47-1.42 (m, 2H).; ^{13}C NMR: (125 MHz, $CDCl_3$) δ 196.1, 189.2,

155.4, 152.3, 147.4, 135.8, 128.7, 126.5, 124.7, 36.4, 30.67, 30.56, 29.3, 28.9, 28.32, 28.26; IR (cm^{-1}): 3497, 3386, 2925, 2858, 1707, 1688, 1649, 1608, 1491, 1340, 1279, 1139, 1112, 1043, 948, 922, 910, 843; HRMS (ESI) *m/z* calculated for $C_{16}H_{19}NO_3S$ $(M + Na)^+$: 328.0983, found: 328.0993.

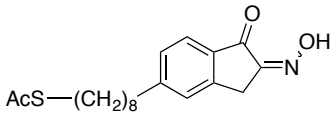

8-Carbon chain thioacetate oxime (47). R_f 0.36 (40% EtOAc/Hex); ^1H NMR: (500 MHz, $CDCl_3$) δ 7.82 (d, *J* = 7.9 Hz, 1H), 7.33 (s, 1H), 7.26 (d, *J* = 8.0 Hz, 1H), 3.85 (s, 2H), 2.87 (t, *J* = 7.4 Hz, 2H), 2.72 (t, *J* = 7.7 Hz, 2H), 2.34 (s, 3H), 1.69-1.63 (m, 2H), 1.60-1.54 (m, 2H), 1.34-1.28 (m, 9H); ^{13}C NMR: (125 MHz, $CDCl_3$) 196.2, 189.0, 155.4, 152.6, 147.2, 135.7, 128.6, 126.4, 124.6, 36.6, 31.0, 30.6, 29.4, 29.2, 29.1, 29.0, 28.9, 28.6, 28.2; IR (cm^{-1}): 3247, 2922, 2852, 1726, 1686, 1655, 1608, 1469, 1434, 1407, 1332, 1302, 1273, 1126, 1109, 1037, 959, 946, 924, 905, 832, 773, 755, 691, 634; HRMS (ESI) *m/z* calculated for $C_{19}H_{25}NO_3S$ $(M + Na)^+$: 370.1453, found: 370.1453.

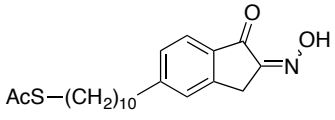

10-Carbon chain thioacetate oxime (48). R_f 0.39 (40% EtOAc/Hex); ^1H NMR: (500 MHz, $CDCl_3$) δ 7.81 (d, *J* = 7.9 Hz, 1H), 7.33 (s, 1H), 7.26 (d, *J* = 7.9 Hz, 1H), 3.85 (s, 2H), 2.87 (t, *J* = 7.4 Hz, 2H), 2.71 (t, *J* = 7.7 Hz, 2H), 2.34 (s, 3H), 1.66 (dq, *J* = 13.8, 6.9 Hz, 3H), 1.60-1.54 (m, 3H), 1.34-1.28 (m, 11H).; ^{13}C NMR: (125 MHz, $CDCl_3$) 196.2, 189.2, 155.3, 152.8, 147.3, 135.6, 128.7, 126.4, 124.5, 36.6, 31.1, 30.6, 29.4, 29.37, 29.34, 29.2, 29.1, 29.0, 28.7, 28.2; IR (cm^{-1}): 3248, 2919, 2851,

1725, 1685, 1655, 1609, 1581, 1469, 1435, 1409, 1352, 1331, 1302, 1269, 1201, 1132, 1111, 1037, 958, 923, 907, 833, 774, 755, 690, 665, 637; HRMS (ESI) *m/z* calculated for $C_{21}H_{29}NO_3S$ $(M + Na)^+$: 376.1922, found: 376.1940.

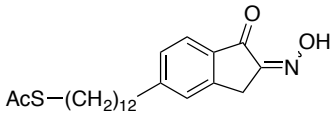

12-Carbon chain thioacetate oxime (49). R_f 0.5 (40% EtOAc/Hex); ^1H NMR: (500 MHz, $CDCl_3$) δ 7.82 (d, *J* = 7.9 Hz, 1H), 7.34 (s, 1H), 7.26 (s, 1H), 3.85 (s, 2H), 2.88 (t, *J* = 7.4 Hz, 2H), 2.72 (t, *J* = 7.7 Hz, 2H), 2.34 (s, 3H), 1.70-1.64 (m, 2H), 1.60-1.54 (m, 2H), 1.36-1.27 (m, 17H); ^{13}C NMR: (125 MHz, $CDCl_3$) 196.2, 189.0, 155.4, 152.7, 147.2, 135.7, 128.7, 126.4, 124.5, 36.6, 31.1, 30.6, 29.53, 29.5, 29.46, 29.42, 29.3, 29.2, 29.1, 29.0, 28.7, 28.2; IR (cm^{-1}): 3258, 2916, 2851, 1726, 1685, 1655, 1610, 1581, 1470, 1406, 1353, 1332, 1303, 1272, 1113, 1037, 960, 922, 906, 832, 755, 756, 689, 640; HRMS (ESI) *m/z* calculated for $C_{23}H_{33}NO_3S$ $(M + Na)^+$: 426.2079, found: 426.2081.

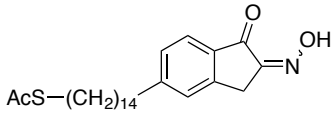

14-Carbon chain thioacetate oxime (50). R_f 0.53 (40% EtOAc/Hex); ^1H NMR: (500 MHz, $CDCl_3$) δ 7.81 (d, *J* = 7.8 Hz, 1H), 7.33 (s, 1H), 7.28 (d, *J* = 2.7 Hz, 1H), 3.85 (s, 2H), 2.87 (t, *J* = 7.2 Hz, 2H), 2.72 (t, *J* = 7.3 Hz, 2H), 2.33 (s, 3H), 1.67-1.63 (m, 2H), 1.60-1.54 (m, 2H), 1.34-1.32 (m, 21H); ^{13}C NMR: (125 MHz, $CDCl_3$) 196.2, 189.1, 155.3, 152.7, 147.3, 135.7, 128.7, 126.4, 124.5, 36.6, 31.1, 30.6, 29.57, 29.53, 29.4, 29.3, 29.2, 29.1, 29.0, 28.7, 28.2; IR (cm^{-1}): 3252, 2916, 2849, 1726, 1685, 1655, 1609, 1470, 1435, 1353, 1332, 1303, 1270, 1139, 1120, 1037, 959, 923, 907,

833, 774, 754, 690, 663, 639; HRMS (ESI) *m/*z calculated for $C_{25}H_{37}NO_3S$ $(M + Na)^+$: 454.2392, found: 454.2387.

General procedure for 1,2-indanedione synthesis

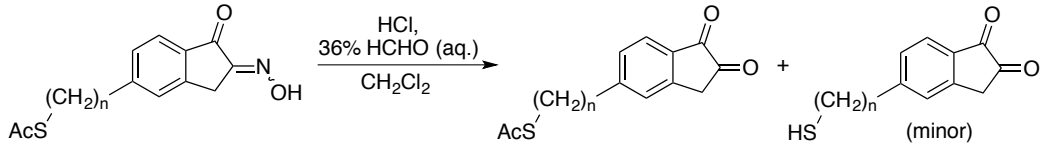

To a stirred solution of **47** (189 mg, 0.543 mmol) in CH_2Cl_2 (5.4 mL) was added aqueous formaldehyde (37% in water, 0.3 mL) followed by conc. HCl (0.6 mL). The resulting mixture was left to stir at room temperature overnight. The reaction was quenched with cold H_2O (5 mL), and the layers were separated. The aqueous layer was extracted with CH_2Cl_2 (5 mL, three times), and the organic layers were combined. The organic layer was washed with brine (5 mL), dried over $MgSO_4$, filtered, and concentrated to afford **52** as a mixture with thioacetate removed thiol, which was used without further purification.

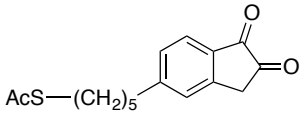

5-Carbon chain thioacetate 1,2-indanedione (51). R_f 0.52 (40% EtOAc/Hex); ^{1}H NMR: (500 MHz, $CDCl_3$) δ 7.84 (d, *J* = 7.9 Hz, 1H), 7.37 (s, 1H), 7.31 (d, *J* = 7.9 Hz, 1H), 3.60 (s, 2H), 2.87 (t, *J* = 7.3 Hz, 2H), 2.75 (t, *J* = 7.7 Hz, 2H), 2.33 (s, 3H), 1.74-1.60 (m, 6H), 1.48-1.41 (m, 4H); ^{13}C NMR: (125 MHz, $CDCl_3$) 200.2, 195.8, 186.4, 154,0, 146.9, 135.1, 129.2, 126.9, 125.7, 36.6, 36.5, 30.5, 30.3, 29.2, 28.7, 28.2; IR (cm^{-1}): 2932, 2858, 1764, 1719, 1688, 1609, 1437, 1391, 1353, 1263, 1134, 949, 837, 752, 627; HRMS (ESI) *m/*z calculated for $C_{16}H_{18}O_3S$ $(M + H)^+$: 291.1055, found: 291.1060.

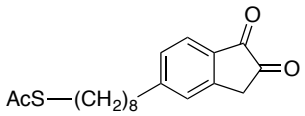

8-Carbon chain thioacetate 1,2-indanedione (52). R_f 0.6 (40% EtOAc/Hex); ^{1}H NMR: (500 MHz, $CDCl_3$) δ 7.83 (d, *J* = 7.9 Hz, 1H), 7.37 (s, 1H), 7.31 (d, *J* = 8.0 Hz, 1H), 3.60 (s, 2H), 2.85 (t, *J* = 7.4 Hz, 2H), 2.74 (t, *J* = 7.7 Hz, 2H), 2.32 (s, 3H), 1.70-1.64 (m, 3H), 1.56 (dt, *J* = 14.6, 7.3 Hz, 3H), 1.35 (dd, *J* = 13.3, 5.8 Hz, 6H).; ^{13}C NMR: (125 MHz, $CDCl_3$) 200.3, 195.9, 186.4, 154.4, 146.8, 135.1, 129.2, 126.9, 125.6, 36.8, 36.5, 30.8, 30.5, 29.4, 29.1, 29.0, 28.9, 28.8, 28.6; IR (cm^{-1}): 3520, 2421, 3354, 3050, 2921, 2852, 2254, 1900, 1768, 1714, 1613, 1580, 1468, 1434, 1386, 1354, 1329, 1304, 1261, 1203, 1118, 1099, 951, 824, 755, 724, 667, 632; HRMS (ESI) *m/*z calculated for $C_{19}H_{24}O_3S$ $(M + H)^+$: 333.1524, found: 333.1521.

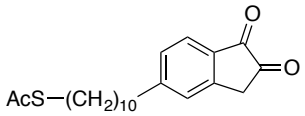

10-Carbon chain thioacetate 1,2-indanedione (53). R_f 0.65 (40% EtOAc/Hex); ^{1}H NMR: (500 MHz, $CDCl_3$) δ 7.86 (d, *J* = 7.9 Hz, 1H), 7.38 (s, 1H), 7.33 (d, *J* = 7.9 Hz, 1H), 3.61 (s, 2H), 2.89-2.86 (m, 2H), 2.76 (t, *J* = 7.7 Hz, 2H), 2.34 (s, 3H), 1.72-1.64 (m, 3H), 1.62-1.54 (m, 3H), 1.38-1.28 (m, 10H); ^{13}C NMR: (125 MHz, $CDCl_3$) 200.3, 196.0, 186.4, 154.6, 146.8, 135.1, 129.2, 126.9, 125.7, 36.9, 36.6, 30.9, 30.6, 29.6, 29.4, 29.37, 29.34, 29.2, 29.1, 29.0, 28.7; IR (cm^{-1}): 2920, 2851, 1765, 1715, 1686, 1612, 1468, 1435, 1352, 1331, 1302, 1268, 1201, 1117, 1098, 954, 923, 907, 833, 774, 755, 690, 637; HRMS (ESI) *m/*z calculated for $C_{21}H_{28}O_3S$ $(M + Na)^+$: 383.1657, found: 383.1644.

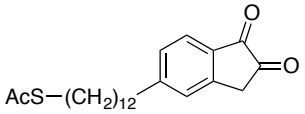

12-Carbon chain thioacetate 1,2-indanedione (54). R_f 0.71 (40% EtOAc/Hex); ^{1}H NMR: (500 MHz, $CDCl_3$) δ 7.85 (d, *J* = 7.9 Hz, 1H), 7.38 (s, 1H), 7.33-7.32 (m, 1H), 3.61 (s, 2H), 2.87 (t, *J* = 7.3 Hz, 2H), 2.75 (t, *J* = 7.7 Hz, 2H), 2.34 (s, 3H), 1.71-1.65 (m, 3H), 1.60-1.54 (m, 3H), 1.36-1.27 (m, 14H).; ^{13}C NMR: (125 MHz, $CDCl_3$) 200.4, 196.0, 186.4, 154.6, 146.8, 135.1, 129.2, 126.9, 125.7, 36.9, 36.5, 30.9, 30.6, 29.5, 29.49, 29.45, 249.41, 29.3, 29.2, 29.1, 29.0, 28.7; IR (cm^{-1}): 2918, 2850, 1766, 1716, 1694, 1611, 1469, 1434, 1384, 1353, 1328, 1304, 1267, 1136, 1118, 951, 8223, 718, 630; HRMS (ESI) *m/*z calculated for $C_{23}H_{32}O_3S$ $(M + Na)^+$: 411.1970, found: 411.1973.

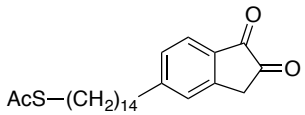

14-Carbon chain thioacetate 1,2-indanedione (55). R_f 0.7 (40% EtOAc/Hex); ^{1}H NMR: (500 MHz, $CDCl_3$) δ 7.85 (d, *J* = 8.0 Hz, 1H), 7.38 (s, 1H), 7.33 (d, *J* = 8.0 Hz, 1H), 3.61 (s, 2H), 2.87 (t, *J* = 7.4 Hz, 2H), 2.75 (t, *J* = 7.7 Hz, 2H), 2.33 (s, 3H), 1.71-1.54 (m, 8H), 1.36-1.27 (m, 16H); ^{13}C NMR: (125 MHz, $CDCl_3$) 200.4, 196.0, 186.4, 154.6, 146.8, 135.1, 129.2, 126.9, 125.7, 36.9, 36.5, 30.9, 30.6, 29.6, 29.5, 29.47, 29.43, 29.3, 29.2, 29.1, 29.0, 28.7; IR (cm^{-1}): 2919, 2849, 1765, 1719, 1693, 1610, 1470, 1437, 1385, 1351, 1328, 1262, 1118, 948, 823, 718, 630; HRMS (ESI) *m/*z calculated for $C_{25}H_{36}O_3S$ $(M + Na)^+$: 439.2283, found: 439.2278.

General procedure for synthesis and functionalization of AuNPs with 1,2-indanedione analogues

Following Klabunde's procedure,[45] a solution of dodecyldimethylammonium bromide (0.02 M) was prepared in 2.5 mL of anhydrous toluene. To this was added $AuCl_3$ (8.5

mg), and the resulting mixture was sonicated until complete dissolution was evident (homogeneous dark orange solution). Freshly prepared 9.4 M aqueous solution of $NaBH_4$ (50 μL) was quickly added to the vortex of the vigorously stirring solution. The resulting mixture was left to stir vigorously for additional 15-20 min to afford the "as-prepared" gold colloid. In a separate vial containing **53** (151 mg, 0.420 mmol) dissolved in anhydrous toluene (2 mL) was added to the solution containing gold colloid via syringe. The resulting mixture was left to stir vigorously for 24 h at room temperature to allow ligand exchange. The functionalized AuNPs were isolated by precipitation with ethanol (10 mL). The tube containing the functionalized AuNPs were centrifugated at 5000 rpm for 5 min cycles three times. After each cycle, the supernatant was decanted and discarded, and fresh EtOH (10 mL) was added. After final centrifugation, the supernatant was decanted, and the resulting AuNPs were dried under vacuum. The dried AuNPs were redispersed in acetonitrile (2.5 mL) to be used as part of the working solution for fingerprint development.

General procedure for development of fingerprints on paper

Following Almog's procedure,[34] the paper substrate containing latent fingerprint deposits was immersed in an aqueous solution of maleic acid (2.5% w/v in water) for 10 min or until no bubbles were apparent. The paper was then air-dried, and subsequently immersed in the working solution containing functionalized AuNPs (5 min-30 min). The paper was air-dried, and immersed in the Ag-PD solution (Arrowhead Scientific Inc.) until visible marks appeared (1-2 min). The paper substrate was then removed and washed with two successive water baths: Milli-Q followed by tap water.

5.8) References

[1] Forensic Science Central forensicsciencecentral.co.uk/edmondlocard.shtml (accessed in July 1, 2014).

[2] Jelly, R., Patton, E. L. T., Lennard, C., Lewis, S. W., Lim, K. F. "The detection of latent fingermarks on porous surfaces using amino acid sensitive reagents: A review." *Analytica Chim. Acta* **2009**, *652*, 128-142.

[3] Ramotowski, R. Composition of latent print residue. In *Advances in Fingerprint Technology Second Edition*; Lee, H. C., Gaensslen, R. E. Eds.; CRC Press: Boca Raton, FL, 2001; pp 63-104.

[4] Bramble, S. K., Brennan, J. S. Fingerprints (dactyloscopy): chemistry of print residue. In *Encyclopedia of Forensic Sciences*; Siegel, J., Saukko, P., Knupfer, G. Eds.; Academic Press; Oxford, 2000; pp 862-869.

[5] Ruhemann, S. "Cyclic di- and tri-ketones." *Trans. Chem. Soc.* **1910**, *97*, 1438-1449.

[6] Odén, S., von Hofsten, B. "Detection of fingerprints by the ninhydrin reaction." *Nature* **1954**, *173*, 449-450.

[7] Friedman, M., Williams, L. D. "Stoichiometry of formation of Ruhemann's purple in the ninhydrin reaction." *Bioorg. Chem.* **1974**, *3*, 267-280.

[8] Grigg, R., Malone, J. F., Mongkolaussavaratana, T., Thianpatanagul, S. "Cycloaddition reaction relevant to the mechanism of the ninhydrin reaction. X-Ray crystal structure of protonated Ruhemann's purple, a stable 1,3-dipole." *J. Chem. Soc., Chem. Commun.* **1986**, 421-422.

[9] Hansen, D. B., Joullié, M. M. "The development of novel ninhydrin analogues." *Chem. Soc. Rev.* **2005**, *34*, 408-417.

[10] (a) Hark, R. R., Hauze, D. B., Petrovskaia, O., Joullié, M. M. "Synthetic studies of novel ninhydrin analogs." *Can. J. Chem.* **2001**, *79*, 1632-1654. (b) R. R. Hark, "Synthesis of ninhydrin analogues." University of Pennsylvania, Philadelphia, PA, 1996.

[11] Herod, D. W., Menzel, E. R. "Laser detection of latent fingerprints: Ninhydrin followed by zinc chloride." *J. Forensic. Sci.* **1982**, *27*, 200-204.

[12] Kobus, H. J., Stoilovic, M., Warrener, R. N. "A simple luminescent post-ninhydrin treatment for the improved visualization of fingerprints on documents in cases where ninhydrin alone gives poor results." *Forensic Sci. Int.* **1983**, *22*, 161-170.

[13] (a) Druey, J., Schmidt, P. "Phenanthrolinchinone and diazafluorene." *Helv. Chim. Acta.* **1950**, *33*, 1080-1087. (b) Bonhôte, P., Wrighton, M. S. "Facile synthesis of tetrapyrido[2,3-a:3',2'-c:2'',3''-h:3''',2'''-j]phenazine." *Synlett* **1997**, *8*, 897-898.

[14] Grigg, R., Mongkolaussavaratana, T., Pounds, C. A., Sivagnanam, S. "1,8-Diazafluorenone and related compounds. A new reagent for the detection of a-amino acids and latent fingerprints." *Tetrahedron Lett.* **1990**, *31*, 7215-7218.

[15] (a) Hauze, D. B., Petrovskaia, O., Taylor, B., Joullié, M. M., Ramotowski, R., Cantu, A. A. "1,2-Indanediones: New reagents for visualizing the amino acid components of latent prints." *J. Forensic Sci.* **1998**, *43*, 744-747. (b) Ramotwoski, R., Cantu, A. A., Joullié, M. M., Petrovskaia, O. "1,2-Indanediones: a preliminary evaluation of a new class of amino acid visualizing compounds." *Fingerprint Whorld* **1997**, *23*, 131-140.

[16] Taylor, B. M., Joullié, M. M. "Reaction of 1,2-indanedione with 3,5-dimethoxyaniline." *Tetrahedron* **1998**, *54*,, 15121-15126.

[17] Petrovskaia, O., Taylor, B. M., Hauze, D. B., Carroll, P. J., Joullié, M. M. "Investigations of the reaction mechanism of 1,2-indanediones with amino acids." *J. Org. Chem.* **2001**, *66*, 7666-7675.

[18] Almog, J., Glasner, H. "Ninhydrin thiohemiketals: Basic research towards improved fingermark detection techniques employing nano-technology." *J. Forensic Sci.* **2010**, *55*, 215-220.

[19] Wallace-Kunkel, C., Lennard, C., Stoilovic, M., Roux, C. "Optimisation and evaluation of 1,2-indanedione for use as a fingermark reagent and its application to real samples." *Forensic Sci. Int.* **2007**, *168*, 14-26.

[20] Wilkinson, D. "Spectroscopic study of 1,2-indanedione." *Forensic Sci. Int.* **2000**, *114*, 123-132.

[21] Roux, C., Jones, N., Lennard, C., Stoilovic, M. "Evaluation of 1,2-indanedione and 5,6-dimethoxy-1,2-indanedione for the detection of latent fingerprints on porous surfaces." *J. Forensic. Sci.* **2000**, *45*, 761-769.

[22] Bicknell, D. E., Ramotowski, R. S. "Use of an optimized 1,2-indanedione process for the development of latent prints." *J. Forensic. Sci.* **2008**, *53*, 1108-1116.

[23] Spindler, X., Shimmon, R., Roux, C., Lennard, C. "The effect of zinc chloride, humidity and the substrate on the reaction of 1,2-indanedione-zinc with amino acids in latent fingermark secretions." *Forensic Sci. Int.* **2011**, *212*, 150-157.

[24] Stoilovic, M., Lennard, C., Wallace-Kunkel, C., Roux, C. "Evaluation of a 1,2-indanedione formulation containing zinc chloride for improved fingermark detection on paper." *J. Forensic Ident.* **2007**, *57*, 4-18.

[25] Marriott, C., Lee, R., Wilkes, Z., Comber, B., Spindler, X., Roux, C., Lennard, C. "Evaluation of fingermark detection sequences on paper substrates." *Forensic Sci. Int.* **2014**, *236*, 30-37.

[26] Selected recent examples: (a) Fritz, P., van Bronswijk, W., Lewis, S. W. "*p*-Dimethylaminobenzaldehyde: preliminary investigations into a novel reagent for the detection of latent fingermarks on paper surfaces." *Anal. Methods.* **2013**, *5*, 3207-3215. (b) Frick, A. A., Busetti, F., Cross, A., Lewis, S. W. "Aqueous nile blue: a simple, versatile and safe reagent for the detection of latent fingermarks." *Chem. Commun.* **2014**, *50*, 3341-3343. (c) Bentolila, A., Totre, J., Zozulia, I., Levin-Elad, M., Domb, A. J. "Fluorescent cyanoacrylate monomers and polymers for fingermark development." *Macromolecules* **2013**, *46*, 4822-4828.

[27] (a) Cantu, A. A. "Silver physical developers for the visualization of latent prints on paper." *Forensic Sci. Rev.* **2001**, *13*, 29-64. (b) Burow, D., Seifert, D., Cantu, A. A. "Modifications to the silver physical developer." *J. Forensic Sci.* **2003**, *48*, 1094-1101.

[28] (a) Cantu, A. A., Johnson, J. L. Silver physical development of latent prints. In *Advances in Fingerprint Technology Second Edition*; Lee, H. C., Gaensslen, R. E. Eds.; CRC Press: Boca Raton, FL, 2001; pp 241-274. (b) Schnetz, B., Margot, P. "Technical note: latent fingermarks, colloidal gold and multimetal deposition (MMD). Optimisation of the method." *Forensic Sci. Int.* **2001**, *118*, 21-28.

[29] Stauffer, E., Becue, A., Singh, K. V., Thampi, K. R., Champod, C., Margot, P. "Single-metal deposition (SMD) as a latent fingermark enhancement technique: An alternative to multimetal deposition (MMD)." *Forensic Sci. Int.* **2007**, *168*, e5-e9.

[30] Selected references: (a) Hazarika, P., Russell, D. A. "Advances in fingerprint analysis." *Angew. Chem. Int. Ed.* **2012**, *51*, 3524-3531. (b) Becue, A., Scoundrianos, A., Champod, C., Margot, P. "Fingermark detection based on the in situ growth of luminescent nanoparticles—Towards a new generation of multimetal deposition." *Forensic Sci. Int.* **2008**, *179*, 39-43. (c) Becue, A., Champod, C., Margot, P. "Use of gold nanoparticles as molecular intermediates for the detection of fingermarks." *Forensic Sci. Int.* **2007**, *168*, 169-176. (d) Spindler, X., Hofstetter, O., McDonagh, A. M., Roux, C., Lennard, C. "Enhancement of latent fingermarks on non-porous surfaces using anti-L-amino acid antibodies conjugated to gold nanoparticles." *Chem. Commun.* **2011**, *47*, 5602-5604.

[31] Aslam, M., Mulla, I. S., Vijayamohanan K. "Hydrophobic organization of monolayer-protected Au clusters on thiol-functionalized Au(111) surfaces." *Langmuir* **2001**, *17*, 7487-7493.

[32] Sametband, M., Shweky, I., Banin, U., Mandler, D., Almog, J. "Application of nanoparticles for the enhancement of latent fingerprints." *Chem. Commun.* **2007**, 1141-1144.

[33] Takatsu, M., Kageyama, H., Hirata, K., Akashi, S., Yoko, T., Tatsuo S., et al. "Development of a new method to detect latent fingerprint on thermal paper with o-alkyl derivative of ninhydrin." *Tokyo: National Research Institute of Police Science* **1991**, *44*, 1-6.

[34] Jaber, N., Lesniewski, A., Gabizon, H., Shenawi, S., Mandler, D., Almog, J. "Visualization of latent fingermarks by nanotechnology: Reversed development on paper—a remedy to the variation in sweat composition." *Angew. Chem. Int. Ed.* **2012**, *51*, 12224-12227.

[35] Shenawi, S., Jaber, N., Almog, J., Mandler, D. "A novel approach to fingerprint visualization on paper using nanotechnology: reversing the appearance by tailoring the gold nanoparticles' capping ligands." *Chem. Commun.* **2013**, *49,* 3688-3690.

[36] (a) Selvam, T., Chiang, C.-M., Chi, K.-H. "Organic-phase synthesis of self-assembled gold nanosheets." *J. Nanopart. Res.* **2011**, *13*, 3275-3286. (b) Cho, E. C., Choi, S.-W., Camargo, P. H. C., Xia, Y. "Thiol-induced assembly of Au nanoparticles into chainlike structures and their fixing by encapsulation in silica shells or gelatin microspheres." *Langmuir* **2010**, *26*, 10005-10012. (c) Wang, G., Guo, R., Kalyuzhny, G., Choi, J.-P., Murray, R. W. "NIR luminescence intensities increase linearly with proportion of polar thiolate ligands in protecting monolayers of Au_{38} and Au_{140} quantum dots." *J. Phys. Chem. B.* **2006**, *110*, 20282-20289.

[37] Corsaro, A., Chiacchio, U., Pistarà, V. "Regeneration of carbonyl compounds from the corresponding oximes." *Synthesis* **2001**, 1903-1931.

[38] Gupta, P. K., Manral, L., Ganesan, K. "An efficient approach for the conversion of oximes into carbonyl compounds using dichloramine-T." *Synthesis* **2007**, 1930-1932.

[39] Fréchet, J. M. J., Darling, P., Farrall, M. J. "Poly(vinylpyridinium dichromate): An inexpensive recyclable polymeric reagent." *J. Org. Chem.* **1981**, *46*, 1728-1730.

[40] Quan, N., Shi, X.-X., Nie, L.-D., Dong, J., Zhu, R.-H. "A green chemistry method for the regeneration of carbonyl compounds from oximes by using cupric chloride dehydrate as a recoverable promoter for hydrolysis." *Synlett* **2011**, 1028-1032.

[41] Dreher, S. D., Lim, S.-E., Sandrock, D. L., Molander, G. A. "Suzuki-Miyaura cross-coupling reactions of primary alkyltrifluoroborates with aryl chlorides." *J. Org. Chem.* **2009**, *74*, 3626-3631.

[42] Biscoe, M. R., Fors, B. P., Buchwald, S. L. "A new class of easily activated palladium precatalysts for facile C—N cross-coupling reactions and the low temperature oxidative addition of aryl chlorides." *J. Am. Chem. Soc.* **2008**, *130*, 6686-6687.

[43] Kinzel, T., Zhang, Y., Buchwald, S. L. "A new palladium precatalyst allows for the fast Suzuki-miyaura coupling reactions of unstable polyfluorophenyl and 2-heteroaryl boronic acids." *J. Am. Chem. Soc.* **2010**, *132*, 14073-14075.

[44] Kotiaho, A., Lahtinen, R., Efimov, A., Metsberg, H., Sariola, E., Lehtivuori, H., Tkachenko, N. V., Lemmetyinen, H. "Photoinduced charge and energy transfer in phthalocyanine-functionalized gold nanoparticles." *J. Phys. Chem. C* **2010**, *114*, 162-168.

[45] Prasad, B. L. V., Stoeva, S. I., Sorensen, C. M., Klabunde, K. J. "Digestive ripening of thiolated gold nanoparticles: The effect of alkyl chain length." *Langmuir* **2002**, *18*, 7515-7520.

[46] Kotiaho, A., Lahtinen, R., Efimov, A., Lehtivuori, H., Tkachenko, N. V., Kanerva, T., Lemmetyinen, H. "Synthesis and time-resolved fluorescence study of porphyrin-functionalized gold nanoparticles." *J. Photochem. Photobiol. A—Chemistry* **2010**, *212*, 129-134.

[47] Fritz, P., van Bronswijk, W., Patton, E., Lewis, S. W. "Variability in visualization of latent fingermarks developed with 1,2-indanedione—zinc chloride." *J. Forensic Ident.* **2013**, *63*, 798-713.

[48] Sauzier, G., Frick, A. A., Lewis, S. W. "Investigation into the performance of physical developer formulations for visualizing latent fingerprints on paper." *J. Forensic Ident.* **2013**, *63*, 70-89.

5.9) Appendix D. Nuclear Magnetic Resonance, Infrared, and UV-Vis Spectra Relevant to Chapter 5

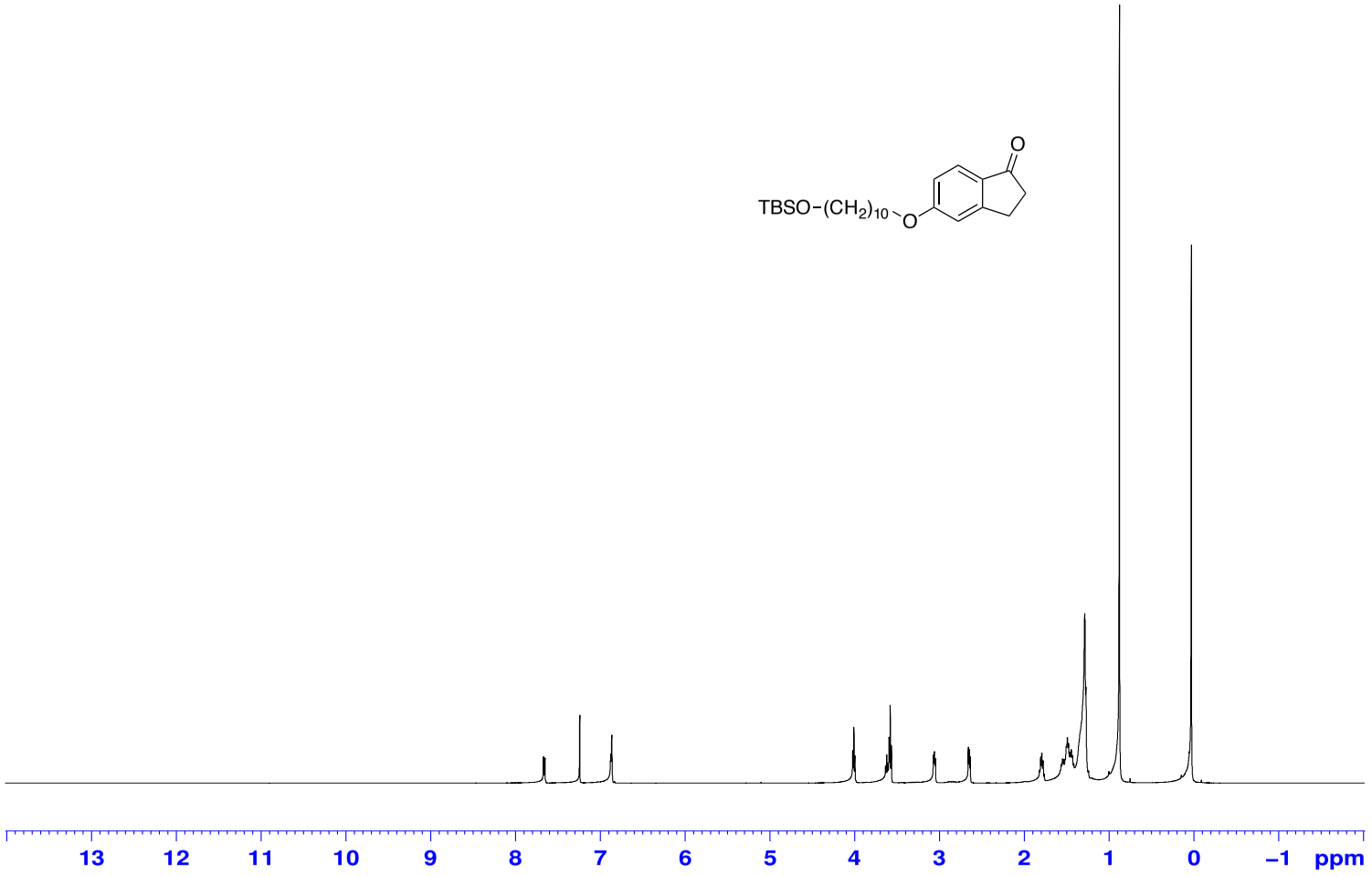

Figure 1: ^{1}H NMR ($CDCl_3$, 500 MHz) of **6**

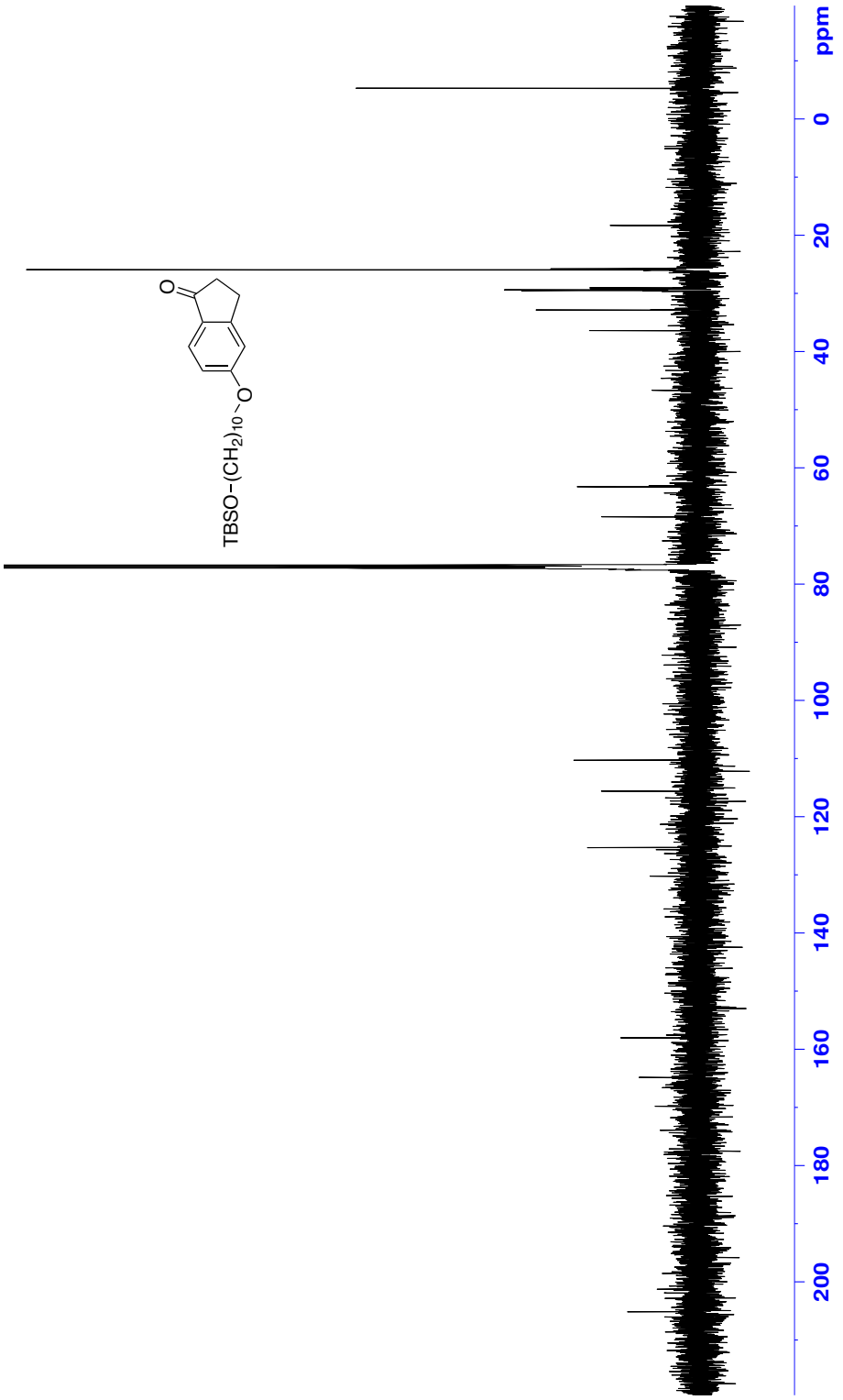

Figure 2: ^{13}C NMR ($CDCl_3$, 125 MHz) of **6**

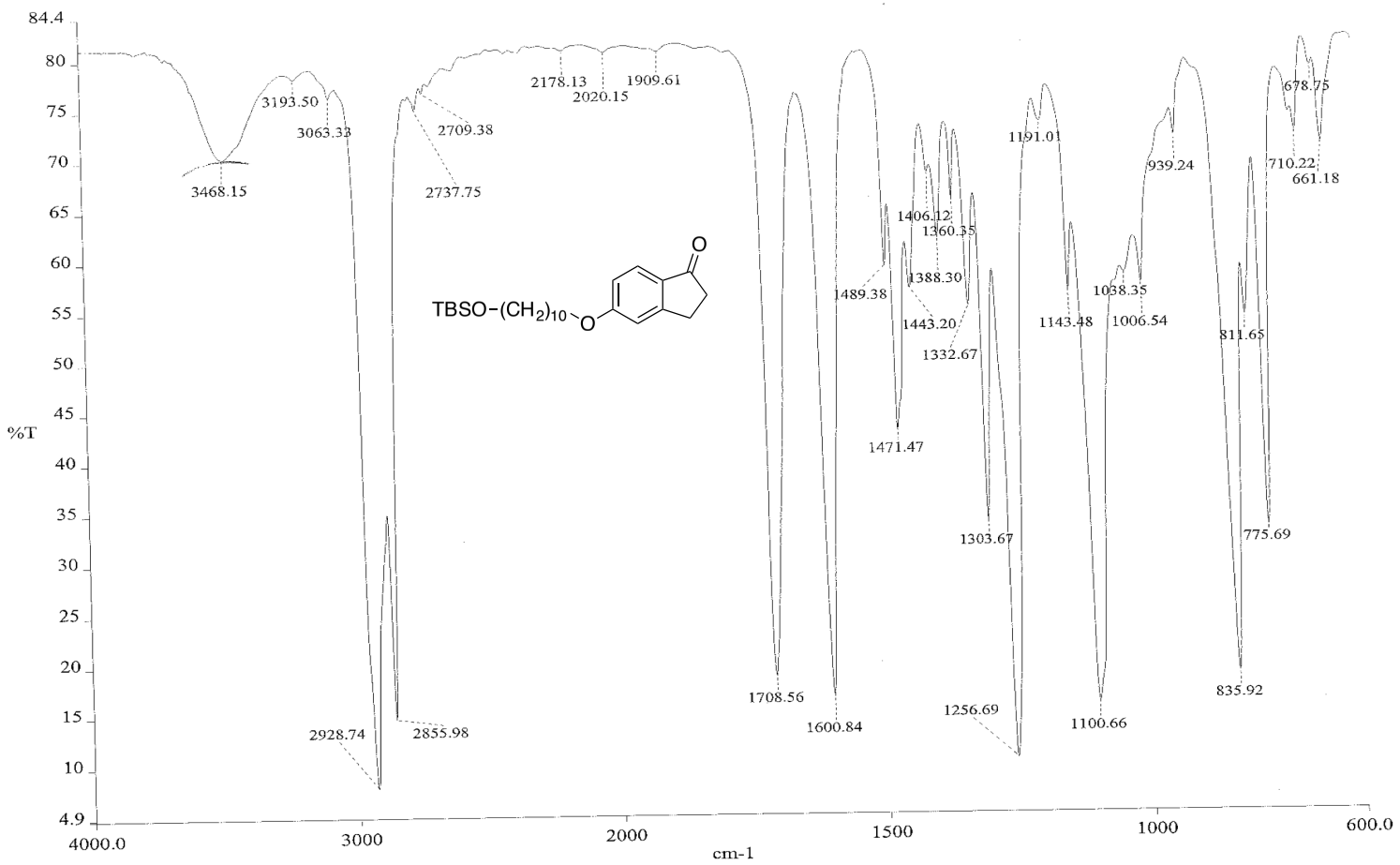

Figure 3: Infrared spectra (neat) of **6**

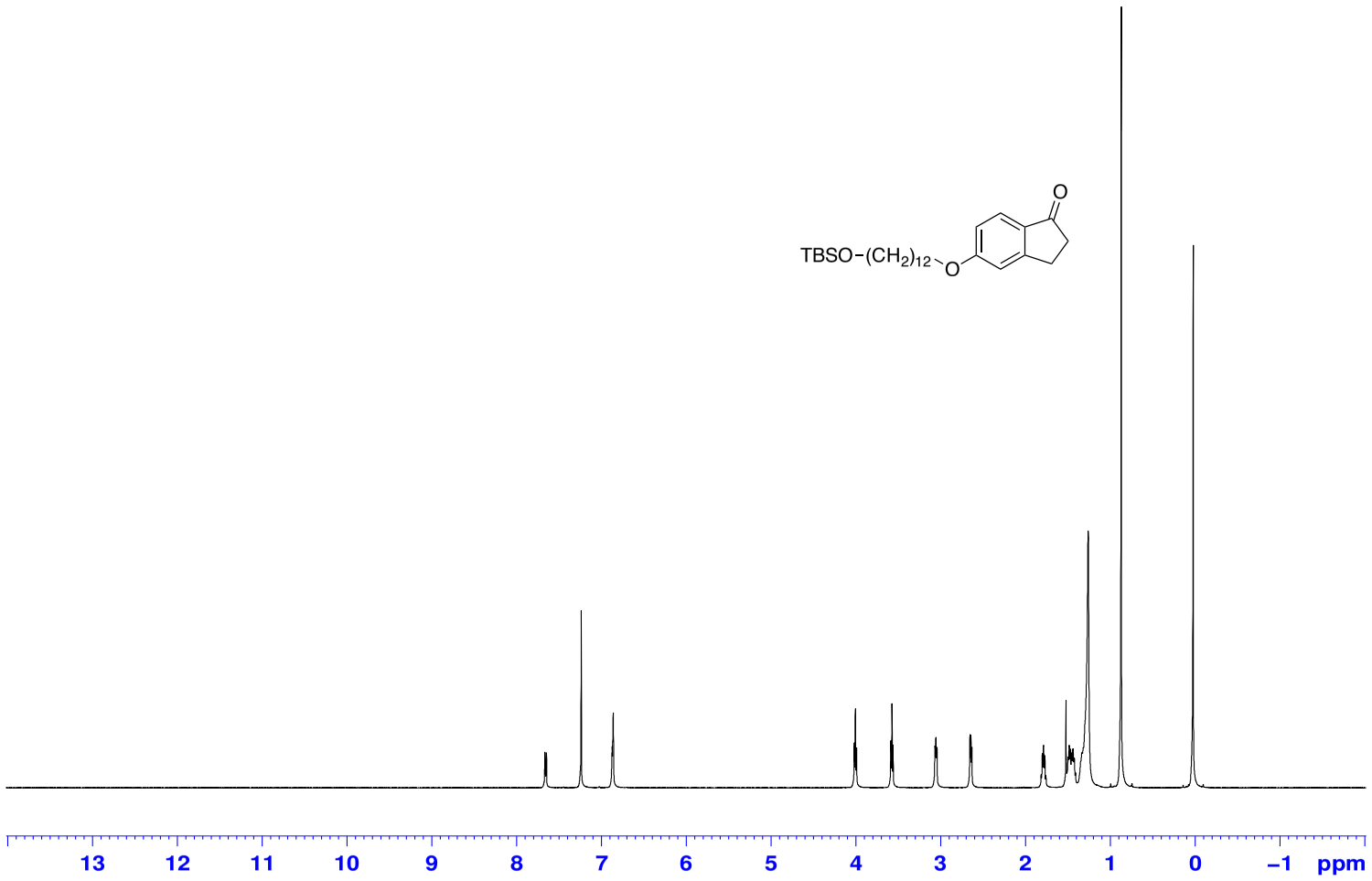

Figure 4: ^{1}H NMR ($CDCl_3$, 500 MHz) of **7**

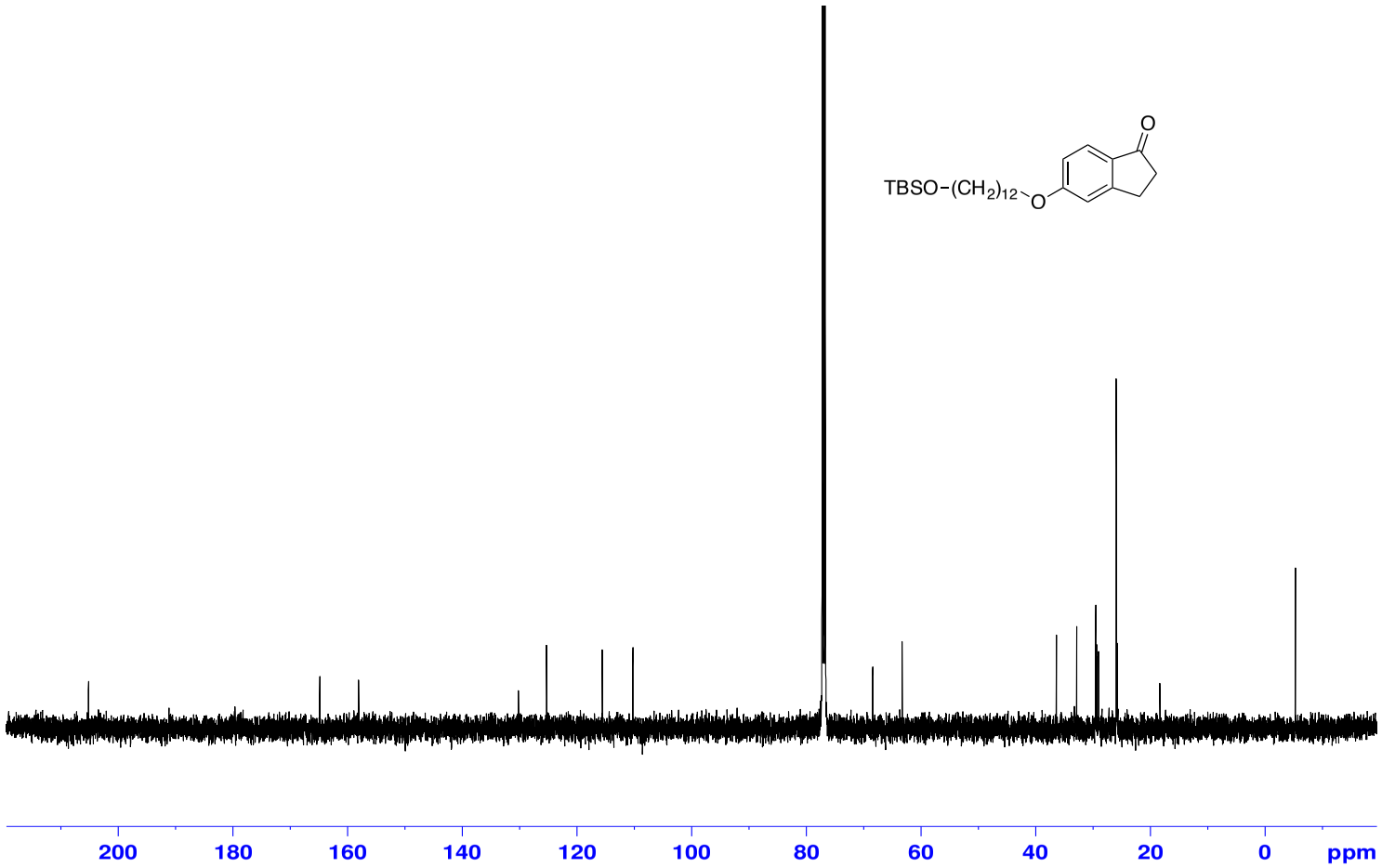

Figure 5: ^{13}C NMR ($CDCl_3$, 125 MHz) of **7**

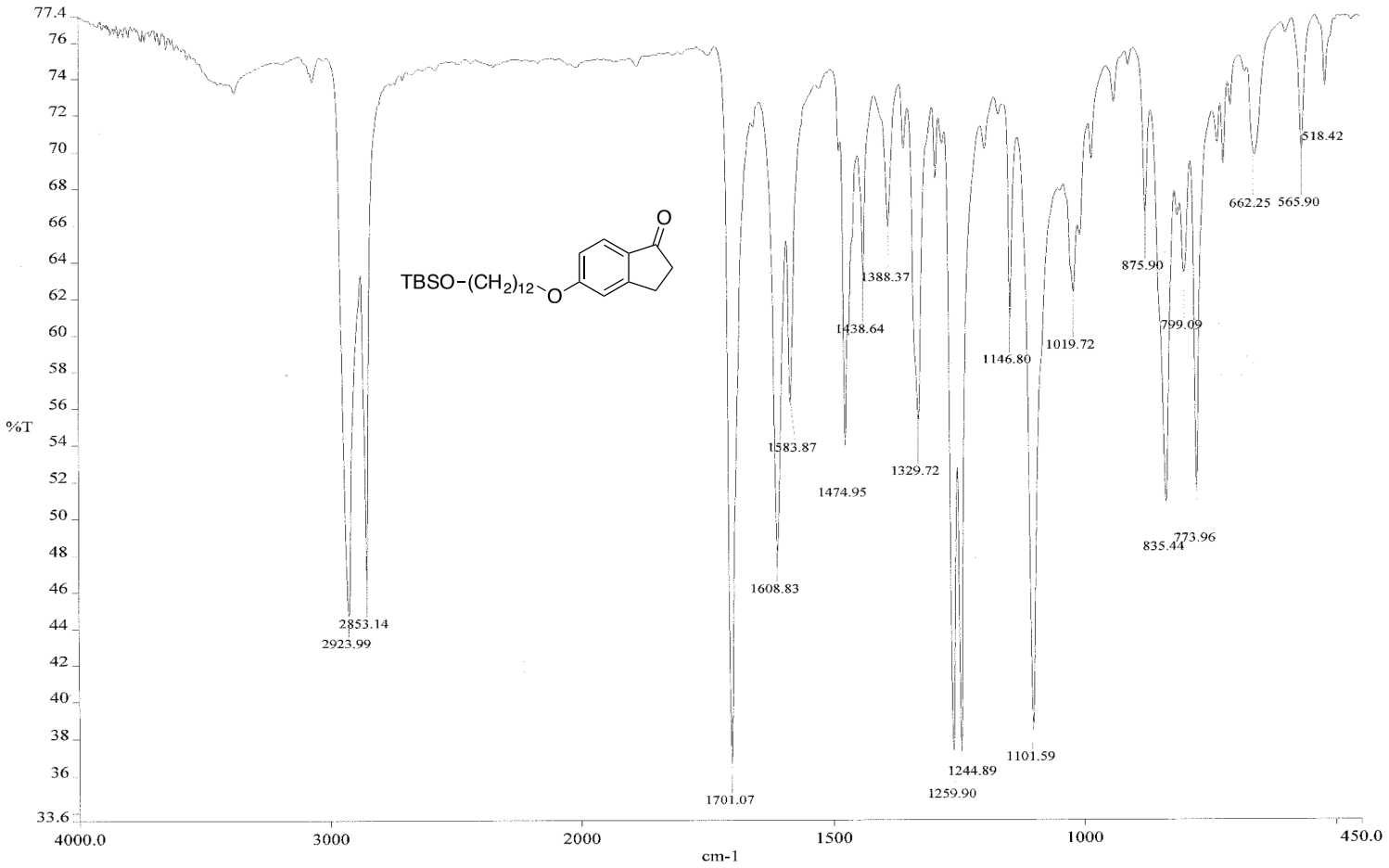

Figure 6: Infrared spectra (neat) of **7**

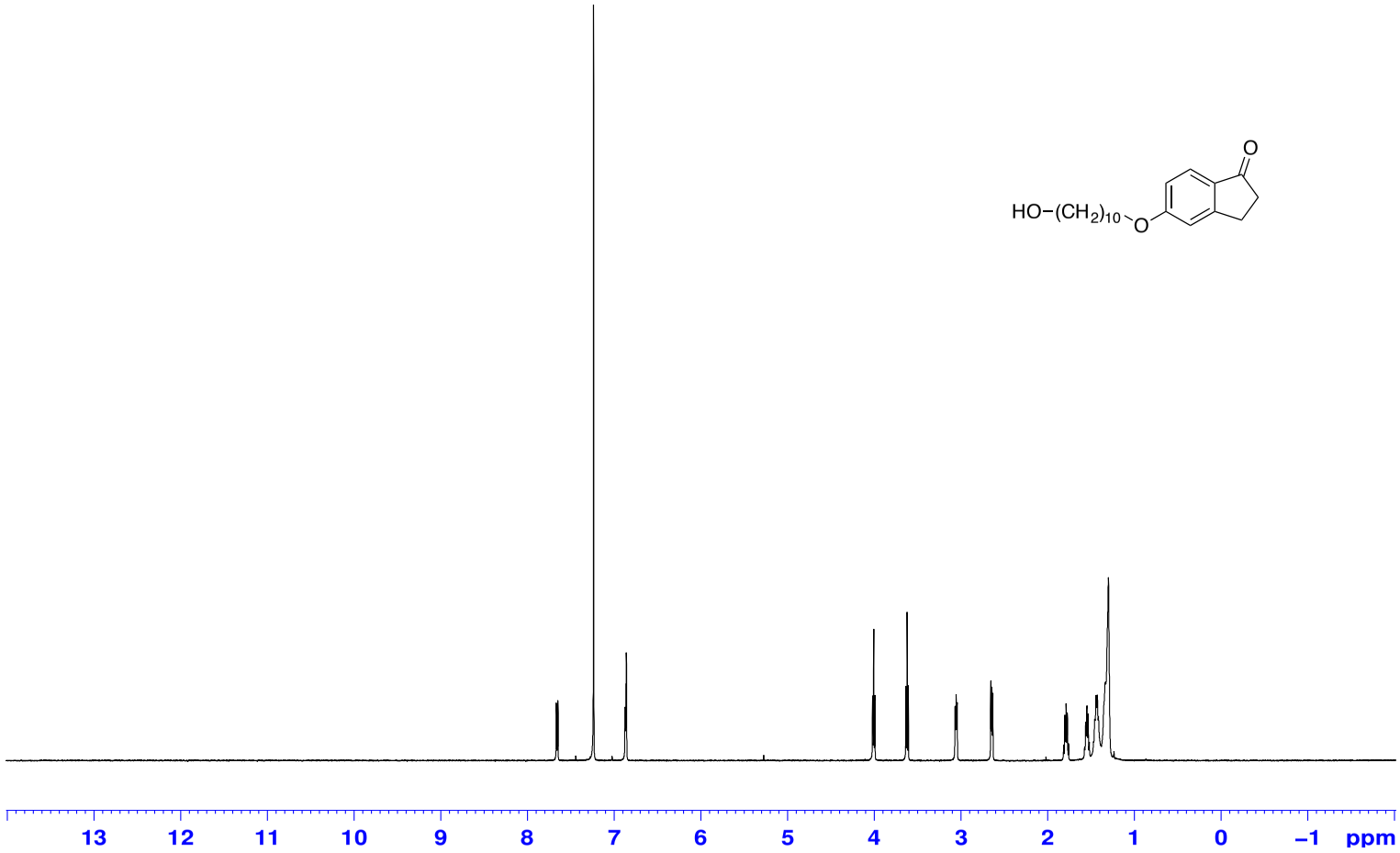

Figure 7: ^{1}H NMR ($CDCl_3$, 500 MHz) of **8**

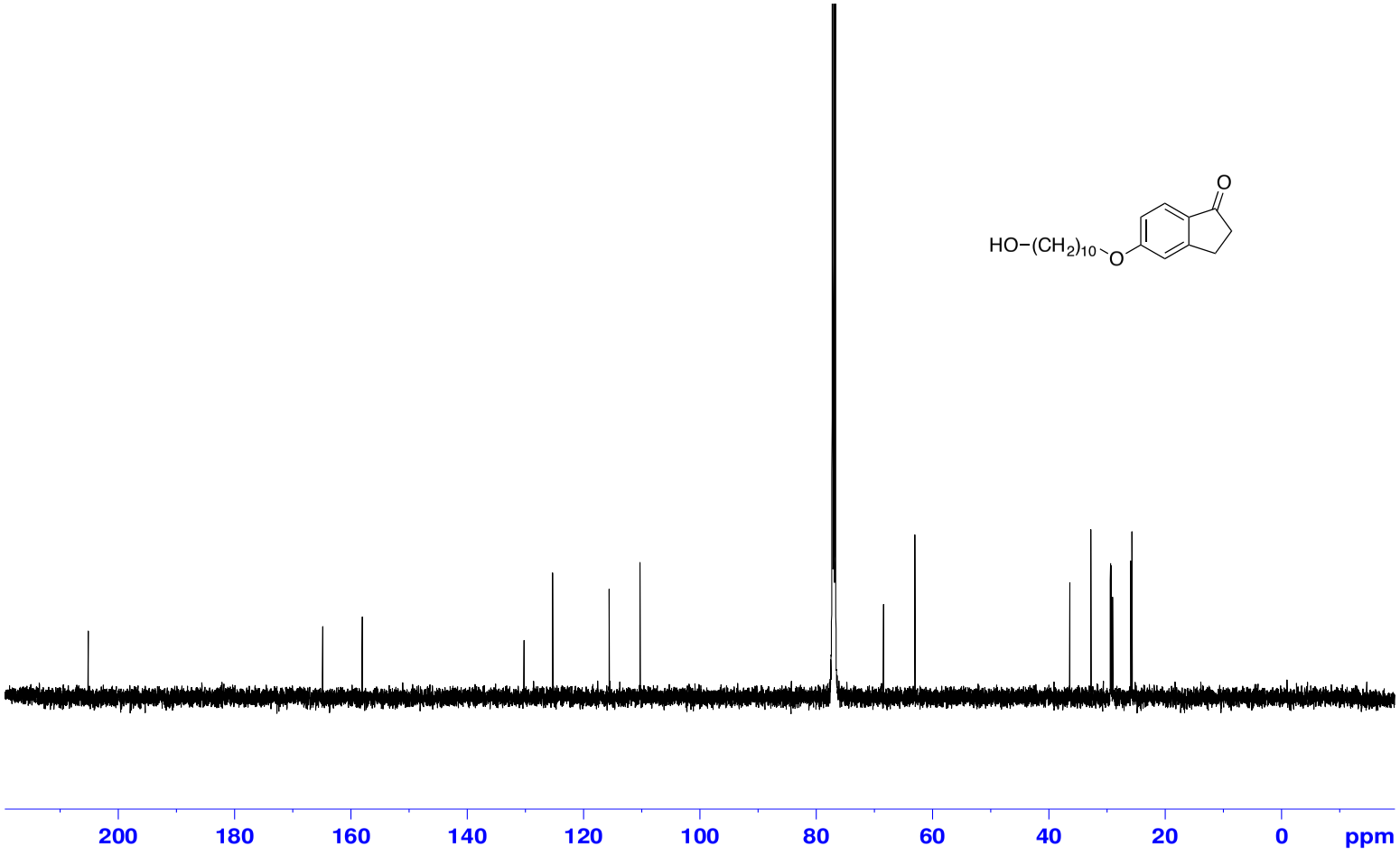

Figure 8: ^{13}C NMR ($CDCl_3$, 125 MHz) of **8**

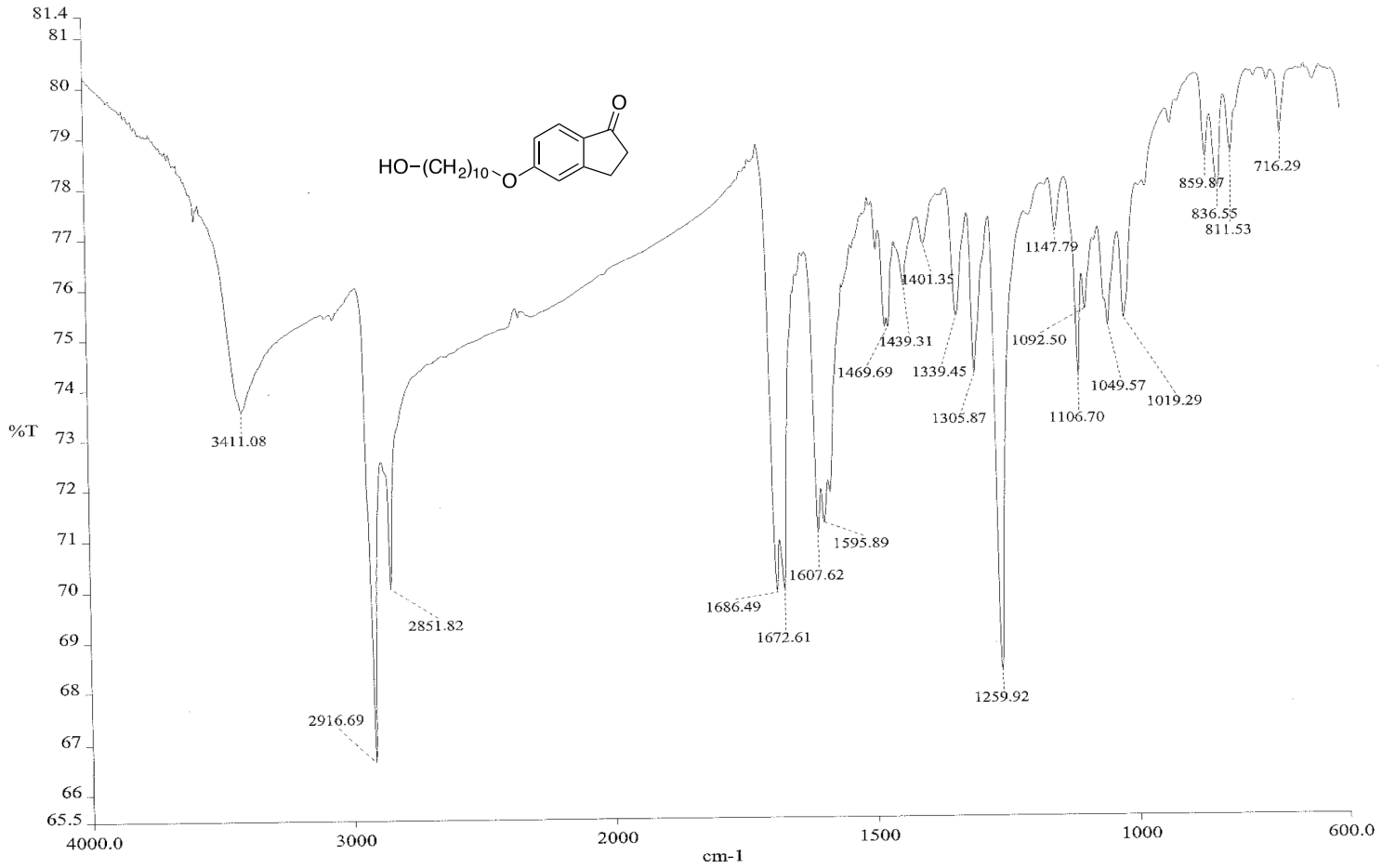

Figure 9: Infrared spectra (neat) of **8**

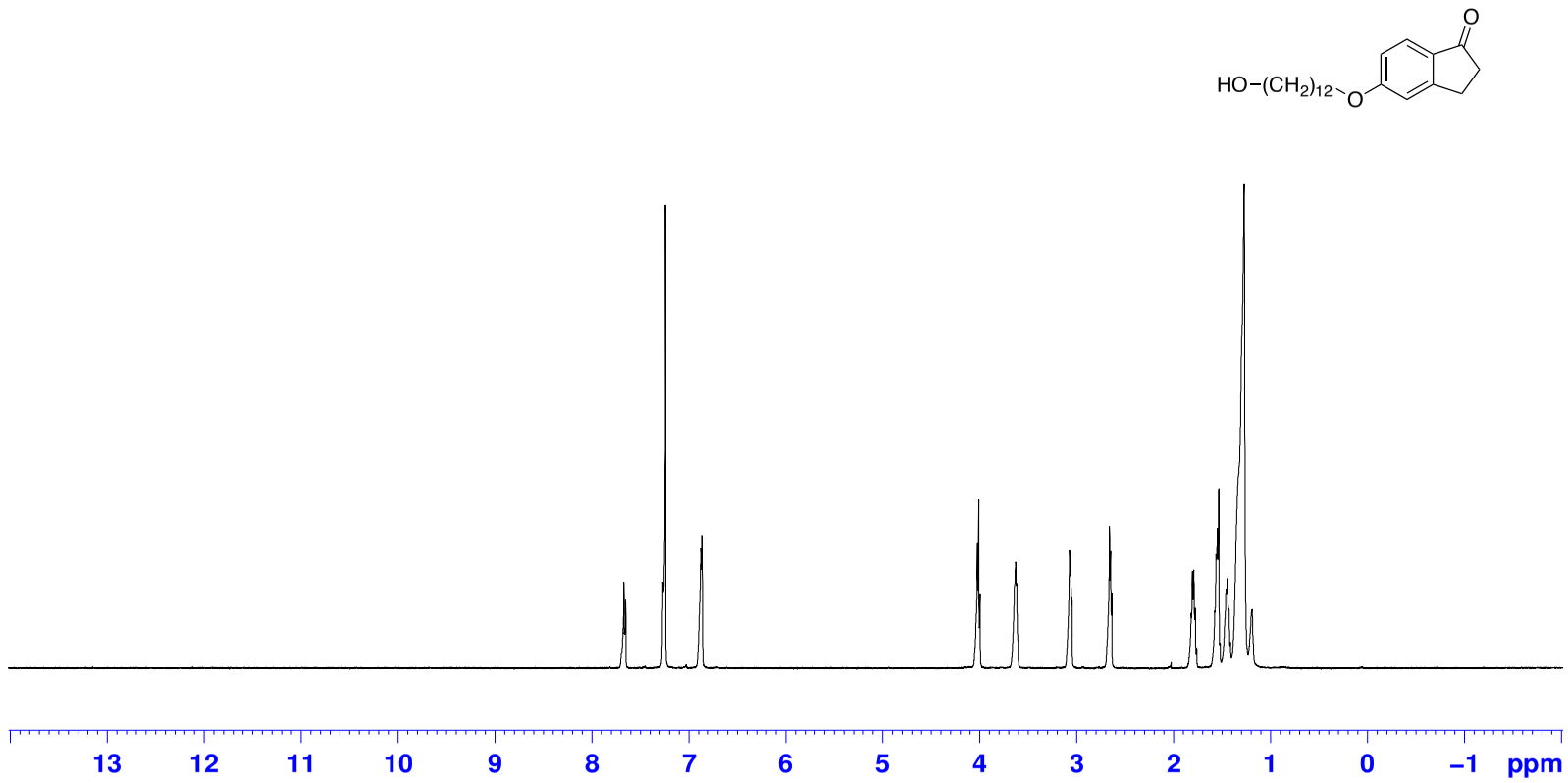

Figure 10: ^{1}H NMR ($CDCl_3$, 500 MHz) of **9**

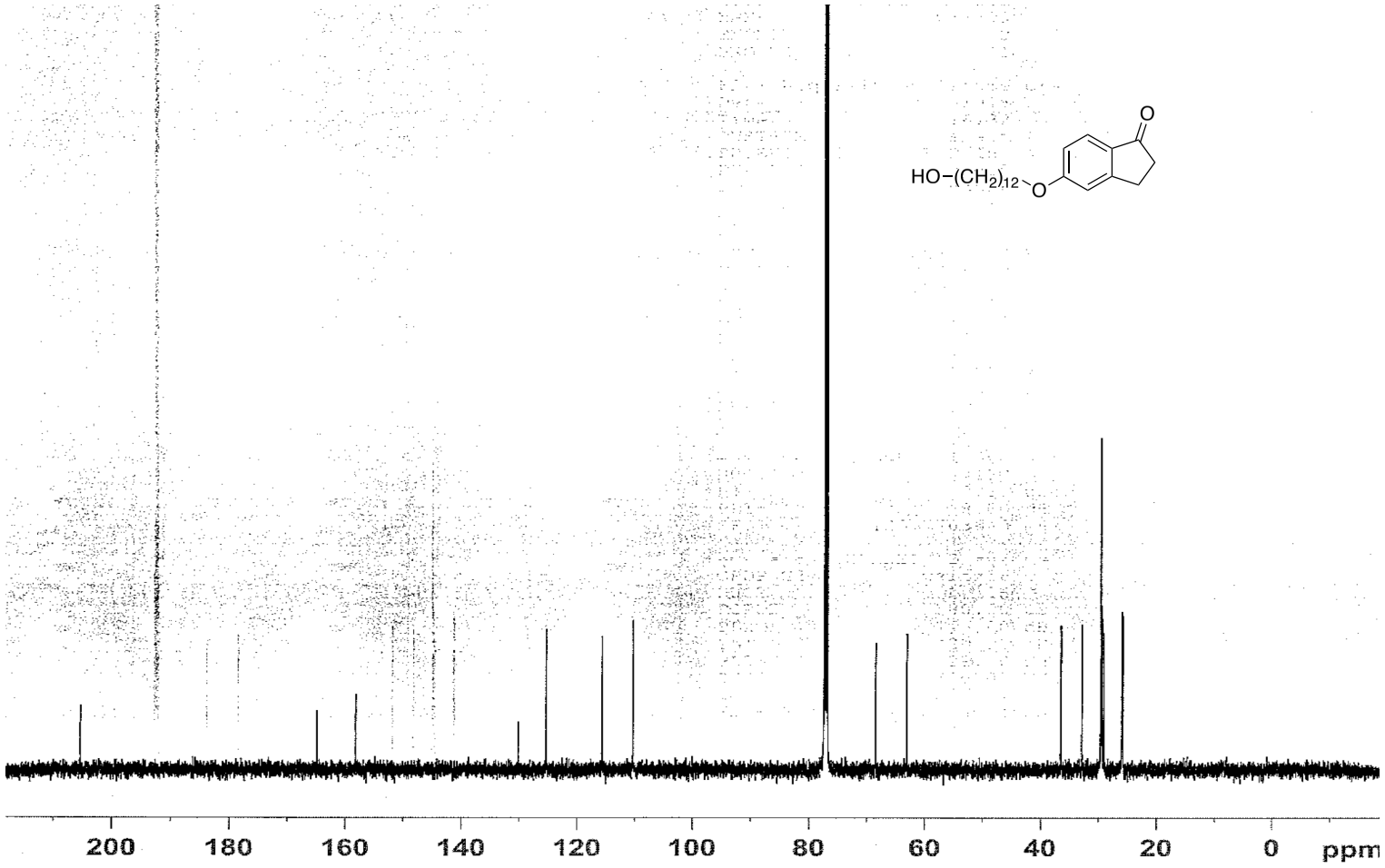

Figure 11: ^{13}C NMR ($CDCl_3$, 125 MHz) of **9**

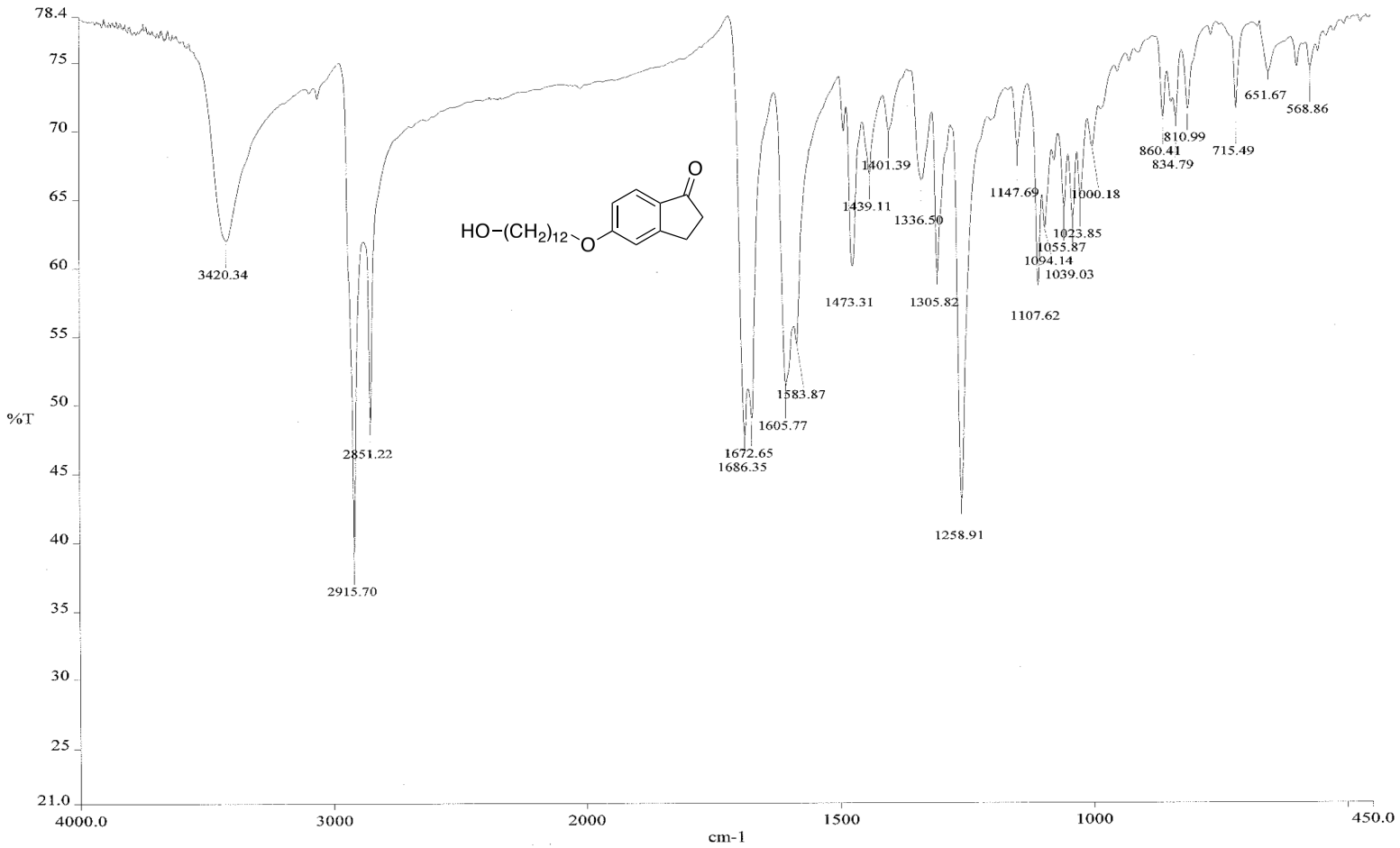

Figure 12: Infrared spectra (neat) of **9**

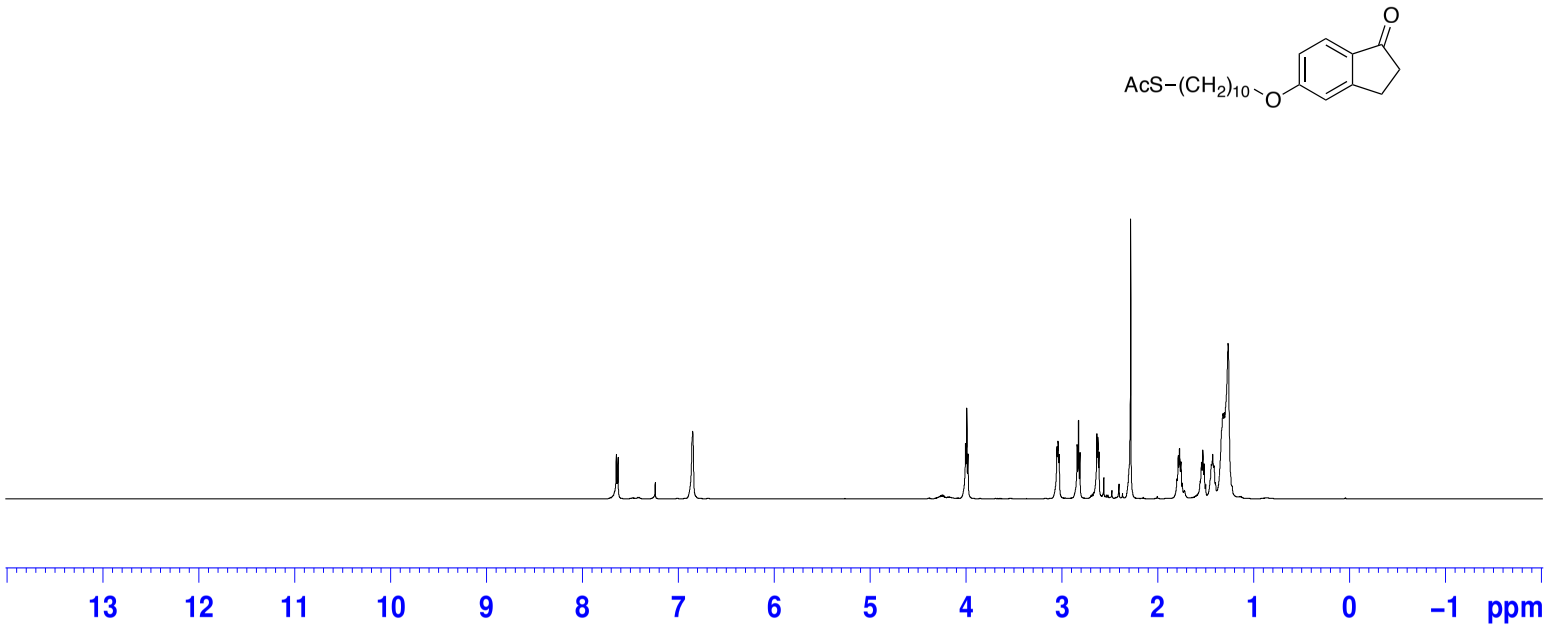

Figure 13: ^{1}H NMR ($CDCl_3$, 500 MHz) of **10**

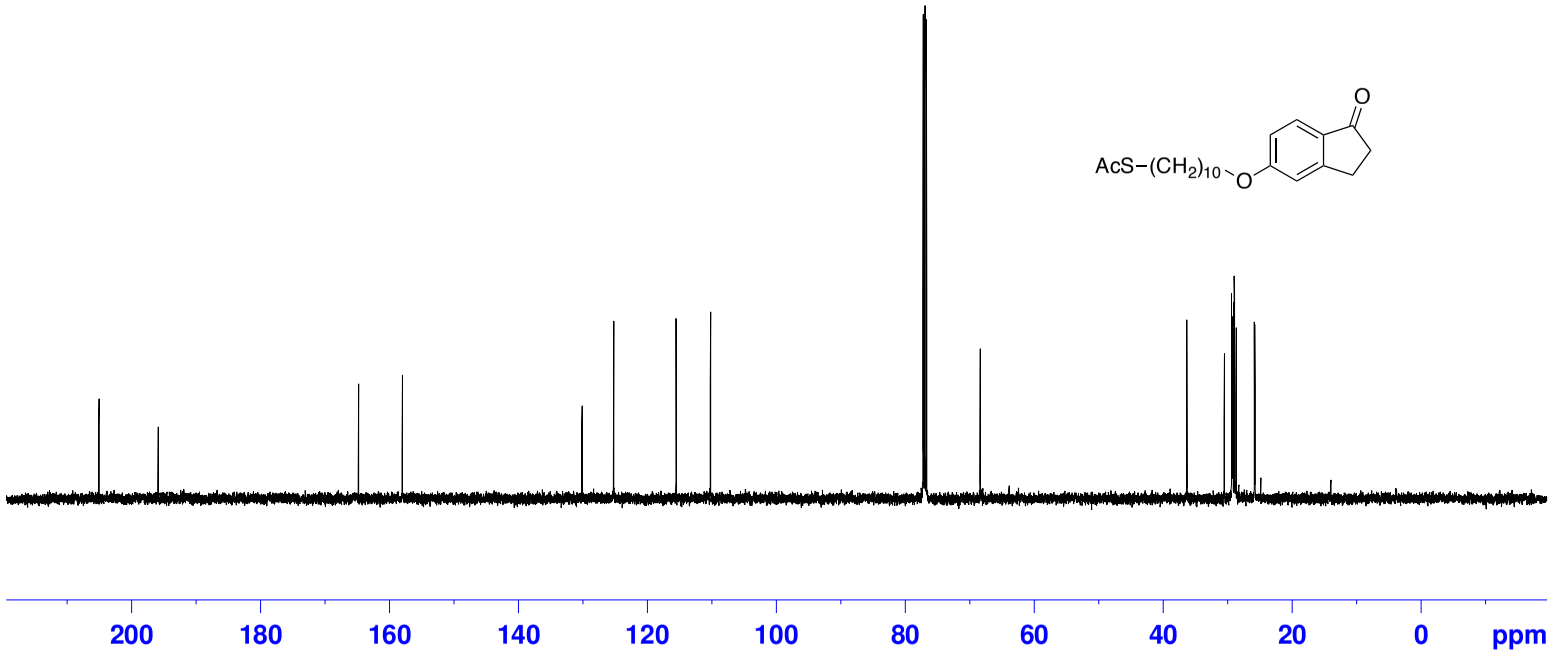

Figure 14: ^{13}C NMR ($CDCl_3$, 125 MHz) of **10**

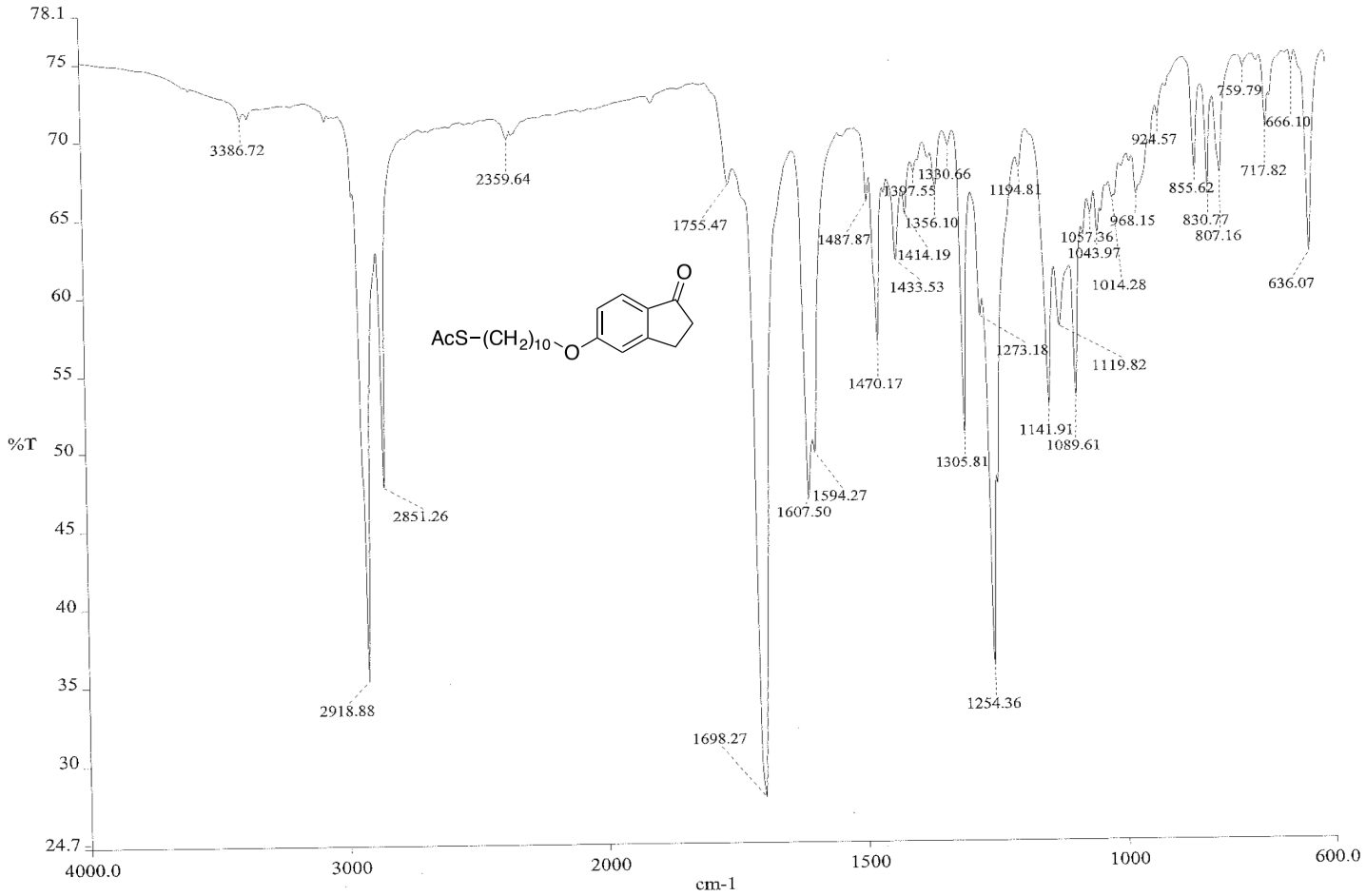

Figure 15: Infrared spectra (neat) of **10**

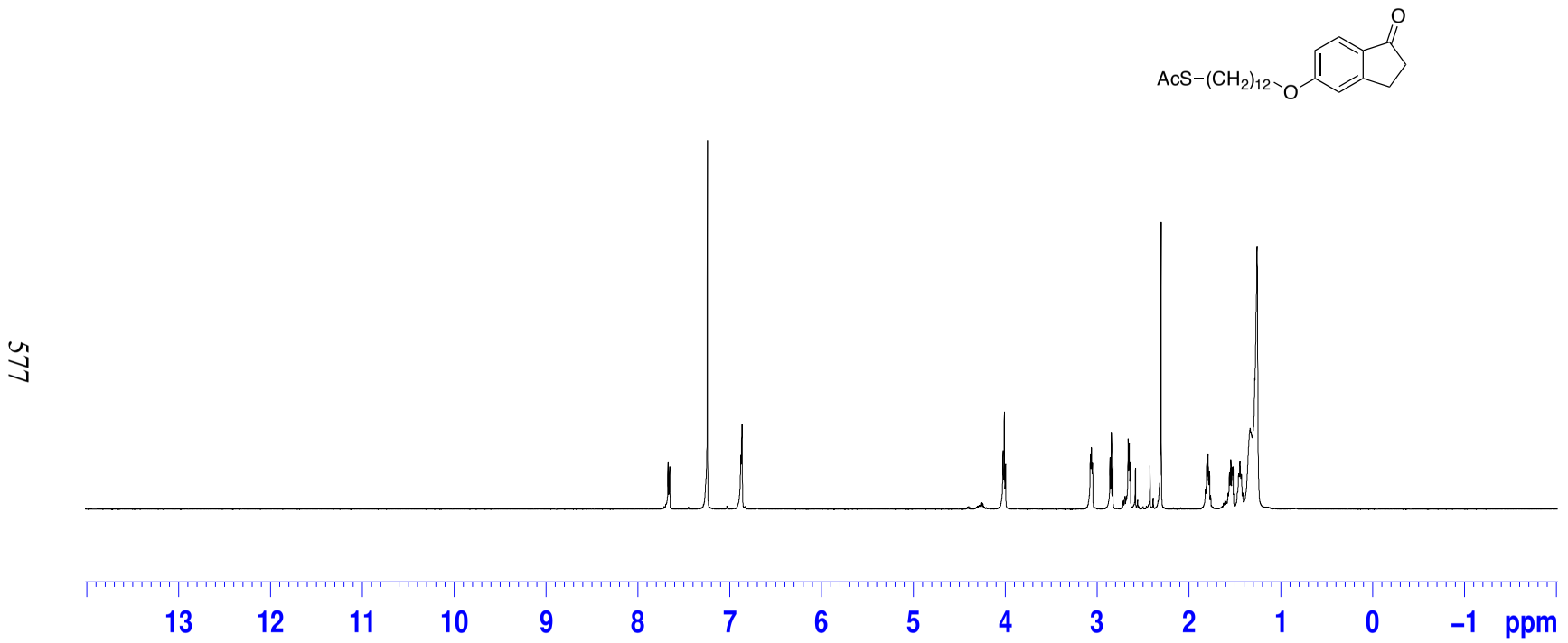

Figure 16: ^{1}H NMR ($CDCl_3$, 500 MHz) of **11**

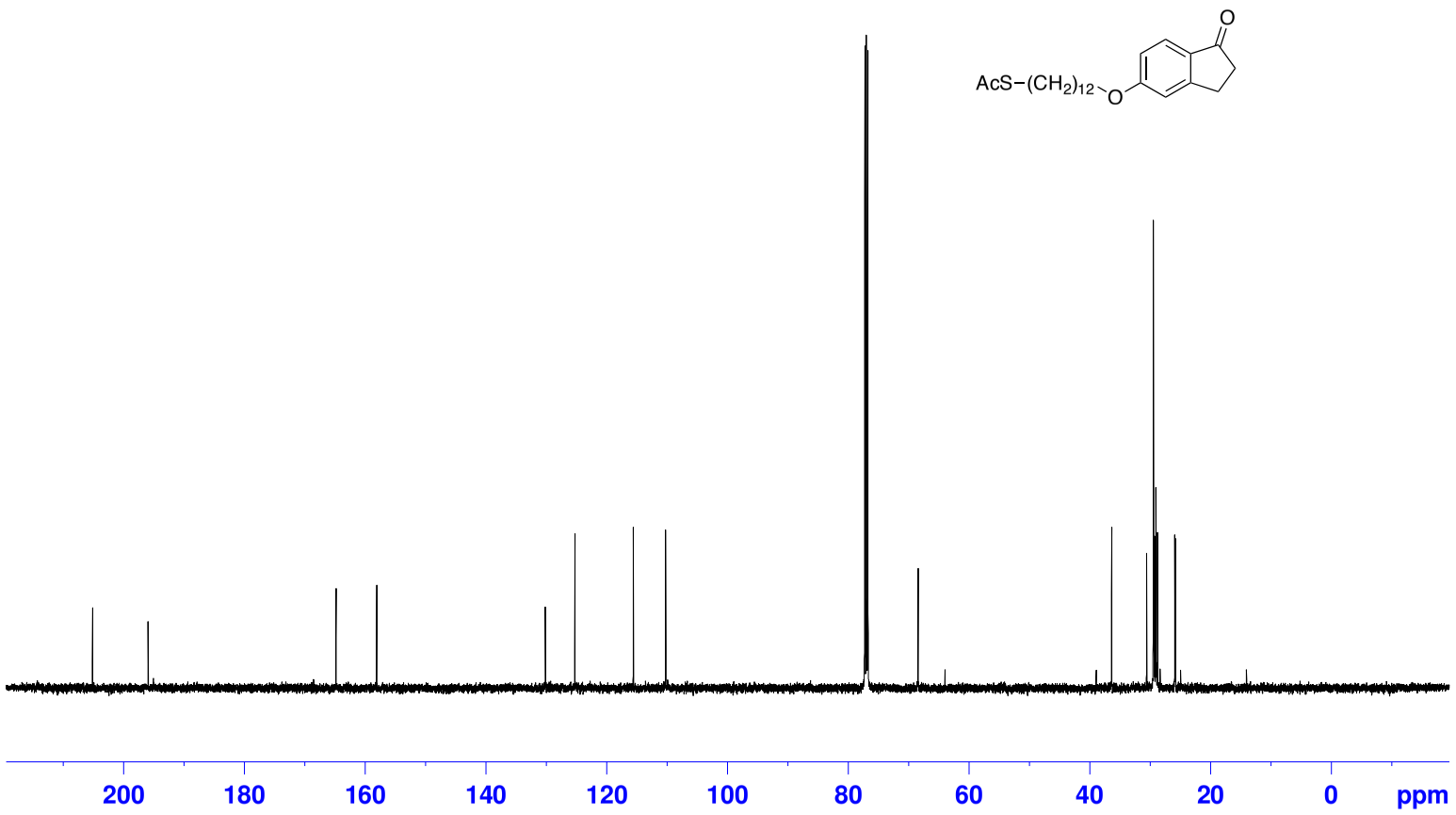

Figure 17: ^{13}C NMR ($CDCl_3$, 125 MHz) of **11**

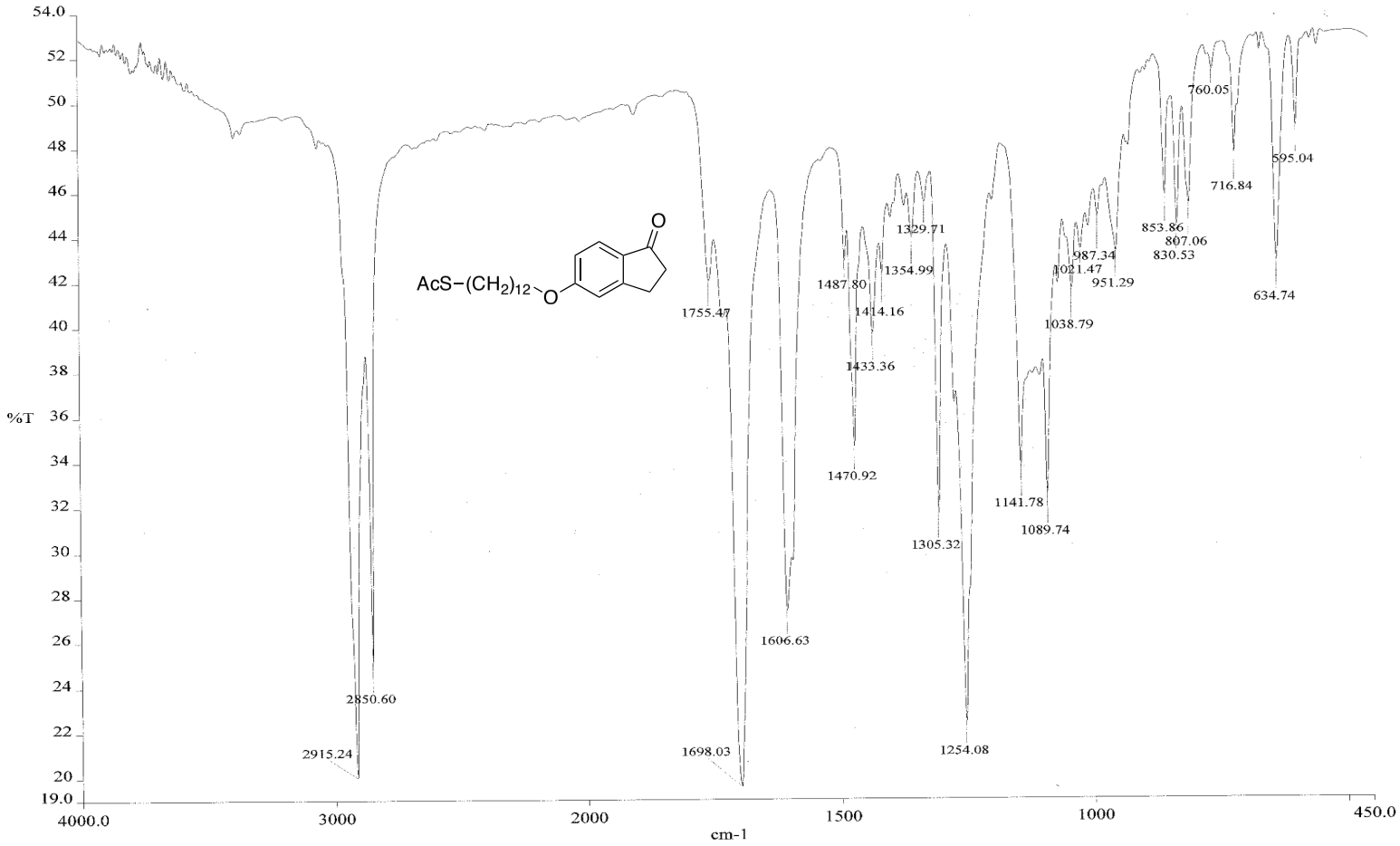

Figure 18: Infrared spectra (neat) of **11**

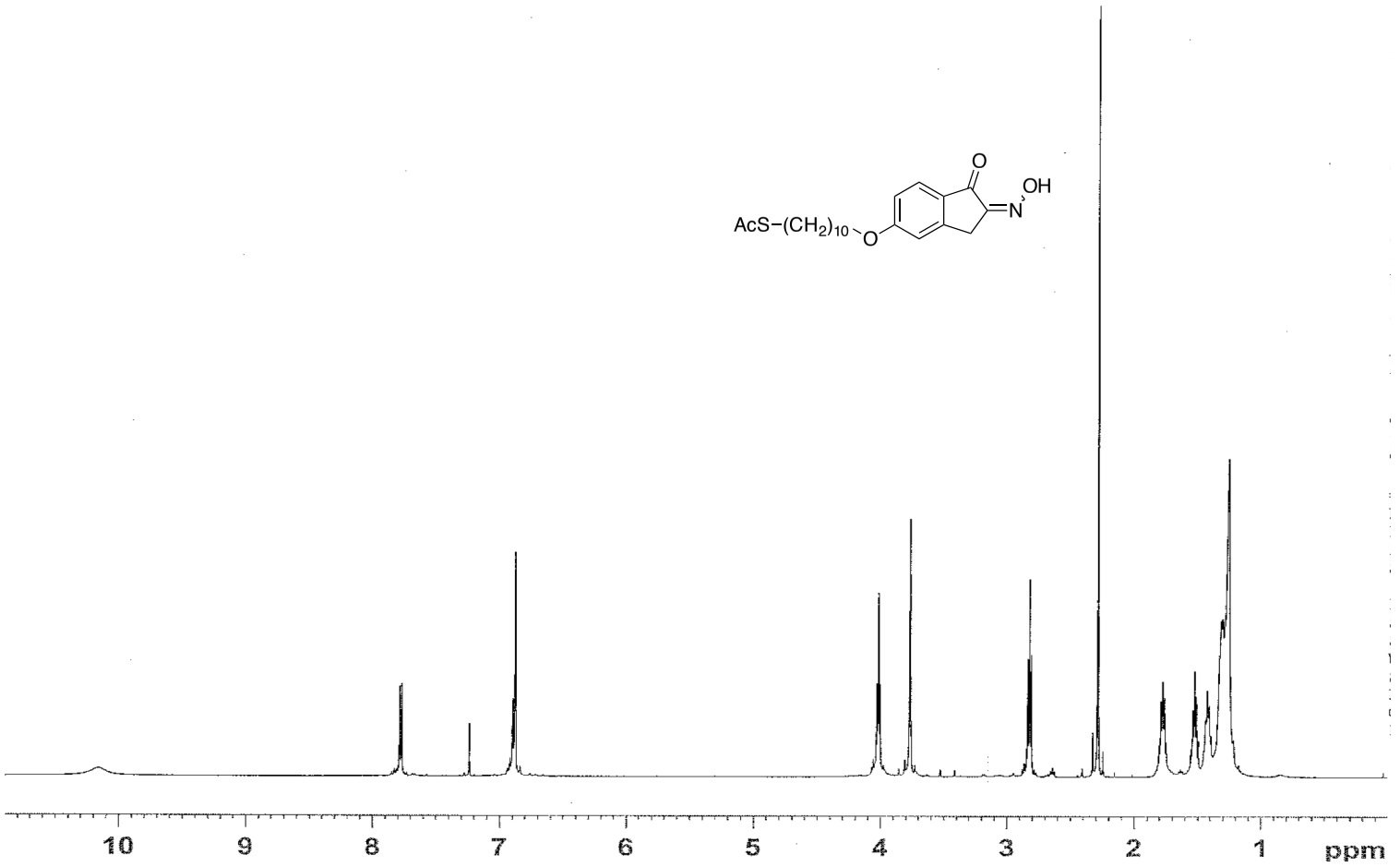

Figure 19: ^{1}H NMR ($CDCl_3$, 500 MHz) of **12**

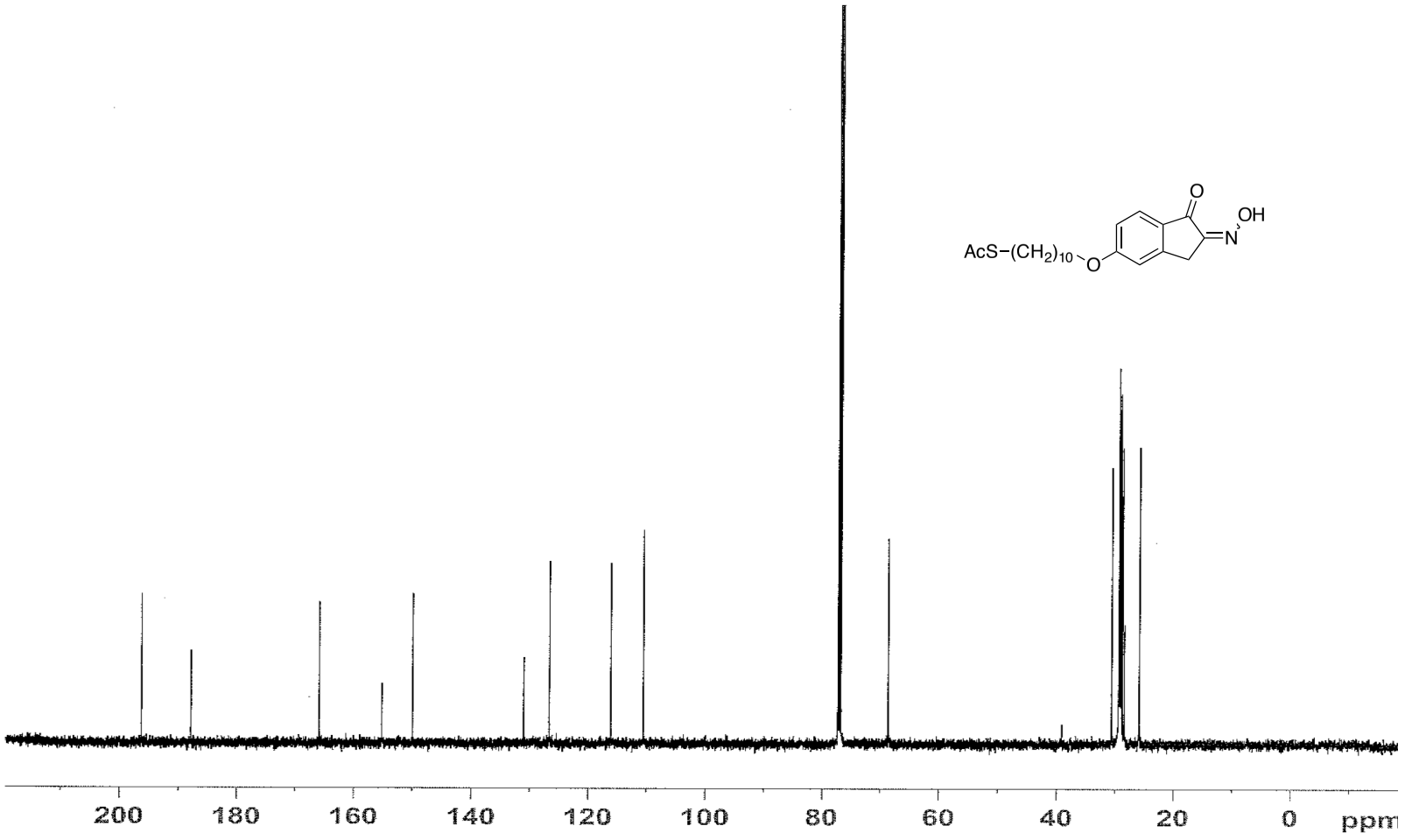

Figure 20: ^{13}C NMR ($CDCl_3$, 125 MHz) of **12**

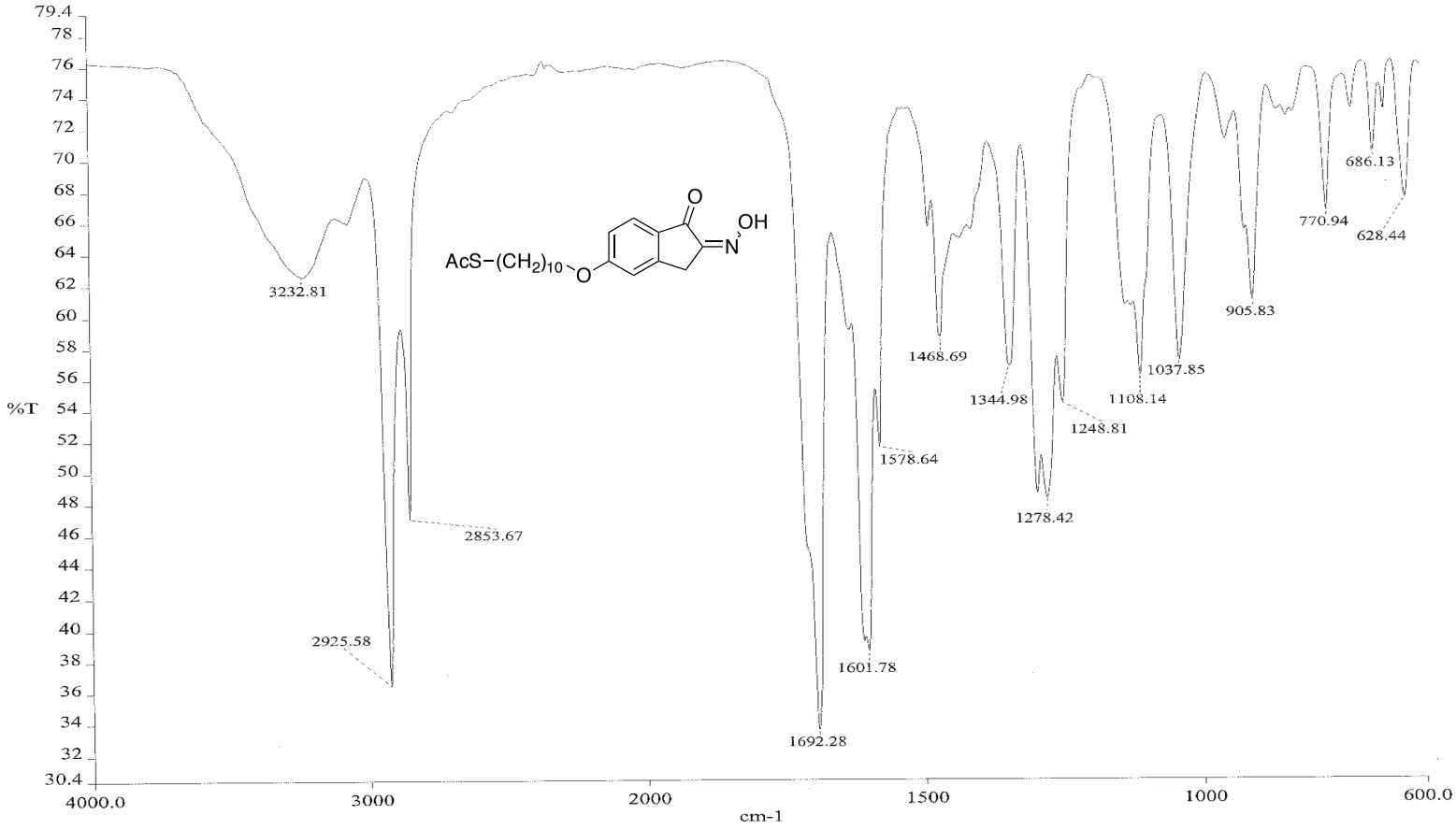

Figure 21: Infrared spectra (neat) of **12**

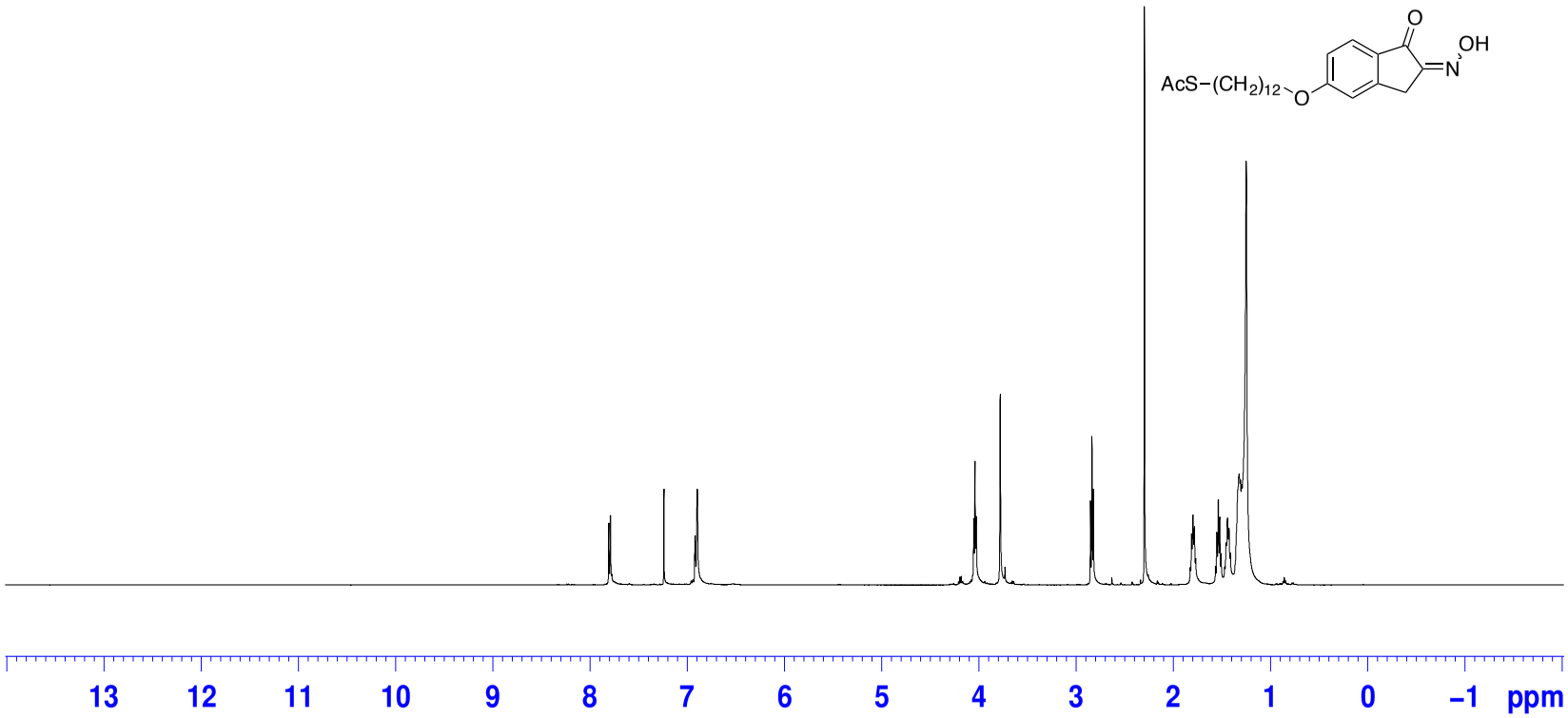

Figure 22: ^{1}H NMR ($CDCl_3$, 500 MHz) of **13**

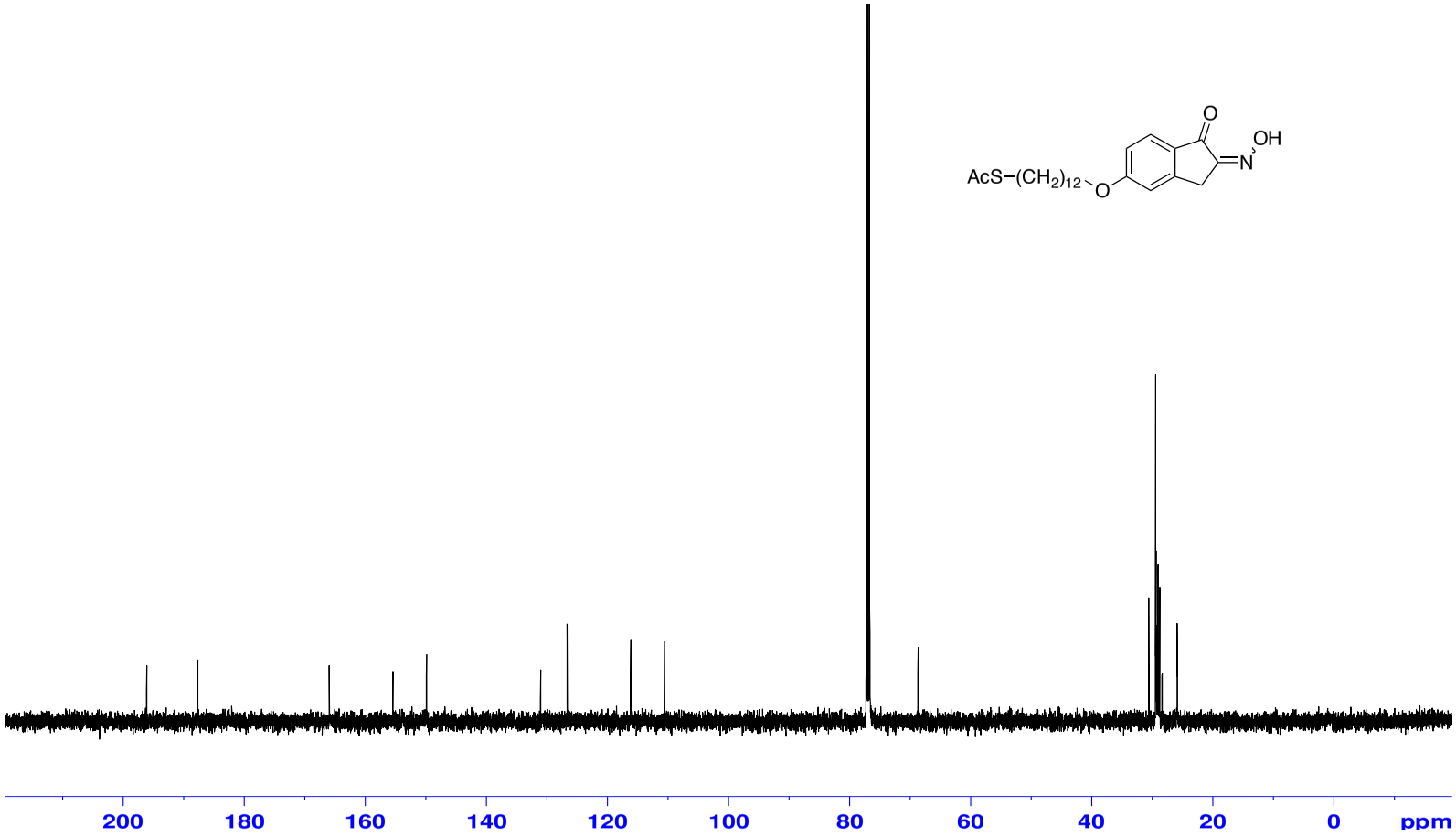

Figure 23: ^{13}C NMR ($CDCl_3$, 125 MHz) of **13**

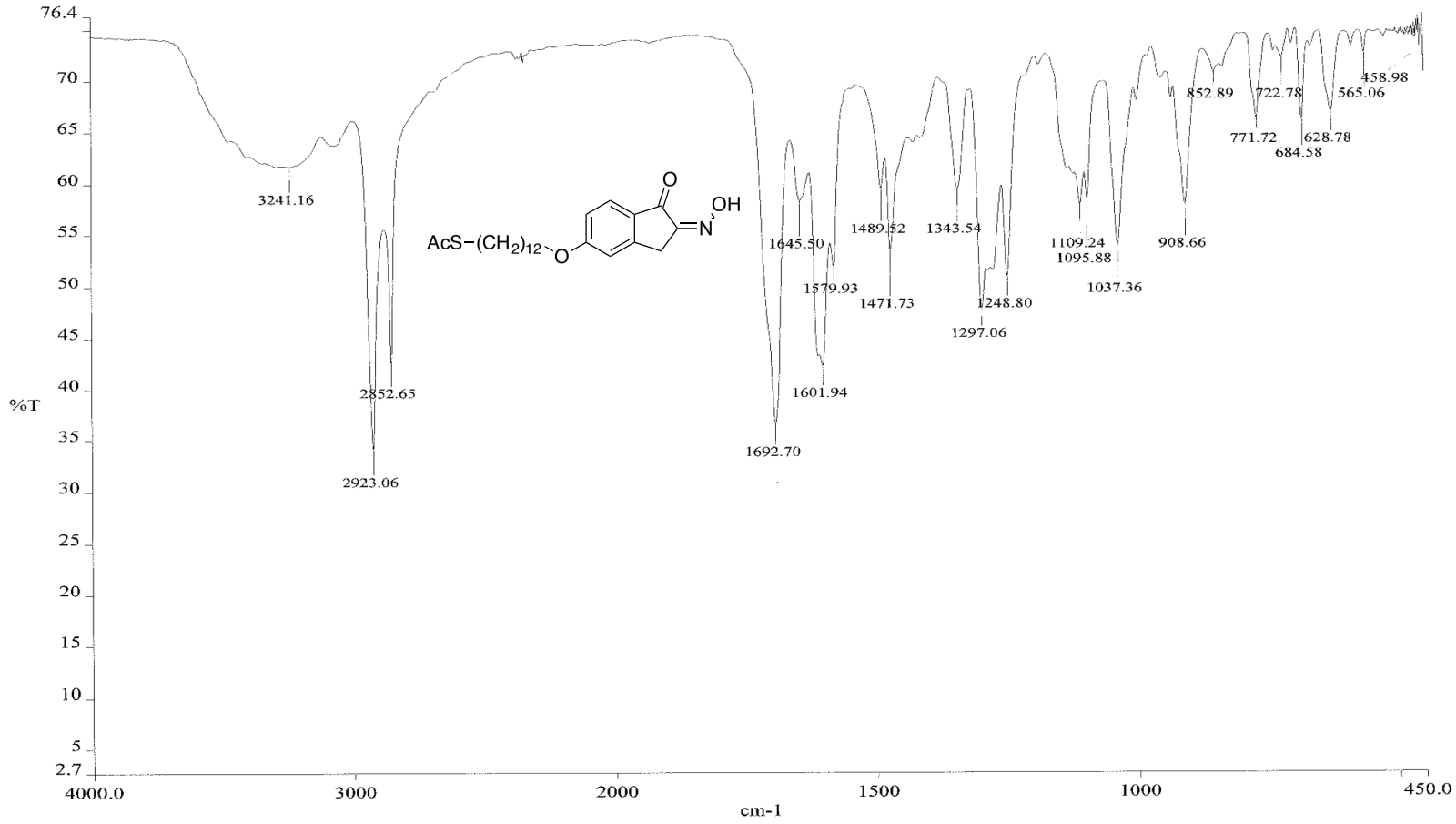

Figure 24: Infrared spectra (neat) of **13**

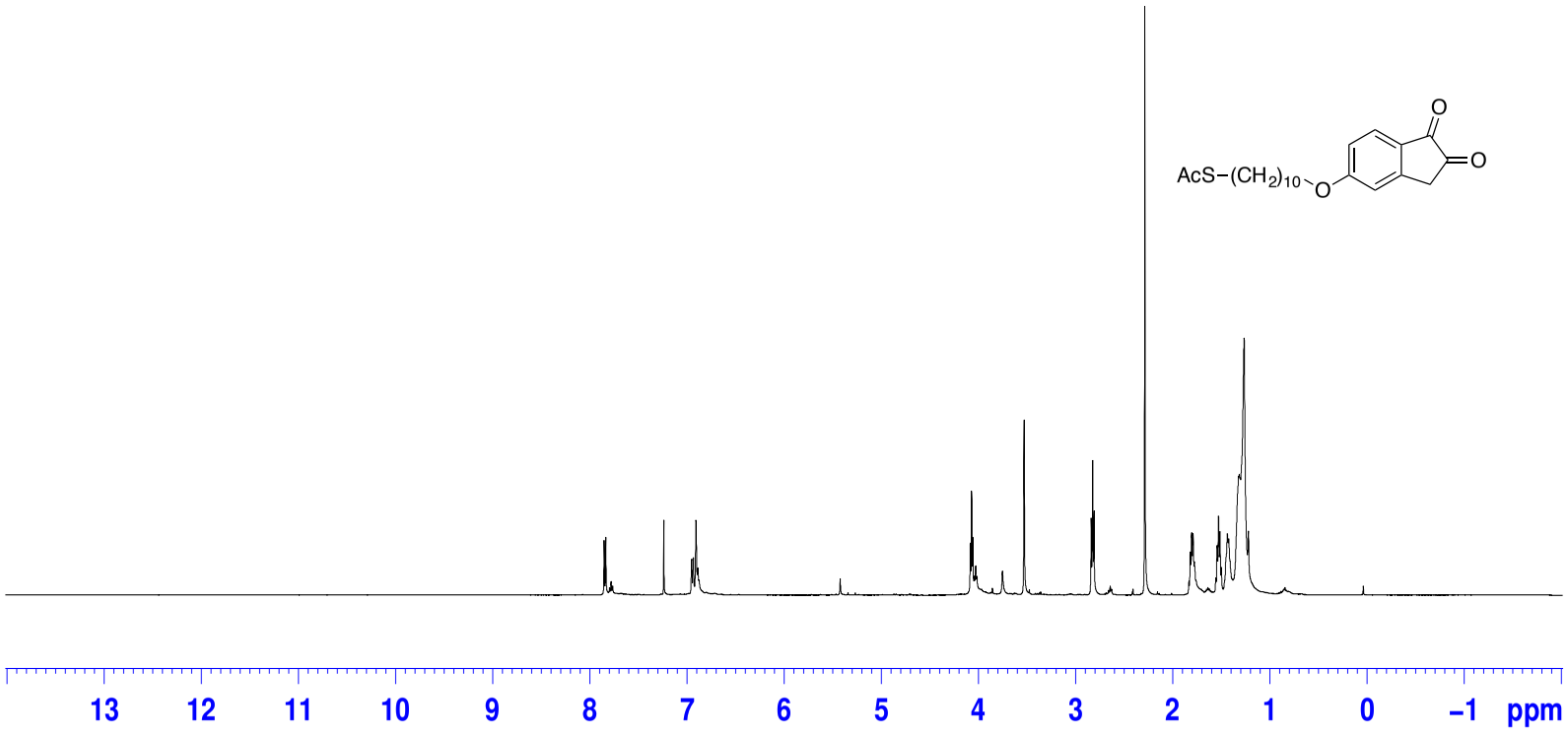

Figure 25: ^{1}H NMR ($CDCl_3$, 500 MHz) of **14**

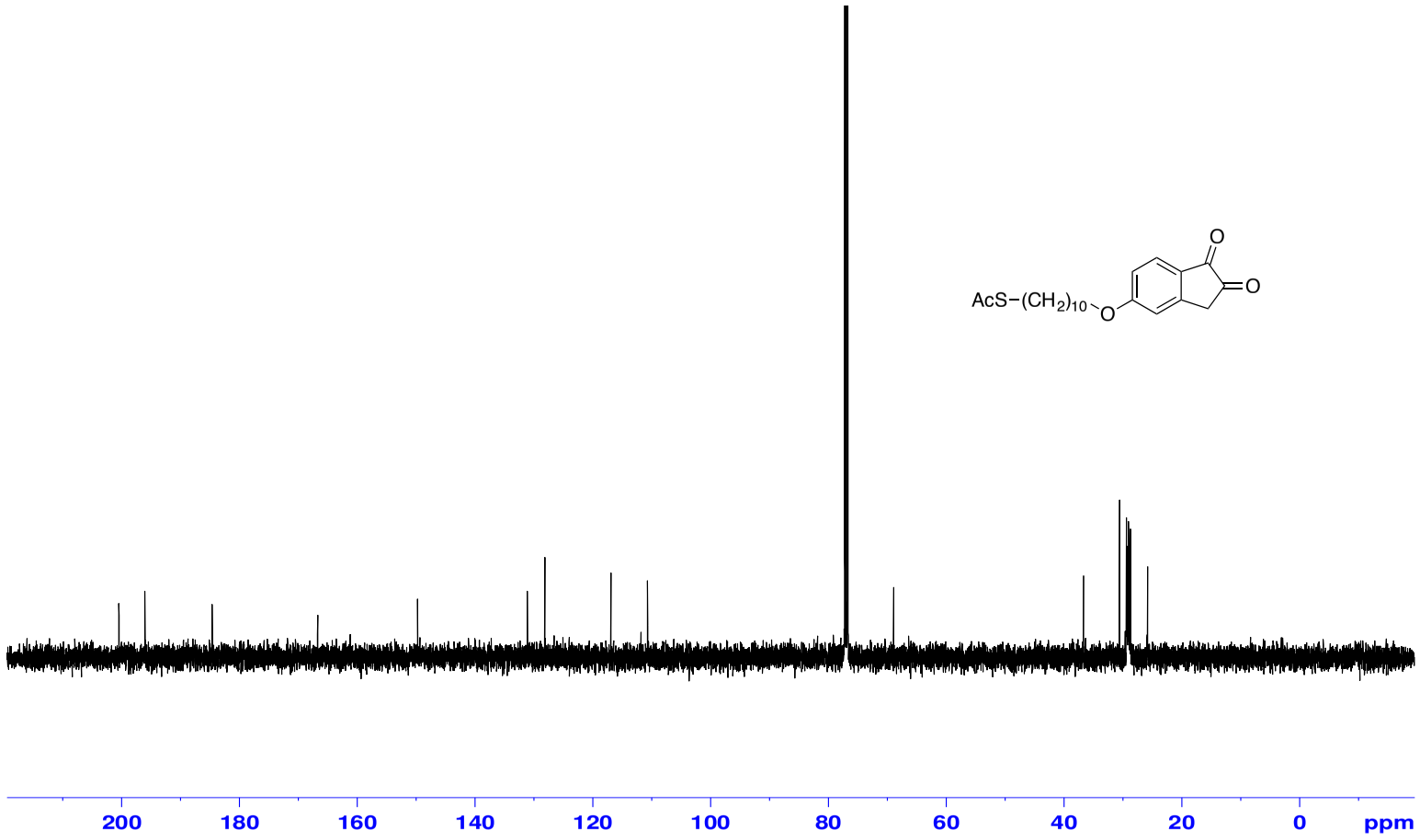

Figure 26: ^{13}C NMR ($CDCl_3$, 125 MHz) of **14**

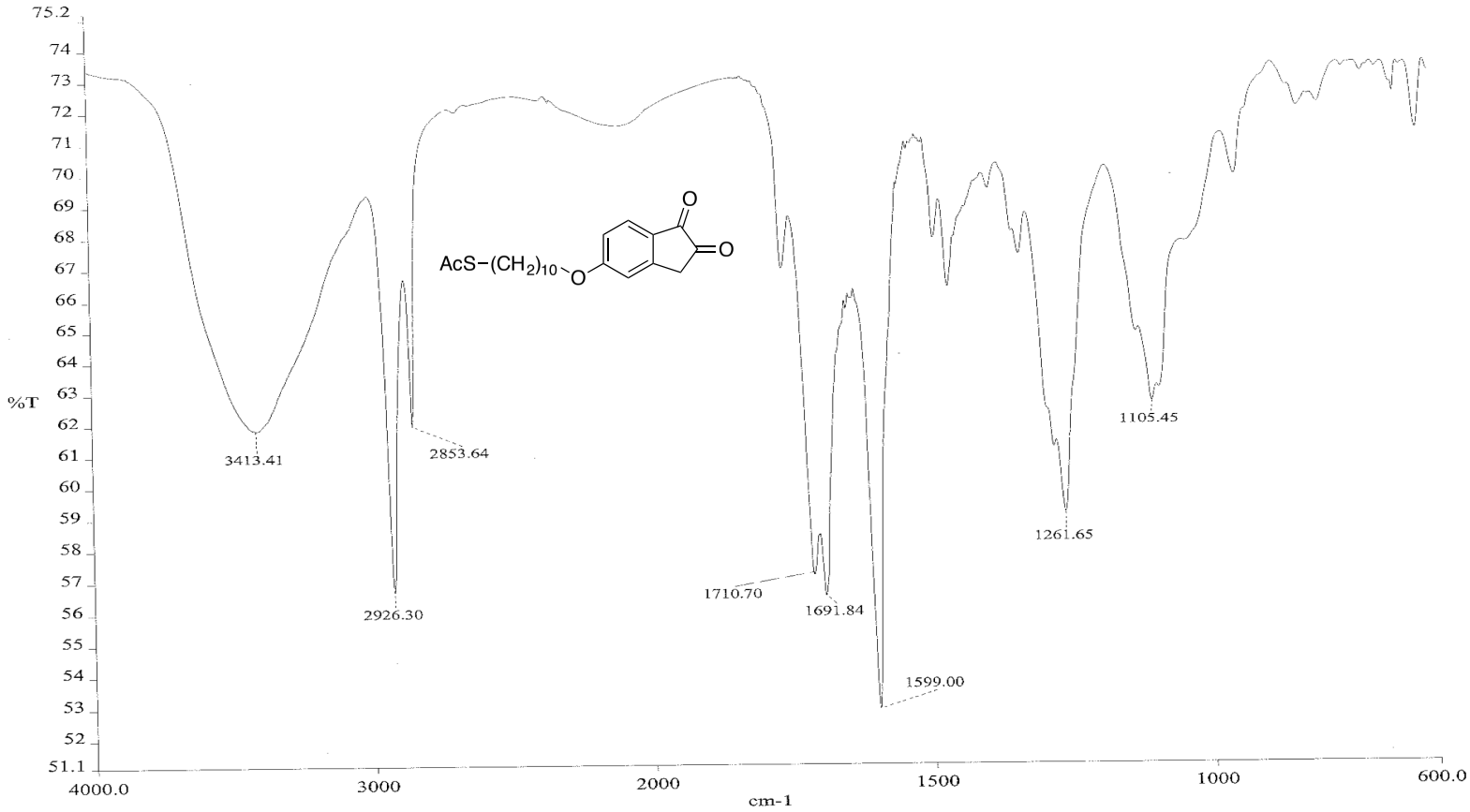

Figure 27: Infrared spectra (neat) of **14**

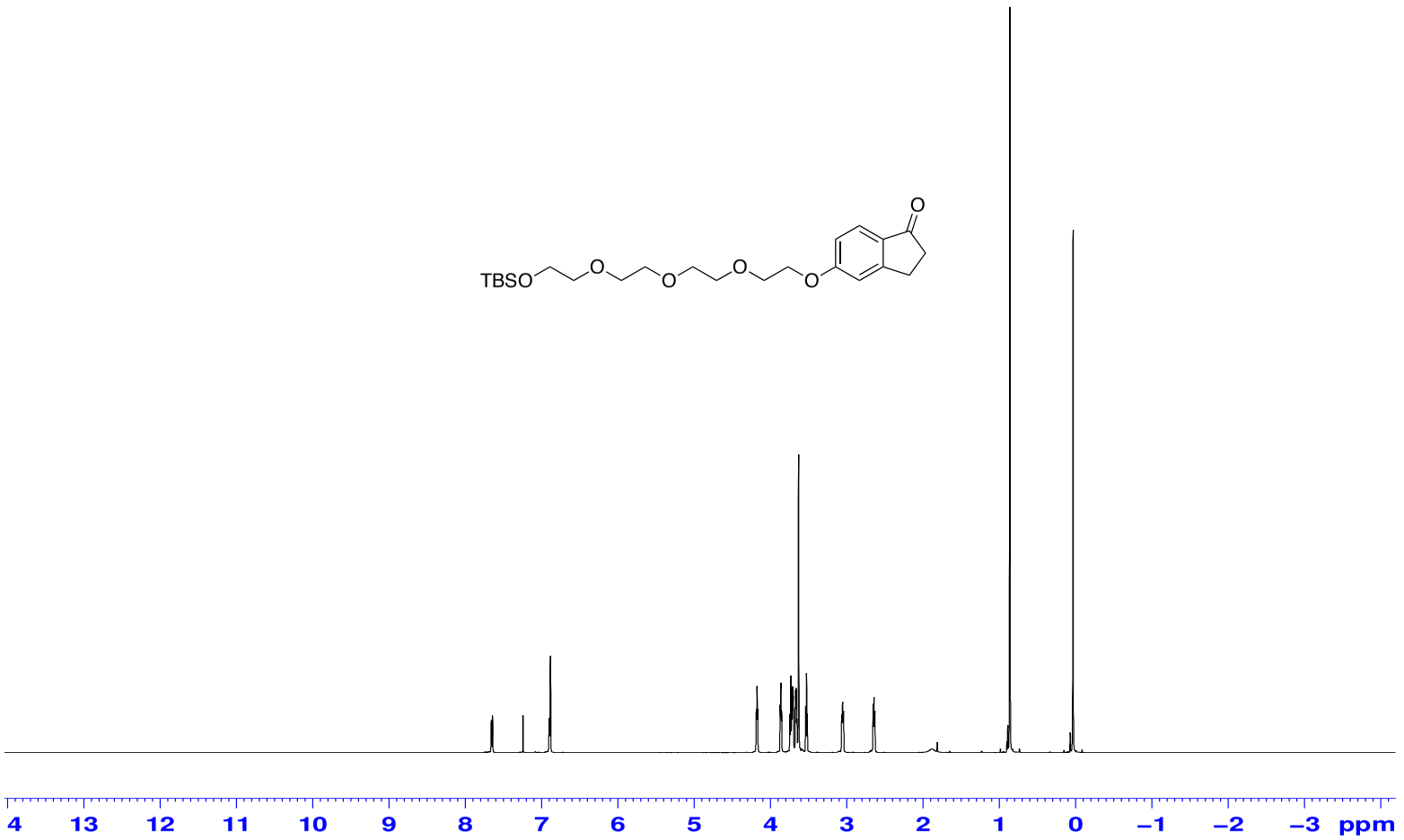

Figure 28: ^{1}H NMR ($CDCl_3$, 500 MHz) of **15**

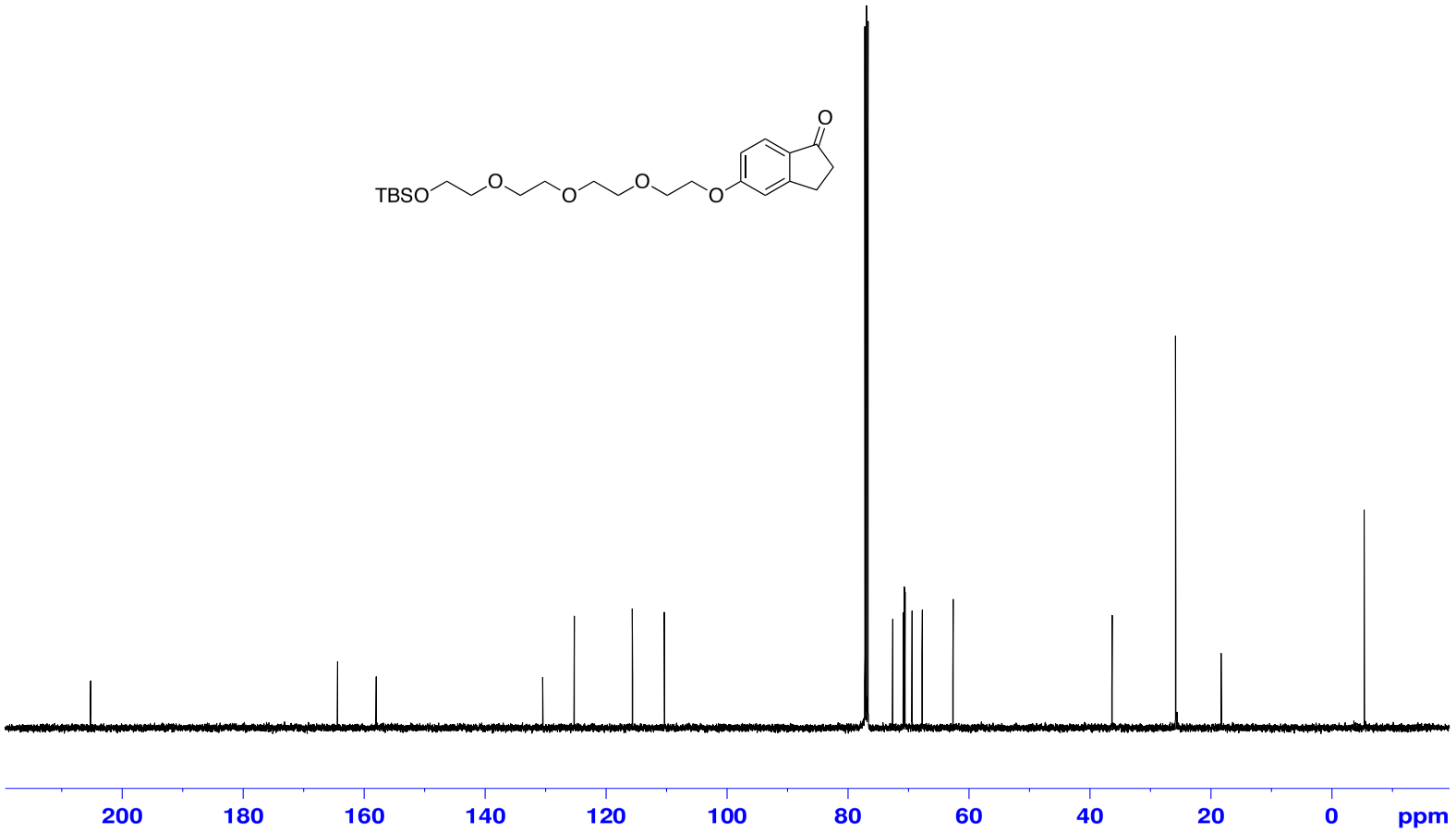

Figure 29: ^{13}C NMR ($CDCl_3$, 125 MHz) of **15**

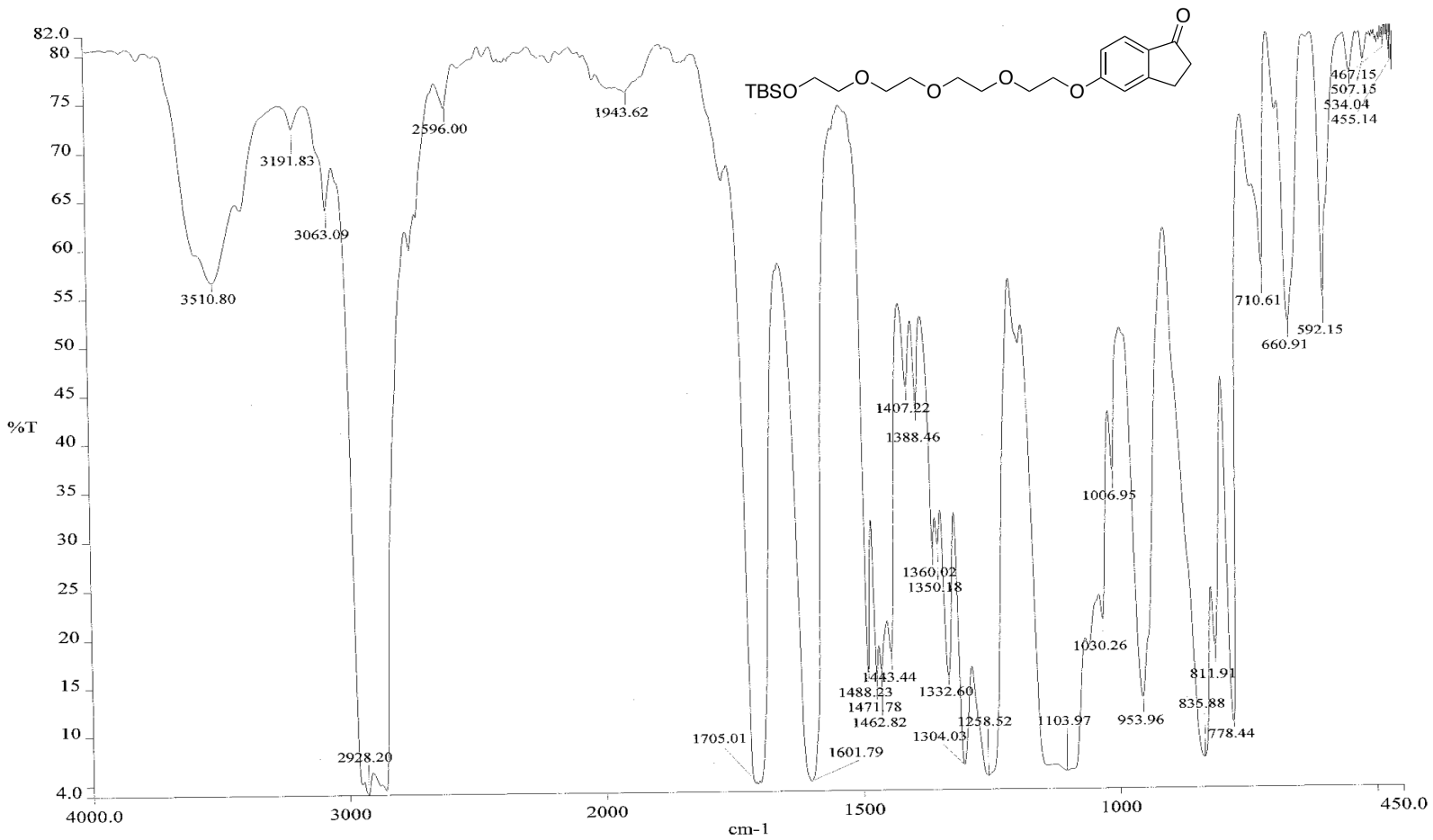

Figure 30: Infrared spectra (neat) of **15**

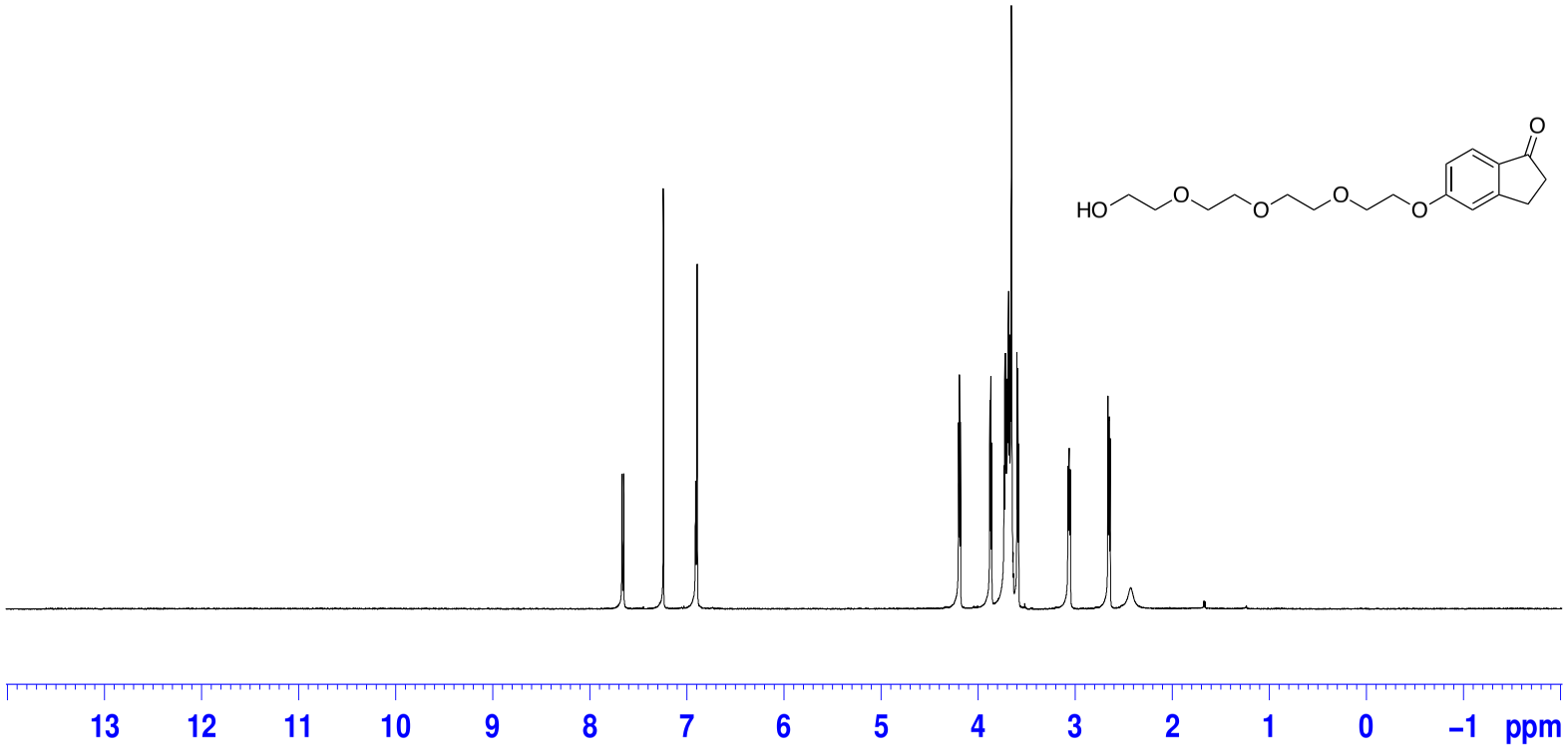

Figure 31: ^{1}H NMR ($CDCl_3$, 500 MHz) of **16**

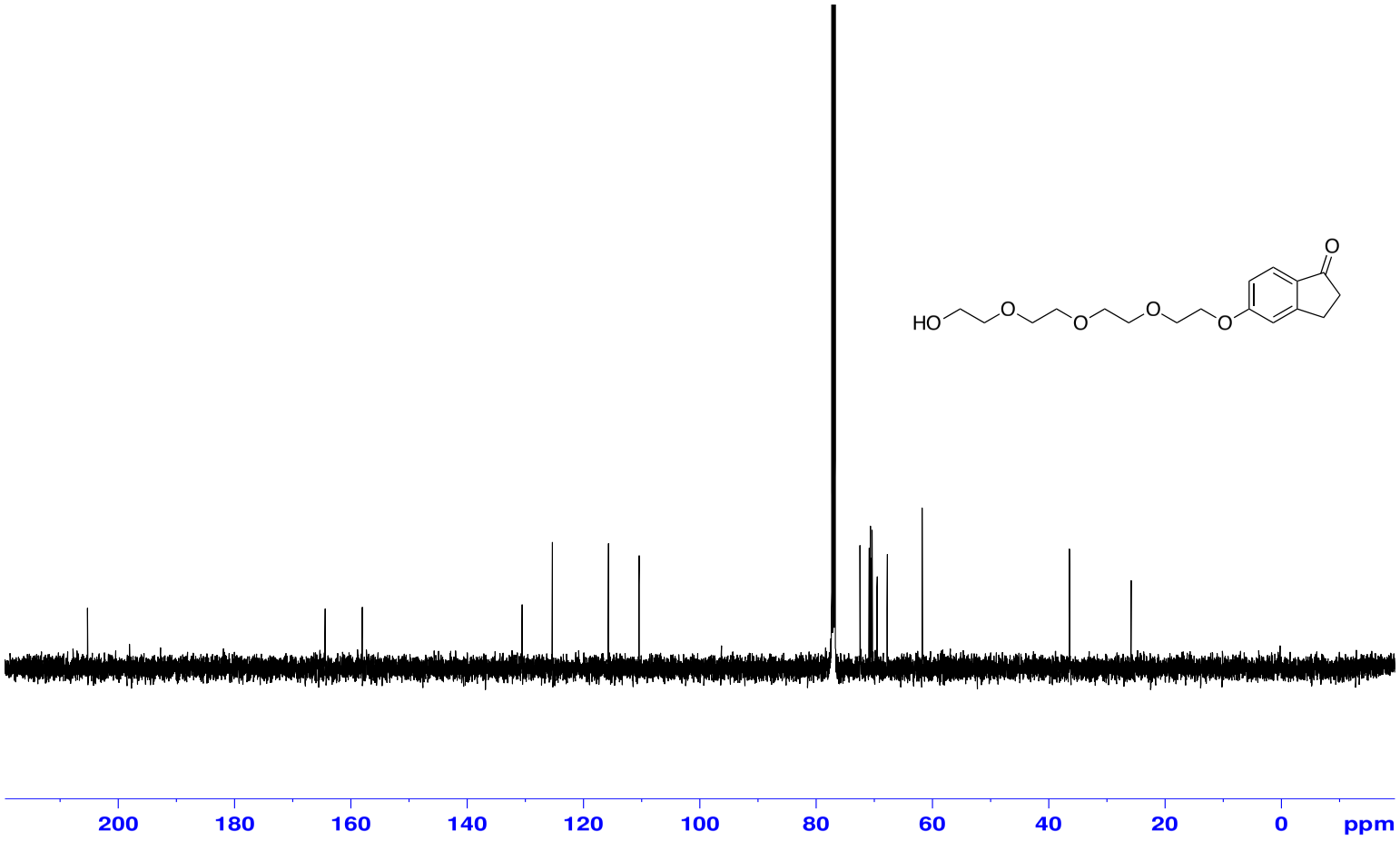

Figure 32: ^{13}C NMR ($CDCl_3$, 125 MHz) of **16**

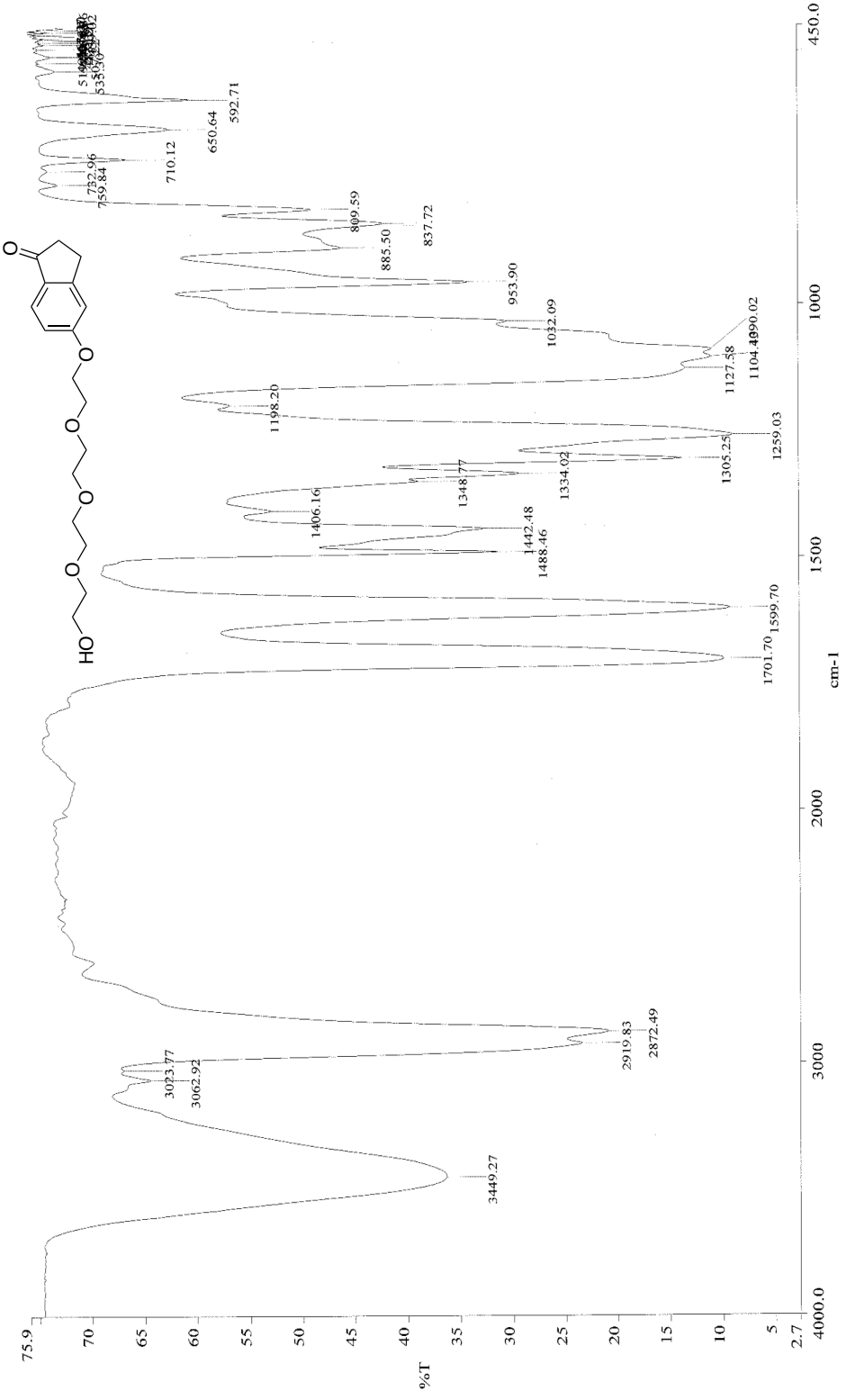

Figure 33: Infrared spectra (neat) of **16**

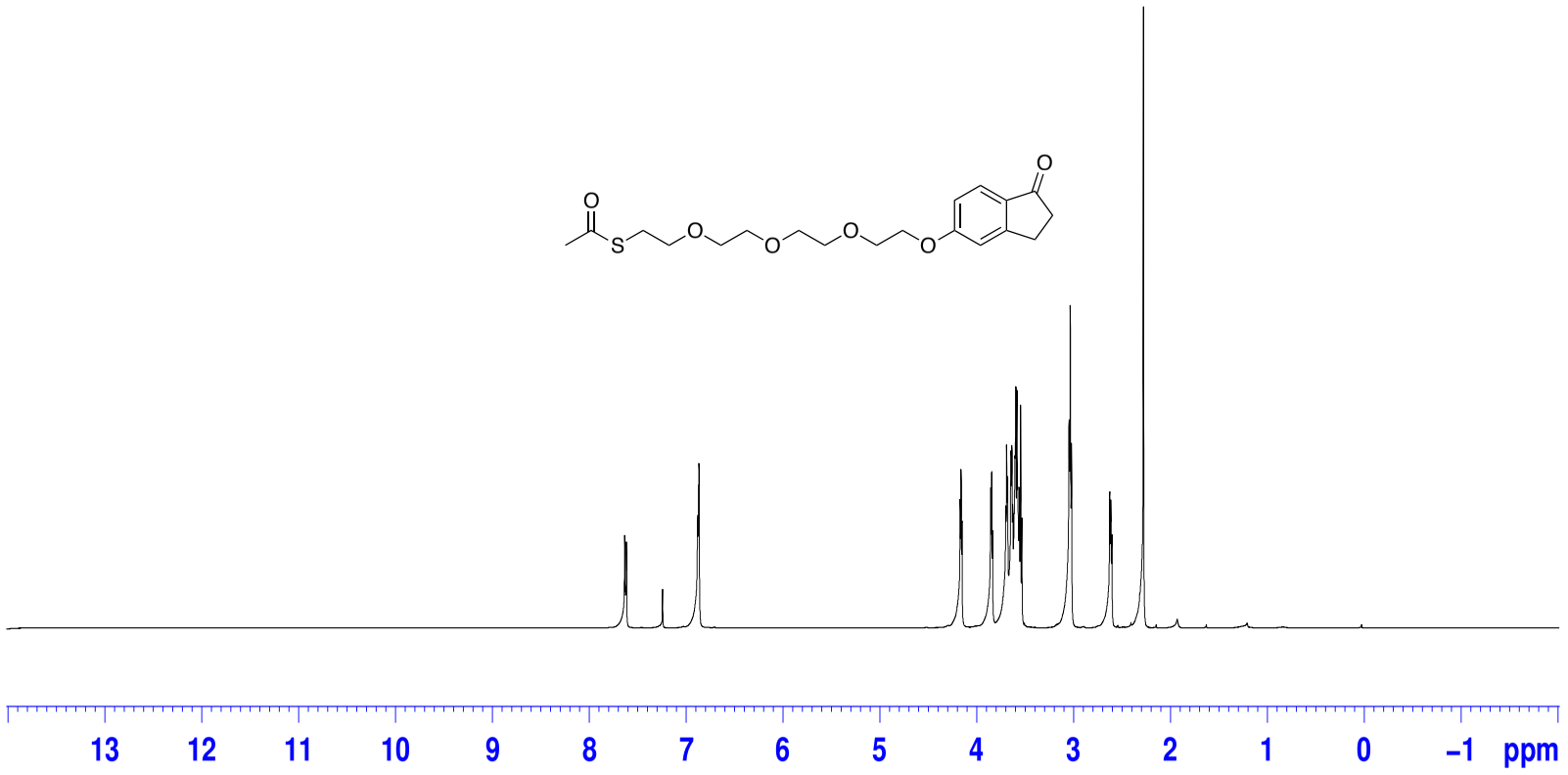

Figure 34: ^{1}H NMR ($CDCl_3$, 500 MHz) of **17**

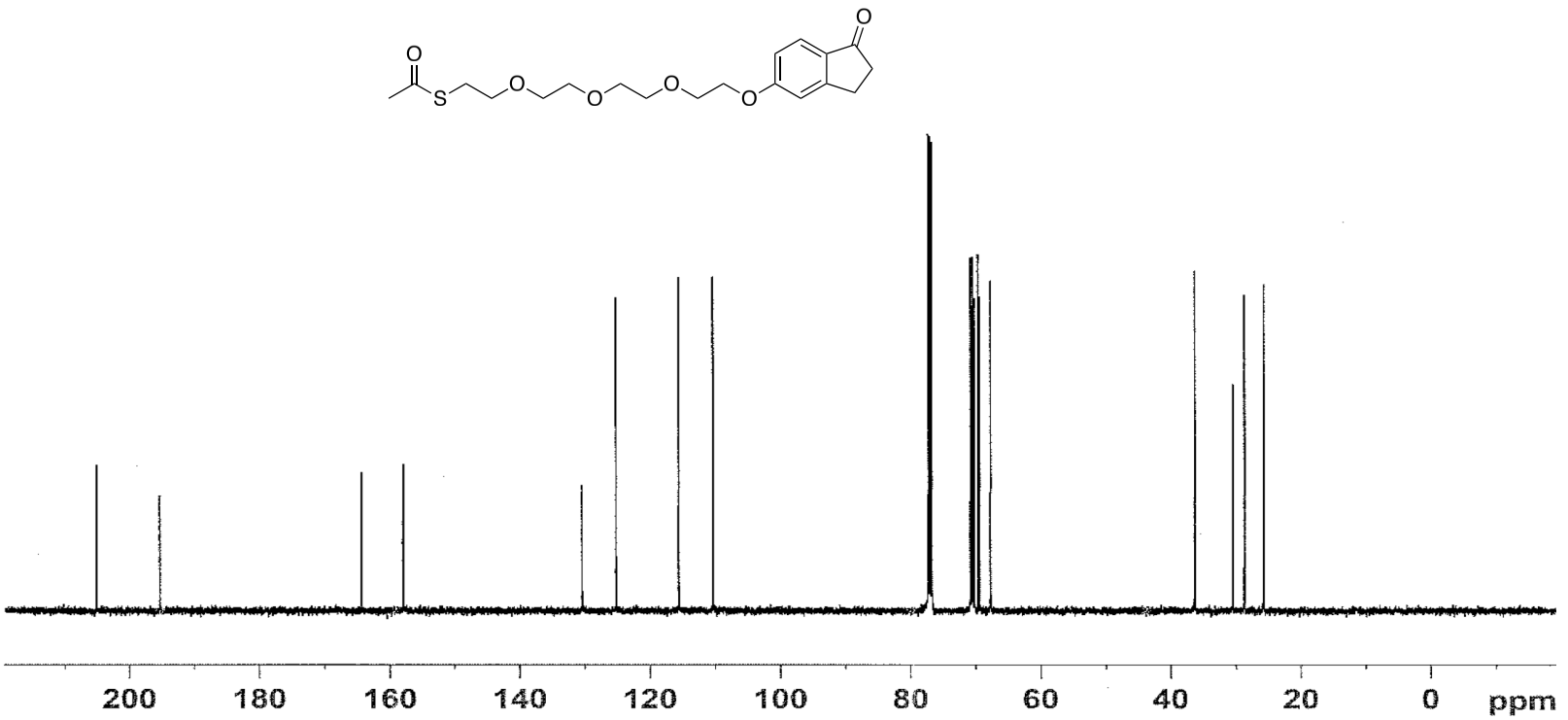

Figure 35: ^{13}C NMR ($CDCl_3$, 125 MHz) of **17**

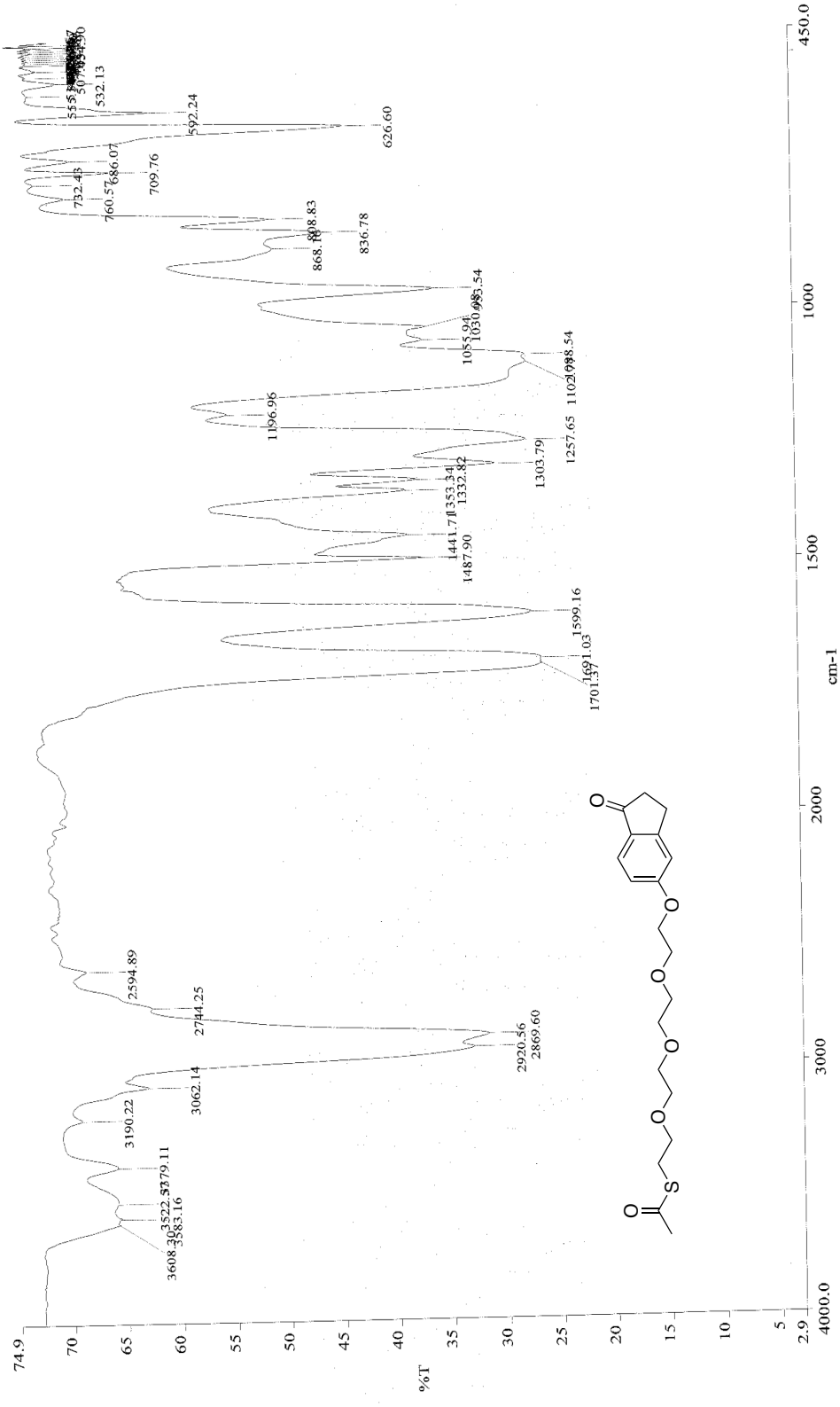

Figure 36: Infrared spectra (neat) of **17**

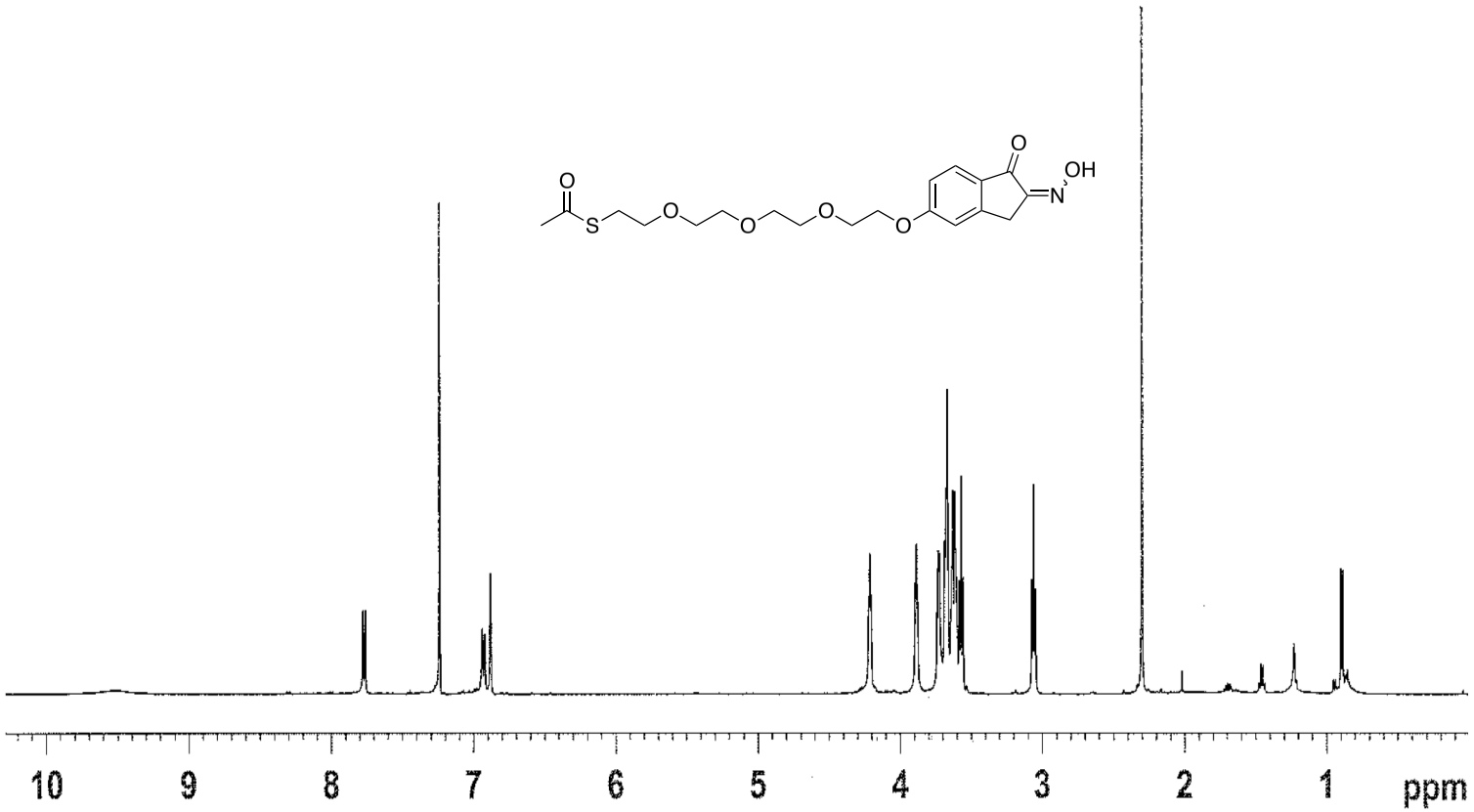

Figure 37: ^{1}H NMR ($CDCl_3$, 500 MHz) of **18**

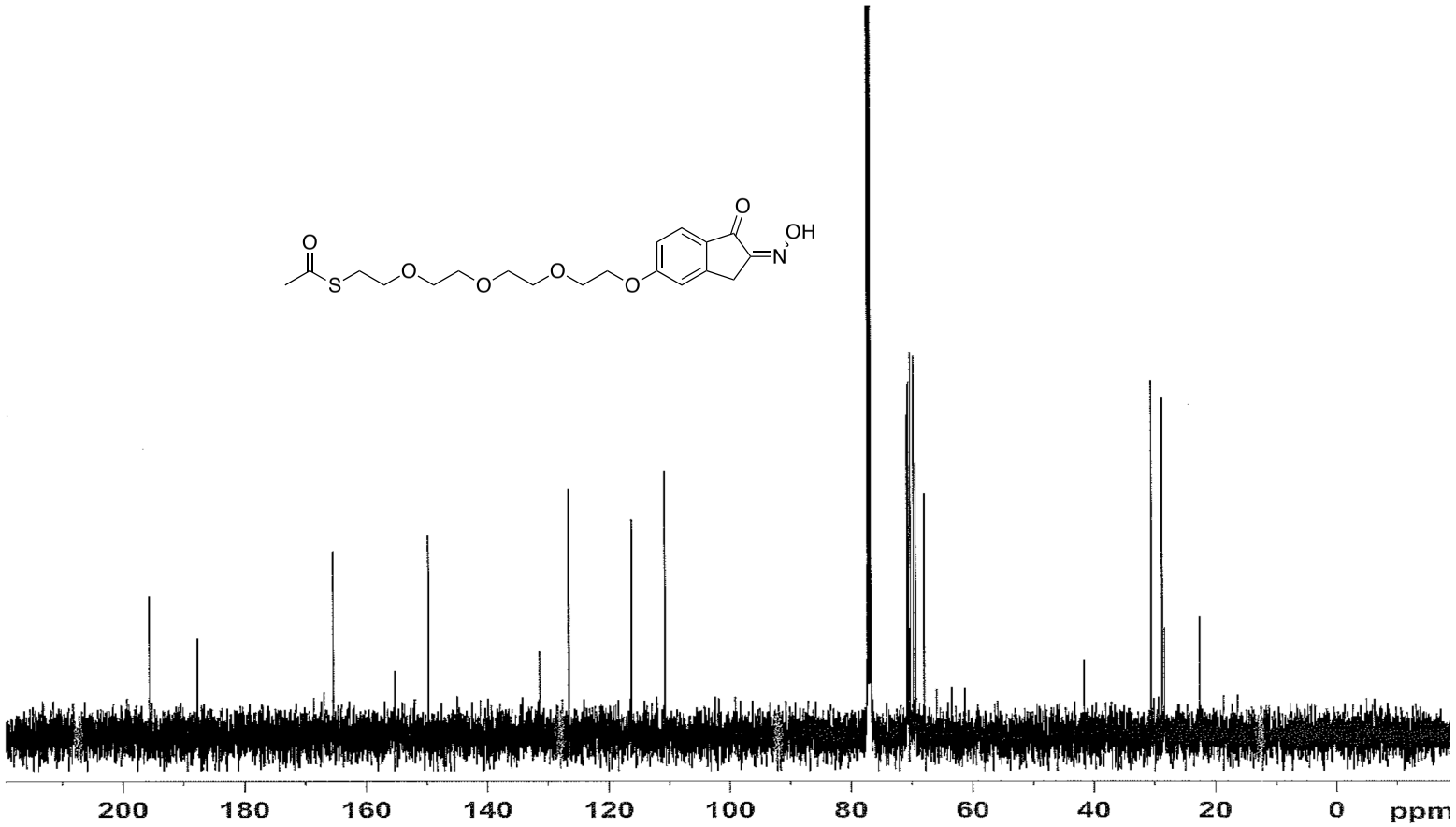

Figure 38: ^{13}C NMR ($CDCl_3$, 125 MHz) of **18**

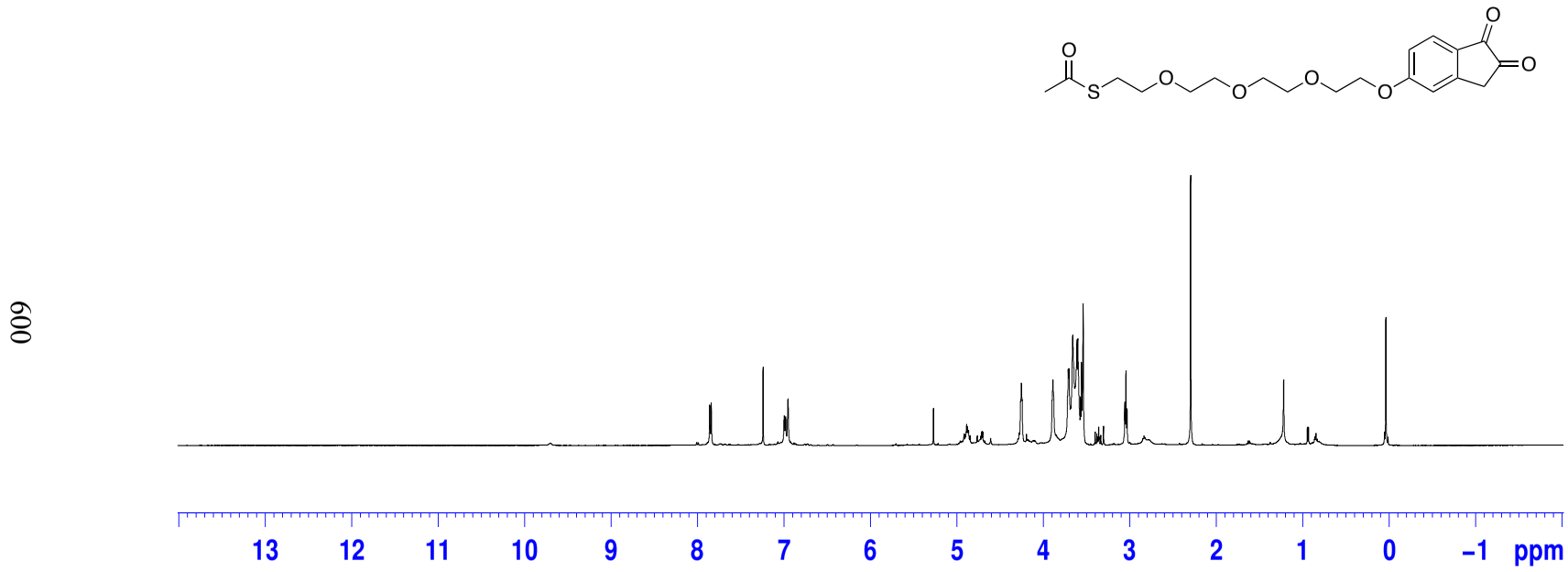

Figure 39: ^{1}H NMR ($CDCl_3$, 500 MHz) of **19**

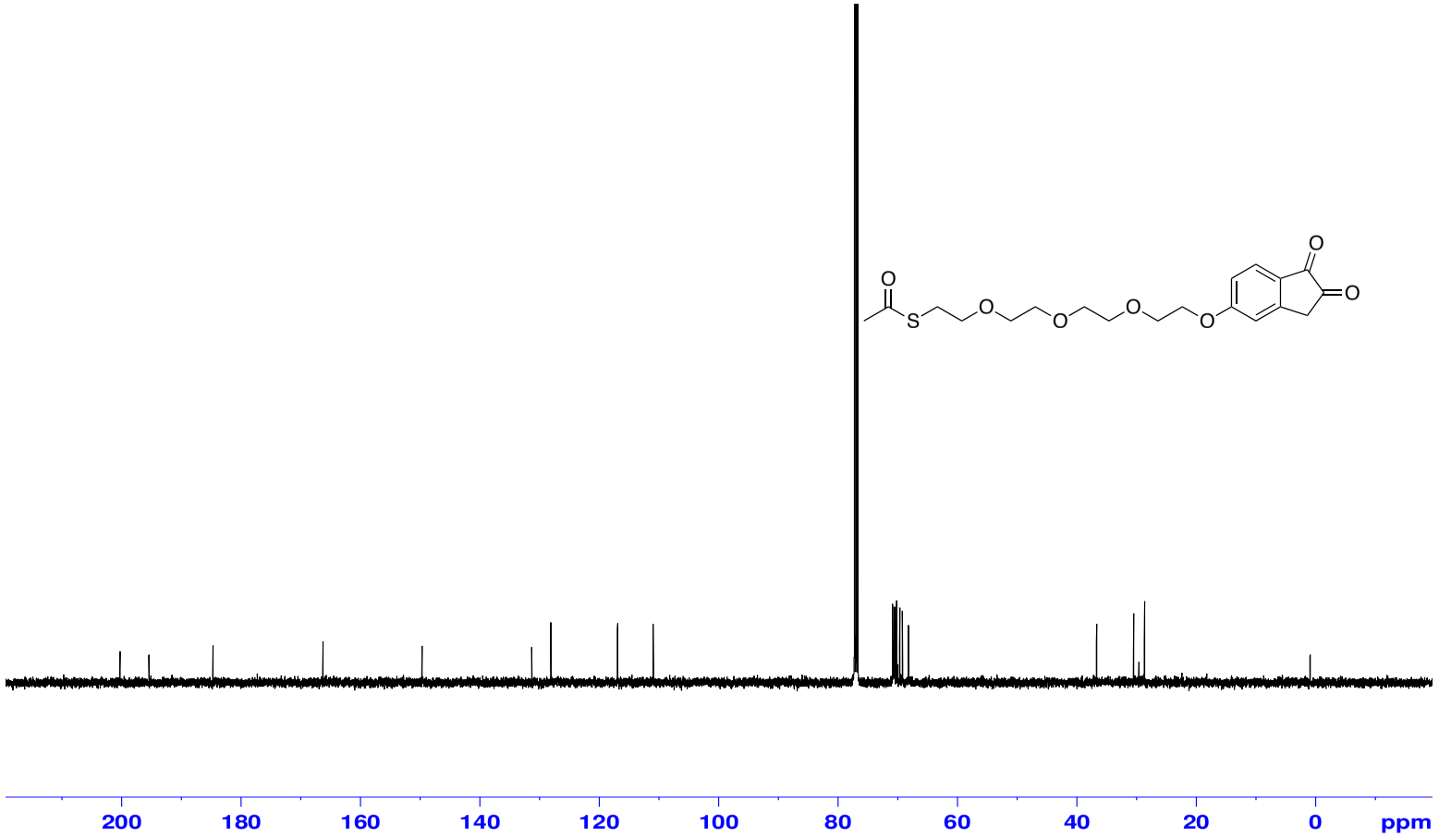

Figure 40: ^{13}C NMR ($CDCl_3$, 125 MHz) of **19**

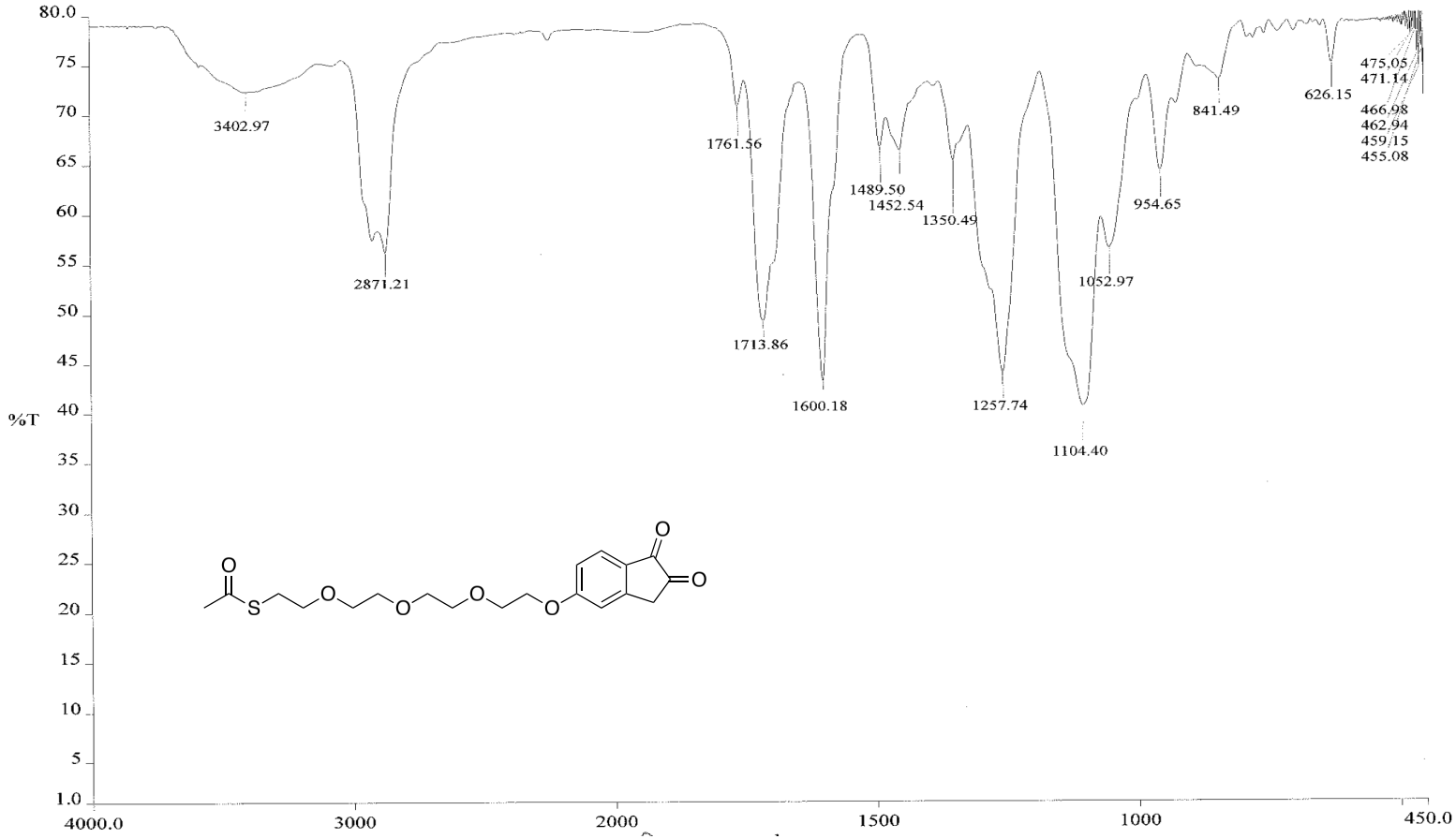

Figure 41: Infrared spectra (neat) of **19**

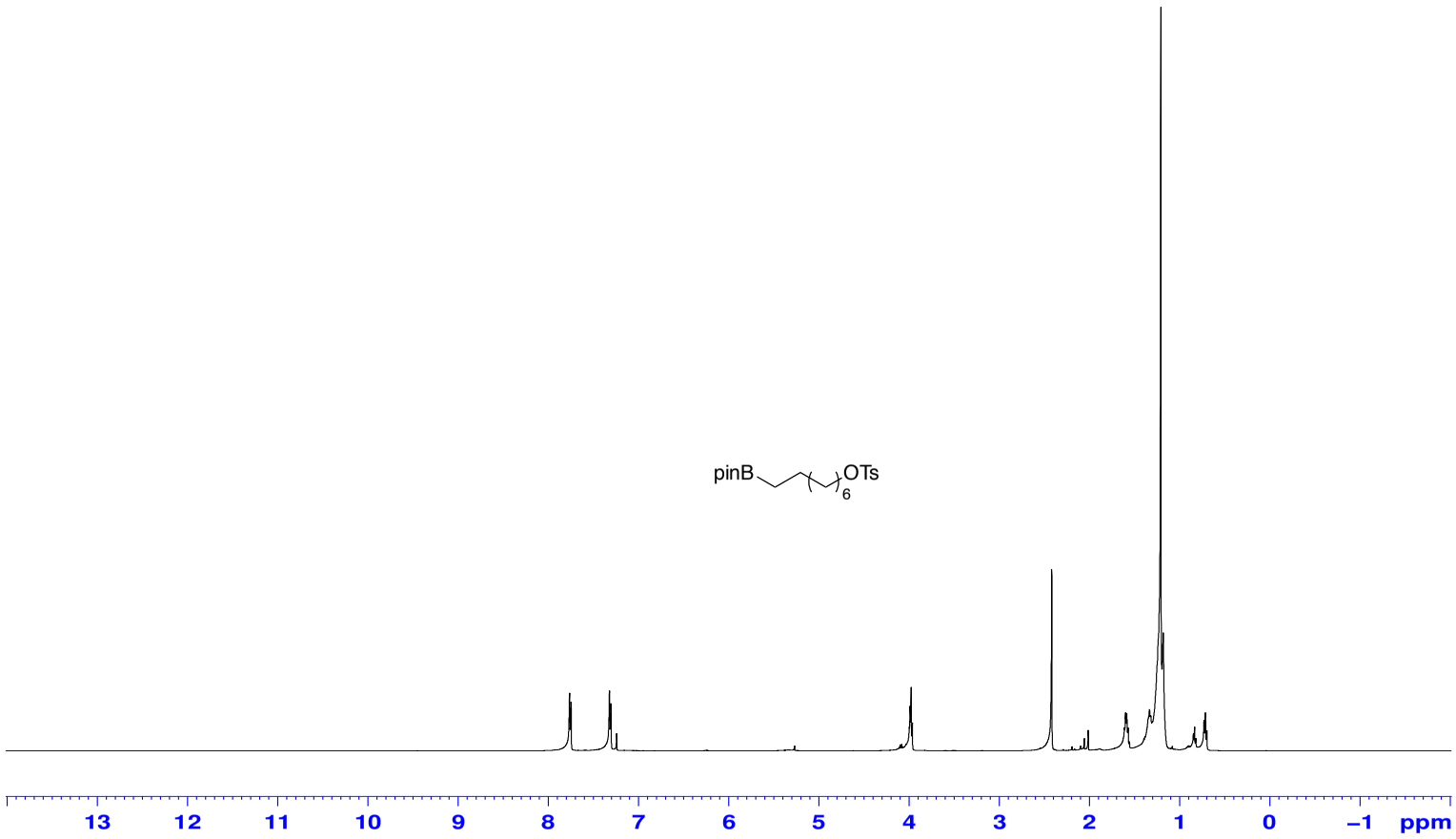

Figure 42: ^{1}H NMR ($CDCl_3$, 500 MHz) of **27**

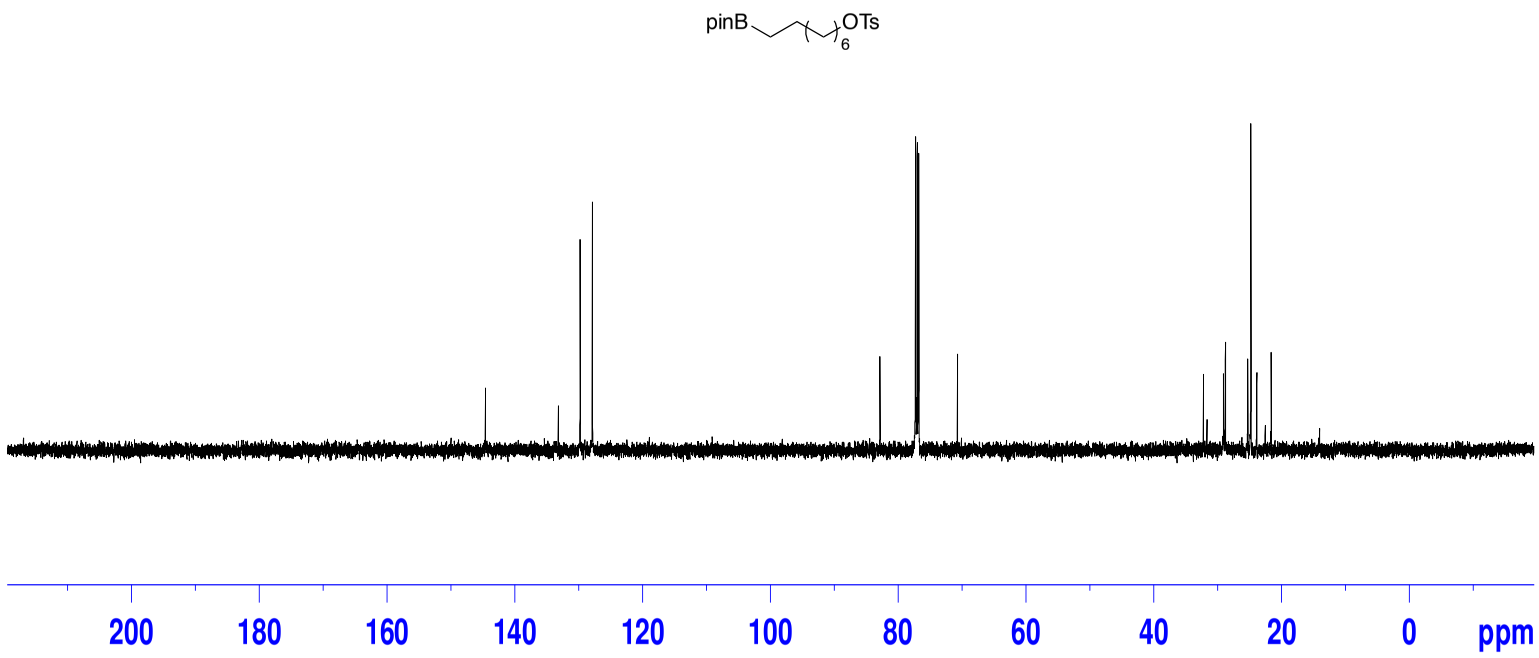

Figure 43: ^{13}C NMR ($CDCl_3$, 125 MHz) of **27**

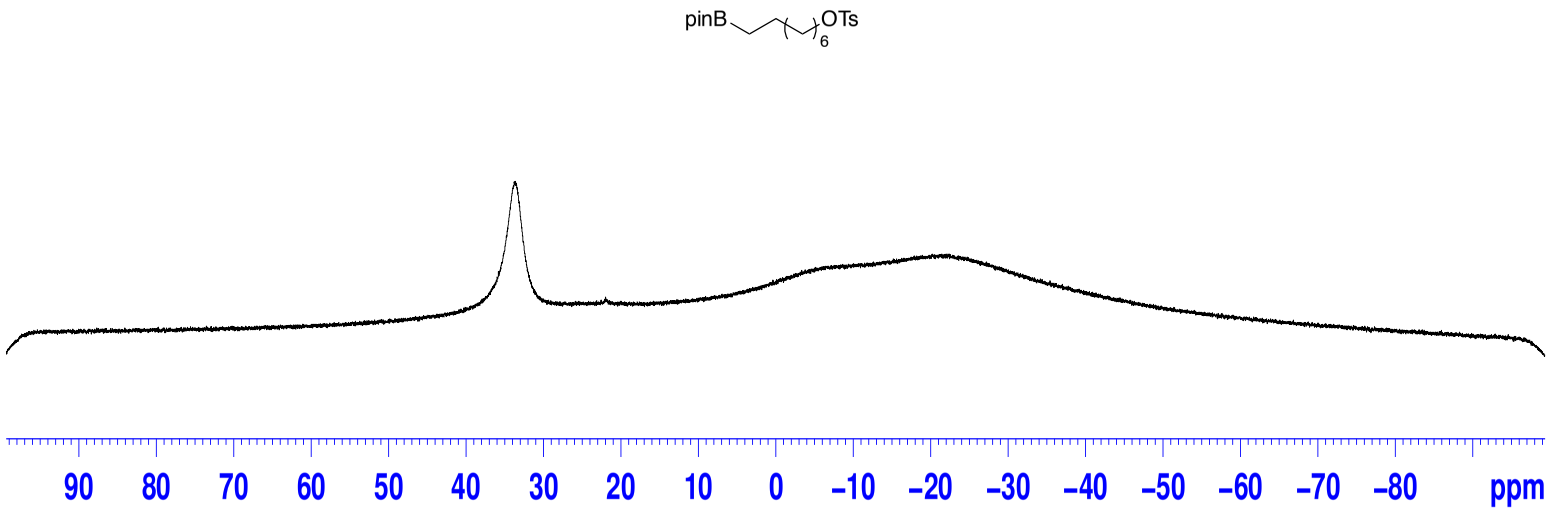

Figure 44: ^{11}B NMR ($CDCl_3$, 128.4 MHz) of **27**

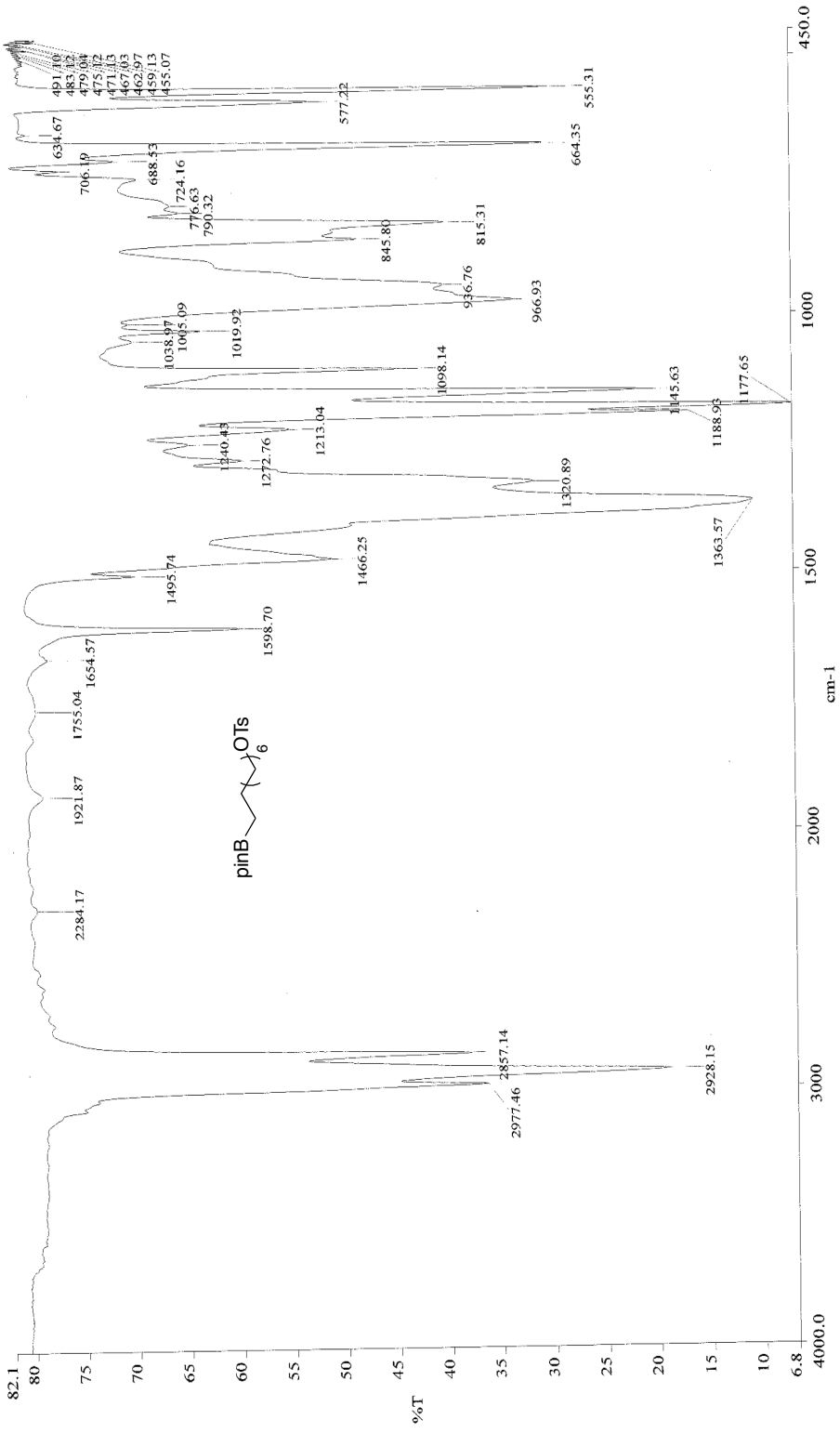

Figure 45: Infrared spectra (neat) of **27**

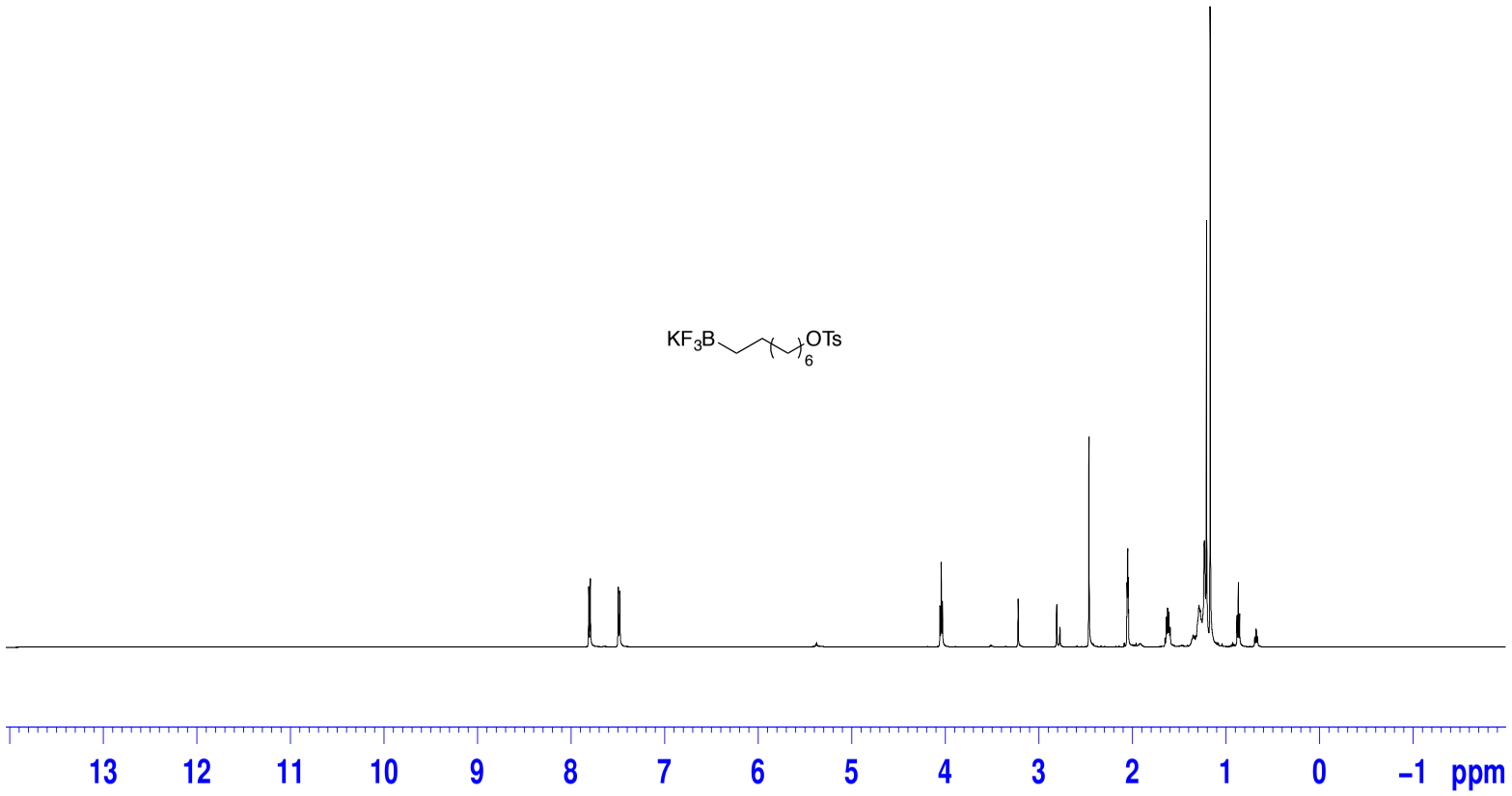

Figure 46: ^{1}H NMR (Acetone-d_6, 500 MHz) of **32**

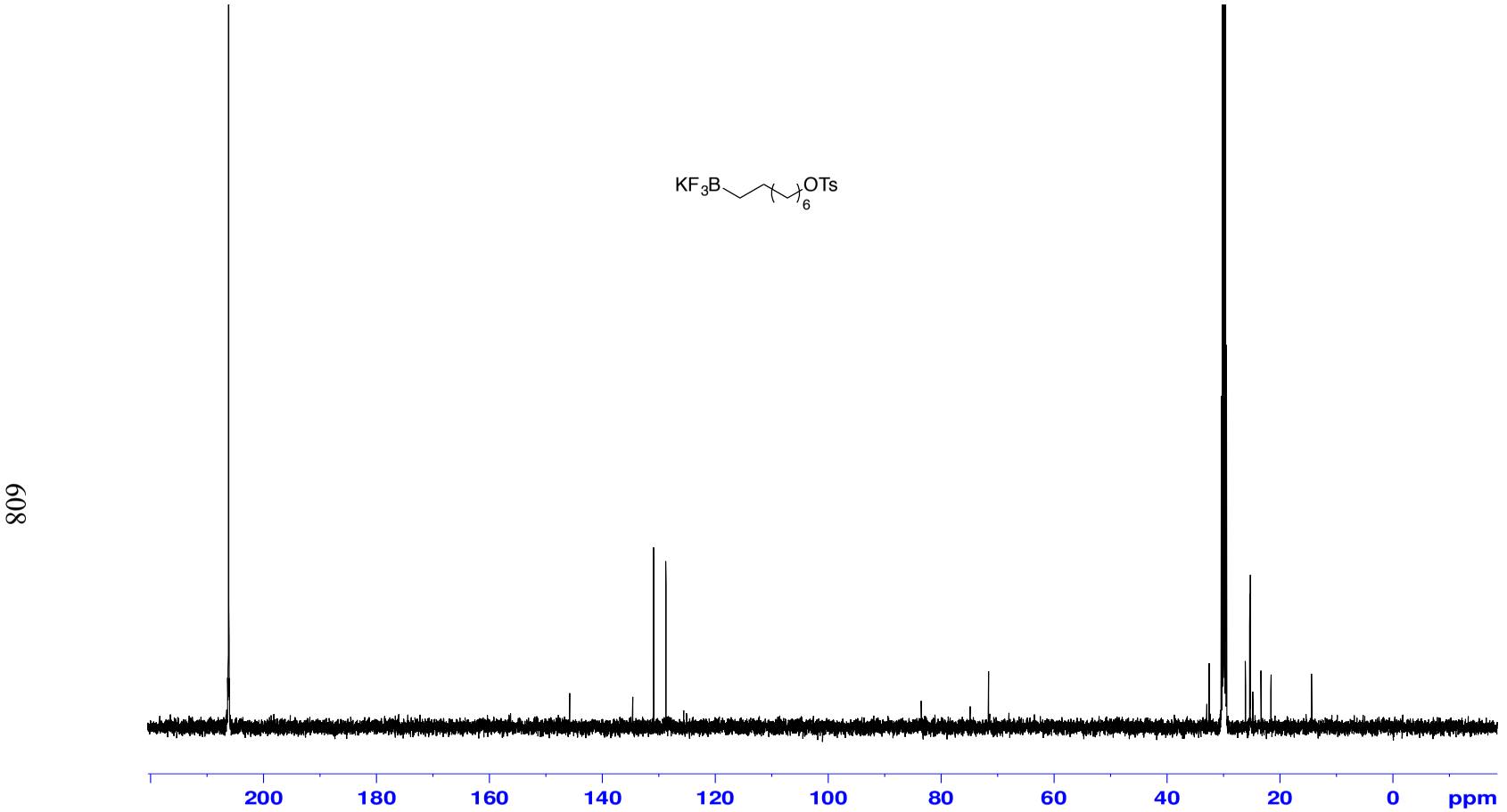

Figure 47: ^{13}C NMR (Acetone-d_6, 125 MHz) of **32**

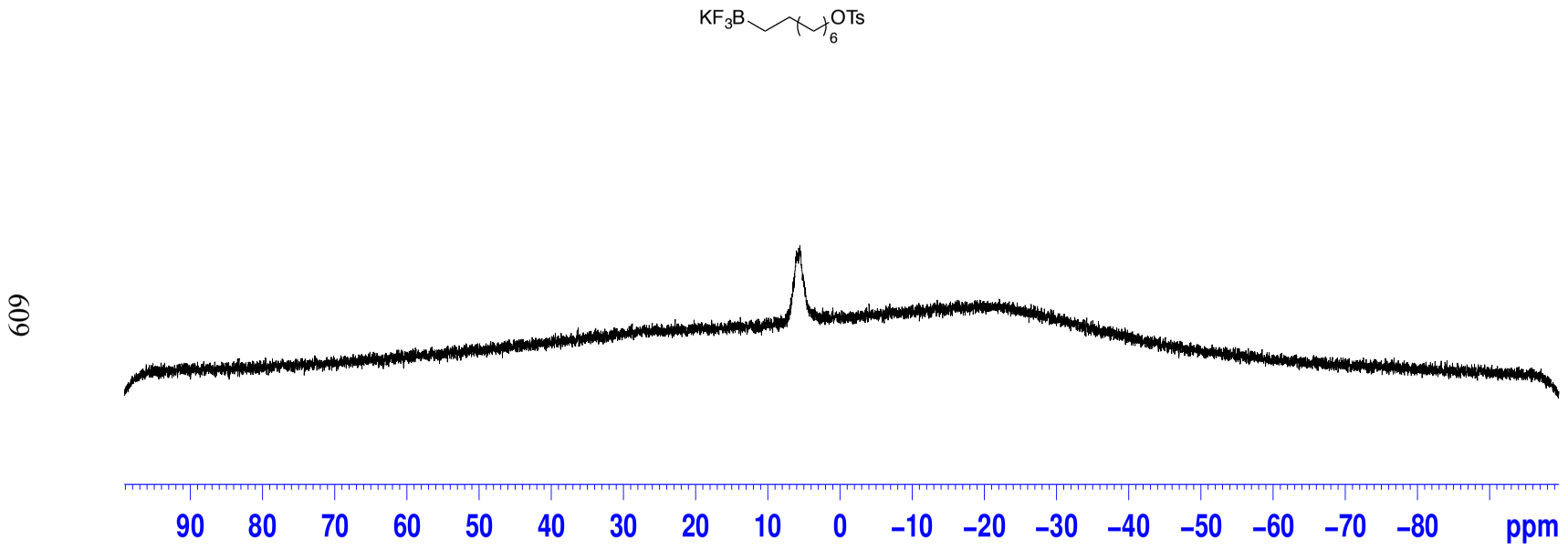

Figure 48: ^{11}B NMR (Acetone-d_6, 128.4 MHz) of **32**

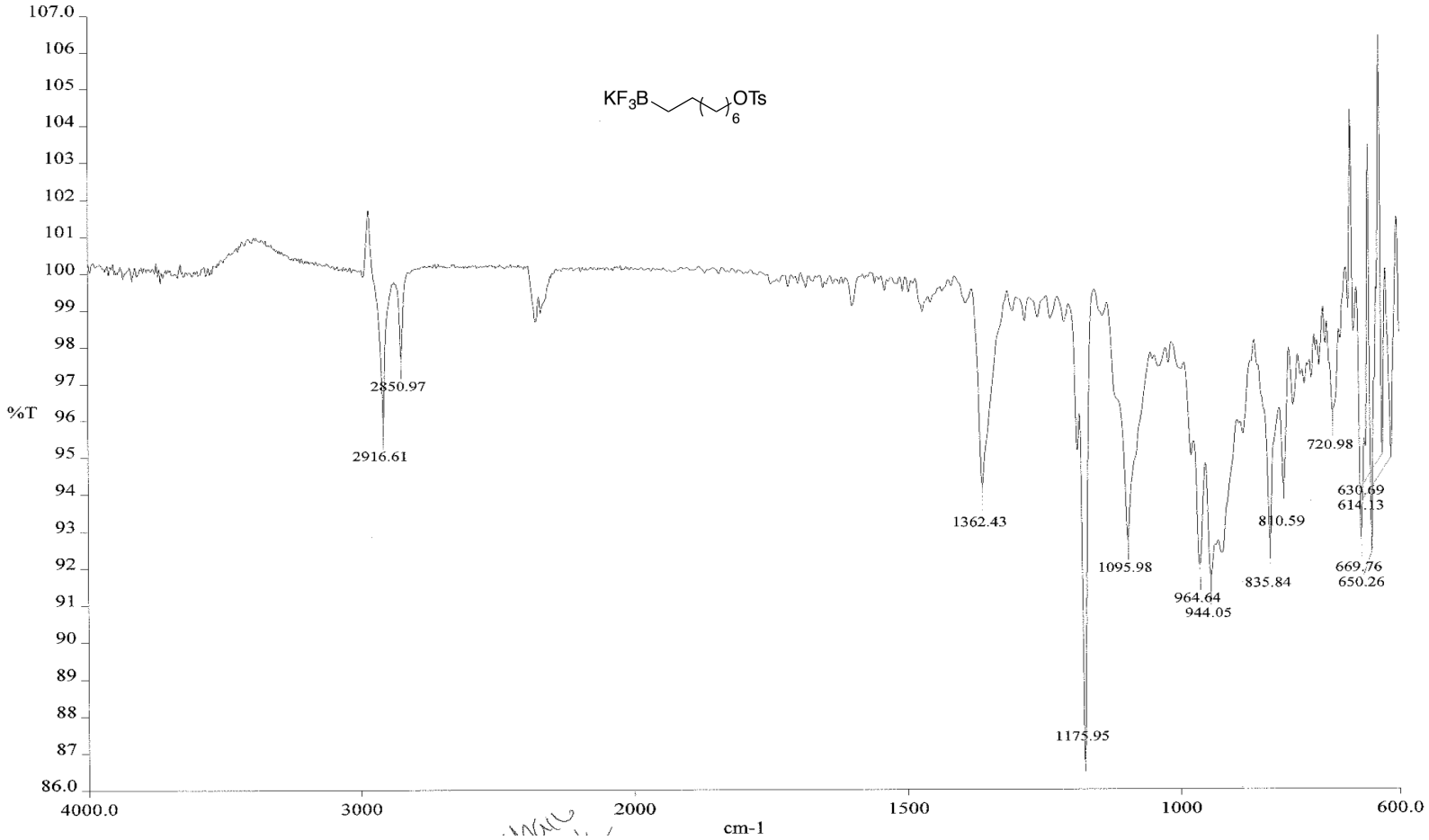

Figure 49: Infrared spectra (neat) of **32**

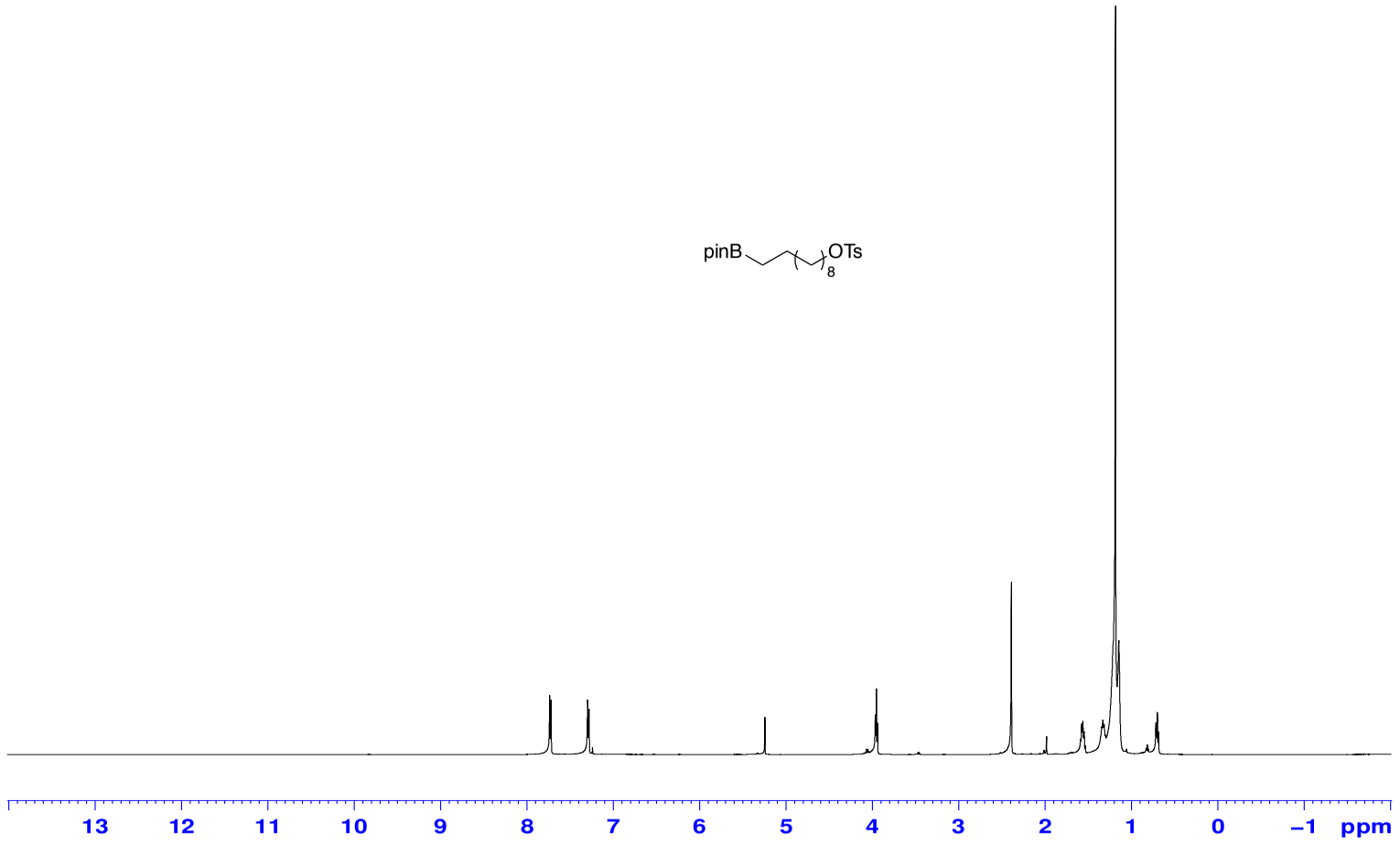

Figure 50: ^{1}H NMR ($CDCl_3$, 500 MHz) of **28**

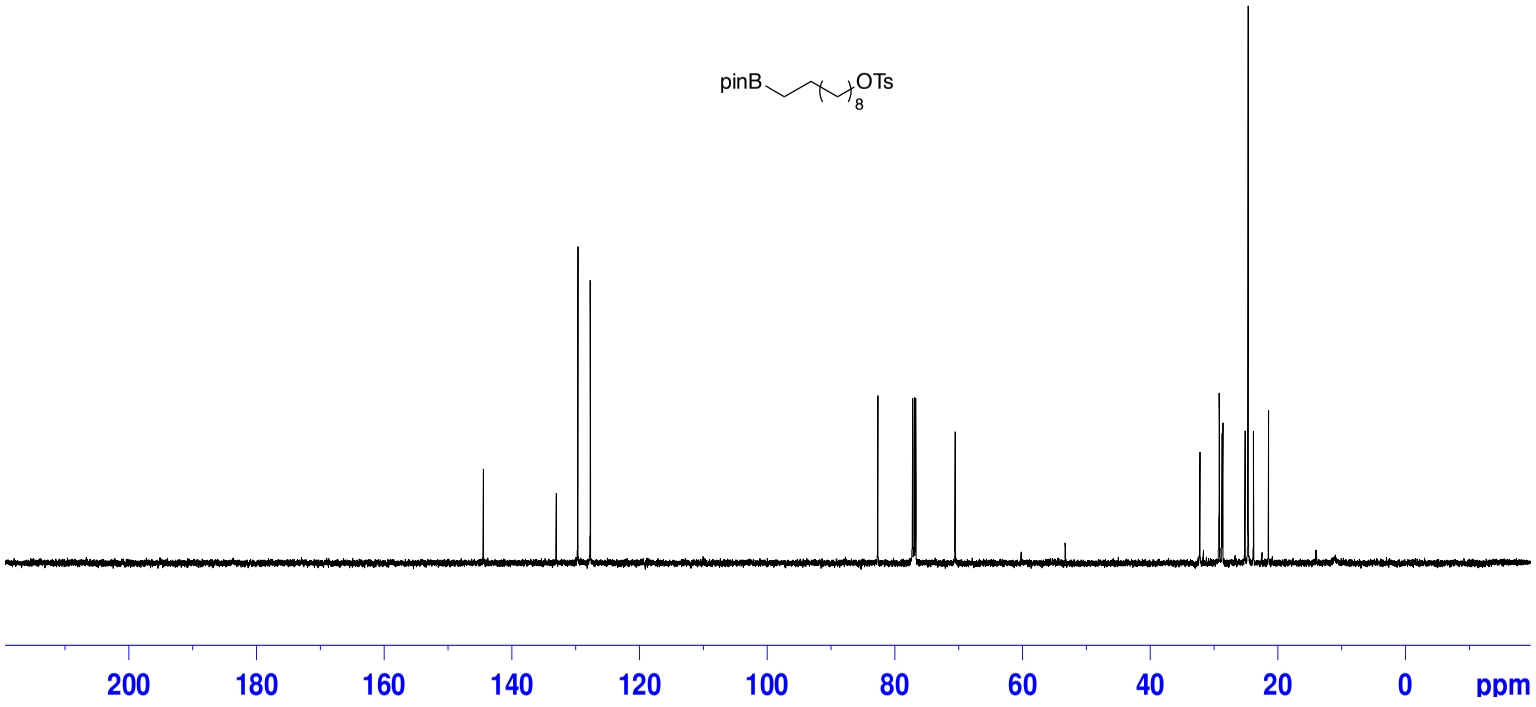

Figure 51: ^{13}C NMR ($CDCl_3$, 125 MHz) of **28**

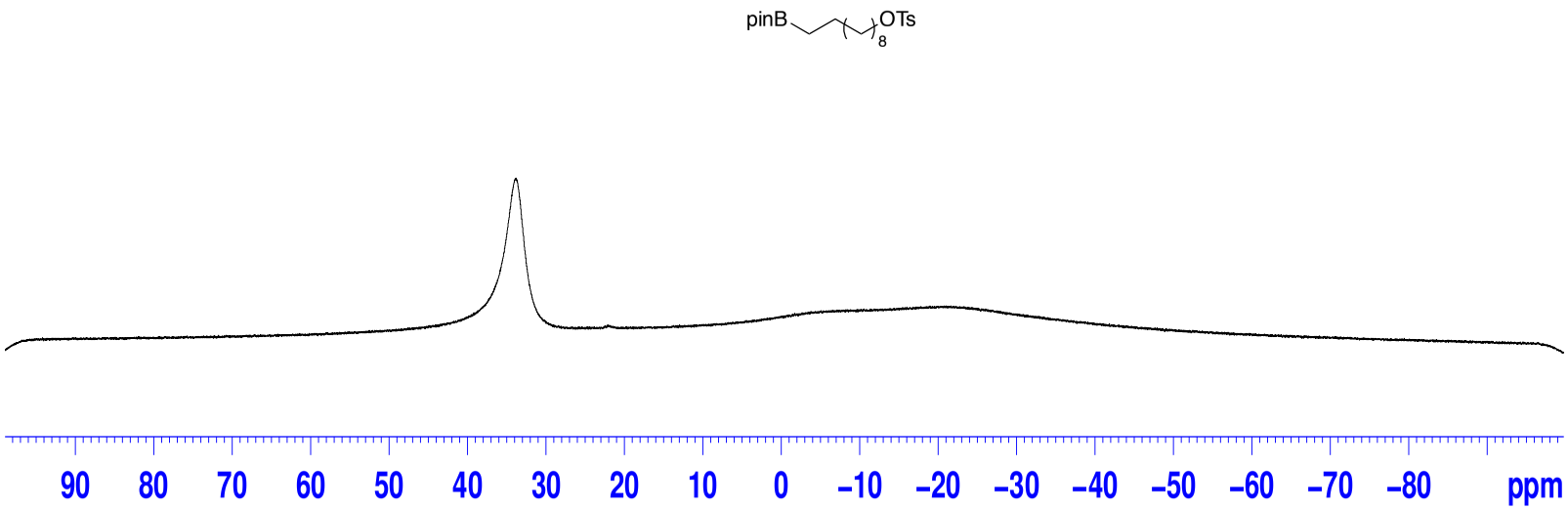

Figure 52: ^{11}B NMR ($CDCl_3$, 128.4 MHz) of **28**

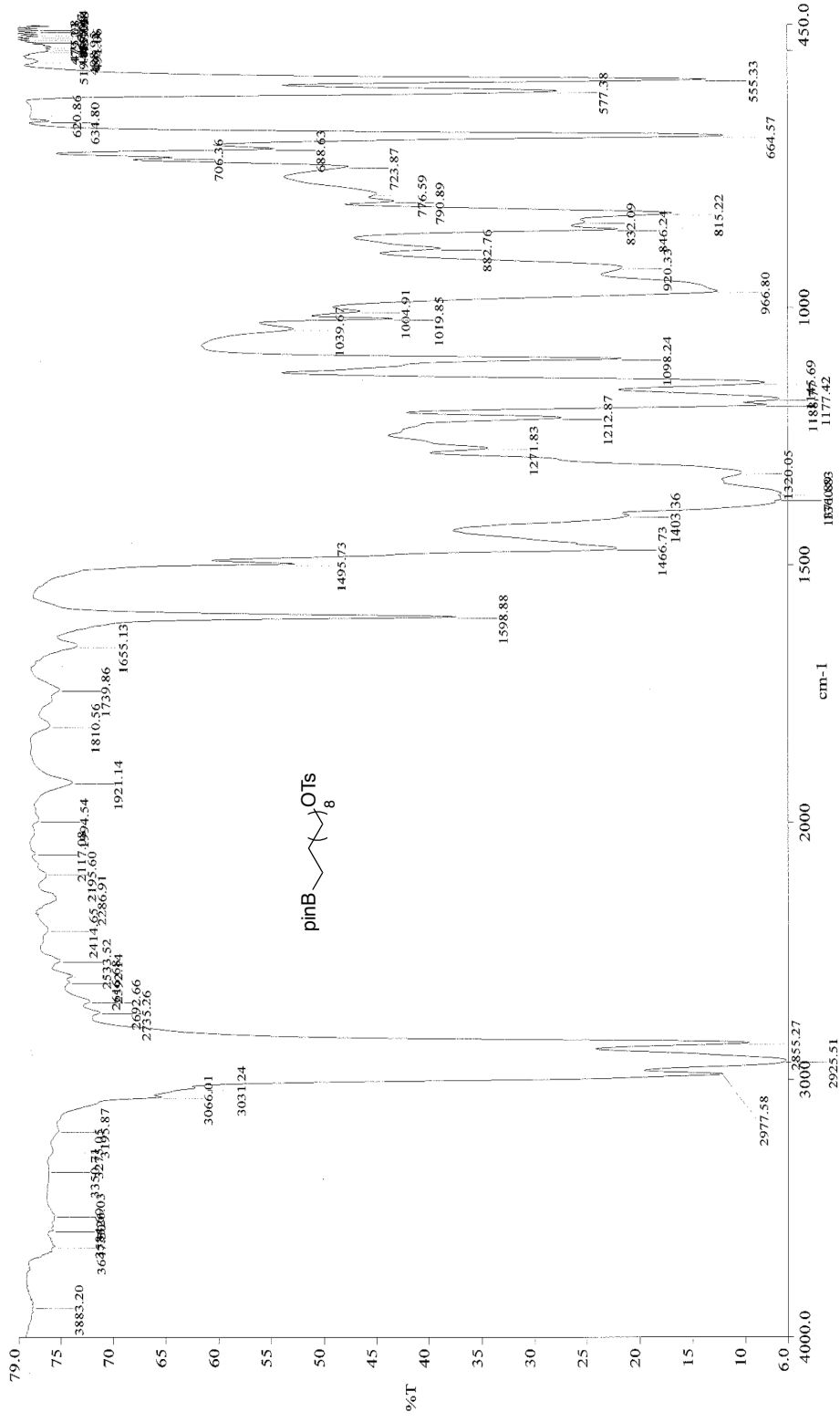

Figure 53: Infrared spectra (neat) of **28**

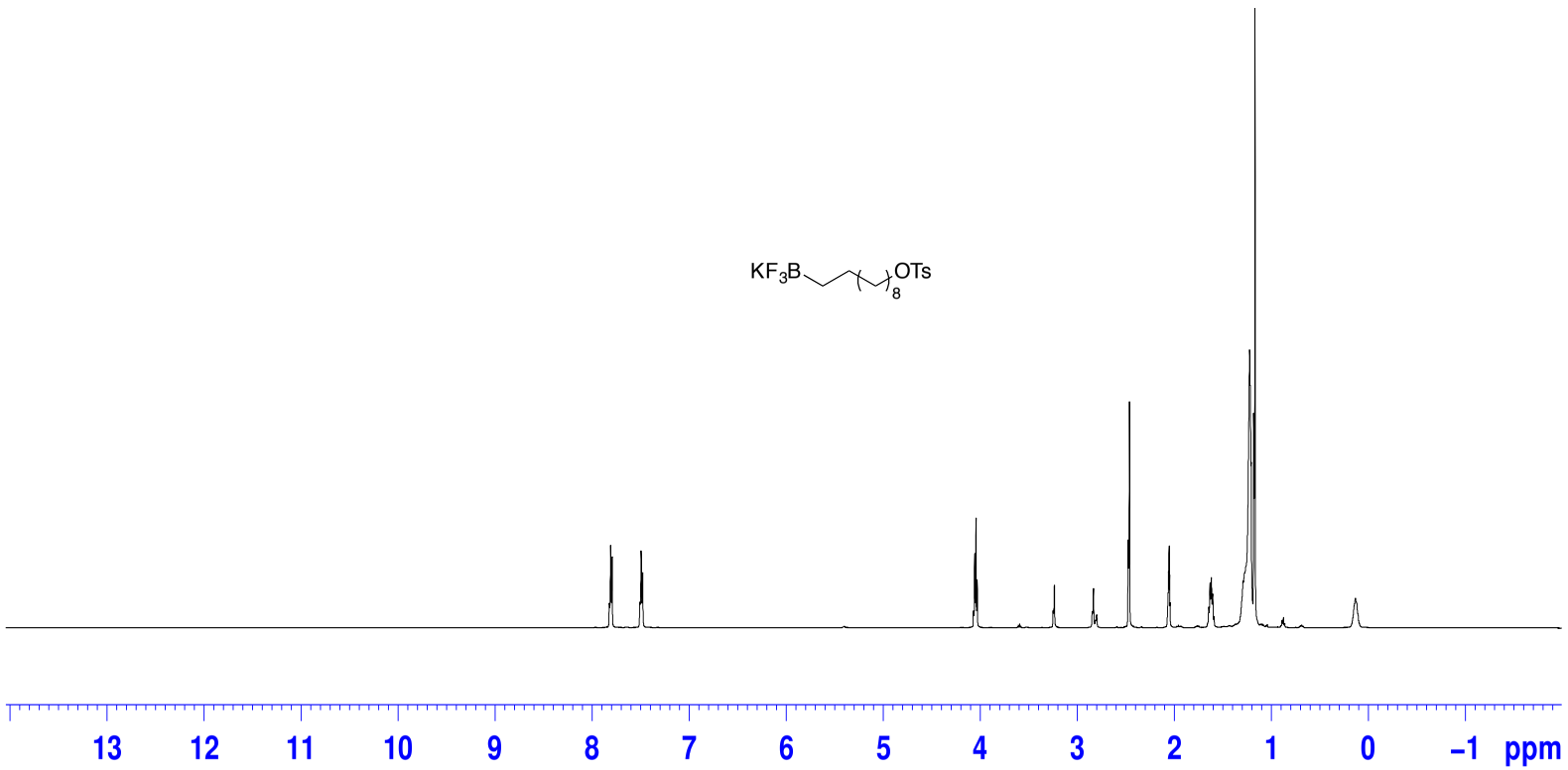

Figure 54: ^{1}H NMR (Acetone-$d_{6,}$ 500 MHz) of **33**

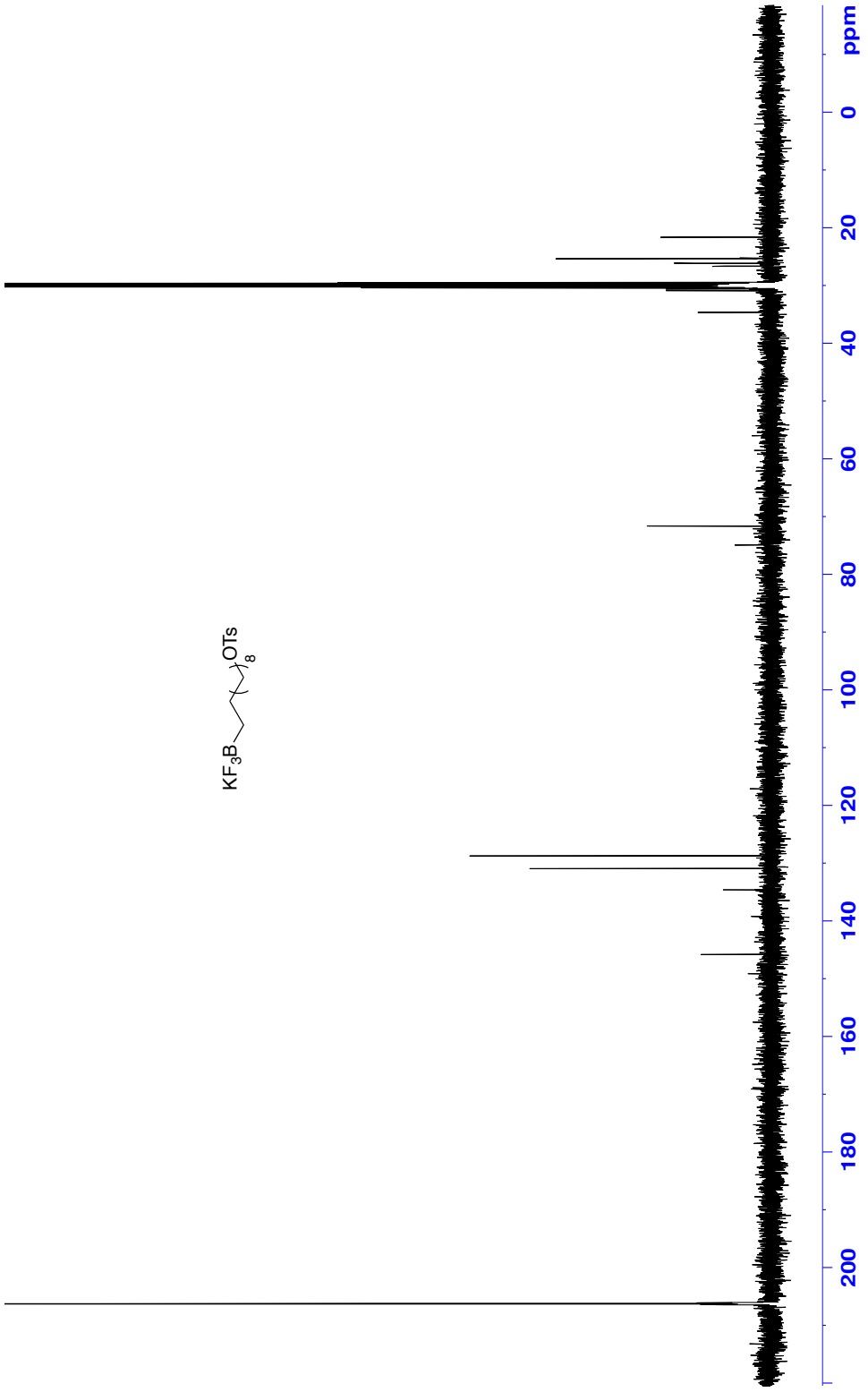

Figure 55: ^{13}C NMR (Acetone-d_6, 125 MHz) of **33**

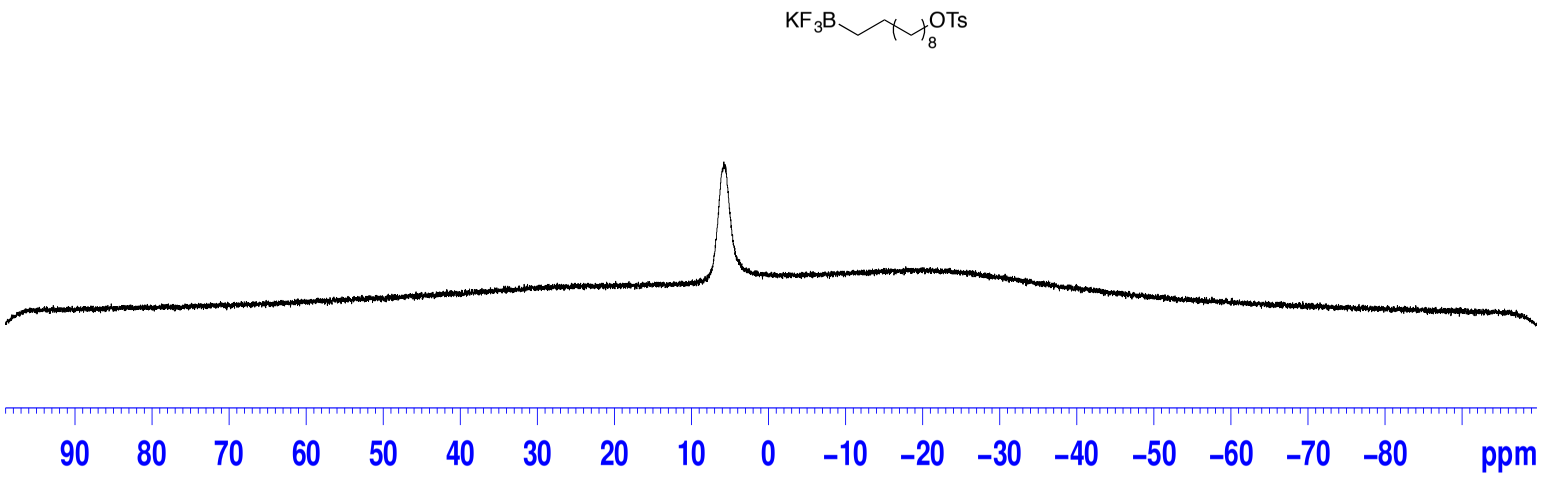

Figure 56: ^{11}B NMR (Acetone-d_6, 128.4 MHz) of **33**

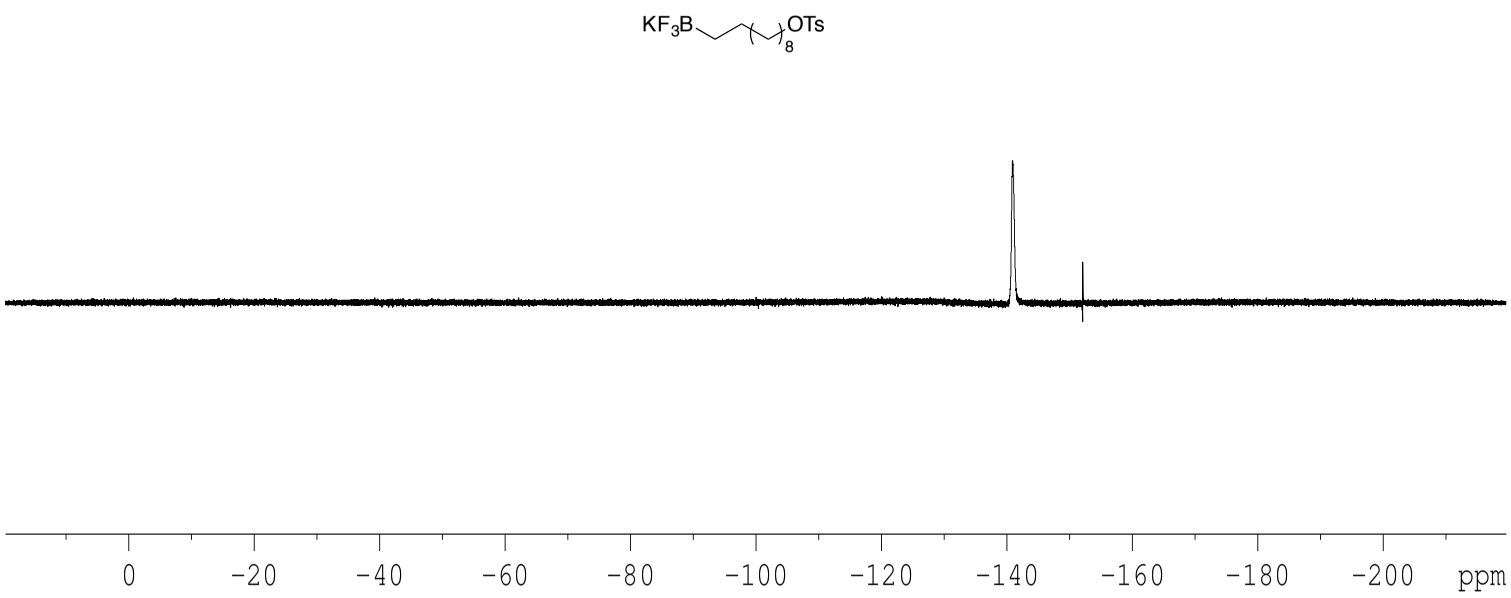

Figure 57: ^{19}F NMR (Acetone-d_6, 470.8 MHz) of **33**

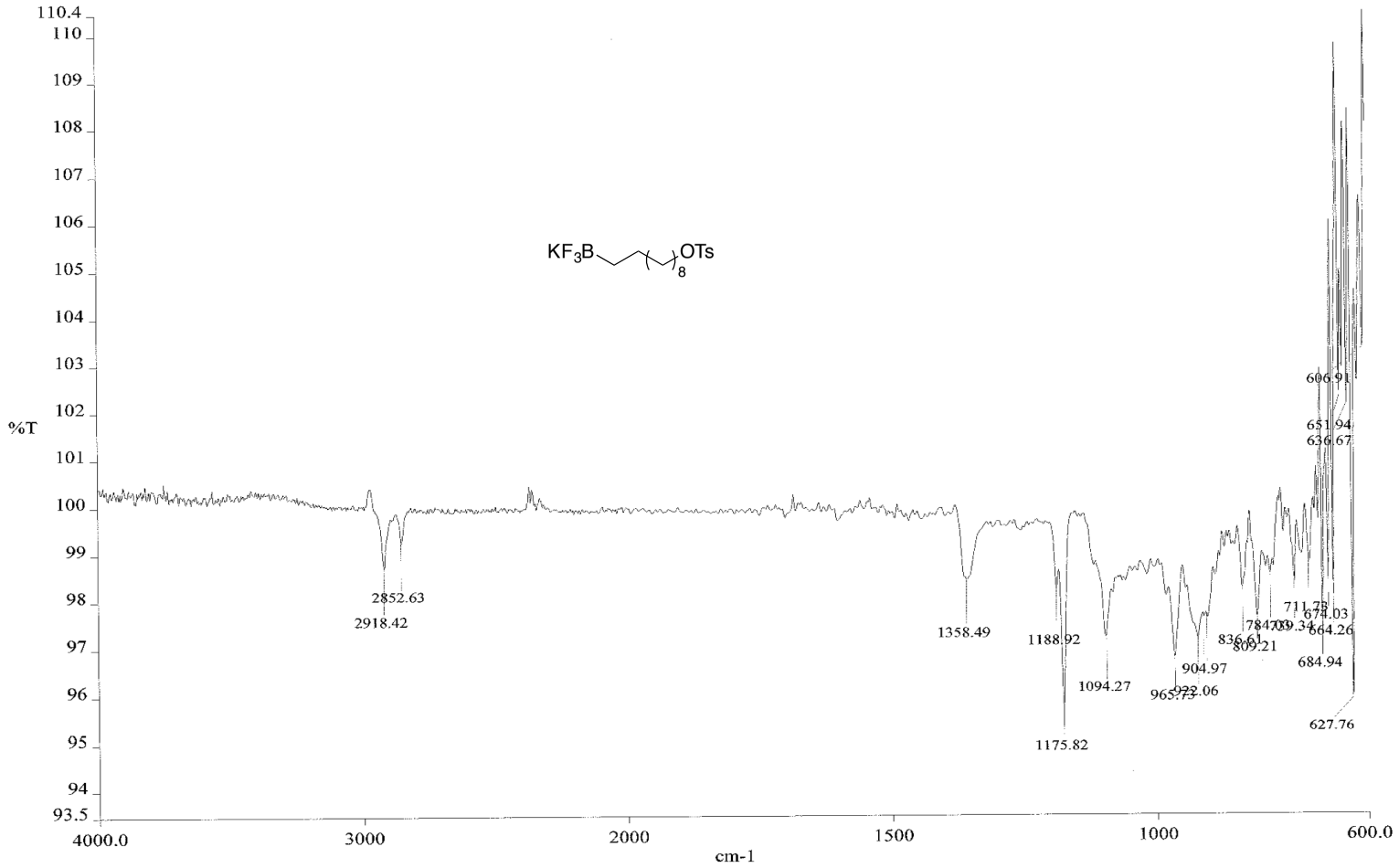

Figure 58: Infrared spectra (neat) of **33**

Figure 59: ^{1}H NMR ($CDCl_3$, 500 MHz) of **29**

v

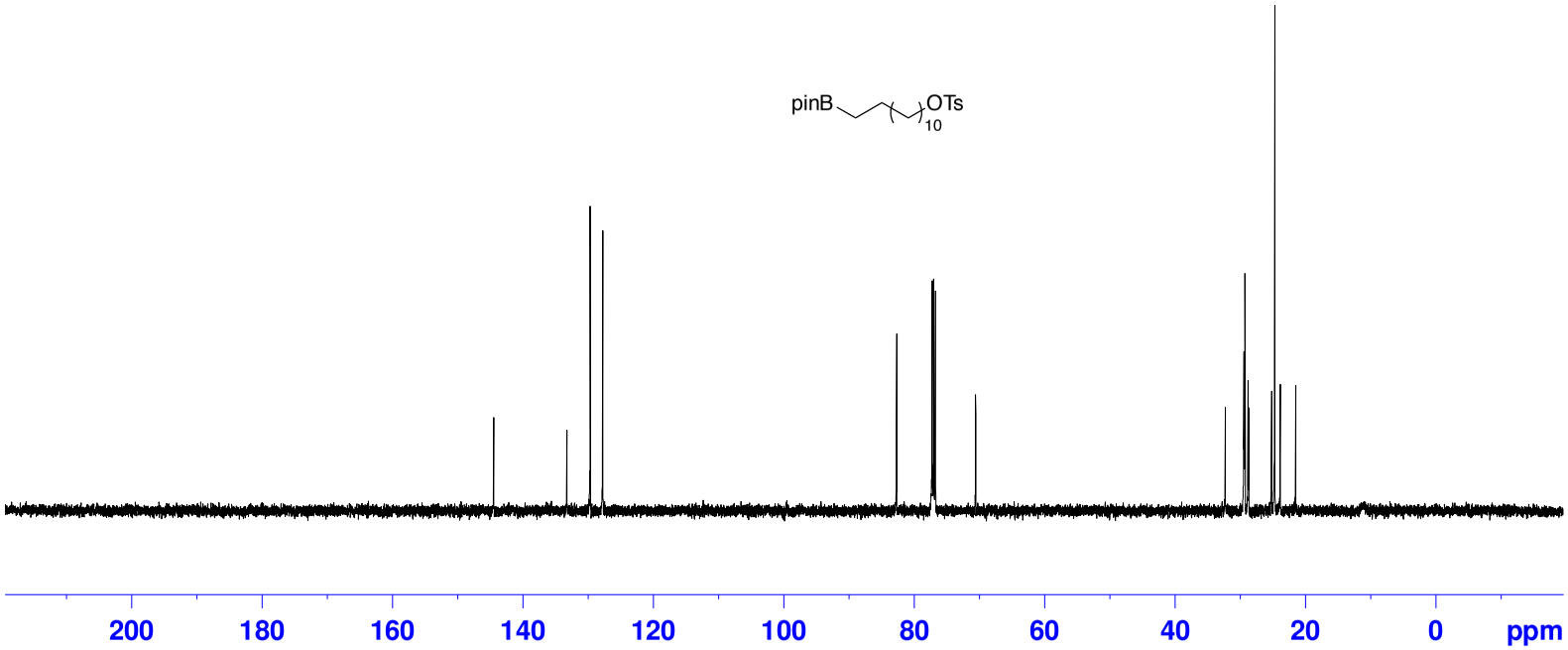

Figure 60: ^{13}C NMR ($CDCl_3$, 125 MHz) of **29**

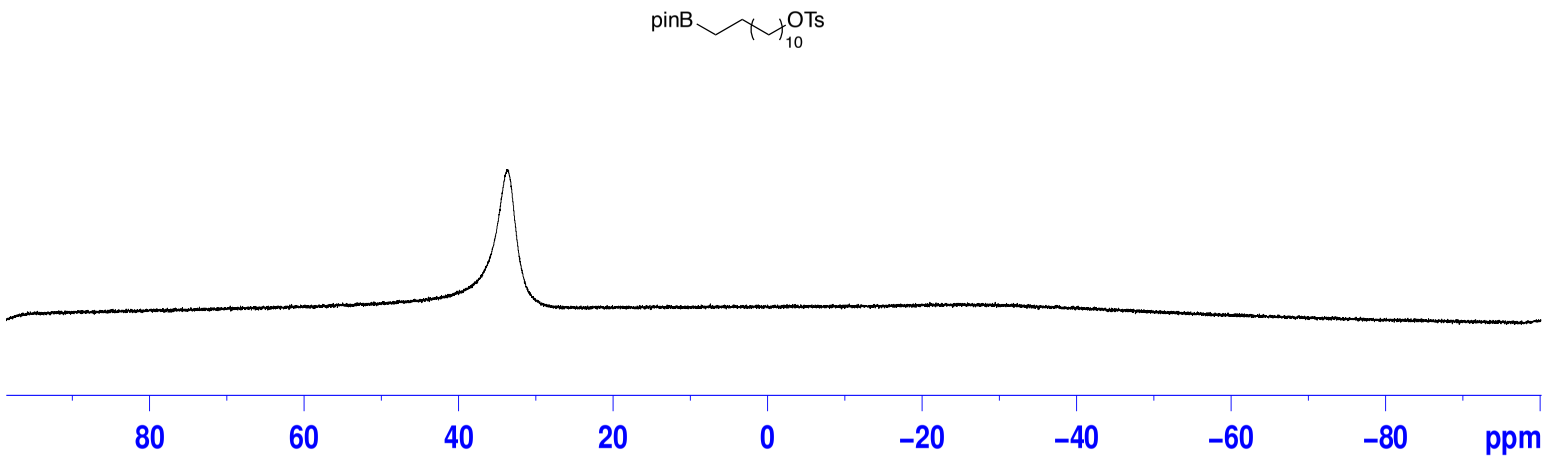

Figure 61: ^{11}B NMR ($CDCl_3$, 128.4 MHz) of **29**

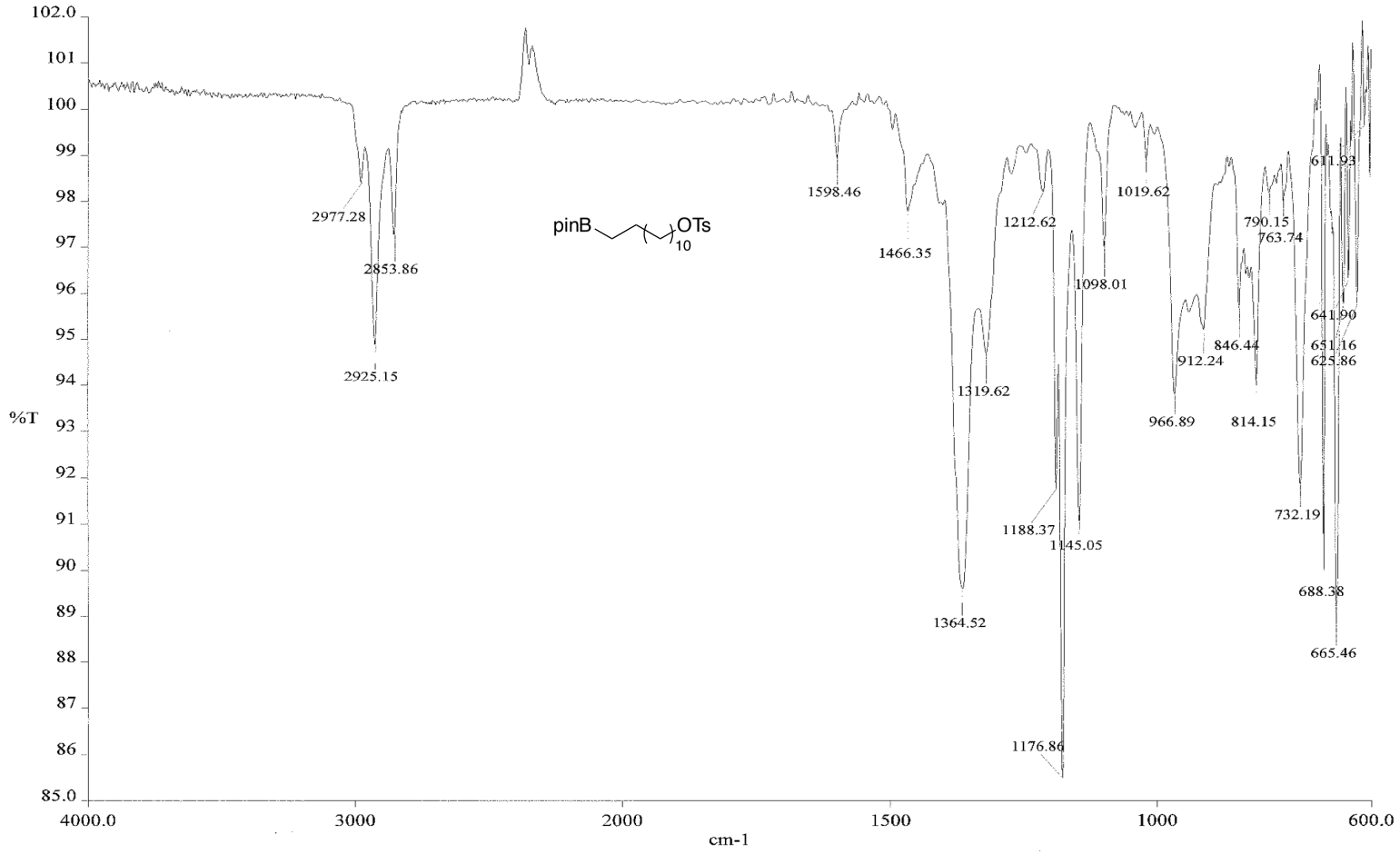

Figure 62: Infrared spectra (neat) of **29**

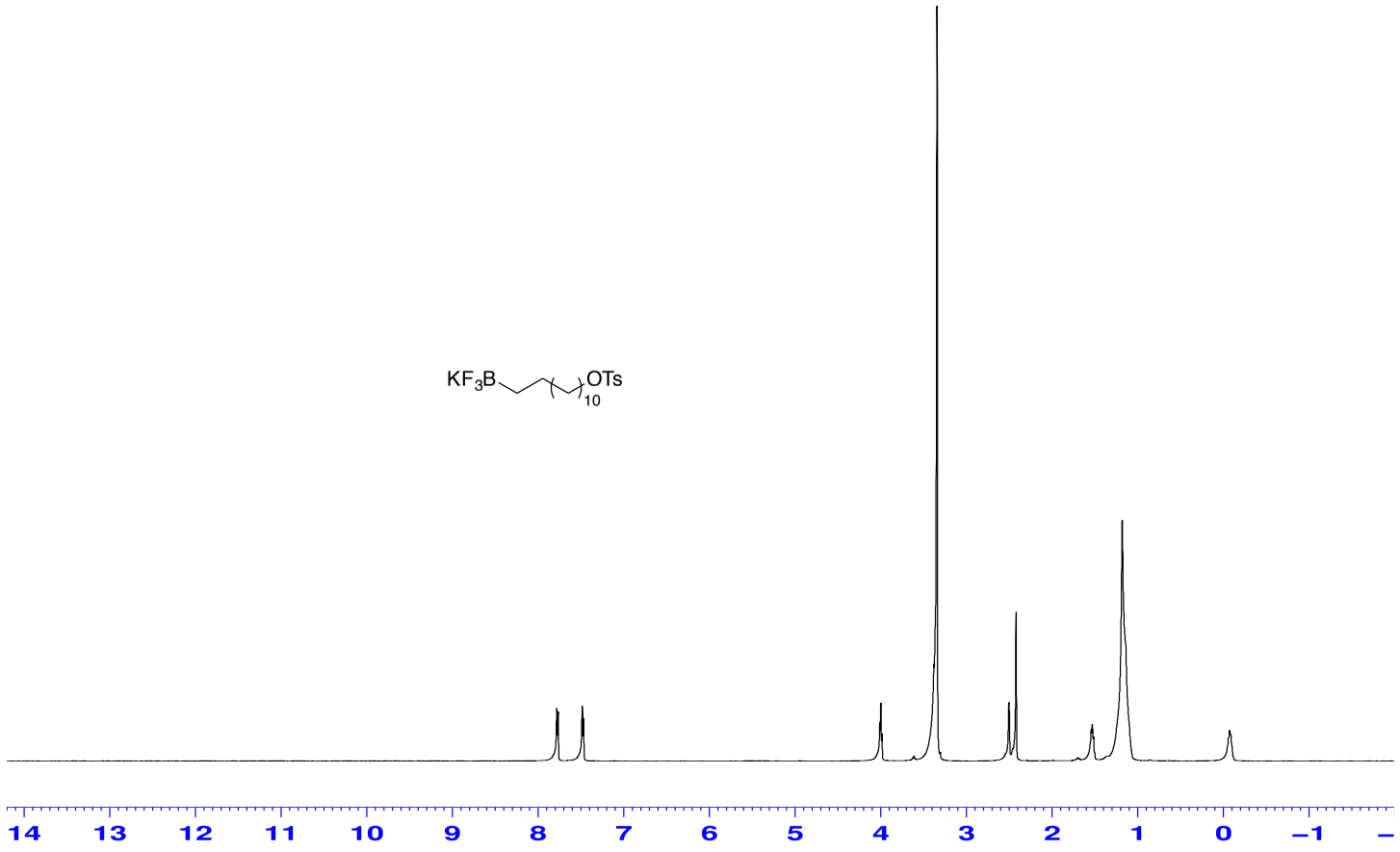

Figure 63: ^{1}H NMR (DMSO-d_6, 500 MHz) of **34**

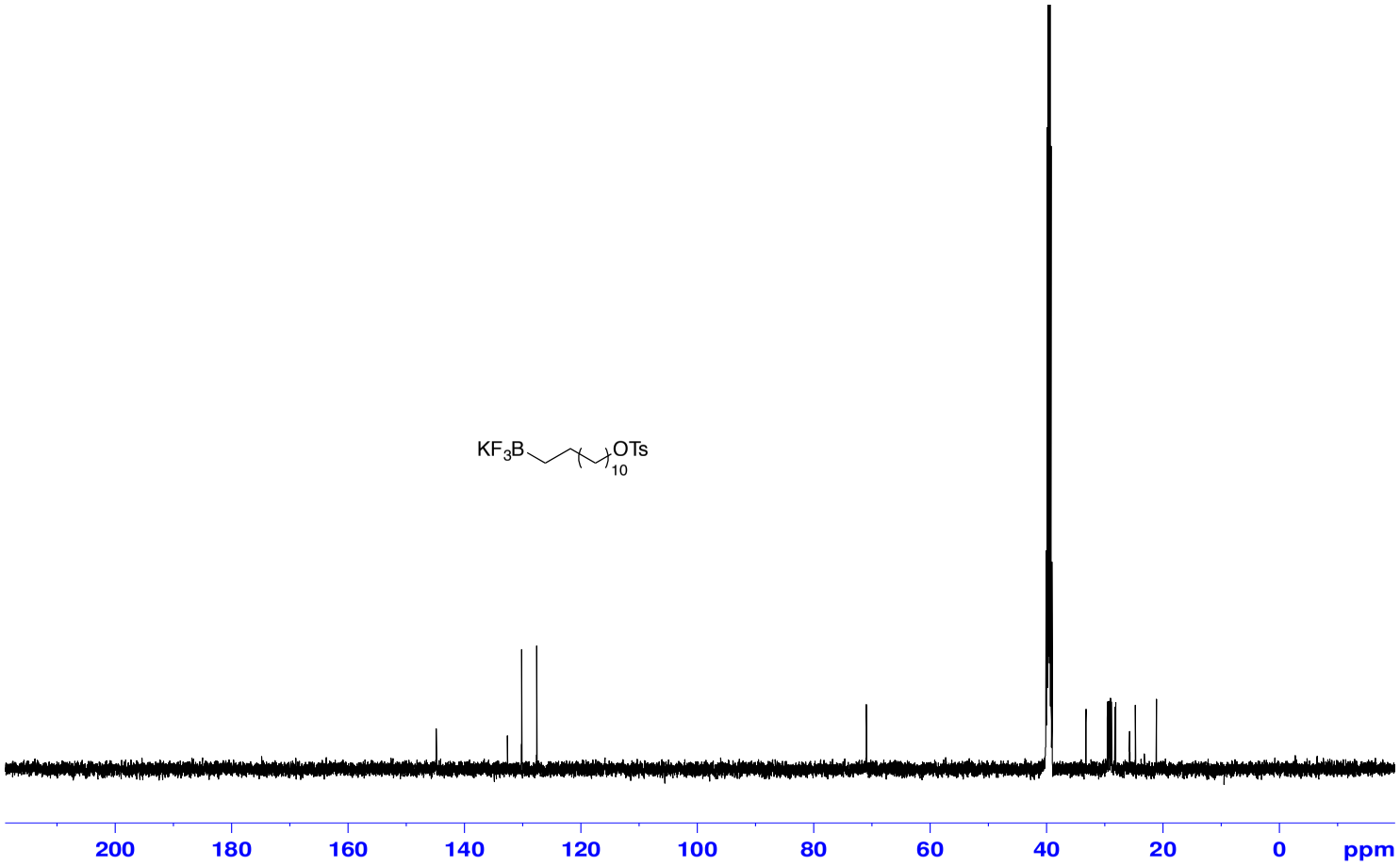

Figure 64: ^{13}C NMR (DMSO-d_6, 125 MHz) of **34**

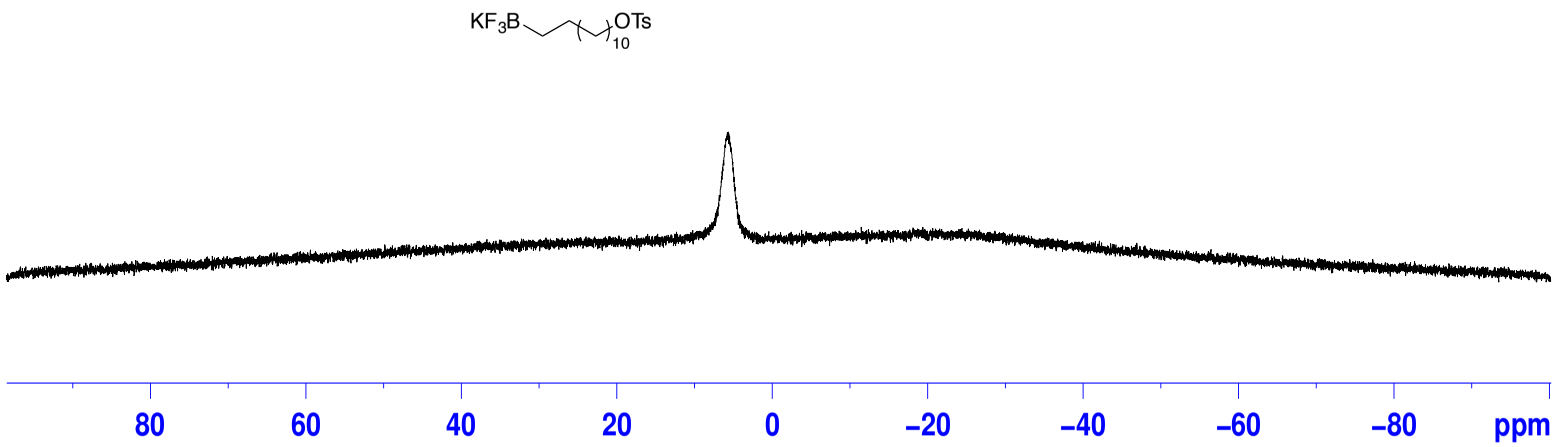

Figure 65: ^{11}B NMR (DMSO-d_6, 128.4 MHz) of **34**

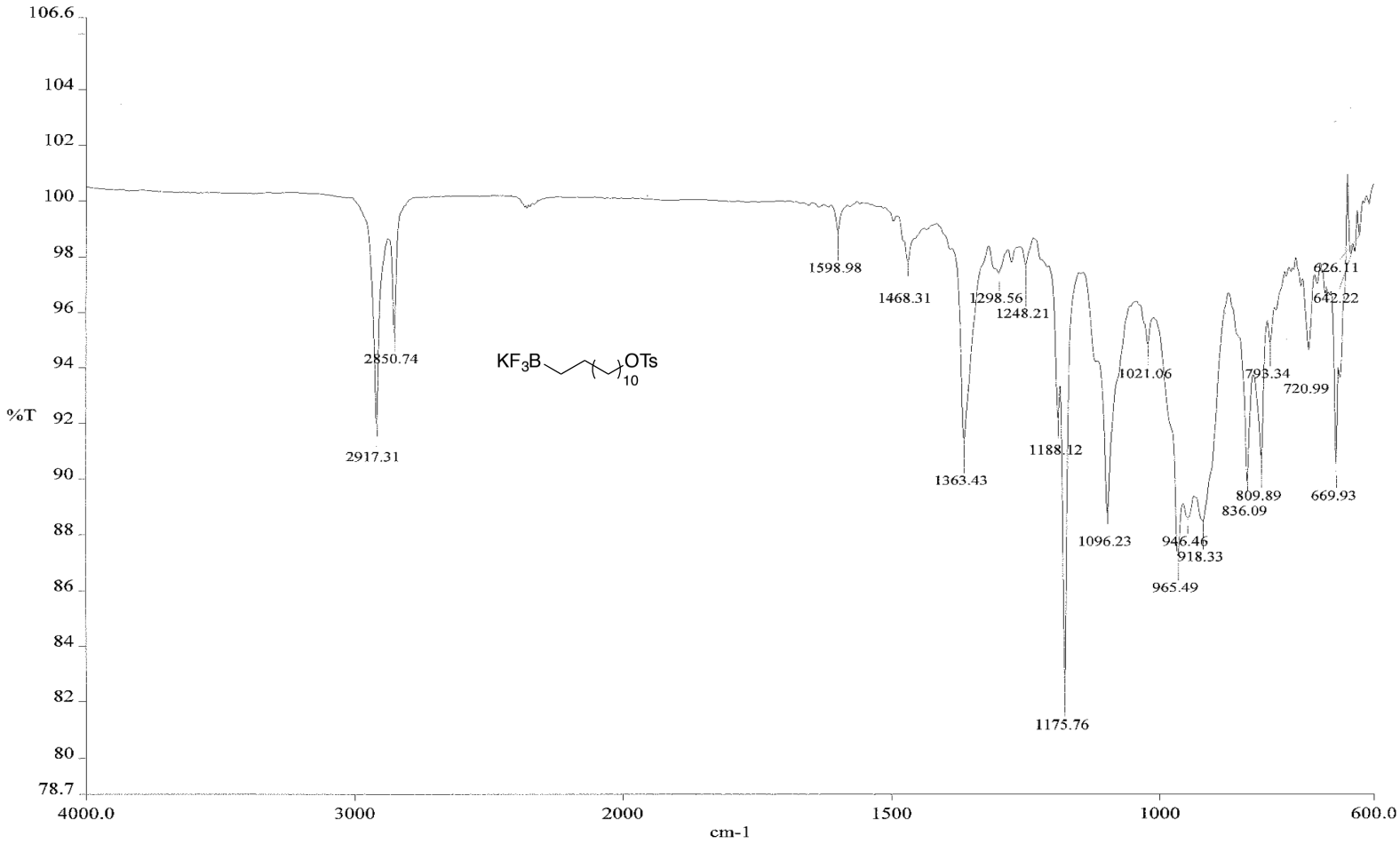

Figure 66: Infrared spectra (neat) of **34**

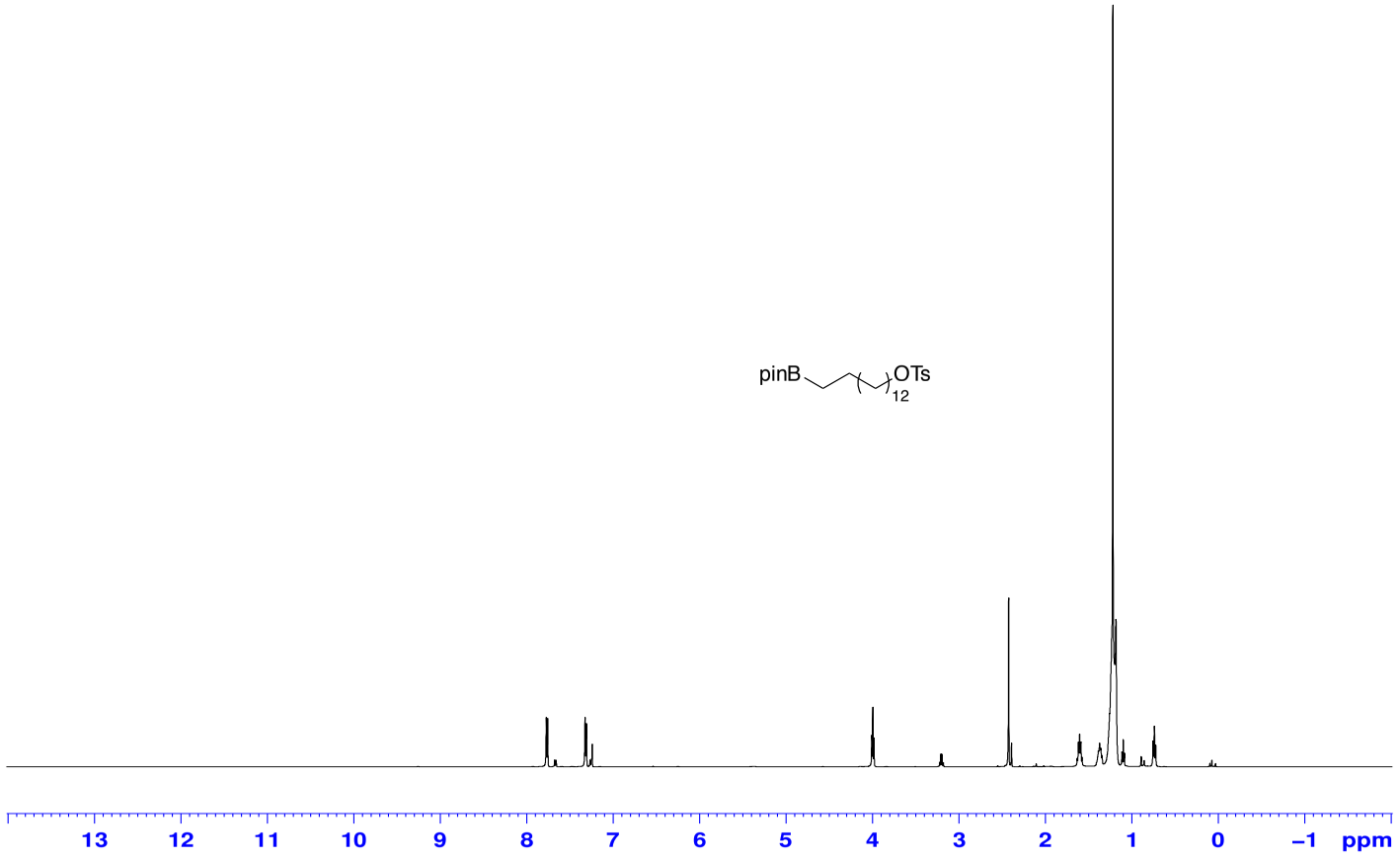

Figure 67: ^{1}H NMR ($CDCl_3$, 500 MHz) of **30**

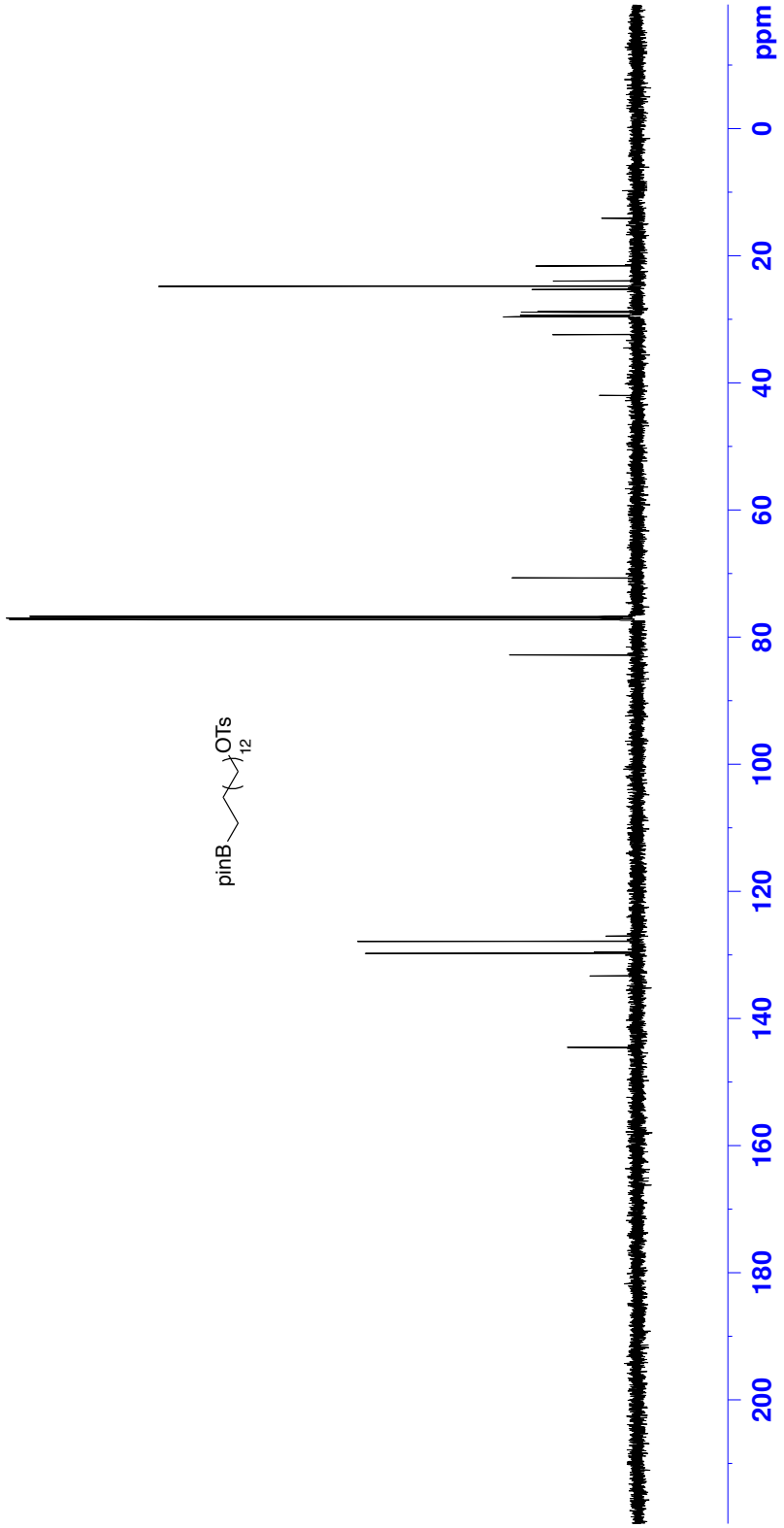

Figure 68: ^{13}C NMR ($CDCl_3$, 125 MHz) of **30**

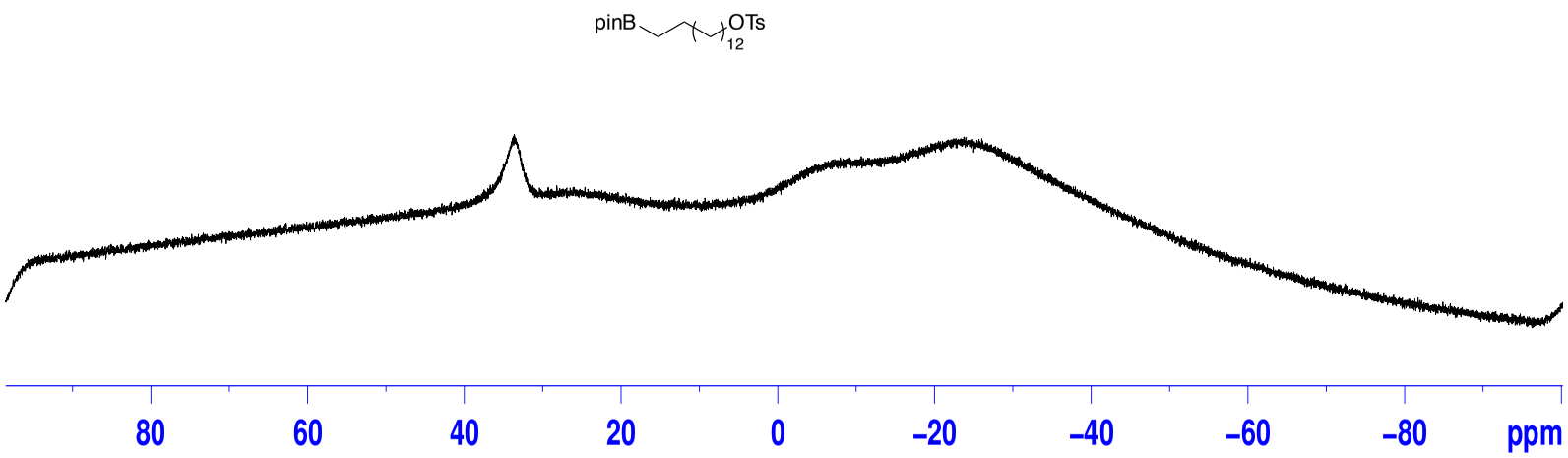

Figure 69: ^{11}B NMR ($CDCl_3$, 128.4 MHz) of **30**

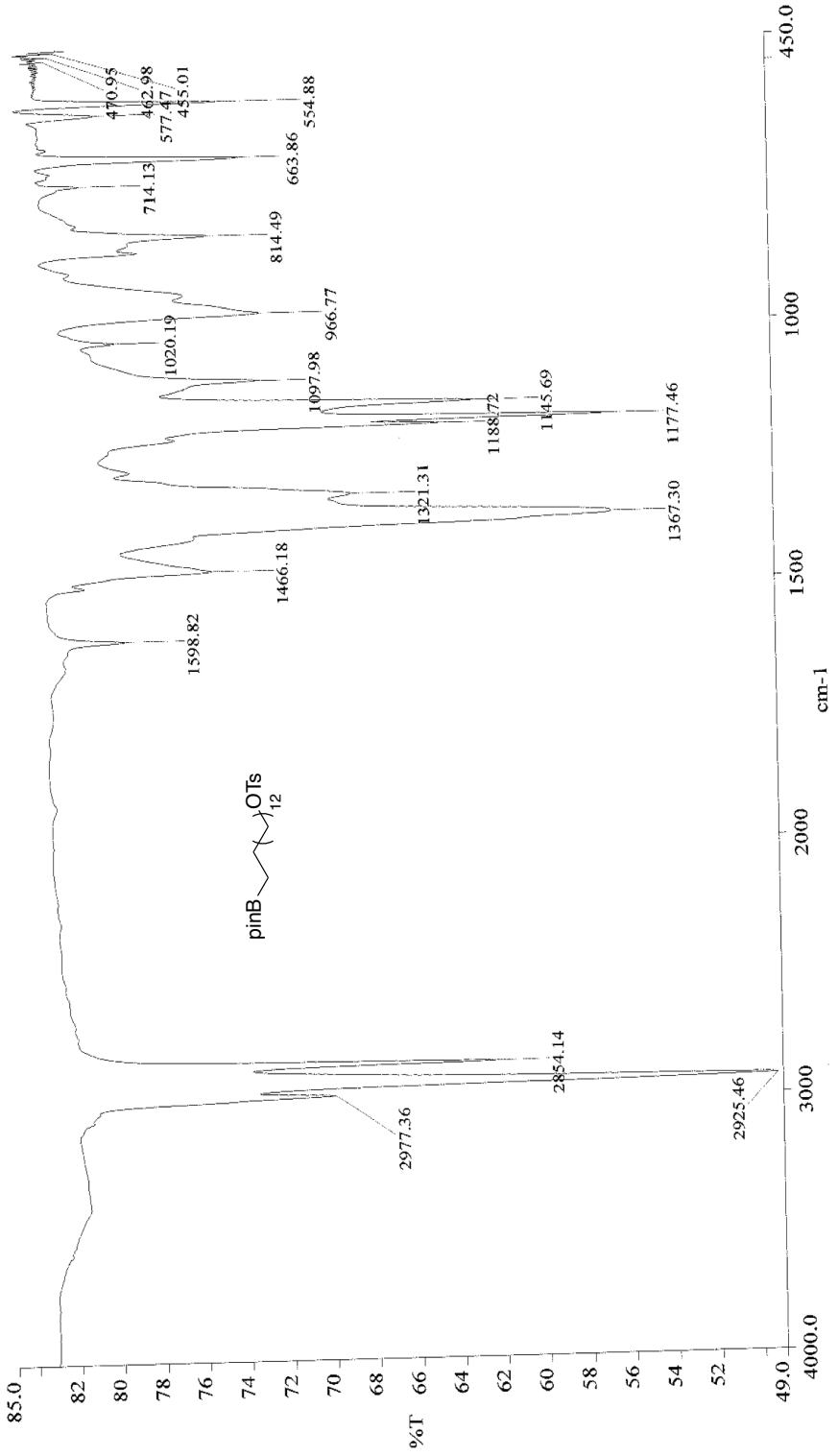

Figure 70: Infrared spectra (neat) of **30**

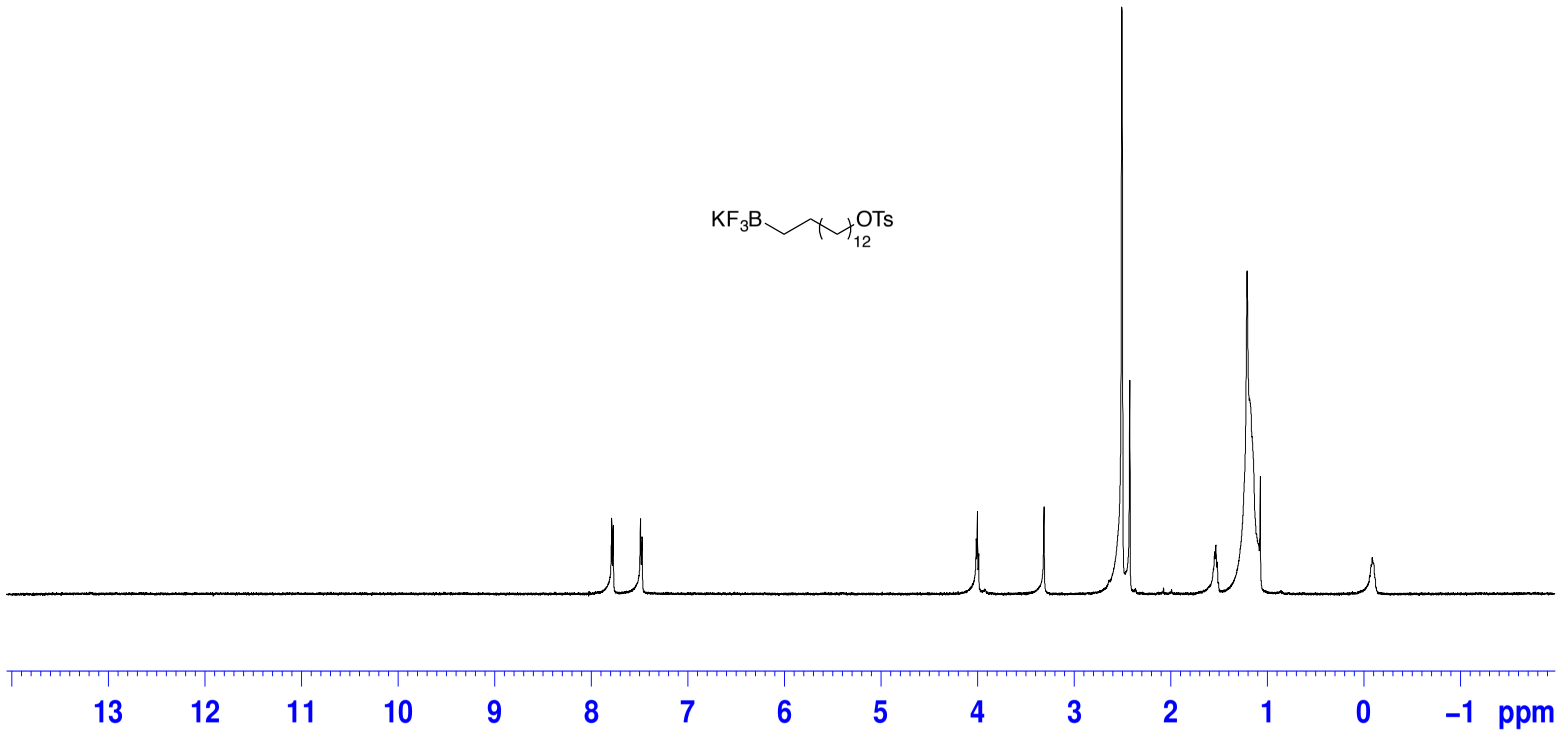

Figure 71: ^{1}H NMR (DMSO-d_6, 500 MHz) of **35**

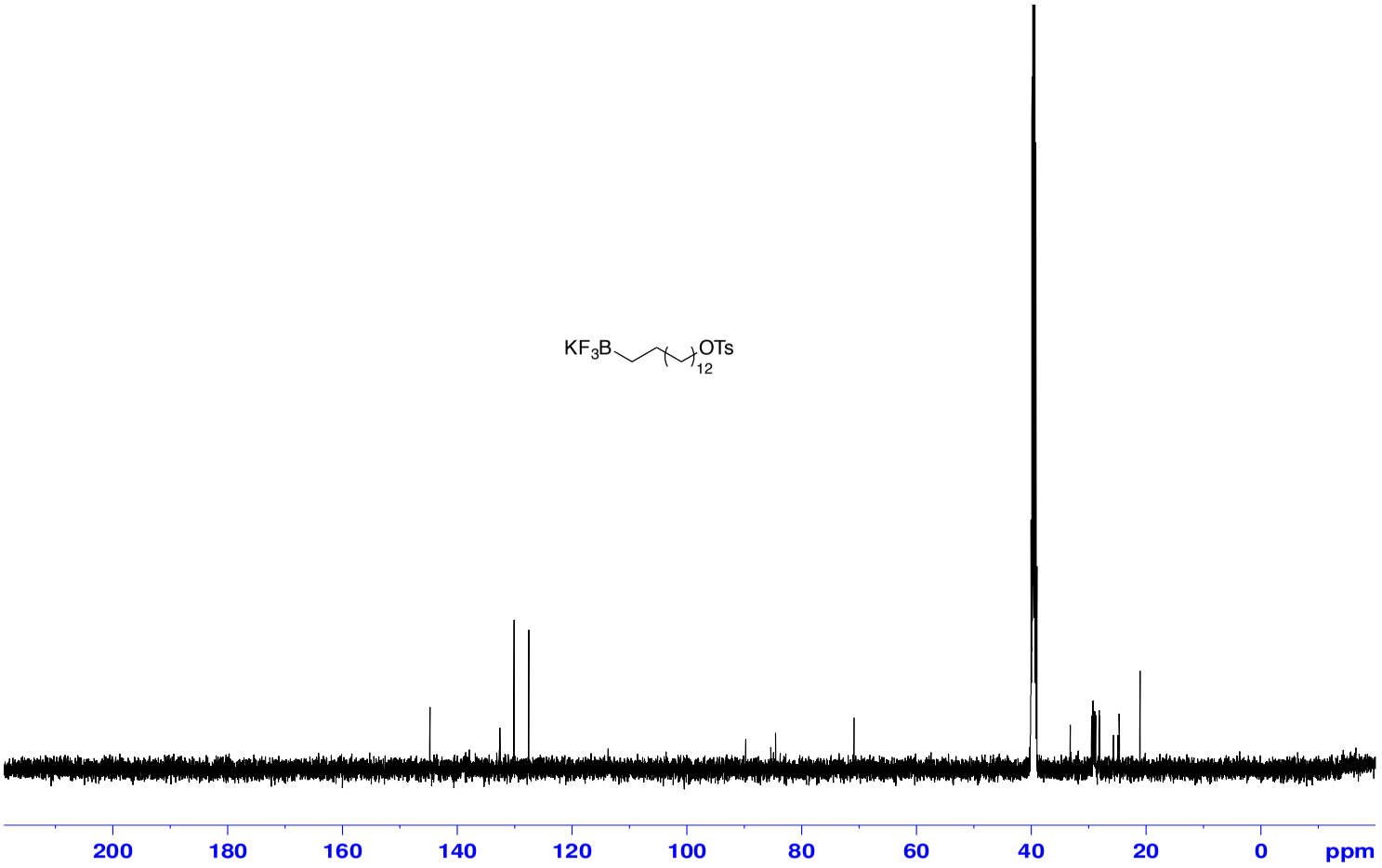

Figure 72: ^{13}C NMR (DMSO-d_6, 125 MHz) of **35**

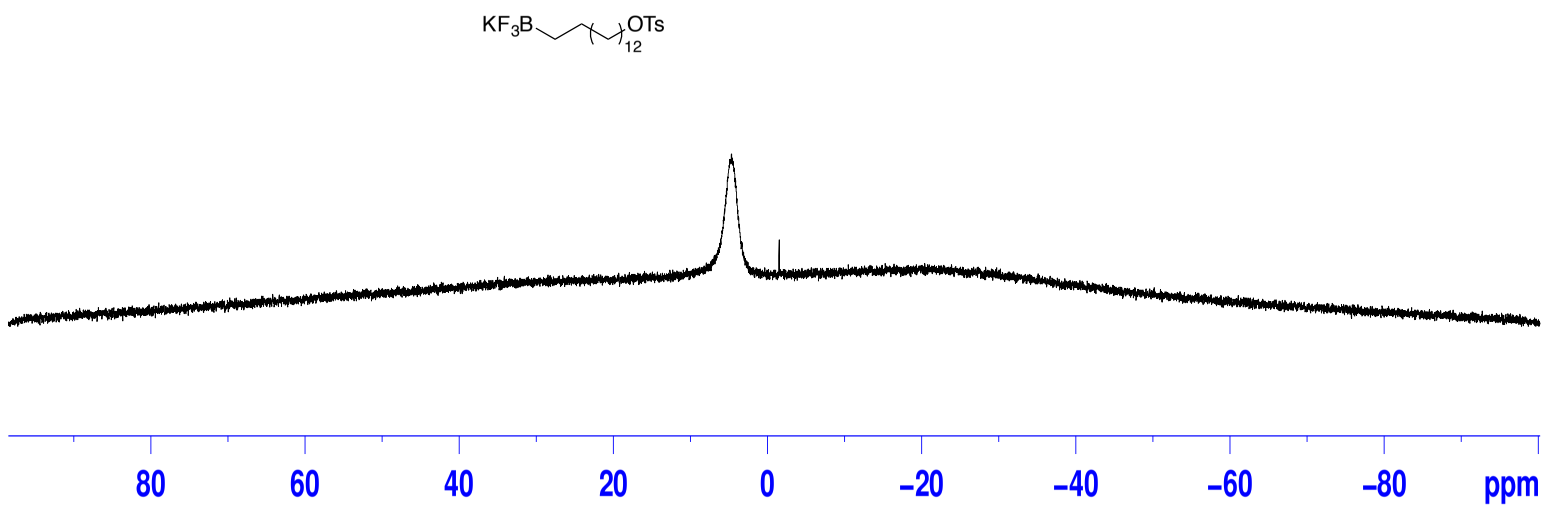

Figure 73: ^{11}B NMR (DMSO-d_6, 128.4 MHz) of **35**

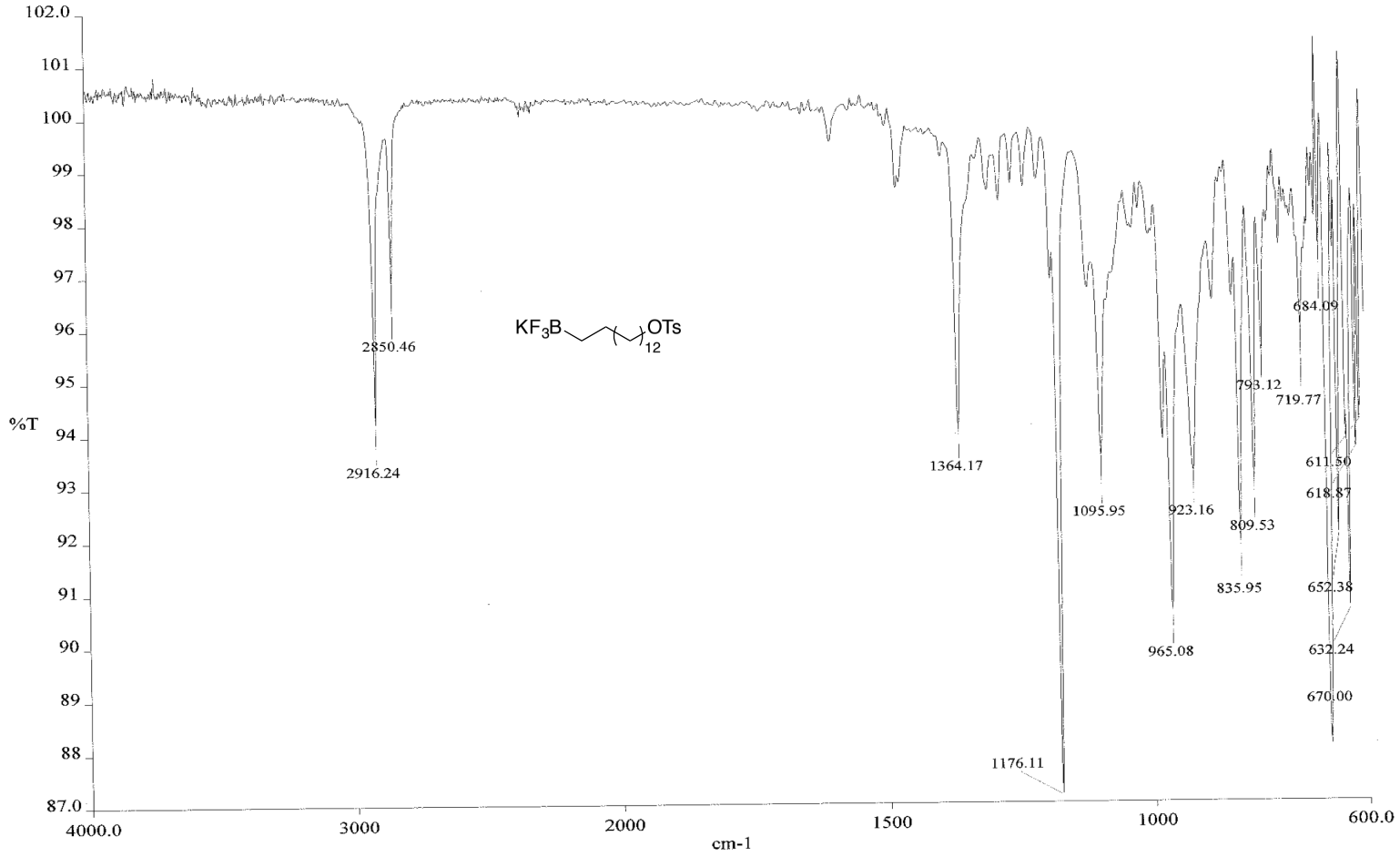

Figure 74: Infrared spectra (neat) of **35**

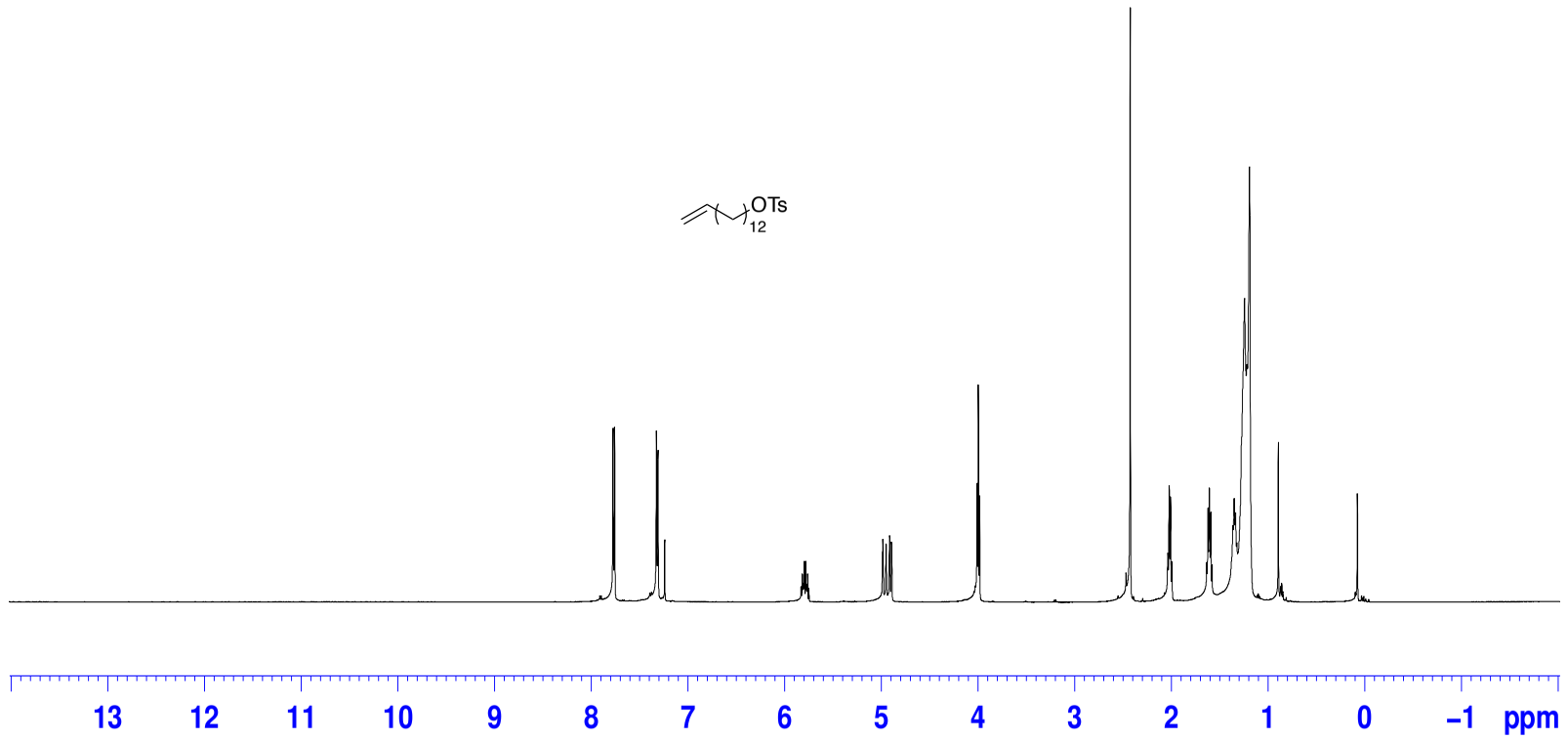

Figure 75: ^{1}H NMR ($CDCl_3$, 500 MHz) of **25**

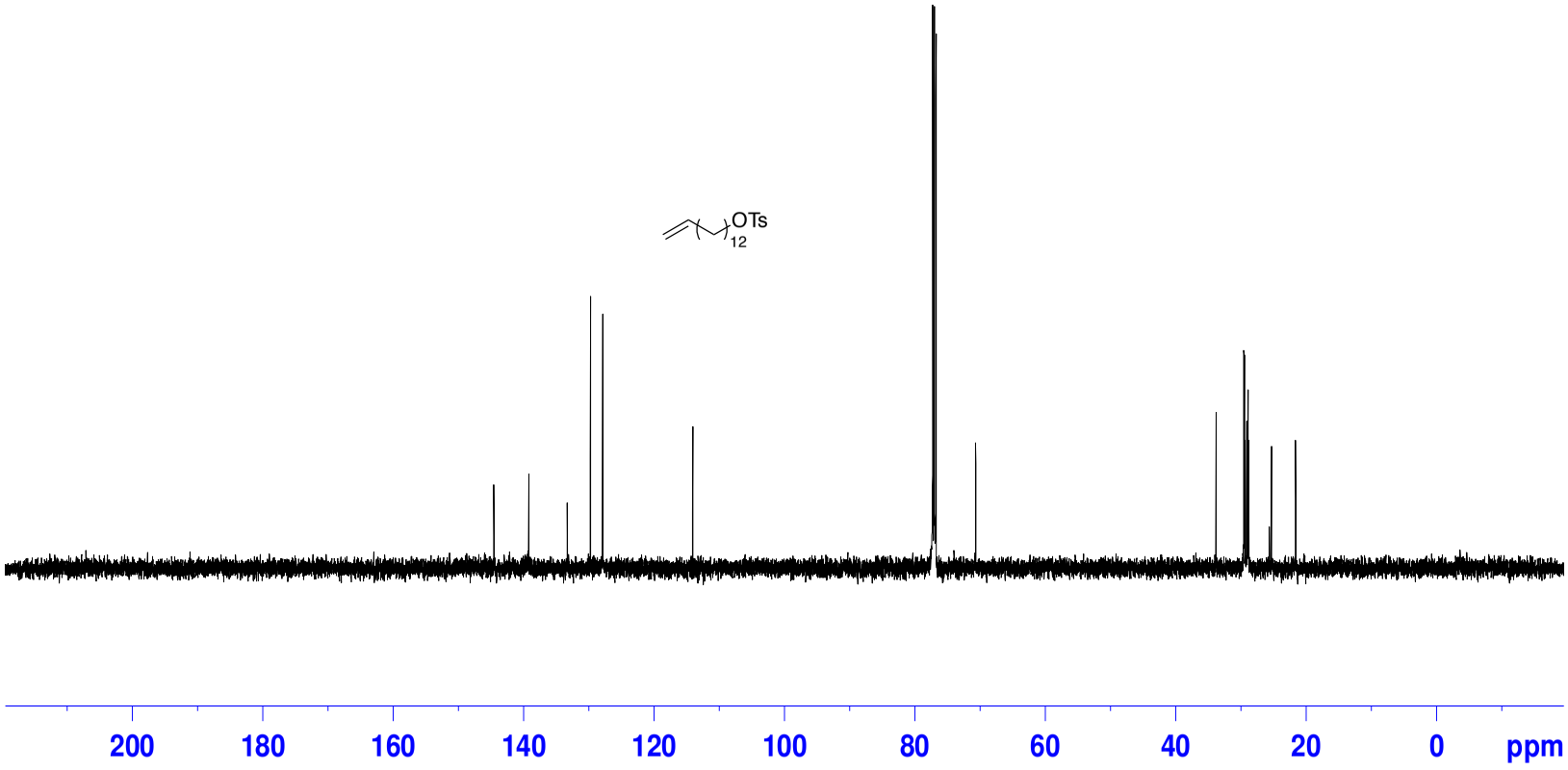

Figure 76: ^{13}C NMR ($CDCl_3$, 125 MHz) of **25**

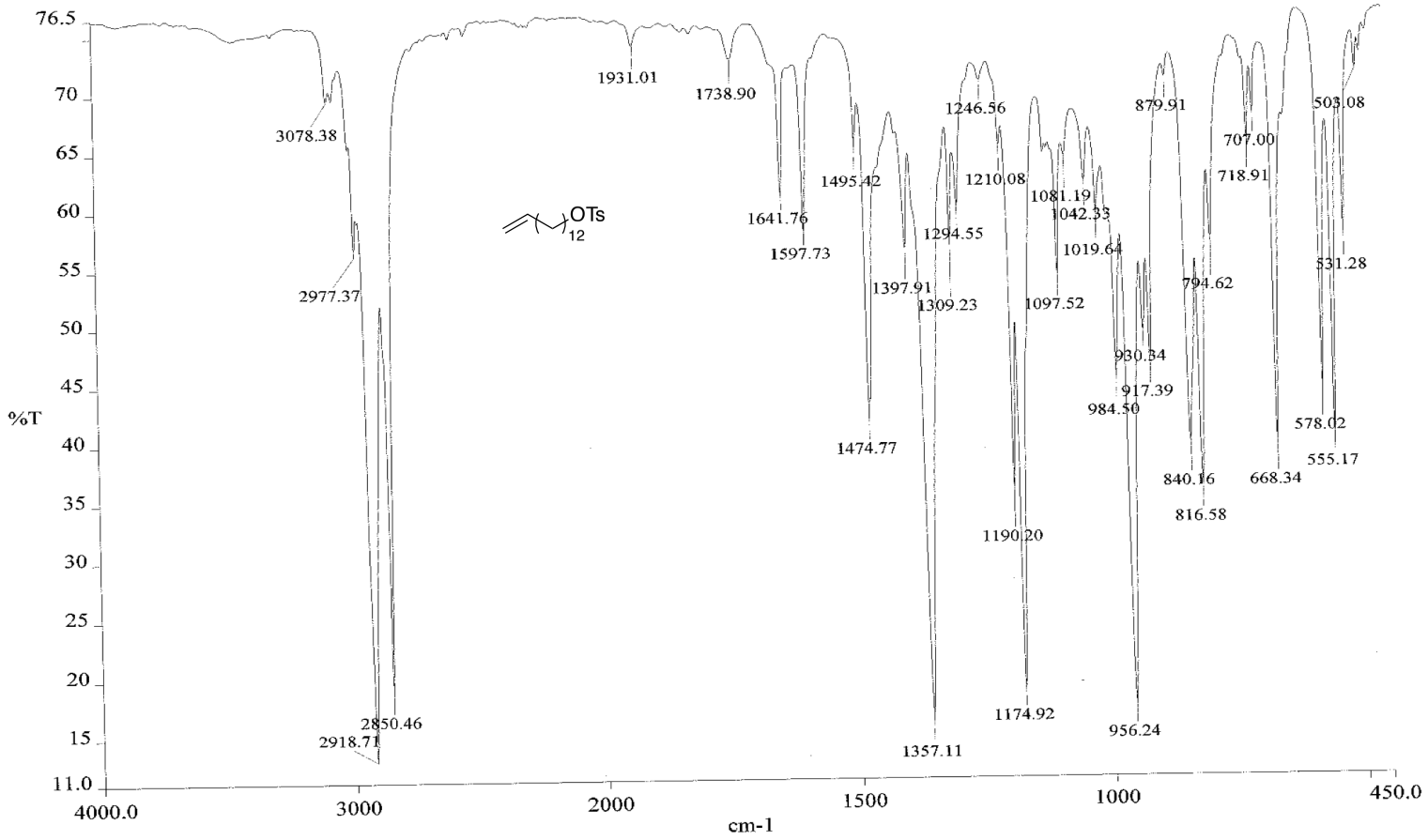

Figure 77: Infrared spectra (neat) of **25**

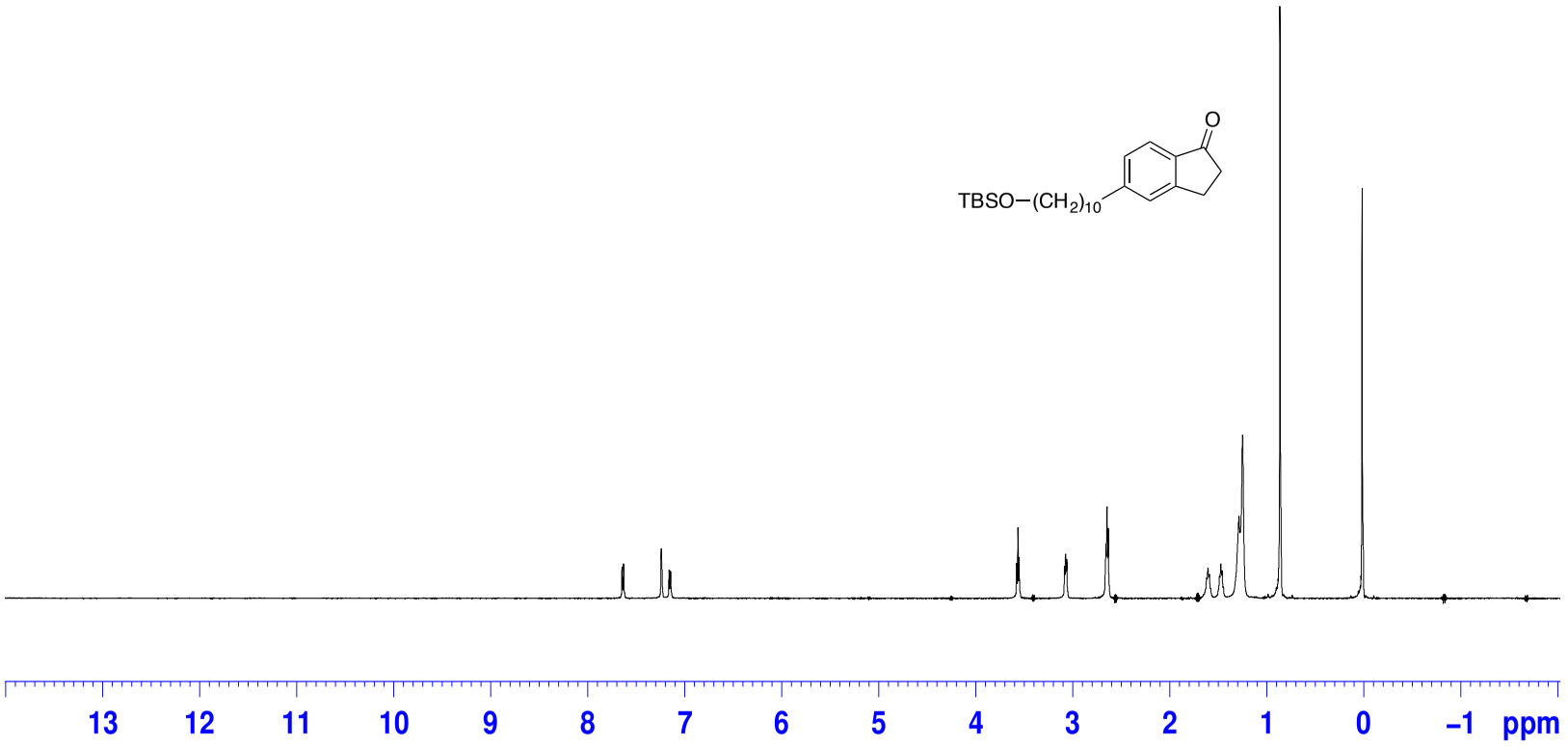

Figure 78: ^{1}H NMR ($CDCl_3$, 500 MHz) of **20**

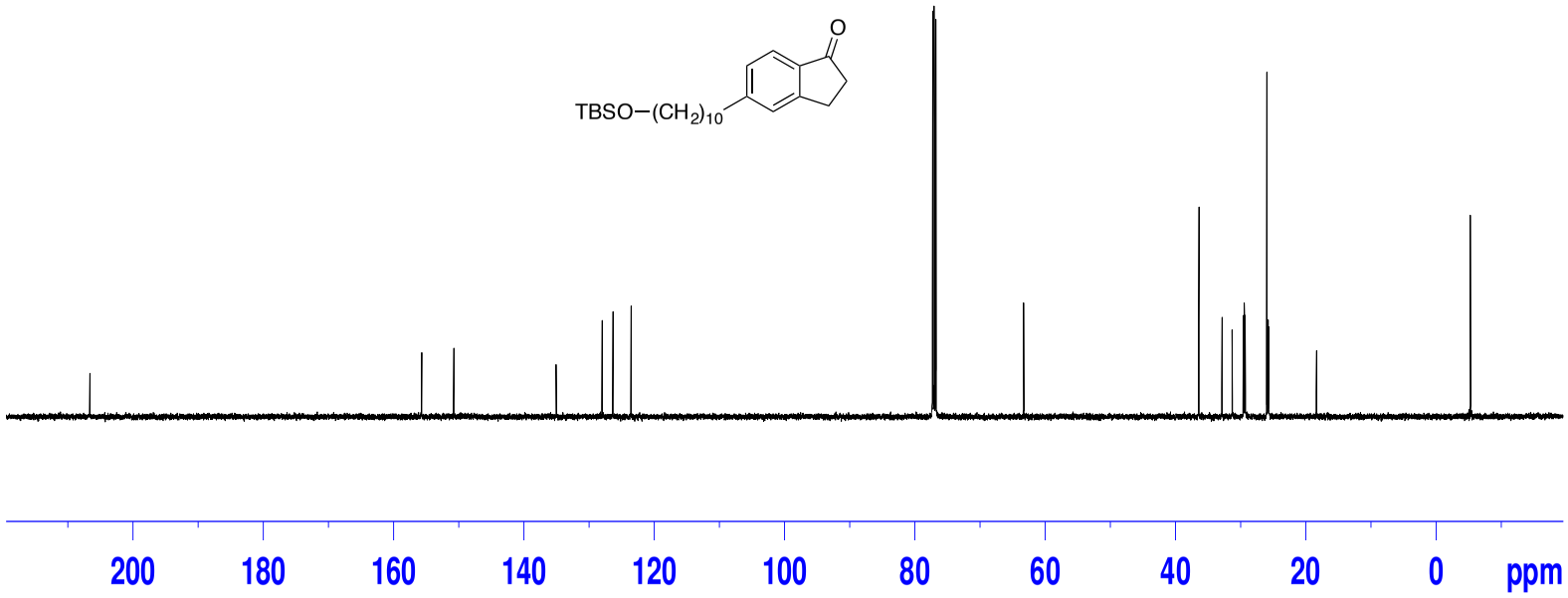

Figure 79: ^{13}C NMR ($CDCl_3$, 125 MHz) of **20**

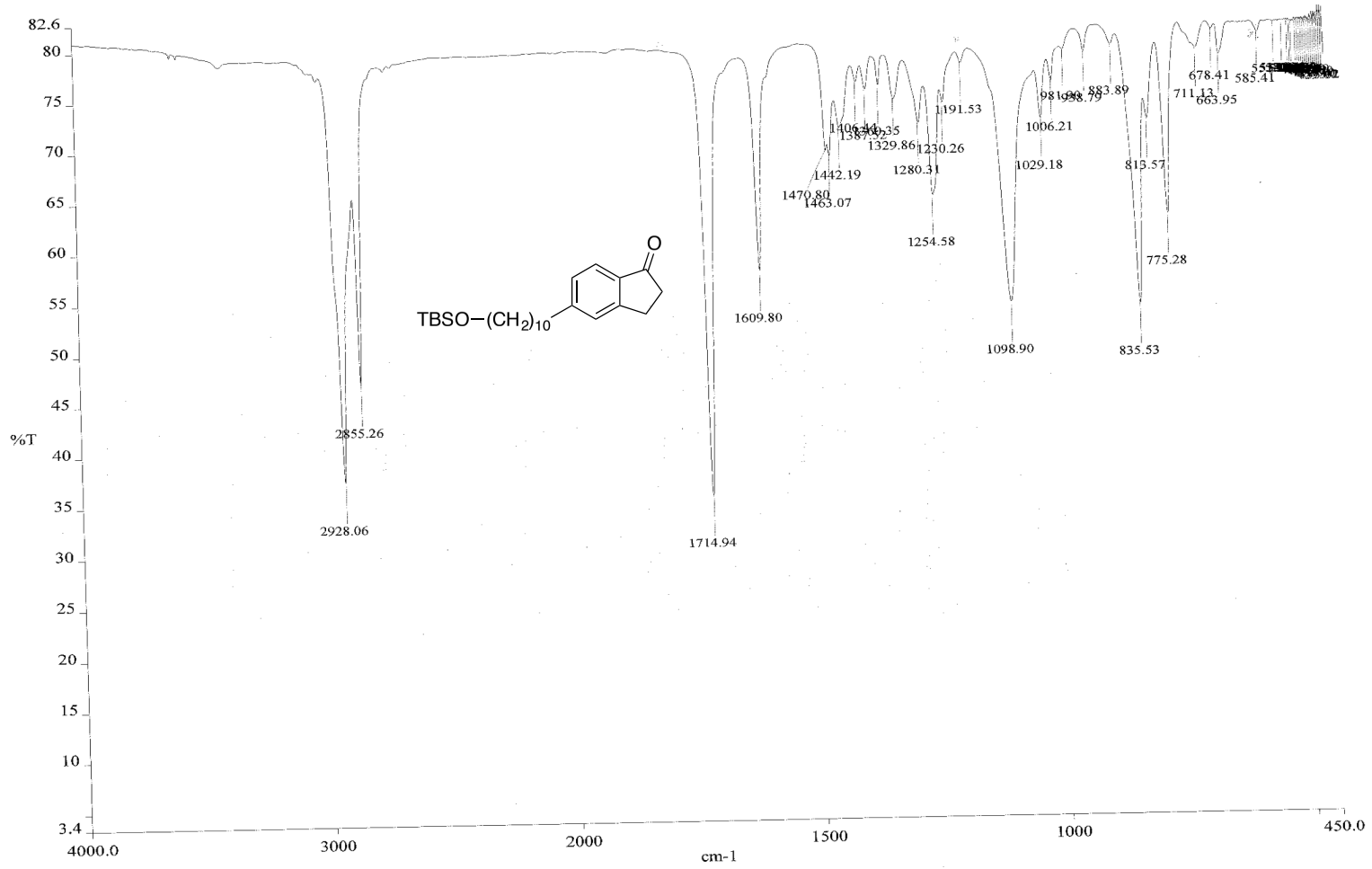

Figure 80: Infrared spectra (neat) of **20**

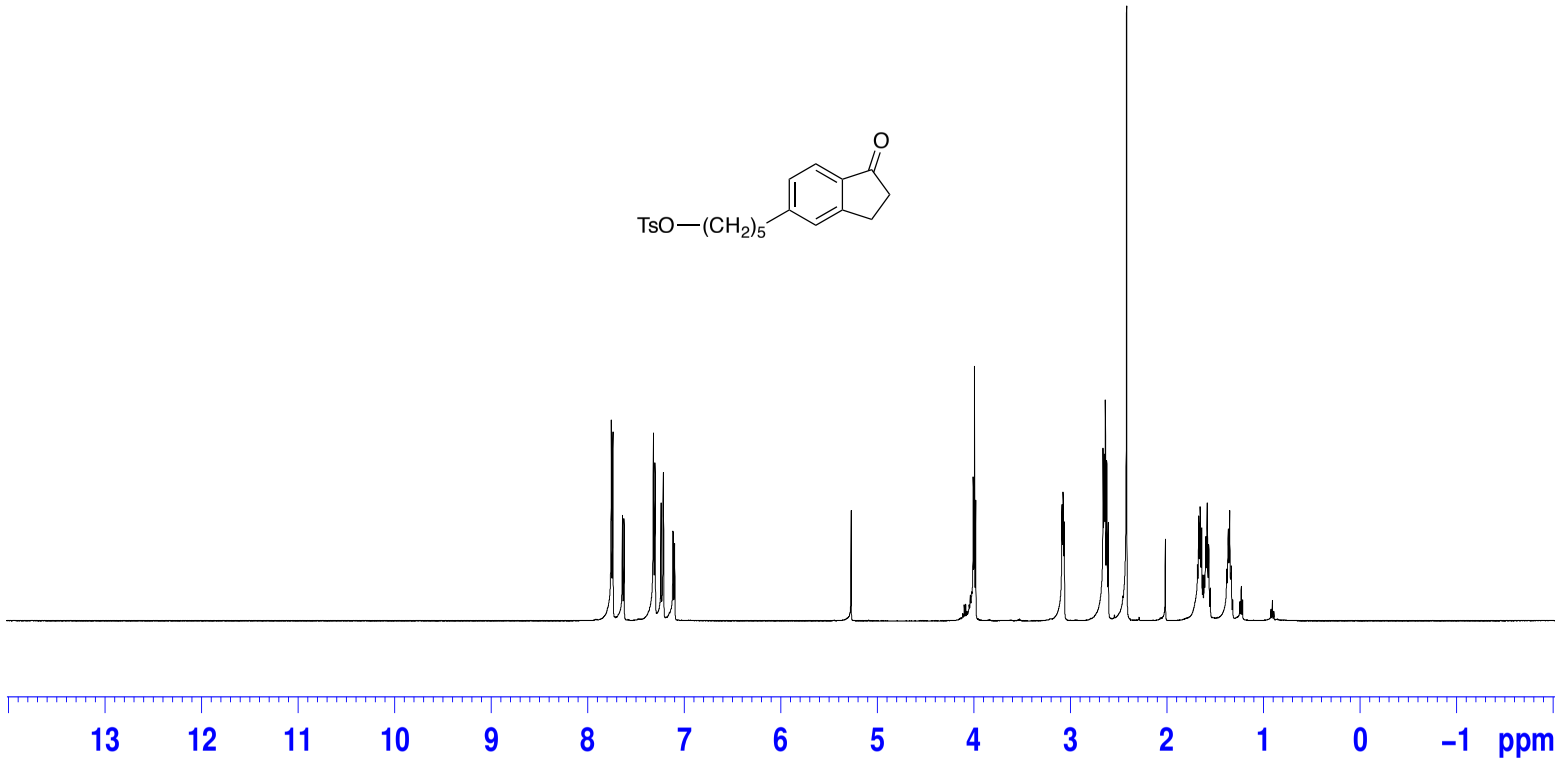

Figure 81: ^{1}H NMR ($CDCl_3$, 500 MHz) of **36**

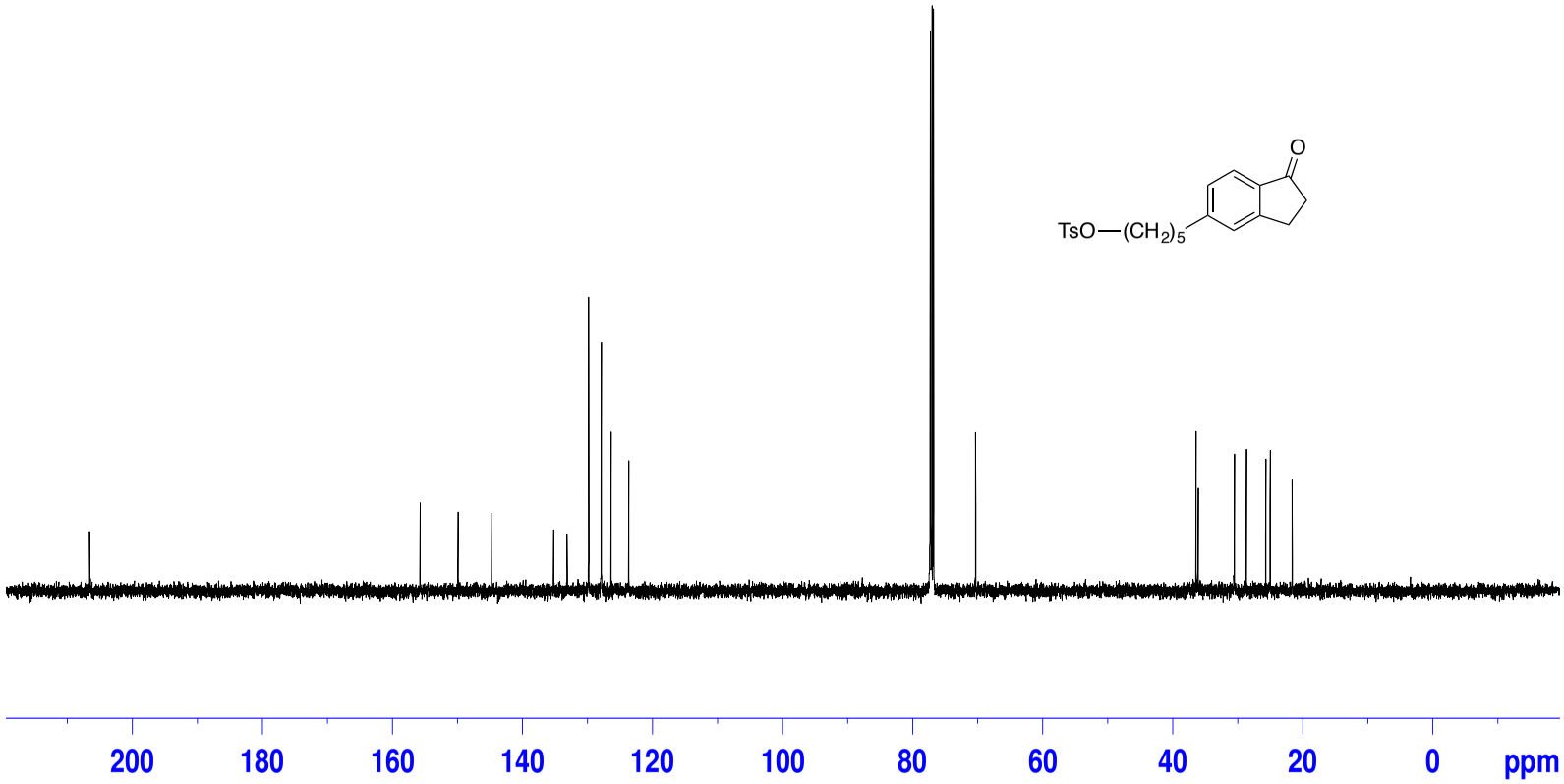

Figure 82: ^{13}C NMR ($CDCl_3$, 125 MHz) of **36**

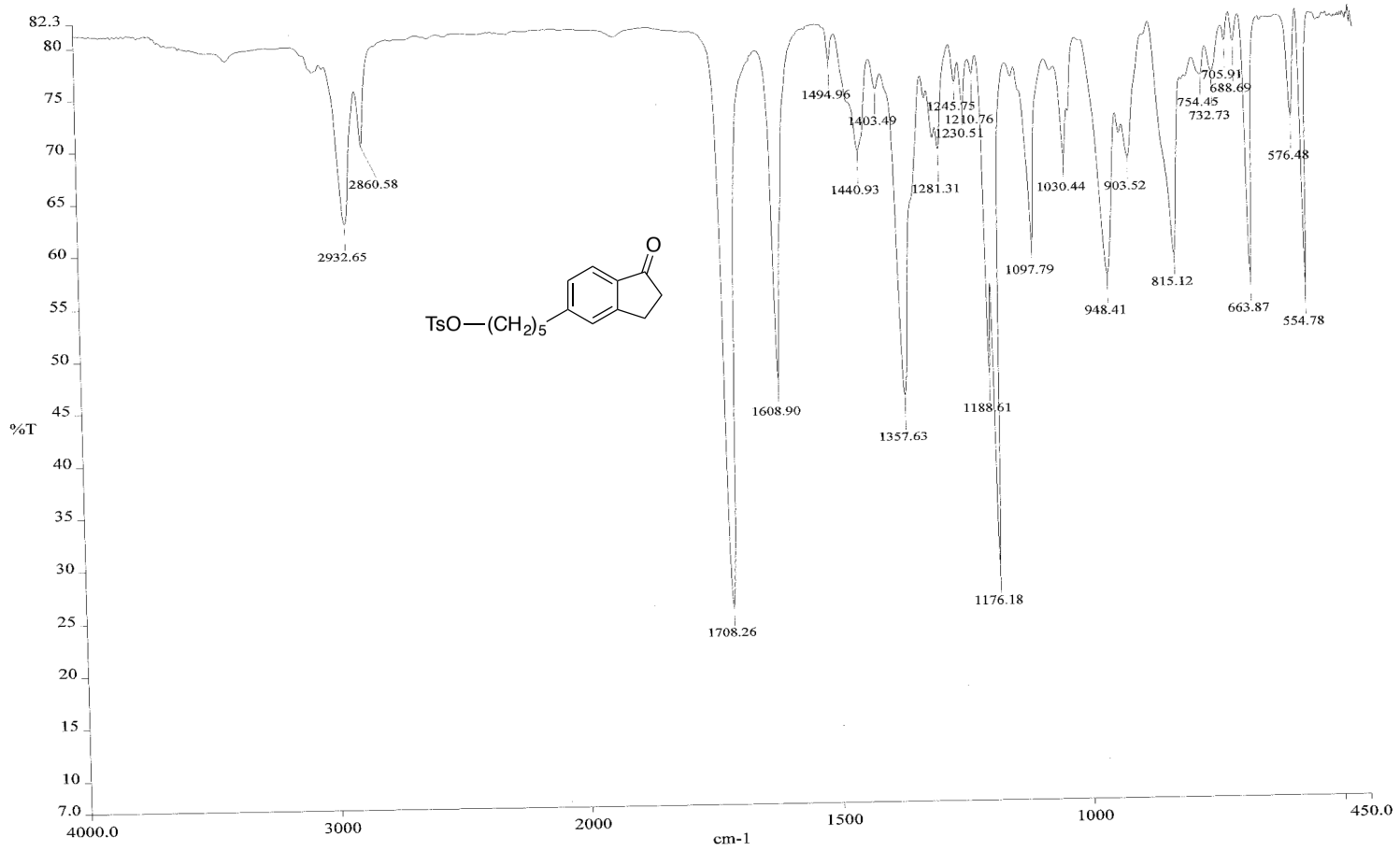

Figure 83: Infrared spectra (neat) of **36**

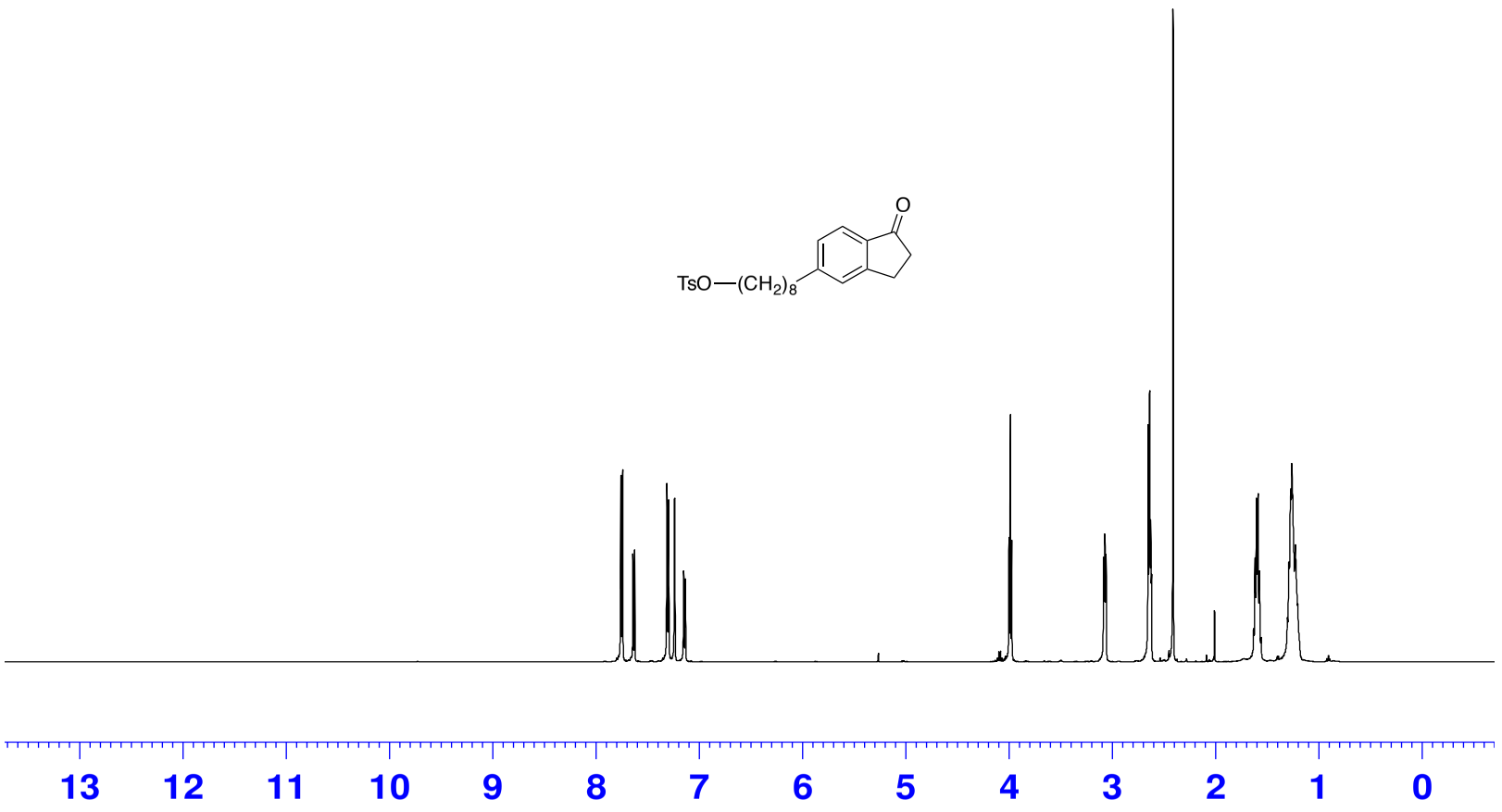

Figure 84: ^{1}H NMR ($CDCl_3$, 500 MHz) of **37**

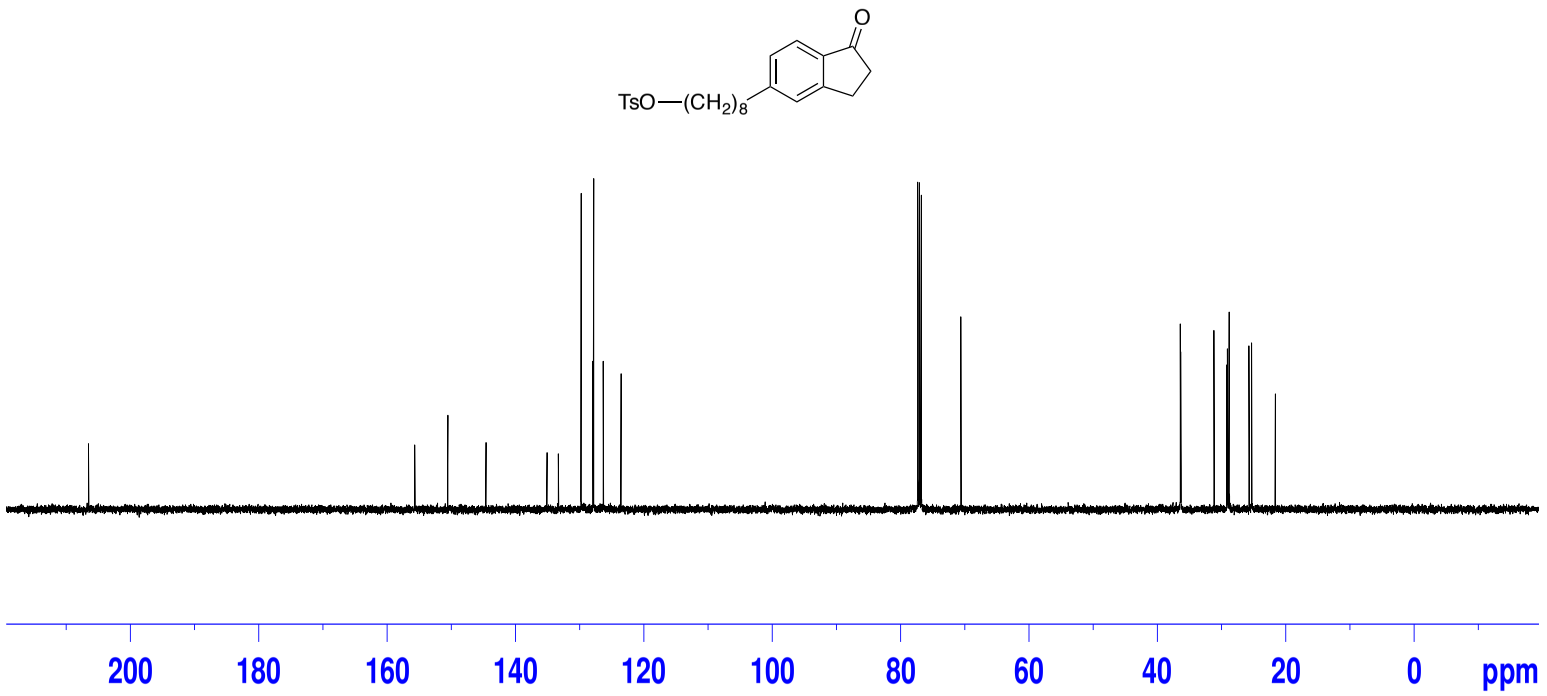

Figure 85: ^{13}C NMR ($CDCl_3$, 125 MHz) of **37**

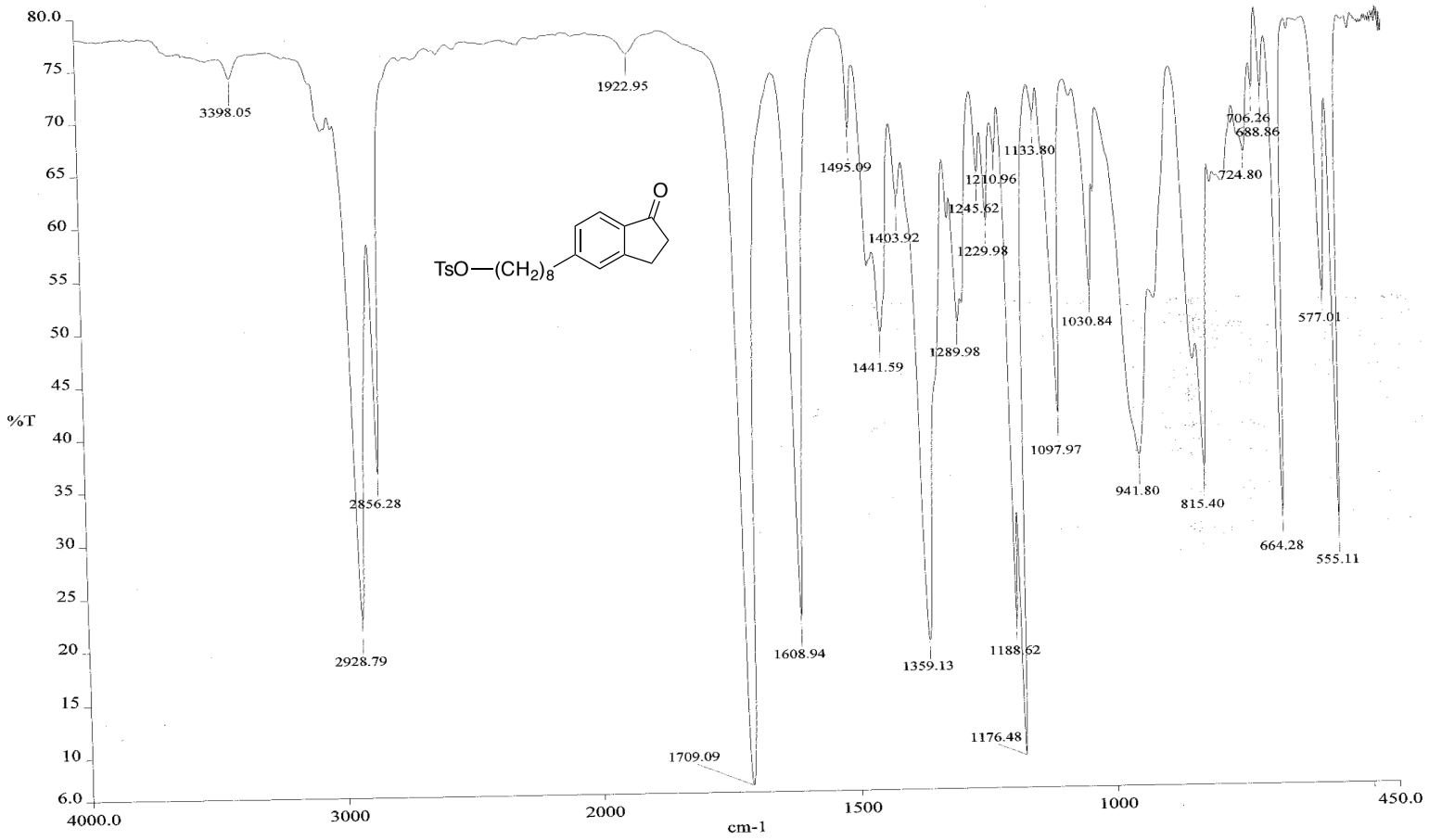

Figure 86: Infrared spectra (neat) of **37**

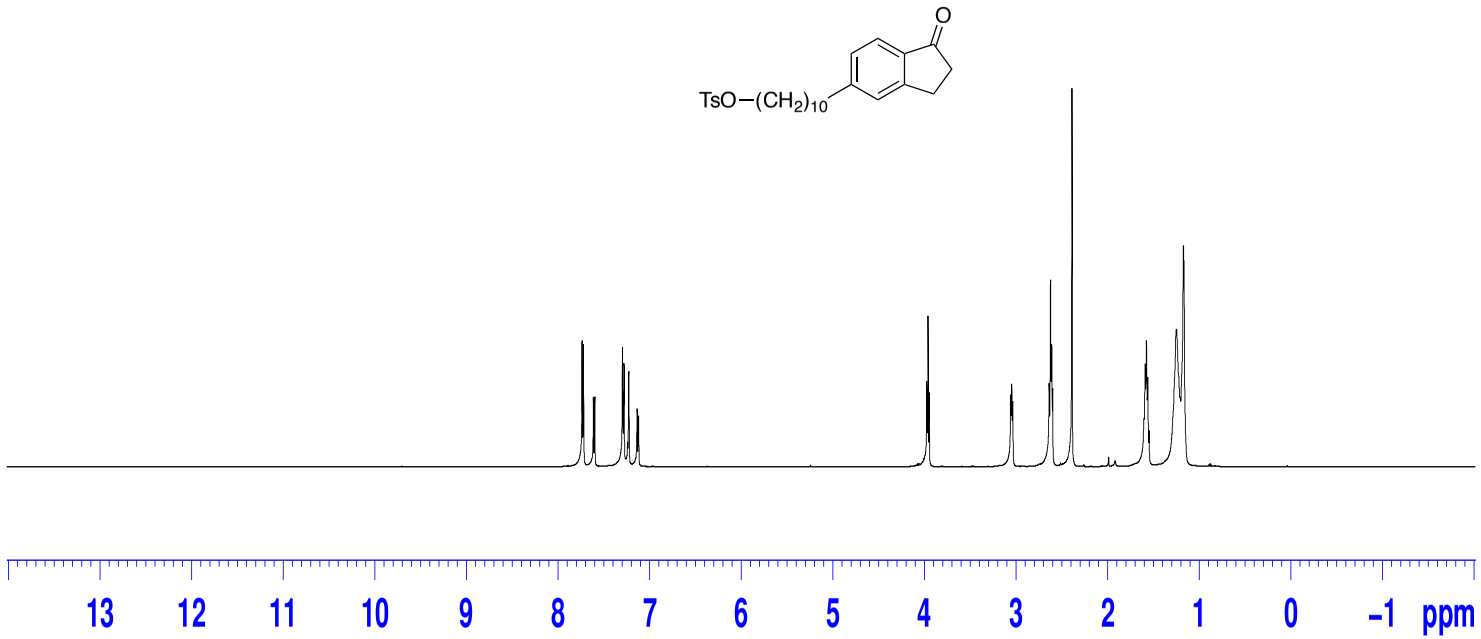

Figure 87: ^{1}H NMR ($CDCl_3$, 500 MHz) of **38**

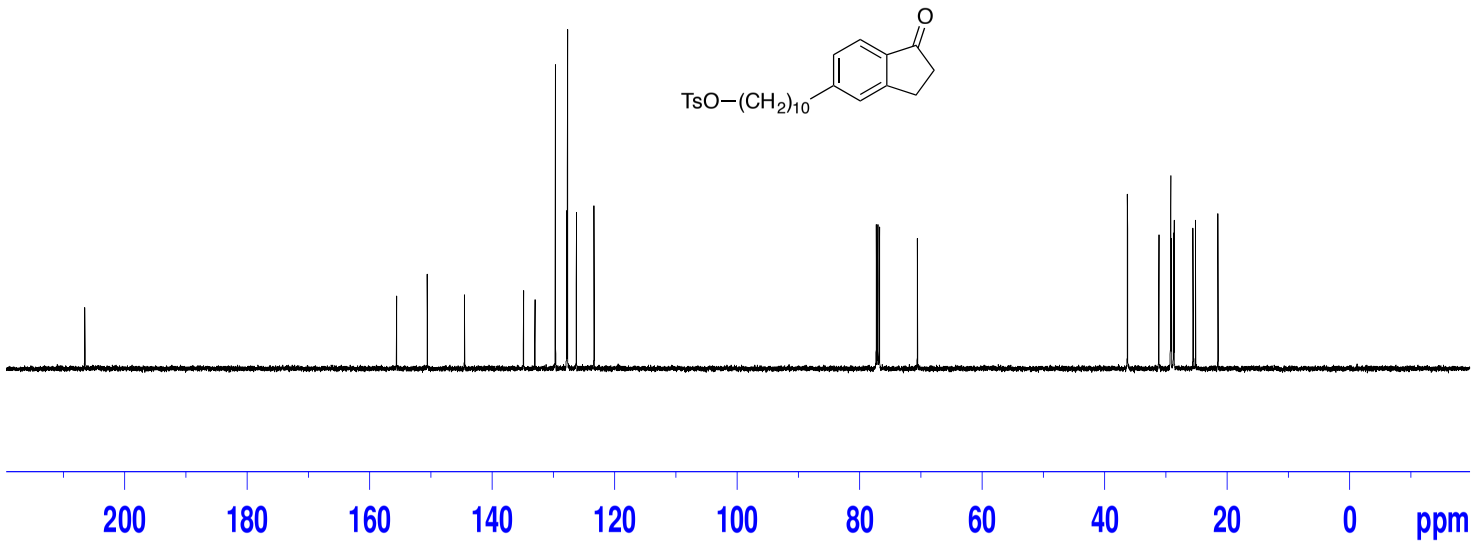

Figure 88: ^{13}C NMR ($CDCl_3$, 125 MHz) of **38**

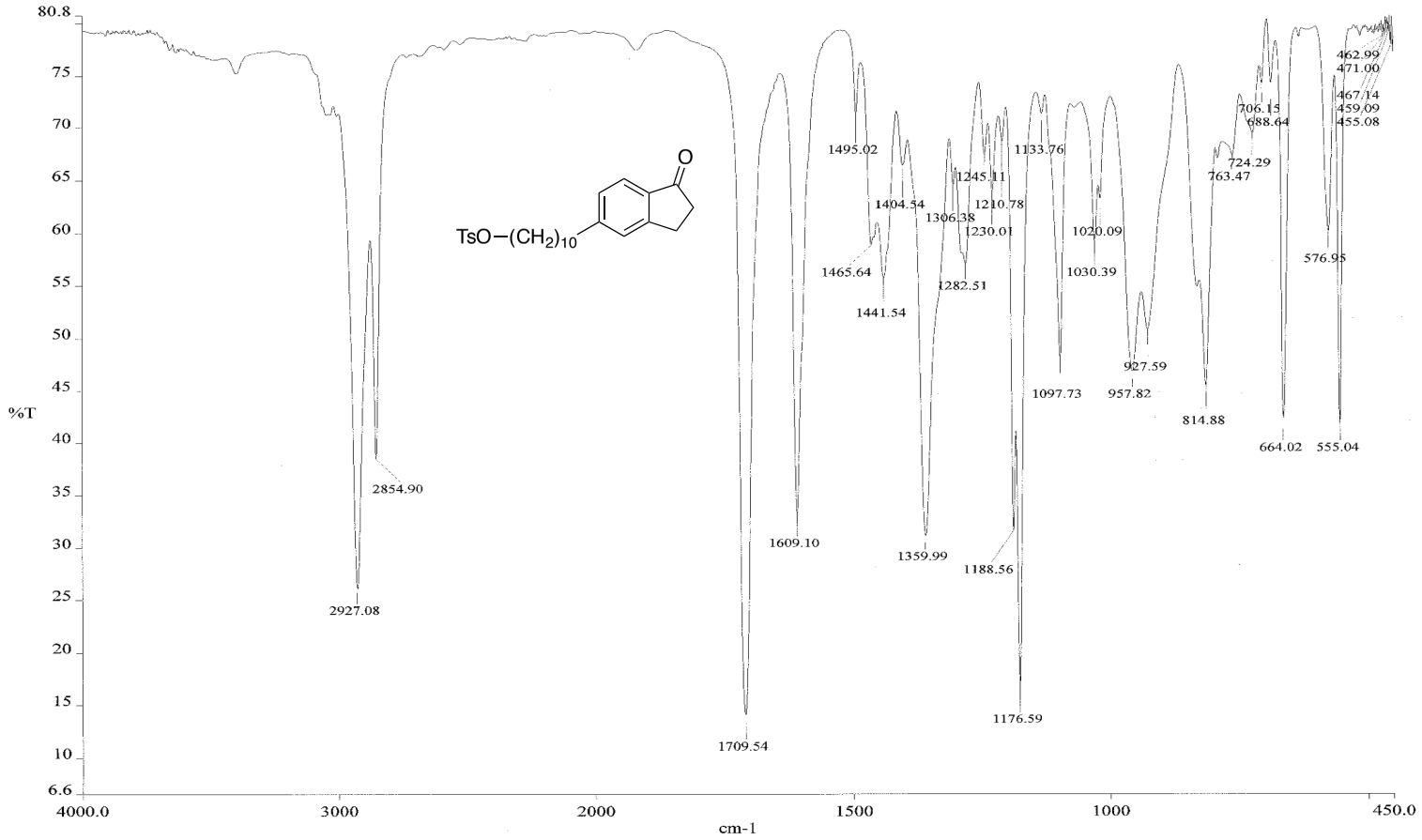

Figure 89: Infrared spectra (neat) of **38**

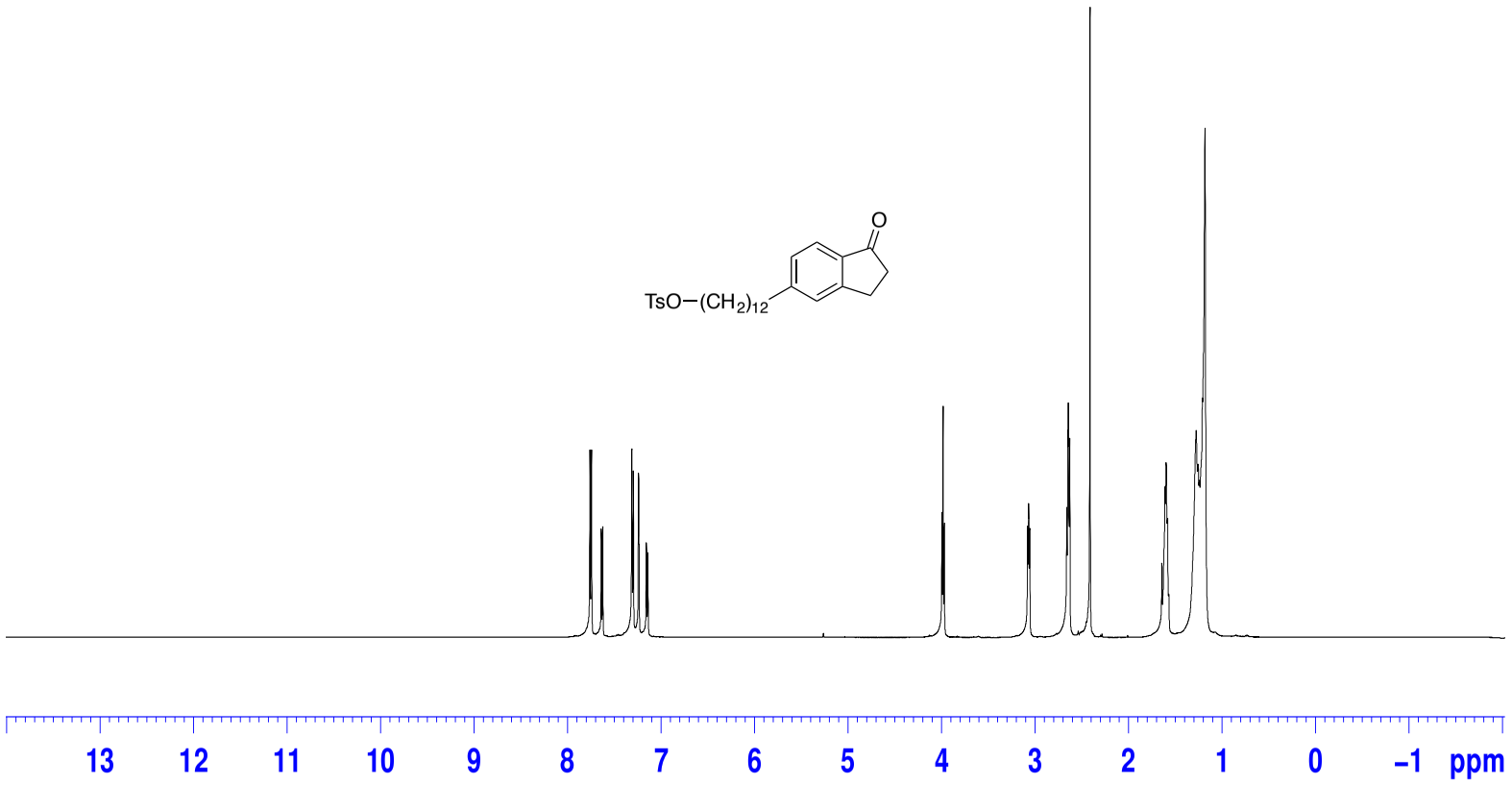

Figure 90: ^{1}H NMR ($CDCl_3$, 500 MHz) of **39**

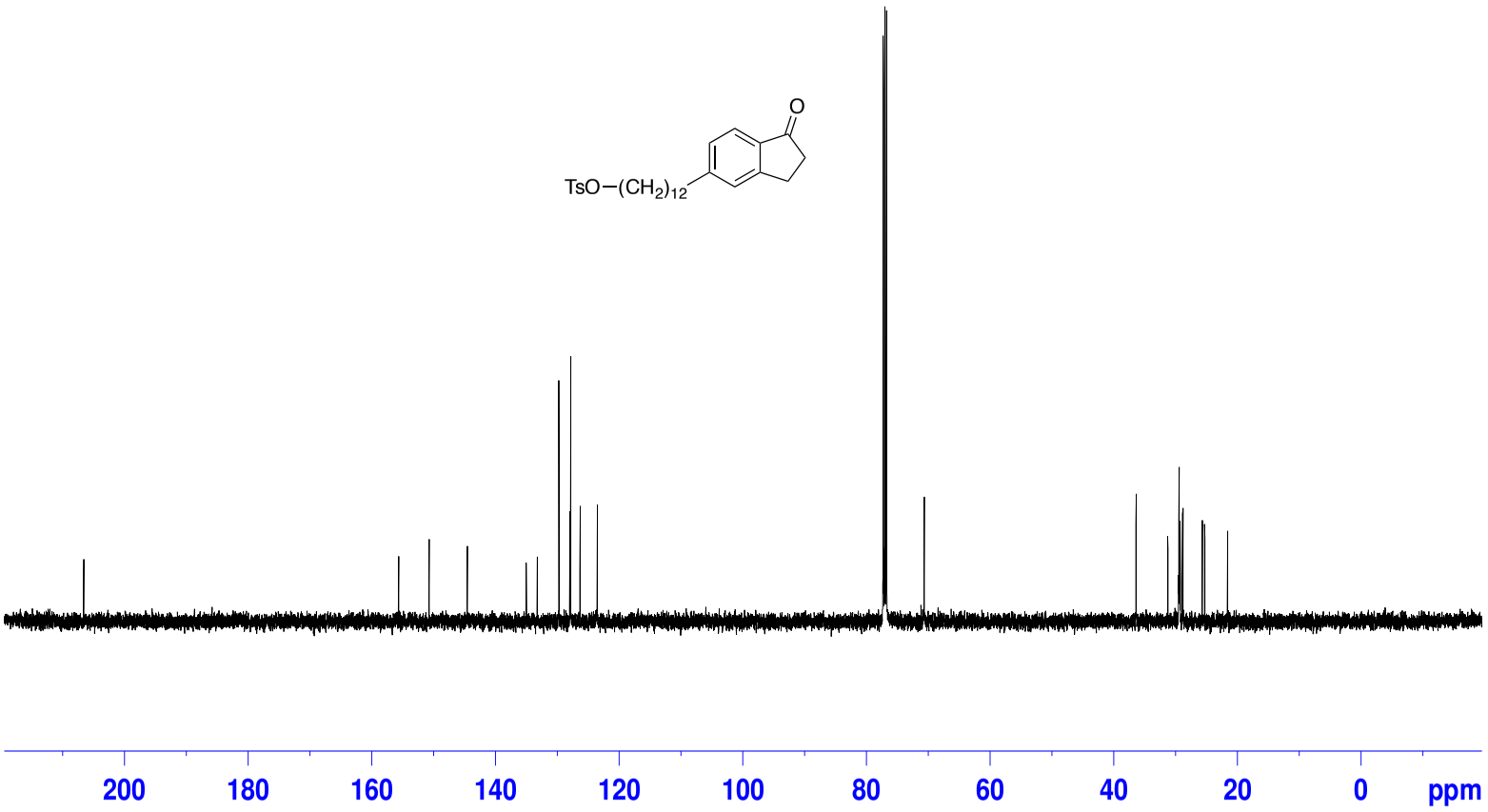

Figure 91: ^{13}C NMR ($CDCl_3$, 125 MHz) of **39**

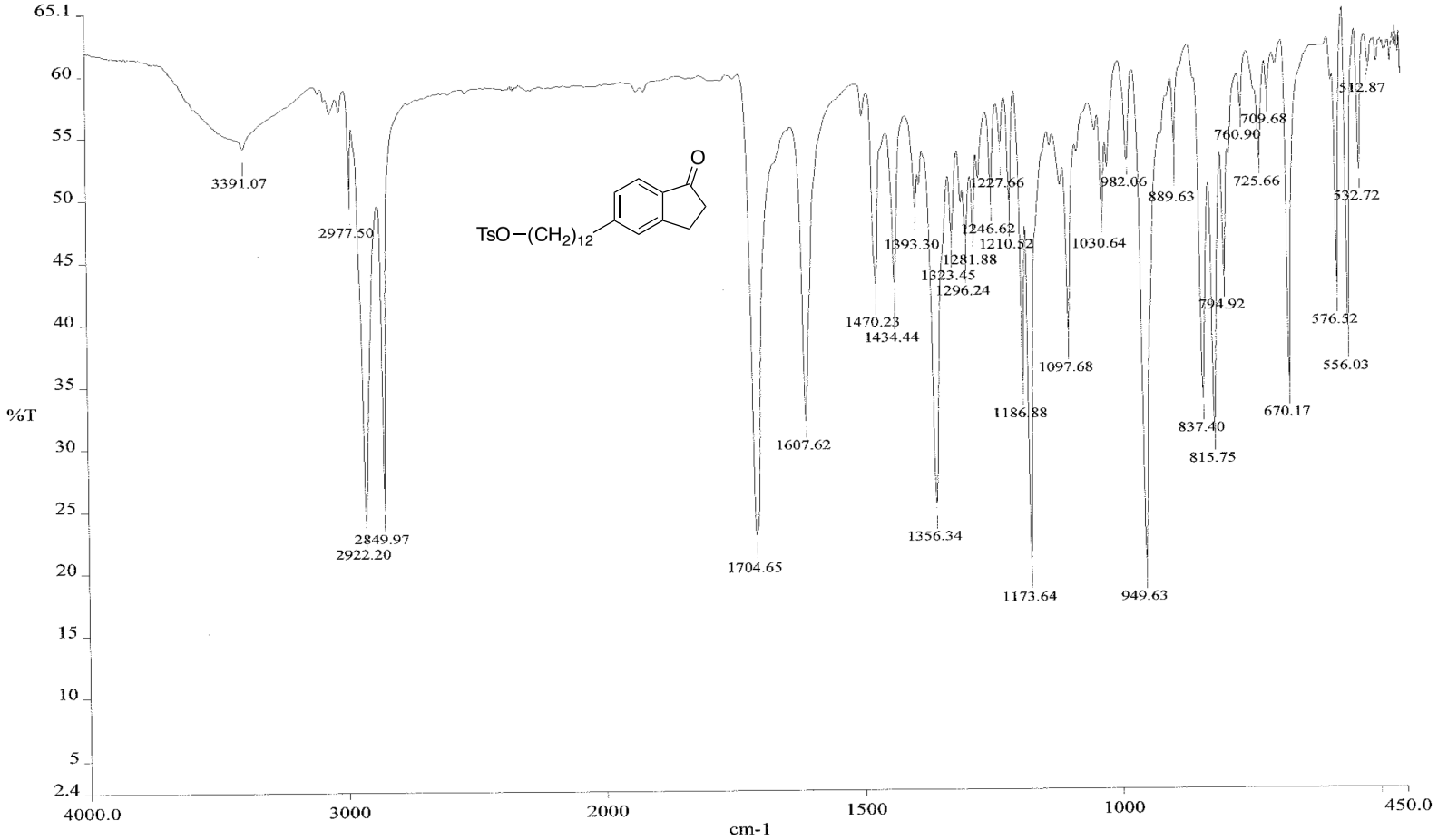

Figure 92: Infrared spectra (neat) of **39**

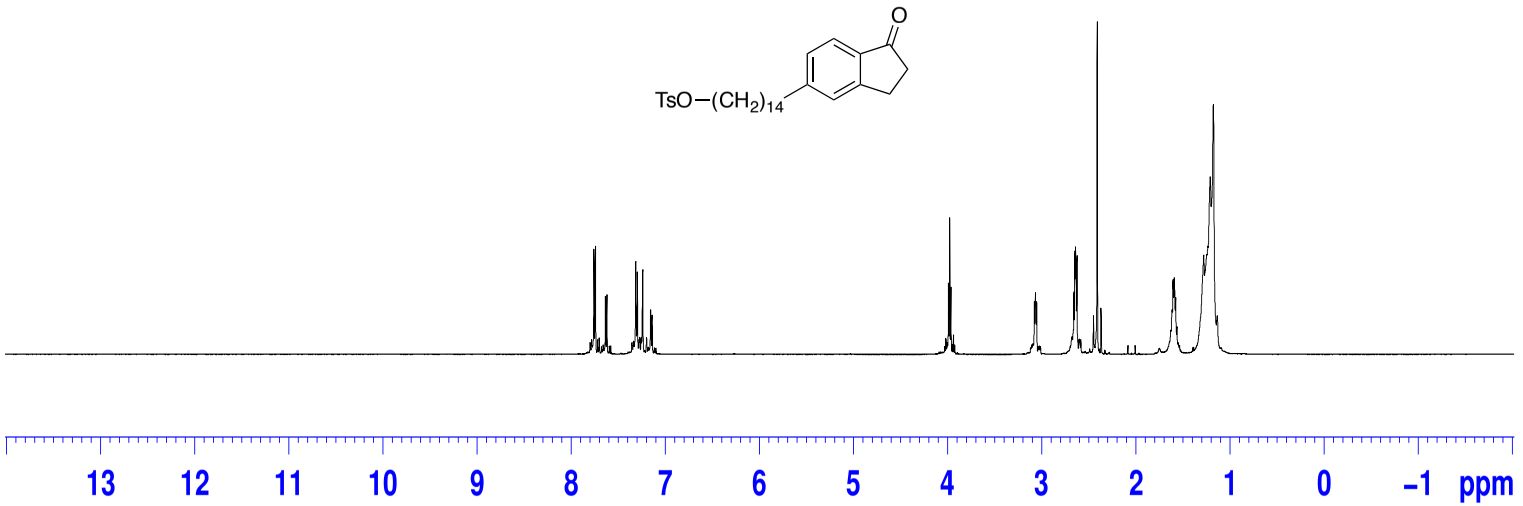

Figure 93: ^{1}H NMR ($CDCl_3$, 500 MHz) of **40**

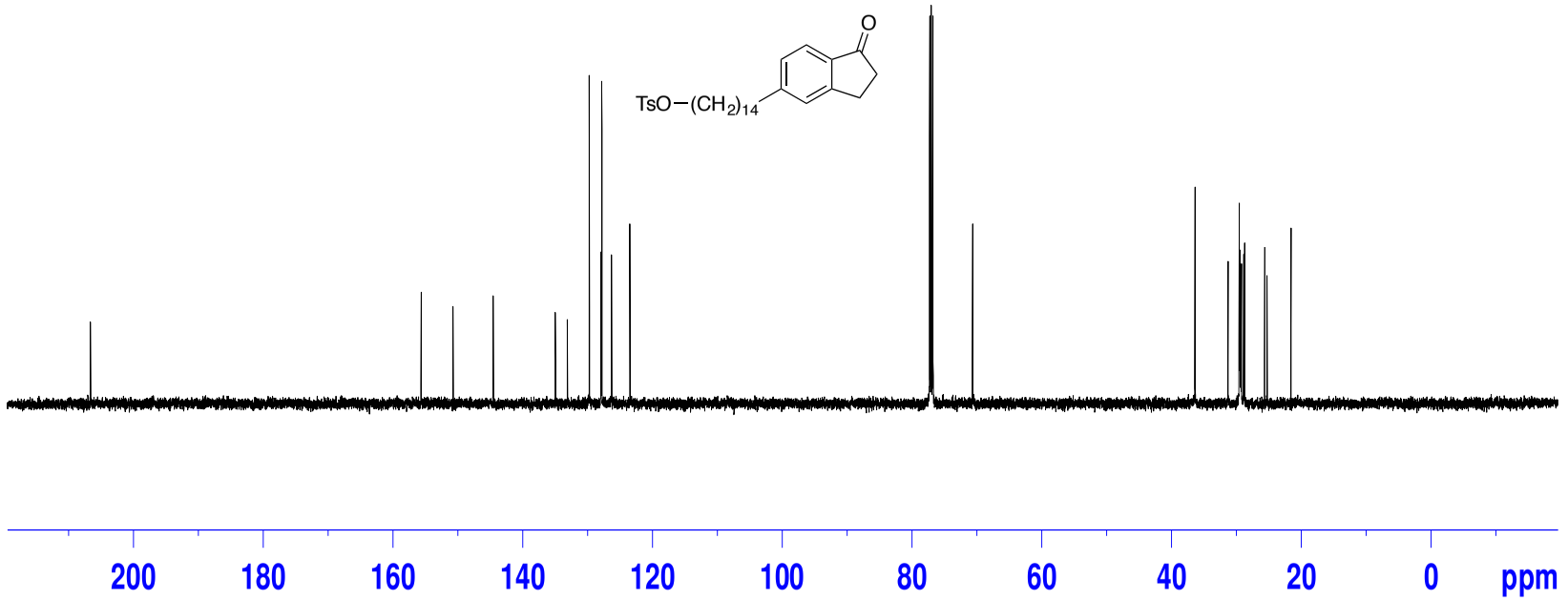

Figure 94: ^{13}C NMR ($CDCl_3$, 125 MHz) of **40**

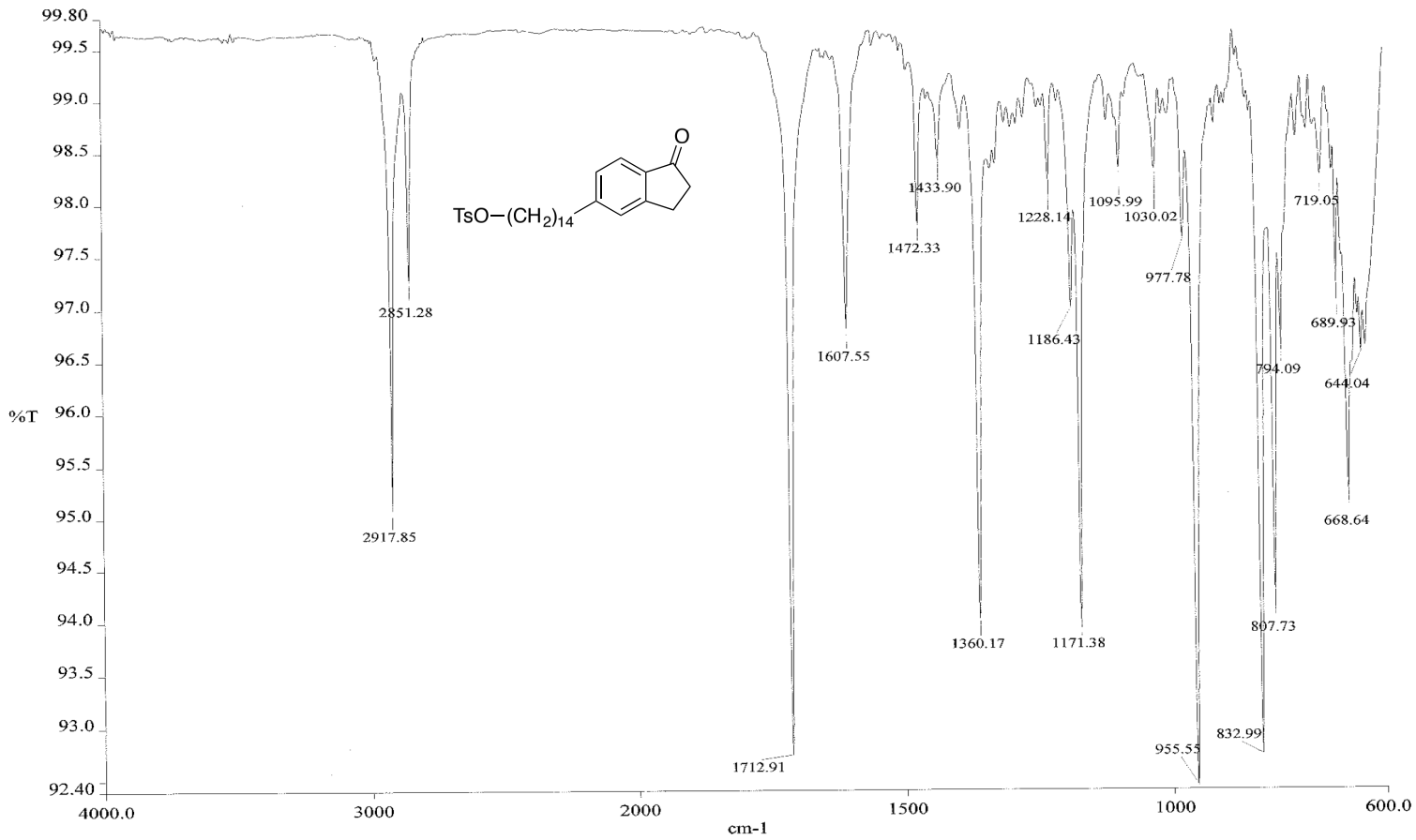

Figure 95: Infrared spectra (neat) of **40**

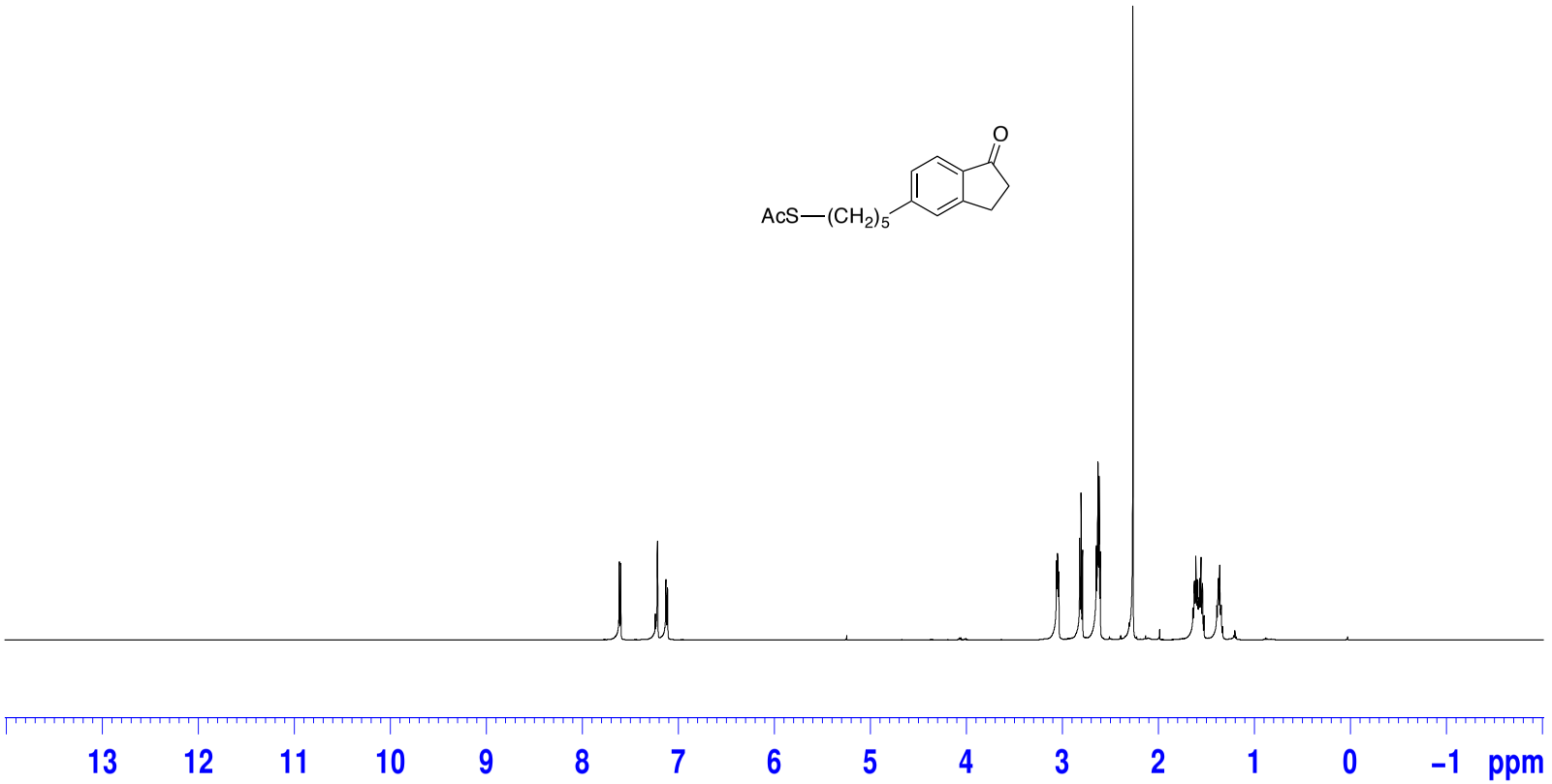

Figure 96: ^{1}H NMR ($CDCl_3$, 500 MHz) of **41**

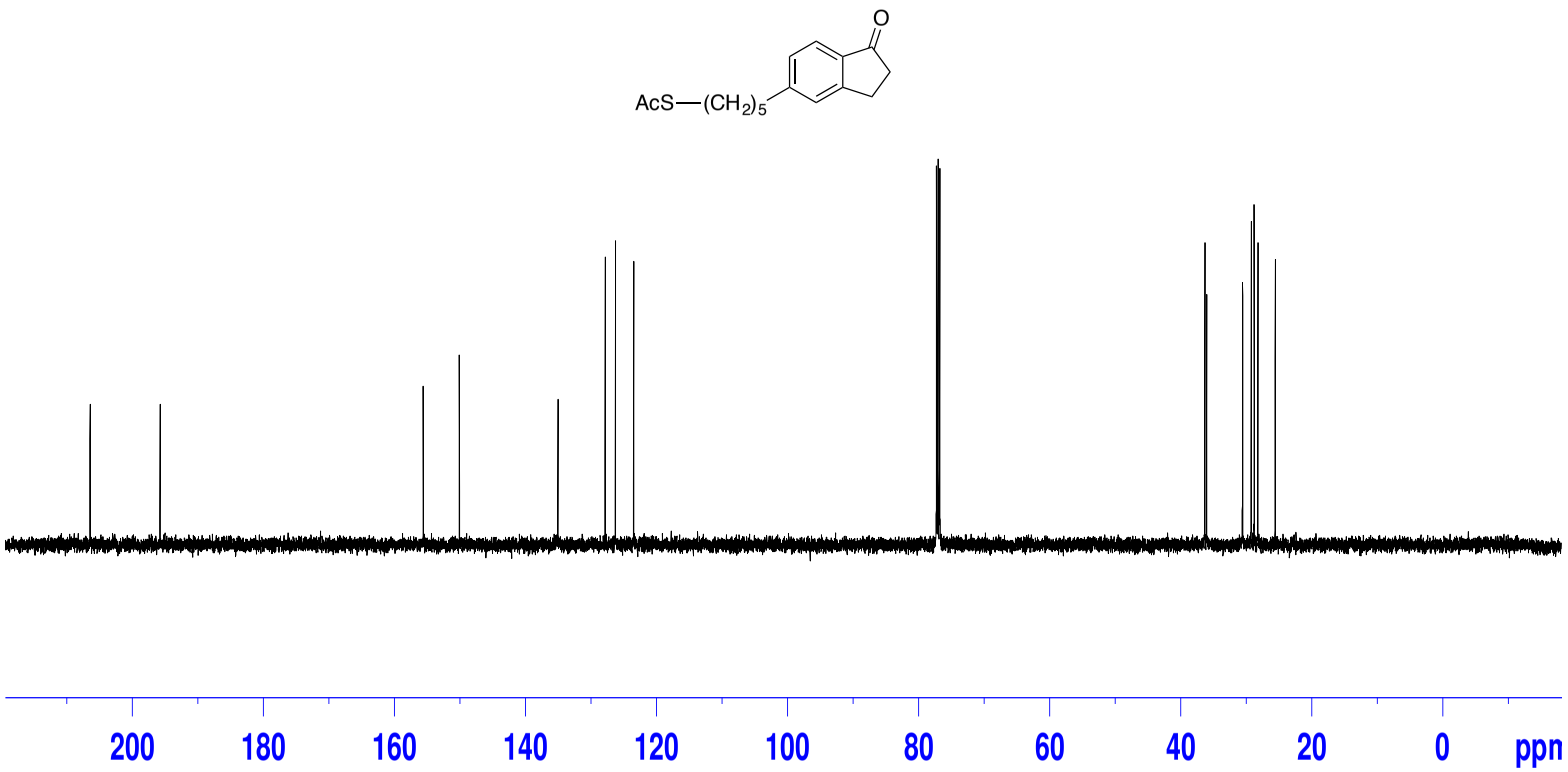

Figure 97: ^{13}C NMR ($CDCl_3$, 125 MHz) of **41**

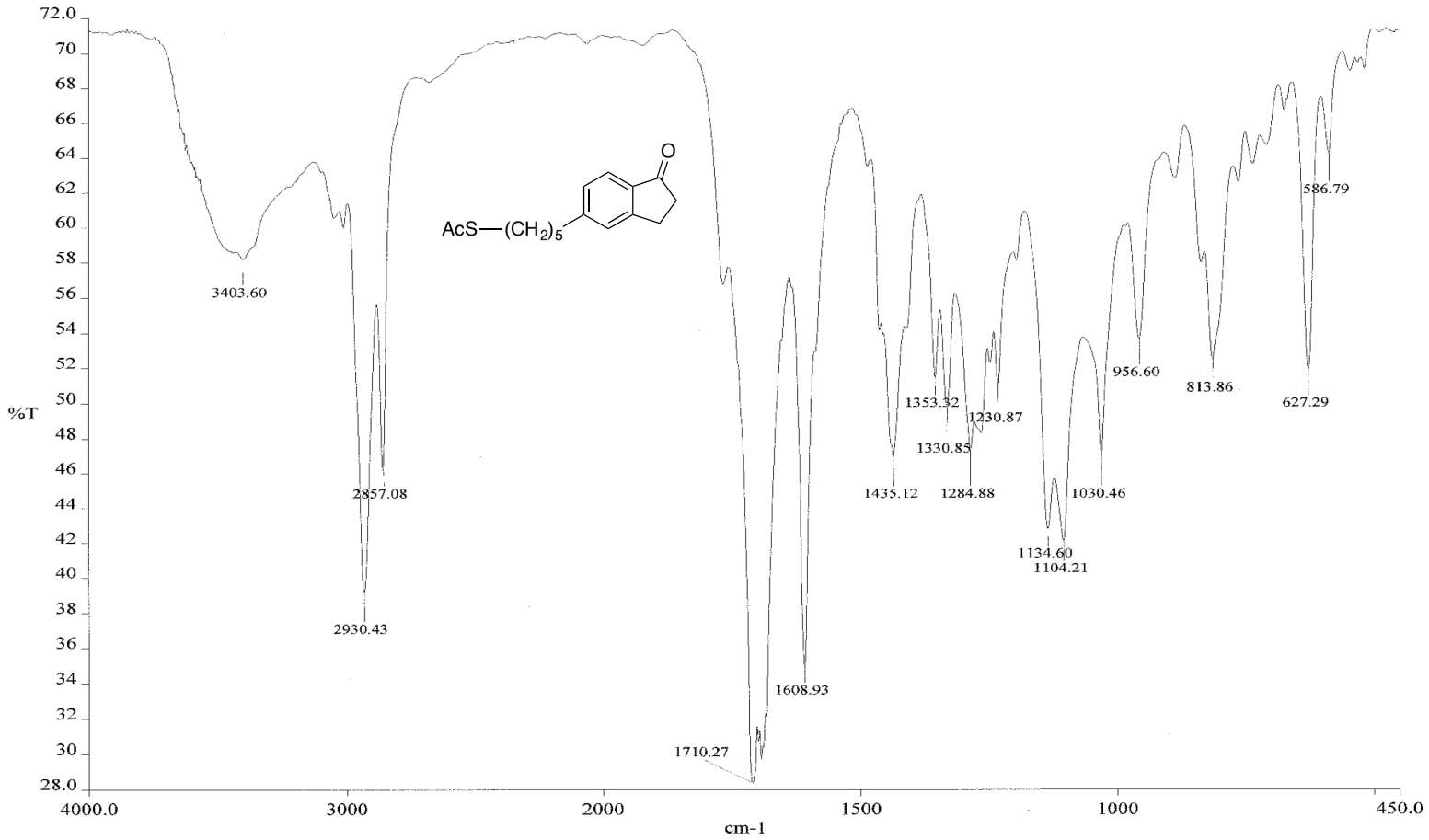

Figure 98: Infrared spectra (neat) of **41**

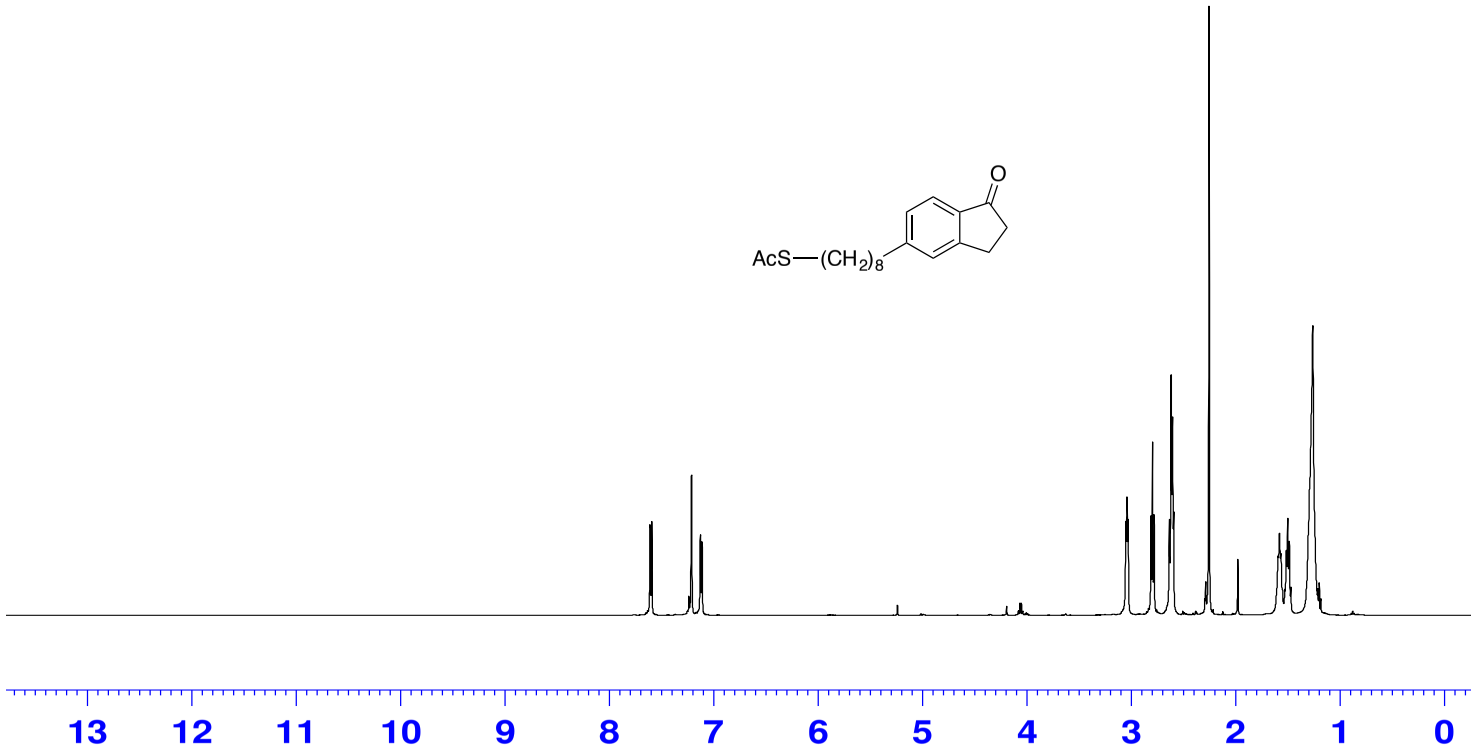

Figure 99: ^{1}H NMR ($CDCl_3$, 500 MHz) of **42**

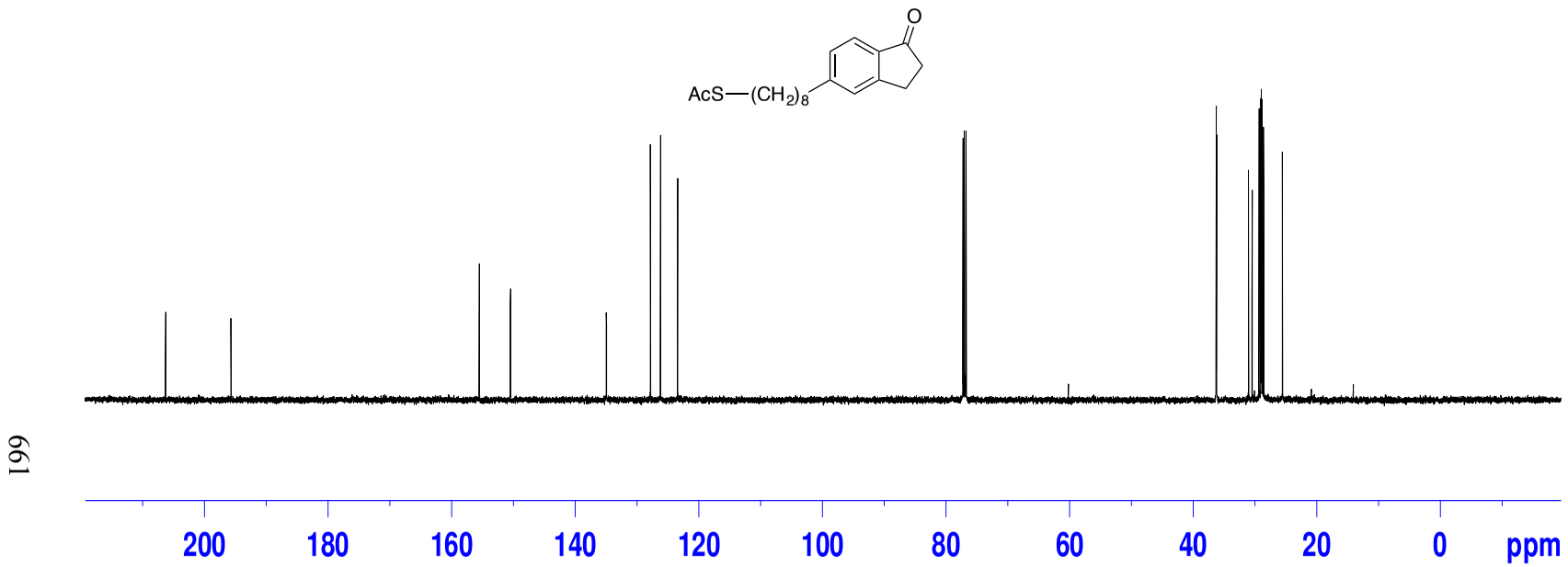

Figure 100: ^{13}C NMR ($CDCl_3$, 125 MHz) of **42**

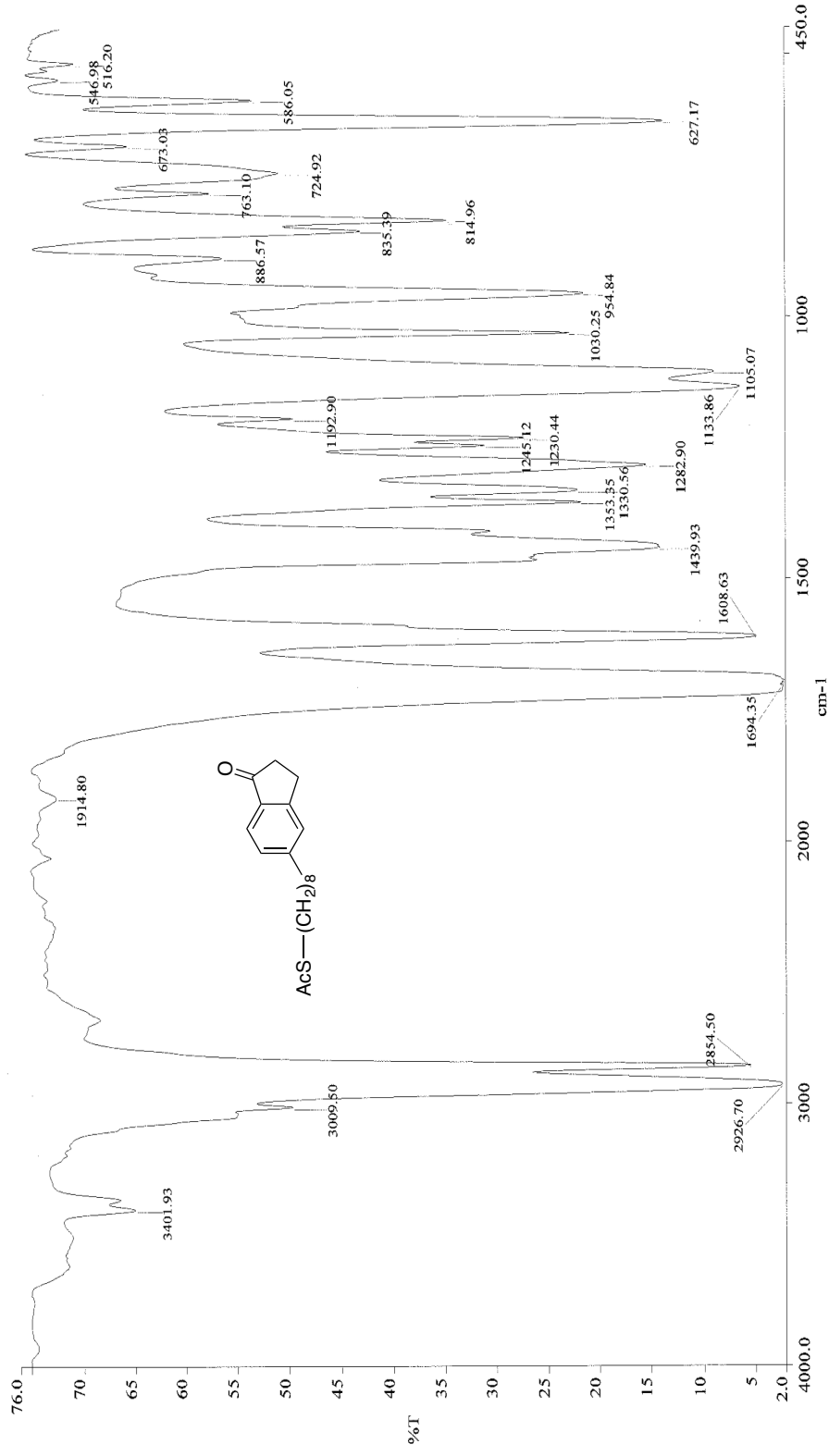

Figure 101: Infrared spectra (neat) of **42**

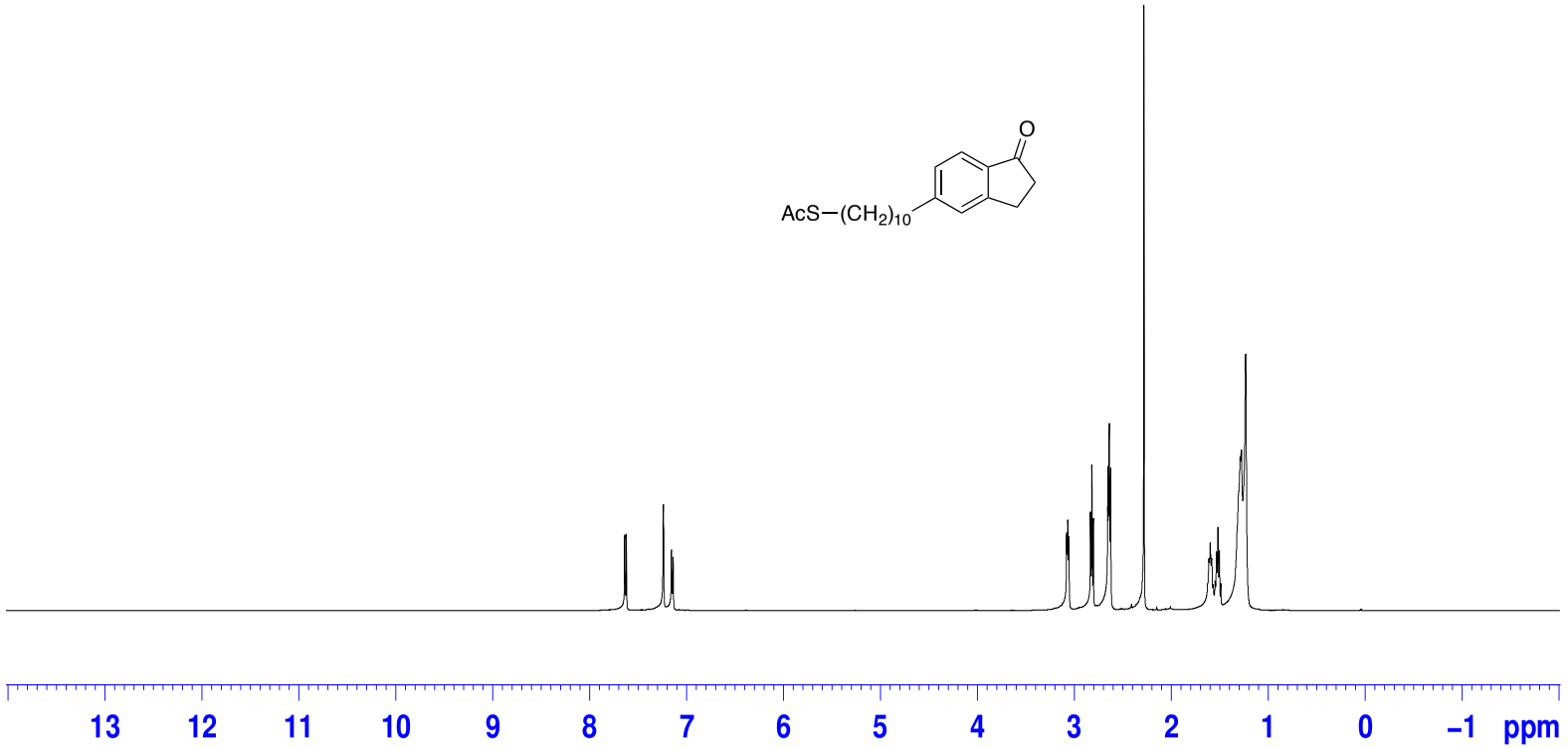

Figure 102: ^{1}H NMR ($CDCl_3$, 500 MHz) of **43**

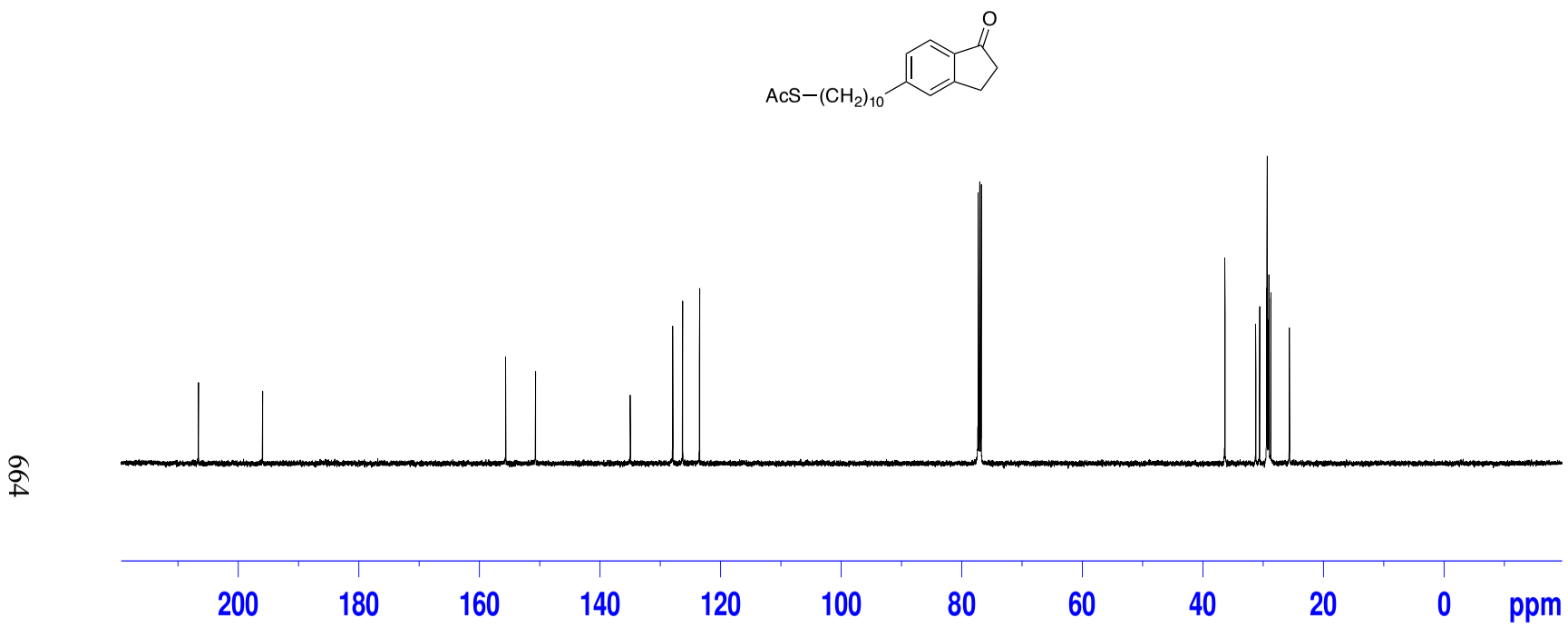

Figure 103: ^{13}C NMR ($CDCl_3$, 125 MHz) of **43**

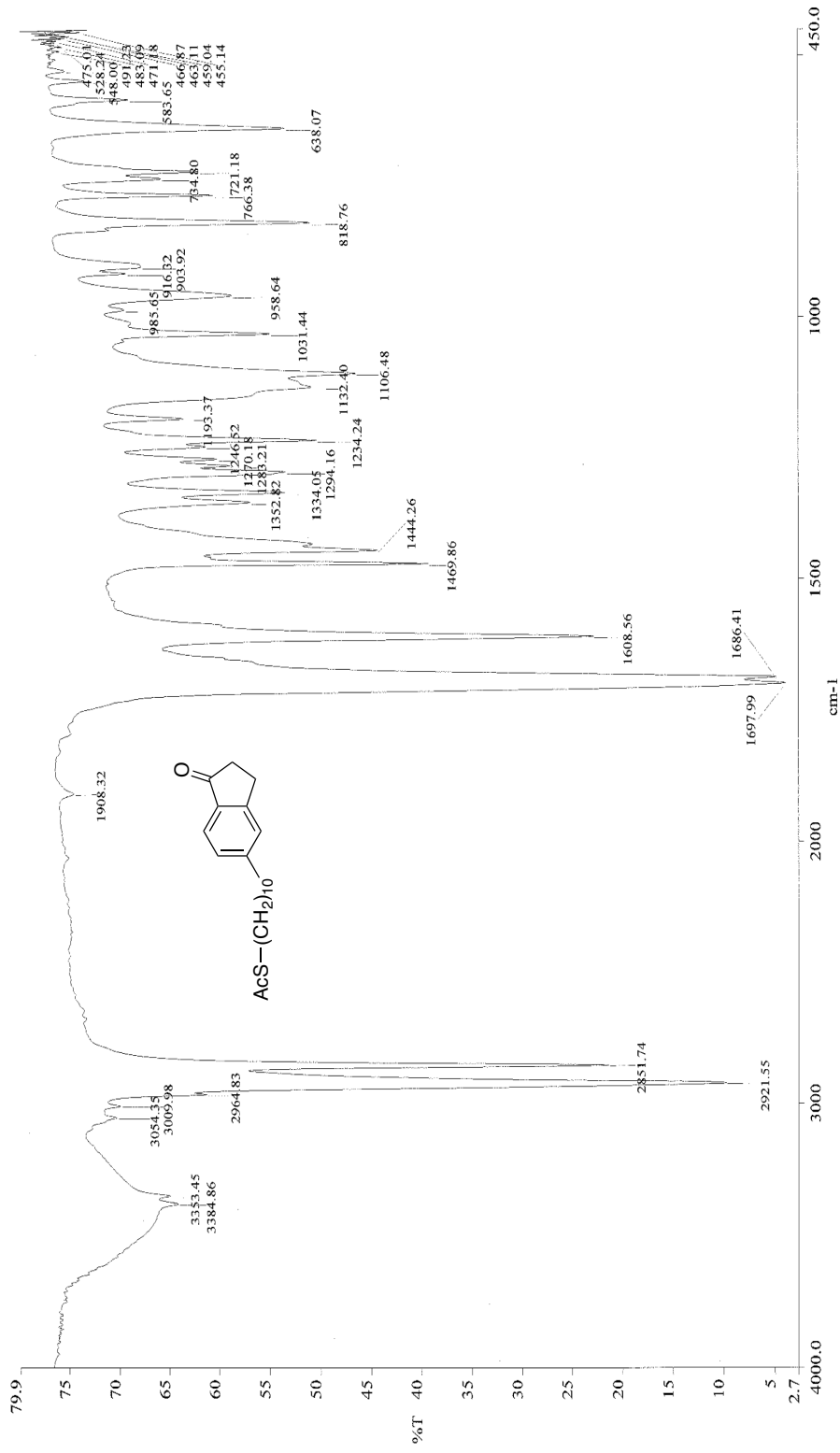

Figure 104: Infrared spectra (neat) of **43**

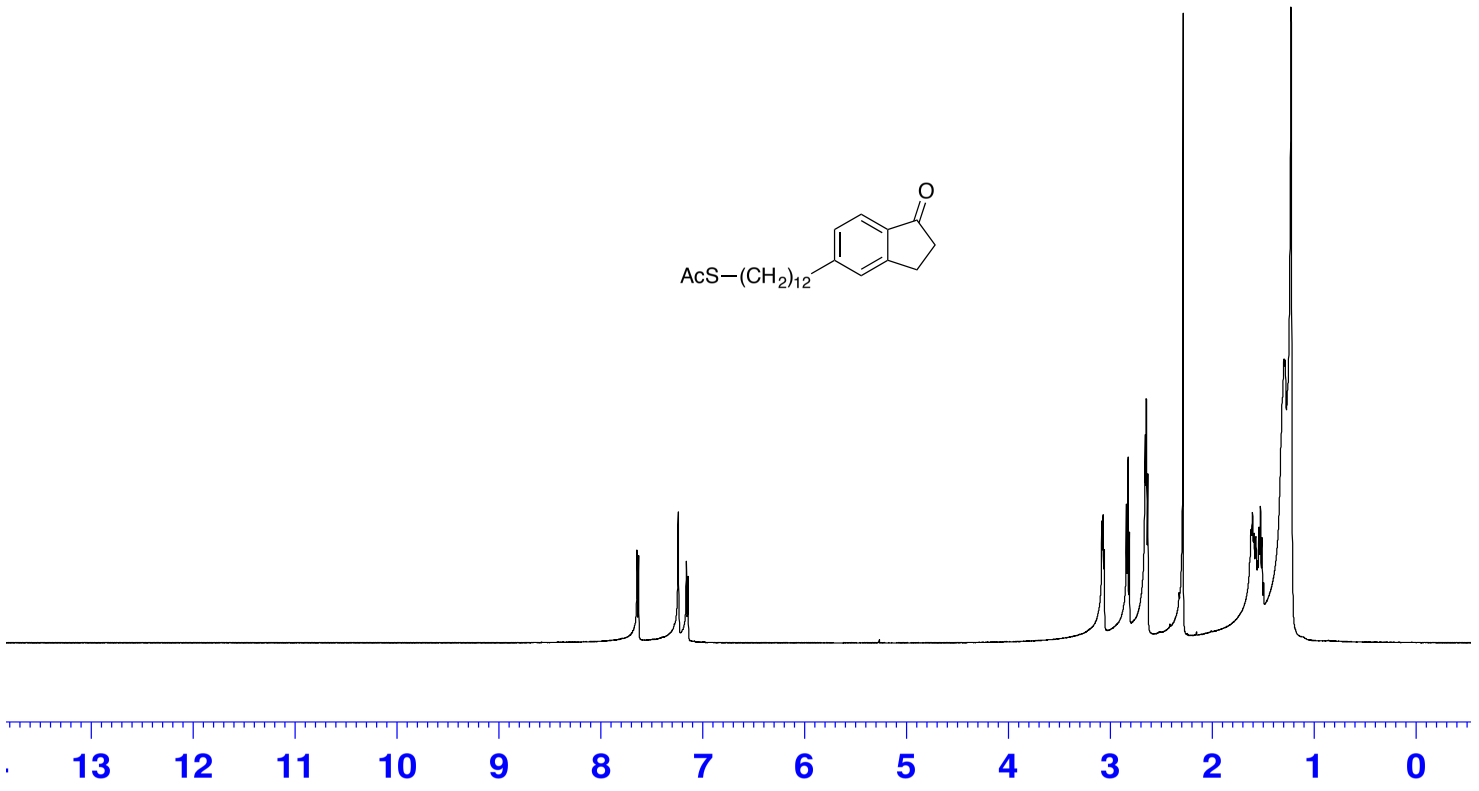

Figure 105: ^{1}H NMR ($CDCl_3$, 500 MHz) of **44**

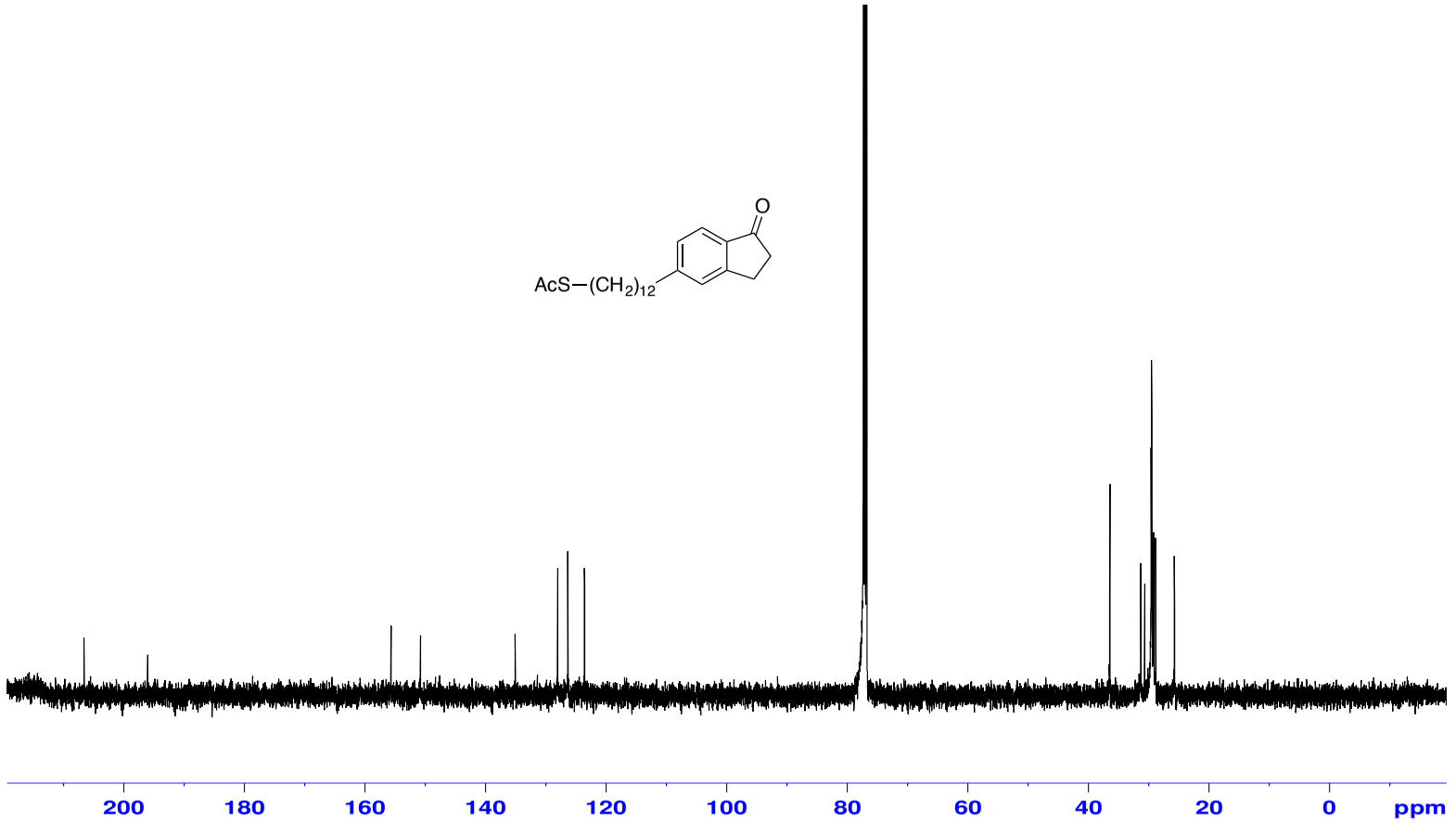

Figure 106: ^{13}C NMR ($CDCl_3$, 125 MHz) of **44**

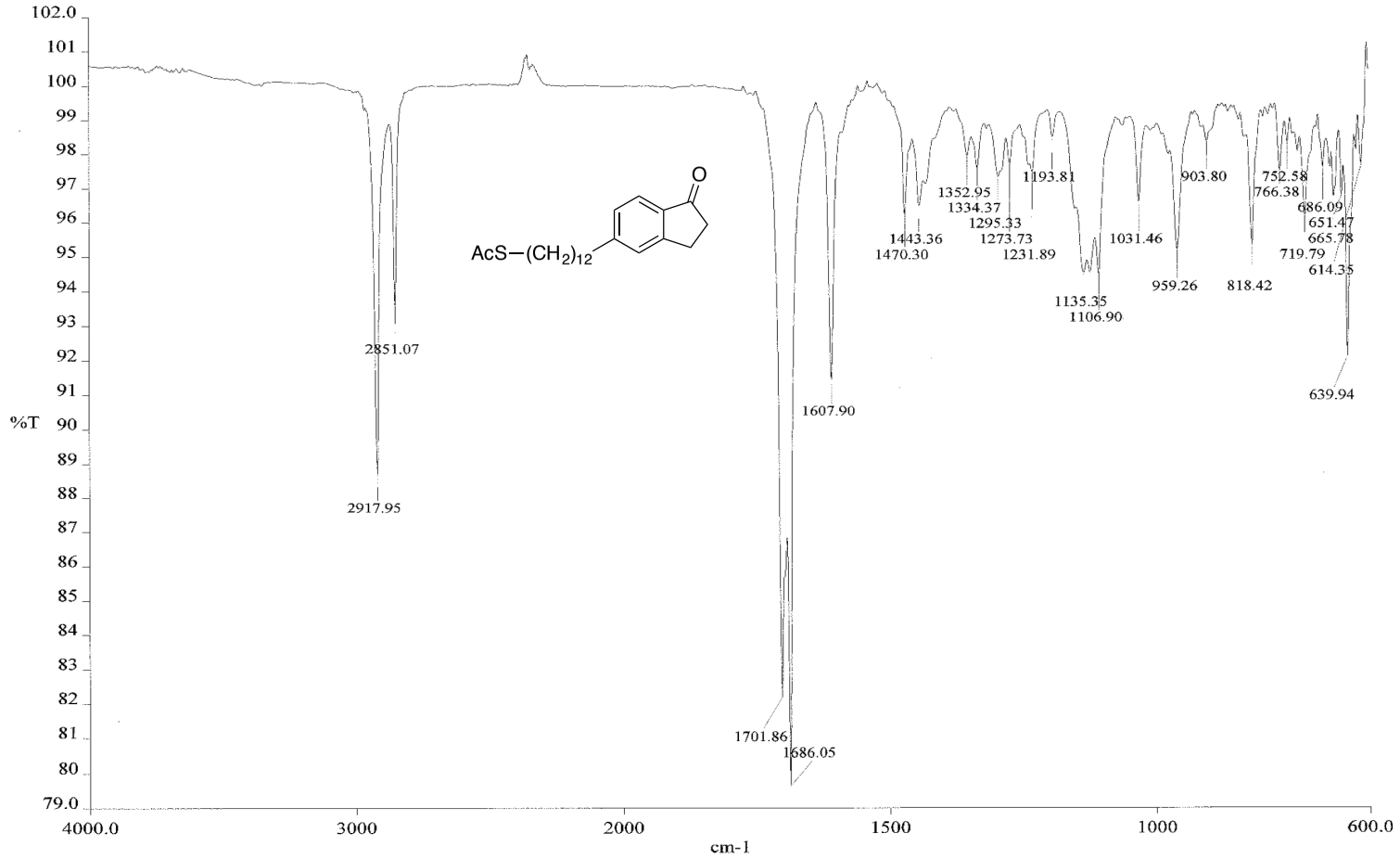

Figure 107: Infrared spectra (neat) of **44**

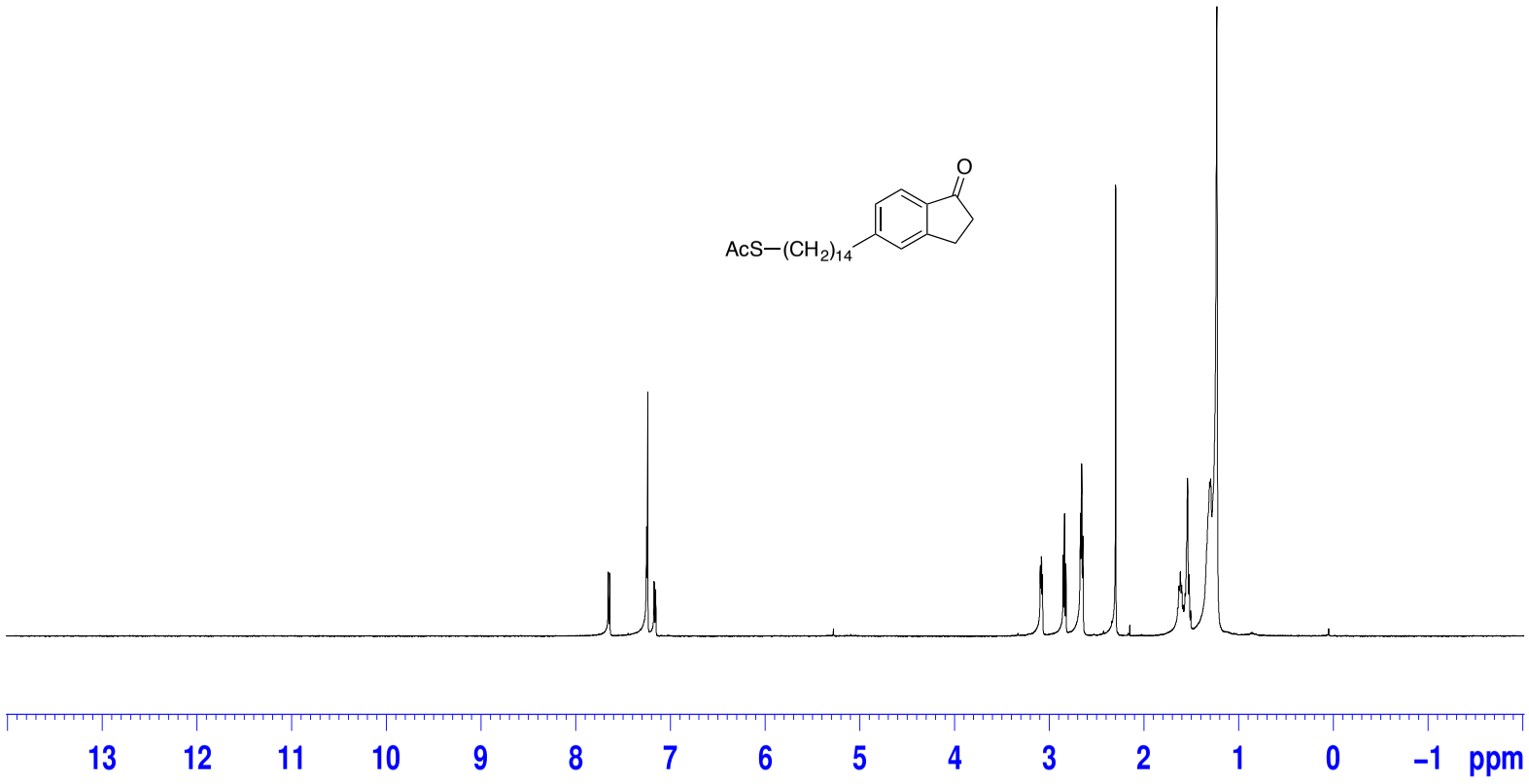

Figure 108: ^{1}H NMR ($CDCl_3$, 500 MHz) of **45**

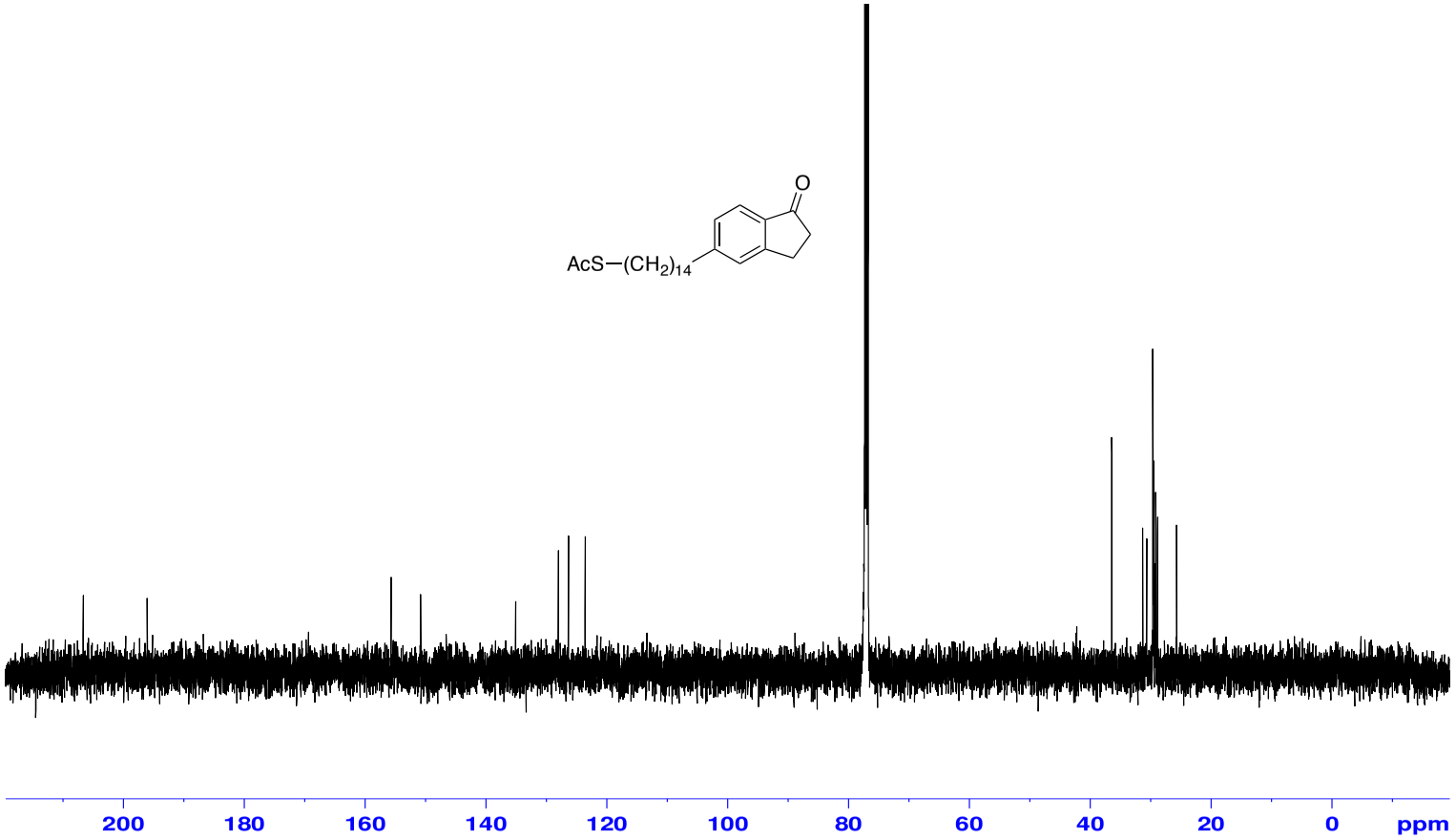

Figure 109: ^{13}C NMR ($CDCl_3$, 125 MHz) of **45**

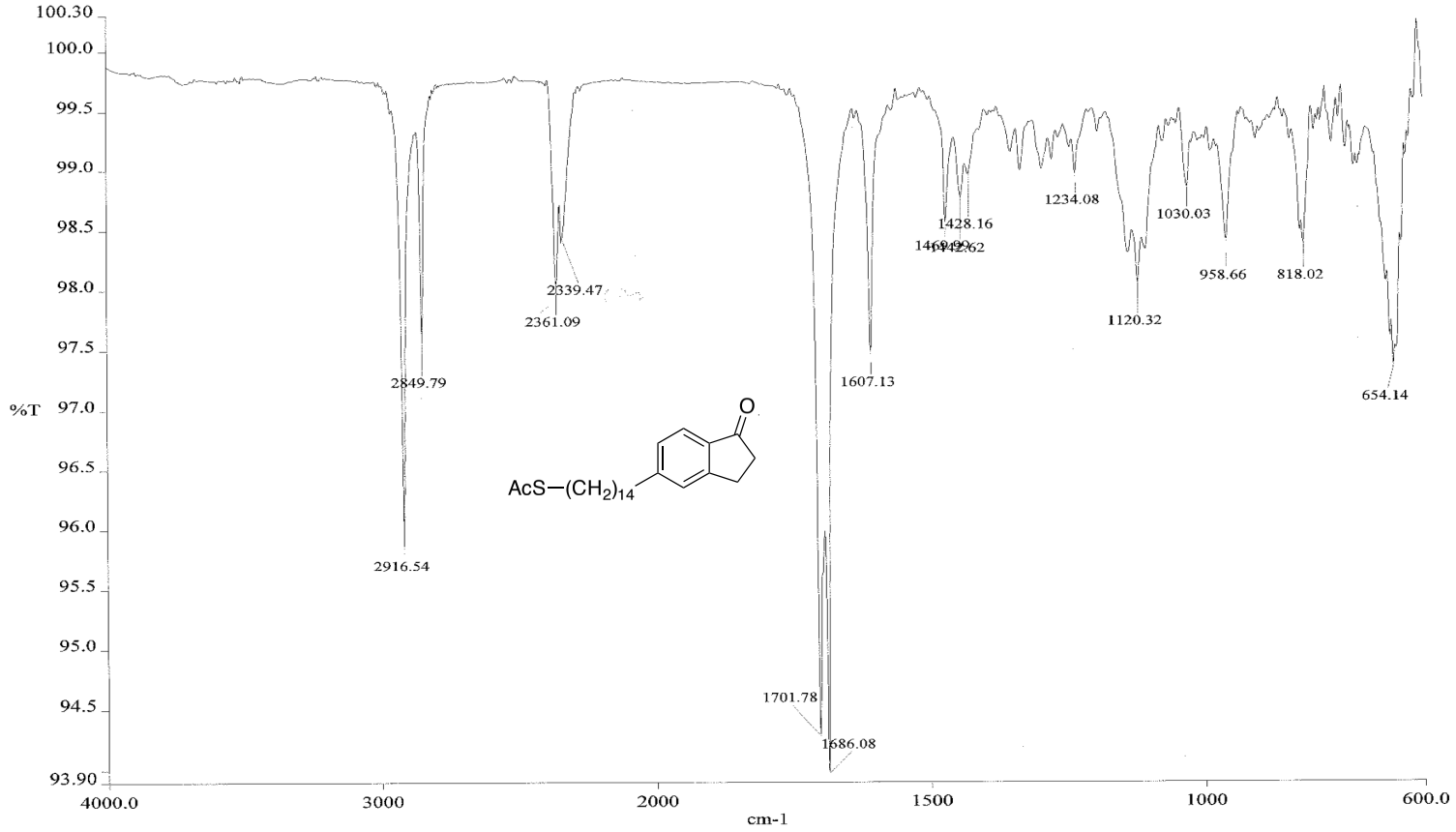

Figure 110: Infrared spectra (neat) of **45**

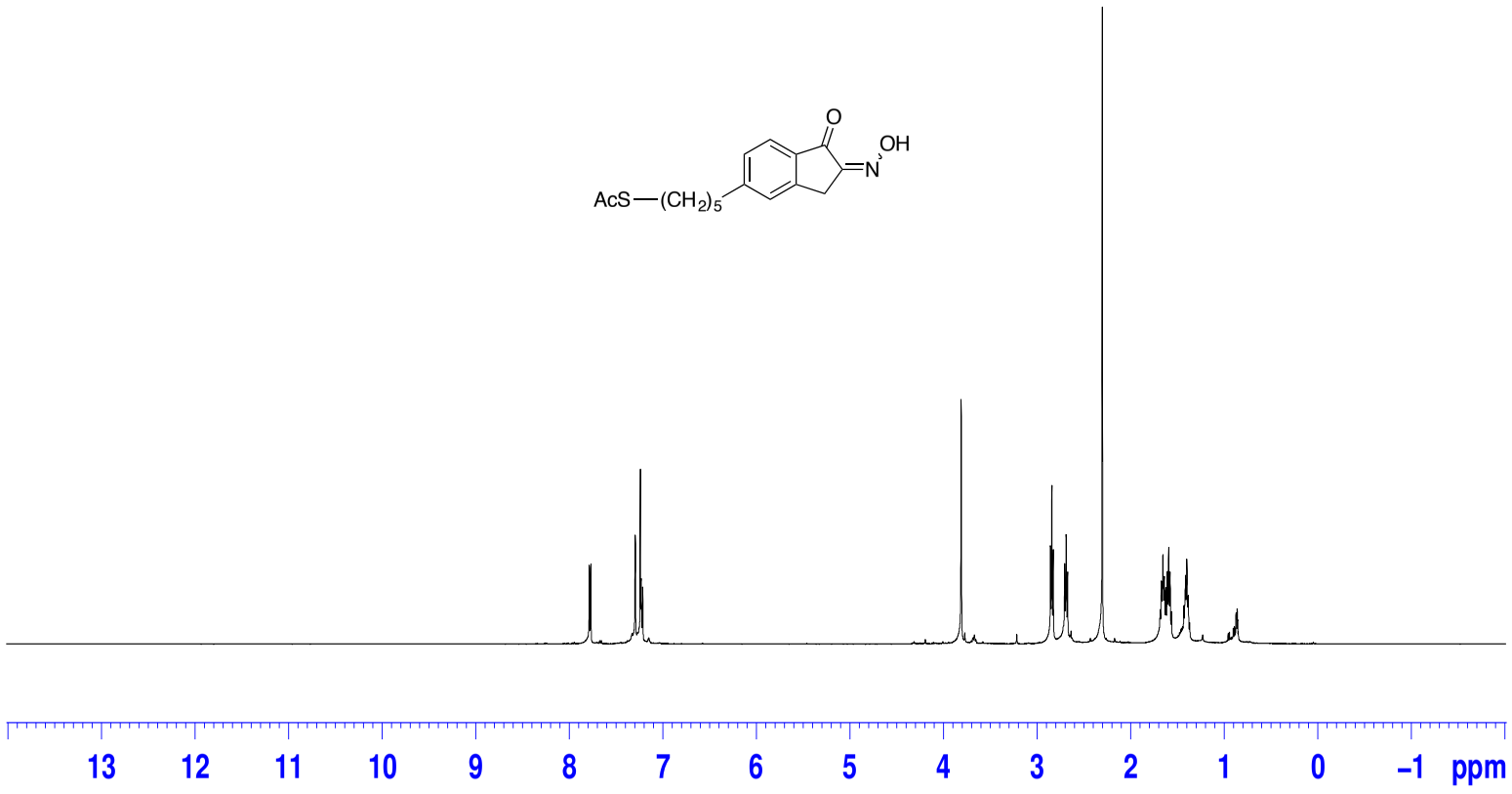

Figure 111: ^{1}H NMR ($CDCl_3$, 500 MHz) of **46**

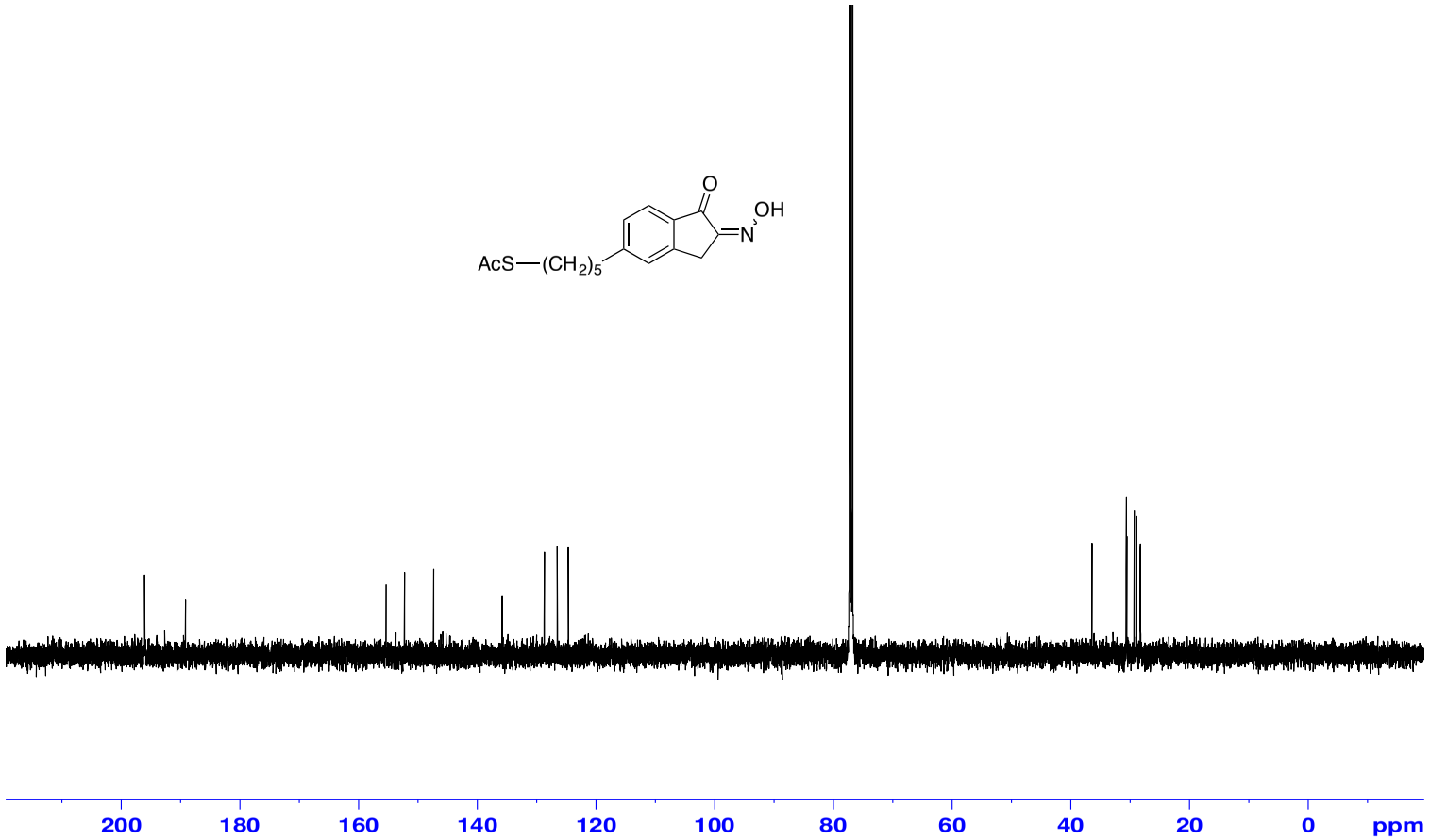

Figure 112: ^{13}C NMR ($CDCl_3$, 125 MHz) of **46**

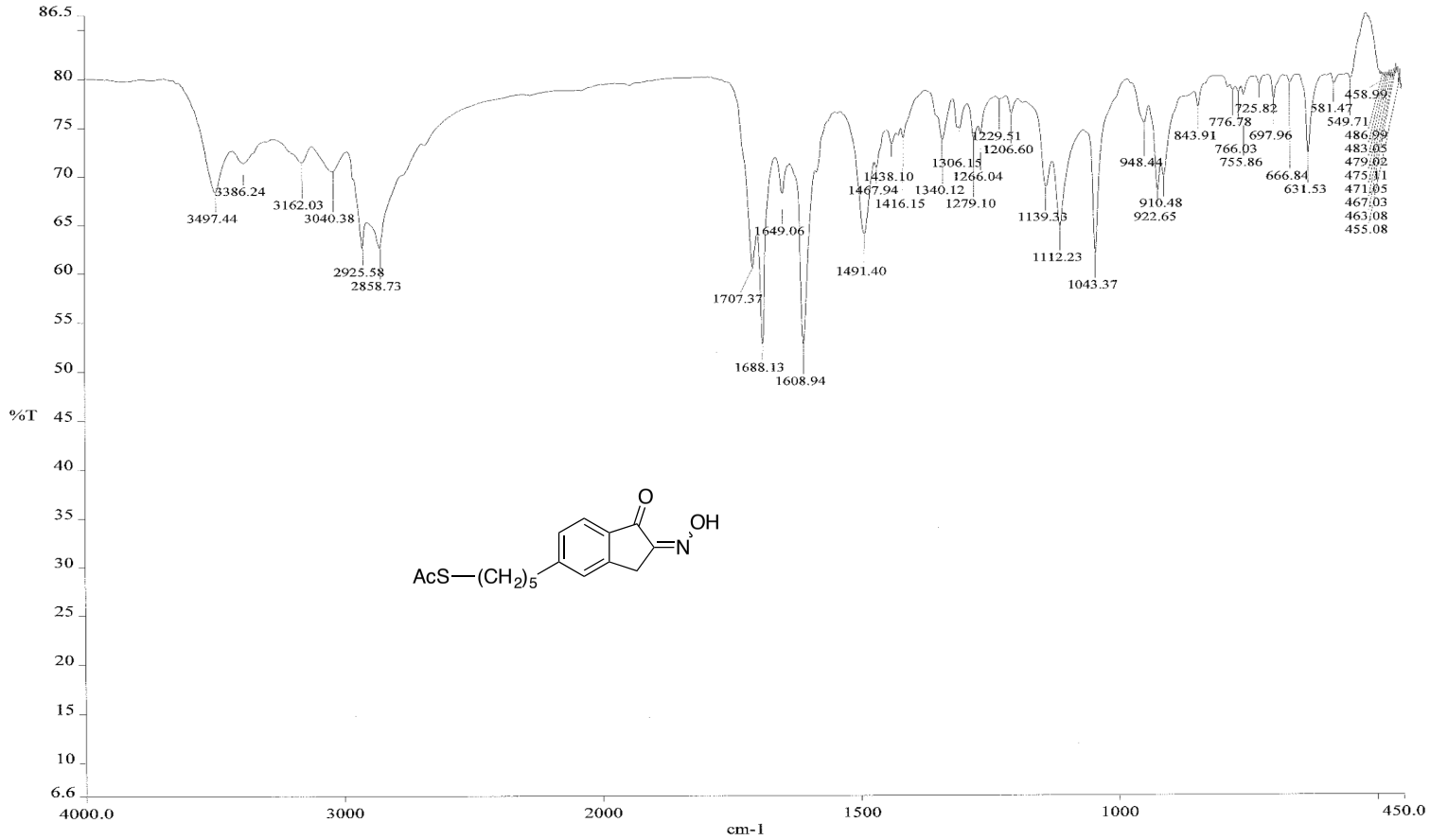

Figure 113: Infrared spectra (neat) of **46**

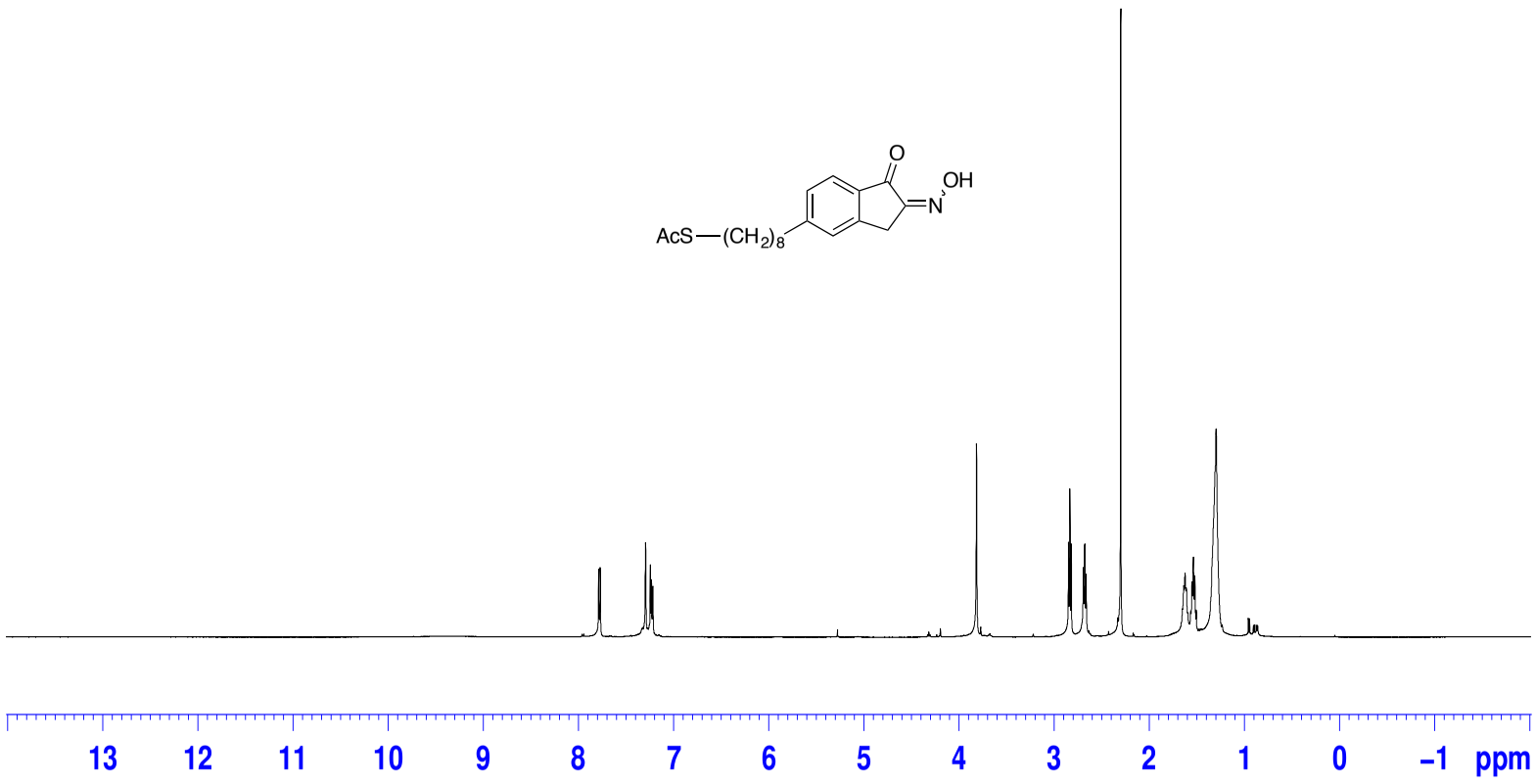

Figure 114: ^{1}H NMR ($CDCl_3$, 500 MHz) of **47**

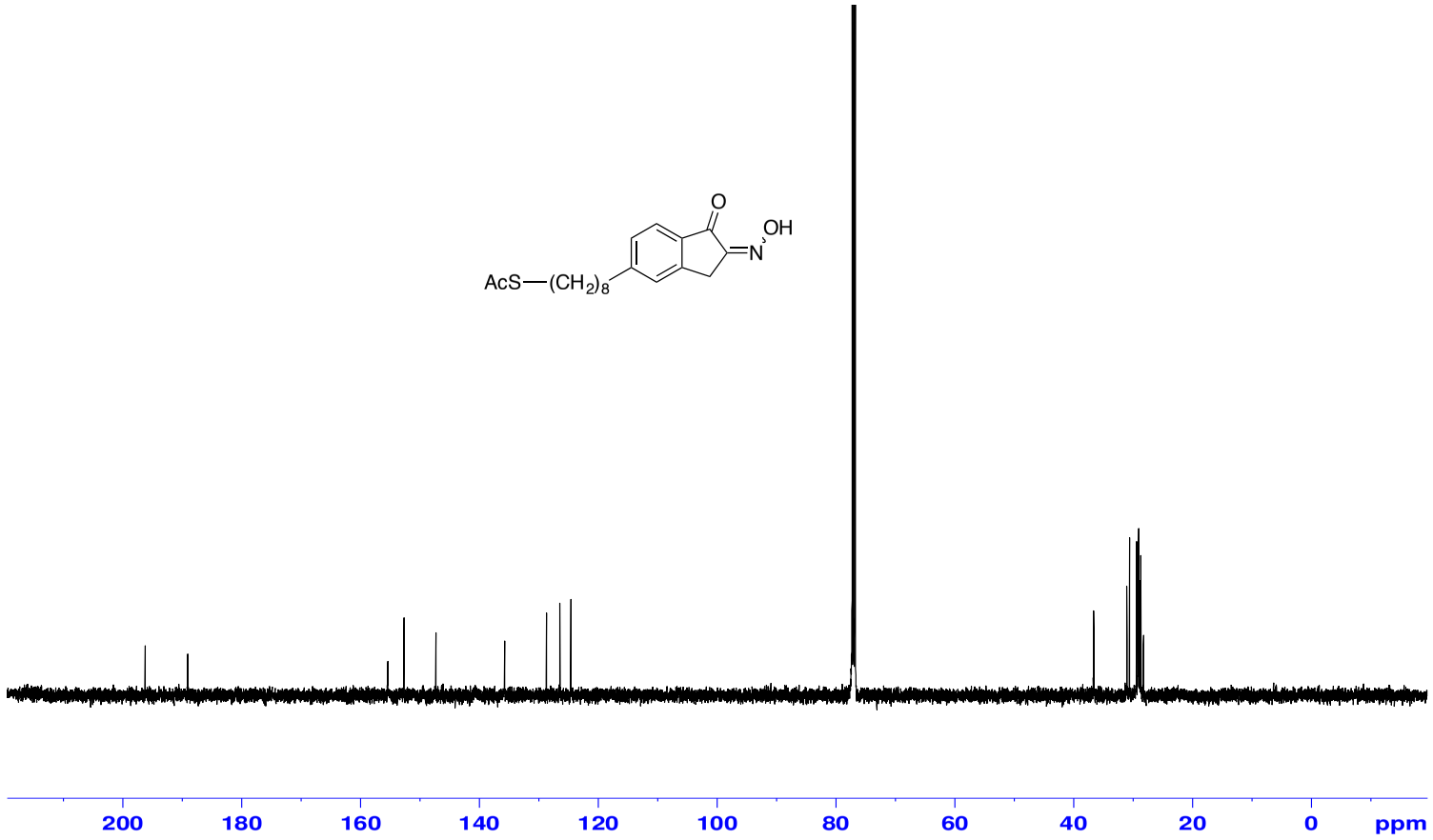

Figure 115: ^{13}C NMR ($CDCl_3$, 125 MHz) of **47**

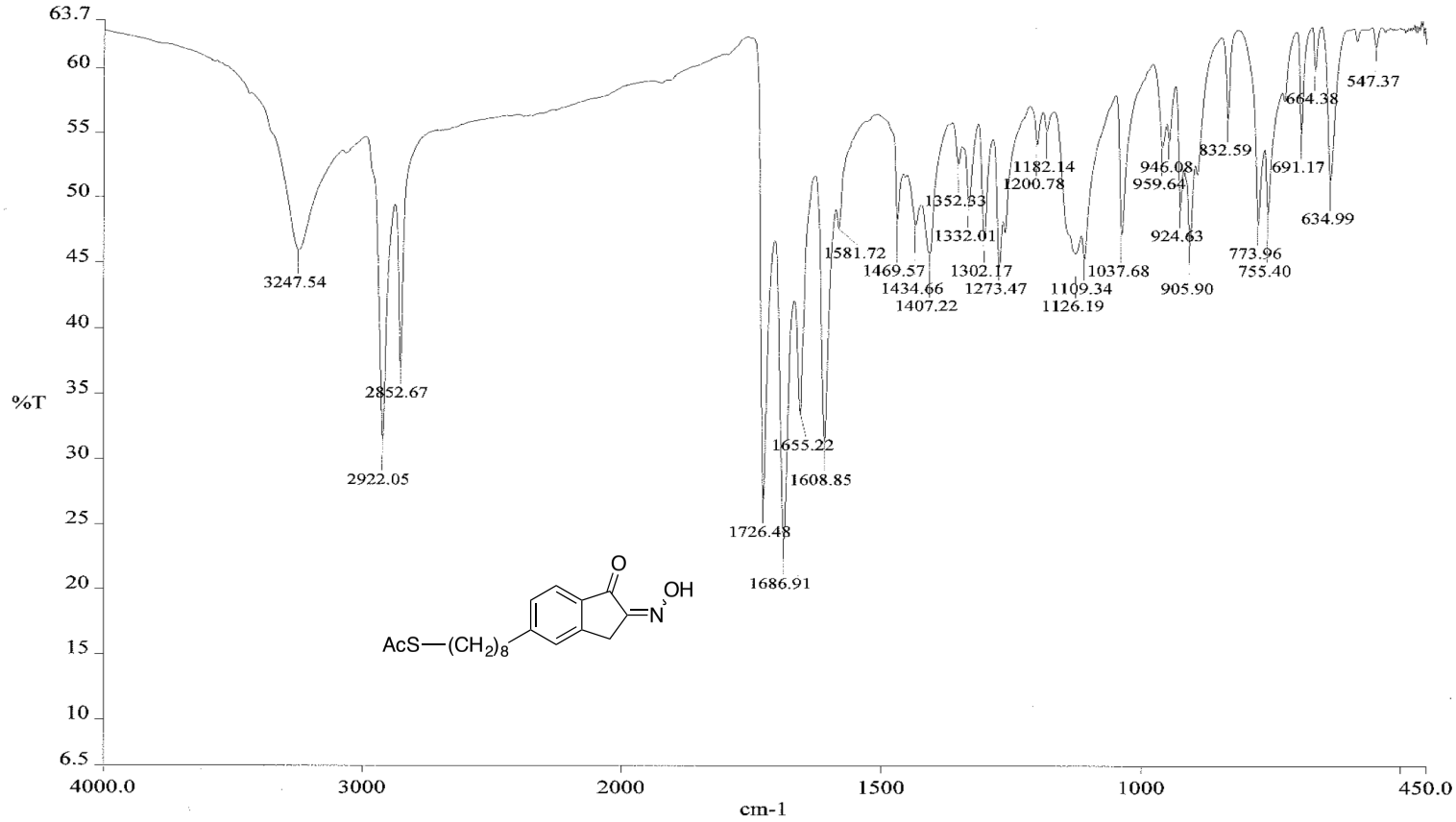

Figure 116: Infrared spectra (neat) of **47**

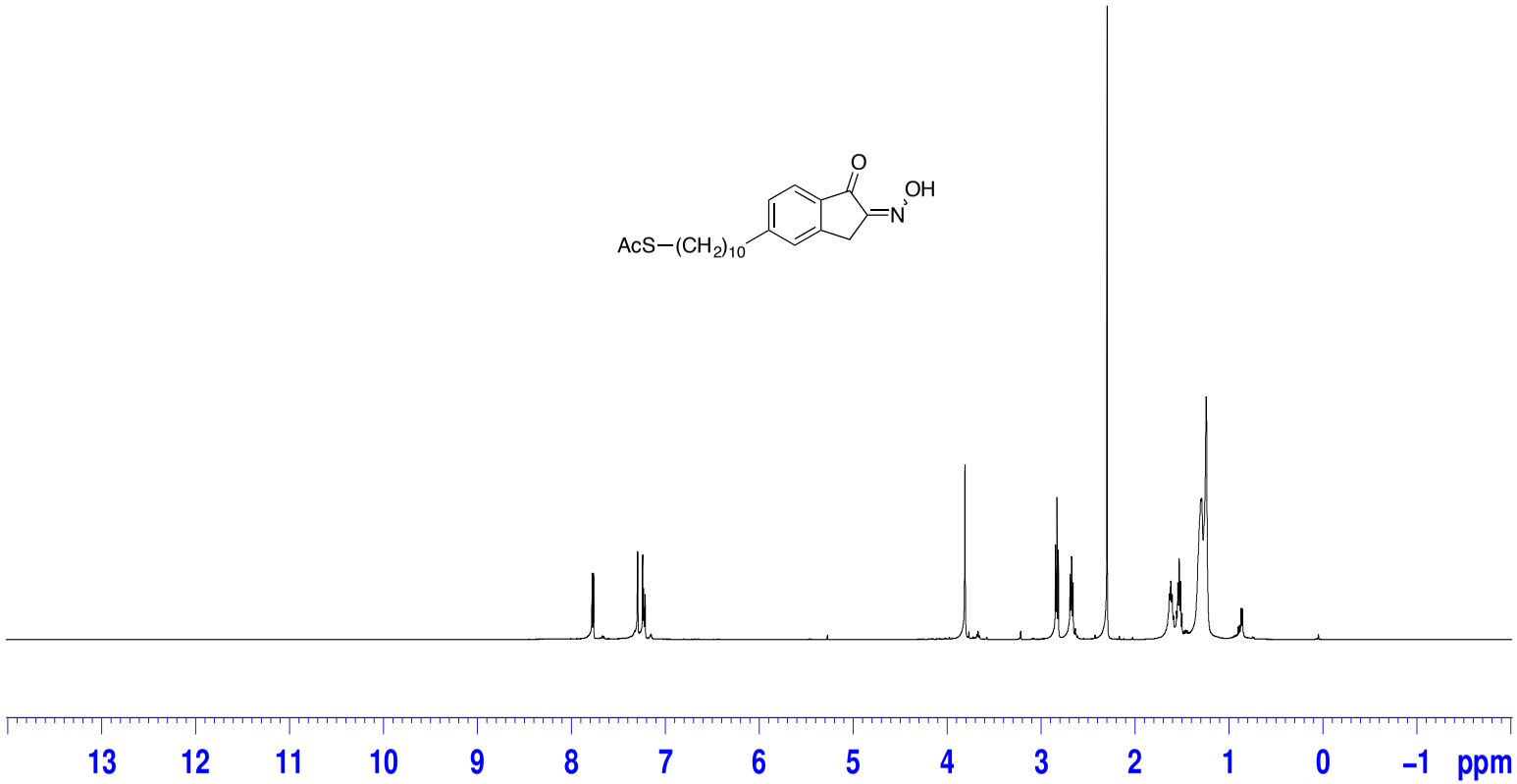

Figure 117: ^{1}H NMR ($CDCl_3$, 500 MHz) of **48**

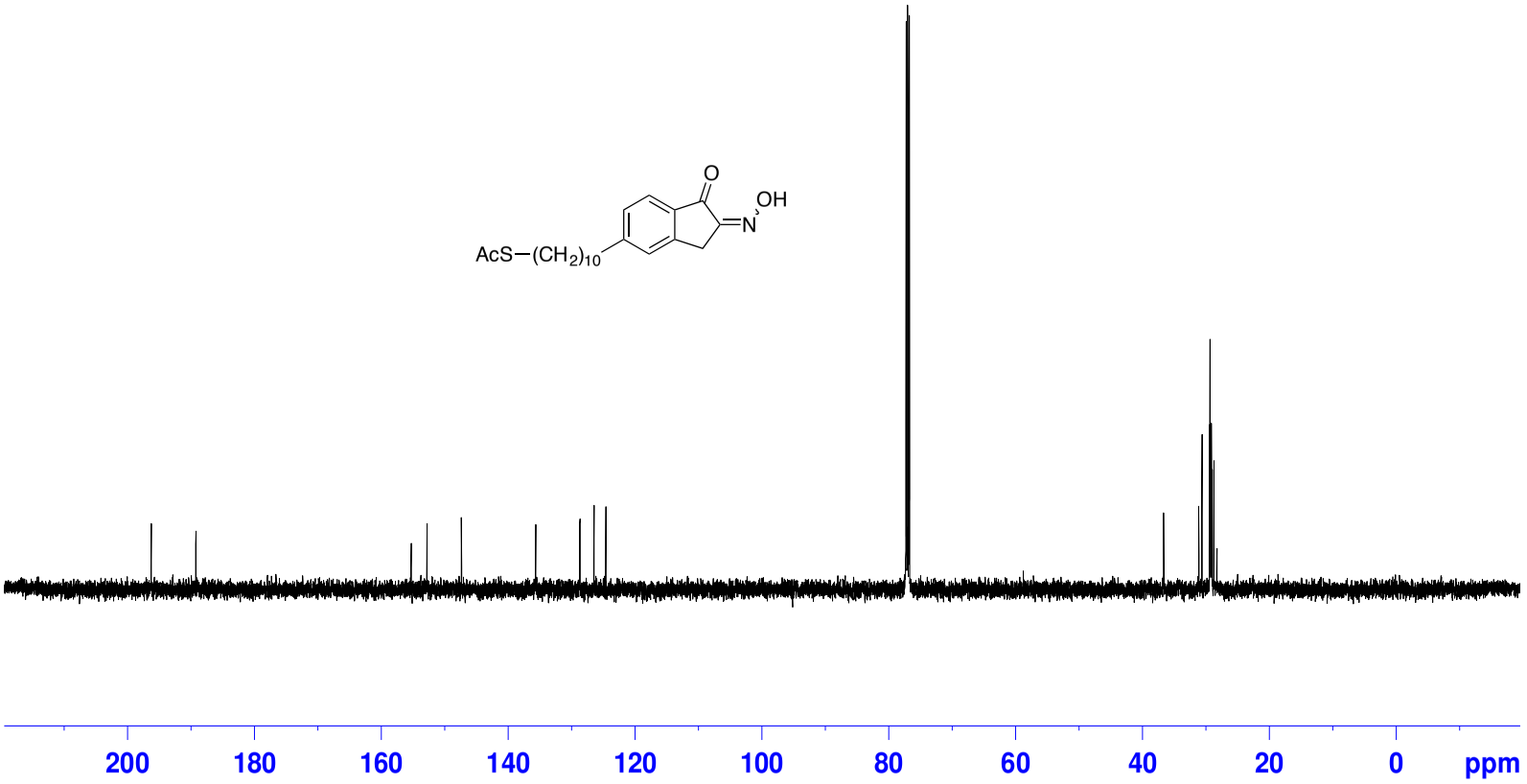

Figure 118: ^{13}C NMR ($CDCl_3$, 125 MHz) of **48**

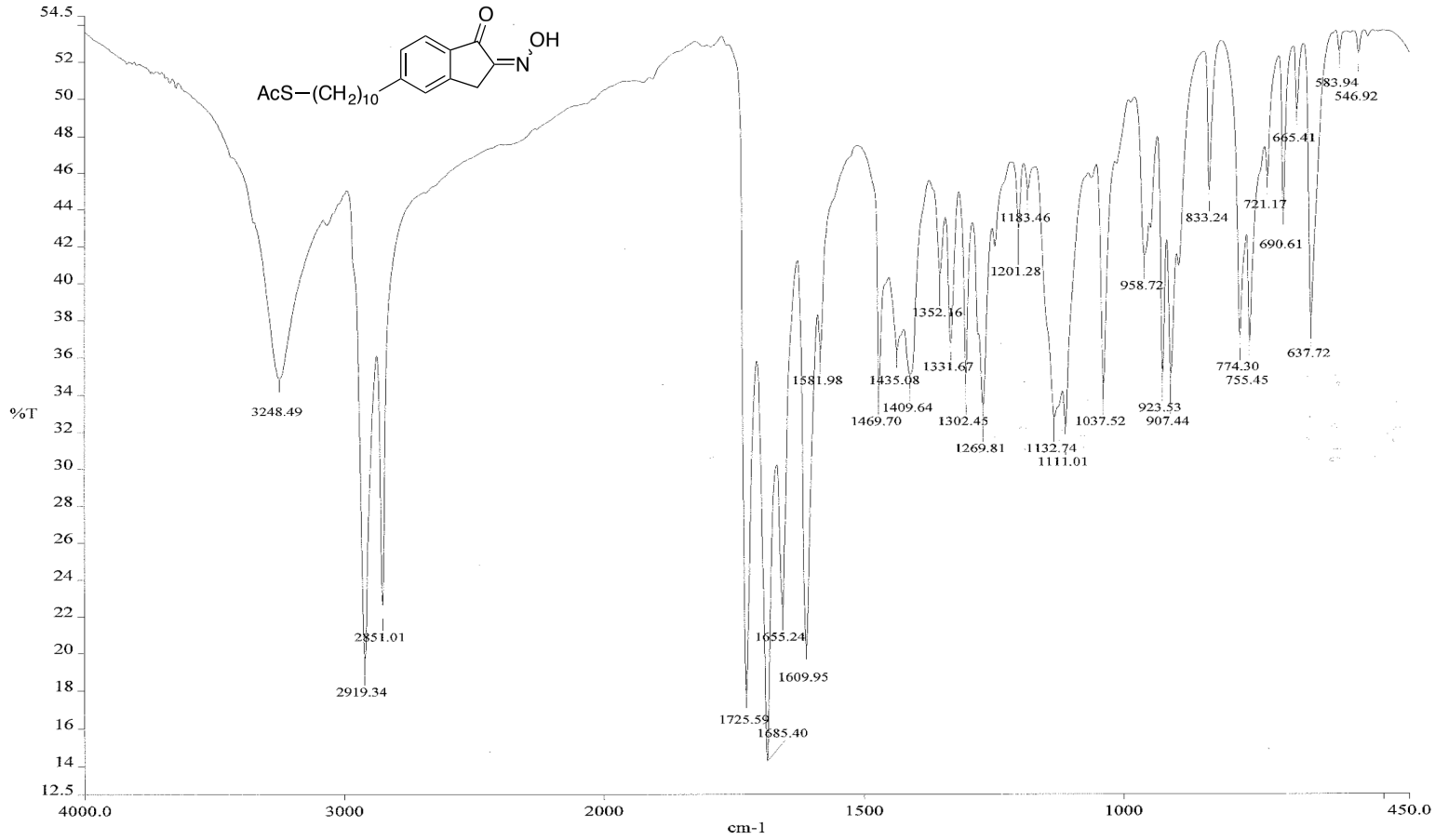

Figure 119: Infrared spectra (neat) of **48**

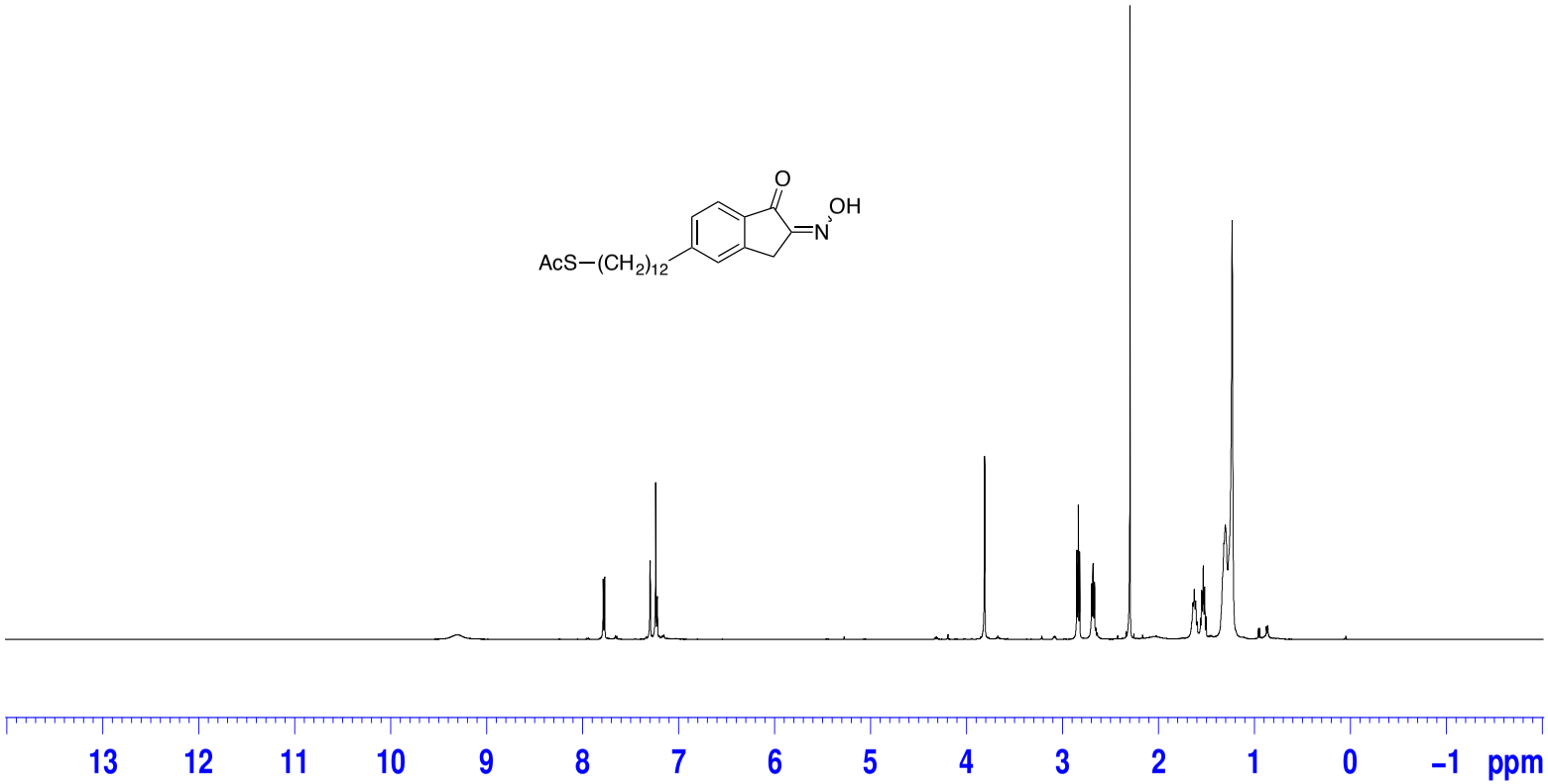

Figure 120: ^{1}H NMR ($CDCl_3$, 500 MHz) of **49**

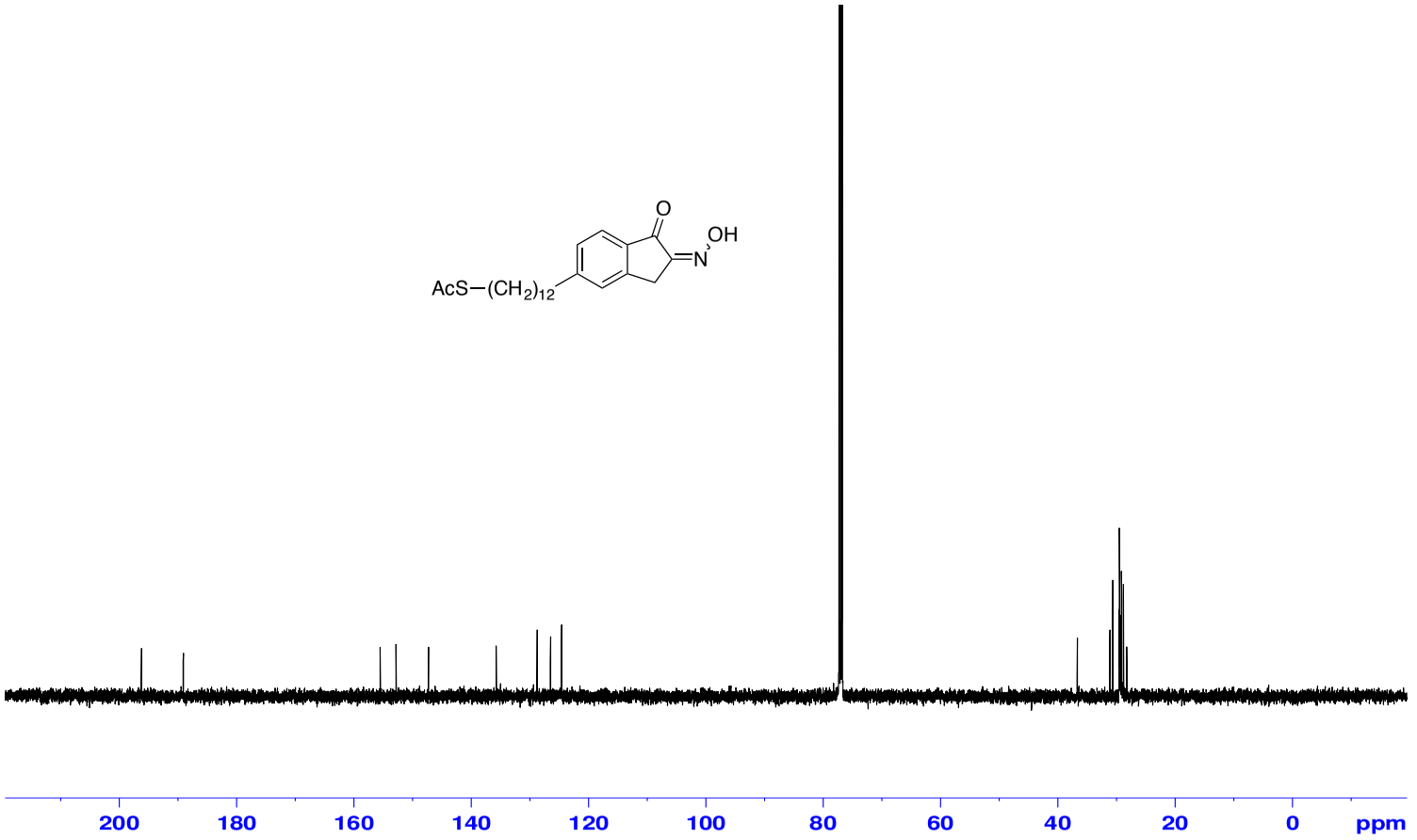

Figure 121: ^{13}C NMR ($CDCl_3$, 125 MHz) of **49**

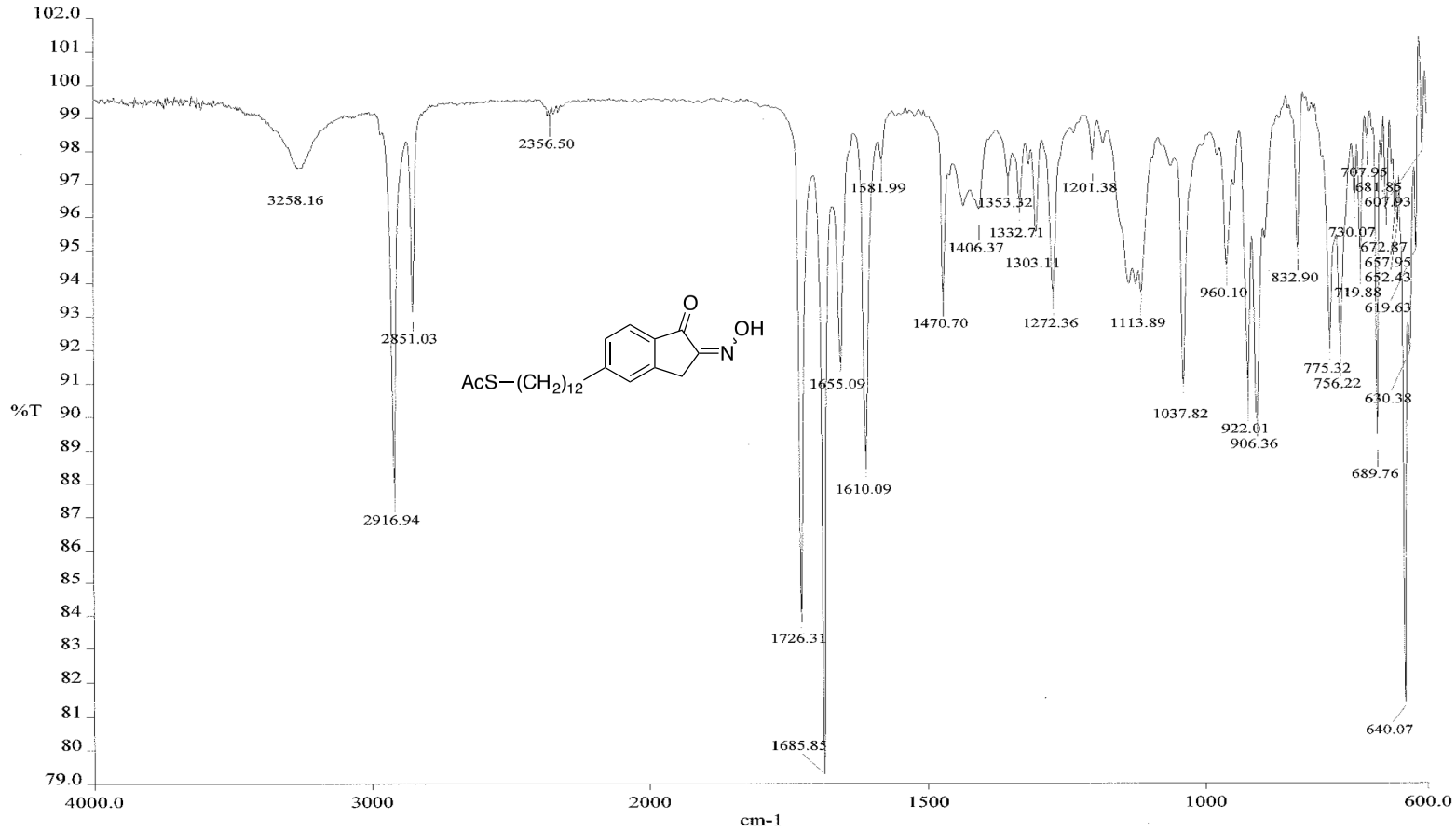

Figure 122: Infrared spectra (neat) of **49**

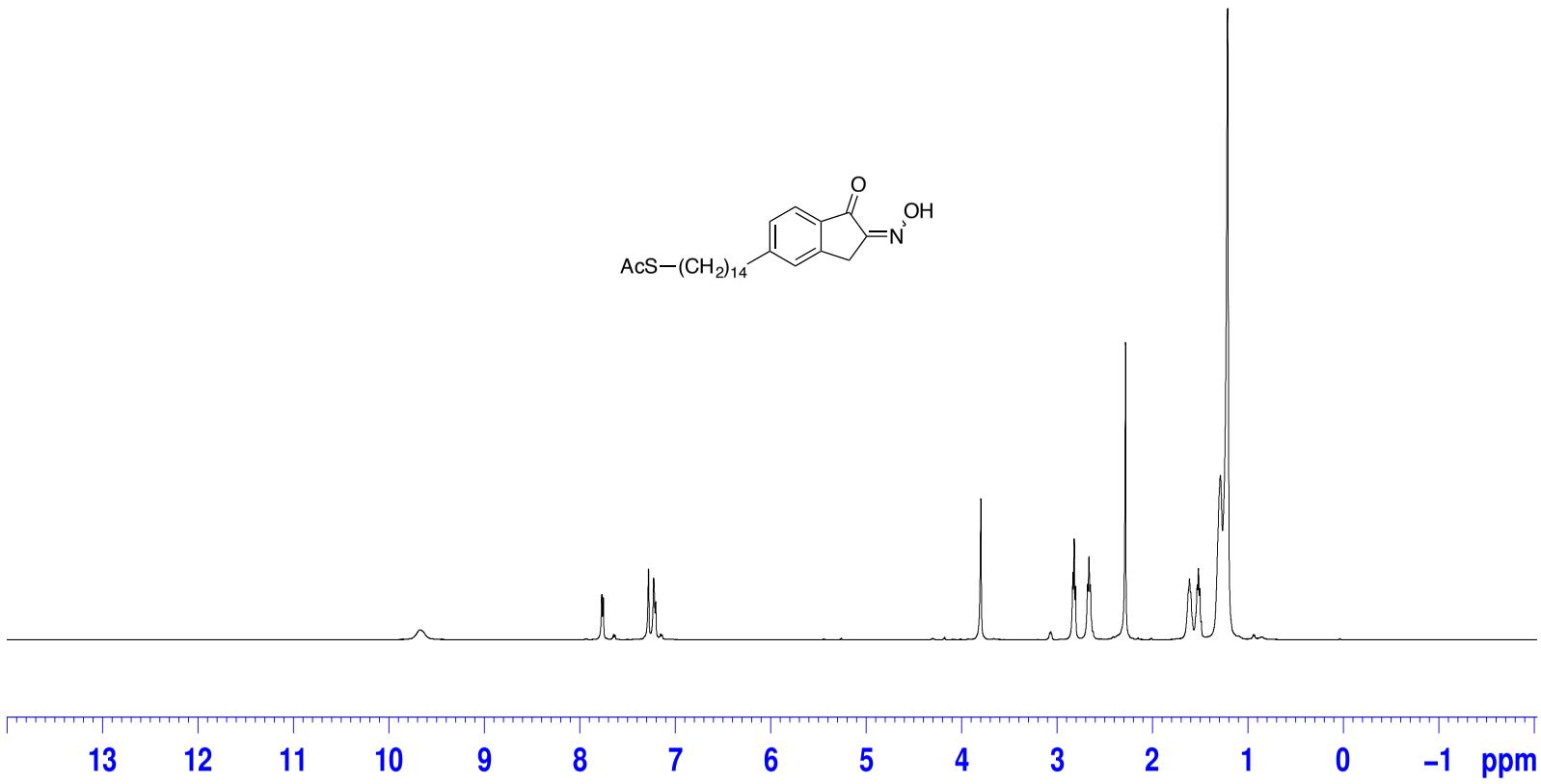

Figure 123: ^{1}H NMR ($CDCl_3$, 500 MHz) of **50**

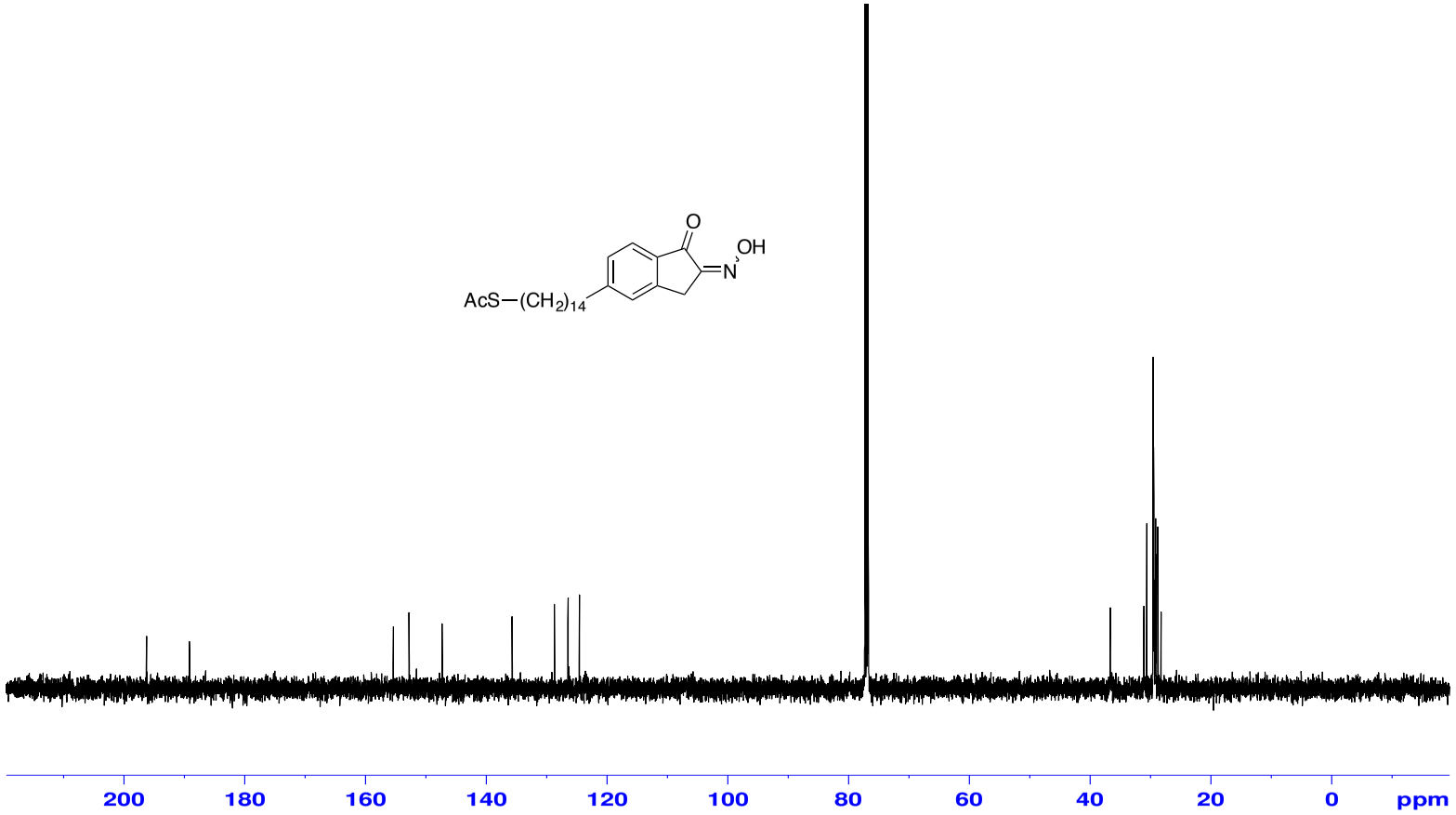

Figure 124: ^{13}C NMR ($CDCl_3$, 125 MHz) of **50**

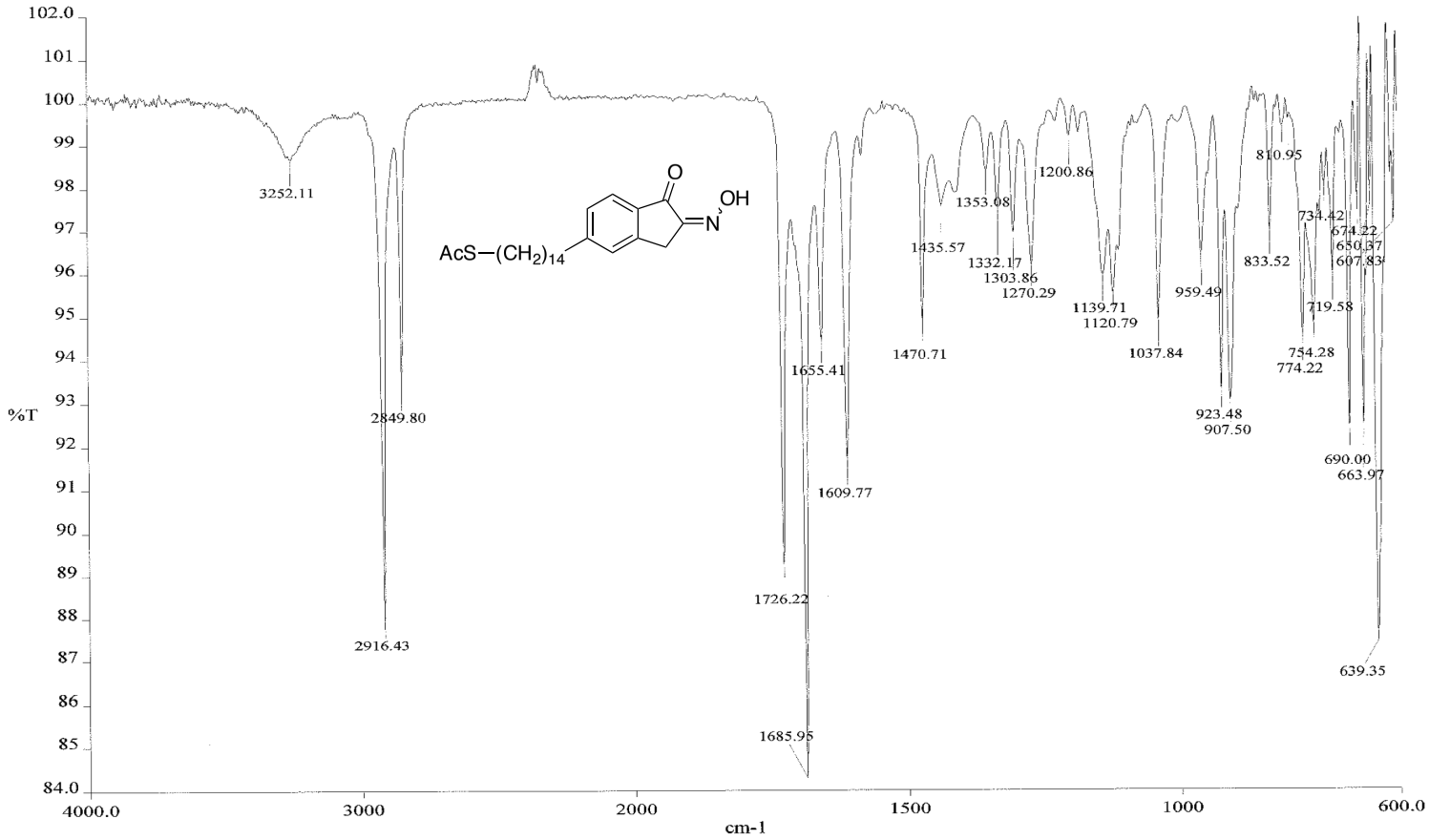

Figure 125: Infrared spectra (neat) of **50**

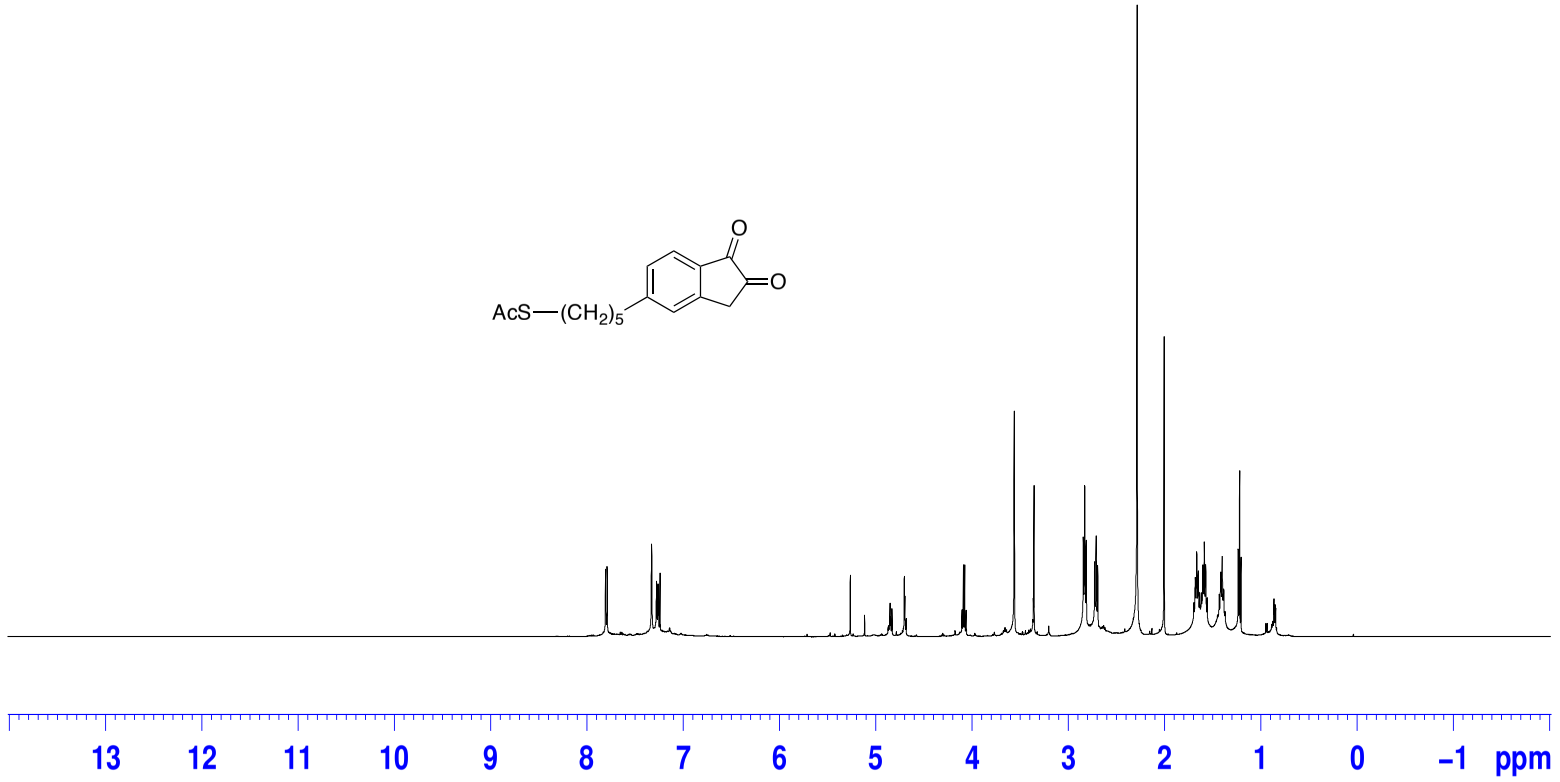

Figure 126: ^{1}H NMR ($CDCl_3$, 500 MHz) of **51**

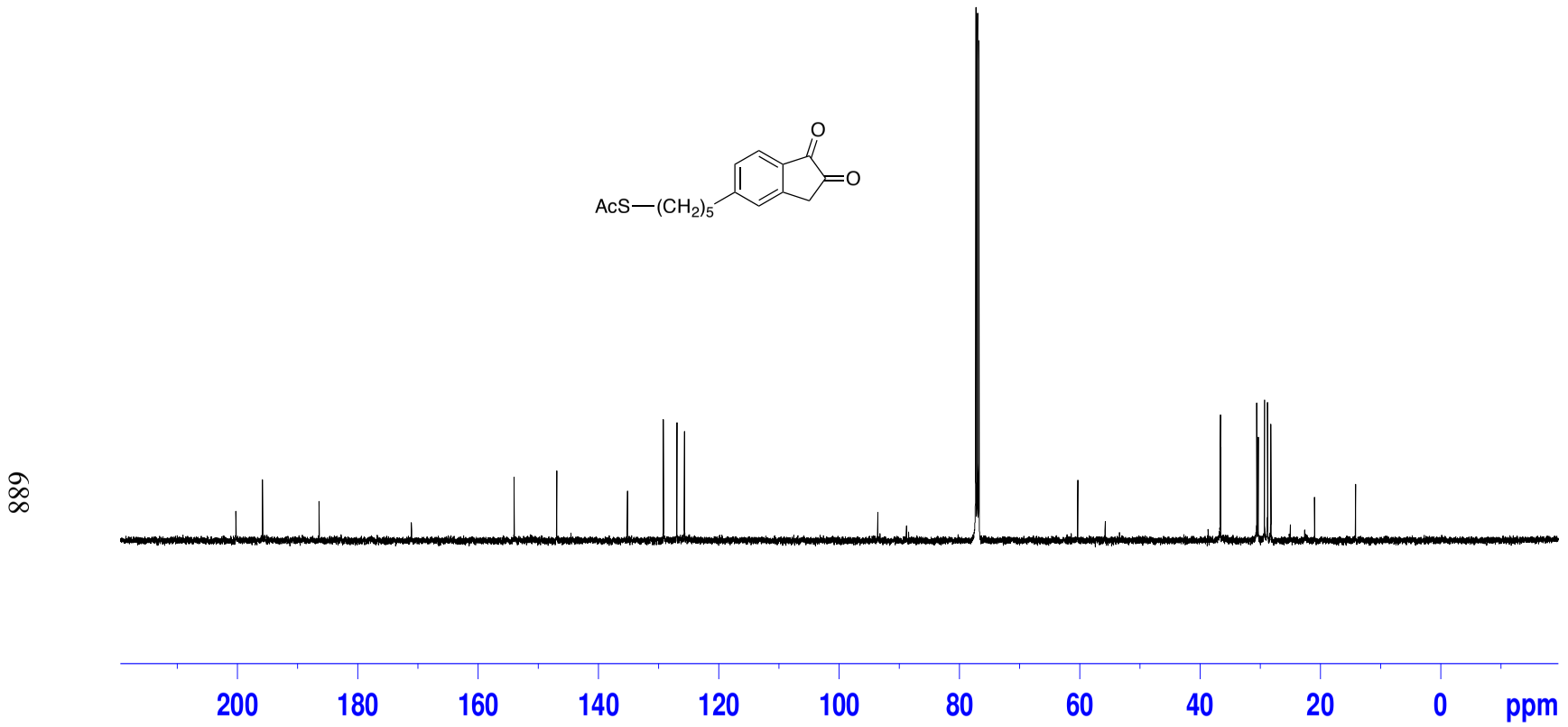

Figure 127: ^{1}H NMR ($CDCl_3$, 500 MHz) of **51**

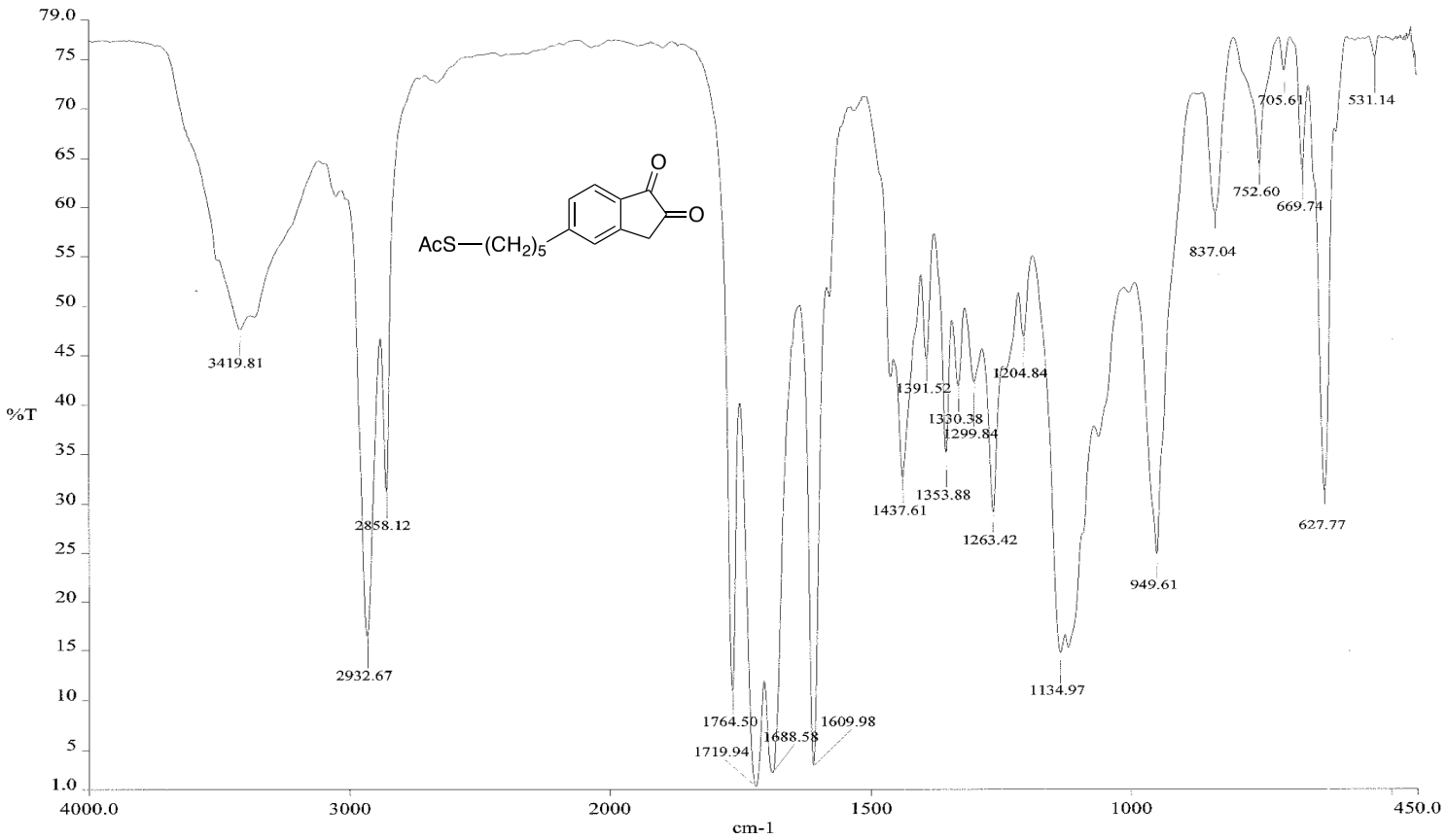

Figure 128: Infrared spectra (neat) of **51**

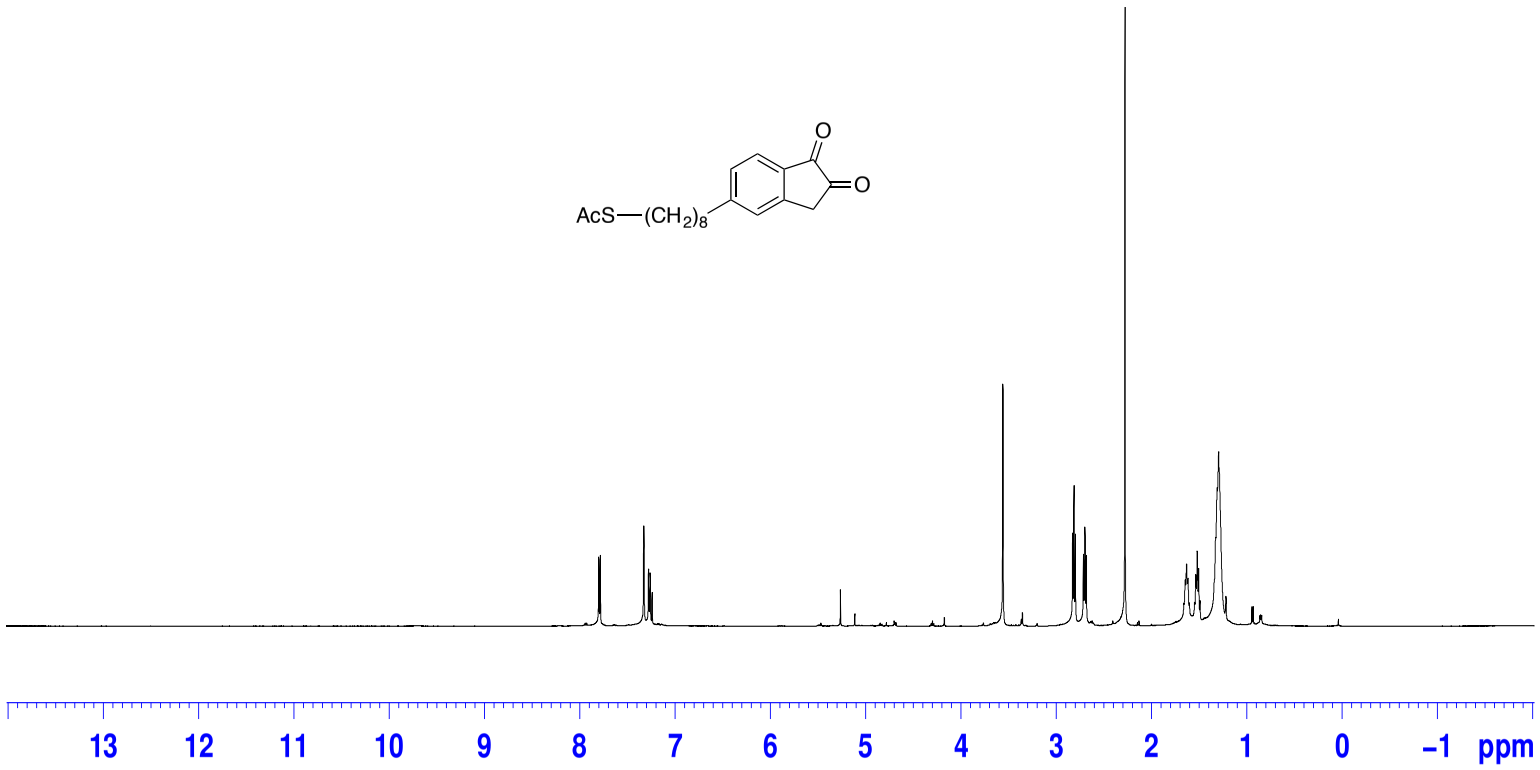

Figure 129: ^{1}H NMR ($CDCl_3$, 500 MHz) of **52**

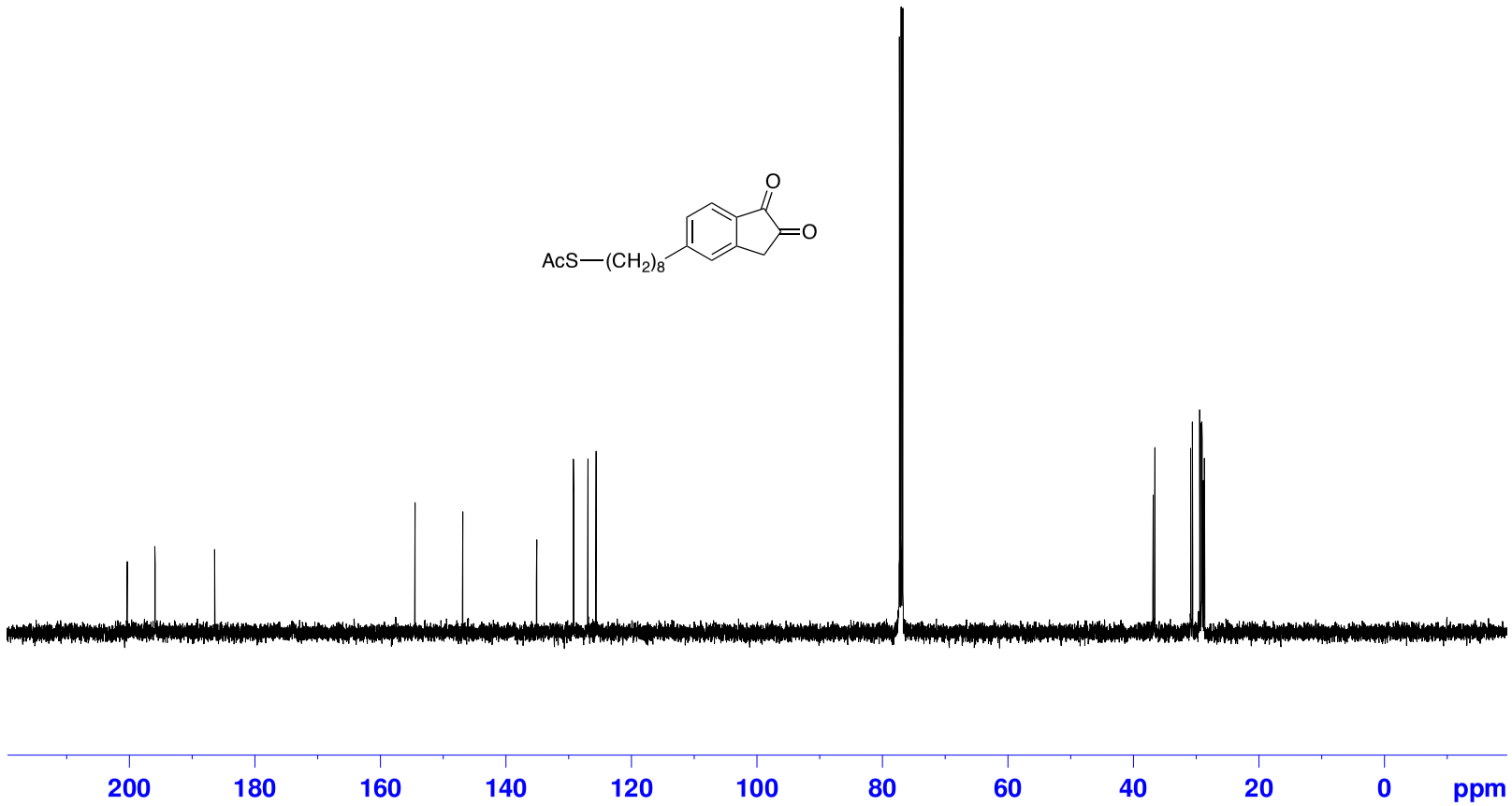

Figure 130: ^{1}H NMR ($CDCl_3$, 500 MHz) of **52**

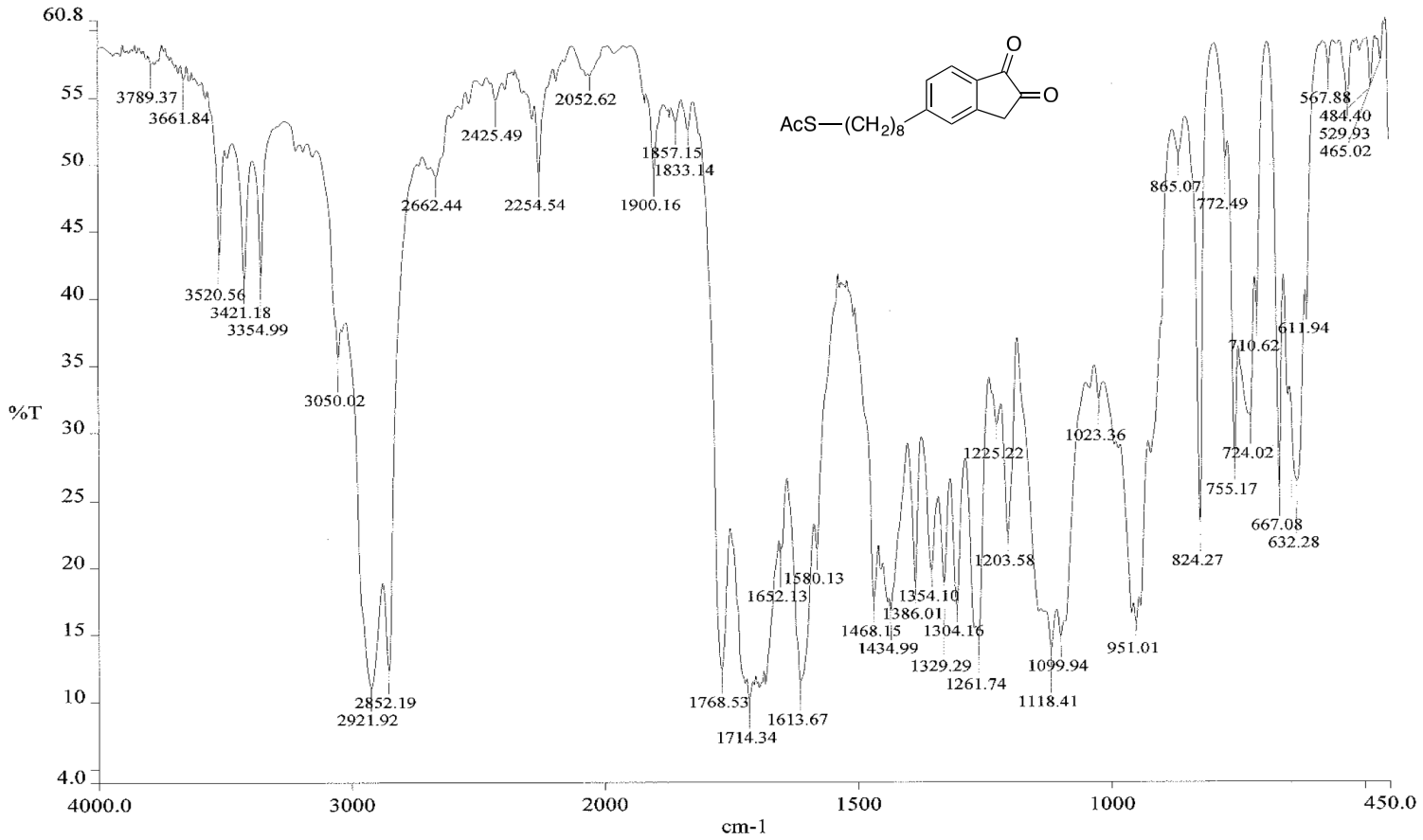

Figure 131: Infrared spectra (neat) of **52**

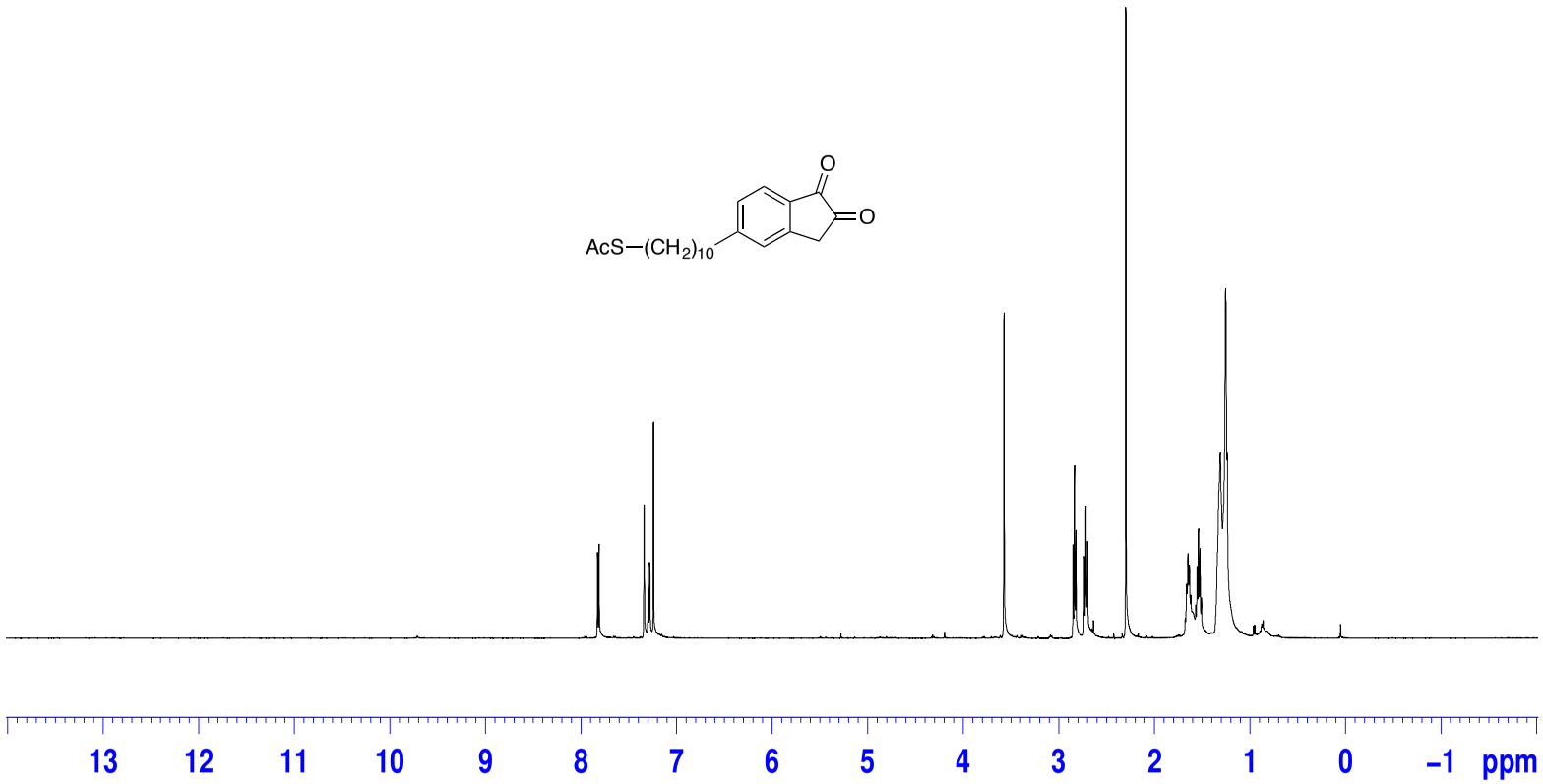

Figure 132: ^{1}H NMR ($CDCl_3$, 500 MHz) of **53**

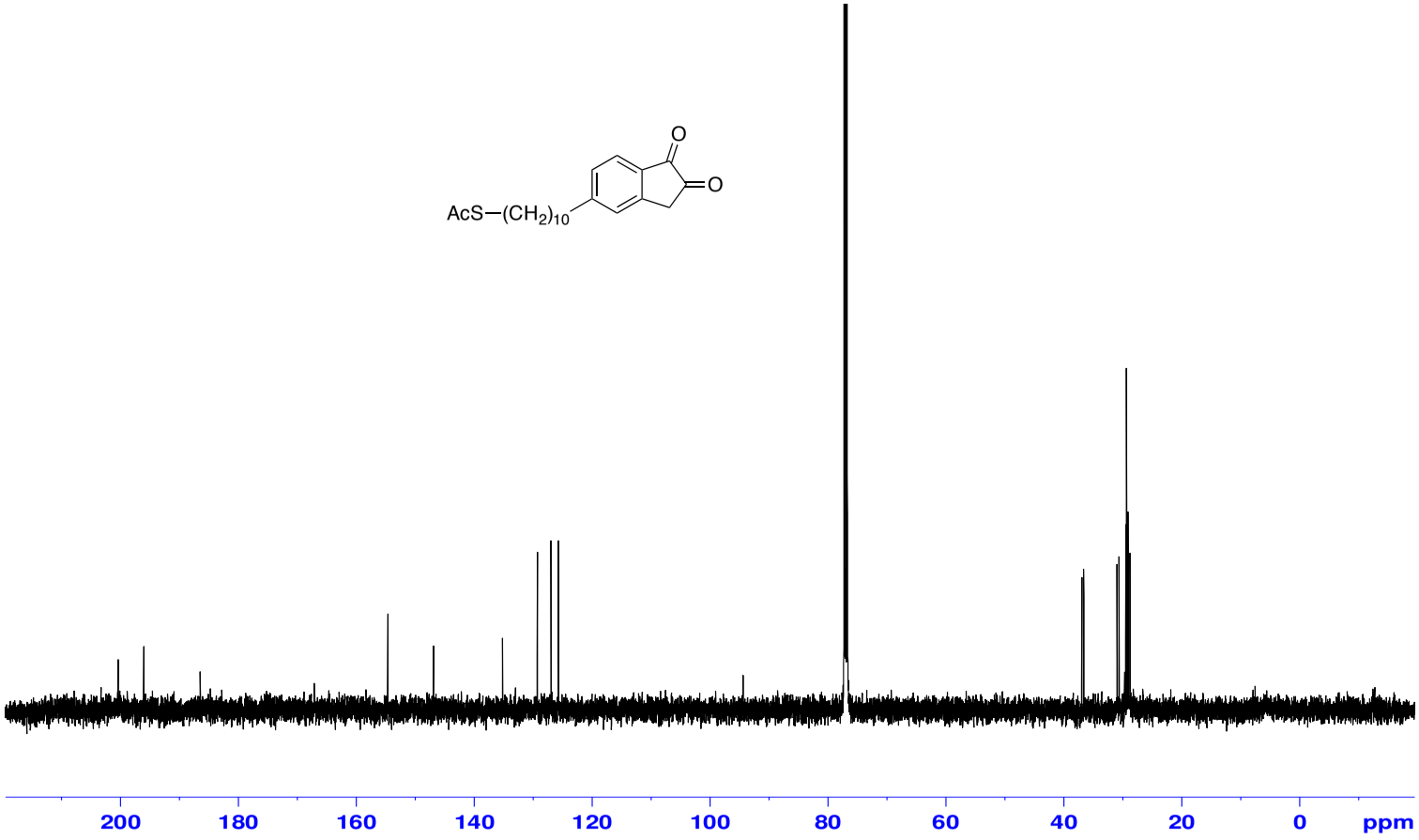

Figure 133: ^{1}H NMR ($CDCl_3$, 500 MHz) of **53**

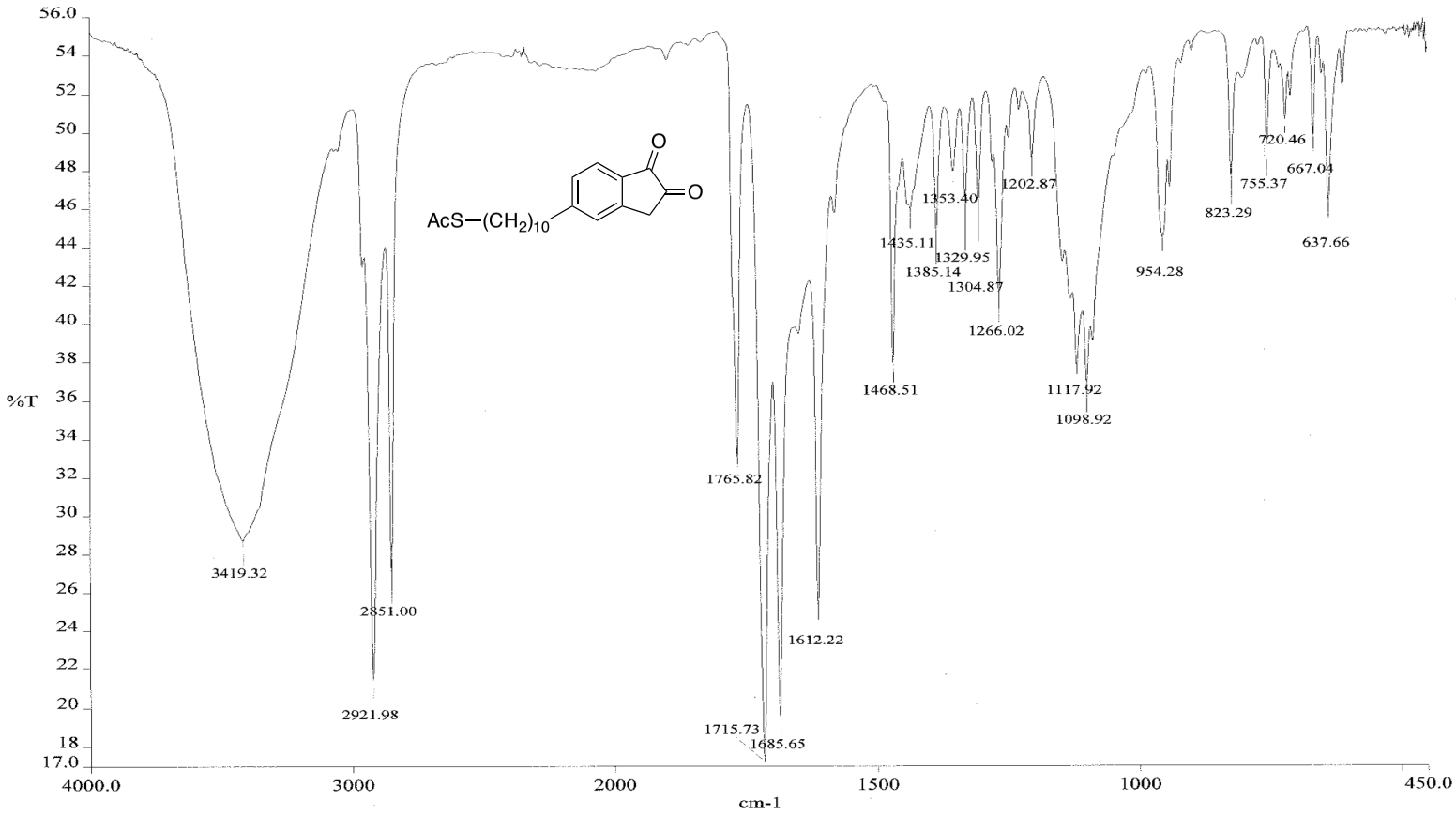

Figure 134: Infrared spectra (neat) of **53**

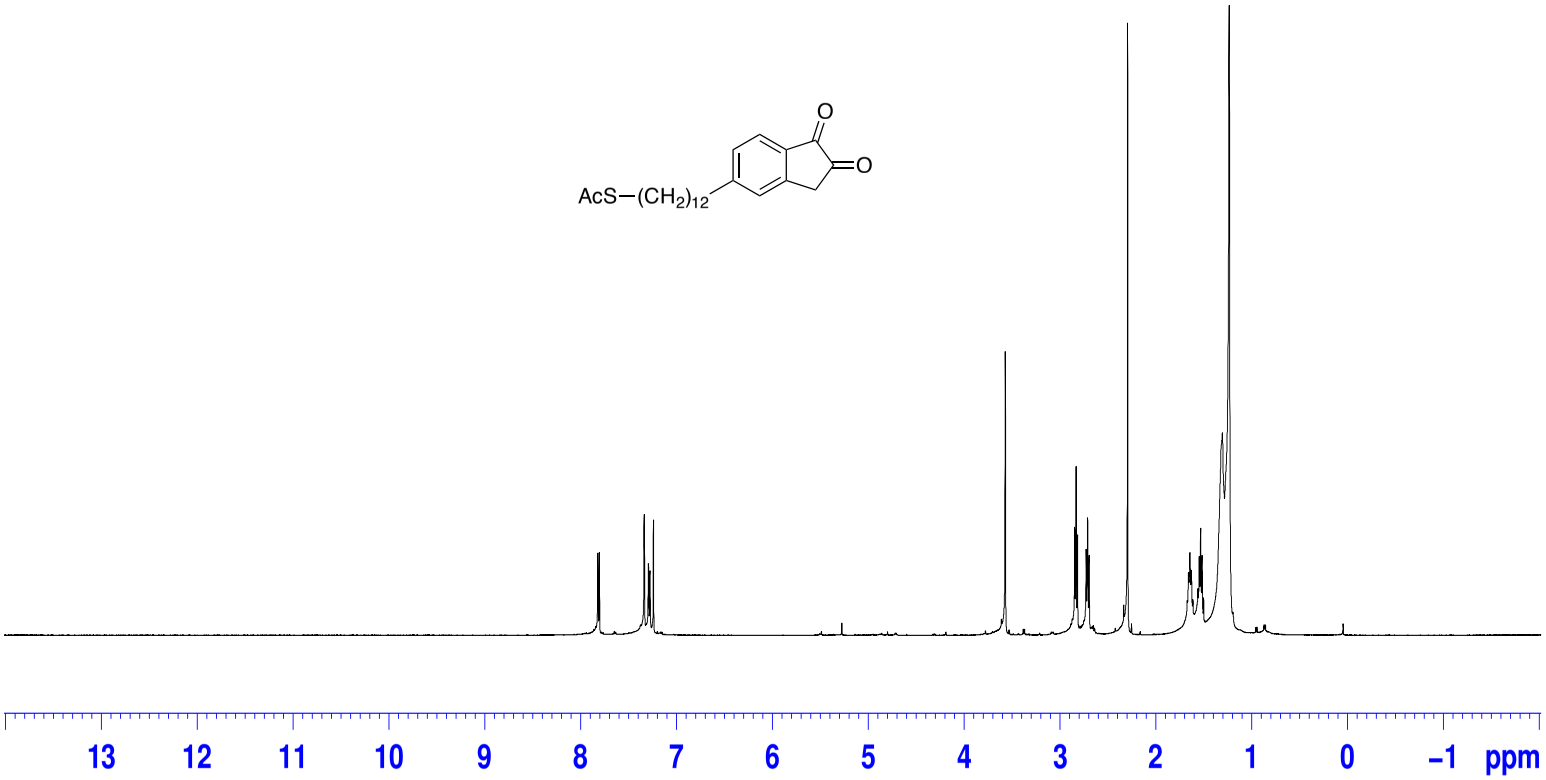

Figure 135: ^{1}H NMR ($CDCl_3$, 500 MHz) of **54**

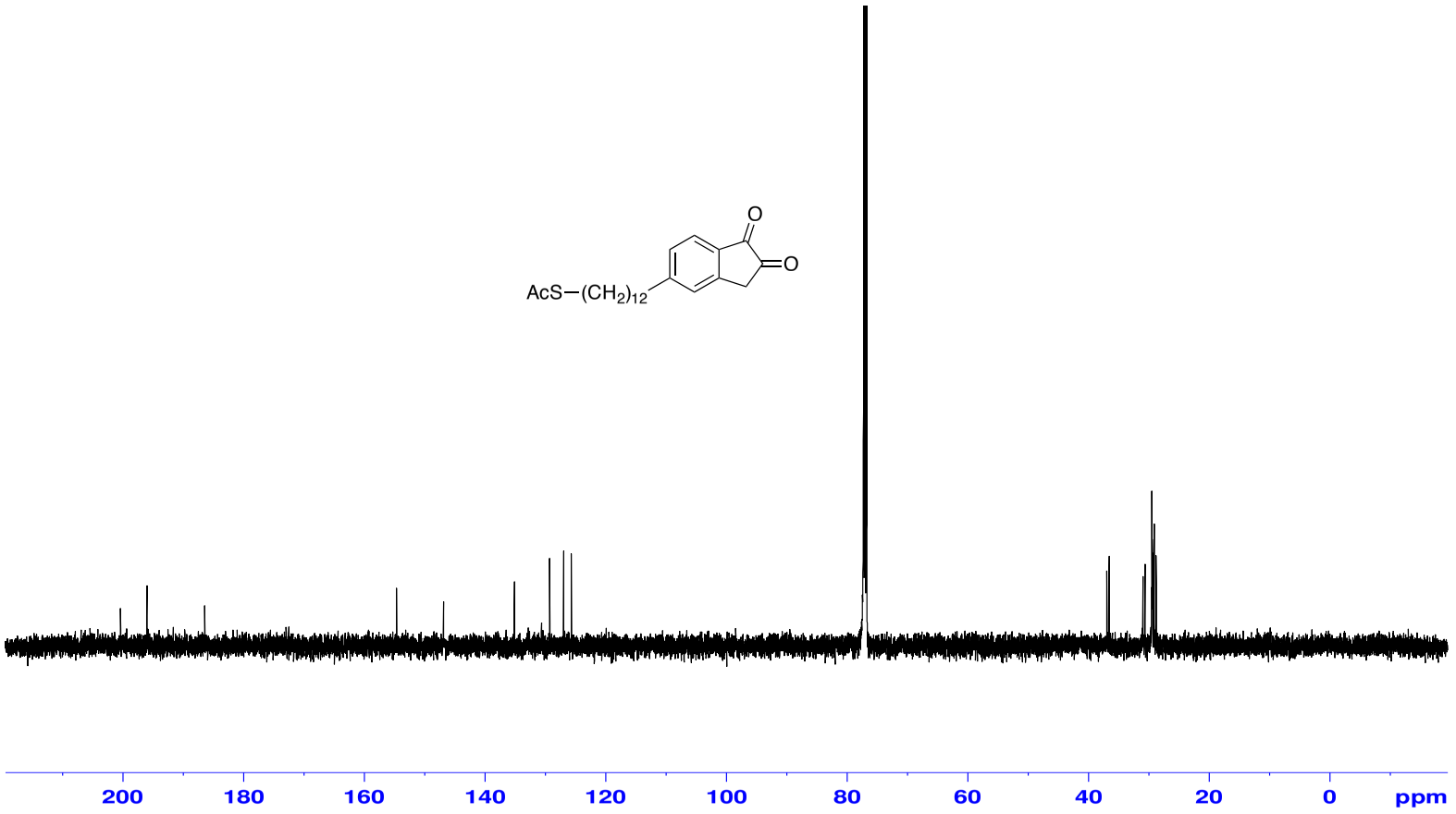

Figure 136: ^{1}H NMR ($CDCl_3$, 500 MHz) of **54**

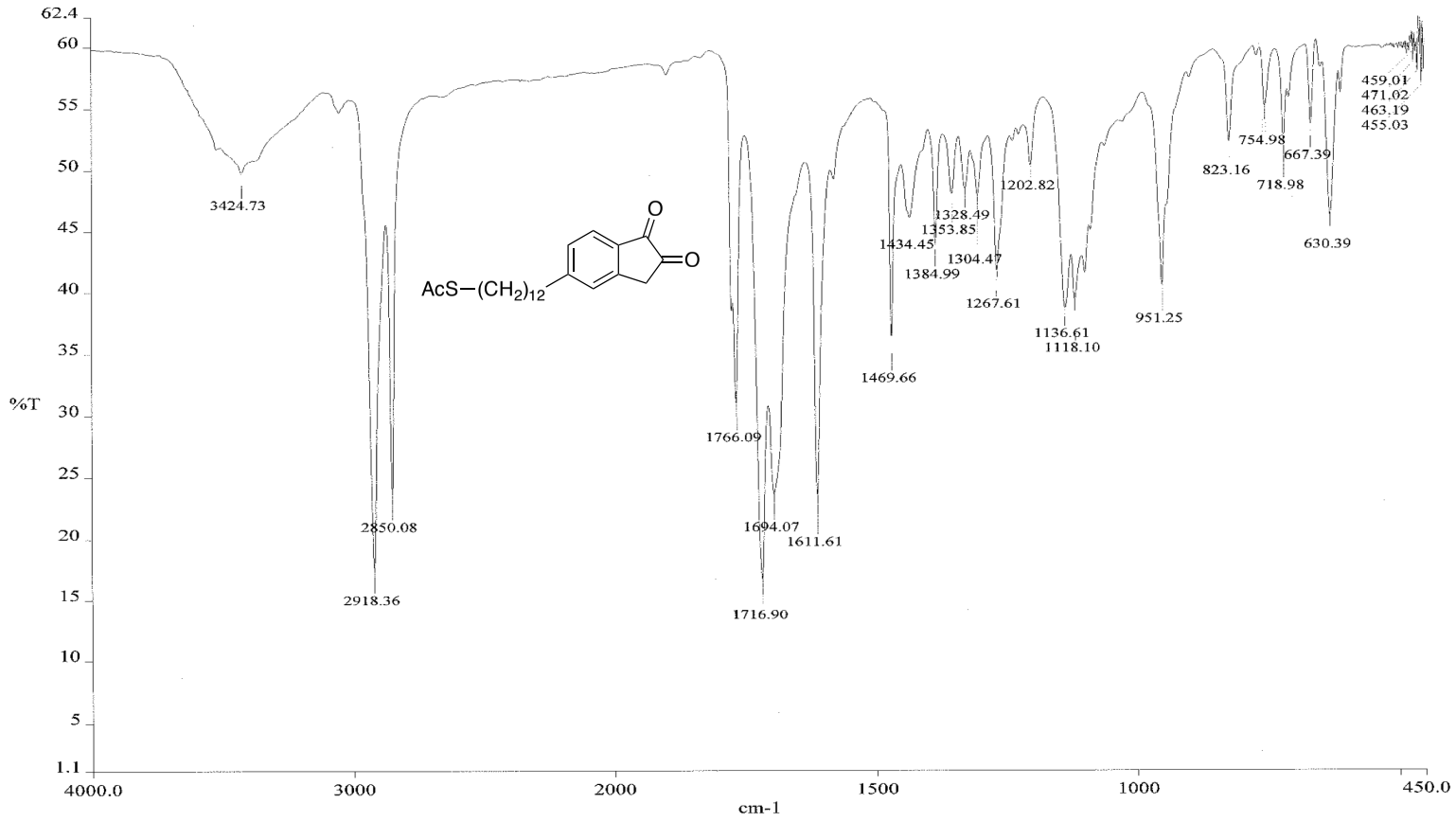

Figure 137: Infrared spectra (neat) of **54**

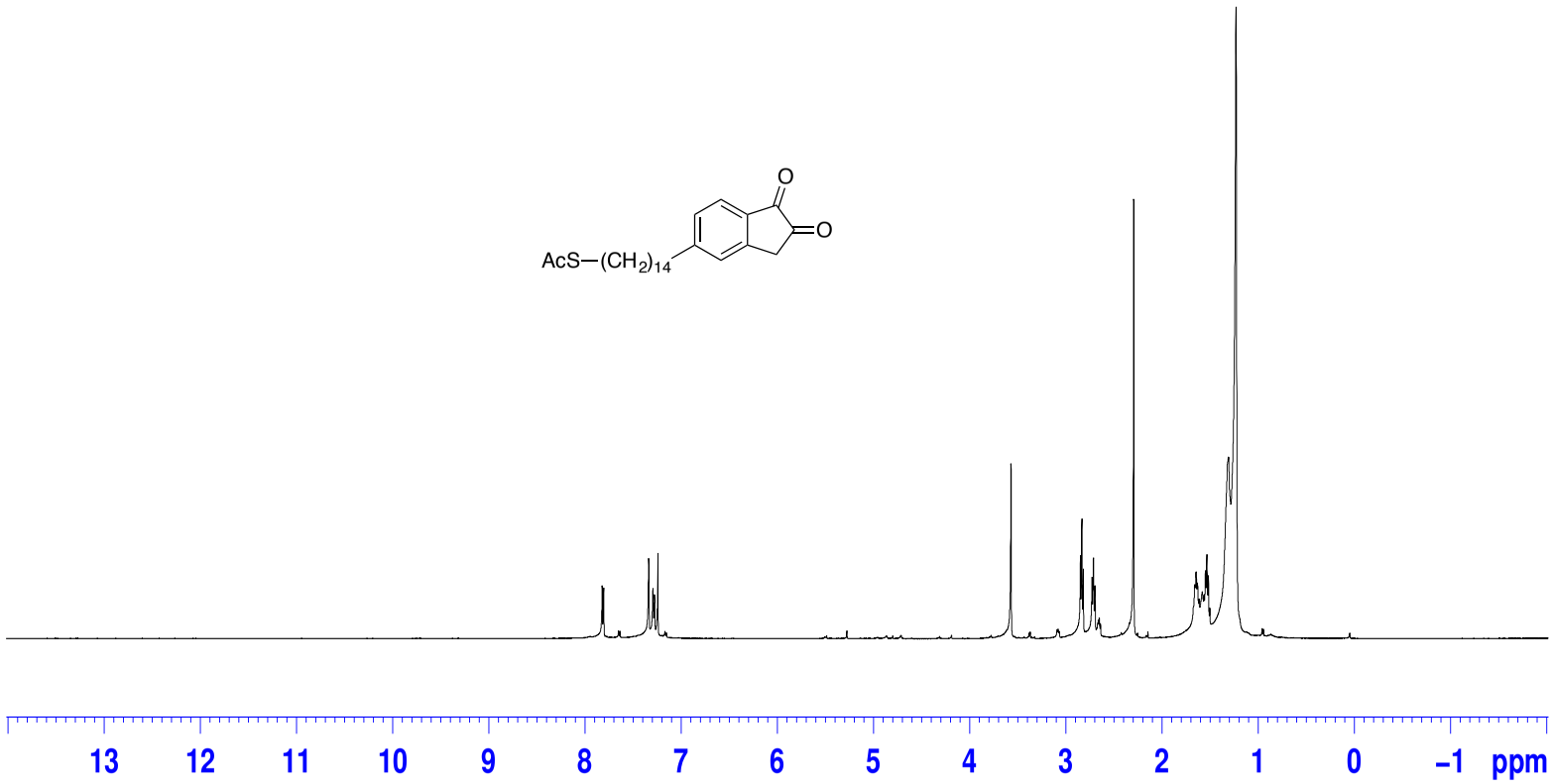

Figure 138: ^{1}H NMR ($CDCl_3$, 500 MHz) of **55**

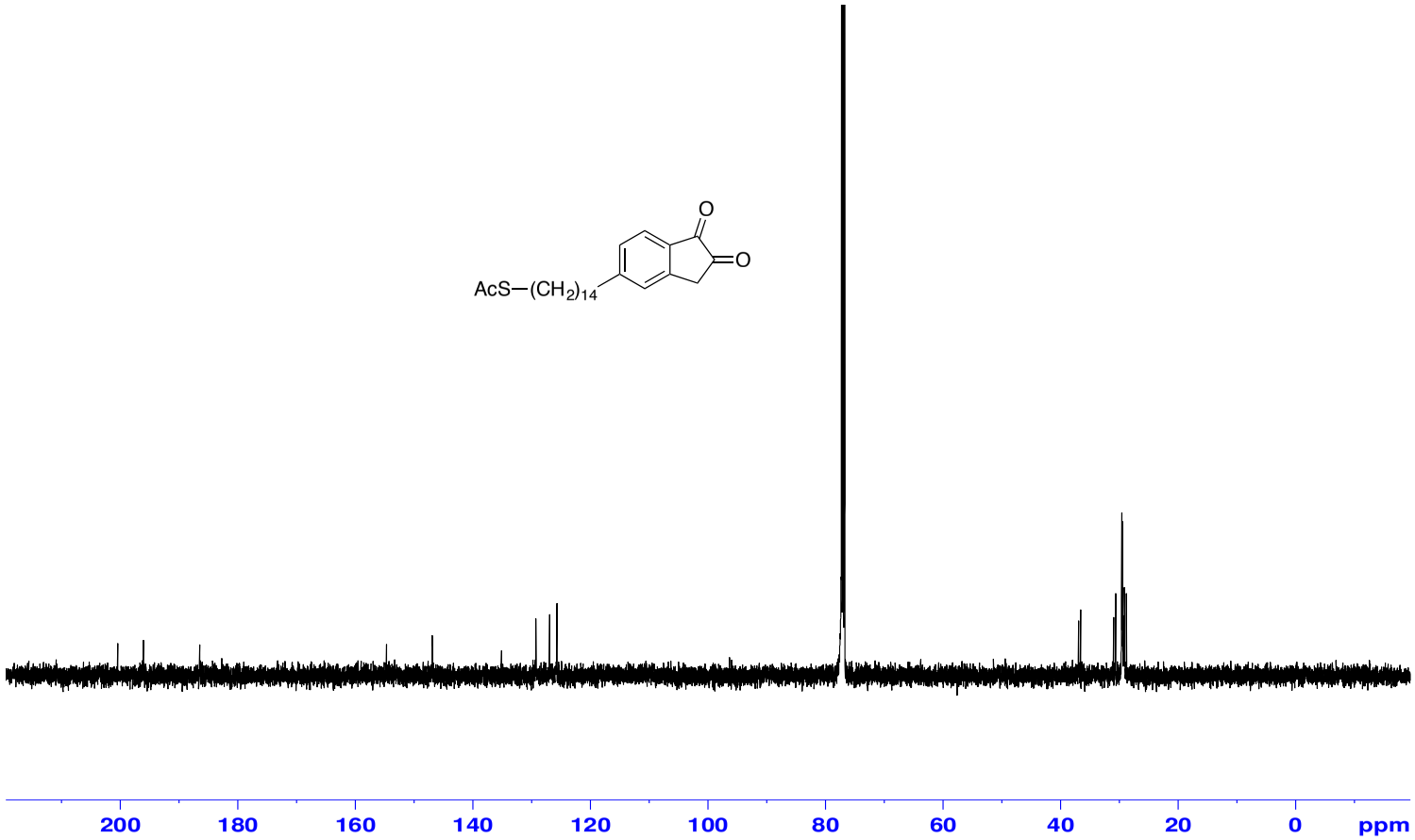

Figure 139: ^{1}H NMR ($CDCl_3$, 500 MHz) of **55**

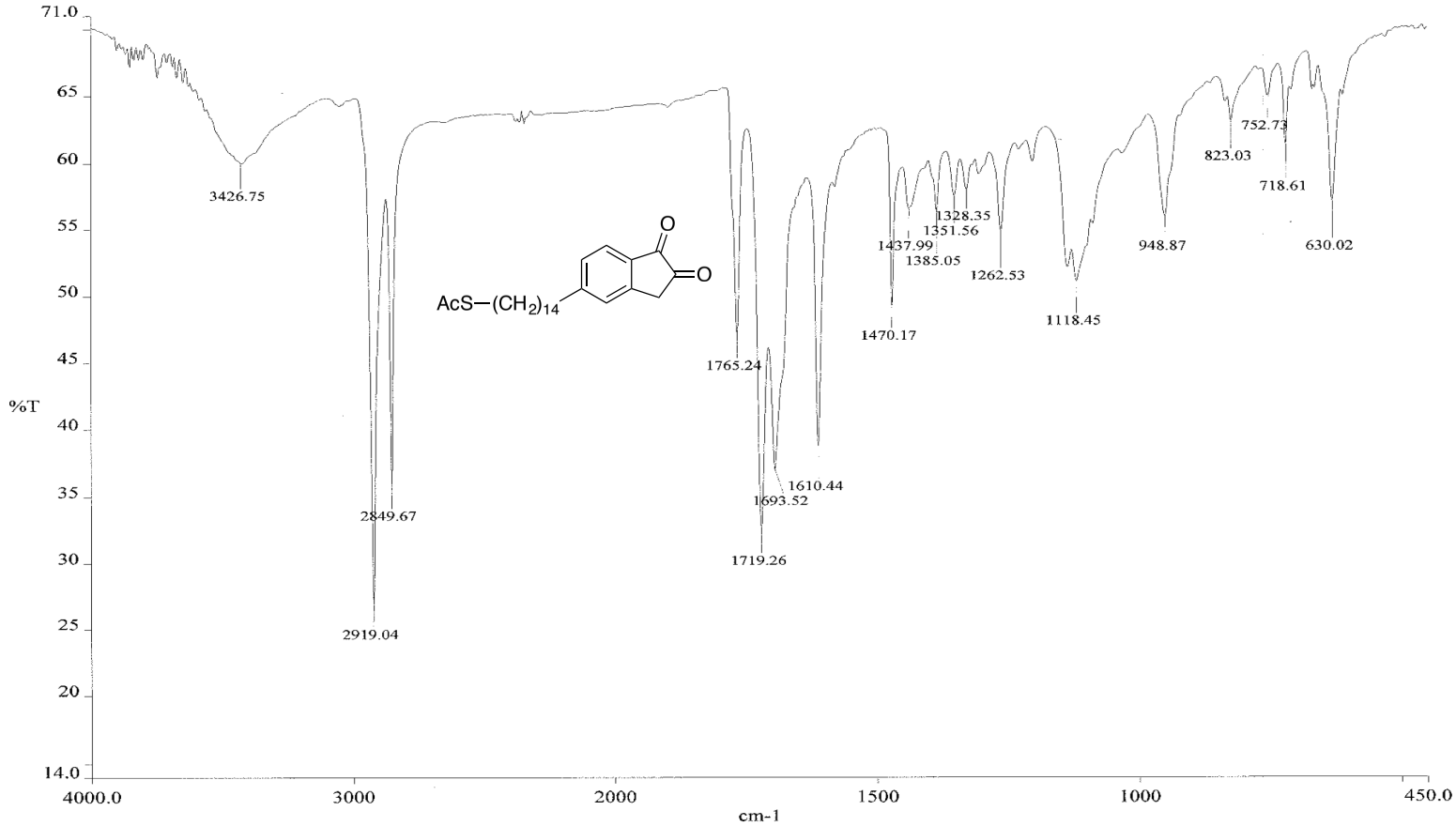

Figure 140: Infrared spectra (neat) of **55**

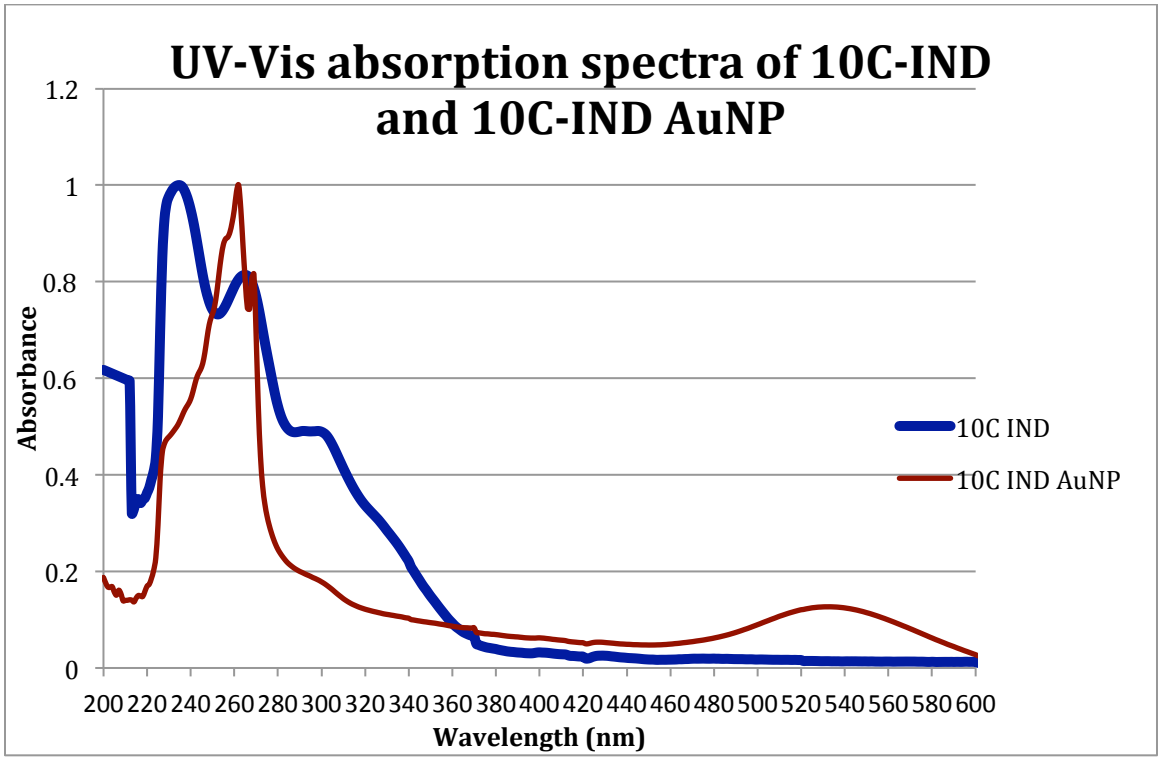

UV Absorption spectra of **53** (10C IND) in CH_2Cl_2 and gold nanoparticles functionalized with **53** (10C IND AuNP) in CH_2Cl_2.